University of KwaZulu-Natal

Synthesis, Characterisation and Antibacterial Activity of New Quinoline and Quinoxaline Hybrid Molecules

2018

Shirveen Sewpersad

Synthesis, Characterisation and Antibacterial Activity of New Quinoline and Quinoxaline Hybrid Molecules

A Thesis

submitted in partial fulfillment for the requirements

for the award of the degree of

Doctor of Philosophy

in the

School of Chemistry and Physics

College of Agriculture, Engineering & Science, University of KwaZulu-Natal,

Westville,

By

Shirveen Sewpersad

2018

Supervisor: Prof. N.A. Koorbanally

Synthesis, Characterisation and Antibacterial Activity of New Quinoline and Quinoxaline Hybrid Molecules

by

Shirveen Sewpersad

2018

A thesis submitted to the School of Chemistry and Physics, College of Agriculture, Engineering and Science, University of KwaZulu-Natal, for the degree of Doctor of Philosophy.

This thesis has been prepared according to **Format 4** as outlined in the guidelines from the College of Agriculture, Engineering and Science which states:

This is a thesis in which chapters are written as a set of discrete research papers, with an overall introduction and final discussion, where one (or all) of the chapters have either been submitted for publication or already been published. Typically these chapters will have been published in internationally recognized, peer- reviewed journals.

To my family, in memory of my Dad

If- *by Rudyard Kipling*

If you can keep your head when all about you
   Are losing theirs and blaming it on you;
If you can trust yourself when all men doubt you,
   But make allowance for their doubting too;
If you can wait and not be tired by waiting,
   Or, being lied about, don't deal in lies,
Or, being hated, don't give way to hating,
   And yet don't look too good, nor talk too wise;

If you can dream—and not make dreams your master;
   If you can think—and not make thoughts your aim;
If you can meet with triumph and disaster
   And treat those two impostors just the same;
If you can bear to hear the truth you've spoken
   Twisted by knaves to make a trap for fools,
Or watch the things you gave your life to broken,
   And stoop and build 'em up with wornout tools;

If you can make one heap of all your winnings
   And risk it on one turn of pitch-and-toss,
And lose, and start again at your beginnings
   And never breathe a word about your loss;
If you can force your heart and nerve and sinew
   To serve your turn long after they are gone,
And so hold on when there is nothing in you
   Except the Will which says to them: "Hold on";

If you can talk with crowds and keep your virtue,
   Or walk with kings—nor lose the common touch;
If neither foes nor loving friends can hurt you;
   If all men count with you, but none too much;
If you can fill the unforgiving minute
With sixty seconds' worth of distance run—
   Yours is the Earth and everything that's in it,
And—which is more—you'll be a Man, my son!

Preface

I hereby declare that the thesis entitled "**Synthesis, Characterisation and Antibacterial Activity of New Quinoline and Quinoxaline Hybrid Molecules**" submitted to the University of KwaZulu-Natal for the award of degree of Doctor of Philosophy in Chemistry under the supervision of Professor Neil A. Koorbanally represents original work by the author and has not been submitted in full or part for any degree or diploma at this or any other University. Where use was made of the work of others it has been duly acknowledged in the text. This work was carried out at the School of Chemistry and Physics, University of KwaZulu-Natal, Westville campus, Durban, South Africa.

Signed: ____________________

Shirveen Sewpersad, MSc (UKZN)

As the candidate's supervisor, I have approved this dissertation for submission

Signed: ____________________

Prof. Neil A. Koorbanally, PhD (Natal)

Declaration - Plagiarism

I, **Shirveen Sewpersad**, declare that:

1. The research reported in this thesis, except where otherwise indicated is my original research.

2. This thesis has not been submitted for any degree or examination at any other university.

3. This thesis does not contain other persons' data, pictures, graphs or other information, unless specifically acknowledged as being sourced from other persons.

4. This thesis does not contain other persons' writing, unless specifically acknowledged as being sourced from other researchers. Where other written sources have been quoted, then,

a) their words have been re-written but the general information attributed to them has been referenced or

b) where their exact words have been used, then their writing has been placed in italics and inside quotation marks, and referenced.

5. This thesis does not contain text, graphics or tables copied and pasted from the internet, unless specifically acknowledged, and the source being detailed in the thesis and in the reference list.

Signed ……………………………………..

Acknowledgements

I would to thank my supervisor Prof. Neil A. Koorbanally, for giving me the opportunity to persue my doctoral research; your guidance and dedication has shaped my outlook on academia and given me something to aspire to, as a chemist and as a person. Your kindness, patience and generosity above all else will stay with me.

To my family, your sacrifices and support have given me the opportunity to persue my studies, the understanding you have shown on this long journey is something I will always be thankful for and I hope to have made you proud.

To my campus family Vashen and Kaalin, for contending with all my crises or irrationalities and sharing the fun times, know that I appreciate the times we have shared immensely. Kaalin, I owe a great deal of this study to your constant encouragement and drive, for this I am thankful.

To my labmates, your help, whether it be brainstorming ideas or troubleshooting, has taught me a great deal and helped me develop as a chemist.

To my friends Sasha, Shaun, Rishab, Kamal, Ashvir, Kyle, Sam and Kavashan for helping me relax when needed and also understanding all my work related abscences

To the technical and support staff of the School of Chemistry and Physics, namely; Malini, Brian, Renee, Anita, Raj, Miler, Shannon and Greg for always trying their best to fulfil my requests regardless of how big or small.

To Mr Sizwe Zamisa for crystallographic data collection and refinement, Mrs Caryl Janse van Rensburgh for conducting HRMS and Dr Chunderika Mocktar for her assistance in conducting antibacterial assays.

Finally to the National Research Foundation for a generous Scarce Skills grant which provided invaluable assistance throughout this study

Abstract

This thesis focussed on the synthesis of three series of hybrid molecules, all related to the quinoline or quinoxaline scaffolds. These are (i) 2-(1*H*-benzo[d]imidazol-2-yl)quinolines, (ii) quinoxaline-chalcones and their pyrazoline derivatives, and (iii) 5-(quinolin-2-ylmethylene)-2-thioxothiazolidin-4-ones. The target molecules were fully characterized particularly by 2D NMR and verified by high resolution mass spectrometry. The synthesised compounds were tested for their antibacterial activity against two Gram +ve species, *Staphylococcus aureus* and MRSA and four Gram -ve bacteria, *Pseudomonas aeruginosa*, *Klebsiella pneumoniae*, *Escherichia coli* and *Salmonella typhimurium* to identify lead compounds which could be developed into active pharmaceutical ingredients for antibiotics. A total of fifty-six compounds were synthesised based on these scaffolds.

The 2-(1*H*-benzo[*d*]imidazol-2-yl)quinolines were synthesised by the Doebner-Miller reaction of crotonaldehyde and substituted anilines, followed by oxidation and benzimidazole formation with *o*-phenylenediamine. The series of compounds consisted of 6- and 8- substituted halogen, methoxy and methyl groups. A complete structural elucidation of all compounds was carried out and the effects that the different substituents had on the resonances of the quinoline scaffold reported. The quinoxaline-chalcone and quinoxaline-chalcone-quinoline hybrids were synthesised from a quinoxaline acetophenone derivative and various 2- or 4- substituted benzaldehydes and 6- or 8- substituted quinoline-2-carbaldehydes *via* the Claisen-Schmidt condensation. These molecules were then converted to their respective pyrazoline derivatives using hydrazine hydrate. The 5-(quinolin-2-ylmethylene)-2-thioxothiazolidin-4-ones were synthesised from the Knoevenagel reaction of various 8- and 6-substituted quinoline-2-carbaldehydes and rhodanine. The method described is a convenient way to tag a rhodanine moeity onto a quinoline ring.

Of the three sets of compounds synthesised, only the quinoxaline-chalcone-quinoline hybrids showed appreciable antibacterial activity, being active against the Gram +ve *S. aureus* and MRSA and not against the Gram -ve species, with the activity against *S. aureus* being much higher than that for MRSA. Quinoxaline chalcones showed no activity against the bacterial strains tested, however, when a quinoline moiety replaced the aromatic ring, eight derivatives showed enhanced antibacterial activity, having MBC values between 0.151-0.360 μM against *S. aureus* and 10.9-618 μM against MRSA. The quinoxaline-chalcone-quinoline hybrids showed antibacterial activity two orders of magnitude greater than ciprofloxacin and levofloxacin against *S. aureus* and comparable activity to these standards against MRSA. Interestingly, the 4'-Br and 4'-Cl pyrazoline derivatives of the quinoxaline chalcones (having MBC values of 11 and 12 μM, respectively) showed comparable activity to levofloxacin and ciprofloxacin.

List of Abbreviations

°C	degrees Celsius
^{13}C NMR	carbon-13 nuclear magnetic resonance spectroscopy
^{1}H NMR	proton nuclear magnetic resonance spectroscopy
aq	aqueous
br	broad
$CDCl_3$	deuterated chloroform
COSY	homonuclear correlation spectroscopy
d	doublet
dd	doublet of doublets
ddd	doublet of doublet of doublets
dddd	doublet of doublet of doublet of doublets
DMF	dimethylformamide
DMSO	dimethyl sulfoxide
DMSO-d_6	deuterated dimethyl sulfoxide
EtOAc	ethyl acetate
EtOH	ethanol
FID	free induction decay
FTIR	Fourier transform infrared
h	hour
HMBC	heteronuclear multiple bond correlation
HRMS	high resolution mass spectrometry
HSQC	heteronuclear single quantum coherence
Hz	hertz
IR	infrared
µM	micromolar
m	multiplet
MBC	minimum bactericidal concentration
MeOH	methanol
MHA	Mueller-Hinton agar

MHz	megahertz
min	minutes
mL	millilitre
mmol	millimole
mp	melting point
MW	microwave irradiation
NC	nanocomposite
NHP	*N*-hydroxyphthalimide
NMP	*N*-methylpyrrolidine
ORTEP	Oak Ridge thermal ellipsoid plot
PIDA	phenyliodine(III) diacetate
PPA	polyphosphoric acid
RT	room temperature
s	singlet
t	triplet
td	triplet of doublets
THF	tetrahydrofuran
TLC	thin layer chromatography
TMS	tetramethylsilane
TMSCl	trimethylsilyl chloride
UV	ultraviolet

List of Compounds in Chapter 2

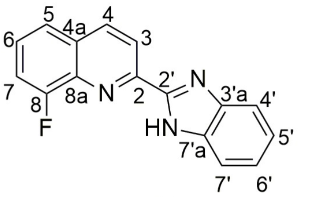

A5a

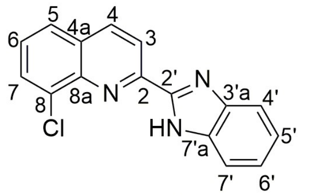

A5b

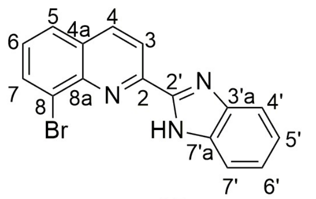

A5c

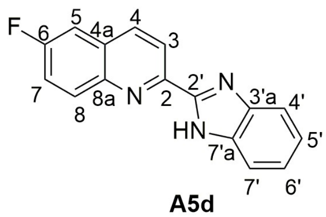

A5d

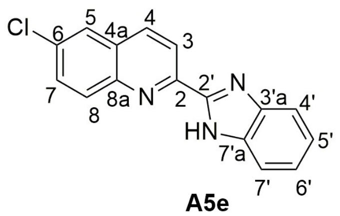

A5e

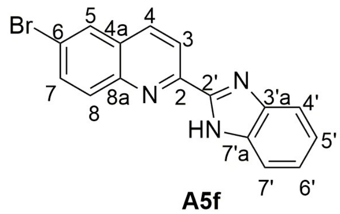

A5f

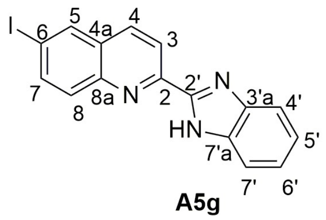

A5g

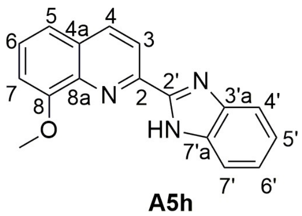

A5h

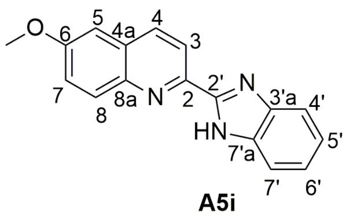

A5i

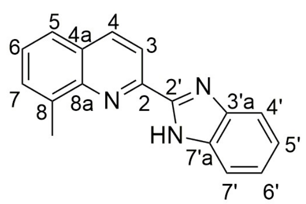

A5j

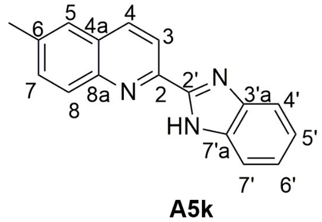

A5k

List of Compounds in Chapter 3

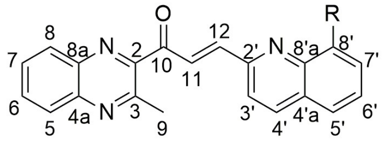

B7a: R = F
B7b: R = Cl
B7c: R = Br
B7d: R = CH_3

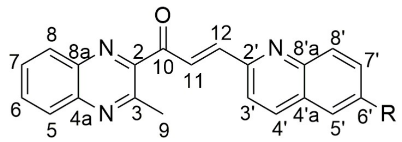

B7e: R = F
B7f: R = Cl
B7g: R = Br
B7h: R = CH_3
B7i: R = OCH_3

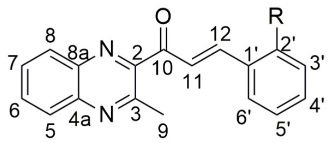

B10a: R = F
B10b: R = Cl
B10c: R = Br
B10d: R = CH_3

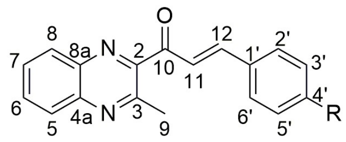

B10e: R = F
B10f: R = Cl
B10g: R = Br
B10h: R = CH_3
B10i: R = OCH_3

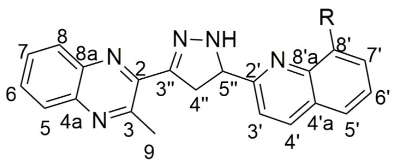

B8a: R = F
B8b: R = Cl
B8c: R = Br
B8d: R = CH_3

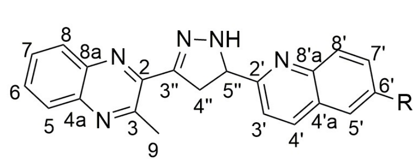

B8e: R = F
B8f: R = Cl
B8g: R = Br
B8h: R = CH_3

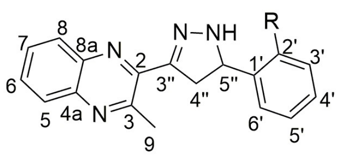

B11a: R = F
B11b: R = Cl
B11c: R = Br
B11d: R = CH_3

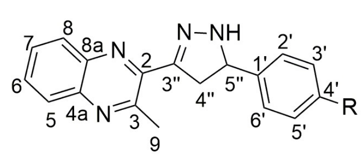

B11e: R = F
B11f: R = Cl
B11g: R = Br
B11h: R = CH_3
B11i: R = OCH_3

List of Compounds in Chapter 4

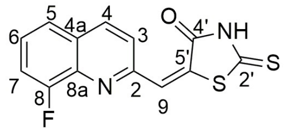

C5a

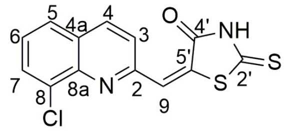

C5b

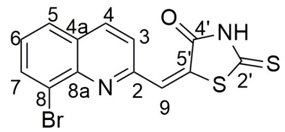

C5c

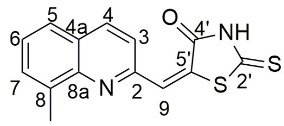

C5d

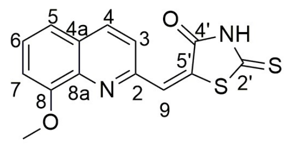

C5e

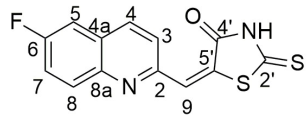

C5f

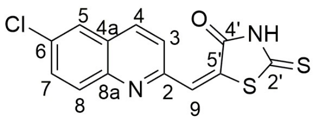

C5g

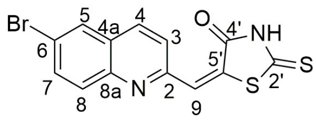

C5h

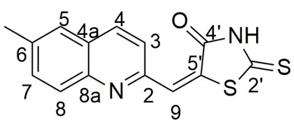

C5i

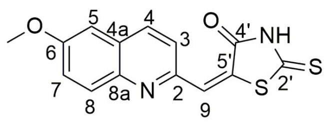

C5j

Table of Contents

List of Schemes

List of Figures

List of Tables

Chapter 1. Introduction

The pharmaceutical industry is constantly in a quest for new and improved drugs to combat a number of diseases, ailments and medical conditions. It is what makes them profitable and ensures a better quality of life. Historically people have died of fever, measles and even the common cold. Drugs and vaccines have totally overcome fatalities associated with these. In the future, HIV and cancer will become a thing of the past through the search for molecular entities that can control or fight against the pathogens or processes leading to these diseases.

Amongst the fight against pathogens which threaten the well-being of human life, antibacterial resistance is at the forefront. Overuse of antibiotics and prescription of broad spectrum antibiotics when not needed are some of the causes of antibacterial resistance (Davies and Davies, 2010). If left unaddressed, this could lead to pandemics in modern society. There is thus a need to produce new and improved antibiotics to lead the fight against bacterial pathogens.

One approach to developing novel antibiotics is using the molecular hybrid approach. This method combines two or more pharmacophores into a single molecule. The aim is to enhance bioactivity by gaining the best of both worlds, allowing each pharmacophore to act on enzymes or other biological targets and thus enhance the activity that each individual pharmacophore may have on its own. The new hybrid drug may be more potent, safer or cheaper or possess fewer side effects than known drugs. Molecular hybrids are engineered using synthetic organic designs, placing one pharmacophore on another through a reaction of functional groups or forming new pharmacophores on existing scaffolds through organic transformations (Viegas-Junior et al., 2007).

1.1. Quinoline

Quinoline is composed of a pyridine ring fused to a benzene ring. Quinoline derived heterocycles are found to have a wide range of biological activities (Prajapati et al., 2014; Jain et al., 2016) and are found in a number of naturally occurring therapeutic compounds such as quinine (an antimalarial isolated from the cinchona tree), and camptothecin (an anticancer drug extracted from the *Camptotheca acuminata*) (**Figure 1-1**) (Sriram et al., 2005; Achan et al., 2011). The efficacy of such natural products has formed the basis for the development of new and more potent drugs.

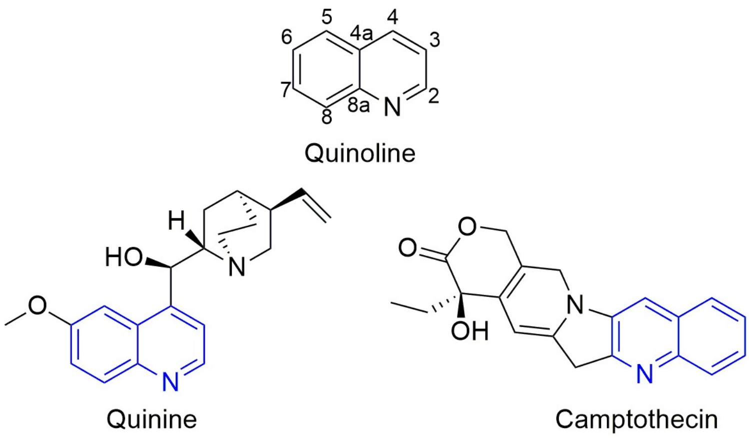

Figure 1-1 The basic structure of quinoline and two examples of naturally occurring quinoline containing therapeutic agents

Quinoline compounds have demonstrated a myriad of therapeutic activities (Kumar et al., 2009; Marella et al., 2013) such as antibacterial (Musiol et al., 2011), anticancer (Solomon and Lee 2011; Afzal et al., 2015; Gopaul et al., 2015), anticonvulsant (Siddiqui et al., 2010), antifungal (Musiol et al., 2010), antileishmanial (Gopinath et al., 2013; Gopinath et al., 2014), antimalarial (Foley and Tilley, 1998; van Schalkwyk and Egan, 2006; Vandekerckhove and D'hooghe, 2015), antimycobacterial (Eswaran et al., 2010), anti-oxidant (Maddela et al., 2015), anti-HIV (Luo et al., 2009), anti-inflammatory and cardiovascular applications (Kumar et al., 2009). The commercial use of quinoline-based drugs is also widespread and include levofloxacin (antibiotic), ciprofloxacin (antibiotic), clioquinol (antifungal), montelukast (anti-asthmatic), bosutinib (antileukaemic), bedaquine (antitubercular) and saquinavir (anti-HIV) (**Figure 1-2**). Thus, the quinoline moiety is an attractive scaffold for new lead drugs *via* molecular hybridisation with other moieties with the aim of either finding new pharmaceutical agents or improving on the activity of existing drugs.

1.1.1. Classical approaches to quinoline synthesis

Depending on the synthetic method employed, the quinoline scaffold may be functionalised at a number of positions on the bicyclic system. Classical procedures for quinoline synthesis involve the reaction of anilines or aniline derivatives with various electrophiles (Marella et al., 2013). These include the Camps, Combes, Conrad-Limpach, Doebner, Doebner-von Miller, Friedlander, Knorr, Niementowski, Pfitzinger, Povarov and Skraup syntheses (Madapa et al., 2008; Ramann and Cowen, 2016).

The Combes synthesis (**Scheme 1-1**) comprises the reaction of substituted anilines with *β*-diketones resulting in 2,4-disubstituted quinoline products. The reaction proceeds *via* a *β*-amino-enone intermediate prior to an acid catalysed cyclisation (Kouznetsov et al., 2005; Aribi et al., 2016).

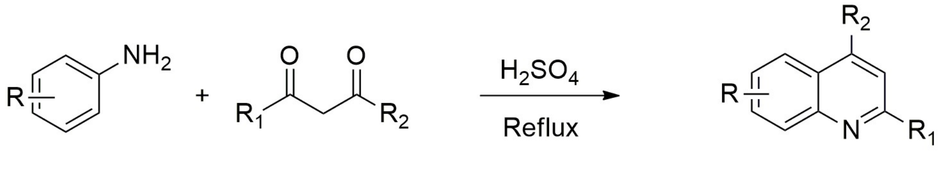

Scheme 1-1 The Combes synthesis of quinolines

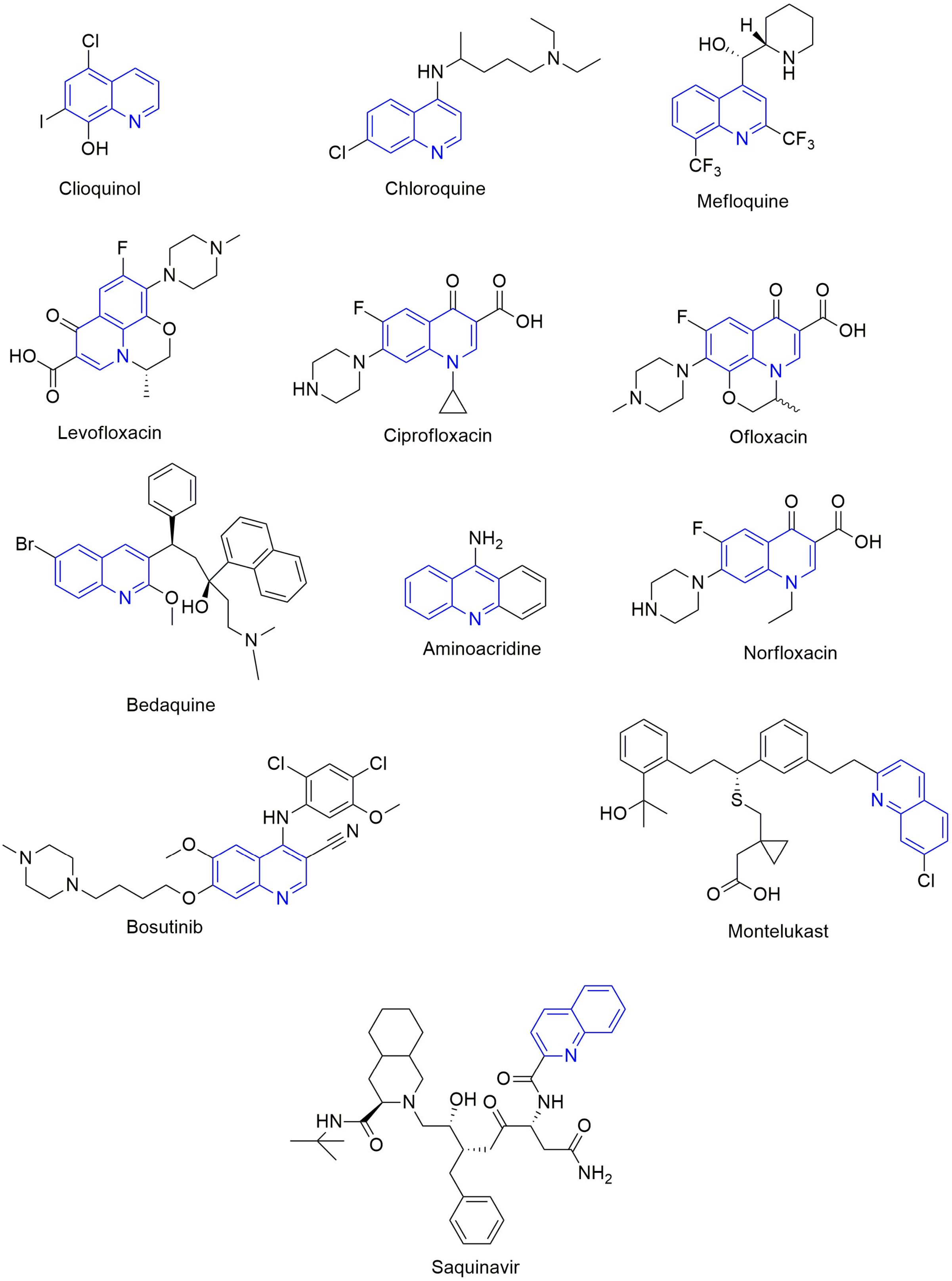

Figure 1-2 Commercially available drugs containing the quinoline scaffold

The Knorr synthesis (Route B, **Scheme 1-2**) and the Conrad-Limpach synthesis (Route A, **Scheme 1-2**), from which it is derived, both involve the reaction of anilines with *β*-ketoesters forming either 4- or 2-hydroxyquinolines. The Conrad-Limpach synthesis is carried out at room temperature using iodine or acid catalysts, with the kinetic 4-hydroxy derivative being favoured over the thermodynamic 2-hydroxy product. This is ascribed to the formation of an alkyl crotonate intermediate. However, at elevated temperatures (~140°C) used in the Knorr modification, an intermediate anilide forms resulting in selective formation of the thermodynamically favoured 2-hydroxy product. The quinolinol products often undergo keto-enol tautomerization with the quinolone form being predominant (Wang, 2010).

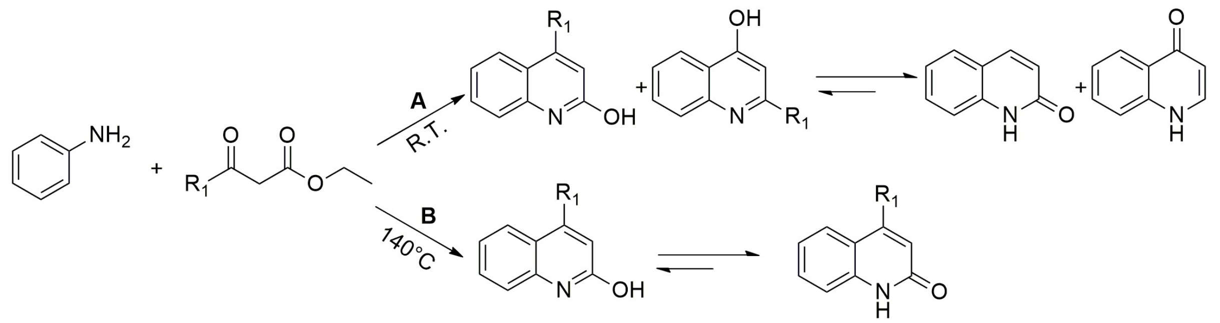

Scheme 1-2 The Conrad-Limpach (A) and Knorr syntheses (B) of quinolones

The Doebner reaction (**Scheme 1-3**) makes use of anilines, aromatic aldehydes and pyruvic acid to form 2-phenylquinoline-4-carboxylic acids. Catalysts such as trifluoroacetic acid (TFA) and acetic acid have been used with solvents varying from ethanol to excess acetic acid (Garudachari et al., 2012; Wang et al., 2016).

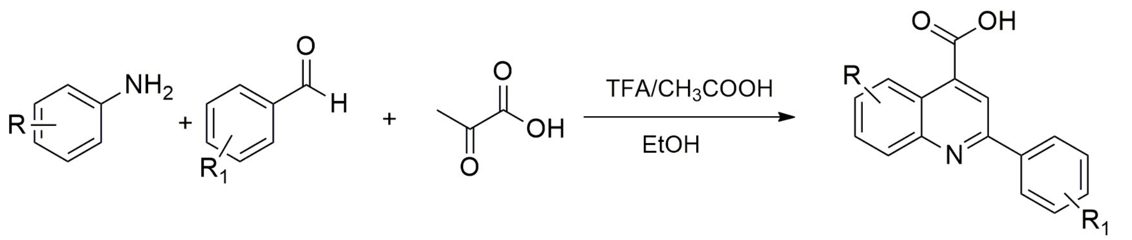

Scheme 1-3 The Doebner reaction of anilines with pyruvic acid and aromatic aldehydes

The reaction of *o*-aminobenzaldehydes with ketones or aldehydes (containing an *α*-methylene group) result in the formation of either C-2, C-3 or C-2 and C-3 substituted quinolines, depending on the choice of ketone or aldehyde in what is known as the Friedlander synthesis (**Scheme 1-4**). This reaction has been carried out using acidic and basic catalysts in aqueous and ethanolic media or at elevated temperatures without catalysts (Madapa et al., 2008; Shiri et al., 2011).

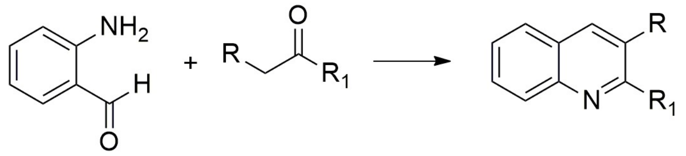

Scheme 1-4 The Friedlander synthesis of *o*-aminobenzaldehydes with aldehydes or ketones

The Niementowski synthesis (**Scheme 1-5**) is similar to the Friedlander reaction above, however, *o*-aminobenzoic acids are used instead of *o*-aminobenzaldehydes. This change resulted in a hydroxyl group at C-4 (Poronik et al., 2017).

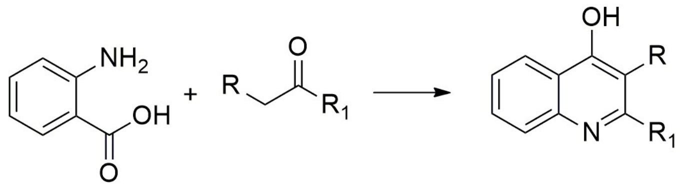

Scheme 1-5 The Niementowski reaction of *o*-aminobenzoic acids with aldehydes or ketones

4-Hydroxyquinolines can also be formed by the reaction of anilines with ethyl ethoxymethylenemalonate in the Gould-Jacobs synthesis (**Scheme 1-6**). Anilines bearing electron donating groups *meta* to the amine group show superior yields to those with electron withdrawing substituents (Li, 2007; Wang, 2010).

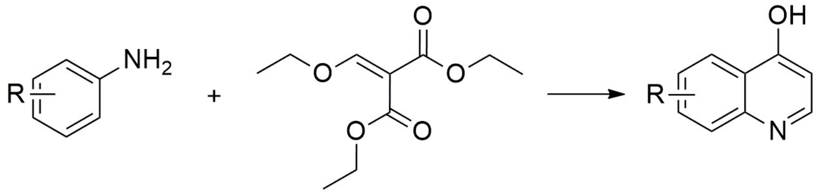

Scheme 1-6 The Gould-Jacobs quinoline synthesis

The base promoted cyclisation of *o*-acylaminoacetophenones is known as the Camps quinoline synthesis (**Scheme 1-7**). This results in either C-2, C-4 or a mixture of C-2 and C-4 hydroxylated products. The products are however believed to exist predominantly in the keto form resulting in quinolones rather than quinolines (Jones et al., 2007; Wang, 2010).

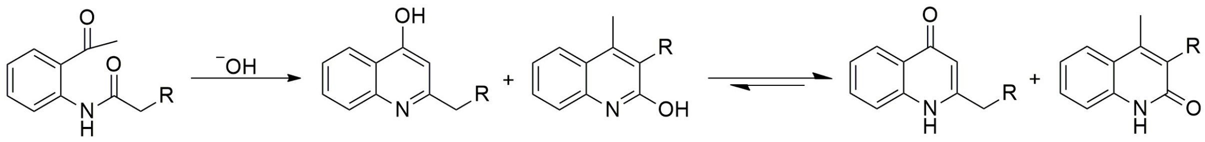

Scheme 1-7 The Camps quinoline synthesis

The Povarov synthesis (**Scheme 1-8**) begins with the reaction of aniline and a benzaldehyde, forming a Schiff base. A Lewis acid such as $BF_3{\cdot}OEt$ is required to activate the resulting imine, which then reacts with an electron rich alkene in a [4+2] cycloaddition reaction forming a quinoline *via* a four membered ring intermediate (Kouznetsov, 2009).

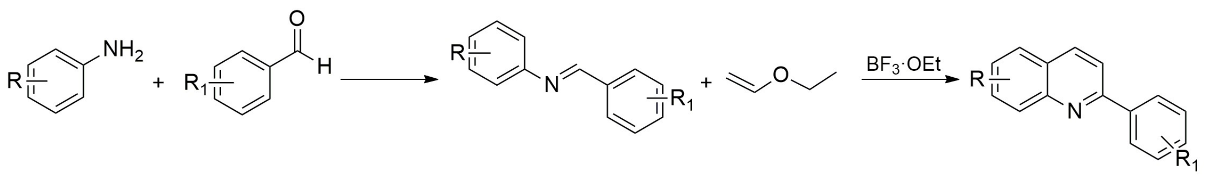

Scheme 1-8 The Povarov synthesis

The Pfitzinger reaction (**Scheme 1-9**) is the base promoted reaction of isatin (1*H*-indole-2,3-dione) with ketones, forming quinolines containing a carboxylic acid at C-4. Disubstitution may occur at C-2 and C-3, depending on the ketone used while substitution on the B-ring of the quinoline moiety may be introduced by using substituted isatin precursors (Shvekhgeimer, 2004; Sangshetti et al., 2014).

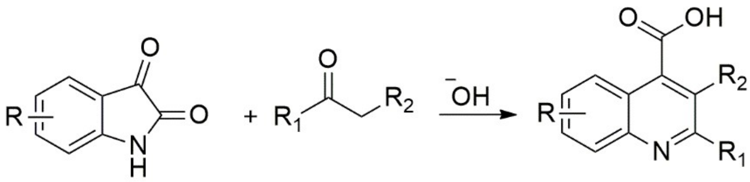

Scheme 1-9 The Pfitzinger reaction of isatin with ketones

The Vilsmeier-Haack reaction may also be used to synthesise quinolines from aniline based starting materials in three ways. The first method entails converting an aniline to its anilide, which then reacts with a Vilsmeier reagent (generated *in situ* from $POCl_3$ and DMF), forming a chloromethylene iminium salt, which then cyclises to form 2-chloroquinoline 3-carbaldehydes (Route A, **Scheme 1-10**) (Abdel-Wahab and Khidre, 2013). The remaining two methods involve the reaction of $POCl_3$ and DMF with *o*-aminoacetophenones (Route B, **Scheme 1-10**) (Wang et al., 2015) and 2'-aminochalcones (Route C, **Scheme 1-10**) (Akila et al., 2001) forming 4-chloroquinoline-3-carbaldehydes and 4-chloro-2-phenylquinoline-1-carbaldehydes, respectively.

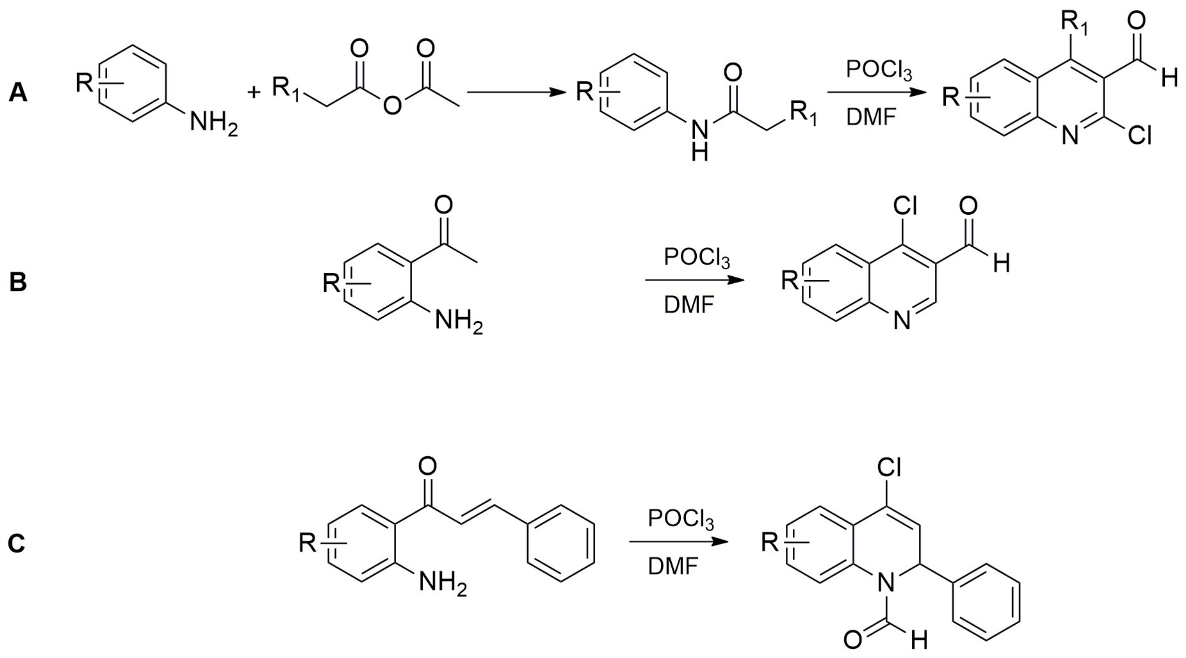

Scheme 1-10 Applications of the Vilsmeier-Haack reaction in quinoline synthesis

In the Skraup synthesis (**Scheme 1-11**), substituted anilines and glycerol are reacted in the presence of sulfuric acid and nitrobenzene, the sulfuric acid acting as both catalyst and dehydrating agent, and nitrobenzene acting as an oxidising agent (Madapa et al., 2008).

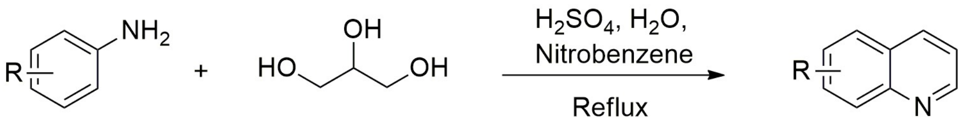

Scheme 1-11 The Skraup quinoline synthesis

The Doebner-von Miller reaction (**Scheme 1-12**) is a modification of the Skraup synthesis using an *α,β*-unsaturated ketone or aldehyde instead of glycerol producing either a monosubstituted or disubstituted quinoline at C-2, C-4 or both C-2 and C-4 (Matsugi et al., 2000).

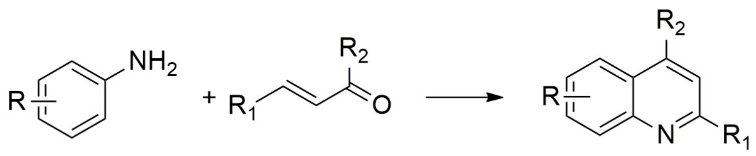

Scheme 1-12 The Doebner-von Miller reaction

Synthesis of 2-methylquinoline (Quinaldine)

Quinaldine is produced by the Doebner-von Miller reaction of substituted aniline with crotonaldehyde. This reaction is favoured over the Skraup synthesis as the latter is violently exothermic (Gilchrist, 1985). The reaction was pioneered by Doebner and von Miller in 1881 (Doebner and von-Miller, 1881). Strong acids such as hydrochloric acid are employed as catalysts for the reaction. However, these strong acids may lead to polymerisation of the *α,β*-unsaturated aldehyde. To minimize this, a biphasic approach was used where the aldehyde was partitioned in an organic solvent such as toluene, while the aniline and acid were retained in aqueous medium. The reaction occurs at the phase boundary of the two immiscible solvents (Matsugi et al., 2000).

Mechanism of the Doebner-Miller reaction

Under strongly acidic conditions, aniline condenses with *α,β*-unsaturated aldehydes forming a conjugated imine. A 2+2 cycloaddition of two imine fragments result in the formation of a four membered intermediate which converts to a neutral six membered intermediate by ring opening and cyclisation steps. Protonation of this neutral intermediate causes the six membered heterocycle bearing the two nitrogen atoms to open. Cyclisation then occurs where the lone pair of the nitrogen adds to the double bond of the alkene moiety bonded to the aromatic ring, which releases an aromatic imine. The last step is an oxidative dehydrogenation yielding quinaldine (**Scheme 1-13**) (Li, 2007).

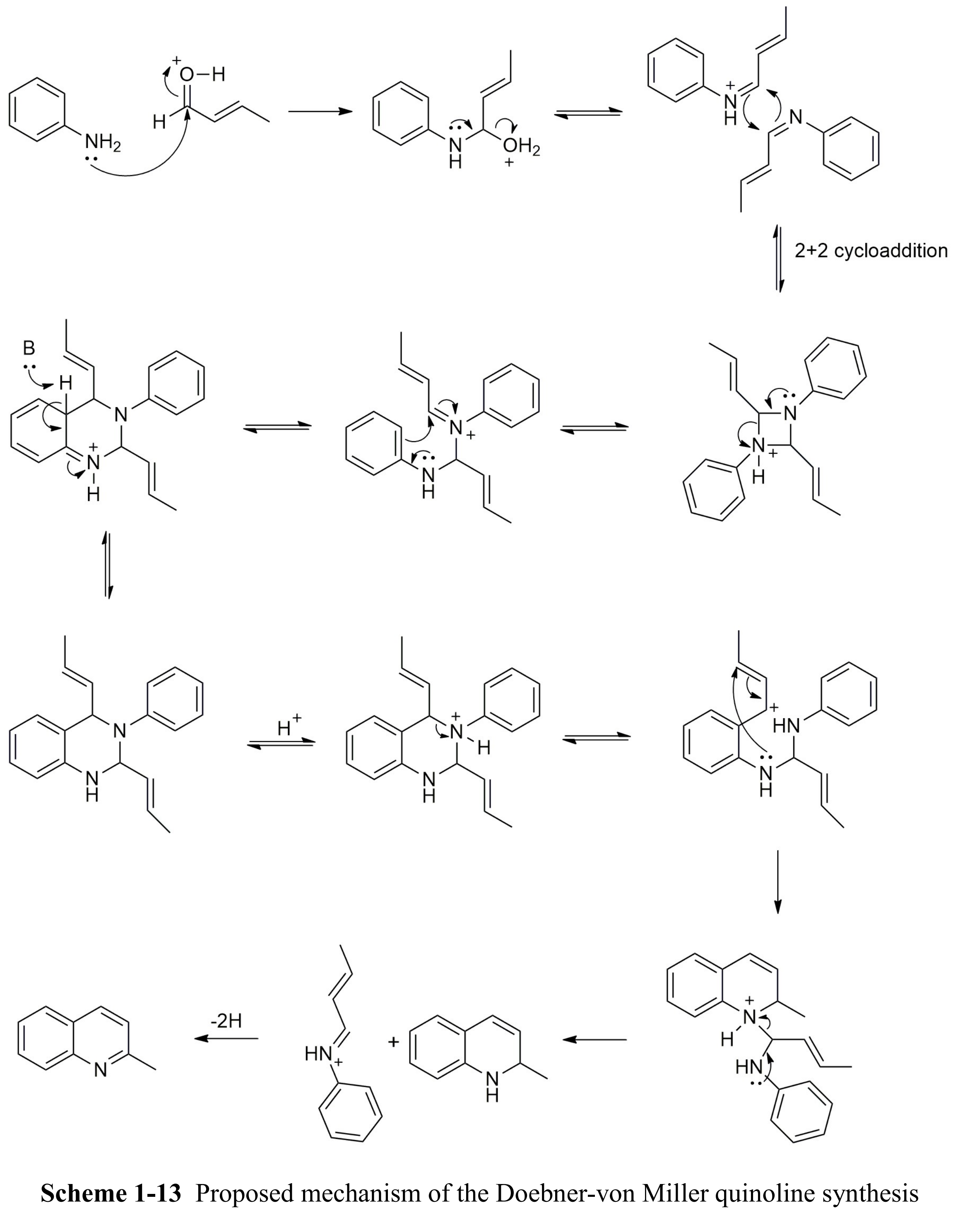

Scheme 1-13 Proposed mechanism of the Doebner-von Miller quinoline synthesis

1.1.2. Alternate and modified approaches to quinaldine synthesis

Beside the classical approaches to synthesising quinolines, several other approaches to quinoline synthesis have also been documented. These methods either improve on existing methods or develop greener procedures.

Microwave-assisted synthetic methods

Microwave irradiation has found a great deal of interest in synthetic chemistry due to reduced reaction times and environmentally benign conditions (Nadaraj and Thamarai Selvi, 2007; Safari et al., 2009). Safari and co-workers (2009) condensed anilines with acetaldehyde in aqueous HCl within seven minutes using an alumina catalyst and achieved good yields of 73-96% (**Scheme 1-14**). The reagents were used in a 1:2 ratio of aniline to aldehyde.

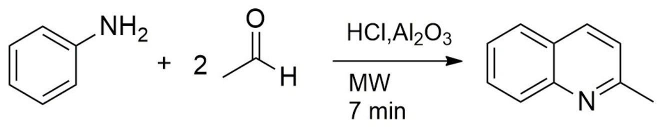

Scheme 1-14 Microwave assisted condensation of aniline and acetaldehyde

Nadaraj and Thamarai Selvi (2007) synthesised ethyl *β*-anilinocrotonates from anilines and acetylacetonate in HCl at room temperature, then cyclised the intermediate to 2-methylquinolin-4-ones with application of microwave irradiation (Route A, **Scheme 1-15**). However, when the same starting materials were subjected to microwave irradiation in the presence of *para* toluene sulfonic acid, acetoacetanilide intermediates were formed and cyclised *in situ* to 4-methylquinoline-2-ones (Route B, **Scheme 1-15**) (Nadaraj and Thamarai Selvi, 2007).

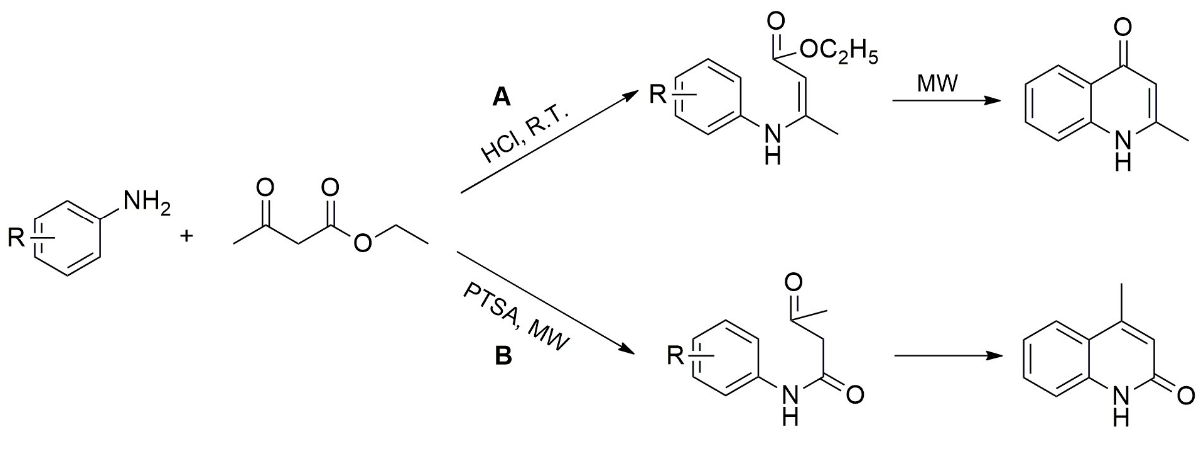

Scheme 1-15 Microwave reactions of anilines and acetylacetonate

Platinum group metal catalysed methods

Platinum group metal catalysts have also been used in quinoline synthesis. Ruthenium catalysts have been used to synthesise quinolines in the Friedlander synthesis from 2-aminobenzyl alcohol and ketones or aldehydes with an α proton (**Scheme 1-16**) (Cho et al., 2001; Van der Mierde et al., 2007a, 2007b).

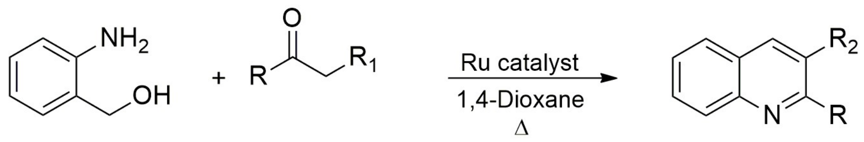

Scheme 1-16 Ruthenium catalysed synthesis of quinolines

Yi and Yun (2005) also used a Ru based catalyst in a hydroamination reaction to form quinaldine from aniline and ethylene (Route A, **Scheme 1-17**), while Monrad and Madsen (2011) formed similar products using aniline and butan-1,3-diol using a $RuCl_3$ catalyst with piperidine and various additives (Route B, **Scheme 1-17**).

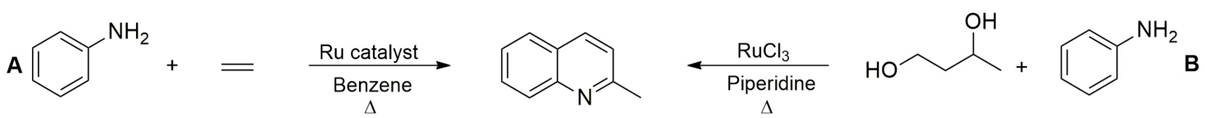

Scheme 1-17 Ruthenium catalysed reactions of aniline with ethylene and 1,3-butanediol

Platinum (Route A, **Scheme 1-18**) and palladium (Route B, **Scheme 1-18**) based catalysts have also been used to synthesise quinolines with anilines and ethylene or ethyl vinyl ether, respectively to produce quinaldine (Matsubara et al., 2011; Béthegnies et al., 2013; Rodriguez-Zubiri et al., 2013; Verma et al., 2014).

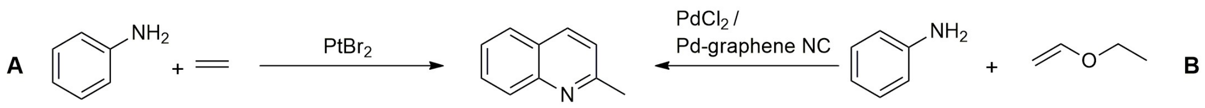

Scheme 1-18 Pt and Pd catalysed synthesis of quinaldine

Transition metal catalysed methods

Nickel and iron catalysts have also been used to form quinolines from alcohols, anilines and carbon tetrachloride (**Scheme 1-19**) (Khusnutdinov et al., 2012, 2013, 2016).

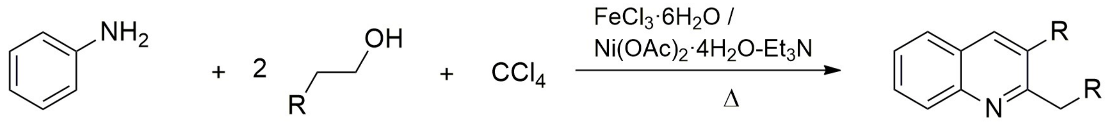

Scheme 1-19 Transition metal catalysed quinoline synthesis

Zeolites

Zeolites were used to methylate quinoline at the 2 position (Route A, **Scheme 1-20**) (Ram Reddy et al., 1998) as well as mediate vapour phase reactions of aniline with acetaldehyde towards 2- and 4-quinolines. Products varied depending on the zeolite used and temperature applied (Route B, **Scheme 1-20**) (Brosius et al., 2006).

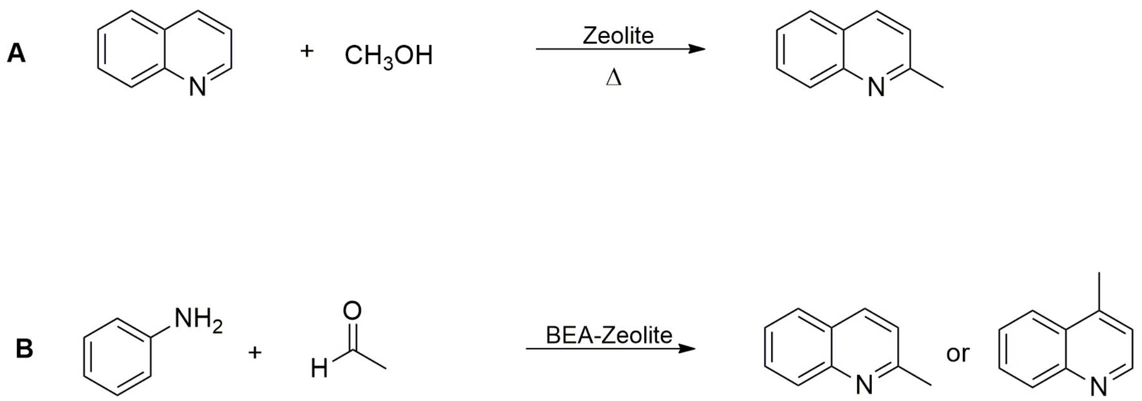

Scheme 1-20 Zeolite mediated syntheses of 2- and 4- methyl quinoline

Heteropoly acids

Heteropoly acids such as phosphomolybdic and phosphotungstic acid have been used in microwave reactions and in conjunction with micellar media in the Doebner-von Miller quinoline synthesis (Sivaprasad et al., 2006, Chaskar et al., 2010).

Photocatalytic reactions

Titania (TiO_2) and titania doped with gold or nitrogen (in the form of hydrazine hydrate) were used in photocatalytic reactions between anilines and ethanol to synthesise quinaldine derivatives (**Scheme 1-21**) (Matsui et al., 2002; Selvam and Swaminathan, 2010, 2013).

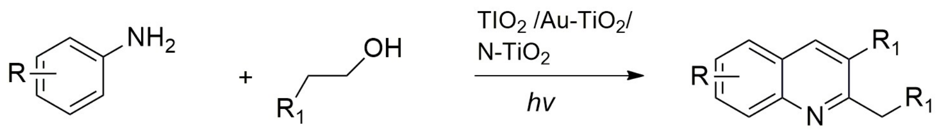

Scheme 1-21 Photocatalytic synthesis of quinolines using titania based catalysts

Blue light

A recent study making use of blue light emitting diodes without the aid of photocatalysts or heat formed quinaldine and other 2-substituted quinolines from *o*-amino-*α,β*-unsaturated ketones (**Scheme 1-22**). The study achieved an impressive 99% conversion of (*E*)-4-(2-aminophenyl)but-3-en-2-one to quinaldine. The method is predicated on the ability of blue light to isomerize the ketone to its *Z*-isomer. This method represents a fast, energy and atom efficient route to quinaldines (Chen et al., 2017).

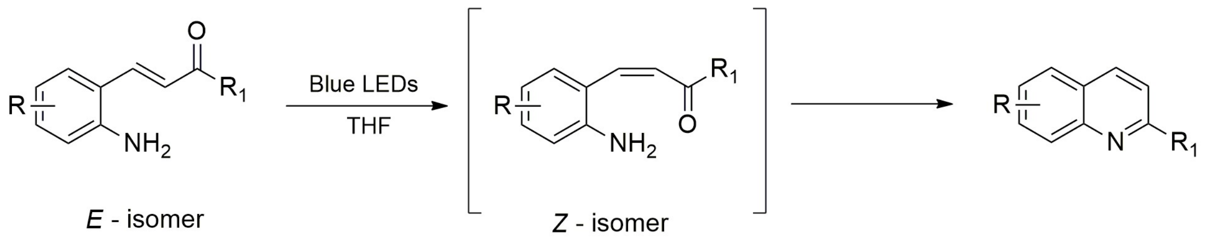

Scheme 1-22 Blue light double bond isomerization in quinoline synthesis

Lu and co-workers (2017) recently used trimethylsilyl chloride (TMSCl) to mediate Pfitzinger reactions between isatin, 1,3-dicarbonyl compounds and alcohols to form quinaldine derivatives (**Scheme 1-23**). This synthesis incorporated cyclization and esterification into a single step cascade process forming a carboxylate at C-4 (Lu et al., 2017).

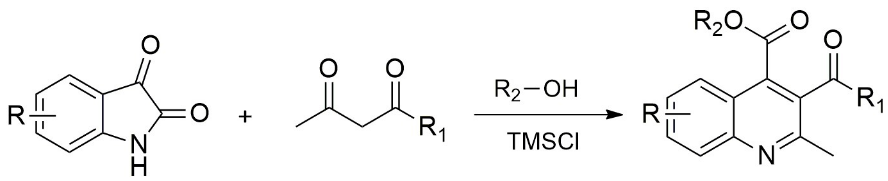

Scheme 1-23 Trimethylsilyl chloride mediated Pfitzinger reactions

Miscellaneous methods

Zhang and Deng (2016) reported a retro-aldol approach to the Friedlander synthesis wherein mild conditions in conjunction with a Cu-catalyst are applied to the synthesis of quinolines and naphthyridines from *ß*-hydroxy ketones and *o*-aminobenzaldehydes, nicotin aldehydes or aryl ketones (**Scheme 1-24**). This marked an improvement on the traditional method due to enhanced chemo- and regioselectivity (Zhang and Deng, 2016).

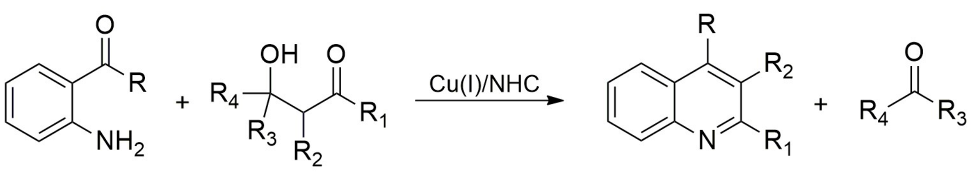

Scheme 1-24 A chemo- and regioselective retro-aldol approach to the Friedlander synthesis

1.1.3. Oxidation of quinaldine

The oxidation of quinaldine to its carbaldehyde or carboxylic acid analogues creates an electrophilic centre which can be further functionalised with other pharmacophores or moieties, provided they have a nucleophilic site.

Selenium dioxide oxidative methods

Selenium dioxide is a common reagent used to carry out this oxidation and is particularly useful for the oxidation of quinaldines to their respective carbaldehydes (**Scheme 1-25**) (Musiol et al., 2009; Chandrasekhar et al., 2011; Ding et al., 2013; George et al., 2013; Gopinath et al., 2013; Gopaul and Koorbanally, 2016). The reaction takes place in boiling aprotic solvents such as 1,4-dioxane, achieving maximum conversion of 82% (Gopaul and Koorbanally, 2016), or xylene, in yields of 50-80% (Pérez-Melero et al., 2004). Dioxane is a good choice of solvent for this purpose since it has the high boiling point required to carry out the reaction at just above 100 °C and can easily be removed by biphasic extraction using water, with the product being extracted with an immiscible organic solvent. A solvent free method has been reported, wherein unsubstituted quinaldine was reacted with SeO_2 at high temperatures of ~170 °C producing the aldehyde in a yield of 81% (Ding et al., 2013). The oxidation of quinaldine to the aldehyde has been reported to take place within an hour (Gopaul and Koorbanally, 2016). If left longer, oxidation to quinoline-2-carboxylic acids occur provided SeO_2 is present in stoichiometric excess (Jampilek et al., 2005; Musiol et al., 2009; Chandrasekhar et al., 2011).

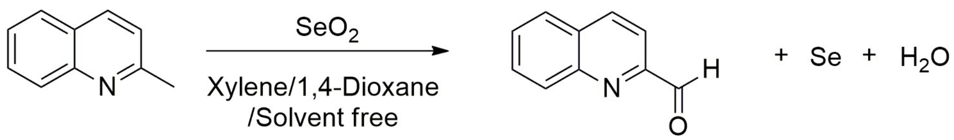

Scheme 1-25 The oxidation of quinaldine to quinoline-2-carbaldehyde by selenium dioxide

The mechanism of selenium dioxide oxidation of quinaldine to quinoline-2-carbaldehyde

The mechanism proposed for the selenium dioxide oxidation of quinaldine to quinoline-2-carbaldehyde begins with the nucleophilic attack of the nitrogen lone pair in quinaldine on selenium dioxide. A proton transfer results in the formation of an unstable four membered cyclic intermediate. Oxygen then adds to the methylene group, causing the C-Se bond to break thereby opening the four-membered ring. Finally the hydroxyl oxygen bound to selenium abstracts the proton from the 2-methylene group producing the desired quinoline-2-carbaldehyde while releasing selenium and water (**Scheme 1-26**) (Trump and Zhou, 1993).

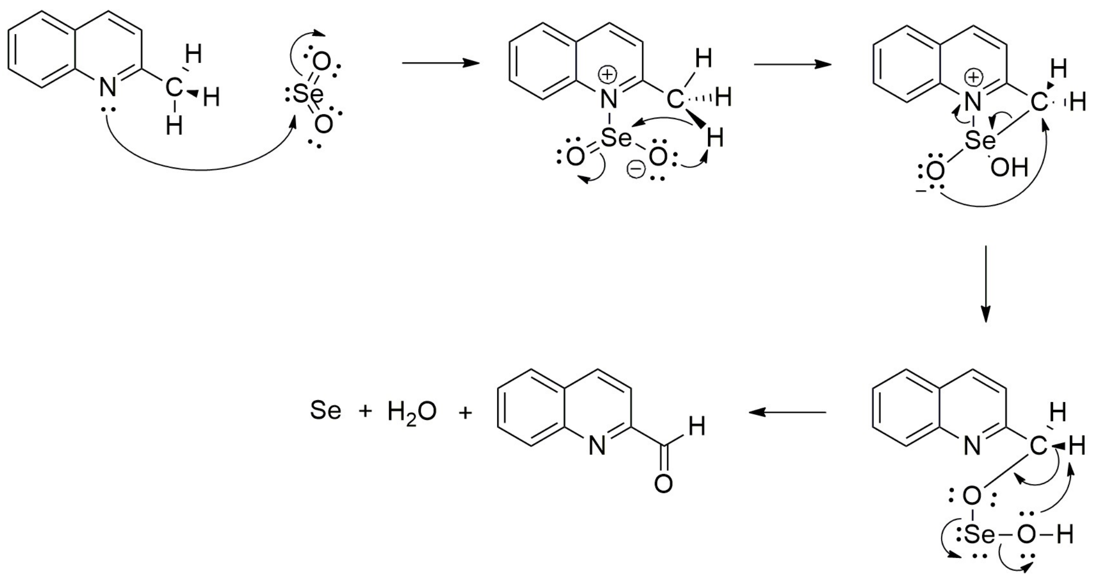

Scheme 1-26 The mechanism for the oxidation of quinaldine to quinoline-2-carbaldehyde using SeO_2

Alternate oxidation methods

Other than selenium dioxide, oxidation of quinaldine to the aldehyde was also carried out by aerobic methods using copper catalysts in DMF at 130 °C in 12 hours (Route A, **Scheme 1-27**) (Liu et al., 2016; Zheng et al., 2016), by a microwave reaction with phenyliodine (III) diacetate (PIDA) as a catalyst in DMSO in short periods of 18 to 42 minutes (Route B, **Scheme 1-27**) (Jiang et al., 2016) and a metal free photo-oxidative method using TFA and I_2 under oxygen for 20 hours (Route C, **Scheme 1-27**) (Nagasawa et al., 2016). Method C formed the aldehyde in a green approach with yields of 65%.

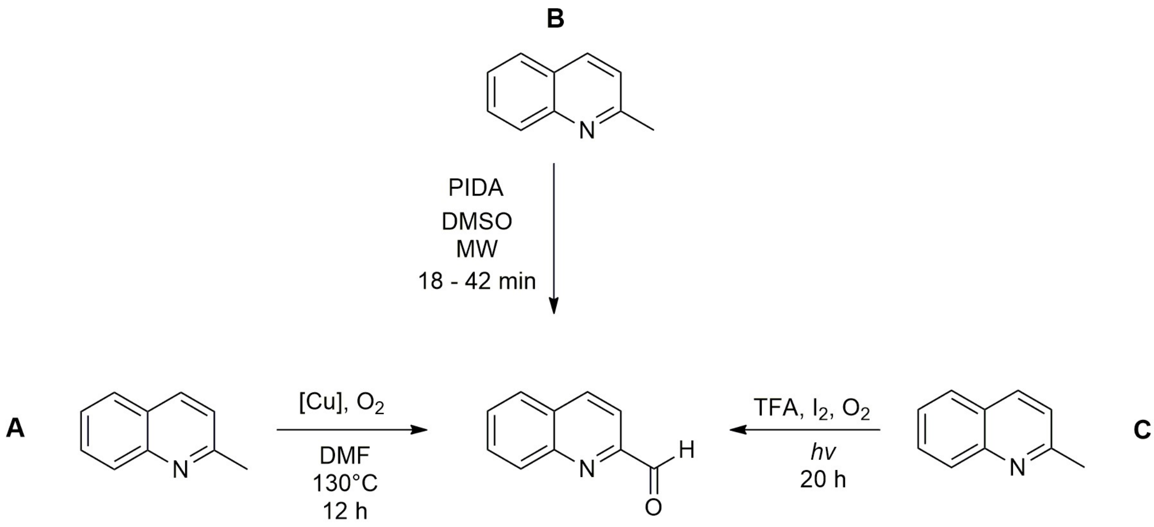

Scheme 1-27 Alternative oxidative methods from quinaldine to quinoline-2-carbaldehyde

Oxidation to quinaldic acid from quinaldine was also carried out with other reagents such as *N*-hydroxyphthalimide (NHP) and $Co(OAc)_2/Mn(OAc)_2$ as a catalyst in the presence of NO_2 (**Scheme 1-28**) (Sakaguchi et al., 2002). There were also cases where conversion to the carboxylic acid was poor using SeO_2 and dioxane, in which case the reaction was followed by the Pinnick oxidation ($NaClO_2$, NaH_2PO_4, *tert*-butanol) to drive the reaction to completion (Contour-Galcéra et al., 2005; George et al., 2013).

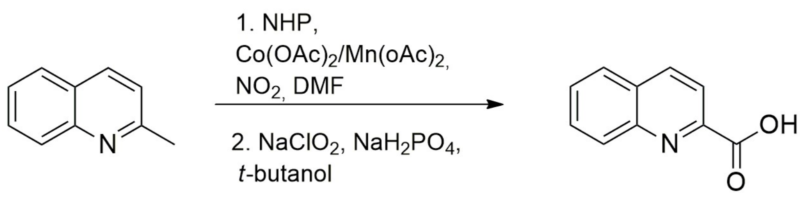

Scheme 1-28 Oxidation of quinaldine to quinaldic acid

There have also been reports of quinoline-2-carbaldehyde being formed first and in a subsequent step oxidized by hydrogen peroxide in either formic acid (Dodd and Le Hyaric, 1993) or in water with the aid of a sulfoxyalkyl-substituted *N*-heterocyclic carbene catalyst (**Scheme 1-29**) (Yoshida et al., 2009). The two step oxidation using SeO_2 to first oxidize quinaldine to quinoline-2-carbaldehyde, and then oxidise the aldehyde to the acid, once selenium is removed, is preferred as quinaldic acids form stable compounds with excess selenous acid (formed from mixing SeO_2 with water), thus making isolation of quinaldic acid difficult (Achremowicz, 1996).

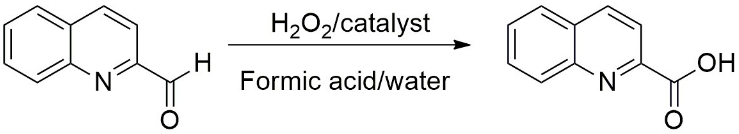

Scheme 1-29 The oxidation of quinoline-2-carbaldehyde to quinaldic acid

1.2. Benzimidazole

The benzimidazole moiety is comprised of a benzene ring fused to a 1,3-diazole (imidazole) ring at C-4 and C-5 of imidazole. They are generally present in two equivalent tautomeric forms (**Figure 1-3**), where the proton rapidly exchanges between two nitrogen atoms (Nieto et al., 2014; Diaz et al., 2015).

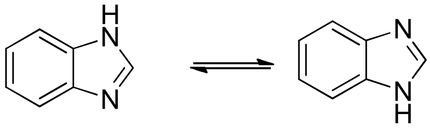

Figure 1-3 The two tautomeric forms of benzimidazole

The benzimidazole nucleus has been identified as a key component of vitamin B12 (α-(5,6-dimethylbenzimidazolyl)cobamidcyanide), a naturally occurring compound. Few other naturally derived benzimidazoles have been identified. One such compound however is kealiiquinone, an alkaloid isolated from the marine *Leucetta* sponges (**Figure 1-4**) (Faulkner, 1992; Jin, 2011).

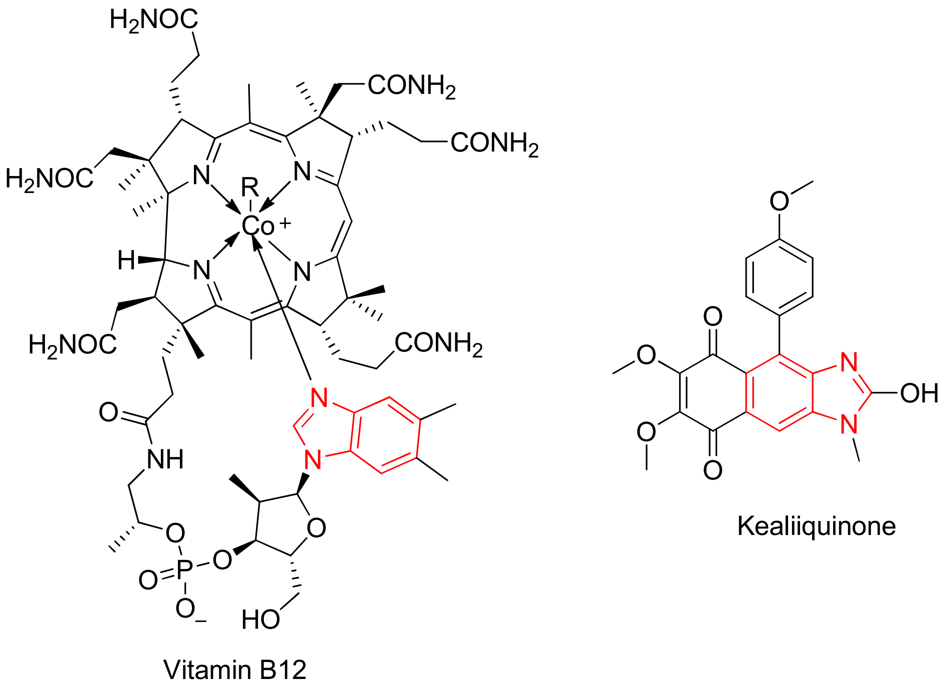

Figure 1-4 Naturally occurring compounds containing the benzimidazole scaffold

1.2.1. Applications of benzimidazoles

The application of the benzimidazole scaffold in pharmaceuticals is well documented, being present in a variety of commercially available drugs (**Figure 1-5**) including omeprazole and lansoprazole (anti-ulcer), pantoprazole (antacid), albendazole (anthelmintic), mebendazole (antimicrobial), thiabendazole (antifungal), astemizole (antihistaminic), telmisartan (antihypertensive), candesartan cilexitil (antihypertensive), bendamustine (anticancer) and enviradine (antiviral) (**Figure 1-5**) (Bansal and Silakari, 2012; Yadav and Ganguly, 2015). Other promising biological activities include anti-inflammatory, antidiabetic, anti-oxidant, anticoagulant, anticonvulsant, psychoactive and lipid modulating properties (Bansal and Silakari, 2012; Rehman et al., 2013).

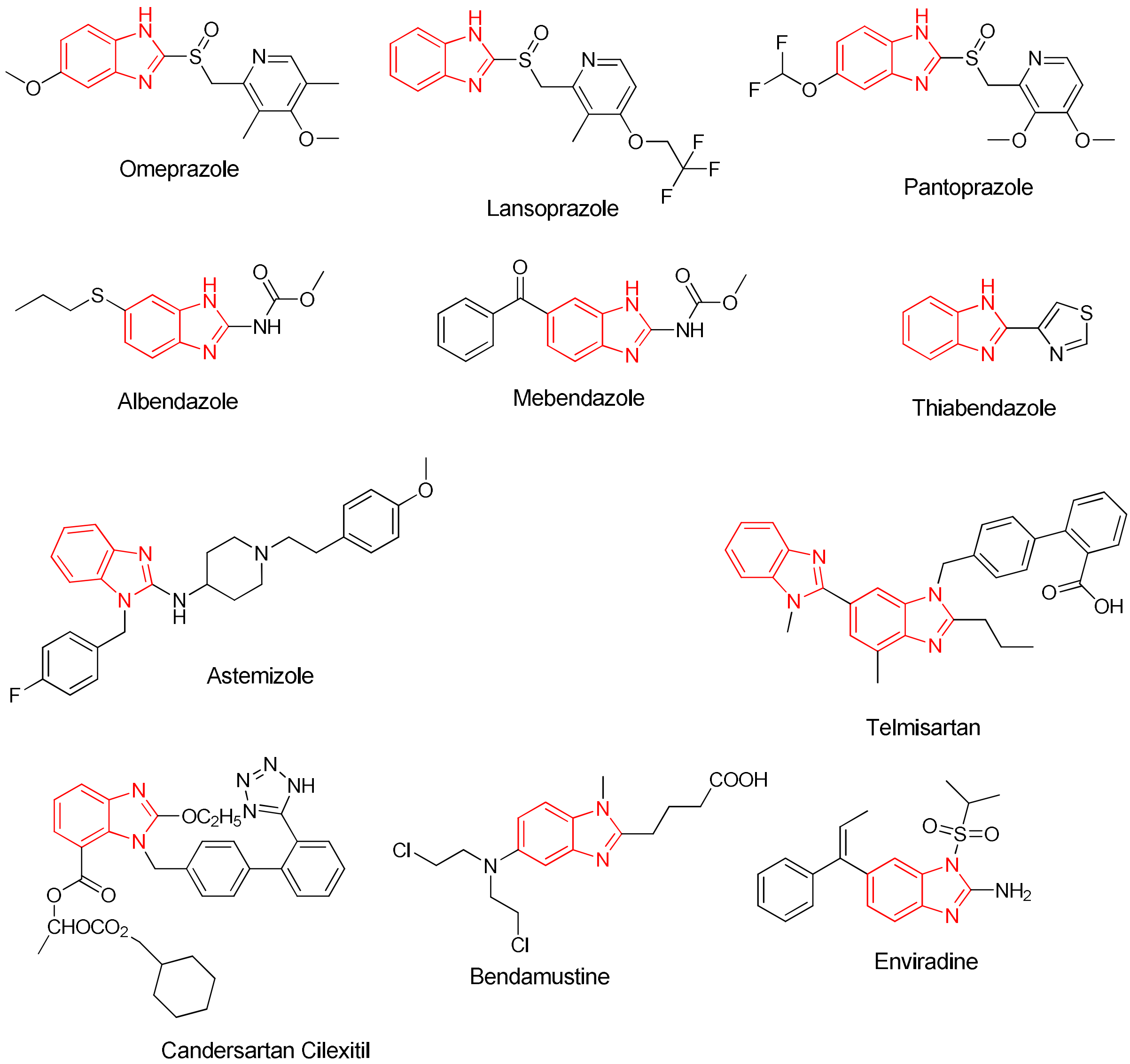

Figure 1-5 Drugs containing the benzimidazole scaffold

In addition, some benzimidazole sulfonic acid salts have shown promise in dental care applications (Rehman et al., 2013), while 5-methylbenzimidazole has also been used as a camphor substitute (Wright, 1951). Benzimidazoles have also found applications as organocatalyts (Nájera and Yus, 2015; Sánchez et al., 2016), in the production of semi-conductors (Mamada et al., 2011; Tozlu et al., 2013), as organometallic ligands (Stibrany et al., 2004; Malik et al., 2015), in dyes (Malathi et al., 2009; Fleischmann et al., 2015; Bodedla et al., 2016), sunscreens (Manescu et al., 2015) and polymeric materials (Berrada et al., 2002; Kim et al., 2012).

1.2.2. Synthesis of benzimidazoles

In general, benzimidazoles are synthesised by the reaction of *o*-phenylenediamine with carboxylic acids, or aldehydes (Alaqeel, 2017). With carboxylic acids, the amino group adds to the carbonyl carbon forming an amide intermediate. Activation of the carboxylic acid is facilitated using acidic catalysts such as polyphosphoric acid (PPA) and hydrochloric acid. The amide is then attacked by the lone pair of electrons on the remaining amino group forming an alcohol intermediate, which is subsequently dehydrated forming the benzimidazole (**Scheme 1-30**).

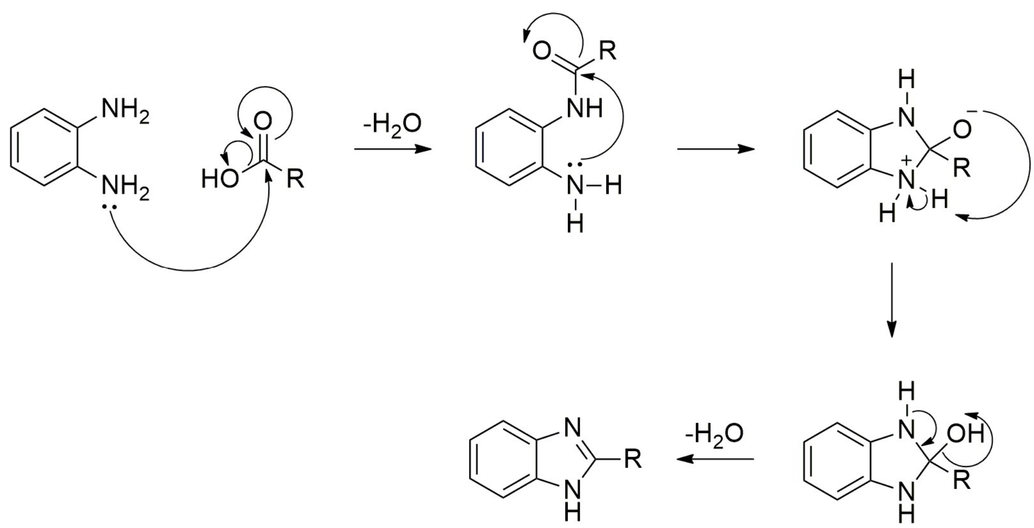

Scheme 1-30 Proposed mechanism of benzimidazole formation from carboxylic acids

When aldehydes are used in benzimidazole synthesis, a sodium sulfite catalyst first adds to the aldehyde, forming a hydroxy sulfite intermediate, which is then attacked by one of the amino groups of *o*-phenylenediamine, substituting the hydroxy group of the sulfite intermediate. The remaining amino group of the diamine then adds to the carbon of the sulfite intermediate resulting in the sulfite group being substituted and the benzimidazole being formed (**Scheme 1-31**) (Eren and Bekdemir, 2014).

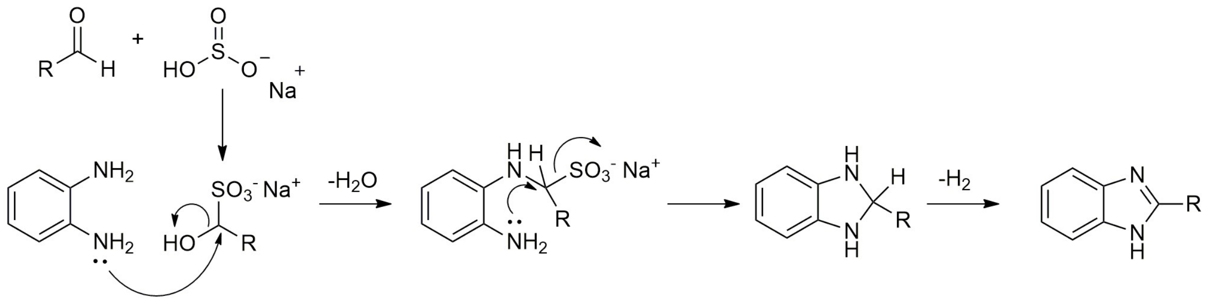

Scheme 1-31 Mechanism of benzimidazole formation from aldehydes

1.2.3. 2-(1*H*-benzo[*d*]imidazol-2-yl) quinolines

2-(1*H*-benzo[*d*]imidazol-2-yl) quinolines are hybrid molecules where a benzimidazole is attached to a quinoline *via* C-2 of each molecular scaffold (**Figure 1-6**).

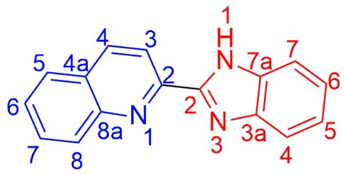

Figure 1-6 2-(1*H*-benzo[*d*]imidazol-2-yl) quinoline scaffold

Such hybrids have shown good antimicrobial and antifungal activities (Hisano et al., 1982), and were shown to act as receptor agonists to aid colon motility (Cosimelli et al., 2011). Metal complexes of 2-(1*H*-benzo[*d*]imidazol-2-yl) quinolines displayed catalytic (Li et al., 2013; Dayan et al., 2016; Sinha et al., 2017), fluorescent (Hu et al., 2015; Li et al., 2016) and luminescent properties (Chen, 2005; Yeh, 2005; Cao et al., 2013; Sinha et al., 2017).

Synthesis of 2-(1H-benzo[d]imidazol-2-yl) quinolines

The most popular routes to synthesise these hybrid molecules involve the reaction of *o*-phenylenediamine with quinaldic acids, quinoline-2-carbaldehydes or quinaldines.

With quinaldic acid precursors (Route A, **Scheme 1-32**), temperatures of 180-200 °C and catalysts such as HCl (Govindan, 1956) and PPA (Case, 1967; Chen, 2005) were used, the latter now being the preferred method, taking approximately 4 hours to complete.

When quinoline-2-carbaldehydes are used instead of quinaldic acids (Route B, **Scheme 1-32**), sodium bisulfite (Hu et al., 2015) and ammonium chloride (Sinha et al., 2017) are the common catalysts. In some cases, the reaction proceeded without a catalyst (Li et al., 2016). They are normally formed under reflux conditions in ethanol (Li et al., 2016) or mixtures of ethanol with DMF (Hu et al., 2015).

The predominant method for the synthesis of quinoline-2-benzimidazoles with *o*-phenylenediamine from quinaldine (Route C, **Scheme 1-32**) proceeds *via* oxidation processes. Oxidation occurs in the presence of elemental sulfur (Hisano and Ichikawa, 1974; Wang et al., 2009; Li et al., 2014) or iodine in DMSO (Baig et al., 2017; Yaragorla and Vijaya Babu, 2017).

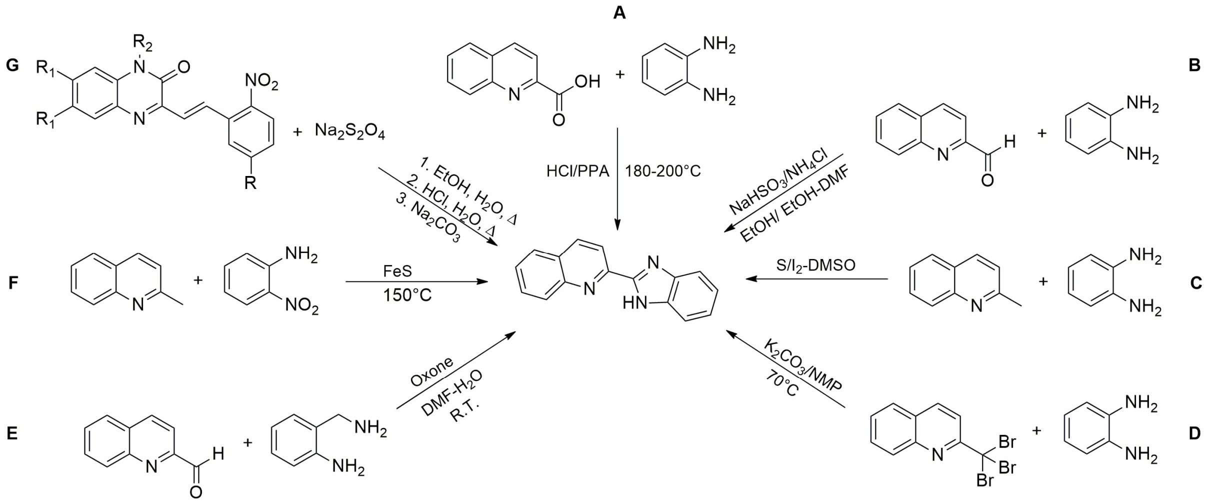

Scheme 1-32 Various methods for the synthesis of 2-(1*H*-benzo[*d*]imidazol-2-yl) quinolines

Several alternative methods in 2-(1*H*-benzo[*d*]imidazol-2-yl) quinoline synthesis have been reported. These include the base catalysed (K_2CO_3) synthesis of quinoline-2-benzimidazoles using a substituted quinaldine (2-(tribromomethyl)quinoline) and *N*-methylpyrrolidine together with *o*-phenylenediamine (Route D, **Scheme 1-32**) (Tynebor and Millings, 2013); using 2-aminobenzylamine instead of *o*-phenylenediamine together with quinoline-2-carbaldehyde in the presence of oxone (Route E, **Scheme 1-32**) (Hati et al., 2016); reacting 2-nitroaniline with methyl hetarenes including quinaldine together with FeS acting as a reducing agent (Route F, **Scheme 1-32**) (Nguyen et al., 2013); and the acid catalysed rearrangement of 3-(2-nitrostyryl)quinoxalin-2(1*H*)ones (Route G, **Scheme 1-32**)(Mamedov et al., 2010).

1.3. Quinoxaline

Quinoxaline is a heterocyclic compound composed of a benzene ring fused to a pyrazine ring. This moiety is a component of many naturally occurring compounds such as vitamin B2 (riboflavin) (**Figure 1-7**). Quinoxalines have shown an array of biological activities including antibacterial (Zhang et al., 2017), antifungal (Zhang et al., 2014), anticancer (El Newahie et al., 2016), antiviral (Shibinskaya et al., 2010), anti-inflammatory (Ismail et al., 2005), and antimalarial (van Heerden et al., 2012) properties.

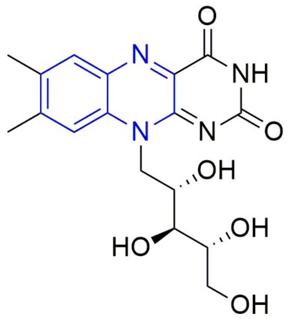

Figure 1-7 Vitamin B2 (riboflavin), a naturally occurring quinoxaline

1.3.1. Pharmaceutical applications of quinoxaline

The quinoxaline core is found in a wide array of drugs such as the antibiotics, echinomycin, quinacillin, olaquindox and carbadox, a veterinary antibiotic, sulfaquinoxaline, a nicotine replacement therapy drug, varenicline, a compound in eye drops, brimonidine and an anticancer agent, chloroquinoxaline sulfonamide (**Figure 1-8**). The quinoxaline scaffold is also present in solar cell dyes (Jung et al., 2015), organic semiconductors (O'Brien et al., 1996; Dailey et al., 2001), dehydroannulenes (Ott and Faust, 2004), and cavitands (Castro et al., 2004).

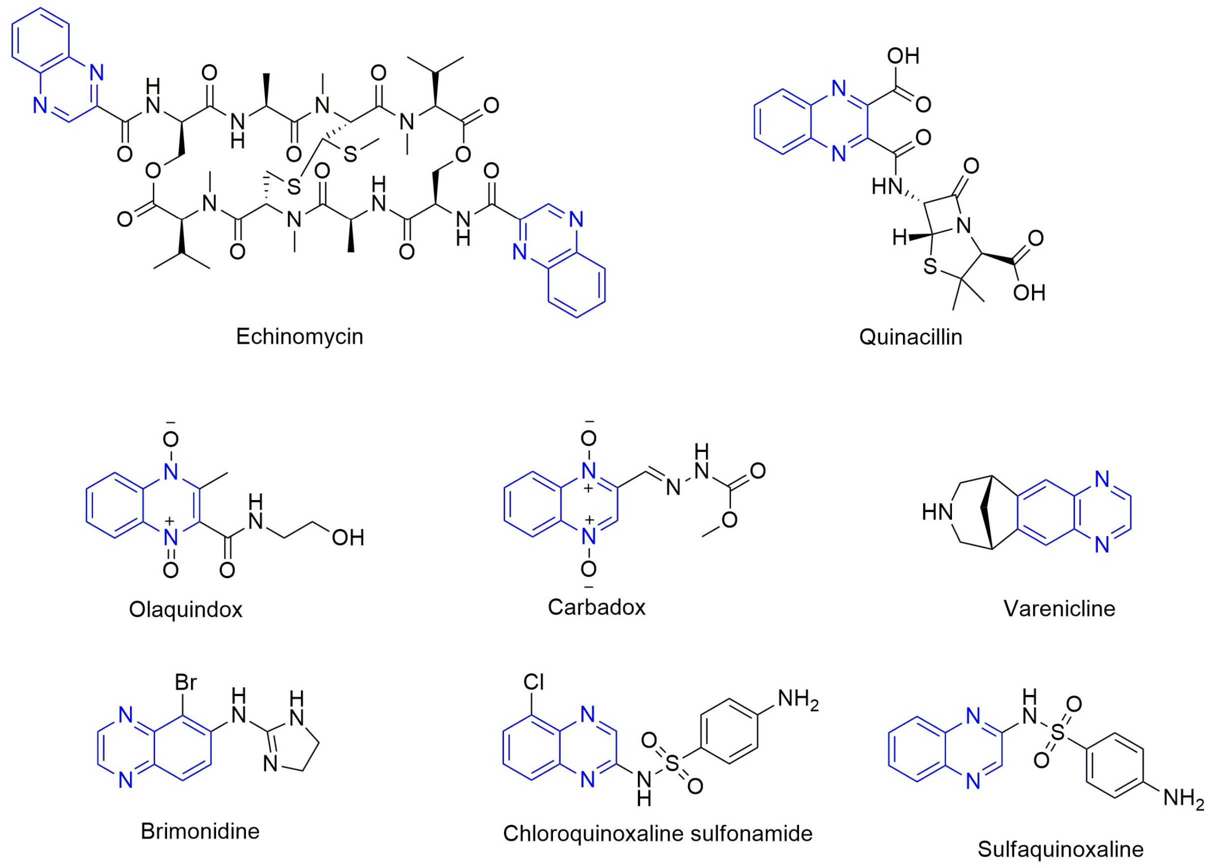

Figure 1-8 Quinoxaline containing drugs

1.3.2. The synthesis of quinoxalines

The quinoxaline nucleus is synthesised by a wide variety of methods and shown as a number of routes depicted in **Scheme 1-33** (Brown, 2004). Popular routes include the condensation of *o*-phenylenediamines (Routes A-G) with *α*-diketones (Route A) (Bhosale et al., 2005; More et al., 2005), phenacyl bromides (Route B) (Nagarapu et al., 2014), 1,4-addition to diazenylbutenes (Route C) (Aparicio et al., 2006), oxidative coupling with epoxides (Route D) (Antoniotti and Duñach, 2002), oxidative cyclization with terminal or internal alkynes (Route E) (Wang et al., 2011), base catalysed surfactant mediated reactions with ketones (Route F) (Cho et al., 2007), and cascade reactions with vicinal diols, *α*-hydroxy ketones and *α*-bromoketones (Raw et al., 2004; Kim et al., 2005; Cho and Oh, 2006; Wan et al., 2009) (Route G).

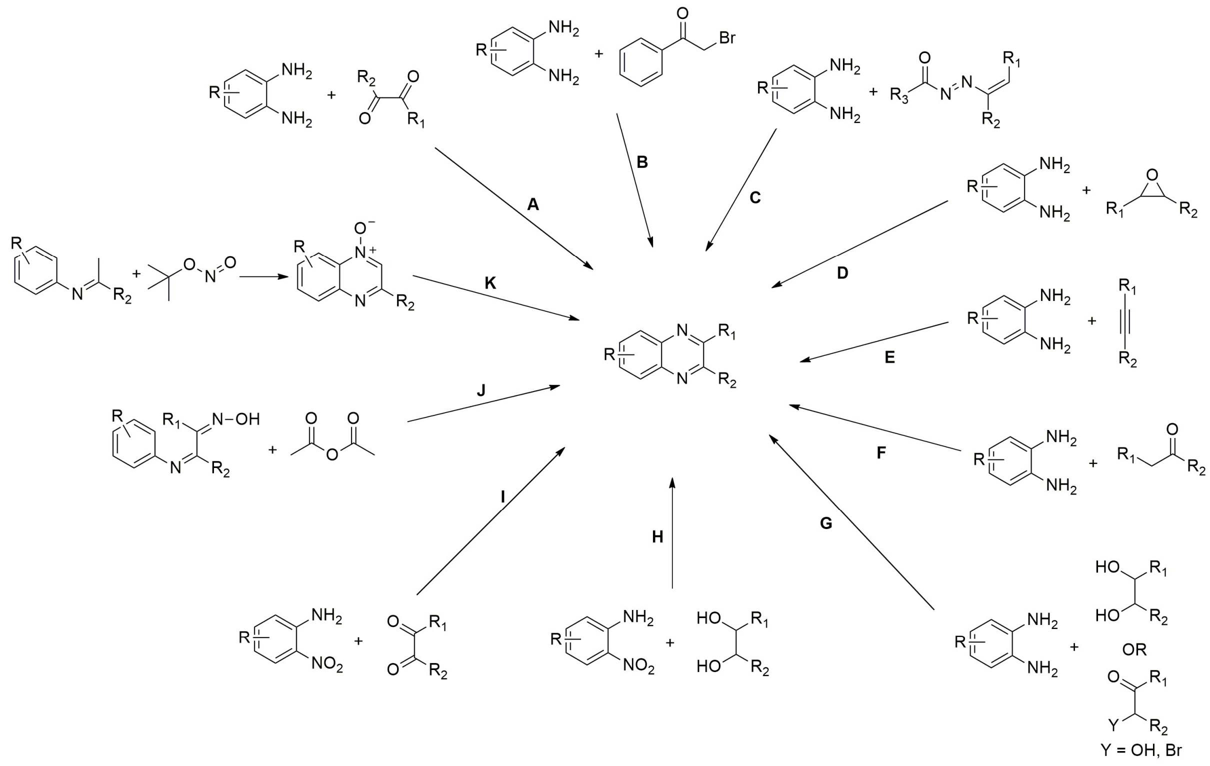

Scheme 1-33 Synthetic routes towards quinoxalines

Ortho-nitroanilines are also used as precursors together with Ru based catalysts and vicinal diols (Route H) (Xie et al., 2015) and in $SnCl_2$ mediated reactions with α–diketones (Route I) (Shi et al., 2008). Quinoxalines are also formed from the cyclization of α-arylimino oximes (Route J) (Xekoukoulotakis et al., 2000) and deoxygenation of quinoxaline *N*-oxides which were formed from the reaction of aryl imines with *tert*-butyl nitrite (Route K) (Chen et al., 2014).

The synthesis of 1-(3-methylquinoxalin-2-yl)ethanone

The introduction of functionalities such as reactive carbonyl groups to the quinoxaline scaffold makes further reactions possible. When these reactions occur with other bioactive organic scaffolds, hybrid compounds containing the quinoxaline core can be developed. One such reactive quinoxaline based species is 1-(3-methylquinoxalin-2-yl)ethanone. This versatile compound, which is also known as 1,4-bisdesoxymequindox, may be synthesised by a number of routes (**Scheme 1-34**).

Popular methods used to form 1-(3-methylquinoxalin-2-yl)ethanone involve using *o*-phenylenediamine with *β*-diketone based starting materials (**Scheme 1-34**), including *α*-brominated acetylacetone (Route A) (Anil Kumar et al., 2011), an *α*-aminoxylated acetylacetone (Route B) (Yan et al., 2016), a pentane-2,3,4-trione (Route C) (Goswami et al., 2016), and a 3-diazopentane-2,4-dione (Route D) (Pandit et al., 2016). Early reports involved the reaction of *o*-nitrosoaniline with acetyl acetone (Route E) (Haddadin et al., 1979). A more recent publication detailed the cyclisation of a *β*-(*N*-2-nitroaryl)-*α,β*-unsaturated ketone intermediate with a Mo(VI) catalyst (Route F) (Vodnala et al., 2016). However, this procedure delivered poor yields of 18%, unlike the methods above which resulted in yields of 70% or greater. An electrocatalytic process involving the acylation of 2-methyl quinoxaline with pyruvic acid mediated by NH_4I (Route G) was also used (Wang et al., 2017).

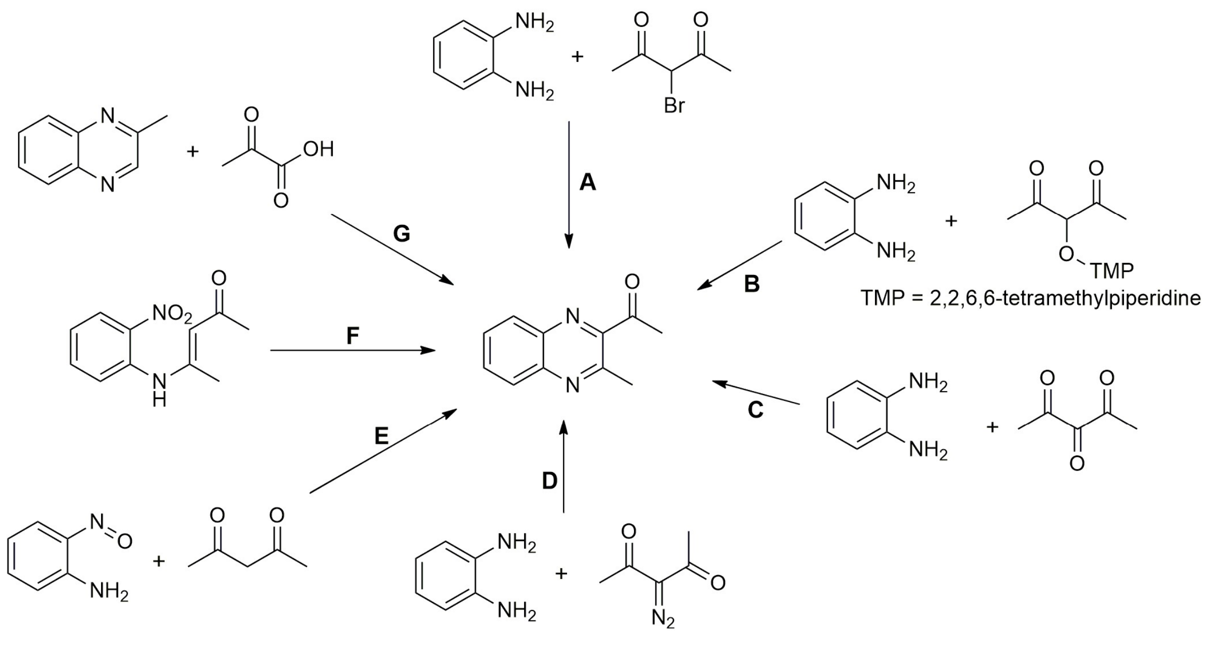

Scheme 1-34 Popular methods used to synthesise 1-(3-methylquinoxalin-2-yl)ethanone

1.4. Chalcones

Chalcones are formed by the Claisen-Schmidt condensation, a variation of the aldol condensation, between an aromatic aldehyde and acetophenone (Wang, 2010). Chalcones have shown a wide variety of biological properties including anticancer, antimicrobial, anti-oxidant, antimalarial, antiulcer, antiviral, antiprotozoal and antihistaminic activities (Singh et al., 2012; Yazdan et al., 2015; Zhuang et al., 2017). They are also found in drugs such as metochalcone (choleretic), sofalcone (antiulcer) and hesperidine methylchalcone (antioxidant) (**Figure 1-9**) (Pinho-Ribeiro et al., 2015; Zhuang et al., 2017). Chalcones also occur naturally as intermediates in biosynthetic plant processes *en route* to flavonoids (Wagner and Farkas, 1975).

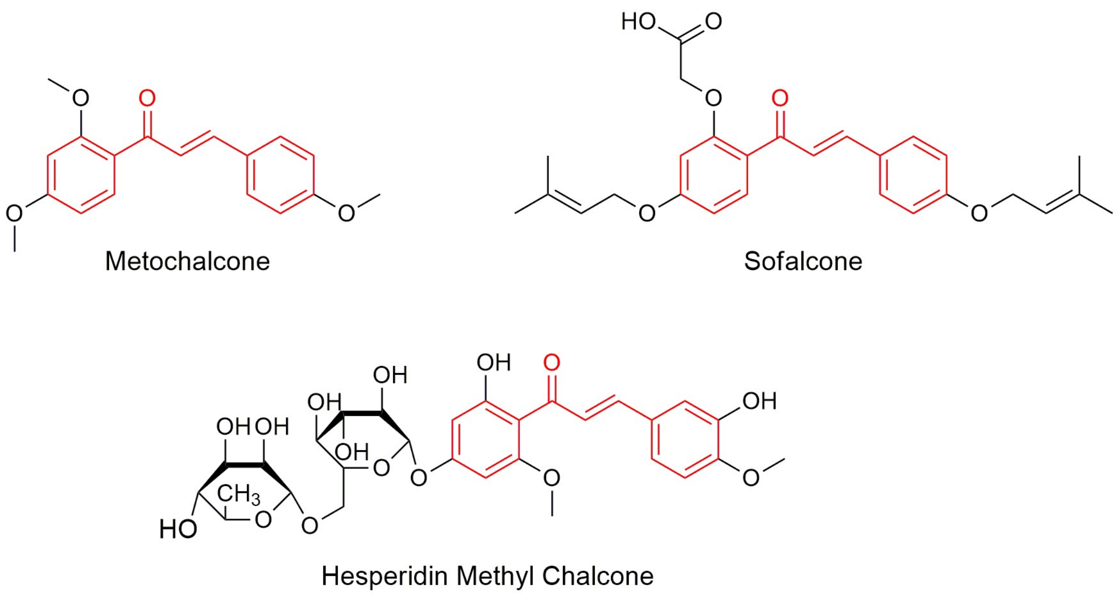

Figure 1-9 Pharmaceutical agents containing the chalcone moiety

1.4.1. The Claisen-Schmidt Condensation

Chalcone synthesis was pioneered simultaneously in 1881 by Claisen (Claisen and Claparède, 1881) and Schmidt (Schmidt, 1881). This condensation may be catalysed by either acidic

(Tseng et al., 2013; Gopinath et al., 2014) or basic media (Tseng et al., 2013; Tseng et al., 2015; Gopaul and Koorbanally, 2016). Under basic conditions an *α*-hydrogen of the ketone is abstracted, forming an enolate ion. This nucleophilic intermediate then attacks the carbonyl group of the aldehyde resulting in formation of an alkoxide, which is subsequently protonated to form the alcohol and followed by elimination of water forming the chalcones (**Scheme 1-35**) (Wang, 2010).

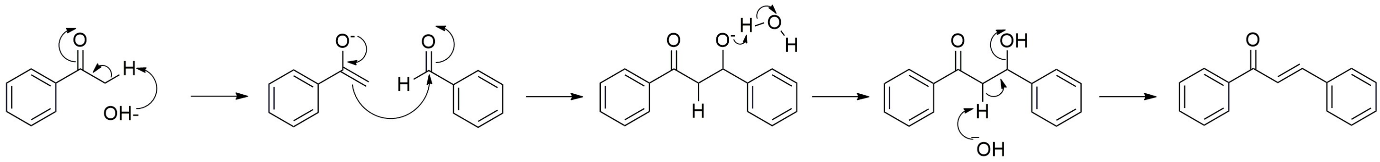

Scheme 1-35 Base catalysed Claisen-Schmidt condensation to form chalcones

1.4.2. Quinoxaline-chalcones

Hybrid molecules incorporating both the quinoxaline and *α,β*-unsaturated ketone moieties have previously been reported with good antitubercular, antibacterial, antimalarial and anticancer activities (Gil et al., 2014; Santivañez-Veliz et al., 2016; Desai et al., 2017; Zhang et al., 2017). In addition, the oxygenated quinoxaline chalcone, quinocetone is a commercially available feedstock additive used as both a growth promoter and antibacterial agent (**Figure 1-10**) (Zhang et al., 2013).

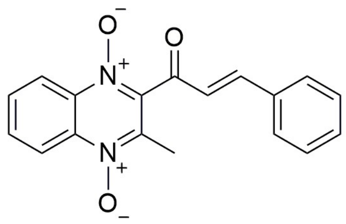

Figure 1-10 The feedstock additive quinocetone

The synthesis of quinoxaline-2-chalcones

Quinoxaline-2-chalcones have previously been synthesised from the reaction of 2-acetyl quinoxaline with benzaldehyde (Route A, **Scheme 1-36**) (Zhang et al., 2012; Zhang et al., 2017) or quinoxaline-2-carbaldehyde with various acetophenones (Route B, **Scheme 1-36**) (Desai et al., 2017). These reactions are conducted in alcoholic media and catalysed using bases such as NaOH (Zhang et al., 2012; Desai et al., 2017) and diethylamine (Zhang et al., 2017). Similarly the synthesis of 1,4-dioxygenated quinoxaline-2-chalcones involves the base catalysed condensation of 1,4-dioxide-2-acetylquinoxaline with aldehydes (Abd El-Halim et al., 1995; Santivañez-Veliz et al., 2016).

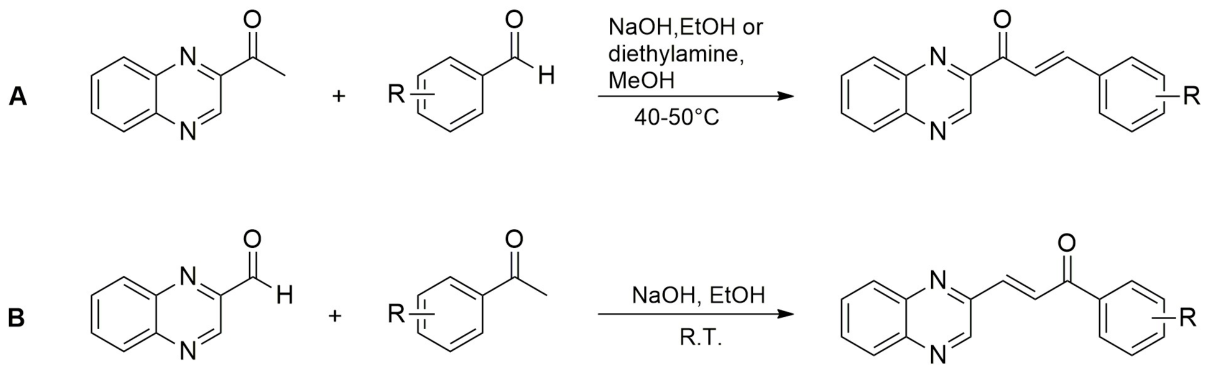

Scheme 1-36 The synthesis of quinoxaline-2-chalcones

1.4.3. Quinoline-chalcones

Compounds containing the quinoline skeleton and the *α,β* -ketone system have previously been synthesised and have shown antimalarial (Gutteridge et al., 2006), antileishmanial (Gopinath et al., 2014), antibacterial (Desai et al., 2012), antifungal (Ashok et al., 2016) and anticancer activities (Tseng et al., 2013).

The synthesis of quinoline-2-chalcones

Synthesis of compounds in which the quinoline backbone is functionalised at C-2 have previously been reported and involve the condensation of quinoline-2-carbaldehydes with various acetophenones (Gutteridge et al., 2006; Rajendra Prasad et al., 2008; Gopinath et al., 2014; Gopaul and Koorbanally, 2016). Base catalysed reactions using sodium hydroxide (Gopaul and Koorbanally, 2016) or potassium hydroxide (Rajendra Prasad et al., 2008) in ethanolic media are the most popular. Barium hydroxide in methanol has also been used to synthesise quinoline-2-chalcones (Gutteridge et al., 2006) and an acid catalysed method using sulfuric acid in acetic acid was previously reported (**Scheme 1-37**) (Gopinath et al., 2014).

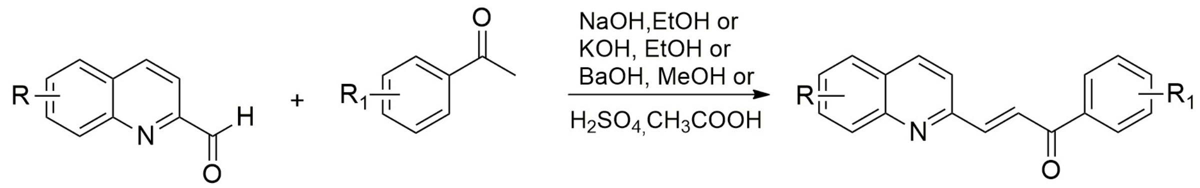

Scheme 1-37 The synthesis of quinoline-2-chalcones

1.5. Pyrazolines from *α,β*-unsaturated ketones

The *α,β*-ketone is attractive, not only due to its pharmacological activity, but because it is highly reactive and can readily be transformed into other more potent pharmacophores such as epoxides (Tseng et al., 2015), aurones (Litkei et al., 1995; Detsi et al., 2009), pyrimidines (Rostom et al., 2011; Desai et al., 2012), isoxazoles (Voskienė and Mickevičius, 2009) and pyrazolines (**Scheme 1-38**) (Desai et al., 2012; Desai et al., 2013; Kendre and Baseer, 2013; Ahmad et al., 2016; Desai et al., 2017).

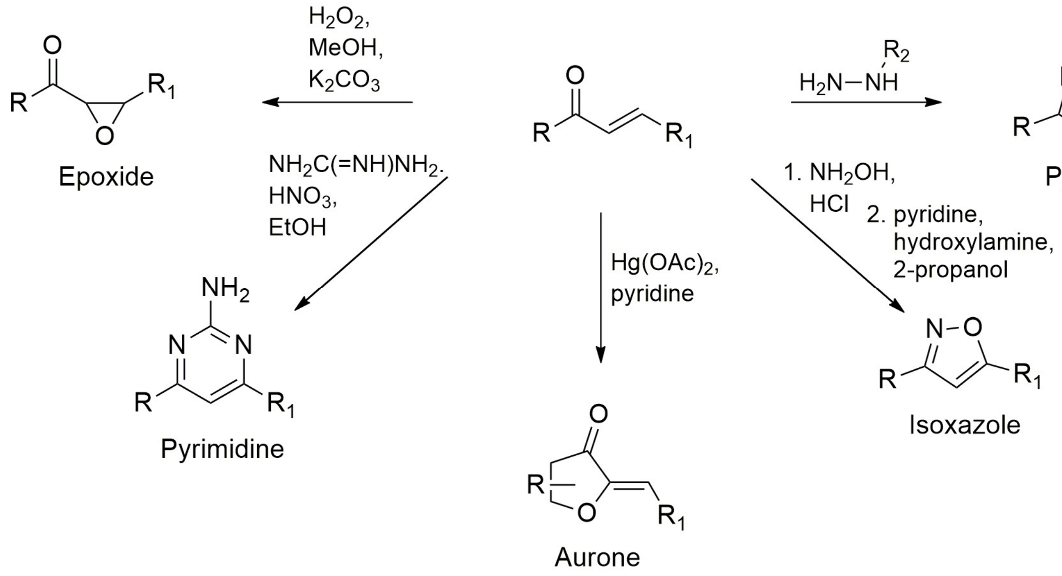

Scheme 1-38 Reactions of the *α,β*-unsaturated moiety forming a wide variety of pharmacophores

The condensation of hydrazines with chalcones is widely reported and results in the formation of pyrazolines (Desai et al., 2012, 2013; Ahmad et al., 2016; Desai et al., 2017). Reports suggest this conversion may enhance pharmacological activity (Desai et al., 2013; Kendre and Baseer, 2013). The pyrazoline moiety has shown antitubercular (Ali et al., 2007), antidepressant, anticonvulsant (Özdemir et al., 2007), anticancer (Yar et al., 2007; Shaharyar et al., 2010), anti-inflammatory and analgesic activities (Joshi et al., 2010). It is found in commercial drugs such as metamizole phenazone, aminophenazone and propylphenazone, which are used as analgesics, antipyretics, anti-inflammatories and antispasmodics (**Figure 1-11**).

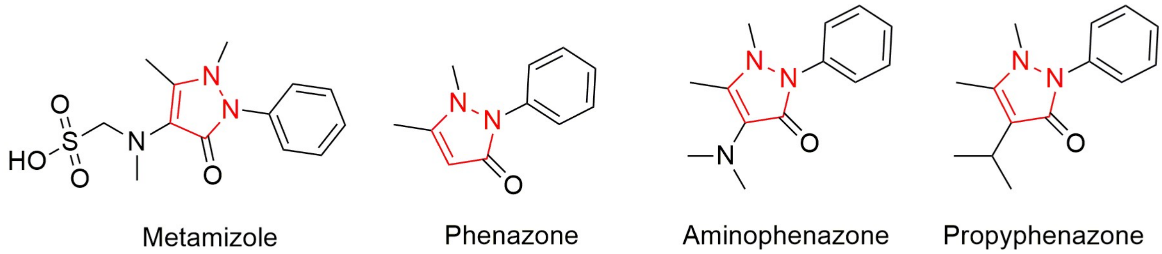

Figure 1-11 Pyrazoline containing drugs

1.5.1. Pyrazoline synthesis from chalcones

The formation of pyrazolines from chalcones occurs in ethanol with hydrazine hydrate or substituted hydrazines (**Scheme 1-38**) (Kendre and Baseer, 2013; Yusuf and Jain, 2014). If hydrazine hydrate is used, acylation of the resulting N-H proton can be carried out *in situ* by substituting ethanol with carboxylic acids such as acetic acid or formic acid as the reaction solvent (Rostom et al., 2011). Use of substituted hydrazine derivatives such as phenyl hydrazine predictably leads to *N*-substituted pyrazolines. This additional substitution was shown to enhance biological properties (Desai et al., 2012; Havrylyuk et al., 2013; Ahmad et al., 2016; Desai et al., 2017).

Hydrazines react with *α,β*-unsaturated ketones in protic media *via* a Michael addition. In acidic conditions, the nucleophilic hydrazine attacks the *β* carbon of the activated ketone. Proton transfer then occurs followed by cyclization through a Claisen addition. A dehydration step produces the final pyrazoline (**Scheme 1-39**).

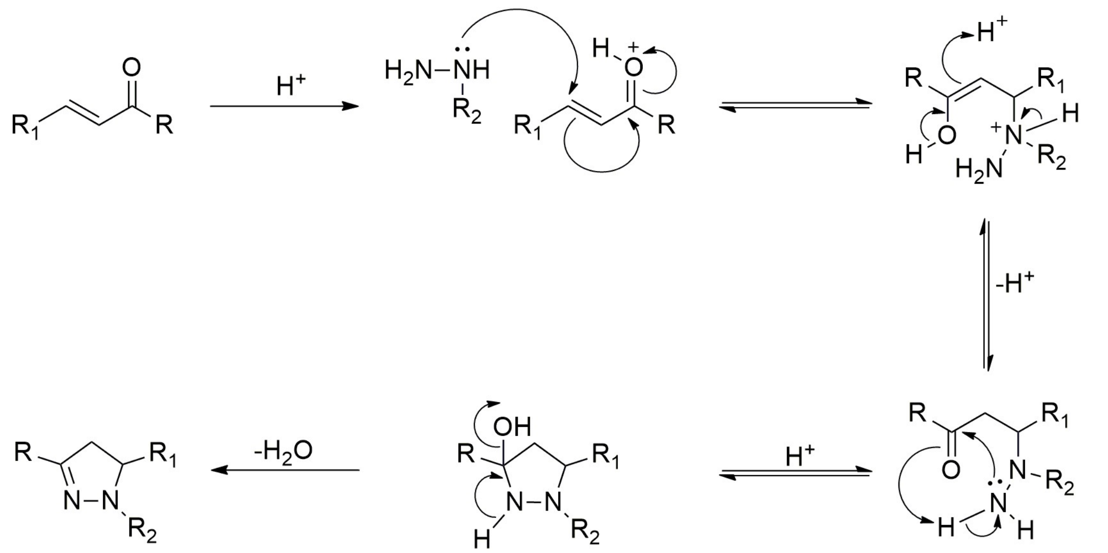

Scheme 1-39 The mechanism of pyrazoline formation from *α,β*-unsaturated carbonyl compounds

1.5.2. Quinoline and quinoxaline pyrazoline hybrid molecules

Molecules containing the quinoxaline core directly bonded to a pyrazoline moiety are rare in the literature with a single report of pyrazoline being formed from an *α,β*-unsaturated ketone specifically at C-2 of the quinoxaline ring (**Figure 1-12**) (Fadda et al., 2011). While the synthesis and spectroscopic data is present in the literature, bioactivity on these compounds are absent.

On the other hand, quinoline-pyrazoline hybrids with antifungal and antibacterial activities have been reported (Desai et al., 2012; Desai et al., 2013; Schowtka et al., 2014; Desai et al., 2017). Quinoline-2-pyrazoline compounds are however rare in literature with only one example of quinoline-2-pyrazole being reported (**Figure 1-12**) (Schowtka et al., 2014). These have generally been synthesised by the conventional methods detailed above.

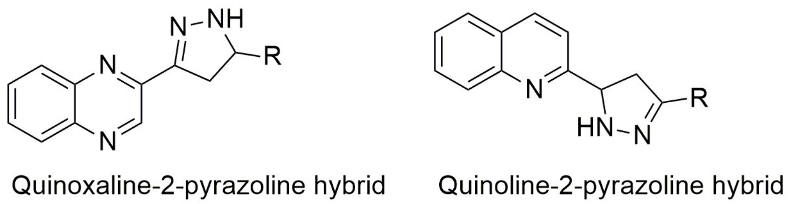

Figure 1-12 Typical structures of quinoxaline 2-pyrazoline and quinoline 2-pyrazoline hybrids

1.6. Rhodanine

Rhodanine is a five-membered heterocyclic ring based on a thiazolidine core. It was first discovered in 1877 by Nencki (Nencki, 1877). This heterocycle is synthesised by reacting carbon disulfide with ammonia and sodium chloroacetate in acidic media (Gagoria et al., 2008a, 2008b). *N*-functionalization of rhodanine was carried out with amines in conjunction with an ammonia rich environment in the reaction with carbon disulfide and sodium chloroacetate (**Scheme 1-40**) (Wolfe and Schreiner, 2007; Ramesh et al., 2014).

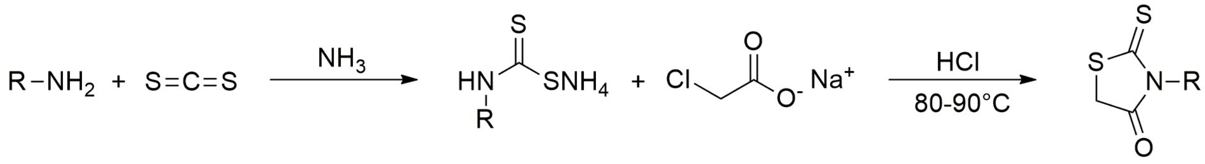

Scheme 1-40 Reaction for the preparation of rhodanine

1.6.1. Applications of rhodanine

The rhodanine scaffold is versatile in its range of biological activities having antibacterial (Grant et al., 2000; Pardasani et al., 2001), antifungal (Habib et al., 1997; Inamori et al., 1998; Siddiqui et al., 2005), antiviral (Sing et al., 2001), antimalarial (Takasu et al., 2002; Kumar et al., 2007), antitumor (Kawakami et al., 1997), anti-inflammatory (Irvine et al., 2008) and anti-diabetic activities (Terashima et al., 1984). Epalrestat, a carboxylic acid derivative of rhodanine, is a commercially available drug used in the treatment of neuropathy associated with type II diabetes (**Figure 1-13**).

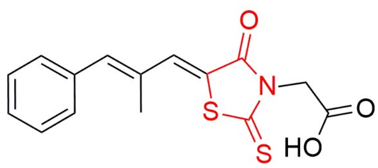

Figure 1-13 Epalrestat, a rhodanine derived drug

1.6.2. Rhodanine and the Knoevenagel condensation

Rhodanine moieties are most popularly hybridized with organic scaffolds using the Knoevenagel condensation of rhodanine with aldehydes (**Scheme 1-41**). Sodium acetate-acetic acid (Ramesh et al., 2014; Li et al., 2015; Mariano et al., 2016), ammonium acetate-acetic acid (Chauhan et al., 2013; Matsui et al., 2010; Meyer et al., 2012; Min et al., 2013), piperidine-ethanol (Guo et al., 2013; Bataille et al., 2017, Zvarec et al., 2012) and ionic liquids (DBU-acetate) (Subhedar et al., 2017) have all been used to perform the condensation.

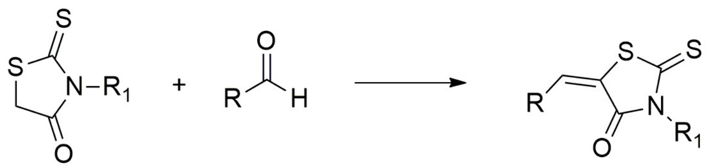

Scheme 1-41 Knoevenagel condensation of rhodanine with aldehydes

The Knoevenagel condensation begins with abstraction of a methylene proton from rhodanine and protonation of the aldehydic precursor. Thereafter, the newly formed rhodanine carbanion attacks the activated aldehyde forming an alcoholic intermediate, followed by dehydration (**Scheme 1-42**) (Sandhu, 2013).

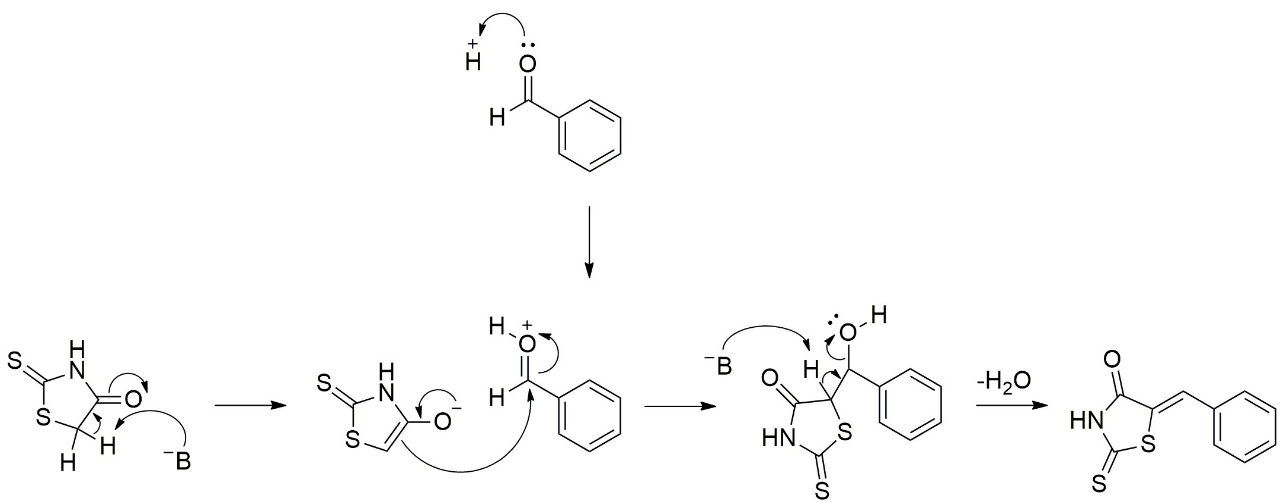

Scheme 1-42 Proposed mechanism for the Knoevenagel condensation between rhodanine and benzaldehyde

1.6.3. Quinoline-rhodanine hybrids

Compounds containing both the quinoline nucleus and rhodanine moiety have previously been reported, taking the form of 7-chloro-4-aminoquinoline-rhodanine hybrids (Chauhan et al., 2013), quinoline-6-rhodanine hybrids (Mariano et al., 2016), 2-chloroquinoline-3-rhodanine hybrids (Guo et al., 2013; Ramesh et al., 2014; Subhedar et al., 2017) and quinoline-2-rhodanine hybrids (Phillips, 1945; Allan et al., 1958; Li et al., 2015; Bataille et al., 2017). These compounds have exhibited good antibacterial (Guo et al., 2013), anticancer (Ramesh et al., 2014; Mariano et al., 2016; Bataille et al., 2017), antifungal (Subhedar et al., 2017), antimalarial (Chauhan et al., 2013) and antitubercular activities (Chauhan et al., 2013; Subhedar et al., 2017) as well as providing leads in Alzheimer's related therapies (Mariano et al., 2016). Guo and co-workers (2013) effectively illustrated that hybridizing quinoline and rhodanine produced compounds that were two to four fold more active against MRSA and QRSA than quinolone based antibiotics.

The 7-chloro-4-aminoquinoline-rhodanine hybrids were synthesised by first condensing 4,7 dichloroquinoline with various diamines and then reacting the intermediate with carbon disulfide and ethylbromoacetate, forming a rhodanine moiety linked to the quinoline scaffold *via* an amine linker. Further functionalisation of the rhodanine scaffold was made using the Knoevenagel condensation with various aromatic and heteroaromatic aldehydes (**Scheme 1-43**) (Chauhan et al., 2013).

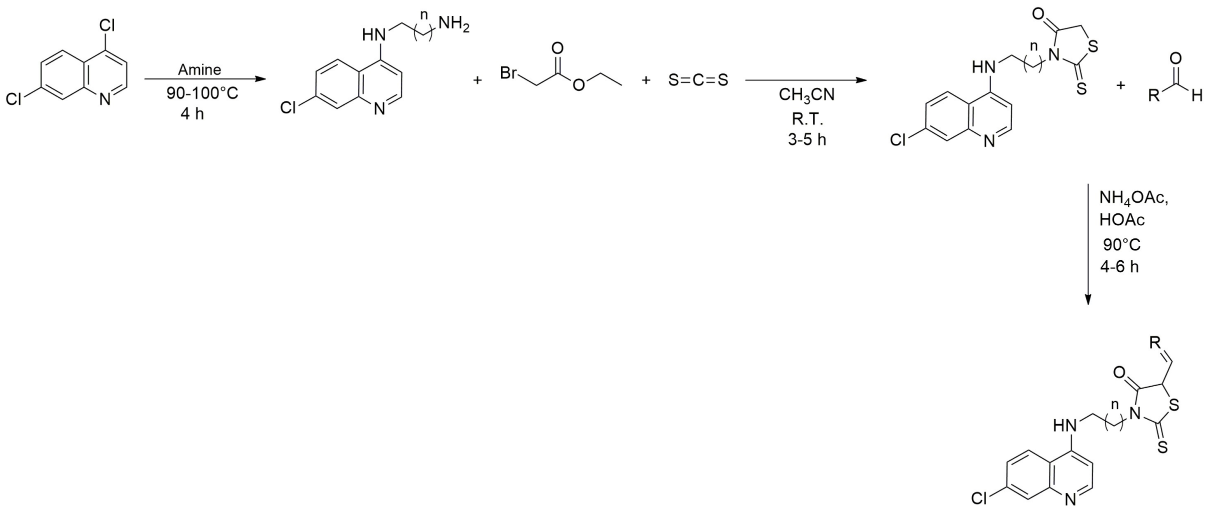

Scheme 1-43 The synthesis of 7-chloro-4-aminoquinoline-rhodanine hybrids

The remaining quinoline-rhodanine hybrids were formed by the methods discussed above, namely the Knoevenagel condensation of the respective quinoline carbaldehydes with rhodanine or substituted rhodanine species. An example is shown in **Scheme 1-44**.

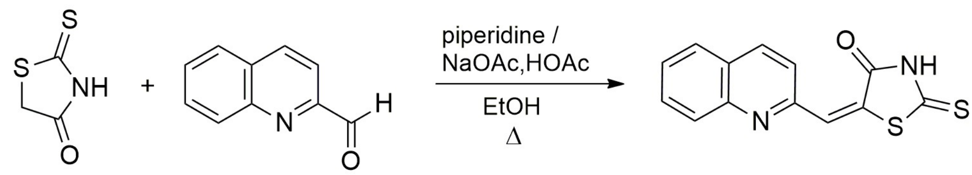

Scheme 1-44 The synthesis of quinoline-2-rhodanine hybrids

1.7. Aims and hypothesis

Hypothesis

The quinoline scaffold is diverse in its range of pharmacological activities and synthetic methods. Hybridising this scaffold with other pharmacophores such as benzimidazole, quinoxaline, chalcone, pyrazoline and rhodanine may thus afford activities which both combine and enhance the activity of their parent moieties, thus leading to novel lead compounds for the pharmaceutical industry.

Aims

To synthesise small libraries of hybrid molecules based on the quinoline or quinoxaline scaffolds with the bioactive pharmacophores of benzimidazoles, chalcones, pyrazolines and thioxothiazolidines and to test each set of compounds for their antibacterial activity for identification of lead compounds, that could be developed into antibiotics for drug resistant bacteria.

Specific aims

- To synthesise three small libraries of quinoline or quinoxaline hybrid molecules with other bioactive pharmacophores mentioned above.
- To characterise the synthesised compounds and document the novel compounds.
- To test the synthesised compounds for their antibacterial activity.

1.8. References

Abd El-Halim, M. S., El-Ahl, A. S., Etman, H. A., Ali, M. M., Fouda, A. and Fadda, A. A. A new route for the synthesis of phenazine di-*N*-oxides. Monatsh. Chem., **1995**, 126, 1217-1223.

Abdel-Wahab, B. F. and Khidre, R. E. 2-Chloroquinoline-3-carbaldehyde II: Synthesis, reactions, and applications. J. Chem., **2013**, 2013, 13.

Achan, J., Talisuna, A. O., Erhart, A., Yeka, A., Tibenderana, J. K., Baliraine, F. N., Rosenthal, P. J. and D'Alessandro, U. Quinine, an old anti-malarial drug in a modern world: role in the treatment of malaria. Malar. J., **2011**, 10, 144.

Achremowicz, L. A new approach to the oxidation of methylquinolines with selenium dioxide. Synth. Commun., **1996**, 26, 1681-1684.

Afzal, O., Kumar, S., Haider, M. R., Ali, M. R., Kumar, R., Jaggi, M. and Bawa, S. A review on anticancer potential of bioactive heterocycle quinoline. Eur. J. Med. Chem., **2015**, 97, 871-910.

Ahmad, A., Husain, A., Khan, S. A., Mujeeb, M. and Bhandari, A. Synthesis, antimicrobial and antitubercular activities of some novel pyrazoline derivatives. J. Saudi Chem. Soc., **2016**, 20, 577-584.

Akila, S., Selvi, S. and Balasubramanian, K. The Vilsmeier cyclization of 2′-azido and 2′-aminochalcones—a mild one pot synthesis of 2-aryl-4-chloroquinoline and its *N*-formyl-1,2-dihydro derivatives. Tetrahedron, **2001**, 57, 3465-3469.

Alaqeel, S. I. Synthetic approaches to benzimidazoles from *o*-phenylenediamine: A literature review. J. Saudi Chem. Soc., **2017**, 21, 229-237.

Ali, M. A., Shaharyar, M. and Siddiqui, A. A. Synthesis, structural activity relationship and anti-tubercular activity of novel pyrazoline derivatives. Eur. J. Med. Chem., **2007**, 42, 268-275.

Allan, F., Allan, G. and Thomson, J. Condensation of rhodanine with pyridine and quinoline aldehydes. J. Org. Chem., **1958**, 23, 112-113.

Anil Kumar, B. S. P., Madhav, B., Harsha Vardhan Reddy, K. and Nageswar, Y. V. D. Quinoxaline synthesis in novel tandem one-pot protocol. Tetrahedron Lett., **2011**, 52, 2862-2865.

Antoniotti, S. and Duñach, E. Direct and catalytic synthesis of quinoxaline derivatives from epoxides and ene-1,2-diamines. Tetrahedron Lett., **2002**, 43, 3971-3973.

Aparicio, D., Attanasi, O. A., Filippone, P., Ignacio, R., Lillini, S., Mantellini, F., Palacios, F. and de los Santos, J. M. Straightforward access to pyrazines, piperazinones, and quinoxalines by reactions of 1,2-diaza-1,3-butadienes with 1,2-diamines under solution, solvent-free, or solid-phase conditions. J. Org. Chem., **2006**, 71, 5897-5905.

Aribi, F., Schmitt, E., Panossian, A., Vors, J.-P., Pazenok, S. and Leroux, F. R. A new approach toward the synthesis of 2,4-bis(fluoroalkyl)-substituted quinoline derivatives using fluoroalkyl amino reagent chemistry. Org. Chem. Frontiers, **2016**, 3, 1392-1415.

Ashok, D., Elsanoosi, M., Alanab, B. F. H., Sarasija, M. and Ravi, S. Solvent-free microwave assisted synthesis of morpholine–piperidine–pyrrolidine annulated quinoline-naphthyl based chalcones and their antimicrobial activity. Russ. J. Gen. Chem., **2016**, 86, 1120-1125.

Baig, M. F., Shaik, S. P., Nayak, V. L., Alarifi, A. and Kamal, A. Iodine-catalyzed C_{sp3}-H functionalization of methylhetarenes: One-pot synthesis and cytotoxic evaluation of heteroarenyl-benzimidazoles and benzothiazole. Bioorg. Med. Chem. Lett., **2017**, 27, 4039-4043.

Bansal, Y. and Silakari, O. The therapeutic journey of benzimidazoles: A review. Bioorg. Med. Chem., **2012**, 20, 6208-6236.

Bataille, C. J. R., Brennan, M. B., Byrne, S., Davies, S. G., Durbin, M., Fedorov, O., Huber, K. V. M., Jones, A. M., Knapp, S., Liu, G., Nadali, A., Quevedo, C. E., Russell, A. J., Walker, R. G., Westwood, R. and Wynne, G. M. Thiazolidine derivatives as potent and selective inhibitors of the PIM kinase family. Bioorg. Med. Chem., **2017**, 25, 2657-2665.

Bergstrom, F. W. Heterocyclic nitrogen compounds. Part IIA. Hexacyclic Compounds: Pyridine, quinoline, and isoquinoline. Chem. Rev., **1944**, 35, 77-277.

Berrada, M., Carriere, F., Abboud, Y., Abourriche, A., Benamara, A., Lajrhed, N., Kabbaj, M. and Berrada, M. Preparation and characterization of new soluble benzimidazole-imide copolymers. J. Mater. Chem., **2002**, 12, 3551-3559.

Béthegnies, A. l., Dub, P. A. and Poli, R. Platinum-catalyzed assembly of quinaldine from aniline and ethylene. Organometallics, **2013**, 32, 1882-1891.

Bhosale, R. S., Sarda, S. R., Ardhapure, S. S., Jadhav, W. N., Bhusare, S. R. and Pawar, R. P. An efficient protocol for the synthesis of quinoxaline derivatives at room temperature using molecular iodine as the catalyst. Tetrahedron Lett., **2005**, 46, 7183-7186.

Bodedla, G. B., Justin Thomas, K. R., Fan, M.-S. and Ho, K.-C. Benzimidazole-branched isomeric dyes: Effect of molecular constitution on photophysical, electrochemical, and photovoltaic properties. J. Org. Chem., **2016**, 81, 640-653.

Brosius, R., Gammon, D., Van Laar, F., van Steen, E., Sels, B. and Jacobs, P. Vapour-phase synthesis of 2-methyl- and 4-methylquinoline over BEA* zeolites. J. Catal., **2006**, 239, 362-368.

Brown, D. J., Primary syntheses. Quinoxalines, John Wiley & Sons, Inc., **2004**, p. 1-92.

Cao, H., Shan, G., Wen, X., Sun, H., Su, Z., Zhong, R., Xie, W., Li, P. and Zhu, D. An orange iridium(III) complex with wide-bandwidth in electroluminescence for fabrication of high-quality white organic light-emitting diodes. J. Mater. Chem. C, **2013**, 1, 7371-7379.

Case, F. H. The preparation of 2-substituted benzimidazole derivatives containing the ferroin group. J. Heterocycl. Chem., **1967**, 4, 157-159.

Castro, P. P., Zhao, G., Masangkay, G. A., Hernandez, C. and Gutierrez-Tunstad, L. M. Quinoxaline excision: A novel approach to tri- and diquinoxaline cavitands. Org. Lett., **2004**, 6, 333-336.

Chandrasekhar, R., Gopalan, B. and Nanjan, M. Synthesis and characterisation of 3-hydroxy-4, 5-dihydro [1, 2, 3] oxadiazolo [3, 4-a] quinolin-10-ium and its fluoro derivative. Int. J. ChemTech. Res., **2011**, 3, 1125-1128.

Chaskar, A., Padalkar, V., Phatangare, K., Langi, B. and Shah, C. Miceller-mediated phosphomolybdic acid: Highly effective reusable catalyst for synthesis of quinoline and its derivatives. Synth. Commun., **2010**, 40, 2336-2340.

Chauhan, K., Sharma, M., Saxena, J., Singh, S. V., Trivedi, P., Srivastava, K., Puri, S. K., Saxena, J. K., Chaturvedi, V. and Chauhan, P. M. S. Synthesis and biological evaluation of a new class of 4-aminoquinoline–rhodanine hybrid as potent anti-infective agents. Eur. J. Med. Chem., **2013**, 62, 693-704.

Chen, F., Huang, X., Li, X., Shen, T., Zou, M. and Jiao, N. Dehydrogenative *N*-incorporation: A direct approach to quinoxaline *N*-oxides under mild conditions. Angew. Chem. Int. Ed., **2014**, 53, 10495-10499.

Chen, T.-R. Luminescence and electroluminescence of bis (2-(benzimidazol-2-yl) quinolinato) zinc. Exciplex formation and energy transfer in mixed film of bis (2-(benzimidazol-2-yl) quinolinato) zinc and *N,N′*-bis-(1-naphthyl)-*N,N′*-diphenyl-1,1′-biphenyl-4,4′-diamine. J. Mol. Struct., **2005**, 737, 35-41.

Chen, T.-R. Synthesis, structure, and field-effect property of 2-(benzimidazol-2-yl) quinoline. Mater. Lett., **2005**, 59, 1050-1052.

Chen, X., Qiu, S., Wang, S., Wang, H. and Zhai, H. Blue-light-promoted carbon-carbon double bond isomerization and its application in the syntheses of quinolines. Org. Biomol. Chem., **2017**, 15, 6349-6352.

Cho, C. S., Kim, B. T., Kim, T.-J. and Shim, S. C. Ruthenium-catalysed oxidative cyclisation of 2-aminobenzyl alcohol with ketones: Modified Friedlaender quinoline synthesis. Chem. Commun., **2001**, 2576-2577.

Cho, C. S. and Oh, S. G. A new ruthenium-catalyzed approach for quinoxalines from *o*-phenylenediamines and vicinal-diols. Tetrahedron Lett., **2006**, 47, 5633-5636.

Cho, C. S., Ren, W. X. and Shim, S. C. Ketones as a new synthon for quinoxaline synthesis. Tetrahedron Lett., **2007**, 48, 4665-4667.

Claisen, L. and Claparède, A. Condensationen von ketonen mit aldehyden. Ber. Dtsch. Chem. Ges., **1881**, 14, 2460-2468.

Contour-Galcéra, M.-O., Sidhu, A., Plas, P. and Roubert, P. 3-Thio-1,2,4-triazoles, novel somatostatin sst_2/sst_5 agonists. Bioorg. Med. Chem. Lett., **2005**, 15, 3555-3559.

Cosimelli, B., Taliani, S., Greco, G., Novellino, E., Sala, A., Severi, E., Da Settimo, F., La Motta, C., Pugliesi, I., Antonioli, L., Fornai, M., Colucci, R., Blandizzi, C., Daniele, S., Trincavelli, M. L. and Martini, C. Derivatives of benzimidazol-2-ylquinoline and benzimidazol-2-ylisoquinoline as selective A_1 adenosine receptor antagonists with stimulant activity on human colon motility. ChemMedChem, **2011**, 6, 1909-1918.

Dailey, S., Feast, W. J., Peace, R. J., Sage, I. C., Till, S. and Wood, E. L. Synthesis and device characterisation of side-chain polymer electron transport materials for organic semiconductor applications. J. Mater. Chem., **2001**, 11, 2238-2243.

Davies, J. and Davies, D. Origins and evolution of antibiotic resistance. Microbiol. Mol. Biol. Rev., **2010**, 74, 417-433.

Dayan, O., Tercan, M. and Özdemir, N. Syntheses and molecular structures of novel Ru(II) complexes with bidentate benzimidazole based ligands and their catalytic efficiency for oxidation of benzyl alcohol. J. Mol. Struct., **2016**, 1123, 35-43.

Desai, N. C., Joshi, V. V., Rajpara, K. M., Vaghani, H. V. and Satodiya, H. M. Synthesis of quinoline-pyrazoline based thiazole derivatives endowed with antimicrobial activity. Indian J. Chem., Sect B: Org. Chem. Incl. Med. Chem., **2013**, 52B, 1191-1201.

Desai, N. C., Patel, B. Y. and Dave, B. P. Synthesis and antimicrobial activity of novel quinoline derivatives bearing pyrazoline and pyridine analogues. Med. Chem. Res., **2017**, 26, 109-119.

Desai, N. C., Rajpara, K. M. and Joshi, V. V. Synthesis and characterization of some new quinoline based derivatives endowed with broad spectrum antimicrobial potency. Bioorg. Med. Chem. Lett., **2012**, 22, 6871-6875.

Desai, V., Desai, S., Gaonkar, S. N., Palyekar, U., Joshi, S. D. and Dixit, S. K. Novel quinoxalinyl chalcone hybrid scaffolds as enoyl ACP reductase inhibitors: Synthesis, molecular docking and biological evaluation. Bioorg. Med. Chem. Lett., **2017**, 27, 2174-2180.

Detsi, A., Majdalani, M., Kontogiorgis, C. A., Hadjipavlou-Litina, D. and Kefalas, P. Natural and synthetic 2′-hydroxy-chalcones and aurones: Synthesis, characterization and evaluation of the antioxidant and soybean lipoxygenase inhibitory activity. Bioorg. Med. Chem., **2009**, 17, 8073-8085.

Diaz, C., Llovera, L., Echevarria, L. and Hernández, F. E. Assessment of the tautomeric population of benzimidazole derivatives in solution: A simple and versatile theoretical-experimental approach. J. Comput. Aided Mol. Des., **2015**, 29, 143-154.

Ding, D., Dwoskin, L. P. and Crooks, P. A. Efficient synthesis of *cis*-2,6-di-(2-quinolylpiperidine). Tetrahedron Lett., **2013**, 54, 5211-5213.

Dodd, R. H. and Le Hyaric, M. The Oxidation of aromatic aldehydes to carboxylic acids using hydrogen peroxide in formic acid. Synthesis, **1993**, 1993, 295-297.

Doebner, O. and v. Miller, W. Ueber eine dem chinolin homologe base. Ber. Dtsch. Chem. Ges., **1881**, 14, 2812-2817.

El Newahie, A. M. S., Ismail, N. S. M., Abou El Ella, D. A. and Abouzid, K. A. M. Quinoxaline-based scaffolds targeting tyrosine kinases and their potential anticancer activity. Arch. Pharm., **2016**, 349, 309-326.

Eren, B. and Bekdemir, Y. Simple, mild, and highly efficient synthesis of 2-substituted benzimidazoles and bis-benzimidazoles. Quim. Nova, **2014**, 37, 643-647.

Eswaran, S., Adhikari, A. V., Chowdhury, I. H., Pal, N. K. and Thomas, K. D. New quinoline derivatives: Synthesis and investigation of antibacterial and antituberculosis properties. Eur. J. Med. Chem., **2010**, 45, 3374-3383.

Fadda, A. A., Abdelrazek, F. M. and Fouda, A. M. Studies with aza-heterocyclic *N*-oxides: Synthesis of some new aromatic *N*-oxide derivatives. Eur. J. Chem., **2011**, 2, 51-57.

Faulkner, D. J. Marine natural products. Nat. Prod. Rep., **1992**, 9, 323-364.

Fleischmann, C., Lievenbrück, M. and Ritter, H. Polymers and dyes: developments and applications. Polymers, **2015**, 7, 717-746.

Foley, M. and Tilley, L. Quinoline antimalarials: Mechanisms of action and resistance and prospects for new agents. Pharmacol. Ther., **1998**, 79, 55-87.

Gagoria, J., Khatkar, A., Khatkar, S., Rao, R., Singh, K. and Nanda, A. 2-((4-oxo-2-thiazolidin-5-ylidine) methyl) phenoxy)acetamides as anticonvulsant agents. Orient. J. Chem, **2008**, 24, 673-676.

Gagoria, J., Singh, K., Jain, S. K., Khatkar, A. and khatkar, G. Synthesis and anti-convulsant study of benzylidine rhodanine derivatives. Orient. J. Chem, **2008**, 24, 713-716.

Garudachari, B., Satyanarayana, M. N., Thippeswamy, B., Shivakumar, C. K., Shivananda, K. N., Hegde, G. and Isloor, A. M. Synthesis, characterization and antimicrobial studies of some new quinoline incorporated benzimidazole derivatives. Eur. J. Med. Chem., **2012**, 54, 900-906.

George, I. R., Lewis, W. and Moody, C. J. Synthesis of iodopyridone. Tetrahedron, **2013**, 69, 8209-8215.

Gil, A., Pabón, A., Galiano, S., Burguete, A., Pérez-Silanes, S., Deharo, E., Monge, A. and Aldana, I. Synthesis, biological evaluation and structure-activity relationships of new quinoxaline derivatives as anti-plasmodium falciparum agents. Molecules, **2014**, 19, 2166.

Gilchrist, T. L. Heterocyclic Chemistry, Pitman Publishing, London, **1985**, p. 270-272

Gopaul, K. and Koorbanally, N. A. Synthesis and structure elucidation of a series of chloroquinoline-2-chalcones by the Doebner-Miller reaction. Magn. Reson. Chem., **2016**, 54, 677-683.

Gopaul, K., Shintre, S. A. and Koorbanally, N. A. A review on the synthesis and anti-cancer activity of 2-substituted quinolines. Anti-Cancer Agents Med. Chem., **2015**, 15, 631-646.

Gopinath, V. S., Pinjari, J., Dere, R. T., Verma, A., Vishwakarma, P., Shivahare, R., Moger, M., Kumar Goud, P. S., Ramanathan, V., Bose, P., Rao, M. V. S., Gupta, S., Puri, S. K., Launay, D. and Martin, D. Design, synthesis and biological evaluation of 2-substituted quinolines as potential antileishmanial agents. Eur. J. Med. Chem., **2013**, 69, 527-536.

Gopinath, V. S., Rao, M., Shivahare, R., Vishwakarma, P., Ghose, S., Pradhan, A., Hindupur, R., Sarma, K. D., Gupta, S., Puri, S. K., Launay, D. and Martin, D. Design, synthesis, ADME characterization and antileishmanial evaluation of novel substituted quinoline analogs. Bioorg. Med. Chem. Lett., **2014**, 24, 2046-2052.

Goswami, S., Das, M. K., Maity, A. C., Quah, C. K. and Fun, H.-K. Synthesis of 7-methyl-6-indolopterin and 7-methyl-6-indoloquinoxaline. Synth. Commun., **2016**, 46, 1529-1536.

Govindan, T. K. Heterocyclic compounds. Proc. Indian Acad. Sci. - Sect. A, **1956**, 44, 123-125.

Grant, E. B., Guiadeen, D., Baum, E. Z., Foleno, B. D., Jin, H., Montenegro, D. A., Nelson, E. A., Bush, K. and Hlasta, D. J. The synthesis and SAR of rhodanines as novel class C *β*-lactamase inhibitors. Bioorg. Med. Chem. Lett., **2000**, 10, 2179-2182.

Guo, M., Zheng, C.-J., Song, M.-X., Wu, Y., Sun, L.-P., Li, Y.-J., Liu, Y. and Piao, H.-R. Synthesis and biological evaluation of rhodanine derivatives bearing a quinoline moiety as potent antimicrobial agents. Bioorg. Med. Chem. Lett., **2013**, 23, 4358-4361.

Gutteridge, C. E., Nichols, D. A., Curtis, S. M., Thota, D. S., Vo, J. V., Gerena, L., Montip, G., Asher, C. O., Diaz, D. S., DiTusa, C. A., Smith, K. S. and Bhattacharjee, A. K. *In vitro* and *in vivo* efficacy and *in vitro* metabolism of 1-phenyl-3-aryl-2-propen-1-ones against *Plasmodium falciparum*. Bioorg. Med. Chem. Lett., **2006**, 16, 5682-5686.

Habib, N. S., Rida, S. M., Badawey, E. A. M., Fahmy, H. T. Y. and Ghozlan, H. A. Synthesis and antimicrobial activity of rhodanine derivatives. Eur. J. Med. Chem., **1997**, 32, 759-762.

Haddadin, M. J., Bitar, H. E. and Issidorides, C. H. Synthesis and some reactions of *o*-nitrosoaniline. Heterocycles, **1979**, 12, 323-327.

Hati, S., Kumar Dutta, P., Dutta, S., Munshi, P. and Sen, S. Accessing benzimidazoles *via* a ring distortion strategy: An oxone mediated tandem reaction of 2-aminobenzylamines. Org. Lett., **2016**, 18, 3090-3093.

Havrylyuk, D., Zimenkovsky, B., Vasylenko, O. and Lesyk, R. Synthesis and anticancer and antiviral activities of new 2-pyrazoline-substituted 4-thiazolidinones. J. Heterocycl. Chem., **2013**, 50, E55-E62.

Hisano, T. and Ichikawa, M. Acidic properties of benzimidazoles and substituents effects. I. Correlation between acid dissociations and hydrogen bondings of some benzimidazoles. Chem. Pharm. Bull., **1974**, 22, 1923-1927.

Hisano, T., Ichikawa, M., Tsumoto, K. and Tasaki, M. Synthesis of benzoxazoles, benzothiazoles and benzimidazoles and evaluation of their antifungal, insecticidal and herbicidal activities. Chem. Pharm. Bull., **1982**, 30, 2996-3004.

Hsu, K.-K., Sun, S.-W. and Chen, Y.-H. Synthesis of 2-(4-quinolyl) and 2-(3-quinolyl) chromone derivatives. J. Chin. Chem. Soc., **1982**, 29, 29-37.

Hu, J., Li, J., Qi, J. and Chen, J. Highly selective and effective mercury(II) fluorescent sensors. New J. Chem., **2015**, 39, 843-848.

Inamori, Y., Okamoto, Y., Takegawa, Y., Tsujibo, H., Sakagami, Y., Kumeda, Y., Shibata, M. and Numata, A. Insecticidal and antifungal activities of aminorhodanine derivatives. Biosci. Biotechnol. Biochem., **1998**, 62, 1025-1027.

Irvine, M. W., Patrick, G. L., Kewney, J., Hastings, S. F. and MacKenzie, S. J. Rhodanine derivatives as novel inhibitors of PDE4. Bioorg. Med. Chem. Lett., **2008**, 18, 2032-2037.

Ismail, M. M. F., Ammar, Y. A., Ibrahim, M. K., El-Zahaby, H. S. A. and Mahmoud, S. S. Synthesis and pharmacological evaluation of novel quinoxalines as potential nonulcerogenic anti-inflammatory and analgesic agents. Arzneim. Forsch., **2005**, 55, 738-743.

Jain, S., Chandra, V., Kumar Jain, P., Pathak, K., Pathak, D. and Vaidya, A. Comprehensive review on current developments of quinoline-based anticancer agents. Arabian J. Chem., **2016**, in press

Jampilek, J., Dolezal, M., Kunes, J., Buchta, V., Silva, L. and Kralova, K. Quinaldine derivatives: Preparation and biological activity. Med. Chem., **2005**, 1, 591-599.

Jiang, L., Huang, Y., Yan, Y. and Xie, Y. Metal-free C(sp^3)-H oxidation of 2-methylquinolines with PIDA under microwave irradiation. Tetrahedron Lett., **2016**, 57, 4149-4151.

Jin, Z. Muscarine, imidazole, oxazole, and thiazole alkaloids. Nat. Prod. Rep., 2011, 28, 1143-1191.

Jones, C. P., Anderson, K. W. and Buchwald, S. L. Sequential Cu-catalyzed amidation-base-mediated Camps cyclization: A two-step synthesis of 2-aryl-4-quinolones from *o*-halophenones. J. Org. Chem., **2007**, 72, 7968-7973.

Joshi, R. S., Mandhane, P. G., Diwakar, S. D., Dabhade, S. K. and Gill, C. H. Synthesis, analgesic and anti-inflammatory activities of some novel pyrazolines derivatives. Bioorg. Med. Chem. Lett., **2010**, 20, 3721-3725.

Jung, C. Y., Song, C. J., Yao, W., Park, J. M., Hyun, I. H., Seong, D. H. and Jaung, J. Y. Synthesis and performance of new quinoxaline-based dyes for dye sensitized solar cell. Dyes Pigm., **2015**, 121, 204-210.

Kawakami, M., Koya, K., Ukai, T., Tatsuta, N., Ikegawa, A., Ogawa, K., Shishido, T. and Chen, L. B. Synthesis and evaluation of novel rhodacyanine dyes that exhibit antitumor activity. J. Med. Chem., **1997**, 40, 3151-3160.

Kendre, M. and Baseer, M. Synthesis and evaluation of some new pyrazoline derivatives as antimicrobial agents. Orient. J. Chem, **2013**, 29, 253-256.

Khusnutdinov, R., Bayguzina, A., Aminov, R. and Dzhemilev, U. Quinoline synthesis by the reaction of anilines with 1,2-diols catalyzed by iron compounds. J. Heterocycl. Chem., **2016**, 53, 1022-1029.

Khusnutdinov, R. I., Baygusina, A. R., Aminov, R. I. and Dzhemilev, U. M. Synthesis of *N*-alkylanilines and substituted quinolines by reaction of aniline with alcohols and CCl_4 effected with Ni-containing catalysts. Russ. J. Org. Chem., **2012**, 48, 690-693.

Khusnutdinov, R. I., Bayguzina, A. R. and Aminov, R. I. Synthesis of substituted quinolines by the reaction of anilines with alcohols and CCl_4 in the presence of Fe-containing catalysts. Russ. Chem. Bull., **2013**, 62, 133-137.

Kim, S.-K., Ko, T., Choi, S.-W., Park, J. O., Kim, K.-H., Pak, C., Chang, H. and Lee, J.-C. Durable cross-linked copolymer membranes based on poly(benzoxazine) and poly(2,5-benzimidazole) for use in fuel cells at elevated temperatures. J. Mater. Chem., **2012**, 22, 7194-7205.

Kim, S. Y., Park, K. H. and Chung, Y. K. Manganese(IV) dioxide-catalyzed synthesis of quinoxalines under microwave irradiation. Chem. Commun., **2005**, 1321-1323.

Kouznetsov, V. V. Recent synthetic developments in a powerful imino Diels-Alder reaction (Povarov reaction): Application to the synthesis of *N*-polyheterocycles and related alkaloids. Tetrahedron, **2009**, 65, 2721-2750.

Kouznetsov, V. V., Vargas Mendez, L., Y. and Melendez Gomez, C. M. Recent Progress in the Synthesis of Quinolines. Curr. Org. Chem., **2005**, 9, 141-161.

Kumar, G., Parasuraman, P., Sharma, S. K., Banerjee, T., Karmodiya, K., Surolia, N. and Surolia, A. Discovery of a rhodanine class of compounds as inhibitors of *Plasmodium falciparum* enoyl-acyl carrier protein reductase. J. Med. Chem., **2007**, 50, 2665-2675.

Kumar, S., Bawa, S. and Gupta, H. Biological activities of quinoline derivatives. Mini-Rev. Med. Chem., **2009**, 9, 1648-1654.

Li, G., Zhang, D., Liu, G. and Pu, S. A highly selective fluorescent probe for Cd^{2+} and Zn^{2+} based on a new diarylethene with quinoline-benzimidazole conjugated system. Tetrahedron Lett., **2016**, 57, 5205-5210.

Li, J. J. Name reactions: A collection of detailed reaction mechanisms, 3rd Edition, Springer, Berlin. **2007**

Li, L., Zhang, X., Zhang, W., Li, W., Sun, W.-H. and Redshaw, C. Zinc 2-((2-(benzoimidazol-2-yl)quinolin-8-ylimino)methyl)phenolates: Synthesis, characterization and photoluminescence behavior. Spectrochim. Acta. Part A, **2014**, 118, 1047-1055.

Li, S., Zhang, B. and Kühn, F. E. Benzimidazolic complexes of methyltrioxorhenium(VII): Synthesis and application in catalytic olefin epoxidation. J. Organomet. Chem., **2013**, 730, 132-136.

Litkei, D., Khilya, V. P., Tokesh, A. L., Antush, S. and Turov, A. V. Reaction of chalcones with *N*-bromosuccinimide. Synthesis of aurones. Chem. Heterocycl. Compd., **1995**, 31, 432-440.

Liu, M., Chen, T. and Yin, S.-F. Copper-catalysed aerobic oxidative esterification of *N*-heteroaryl methanes with alcohols. Catal. Sci. Technol., **2016**, 6, 690-693.

Lu, L., Zhou, P., Hu, B., Li, X., Huang, R. and Yu, F. An improved Pfitzinger reaction: Eco-efficient synthesis of quinaldine-4-carboxylates by TMSCl-mediated. Tetrahedron Lett., **2017**, 58, 3658-3661.

Luo, Z.-g., Zeng, C.-c., Wang, F., He, H.-q., Wang, C.-X., Du, H.-G. and Hu, L.-M. Synthesis and biological activities of quinoline derivatives as HIV-1 integrase inhibitors. Chem. Res. Chin. Univ., **2009**, 25, 841-845.

Madapa, S., Tusi, Z. and Batra, S. Advances in the syntheses of quinoline and quinoline-annulated ring systems. Curr. Org. Chem., **2008**, 12, 1116-1183.

Maddela, S., Venugopal, M., Maddela, R. and Ajitha, M. Design and synthesis of new *N′*-substituted-2-methylquinoline-3-carbohydrazides with antioxidant and antimicrobial activity. Indian J. Chem., Sect. B: Org. Chem. Incl. Med. Chem., **2015**, 54, 930-935.

Malathi, M., Mohan, P. S., Butcher, R. J. and Venil, C. K. Benzimidazole quinoline derivatives - An effective green fluorescent dye for bacterial imaging. Can. J. Chem., **2009**, 87, 1692-1703.

Malik, S., Singh, A. and Ahmed, N. Spectral and biological behaviour of complexes derived some bivalent metals and Schiff base. Der Chemica Sinica, **2015**, 6, 1-6.

Mamada, M., Pérez-Bolívar, C. and Anzenbacher, P. Green synthesis of polycyclic benzimidazole derivatives and organic semiconductors. Org. Lett., **2011**, 13, 4882-4885.

Mamedov, V. A., Saifina, D. F., Gubaidullin, A. T., Ganieva, V. R., Kadyrova, S. F., Rakov, D. V., Rizvanov, I. d. K. and Sinyashin, O. G. Acid-catalyzed rearrangement of 3-(β-2-aminostyryl)quinoxalin-2(1*H*)ones-A new and efficient method for the synthesis of 2-benzimidazol-2-ylquinolines. Tetrahedron Lett., **2010**, 51, 6503-6506.

Manescu, I. G., Badea, G., Iscrulescu, L., Iovu, M. and Balaci, T. Incorporation of new benzimidazole compounds into lipid nanostructures in order to obtain photoprotective formulations. Farmacia, **2015**, 63, 518-525.

Marella, A., Tanwar, O. P., Saha, R., Ali, M. R., Srivastava, S., Akhter, M., Shaquiquzzaman, M. and Alam, M. M. Quinoline: A versatile heterocyclic. Saudi Pharm. J., **2013**, 21, 1-12.

Mariano, M., Hartmann, R. W. and Engel, M. Systematic diversification of benzylidene heterocycles yields novel inhibitor scaffolds selective for Dyrk1A, Clk1 and CK2. Eur. J. Med. Chem., **2016**, 112, 209-216.

Matsubara, Y., Hirakawa, S., Yamaguchi, Y. and Yoshida, Z.-i. Assembly of substituted 2-alkylquinolines by a sequential palladium-catalyzed C-N and C-C bond formation. Angew. Chem. Int. Ed., **2011**, 50, 7670-7673.

Matsugi, M., Tabusa, F. and Minamikawa, J.-i. Doebner-Miller synthesis in a two-phase system: Practical preparation of quinolines. Tetrahedron Lett., **2000**, 41, 8523-8525.

Matsui, M., Asamura, Y., Kubota, Y., Funabiki, K., Jin, J., Yoshida, T. and Miura, H. Highly efficient substituted triple rhodanine indoline dyes in zinc oxide dye-sensitized solar cell. Tetrahedron, **2010**, 66, 7405-7410.

Matsui, M., Furukawa, K. and Shibata, K. Preparation of 2-alkylquinolines by TiO_2-photocatalysed reaction of arylamines in alcohols. J. Jpn. Soc. Colour Mater., **2002**, 75, 319-323.

Meyer, T., Ogermann, D., Pankrath, A., Kleinermanns, K. and Müller, T. J. J. Phenothiazinyl rhodanylidene merocyanines for dye-sensitized solar cells. J. Org. Chem., **2012**, 77, 3704-3715.

Michael, J. P. Quinoline, quinazoline and acridone alkaloids. Nat. Prod. Rep., **2008**, 25, 166-187.

Min, G., Lee, S.-K., Kim, H.-N., Han, Y.-M., Lee, R.-H., Jeong, D. G., Han, D. C. and Kwon, B.-M. Rhodanine-based PRL-3 inhibitors blocked the migration and invasion of metastatic cancer cells. Bioorg. Med. Chem. Lett., **2013**, 23, 3769-3774.

Monrad, R. N. and Madsen, R. Ruthenium-catalysed synthesis of 2-and 3-substituted quinolines from anilines and 1, 3-diols. Org. Biomol. Chem., **2011**, 9, 610-615.

More, S. V., Sastry, M. N. V., Wang, C.-C. and Yao, C.-F. Molecular iodine: A powerful catalyst for the easy and efficient synthesis of quinoxalines. Tetrahedron Lett., **2005**, 46, 6345-6348.

Musiol, R., Jampilek, J., Podeszwa, B., Finster, J., Tabak, D., Dohnal, J. and Polanski, J. RP-HPLC determination of lipophilicity in series of quinoline derivatives. Cent. Eur. J. Chem., **2009**, 7, 586-597.

Musiol, R., Magdziarz, T. and Kurczyk, A. Quinoline scaffold as a privileged substructure in antimicrobial drugs. Science against microbial pathogens: Communicating current research and technological advances. Méndez-Vilas, A. (Ed), Formatex, Badajoz, Spain, **2011**, p. 72-83.

Musiol, R., Serda, M., Hensel-Bielowka, S. and Polanski, J. Quinoline-based antifungals. Curr. Med. Chem., **2010**, 17, 1960-1973.

Nadaraj, V. and Thamarai Selvi, S. Microwave-assisted solvent-free synthesis of 4-methyl-2-hydroxy- and 2-methyl-4-hydroxyquinolines. Indian J. Chem., Sect. B: Org. Chem. Incl. Med. Chem., **2007**, 46B, 1203-1207.

Nagarapu, L., Palem, J. D., Reddy Aruva, R. K. and Bantu, R. A facile and efficient synthesis of quinoxalines from phenacyl bromides and *ortho* phenylenediamine promoted by zirconium tungstate. Org. Chem. Curr. Res., **2014**, S4.

Nagasawa, Y., Tachikawa, Y., Yamaguchi, E., Tada, N., Miura, T. and Itoh, A. Catalytic aerobic photo-oxidation of a methyl group on a heterocycle to produce an aldehyde *via* homolytic C-I bond cleavage caused by irradiation with visible light. Adv. Synth. Catal., **2016**, 358, 178-182.

Nájera, C. and Yus, M. Chiral benzimidazoles as hydrogen bonding organocatalysts. Tetrahedron Lett., **2015**, 56, 2623-2633.

Nencki, M. Ueber die einwirkung der monochloressigsäure auf sulfocyansäure und ihre salze. J. Prakt. Chem., **1877**, 16, 1-17.

Nguyen, T. B., Ermolenko, L. and Al-Mourabit, A. Iron sulfide catalyzed redox/condensation cascade reaction between 2-amino/hydroxy nitrobenzenes and activated methyl groups: A straightforward atom economical approach to 2-hetaryl-benzimidazoles and -benzoxazoles. J. Am. Chem. Soc., **2013**, 135, 118-121.

Nieto, C. I., Cabildo, P., García, M. Á., Claramunt, R. M., Alkorta, I. and Elguero, J. An experimental and theoretical NMR study of NH-benzimidazoles in solution and in the solid state: Proton transfer and tautomerism. Beilstein J. Org. Chem., **2014**, 10, 1620-1629.

O'Brien, D., Weaver, M. S., Lidzey, D. G. and Bradley, D. D. C. Use of poly(phenyl quinoxaline) as an electron transport material in polymer light-emitting diodes. Appl. Phys. Lett., **1996**, 69, 881-883.

Ott, S. and Faust, R. Quinoxalinodehydroannulenes: A novel class of carbon-rich materials. Synlett, **2004**, 2004, 1509-1512.

Özdemir, Z., Kandilci, H. B., Gümüşel, B., Çalış, Ü. and Bilgin, A. A. Synthesis and studies on antidepressant and anticonvulsant activities of some 3-(2-furyl)-pyrazoline derivatives. Eur. J. Med. Chem., **2007**, 42, 373-379.

Pandit, R. P., Kim, S. H. and Lee, Y. R. Iron-catalyzed annulation of 1,2-diamines and diazodicarbonyls for diverse and polyfunctionalized quinoxalines, pyrazines, and benzoquinoxalines in water. Adv. Synth. Catal., **2016**, 358, 3586-3599.

Pardasani, R., Pardasani, P., Sherry, D. and Chaturvedi, V. Synthetic and antibacterial studies of rhodanine derivatives with indol-2, 3-diones. Indian J. Chem., Sect. B: Org. Chem. Incl. Med. Chem., **2001**, 40, 1275-1278.

Pérez-Melero, C., Maya, A. B. S., del Rey, B., Peláez, R., Caballero, E. and Medarde, M. A new family of quinoline and quinoxaline analogues of combretastatins. Bioorg. Med. Chem. Lett., **2004**, 14, 3771-3774.

Phillips, A. P. Condensation reactions of cinchoninaldehyde and quinaldaldehyde with some heterocyclic methylene compounds. I. J. Am. Chem. Soc., **1945**, 67, 744-748.

Pinho-Ribeiro, F. A., Hohmann, M. S. N., Borghi, S. M., Zarpelon, A. C., Guazelli, C. F. S., Manchope, M. F., Casagrande, R. and Verri, W. A. Protective effects of the flavonoid hesperidin methyl chalcone in inflammation and pain in mice: Role of TRPV1, oxidative stress, cytokines and NF-κB. Chem.-Biol. Interact.., **2015**, 228, 88-99.

Poronik, Y. M., Klajn, J., Borzęcka, W. and Gryko, D. T. The Niementowski reaction of anthranilic acid with ethyl acetoacetate revisited: a new access to pyrano[3,2-c]quinoline-2,5-dione. ARKIVOC, **2017**, Part II, 7-11.

Prajapati, S. M., Patel, K. D., Vekariya, R. H., Panchal, S. N. and Patel, H. D. Recent advances in the synthesis of quinolines: A review. RSC Adv., **2014**, 4, 24463-24476.

Rajendra Prasad, Y., Srinivasa Rao, A., Sridhar, S. and Rambabu, R. Synthesis and studies of anti-inflammatory and antimicrobial activity of some new 4-amino chalcones. Int. J. Chem. Sci., **2008**, 6, 234-244.

Ram Reddy, P., Subba Rao, K. V. and Subrahmanyam, M. Selective synthesis of 2-methylquinoline over zeolites. Catal. Lett., **1998**, 56, 155-158.

Ramann, G. and Cowen, B. Recent advances in metal-free quinoline synthesis. Molecules, **2016**, 21, 986.

Ramesh, V., Ananda Rao, B., Sharma, P., Swarna, B., Thummuri, D., Srinivas, K., Naidu, V. G. M. and Jayathirtha Rao, V. Synthesis and biological evaluation of new rhodanine analogues bearing 2-chloroquinoline and benzo[*H*]quinoline scaffolds as anticancer agents. Eur. J. Med. Chem., **2014**, 83, 569-580.

Raw, S. A., Wilfred, C. D. and Taylor, R. J. K. Tandem oxidation processes for the preparation of nitrogen-containing heteroaromatic and heterocyclic compounds. Org. Biomol. Chem., **2004**, 2, 788-796.

Rehman, M. u., Imran, M., Arif, M. and Farooq, M. Mannich base derivatives of benzimidazole: Synthesis and antimicrobial properties - A short review. World Applied Programming, **2013**, 3, 558-564.

Rodriguez-Zubiri, M., Anguille, S., Brunet, J.-J. and Daran, J.-C. Pt-catalysed intermolecular hydroamination of non-activated olefins using a novel family of catalysts: Arbuzov-type phosphorus metal complexes. J. Mol. Catal. A: Chem., **2013**, 379, 103-111.

Rostom, S. A. F., Badr, M. H., Abd El Razik, H. A., Ashour, H. M. A. and Abdel Wahab, A. E. Synthesis of some pyrazolines and pyrimidines derived from polymethoxy chalcones as anticancer and antimicrobial agents. Arch. Pharm., **2011**, 344, 572-587.

Safari, J., Banitaba, S. H. and Samiei, S. S. One-pot synthesis of quinaldine derivatives by using microwave irradiation without any solvent - A green chemistry approach. J. Chem. Sci., **2009**, 121, 481-484.

Sakaguchi, S., Shibamoto, A. and Ishii, Y. Remarkable effect of nitrogen dioxide for *N*-hydroxyphthalimide-catalyzed aerobic oxidation of methylquinolines. Chem. Commun., **2002**, 180-181.

Sánchez, D. S., Baeza, A. and Alonso, D. A. Organocatalytic asymmetric α-chlorination of 1, 3-dicarbonyl compounds catalyzed by 2-aminobenzimidazole derivatives. Symmetry, **2016**, 8, 3.

Sandhu, S., Sandhu J. S. Ultrasound-assisted synthesis of 2,4-thiazolidinedione and rhodanine derivatives catalyzed by task-specific ionic liquid: [TMG][Lac]. Org. and Med. Chem. Lett. **2013**, 3, 2-6

Sangshetti, J. N., Zambare, A. S., Gonjari, I. and Shinde, D. B. Pfitzinger reaction in the synthesis of bioactive compounds - A review. Mini Rev. Org. Chem., **2014**, 11, 225-250.

Santivañez-Veliz, M., Pérez-Silanes, S., Torres, E. and Moreno-Viguri, E. Design and synthesis of novel quinoxaline derivatives as potential candidates for treatment of multidrug-resistant and latent tuberculosis. Bioorg. Med. Chem. Lett., **2016**, 26, 2188-2193.

Schmidt, J. G. Ueber die einwirkung von aceton auf furfurol und auf bittermandelöl bei gegenwart von alkalilauge. Ber. Dtsch. Chem. Ges., **1881**, 14, 1459-1461.

Schowtka, B., Müller, C., Görls, H. and Westerhausen, M. Synthesis, structures, and spectroscopic properties of 3-aryl-5-(2-pyridyl)pyrazoles and related pyrazoles. Z. Anorg. Allg. Chem., **2014**, 640, 916-925.

Selvam, K. and Swaminathan, M. Au-doped TiO_2 nanoparticles for selective photocatalytic synthesis of quinaldines from anilines in ethanol. Tetrahedron Lett., **2010**, 51, 4911-4914.

Selvam, K. and Swaminathan, M. Facile synthesis of 2-methylquinolines from anilines on mesoporous *N*-doped TiO_2 under UV and visible light. Synth. React. Inorg., Met.-Org., Nano-Met. Chem., **2013**, 43, 500-508.

Shaharyar, M., Abdullah, M. M., Bakht, M. A. and Majeed, J. Pyrazoline bearing benzimidazoles: Search for anticancer agent. Eur. J. Med. Chem., **2010**, 45, 114-119.

Shi, D.-Q., Dou, G.-L., Ni, S.-N., Shi, J.-W. and Li, X.-Y. An efficient synthesis of quinoxaline derivatives mediated by stannous chloride. J. Heterocycl. Chem., **2008**, 45, 1797-1801.

Shibinskaya, M. O., Lyakhov, S. A., Mazepa, A. V., Andronati, S. A., Turov, A. V., Zholobak, N. M. and Spivak, N. Y. Synthesis, cytotoxicity, antiviral activity and interferon inducing ability of 6-(2-aminoethyl)-6*H*-indolo[2,3-b]quinoxalines. Eur. J. Med. Chem., **2010**, 45, 1237-1243.

Shiri, M., Zolfigol, M. A., Kruger, H. G. and Tanbakouchian, Z. Friedländer annulation in the synthesis of azaheterocyclic compounds. Adv. Heterocycl. Chem. A. R. Katritzky, Academic Press. **2011**, 102, 139-227.

Shvekhgeimer, M. G.-A. The Pfitzinger reaction. (review). Chem. Heterocycl. Compd., **2004**, 40, 257-294.

Siddiqui, I. R. , Singh, P. K., Singh, J. and Singh, J. Facile synthesis and fungicidal activity of novel 4, 4'-bis [2"-(5'''-substituted rhodanin-3'''-yl) thiazol-4"-yl] bibenzyls. Indian J. Chem., Sect. B: Org. Chem. Incl. Med. Chem., **2005**, 44, 2102-2106.

Siddiqui, N. An updated review: emerging anticonvulsants. Int. J. Pharm. Biol. Arch., **2010**, 1, 404-415.

Sing, W. T., Lee, C. L., Yeo, S. L., Lim, S. P. and Sim, M. M. Arylalkylidene rhodanine with bulky and hydrophobic functional group as selective HCV NS3 protease inhibitor. Bioorg. Med. Chem. Lett., **2001**, 11, 91-94.

Singh, N., Ahmad, S. and Alam, M. S. Biological potentials of chalcones: A review. Int. J. Pharm. Biol. Arch., **2012**, 3, 1298-1303.

Sinha, S., Berdichevsky, E. K. and Warren, J. J. Electrocatalytic CO_2 reduction using rhenium(I) complexes with modified 2-(2′-pyridyl)imidazole ligands. Inorg. Chim. Acta, **2017**, 460, 63-68.

Sivaprasad, G., Rajesh, R. and Perumal, P. T. Synthesis of quinaldines and lepidines by a Doebner-Miller reaction under thermal and microwave irradiation conditions using phosphotungstic acid. Tetrahedron Lett., **2006**, 47, 1783-1785.

Solomon, V. R., Hu, C. and Lee, H. Design and synthesis of anti-breast cancer agents from 4-piperazinylquinoline: A hybrid pharmacophore approach. Bioorg. Med. Chem., **2010**, 18, 1563-1572.

Solomon, V. R. and Lee, H. Quinoline as a privileged scaffold in cancer drug discovery. Curr. Med. Chem., **2011**, 18, 1488-1508.

Sriram, D., Yogeeswari, P., Thirumurugan, R. and Ratan Bal, T. Camptothecin and its analogues: A review on their chemotherapeutic potential. Nat. Prod. Res., **2005**, 19, 393-412.

Stibrany, R. T., Lobanov, M. V., Schugar, H. J. and Potenza, J. A. A geometrically constraining bis(benzimidazole) ligand and its nearly tetrahedral complexes with Fe(II) and Mn(II). Inorg. Chem., **2004**, 43, 1472-1480.

Subhedar, D. D., Shaikh, M. H., Shingate, B. B., Nawale, L., Sarkar, D., Khedkar, V. M., Kalam Khan, F. A. and Sangshetti, J. N. Quinolidene-rhodanine conjugates: Facile synthesis and biological evaluation. Eur. J. Med. Chem., **2017**, 125, 385-399.

Takasu, K., Inoue, H., Kim, H.-S., Suzuki, M., Shishido, T., Wataya, Y. and Ihara, M. Rhodacyanine dyes as antimalarials. 1. Preliminary evaluation of their activity and toxicity. J. Med. Chem., **2002**, 45, 995-998.

Terashima, H., Hama, K., Yamamoto, R., Tsuboshima, M., Kikkawa, R., Hatanaka, I. and Shigeta, Y. Effects of a new aldose reductase inhibitor on various tissues *in vitro*. J. Pharmacol. Exp. Ther., **1984**, 229, 226-230.

Tozlu, C., Erten-Ela, S., Singh, T. B., Sariciftci, N. S. and İçli, S. Comparative study of arylene bisimides substituted with imidazole side group for different dielectrics on the OFET application. Synth. Met., **2013**, 172, 5-10.

Trump, E. L. and Zhou, M. X. The use of selenium (IV) oxide to oxidize aromatic methyl groups. Trans. Kans. Acad. Sci., **1993**, 96, 167-180.

Tseng, C.-H., Chen, Y.-L., Hsu, C.-Y., Chen, T.-C., Cheng, C.-M., Tso, H.-C., Lu, Y.-J. and Tzeng, C.-C. Synthesis and antiproliferative evaluation of 3-phenylquinolinylchalcone derivatives against non-small cell lung cancers and breast cancers. Eur. J. Med. Chem., **2013**, 59, 274-282.

Tseng, C.-H., Tzeng, C.-C., Hsu, C.-Y., Cheng, C.-M., Yang, C.-N. and Chen, Y.-L. Discovery of 3-phenylquinolinylchalcone derivatives as potent and selective anticancer agents against breast cancers. Eur. J. Med. Chem., **2015**, 97, 306-319.

Tynebor, R. and Millings, E. Novel method of synthesizing various five membered heterocycles from an aryl tribromomethyl group. Synth. Commun., **2013**, 43, 1902-1908.

van Heerden, L., Cloete, T. T., Breytenbach, J. W., de Kock, C., Smith, P. J., Breytenbach, J. C. and N'Da, D. D. Synthesis and *in vitro* antimalarial activity of a series of bisquinoline and bispyrrolo[1,2a]quinoxaline compounds. Eur. J. Med. Chem., **2012**, 55, 335-345.

van Schalkwyk, D. A. and Egan, T. J. Quinoline-resistance reversing agents for the malaria parasite *Plasmodium falciparum*. Drug Resistance Updates, **2006**, 9, 211-226.

Vandekerckhove, S. and D'hooghe, M. Quinoline-based antimalarial hybrid compounds. Bioorg. Med. Chem., **2015**, 23, 5098-5119.

Vander Mierde, H., Ledoux, N., Allaert, B., Van Der Voort, P., Drozdzak, R., De Vos, D. and Verpoort, F. Improved ruthenium catalysts for the modified Friedlaender quinoline synthesis. New J. Chem., **2007**, 31, 1572-1574.

Vander Mierde, H., Van Der Voort, P., De Vos, D. and Verpoort, F. A Ruthenium-catalyzed approach to the Friedländer quinoline synthesis. Eur. J. Org. Chem., **2008**, 2008, 1625-1631.

Verma, S., Verma, D. and Jain, S. L. Magnetically separable palladium-graphene nanocomposite as heterogeneous catalyst for the synthesis of 2-alkylquinolines *via* one pot reaction of anilines with alkenyl ethers. Tetrahedron Lett., **2014**, 55, 2406-2409.

Viegas-Junior, C., Danuello, A., da Silva Bolzani, V., Barreiro, E. J. and Fraga, C. A. M. Molecular hybridization: a useful tool in the design of new drug prototypes. Curr. Med. Chem. **2007**, 14, 1829-1852

Vodnala, N., Kaldhi, D., Gupta, R., Linthoinganbi, R. K., Putta, V. P. R. K., Polina, S., Singh, V. and Malakar, C. C. Novel domino routes for the synthesis of *N*-heterocycles *via* reductive cyclization of *β*-(*N*-2-nitroaryl)-*α,β*-unsaturated ketones. ChemistrySelect, **2016**, 1, 5784-5788.

Voskienė, A. and Mickevičius, V. Cyclization of chalcones to isoxazole and pyrazole derivatives. Chem. Heterocycl. Compd., **2009**, 45, 1485-1488.

Wagner, H. and Farkas, L. Synthesis of flavonoids. <u>The Flavonoids</u>. Harborne, J. B., Mabry, T. J. and Mabry, H. (Eds), Springer US, Boston, MA. **1975**, 127-213

Wan, J.-P., Gan, S.-F., Wu, J.-M. and Pan, Y. Water mediated chemoselective synthesis of 1,2-disubstituted benzimidazoles using *o*-phenylenediamine and the extended synthesis of quinoxalines. Green Chem., **2009**, 11, 1633-1637.

Wang, C., Tang, C., Li, Z. and Wang, Q. Palladium-catalyzed synthesis of 1*H*-Pyrazolo [4, 3-c] quinolines and 4-anilinoquinoline-3-carbonitriles from 4-chloroquinoline-3-carbaldehydes. Synthesis, **2015**, 47, 3139-3146.

Wang, K., Shen, M. and Sun, W.-H. Synthesis, characterization and ethylene oligomerization of nickel complexes bearing *N*-(2-(1*H*-benzo[*d*]imidazol-2-yl)quinolin-8-yl)benzamide derivatives. Dalton Trans., **2009**, 0, 4085-4095.

Wang, L., Hou, X., Fu, H., Pan, X., Xu, W., Tang, W. and Fang, H. Design, synthesis and preliminary bioactivity evaluations of substituted quinoline hydroxamic acid derivatives as novel histone deacetylase (HDAC) inhibitors. Bioorg. Med. Chem., **2015**, 23, 4364-4374.

Wang, Q.-Q., Xu, K., Jiang, Y.-Y., Liu, Y.-G., Sun, B.-G. and Zeng, C.-C. Electrocatalytic minisci acylation reaction of *N*-heteroarenes mediated by NH_4I. Org. Lett., **2017**, 19, 5517-5520.

Wang, W., Shen, Y., Meng, X., Zhao, M., Chen, Y. and Chen, B. Copper-catalyzed synthesis of quinoxalines with *o*-phenylenediamine and terminal alkyne in the presence of bases. Org. Lett., **2011**, 13, 4514-4517.

Wang, X., Xie, X., Cai, Y., Yang, X., Li, J., Li, Y., Chen, W. and He, M. Design, synthesis and antibacterial evaluation of some new 2-phenyl-quinoline-4-carboxylic acid derivatives. Molecules, **2016**, 21, 340.

Wang, Z. Comprehensive organic name reactions and reagents, John Wiley & Sons, Inc. **2010**

Wolfe, D. M. and Schreiner, P. R. Oxidative desulfurization of azole-2-thiones with benzoyl peroxide: Syntheses of ionic liquids and other azolium salts. Eur. J. Org. Chem., **2007**, 2007, 2825-2838.

Wright, J. B. The chemistry of the benzimidazoles. Chem. Rev., **1951**, 48, 397-541.

Xekoukoulotakis, N. P., Hadjiantoniou-Maroulis, C. P. and Maroulis, A. J. Synthesis of quinoxalines by cyclization of *α*-arylimino oximes of *α*-dicarbonyl compounds. Tetrahedron Lett., **2000**, 41, 10299-10302.

Xie, F., Zhang, M., Jiang, H., Chen, M., Lv, W., Zheng, A. and Jian, X. Efficient synthesis of quinoxalines from 2-nitroanilines and vicinal diols *via* a ruthenium-catalyzed hydrogen transfer strategy. Green Chem., **2015**, 17, 279-284.

Yadav, G. and Ganguly, S. Structure activity relationship (SAR) study of benzimidazole scaffold for different biological activities: A mini-review. Eur. J. Med. Chem., **2015**, 97, 419-443.

Yan, J., Xu, Y., Zhuang, F., Tian, J. and Zhang, G. Highly efficient synthesis of quinoxaline derivatives from 1,2-benzenediamine and *α*-aminoxylated 1,3-dicarbonyl compounds. Mol. Diversity, **2016**, 20, 567-573.

Yar, M. S., Siddiqui, A. A., Ali, M. A., Murugan, V. and Chandrashekhar, R. Synthesis and cytotoxic activity of novel pyrazoline derivatives against human lung tumor cell line (A549). J. Chin. Chem. Soc., **2007**, 54, 81-86.

Yaragorla, S. and Vijaya Babu, P. Oxidative C_{sp3}-H functionalization of 2-methylazaarenes: A practical synthesis of 2-azaarenyl-benzimidazoles and benzothiazoles. Tetrahedron Lett., **2017**, 58, 1879-1882.

Yazdan, S. K., Sagar, D. V. and Shaik, A. B. Chemical and biological potentials of chalcones: A review. Org. Med. Chem. Int. J., **2015**, 1, 001-009.

Yeh, A. Synthesis and electroluminescent property of bis (2-(benzimidazol-2-yl) quinolinato) zinc. Mater. Lett., **2005**, 59, 1811-1814.

Yi, C. S. and Yun, S. Y. Ruthenium-catalyzed intermolecular coupling reactions of arylamines with ethylene and 1,3-dienes: mechanistic insight on hydroamination vs *ortho*-C-H bond activation. Org. Lett., **2005**, 7, 2181-2183.

Yoshida, M., Katagiri, Y., Zhu, W.-B. and Shishido, K. Oxidative carboxylation of arylaldehydes with water by a sulfoxylalkyl-substituted *N*-heterocyclic carbene catalyst. Org. Biomol. Chem., **2009**, 7, 4062-4066.

Yusuf, M. and Jain, P. Synthetic and biological studies of pyrazolines and related heterocyclic compounds. Arabian J. Chem., **2014**, 7, 553-596.

Zhang, C., Wang, C., Tang, S., Sun, Y., Zhao, D., Zhang, S., Deng, S., Zhou, Y. and Xiao, X. TNFR1/TNF-*α* and mitochondria interrelated signaling pathway mediates quinocetone-induced apoptosis in HepG2 cells. Food Chem. Toxicol., **2013**, 62, 825-838.

Zhang, J., Li, M., Li, L., Li, Y., Peng, B., Zhang, S., Gao, H. and Zhou, W. Investigation of the ultrasound effect and target analyte selectivity of dispersive liquid-liquid microextraction and its application to a quinocetone pharmacokinetic study. J. Chromatogr. A, **2012**, 1268, 1-8.

Zhang, K., Wang, C., Wang, X., Zheng, H., Zhao, J., Wang, M., Xiao, S., Fei, C., Zheng, W., Zhang, L. and Xue, F. Synthesis, *in-vitro* activity and metabolic properties of quinocetone and structurally similar compounds. Iranian J. Pharm. Res., **2017**, 16, 569-585.

Zhang, M., Dai, Z.-C., Qian, S.-S., Liu, J.-Y., Xiao, Y., Lu, A.-M., Zhu, H.-L., Wang, J.-X. and Ye, Y.-H. Design, synthesis, antifungal, and antioxidant activities of (*E*)-6-((2-phenylhydrazono)methyl)quinoxaline derivatives. J. Agric. Food Chem., **2014**, 62, 9637-9643.

Zhang, S.-L. and Deng, Z.-Q. Synthesis of quinolines and naphthyridines *via* catalytic retro-aldol reaction of *β*-hydroxyketones with *ortho*-aminobenzaldehydes or nicotinaldehydes. Org. Biomol. Chem., **2016**, 14, 8966-8970.

Zhang, Y., Ming, Q., Wu, L., Rahman, K. and Qin, L. Alkaloids produced by endophytic fungi: A Review. Nat. Prod. Commun., **2012**, 7, 963-968.

Zheng, G., Liu, H. and Wang, M. Copper-catalyzed aerobic oxidation of azinylmethanes for access to trifluoromethylazinylols. Chin. J. Chem . **2016**, 34, 519-523.

Zhuang, C., Zhang, W., Sheng, C., Zhang, W., Xing, C. and Miao, Z. Chalcone: A privileged structure in medicinal chemistry. Chem. Rev., **2017**, 117, 7762-7810.

Zvarec, O., Polyak, S. W., Tieu, W., Kuan, K., Dai, H., Pedersen, D. S., Morona, R., Zhang, L., Booker, G. W. and Abell, A. D. 5-Benzylidenerhodanine and 5-benzylidene-2-4-thiazolidinedione based antibacterials. Bioorg. Med. Chem. Lett., **2012**, 22, 2720-2722.

Chapter 2. Synthesis and structural elucidation of a series of quinoline benzimidazole hybrid molecules

Abstract

A total of eleven 2-(1*H*-benzo[*d*]imidazol-2-yl)quinolines were synthesised by the Doebner-von Miller reaction of crotonaldehyde and substituted anilines, followed by oxidation and benzimidazole formation with *o*-phenylenediamine. The series of compounds consisted of 6- and 8- substituted halogen, methoxy and methyl groups. A complete structural elucidation of all compounds is provided, studying the effects that the different substituents had on the resonances of the quinoline scaffold.

Keywords: quinolines; benzimidazoles; 2-(1*H*-benzo[*d*]imidazol-2-yl)quinolines; structural elucidation; NMR

2.1. Introduction

Quinoline and benzimidazole scaffolds are composed of pyridine and imidazole rings fused to benzene respectively. Quinoline-benzimidazole hybrids have shown good antimicrobial and antifungal activity (Hisano et al., 1982). A recent study has shown 2-(1*H*-benzo[*d*]imidazol-2-yl)quinolines to aid colon motility by acting as receptor agonists (Cosimelli et al., 2011). When these hybrid molecules were complexed with metals, they showed catalytic, fluorescent and electroluminescent properties (Chen, 2005; Yeh et al., 2005; Cao et al., 2013; Li et al., 2013; Hu et al., 2015; Dayan et al., 2016; Li et al., 2016; Sinha et al., 2017).

The synthesis of 2-(1*H*-benzo[*d*]imidazol-2-yl) quinolines generally consist of a reaction involving *o*-phenylenediamine with quinaldic acids, quinoline-2-carbaldehydes or quinaldines. Early reports on the synthesis of 2-(1*H*-benzo[*d*]imidazol-2-yl) quinolines made use of solvent free reactions of *o*-phenylenediamine with quinaldic acid at 180 °C, however, poor yields of 17% were reported (Govindan, 1956). The most popular method used to synthesise these compounds is the condensation of quinaldic acid with *o*-phenylenediamine in the presence of polyphosphoric acid (PPA), which occur at temperatures exceeding 200 °C in ~4 hours, achieving 80% yields (Chen, 2005; Dayan et al., 2016).

Another frequently used method makes use of quinoline-2-carbaldehydes in a condensation reaction with *o*-phenylenediamine (Hu et al., 2015; Li et al., 2016; Gong et al., 2017; Sinha et al., 2017). They can also be synthesised directly from 2-methylquinoline (quinaldine) and *o*-phenylenediamine using oxidising agents such as elemental sulfur and iodine (Hisano and Ichikawa, 1974; Wang et al., 2009; Li et al., 2014; Yaragorla et al., 2017). An alternate method involving the reaction of quinaldine with 2-nitroaniline using elemental sulfur and Fe by a cascade reaction has also been carried out (Nguyen et al., 2013). Other miscellaneous methods include using 2-(tribromomethyl)quinoline with *o*-phenylenediamine or by rearrangement of quinoxaline-2-one derivatives (Mamedov et al., 2010; Tynebore and Millings, 2013; Mamedov et al., 2014).

To the best of our knowledge, there have been no reports on the structural elucidation of 2-(1*H*-benzo[*d*]imidazol-2-yl) quinolines, hence we report on the synthesis and complete structural elucidation of a series of quinoline-benzimidazole hybrids.

2.2. Experimental

General Procedures

All reagents and chemicals used in this study were purchased from Sigma-Aldrich *via* Capital Lab, South Africa and were reagent grade. All organic solvents were distilled prior to use. Thin-layer chromatography (TLC) was performed using Merck Kieselgel 60 F_{254} plates. Crude compounds were purified with column chromatography using silica gel (60–120 mesh), as the stationary phase, with various combinations of solvents, depending on the sample to be purified. The melting points were measured using a sealed capillary tube in an Electrothermal IA9100 melting point apparatus. Infrared (IR) spectra were recorded on a Perkin Elmer Spectrum 100 FT-IR spectrometer with universal attenuated total reflectance sampling accessory. Ultraviolet (UV) spectra were obtained on a Shimadzu UV-3600 spectrophotometer in dichloromethane. High-resolution mass spectrometry was carried out using a Waters Micromax LCT Premier TOF-MS instrument, operating at ambient temperatures, with a sample concentration of approximately 1 ppm. The ^{1}H and ^{13}C NMR spectra were recorded at 298 K with 5 to 10 mg samples dissolved in 0.5 mL DMSO-d_6 in 5 mm NMR tubes using a

Bruker Avance 400 MHz NMR spectrometer (9.4 T; Bruker, Germany) (400.22 MHz for ^{1}H and 100.63 MHz for ^{13}C). The free induction decay (FID) resolution was 0.501 Hz/pt for ^{1}H and 0.734 Hz/pt for ^{13}C spectra. Chemical shifts are reported in ppm and coupling constants (*J*) in Hz. The ^{1}H and ^{13}C chemical shifts of the deuterated solvent were 2.50 and 39.51, respectively, referenced to the internal standard, tetramethylsilane (TMS). All data was analysed using Bruker TopSpin 3.5 software.

Crystallographic data collection and refinement of **5k** was conducted using a Bruker Smart APEX II diffractometer, using graphite monochromated MoKα radiation (λ = 0.71073 Å). Data reduction was performed using *SAINT* software and the scaling and absorption corrections were applied using *SADABS* multi-scan technique (Bruker, 2009). The structural data collected was solved by direct methods and refined employing full-matrix least-squares with SHELXL (Sheldrick, 2008) refining on F2. All hydrogen atoms were found in the difference electron density maps, placed in idealised positions and refined with geometrical constraints. Crystallographic images were prepared using ORTEP-3 (Farrugia, 2012).

Preparation of quinoline-2-carbaldehydes

Substituted anilines (**1h-k**) (45.0 mmol) were dissolved in HCl:water (1:2) and heated to 60 °C. Crotonaldehyde (**2**) (67.5 mmol; 5.6 mL) dissolved in toluene (20 mL) was added slowly to the aniline mixture and heated under reflux for 4 hours. Upon completion, the aqueous layer was separated from the resultant biphasic reaction mixture, adjusted to pH 8, extracted with 3 × 50 mL portions of ethyl acetate (EtOAc) and dried over anhydrous $MgSO_4$. The solvent was then removed *in vacuo*. The residue was then dissolved in 1,4-dioxane and SeO_2 (45.4 mmol; 5.0 g) was added. The resulting suspension was left to reflux for 15 to 180 minutes depending on the substituent and the reaction monitored by TLC. Upon completion, the reaction mixture was filtered hot through celite, diluted with water (40 mL) and extracted with 3 × 50 mL portions of ethyl acetate, combined, washed with 2 x 50 mL portions of water, dried over anhydrous $MgSO_4$ and the solvent removed. The residues were purified by column chromatography (hexane: EtOAc, 85:15 v/v) to yield the carbaldehydes (**3h-k**).

Preparation of quinoline-2-carboxylic acids

The carbaldehydes **3a-g** were prepared as above. The resultant residues were then dissolved in 20 mL THF, 10 mL 30% hydrogen peroxide added and the mixture refluxed for 3 hours. Upon completion, excess hydrogen peroxide was neutralized with sodium bicarbonate and the reaction mixture acidified to pH 3, upon which the halogenated quinoline-2-carboxylic acids (**4a-g**) precipitated out of solution.

Preparation of quinoline-2-benzimidazoles

Quinoline-2-carboxylic acids (**4a-g**) (1 eq) and polyphosphoric acid (~4 g) were heated and stirred until complete dissolution occurred. Thereafter *o*-phenylenediamine (1 eq) was added and the reaction mixture heated to 250 °C for 2 hours. The hot reaction mixture was then poured into 20 mL 30% sodium carbonate in water. The resulting precipitates were collected by vacuum filtration and purified by column chromatography (hexane:EtOAc, 80:20 v/v) yielding **5a-g**.

Preparation of quinoline-2-benzimidazoles

Quinoline-2-carbaldehydes (**3h-k**) (1 eq) and sodium metabisulfite (1 eq) were then dissolved in ethanol and allowed to stir for 4 hours. A solution of *o*-phenylenediamine (1 eq) in DMF was added to the ethanol mixture and refluxed for 2 hours. The reaction mixture was then cooled to room temperature, 100 mL water added and the suspension extracted with 3 × 20 mL ethyl acetate. The organic extracts were combined, dried over anhydrous $MgSO_4$ and purified by column chromatography, hexane:EtOAc (80:20) yielding **5h**-**k**.

2-(1H-benzo[d]imidazol-2-yl)-8-fluoroquinoline (**5a**), yellow powder; yield 66%; mp 194 °C; IR (neat) υ_{max} 2923, 1592, 1499 cm^{-1}; λ_{max} (log ε) = 291 (4.32), 337 (4.35), 351 (4.37); HRMS (*neg*) *m/z* 262.0787 [M-H] (calcd. for $C_{16}H_9FN_3$ 262.0781)

2-(1H-benzo[d]imidazol-2-yl)-8-chloroquinoline (**5b**), yellow crystals; yield 79%; mp 228 °C; IR (neat) υ_{max} 3073, 1599, 1495 cm^{-1}; λ_{max} (log ε) = 292 (4.44), 342 (4.44), 355 (4.47); HRMS (*neg*) *m/z* 278.0489 [M-H] (calcd. for $C_{16}H_9ClN_3$ 278.0485)

2-(1H-benzo[d]imidazol-2-yl)-8-bromoquinoline (**5c**), yellow crystals; yield 57%; mp 231 °C; IR (neat) υ_{max} 3072, 1598, 1491cm^{-1}; λ_{max} (log ε) = 292 (4.47), 344 (4.46), 356 (4.48); HRMS (*neg*) *m/z* 321.9982 [M-H] (calcd. for $C_{16}H_9BrN_3$ 321.9980)

2-(1H-benzo[d]imidazol-2-yl)-6-fluoroquinoline (**5d**), brown crystals; yield 58%; mp 159 °C; IR (neat) υ_{max} 3050, 1603, 1503 cm^{-1}; λ_{max} (log ε) = 288 (4.15), 302 (4.07), 315 (4.02), 338 (4.21), 351 (4.24); HRMS (*neg*) *m/z* 262.0789 [M-H] (calcd. for $C_{16}H_9FN_3$ 262.0781)

2-(1H-benzo[d]imidazol-2-yl)-6-chloroquinoline (**5e**), yellow crystals; yield 59%; mp 205 °C; IR (neat) υ_{max} 3073, 1599, 1495 cm^{-1}; λ_{max} (log ε) = 290 (4.42), 309 (4.39), 323 (4.38), 343 (4.55), 356 (4.60); HRMS (*neg*) *m/z* 278.0486 [M-H] (calcd. for $C_{16}H_9ClN_3$ 278.0485)

2-(1H-benzo[d]imidazol-2-yl)-6-bromoquinoline (**5f**), yellow crystals; yield 55%; mp 219 °C; IR (neat) υ_{max} 3072, 1598, 1491 cm^{-1}; λ_{max} (log ε) = 291 (4.52), 309 (4.49), 323 (4.49), 344 (4.65), 356 (4.69); HRMS (*neg*) *m/z* 321.9982 [M-H] (calcd. for $C_{16}H_9BrN_3$ 321.9980)

2-(1H-benzo[d]imidazol-2-yl)-6-iodoquinoline (**5g**), white powder; yield 50%; mp 232 °C; IR (neat) υ_{max} 3435, 1595, 1417 cm^{-1}; λ_{max} (log ε) = 296 (4.63), 310 (4.61), 325 (4.61), 346 (4.79), 359 (4.85); HRMS (*neg*) *m/z* 369.9843 [M-H] (calcd. for $C_{16}H_9IN_3$ 369.9841)

2-(1H-benzo[d]imidazol-2-yl)-8-methoxyquinoline (**5h**), white crystals; yield 62%; mp 210 °C; IR (neat) υ_{max} 3124, 1660, 1601 cm^{-1}; λ_{max} (log ε) = 300 (4.67), 345 (4.57); HRMS (*neg*) *m/z* 274.0984 [M-H] (calcd. for $C_{17}H_{12}N_3O$ 274.0980)

2-(1H-benzo[d]imidazol-2-yl)-6-methoxyquinoline (**5i**), yellow powder; yield 65%; mp 227 °C; IR (neat) υ_{max} 3063, 1619, 1499 cm^{-1}; λ_{max} (log ε) = 296 (4.39), 309 (4.32), 321 (4.27), 345 (4.41), 359 (4.48); HRMS (*neg*) *m/z* 274.0984 [M-H] (calcd. for $C_{17}H_{12}N_3O$ 274.0980)

2-(1H-benzo[d]imidazol-2-yl)-8-methylquinoline (**5j**), yellow crystals; yield 58%; mp 234 °C; IR (neat) υ_{max} 3042, 1598, 1501 cm^{-1}; λ_{max} (log ε) = 289 (4.49), 336 (4.53), 351 (4.54); HRMS (*pos*) *m/z* 260.1188 [M+H] (calcd. for $C_{17}H_{14}N_3$ 260.1188)

2-(1H-benzo[d]imidazol-2-yl)-6-methylquinoline (**5k**), yellow crystals; yield 66%; mp 224 °C; IR (neat) υ_{max} 3064, 1659, 1597 cm^{-1}; λ_{max} (log ε) =289 (4.56), 306 (4.43), 323 (4.48), 338 (4.61), 352 (4.68); HRMS (*pos*) *m/z* 260.1189 [M+H] (calcd. for $C_{17}H_{14}N_3$ 260.1188)

2.3. Results and Discussion

Synthesis

The 2-(1*H*-benzo[*d*]imidazol-2-yl) quinolines were synthesised by two alternative methods, either using quinoline-2-carboxylic acid or quinoline-2-carboxaldehyde precursors. The Doebner-von Miller reaction was used to synthesise substituted 2-methylquinolines using substituted anilines and crotonaldehyde and subsequently oxidised with selenium dioxide resulting in quinoline carbaldehydes. Without purifying the carbaldehydes, they were further oxidised using hydrogen peroxide to carboxylic acids before forming benzimidazoles **5a-g**. By avoiding purification of both 2-methylquinoline and quinoline-2-carbaldehyde we have developed a more efficient approach since the solvents and time spent on purification is avoided. We found that this made no difference to the yields of final product. The 8-iodo substituted derivative was not synthesised. Attempts to synthesise this resulted in substitution of the iodo group by chlorine from HCl. Efforts to modify the procedure using hydroiodic and phosphomolybdic acid were unsuccessful. Previous reports on these reactions all include purification of 2-methylquinoline and/or carbaldehyde (Chandrasekhar et al., 2011; George et al., 2013; Gopaul and Koorbanally, 2016).

The final step in the synthesis involved condensation with *o*-phenylenediamine, consistent with those reported in the literature (Hisano et al., 1982; Chen, 2005). Although this reaction worked for most precursors, the electron donating methoxy and methyl groups at C-6 and C-8 seemed to somehow prevent the acid from condensing with the *o*-phenylenediamine, probably through increasing electron density at the carbonyl carbon of the acid, preventing nucleophilic substitution from occurring. For these precursors, the carbaldehydes (**3h-k)** were purified by column chromatography and then condensed with *o*-phenylenediamine to obtain the benzimidazoles, **5h-k**. There were a few reports in the literature which used a similar method (Hu et al., 2015; Gong et al., 2017). In comparison to the route involving the carboxylic acid, this procedure is more time consuming and involves an additional purification step by column chromatography. The carboxylic acids precipitated out of solution hence, this purification step was not necessary in proceeding through the carboxylic acid route.

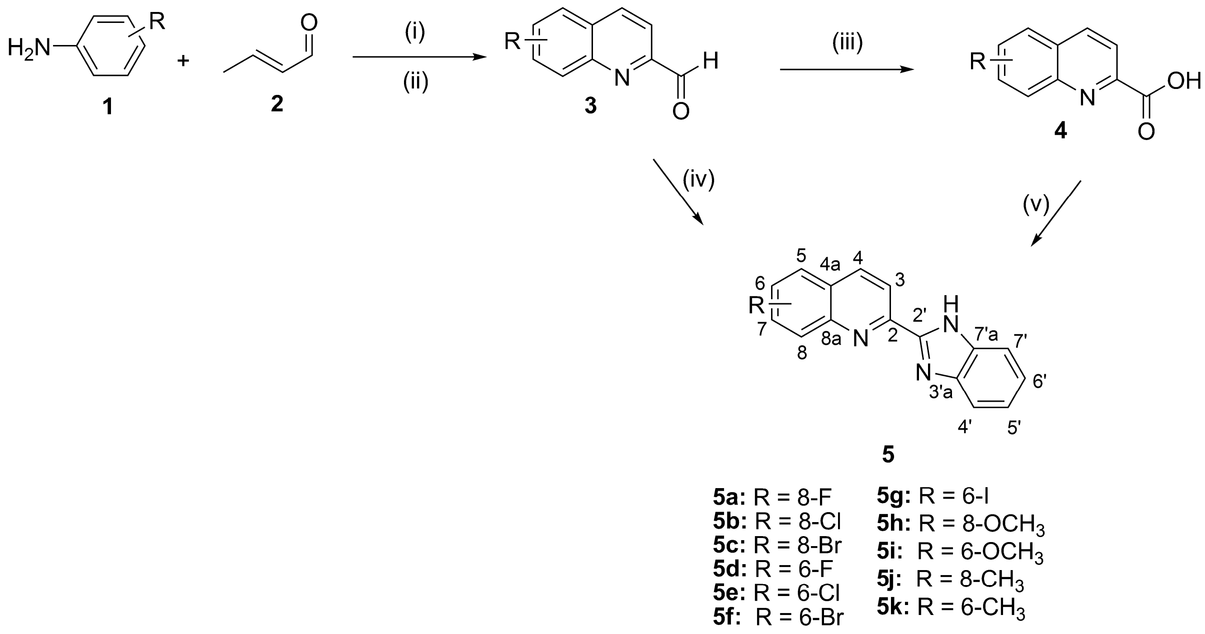

Scheme 2-1 Synthetic scheme for quinoline-2-benzimidazoles (**5a-k**). (i) HCl(aq), toluene, reflux, 100 °C; (ii) SeO_2, 1,4-dioxane, reflux, 101 °C; (iii) H_2O_2, THF, reflux, 66 °C; (iv) *o*-phenylenediamine, $Na_2S_2O_5$, ethanol, DMF, 100 °C; (v) *o*-phenylenediamine, PPA, 250 °C

Structural elucidation

The full characterisation (^{1}H and ^{13}C NMR assignments) of the 2-(1*H*-benzo[*d*]imidazol-2-yl) quinolines (**5a–k**) are shown in **Table 2-1** and **Table 2-2** and made with the aid of 2D NMR spectra.

For the 8-substituted quinoline-benzimidazole hybrids, for example, the 8-chloro substituted derivative **5b**, the ^{1}H NMR spectrum contained seven resonances in the aromatic region and a NH proton resonance at δ_H 12.93, which occurred as a broadened singlet. H-3 and H-4 are seen as two distinct doublets at δ_H 8.55 and 8.63 with a *J* value of 8.5 Hz. The H-5 and H-7 resonances occur as double doublets at δ_H 8.07 (*J* = 7.7, 1.1 Hz) and 8.03 (*J* = 7.7, 1.1 Hz), which coalesce resulting in these resonances taking the form of a triplet of doublets. The H-6 resonance occurs as a triplet at δ_H 7.65 (*J* = 7.7 Hz) and the benzimidazole protons are present at δ_H 7.29 and 7.74 as two broadened resonances, attributed to H-5'/6' and H-4'/7'. The H-5 and H-7 resonance at δ_H 8.03 was differentiated by an HMBC correlation between H-5 and C-4. The singlet carbon resonances C-2 and C-2' at δ_C 149.2 and 150.1 respectively, were made by an HMBC correlation between H-4 and C-2 whilst that of C-8a, C-8 and C-4a at δ_C 143.2, 132.2 and 130.5 respectively were assigned using HMBC correlations: H-3 and H-6 to C-4a; H-6 to C-8; and H-4, H-5 and H-7 to C-8a.

Since both H-5'/6' and H-4'/7' coalesce in **5b**, the assignments of the benzimidazole portion of the molecule was made using **5g**, the iodo compound, as an example, where H-4' to H-7' all occurred as separate resonances. In addition, all the carbon resonances, including singlet carbon resonances were seen. This was not the case for other compounds due to tautomeric effects (Nieto et al., 2014). In **5g**, H-4' and H-7' each appeared as doublets more deshielded than the H-5' and H-6' resonances, which were seen as triplets due to each having two adjacent protons. The H-4' and H-7' resonances in this spectrum were differentiated by the NH proton resonance of the benzimidazole moiety having an HMBC correlation to C-7'. C-3'a and C-7'a were identified by their HMBC correlations to H-5' and H-6' respectively.

The H-5 and H-7 resonances for **5a-c** are more shielded for the fluoro derivative, followed by the chloro and then the bromo derivative (**Figure 2-1**). This indicates that the resonance effects of the halogen at C-8 has a greater influence on the chemical shift of these two protons than an inductive effect leading to a build-up of electron density at these positions. The same trend occurs for C-5 and C-7. For the 8-fluoro and 8-chloro derivatives, H-5 is more deshielded than H-7, however, the build-up of electron density at H-7 occurs the least in the 8-bromo derivative, such that H-7 is more deshielded than H-5. In general, the same trends are seen in the 6-halogenated derivatives (**Figure 2-2**), however, there is a notable downfield shift for H-5 going from the 6-fluoro to the 6-iodo derivative. The same effect is observed for H-7, however, not as noticeable as that for H-5.

The ^{1}H and ^{13}C NMR spectra of the fluorinated derivatives contain more splitting, resulting in more complex spectra, since the protons and carbons are also split by the fluorine atoms. These were discussed in an earlier publication (Gopaul and Koorbanally, 2016).

In addition to NMR, the structures of the compounds were confirmed by X-ray crystallography. A crystal structure of **5f** (6-bromo derivative) was solved in the monoclinic space group C 2/c, with eight molecules in the asymmetric unit. The entire molecule is planar. In addition, the NH group is clearly seen in the vicinity of H-7'. An ORTEP diagram of **5k** is provided in **Figure 2-3**.

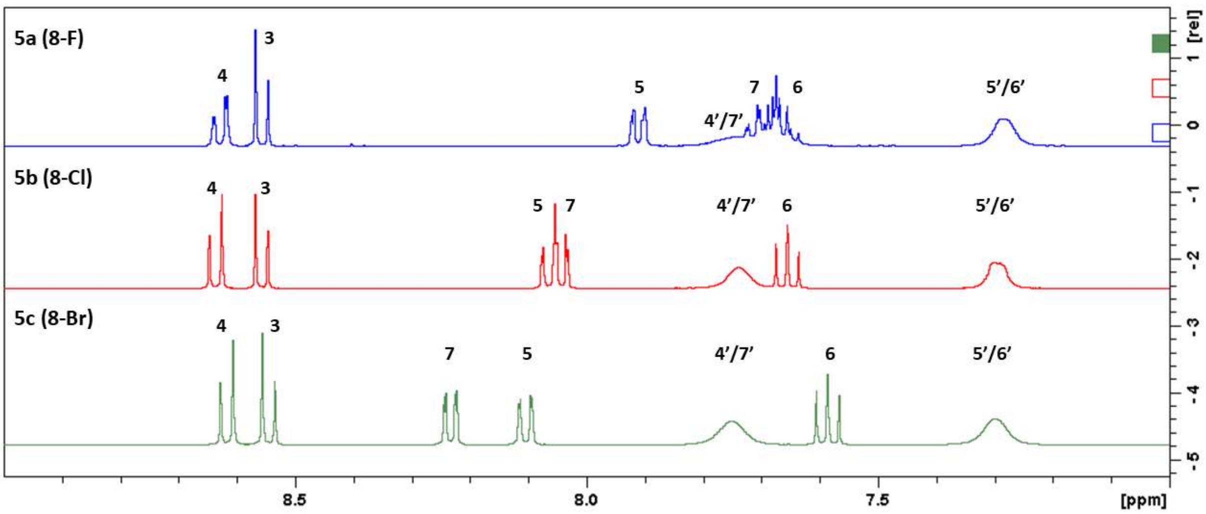

Figure 2-1 Overlay of ^{1}H NMR spectra of 8-substituted derivatives **5a-c** showing differences in NMR shifts of H-5 and H-7

Table 2-1 [1]H NMR data of 2-(1*H*-benzo[*d*]imidazol-2-yl)quinolines **5a-k** (DMSO-*d*6, 400 MHz)

Pos.	**5a**	**5b**	**5c**	**5d**	**5e**	**5f**	**5g**	**5h**	**5i**	**5j**	**5k**
3	8.55 (d, 8.6)	8.56 (d, 8.5)	8.54 (d, 8.6)	8.50 (d, 8.7)	8.51 (d 8.7)	8.50 (d, 8.7)	8.48 (s)	8.48 (d, 8.6)	8.42 (s)	8.45 (d, 8.6)	8.41 (d, 9.1)
4	8.63 (dd, 8.6, 1.4)	8.63 (d, 8.5)	8.62 (d, 8.6)	8.54 (d, 8.7)	8.54 (d 8.7)	8.52 (d, 8.7)	8.48 (s)	8.52 (d, 8.6)	8.42 (s)	8.50 (d, 8.6)	8.44 (d, 9.1)
5	7.91 (dd, 7.6, 1.7)	8.07 (dd, 7.7, 1.1)	8.10 (dd, 7.8, 1.1)	7.89 (dd, 9.3, 2.9)	8.23 (d 2.4)	8.38 (d, 2.2)	8.55 (d, 1.9)	7.63-7.57 (m)	7.47 (d, 2.8)	7.86 (d, 8.0)	7.80 (s)
6	7.67 (ddd, 7.6, 7.6, 2.4)	7.66 (dd, 7.7, 7.7)	7.58 (dd, 7.8, 7.8)	-	-	-	-	7.32-7.30 (m)	-	7.55 (dd, 7.6, 7.6)	-
7	7.70 (ddd, 7.6, 7.6, 1.5)	8.03 (dd, 7.7, 1.1)	8.23 (dd, 7.8, 1.1)	7.77 (ddd, 8.9, 8.9, 2.9)	7.87 (dd 2.4, 9.0)	7.97 (dd, 8.8, 2.2)	8.10 (dd, 8.8, 1.9)	7.63-7.57 (m)	7.50 (dd, 9.1, 2.8)	7.69 (d, 7.0)	7.69 (dd, 8.6, 1.8)
8	-	-	-	8.20 (dd, 9.3, 5.4)	8.15 (d 9.0)	8.07 (d, 8.8)	7.91 (d, 8.8)	-	8.06 (d, 9.1)	-	8.05 (d, 8.6)
4'	7.75 (bs)	7.74 (bs)	7.75 (bs)	7.69 (s)	7.69 (s)	7.69 (s)	7.61 (d, 7.8)	7.73 (d, 6.0)*	7.60 (d, 8.3)**	7.72 (bs)	7.70-7.67 (m)
5'	7.28 (bs)	7.29 (bs)	7.30 (bs)	7.28 (m)	7.28 - 7.27	7.29 - 7.26	7.30 (ddd, 7.0,7.0, 1.2)	7.32-7.30 (m)	7.29-7.22 (m)	7.28 (dd, 5.7, 2.7)	7.26 (dd, 6.0, 1.3)
6'	7.28 (bs)	7.29 (bs)	7.30 (bs)	7.28 (m)	7.28 - 7.27	7.29 - 7.26	7.24 (ddd, 7.0,7.0, 1.2)	7.32-7.30 (m)	7.29-7.22 (m)	7.28 (dd, 5.7, 2.7)	7.26 (dd, 6.0, 1.3)
7'	7.75 (bs)	7.74 (bs)	7.75 (bs)	7.69 (s)	7.69 (s)	7.69 (s)	7.76 (d, 7.9)	7.74 (d, 6.0)*	7.74 (d, 7.48)**	7.72 (bs)	7.70-7.67 (m)
NH	13.11 (s)	12.94 (s)	12.85 (s)	13.20 (s)	13.24 (s)	13.22 (s)	13.21 (s)		13.09 (s)	12.93 (bs)	13.15 (bs)
OCH_3	-	-	-	-	-	-	-	4.07 (s)	3.94 (s)		
CH_3	-	-	-	-	-	-	-			2.93 (s)	2.52 (s)

*,** assignments are interchangeable

Table 2-2 ^{13}C NMR data of 2-(1*H*-benzo[*d*]imidazol-2-yl)quinolines **5a-k** (DMSO-*d*6, 100 MHz)

Pos.	**5a**	**5b**	**5c**	**5d**	**5e**	**5f**	**5g**	**5h**	**5i**	**5j**	**5k**
2	148.9	149.2	150	148.3 (d, 2.6)	149.1	149.2	149.1	146.4	146.3	150.9*	147.8
3	120.2	120.1	120.2	120.0	120.2	120.2	119.9	119.7	119.4	118.7	119.2
4	137.1 (d, 11.8)	138.1	138.3	136.9 (d, 5.3)	136.8	136.6	136.3	137.3	136.0	135.6	136.6
4a	129.7	130.5	129.5	128.8 (d, 10.7)	128.9	129.3	129.8	139.0	129.4	128.0	128.0
5	124.1 (d, 4.5)	129.5	128.3	111.4 (d, 22.0)	126.9	130.2	136.6	128.0	106.0	125.9	126.9
6	127.3 (d, 7.9)	127.5	128.0	160.0 (d, 246.6)	131.5	120.1	93.5	109.4	157.9	127.0	137.0
7	114.6 (d, 18.7)	127.6	134.0	120.5 (d, 25.9)	131.0	133.5	138.8	119.6	122.9	130.2	132.5
8	157.1 (d, 255.7)	132.2	123.7	131.5 (d, 9.5)	130.8	130.8	130.5	155.1	130.2	136.8	128.5
8a	137.4	143.2	144.0	144.3	145.6	145.8	146.1	129.2	143.1	146.1	145.7
2'	150.2	150.1	149.4	150.5	150.3	150.3	150.3	150.3	151.0	147.4*	150.8
3'a	-	-	-	-	-	-	135.2	-	135.1	-	-
4'	-	-	-	122.8	-	-	112.3	115.7	112.1	-	112.5
5'	-	-	-	122.8	-	-	123.7	123.2	123.3	-	122.8
6'	-	-	-	122.8	-	-	122.1	123.2	121.9	-	122.8
7'	-	-	-	122.8	-	-	119.6	115.7	119.3	-	112.5
7'a	-	-	-		-	-	143.9		143.9	-	-
OCH_3	-	-	-	-	-	-	-	55.8	55.6	-	-
CH_3	-	-	-	-	-	-	-	-	-	17.5	21.1

* assignments are interchangeable

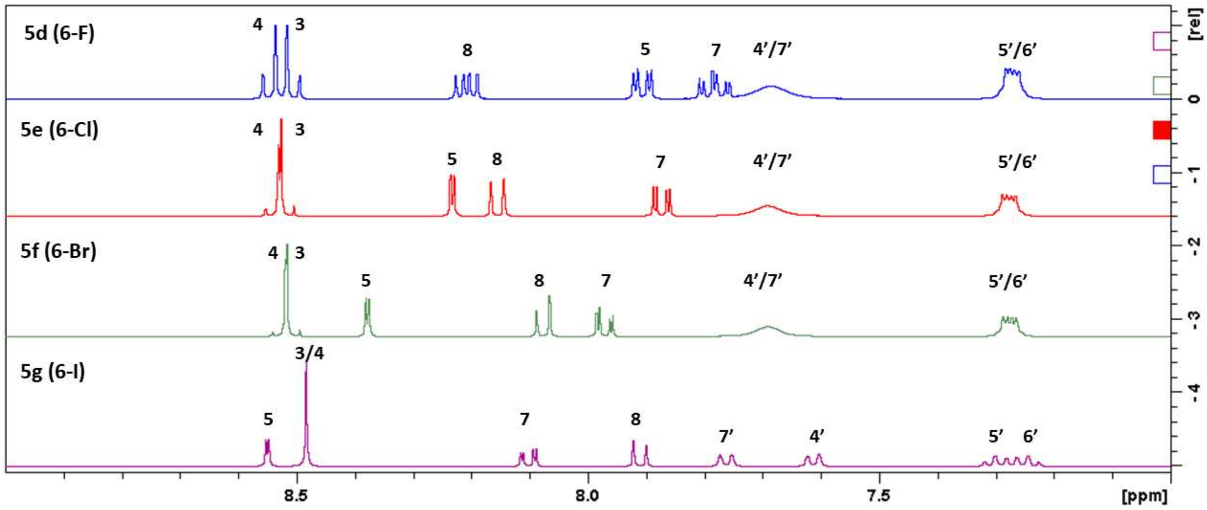

Figure 2-2 Overlay of ^{1}H NMR spectra of 6-substituted derivatives **5d-g** showing differences in NMR shifts of H-5 and H-7

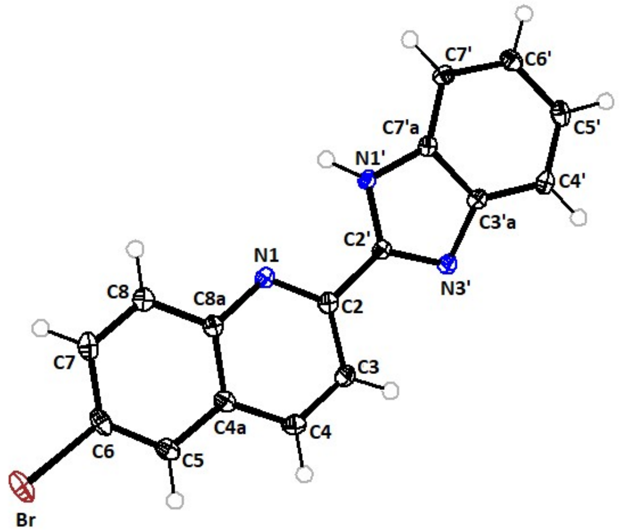

Figure 2-3 Ortep diagram of **5f**

2.4. Conclusion

Both 6- and 8- substituted quinoline-2-benzimidazoles were synthesised by an easy, efficient reaction scheme consisting of synthesising the 2-methylquinoline backbone, oxidising this to either the aldehyde or acid and then condensing this with *o*-phenylenediamine to produce the target compounds. Electron donating methoxy and methyl groups prevented the condensation of *o*-phenylenediamine with the carboxylic acid and hence the target molecules in this instance were synthesised through the carbaldehyde route. The *ortho* position in the molecules was most affected by electron donation leading to a build-up of electron density in the order of F>Cl>Br>I. This was indicated by the *ortho* proton resonance being most shielded for the fluoro derivatives, followed by Cl, then Br and I.

2.5. References

Bruker, *SADABS* and *SAINT*. Madison, Wisconsin, USA, Vol. Bruker AXS Inc., **2009**

Cao, H., Shan, G., Wen, X., Sun, H., Su, Z., Zhong, R., Xie, W., Li, P. and Zhu, D. An orange iridium(III) complex with wide-bandwidth in electroluminescence for fabrication of high-quality white organic light-emitting diodes. J. Mater. Chem. C, **2013**, 1, 7371-7379.

Chandrasekhar, R., Gopalan, B. and Nanjan, M. Synthesis and characterisation of 3-hydroxy-4, 5-dihydro[1,2,3]oxadiazolo [3,4-a]quinolin-10-ium and its fluoro derivative. Int. J. ChemTech Res., **2011**, 3, 1125-1128.

Chen, T.-R. Luminescence and electroluminescence of bis (2-(benzimidazol-2-yl) quinolinato) zinc. Exciplex formation and energy transfer in mixed film of bis (2-(benzimidazol-2-yl)quinolinato) zinc and *N*,*N′*-bis-(1-naphthyl)-*N*,*N′*-diphenyl-1,1′-biphenyl-4,4′-diamine. J. Mol. Struct., **2005**, 737, 35-41.

Cosimelli, B., Taliani, S., Greco, G., Novellino, E., Sala, A., Severi, E., Da Settimo, F., La Motta, C., Pugliesi, I., Antonioli, L., Fornai, M., Colucci, R., Blandizzi, C., Daniele, S., Trincavelli, M. L. and Martini, C. Derivatives of benzimidazol-2-ylquinoline and benzimidazol-2-ylisoquinoline as selective A_1 adenosine receptor antagonists with stimulant activity on human colon motility. ChemMedChem, **2011**, 6, 1909-1918.

Dayan, O., Tercan, M. and Özdemir, N. Syntheses and molecular structures of novel Ru(II) complexes with bidentate benzimidazole based ligands and their catalytic efficiency for oxidation of benzyl alcohol. J. Mol. Struc., **2016**, 1123, 35-43.

Farrugia, L. WinGX and ORTEP for Windows: An update. J. Appl. Crystallogr., **2012**, 45, 849-854.

George, I. R., Lewis, W. and Moody, C. J. Synthesis of iodopyridone. Tetrahedron, **2013**, 69, 8209-8215.

Gong, D.-P., Gao, T.-B., Cao, D.-K. and Ward, M. D. Cyclometalated Ir(III) complexes containing quinoline-benzimidazole-based *N*,*N* ancillary ligands: Structural and luminescence modulation by varying the substituent groups or the protonation/deprotonation state of imidazole units. Dalton Trans., **2017**, 46, 275-286.

Gopaul, K. and Koorbanally, N. A. Synthesis and structure elucidation of a series of chloroquinoline-2-chalcones by the Doebner-Miller reaction. Magn. Reson. Chem., **2016**, 54, 677-683.

Govindan, T. K. Heterocyclic compounds. Proc. Indian Acad. Sci. - Sect. A, **1956**, 44, 123-125.

Hisano, T. and Ichikawa, M. Acidic properties of benzimidazoles and substituents effects. I. correlation between acid dissociations and hydrogen bondings of some benzimidazoles. Chem. Pharm. Bull., **1974**, 22, 1923-1927.

Hisano, T., Ichikawa, M., Tsumoto, K. and Tasaki, M. Synthesis of benzoxazoles, benzothiazoles and benzimidazoles and evaluation of their antifungal, insecticidal and herbicidal activities. Chem. Pharm. Bull., **1982**, 30, 2996-3004.

Hu, J., Li, J., Qi, J. and Chen, J. Highly selective and effective mercury(II) fluorescent sensors. New J. Chem., **2015**, 39, 843-848.

Li, G., Zhang, D., Liu, G. and Pu, S. A highly selective fluorescent probe for Cd^{2+} and Zn^{2+} based on a new diarylethene with quinoline-benzimidazole conjugated system. Tetrahedron Lett., **2016**, 57, 5205-5210.

Li, L., Zhang, X., Zhang, W., Li, W., Sun, W.-H. and Redshaw, C. Zinc 2-((2-(benzoimidazol-2-yl)quinolin-8-ylimino)methyl)phenolates: Synthesis, characterization and photoluminescence behavior. Spectrochim. Acta A, **2014**, 118, 1047-1055.

Li, S., Zhang, B. and Kühn, F. E. Benzimidazolic complexes of methyltrioxorhenium(VII): Synthesis and application in catalytic olefin epoxidation. J. Organomet. Chem., **2013**, 730, 132-136.

Mamedov, V. A., Kadyrova, S. F., Zhukova, N. A., Galimullina, V. R., Polyancev, F. M. and Latypov, S. K. Friedländer reaction/quinoxalinone-benzimidazole rearrangement sequence: Expeditious entry to diverse quinoline derivatives with the benzimidazole moieties. Tetrahedron, **2014**, 70, 5934-5946.

Mamedov, V. A., Saifina, D. F., Gubaidullin, A. T., Ganieva, V. R., Kadyrova, S. F., Rakov, D. V., Rizvanov, I. D. K. and Sinyashin, O. G. Acid-catalyzed rearrangement of 3-(*β*-2-aminostyryl)quinoxalin-2(1*H*)ones-A new and efficient method for the synthesis of 2-benzimidazol-2-ylquinolines. Tetrahedron Lett., **2010**, 51, 6503-6506.

Nguyen, T. B., Ermolenko, L. and Al-Mourabit, A. Iron sulfide catalyzed redox/condensation cascade reaction between 2-amino/hydroxy nitrobenzenes and activated methyl groups: A straightforward atom economical approach to 2-hetaryl-benzimidazoles and benzoxazoles. J. Am. Chem. Soc., **2013**, 135, 118-121.

Nieto, C. I., Cabildo, P., García, M. Á., Claramunt, R. M., Alkorta, I. and Elguero, J. An experimental and theoretical NMR study of NH-benzimidazoles in solution and in the solid state: Proton transfer and tautomerism. Beilstein J. Org. Chem., **2014**, 10, 1620-1629.

Sheldrick, G. A short history of SHELX. Acta Crystallogr. A, **2008**, 64, 112-122.

Sinha, S., Berdichevsky, E. K. and Warren, J. J. Electrocatalytic CO_2 reduction using rhenium(I) complexes with modified 2-(2′-pyridyl)imidazole ligands. Inorg. Chim. Acta, **2017**, 460, 63-68.

Tynebor, R. and Millings, E. Novel method of synthesizing various five membered heterocycles from an aryl tribromomethyl group. Synth. Commun., **2013**, 43, 1902-1908.

Wang, K., Shen, M. and Sun, W.-H. Synthesis, characterization and ethylene oligomerization of nickel complexes bearing *N*-(2-(1*H*-benzo[*d*]imidazol-2-yl)quinolin-8-yl)benzamide derivatives. Dalton Trans., **2009**, 4085-4095.

Yaragorla, S. and Vijaya Babu, P. Oxidative C_{sp3}-H functionalization of 2-methylazaarenes: A practical synthesis of 2-azaarenyl-benzimidazoles and benzothiazoles. Tetrahedron Lett., **2017**, 58, 1879-1882.

Yeh, A. Synthesis and electroluminescent property of bis (2-(benzimidazol-2-yl)quinolinato) zinc. Mater. Lett., **2005**, 59, 1811-1814.

Chapter 3. Synthesis and antibacterial activity of a series of quinoxaline-chalcone-quinoline hybrids

Abstract

A small library of nine quinoxaline-chalcones and nine quinoxaline-chalcone-quinoline hybrids were synthesised and converted to their respective pyrazoline derivatives using hydrazine hydrate. These molecules were synthesised from a quinoxaline acetophenone derivative and various 2- or 4- substituted benzaldehydes and 6- or 8- substituted quinoline-2-carbaldehydes *via* the Claisen-Schmidt condensation. The compounds were characterised using ^{1}H and ^{13}C NMR spectroscopy using 2D NMR spectroscopy. All synthesised compounds were tested for their antibacterial activity against two Gram +ve species, *Staphylococcus aureus* and MRSA and four Gram -ve bacteria, *Pseudomonas aeruginosa*, *Klebsiella pneumoniae*, *Escherichia coli* and *Salmonella typhimurium*. The synthesised compounds showed activity against the Gram +ve *S. aureus* and MRSA and not against the Gram -ve species. The activity against *S. aureus* was much higher than that for MRSA. Quinoxaline chalcones showed no activity against the bacteria tested against, however, when a quinoline moiety replaced the aromatic ring, eight derivatives showed enhanced antibacterial activity, having MBC values between 0.151-0.360 μM against *S. aureus* and 10.9-618 μM against MRSA. The quinoxaline-chalcone-quinoline hybrids showed antibacterial activity two orders of magnitude better than ciprofloxacin and levofloxacin against *S. aureus* and comparable activity to these standards against MRSA. Interestingly, the 4'-Br and 4'-Cl pyrazoline derivatives of the quinoxaline chalcones (having MBC values of 11 and 12 μM, respectively) showed comparable activity to levofloxacin and ciprofloxacin.

Keywords: quinolines; quinoxalines; chalcones; molecular hybrids; antibacterial activity

3.1. Introduction

Hybrid molecules are chemical compounds in which two or more scaffolds are joined together in a single molecule. This offers a new and exciting approach to drug discovery, since the new molecule may have the combined effects of the respective scaffolds. Quinoxaline chalcones are an example of these hybrid molecules, consisting of a quinoxaline scaffold linked *via* a highly reactive *α,β*-unsaturated ketone to an aromatic ring. Both quinoxalines and chalcones are well known pharmacophores showing an array of biological activities (Batovska and Todorova, 2010), including antibacterial (Zhang et al., 2017), antifungal (Zhang et al., 2014), anticancer (El Newahie et al., 2016), antiviral (Shibinskaya et al., 2010), anti-inflammatory (Ismail et al., 2005), and antimalarial (van Heerden et al., 2012) activities. In addition, the oxygenated quinoxaline chalcone quinocetone is a commercially available feedstock additive used as both a growth promoter and antibacterial agent (Carta et al., 2005).

Several quinoxaline chalcones with hydroxy, methoxy, nitro, chloro and *N*-dimethyl groups have previously been synthesised and showed little antibacterial activity, but when converted to *N*-oxides, their antibacterial activity increased dramatically (Zhang et al., 2017). However, the study lacked a systematic approach to electron withdrawing halogen substitution and electron donating methyl and methoxy substitution. In the same study, the authors replaced the aromatic ring with a furan ring (Zhang et al., 2017). To the best of our knowledge no other scaffold was combined with a quinoxaline by an *α,β*-unsaturated linker. There are reports in literature of *α,β*-unsaturated moieties being converted to pyrazolines, which enhanced antibacterial activity (Desai et al., 2013; Kendre and Baseer, 2013). A quinocetone derivative was also reported to have been converted to the pyrazoline moiety using hydrazine hydrate or phenylhydrazine (Fadda et al., 2011).

The quinoline moiety was identified as an excellent candidate to replace the aromatic ring at the alkene end of the *α,β*-unsaturated fragment as methyl quinolines could easily be converted to aldehydes (Gopaul and Koorbanally, 2016), a functional group needed to join a scaffold to the alkene end. Furthermore, quinoline chalcone hybrids have proven to be promising lead compounds possessing a wide array of biological activities such as antimalarial (Gutteridge et al., 2006), antileishmanial (Gopinath et al., 2014), antibacterial (Desai et al., 2012), antifungal (Ashok et al., 2016) and anticancer (Tseng et al., 2013) activities. The synthesis of organic hybrid molecules containing both the quinoxaline and quinoline scaffolds is a novel approach, which does not appear in the literature.

3.2. Experimental

Chemistry

General Procedures

Reagents used in the synthesis were reagent grade. Selenium dioxide was purchased from Merck, South Africa. Crotonaldehyde was purchased from B&M Scientific, South Africa. All other reagents were purchased from Sigma Aldrich, South Africa. Solvents used in the synthesis were distilled prior to being used. Merck Kieselgel 60 F_{254} plates were used for thin layer chromatography (TLC). Where required, column chromatography was carried out using silica gel (60–120 mesh) as the stationary phase and varying ratios of organic solvents as the mobile phase depending on the compound to be purified. Infrared (IR) spectra were collected on a Perkin Elmer Spectrum 100 FT-IR spectrometer with universal attenuated total reflectance sampling accessory. Ultraviolet (UV) spectra were recorded on a Shimadzu UV-3600 spectrophotometer in dichloromethane (DCM) as the samples were not soluble in methanol (MeOH). Melting points were determined in a sealed capillary tube in an Electrothermal IA9100 instrument. High resolution mass spectrometry (HRMS) was conducted using a

Waters Micromax LCT Premier TOF-MS instrument, operating at ambient temperature. ^{1}H and ^{13}C NMR spectra were recorded using a Bruker Avance 400 MHz NMR spectrometer (9.4 T; Bruker, Germany) (400.22 MHz for ^{1}H and 100.63 MHz for ^{13}C) at 298 K. Chemical shifts (δ) are reported in ppm and coupling constants (J) in Hz. Chemical shifts were referenced to the solvent peak of chloroform at δ 7.24 and 77.0 for ^{1}H and ^{13}C NMR, respectively. NMR data was analysed using Bruker TopSpin 3.5 software.

Preparation of quinoline-2-carbaldehydes

Substituted anilines (**1a-i**) (45.0 mmol) were dissolved in HCl:water (1:2) and heated to 60 °C. Crotonaldehyde (**2**) (67.5 mmol; 5.6 mL) dissolved in toluene (20 mL) was added slowly to the aniline mixture and heated under reflux for 4 hours. The aqueous layer was then separated from the biphasic mixture and the pH adjusted to 8. The solution was then extracted with 3 × 50 mL portions of ethyl acetate (EtOAc), dried over anhydrous $MgSO_4$ and the solvent removed under reduced pressure. The resultant residue was dissolved in 1,4-dioxane (20 mL) to which SeO_2 (45.4 mmol; 5.0 g) was added and the resulting suspension refluxed for 15 to 180 minutes depending on the substituent and the reaction monitored by TLC. Upon completion, the mixture was filtered, diluted with water (40 mL) and the contents extracted with 3 × 50 mL portions of EtOAc. The combined extract was washed with 2 × 50 mL portions of water, dried using anhydrous $MgSO_4$ and the solvent removed under vacuum. The residues were purified by column chromatography (hexane:ethyl acetate, 85:15 v/v) to yield the carbaldehydes (**3a-i**) in yields of between 70-90% depending on the substituent.

Preparation of 1-(3-methylquinoxalin-2-yl)ethanone

Acetylacetone (**5**) (20.0 mL, 0.20 mol) and *N*-bromosuccinamide (42.0 g, 0.24 mol) were stirred in 150 mL water at 70 °C until clear (~20 minutes). Thereafter *o*-phenylenediamine (**4**)

(21.6 g, 0.20 mol) was added and the mixture refluxed for an hour. The reaction mixture was extracted with EtOAc (3 × 100 mL) and the organic layers combined before being washed with water and saturated brine. The extracts were then dried over anhydrous Na_2SO_4, the solvent removed *in vacuo* and the residue purified by column chromatography (hexane: EtOAc, 85:15 v/v) to yield **6** in a yield of 64%.

Preparation of (E)-1-(3-methylquinoxalin-2-yl)-3-(quinolin-2-yl)prop-2-en-1-ones and (E)-1-(3-methylquinoxalin-2-yl)-3-phenylprop-2-en-1-ones

1-(3-Methylquinoxalin-2-yl)ethanone (**6**) (150 mg, 0.806 mmol) was dissolved in ethanol (EtOH), to which 5 drops of 40% NaOH and quinoline aldehyde (**3a-i**) or benzaldehyde (**9a-i**) (0.806 mmol) added. The reaction was allowed to proceed until the chalcone precipitated out of solution. In cases where precipitate did not form, ice water (10 mL) was added and the reaction mixture stirred at 0 °C until a precipitate formed. The products were collected under filtration and recrystallized in 15 mL DCM:EtOH (2:1 v/v) yielding compounds **7a-i** and **10a-i** respectively.

(*E*)*-3-(8-fluoroquinolin-2-yl)-1-(3-methylquinoxalin-2-yl)prop-2-en-1-one* (**7a**), Yield: 47%; pale yellow powder, mp 178 °C; IR (neat) υ_{max} 1671 cm^{-1} (C=O); λ_{max} (log ε) = 335 (4.34); ^{1}H NMR ($CDCl_3$, 400 MHz) δ 8.47 (1H, d, J = 16.1 Hz, H-12), 8.24 (1H, dd, J = 8.6, 1.0 Hz, H- 4'), 8.20 (1H, dd, J = 8.4, 1.1 Hz, H-5*), 8.07 (1H, dd, J = 8.2, 1.1 Hz, H-8*), 8.04 (1H, d, J = 16.1 Hz, H-11), 7.86 (1H, d, J = 8.6 Hz, H-3'), 7.84 (1H, td, J = 8.2, 1.5 Hz, H-6$^\#$), 7.77 (1H, td, J = 8.3, 1.3 Hz, H-7$^\#$), 7.61 (1H, d, J = 8.2 Hz, H-5'), 7.50 (1H, td, J = 7.9, 4.9 Hz, H-6'), 7.42 (1H, ddd, J = 8.9, 7.6, 1.0 Hz, H-7'), 3.00 (3H, s, H-9); ^{13}C NMR ($CDCl_3$, 100 MHz) δ 191.2 (C=O, C-10), 158.3 (C, d, J = 258.7 Hz, C-8'), 154.0 (C, C-2'), 153.6 (C, C-2), 148.1 (CH, C-3), 144.4 (CH, C-11), 142.6 (C, C- 4a$^\$$), 139.8 (C, C-8a$^\$$), 138.8 (C, d, J = 12.4

Hz, C-8'a), 136.6 (CH, d, J = 2.9 Hz,C-4'), 132.0 (CH, C-6$^{\#}$), 129.9 (CH, C-5*), 129.72 (CH, C-7$^{\#}$), 129.67 (C, C-4'a), 129.5 (CH, C-3'), 129.1 (CH, C-12), 128.6 (CH, C-8*), 127.4 (CH, d, J = 8.1 Hz, C-6'), 123.0 (CH, d, J = 4.8 Hz, C-5'), 114.2 (CH, d, J = 19.1 Hz, C-7'), 24.0 (CH_3, C-9); HRMS (*pos*) *m/z* 344.1196 [M+H] (calcd. for $C_{21}H_{15}FN_3O$ 344.1199).

*, $^{\#}$, $^{\$}$ indicates assignments are interchangeable

(E)-3-(8-chloroquinolin-2-yl)-1-(3-methylquinoxalin-2-yl)prop-2-en-1-one (**7b**), Yield: 95%; pale yellow powder, mp 188 °C; IR (neat) υ_{max} 1669 cm^{-1} (C=O); λ_{max} (log ε) = 338 (4.30); ^{1}H NMR ($CDCl_3$, 400 MHz) δ 8.56 (1H, d, J = 16.0 Hz, H-12), 8.23 (2H, d, J = 8.6 Hz, H-5*), 8.20 (1H, d, J = 8.8 Hz, H-4'), 8.08 (1H, d, J = 6.5 Hz, H-8*), 8.05 (1H, d, J = 16.0 Hz, H-11), 7.86-7.83 (3H, m, H-5'/6/7), 7.79 (1H, d, J = 7.5 Hz, H-3'), 7.75 (1H, d, J = 8.4 Hz, H-7'), 7.47 (1H, dd, J = 7.8, 7.8 Hz, H-6'), 3.01 (3H, s, H-9); ^{13}C NMR ($CDCl_3$, 100 MHz) δ 191.1 (C=O, C-10), 154.3 (C, C-2'), 153.6 (C, C-2), 148.2 (C, C-3), 144.6 (C, C-8'a), 144.3 (CH, C-11), 142.5 (C, C-4a$^{\$}$), 139.8 (C, C-8a$^{\$}$), 137.3 (CH, C-4'), 134.3 (C, C-4'a), 132.1 (CH, C-6$^{\#}$), 130.3 (CH, C-7$^{\#}$), 129.9 (CH, C-3'), 129.8 (CH, C-5*), 129.5 (C, C-8'), 129.1(CH, C-12), 128.5 (CH, C-8*), 127.4 (CH, C-6'), 126.7 (CH, C-7'), 121.6 (CH, C-5'), 24.0 (CH_3, C-9); HRMS (*pos*) *m/z* 360.0900 [M+H] (calcd. for $C_{21}H_{15}ClN_3O$ 360.0904).

*, $^{\#}$, $^{\$}$ indicates assignments are interchangeable

(E)-3-(8-bromoquinolin-2-yl)-1-(3-methylquinoxalin-2-yl)prop-2-en-1-one (**7c**), Yield: 40%; yellow powder, mp 179 °C; IR (neat) υ_{max} 1669 cm^{-1} (C=O); λ_{max} (log ε) = 341 (4.32); ^{1}H NMR ($CDCl_3$, 400 MHz) δ 8.60 (1H, d, J = 16.0 Hz, H-12), 8.19 (2H, d, J = 8.4 Hz, H-4'/5*), 8.08-8.05 (2H, m, H-5'/8*), 8.04 (1H, d, J = 16.0 Hz, H-11), 7.84 (1H, td, J = 8.5, 1.3 Hz, H-6$^{\#}$), 7.80 (1H, d, J = 8.4 Hz, H-3'), 7.78 (2H, m, H-7'/7$^{\#}$), 7.39 (1H, t, J = 7.8 Hz, H-6'), 3.01 (3H, s, H-9); ^{13}C NMR ($CDCl_3$, 100 MHz) δ 191.1 (C=O, C-10), 154.4 (C, C-2'), 153.6 (C, C-2), 148.2 (C, C-3), 145.4 (C, C-8'a), 144.1 (CH, C-11), 142.4 (C, C-4a$^{\$}$), 139.8 (C, C-8a$^{\$}$), 137.4 (CH, C-4'), 133.8 (CH, C-5'), 132.1 (CH, C-6$^{\#}$), 130.0 (CH, C-5*), 129.8 (CH, C-

7$^{\#}$), 129.4 (C, C-4'a), 129.1 (CH, C-12), 128.4 (CH, C-8*), 127.8 (CH, C-6'), 127.4 (CH, C-7'), 125.7 (C, C-8'), 121.8 (CH, C-3'), 24.0 (CH_3, C-9); HRMS (*pos*) *m*/*z* 404.0390 [M+H] (calcd. for $C_{21}H_{15}BrN_3O$ 404.0398).

*, $^{\#}$, $^{\$}$ indicates assignments are interchangeable

(E)-3-(8-methylquinolin-2-yl)-1-(3-methylquinoxalin-2-yl)prop-2-en-1-one (**7d**), Yield: 83%; pale yellow powder, mp 159 °C; IR (neat) υ_{max} 1670 cm^{-1} (C=O); λ_{max} (log ε) = 343 (4.43); ^{1}H NMR ($CDCl_3$, 400 MHz) δ 8.49 (1H, d, J = 16.0 Hz, H-12), 8.19 (1H, dd, J = 8.1, 1.2 Hz, H-5*), 8.15 (1H, d, J = 8.4 Hz, H-4'), 8.07 (1H, dd, J = 8.5, 1.0 Hz, H-8*), 8.02 (1H, d, J = 16.0 Hz, H-11), 7.84 (1H, td, J = 8.4, 1.4 Hz, H-6$^{\#}$), 7.77 (1H, td, J = 8.2, 1.3 Hz, H-7$^{\#}$), 7.74 (1H, d, J = 8.4 Hz, H-3'), 7.64 (1H, d, J = 8.1 Hz, H-5'), 7.56 (1H, d, J = 6.9 Hz, H-7'), 7.44 (1H, dd, J = 7.6, 7.6 Hz, H-6'), 3.00 (3H, s, H-9), 2.85 (3H, s, C$\underline{H}_3$); ^{13}C NMR ($CDCl_3$, 100 MHz) δ 191.5 (C=O, C-10), 153.6 (C, C-2), 152.2 (C, C-2'), 148.5 (C, C-3), 147.4 (C, C-8'a), 145.4 (CH, C-11), 142.5 (C, C-4a$^{\$}$), 139.8 (C, C-8a$^{\$}$), 138.2 (C, C-8'), 136.9 (CH, C-4'), 131.9 (CH, C-6$^{\#}$), 130.1 (CH, C-7'), 129.9 (CH, C-5*), 129.7 (CH, C-7$^{\#}$), 128.5 (CH, C-8*), 128.2 (C, C-4'a), 127.9 (CH, C-12), 127.4 (CH, C-6'), 125.5 (CH, C-5'), 120.7 (CH, C-3'), 24.0 (CH_3, C-9), 17.8 (C$\underline{H}_3$); HRMS (*pos*) *m*/*z* 362.1627 [M+Na] (calcd. for $C_{22}H_{17}N_3ONa$ 362.1269)

*, $^{\#}$, $^{\$}$ indicates assignments are interchangeable

(E)-3-(6-fluoroquinolin-2-yl)-1-(3-methylquinoxalin-2-yl)prop-2-en-1-one (**7e**), yield: 90%; off-white powder, mp 179 °C; IR (neat) υ_{max} 1670 cm^{-1} (C=O); λ_{max} (log ε) = 339 (4.41); ^{1}H NMR ($CDCl_3$, 400 MHz) δ 8.51 (1H, d, J = 16.1 Hz, H-12), 8.22-8.17 (2H, m, H-5*/8'), 8.18 (1H, d, J = 8.9 Hz, H-4'), 8.07 (1H, dd, J = 8.1, 1.4 Hz, H-8*), 8.01 (1H, d, J = 16.1 Hz, H-11), 7.84 (1H, td, J = 6.8, 1.4 Hz, H-6$^{\#}$), 7.81 (1H, d, J = 9.1 Hz, H-3'), 7.78 (1H, td, J = 7.1, 1.3 Hz, H-7$^{\#}$), 7.52 (1H, td, J = 8.9, 2.7 Hz, H-7'), 7.45 (1H, dd, J = 8.7, 2.8 Hz, H-5'), 3.01 (1H, s, H-9); ^{13}C NMR ($CDCl_3$, 100 MHz) δ 191.1 (C=O, C-10), 161.1 (C, d, J = 244.6 Hz, C-

6'), 153.6 (C, C-2), 153.1 (C, C-2'), 148.1 (C, C-3), 144.3 (CH, C-11), 142.6 (C, C-4a$^{\$}$), 139.8 (C, C-8a$^{\$}$), 139.7 (C, C-8'a), 136.1 (CH, d, J = 5.8 Hz, C-4'), 132.6 (CH, d, J = 9.1 Hz, C-8'), 132.0 (CH, C-6$^{\#}$), 129.9 (CH, C-7$^{\#}$), 129.7 (CH, C-5*), 128.9 (C, d, J = 10.9 Hz, C-4'a), 128.6 (CH, C-8*), 128.3 (CH, C-12), 121.6 (CH, C-3'), 120.5 (CH, d, J = 26.0 Hz, C-7'), 110.7 (CH, d, J = 21.8 Hz, C-5'), 24.1 (CH_3, C-9); HRMS (*pos*) *m/z* 344.1201 [M+H] (calcd. for $C_{21}H_{15}FN_3O$ 344.1199)

*, $^{\#}$, $^{\$}$ indicates assignments are interchangeable

(E)-3-(6-chloroquinolin-2-yl)-1-(3-methylquinoxalin-2-yl)prop-2-en-1-one (**7f**); yield: 88%; off-white powder, mp 187 °C; IR (neat) υ_{max} 1671 cm^{-1} (C=O); λ_{max} (log ε) = 344 (4.45); ^{1}H NMR ($CDCl_3$, 400 MHz) δ 8.51 (1H, d, J = 16.0 Hz, H-12), 8.20 (1H, dd, J = 8.6, 1.5 Hz, H-5*), 8.12 (1H, d, J = 8.6 Hz, H-4'), 8.07 (2H, d, J = 9.0 Hz, H-8*/8'), 7.98 (1H, d, J = 16.0 Hz, H-11), 7.84 (1H, td, J = 7.6, 1.3 Hz, H-6$^{\#}$), 7.81 (1H, d, J = 2.3 Hz, H-5'), 7.81-7.75 (1H, m, H-7$^{\#}$), 7.80 (1H, d, J = 8.6 Hz, H-3'), 7.67 (1H, dd, J = 9.0, 2.3 Hz, H-7'), 3.01 (1H, s, H-9); ^{13}C NMR ($CDCl_3$, 100 MHz) δ 191.1 (C=O, C-10), 153.9 (C, C-2'), 153.7 (C, C-2), 148.1 (C, C-3), 146.8 (C, C-8'a), 144.1 (CH, C-11), 142.6 (C, C-4a$^{\$}$), 139.8 (C, C-8a$^{\$}$), 135.8 (CH, C-4'), 133.4 (C, C-6'), 132.1 (CH, C-6$^{\#}$), 131.6 (CH, C-8'), 131.1 (CH, C-7'), 129.9 (CH, C-5*), 129.7 (CH, C-7$^{\#}$), 128.7 (C, C-4'a), 128.6 (CH, C-8*), 128.6 (CH, C-12), 126.3 (CH, C-5'), 121.8 (CH, C-3'), 24.1 (CH_3, C-9); HRMS (*pos*) *m/z* 360.0900 [M+H] (calcd. for $C_{21}H_{15}ClN_3O$ 360.0904)

*, $^{\#}$, $^{\$}$ indicates assignments are interchangeable

(E)-3-(6-bromoquinolin-2-yl)-1-(3-methylquinoxalin-2-yl)prop-2-en-1-one (**7g**), Yield: 63%; off-white powder, mp 184 °C; IR (neat) υ_{max} 1673 cm^{-1} (C=O); λ_{max} (log ε) = 325 (4.21); ^{1}H NMR ($CDCl_3$, 400 MHz) δ 8.52 (1H, d, J = 16.0 Hz, H-12), 8.20 (1H, dd, J = 8.5, 1.0 Hz, H-5*), 8.12 (1H, d, J = 8.5 Hz, H-4'), 8.07 (1H, dd, J = 8.6, 1.4 Hz, H-8*), 8.00 (1H, d, J = 8.2 Hz, H-8'), 7.97 (1H, d, J = 16.1 Hz, H-11), 7.97 (1H, d, J = 2.2 Hz, H-5'), 7.85 (1H, td, J = 7.6,

1.5 Hz, H-6$^{\#}$), 7.81-7.75 (2H, m, H-7$^{\#}$/7'), 7.81 (1H, d, J = 8.5 Hz, H-3'), 3.01 (1H, s, H-9); ^{13}C NMR ($CDCl_3$, 100 MHz) δ 191.0 (C=O, C-10), 154.0 (C, C-2'), 153.7 (C, C-2), 148.1 (C, C-3), 147.0 (C, C-8'a), 144.1 (CH, C-11), 142.6 (C, C-4a$^{\$}$), 139.8 (C, C-8a$^{\$}$), 135.8 (CH, C-4'), 133.7 (CH, C-7'), 132.1(CH, C-6$^{\#}$), 131.6 (CH, C-5'), 129.9 (CH, C-5*), 129.7 (CH, C-7$^{\#}$), 129.6 (CH, C-8'), 129.2 (C, C-4'a), 128.7 (CH, C-12), 128.6 (CH, C-8*), 121.8 (CH, C-3'), 121.6 (C, C-6'), 24.1 (CH_3, C-9); HRMS (*pos*) *m*/*z* 404.0398 [M+H] (calcd. for $C_{21}H_{15}FN_3O$ 404.0398)

*, $^{\#}$, $^{\$}$ indicates assignments are interchangeable

(E)-3-(6-methylquinolin-2-yl)-1-(3-methylquinoxalin-2-yl)prop-2-en-1-one (**7h**), Yield: 80%; pale yellow fibrous solid, mp 161 °C; IR (neat) υ_{max} 1669 cm^{-1} (C=O); λ_{max} (log ε) = 345 (4.36); ^{1}H NMR ($CDCl_3$, 400 MHz) δ 8.42 (1H, d, J = 16.1 Hz, H-12), 8.19 (1H, dd, J = 8.3, 1.2 Hz, H-5*), 8.10 (1H, d, J = 8.5 Hz, H-4'), 8.06 (1H, dd, J = 8.4, 1.1 Hz, H-8*), 8.01 (1H, d, J = 9.9 Hz, H-8'), 7.98 (1H, d, J = 16.2 Hz, H-11), 7.83 (1H, td, J = 8.2, 1.3 Hz, H-6$^{\#}$), 7.76 (1H, td, J = 8.2, 1.4 Hz, H-7$^{\#}$), 7.74 (1H, d, J = 8.4 Hz, H-3'), 7.56 (1H, dd, J = 7.9, 1.8 Hz, H-7'), 7.54 (1H, d, J = 1.8, Hz, H-5'), 2.99 (3H, s, H-9), 2.53 (3H, s, C<u>H</u>$_3$); ^{13}C NMR ($CDCl_3$, 100 MHz) δ 191.4 (C=O, C-10), 153.5 (C, C-2), 152.7 (C, C-2'), 148.4 (C, C-3), 147.1 (C, C-8'a), 145.1 (CH, C-11), 142.5 (C, C-4a$^{\$}$), 139.8 (C, C-8a$^{\$}$), 137.8 (C, C-6'), 136.0 (CH, C-4'), 132.5 (CH, C-7'), 131.9 (CH, C-6$^{\#}$), 129.9 (CH, C-5*), 129.7 (CH, C-7$^{\#}$), 129.6 (CH, C-8'), 128.5 (CH, C-8*), 128.3 (C, C-4'a), 127.9 (CH, C-12), 126.4 (CH, C-5'), 120.9 (C, C-3'), 24.0 (CH_3, C-9), 21.7 (<u>C</u>H$_3$); HRMS (*pos*) *m*/*z* 362.1627 [M+Na] (calcd. for $C_{22}H_{17}N_3ONa$ 362.1269)

*, $^{\#}$, $^{\$}$ indicates assignments are interchangeable

(E)-3-(6-methoxyquinolin-2-yl)-1-(3-methylquinoxalin-2-yl)prop-2-en-1-one (**7i**), Yield: 57%; yellow powder, mp 162 °C; IR (neat) υ_{max} 1670 cm^{-1} (C=O); λ_{max} (log ε) = 361 (4.39); ^{1}H NMR ($CDCl_3$, 400 MHz) δ 8.39 (1H, d, J = 16.0 Hz, H-12), 8.20 (1H, dd, J = 8.2, 1.3 Hz, H-5*), 8.09 (1H, d, J = 8.5 Hz, H-4'), 8.06 (1H, dd, J = 9.6, 1.5 Hz, H-8*), 8.02 (1H, d, J = 9.2

Hz, H-8'), 7.97 (1H, d, J = 16.0 Hz, H-11), 7.84 (1H, td, J = 7.8, 1.4 Hz, H-6$^{\#}$), 7.77 (1H, td, J = 7.0, 1.4 Hz, H-7$^{\#}$), 7.74 (1H, d, J = 8.4 Hz, H-3'), 7.38 (1H, dd, J = 9.3, 2.8 Hz, H-7'), 7.07 (1H, d, J = 2.8, Hz, H-5'), 3.94 (3H, s, OC<u>H</u>$_3$), 3.00 (3H, s, H-9); ^{13}C NMR ($CDCl_3$, 100 MHz) δ 191.5 (C=O, C-10), 158.8 (C, C-6'), 153.5 (C, C-2), 151.2 (C, C-2'), 148.6 (C, C-3), 145.2 (CH, C-11), 144.6 (C, C-8'a), 142.5 (C, C-4a$^{\$}$), 139.8 (CH, C-8a$^{\$}$), 135.3 (CH, C-4'), 131.9 (CH, C-6$^{\#}$), 131.5 (CH, C-8'), 129.9 (CH, C-7$^{\#}$), 129.7 (CH, C-5*), 129.5 (C, C-4'a), 128.5 (CH, C-8*), 127.3 (CH, C-12), 123.1 (CH, C-7'), 121.3 (CH, C-3'), 105.0 (C, C-5'), 55.6 (O<u>C</u>H$_3$), 24.0 (CH_3, C-9); HRMS (*pos*) *m/z* 356.1395 [M+H] (calcd. for $C_{22}H_{18}N_3O_2$ 356.1399)

*, $^{\#}$, $^{\$}$ indicates assignments are interchangeable

(E)-3-(2-fluorophenyl)-1-(3-methylquinoxalin-2-yl)prop-2-en-1-one (**10a**), Yield: 98%; pale yellow solid; mp 163 °C; IR (neat) υ_{max} 1670 cm^{-1} (C=O); λ_{max} (log ε) = 324 (4.50); ^{1}H NMR ($CDCl_3$, 400 MHz) δ 8.15 (1H, dd, J = 8.3, 1.2 Hz, H-5*), 8.10 (1H, d, J = 16.3 Hz, H-11), 8.04 (1H, dd, J = 8.5, 1.1 Hz, H-8*), 7.99 (1H, d, J = 16.3 Hz, H-12), 7.82 (1H, td, J = 8.2, 1.4 Hz, H-6$^{\#}$), 7.75 (1H, td, J = 8.3, 1.4 Hz, H-7$^{\#}$), 7.73 (1H, td, J = 8.1, 1.6 Hz, H-6'), 7.41-7.35 (1H, m, H-4'), 7.19 (1H, d, J = 7.3 Hz, H-5'), 7.14-7.09 (1H, m, H-3'), 2.99 (3H, s, H-9); ^{13}C NMR ($CDCl_3$, 100 MHz) δ 190.9 (C=O, C-10), 161.8 (C, d, J = 254.7 Hz, C-2'), 153.7 (C, C-2), 148.3 (C, C-3), 142.5 (C, C-4a$^{\$}$), 139.7 (C, C-8a$^{\$}$), 137.8 (CH, d, J = 3.0 Hz, C-11), 132.2 (CH, d, J = 8.8 Hz, C-4'), 131.9 (CH, C-6$^{\#}$), 129.8 (CH, C-5*), 129.7 (CH, C-7$^{\#}$), 129.4 (CH, d, J = 2.8 Hz, C-6'), 128.5 (CH, C-8*), 125.4 (CH, d, J = 5.9 Hz, C-12), 124.5 (CH, d, J = 3.6 Hz, C-5'), 123.0 (C, d, J = 11.6 Hz, C-1'), 116.3 (CH, d, J = 21.8, C-3'), 24.1 (CH_3, C-9); HRMS (*pos*) *m/z* 293.1079 [M+H] (calcd. for $C_{18}H_{14}FN_2O$ 293.1090)

*, $^{\#}$, $^{\$}$ indicates assignments are interchangeable

(E)-3-(2-chlorophenyl)-1-(3-methylquinoxalin-2-yl)prop-2-en-1-one (**10b**),Yield: 86%; pale yellow solid, mp 150 °C; IR (neat) υ_{max} 1670 cm^{-1} (C=O); λ_{max} (log ε) = 325 (4.35); ^{1}H NMR ($CDCl_3$, 400 MHz) δ 8.29 (1H, d, J = 16.1 Hz, H-11), 8.15 (1H, dd, J = 8.3, 1.2 Hz, H-

5*), 8.05 (1H, dd, J = 8.3, 1.2 Hz, H-8*), 8.04 (1H, d, J = 16.1 Hz, H-12), 7.86 (1H, d, J = 9.6 Hz, H-6'), 7.83 (1H, ddd, J = 8.4, 8.4, 1.4 Hz, H-6$^{\#}$), 7.76 (1H, ddd, J = 8.3, 8.3, 1.4 Hz, H-7$^{\#}$), 7.44-7.42 (H, m, H-4'), 7.35-7.30 (2H, m, H-3'/5'), 3.00 (3H, s, H-9); ^{13}C NMR ($CDCl_3$, 100 MHz) δ 190.6 (C=O, C-10), 153.8 (C, C-2), 148.1 (C, C-3), 142.5 (C, C-4a$^{\$}$), 141.1 (CH, C-11), 139.7 (C, C-8a$^{\$}$), 135.9 (C, C-1'), 133.1 (C, C-2'), 132.0 (CH, C-6$^{\#}$), 131.5 (CH, C-3'†), 130.3 (CH, C-4'), 129.8 (CH, C-5*), 129.7 (CH, C-7$^{\#}$), 128.6 (CH, C-8*), 128.0 (CH, C-6'), 127.1 (CH, C-5'†), 125.5 (CH, C-12), 24.2 (CH_3, C-9); HRMS (*pos*) m/z 309.0799 [M+H] (calcd. for $C_{18}H_{14}ClN_2O$ 309.0795)

*, $^{\#}$, $^{\$}$, † indicates assignments are interchangeable

(E)-3-(2-bromophenyl)-1-(3-methylquinoxalin-2-yl)prop-2-en-1-one (**10c**), Yield: 58%; pale yellow powder; mp 140 °C; IR (neat) υ_{max} 1670 cm^{-1} (C=O); λ_{max} (log ε) = 321 (4.33); ^{1}H NMR ($CDCl_3$, 400 MHz) δ 8.24 (1H, d, J = 16.0 Hz, H-11), 8.15 (1H, dd, J = 8.2, 1.2 Hz, H-5*), 8.06 (1H, dd, J = 8.2, 0.9 Hz, H-8*), 8.00 (1H, d, J = 16.0 Hz, H-12), 7.85 (1H, d, J = 7.7 Hz, H-3'), 7.84 (1H, ddd, J = 8.6, 8.6, 1.5 Hz, H-6$^{\#}$), 7.76 (1H, td, J = 8.2, 1.3 Hz, H-7$^{\#}$), 7.63 (H, dd, J = 8.0, 1.1 Hz, H-6'), 7.37 (1H, t, J = 7.3 Hz, H-4'), 7.25 (1H, ddd, J = 7.9, 7.9, 1.6 Hz, H-5'), 3.01 (3H, s, H-9); ^{13}C NMR (CDCl3, 100 MHz) δ 190.6 (C=O, C-10), 153.8 (C, C-2), 148.1 (C, C-3), 143.7 (CH, C-11), 142.6 (C, C-4a$^{\$}$), 139.7 (C, C-8a$^{\$}$), 134.9 (C, C-2'), 133.6 (CH, C-6'), 132.0 (CH, C-3'), 131.6 (CH, C-5'), 129.8 (CH, C-5*), 129.7 (CH, C-6$^{\#}$), 128.6 (CH, C-8*), 128.1 (CH, C-7$^{\#}$), 127.7 (CH, C-4'), 126.3 (C, C-1'), 125.7 (CH, C-12), 24.2 (CH_3, C-9); HRMS (*pos*) m/z 353.0293 [M+H] (calcd. for $C_{18}H_{14}BrN_2O$ 353.0289)

*, $^{\#}$, $^{\$}$ indicates assignments are interchangeable

(E)-1-(3-methylquinoxalin-2-yl)-3-o-tolylprop-2-en-1-one (**10d**), Yield: 52%; pale yellow solid; mp 134 °C; IR (neat) υ_{max} 1667 cm^{-1} (C=O); λ_{max} (log ε) = 334 (4.26); ^{1}H NMR ($CDCl_3$, 400 MHz) δ 8.18 (1H, d, J = 15.9 Hz, H-11), 8.15 (1H, dd, J = 8.7, 1.4 Hz, H-5*), 8.05 (1H, dd, J = 8.5, 1.1 Hz, H-8*), 7.96 (1H, d, J = 15.9 Hz, H-12), 7.82 (1H, td, J = 8.4, 1.4 Hz, H-

6#), 7.79 (1H, dd, J = 7.8, 1.7 Hz, H-6'), 7.75 (1H, td, J = 8.2, 1.3 Hz, H-7#), 7.30 (H, ddd, J = 7.4, 7.4, 1.3 Hz, H-4'), 7.26 (1H, t, J = 7.4 Hz, H-5'), 7.22 (1H, d, J = 7.7 Hz, H-3'), 3.00 (3H, s, H-9); 2.48 (3H, s, C<u>H</u>$_3$); ^{13}C NMR ($CDCl_3$, 100 MHz) δ 191.0 (C=O, C-10), 153.7 (C, C-2), 148.6 (C, C-3), 143.0 (CH, C-11), 142.5 (C, C-4a$), 139.8 (C, C-8a$), 138.7 (C, C-2'), 133.7 (C, C-1'), 131.8 (CH, C-6#), 131.0 (CH, C-3'), 130.6 (CH, C-4'), 129.8 (CH, C-5*), 129.6 (CH, C-7#), 128.5 (CH, C-8*), 126.8 (CH, C-6'), 126.4 (CH, C-5'), 124.2 (CH, C-12), 24.2 (CH_3, C-9), 19.9 (<u>C</u>H$_3$); HRMS (*pos*) m/z 289.1337 [M+H] (calcd. for $C_{19}H_{17}N_2O$ 289.9341)

*, #, $ indicates assignments are interchangeable

(E)-3-(4-fluorophenyl)-1-(3-methylquinoxalin-2-yl)prop-2-en-1-one (**10e**), Yield: 79%; pale yellow powder, mp 163 °C; IR (neat) υ_{max} 1667 cm^{-1} (C=O); λ_{max} (log ε) = 329 (4.31); ^{1}H NMR ($CDCl_3$, 400 MHz) δ 8.16 (1H, dd, J = 8.2, 1.2 Hz, H-5*), 8.06 (1H, dd, J = 8.5, 1.1 Hz, H-8*), 7.96 (1H, d, J = 16.0 Hz, H-11), 7.86 (1H, td, J = 8.4, 1.5 Hz, H-6#), 7.80 (1H, d, J = 16.0 Hz, H-12), 7.79 (1H, td, J = 8.2, 1.3 Hz, H-7#), 7.70 (2H, dd, J = 8.7, 5.4 Hz, H-2'/6'), 7.11 (2H, t, J = 8.6 Hz, H-3'/5'), 2.99 (3H, s, H-9); ^{13}C NMR ($CDCl_3$, 100 MHz) δ 190.9 (C=O, C-10), 164.3 (C, d, J = 254.8 Hz, C-4'), 154.0 (C, C-2), 148.5 (C, C-3), 144.2 (CH, C-12), 142.7 (C, C-4a$), 139.9 (C, C-8a$), 131.9 (CH, C-6#), 131.1 (C, d, J = 2.7 Hz, C-1'), 130.8 (CH, d, J = 8.7 Hz, C-2'/6'), 129.7 (CH, C-5*), 129.7 (CH, C-7#), 128.6 (CH, C-8*), 123.3 (CH, C-11), 116.2 (CH, d, J = 22.0 Hz, C-3'/5'), 24.1 (CH_3, C-9); HRMS (*pos*) m/z 293.1086 [M+H] (calcd. for $C_{18}H_{14}FN_2O$ 293.1090)

*, #, $ indicates assignments are interchangeable

(E)-3-(4-chlorophenyl)-1-(3-methylquinoxalin-2-yl)prop-2-en-1-one (**10f**), Yield 90%; pale yellow powder; mp 159 °C; IR (neat) υ_{max} 1668 cm^{-1} (C=O); λ_{max} (log ε) = 331 (4.13); ^{1}H NMR ($CDCl_3$, 400 MHz) δ 8.16 (1H, dd, J = 8.2, 1.3 Hz, H-5*), 8.05 (1H, dd, J = 8.5, 1.2 Hz, H-8*), 8.02 (1H, d, J = 16.1 Hz, H-11), 7.82 (1H, td, J = 8.4, 1.5 Hz, H-6#), 7.79 (1H, d, J = 16.1 Hz, H-12), 7.76 (1H, td, J = 8.4, 1.4 Hz, H-7#), 7.62 (2H, d, J = 8.5 Hz, H-2'/6'), 7.39

(2H, d, J = 8.5 Hz, H-3'/5'), 2.99 (3H, s, H-9); ^{13}C NMR ($CDCl_3$, 100 MHz) δ 190.7 (C=O, C-10), 153.7 (C, C-2), 148.3 (C, C-3), 143.9 (CH, C-12), 142.5 (C, C-4a$^{\$}$), 139.7 (C, C-8a$^{\$}$), 136.8 (C, C-4'), 133.3 (C, C-1'), 131.9 (CH, C-6$^{\#}$),129.9 (CH, C-2'/6'), 129.8 (CH, C-7$^{\#}$), 129.7 (CH, C-5*), 129.3 (CH, C-3'/5'), 128.5 (CH, C-8*), 123.7 (CH, C-11), 24.1 (CH_3, C-9) ; HRMS (*pos*) *m*/*z* 309.0787 [M+H] (calcd. for $C_{18}H_{14}ClN_2O$ 309.0795)

*, $^{\#}$, $^{\$}$ indicates assignments are interchangeable

(E)-3-(4-bromophenyl)-1-(3-methylquinoxalin-2-yl)prop-2-en-1-one (**10g**),Yield: 88%; pale yellow powder; mp 164 °C; IR (neat) υ_{max} 1669 cm^{-1} (C=O); λ_{max} (log ε) = 331 (4.10); ^{1}H NMR ($CDCl_3$, 400 MHz) δ 8.15 (1H, dd, J = 8.3, 1.3 Hz, H-5*), 8.05 (1H, dd, J = 8.4, 1.2 Hz, H-8*), 8.03 (1H, d, J = 16.0 Hz, H-11), 7.83 (1H, td, J = 8.2, 1.5 Hz, H-6$^{\#}$), 7.78-7.74 (1H, m, H-7$^{\#}$), 7.76 (1H, d, J = 16.0 Hz, H-12), 7.54 (4H, s, H-2'/3'/5'/6'), 2.99 (3H, s, H-9); ^{13}C NMR ($CDCl_3$, 100 MHz) δ 190.7 (C=O, C-10), 153.7 (C, C-2), 148.2 (C, C-3), 144.0 (CH, C-12), 142.5 (C, C-4a$^{\$}$), 139.7 (C, C-8a$^{\$}$), 133.8 (C, C-1'), 132.3 (CH, C-2'/6'$^{\&}$), 132.0 (CH, C-6$^{\#}$), 130.2 (CH, C-3'/5'$^{\&}$), 129.8 (CH, C-7$^{\#}$), 129.7 (CH, C-5*), 128.6 (CH, C-8*), 125.2 (C, C-4'), 123.8 (CH, C-11), 24.2 (CH_3, C-9) ; HRMS (*pos*) *m*/*z* 353.0293 [M+H] (calcd. for $C_{18}H_{14}BrN_2O$ 353.0289)

*, $^{\#}$, $^{\$}$,$^{\&}$ indicates assignments are interchangeable

(E)-1-(3-methylquinoxalin-2-yl)-3-p-tolylprop-2-en-1-one (**10h**),Yield: 84%; pale yellow powder; mp 145 °C; IR (neat) υ_{max} 1665 cm^{-1} (C=O); λ_{max} (log ε) = 339 (4.36); ^{1}H NMR ($CDCl_3$, 400 MHz) δ 8.15 (1H, dd, J = 8.1, 1.4 Hz, H-5*), 8.05 (1H, dd, J = 8.0, 1.4 Hz, H-8*), 7.92 (1H, d, J = 16.1 Hz, H-11), 7.82 (1H, td, J = 8.6, 1.4 Hz, H-6$^{\#}$), 7.80 (1H, d, J = 16.1 Hz, H-12), 7.75 (1H, td, J = 8.2, 1.3 Hz, H-7$^{\#}$), 7.57 (2H, d, J = 8.1 Hz, H-2'/6'), 7.22 (2H, d, J = 8.0 Hz, H-3'/5'), 2.97 (3H, s, H-9), 2.38 (3H, s, C$\underline{H}_3$); ^{13}C NMR ($CDCl_3$, 100 MHz) δ 191.3 (C=O, C-10), 153.5 (C, C-2), 148.9 (C, C-3), 145.9 (CH, C-12), 142.4 (C, C-4a$^{\$}$), 141.5 (C, C-4'), 139.7 (C, C-8a$^{\$}$), 132.1 (C, C-1'), 131.7 (CH, C-6$^{\#}$), 129.7 (CH, C-3'/5'), 129.7 (CH, C-7$^{\#}$),

129.6 (CH, C-5*), 128.9 (CH, C-2'/6'), 128.5 (CH, C-8*), 122.5 (CH, C-11), 24.0 (CH_3, C-9), 21.5 ($\underline{C}H_3$) ; HRMS (*pos*) *m/z* 311.1158 [M+Na] (calcd. for $C_{19}H_{16}N_2ONa$ 311.1160)

*, #, $, & indicates assignments are interchangeable

(E)-3-(4-methoxyphenyl)-1-(3-methylquinoxalin-2-yl)prop-2-en-1-one (**10i**), Yield: 41%; yellow solid; mp 140 °C; IR (neat) υ_{max} 1663 cm^{-1} (C=O); λ_{max} (log ε) = 339 (4.20); ^{1}H NMR ($CDCl_3$, 400 MHz) δ 8.15 (1H, dd, J = 8.3, 1.3 Hz, H-5*), 8.05 (1H, dd, J = 8.4, 1.3 Hz, H-8*), 7.84 (1H, td, J = 8.4, 1.5 Hz, H-6#), 7.78 (1H, s, H-11&), 7.79 (1H, s, H-12&), 7.75 (1H, td, J = 8.4, 1.5 Hz, H-7#), 7.64 (2H, d, J = 8.5 Hz, H-2'/6'), 6.93 (2H, d, J = 8.5 Hz, H-3'/5'), 3.85 (3H, s, $OC\underline{H}_3$), 2.96 (3H, s, H-9); ^{13}C NMR ($CDCl_3$, 100 MHz) δ 191.3 (C=O, C-10), 162.0 (C, C-4'), 153.5 (C, C-2), 149.2 (C, C-3), 145.8 (CH, C-12), 142.4 (C, C-4a$), 139.8 (C, C-8a$), 131.6 (CH, C-6#), 130.7 (CH, C-2'/6'), 129.7 (CH, C-5*), 129.6 (CH, C-7#), 128.5 (CH, C-8*), 127.6 (C, C-1'), 121.2 (CH, C-11), 114.5 (CH, C-3'/5'), 55.4 ($O\underline{C}H_3$), 24.0 (CH_3, C-9) ; HRMS (*pos*) *m/z* 305.1291 [M+H] (calcd. for $C_{19}H_{17}N_2O_2$ 305.1290)

*, #, $ indicates assignments are interchangeable; &resonances are coalescing and therefore appear as singlets. Assignments can be interchanged.

Preparation of 2-(3-(quinolin-2-yl)-4,5-dihydro-1H-pyrazol-5-yl)quinoxalines and preparation of 2-(3-phenyl-4,5-dihydro-1H-pyrazol-5-yl)quinoxalines

Hydrazine hydrate (2 eq) was added to a suspension of chalcone (**7a-h** or **10a-i**) (200 mg) in EtOH (15 mL) and the mixture refluxed for 12 hours. Upon completion the reaction was cooled and allowed to stand overnight where the pyrazoline compounds crystallised out of solution (**8a-h** and **11a-i**) and were collected by filtration.

2-(5-(8-fluoroquinolin-2-yl)-4,5-dihydro-1H-pyrazol-3-yl)-3-methylquinoxaline (**8a**), Yield 80%; pale yellow powder; mp 197-198 °C; IR (neat) υ_{max} 3217 cm^{-1} (N-H); λ_{max} (log ε)

= 358 (4.24); ^{1}H NMR ($CDCl_3$, 400 MHz) δ 8.18 (1H, dd, J = 8.6, 1.3 Hz, H- 4'), 7.98 (1H, dd, J = 7.6, 1.9 Hz, H-5*), 7.94 (1H, dd, J = 7.7, 2.0 Hz, H-8*), 7.66 (1H, td, J = 6.9, 1.7 Hz, H-6$^{\#}$), 7.65-7.61 (1H, m, H-7$^{\#}$), 7.64 (1H, d, J = 8.6 Hz, H-3'), 7.57 (1H, d, J = 7.8 Hz, H-5'), 7.47-7.41 (1H, m, H-6'), 7.38 (1H, td, J = 7.4, 1.3 Hz, H-7'), 5.32 (1H, dd, J = 11.7, 8.1 Hz, H-5''), 3.98 (1H, dd, J = 17.4, 11.7 Hz, H-4''a), 3.68 (1H, dd, J = 17.4, 8.1 Hz, H-4''b), 3.07 (3H, s, H-9); ^{13}C NMR ($CDCl_3$, 100 MHz) δ 161.9 (C, C-2'), 157.9 (C, d, J = 256.9 Hz, C-8'), 153.6 (C, C-2), 152.2 (C, C-3''), 146.3 (C, C-3), 140.5 (C, C-4a$^{\$}$), 139.9 (C, C-8a$^{\$}$), 137.4 (C, d, J = 11.0 Hz, C-8'a), 137.2 (CH, d, J = 2.9 Hz, C-4'), 129.9 (CH, C-6$^{\#}$), 129.2 (C, d, J = 2.2 Hz, C-4'a), 129.1 (CH, C-5*), 128.9 (CH, C-7$^{\#}$), 128.0 (CH, C-8*), 126.4 (CH, d, J = 8.0 Hz, C-6'), 123.2 (CH, d, J = 4.5 Hz, C-5'), 119.6 (CH, C-3'), 114.1 (CH, d, J = 19.1 Hz, C-7'), 64.6 (CH, C-5''), 41.1 (CH_2, C-4''), 26.1 (CH_3, C-9) ; HRMS (*pos*) *m*/*z* 380.1283 [M+Na] (calcd. for $C_{21}H_{16}FN_5Na$ 380.1287)

*, $^{\#}$, $^{\$}$ indicates assignments are interchangeable

2-(5-(8-chloroquinolin-2-yl)-4,5-dihydro-1H-pyrazol-3-yl)-3-methylquinoxaline (**8b**), Yield 37%; off-white powder; mp 198 °C; IR (neat) υ_{max} 3295 cm^{-1} (N-H); λ_{max} (log ε) = 348 (4.22); ^{1}H NMR ($CDCl_3$, 400 MHz) δ 8.18 (1H, d, J = 8.6 Hz, H- 4'), 7.94 (1H, dd, J = 8.2, 2.0 Hz, H-5*), 7.81 (1H, dd, J = 7.5, 1.0 Hz, H-7'), 7.70 (1H, dd, J = 8.2, 1.0 Hz, H-5'), 7.67 (1H, dd, J = 8.2, 1.9 Hz, H-8*), 7.66 (1H, td, J = 8.2, 1.8 Hz, H-6$^{\#}$), 7.65-7.60 (1H, m, H-7$^{\#}$), 7.61 (1H, d, J = 8.6 Hz, H-3'), 7.42 (1H, t, J = 7.8 Hz, H-6'), 5.30 (1H, dd, J = 11.7, 7.1 Hz, H-5''), 3.98 (1H, dd, J = 17.3, 11.7 Hz, H-4''a), 3.73 (1H, dd, J = 17.3, 7.1 Hz, H-4''b), 3.06 (3H, s, H-9); ^{13}C NMR ($CDCl_3$, 100 MHz) δ 162.1 (C, C-2'), 153.8 (C, C-2), 152.3 (C, C-3''), 146.4 (C, C-3), 143.4 (C, C-8'a), 140.5 (C, C-4a$^{\$}$), 140.1 (C, C-8a$^{\$}$), 137.8 (CH, C-4'), 133.5 (C, C-8'), 130.0 (CH, C-7'), 129.8 (CH, C-6$^{\#}$), 129.0 (CH, C-7$^{\#}$), 128.9 (CH, C-5*), 128.8 (C, C-4'a), 128.1 (CH, C-8*), 126.7 (CH, C-5'), 126.5 (CH, C-6'), 119.5 (CH, C-3'), 64.1 (CH, C-5''), 40.9

(CH_2, C-4''), 26.2 (CH_3, C-9) ; HRMS (*pos*) *m*/*z* 396.0985 [M+Na] (calcd. for $C_{21}H_{16}ClN_5Na$ 396.0992)

*, #, $ indicates assignments are interchangeable

2-(5-(8-bromoquinolin-2-yl)-4,5-dihydro-1H-pyrazol-3-yl)-3-methylquinoxaline (**8c**), Yield 46%; pale yellow powder; mp 189 °C; IR (neat) υ_{max} 3326 cm^{-1} (N-H); λ_{max} (log ε) = 359 (4.37); ^{1}H NMR ($CDCl_3$, 400 MHz) δ 8.16 (1H, d, *J* = 8.5 Hz, H-4'), 8.03 (1H, d, *J* = 7.5 Hz, H-7'), 8.00 (1H, d, *J* = 8.5 Hz, H-5*), 7.96 (1H, dd, *J* = 7.6, 1.7 Hz, H-8*), 7.76 (1H, d, *J* = 8.1 Hz, H-5'), 7.69-7.62 (2H, m, H-6/7), 7.59 (1H, d, *J* = 8.5 Hz, H-3'), 7.36 (1H, t, *J* = 7.8 Hz, H-6'), 5.30 (1H, dd, *J* = 11.7, 6.6 Hz, H-5''), 3.98 (1H, dd, *J* = 17.3, 11.7 Hz, H-4''a), 3.73 (1H, dd, *J* = 17.3, 6.6 Hz, H-4''b), 3.08 (3H, s, H-9); ^{13}C NMR ($CDCl_3$, 100 MHz) δ 162.3 (C, C-2'), 153.7 (C, C-2), 152.4 (C, C-3''), 146.4 (C, C-3), 144.3 (C, C-8'a), 140.7 (C, C-4a$^\$$), 138.4 (C, C-8a$^\$$), 137.9 (CH, C-4'), 133.6 (CH, C-7'), 130.0 (CH, C-6$^\#$), 129.2 (CH, C-7$^\#$), 128.9 (CH, C-5*), 128.8 (C, C-4'a), 127.8 (CH, C-8*), 127.4 (CH, C-5'), 127.0 (CH, C-6'), 125.1 (C, C-8'), 119.5 (CH, C-3'), 63.8 (CH, C-5''), 40.7 (CH_2, C-4''), 26.0 (CH_3, C-9); HRMS (*pos*) *m*/*z* 440.0485 [M+Na] (calcd. for $C_{21}H_{16}BrN_5Na$ 440.0487)

*, #, $ indicates assignments are interchangeable

2-methyl-3-(5-(8-methylquinolin-2-yl)-4,5-dihydro-1H-pyrazol-3-yl)quinoxaline (**8d**), Yield 82%; off-white powder; mp 167 °C; IR (neat) υ_{max} 3316 cm^{-1} (N-H); λ_{max} (log ε) = 358 (4.42); ^{1}H NMR ($CDCl_3$, 400 MHz) δ 8.16 (1H, d, *J* = 8.5 Hz, H- 4'), 7.97 (1H, dd, *J* = 8.5, 2.1 Hz, H-5*), 7.95 (1H, dd, *J* = 8.2, 2.2 Hz, H-8*), 7.66 (1H, td, *J* = 8.5, 1.9 Hz, H-6$^\#$), 7.65-7.61 (2H, m, H-7$^\#$/5'), 7.55 (1H, d, *J* = 7.6 Hz, H-7'), 7.51 (1H, d, *J* = 8.5 Hz, H-3'), 7.41 (1H, dd, *J* = 7.6, 7.6 Hz, H-6'), 5.32 (1H, dd, *J* = 11.6, 6.2 Hz, H-5''), 3.96 (1H, dd, *J* = 17.2, 11.6 Hz, H-4''a), 3.78 (1H, dd, *J* = 17.2, 6.2 Hz, H-4''b), 3.06 (3H, s, H-9), 2.82 (3H, C$\underline{H_3}$); ^{13}C NMR ($CDCl_3$, 100 MHz) δ 159.7 (C, C-2'), 153.7 (C, C-2), 152.6 (C, C-3''), 146.4 (C, C-3), 145.7 (C, C-8'a), 140.5 (C, C-4a$^\$$), 140.0 (C, C-8a$^\$$), 138.1 (CH, C-4'), 136.9 (C, C-8'), 130.3 (CH, C-7'), 129.8 (CH, C-6#), 129.0 (CH, C-7#), 128.9 (CH, C-5*), 128.1 (CH, C-8*), 127.5 (C, C-4'a), 126.5 (CH, C-6'), 125.5 (CH, C-5'), 118.4 (CH, C-3'), 63.3 (CH, C-5''), 40.8 (CH_2, C-4''), 26.0 (CH_3, C-9), 18.0 (CH_3); HRMS (*pos*) *m/z* 376.1537 [M+Na] (calcd. for $C_{22}H_{19}N_5Na$ 376.1538)

*, #, $ indicates assignments are interchangeable

2-(5-(6-fluoroquinolin-2-yl)-4,5-dihydro-1H-pyrazol-3-yl)-3-methylquinoxaline (**8e**), Yield: 71%; white fibrous solid, mp 180-182 °C; IR (neat) υ_{max} 3320 cm^{-1} (N-H); λ_{max} (log ε) = 358 (4.17); ^{1}H NMR ($CDCl_3$, 400 MHz) δ 8.11 (1H, d, J = 8.5 Hz, H- 4'), 8.06 (1H, dd, J = 9.0, 5.3 Hz, H-8'), 7.96-7.93 (2H, m, H-5/8), 7.67-7.61 (2H, m, H-6/7), 7.56 (1H, d, J = 8.5 Hz, H-3'), 7.45 (1H, td, J = 8.9, 2.2 Hz, H-7'), 7.40 (1H, dd, J = 8.7, 2.1 Hz, H-5'), 5.22 (1H, dd, J = 11.0, 7.9 Hz, H-5''), 3.95 (1H, dd, J = 17.2, 11.0 Hz, H-4''a), 3.71 (1H, dd, J = 17.2, 7.9 Hz, H-4''b), 3.06 (3H, s, H-9); ^{13}C NMR ($CDCl_3$, 100 MHz) δ 160.6 (C, C-2'), 160.5 (C, d, J = 248.1 Hz, C-6'), 153.7 (C, C-2), 152.4 (C, C-3''), 146.3 (C, C-3), 144.4 (C, C-8'a), 140.5 (C, C-4a$), 140.3 (C, C-8a$), 136.7 (CH, d, J = 5.4 Hz, C-4'), 131.7 (CH, d, J = 9.1 Hz, C-8'), 129.8 (CH, C-6#), 129.0 (CH, C-7#), 128.8 (CH, C-5*), 128.2 (CH, C-8*), 128.1 (C, d, J = 9.5 Hz, C-4'a), 120.0 (CH, d, J = 25.6 Hz, C-7'), 119.4 (CH, C-3'), 110.6 (CH, d, J = 21.6 Hz, C-5'), 64.1 (CH, C-5''), 40.9 (CH_2, C-4''), 26.2 (CH_3, C-9) ; HRMS (*pos*) *m/z* 380.1288 [M+Na] (calcd. for $C_{21}H_{16}FN_5Na$ 380.1287)

*, #, $ indicates assignments are interchangeable

2-(5-(6-chloroquinolin-2-yl)-4,5-dihydro-1H-pyrazol-3-yl)-3-methylquinoxaline (**8f**), Yield: 58%; white powder; mp 207-208 °C; IR (neat) υ_{max} 3352 cm^{-1} (N-H); λ_{max} (log ε) = 356 (4.38); ^{1}H NMR ($CDCl_3$, 400 MHz) δ 8.08 (1H, d, J = 8.6 Hz, H- 4'), 7.99 (1H, d, J = 9.0 Hz, H-8'), 7.95 (2H, m, H-5/8), 7.77 (1H, d, J = 2.3 Hz, H-5'), 7.68-7.60 (3H, m, H-6/7/7'), 7.57 (1H, d, J = 8.6 Hz, H-3'), 5.22 (1H, dd, J = 11.6, 7.5 Hz, H-5''), 3.95 (1H, dd, J = 17.3, 11.7 Hz, H-4''a), 3.70 (1H, dd, J = 17.3, 7.5 Hz, H-4''b), 3.06 (3H, s, H-9); ^{13}C NMR ($CDCl_3$, 100

MHz) δ 161.6 (C, C-2'), 153.7 (C, C-2), 152.4 (C, C-3''), 146.3 (C, C-3), 145.7 (C, C-8'a), 140.5 (C, C-4a$^{\$}$), 140.3 (C, C-8a$^{\$}$), 136.4 (CH, C-4'), 132.3 (C, C-6'), 130.8 (CH, C-8'), 130.7 (CH, C-7'), 129.8 (CH, C-6$^{\#}$), 129.0 (CH, C-7$^{\#}$), 128.8 (CH, C-5*), 128.2 (CH, C-8*), 128.1 (C, C-4'a), 126.2 (CH, C-5'), 119.6 (CH, C-3'), 64.2 (CH, C-5''), 40.9 (CH_2, C-4''), 26.2 (CH_3, C-9) ; HRMS (*pos*) *m/z* 396.0990 [M+Na] (calcd. for $C_{21}H_{16}ClN_5Na$ 396.0992)

*, $^{\#}$, $^{\$}$ indicates assignments are interchangeable

2-(5-(6-bromoquinolin-2-yl)-4,5-dihydro-1H-pyrazol-3-yl)-3-methylquinoxaline (**8g**), Yield: 50%; off-white powder; mp 219-220 °C; IR (neat) υ_{max} 3352 cm^{-1} (N-H); λ_{max} (log ε) = 358 (4.16); ^{1}H NMR ($CDCl_3$, 400 MHz) δ 8.07 (1H, d, J = 8.6 Hz, H- 4'), 7.97-7.92 (4H, m, H-5/8/5'/8'), 7.76 (1H, dd, J = 9.0, 2.1 Hz, H-7'), 7.66 (1H, td, J = 7.0, 1.7 Hz, H-6*), 7.63 (1H, td, J = 7.0, 1.7 Hz, H-7*), 7.57 (1H, d, J = 8.6 Hz, H-3'), 5.22 (1H, dd, J = 11.7, 7.5 Hz, H-5''), 3.96 (1H, dd, J = 17.3, 11.7 Hz, H-4''a), 3.70 (1H, dd, J = 17.3, 7.5 Hz, H-4''b), 3.06 (3H, s, H-9); ^{13}C NMR ($CDCl_3$, 100 MHz) δ 161.8 (C, C-2'), 153.7 (C, C-2), 152.4 (C, C-3''), 146.3 (C, C-8'a), 145.9 (C, C-3), 140.5 (C, C-4a$^{\$}$), 140.3 (C, C-8a$^{\$}$), 136.4 (CH, C-4'), 133.3 (CH, C-7'), 130.9 (CH, C-8'), 129.8 (CH, C-6$^{\#}$), 129.6 (CH, C-5'), 129.0 (CH, C-5*), 128.8 (CH, C-7$^{\#}$), 128.6 (C, C-4'a), 128.2 (CH, C-8*), 120.4 (C, C-6'), 119.6 (CH, C-3'), 64.2 (CH, C-5''), 40.9 (CH_2, C-4''), 26.2 (CH_3, C-9); HRMS (*pos*) *m/z* 440.0481 [M+Na] (calcd. for $C_{21}H_{16}BrN_5Na$ 440.0487)

*, $^{\#}$, $^{\$}$ indicates assignments are interchangeable

2-methyl-3-(5-(6-methylquinolin-2-yl)-4,5-dihydro-1H-pyrazol-3-yl)quinoxaline (**8h**), Yield: 79%; off-white powder; mp 180-181 °C; IR (neat) υ_{max} 3351 cm^{-1} (N-H); λ_{max} (log ε) = 358 (4.44); ^{1}H NMR ($CDCl_3$, 400 MHz) δ 8.09 (1H, d, J = 8.6 Hz, H- 4'), 7.99 (1H, d, J = 9.2 Hz, H-8'), 7.96 (1H, dd, J = 8.1, 2.0 Hz, H-5*), 7.94 (1H, dd, J = 8.0, 2.0 Hz, H-8*), 7.66 (1H, td, J = 6.9, 1.7 Hz, H-6$^{\#}$), 7.62 (1H, td, J = 6.9, 1.7 Hz, H-7$^{\#}$), 7.55-7.51 (3H, m, H-3'/5'/7'), 5.28 (1H, dd, J = 11.6, 7.7 Hz, H-5''), 3.96 (1H, dd, J = 17.3, 11.7 Hz, H-4''a), 3.70 (1H, dd, J

= 17.3, 7.7 Hz, H-4''b), 3.06 (3H, s, H-9), 2.51 (3H, s, C<u>H</u>$_3$); ^{13}C NMR ($CDCl_3$, 100 MHz) δ 160.2 (C, C-2'), 153.8 (C, C-2), 152.4 (C, C-3''), 146.4 (C, C-3), 145.4 (C, C-8'a), 140.5 (C, C-4a$^{\$}$), 140.3 (C, C-8a$^{\$}$), 137.2 (CH, C-4'), 136.7 (C, C-6'), 132.4 (CH, C-7'), 129.7 (CH, C-6$^{\#}$), 128.9 (CH, C-5*), 128.8 (CH, C-7$^{\#}$), 128.4 (CH, C-8'), 128.2 (CH, C-8*), 127.6 (C, C-4'a), 126.5 (CH, C-5'), 118.6 (CH, C-3'), 64.0 (CH, C-5''), 41.0 (CH_2, C-4''), 26.2 (CH_3, C-9), 21.6 (<u>C</u>H$_3$); HRMS (*pos*) *m*/*z* 376.1534 [M+Na] (calcd. for $C_{22}H_{19}N_5Na$ 376.1538)

*, #, $ indicates assignments are interchangeable

2-(5-(2-fluorophenyl)-4,5-dihydro-1H-pyrazol-3-yl)-3-methylquinoxaline (**11a**), Yield: 72%; off white fibrous solid; mp 120-121 °C; IR (neat) υ_{max} 3308 cm^{-1} (N-H); λ_{max} (log ε) = 358 (4.41); ^{1}H NMR ($CDCl_3$, 400 MHz) δ 8.04 (1H, dd, *J* = 7.4, 2.0 Hz, H-5*), 7.97 (1H, dd, *J* = 7.4, 2.2 Hz, H-8*), 7.70-7.63 (2H, m, H-6$^{\#}$, H-7$^{\#}$), 7.46 (1H, td, *J* = 7.6, 1.6 Hz, H-5'), 7.29-7.24 (1H, m, H-4'), 7.13 (1H, td, *J* = 7.5, 1.3 Hz, H-6'), 7.07 (1H, ddd, *J* = 8.4, 8.3, 1.7 Hz, H-3'), 5.27 (1H, dd, *J* = 11.1, 9.3 Hz, H-5''), 3.85 (1H, dd, *J* = 17.1, 11.1 Hz, H-4''a), 3.39 (1H, dd, *J* = 17.1, 9.3 Hz, H-4''b), 3.05 (3H, s, H-9); ^{13}C NMR ($CDCl_3$, 100 MHz) δ 160.5 (C, d, *J* = 243.4 Hz, C-2'), 153.6 (C, C-2), 152.4 (C, C-3''), 146.4 (C, C-3), 140.5 (C, C-4a$^{\$}$), 140.3 (C, C-8a$^{\$}$), 129.8 (CH, C-6$^{\#}$), 129.2 (CH, d, *J* = 8.1 Hz, C-4'), 129.1 (C, C-1'), 129.0 (CH, C-7$^{\#}$), 128.9 (CH, C-5*), 128.2 (CH, C-8*), 127.3 (CH, d, *J* = 4.2 Hz, C-5'), 124.5 (CH, d, *J* = 3.5 Hz, C-6'), 115.3 (CH, d, *J* = 21.4 Hz, C-3'), 57.1 (CH, d, *J* = 2.6 Hz, C-5''), 40.6 (CH_2, C-4''), 26.2 (CH_3, C-9); HRMS (*pos*) *m*/*z* 329.1177 [M+Na] (calcd. for $C_{18}H_{15}FN_4Na$ 329.1178)

*, # indicates assignments are interchangeable

2-(5-(2-chlorophenyl)-4,5-dihydro-1H-pyrazol-3-yl)-3-methylquinoxaline (**11b**), Yield: 82%; white fibrous solid; mp 121-122 °C; IR (neat) υ_{max} 3380 cm^{-1} (N-H); λ_{max} (log ε) = 359 (4.27); ^{1}H NMR ($CDCl_3$, 400 MHz) δ 8.04 (1H, dd, *J* = 8.6, 1.5 Hz, H-5*), 7.96 (1H, dd, *J* = 8.2, 2.2 Hz, H-8*), 7.70-7.63 (2H, m, H-6$^{\#}$, H-7$^{\#}$), 7.55 (1H, dd, *J* = 7.5, 1.8 Hz, H-3'), 7.39 (1H, dd, *J* = 7.5, 1.8 Hz, H-6'), 7.25 (1H, td, *J* = 8.8, 1.4 Hz, H-4'), 7.23 (1H, td, *J* = 7.6, 1.4

Hz, H-5'), 5.38 (1H, dd, J = 11.1, 9.3 Hz, H-5''), 3.94 (1H, dd, J = 17.2, 11.1 Hz, H-4''a), 3.29 (1H, dd, J = 17.2, 9.3 Hz, H-4''b), 3.08 (3H, s, H-9); ^{13}C NMR ($CDCl_3$, 100 MHz) δ 153.4 (C, C-2), 151.8 (C, C-3''), 146.6 (C, C-3), 140.7 (C, C-4a/8a), 139.5 (C, C-1'), 132.9 (C, C-2'), 130.0 (CH, C-6$^{\#}$), 129.8 (CH, C-6'), 129.3 (CH, C-7$^{\#}$), 128.9 (CH, C-5*), 128.8 (CH, C-5'), 127.7 (CH, C-8*), 127.3 (CH, C-4'), 126.9 (CH, C-3'), 60.6 (CH, C-5''), 40.7 (CH_2, C-4''), 25.9 (CH_3, C-9); HRMS (*pos*) *m*/*z* 345.0882 [M+Na] (calcd. for $C_{18}H_{15}ClN_4Na$ 345.0883)

*, $^{\#}$ indicates assignments are interchangeable

2-(5-(2-bromophenyl)-4,5-dihydro-1H-pyrazol-3-yl)-3-methylquinoxaline (**11c**), Yield: 51%; white fibrous solid; mp 148-150 °C; IR (neat) υ_{max} 3379 cm^{-1} (N-H); λ_{max} (log ε) = 357 (4.37); ^{1}H NMR ($CDCl_3$, 400 MHz) δ 7.97-7.93 (2H, m, H-5/8), 7.68-7.61 (2H, m, H-6$^{\#}$, H-7$^{\#}$), 7.57 (1H, d, J = 7.8, H-3'), 7.56 (1H, dd, J = 7.8, 1.3 Hz, H-6'), 7.30 (1H, t, J = 7.4 Hz, H-5'), 7.14 (1H, td, J = 7.7, 1.5 Hz, H-4'), 6.49 (1H, N<u>H</u>), 5.33 (1H, dd, J = 11.1, 9.3 Hz, H-5''), 3.95 (1H, dd, J = 17.2, 11.1 Hz, H-4''a), 3.26 (1H, dd, J = 17.2, 9.3 Hz, H-4''b), 3.04 (3H, s, H-9); ^{13}C NMR ($CDCl_3$, 100 MHz) δ 153.6 (C, C-2), 151.9 (C, C-3''), 146.4 (C, C-3), 141.2 (C, C-1'), 140.5 (C, C-4a$^{\$}$), 140.2 (C, C-8a$^{\$}$), 133.0 (CH, C-3'), 129.7 (CH, C-6$^{\#}$), 129.1 (CH, C-4'), 129.0 (CH, C-7$^{\#}$), 128.9 (CH, C-5*), 128.2 (CH, C-8*), 128.0 (CH, C-5'), 127.2 (CH, C-6'), 123.0 (C, C-2'), 62.9 (CH, C-5''), 40.9 (CH_2, C-4''), 26.2 (CH_3, C-9); HRMS (*pos*) *m*/*z* 367.0561[M+H] (calcd. for $C_{18}H_{16}BrN_4$ 367.0558)

*, $^{\#}$, $^{\$}$ indicates assignments are interchangeable

2-methyl-3-(5-o-tolyl-4,5-dihydro-1H-pyrazol-3-yl)quinoxaline (**11d**), Yield: 65%; white solid; mp 150-151 °C; IR (neat) υ_{max} 3387 cm^{-1} (N-H); λ_{max} (log ε) = 360 (4.30); ^{1}H NMR ($CDCl_3$, 400 MHz) δ 7.98 (1H, dd, J = 8.3, 2.1 Hz, H-5*), 7.93 (1H, dd, J = 8.2, 2.1 Hz, H-8*), 7.68-7.61 (2H, m, H-6$^{\#}$, H-7$^{\#}$), 7.45-7.43 (1H, m, H-5'), 7.19–7.17 (3H, m, H-3'/4'/6'), 5.20 (1H, dd, J = 11.1 , 8.8 Hz, H-5''), 3.86 (1H, dd, J = 17.0, 11.1 Hz, H-4''a), 3.23 (1H, dd, J = 17.0, 8.8 Hz, H-4''b), 3.09 (3H, s, H-9), 2.42 (3H, s, C<u>H</u>$_3$); ^{13}C NMR ($CDCl_3$, 100 MHz) δ

153.6 (C, C-2), 151.5 (C, C-3''), 146.6 (C, C-3), 140.6 (C, C-4a/8a), 140.4 (C, C-1'), 135.0 (C, C-2'), 130.7 (CH, C-3'), 129.7 (CH, C-6$^{\#}$), 129.0 (CH, C-7$^{\#}$), 128.8 (CH, C-5*), 128.1 (CH, C-8*), 127.5 (CH, C-4'†), 126.6 (CH, C-6'†), 125.0 (CH, C-5'), 60.5 (CH, C-5''), 41.0 (CH_2, C-4''), 26.2 (CH_3, C-9), 19.5 ($\underline{C}H_3$); HRMS (*pos*) *m*/*z* 303.1617 [M+H] (calcd. for $C_{19}H_{19}N_4$ 303.1610)

$*, ^{\#}, ^{\dagger}$ indicates assignments are interchangeable

2-(5-(4-fluorophenyl)-4,5-dihydro-1H-pyrazol-3-yl)-3-methylquinoxaline (**11e**), Yield 90%; yellow crystals; mp 168 °C; IR (neat) υ_{max} 3240 cm^{-1} (N-H); λ_{max} (log ε) = 361 (4.39); ^{1}H NMR ($CDCl_3$, 400 MHz) δ 7.97 (1H, dd, *J* = 7.8, 1.9 Hz, H-5*), 7.94 (1H, dd, *J* = 7.7, 2.2 Hz, H-8*), 7.69-7.62 (2H, m, H-6$^{\#}$, H-7$^{\#}$), 7.35 (2H, dd, *J* = 8.7, 5.3 Hz, H-2'/6'), 7.03 (2H, t, *J* = 8.7 Hz, H-3'/5'), 6.42 (1H, s, N$\underline{H}$), 4.95 (1H, dd, *J* = 11.0 , 9.4 Hz, H-5''), 3.80 (1H, dd, *J* = 17.2, 11.0 Hz, H-4''a), 3.36 (1H, dd, *J* = 17.2, 9.4 Hz, H-4''b), 3.05 (3H, s, H-9); ^{13}C NMR ($CDCl_3$, 100 MHz) δ 162.4 (C, d, *J* = 246.0 Hz, C-4'), 153.6 (C, C-2), 152.1 (C, C-3''), 146.4 (C, C-3), 140.5 (C, C-4a$^{\$}$), 140.2 (C, C-8a$^{\$}$), 138.2 (C, d, *J* = 2.6 Hz, C-1'), 129.8 (CH, C-6$^{\#}$), 129.0 (CH, C-7$^{\#}$), 128.8 (CH, C-5*), 128.2 (CH, C-8*), 128.0 (CH, d, *J* = 8.1 Hz, C-2'/6'), 115.7 (CH, d, *J* = 21.5 Hz, C-3'/5'), 63.3 (CH, C-5''), 42.4 (CH_2, C-4''), 26.2 (CH_3, C-9); HRMS (*pos*) *m*/*z* 329.1174 [M+Na] (calcd. for $C_{18}H_{15}FN_4Na$ 329.1178)

$*, ^{\#}, ^{\$}$ indicates assignments are interchangeable

2-(5-(4-chlorophenyl)-4,5-dihydro-1H-pyrazol-3-yl)-3-methylquinoxaline (**11f**), Yield: 82%; yellow powder; mp 164 °C; IR (neat) υ_{max} 3369 cm^{-1} (N-H); λ_{max} (log ε) = 358 (4.43); ^{1}H NMR ($CDCl_3$, 400 MHz) δ 7.96 (1H, dd, *J* = 7.8, 1.9 Hz, H-5*), 7.93 (1H, dd, *J* = 7.7, 2.1 Hz, H-8*), 7.68-7.63 (2H, m, H-6$^{\#}$, H-7$^{\#}$), 7.30 (4H, s, H-2'/3'/5'/6'), 6.45 (1H, s, N$\underline{H}$), 4.93 (1H, dd, *J* = 11.1, 9.4 Hz, H-5''), 3.81 (1H, dd, *J* = 17.3, 11.1 Hz, H-4''a), 3.34 (1H, dd, *J* = 17.3, 9.4 Hz, H-4''b), 3.04 (3H, s, H-9); ^{13}C NMR ($CDCl_3$, 100 MHz) δ 153.6 (C, C-2), 152.1 (C, C-3''), 146.3 (C, C-3), 140.9 (C, C-1'), 140.5 (C, C-4a$^{\$}$), 140.2 (C, C-8a$^{\$}$), 133.6 (C, C-4'), 129.8 (CH, C-6$^{\#}$), 129.0 (CH, C-5*/2'/6'$^{\&}$), 128.8 (CH, C-7$^{\#}$), 128.2 (CH, C-8*), 127.8 (CH, C-

3'/5'[&]), 63.3 (CH, C-5''), 42.3 (CH_2, C-4''), 26.2 (CH_3, C-9); HRMS (*pos*) *m*/*z* 345.0872 [M+Na] (calcd. for $C_{18}H_{15}ClN_4Na$ 345.0883)

*, #, $, & indicates assignments are interchangeable

2-(5-(4-bromophenyl)-4,5-dihydro-1H-pyrazol-3-yl)-3-methylquinoxaline (**11g**), Yield: 76%; white powder; mp 155 °C; IR (neat) υ_{max} 3375 cm^{-1} (N-H); λ_{max} (log ε) = 359 (4.23); ^{1}H NMR ($CDCl_3$, 400 MHz) δ 7.97 (1H, dd, *J* = 7.8, 1.8 Hz, H-5*), 7.94 (1H, dd, *J* = 7.8, 1.9 Hz, H-8*), 7.69-7.61 (1H, m, H-6#, H-7#), 7.47 (2H, d, *J* = 8.4 Hz, H-3'/5'), 7.26 (2H, d, *J* = 8.4 Hz, H-2'/6'), 6.42 (1H, s, N<u>H</u>), 4.93 (1H, dd, *J* = 11.0, 9.3 Hz, H-5''), 3.82 (1H, dd, *J* = 17.1, 11.0 Hz, H-4''a), 3.35 (1H, dd, *J* = 17.1, 9.3 Hz, H-4''b), 3.04 (3H, s, H-9); ^{13}C NMR ($CDCl_3$, 100 MHz) δ 153.6 (C, C-2), 152.1 (C, C-3''), 146.3 (C, C-3), 141.4 (C, C-1'), 140.5 (C, C-4a/8a), 133.6 (C, C-4'), 132.0 (CH, 3'/5'), 129.8 (CH, C-6#), 128.9 (CH, C-7#), 128.7 (CH, C-5*), 128.2 (CH, C-8*), 128.1 (CH, 2'/6'), 63.3 (CH, C-5''), 42.3 (CH_2, C-4''), 26.2 (CH_3, C-9); HRMS (*pos*) *m*/*z* 389.0375 [M+Na] (calcd. for $C_{18}H_{15}BrN_4Na$ 389.0378)

*, # indicates assignments are interchangeable

2-methyl-3-(5-p-tolyl-4,5-dihydro-1H-pyrazol-3-yl)quinoxaline (**11h**), Yield: 83%; yellow powder; mp 159-160 °C; IR (neat) υ_{max} 3218 cm^{-1} (N-H); λ_{max} (log ε) = 360 (4.29); ^{1}H NMR ($CDCl_3$, 400 MHz) δ 7.99 (1H, dd, *J* = 7.6, 2.0 Hz, H-5*), 7.94 (1H, dd, *J* = 7.7, 2.0 Hz, H-8*), 7.68-7.61 (2H, m, H-6#, H-7#), 7.25 (2H, d, *J* = 8.1 Hz, H-2'/6'), 7.14 (2H, d, *J* = 8.0 Hz, H-3'/5'), 4.93 (1H, dd, *J* = 10.9, 8.8 Hz, H-5''), 3.77 (1H, dd, *J* = 17.1, 10.9 Hz, H-4''a), 3.40 (1H, dd, *J* = 17.1, 8.8 Hz, H-4''b), 3.06 (3H, s, H-9), 2.32 (3H, s, C<u>H</u>$_3$); ^{13}C NMR ($CDCl_3$, 100 MHz) δ 153.5 (C, C-2), 151.9 (C, C-3''), 146.5 (C, C-3), 140.6 (C, C-4a/8a), 139.4 (C, C-1'), 137.6 (C, C-4'), 129.8 (CH, C-6#), 129.5 (CH, C-3'/5'), 129.1 (CH, C-7#), 128.9 (CH, C-5*), 127.9 (CH, C-8*), 126.2 (CH, C-2'/6'), 63.7 (CH, C-5''), 42.1 (CH_2, C-4''), 26.0 (CH_3, C-9), 21.1 (<u>C</u>H$_3$); HRMS (*pos*) *m*/*z* 325.1417 [M+Na] (calcd. for $C_{19}H_{18}N_4Na$ 325.1429)

*, # indicates assignments are interchangeable

2-(5-(4-methoxyphenyl)-4,5-dihydro-1H-pyrazol-3-yl)-3-methylquinoxaline (**11i**), Yield: 63%; yellow crystalline powder; mp 129-130 °C; IR (neat) υ_{max} 3214 cm^{-1} (N-H); λ_{max} (log ε) = 363 (4.21); ^{1}H NMR ($CDCl_3$, 400 MHz) δ 8.00 (1H, dd, J = 7.6, 2.2 Hz, H-5*), 7.94 (1H, dd, J = 7.6, 2.1 Hz, H-8*), 7.69-7.62 (1H, m, H-6$^\#$, H-7$^\#$), 7.28 (2H, d, J = 8.7 Hz, H-2'/6'), 6.87 (2H, d, J = 8.7 Hz, H-3'/5'), 4.92 (1H, dd, J = 11.0, 8.8 Hz, H-5''), 3.77 (3H, s, OC$\underline{H}_3$), 3.76 (1H, dd, J = 17.1, 11.0 Hz, H-4''a), 3.39 (1H, dd, J = 17.1, 8.8 Hz, H-4''b), 3.05 (3H, s, H-9); ^{13}C NMR ($CDCl_3$, 100 MHz) δ 159.3 (C, C-4'), 153.7 (C, C-2), 152.1 (C, C-3''), 146.6 (C, C-3), 140.6 (C, C-4a$^\$$), 140.2 (C, C-8a$^\$$), 134.6 (C, C-1'), 129.6 (CH, C-6$^\#$), 128.9 (CH, C-7$^\#$), 128.8 (CH, C-5*), 128.2 (CH, C-8*), 127.5 (CH, C-2'/6'), 114.2 (CH, C-3'/5'), 63.4 (CH, C-5''), 55.3 (O$\underline{C}H_3$), 42.1 (CH_2, C-4''), 26.3 (CH_3, C-9); HRMS (*pos*) *m*/*z* 341.1377 [M+Na] (calcd. for $C_{19}H_{18}N_4ONa$ 341.1378)

*, $^\#$, $^\$$ indicates assignments are interchangeable

The antimicrobial activities of compounds **7a-i, 8a-h, 10a-i** and **11a-i** were screened against two Gram +ve strains (*Staphylococcus aureus* ATCC 25923 and methicillin resistant *Staphylococcus aureus* ATCC BAA-1683) and four Gram -ve strains (*Escherichia coli* ATCC 25922, *Pseudomonas aeruginosa* ATCC 27853, *Salmonella typhimurium* ATCC 14026 and *Klebsiella pneumonia* ATCC 314588).

Microbial cultures were grown overnight at 37 °C in nutrient broth (UKZN Biolab, South Africa), adjusted to 0.5 McFarland standard using distilled water. Mueller-Hinton agar (MHA) (Biolab, South Africa) plates were prepared by dissolving 38 g of agar in 1 L of water, pouring them into sterile 60 mm petri dishes and allowing them to set at room temperature. The agar plates were lawn inoculated with each respective strain of bacteria. A disc diffusion method was used for initial screening. A volume of 5 μL of a 10 mg mL^{-1} dimethyl sulfoxide (DMSO) solution of each test compound was then spotted onto antibiotic test discs (12 mm), which had been placed on an MHA plate and allowed to set. They were then left to incubate for 24 hours at 37 °C, following which the zones of inhibition were measured in millimeters.

Screening based on inhibitory zone diameter was used to select compounds and bacterial strains to be further tested in a minimum bactericidal concentration (MBC) study. Testing revealed that only compounds **7a-i** and **11a-h** showed activity, and only against the two Gram +ve bacterial strains.

The MBC study was conducted by swabbing microbial cultures (adjusted to 0.5 McFarland standard), prepared as previously described, evenly over sterile MHA plates. The test compounds were dissolved in DMSO and serially diluted. A volume of 5 µL of concentrations of 1.95 to 1000 µg mL^{-1} were directly spotted on MHA plates containing the respective bacterial strains and incubated at 37 °C for 24 hours to determine the MBC of each compound. The MBC value was taken as the lowest concentration at which a zone of inhibition was observed around the test compound. DMSO was used as a control and showed no zones of inhibition against *Staphylococcus aureus* ATCC 25923 or MRSA (ATCC BAA-1683). Levofloxacin and ciprofloxacin were used as standard drugs for comparison in all antimicrobial studies. All experiments were conducted in triplicate.

3.3. Results and discussion

Two small libraries of quinoxaline-pyrazoline-quinoline and quinoxaline-pyrazoline-phenyl hybrids, in yields of 37-90%, were formed by first synthesising the 2-acetyl-3-methylquinoxaline intermediate in a yield of 64% from *o*-phenylendiamine and acetylacetone (Anil Kumar et al., 2011). The reaction was conducted under mild conditions employing *N*-

bromosuccinamide as the catalyst in a slight molar excess to acetylacetone. This key intermediate was then reacted with two different types of aldehydes, simple aromatic aldehydes and quinoline aldehydes to form *α,β*-unsaturated ketones bridged between phenyl groups and quinoxalines on the one hand and quinolines and quinoxalines on the other.

The quinoline-2-carbaldehydes were synthesised from various anilines, substituted at either the 2- or 4- position, and crotonaldehyde in a Doebner-von Miller reaction, which resulted in substituted quinaldines (2-methylquinolines), which were subsequently oxidized by selenium dioxide to the desired aldehydic analogues. Formation of the pyrazoline derivatives were carried out by condensation of the *α,β*-unsaturated ketones with hydrazine hydrate (**Scheme 3-1**) (Voskienė and Mickevičius, 2009). The reactions proceeded within 4 hours and solid crystals were formed overnight in ethanolic solution in yields of 60-80%.

A slight modification was made to the procedures carried out in literature, which was the quinaldine intermediates not being purified en route to the quinoline aldehydes. Thus, this method is less time consuming than those previously reported (Gopaul and Koorbanally, 2016). The yields of the quinoline 2-carbaldehyde depend on substituent, but, in general, range between 70-90%.

The Claisen-Schmidt condensation producing the *α,β*-unsaturated ketones proceeds readily at room temperature in ethanolic media resulting in solid product precipitates similar to reports in literature with yields of 41-95% (Gopaul and Koorbanally, 2016). The 2'-OCH_3 derivative of the phenyl quinoxaline-chalcone hybrids, and the 8'-OCH_3 derivative of the quinoxaline-quinoline chalcone were not formed despite attempts at modifying the reaction procedure by varying reaction times, temperatures and ratios of reagents. The pyrazoline analogue of the 6'-OCH_3 derivative **8i** also failed even after extended reaction times.

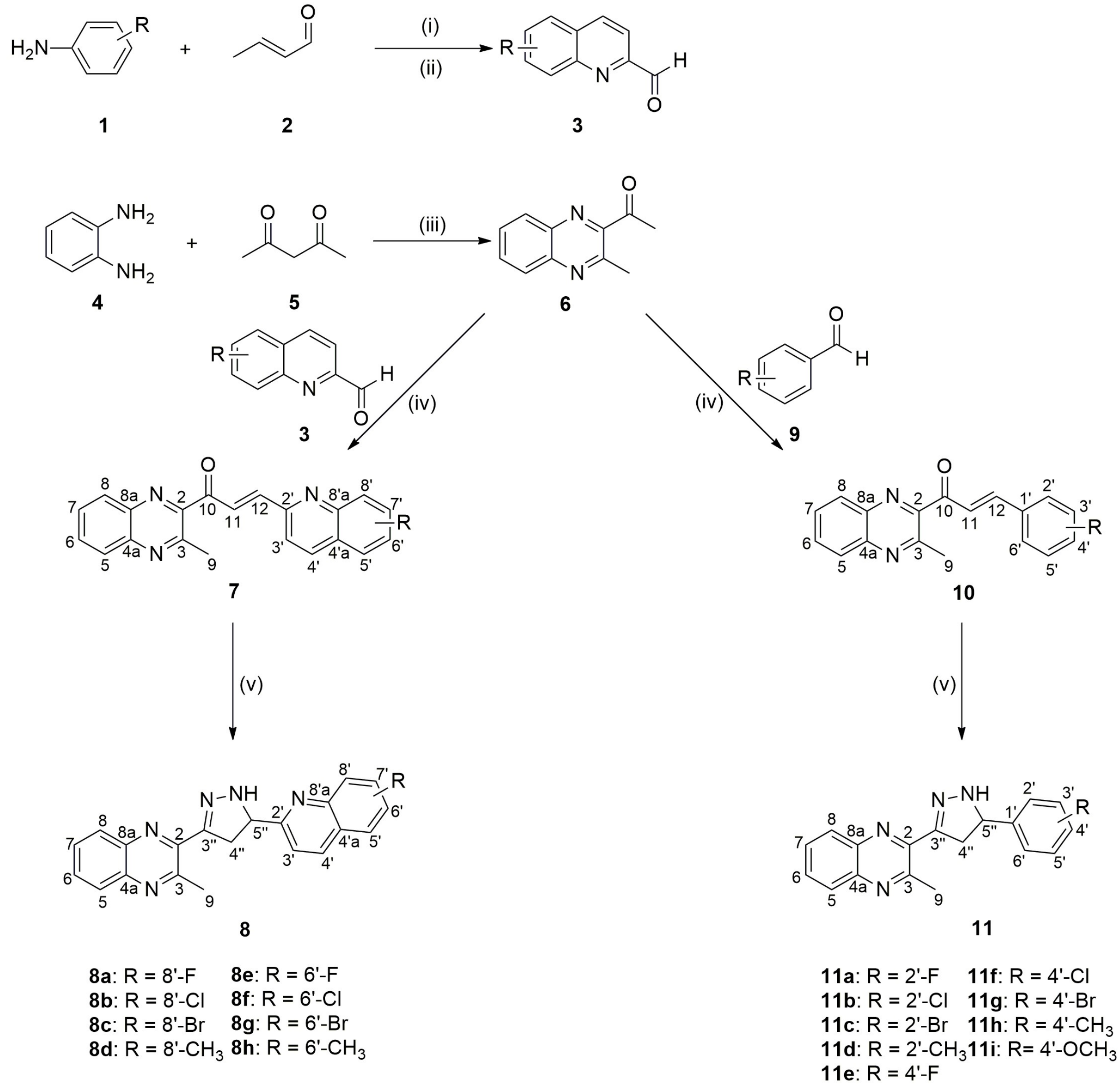

Scheme 3-1 Synthetic scheme for quinoxaline-chalcone and quinoxaline-pyrazoline hybrids (**8a-8h** and **11a-i**). (i) HCl(aq), toluene, reflux, 100 °C; (ii) SeO_2, 1,4-dioxane, reflux, 101 °C; (iii) *N*-bromosuccinamide, water, 100 °C; (iv) NaOH(aq), ethanol; (v) Hydrazine hydrate, ethanol, 78 °C.

A full structural elucidation of the quinoxaline-chalcone-quinoline hybdrids and quinoxaline chalcones and their pyrazoline analogues were carried out with the aid of 2D (HMBC, HSQC and COSY) NMR spectroscopy.

Structural elucidation

The ^{1}H NMR spectrum of the *α,β*-unsaturated ketone **7a** (the 8'-F derivative) contained twelve resonances, eleven of which were in the aromatic region. Both quinoline and quinoxaline resonances as well as the resonances of the *α,β*-unsaturated ketone moiety appear in the same aromatic region, hence HMBC spectra were needed to differentiate between the resonances and assign them to their respective scaffold. The methyl resonance CH_3-9 appeared at δ_H 3.00 in the ^{1}H NMR spectrum and was easily distinguished from the other resonances.

Of the 11 proton resonances in the aromatic region of the spectrum, the *α,β*-unsaturated olefinic resonances, H-11 and H-12 at δ_H 8.04 and δ_H 8.47, respectively could easily be distinguished due to their large J values of 16.1 Hz. The two *para* positioned protons on the quinoxaline scaffold, H-5 and H-8, appeared as double doublets at δ_H 8.20 (J = 8.4, 1.1 Hz) and δ_H 8.07 (J = 8.2, 1.1 Hz). These two resonances could not be distinguished from each other and are interchangeable, as were the H-6 and H-7 resonances, which appeared as triplets of doublets at δ_H 7.84 (J = 8.2, 1.5 Hz) and δ_H 7.77 (J = 8.3, 1.3 Hz).

The aromatic resonances, H-6' and H-7', both show coupling to fluorine at C-8'. H-6' couples to both protons, H-5' and H-7' and to fluorine, resulting in a ddd at δ_H 7.50 (J = 7.9, 7.9, 4.9 Hz). H-7' is also a ddd (δ_H 7.42) coupled to the fluorine (J = 8.9 Hz), H-6' (J = 7.6 Hz) and H-5' (J = 1.0 Hz). The coupled resonances of H-3' and H-4' appeared as doublets and double doublets, respectively at δ_H 7.86 (J = 8.6 Hz) and δ_H 8.24 (1H, dd, J = 8.6, 1.0 Hz), the small

J value of 1.0 Hz being due to either H-4' or F coupling. The assignment of H-3' also allowed us to differentiate between H-11 and H-12 as an HMBC correlation was observed between H-3' and C-12.

The ^{13}C NMR spectrum showed distinct resonances for the methyl group at δ_C 24.0 and the carbonyl group at δ_C 191.2. All protonated carbons were assigned using HSQC correlations to their respective protons. C-8', to which the fluorine is attached, occurs as a doublet at δ_C 158.3 with a large J value of 258.7 Hz and was confirmed by HMBC correlations to both the H-6' and H-7' resonances. Seven other resonances were observed at δ_C 129.7, 138.8, 139.8, 142.6, 148.1, 153.6 and 154.0. The most upfield resonance of this group, C-4'a occurred at δ_C 129.7 and was confirmed by HMBC correlations to H-6' and H-3'. C-4a and C-8a are found at δ_C 142.6 and δ_C 139.8, respectively. These resonances could be differentiated from C-3, C-2 and C-2' by HMBC correlations to the quinoxaline protons H-5 to H-8. However, these could not be unequivocally assigned and are interchangeable. C-2 (δ_C 153.6) and C-3 (δ_C 148.1), both have HMBC correlations to the methyl group at C-9, however, these were differentiated by the HMBC correlation of C-2 to H-11. C-2' (δ_C 154.0) was assigned due to an HMBC correlation with H-4'. **Figure 3-1** shows selected HMBC correlations used to identify the quaternary carbon resonances in the molecule.

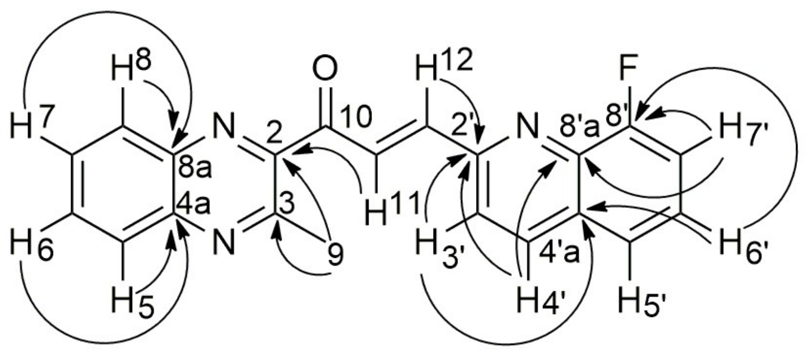

Figure 3-1 Key HMBC correlations used in the structural elucidation of **7a**

Conversion to the respective pyrazoline (**8a**) was indicated by the disappearance of the two *α,β*-unsaturated protons and the appearance of an ABX system with double doublets at δ_H 3.98 (J = 17.4, 11.7 Hz) and δ_H 3.68 (J = 17.4, 8.1 Hz) (H-4"a and H-4"b, respectively) and H-5" at δ_H 5.32 (J = 11.7, 8.1 Hz). This was also accompanied by slight shifts in the proton resonances of the quinoxaline fragment, for example the resonance at δ_H 8.20 attributed to H-5 or H-8 in the chalcone shifted to δ_H 7.94 in the pyrazoline and similarly the resonances at δ_H 7.84 and δ_H 7.77 assigned to H-6 and H-7 shifted to δ_H 7.66 and δ_H 7.61. In the quinoline fragment, only the H-3' resonance, closest to the pyrazoline moiety, shifted upfield significantly from δ_H 7.86 to δ_H 7.64. (**Figure 3-2**). Another distinct difference between the chalcone and pyrazoline derivatives is the shift of the carbonyl resonance at δ_C 191.1 (C-10) in the chalcone to δ_C 152.2 (C-3"), when this carbon now forms part of the pyrazoline moiety.

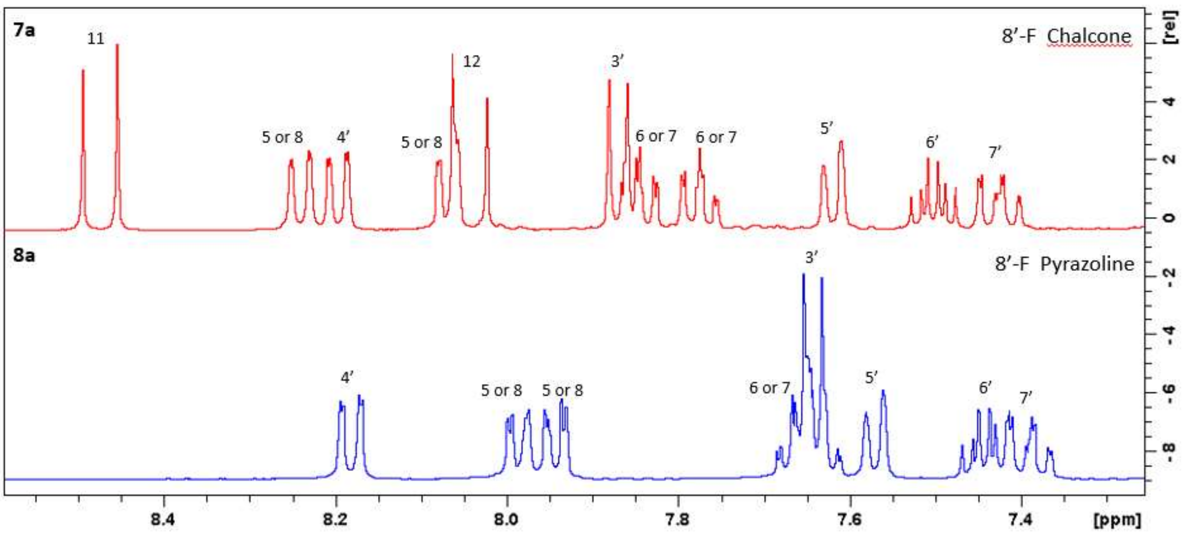

Figure 3-2 Overlaid [1]H NMR spectra of chalcone **7a** and its pyrazoline analogue **8a** showing the differences in chemical shifts of the aromatic protons when derivatisation occurs

Antibacterial activity

The synthesised compounds were tested for their antibacterial activity against two Gram +ve (*Staphylococcus aureus* ATCC 25923 and *S. aureus* ATCC BAA-1683 (MRSA)) and four Gram -ve species (*Klebsiella pneumonia*, *Pseudomonas aeruginosa*, *Escherichia coli* and *Salmonella typhimurium*) by doing a preliminary screen using the disc diffusion method. Of the compounds tested, only 13 compounds showed activity against *S. aureus* ATCC 25923 and 7 compounds against MRSA. In general, replacing the quinoline moiety with an aromatic ring in the quinoxaline chalcones resulted in loss of activtiy. The opposite is true for the pyrazole derivatives where only the quinoxaline pyrazolines with an aromatic ring showed some activity. Another general trend was that the quinoxaline chalcones with quinoline moeities were far more active (by 3 orders of magnitude) than the aromatic pyrazolines against *S. aureus*. There were however two pyrazolines, **11f** and **11g** (4'-Cl and 4'-Br derivatives), which were active at an order of magnitude greater than the other pyrazolines.

Eight quinoxaline-chalcone-quinoline derivatives showed two orders of magnitude better activity than both ciprofloxacin and levofloxacin against *S. aureus*, which had MBC values of 94.3 and 21.6 μM, respectively. The activities of six of the compounds (**7a**-**7c** and **7e**-**7g**) ranged from 0.151 – 0.178 μM, with a further two (**7h** and **7i**) having activities of 0.360 and 0.343 μM. Our results indicated that all derivatives with halogens at either the 6' or 8' positions led to good activity. Loss of activity occurred when electron donating substituents were placed at these positions, such as methyl and methoxy groups. With the exception of **7f** (6'-Cl derivative), the same set of compounds were active against MRSA. Compounds **7a**, **7b**, **7e** and **7i** were active between 10.9-91.0 μM, better than the standards, ciprofloxacin and levofloxacin which were active at 188.6 and 86.5 μM, respectively. All these compounds contained a halogen, with the exception of **7i**, which contained a methoxy group at the 6' position. The bromo derivatives **7c** (8'-Br) and **7g** (6'-Br) showed less potent activity against MRSA at 618 and 309 μM respectively.

Table 3-1 Antibacterial activity of the synthesised compounds (MBC in μM)

No.	*Sa*	MRSA	**No.**	*Sa*	MRSA
7a	0.178	22.8	**11a**	816	-
7b	0.170	10.9	**11b**	387	-
7c	0.151	618	**11c**	681	-
7e	0.178	91.0	**11e**	-	-
7f	0.170	-	**11f**	12	-
7g	0.151	309	**11g**	11	-
7h	0.360	23.0	**Cip**	94.3	188.6
7i	0.343	87.9	**Lev**	21.6	86.5

Sa = Staphylococcus aureus; Cip = Ciprofloxacin; Lev = Levofloxacin

While the quinoxaline-chalcone-quinoline derivatives showed activity against both *S. aureus* ATCC 25923 and MRSA, the quinoxaline-pyrazolines with phenyl groups were only active against *S. aureus* ATCC 25923. In this case, only the halogenated derivatives were active. The three compounds with methyl and methoxy groups did not show any activity. The two *para* substituted compounds **11f** and **11g** (4'-Cl and 4'-Br) showed better activity (12.0 and 11.0 μM, respectively) than ciprofloxacin and levofloxacin (94.3 and 21.6 μM, respectively) but in the same order of magnitude.

3.4. Conclusion

A library of new quinoxaline derived chalcones (**7a-i** and **10a-i**) and their respective pyrazolines (**8a-h** and **11a-i**) were synthesised and evaluated for their *in vitro* antibacterial activity. Chalcones of both substituted benzaldehydes and substituted quinoline-2-carbaldehydes were synthesised by a base catalysed Claisen-Schmidt condensation with 2-

acetyl-3-methylquinoxaline in yields ranging from 41 to 95%. These were readily converted to their pyrazoline analogues using hydrazine hydrate, with the exception of the 6'-OCH_3 derivative, achieving good yields of 60 to 80%. The novel quinoxaline-chalcone-quinoline class showed good activity against the Gram +ve species, *S.aureus* and MRSA, in MBC assays while the aromatic derived chalcones did not. The quinoxaline-chalcone-quinoline derivatives, **7a**-**7c** and **7e-7i**, exhibited better activity (0.151-0.360 μM) against *S.aureus* than the standards, ciprofloxacin and levofloxacin, by two orders of magnitude. These compounds were found to be less active against MRSA, however, compounds **7a**, **7b** and **7h** remained more potent than the standards. Interestingly, the opposite trend was observed for the pyrazoline analogues as conversion of the *α,β*-ketone group to a pyrazoline in the quinoxaline-chalcone-quinoline hybrids resulted in loss of activity. Similar conversion of the aromatic chalcones to their pyrazoline analogues resulted in compounds **11a-c**, **11f** and **11g** showing activity (11-816 μM) against *S. aureus* only with **11f** and **11g** having better activity (12.0 and 11.0 μM respectively) than the standards. The results of the study have revealed promising compounds for further development as antimicrobial agents

3.5. References

Anil Kumar, B. S. P., Madhav, B., Harsha Vardhan Reddy, K. and Nageswar, Y. V. D. Quinoxaline synthesis in novel tandem one-pot protocol. Tetrahedron Lett., **2011**, 52, 2862-2865.

Ashok, D., Elsanoosi, M., Alanab, B. F. H., Sarasija, M. and Ravi, S. Solvent-free microwave assisted synthesis of morpholine–piperidine–pyrrolidine annulated quinoline-naphthyl based chalcones and their antimicrobial activity. Russ. J. Gen. Chem., **2016**, 86, 1120-1125.

Batovska, D. I. and Todorova, I. T. Trends in utilization of the pharmacological potential of chalcones. Curr. Clin. Pharmacol., **2010**, 5, 1-29.

Carta, A., Corona, P. and Loriga, M. Quinoxaline 1,4-dioxide: A versatile scaffold endowed with manifold activities. Curr. Med. Chem., **2005**, 12, 2259-2272.

Desai, N., Joshi, V. V., Rajpara, K. M., Vaghani, H. V. and Satodiya, H. M. Synthesis of quinoline-pyrazoline based thiazole derivatives endowed with antimicrobial activity. Indian J. Chem., Sect. B: Org. Chem. Incl. Med. Chem., **2013**, 52B, 1191-1201.

Desai, N. C., Rajpara, K. M. and Joshi, V. V. Synthesis and characterization of some new quinoline based derivatives endowed with broad spectrum antimicrobial potency. Bioorg. Med. Chem. Lett., **2012**, 22, 6871-6875.

El Newahie, A. M. S., Ismail, N. S. M., Abou El Ella, D. A. and Abouzid, K. A. M. Quinoxaline-based scaffolds targeting tyrosine kinases and their potential anticancer activity. Arch. Pharm., **2016**, 349, 309-326.

Fadda, A. A., Abdelrazek, F. M. and Fouda, A. M. Studies with aza-heterocyclic *N*-oxides: Synthesis of some new aromatic *N*-oxide derivatives. Eur. J. Chem., **2011**, 2(1), 51-57.

Gopaul, K. and Koorbanally, N. A. Synthesis and structure elucidation of a series of chloroquinoline-2-chalcones by the Doebner-Miller reaction. Magn. Reson. Chem., **2016**, 54, 677-683.

Gopinath, V. S., Rao, M., Shivahare, R., Vishwakarma, P., Ghose, S., Pradhan, A., Hindupur, R., Sarma, K. D., Gupta, S., Puri, S. K., Launay, D. and Martin, D. Design, synthesis, ADME characterization and antileishmanial evaluation of novel substituted quinoline analogs. Bioorg. Med. Chem. Lett., **2014**, 24, 2046-2052.

Gutteridge, C. E., Nichols, D. A., Curtis, S. M., Thota, D. S., Vo, J. V., Gerena, L., Montip, G., Asher, C. O., Diaz, D. S., DiTusa, C. A., Smith, K. S. and Bhattacharjee, A. K. *In vitro* and *in vivo* efficacy and *in vitro* metabolism of 1-phenyl-3-aryl-2-propen-1-ones against *Plasmodium falciparum*. Bioorg. Med. Chem. Lett., **2006**, 16, 5682-5686.

Ismail, M. M. F., Ammar, Y. A., Ibrahim, M. K., El-Zahaby, H. S. A. and Mahmoud, S. S. Synthesis and pharmacological evaluation of novel quinoxalines as potential nonulcerogenic anti-inflammatory and analgesic agents. Arzneim. Forsch., **2005**, 55, 738-743.

Kendre, M. and Baseer, M. Synthesis and evaluation of some new pyrazoline derivatives as antimicrobial agents. Orient. J. Chem, **2013**, 29, 253-256.

Shibinskaya, M. O., Lyakhov, S. A., Mazepa, A. V., Andronati, S. A., Turov, A. V., Zholobak, N. M. and Spivak, N. Y. Synthesis, cytotoxicity, antiviral activity and interferon inducing ability of 6-(2-aminoethyl)-6*H*-indolo[2,3-b]quinoxalines. Eur. J. Med. Chem., **2010**, 45, 1237-1243.

Tseng, C.-H., Chen, Y.-L., Hsu, C.-Y., Chen, T.-C., Cheng, C.-M., Tso, H.-C., Lu, Y.-J. and Tzeng, C.-C. Synthesis and antiproliferative evaluation of 3-phenylquinolinylchalcone derivatives against non-small cell lung cancers and breast cancers. Eur. J. Med. Chem., **2013**, 59, 274-282.

van Heerden, L., Cloete, T. T., Breytenbach, J. W., de Kock, C., Smith, P. J., Breytenbach, J. C. and N'Da, D. D. Synthesis and *in vitro* antimalarial activity of a series of bisquinoline and bispyrrolo[1,2a]quinoxaline compounds. Eur. J. Med. Chem., **2012**, 55, 335-345.

Voskienė, A. and Mickevičius, V. Cyclization of chalcones to isoxazole and pyrazole derivatives. Chem. Heterocycl. Compd., **2009**, 45, 1485-1488.

Zhang, K., Wang, C., Wang, X., Zheng, H., Zhao, J., Wang, M., Xiao, S., Fei, C., Zheng, W., Zhang, L. and Xue, F. Synthesis, *in-vitro* activity and metabolic properties of quinocetone and structurally similar compounds. Iranian J. Pharm. Res., **2017**, 16, 569-585.

Zhang, M., Dai, Z.-C., Qian, S.-S., Liu, J.-Y., Xiao, Y., Lu, A.-M., Zhu, H.-L., Wang, J.-X. and Ye, Y.-H. Design, synthesis, antifungal, and antioxidant activities of (*E*)-6-((2-phenylhydrazono)methyl)quinoxaline derivatives. J. Agric. Food Chem., **2014**, 62, 9637-9643.

Chapter 4. Synthesis and antibacterial activity of quinoline-thioxothiazolidin-4-one hybrids

Abstract

A total of 10 new 5-(quinolin-2-ylmethylene)-2-thioxothiazolidin-4-ones were synthesised from the Knoevenagel reaction of various 8- and 6-substituted quinoline-2-carbaldehydes and rhodanine. The method described is a convenient way to tag a rhodanine moeity onto a quinoline ring. Full structural elucidation of the novel compounds was made with the aid of 2D NMR. The 6-substituted compounds showed antibacterial activity against the Gram+ve strains *S. aureus* and MRSA. The 6-Br derivative was found to be the most potent with an MBC value of 356 μM against both MRSA and *S.aureus*.

Keywords: quinolines, thioxothiazolidinones, thiazolidines, antibacterial activity

4.1. Introduction

Hybrid molecules combine two or more classes of organic molecules into a single molecule with the aim of enhancing the activity that each of the individual moieties have on their own. Quinolines and rhodanines are each known to have a range of bioactivities that make them good candidates for molecular hybridisation (Kumar et al., 2009; Tomasic and Masic, 2009). Quinoline is composed of a pyridine ring fused with benzene while rhodanine is a 5 membered heterocycle based on the thiazolidine core having a carbonyl group at C-4.

Quinolines are known to have antimalarial (Vandekerckhove and D'hooghe, 2015), anticancer (Afzal et al., 2015; Gopaul et al., 2015), anti-oxidant (Maddela et al., 2015), anti-HIV (Luo et al., 2009), antimicrobial (Musiol et al., 2011), antileishmanial (Gopinath et al., 2013; Gopinath et al., 2014), antimycobacterial (Eswaran et al., 2010), and anticonvulsant activities (Siddiqui, 2010), and is found in many commercially available drugs such as quinine (antimalarial), levofloxacin (antibiotic), ciprofloxacin (antibiotic), clioquinol (antifungal), montelukast (antiasthmatic), bosutinib (antileukaemic), bedaquiline (antitubercular) and saquinavir (anti-HIV). On the other hand, rhodanine derivatives have reported antibacterial (Grant et al., 2000; Pardasani et al., 2001), antifungal (Habib et al., 1997; Inamori et al., 1998; Siddiqui et al., 2005), antiviral (Sing et al., 2001), antimalarial (Takasu et al., 2002; Kumar et al., 2007), antitumor (Kawakami et al., 1997), anti-inflammatory (Irvine et al., 2008) and antidiabetic (Terashima et al., 1984) activities, and is incorporated in epalrestat, a carboxylic acid derivative commercially available for the treatment of neuropathy associated with type II diabetes.

Rhodanine moeities are tagged onto other organic scaffolds using the Knoevenagel condensation of rhodanine with aldehydes (Bataille et al., 2017) and, in particular, have been tagged onto substituted 2-chloroquinoline-3-carbaldehydes (Guo et al., 2013; Ramesh et al., 2014; Subhedar et al., 2017). These compounds showed potent antibacterial activity against methicillin resistant *Staphylococcus aureus* (MRSA) and quinolone resistant *Staphylococcus aureus* (QRSA) (Guo et al., 2013), anticancer activity (Ramesh et al., 2014) and antitubercular activity (Subhedar et al., 2017). Previously, substituted rhodanines were prepared by the reaction of substituted primary amines, carbon disulfide and sodium chloroacetate (Ramesh et al., 2014). In a slightly different synthetic route, 7-chloro-4-aminoquinoline-rhodanine hybrids were formed using carbon disulfide and ethylbromoacetate, which formed the rhodanine moeity at the amino group on the quinoline itself. These compounds showed good activity as antimalarial and antitubercular compounds with low cytotoxicity (Chauhan et al., 2013). Quinoline-6-rhodanine hybrids formed from rhodanine and quinoline-6-carbaldehyde showed good anticancer and anti-Alzheimer's activity (Mariano et al., 2016).

This paper describes the synthesis of a series of 6- and 8-substituted quinoline-2-rhodanine hybrids and their antibacterial activity against four Gram -ve and two Gram +ve bacterial strains.

4.2. Experimental

Chemistry

General Procedures

All reagents and chemicals used in this study were purchased from Sigma-Aldrich *via* Capital Lab, South Africa and were reagent grade. Crude organic solvents were distilled prior to use. Merck Kieselgel 60 F_{254} plates were used for thin-layer chromatography (TLC). For column chromatography, silica gel (60–120 mesh) was used as the stationary phase and varying ratios of ethyl acetate:hexane as the mobile phase. Melting points were obtained using a sealed capillary tube in an Electrothermal IA9100 melting point apparatus (Cole-Parmer, Staffordshire, UK). Infrared (IR) spectra were recorded on a Perkin Elmer Spectrum 100 FT-IR spectrometer (PerkinElmer Inc.) with universal attenuated total reflectance sampling accessory. Ultraviolet (UV) spectra were collected on a Shimadzu UV-3600 spectrophotometer (Shimadzu, Tokyo) in chlorobenzene. High resolution mass spectrometry (HRMS) was carried out using a Waters Micromax LCT Premier TOF-MS instrument (Microsep Pty, Ltd), operating at ambient temperatures. The ^{1}H and ^{13}C NMR spectra were recorded at 298 K in DMSO-d_6 using a Bruker Avance 400 MHz NMR spectrometer (9.4 T; Bruker, Germany) (400.22 MHz for ^{1}H and 100.63 MHz for ^{13}C). Chemical shifts are reported in ppm and coupling constants (J) in Hz. The ^{1}H and ^{13}C NMR chemical shifts of deuterated DMSO were δ 2.50 and 39.5, respectively, referenced to the internal standard, tetramethylsilane (TMS). All data was analysed using Bruker TopSpin 3.5 software.

Preparation of quinoline-2-carbaldehydes

Various 2- and 4- substituted anilines (**1a-j**) (45.0 mmol) were dissolved in HCl:water (1:2). The mixture was heated to 60 °C. Thereafter, crotonaldehyde (**2**) (67.5 mmol; 5.6 mL) dissolved in toluene (20 mL) was added slowly and the mixture allowed to reflux for 4 hours. The aqueous layer was then collected from the mixture and basified to pH 8. The solution was then extracted with 3 × 50 mL portions of ethyl acetate. The organic extracts were combined and dried over anhydrous $MgSO_4$ before the solvent was removed under vacuum. The residue was dissolved in 1,4-dioxane (20 mL) and SeO_2 (45.4 mmol; 5.0 g) was added. The mixture was then refluxed for 15 to 180 minutes (monitored by TLC). The resultant suspension was then filtered to remove the reduced selenium. The filtrate was diluted with water (40 mL) and the aqueous solution extracted with 3 × 50 mL portions of ethyl acetate. The combined extracts were washed with 2 × 50 mL portions of water and dried over anhydrous $MgSO_4$ and the solvent removed as above. The crude products were purified by column chromatography (hexane:ethyl acetate, 85:15 v/v) resulting in the carbaldehydes (**3a-j**) in yields of between 60-80%, depending on the substituent.

Preparation of quinoline-2-rhodanine derivatives

Acetic acid (30 mL) was added to a mixture of quinoline-2-carbaldehydes (**3a-j**) (1.00 mmol), 2-thioxothiazolin-4-one (**4**) (0.133 g; 1.00 mmol) and sodium acetate (0.246 g; 3.00 mmol) and refluxed for 4 to 6 hours. Once complete the reaction mixture was cooled to ambient temperature and poured into water (50 mL). The crude grey solid was collected by filtration, washed with water (3 x 20 mL) and recrystallized using methanol, resulting in pure products (**5a-j**) in yields of 52-80%.

(E)-5-((8-fluoroquinolin-2-yl)methylene)-2-thioxothiazolidin-4-one (**5a**), Yield 55%; yellow powder; decomp. 300°C; IR (neat) υ_{max} 3040 cm^{-1} (N-H), 1695 cm^{-1} (C=O); λ_{max} (log ε) = 394 (4.58), 313 (4.12), 293 (4.14), 258 (4.52); ^{1}H NMR ($CDCl_3$, 400 MHz) δ 13.75 (1H, s, N<u>H</u>), 8.56 (1H, d, J = 8.5 Hz, H-4), 8.06 (1H, d, J = 8.5 Hz, H-3), 7.85 (1H, d, J = 7.9 Hz, H-5), 7.84 (1H, s, H-9), 7.73-7.62 (2H, m, H-6/7); ^{13}C NMR ($CDCl_3$, 100 MHz) δ 202.6 (C, C-2'), 169.3 (C, C-4'), 157.0 (C, d, J = 256.8 Hz, C-8), 151.8 (C, C-2), 137.3 (CH, C-4), 137.0 (C, d, J = 12.8 Hz, C-8a), 132.6 (C, C-5'), 128.5 (C, C-4a), 127.8 (CH, d, J = 8.0 Hz, C-6), 126.2 (CH, C-9), 125.4 (CH, C-3), 123.9 (CH, d, J = 4.5 Hz, C-5), 114.6 (CH, d, J = 17.8 Hz, C-7); HRMS (*neg*) *m/z* 288.9911 [M-H] (calcd. for $C_{13}H_6FN_2OS_2$ 288.9906)

(E)-5-((8-chloroquinolin-2-yl)methylene)-2-thioxothiazolidin-4-one (**5b**), Yield 54%; yellow powder; decomp. 295°C; IR (neat) υ_{max} 3046 cm^{-1} (N-H), 1690 cm^{-1} (C=O); λ_{max} (log ε) = 396 (4.66), 315 (4.22), 297 (4.22), 259 (4.68); ^{1}H NMR ($CDCl_3$, 400 MHz) δ 13.75 (1H, s, N<u>H</u>), 8.57 (1H, d, J = 8.4 Hz, H-4), 8.07 (1H, d, J = 8.4 Hz, H-3), 8.05 (1H, d, J = 7.8 Hz,

H-7), 8.01 (1H, d, J = 7.8 Hz, H-5), 7.86 (1H, s, H-9), 7.65 (1H, t, J = 7.8 Hz, H-6); ^{13}C NMR ($CDCl_3$, 100 MHz) δ 202.4 (C, C-2'), 169.4 (C, C-4'), 152.2 (C, C-2), 143.3 (C, C-8a), 138.1 (CH, C-4), 132.5 (C, C-5'), 132.4 (C, C-8), 130.7 (CH, C-7), 128.5 (C, C-4a), 127.8 (CH, C-6), 127.4 (CH, C-5), 126.2 (CH, C-9), 125.6 (CH, C-3); HRMS (*neg*) m/z 304.9605 [M-H] (calcd. for $C_{13}H_6ClN_2OS_2$ 304.9610)

(E)-5-((8-bromoquinolin-2-yl)methylene)-2-thioxothiazolidin-4-one (**5c**), Yield 52%; orange powder; decomp. 256°C; IR (neat) υ_{max} 3057 cm^{-1} (N-H), 1689 cm^{-1} (C=O); λ_{max} (log ε) = 398 (4.37), 297 (3.99); ^{1}H NMR ($CDCl_3$, 400 MHz) δ 13.74 (1H, s, N<u>H</u>), 8.57 (1H, d, J = 8.4 Hz, H-4), 8.07 (1H, d, J = 8.4 Hz, H-3), 8.25 (1H, d, J = 7.8 Hz, H-7), 8.06 (1H, d, J = 7.8 Hz, H-5), 7.86 (1H, s, H-9), 7.58 (1H, t, J = 7.8 Hz, H-6); ^{13}C NMR ($CDCl_3$, 100 MHz) δ 202.2 (C, C-2'), 169.5 (C, C-4'), 152.4 (C, C-2), 144.3 (C, C-8a), 138.3 (CH, C-4), 134.4 (CH, C-7), 132.3 (C, C-5'), 128.7 (C, C-4a), 128.3 (CH, C-5), 128.1 (CH, C-6), 126.3 (CH, C-9), 125.8 (CH, C-3), 123.8 (C, C-8); HRMS (*neg*) m/z 348.9105 [M-H] (calcd. for $C_{13}H_6BrN_2OS_2$ 348.9105)

(E)-5-((8-methylquinolin-2-yl)methylene)-2-thioxothiazolidin-4-one (**5d**), Yield 80%; bright yellow powder; decomp. 271°C; IR (neat) υ_{max} 3037 cm^{-1} (N-H), 1687 cm^{-1} (C=O); λ_{max} (log ε) = 394 (4.56), 314 (4.03), 258 (4.56); ^{1}H NMR ($CDCl_3$, 400 MHz) δ 13.75 (1H, s, N<u>H</u>), 8.47 (1H, d, J = 8.4 Hz, H-4), 7.99 (1H, d, J = 8.4 Hz, H-3), 7.86 (1H, d*, H-7), 7.86 (1H, s*, H-9), 7.74 (1H, d, J = 7.5 Hz, H-5), 7.58 (1H, t, J = 7.5 Hz, H-6), 2.82 (3H, s, C<u>H</u>$_3$); ^{13}C NMR ($CDCl_3$, 100 MHz) δ 202.0 (C, C-2'), 169.4 (C, C-4'), 150.3 (C, C-2), 146.5 (C, C-8a), 137.7 (CH, C-4), 136.7 (C, C-8), 130.8 (C, C-5'), 130.6 (CH, C-5), 127.5 (CH, C-6), 127.1 (C, C-4a), 127.1 (CH, C-9), 125.9 (CH, C-7), 124.3 (CH, C-3), 19.3 (<u>C</u>H$_3$); HRMS (*neg*) m/z 285.0161 [M-H] (calcd. for $C_{14}H_9N_2OS_2$ 285.0156)

* resonances overlap, J values cannot be determined.

(E)-5-((8-methoxyquinolin-2-yl)methylene)-2-thioxothiazolidin-4-one (**5e**), Yield 60%; orange powder; mp 288-289 °C; IR (neat) υ_{max} 3038 cm^{-1} (N-H), 1688 cm^{-1} (C=O); λ_{max} (log ε) = 399 (4.66), 328 (4.26), 264 (4.65); ^{1}H NMR (CDCl$_3$, 400 MHz) δ 13.64 (1H, s, N<u>H</u>), 8.41 (1H, d, J = 8.4 Hz, H-4), 7.96 (1H, d, J = 8.4 Hz, H-3), 7.81 (1H, s, H-9), 7.59 (1H, t, J = 7.9 Hz, H-6), 7.52 (1H, d, J = 7.9 Hz, H-5), 7.29 (1H, d, J = 7.9 Hz, H-7), 4.06 (3H, s, OC<u>H</u>$_3$); ^{13}C NMR (CDCl$_3$, 100 MHz) δ 203.6 (C, C-2'), 169.4 (C, C-4'), 155.3 (C, C-8), 149.9 (C, C-2), 139.1 (C, C-8a), 137.0 (CH, C-4), 131.5 (C, C-5'), 128.3 (CH, C-6), 128.0 (C, C-4a), 126.8 (CH, C-9), 124.8 (CH, C-3), 119.1 (CH, C-5), 109.2 (CH, C-7), 56.1 (O<u>C</u>H$_3$); HRMS (*neg*) *m*/*z* 301.0099 [M-H] (calcd. for $C_{14}H_9N_2O_2S_2$ 301.0105)

(E)-5-((6-fluoroquinolin-2-yl)methylene)-2-thioxothiazolidin-4-one (**5f**), Yield 68%; yellow powder; mp 303-305 °C; IR (neat) υ_{max} 3028 cm^{-1} (N-H), 1691 cm^{-1} (C=O); λ_{max} (log ε) = 393 (4.66), 292 (4.21), 257 (4.62); ^{1}H NMR (CDCl$_3$, 400 MHz) δ 13.73 (1H, s, N<u>H</u>), 8.45 (1H, d, J = 8.5 Hz, H-4), 8.19 (1H, dd, J = 9.2, 5.4, H-5), 7.98 (1H, d, J = 8.5 Hz, H-3), 7.81 (1H, d, J = 9.3, 2.7 Hz, H-8), 7.78 (1H, s, H-9), 7.74 (1H, td, J = 8.9, 2.8 Hz, H-7); ^{13}C NMR (CDCl$_3$, 100 MHz) δ 202.2 (C, C-2'), 169.3 (C, C-4'), 160.4 (C, d, J = 248.0 Hz, C-6), 151.2 (C, d, J = 2.7 Hz, C-2), 144.3 (C, C-8a), 136.9 (CH, d, J = 5.5 Hz, C-4), 131.5 (C, C-5'), 131.3 (CH, d, J = 9.5 Hz, C-8), 127.7 (C, d, J = 10.8 Hz, C-4a), 126.6 (CH, C-9), 125.3 (CH, C-3), 120.9 (CH, d, J = 26.2 Hz, C-7), 111.2 (CH, d, J = 22.2 Hz, C-5); HRMS (*neg*) *m*/*z* 288.9908 [M-H] (calcd. for $C_{13}H_6FN_2OS_2$ 288.9906)

(E)-5-((6-chloroquinolin-2-yl)methylene)-2-thioxothiazolidin-4-one (**5g**), Yield 65%; yellow powder; decomp. 290 °C; IR (neat) υ_{max} 3047 cm^{-1} (N-H), 1716 cm^{-1} (C=O); λ_{max} (log ε) = 397 (4.65), 294 (4.21), 258 (4.70); ^{1}H NMR (CDCl$_3$, 400 MHz) δ 13.77 (1H, s, N<u>H</u>), 8.45 (1H, d, J = 8.5 Hz, H-4), 8.16 (1H, d, J = 2.3, H-5), 8.15 (1H, d, J = 9.0 Hz, H-8), 8.01 (1H, d, J = 8.5 Hz, H-3), 7.84 (1H, dd, J = 9.0, 2.3 Hz, H-7), 7.80 (1H, s, H-9); ^{13}C NMR (CDCl$_3$, 100 MHz) δ 202.1 (C, C-2'), 169.3 (C, C-4'), 152.1 (C, C-2), 145.5 (C, C-8a), 136.7 (CH, C-

4), 132.2 (C, C-6), 132.1 (C, C-5'), 131.3 (CH, C-7), 130.4 (CH, C-8), 127.6 (C, C-4a), 126.8 (CH, C-5), 126.4 (CH, C-9), 125.5 (CH, C-3); HRMS (*neg*) *m/z* 304.9605 [M-H] (calcd. for $C_{13}H_6ClN_2OS_2$ 304.9610)

(E)-5-((6-bromoquinolin-2-yl)methylene)-2-thioxothiazolidin-4-one (**5h**), Yield 64%; dark yellow-green powder; decomp. 258 °C; IR (neat) υ_{max} 3047 cm^{-1} (N-H), 1695 cm^{-1} (C=O); λ_{max} (log ε) = 394 (4.66), 313 (4.20), 293 (4.22), 258 (4.60); ^{1}H NMR ($CDCl_3$, 400 MHz) δ 13.75 (1H, s, N<u>H</u>), 8.43 (1H, d, *J* = 8.4 Hz, H-4), 8.30 (1H, d, *J* = 1.7, H-5), 8.05 (1H, d, *J* = 9.0 Hz, H-8), 7.99 (1H, d, *J* = 8.4 Hz, H-3), 7.92 (1H, dd, *J* = 9.0, 1.7 Hz, H-7), 7.78 (1H, s, H-9); ^{13}C NMR ($CDCl_3$, 100 MHz) δ 202.1 (C, C-2'), 169.2 (C, C-4'), 152.1 (C, C-2), 145.6 (C, C-8a), 136.6 (CH, C-4), 133.8 (CH, C-7), 132.1 (C, C-5'), 130.4 (CH, C-8), 130.0 (CH, C-5), 128.0 (C, C-4a), 126.4 (CH, C-9), 125.5 (CH, C-3); 120.9 (C, C-6); HRMS (*neg*) *m/z* 348.9106 [M-H] (calcd. for $C_{13}H_6BrN_2OS_2$ 348.9105)

(E)-5-((6-methylquinolin-2-yl)methylene)-2-thioxothiazolidin-4-one (**5i**), Yield 75%; yellow powder; decomp. 268 °C; IR (neat) υ_{max} 3027 cm^{-1} (N-H), 1690 cm^{-1} (C=O); λ_{max} (log ε) = 394 (4.58), 293 (4.09), 258 (4.60); ^{1}H NMR ($CDCl_3$, 400 MHz) δ 13.70 (1H, s, N<u>H</u>), 8.38 (1H, d, *J* = 8.4 Hz, H-4), 8.05 (1H, d, *J* = 8.6 Hz, H-8), 7.94 (1H, d, *J* = 8.4 Hz, H-3), 7.80 (1H, s, H-9), 7.78 (1H, bs, H-5), 7.70 (1H, d, *J* = 8.6 Hz, H-7), 2.53 (3H, s, $C\underline{H}_3$); ^{13}C NMR ($CDCl_3$, 100 MHz) δ 202.4 (C, C-2'), 169.3 (C, C-4'), 150.7 (C, C-2), 145.7 (C, C-8a), 137.9 (C, C-6), 136.6 (CH, C-4), 133.0 (CH, C-7), 130.9 (C, C-5'), 128.2 (CH, C-8), 127.0 (CH, C-9), 127.0 (C, C-4a), 126.7 (CH, C-5), 124.7 (CH, C-3), 21.2 ($\underline{C}H_3$); HRMS (*neg*) *m/z* 285.0157 [M-H] (calcd. for $C_{14}H_9N_2OS_2$ 285.0156)

(E)-5-((6-methoxyquinolin-2-yl)methylene)-2-thioxothiazolidin-4-one (**5j**), Yield 58%; orange powder; decomp. 270 °C; IR (neat) υ_{max} 3018 cm^{-1} (N-H), 1688 cm^{-1} (C=O); λ_{max} (log ε) = 419 (4.67), 400 (4.70), 295 (4.12), 260 (4.46); ^{1}H NMR ($CDCl_3$, 400 MHz) δ 13.68 (1H, s, N<u>H</u>), 8.35 (1H, d, *J* = 8.4 Hz, H-4), 8.03 (1H, d, *J* = 9.2 Hz, H-8), 7.91 (1H, d, *J* = 8.4 Hz,

H-3), 7.77 (1H, s, H-9), 7.48 (1H, dd, J = 9.2, 2.7 Hz, H-7), 7.41 (1H, d, J = 2.7 Hz, H-5), 3.92 (3H, s, OC$\underline{H}_3$); ^{13}C NMR (CDCl$_3$, 100 MHz) δ 202.3 (C, C-2'), 169.3 (C, C-4'), 158.4 (C, C-6), 149.0 (C, C-2), 143.3 (C, C-8a), 135.9 (CH, C-4), 130.0 (C-8/C-5'), 128.4 (C, C-4a), 127.2 (CH, C-9), 125.0 (CH, C-3), 123.5 (CH, C-7), 105.7 (CH, C-5), 55.7 (O$\underline{C}H_3$); HRMS (*neg*) *m*/*z* 301.0106 [M-H] (calcd. for $C_{14}H_9N_2O_2S_2$ 301.0105)

Antibacterial assays

Compounds **5a-j** were screened against two Gram +ve (*Staphylococcus aureus* ATCC 25923 and methicillin resistant *Staphylococcus aureus* ATCC BAA-1683 (MRSA)) and four Gram -ve bacterial strains (*Escherichia coli* ATCC 25922, *Pseudomonas aeruginosa* ATCC 27853, *Salmonella typhimurium* ATCC 14026 and *Klebsiella pneumonia* ATCC 314588).

Bacterial cultures were grown overnight in nutrient broth (UKZN Biolab, South Africa) at 37 °C and adjusted to a 0.5 McFarland standard using distilled water. Mueller-Hinton agar (MHA) (Biolab, South Africa) plates were prepared by dissolving 38 g of agar in 1 L of water, pouring this into sterile 60 mm petri dishes and allowing them to set at room temperature. Agar plates were thereafter inoculated with the respective bacterial strains. A volume of 5 µL of each test compound (10 mg mL^{-1} DMSO) was then spotted onto antibiotic test discs (12 mm), which had been placed on an MHA plate and incubated for 24 hours at 37 °C. Thereafter, the zones of inhibition were measured using a transparent ruler.

For the MBC assay, agar plates were prepared and inoculated with the two Gram +ve bacterial strains described above. The test compounds were dissolved in DMSO and serially diluted from 1000 to 1.95 µg mL^{-1} and directly spotted on the MHA plates in 5 µL aliquots, which were were incubated at 37 °C for 24 hours to determine the MBC values. The MBC value was taken as the lowest concentration at which a zone of inhibition was observed. No zones of inhibition were observed against *Staphylococcus aureus* ATCC 25923 or MRSA (ATCC BAA-1683) for the DMSO solvent control. Levofloxacin and ciprofloxacin were employed as standard drugs for comparison in all antimicrobial studies. All experiments were conducted in triplicate and an average of the readings taken.

4.3. Results and Discussion

A series of quinoline-rhodanine hybrids were synthesised in a three step reaction, commencing with the preparation of the substituted quinaldines, oxidation to the quinoline-2-carbaldehydes and finally a Knoevenagel condensation with rhodanine (2-thioxo-4-thiazolidinone) (**Scheme 4-1**). For the preparation of the quinaldines, various 2 and 4 substituted anilines were reacted with crotonaldehyde in an acid catalysed Doebner-von Miller reaction. Neutralisation, extraction and concentration steps yielded a crude reaction mixture, which was oxidised in a further step without purification by selenium dioxide, resulting in quinoline-2-carbaldehydes, which were isolated by column chromatography in yields of 60-80%. Avoiding isolation of the quinaldine precursors resulted in less solvent being used and a shorter route to the final product compared to previous procedures reported in literature (Gopaul and Koorbanally, 2016). The final step resulted in various 6- and 8- substituted quinoline-rhodanine hybrids in moderate to good yields of 52-80%. The reaction was conducted in acetic acid and catalysed by sodium acetate.

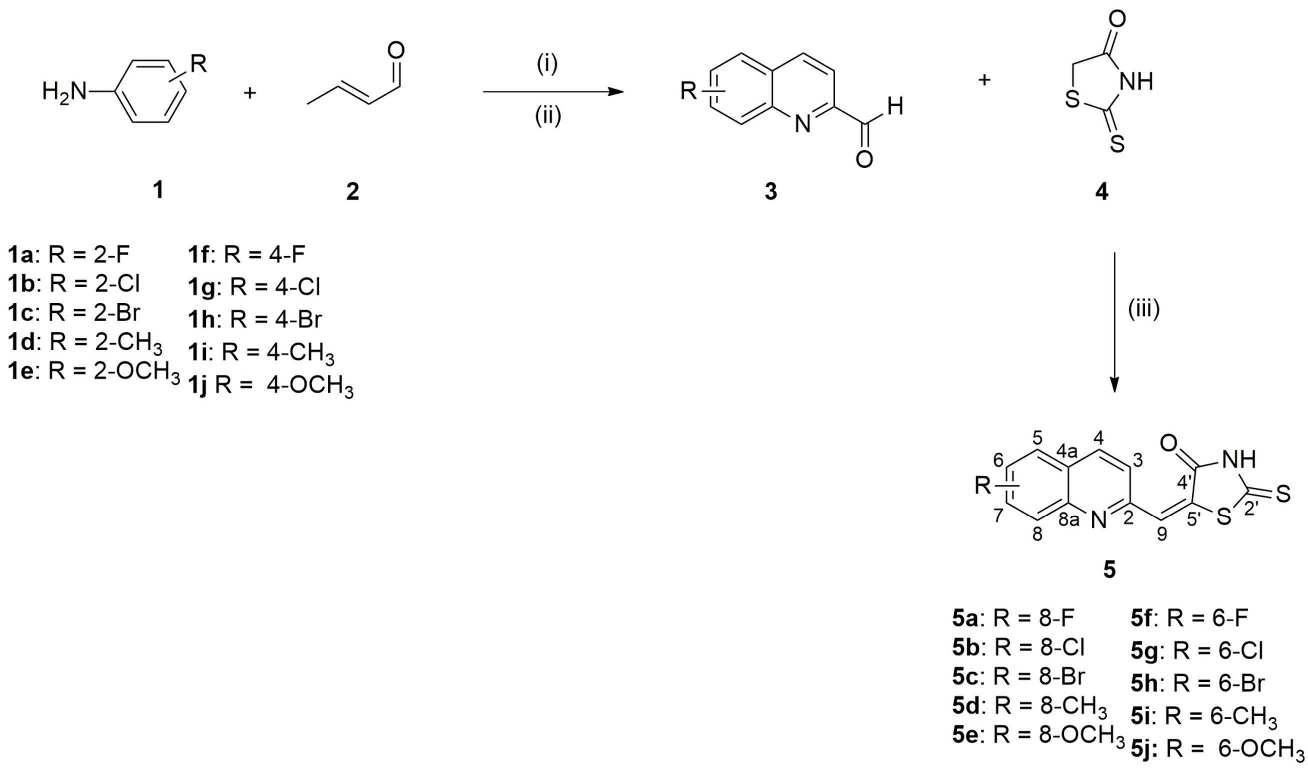

Scheme 4-1 Synthetic scheme to the quinoline rhodanine hybrid molecules (**5a-j**). (i) HCl(aq), toluene, reflux, 100 °C; (ii) SeO_2, 1,4-dioxane, reflux, 101 °C; (iii) CH_3COONa, CH_3COOH, reflux, 100 °C

Unambiguous elucidation of the quinoline-rhodanine hybrids was made using 2D (HMBC, HSQC and COSY) NMR spectroscopy. As an example, the ^{1}H NMR spectrum of **5g**, the 6-Cl derivative, contained seven resonances. The vinylic singlet assigned to H-9 at δ_H 7.80 was characteristic of hybrid formation. Since the chemical shift of H-9 for all compounds were less than δ8.0, they were assigned to the *E* configuration (Mendoza et al., 2014), which is expected since this is the thermodynamically favoured configuration. The distinctive NH proton belonging to the rhodanine moiety is visible as a broad singlet at δ_H 13.77. The five remaining ^{1}H signals were assigned to the quinoline scaffold with H-3 and H-4 appearing as doublets at δ_H 8.01 (J = 8.5 Hz) and δ_H 8.50 (J = 8.5 Hz), respectively. H-4 was differentiated from H-3 by HMBC correlations to C-8a and C-5. H-5 appears as a distinctive doublet at δ_H 8.16 with a small *meta* coupling of 2.3 Hz. H-7 is easily identified as the only doublet of doublets at δ_H 7.84 (J = 9.0, 2.3 Hz). The remaining doublet at δ_H 8.15 (J = 9.0 Hz) was assigned to H-8.

The ^{13}C NMR spectrum contained thirteen signals, with the six protonated carbons occurring at δ_C 125.5 (C-3), δ_C 136.7 (C-4), δ_C 126.8 (C-5), δ_C 131.2 (C-7), δ_C 130.4 (C-8) and δ_C 126.3 (C-9). C-2 was assigned to δ_C 152.1 due to HMBC correlations to H-9, H-3 and H-4. The C-4a and C-8a resonances on the quinoline ring were present at δ_C 127.6 and δ_C 145.5, assigned by their chemical shifts, which was confirmed by the HMBC correlation from H-3 to C-4a. The chlorinated carbon resonance, C-6, was assigned to δ_C 132.2, following HMBC correlations to H-5 and H-8. In the rhodanine moiety, the carbonyl carbon, C-4', was assigned to δ_C 169.4, while C-5' was assigned to δ_C 132.1. Both resonances showed HMBC correlations to H-9. The remaining resonance at δ_C 202.1 was ascribed to C-2'. Relevant HMBC correlations used for the structural elucidation are shown in **Figure 4-1**.

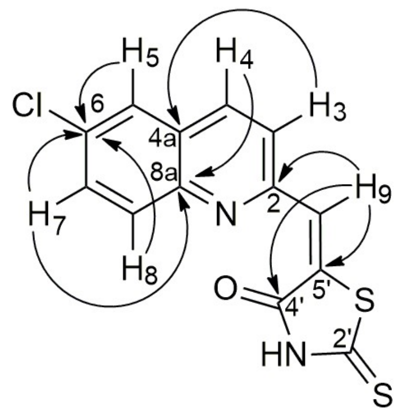

Figure 4-1 Key HMBC correlations used in the structural elucidation of **5g**

Antibacterial activity

The quinoline-rhodanine hybrids were screened for their antibacterial activity against two Gram +ve (*Staphylococcus aureus* ATCC 25923 and *S. aureus* ATCC BAA-1683 (MRSA)) and four Gram -ve strains of bacteria (*Klebsiella pneumonia*, *Pseudomonas aeruginosa*, *Escherichia coli* and *Salmonella typhimurium*). Initial screening using the disc diffusion method indicated that four of the synthesised compounds (**5f-i**) were active against the two Gram +ve bacteria and were further assayed to determine their minimum bactericidal concentration (MBC) values. Only the 6- substituted quinoline hybrids were active while none of the 8- substituted compounds showed any activity. In general, the synthesised compounds were less active than the standards, levofloxacin and ciprofloxacin. The most potent compound, **5h**, the 6-Br derivative, was active at 356 μM against both MRSA and *S. aureus*, the same order of magnitude to ciprofloxacin and an order of magnitude less than levofloxacin.

Table 4-1 Antibacterial activity of quinoline-2-rhodanine hybrids (MBC in μM)

No.	Bacterial strains	
	Sa	MRSA
5f	430	861
5g	1630	815
5h	356	356
5i	1746	1746
Cip	94.3	188.6
Lev	21.6	86.5

Sa = *Staphyloccocus aureus*; Cip = ciprofloxacin; Lev = levofloxacin

4.4. Conclusion

A convenient method to tag a rhodanine moeity onto a quinoline scaffold *via* an aldehyde group at the 2-position on the quinoline framework was carried out. A few of the synthesised molecules were active against *S. aureus* and MRSA, however they were not as active as the standards levofloxacin and ciprofloxacin. The most potent of all the synthesised compounds was the 6-bromo derivative, **5h**, active at 356 μM against both *S. aureus* and MRSA.

4.5. References

Afzal, O., Kumar, S., Haider, M. R., Ali, M. R., Kumar, R., Jaggi, M. and Bawa, S. A review on anticancer potential of bioactive heterocycle quinoline. Eur. J. Med. Chem., **2015**, 97, 871-910.

Bataille, C. J. R., Brennan, M. B., Byrne, S., Davies, S. G., Durbin, M., Fedorov, O., Huber, K. V. M., Jones, A. M., Knapp, S., Liu, G., Nadali, A., Quevedo, C. E., Russell, A. J., Walker, R. G., Westwood, R. and Wynne, G. M. Thiazolidine derivatives as potent and selective inhibitors of the PIM kinase family. Bioorg. Med. Chem., **2017**, 25, 2657-2665.

Chauhan, K., Sharma, M., Saxena, J., Singh, S. V., Trivedi, P., Srivastava, K., Puri, S. K., Saxena, J. K., Chaturvedi, V. and Chauhan, P. M. S. Synthesis and biological evaluation of a new class of 4-aminoquinoline–rhodanine hybrids as potent anti-infective agents. Eur. J. Med. Chem., **2013**, 62, 693-704.

Eswaran, S., Adhikari, A. V., Chowdhury, I. H., Pal, N. K. and Thomas, K. D. New quinoline derivatives: Synthesis and investigation of antibacterial and antituberculosis properties. Eur. J. Med. Chem., **2010**, 45, 3374-3383.

Gopaul, K. and Koorbanally, N. A. Synthesis and structure elucidation of a series of chloroquinoline-2-chalcones by the Doebner-Miller reaction. Magn. Reson. Chem., **2016**, 54, 677-683.

Gopaul, K., Shintre, S. A. and Koorbanally, N. A. A review on the synthesis and anti-cancer activity of 2-substituted quinolines. Anti-Cancer Agents Med. Chem., **2015**, 15, 631-646.

Gopinath, V. S., Pinjari, J., Dere, R. T., Verma, A., Vishwakarma, P., Shivahare, R., Moger, M., Kumar Goud, P. S., Ramanathan, V., Bose, P., Rao, M. V. S., Gupta, S., Puri, S. K., Launay, D. and Martin, D. Design, synthesis and biological evaluation of 2-substituted quinolines as potential antileishmanial agents. Eur. J. Med. Chem., **2013**, 69, 527-536.

Gopinath, V. S., Rao, M., Shivahare, R., Vishwakarma, P., Ghose, S., Pradhan, A., Hindupur, R., Sarma, K. D., Gupta, S., Puri, S. K., Launay, D. and Martin, D. Design, synthesis, ADME characterization and antileishmanial evaluation of novel substituted quinoline analogs. Bioorg. Med. Chem. Lett., **2014**, 24, 2046-2052.

Grant, E. B., Guiadeen, D., Baum, E. Z., Foleno, B. D., Jin, H., Montenegro, D. A., Nelson, E. A., Bush, K. and Hlasta, D. J. The synthesis and SAR of rhodanines as novel class C β-lactamase inhibitors. Bioorg. Med. Chem. Lett., **2000**, 10, 2179-2182.

Guo, M., Zheng, C.-J., Song, M.-X., Wu, Y., Sun, L.-P., Li, Y.-J., Liu, Y. and Piao, H.-R. Synthesis and biological evaluation of rhodanine derivatives bearing a quinoline moiety as potent antimicrobial agents. Bioorg. Med. Chem. Lett., **2013**, 23, 4358-4361.

Habib, N. S., Rida, S. M., Badawey, E. A. M., Fahmy, H. T. Y. and Ghozlan, H. A. Synthesis and antimicrobial activity of rhodanine derivatives. Eur. J. Med. Chem., **1997**, 32, 759-762.

Inamori, Y., Okamoto, Y., Takegawa, Y., Tsujibo, H., Sakagami, Y., Kumeda, Y., Shibata, M. and Numata, A. Insecticidal and antifungal activities of aminorhodanine derivatives. Biosci. Biotechnol. Biochem., **1998**, 62, 1025-1027.

Irvine, M. W., Patrick, G. L., Kewney, J., Hastings, S. F. and MacKenzie, S. J. Rhodanine derivatives as novel inhibitors of PDE4. Bioorg. Med. Chem. Lett., **2008**, 18, 2032-2037.

Kawakami, M., Koya, K., Ukai, T., Tatsuta, N., Ikegawa, A., Ogawa, K., Shishido, T. and Chen, L. B. Synthesis and evaluation of novel rhodacyanine dyes that exhibit antitumor activity. J. Med. Chem., **1997**, 40, 3151-3160.

Kumar, G., Parasuraman, P., Sharma, S. K., Banerjee, T., Karmodiya, K., Surolia, N. and Surolia, A. Discovery of a rhodanine class of compounds as inhibitors of *Plasmodium falciparum* enoyl-acyl carrier protein reductase. J. Med. Chem., **2007**, 50, 2665-2675.

Kumar, S., Bawa, S. and Gupta, H. Biological activities of quinoline derivatives. Mini-Rev. Med. Chem., **2009**, 9, 1648-1654.

Luo, Z.-g., Zeng, C.-c., Wang, F., He, H.-q., Wang, C.-X., Du, H.-G. and Hu, L.-M. Synthesis and biological activities of quinoline derivatives as HIV-1 integrase inhibitors. Chem. Res. Chin. Univ., **2009**, 25, 841-845.

Maddela, S., Venugopal, M., Maddela, R. and Ajitha, M. Design and synthesis of new *N'*-substituted-2-methylquinoline-3-carbohydrazides with antioxidant and antimicrobial activity. Indian J. Chem., Sect. B: Org. Chem. Incl. Med. Chem., **2015**, 54, 930-935.

Mariano, M., Hartmann, R. W. and Engel, M. Systematic diversification of benzylidene heterocycles yields novel inhibitor scaffolds selective for Dyrk1A, Clk1 and CK2. Eur. J. Med. Chem., **2016**, 112, 209-216.

Mendoza, K., Kamila, S. and Biehl, E. R. Synthesis of novel 5-aryl/hetarylidenyl 3-(2-methyl-5,6,7,8-tetrahydrobenzo[4,5]thieno[2,3-d]pyrimidin-4-yl)-2-thioxothiazolidin-4-ones. Heterocycles, **2014**, 88, 741-753.

Musiol, R., Magdziarz, T. and Kurczyk, A. Quinoline scaffold as a privileged substructure in antimicrobial drugs. Science against microbial pathogens: Communicating current research and technological advances. A. Méndez-Vilas (Ed), Badajoz, Spain. **2011**: 72-83.

Pardasani, R., Pardasani, P., Sherry, D. and Chaturvedi, V. Synthetic and antibacterial studies of rhodanine derivatives with indol-2,3-diones. Indian J. Chem., Sect. B: Org. Chem. Incl. Med. Chem., **2001**, 40, 1275-1278.

Ramesh, V., Ananda Rao, B., Sharma, P., Swarna, B., Thummuri, D., Srinivas, K., Naidu, V. G. M. and Jayathirtha Rao, V. Synthesis and biological evaluation of new rhodanine analogues bearing 2-chloroquinoline and benzo[*H*]quinoline scaffolds as anticancer agents. Eur. J. Med. Chem., **2014**, 83, 569-580.

Siddiqui, I., Singh, P. K., Singh, J. and Singh, J. Facile synthesis and fungicidal activity of novel 4,4'-bis[2"-(5'''-substituted rhodanin-3'''-yl) thiazol-4"-yl]bibenzyls. Indian J. Chem., Sect. B: Org. Chem. Incl. Med. Chem., **2005**, 44, 2102-2106.

Siddiqui, N. An updated review: emerging anticonvulsants. Int. J. Pharm. Biol. Arch., **2010**, 1, 404-415.

Sing, W. T., Lee, C. L., Yeo, S. L., Lim, S. P. and Sim, M. M. Arylalkylidene rhodanine with bulky and hydrophobic functional groups as selective HCV NS3 protease inhibitor. Bioorg. Med. Chem. Lett., **2001**, 11, 91-94.

Subhedar, D. D., Shaikh, M. H., Shingate, B. B., Nawale, L., Sarkar, D., Khedkar, V. M., Kalam Khan, F. A. and Sangshetti, J. N. Quinolidene-rhodanine conjugates: Facile synthesis and biological evaluation. Eur. J. Med. Chem., **2017**, 125, 385-399.

Takasu, K., Inoue, H., Kim, H.-S., Suzuki, M., Shishido, T., Wataya, Y. and Ihara, M. Rhodacyanine dyes as antimalarials. 1. Preliminary evaluation of their activity and toxicity. J. Med. Chem., **2002**, 45, 995-998.

Terashima, H., Hama, K., Yamamoto, R., Tsuboshima, M., Kikkawa, R., Hatanaka, I. and Shigeta, Y. Effects of a new aldose reductase inhibitor on various tissues *in vitro*. J. Pharmacol. Exp. Ther., **1984**, 229, 226-230.

Tomasic, T. and Masic, L. P. Rhodanine as a privileged scaffold in drug discovery. Curr. Med. Chem., **2009**, 16, 1596-1629.

Vandekerckhove, S. and D'hooghe, M. Quinoline-based antimalarial hybrid compounds. Bioorg. Med. Chem., **2015**, 23, 5098-5119.

Chapter 5. Conclusion

A series of quinoline-2-carbaldehydes and quinoline-2-carboxylic acids were synthesised by employing the Doebner-von Miller reaction of crotonaldehyde with various 2- and 4-substituted anilines. The resulting 2-methyl quinolines were thus functionalised by varying the anilines used with halogenated, methylated and methoxylated groups being employed. The methyl quinolines were oxidised by selenium dioxide to the aldehydic analogues, with a subsequent oxidation step using hydrogen peroxide to produce the quinaldic acids where required. In this study, we modified literature procedures for the synthesis of quinaldic acids, bypassing the isolation of both the 2-methyl quinolines and quinoline-2-carbaldehydes thus avoiding all column chromatography purifications. This resulted in a faster and more efficient approach to such intermediates.

The halogenated quinaldic acids were condensed in acid catalysed reactions with *ortho* phenylenediamine to yield benzimidazoles. While the quinoline scaffolds containing electron donating methyl and methoxy substitutents required an alternative procedure, namely the reaction of the respective quinoline-2-carbaldehydes with *ortho* phenylenediamine in the presence of sodium metabisulfite. In varying the substituted anilines used, an NMR study examining this substituent effects on the quinoline proton and carbon shifts was conducted.

The quinoline-2-rhodanine hybrids were synthesised by reacting various quinoline-2-carbaldehydes with rhodanine in a Knoevenagel condensation using ammonium acetate and acetic acid.

The synthesis of pyrazoline compounds entailed first producing 1-(3-methylquinoxalin-2-yl)ethanone from the aqueous *N*-bromosuccinamide catalysed reaction of *o*-phenylenediamine and acetyl acetone. This was condensed with previously synthesised quinoline carbaldehydes and also monosubstitued benzaldehydes producing *α,β*-unsaturated compounds. The chalcone compounds were then further condensed with hydrazine hydrate to yield the pyrazolines.

All compounds were characterised fully by IR, UV and HRMS with full structural elucidation being made using 2D NMR techniques. Single crystal X-ray diffractometry was applied to produce a crystal structure of compound **A5f**.

All compounds were screened for their antimicrobial activities against two Gram +ve (*Staphylococcus aureus* and MRSA) and Gram -ve (*Klebsiella pneumonia, Pseudomonas aeruginosa, Escherichia coli* and *Salmonella typhimurium*) strains of bacteria. The 2-(1*H*-benzo[*d*]imidazol-2-yl)quinolines (**A5a-A5k**) showed no appreciable antibacterial activity in the preliminary screening phase (disc diffusion assay) and thus no further testing was conducted.

The novel quinoxaline-chalcone-quinoline compounds showed good activity against the Gram +ve species (*S.aureus* and MRSA) in MBC assays while the aromatic derived chalcones did not. The quinoxaline-chalcone-quinoline derivatives, **B7a-c** and **B7e-i**, exhibited better activity (0.151-0.360 µM) against *S.aureus* than the standards, ciprofloxacin and levofloxacin, by two orders of magnitude. Only compounds **B7a**, **B7b** and **B7h** remained more potent than the standards when tested against MRSA.

When these compounds were converted to their respective pyrazoline analogues, however, an opposite trend was observed as conversion of the *α,β*-ketone group to a pyrazoline in the quinoxaline-chalcone-quinoline hybrids resulted in loss of activity while similar conversion of the aromatic chalcones to their pyrazoline analogues resulted in compounds **B11a-c**, **B11f** and **B11g** showing activity (11-816 µM) against *S. aureus* only with **B11f** and **B11g** having better activity (12.0 and 11.0 µM, respectively) than the standards. The results of the study have revealed promising compounds for further development as antimicrobial agents.

The rhodanine hybrids (**C5f-i)** also showed significant activity only towards the two Gram +ve strains in screening, however, in MBC assays, none of these compounds showed better activity than the antibiotic standards. The most potent of these compounds was **C5h**, the 6-Br derivative, which showed an MBC value of 356 μM.

Future work can be carried out on all novel compounds wherein antimalarial and anticancer assays may be conducted. The rhodanine hybrids can be screened for antidiabetic activity, as compounds containing the rhodanine moiety are known to possess such activity. Molecular modelling computational studies can also be conducted.

University of KwaZulu-Natal

Synthesis, Characterisation and Antibacterial Activity of New Quinoline and Quinoxaline Hybrid Molecules

Appendix A : Characterisation Data

2018

Shirveen Sewpersad

Table of Contents

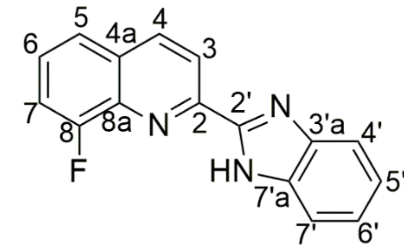

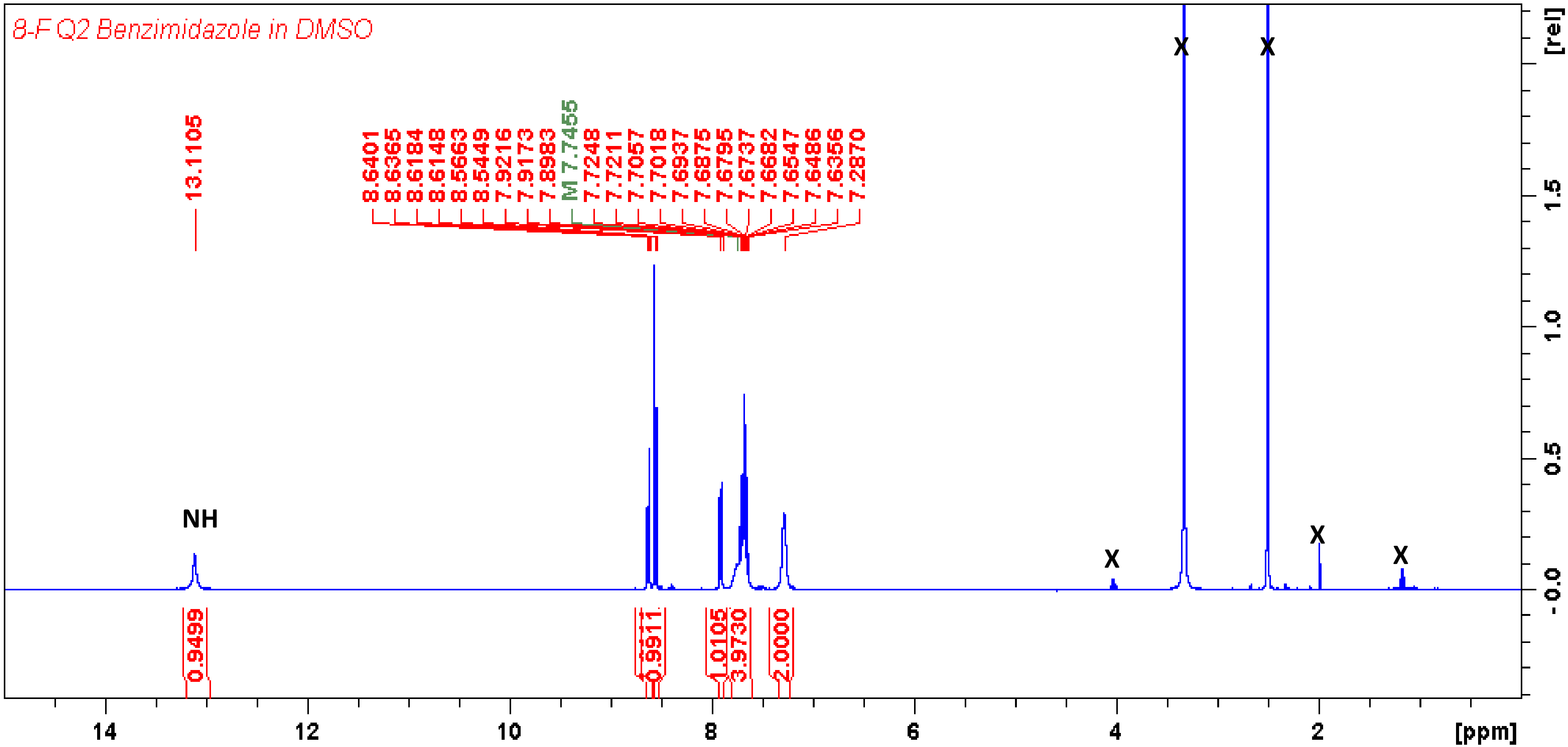

^{1}H NMR spectrum of **A5a**

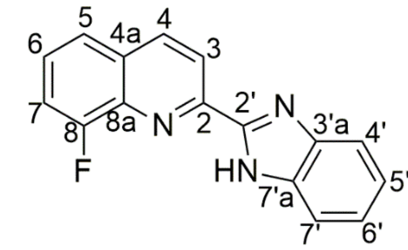

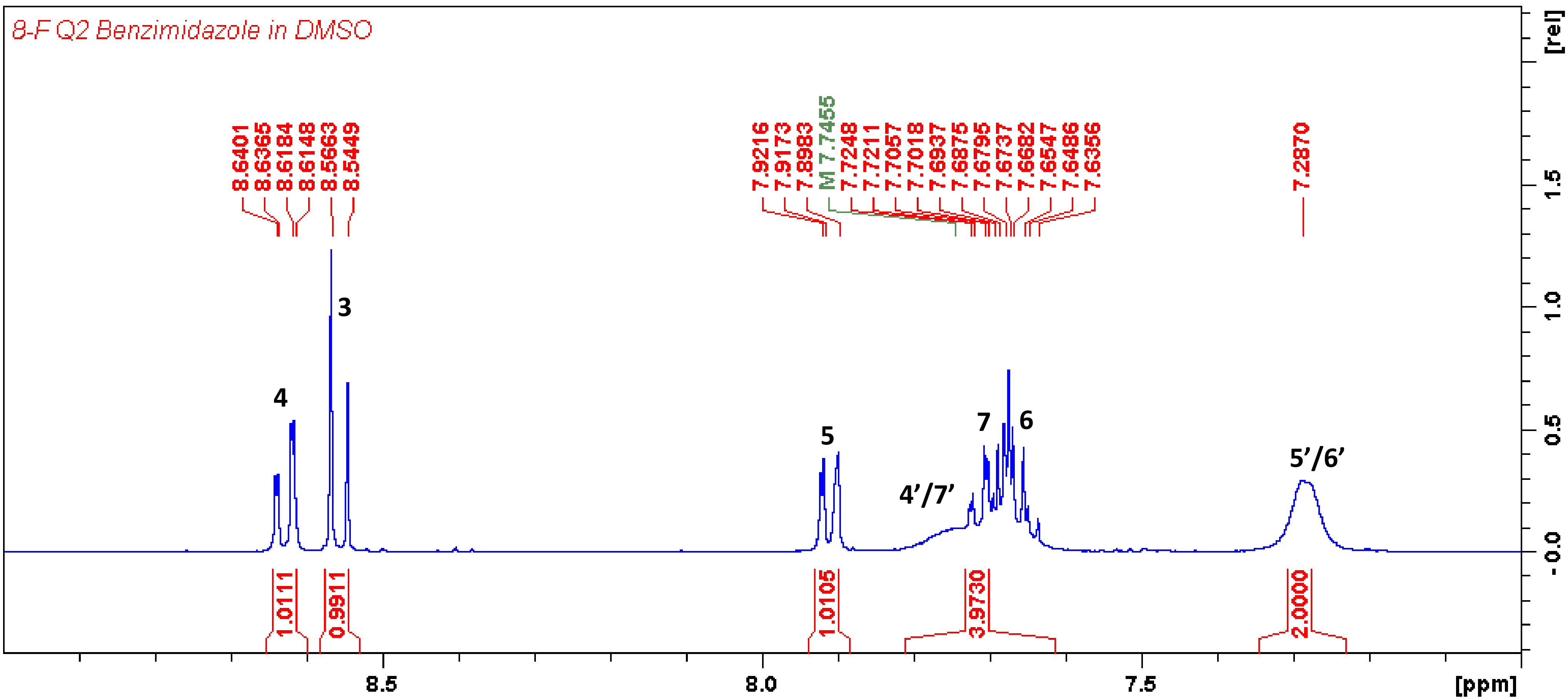

Expanded ^{1}H NMR spectrum of **A5a**

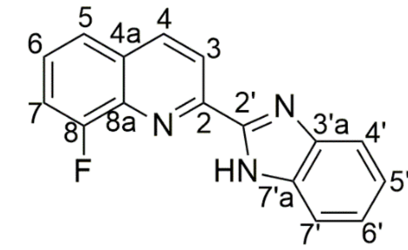

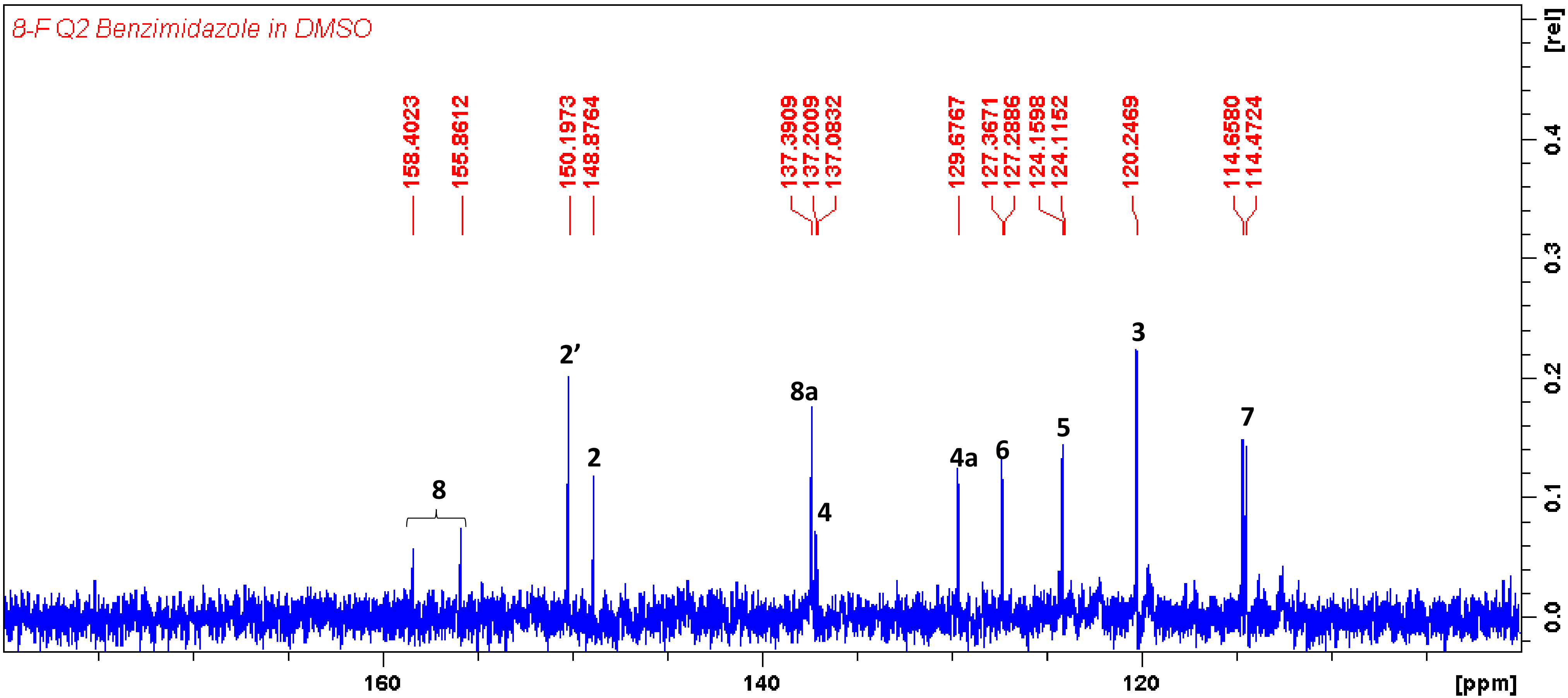

^{13}C NMR spectrum of **A5a**

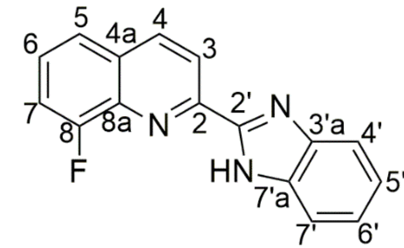
5
4a
4
6
3
7
8a
N
2
2'
N
3'a
4'
8
F
HN
7'a
5'
7'
6'

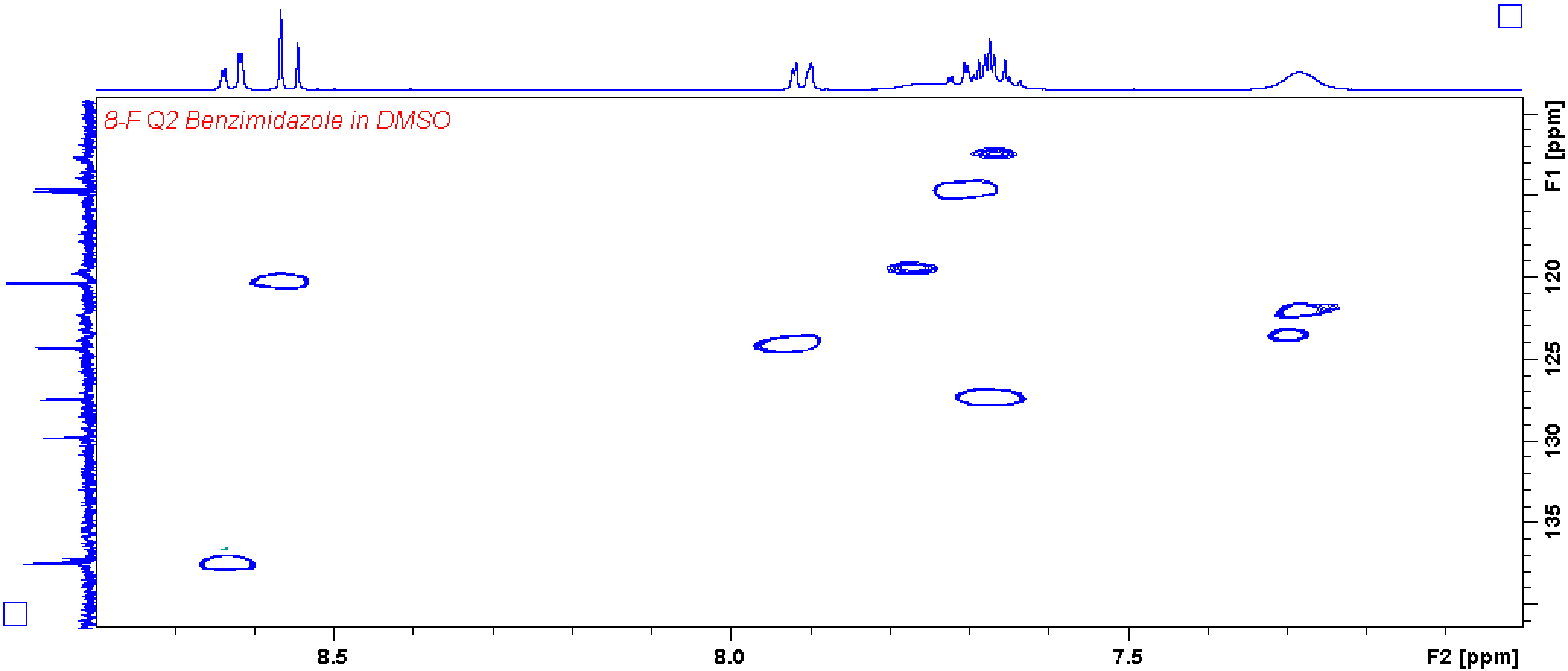
8-F Q2 Benzimidazole in DMSO
F1 [ppm]
120
125
130
135
8.5
8.0
7.5
F2 [ppm]

HSQC of **A5a**

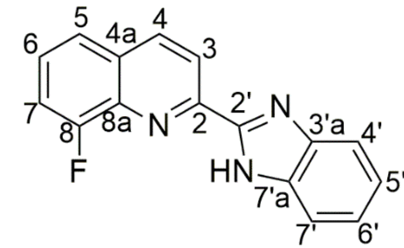

5
4a
4
3
6
7
8
8a
N
2
2'
N
3'a
4'
5'
F
HN
7'a
7'
6'

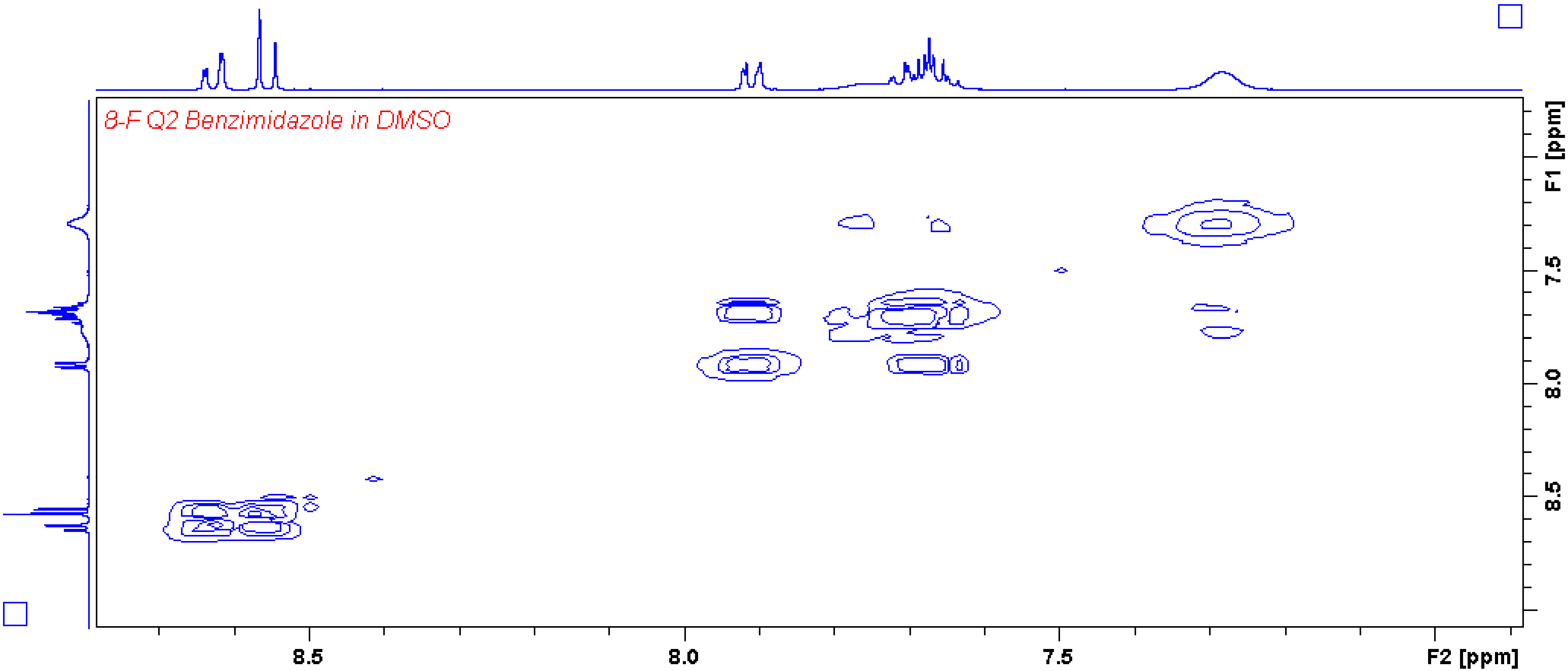

8-F Q2 Benzimidazole in DMSO
F1 [ppm]
7.5
8.0
8.5
F2 [ppm]

COSY of **A5a**

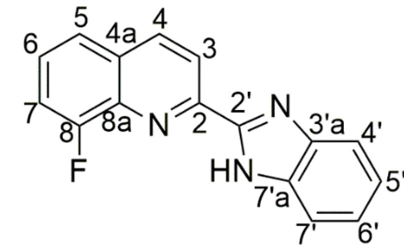
5
4a
4
3
6
7
8
8a
N
2
2'
N
3'a
4'
F
HN
7'a
5'
7'
6'

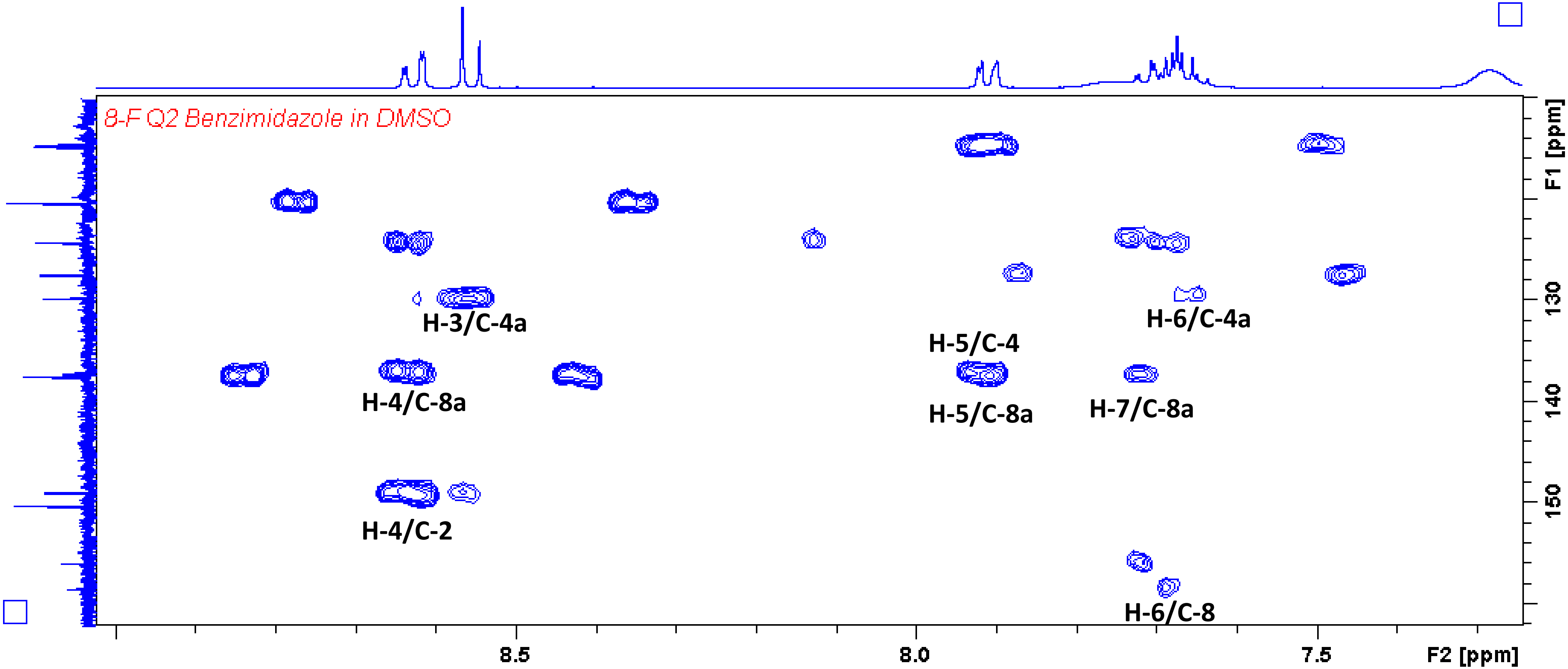
8-F Q2 Benzimidazole in DMSO
H-3/C-4a
H-6/C-4a
H-5/C-4
H-4/C-8a
H-5/C-8a
H-7/C-8a
H-4/C-2
H-6/C-8
F1 [ppm]
130
140
150
8.5
8.0
7.5
F2 [ppm]

HMBC of **A5a**

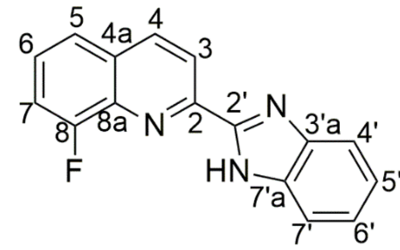

Elemental Composition Report

Single Mass Analysis

Tolerance = 5.0 PPM / DBE: min = -1.5, max = 100.0
Element prediction: Off
Number of isotope peaks used for i-FIT = 3

Monoisotopic Mass, Even Electron Ions
5 formula(e) evaluated with 1 results within limits (up to 20 closest results for each mass)
Elements Used:
C: 15-20 H: 5-10 N: 0-5 F: 0-1
SSQB4 18 (0.574) Cm (1:61)
TOF MS ES-

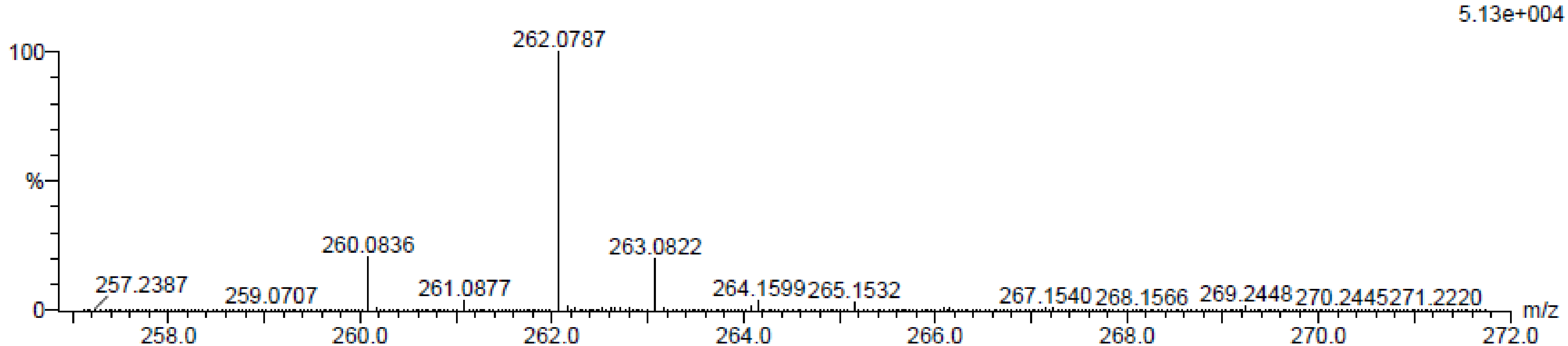

Minimum:				-1.5			
Maximum:		5.0	5.0	100.0			
Mass	Calc. Mass	mDa	PPM	DBE	i-FIT	i-FIT (Norm)	Formula
262.0787	262.0781	0.6	2.3	13.5	533.9	0.0	C16 H9 N3 F

High resolution mass spectrum of **A5a**

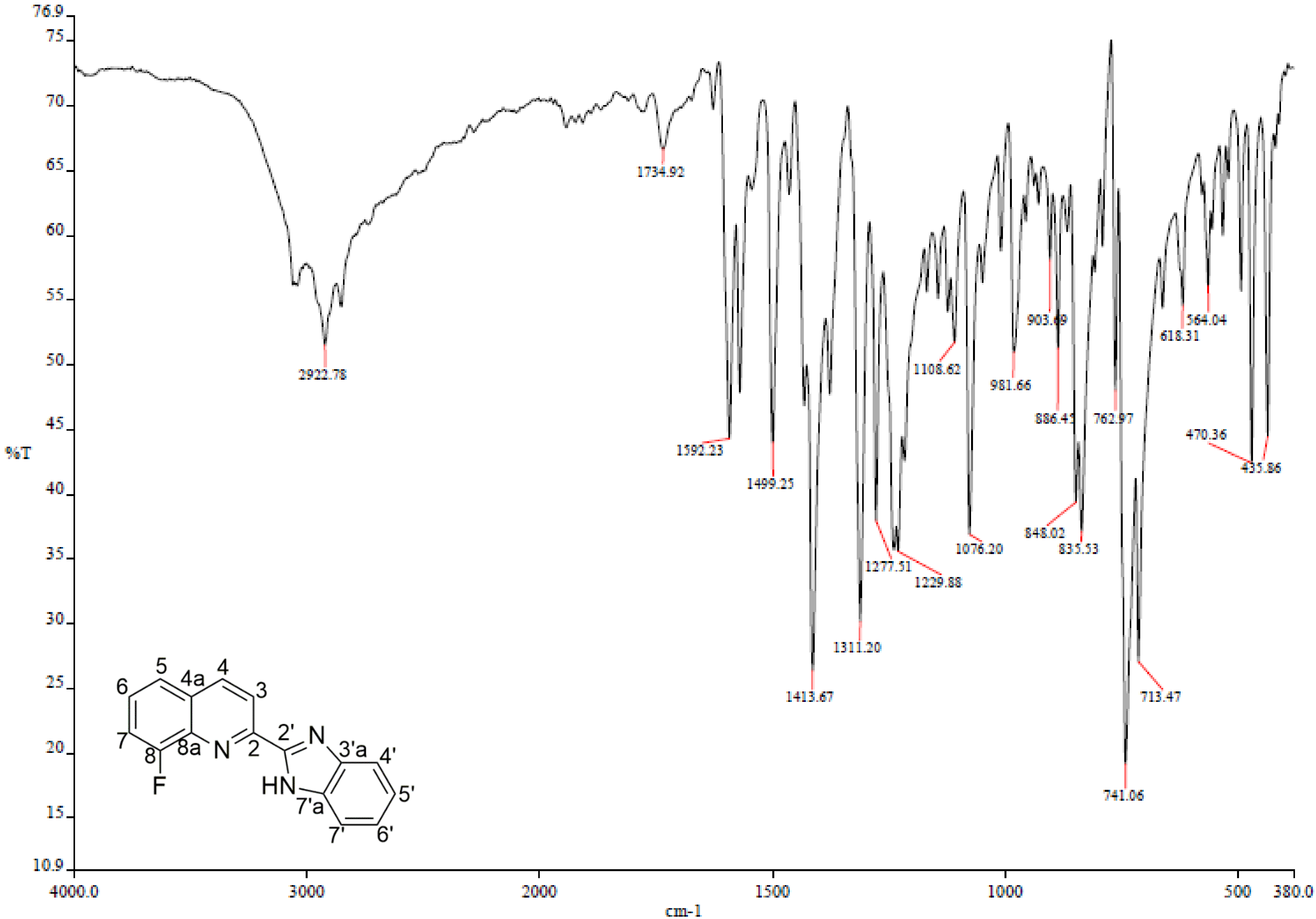

FTIR spectrum of **A5a**

Overlay Spectrum Graph Report

03/08/2017 03:16:59 PM

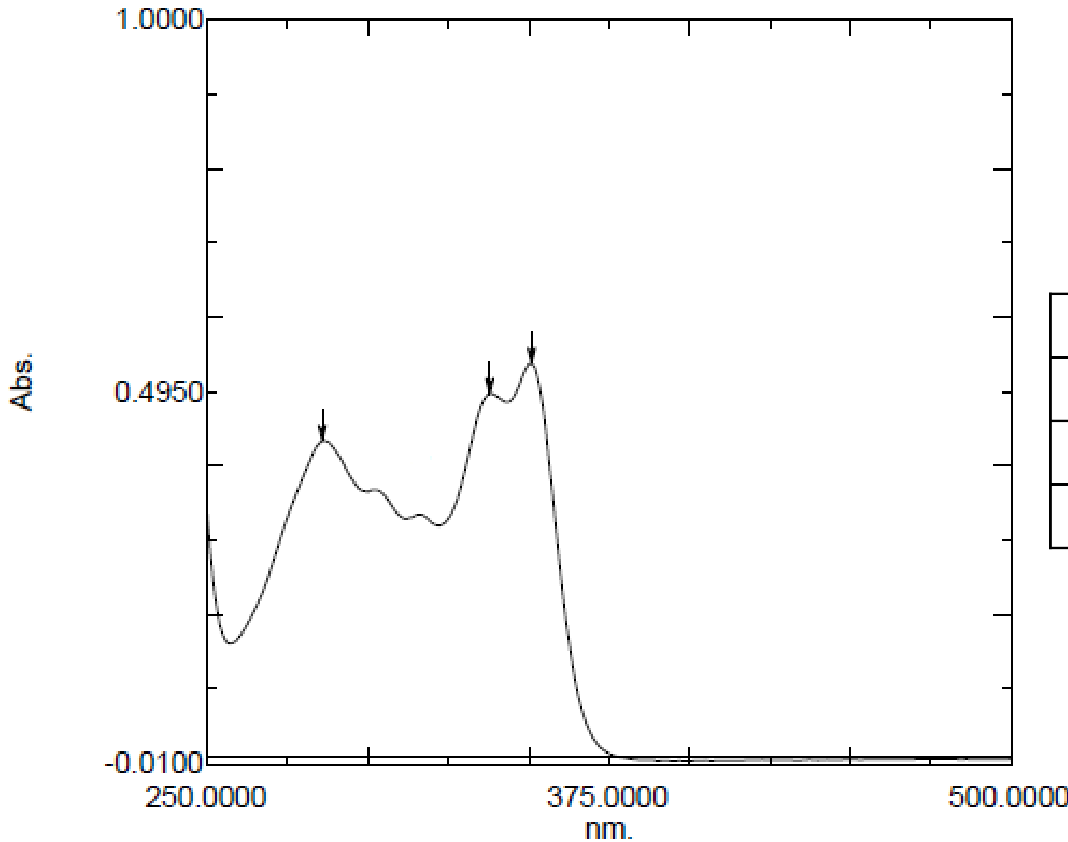

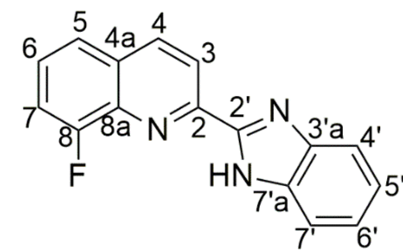

λ	absorbance	logε
291	0.3931	4.32
337	0.4256	4.35
351	0.4444	4.37

Page 1 / 1

UV spectrum of **A5a**

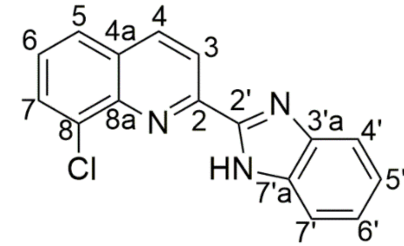

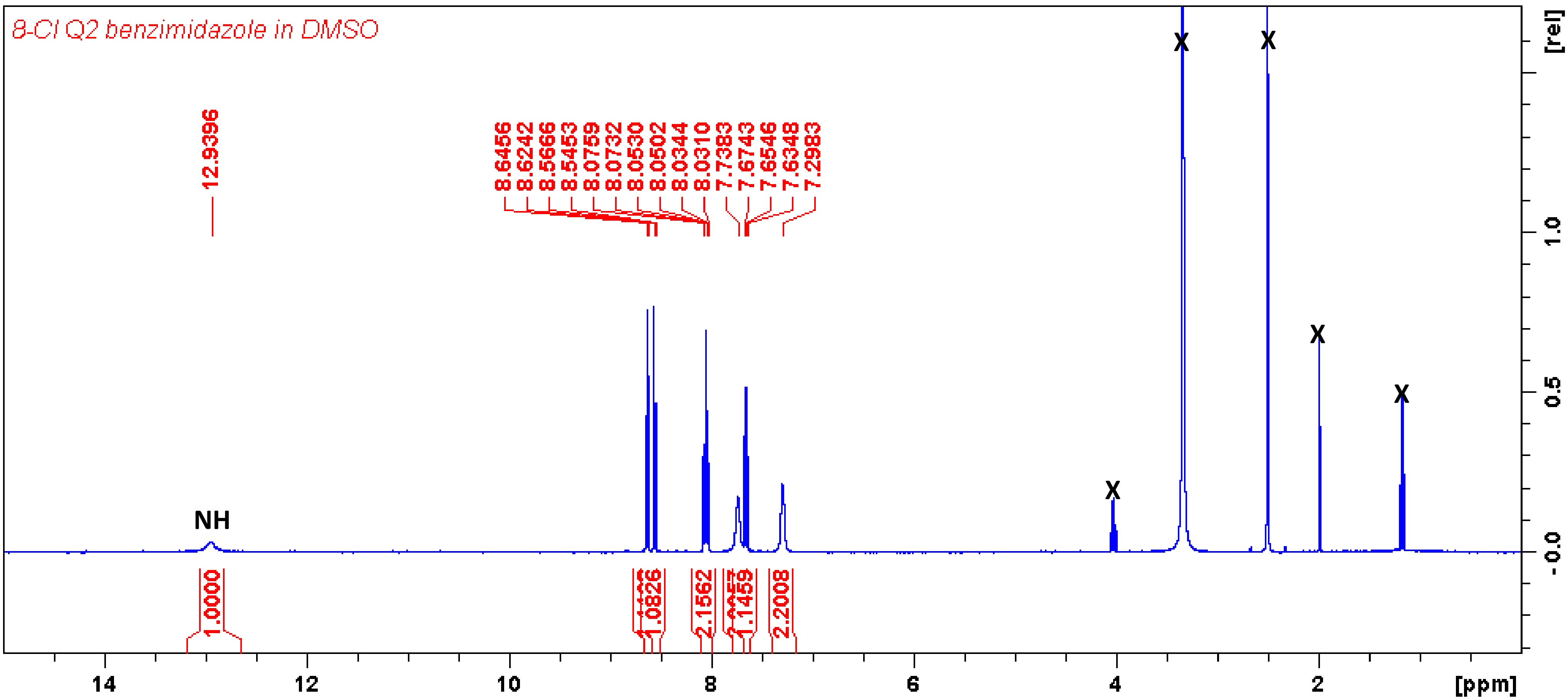

^{1}H NMR spectrum of **A5b**

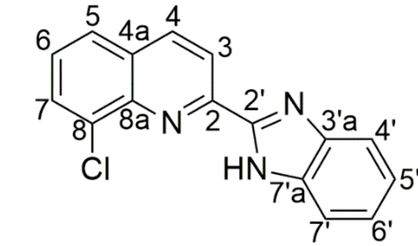

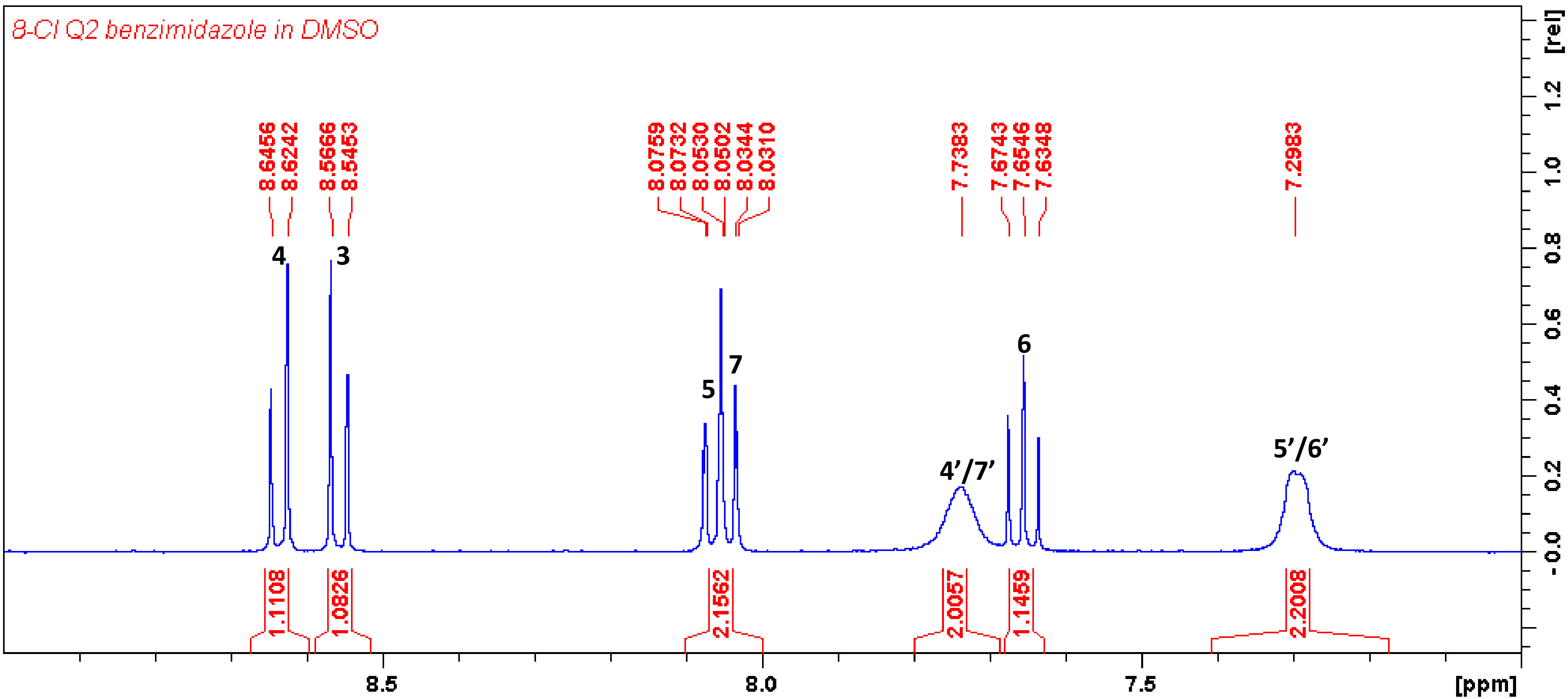

Expanded ^{1}H NMR spectrum of **A5b**

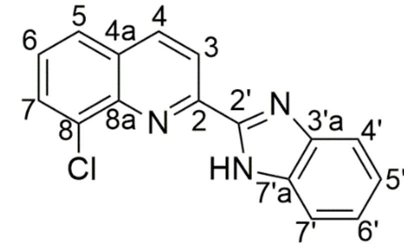

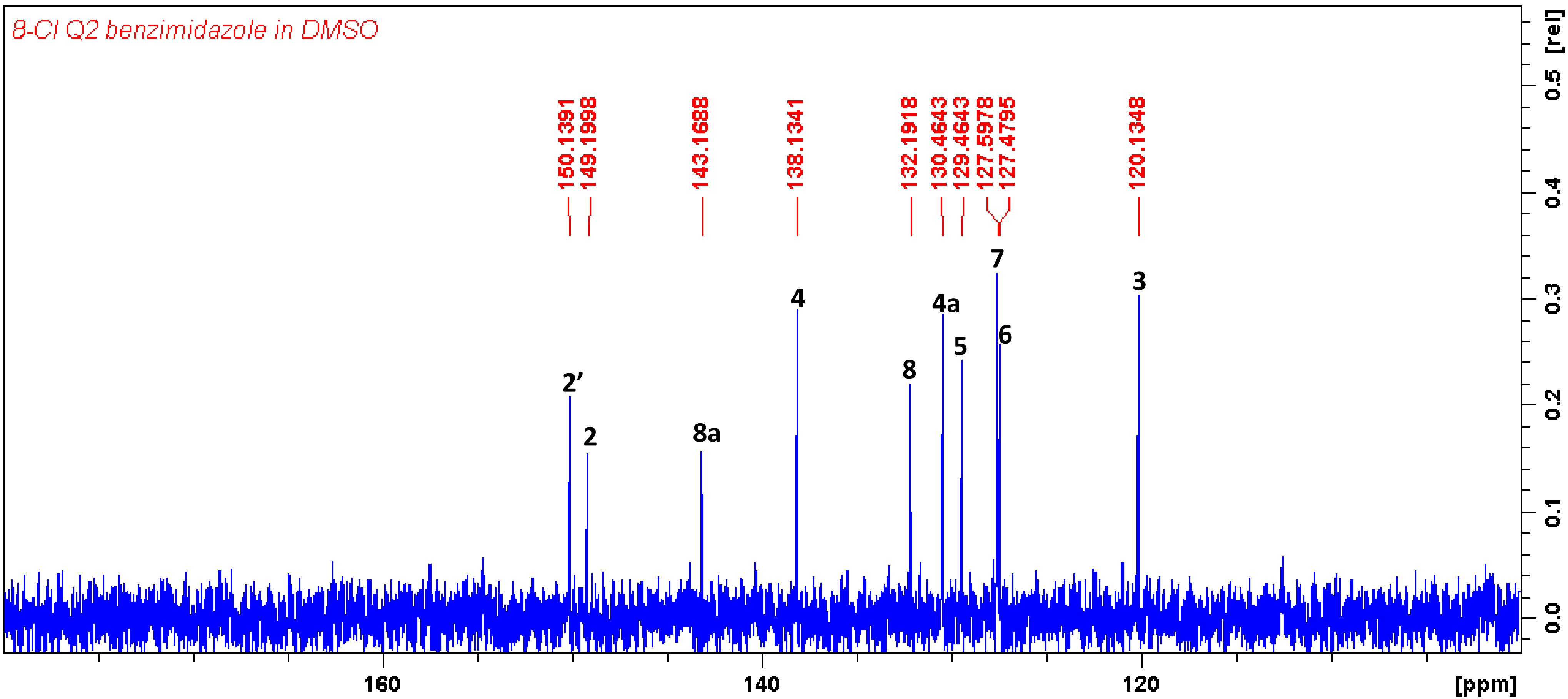

^{13}C NMR spectrum of **A5b**

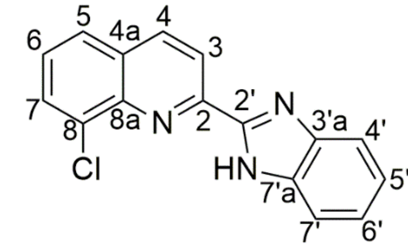

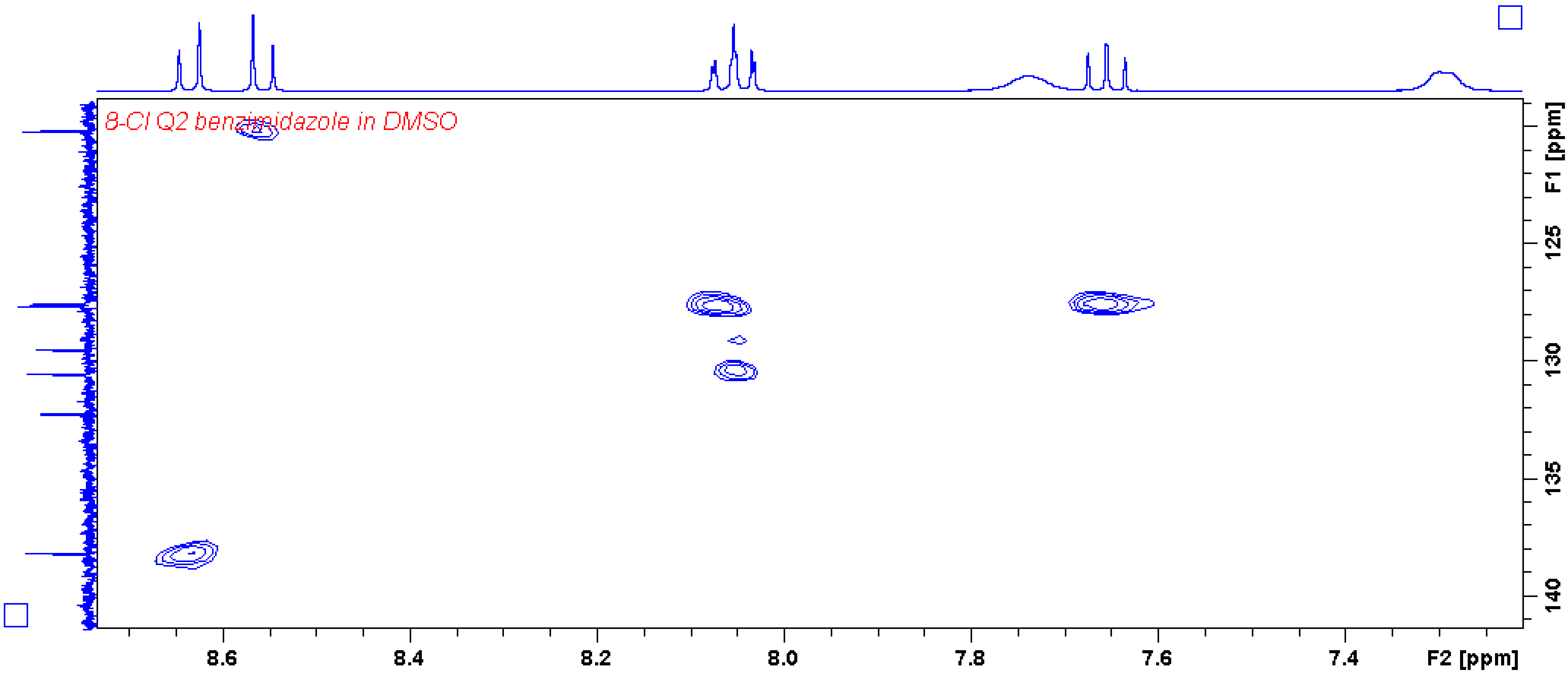

HSQC of **A5b**

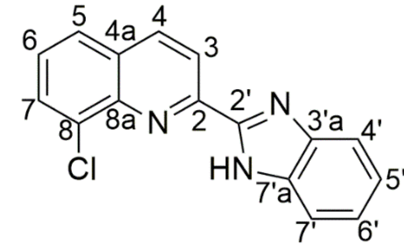

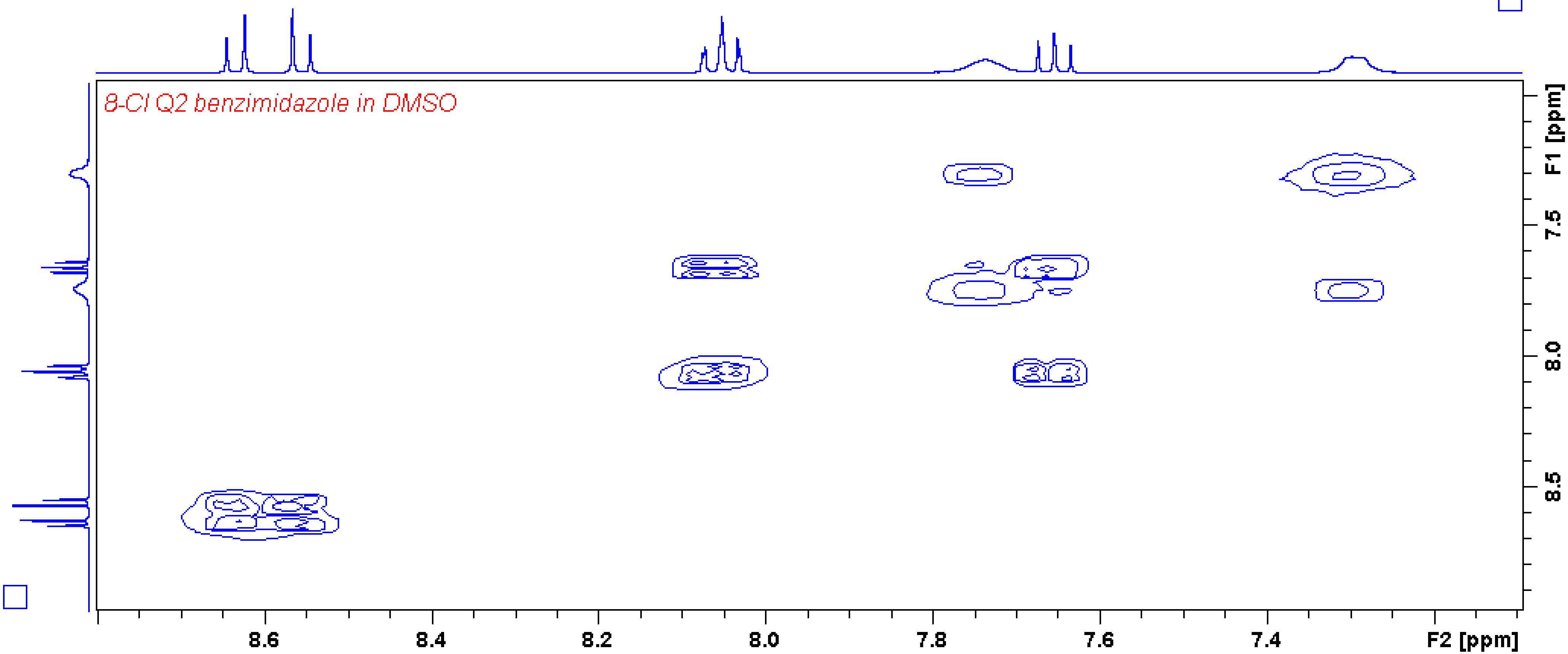

COSY of **A5b**

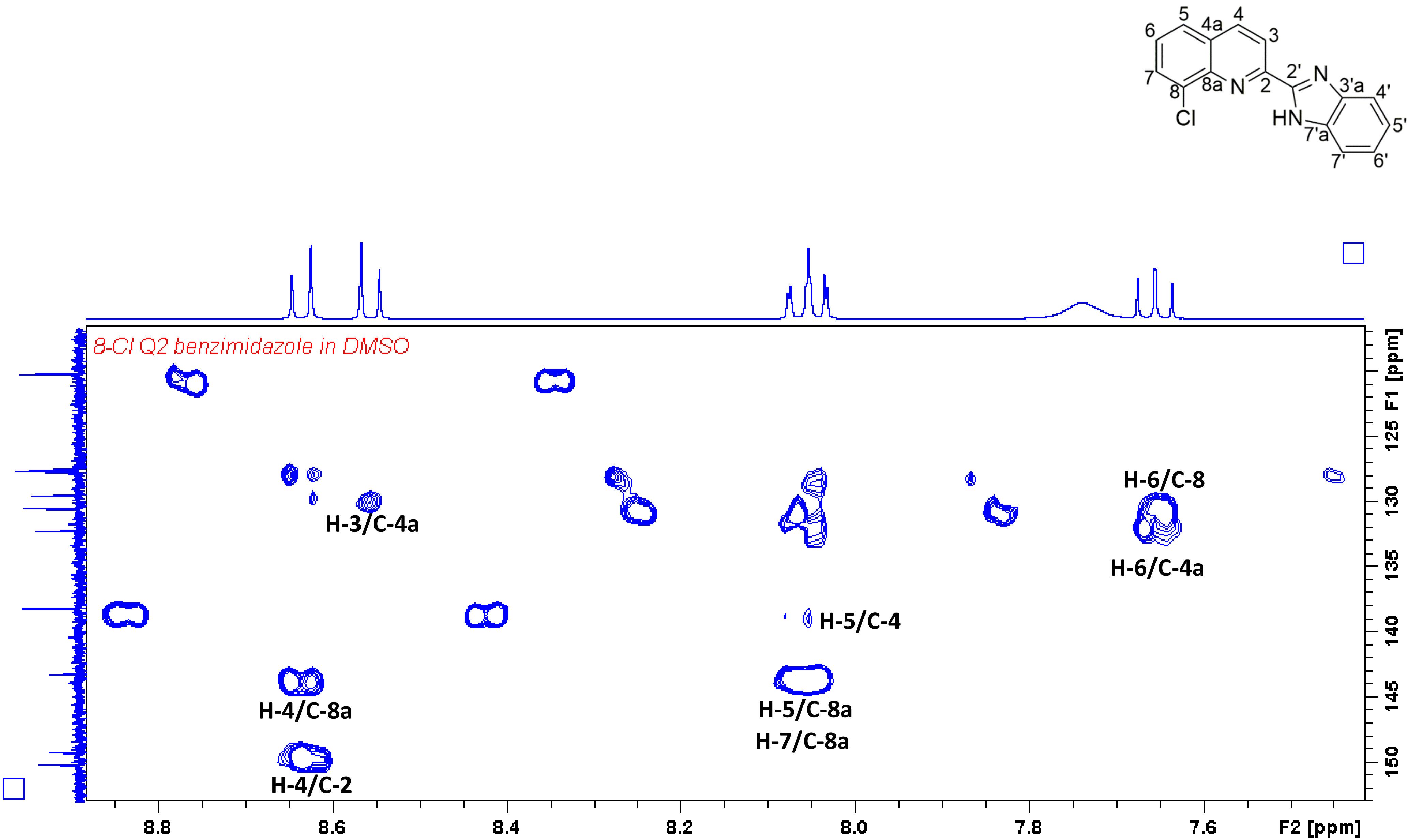
8-Cl Q2 benzimidazole in DMSO
H-3/C-4a
H-6/C-8
H-6/C-4a
H-5/C-4
H-4/C-8a
H-5/C-8a
H-7/C-8a
H-4/C-2
F1 [ppm]
F2 [ppm]
5
6
4a
4
3
7
8
8a
N
2
2'
N
3'a
4'
5'
6'
7'
7'a
HN
Cl

HMBC of **A5b**

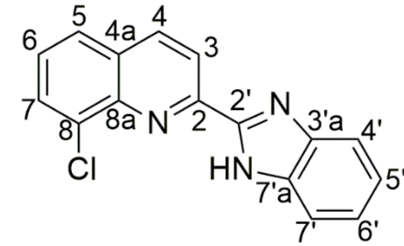

Elemental Composition Report

Single Mass Analysis

Tolerance = 5.0 PPM / DBE: min = -1.5, max = 100.0
Element prediction: Off
Number of isotope peaks used for i-FIT = 3

Monoisotopic Mass, Even Electron Ions
6 formula(e) evaluated with 1 results within limits (up to 20 closest results for each mass)
Elements Used:
C: 15-20 H: 5-10 N: 0-5 Cl: 0-1
SSQB6 2 (0.034) Cm (1:61)
TOF MS ES-

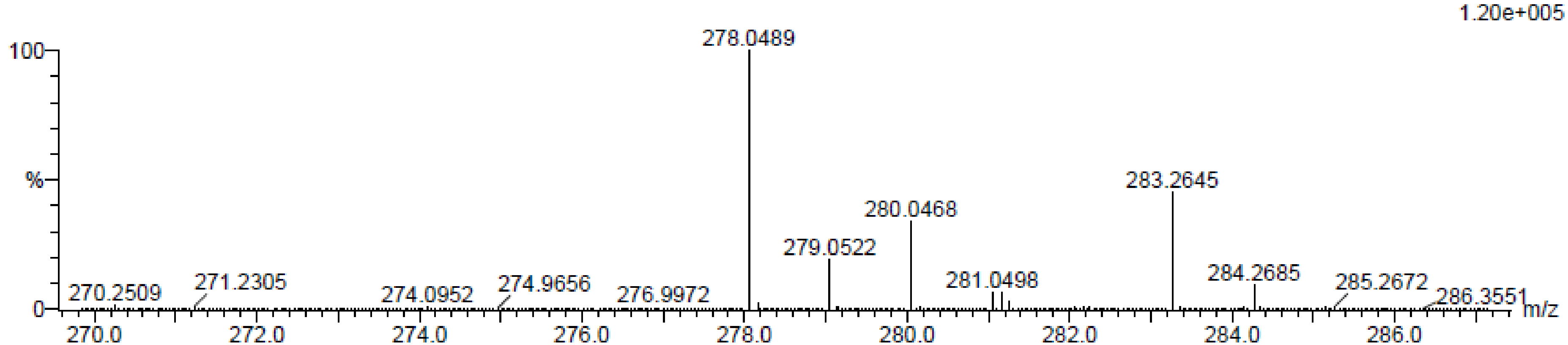

Minimum:				-1.5			
Maximum:		5.0	5.0	100.0			
Mass	Calc. Mass	mDa	PPM	DBE	i-FIT	i-FIT (Norm)	Formula
278.0489	278.0485	0.4	1.4	13.5	589.5	0.0	C16 H9 N3 Cl

High resolution mass spectrum of **A5b**

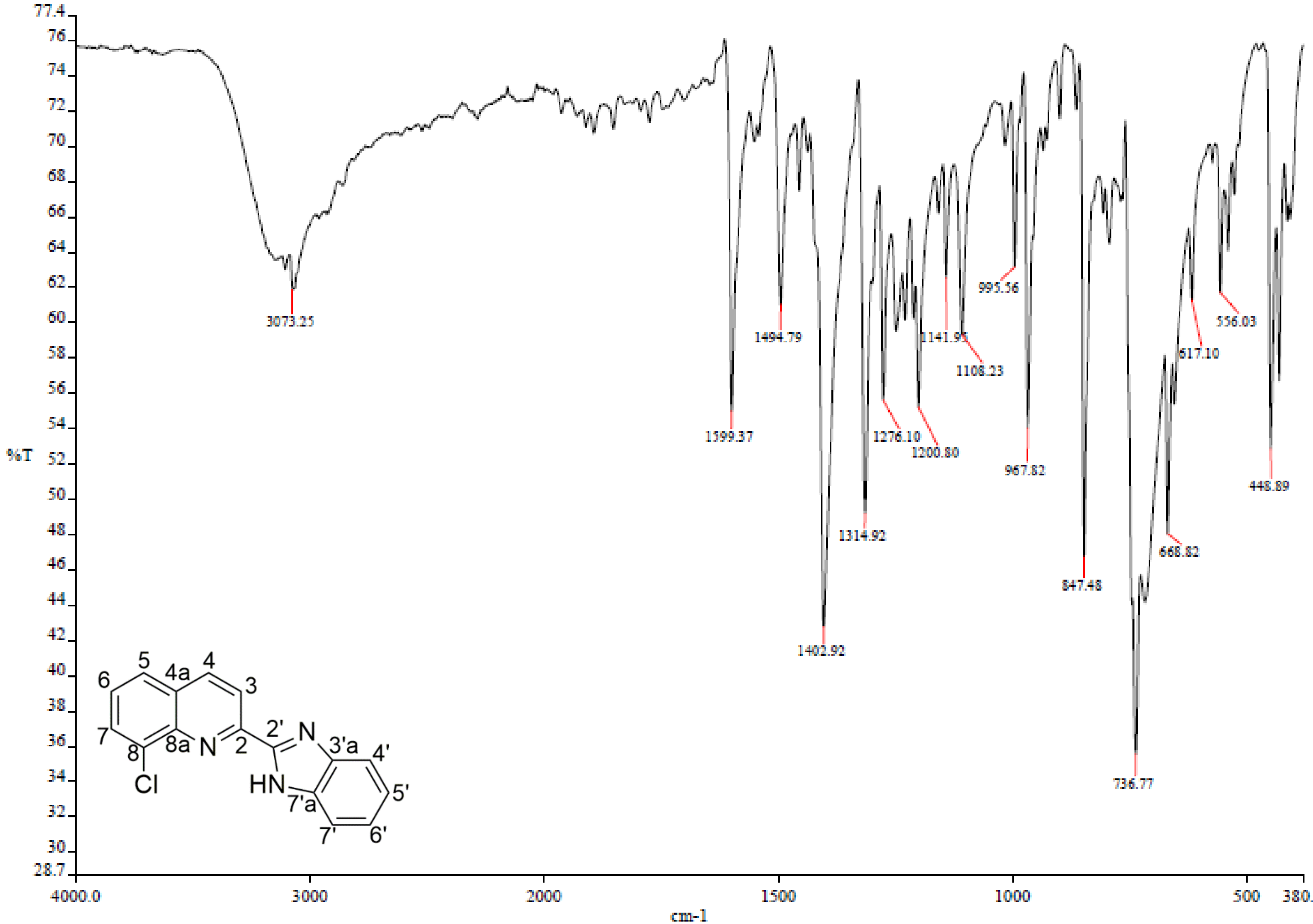

FTIR spectrum of **A5b**

Overlay Spectrum Graph Report

03/08/2017 03:15:26 PM

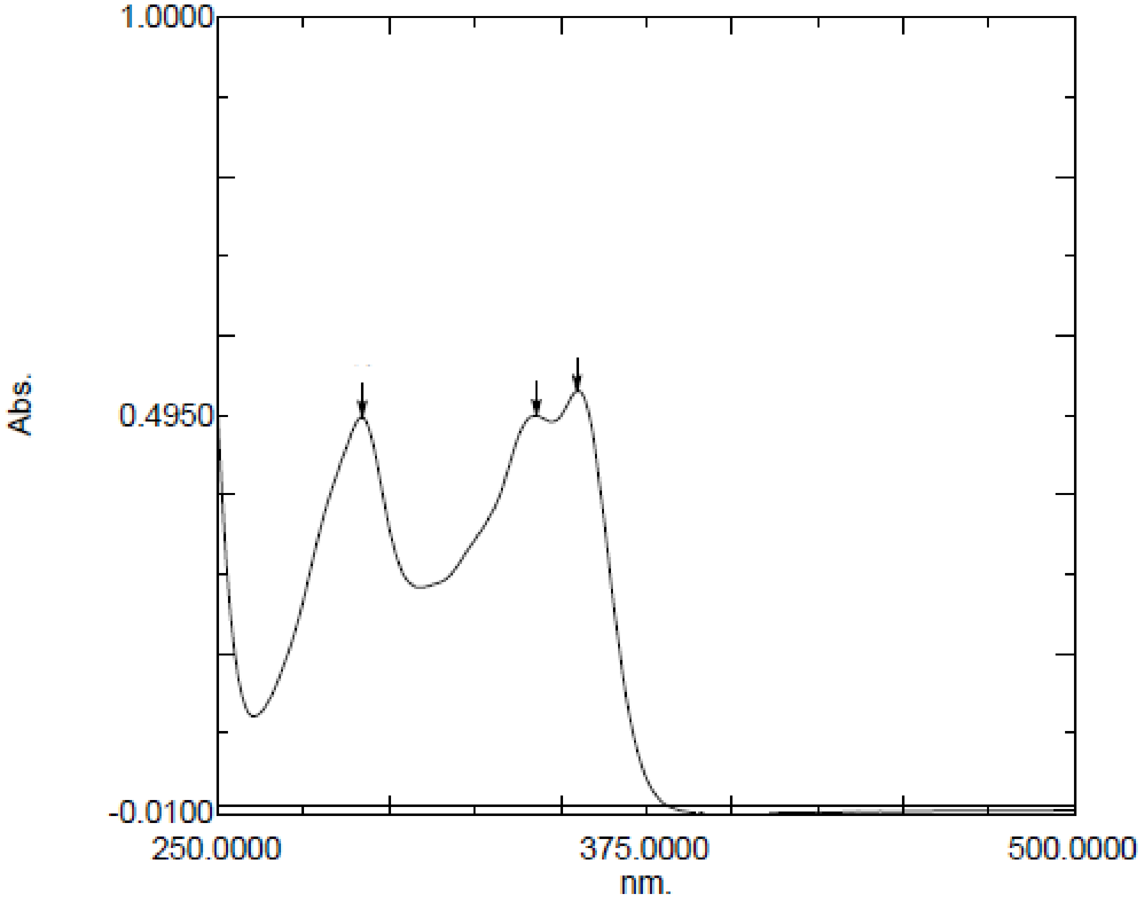

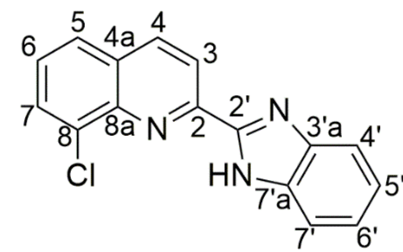

λ	absorbance	logε
292	0.4932	4.44
342	0.4941	4.44
355	0.5258	4.47

Page 1 / 1

UV spectrum of **A5b**

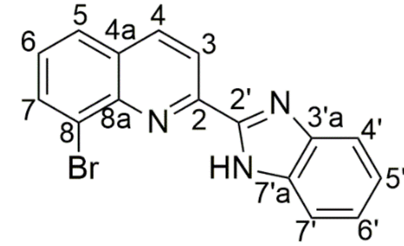

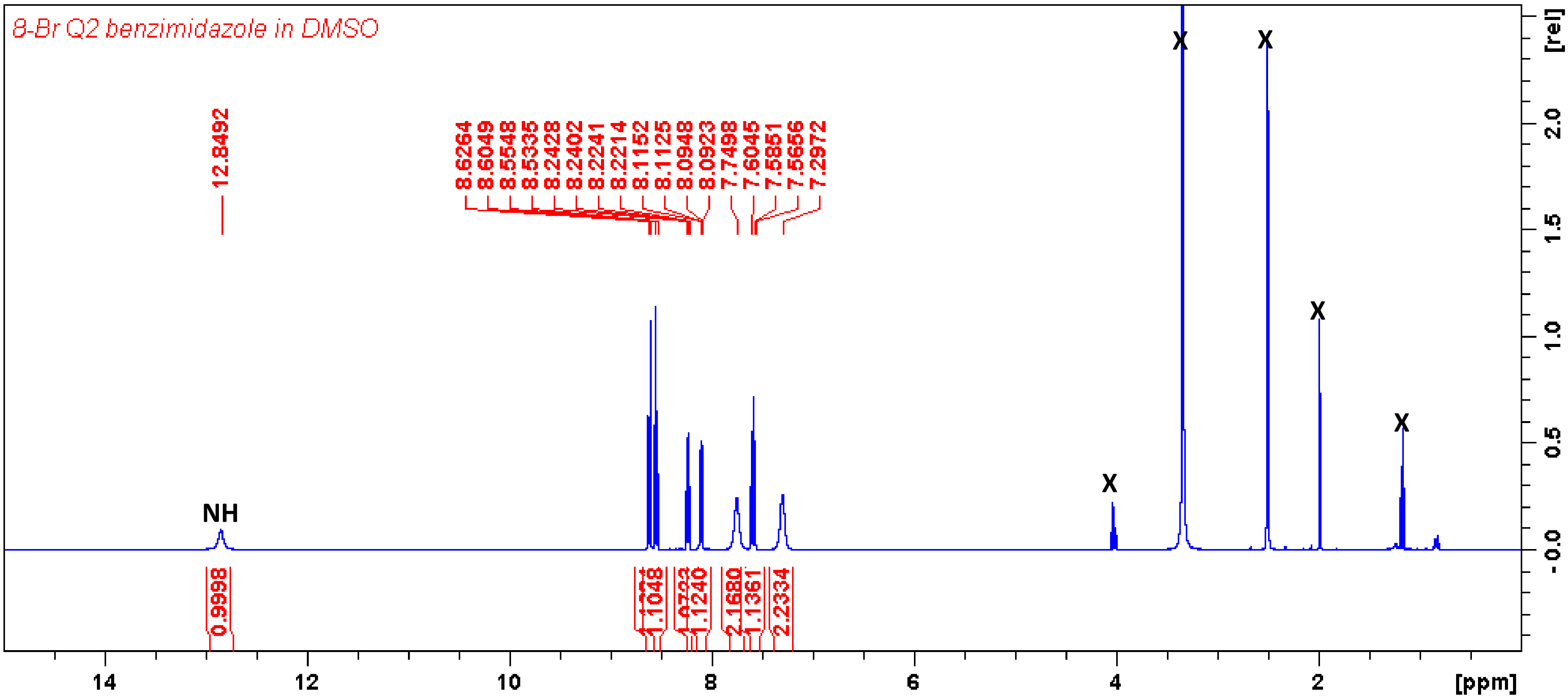

^{1}H NMR spectrum of **A5c**

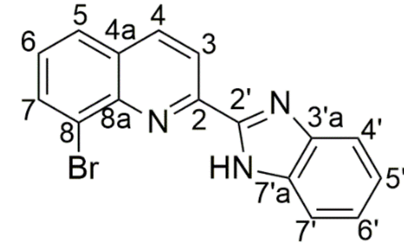

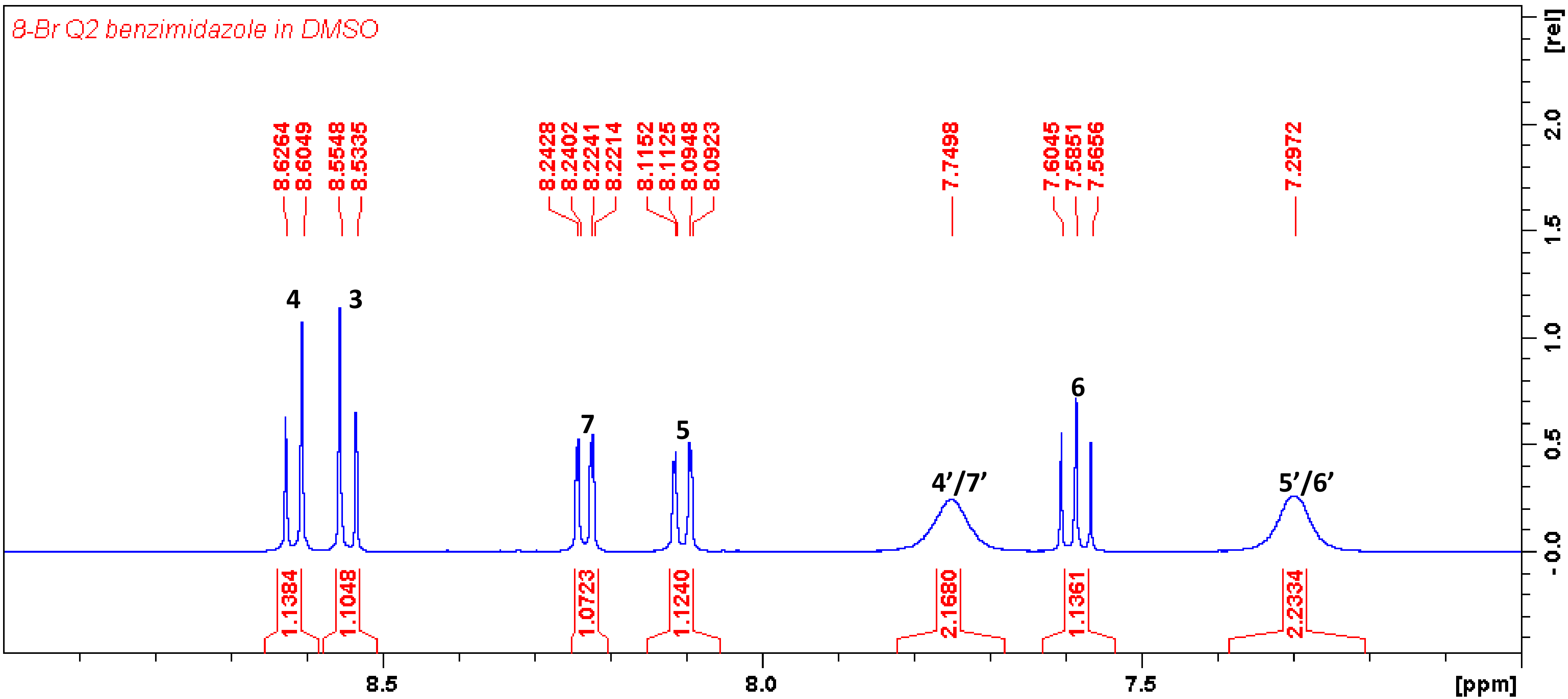

Expanded ^{1}H NMR spectrum of **A5c**

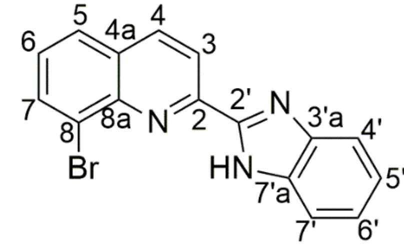

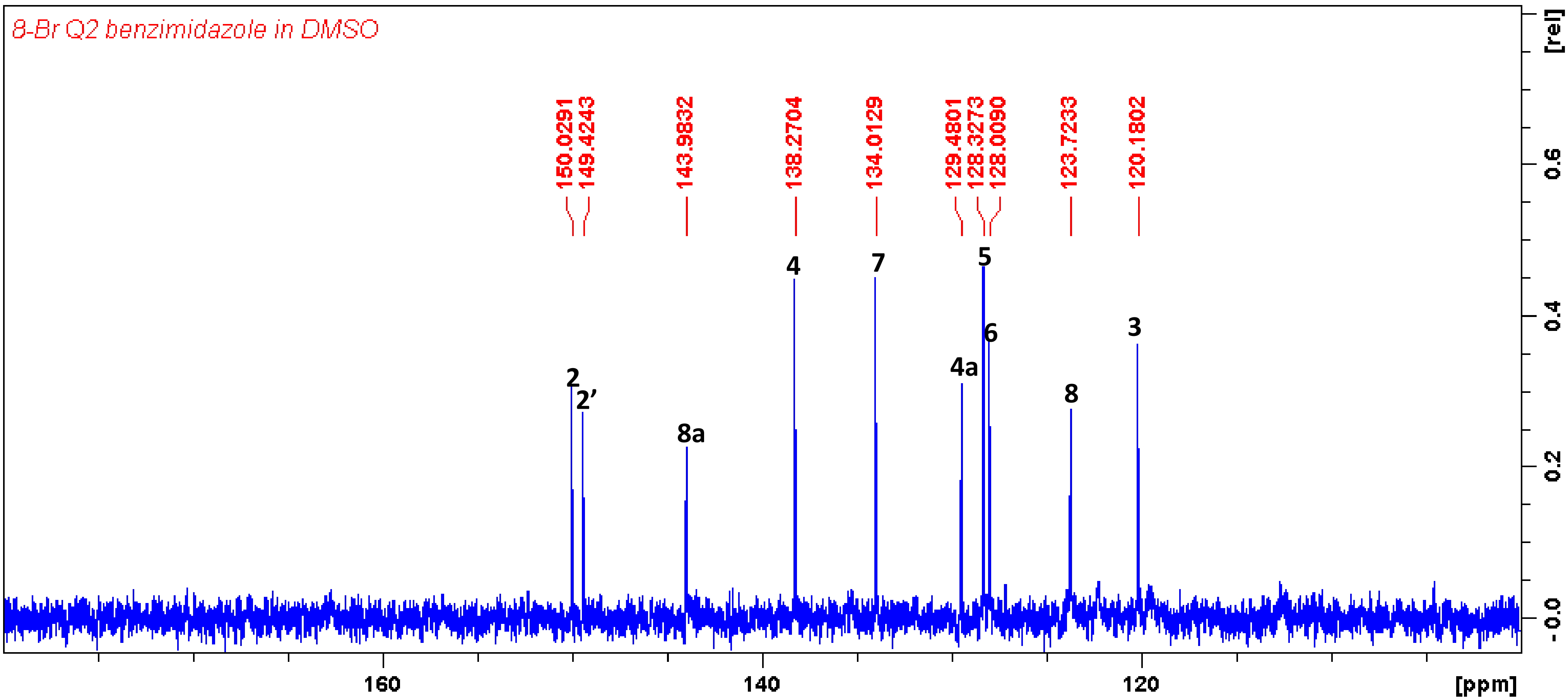

^{13}C NMR spectrum of **A5c**

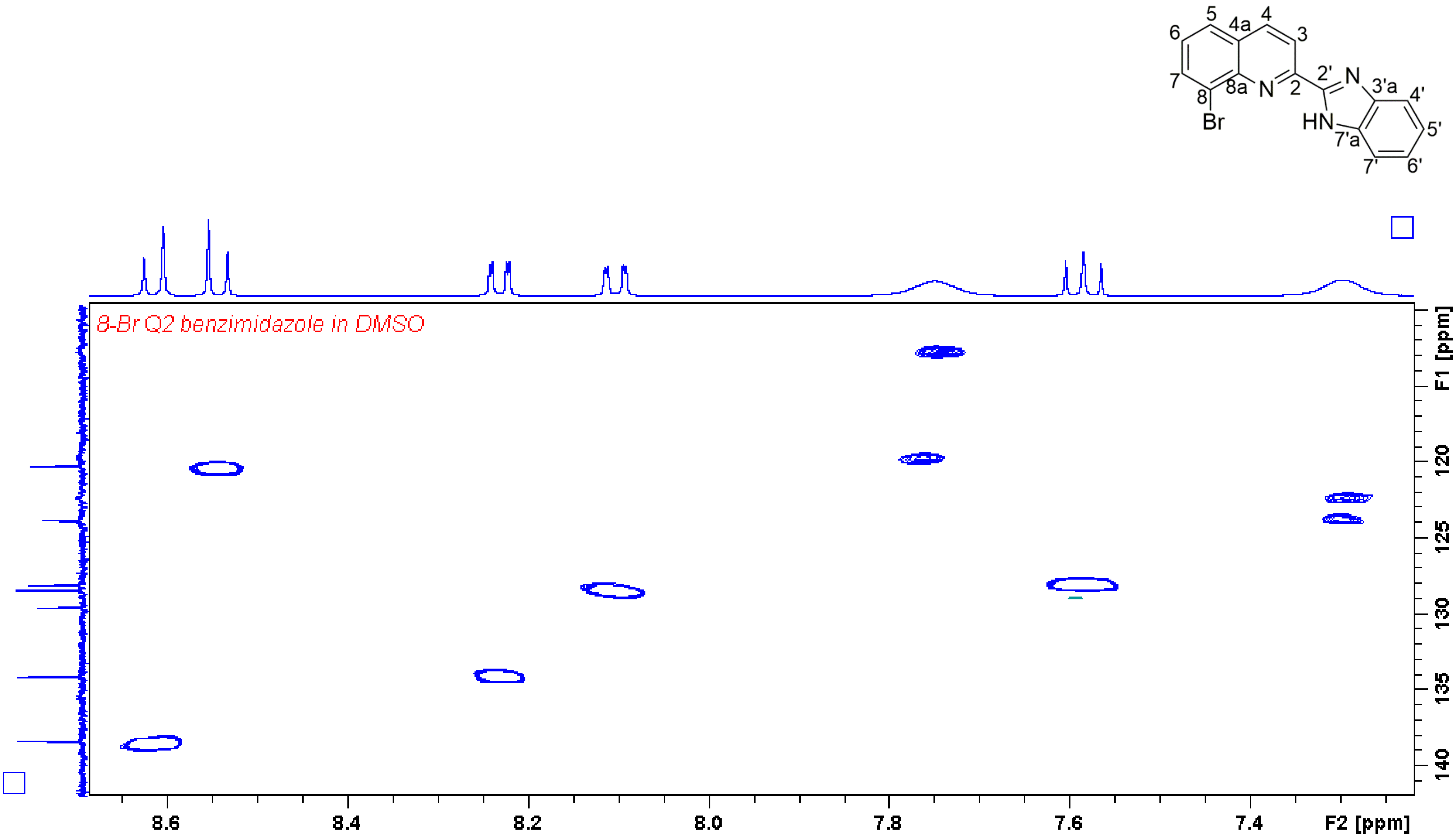

8-Br Q2 benzimidazole in DMSO
F1 [ppm]
F2 [ppm]
8.6
8.4
8.2
8.0
7.8
7.6
7.4
120
125
130
135
140
Br
N
HN

HSQC of **A5c**

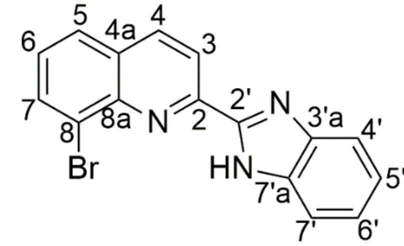

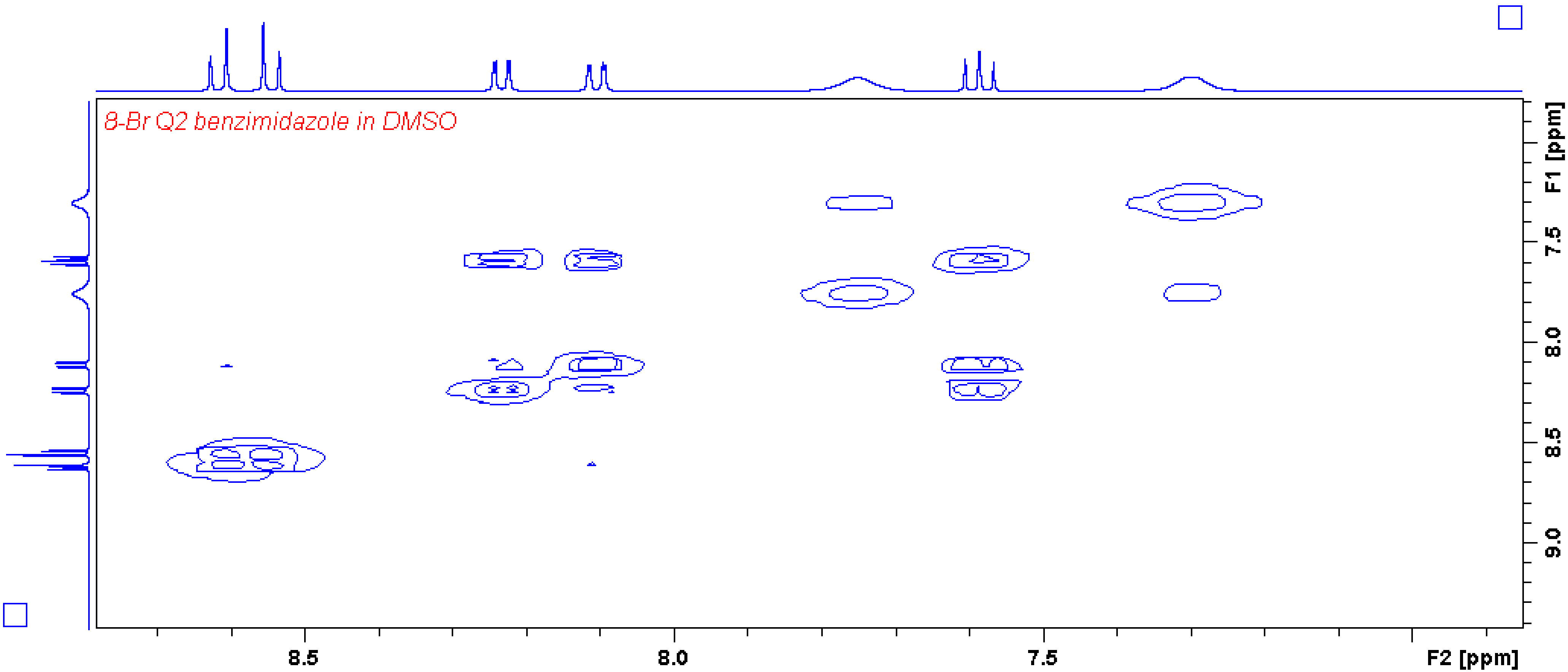

COSY of **A5c**

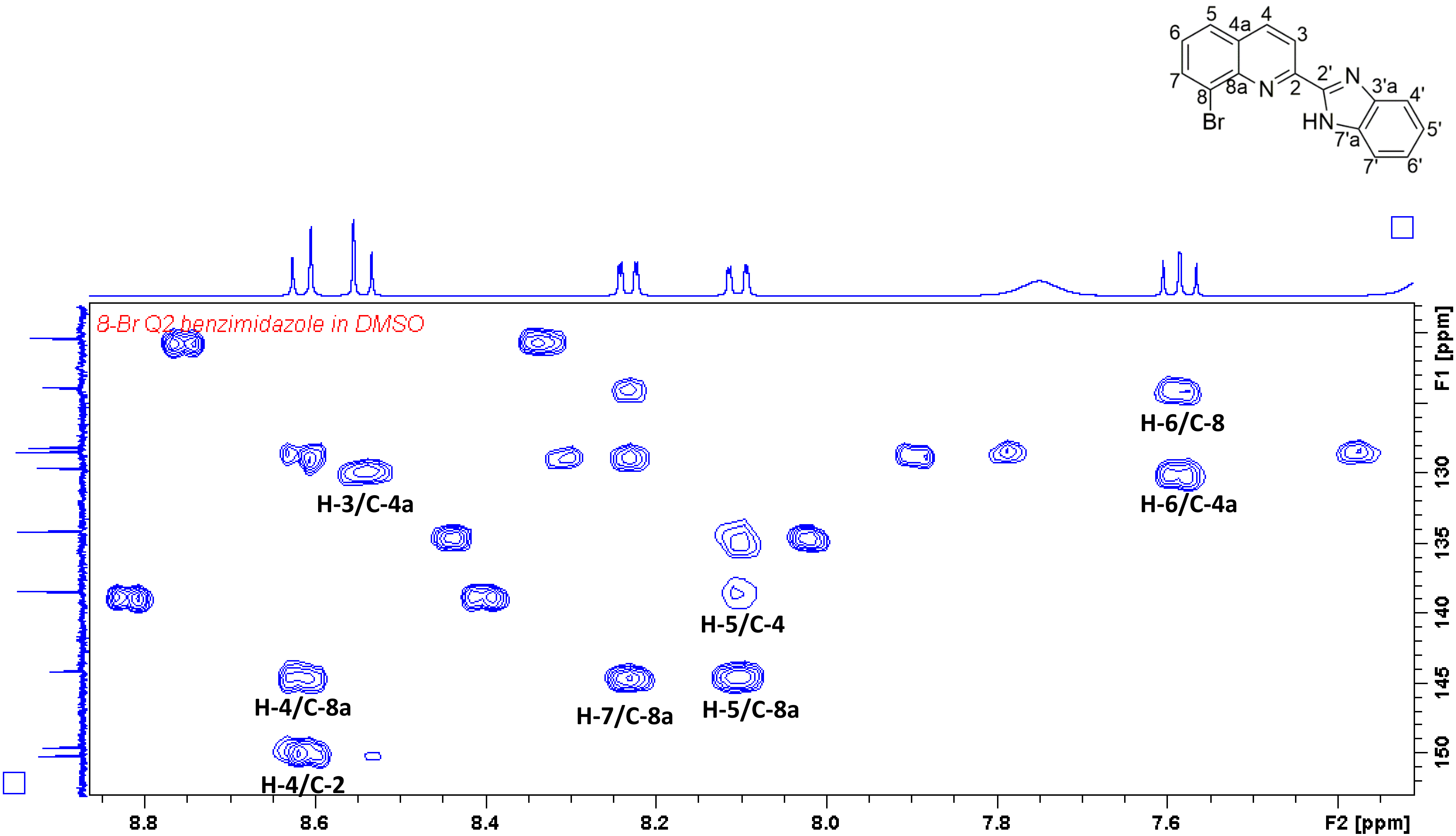
8-Br Q2 benzimidazole in DMSO
H-6/C-8
H-3/C-4a
H-6/C-4a
H-5/C-4
H-4/C-8a
H-7/C-8a
H-5/C-8a
H-4/C-2
F1 [ppm]
F2 [ppm]
Br
N
HN

HMBC of **A5c**

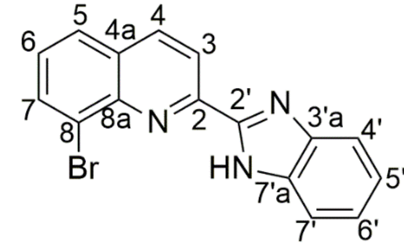

Elemental Composition Report

Single Mass Analysis

Tolerance = 5.0 PPM / DBE: min = -1.5, max = 100.0
Element prediction: Off
Number of isotope peaks used for i-FIT = 3

Monoisotopic Mass, Even Electron Ions
5 formula(e) evaluated with 1 results within limits (up to 20 closest results for each mass)
Elements Used:
C: 15-20 H: 5-10 N: 0-5 Br: 0-1

SSQB2 31 (1.013) Cm (1:61)
TOF MS ES-

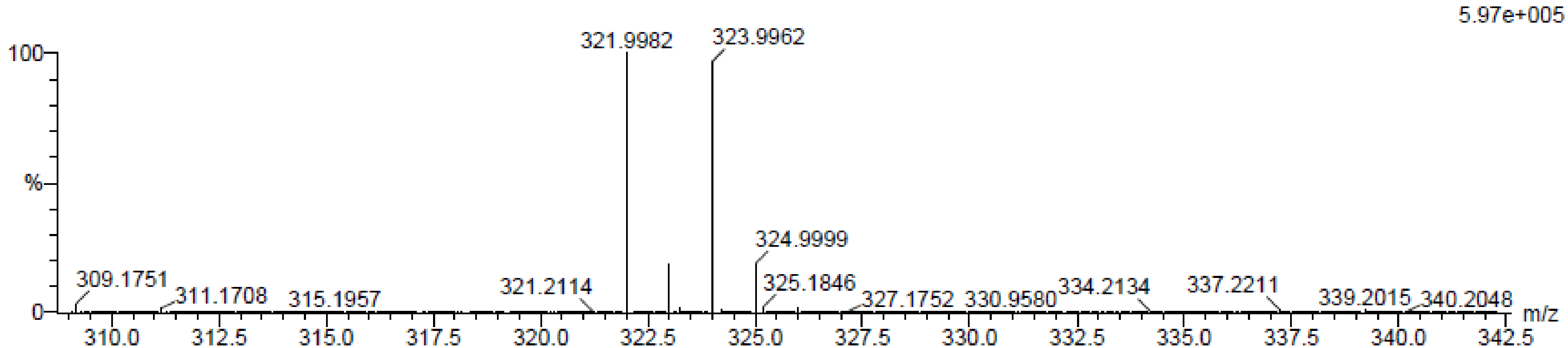

Minimum:				-1.5			
Maximum:		5.0	5.0	100.0			
Mass	Calc. Mass	mDa	PPM	DBE	i-FIT	i-FIT (Norm)	Formula
321.9982	321.9980	0.2	0.6	13.5	622.7	0.0	C16 H9 N3 Br

High resolution mass spectrum of **A5c**

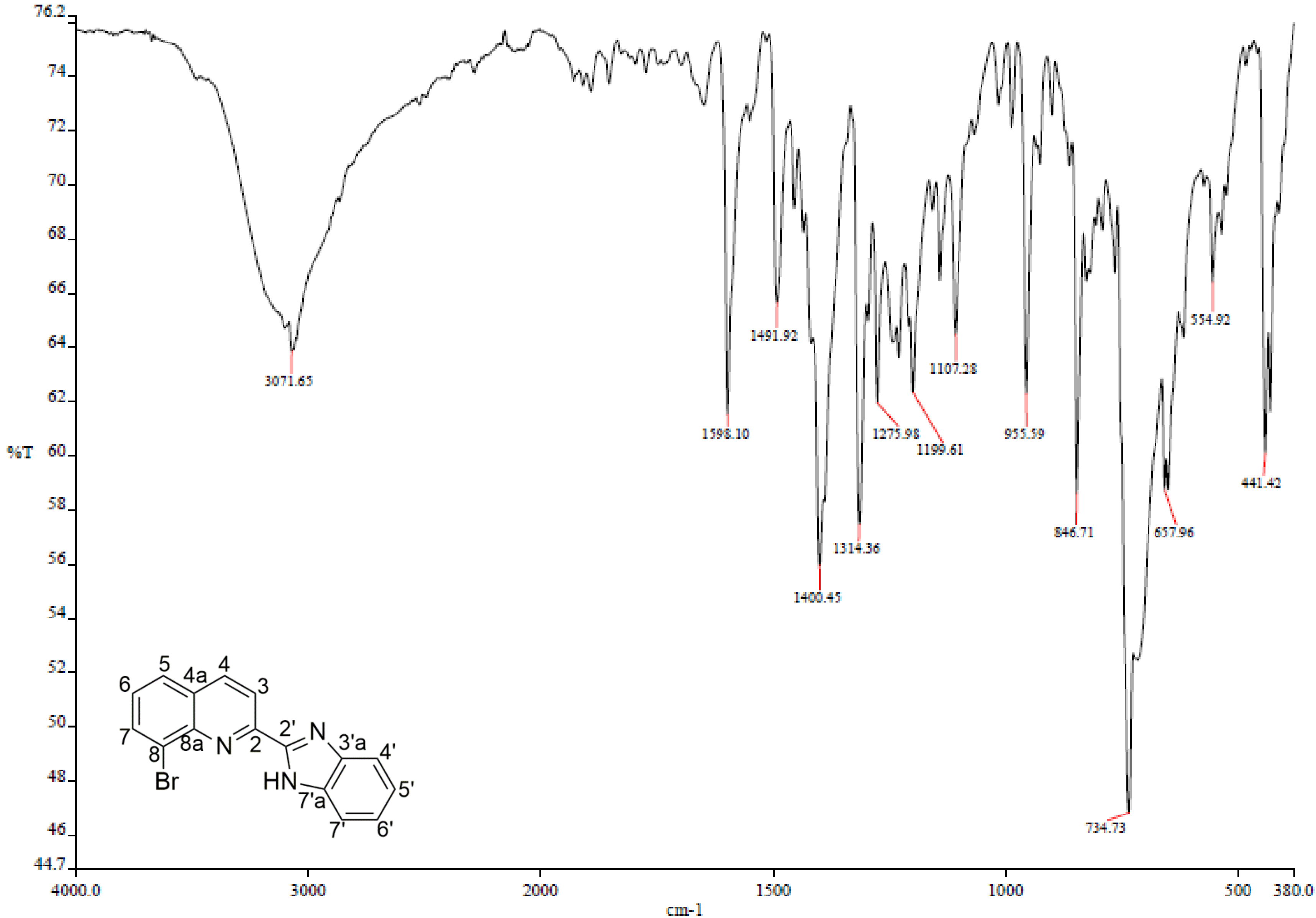

FTIR spectrum of **A5c**

Overlay Spectrum Graph Report

03/08/2017 03:13:37 PM

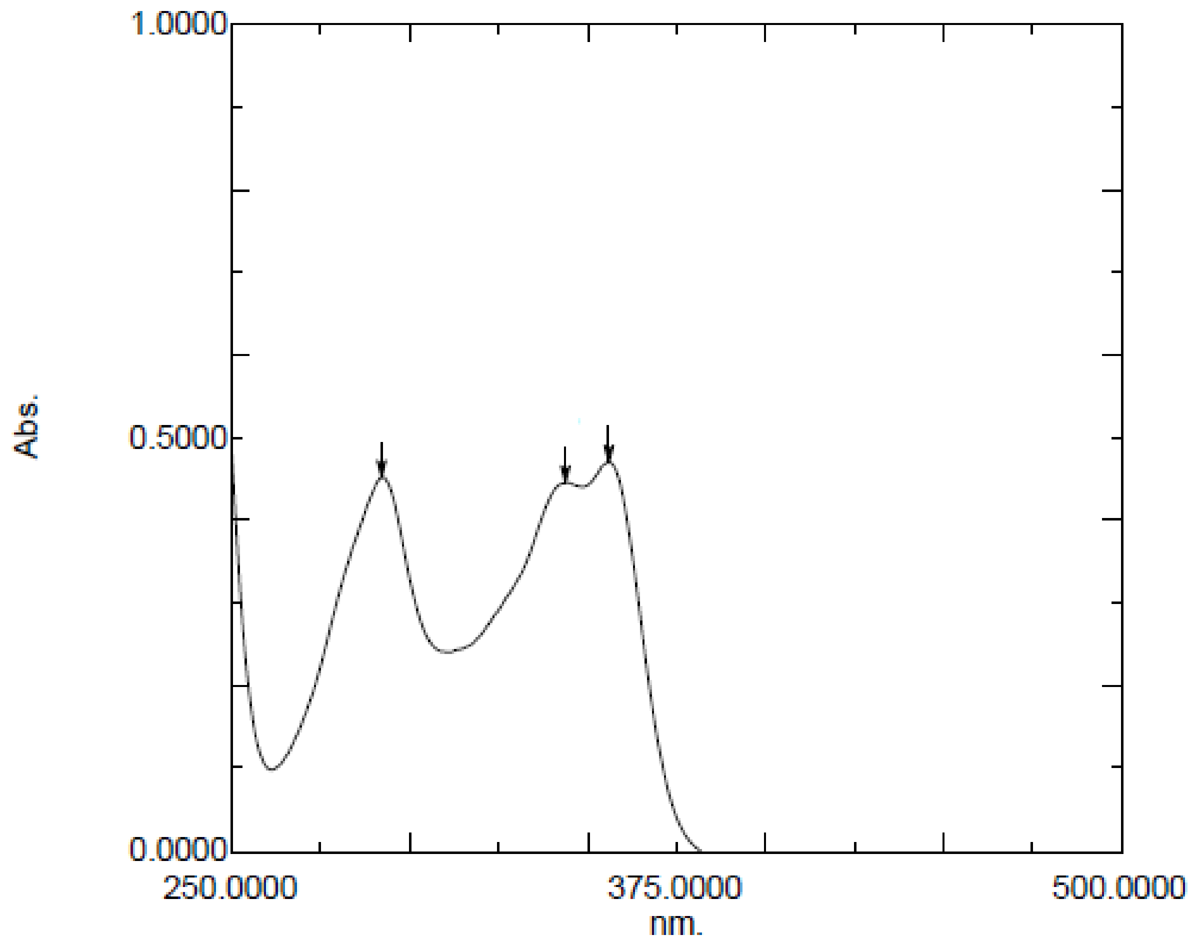

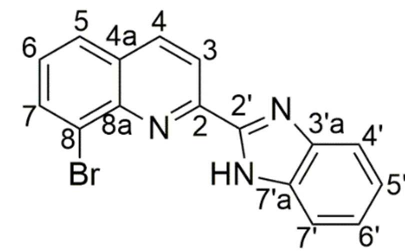

λ	absorbance	logε
292	0.4518	4.47
344	0.4450	4.46
356	0.4705	4.48

UV spectrum of **A5c**

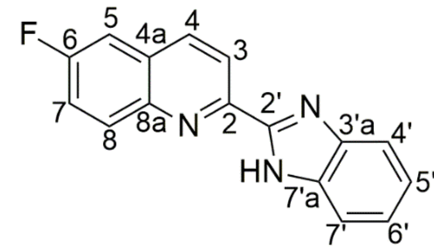

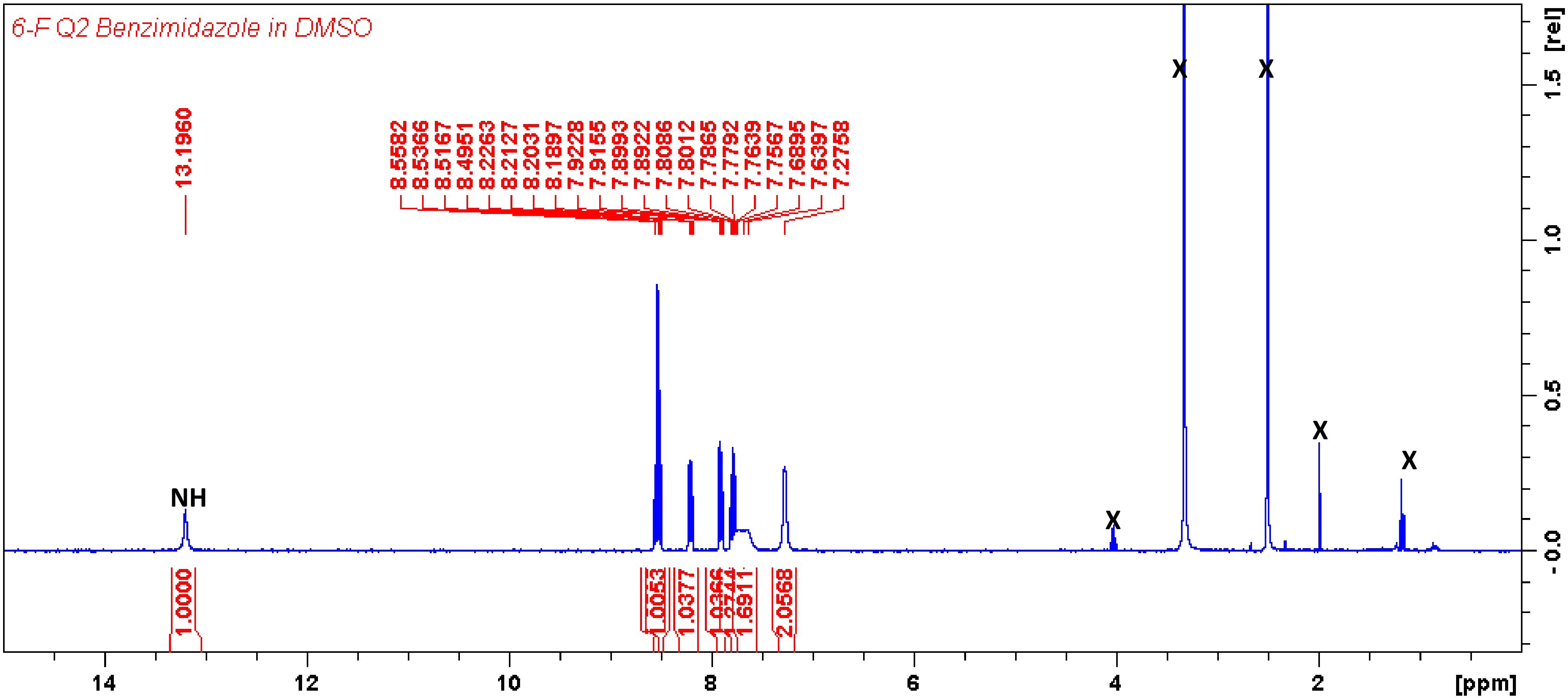

^{1}H NMR spectrum of **A5d**

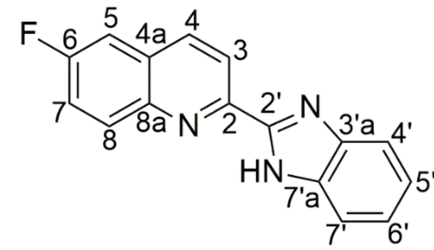

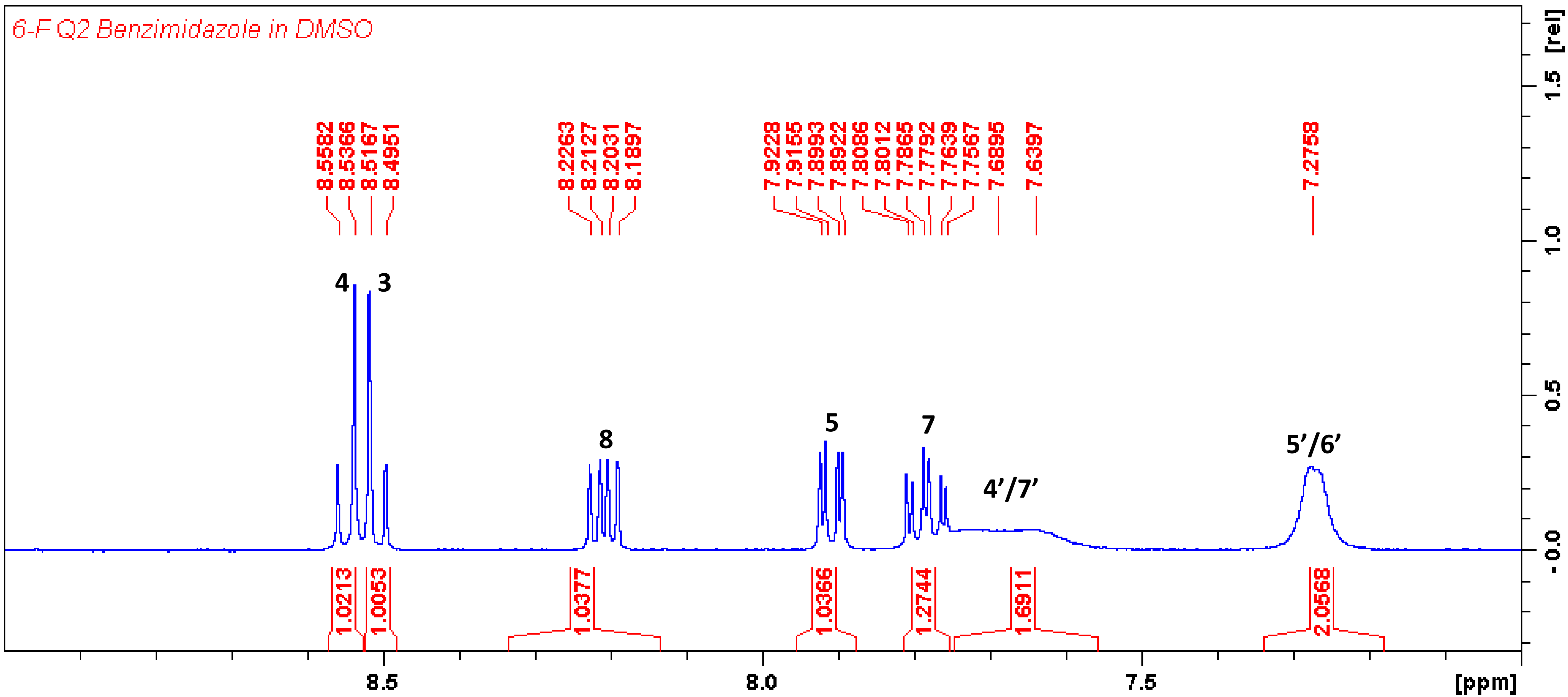

Expanded ^{1}H NMR spectrum of **A5d**

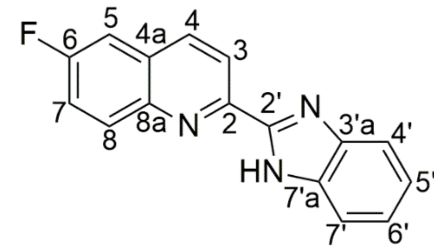

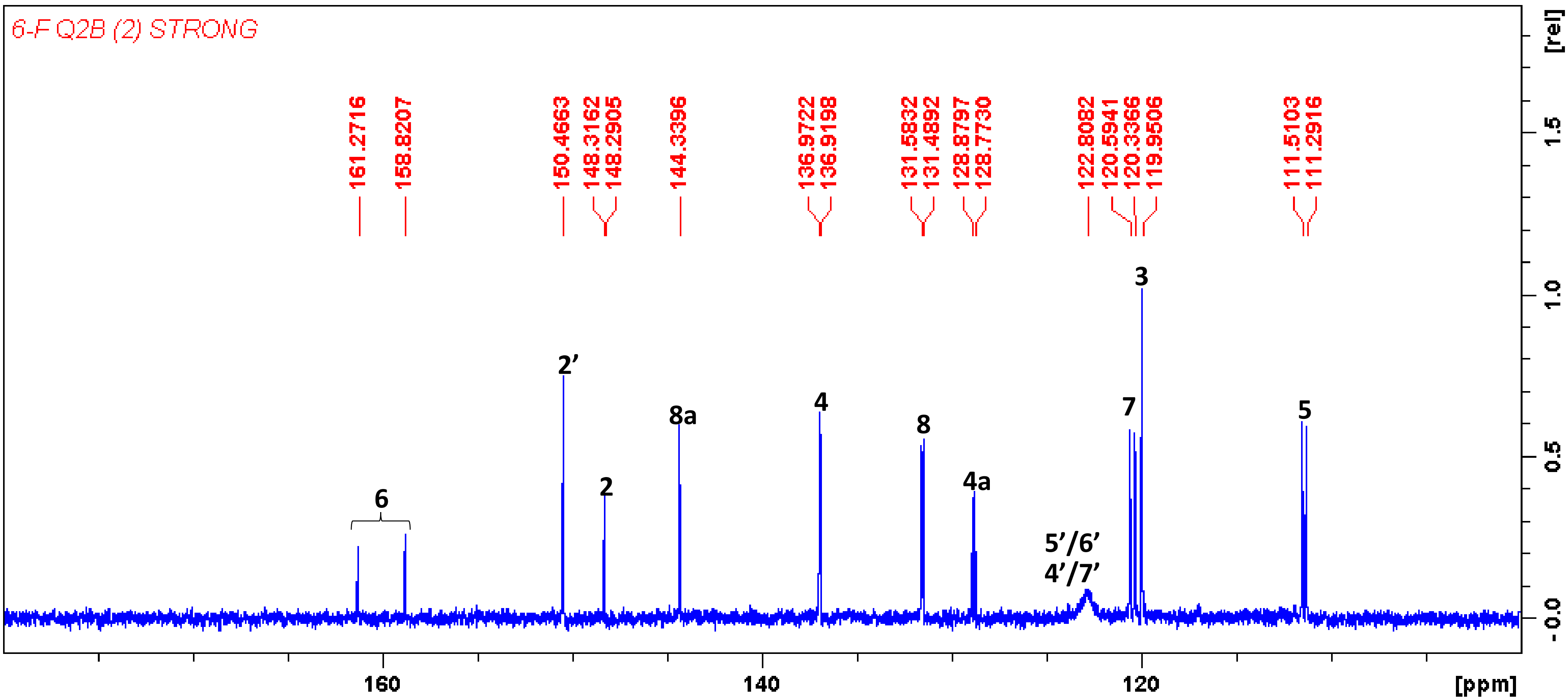

^{13}C NMR spectrum of **A5d**

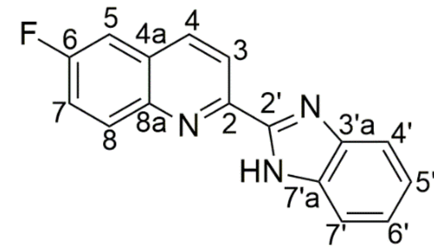

F
6
5
4a
4
3
7
8
8a
N
2
2'
N
3'a
4'
HN
7'a
5'
7'
6'

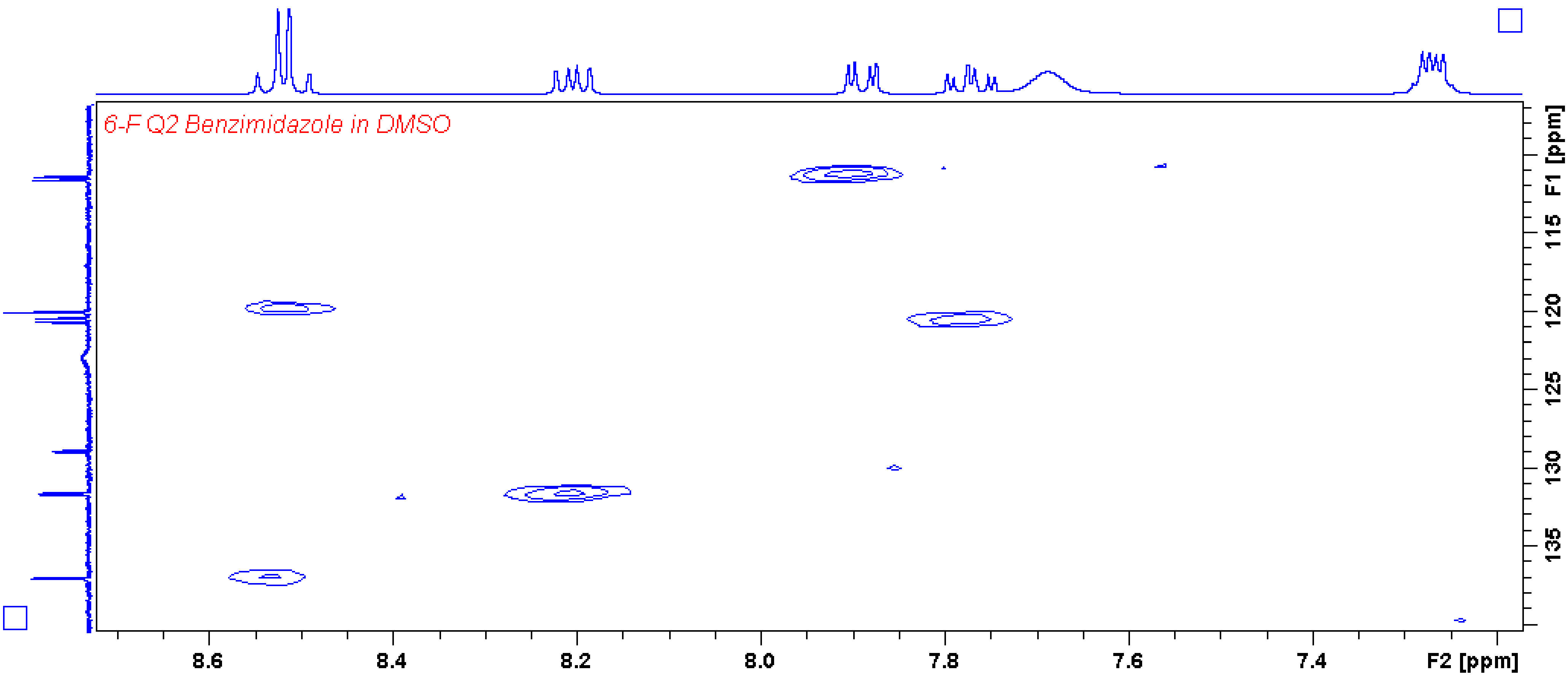

6-F Q2 Benzimidazole in DMSO
F1 [ppm]
115
120
125
130
135
8.6
8.4
8.2
8.0
7.8
7.6
7.4
F2 [ppm]

HSQC of **A5d**

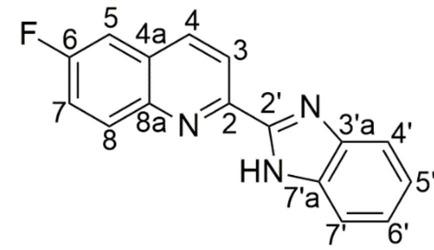
F
6
5
4a
4
3
7
8
8a
N
2
2'
N
3'a
4'
5'
6'
7'
7'a
HN

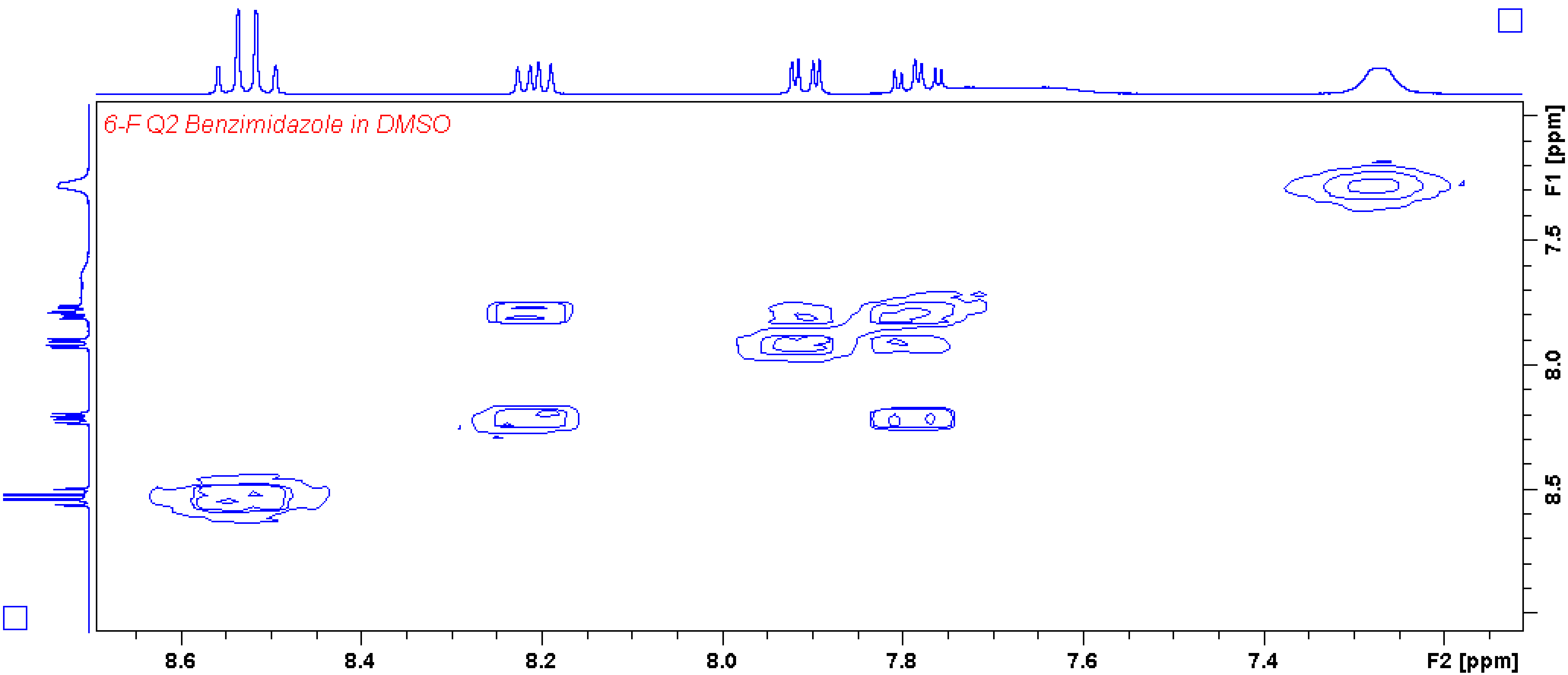
6-F Q2 Benzimidazole in DMSO
F1 [ppm]
7.5
8.0
8.5
8.6
8.4
8.2
8.0
7.8
7.6
7.4
F2 [ppm]

COSY of **A5d**

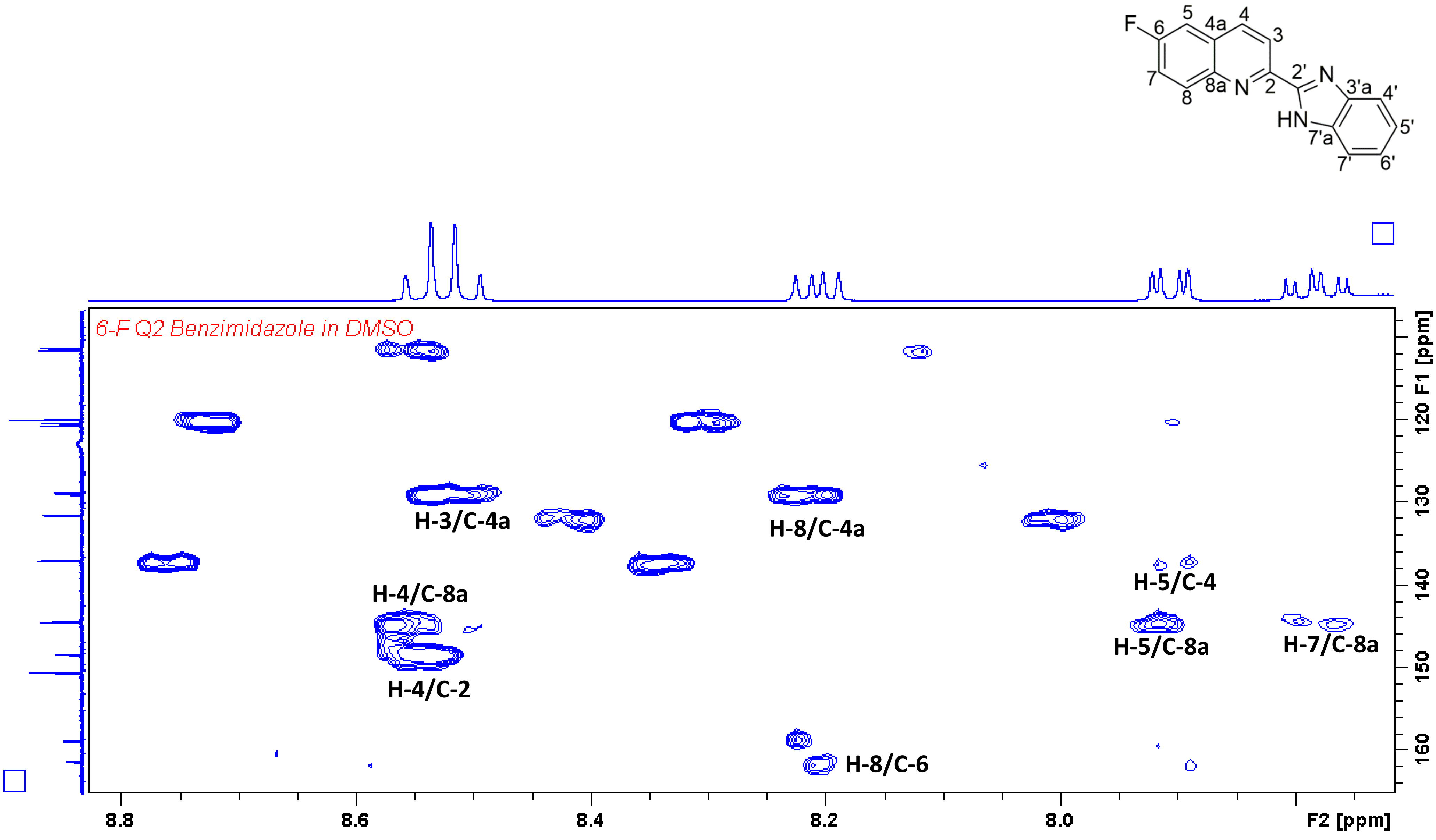
F
6
5
4a
4
3
7
8
8a
N
2
2'
N
3'a
4'
5'
HN
7'a
7'
6'
6-F Q2 Benzimidazole in DMSO
H-3/C-4a
H-8/C-4a
H-4/C-8a
H-4/C-2
H-5/C-4
H-5/C-8a
H-7/C-8a
H-8/C-6
8.8
8.6
8.4
8.2
8.0
F2 [ppm]
120
130
140
150
160
F1 [ppm]

HMBC of **A5d**

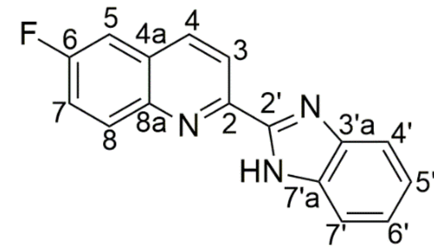

Elemental Composition Report

Single Mass Analysis

Tolerance = 50.0 PPM / DBE: min = -1.5, max = 100.0
Element prediction: Off
Number of isotope peaks used for i-FIT = 3

Monoisotopic Mass, Even Electron Ions
5 formula(e) evaluated with 1 results within limits (up to 20 closest results for each mass)
Elements Used:
C: 15-20 H: 5-10 N: 0-5 F: 0-1
SSQB3 3 (0.068) Cm (1:61)
TOF MS ES-

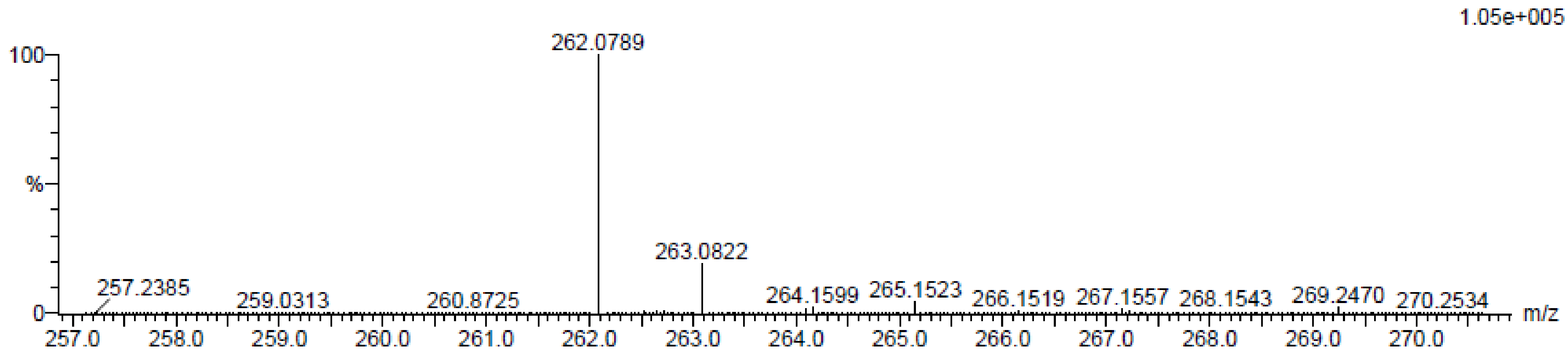

Minimum:				-1.5			
Maximum:		5.0	50.0	100.0			
Mass	Calc. Mass	mDa	PPM	DBE	i-FIT	i-FIT (Norm)	Formula
262.0789	262.0781	0.8	3.1	13.5	585.1	0.0	C16 H9 N3 F

High resolution mass spectrum of **A5d**

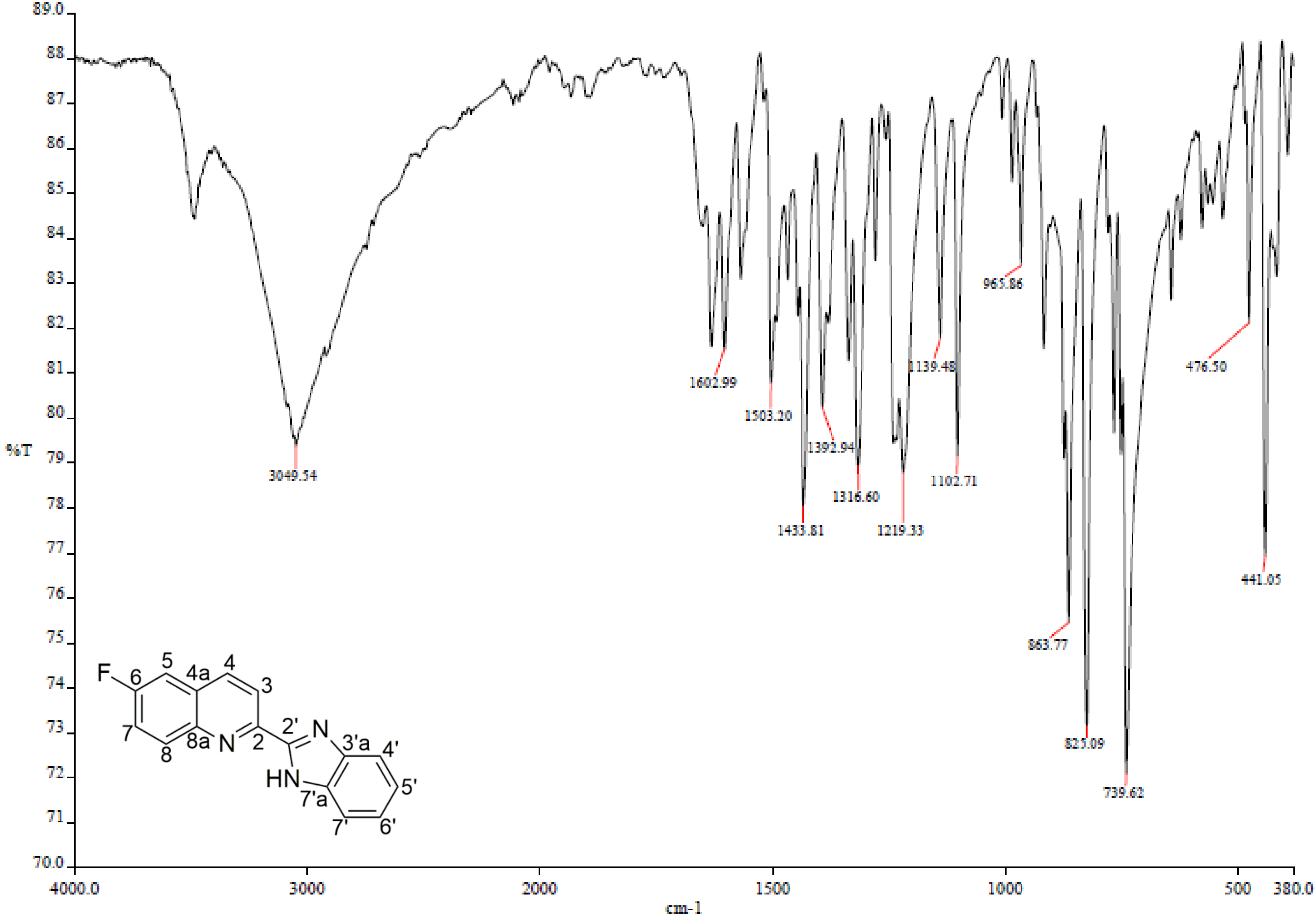

FTIR spectrum of **A5d**

Overlay Spectrum Graph Report

03/08/2017 03:11:40 PM

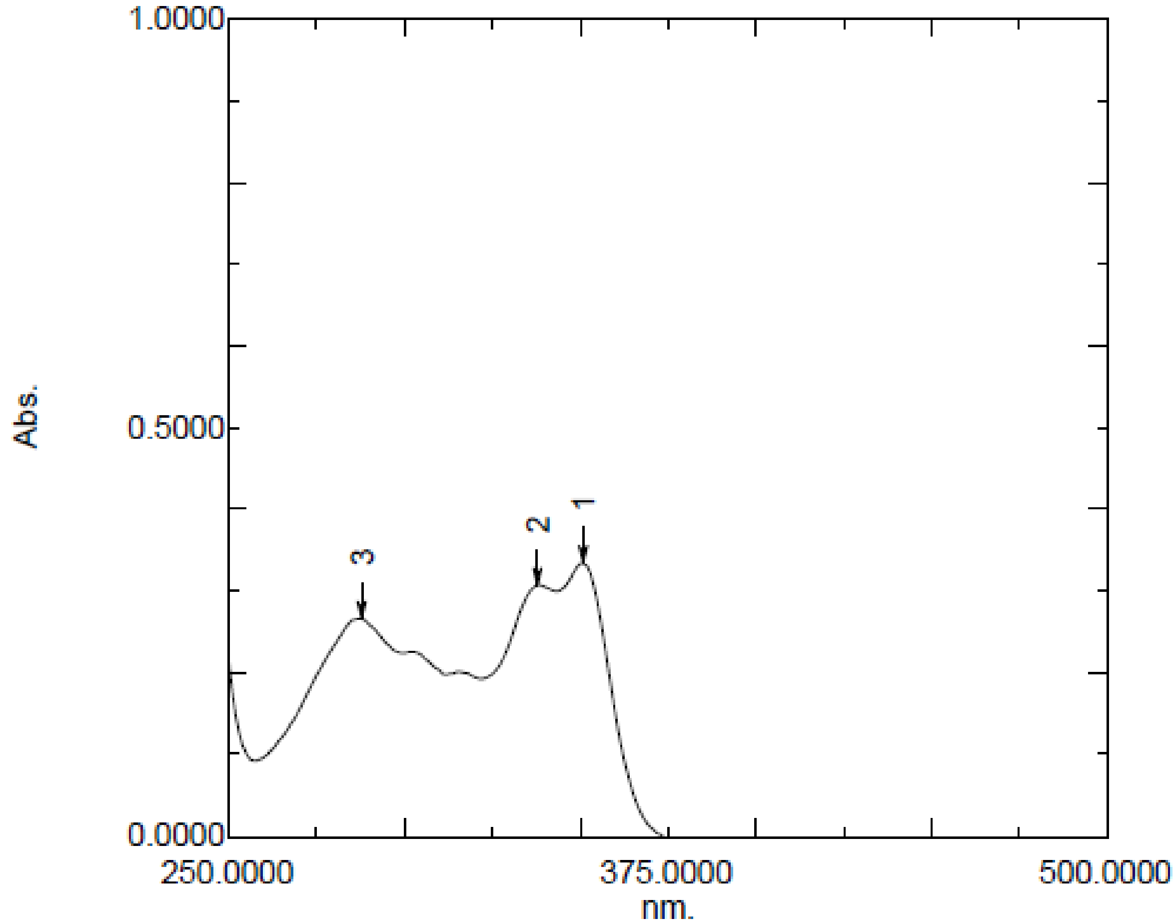

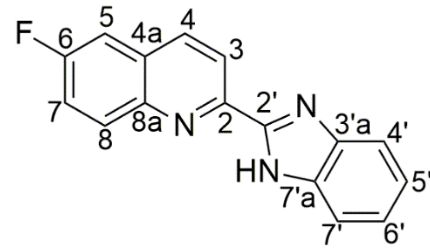

λ	absorbance	logε
288	0.2657	4.15
302	0.2253	4.07
315	0.2006	4.02
338	0.3072	4.21
351	0.3337	4.24

Page 1 / 1

UV spectrum of **A5d**

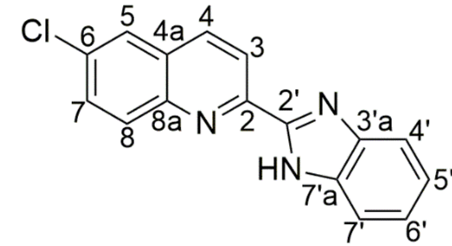

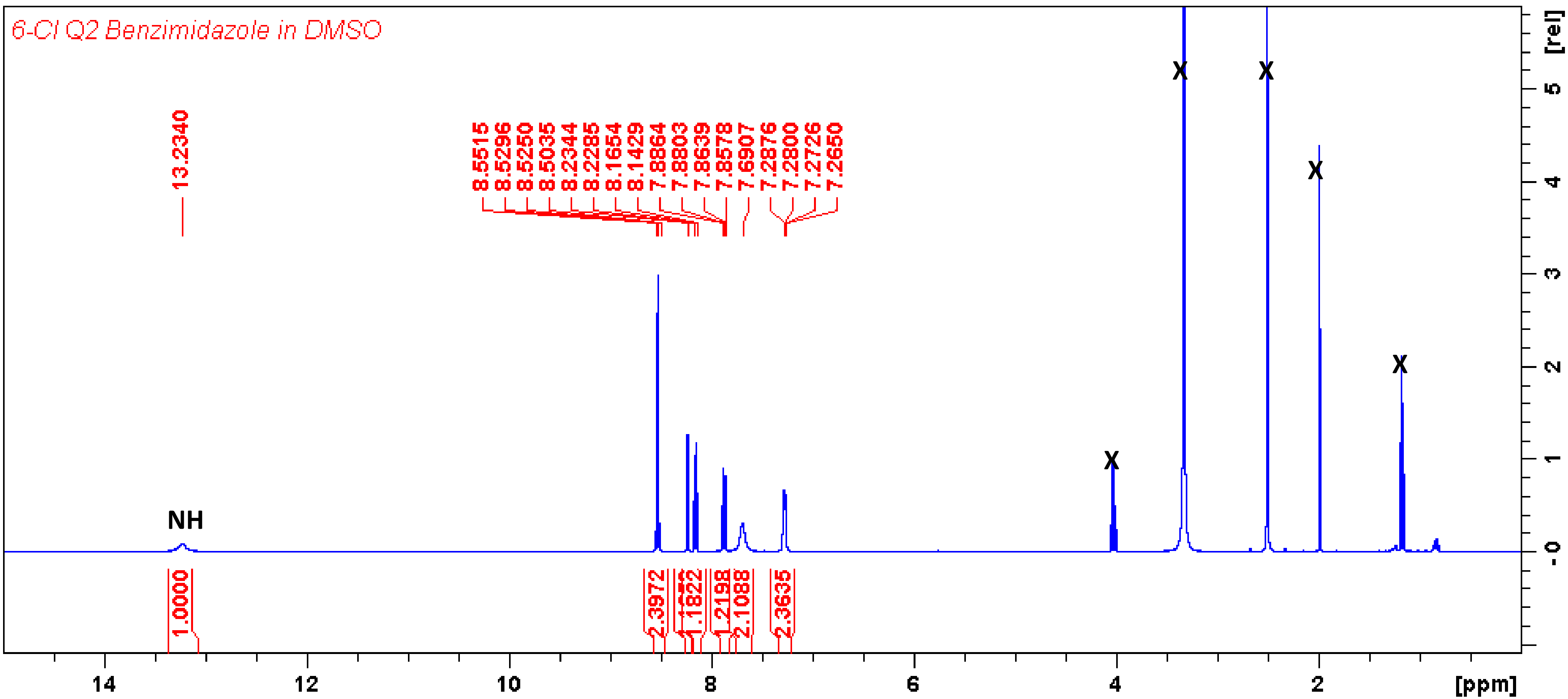

^{1}H NMR spectrum of **A5e**

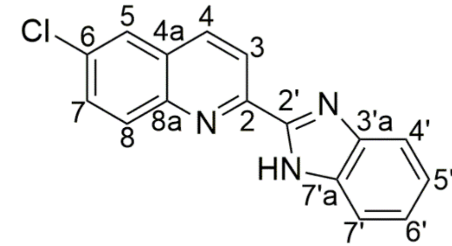

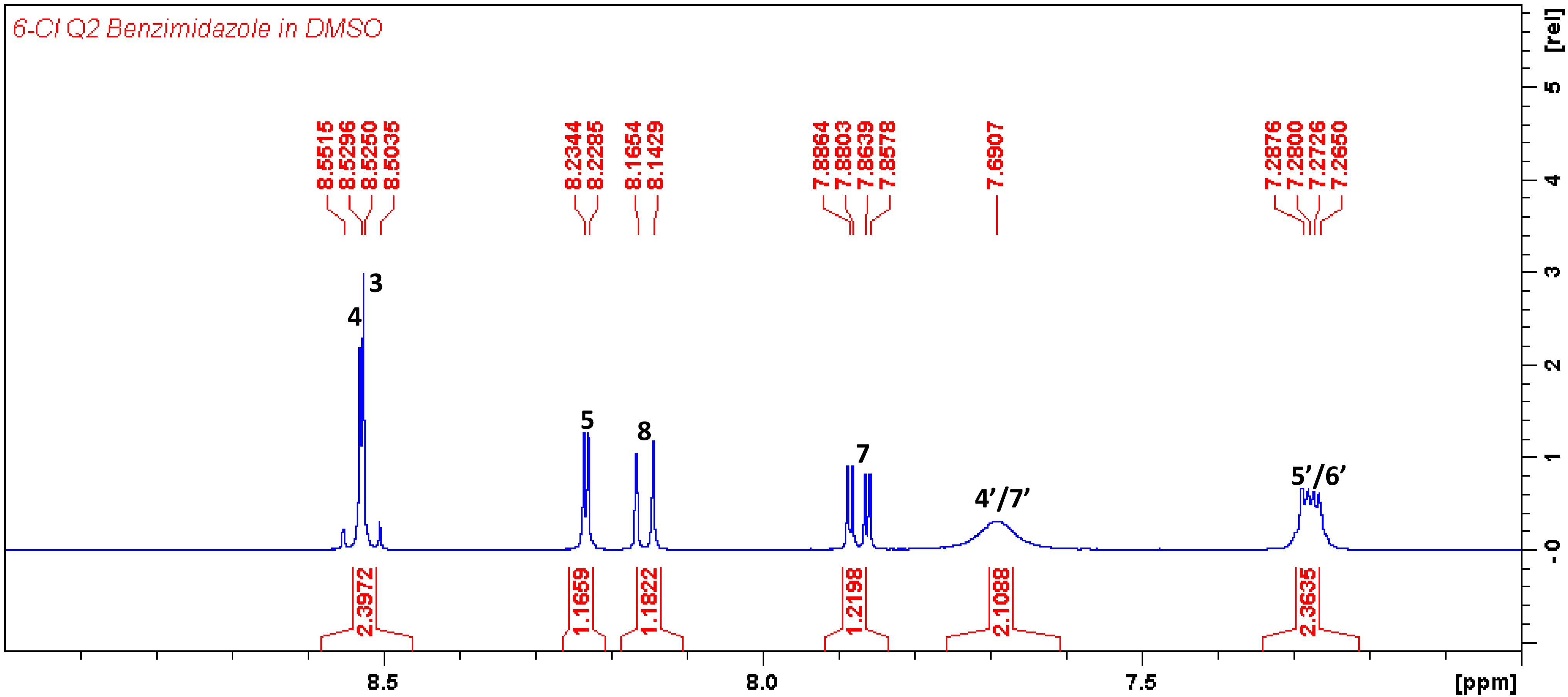

Expanded ^{1}H NMR spectrum of **A5e**

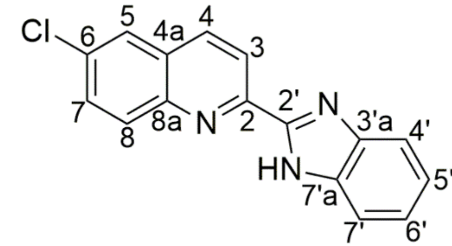

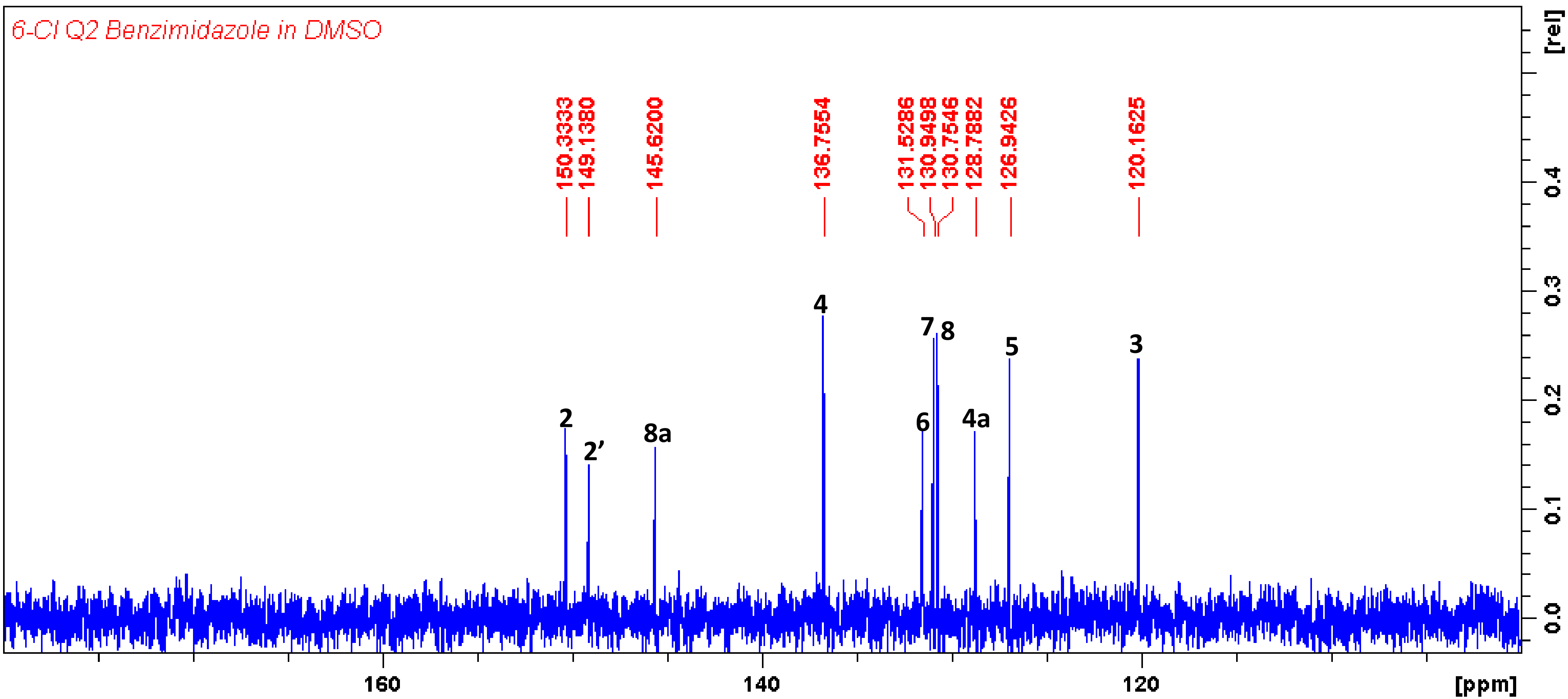

^{13}C NMR spectrum of **A5e**

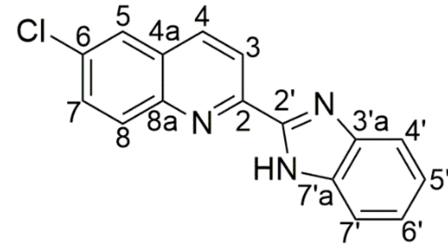

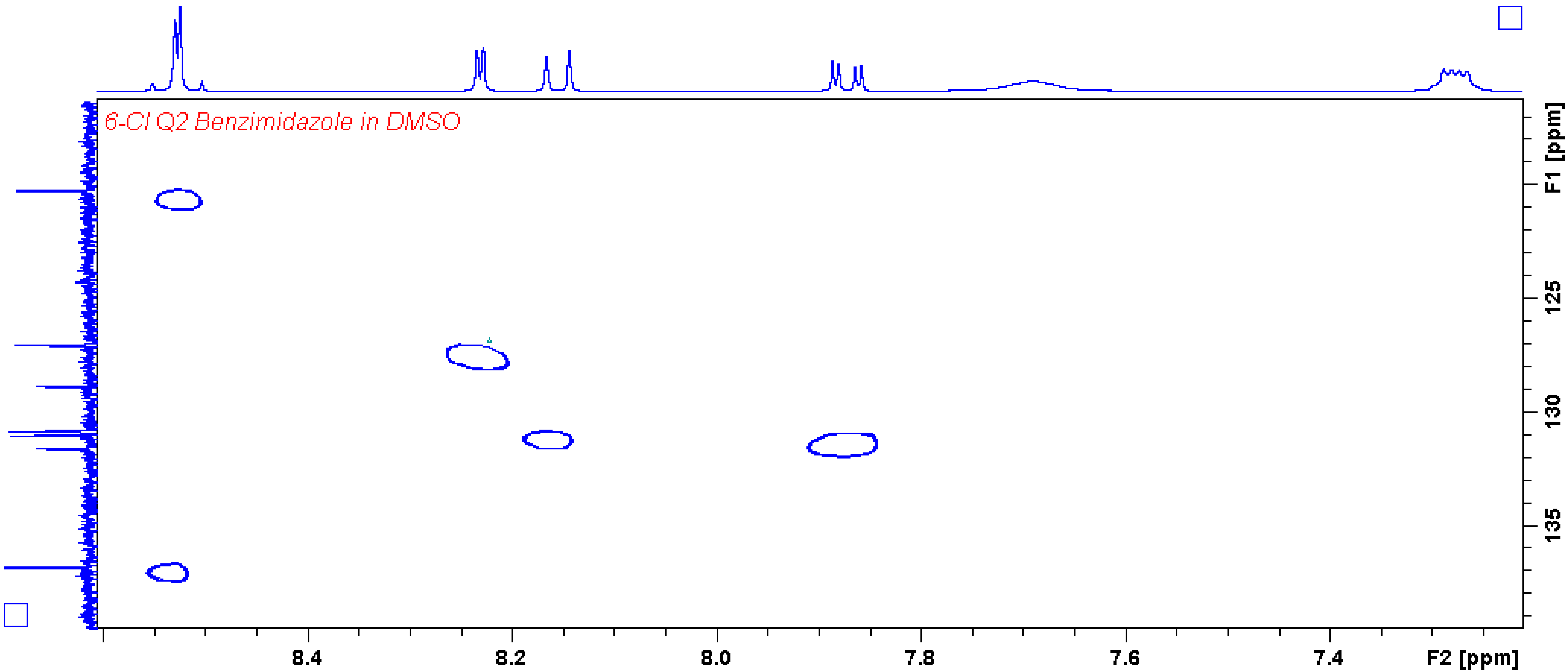

6-Cl Q2 Benzimidazole in DMSO
F1 [ppm]
125
130
135
8.4
8.2
8.0
7.8
7.6
7.4
F2 [ppm]

HSQC of **A5e**

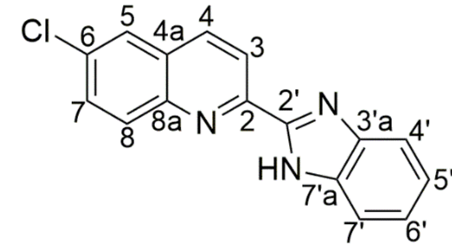
Cl
6
5
4a
4
3
7
8
8a
N
2
2'
N
3'a
4'
HN
7'a
5'
7'
6'

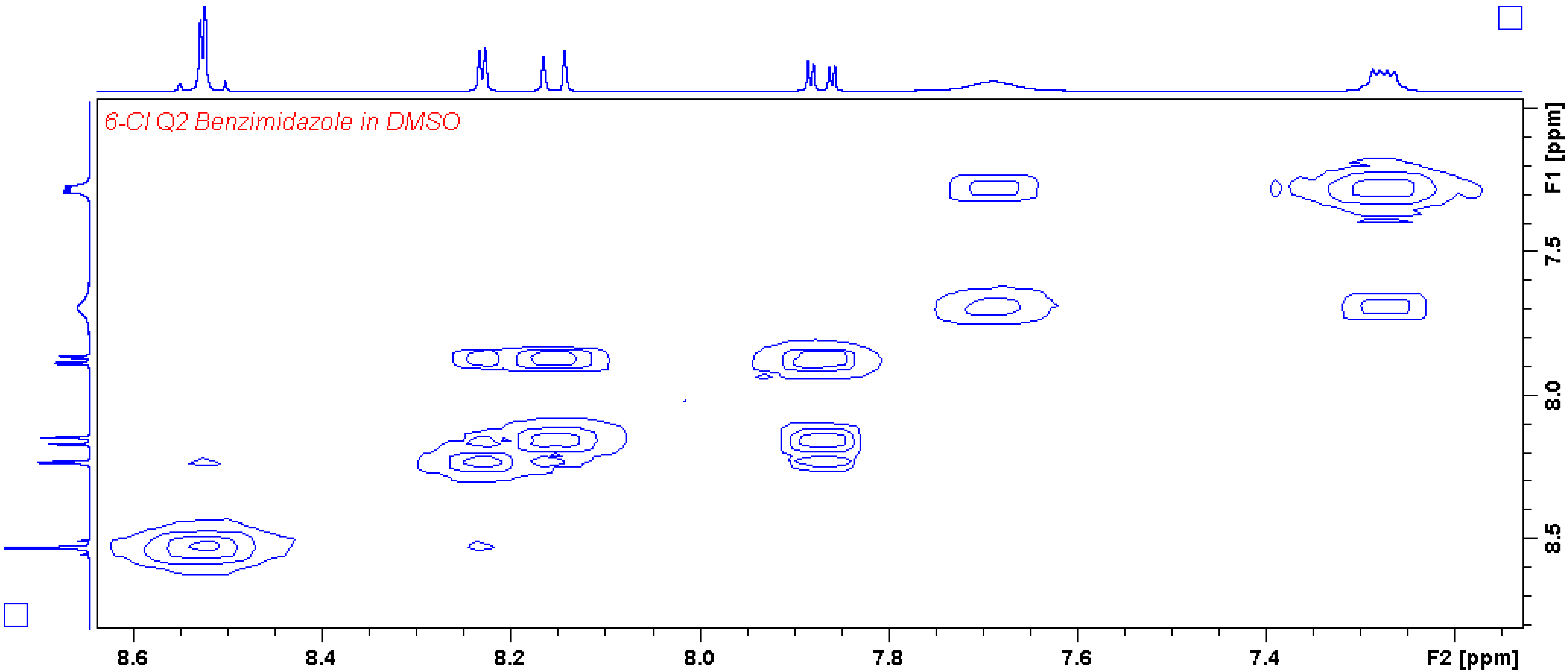
6-Cl Q2 Benzimidazole in DMSO
F1 [ppm]
7.5
8.0
8.5
8.6
8.4
8.2
8.0
7.8
7.6
7.4
F2 [ppm]

COSY of **A5e**

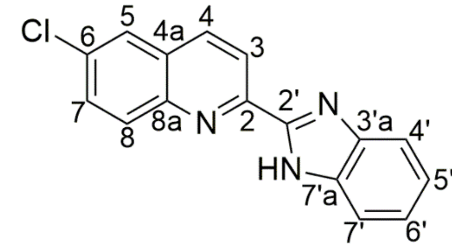

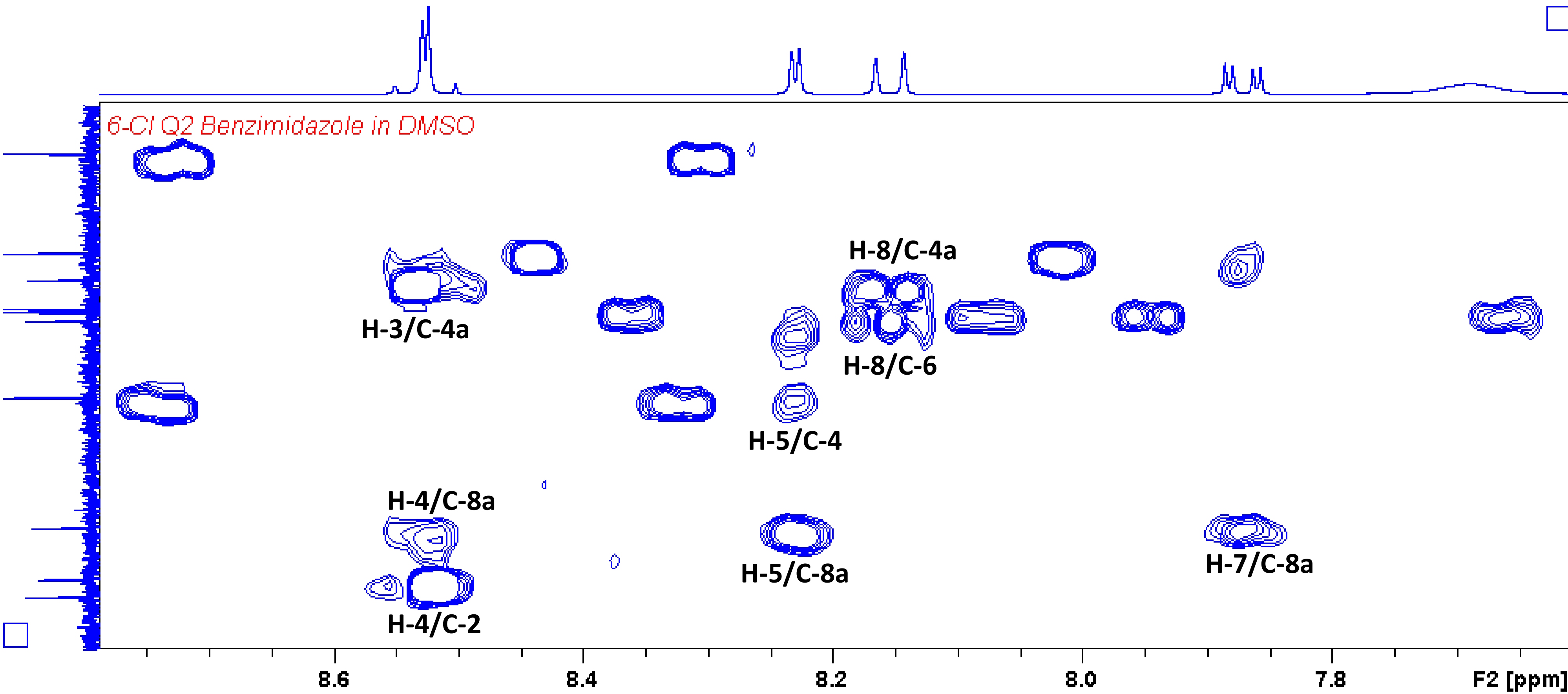

6-Cl Q2 Benzimidazole in DMSO
H-8/C-4a
H-3/C-4a
H-8/C-6
H-5/C-4
H-4/C-8a
H-5/C-8a
H-7/C-8a
H-4/C-2
F1 [ppm]
F2 [ppm]

HMBC of **A5e**

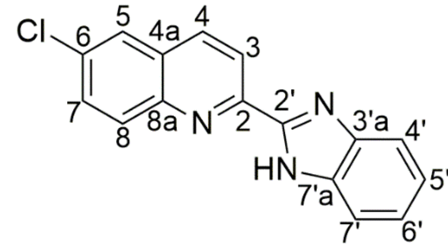

Elemental Composition Report

Single Mass Analysis

Tolerance = 5.0 PPM / DBE: min = -1.5, max = 100.0
Element prediction: Off
Number of isotope peaks used for i-FIT = 3

Monoisotopic Mass, Even Electron Ions
6 formula(e) evaluated with 1 results within limits (up to 20 closest results for each mass)
Elements Used:
C: 15-20 H: 5-10 N: 0-5 Cl: 0-1
SSQB5 58 (1.923) Cm (1:61)
TOF MS ES-

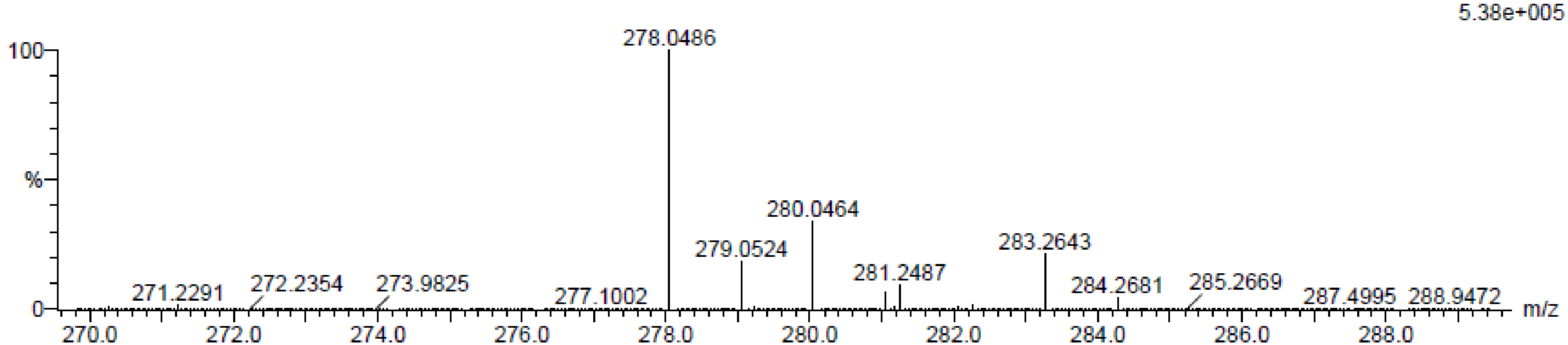

Minimum:				-1.5			
Maximum:		5.0	5.0	100.0			
Mass	Calc. Mass	mDa	PPM	DBE	i-FIT	i-FIT (Norm)	Formula
278.0486	278.0485	0.1	0.4	13.5	644.4	0.0	C16 H9 N3 Cl

High resolution mass spectrum of **A5e**

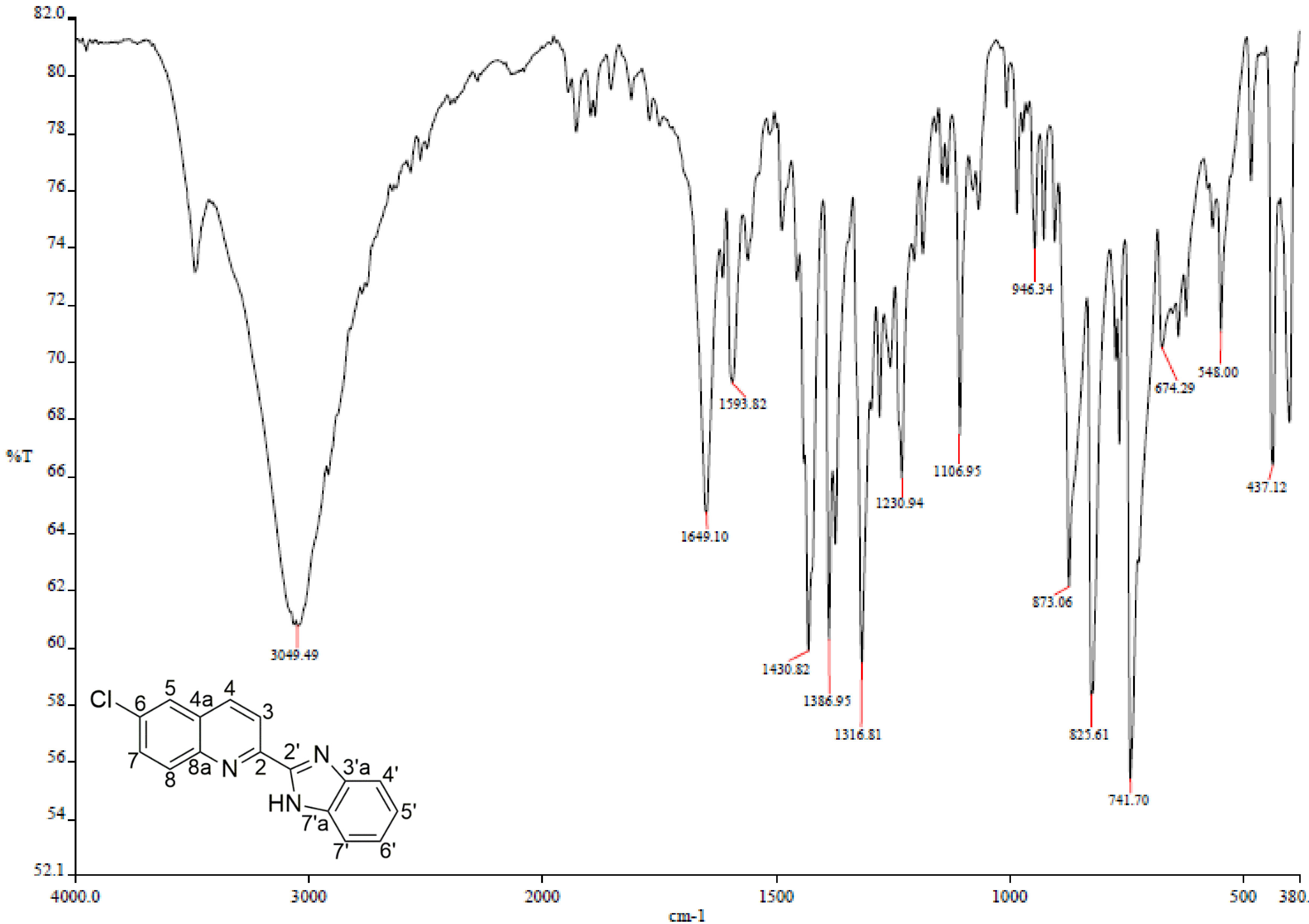

FTIR spectrum of **A5e**

Overlay Spectrum Graph Report

03/08/2017 03:10:07 PM

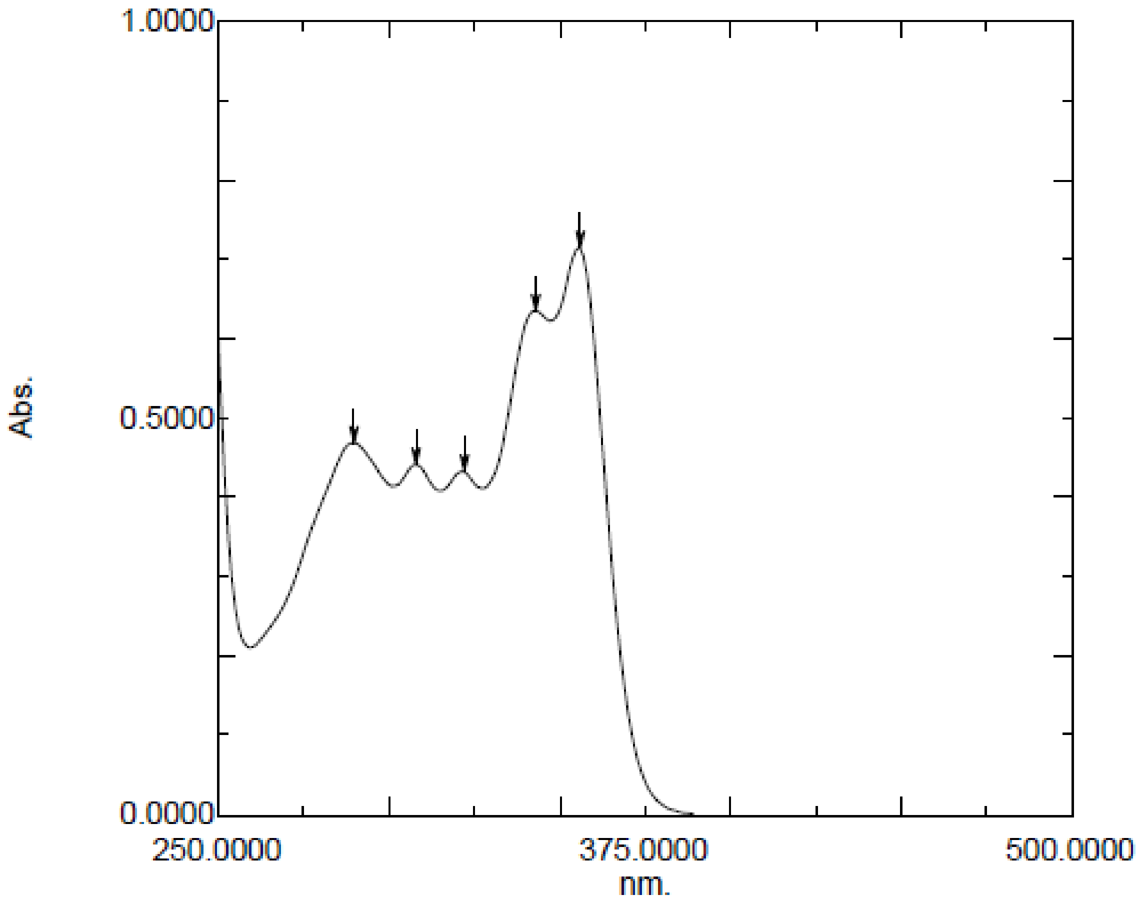

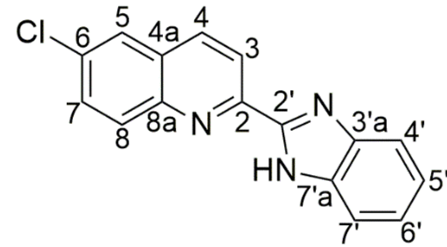

λ	absorbance	logε
290	0.4683	4.42
309	0.4392	4.39
323	0.4290	4.38
343	0.6349	4.55
356	0.7141	4.60

Page 1 / 1

UV spectrum of **A5e**

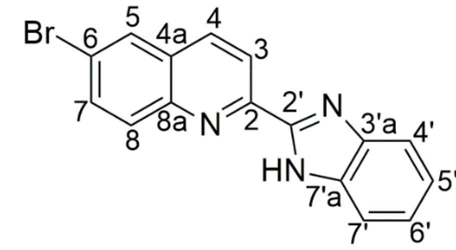

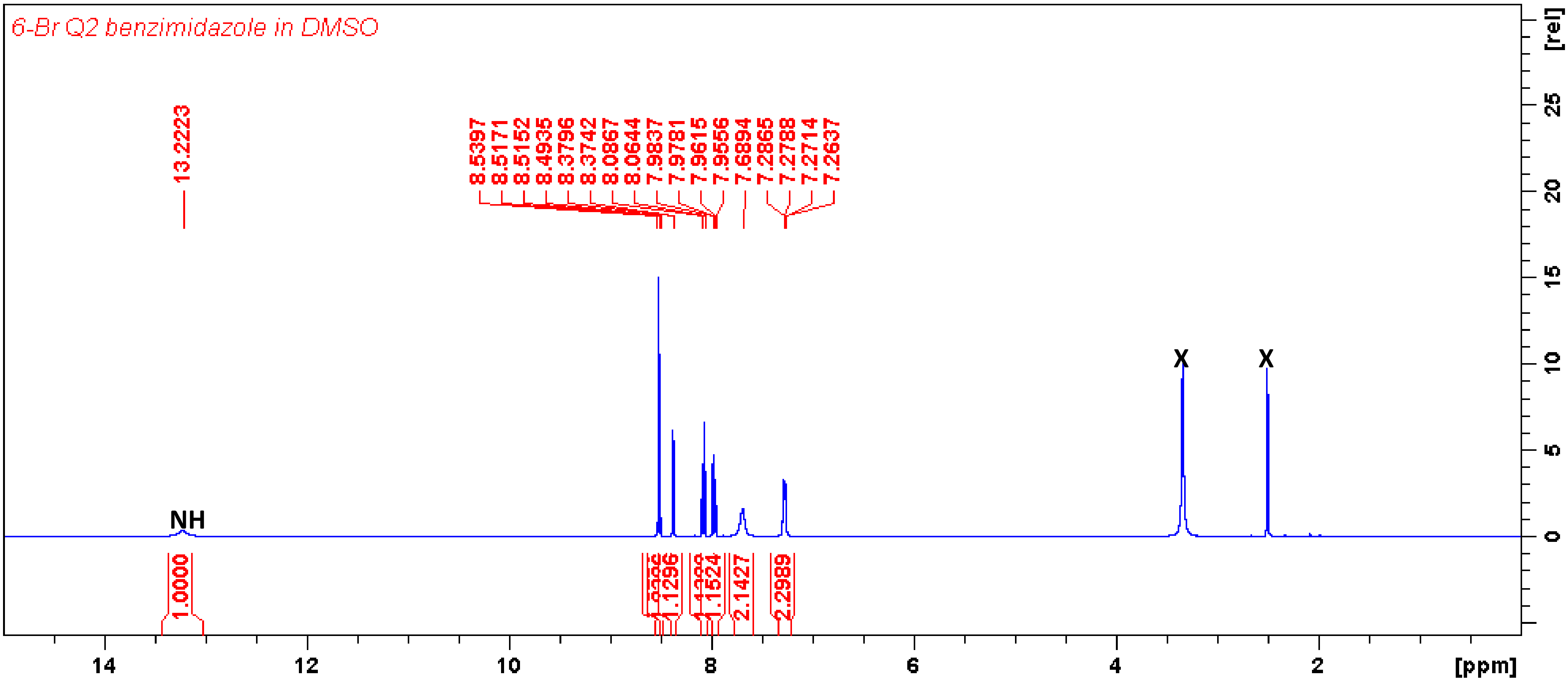

^{1}H NMR spectrum of **A5f**

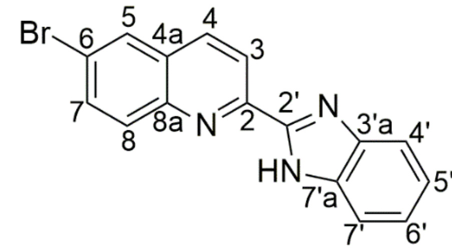

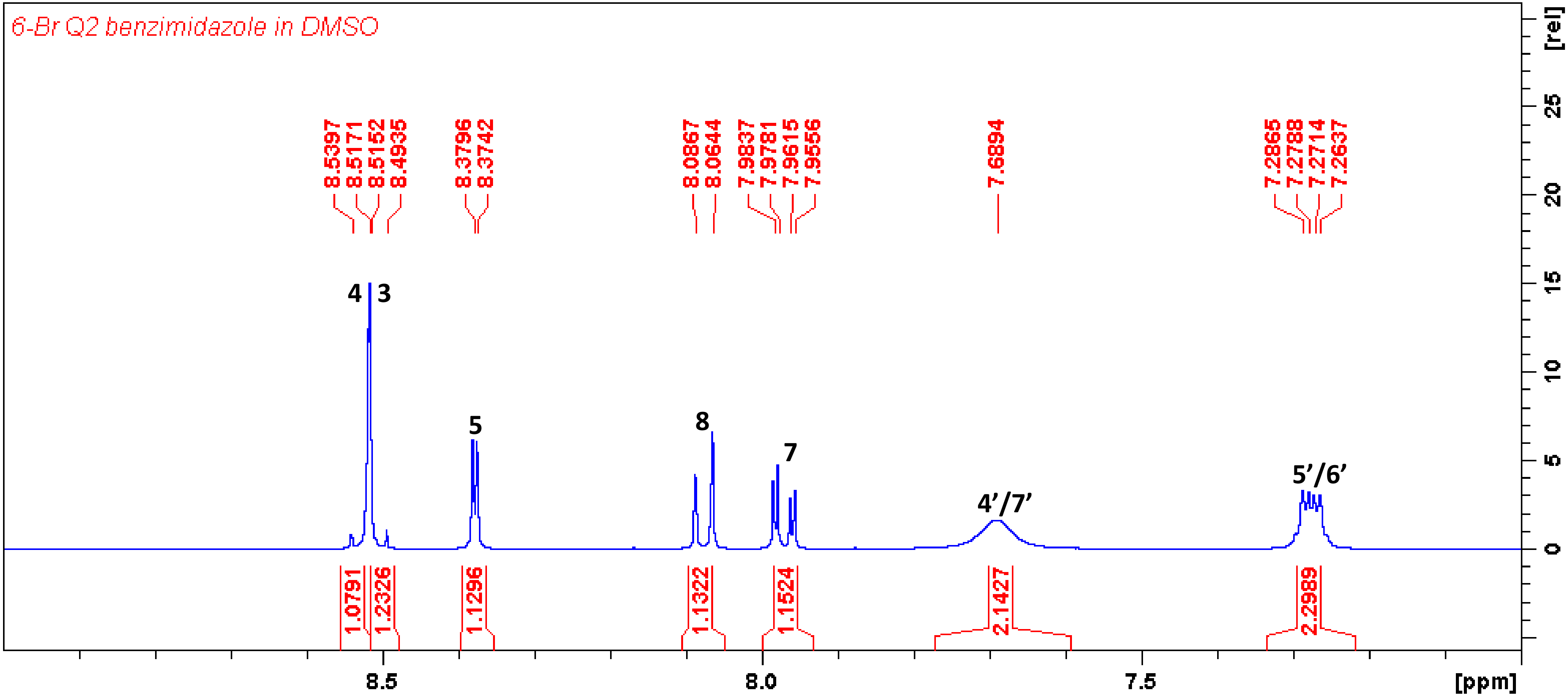

Expanded ^{1}H NMR spectrum of **A5f**

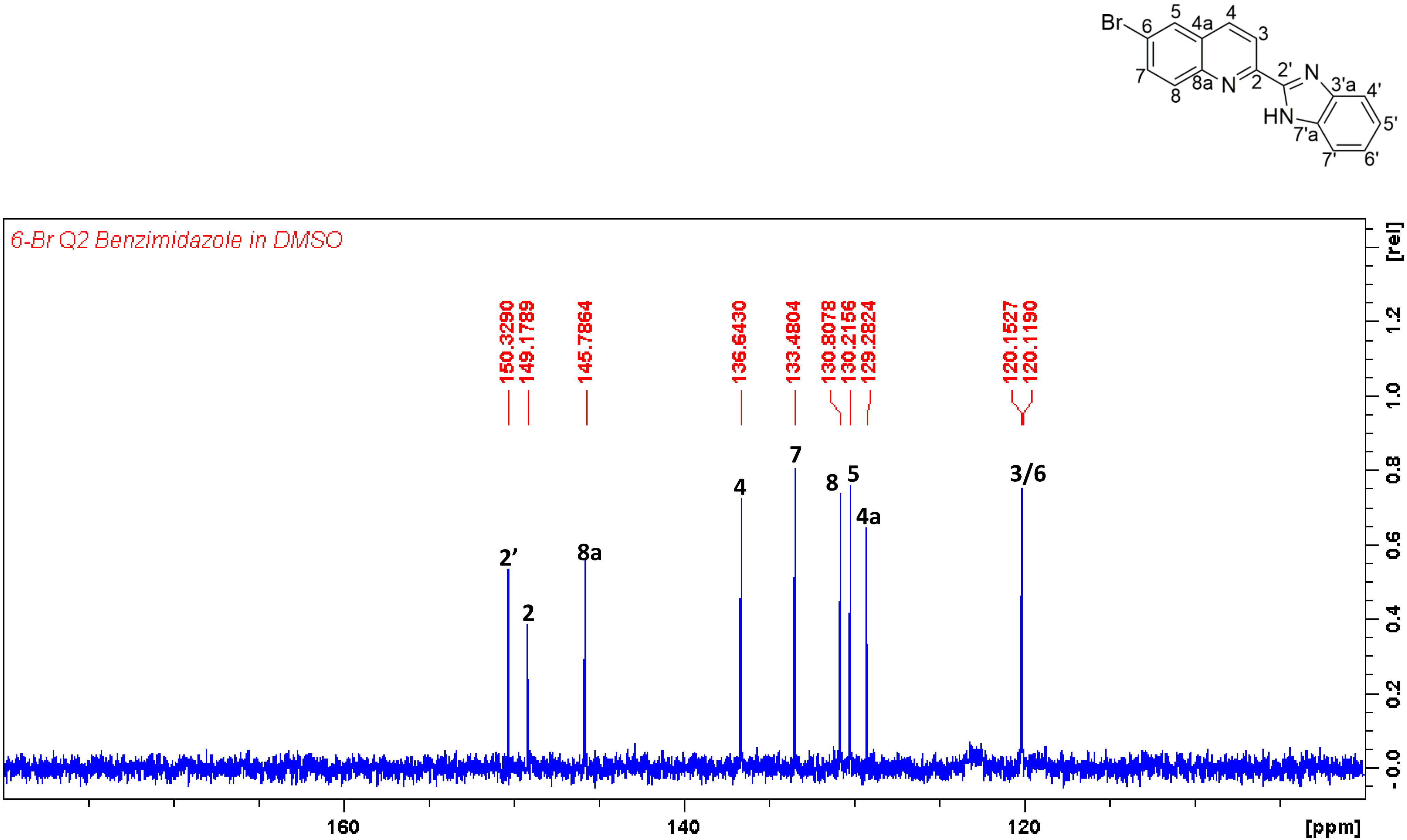

^{13}C NMR spectrum of **A5f**

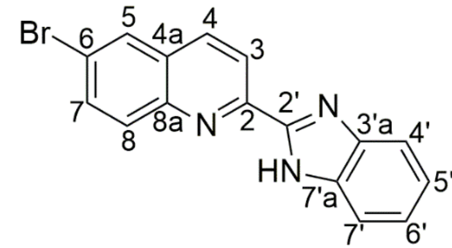
Br
6
5
4a
4
3
7
8
8a
N
2
2'
N
3'a
4'
HN
7'a
5'
7'
6'

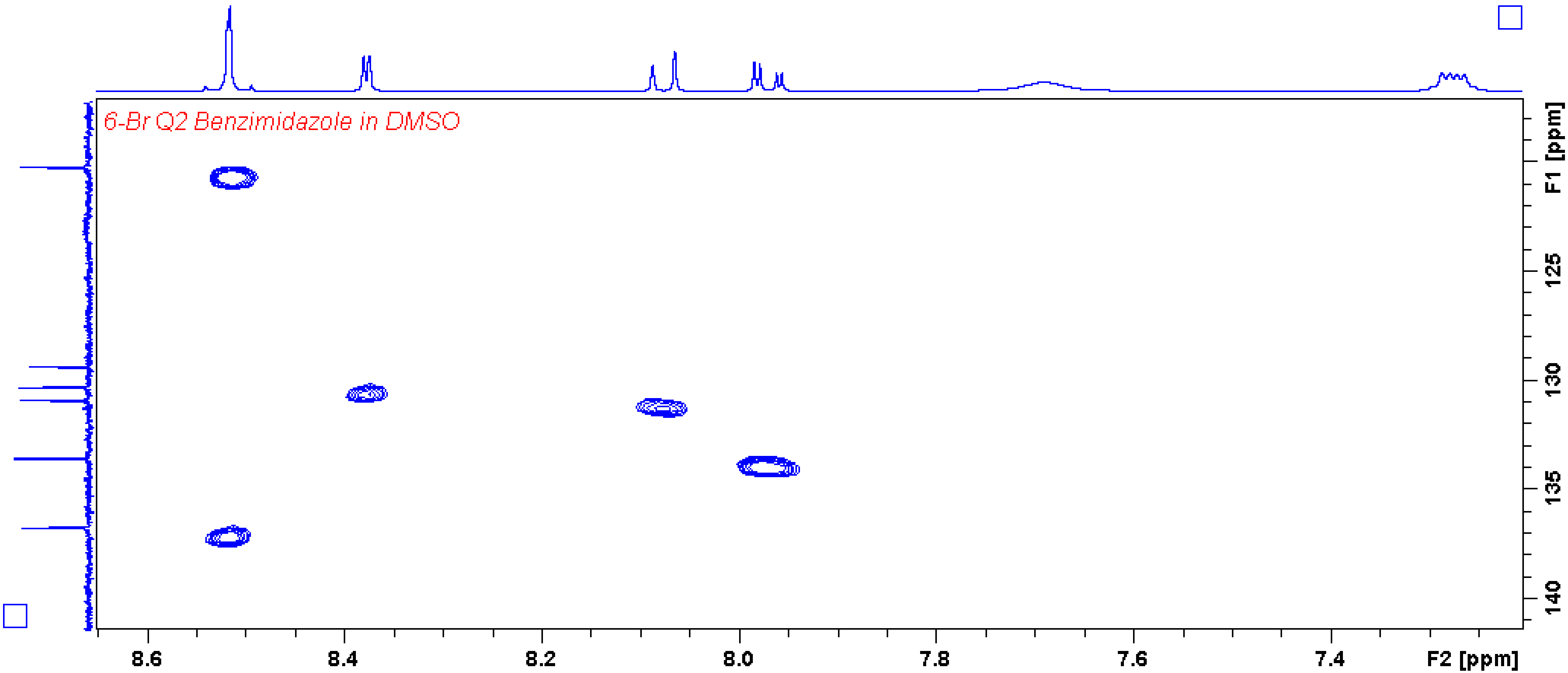
6-Br Q2 Benzimidazole in DMSO
F1 [ppm]
125
130
135
140
8.6
8.4
8.2
8.0
7.8
7.6
7.4
F2 [ppm]

HSQC of **A5f**

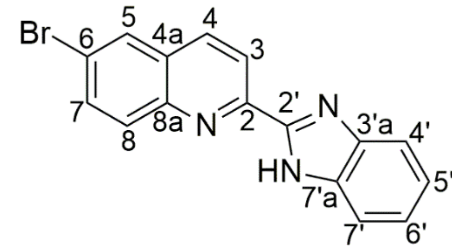
Br
6
5
4a
4
3
7
8
8a
N
2
2'
N
3'a
4'
HN
7'a
5'
7'
6'

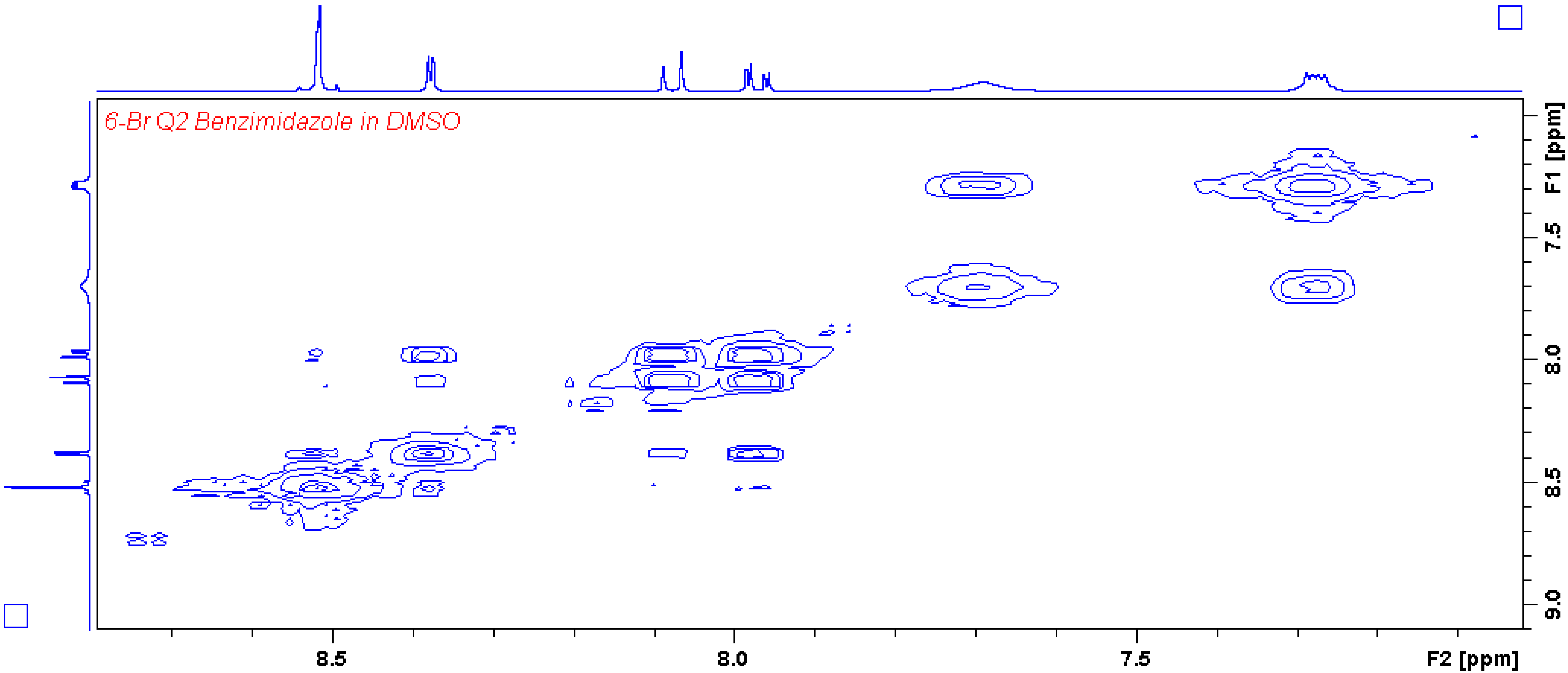
6-Br Q2 Benzimidazole in DMSO
8.5
8.0
7.5
F2 [ppm]
F1 [ppm]
9.0

COSY of **A5f**

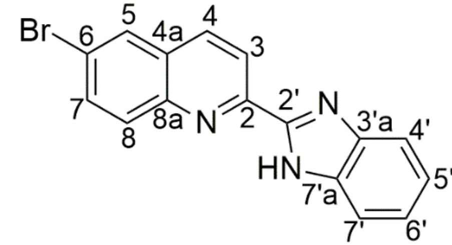
Br
6
5
4a
4
3
7
8
8a
N
2
2'
N
3'a
4'
5'
HN
7'a
7'
6'

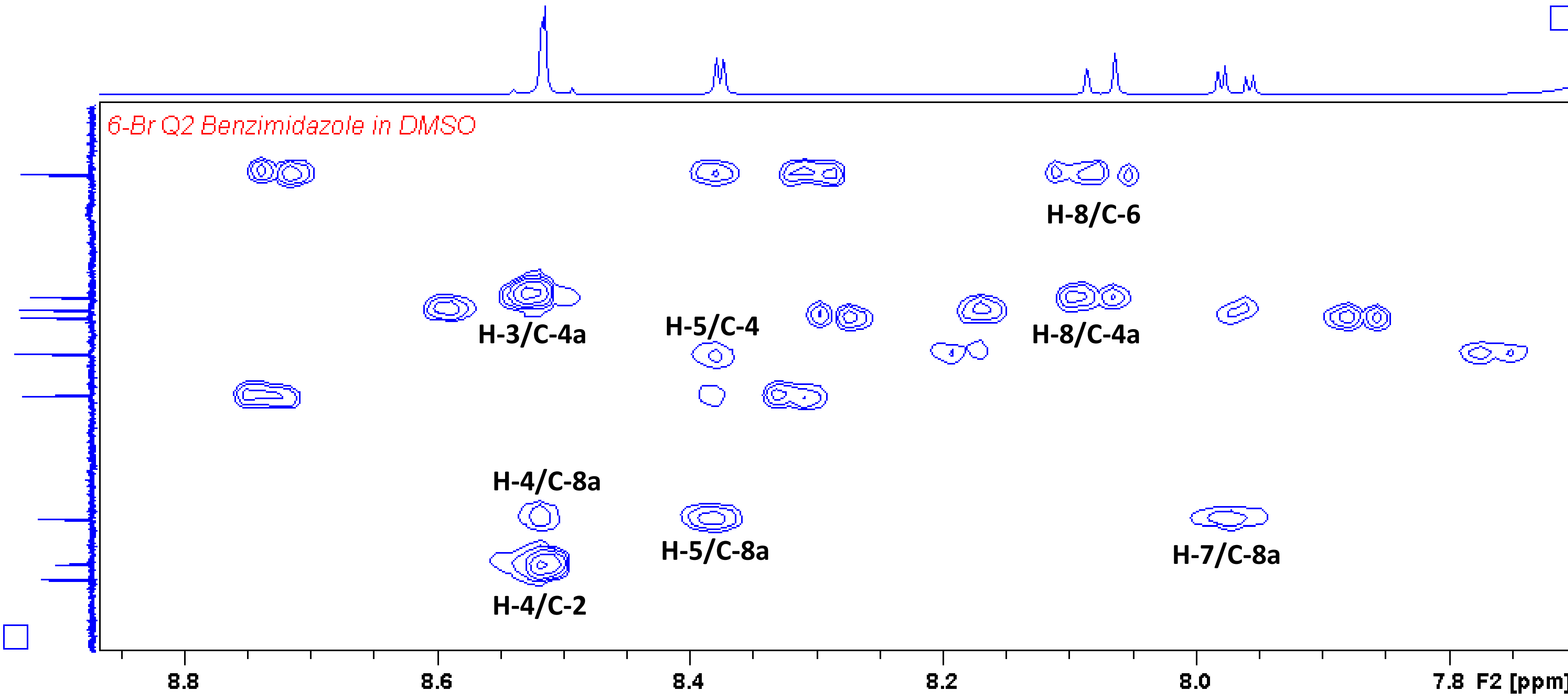
6-Br Q2 Benzimidazole in DMSO
H-8/C-6
H-3/C-4a
H-5/C-4
H-8/C-4a
H-4/C-8a
H-5/C-8a
H-7/C-8a
H-4/C-2
8.8
8.6
8.4
8.2
8.0
7.8
F2 [ppm]
130
140
150
F1 [ppm]

HMBC of **A5f**

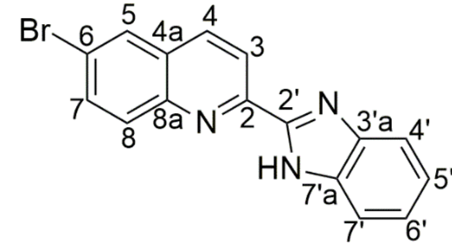

Elemental Composition Report

Single Mass Analysis

Tolerance = 5.0 PPM / DBE: min = -1.5, max = 100.0
Element prediction: Off
Number of isotope peaks used for i-FIT = 3

Monoisotopic Mass, Even Electron Ions
5 formula(e) evaluated with 1 results within limits (up to 20 closest results for each mass)
Elements Used:
C: 15-20 H: 5-10 N: 0-5 Br: 0-1

SSQB1 38 (1.249) Cm (1:61)
TOF MS ES-

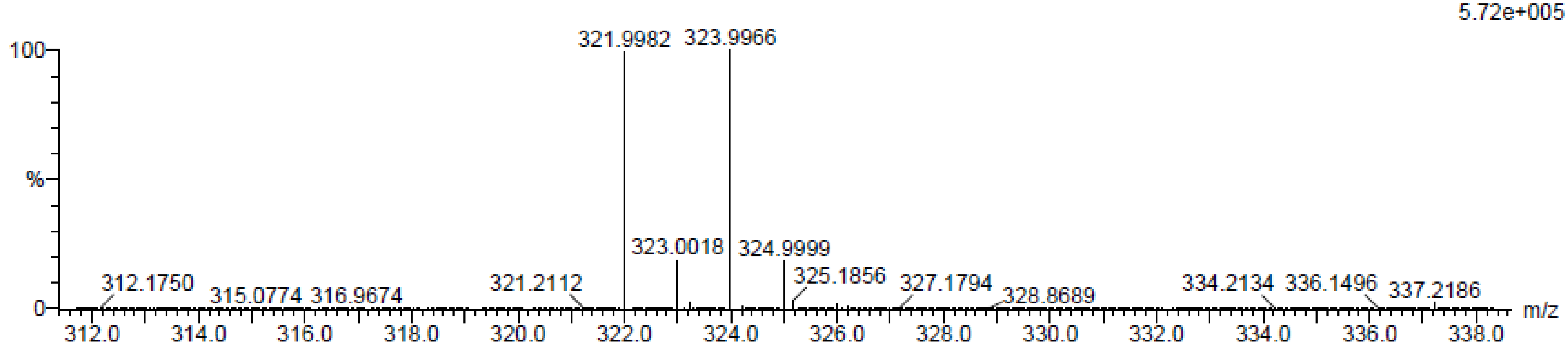

Minimum:				-1.5			
Maximum:		5.0	5.0	100.0			
Mass	Calc. Mass	mDa	PPM	DBE	i-FIT	i-FIT (Norm)	Formula
321.9982	321.9980	0.2	0.6	13.5	605.3	0.0	C16 H9 N3 Br

High resolution mass spectrum of **A5f**

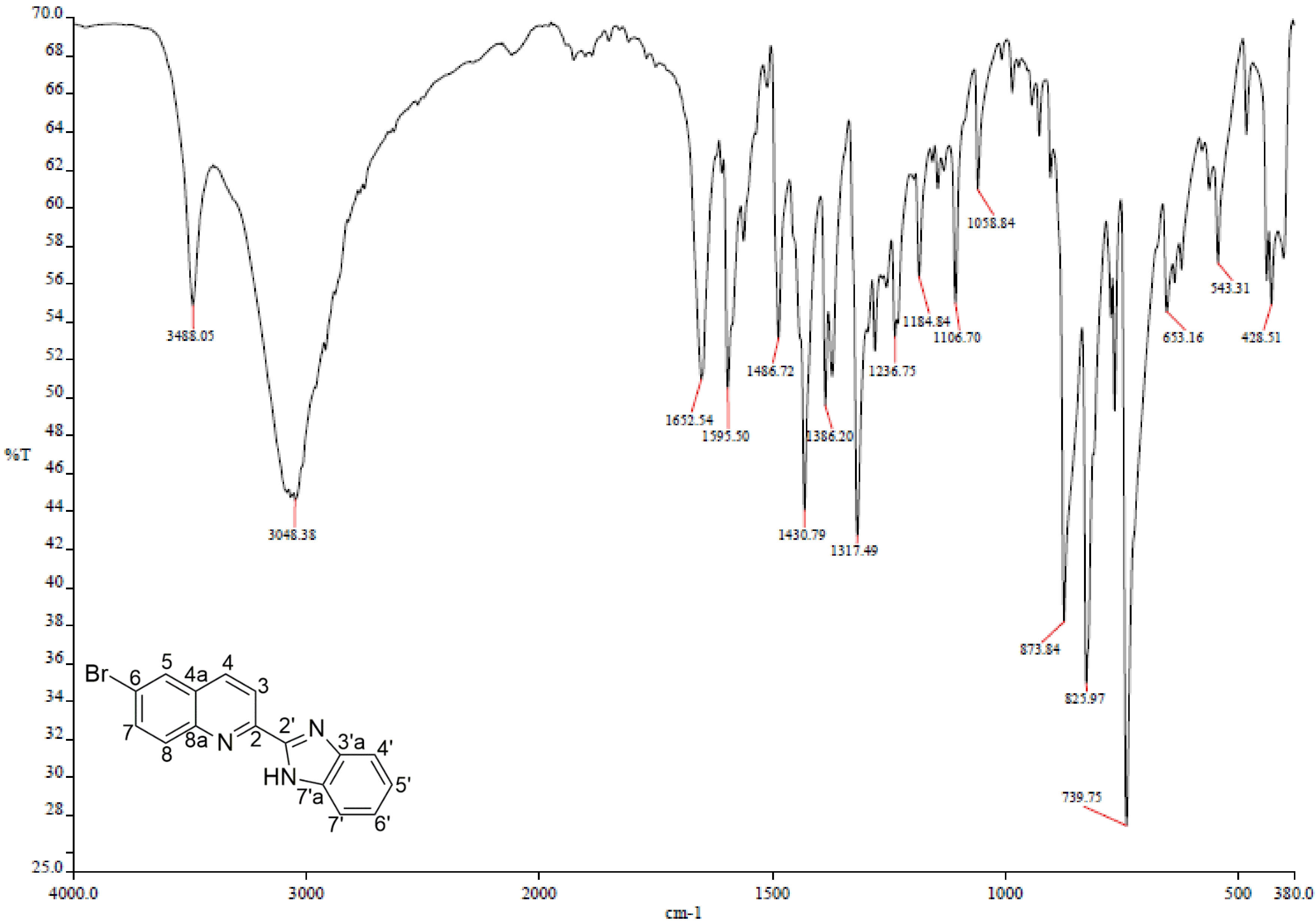

FTIR spectrum of **A5f**

Overlay Spectrum Graph Report

03/08/2017 03:10:31 PM

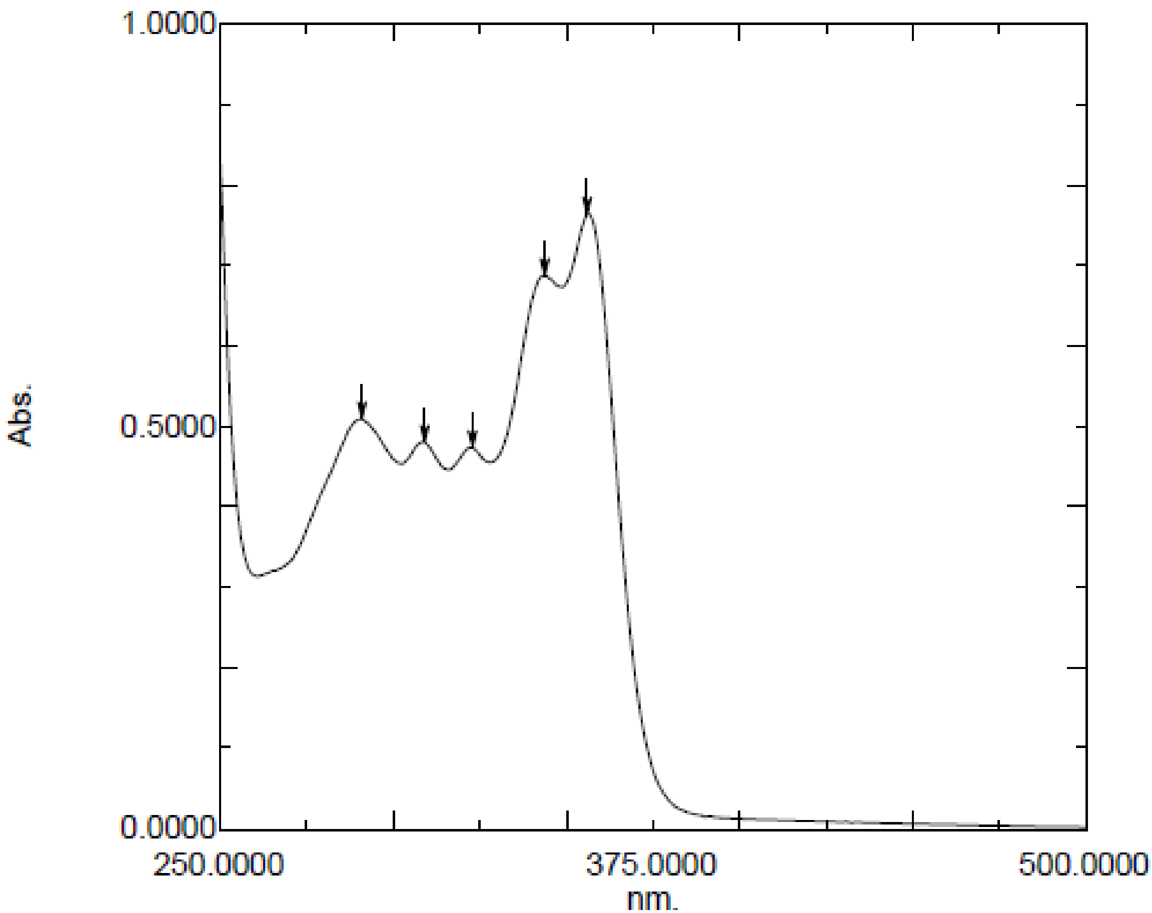

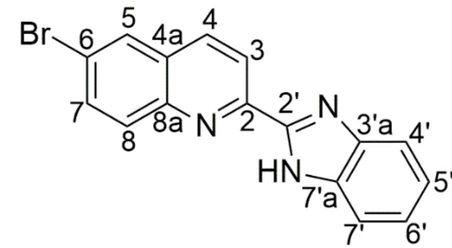

λ	absorbance	logε
291	0.5087	4.52
309	0.4811	4.49
323	0.4732	4.49
344	0.6874	4.65
356	0.7634	4.69

Page 1 / 1

UV spectrum of **A5f**

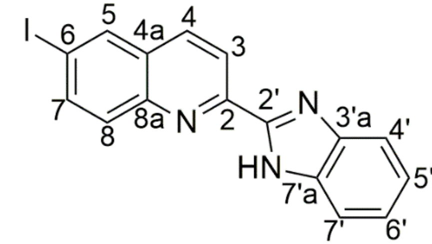

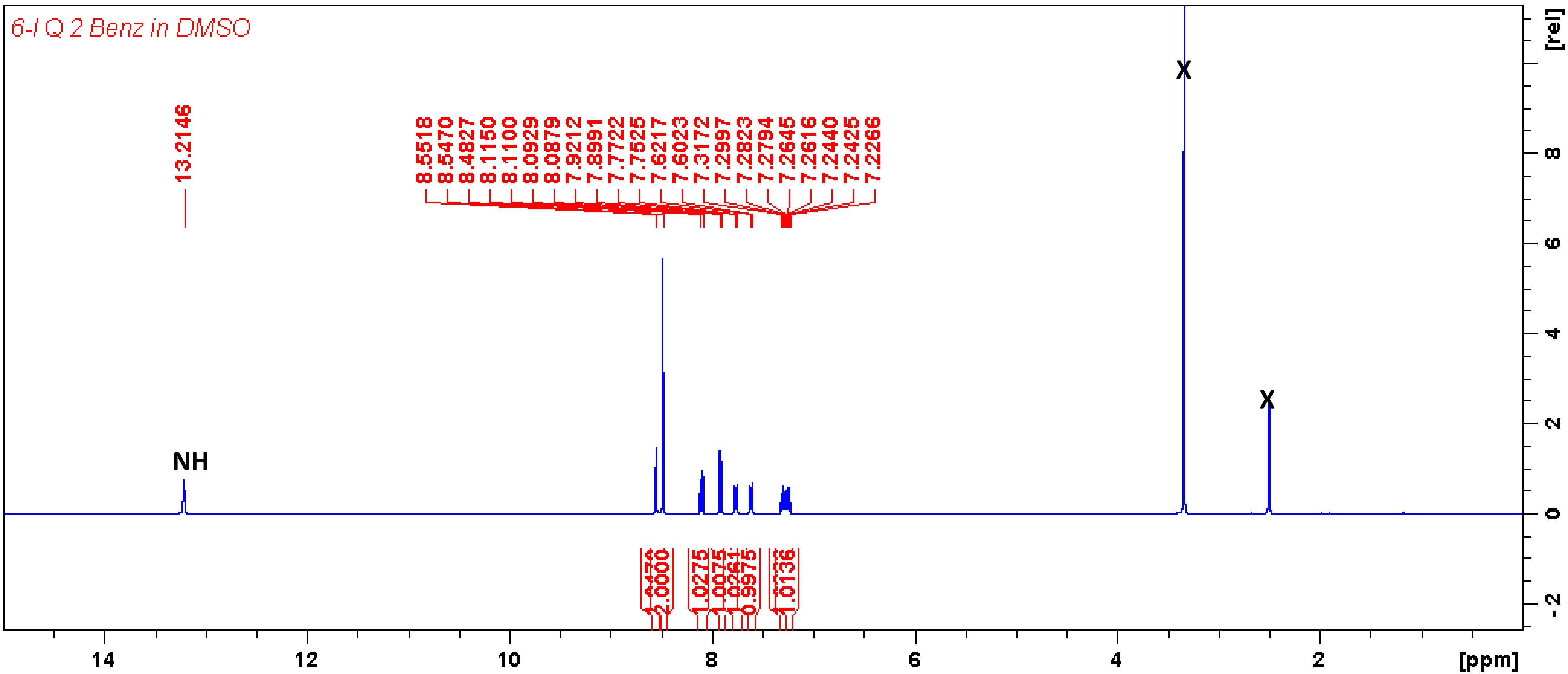

^{1}H NMR spectrum of **A5g**

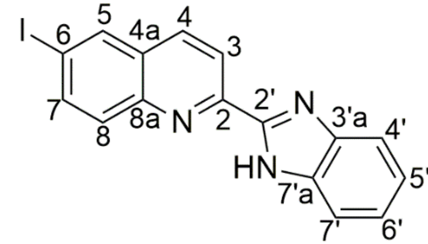

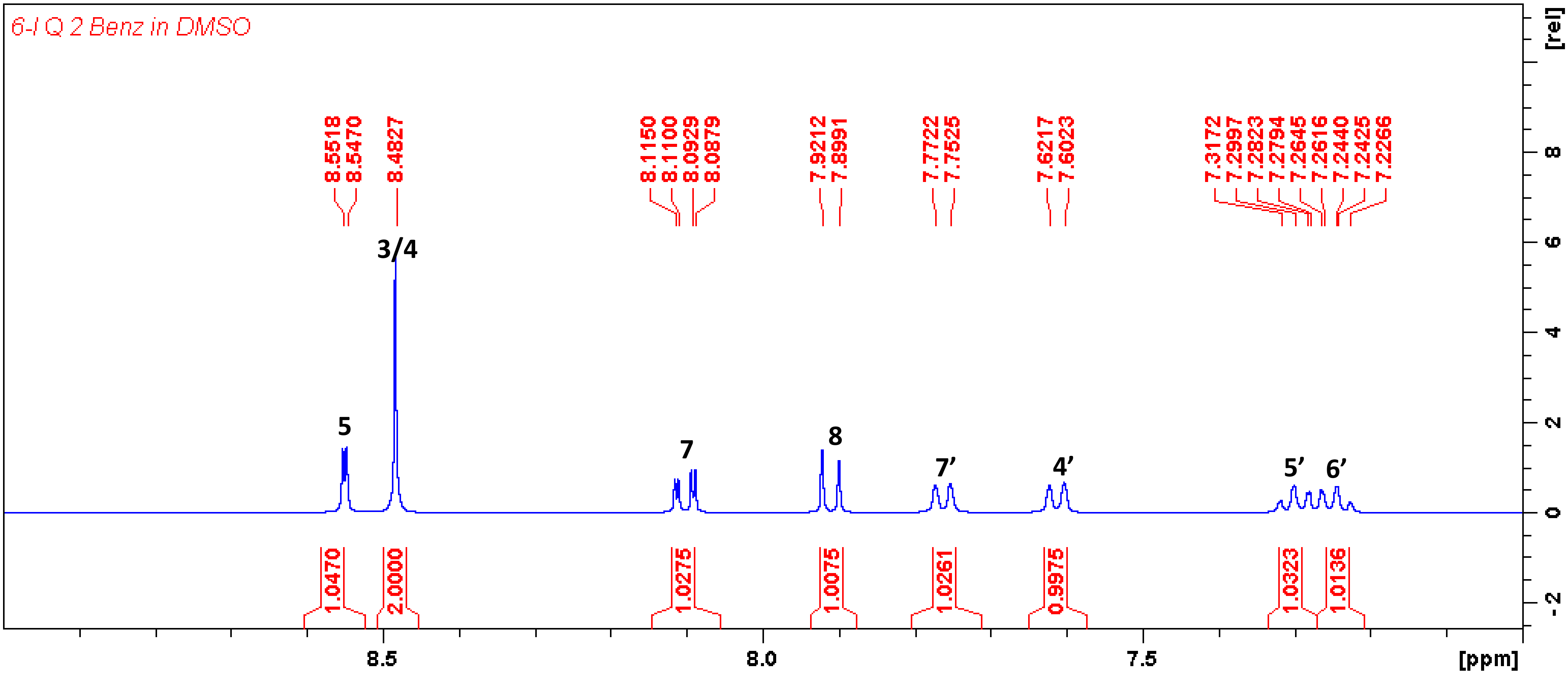

Expanded ^{1}H NMR spectrum of **A5g**

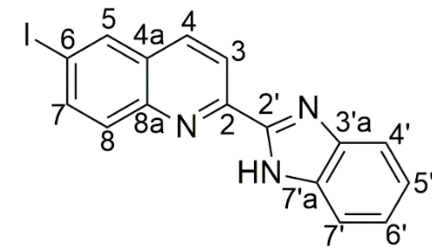

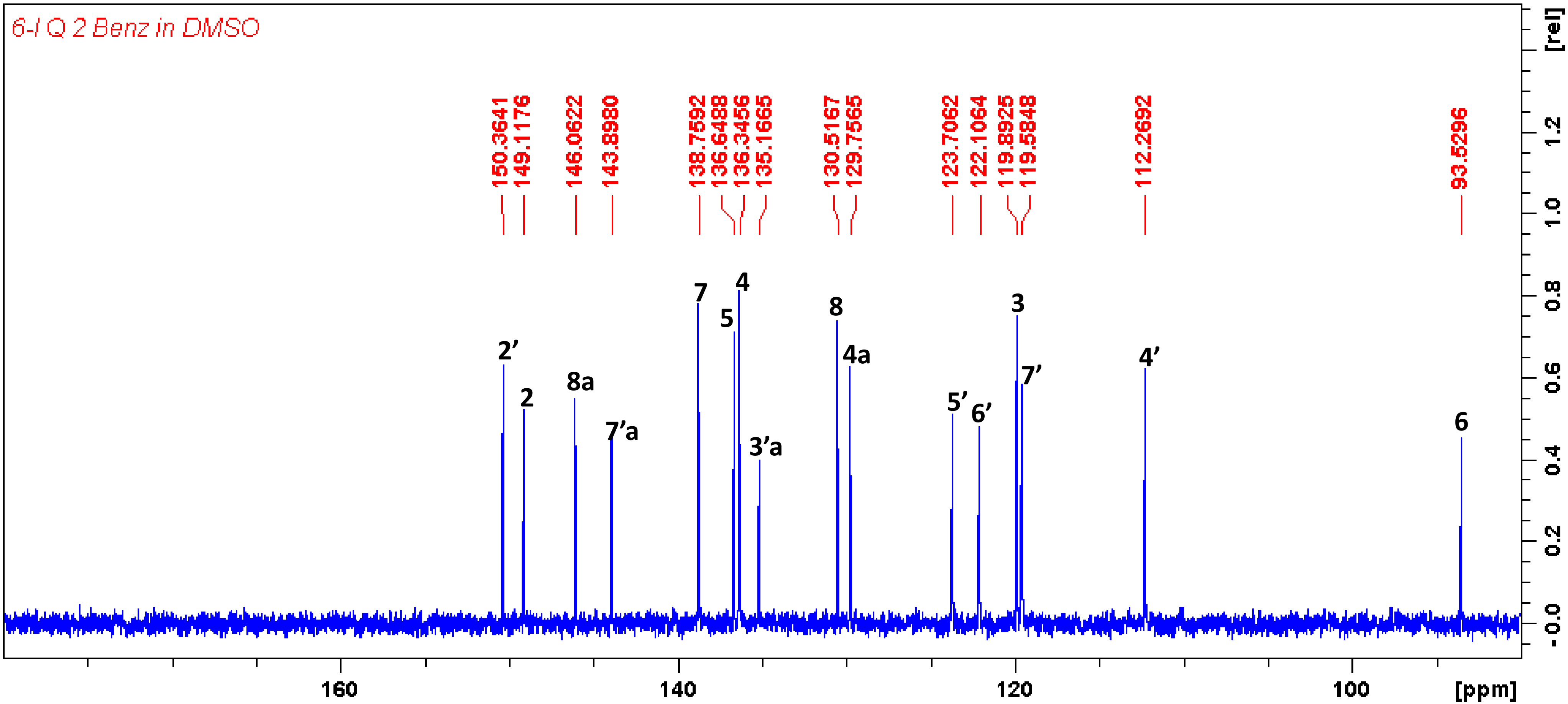

^{13}C NMR spectrum of **A5g**

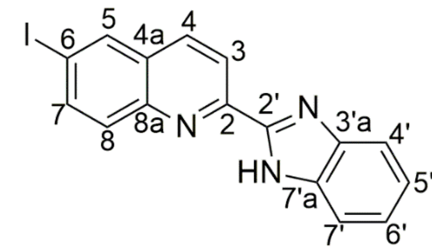

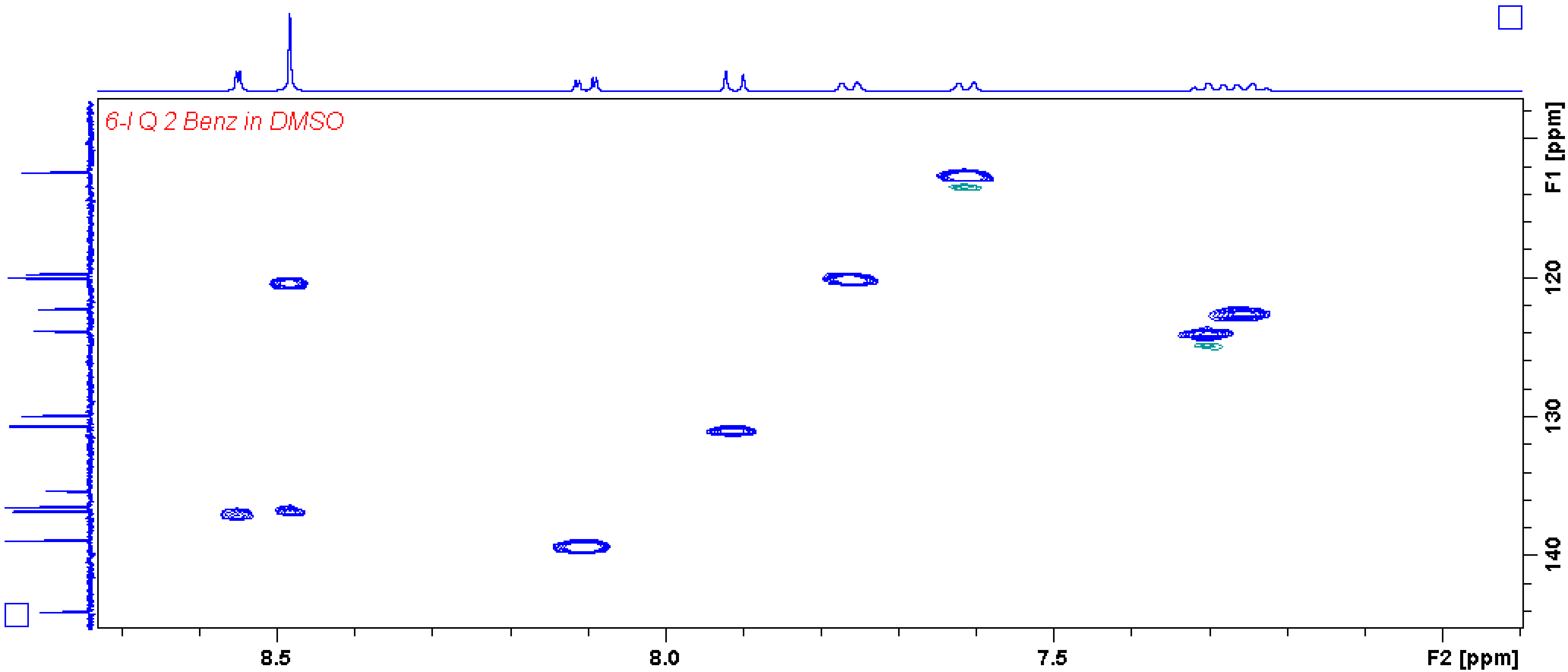

HSQC of **A5g**

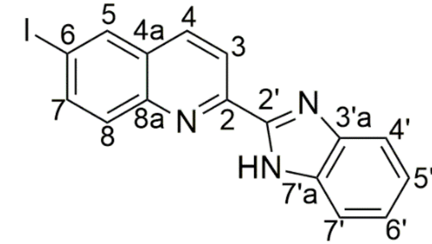
I
6
5
4a
4
3
7
8
8a
N
2
2'
N
3'a
4'
HN
7'a
5'
7'
6'

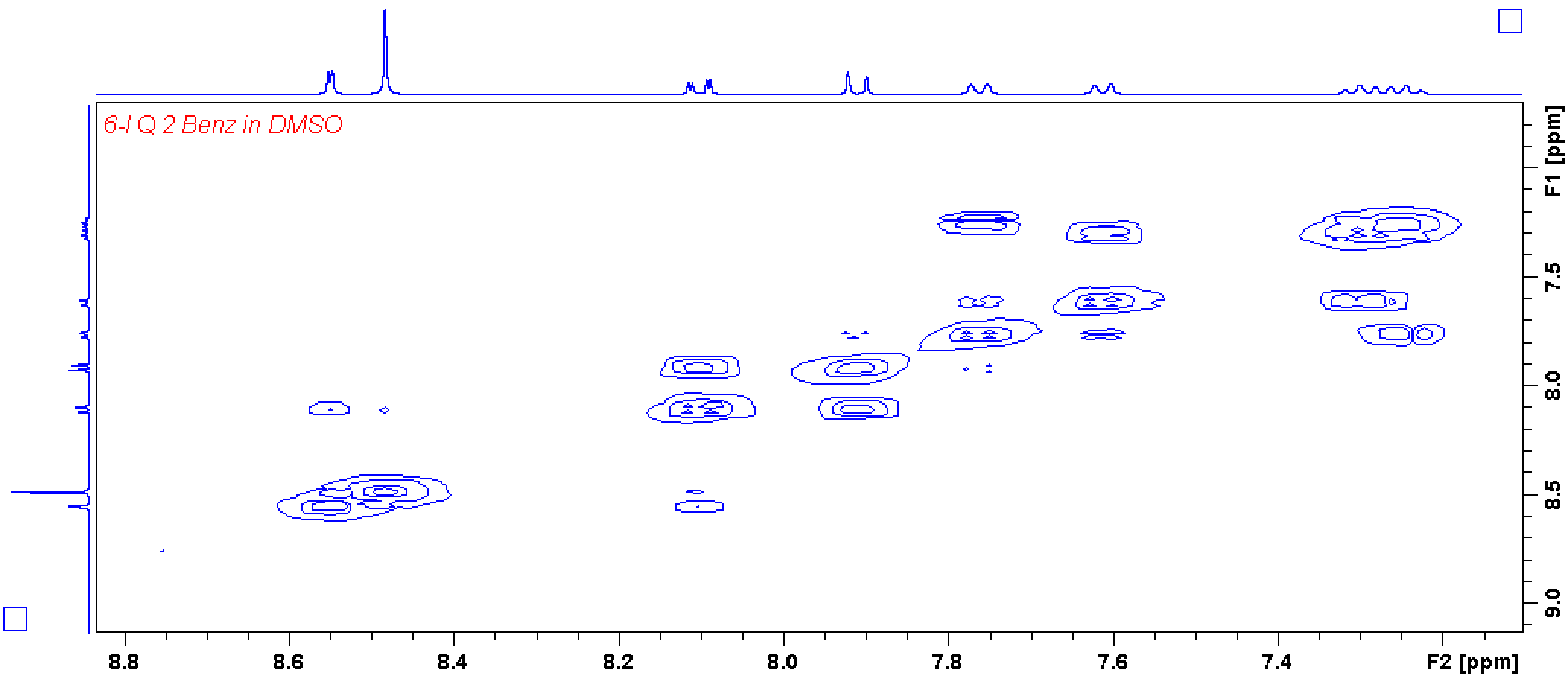
6-I Q 2 Benz in DMSO
F1 [ppm]
7.5
8.0
8.5
9.0
8.8
8.6
8.4
8.2
8.0
7.8
7.6
7.4
F2 [ppm]

COSY of **A5g**

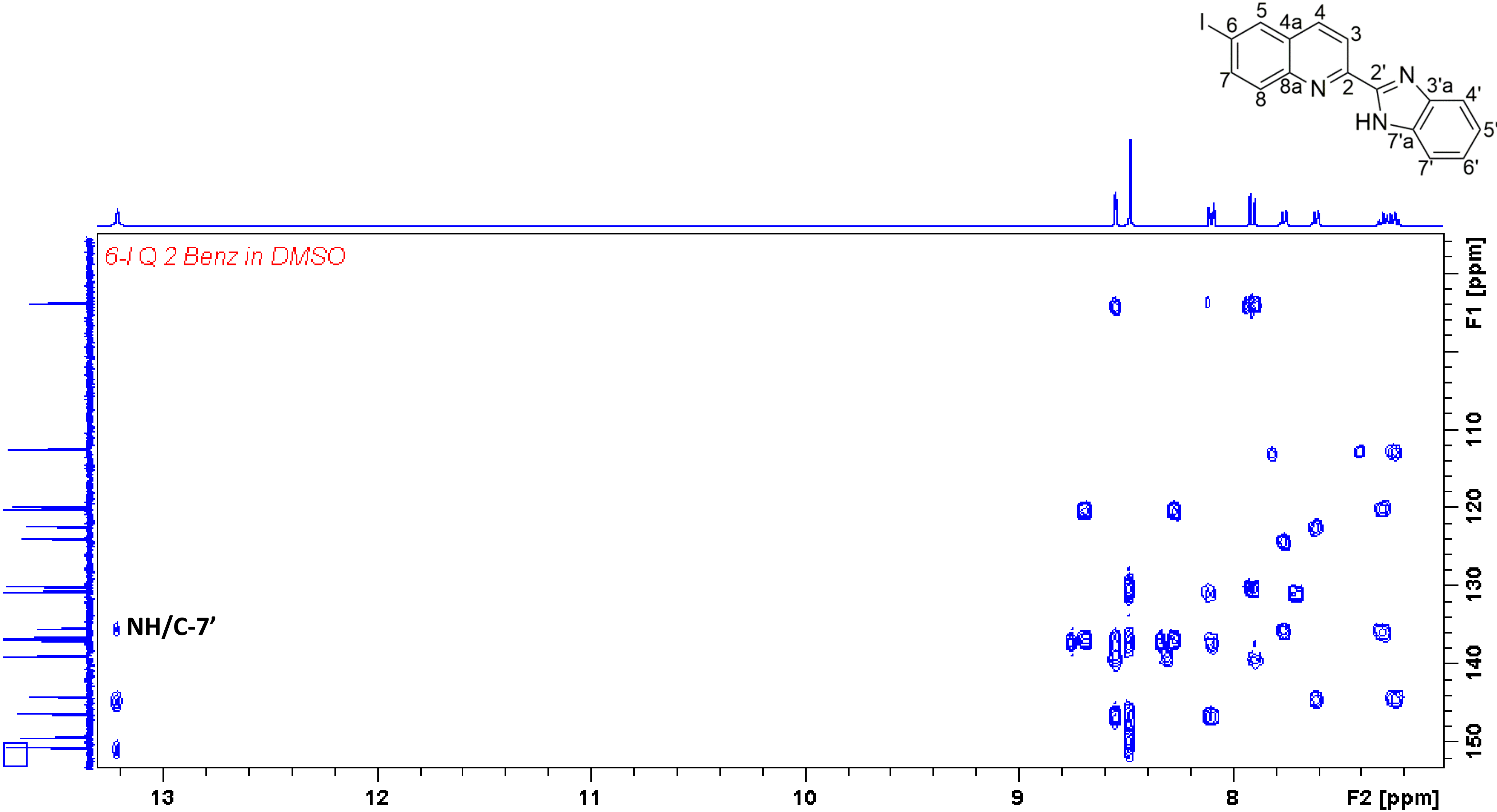
I
6
5
4a
4
3
7
8
8a
N
2
2'
N
3'a
4'
5'
HN
7'a
7'
6'
6-I Q 2 Benz in DMSO
NH/C-7'
F1 [ppm]
110
120
130
140
150
13
12
11
10
9
8
F2 [ppm]

HMBC of **A5g**

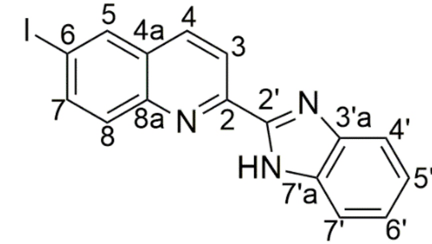

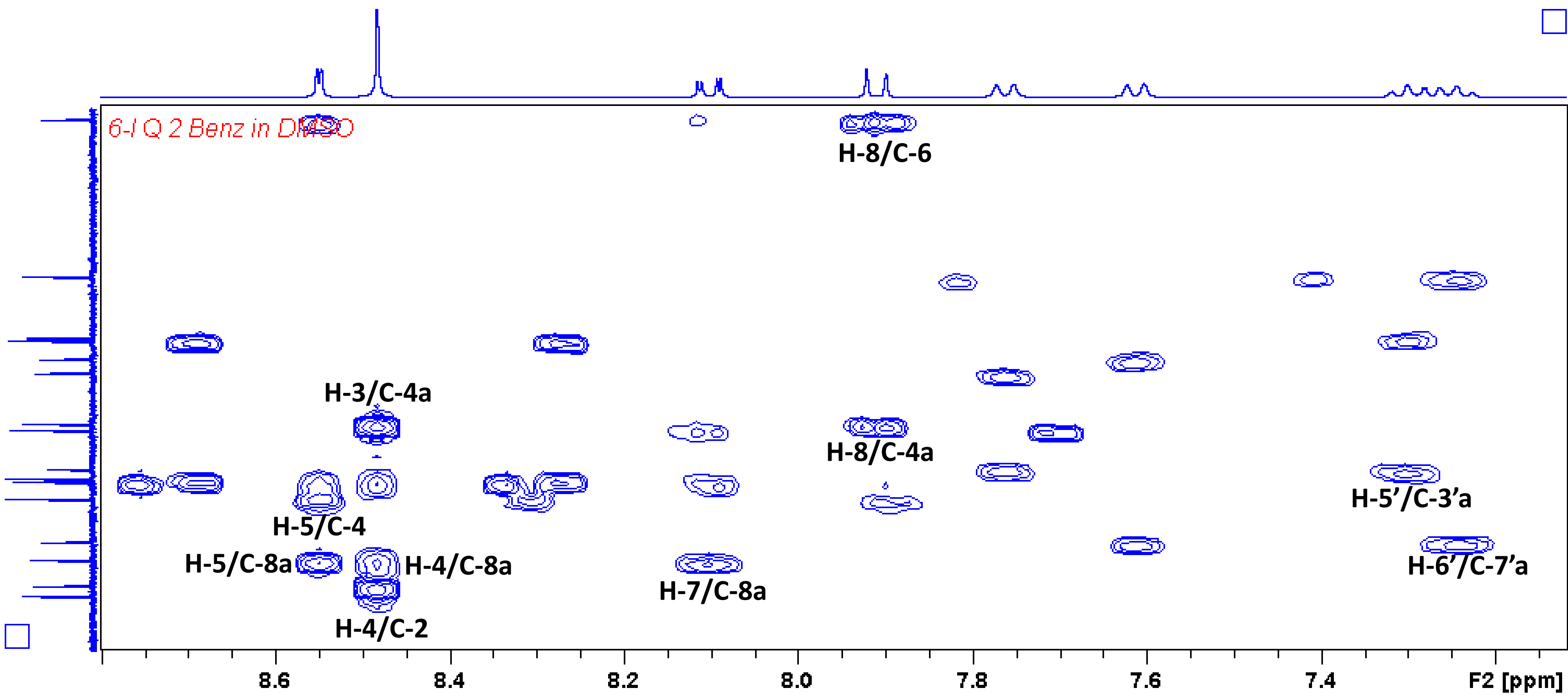

Expanded HMBC of **A5g**

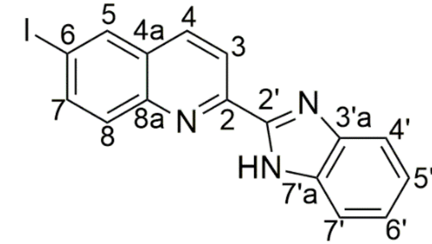

Elemental Composition Report

Single Mass Analysis

Tolerance = 5.0 PPM / DBE: min = -1.5, max = 100.0
Element prediction: Off
Number of isotope peaks used for i-FIT = 3

Monoisotopic Mass, Even Electron Ions
9 formula(e) evaluated with 1 results within limits (up to 20 closest results for each mass)
Elements Used:
C: 15-20 H: 5-10 N: 0-5 I: 0-1

SSQB9 26 (0.843) Cm (1:61)
TOF MS ES-

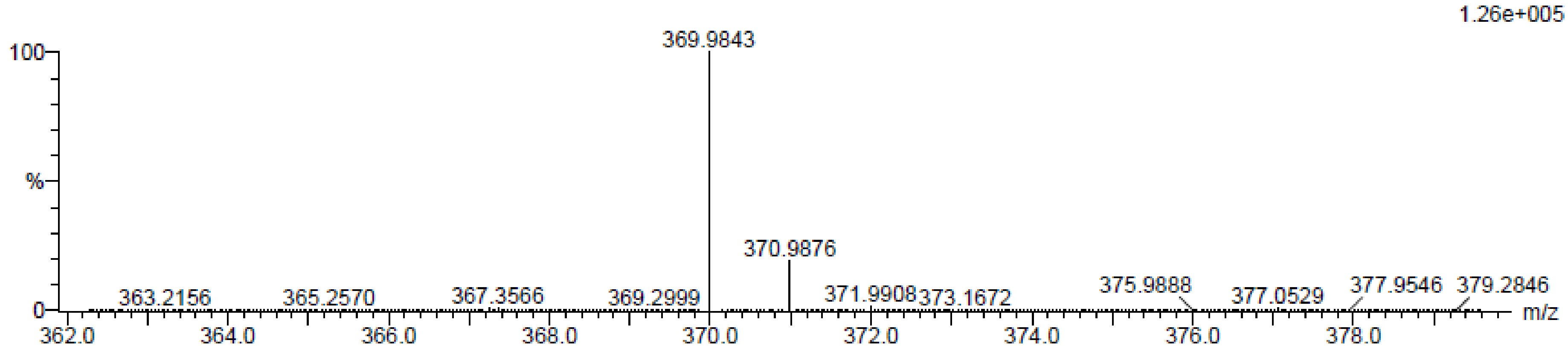

Minimum:				-1.5			
Maximum:		5.0	5.0	100.0			
Mass	Calc. Mass	mDa	PPM	DBE	i-FIT	i-FIT (Norm)	Formula
369.9843	369.9841	0.2	0.5	13.5	523.7	0.0	C16 H9 N3 I

High resolution mass spectrum of **A5g**

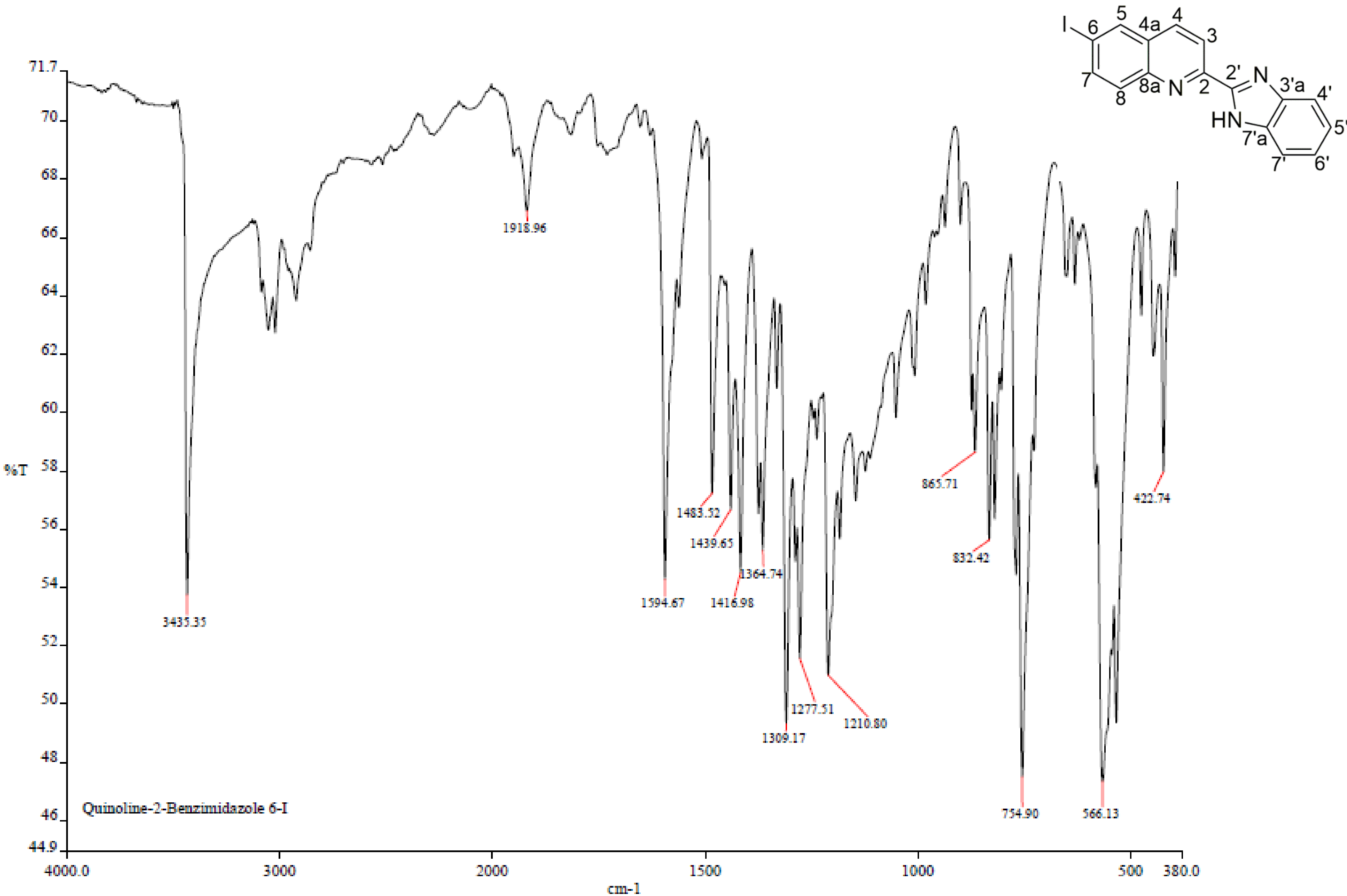

FTIR spectrum of **A5g**

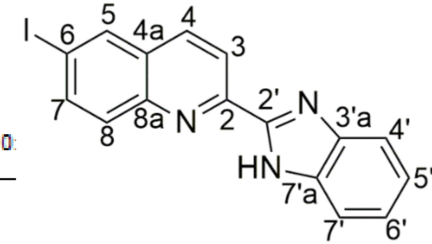

Overlay Spectrum Graph Report

03/08/2017 03:10:

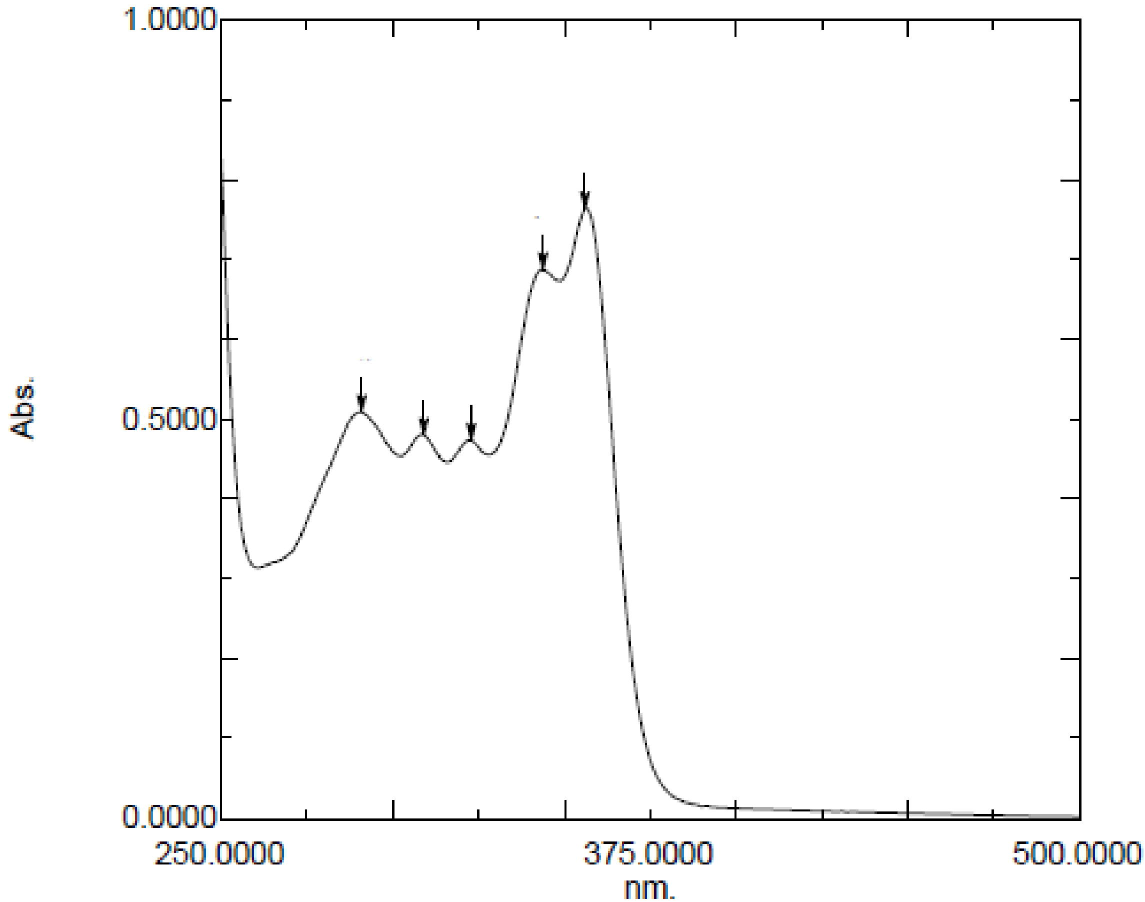

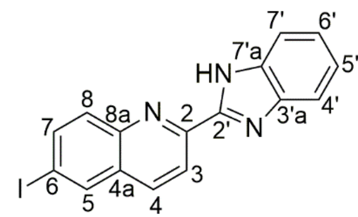

λ	absorbance	logε
296	0.5792	4.85
310	0.5501	4.79
325	0.5449	4.61
346	0.8334	4.61
359	0.9530	4.63

UV spectrum of **A5g**

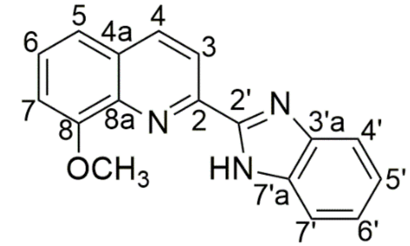

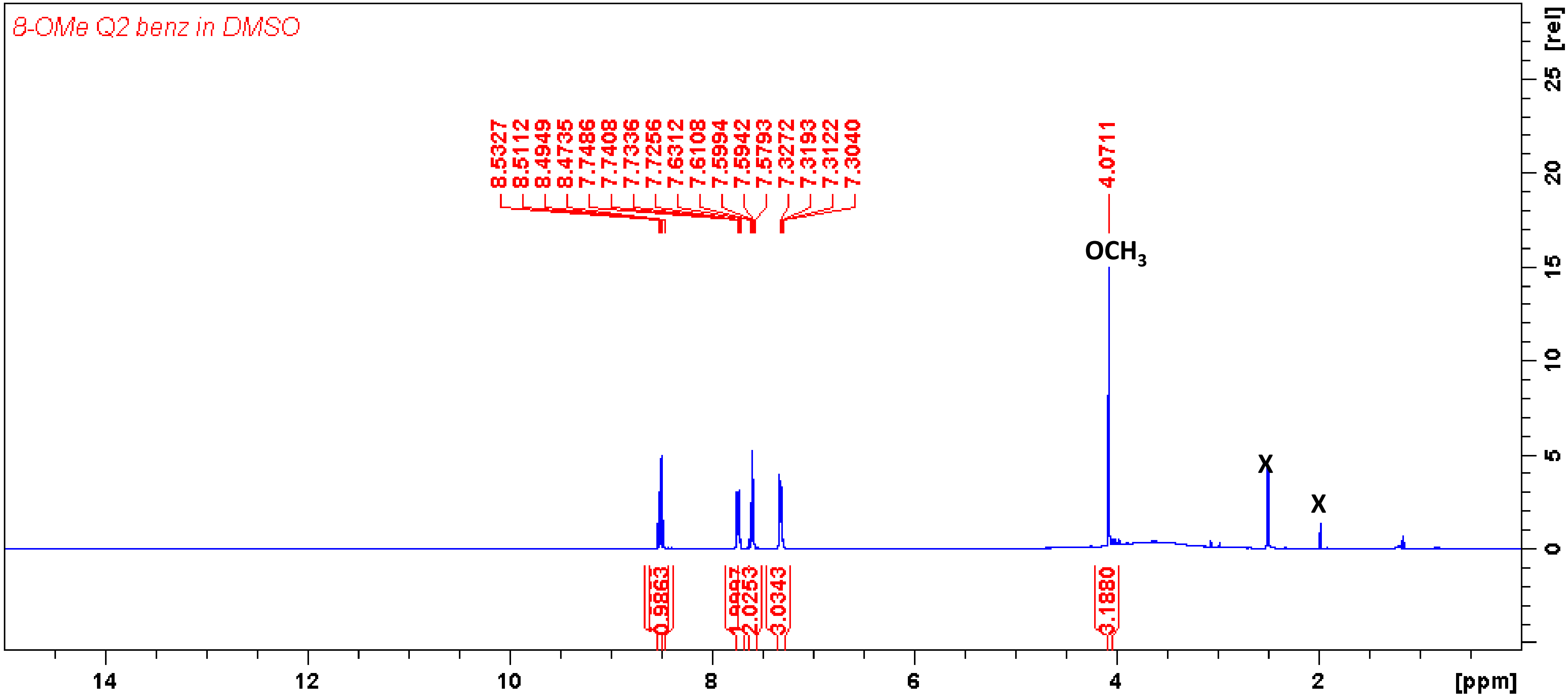

^1H NMR spectrum of **A5h**

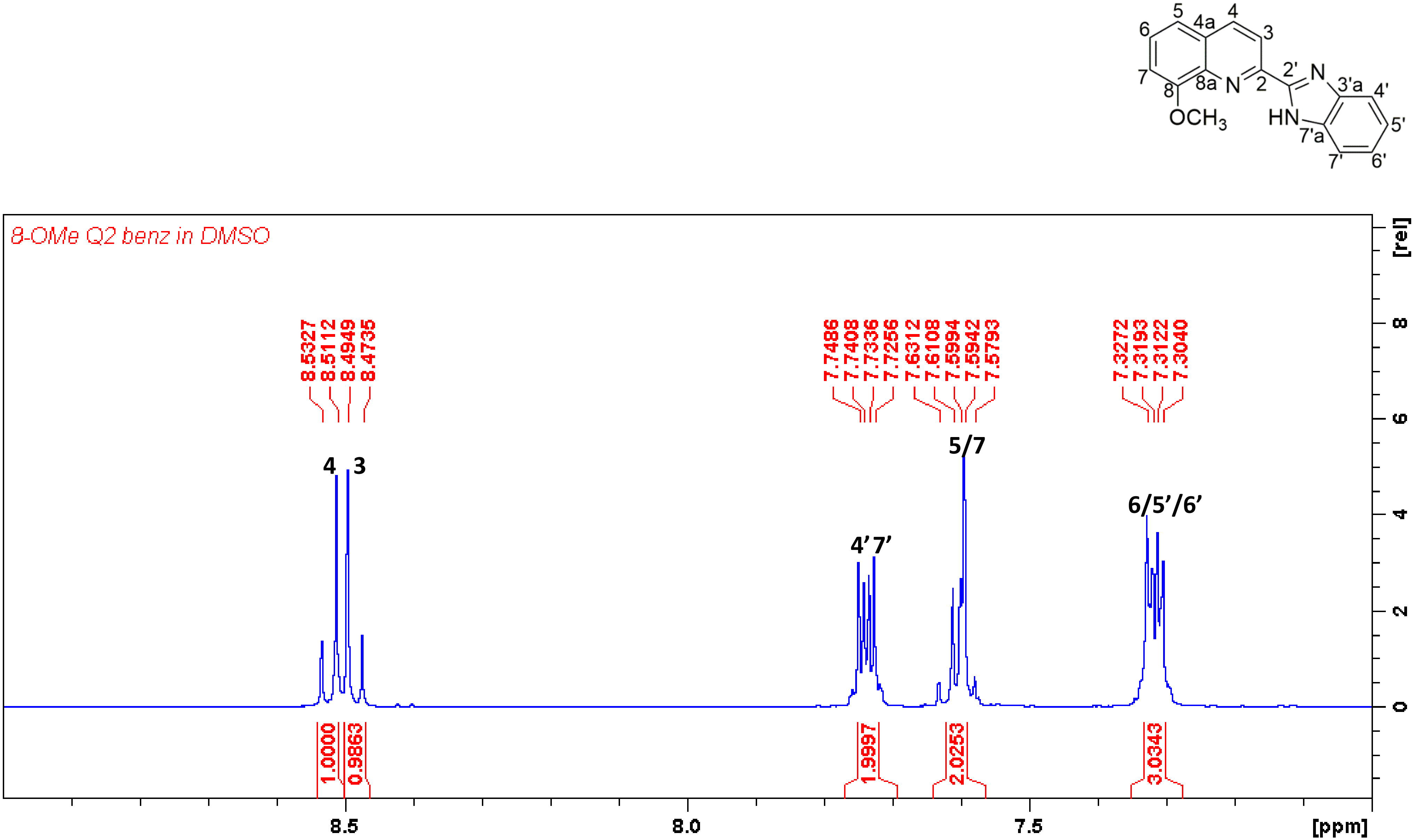

Expanded ^{1}H NMR spectrum of **A5h**

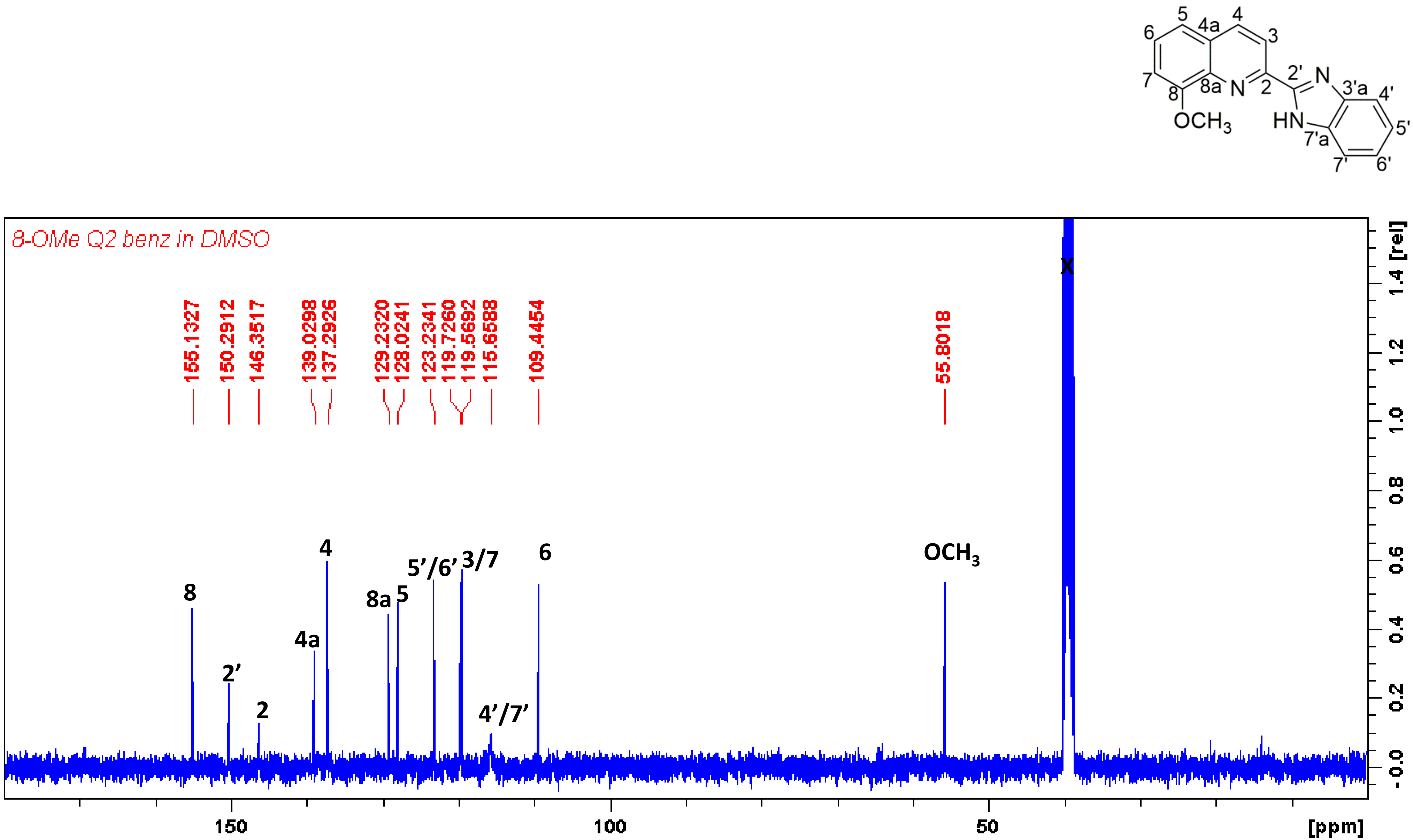

^{13}C NMR spectrum of **A5h**

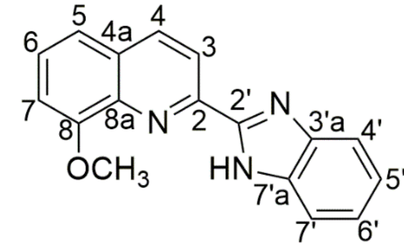

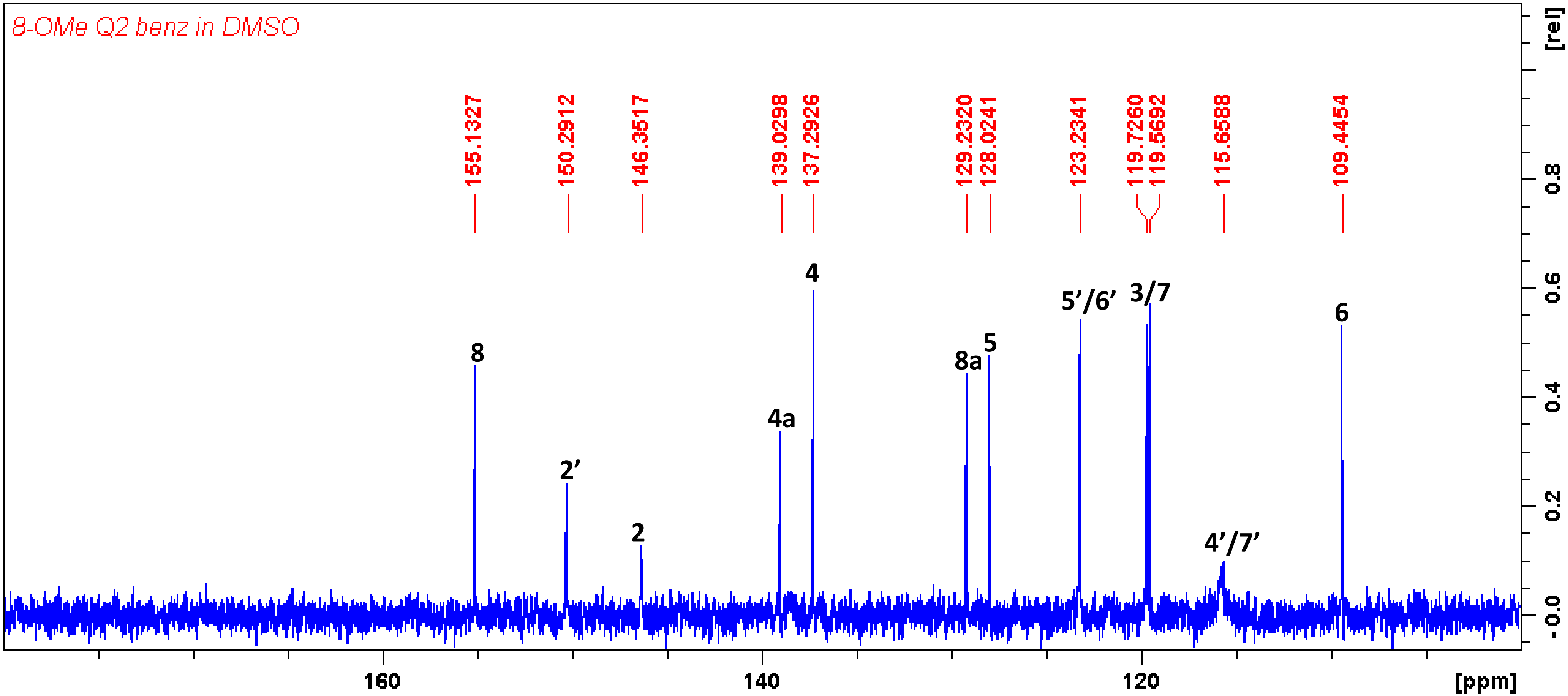

Expanded ^{13}C NMR spectrum of **A5h**

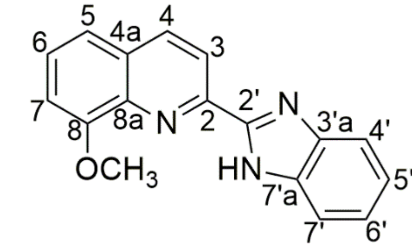

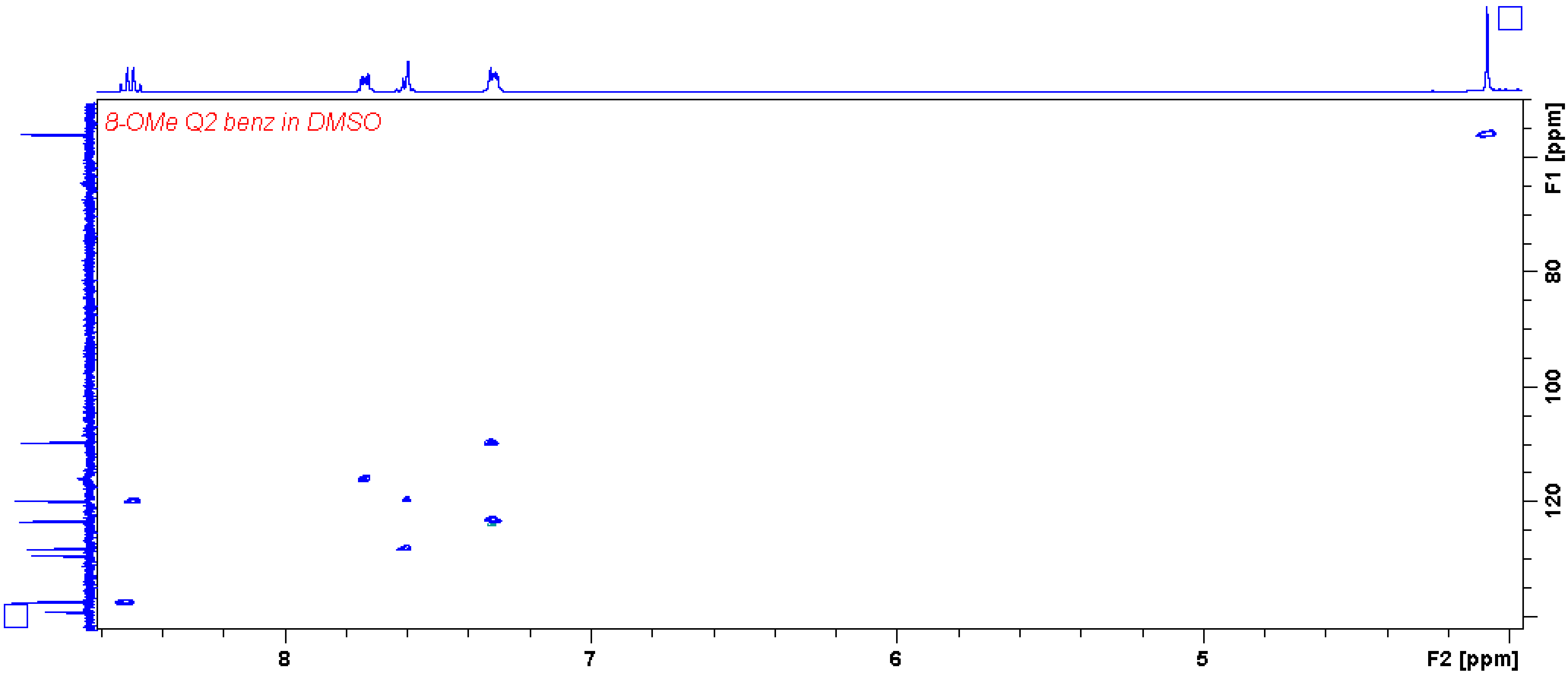

HSQC of **A5h**

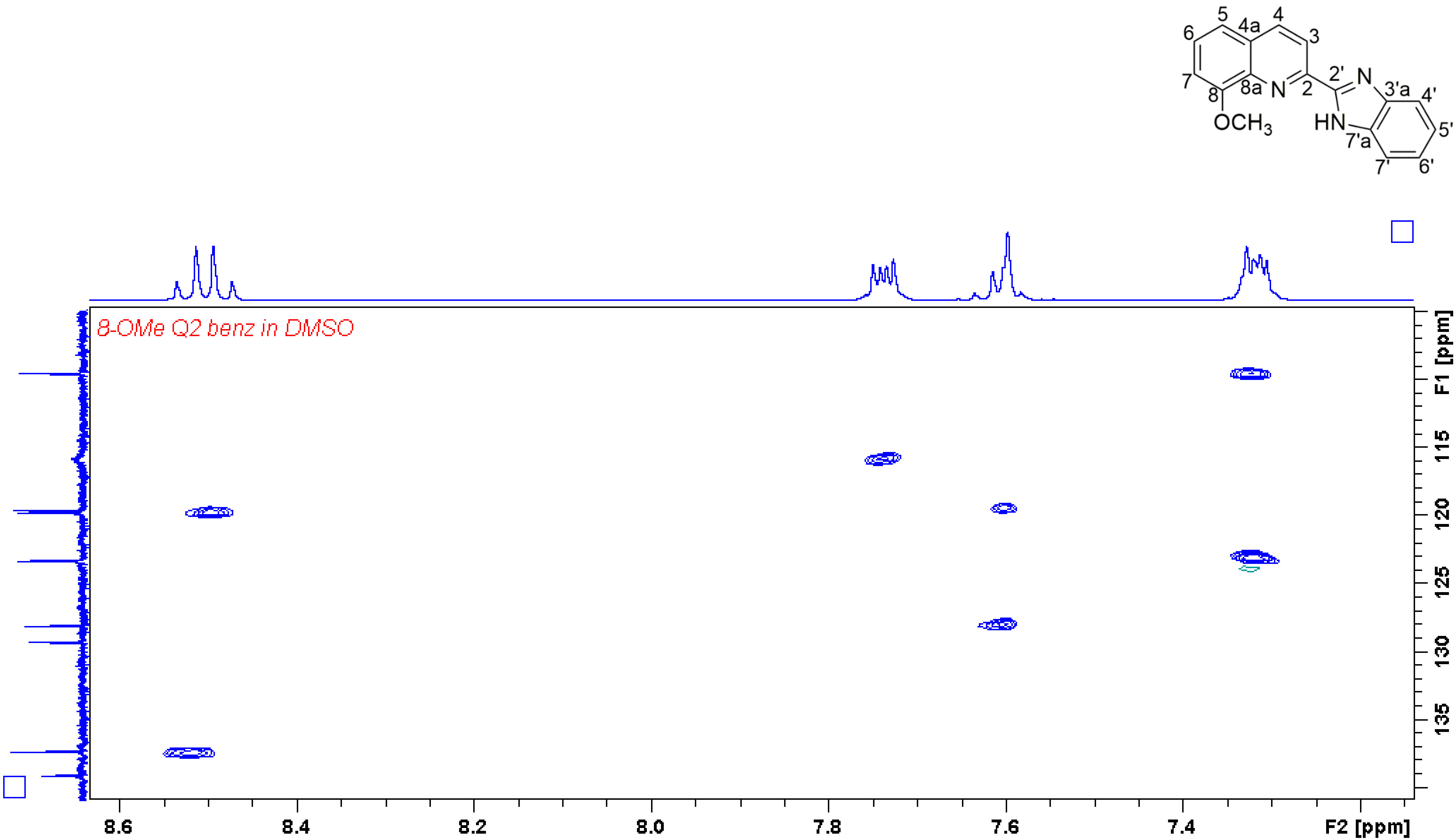

Expanded HSQC of **A5h**

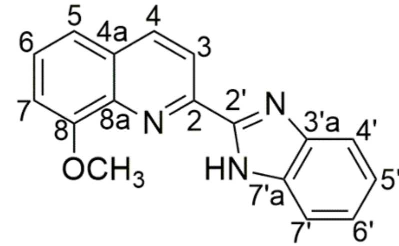

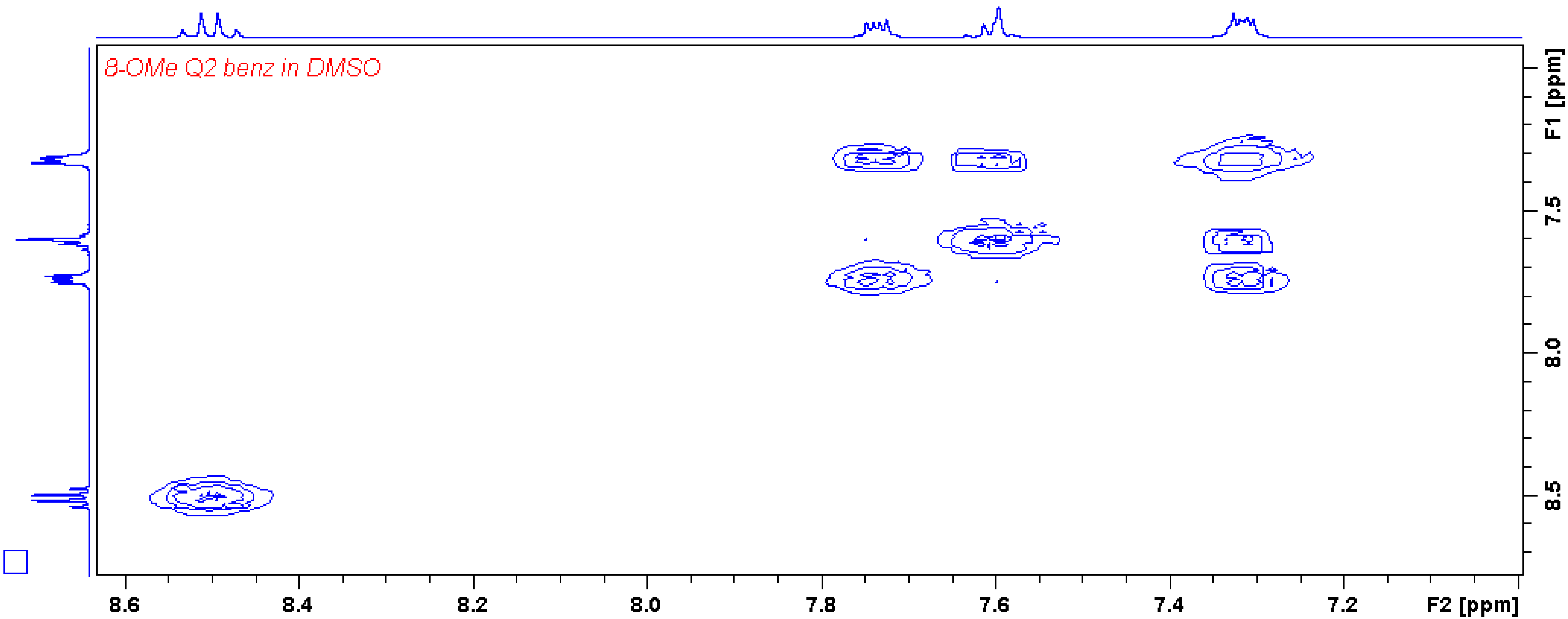

COSY of **A5h**

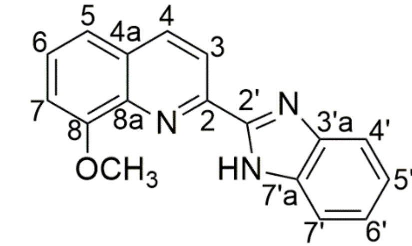
5
4
4a
3
6
7
8a
N
2
2'
N
3'a
4'
8
OCH3
HN
5'
7'a
7'
6'

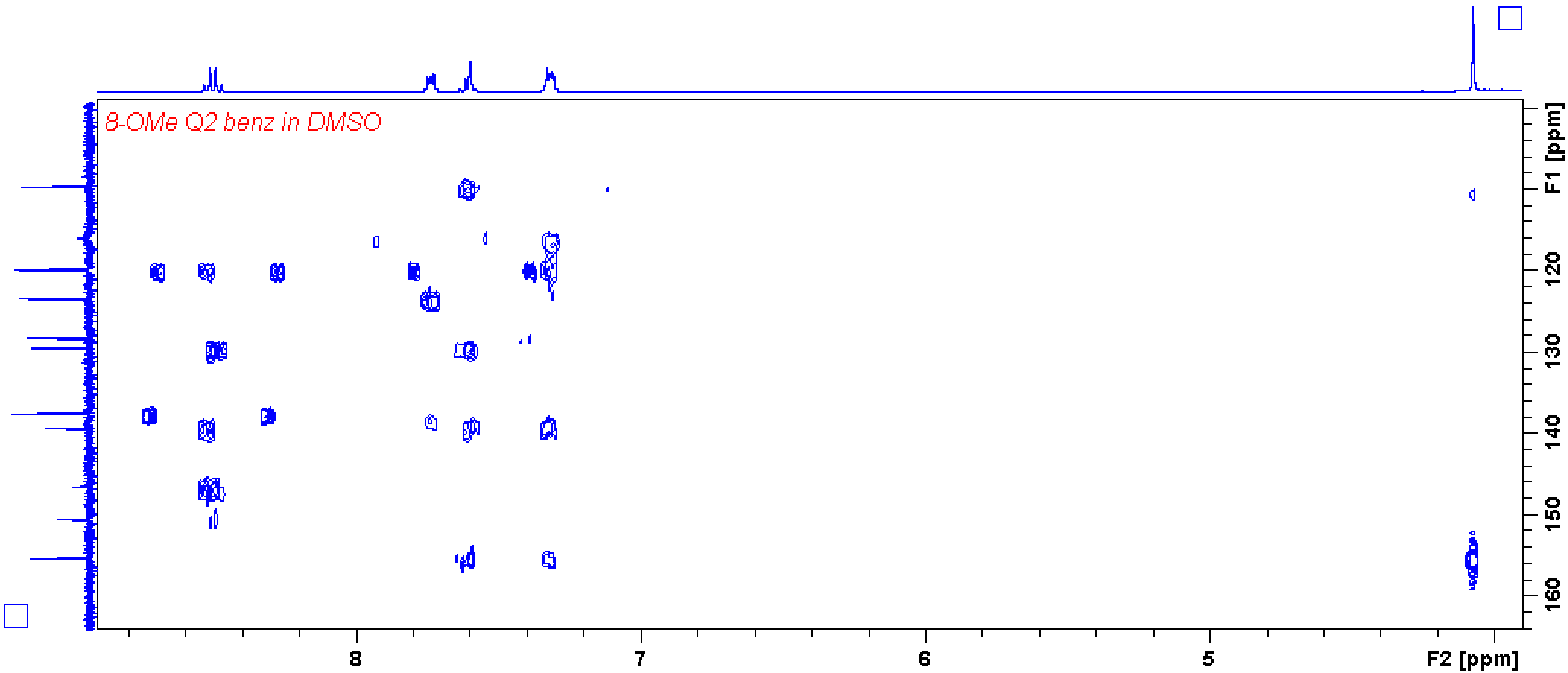
8-OMe Q2 benz in DMSO
F1 [ppm]
120
130
140
150
160
8
7
6
5
F2 [ppm]

HMBC of **A5h**

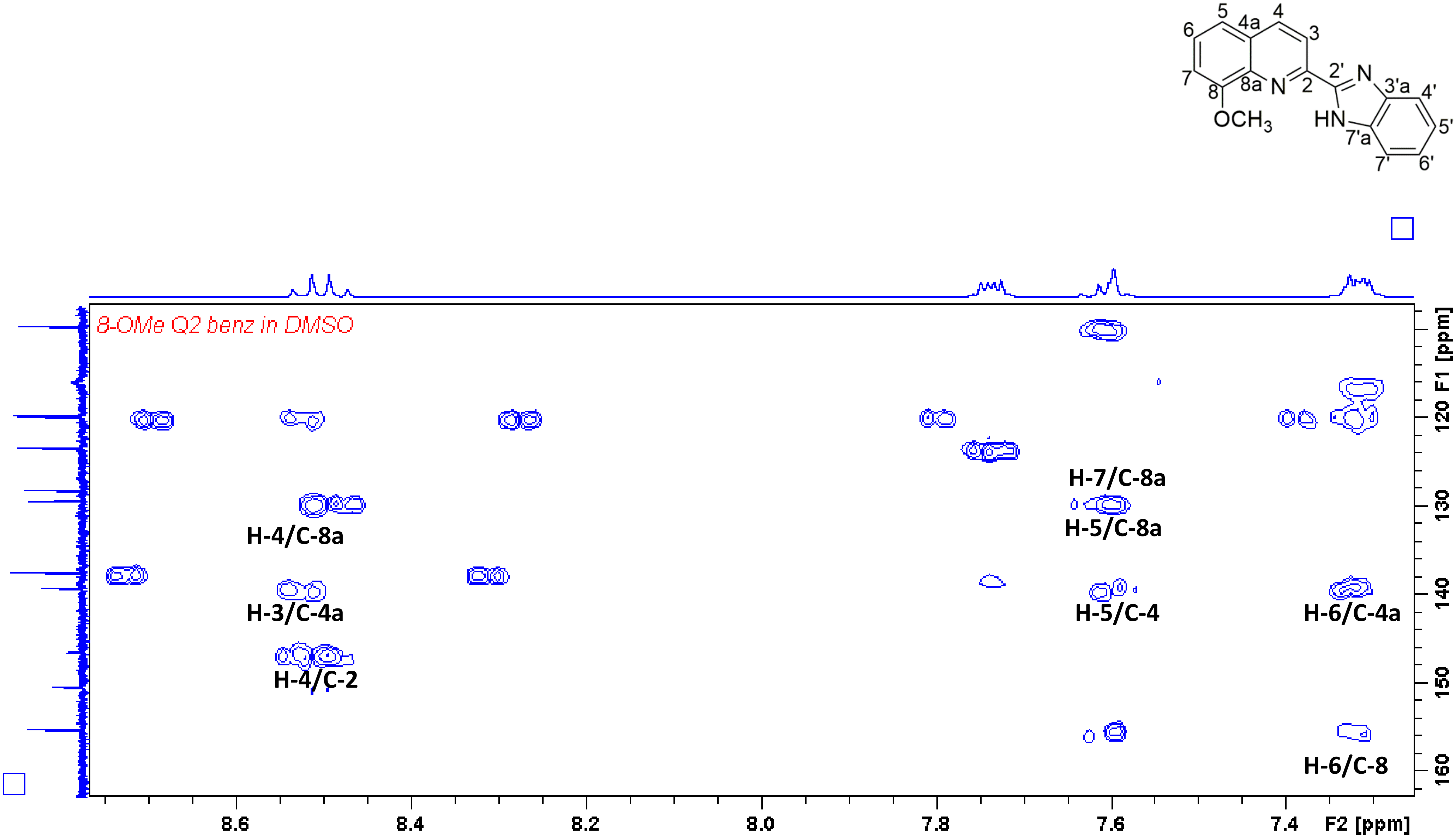

Expanded HMBC of **A5h**

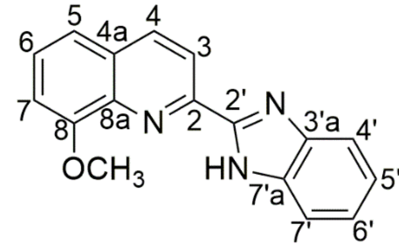

Elemental Composition Report

Single Mass Analysis

Tolerance = 5.0 PPM / DBE: min = -1.5, max = 100.0
Element prediction: Off
Number of isotope peaks used for i-FIT = 3

Monoisotopic Mass, Even Electron Ions
20 formula(e) evaluated with 1 results within limits (up to 20 closest results for each mass)
Elements Used:
C: 15-20 H: 10-15 N: 0-5 O: 0-5
SSQB8 49 (1.653) Cm (1:60)
TOF MS ES-

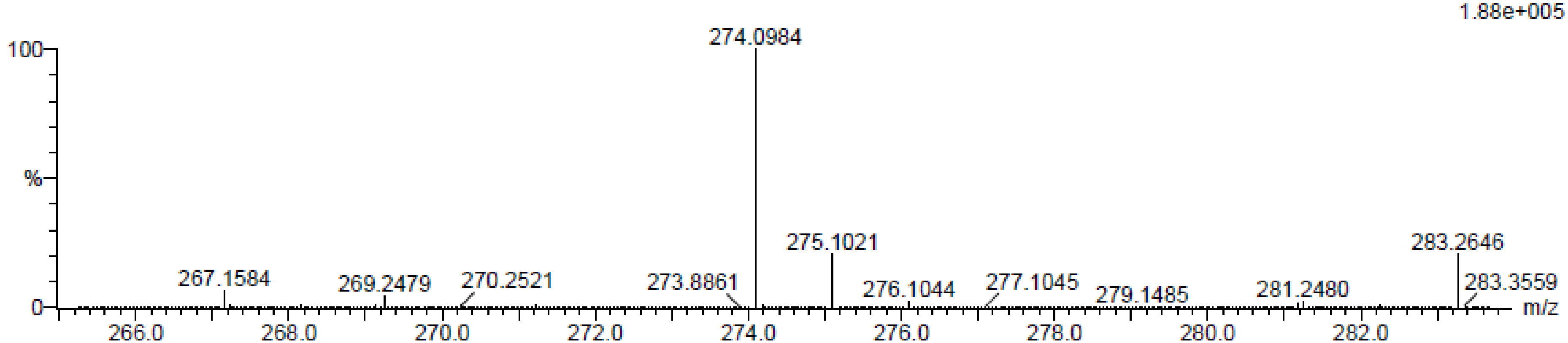

Minimum:				-1.5			
Maximum:		5.0	5.0	100.0			
Mass	Calc. Mass	mDa	PPM	DBE	i-FIT	i-FIT (Norm)	Formula
274.0984	274.0980	0.4	1.5	13.5	601.9	0.0	C17 H12 N3 O

High resolution mass spectrum of **A5h**

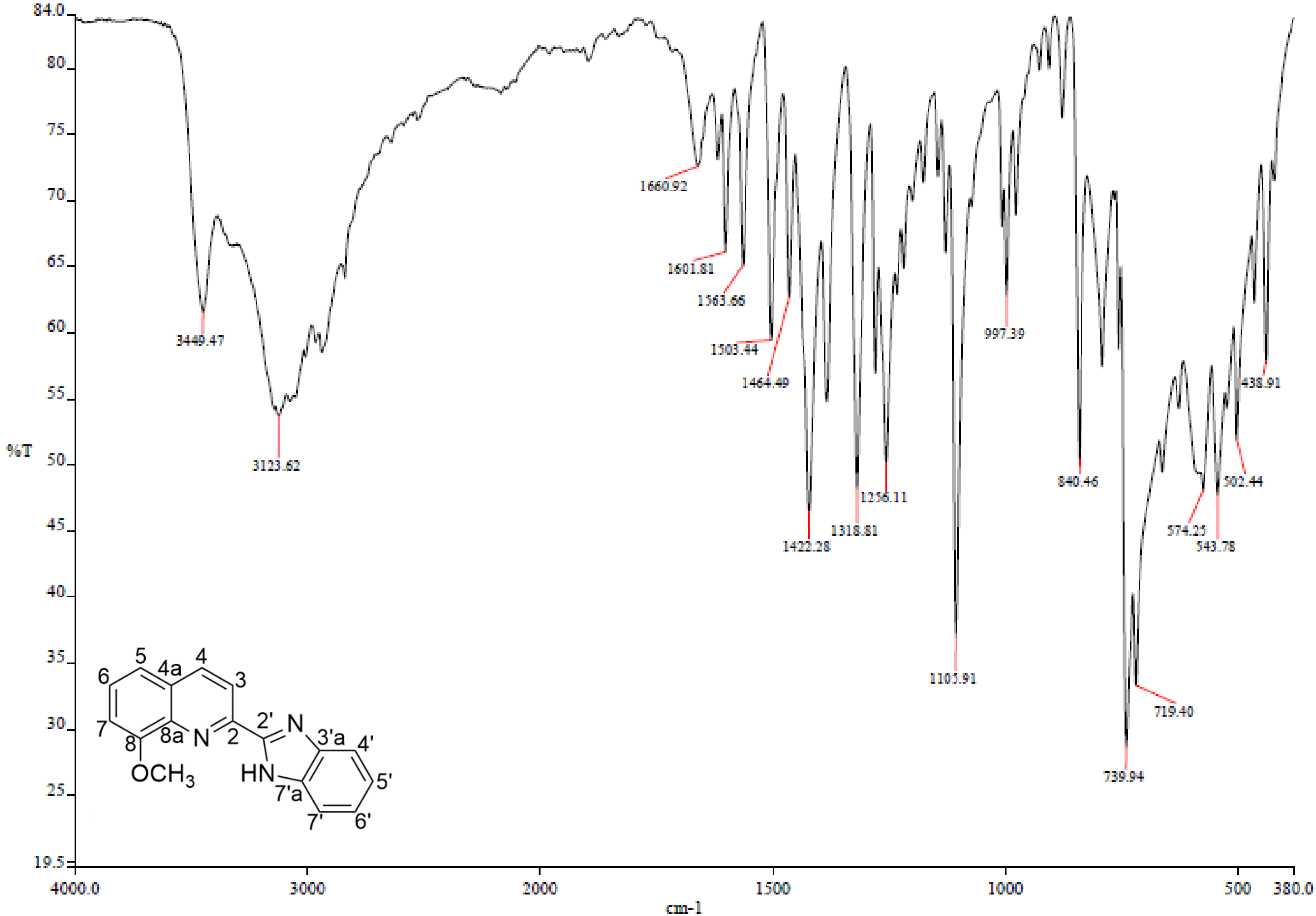

FTIR spectrum of **A5h**

Overlay Spectrum Graph Report

03/08/2017 03:16:05 PM

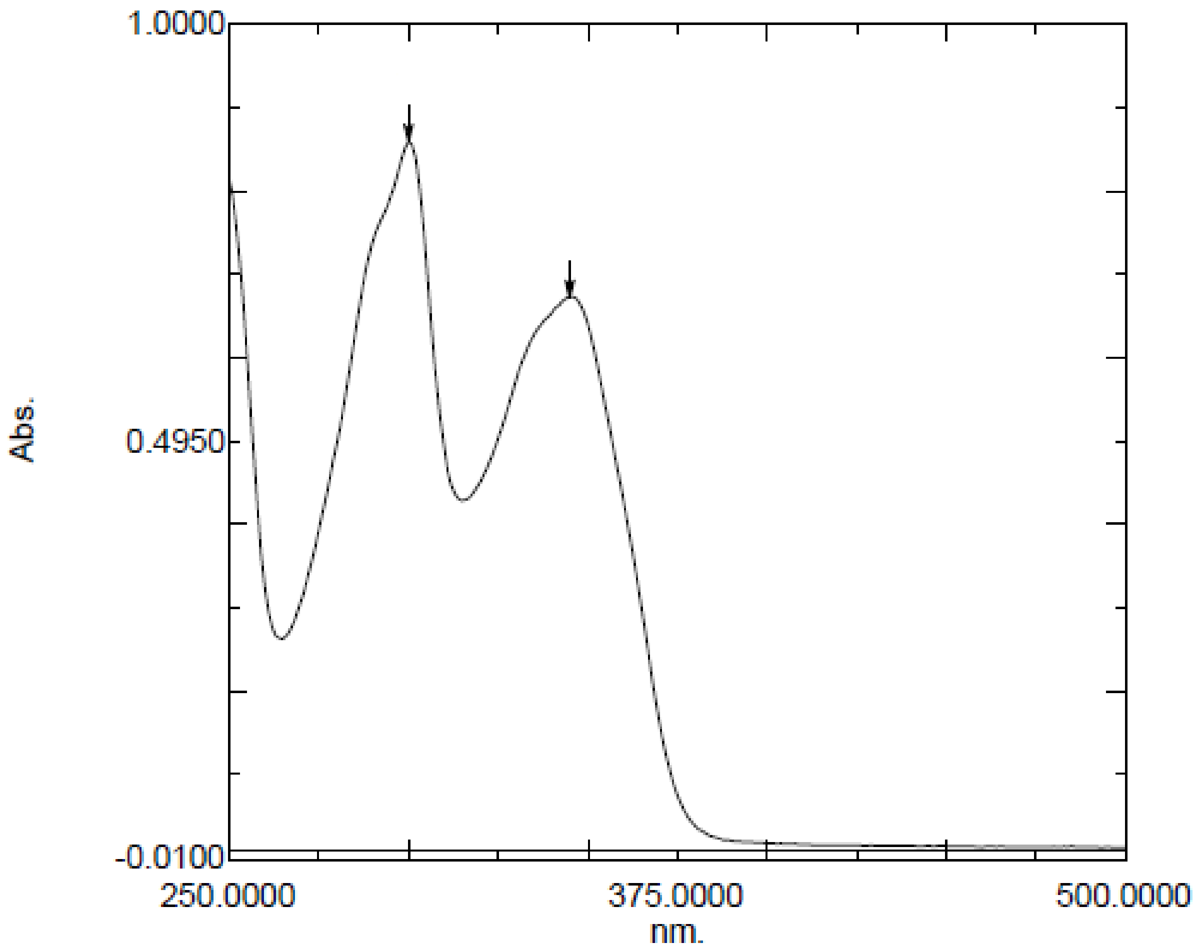

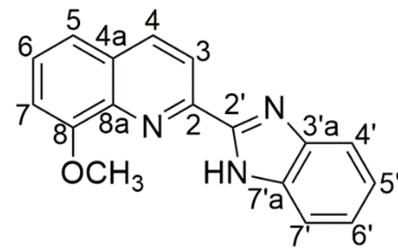

λ	absorbance	logε
300	0.8570	4.67
345	0.6697	4.57

UV spectrum of **A5h**

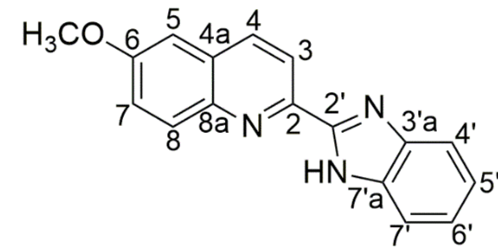

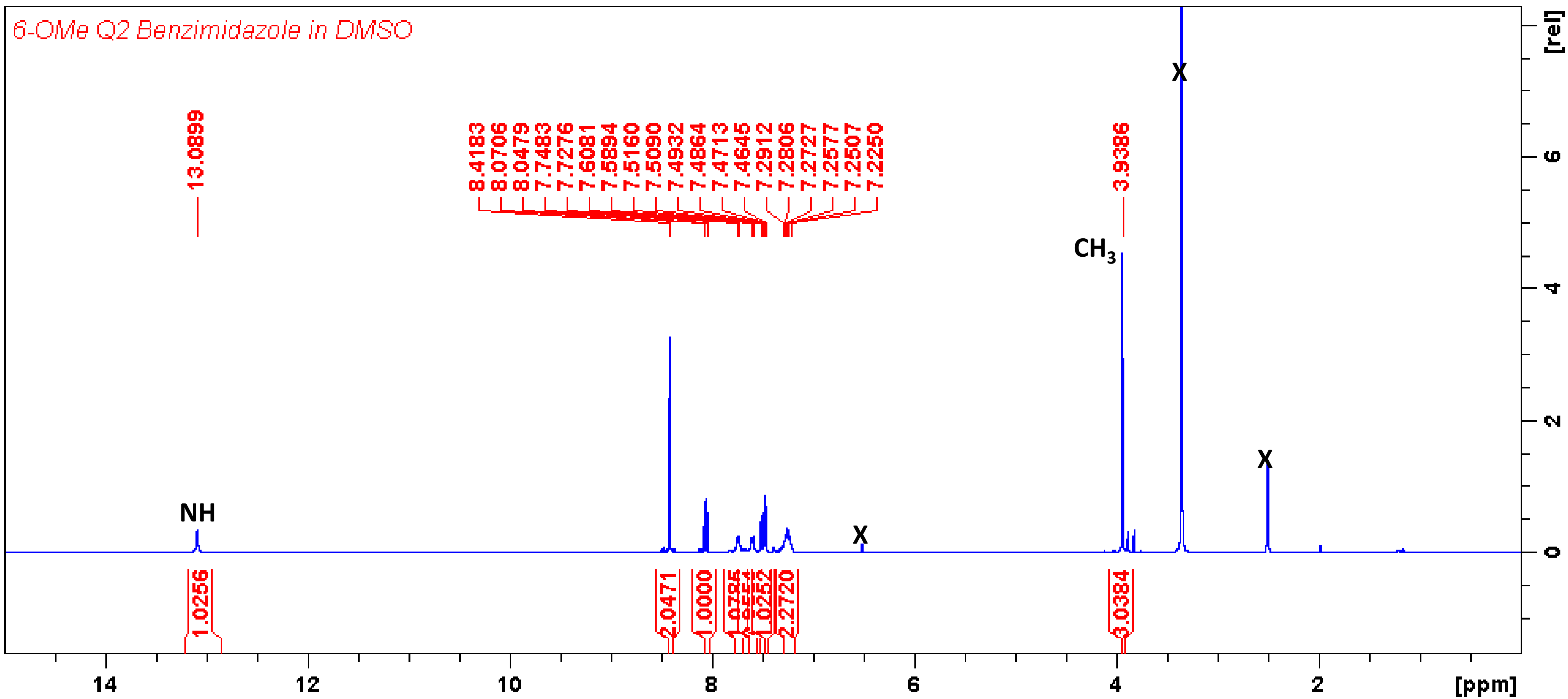

^{1}H NMR spectrum of **A5i**

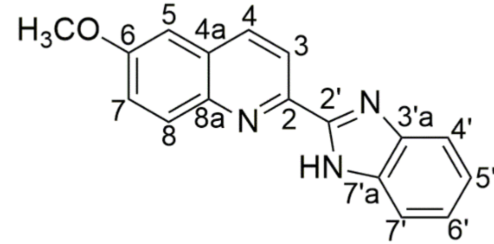

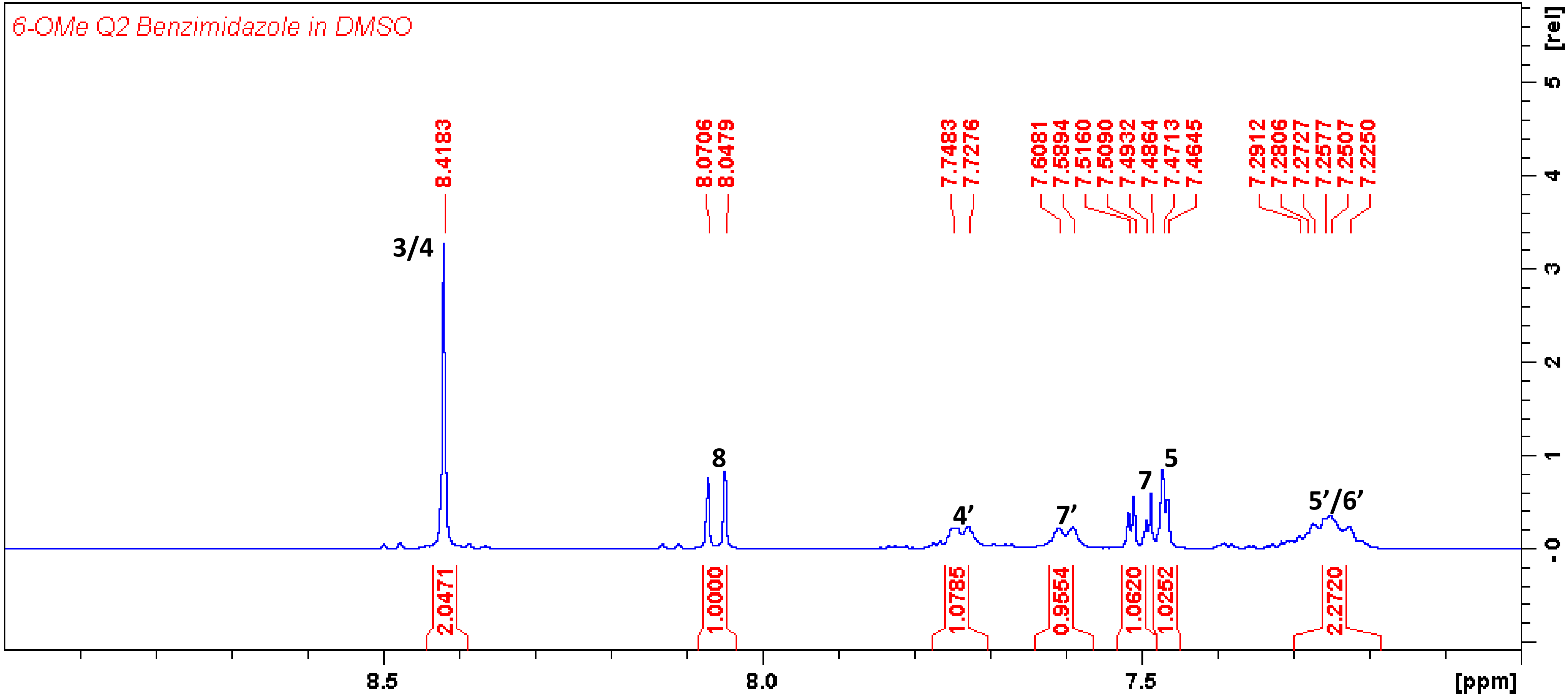

Expanded ^{1}H NMR spectrum of **A5i**

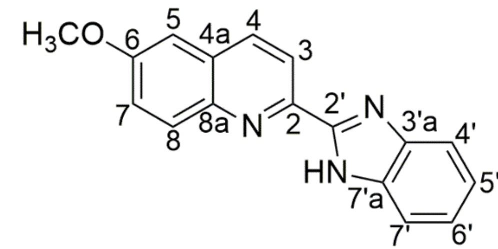

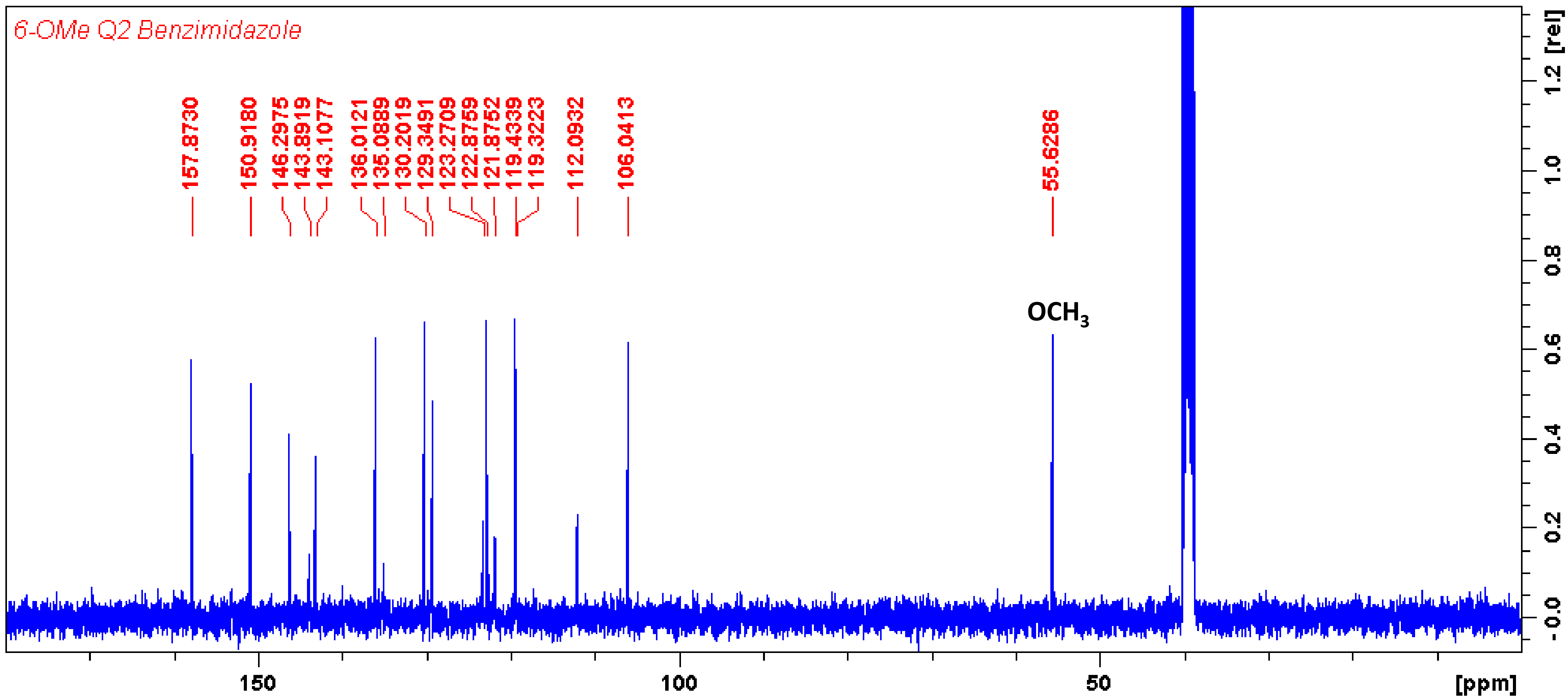

^{13}C NMR spectrum of **A5i**

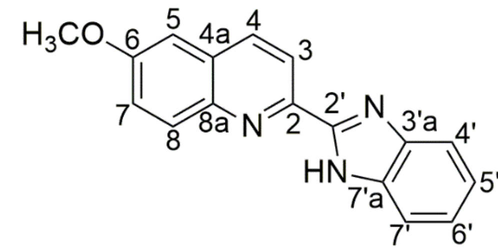

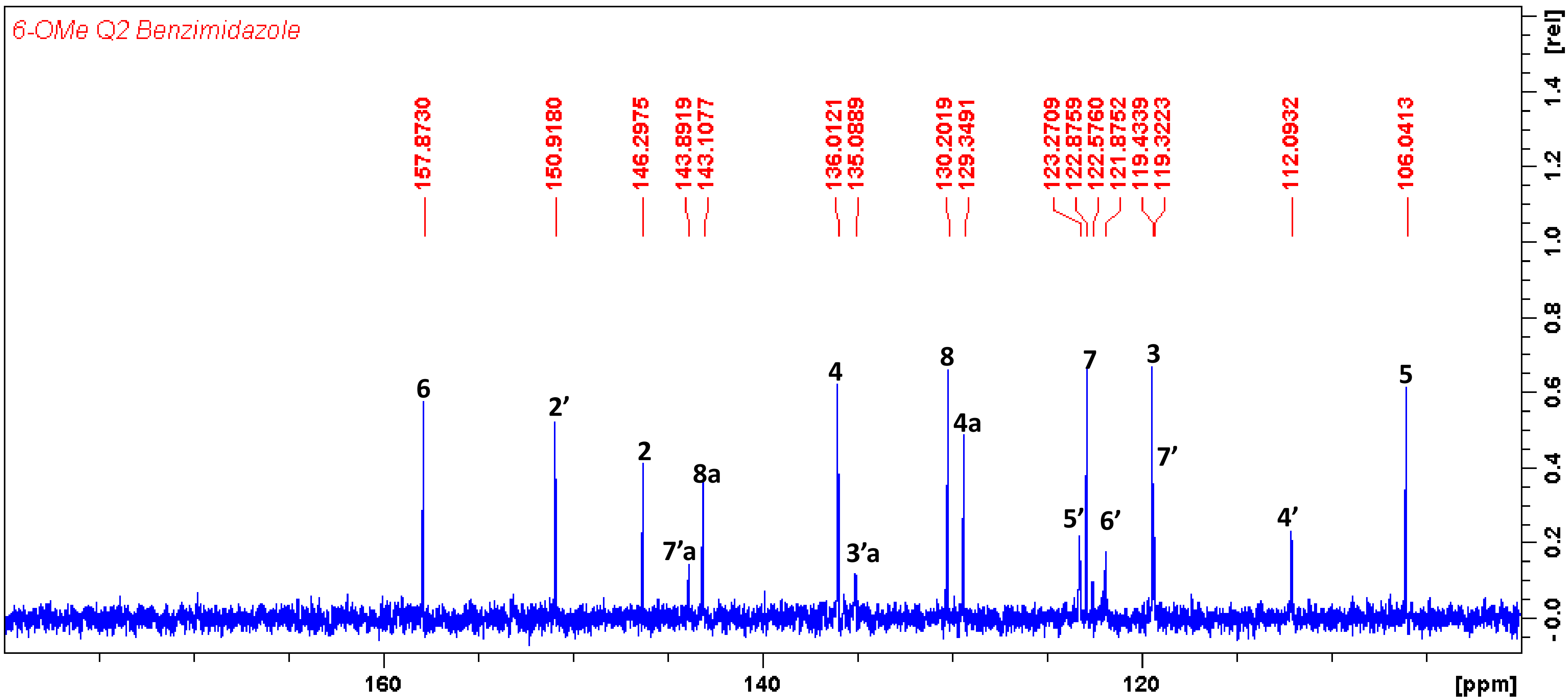

Expanded ^{13}C NMR spectrum of **A5i**

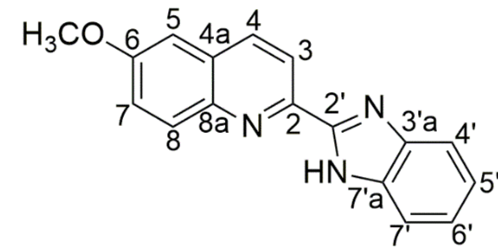

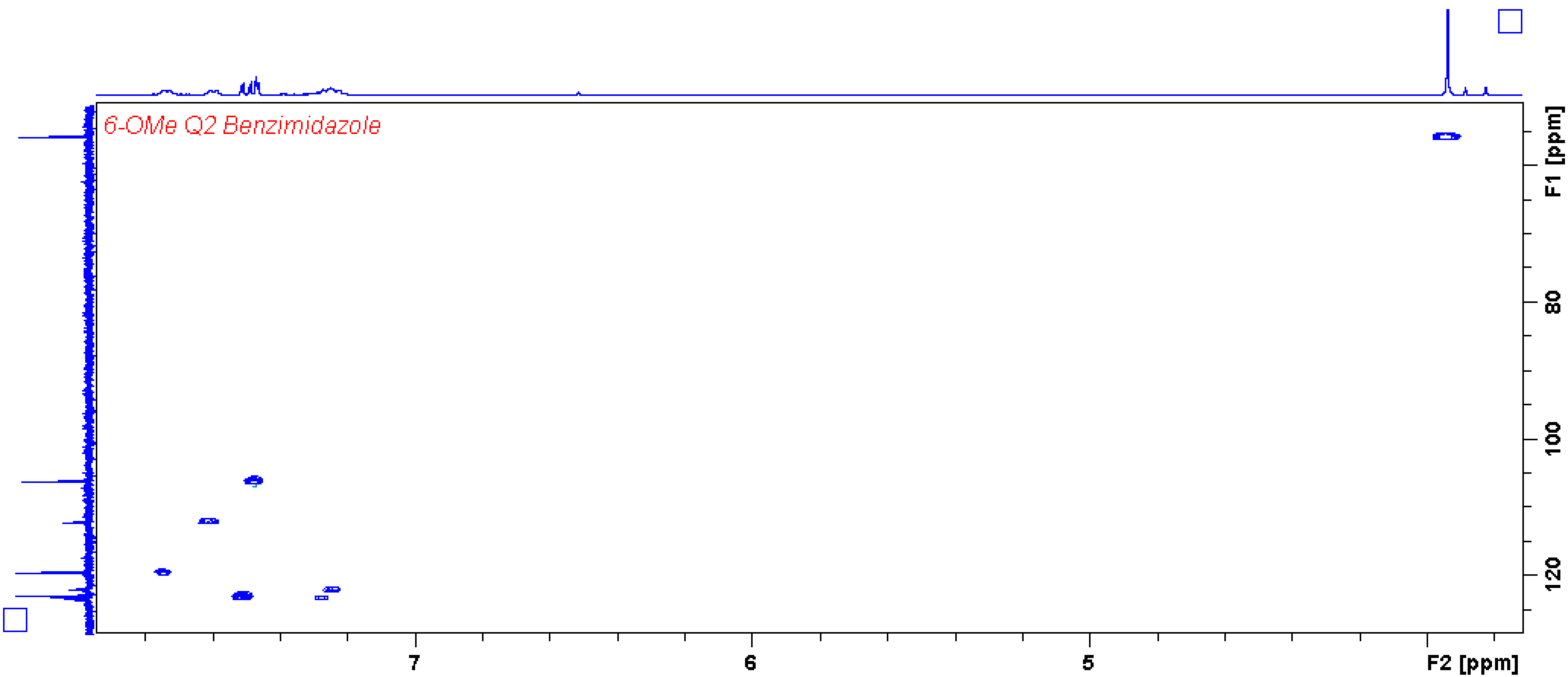

HSQC of **A5i**

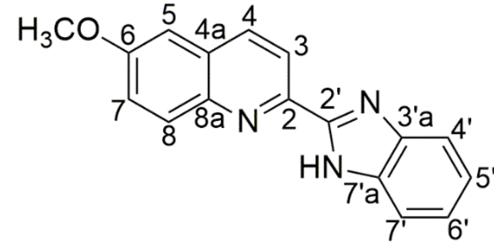

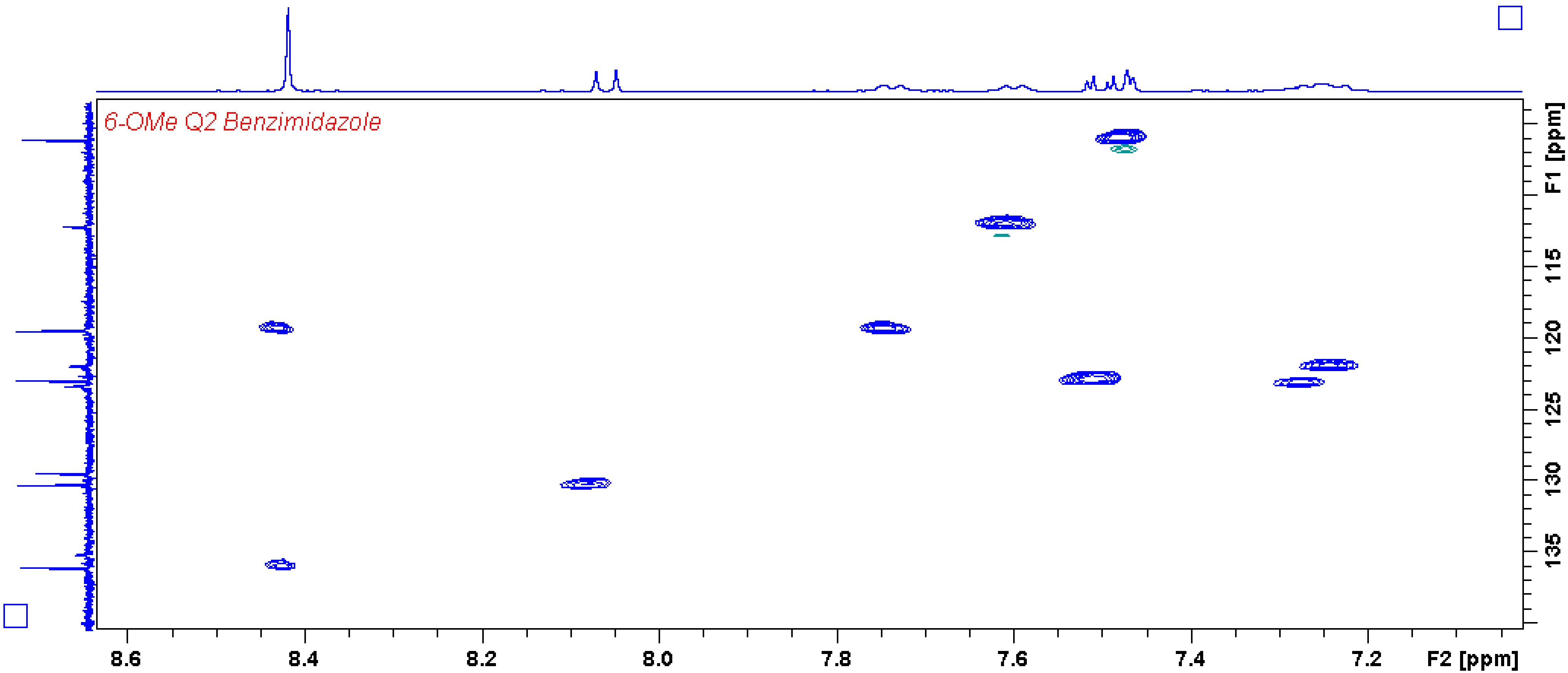

Expanded HSQC of **A5i**

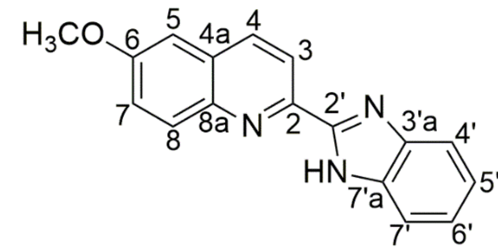
H3CO
6
5
4a
4
3
2'
N
3'a
4'
7
8a
N
2
HN
5'
8
7'a
7'
6'

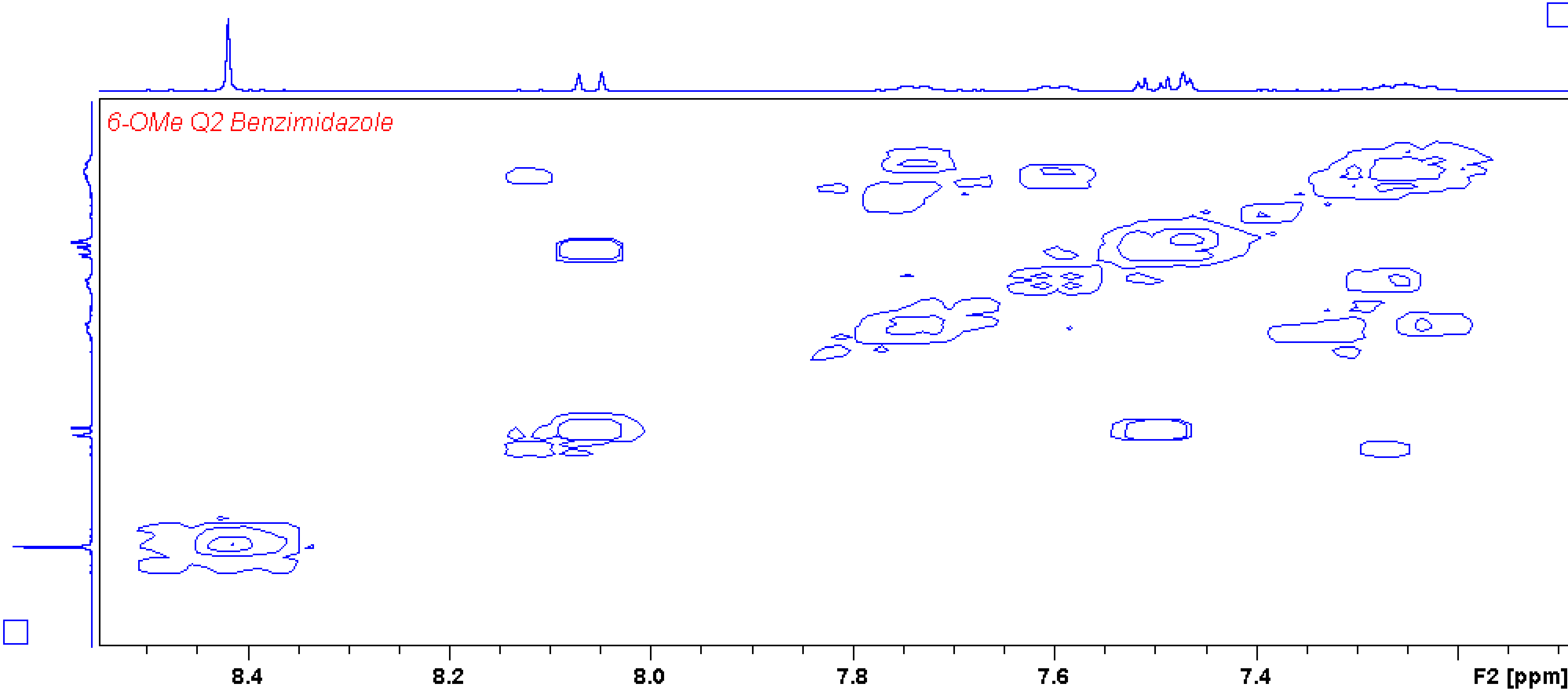
6-OMe Q2 Benzimidazole
F1 [ppm]
7.6
7.8
8.0
8.2
8.4
8.6
8.4
8.2
8.0
7.8
7.6
7.4
F2 [ppm]

COSY of **A5i**

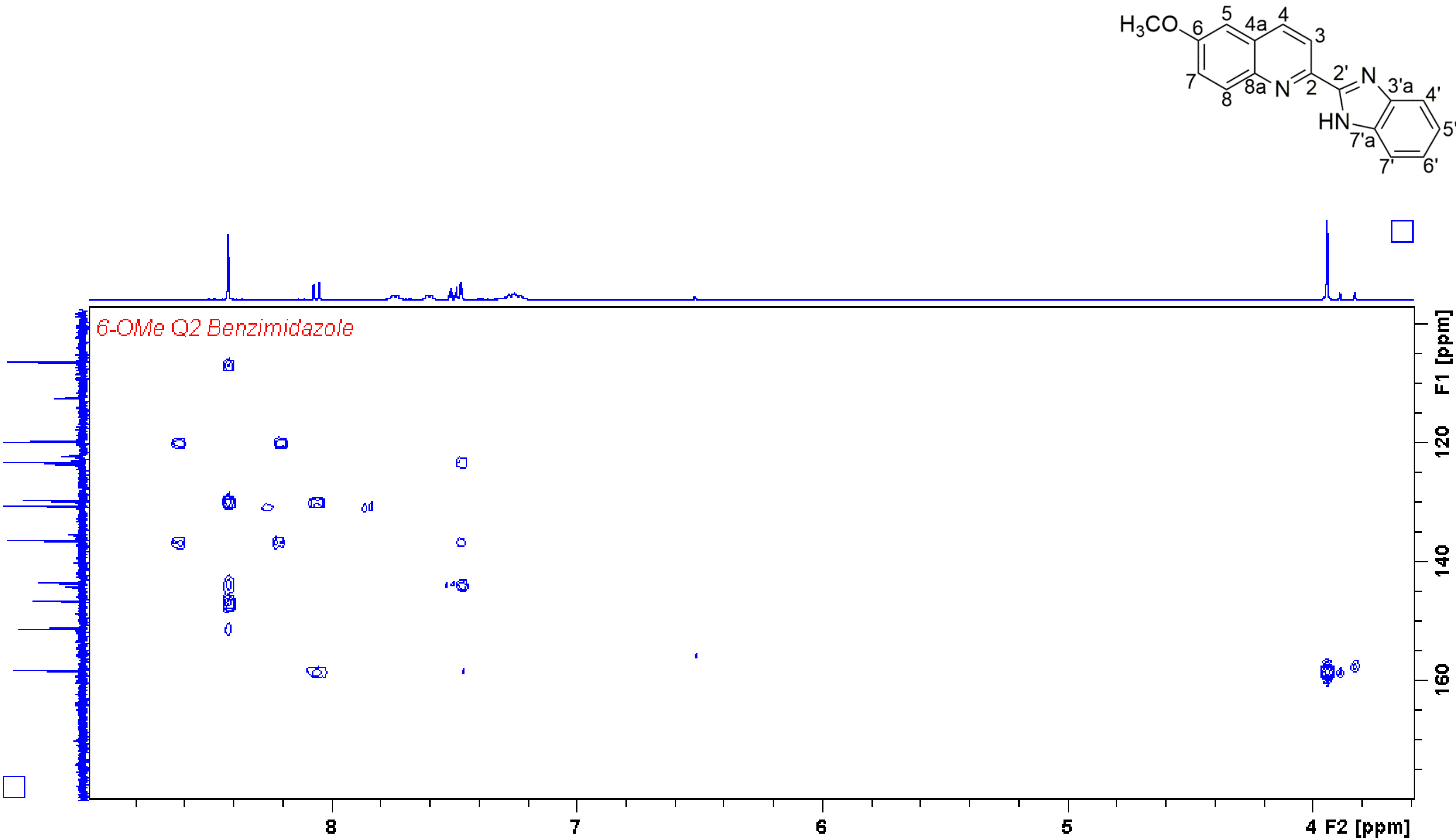

HMBC of **A5i**

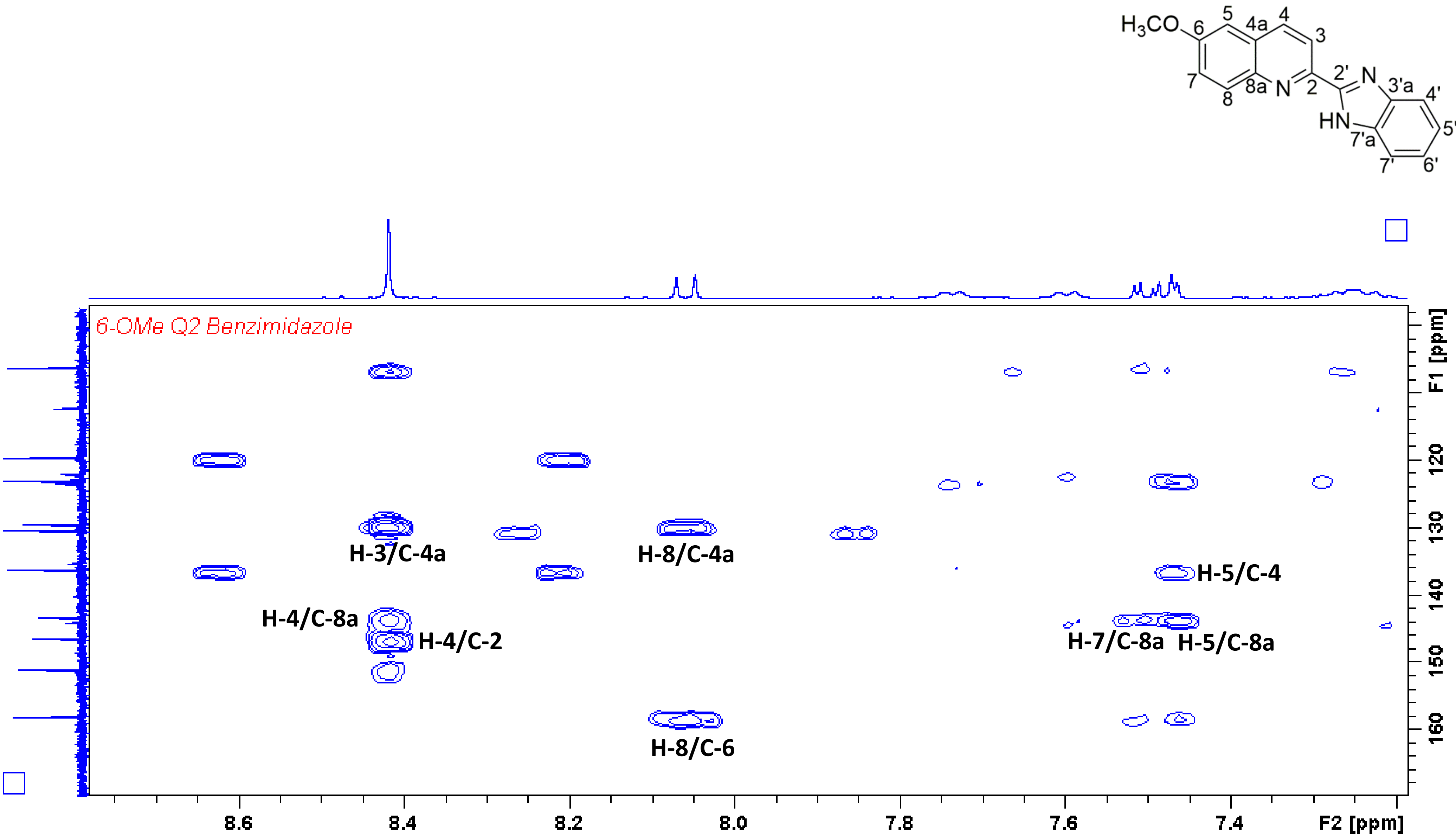

Expanded HMBC of **A5i**

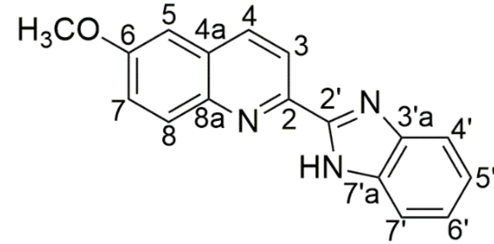

Elemental Composition Report

Single Mass Analysis

Tolerance = 5.0 PPM / DBE: min = -1.5, max = 100.0
Element prediction: Off
Number of isotope peaks used for i-FIT = 3

Monoisotopic Mass, Even Electron Ions
20 formula(e) evaluated with 1 results within limits (up to 20 closest results for each mass)
Elements Used:
C: 15-20 H: 10-15 N: 0-5 O: 0-5
SSQB7 2 (0.034) Cm (1:61)
TOF MS ES-

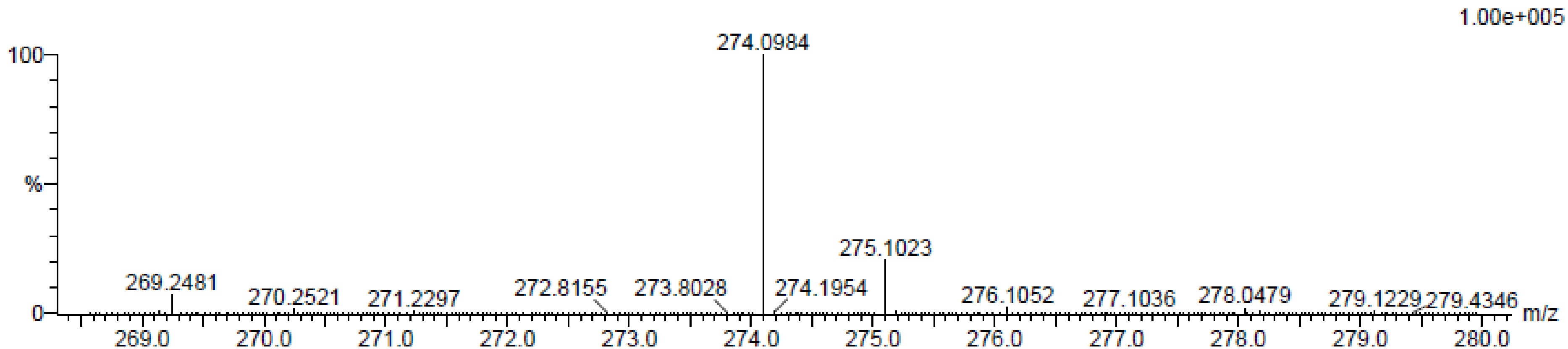

Minimum:				-1.5			
Maximum:		5.0	5.0	100.0			
Mass	Calc. Mass	mDa	PPM	DBE	i-FIT	i-FIT (Norm)	Formula
274.0984	274.0980	0.4	1.5	13.5	541.6	0.0	C17 H12 N3 O

High resolution mass spectrum of **A5i**

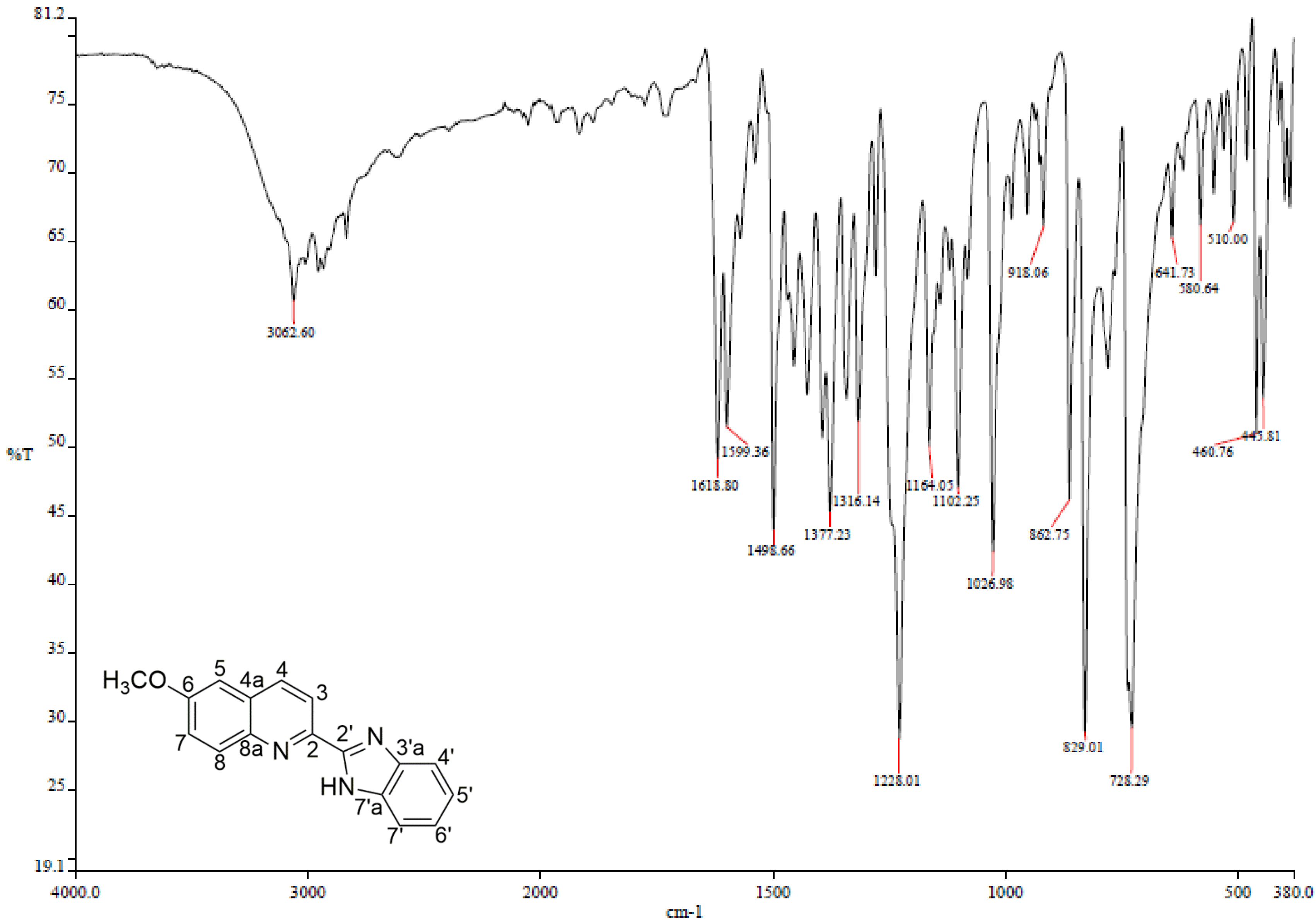

FTIR spectrum of **A5i**

Overlay Spectrum Graph Report

03/08/2017 03:12:31 PM

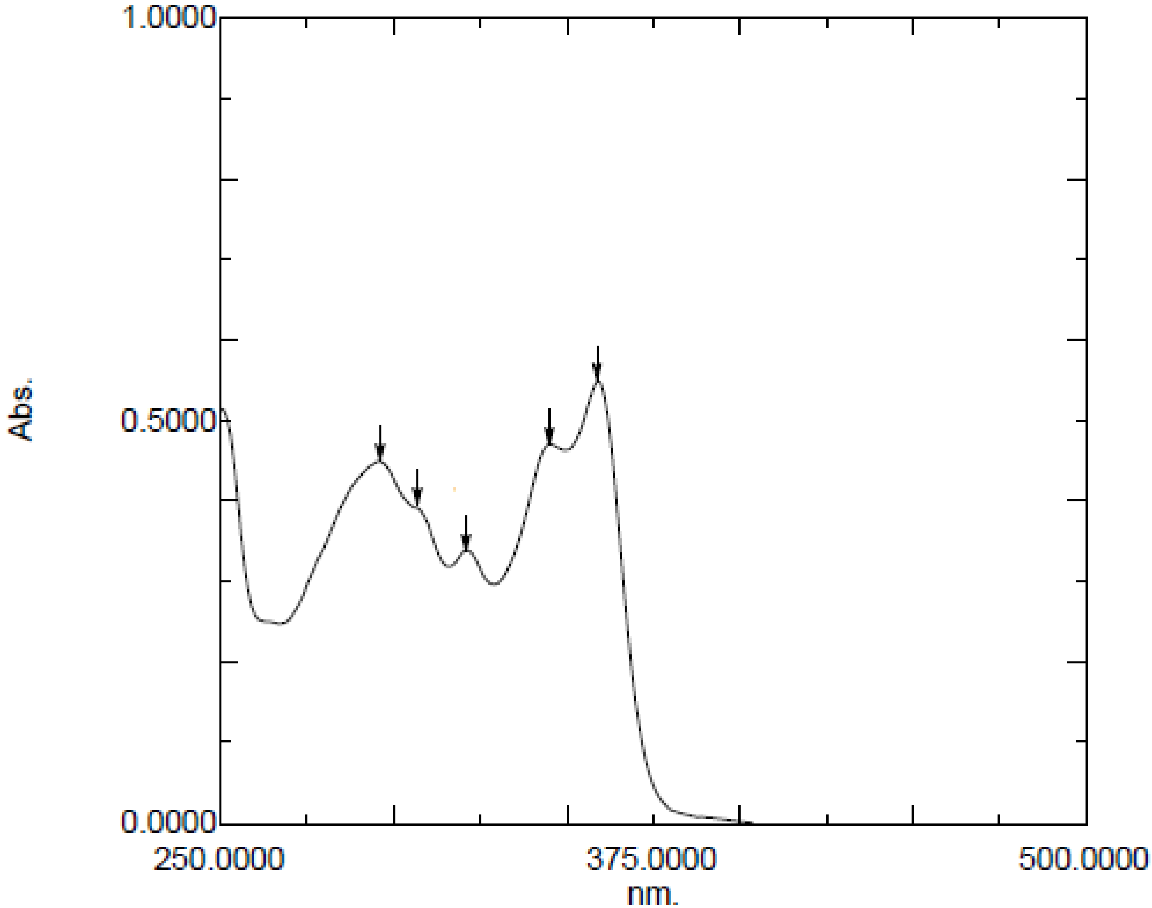

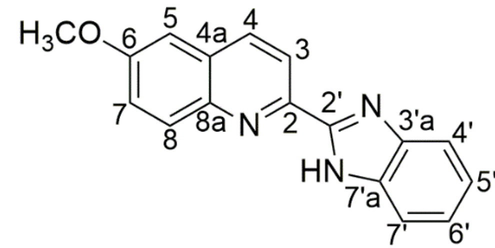

λ	absorbance	logε
296	0.4493	4.39
309	0.3798	4.32
321	0.3387	4.27
345	0.4709	4.41
359	0.5496	4.48

UV spectrum of **A5i**

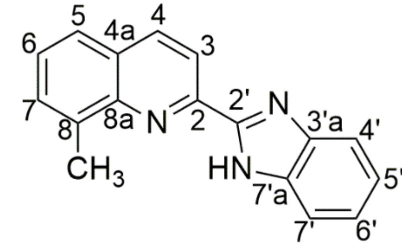

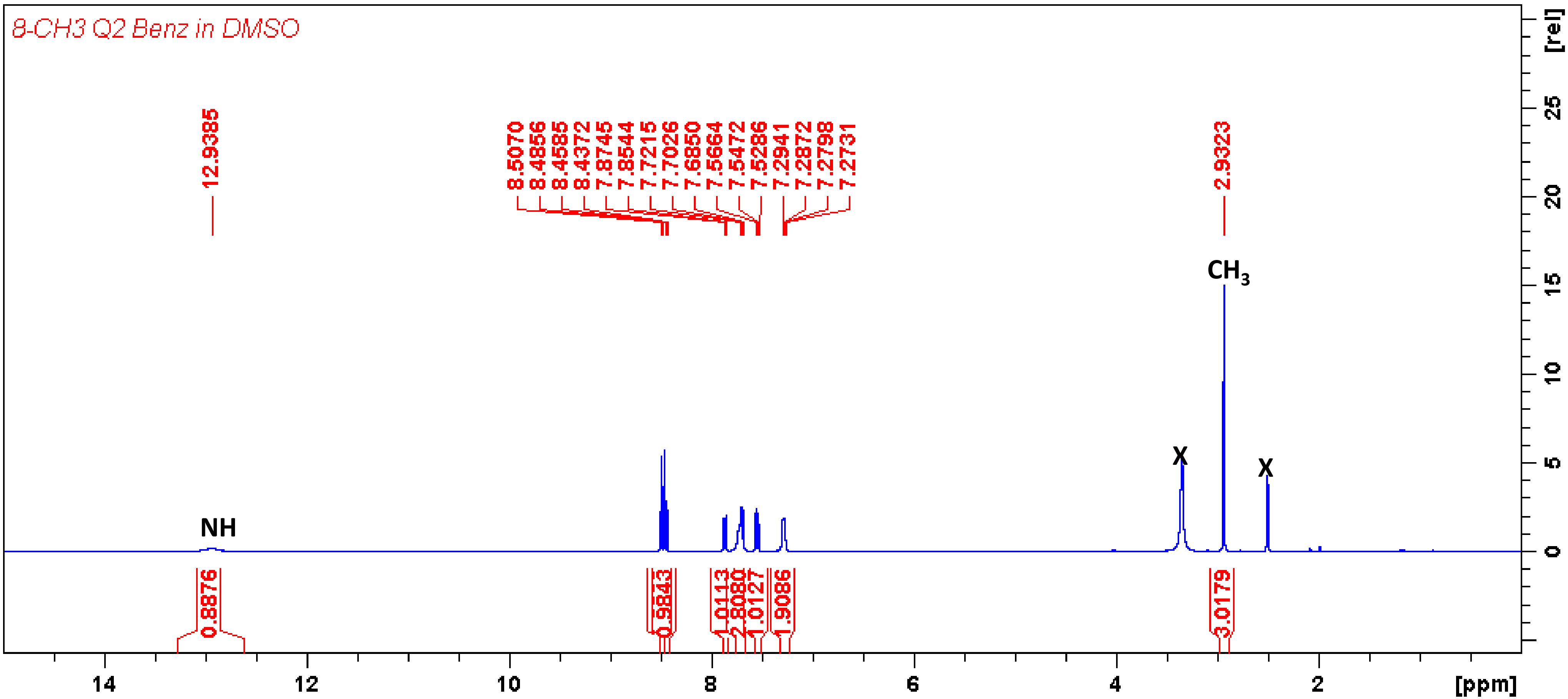

^{1}H NMR spectrum of **A5j**

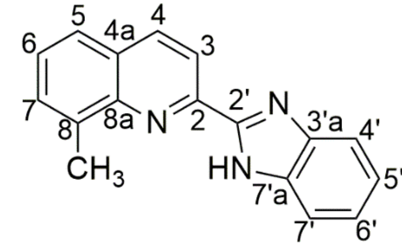

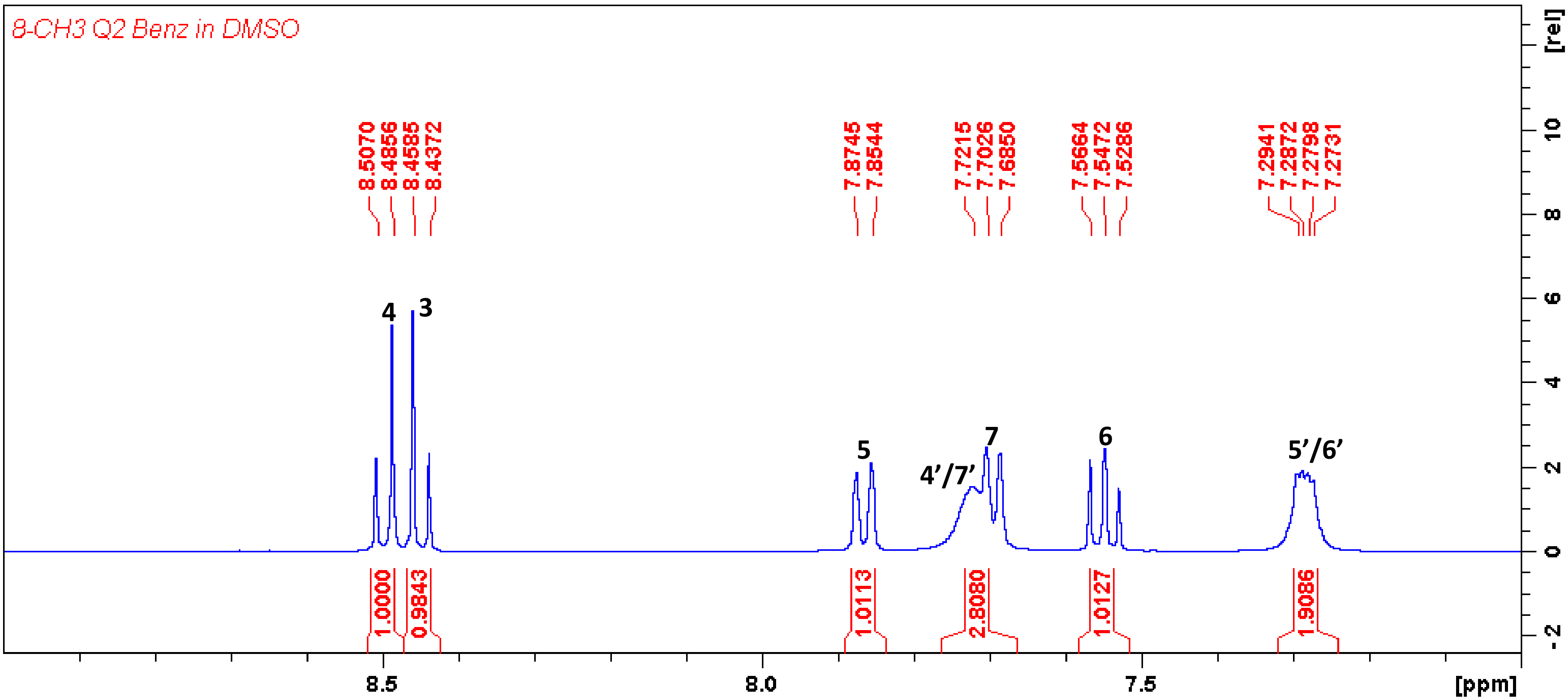

Expanded ^{1}H NMR spectrum of **A5j**

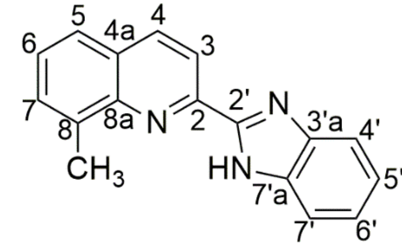

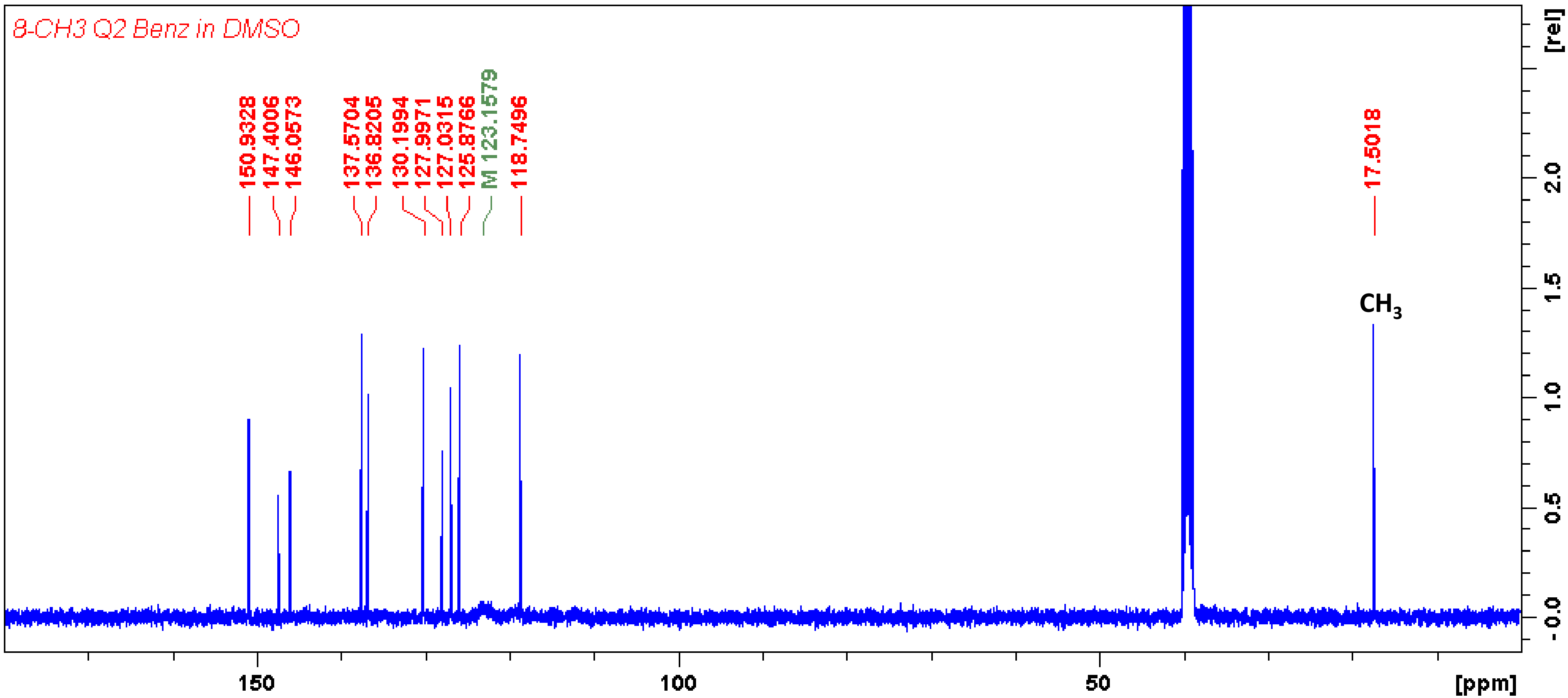

^{13}C NMR spectrum of **A5j**

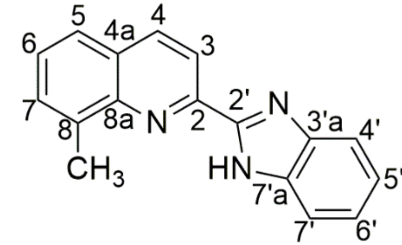

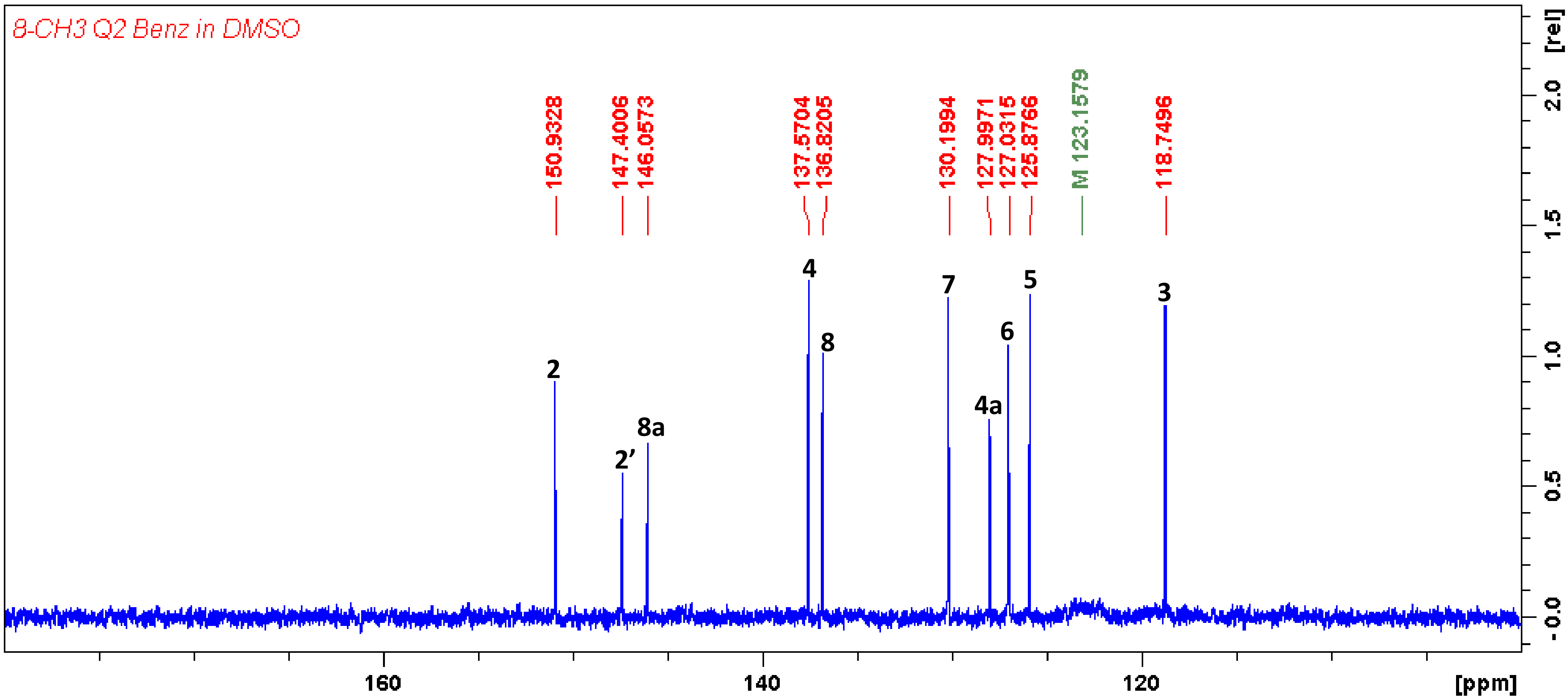

Expanded ^{13}C NMR spectrum of **A5j**

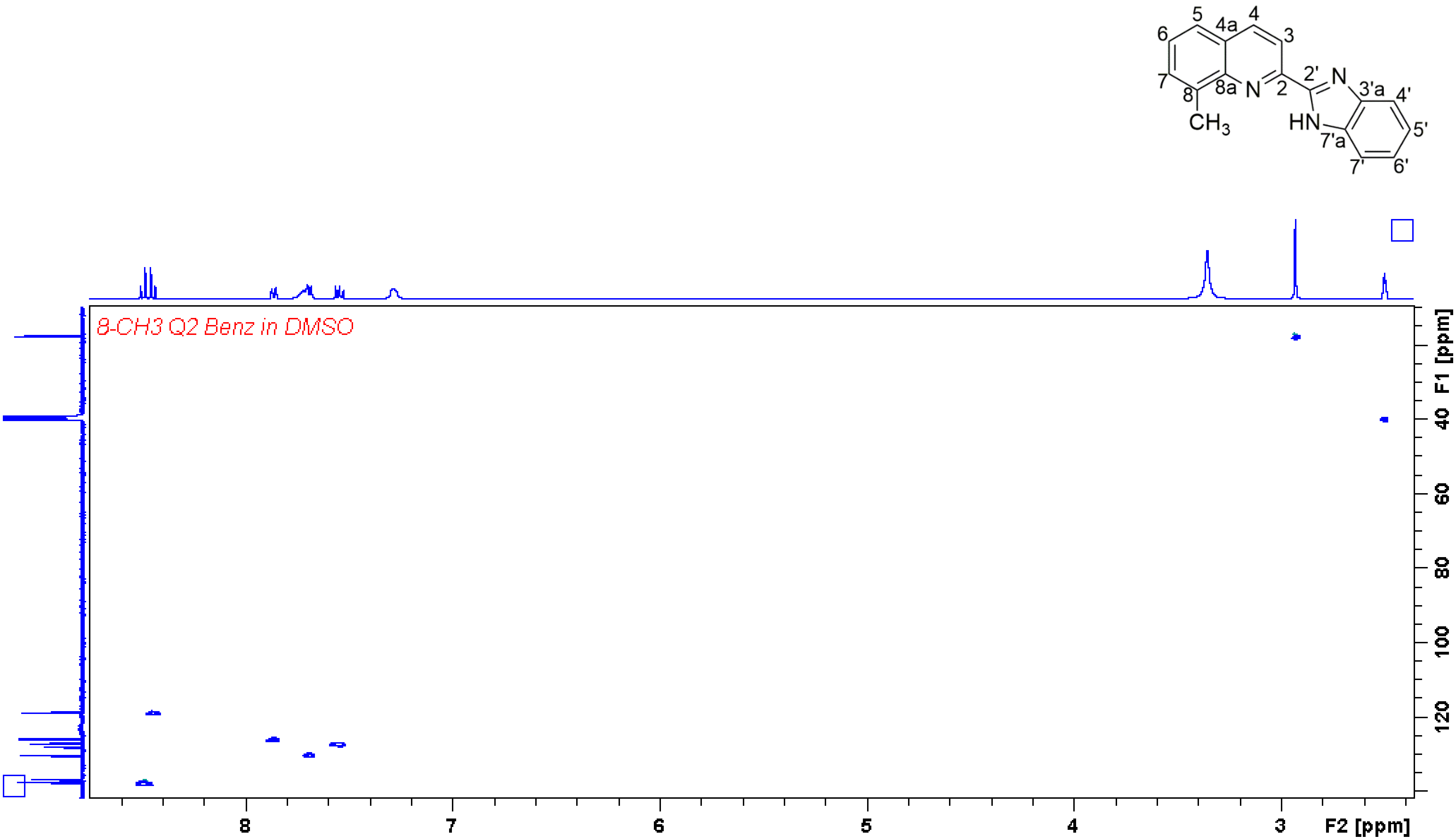

5
4a
4
3
6
7
8
8a
N
2
2'
N
3'a
4'
CH3
HN
7'a
5'
7'
6'
8-CH3 Q2 Benz in DMSO
F1 [ppm]
40
60
80
100
120
8
7
6
5
4
3
F2 [ppm]

HSQC of **A5j**

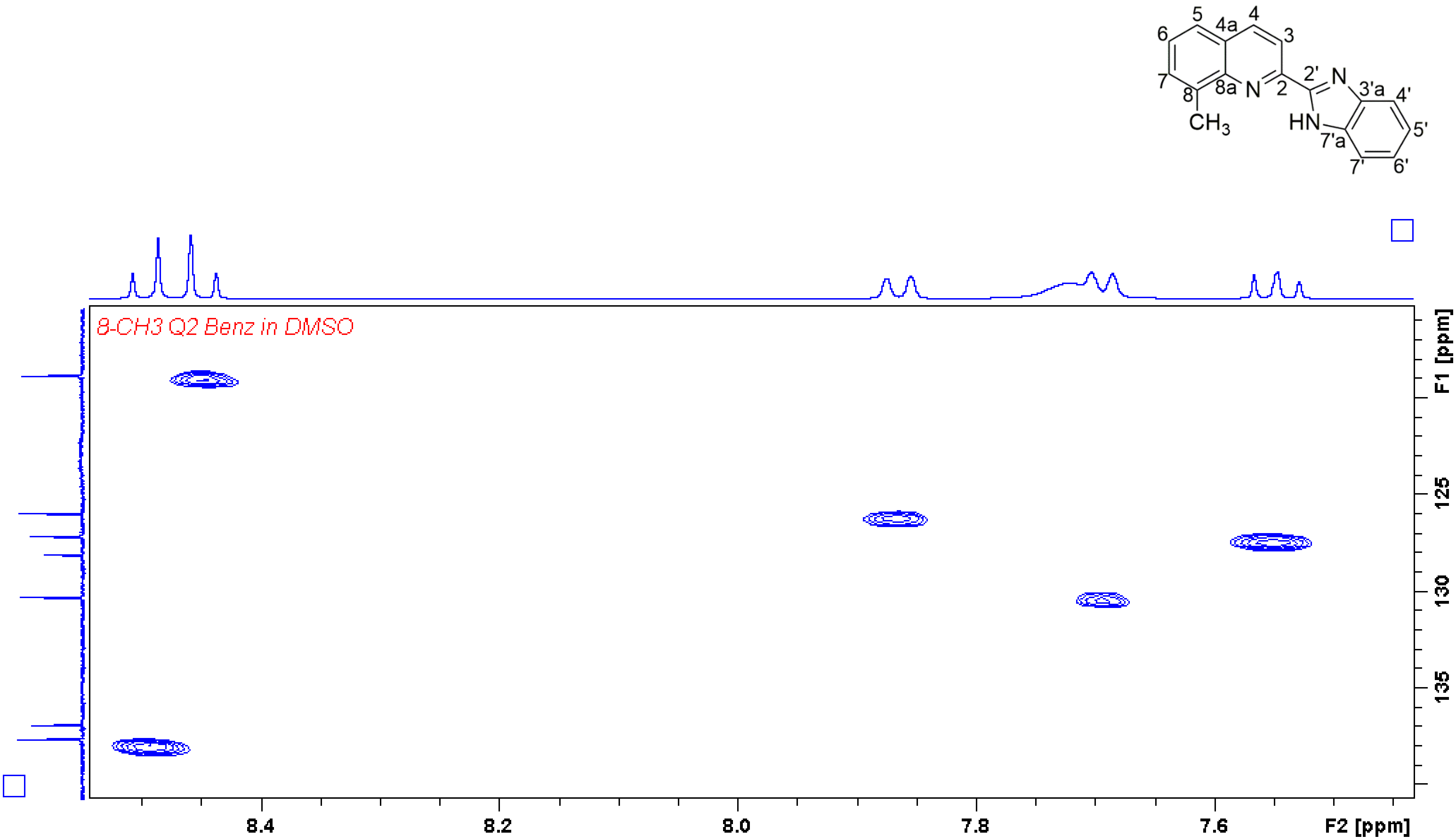

Expanded HSQC of **A5j**

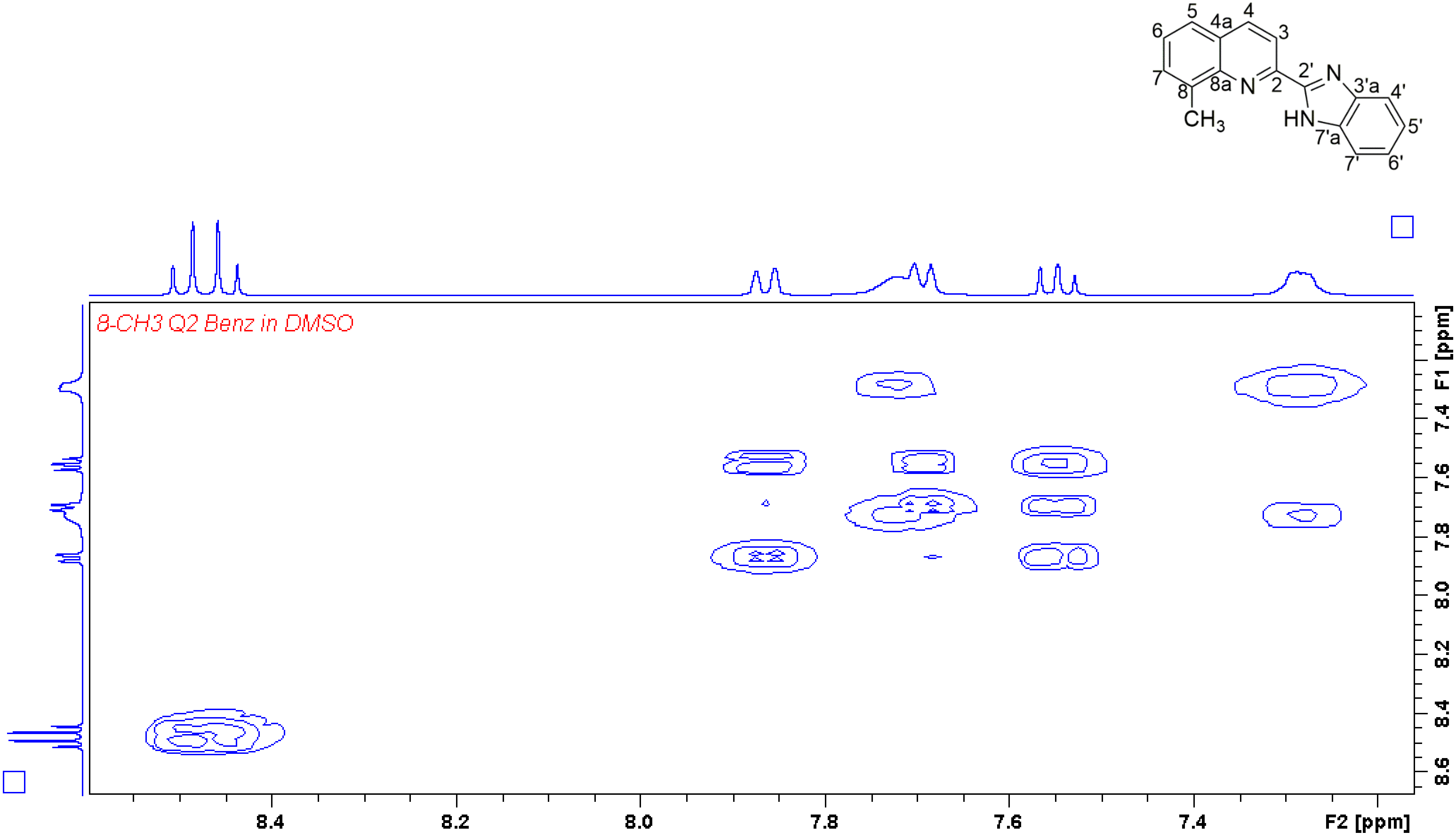
5
4a
4
6
3
7
8a
N
2
2'
N
3'a
4'
8
CH3
HN
7'a
5'
7'
6'
8-CH3 Q2 Benz in DMSO
F1 [ppm]
F2 [ppm]
7.4
7.6
7.8
8.0
8.2
8.4
8.6

COSY of **A5j**

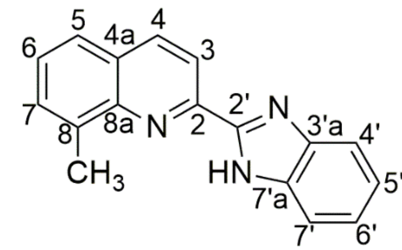
5
4a
4
6
3
2'
N
7
8a
N
2
3'a
4'
8
HN
5'
CH3
7'a
7'
6'

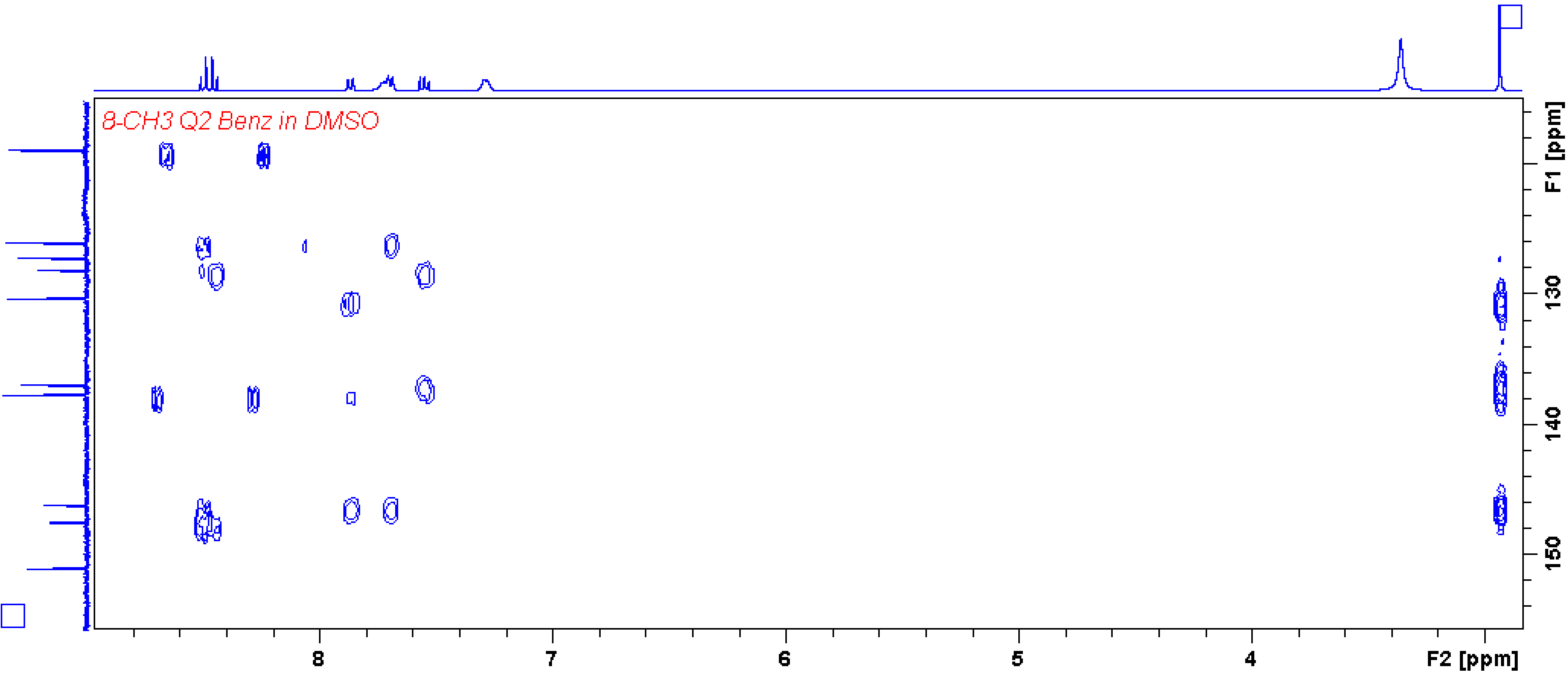
8-CH3 Q2 Benz in DMSO
F1 [ppm]
130
140
150
8
7
6
5
4
F2 [ppm]

HMBC of **A5j**

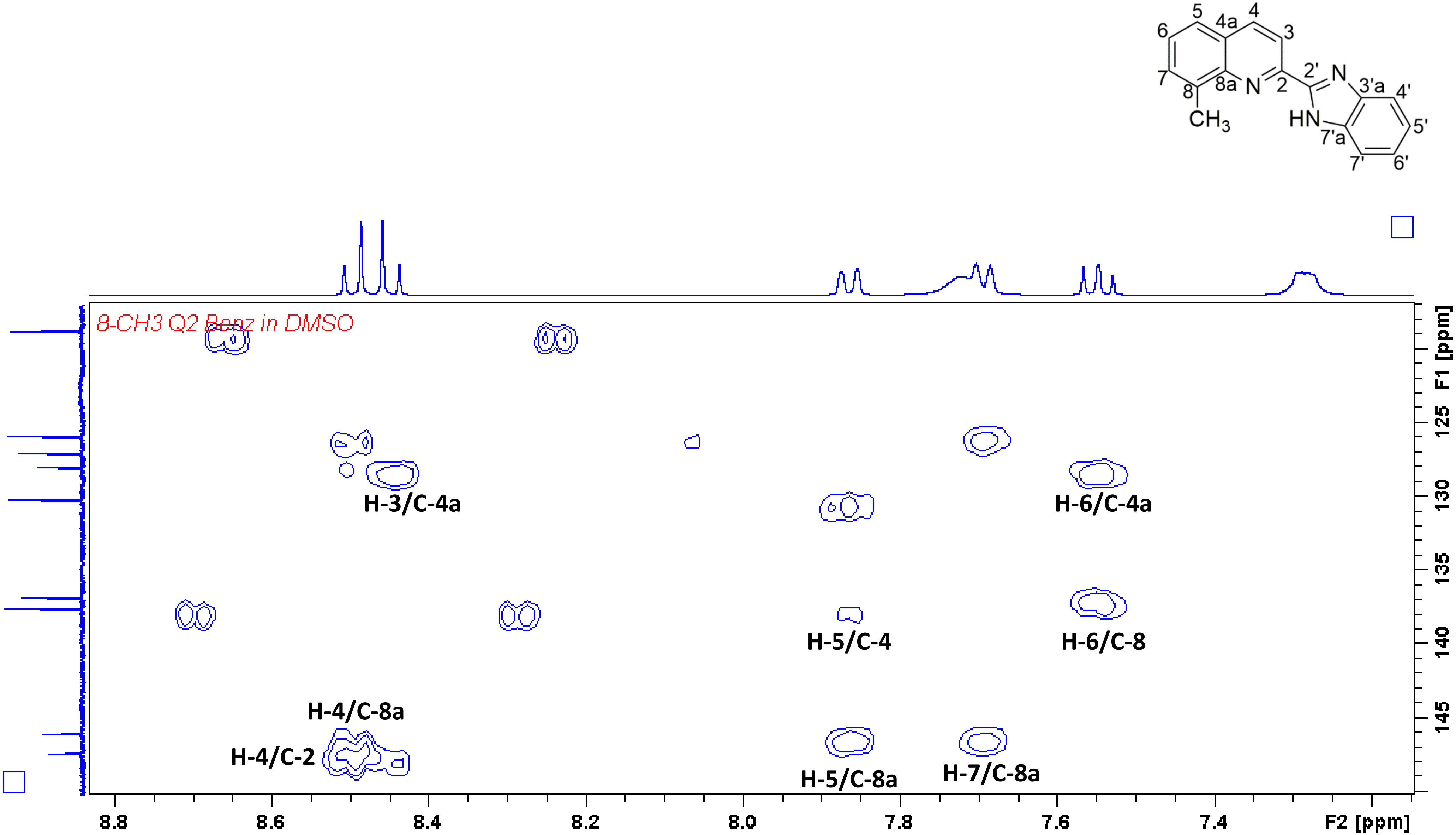

Expanded HMBC of **A5j**

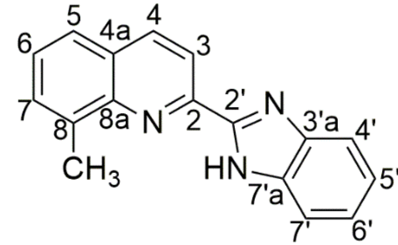

Elemental Composition Report

Single Mass Analysis

Tolerance = 5.0 PPM / DBE: min = -1.5, max = 100.0
Element prediction: Off
Number of isotope peaks used for i-FIT = 3

Monoisotopic Mass, Even Electron Ions
3 formula(e) evaluated with 1 results within limits (up to 20 closest results for each mass)
Elements Used:
C: 15-20 H: 10-15 N: 0-5
SSQB 12 60 (1.990) Cm (1:61)
TOF MS ES+

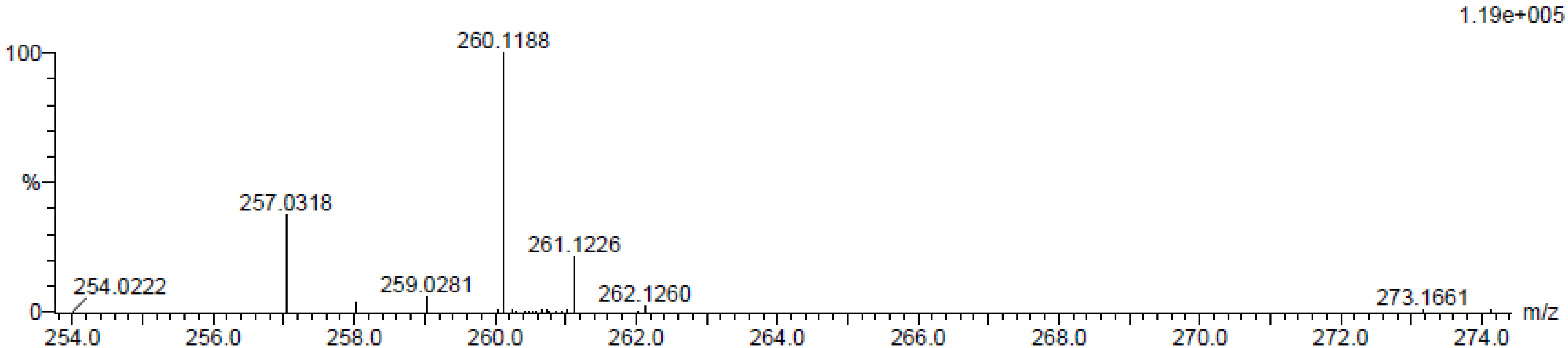

Minimum:				-1.5			
Maximum:		5.0	5.0	100.0			
Mass	Calc. Mass	mDa	PPM	DBE	i-FIT	i-FIT (Norm)	Formula
260.1188	260.1188	0.0	0.0	12.5	177.1	0.0	C17 H14 N3

High resolution mass spectrum of **A5j**

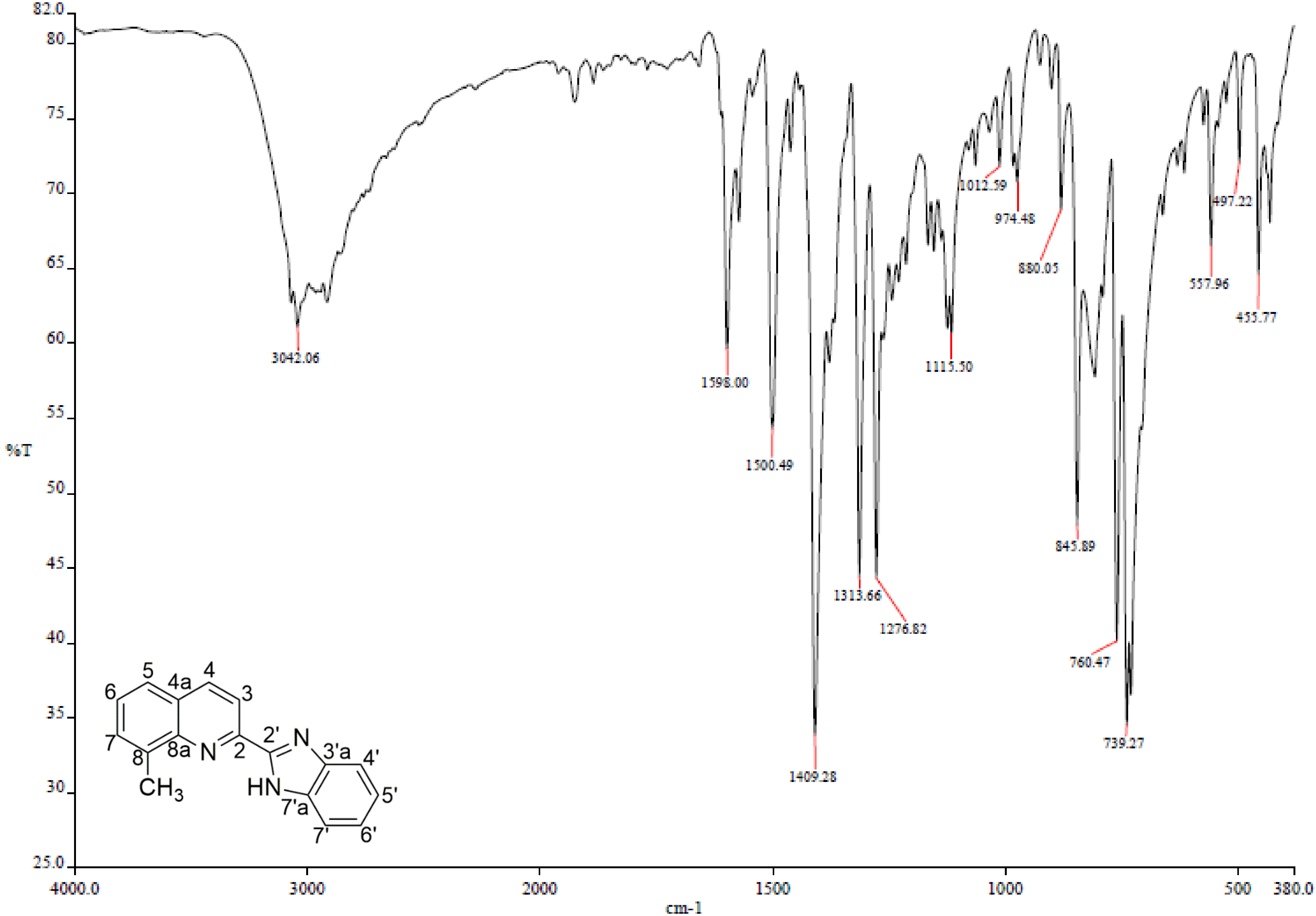

FTIR spectrum of **A5j**

Overlay Spectrum Graph Report

03/08/2017 03:14:44 PM

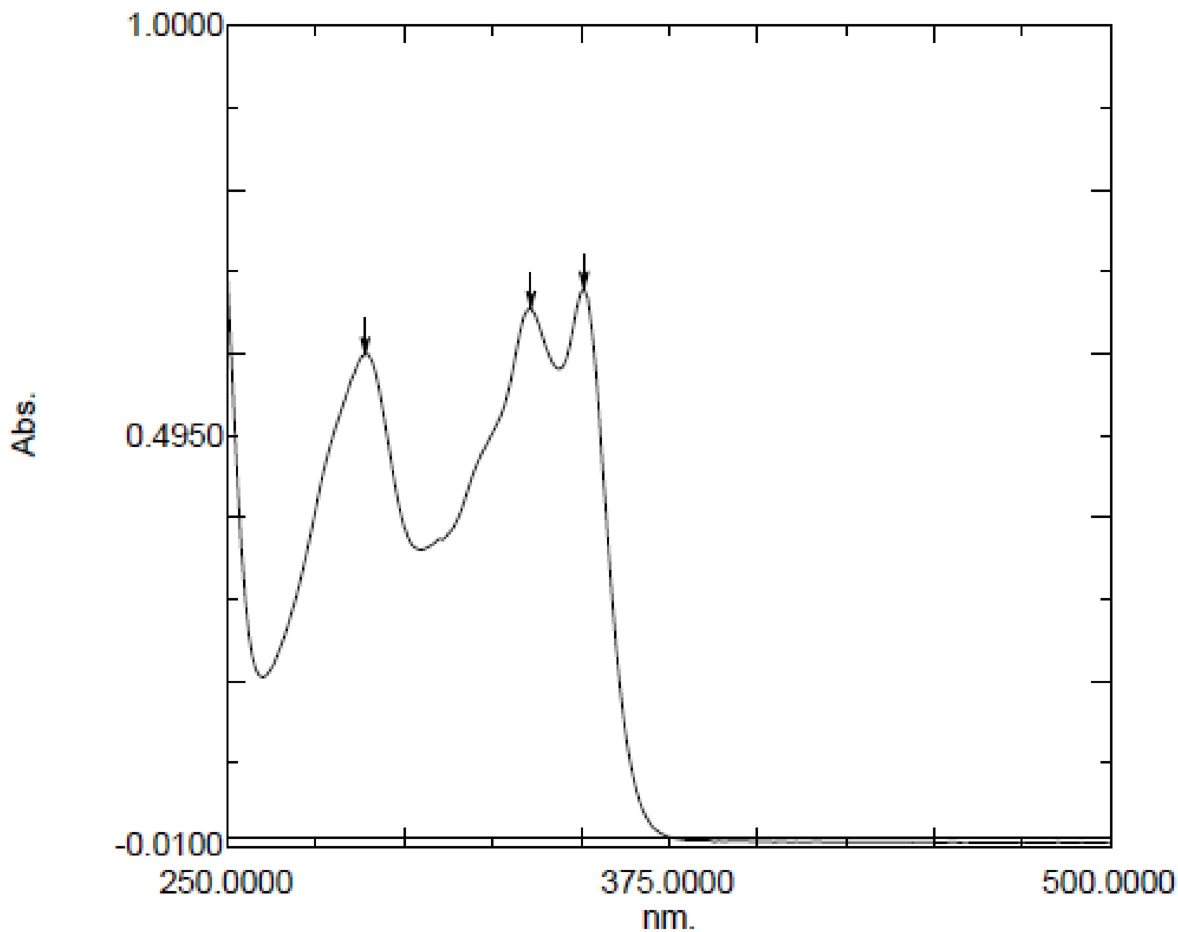

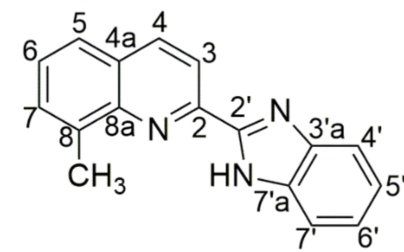

λ	absorbance	logε
289	0.5956	4.49
336	0.6516	4.53
351	0.6756	4.54

Page 1 / 1

UV spectrum of **A5j**

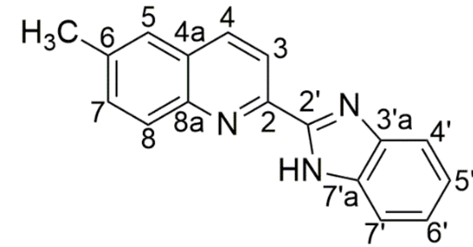

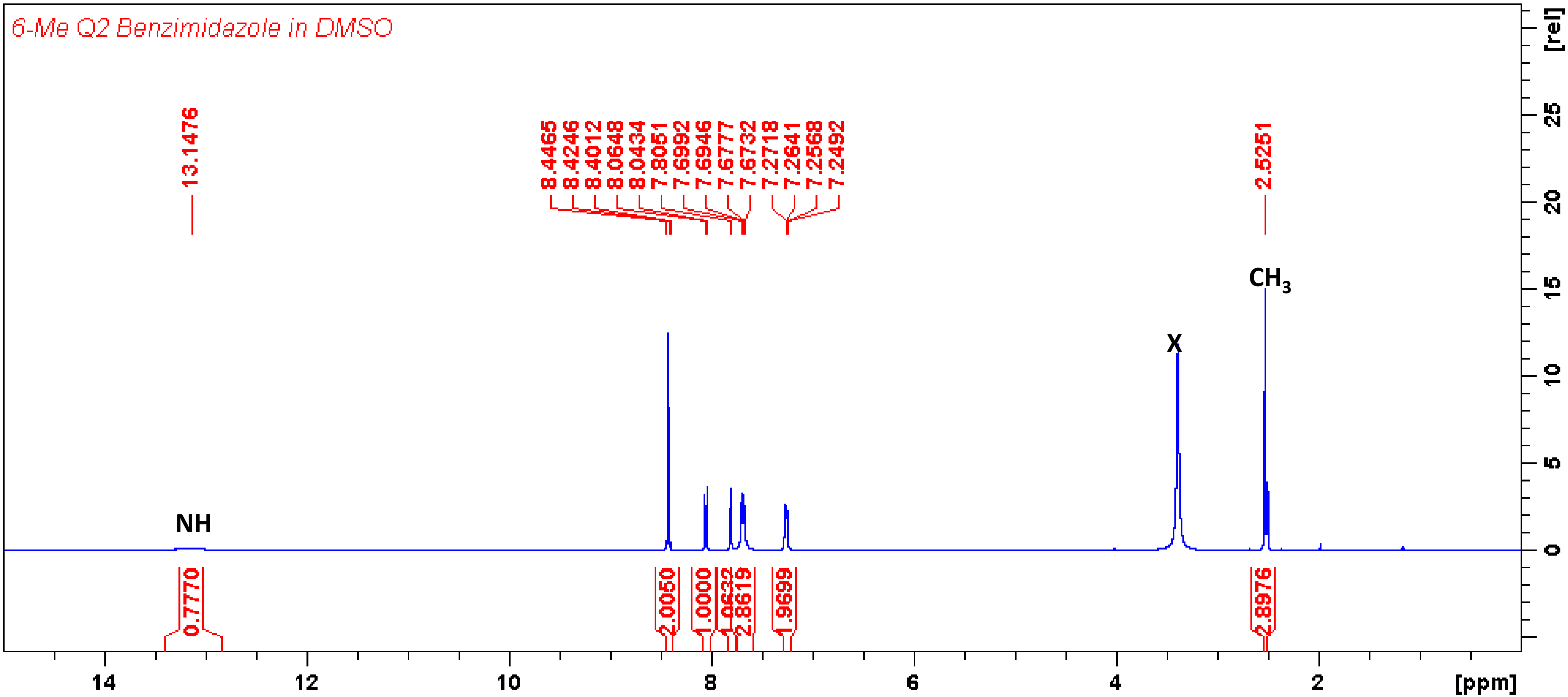

^{1}H NMR spectrum of **A5k**

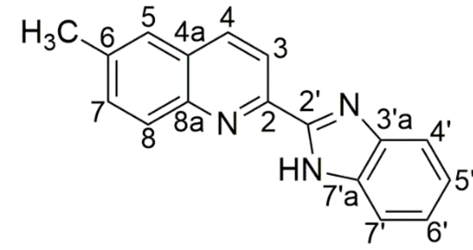

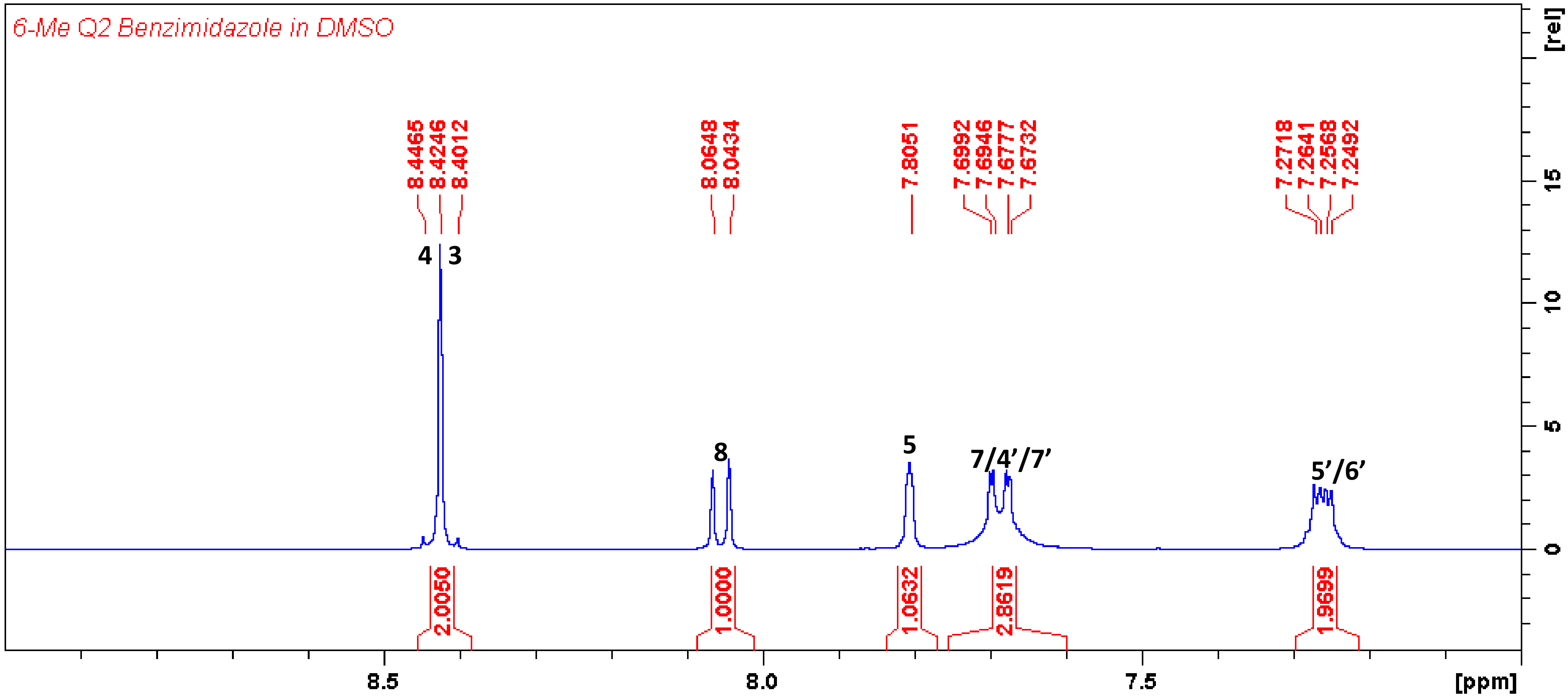

Expanded ^{1}H NMR spectrum of **A5k**

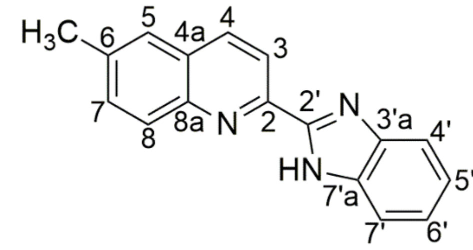

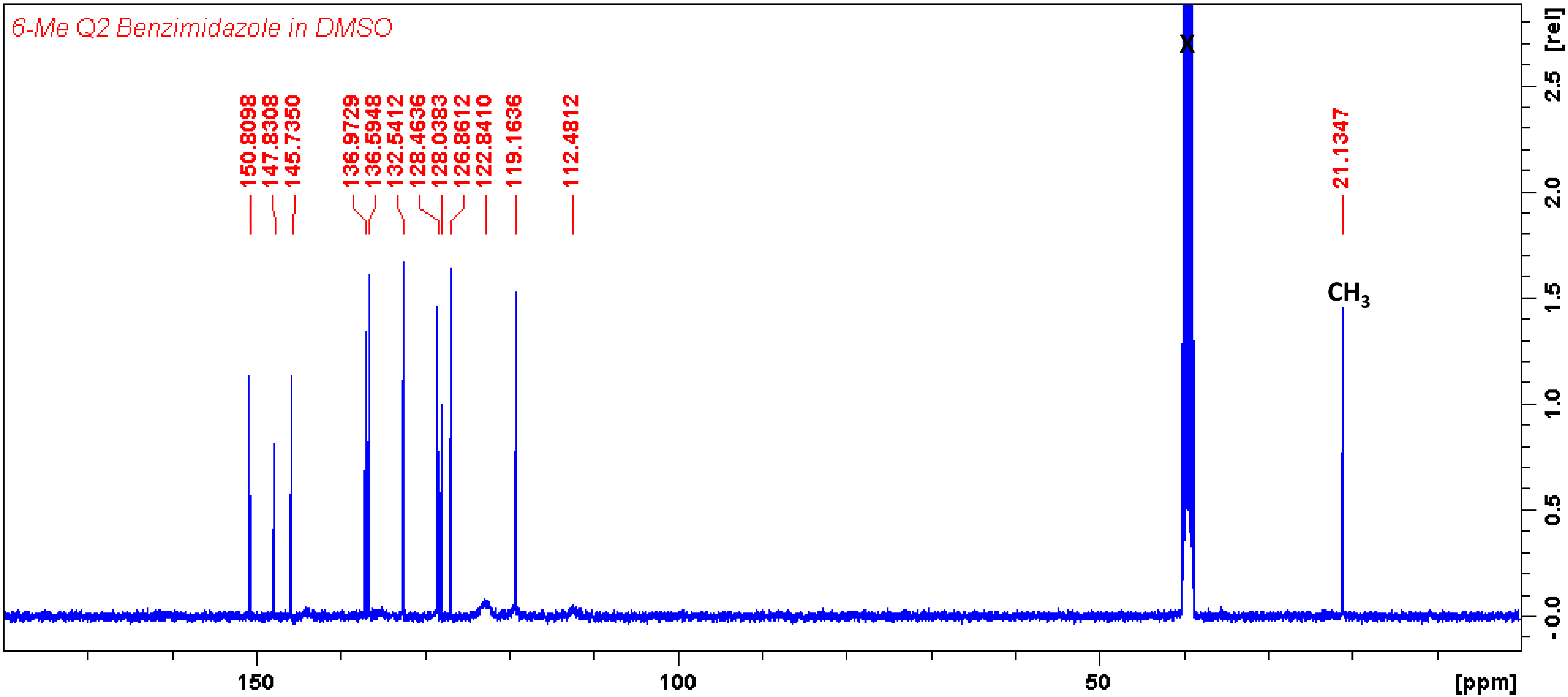

^{13}C NMR spectrum of **A5k**

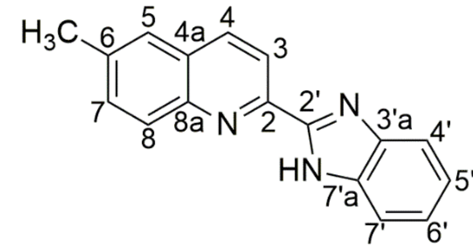

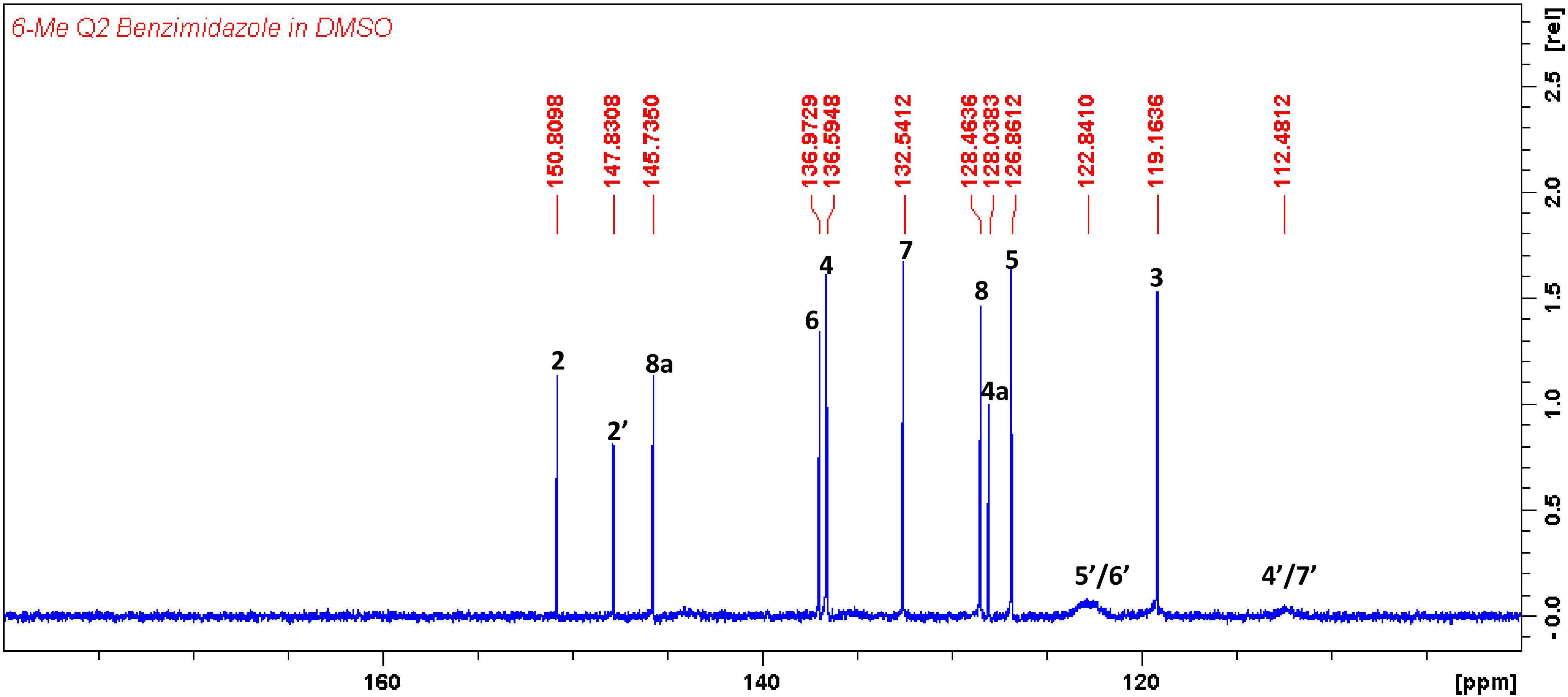

Expanded ^{13}C NMR spectrum of **A5k**

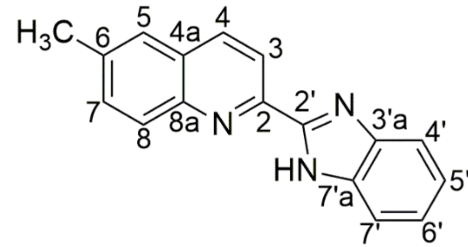

H_3C
6
5
4a
4
3
7
8
8a
N
2
2'
N
3'a
4'
HN
7'a
5'
7'
6'

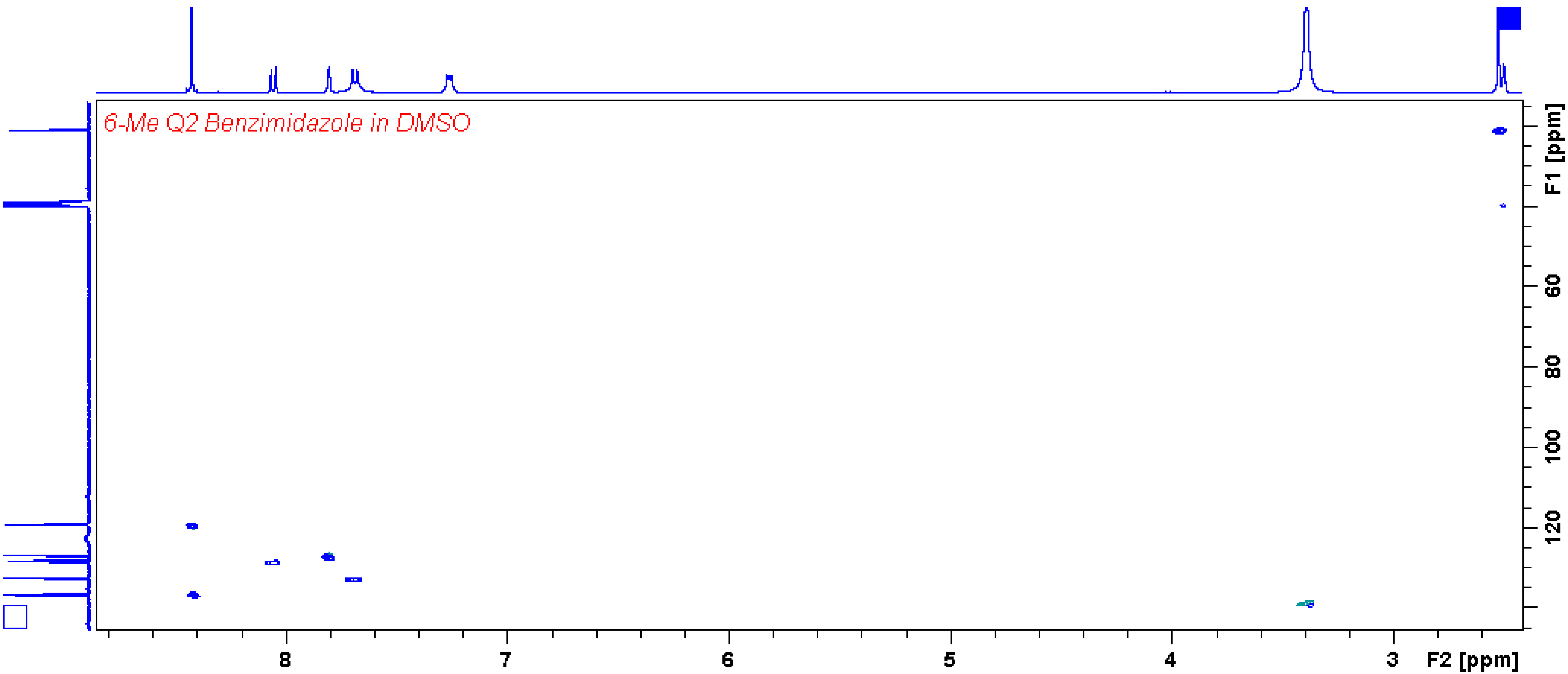

6-Me Q2 Benzimidazole in DMSO
F1 [ppm]
60
80
100
120
8
7
6
5
4
3
F2 [ppm]

HSQC of **A5k**

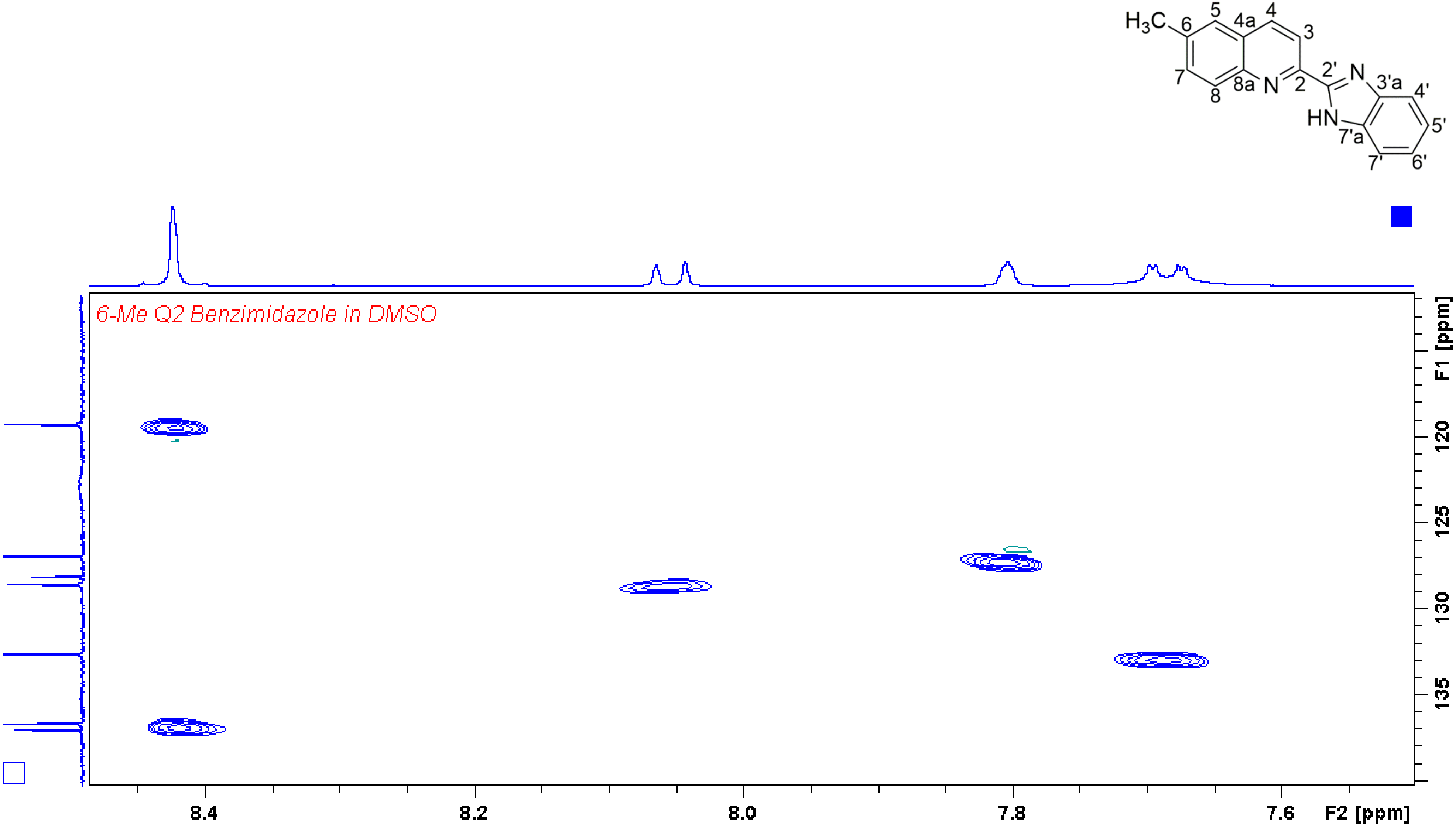

Expanded HSQC of **A5k**

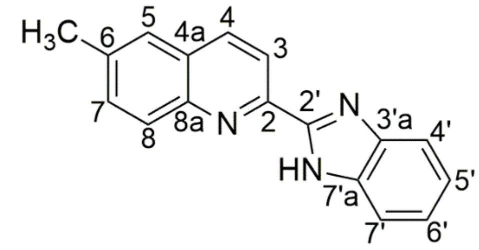

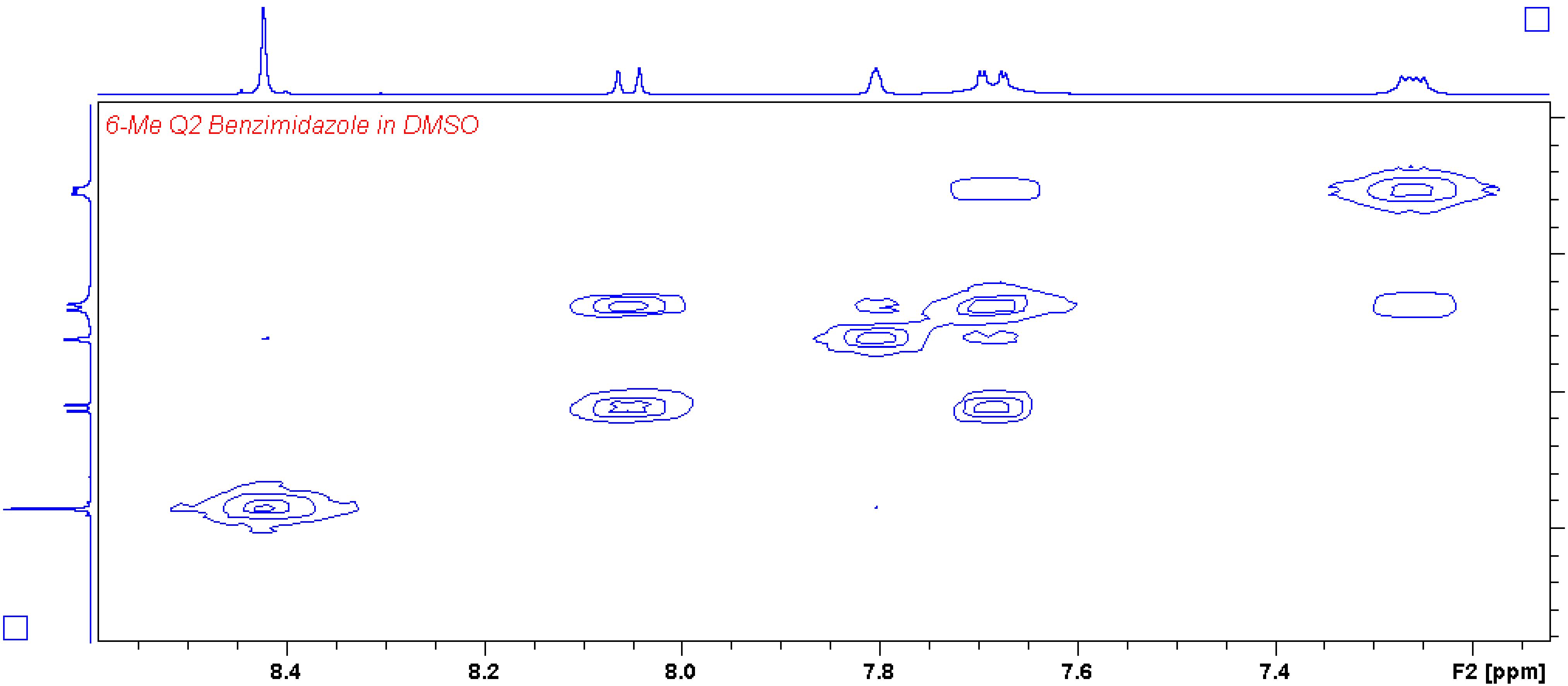
6-Me Q2 Benzimidazole in DMSO
F1 [ppm]
7.5
8.0
8.5
8.4
8.2
8.0
7.8
7.6
7.4
F2 [ppm]

COSY of **A5k**

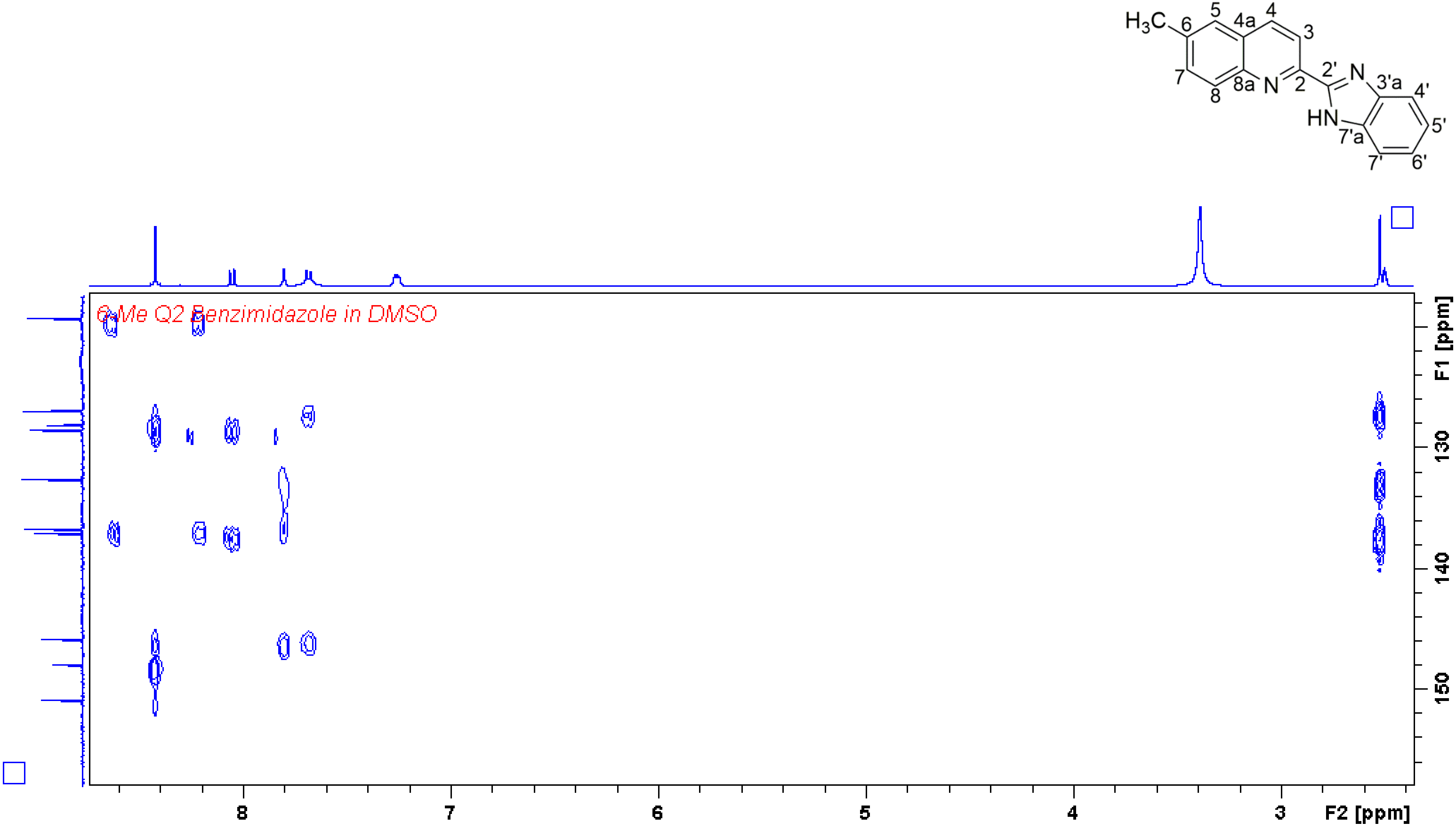

HMBC of **A5k**

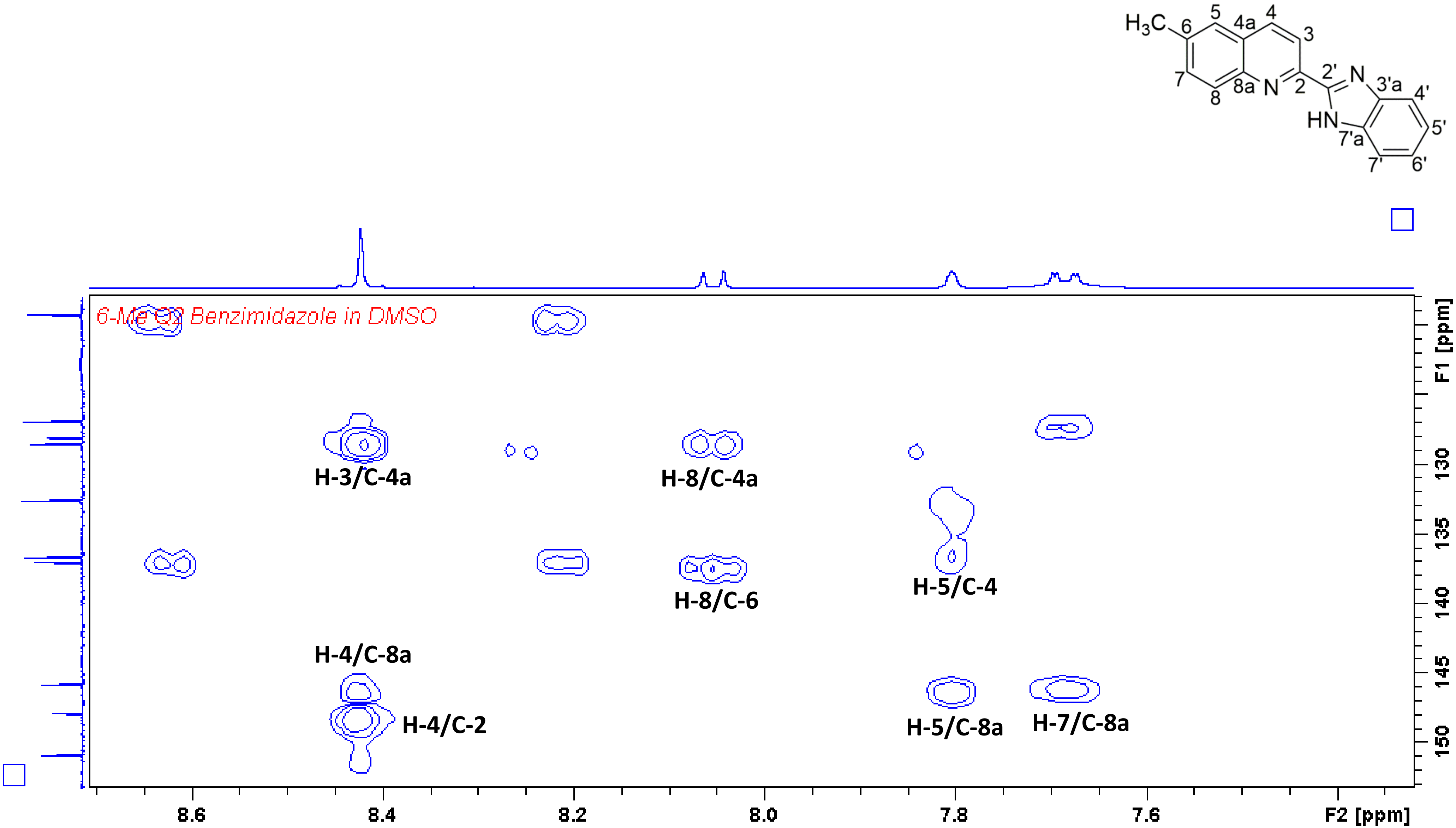

Expanded HMBC of **A5k**

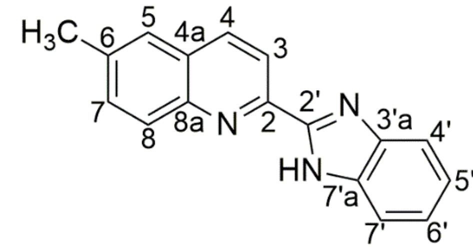

Elemental Composition Report

Single Mass Analysis

Tolerance = 5.0 PPM / DBE: min = -1.5, max = 100.0
Element prediction: Off
Number of isotope peaks used for i-FIT = 3

Monoisotopic Mass, Even Electron Ions
3 formula(e) evaluated with 1 results within limits (up to 20 closest results for each mass)
Elements Used:
C: 15-20 H: 10-15 N: 0-5
SSQB 11 52 (1.721) Cm (1:61)
TOF MS ES+

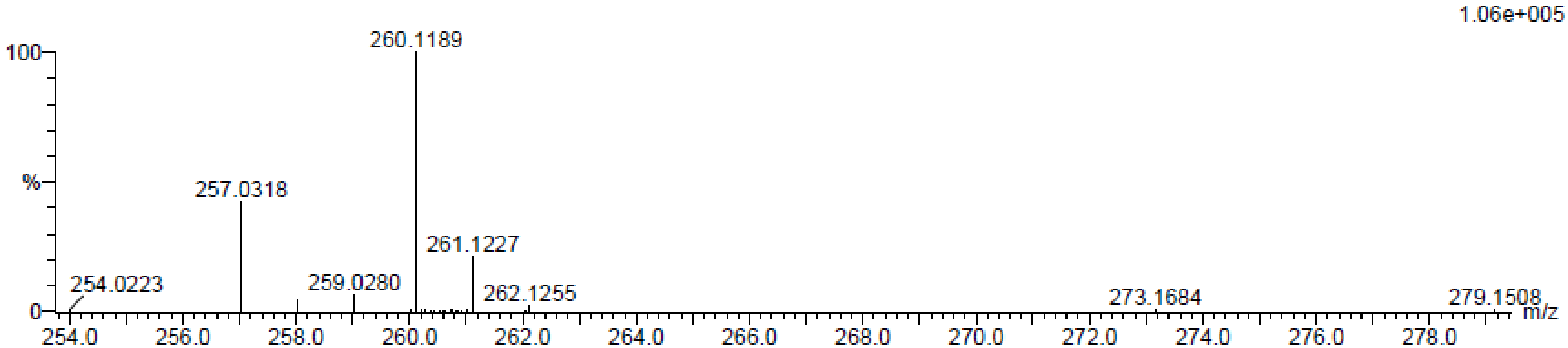

Minimum:				-1.5			
Maximum:		5.0	5.0	100.0			
Mass	Calc. Mass	mDa	PPM	DBE	i-FIT	i-FIT (Norm)	Formula
260.1189	260.1188	0.1	0.4	12.5	184.1	0.0	C17 H14 N3

High resolution mass spectrum of **A5k**

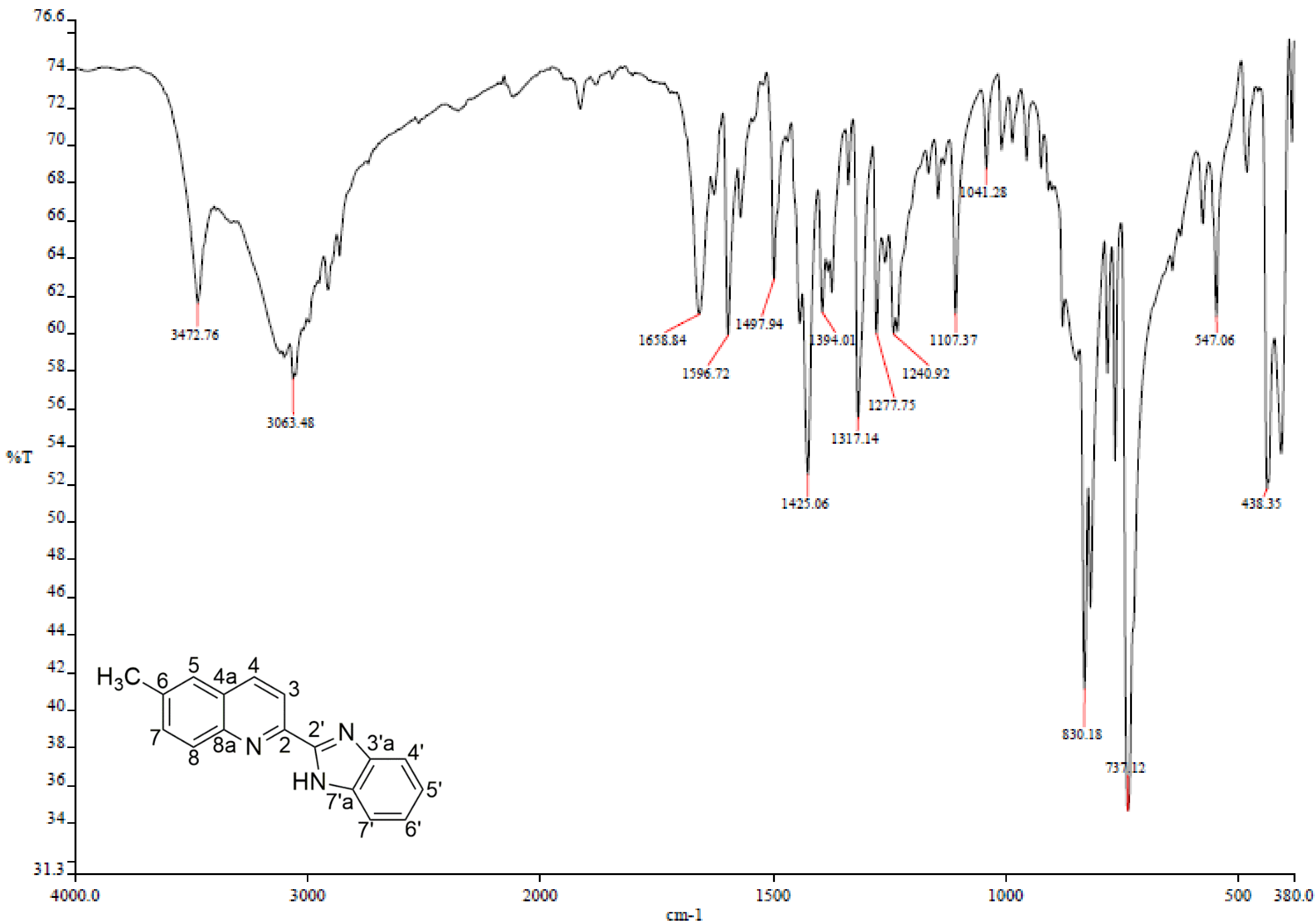

FTIR spectrum of **A5k**

Overlay Spectrum Graph Report

03/08/2017 03:11:02 PM

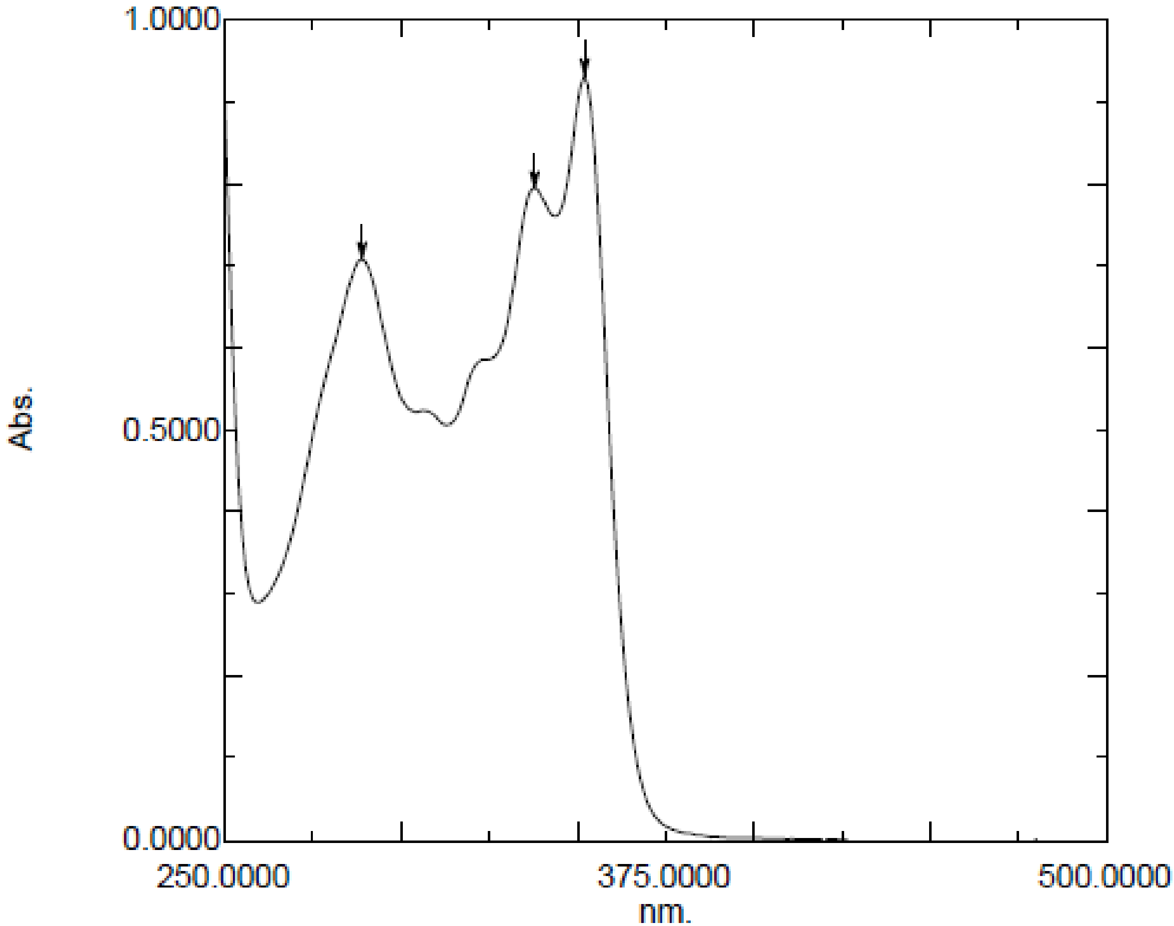

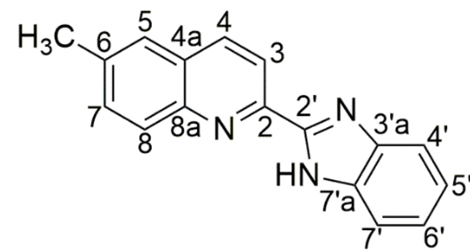

λ	absorbance	logε
289	0.7079	4.56
306	0.5232	4.43
323	0.5854	4.48
338	0.7951	4.61
352	0.9313	4.68

UV spectrum of **A5k**

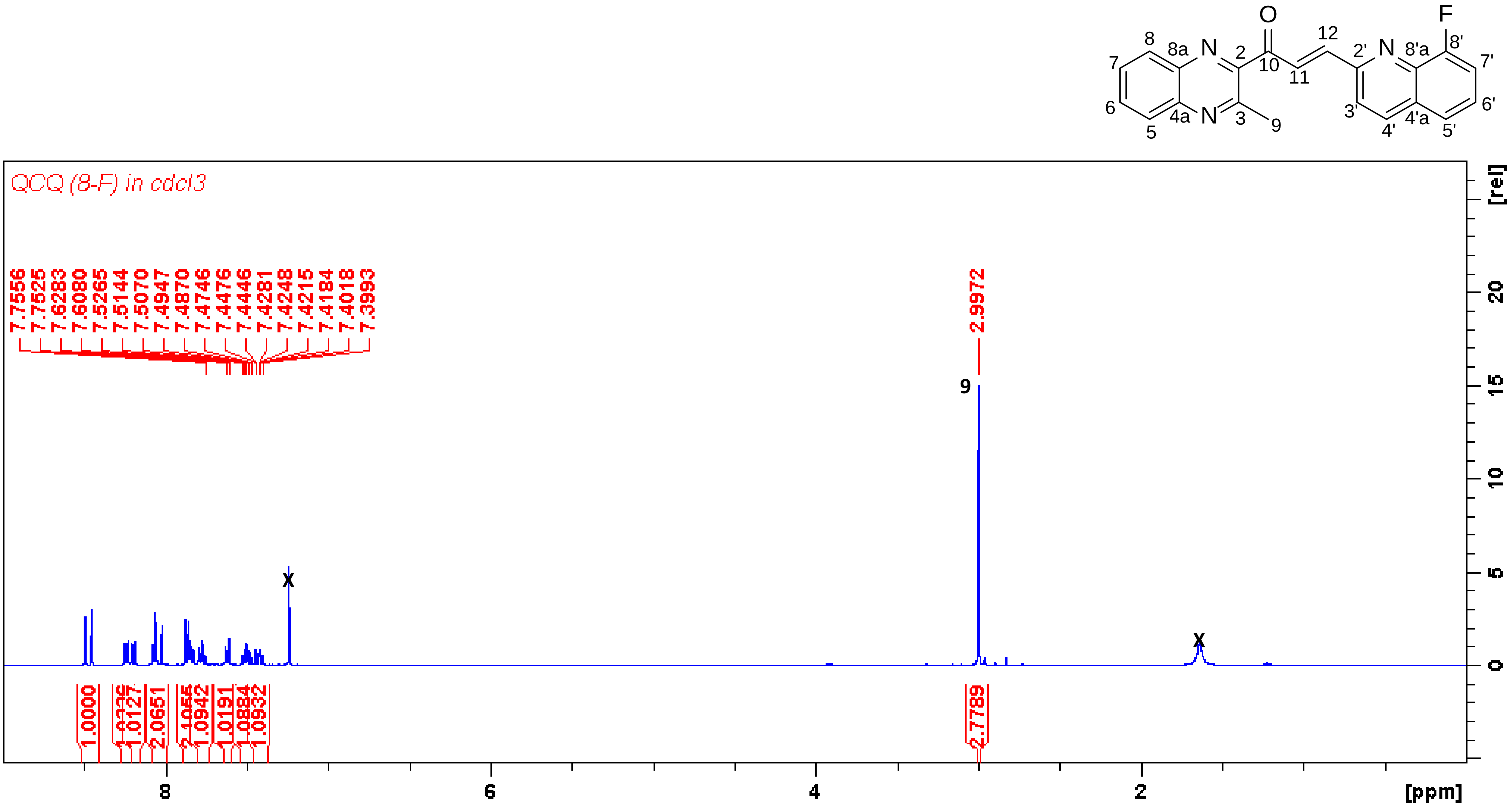

^{1}H NMR spectrum of **B7a**

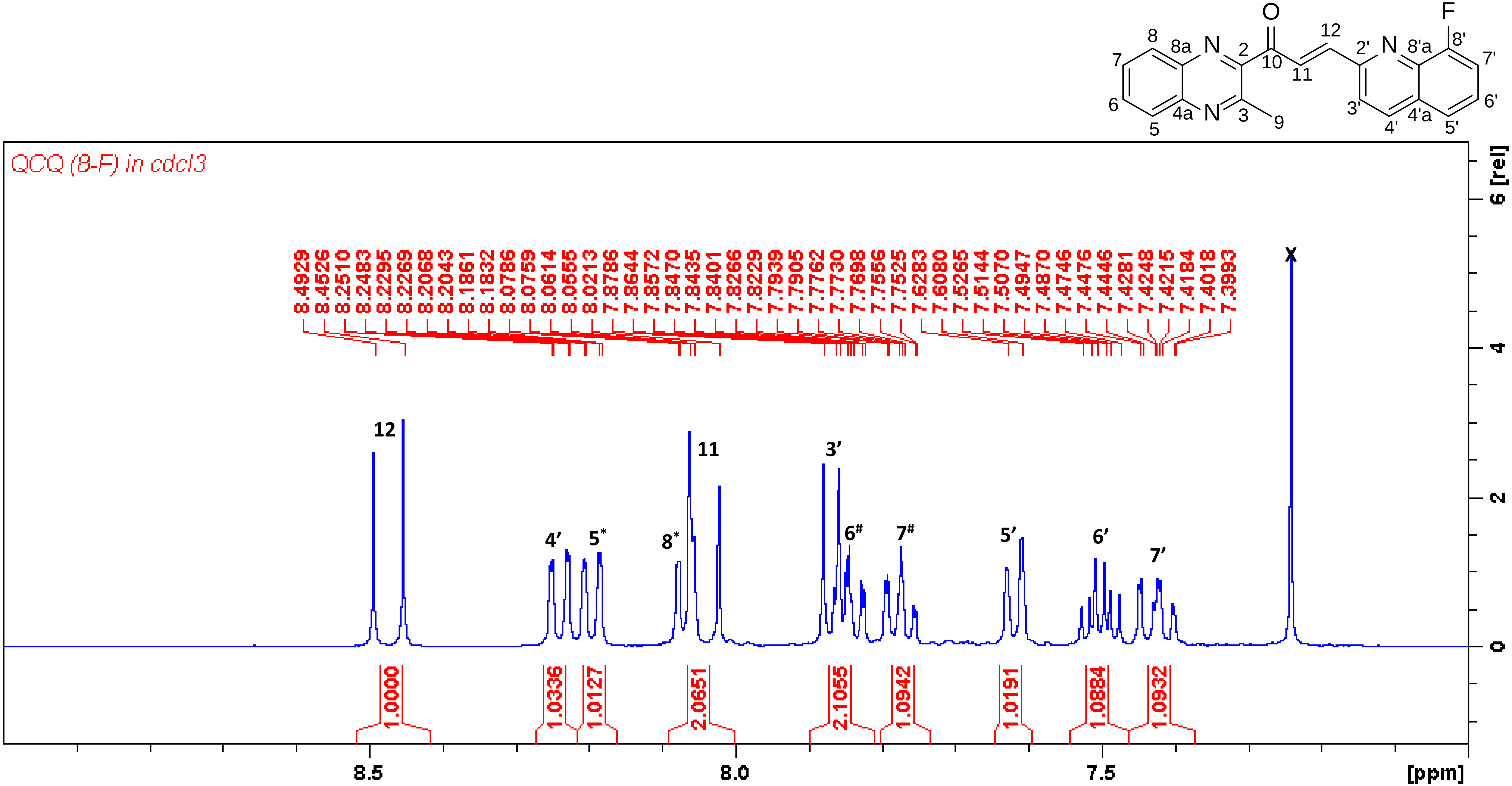

*, # Indicates assignments are interchangeable

Expanded ^{1}H NMR spectrum of **B7a**

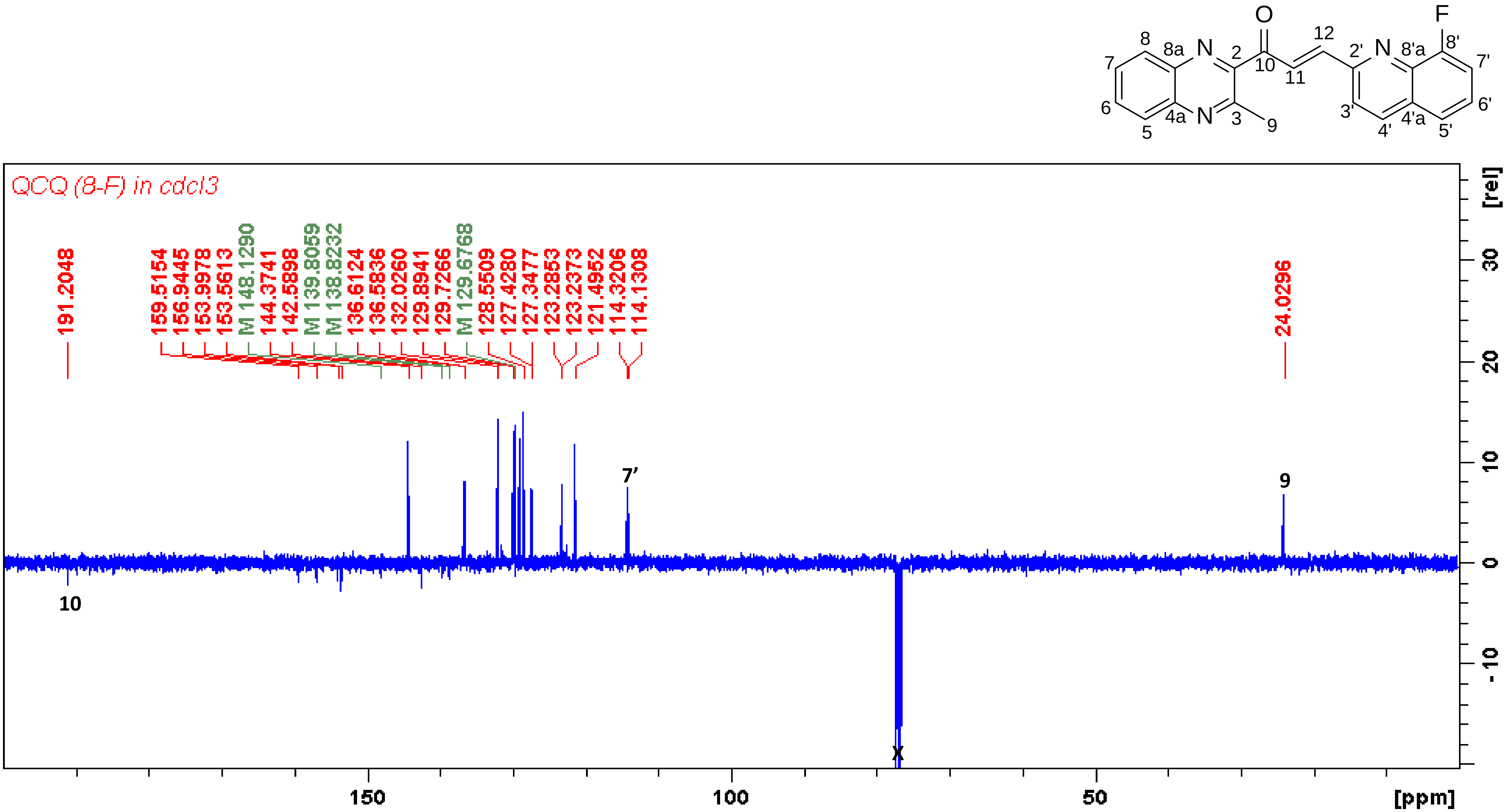

^{13}C NMR spectrum of **B7a**

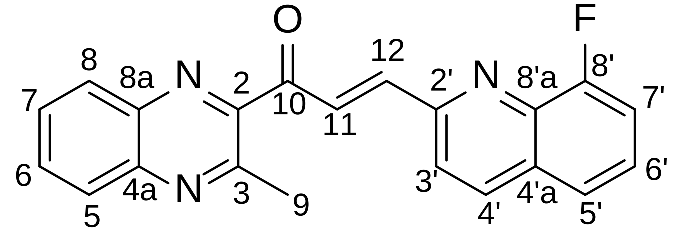

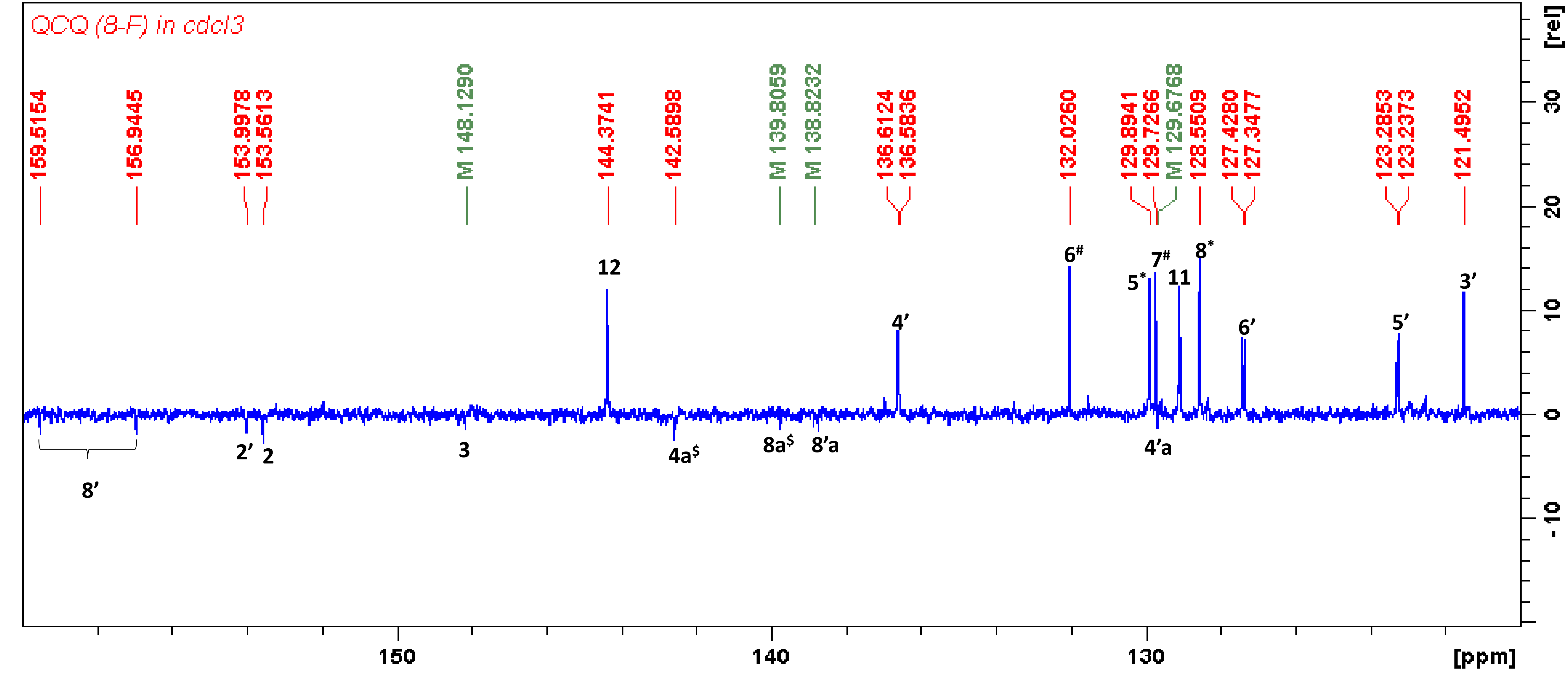

*, #, $ Indicates assignments are interchangeable

Expanded ^{13}C NMR spectrum of **B7a**

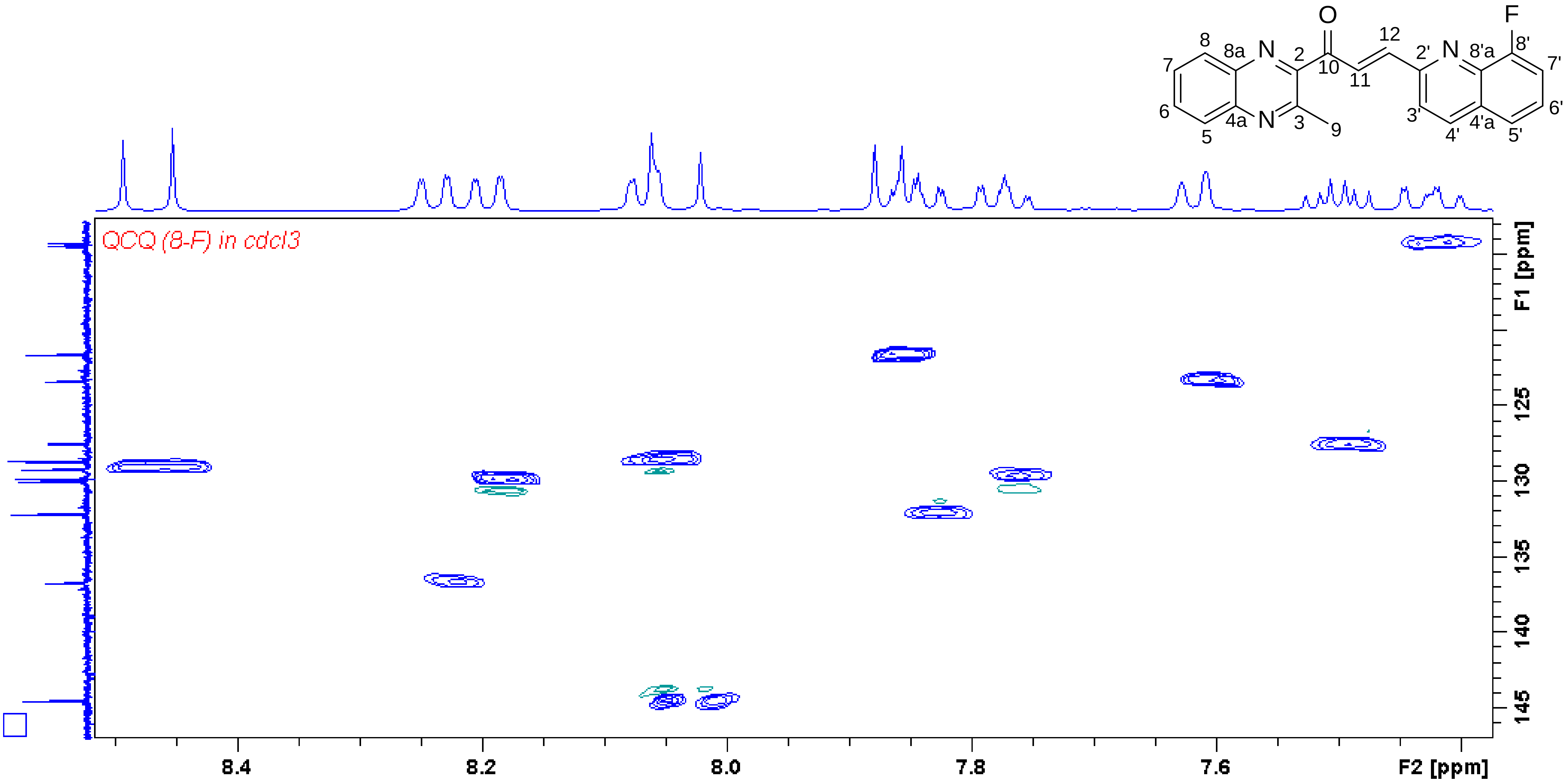

HSQC of **B7a**

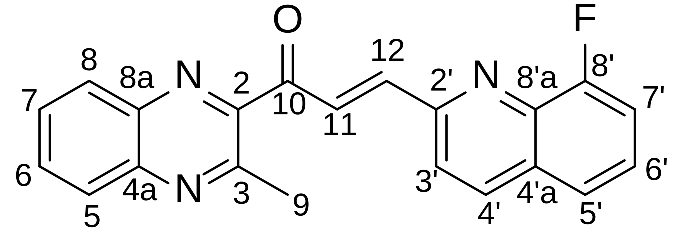
O
F
8
8a
N
2
12
2'
N
8'a
8'
7
10
11
7'
6
3'
6'
4a
N
3
9
4'
4'a
5'
5

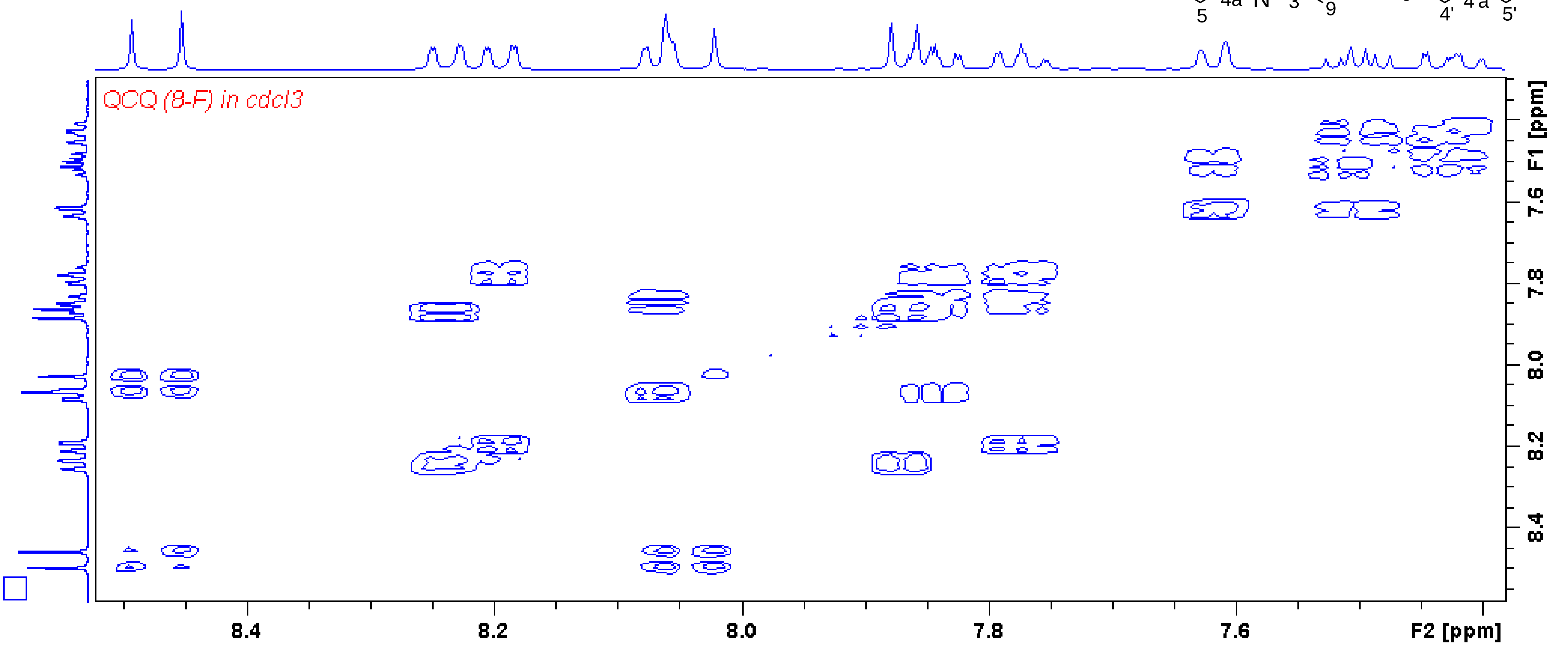
QCQ (8-F) in cdcl3
F1 [ppm]
7.6
7.8
8.0
8.2
8.4
8.4
8.2
8.0
7.8
7.6
F2 [ppm]

COSY of **B7a**

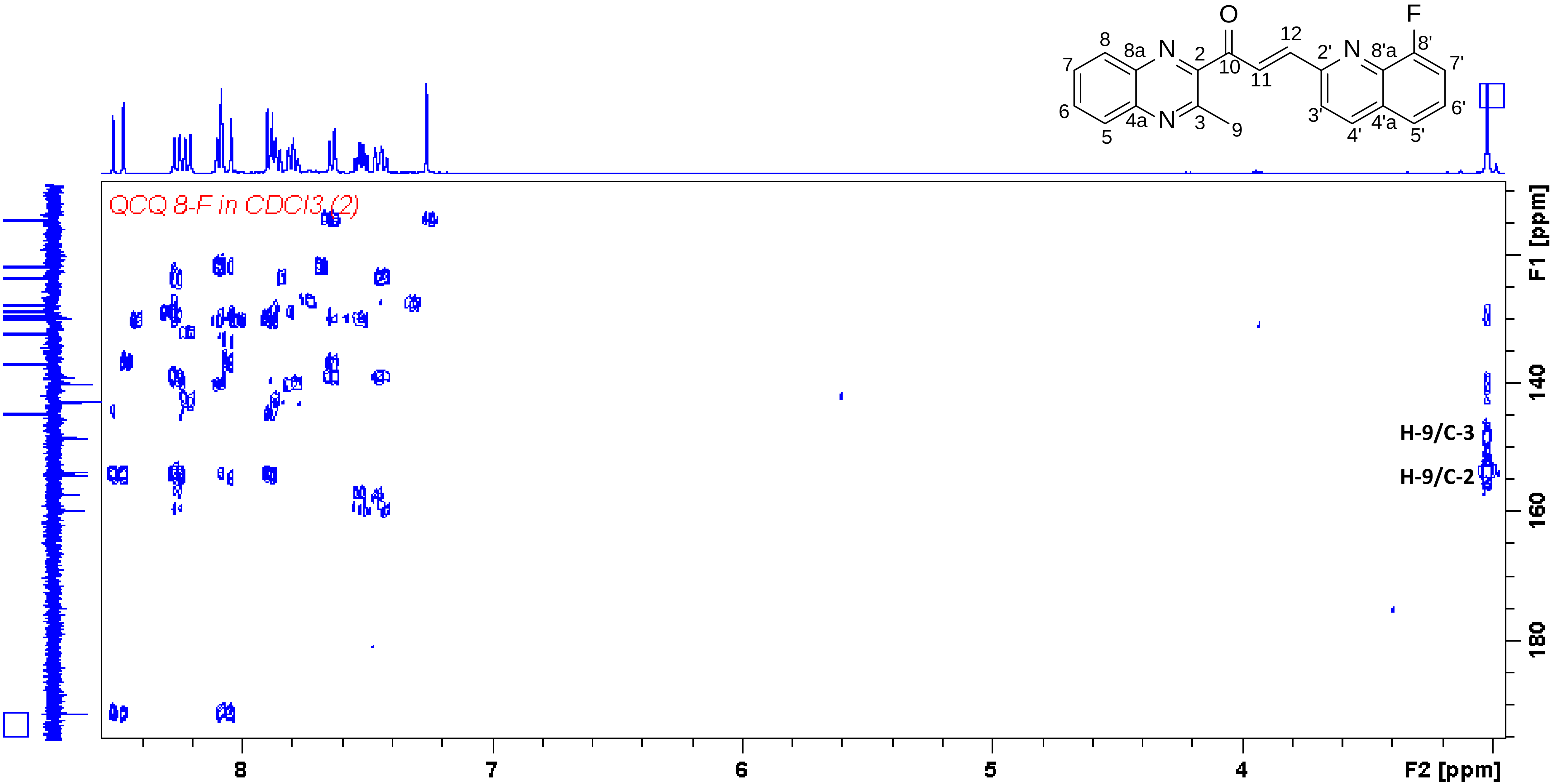
QCQ 8-F in CDCl3 (2)
H-9/C-3
H-9/C-2
F2 [ppm]
F1 [ppm]
8
7
6
5
4
140
160
180
O
F
N
N
N
8
7
6
5
8a
4a
2
3
9
10
11
12
2'
3'
4'
4'a
5'
6'
7'
8'
8'a

HMBC of **B7a**

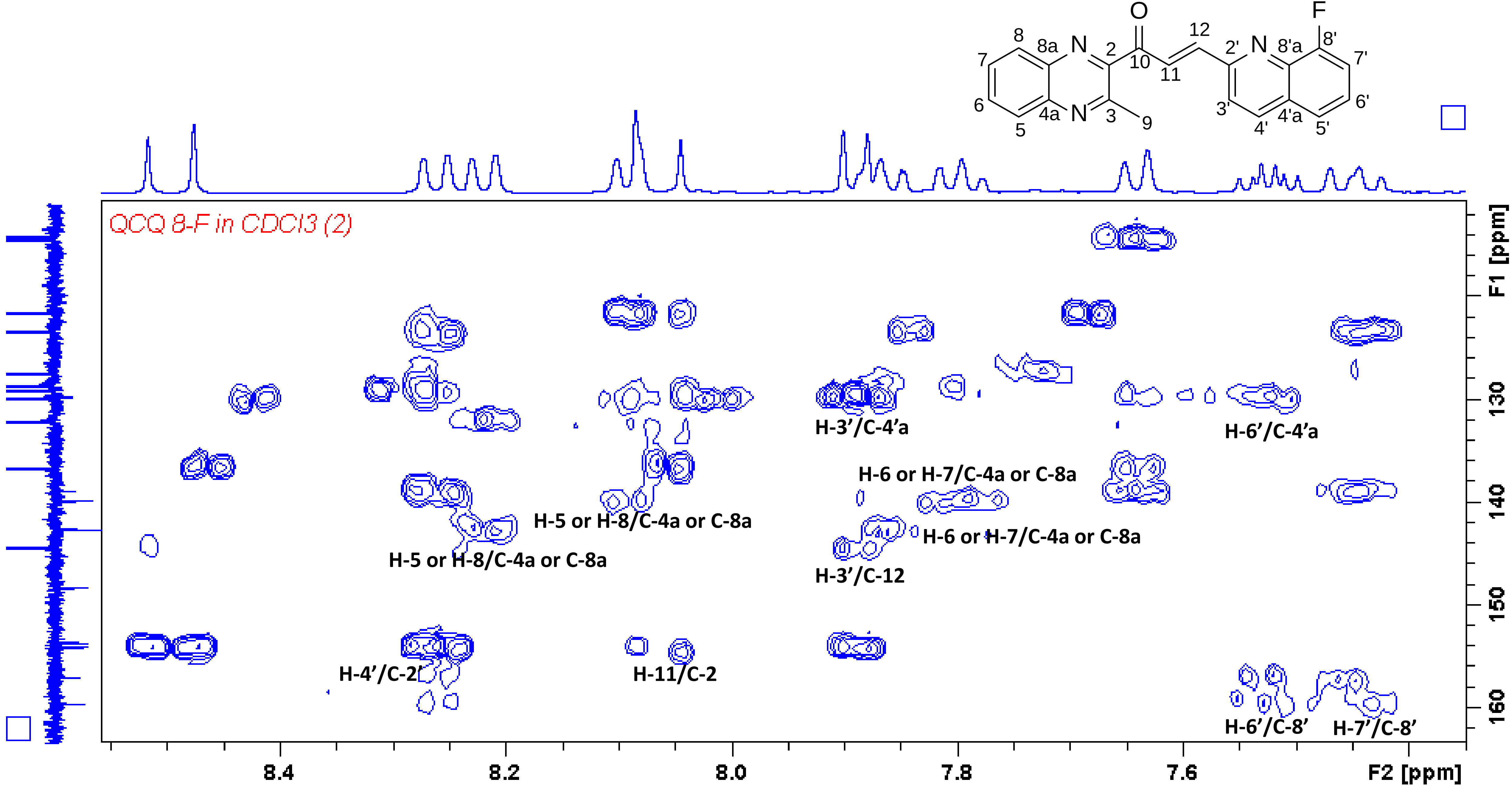

Expanded HMBC of **B7a**

Elemental Composition Report

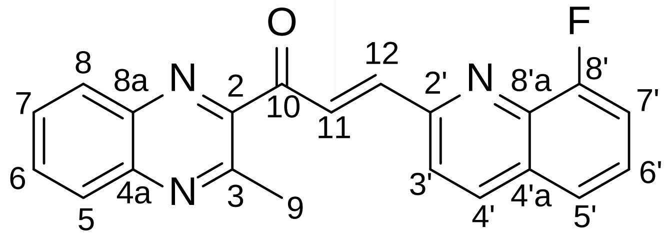

Single Mass Analysis

Tolerance = 5.0 PPM / DBE: min = -1.5, max = 100.0
Element prediction: Off
Number of isotope peaks used for i-FIT = 3

Monoisotopic Mass, Even Electron Ions
35 formula(e) evaluated with 1 results within limits (up to 20 closest results for each mass)
Elements Used:
C: 20-25 H: 10-15 N: 0-5 O: 1-5 F: 0-1
QCQ(8-F) 3 (0.068) Cm (1:61)
TOF MS AP+

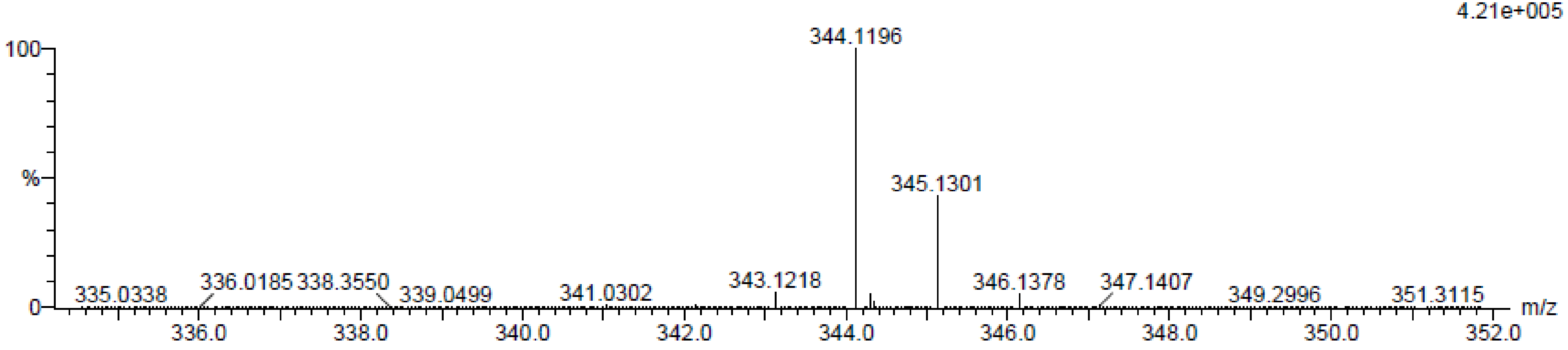

Minimum:				-1.5			
Maximum:		5.0	5.0	100.0			
Mass	Calc. Mass	mDa	PPM	DBE	i-FIT	i-FIT (Norm)	Formula
344.1196	344.1199	-0.3	-0.9	15.5	610.2	0.0	C21 H15 N3 O F

High resolution mass spectrum of **B7a**

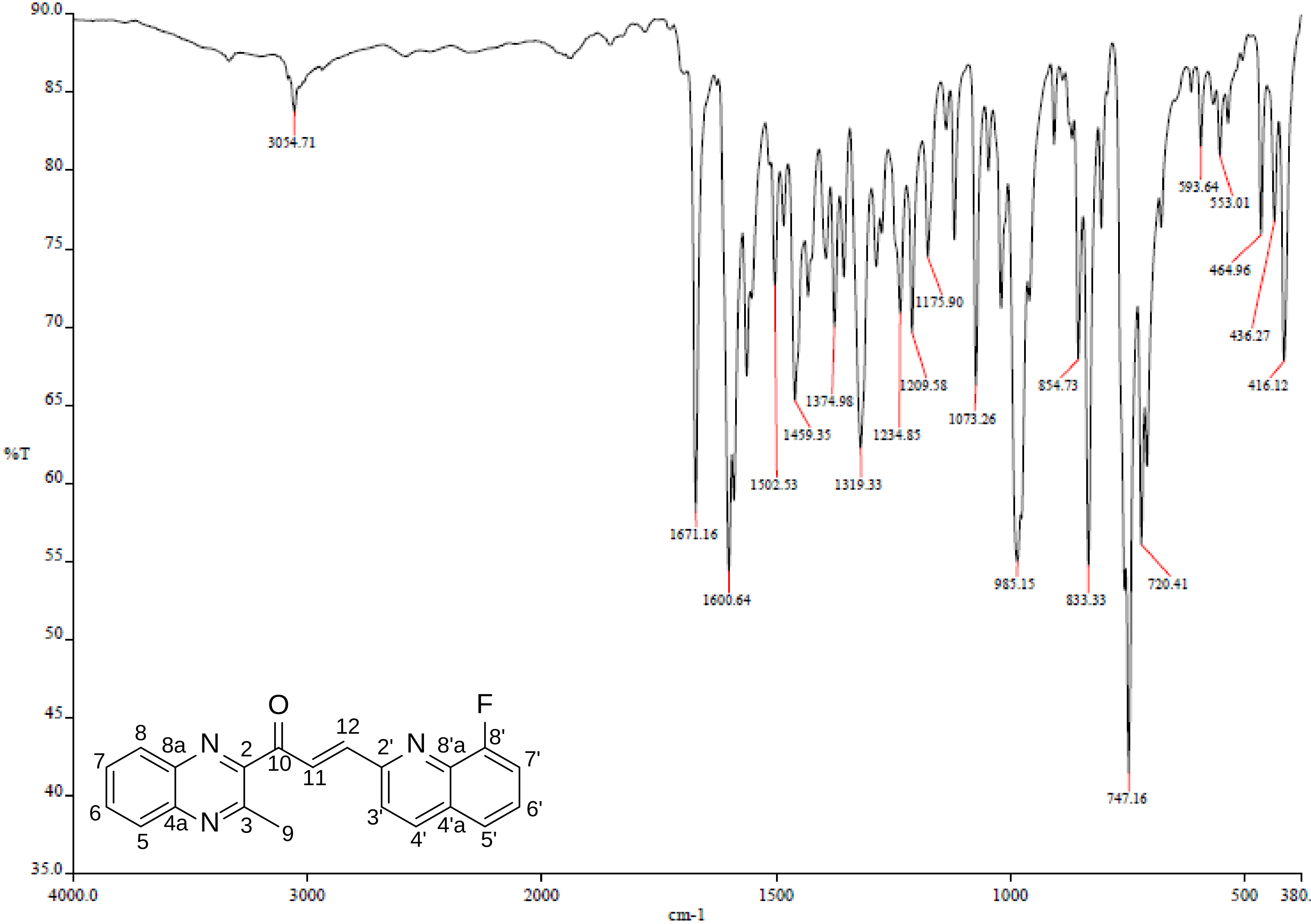

FTIR spectrum of **B7a**

Overlay Spectrum Graph Report

06/10/2017 12:03:32 PM

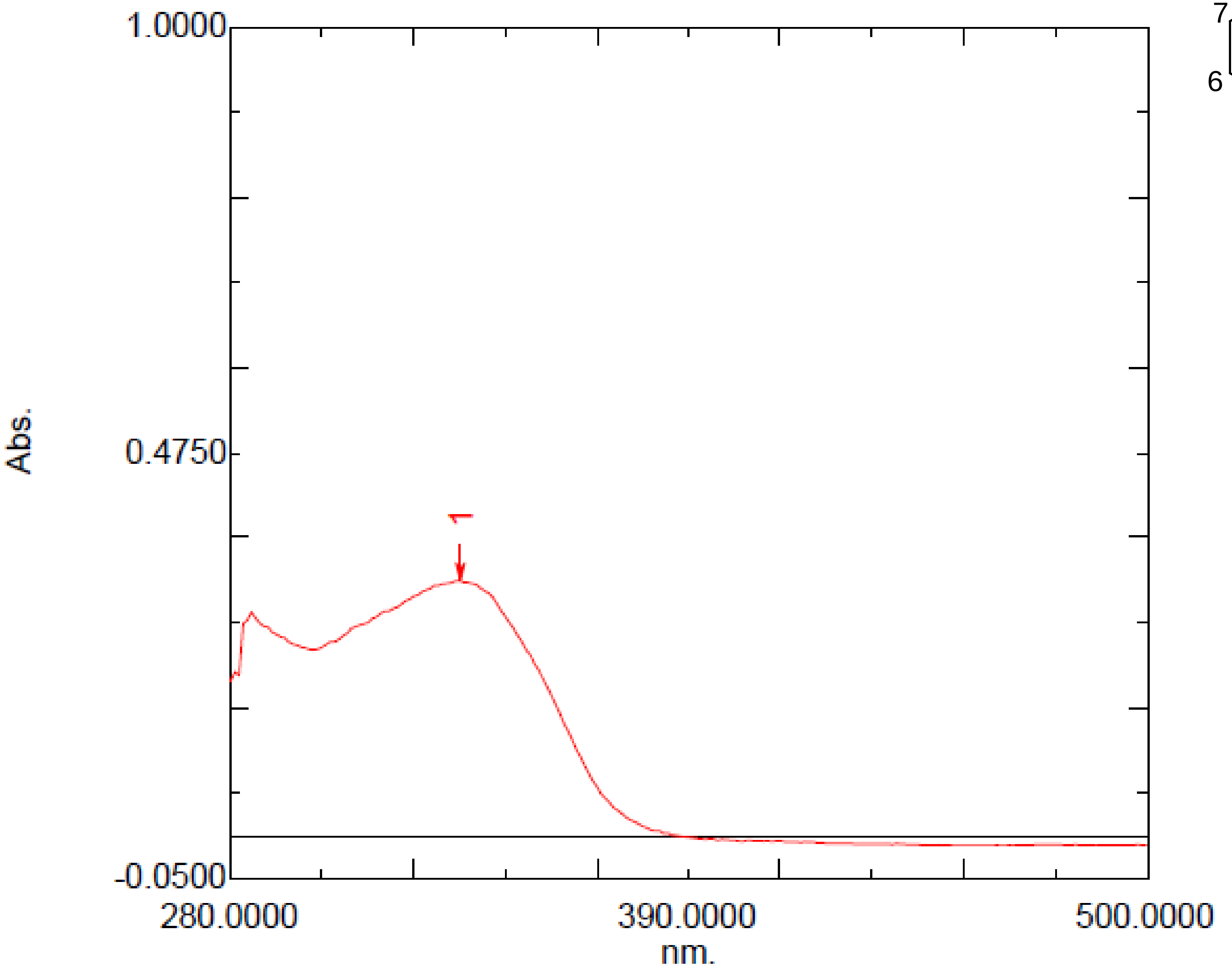

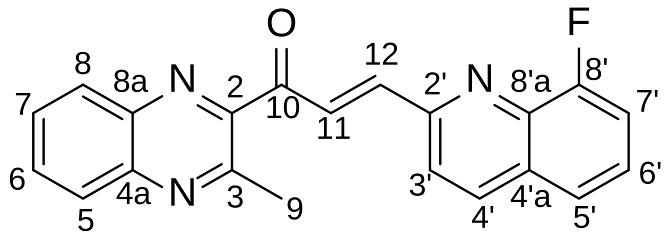

λ	absorbance	logε
335	0.3167	4.34

UV spectrum of **B7a**

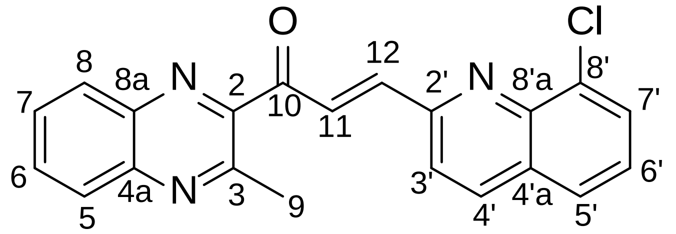

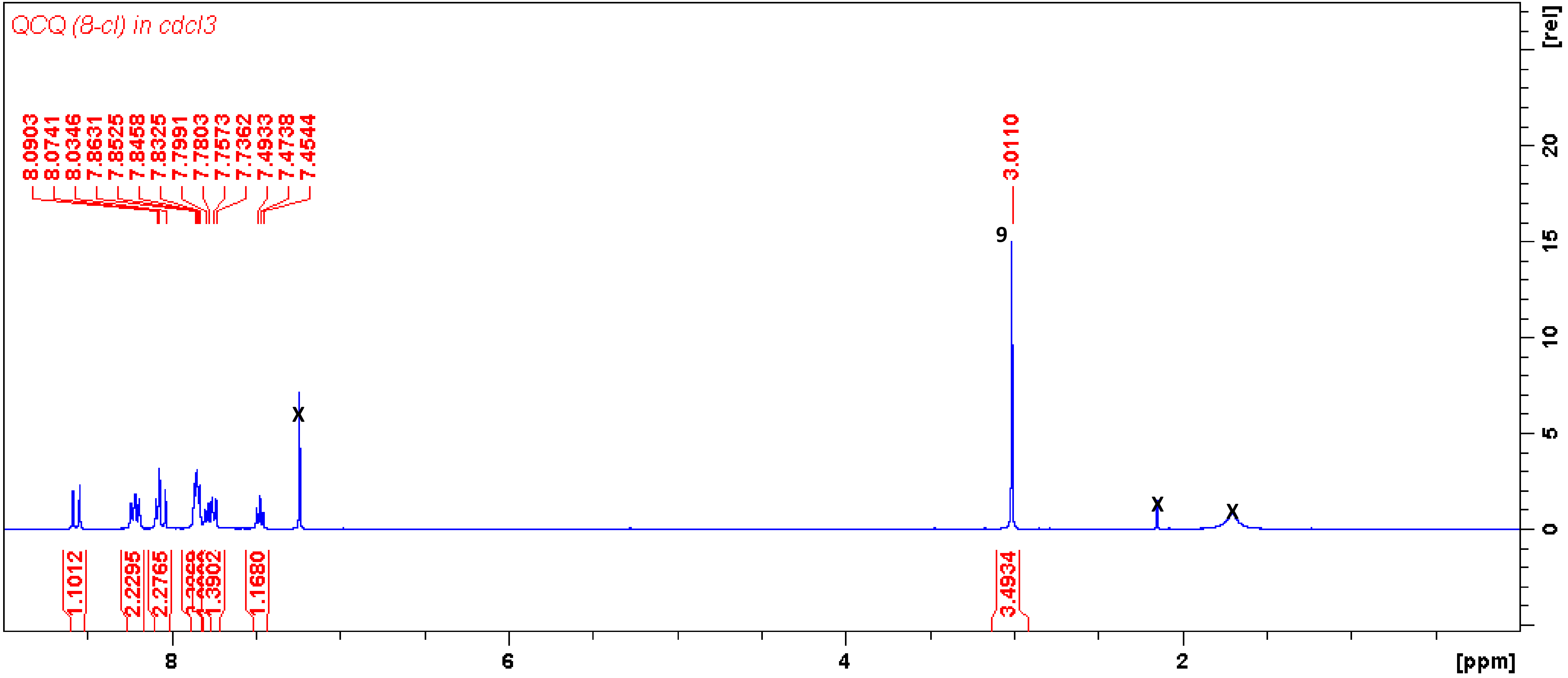

^{1}H NMR spectrum of **B7b**

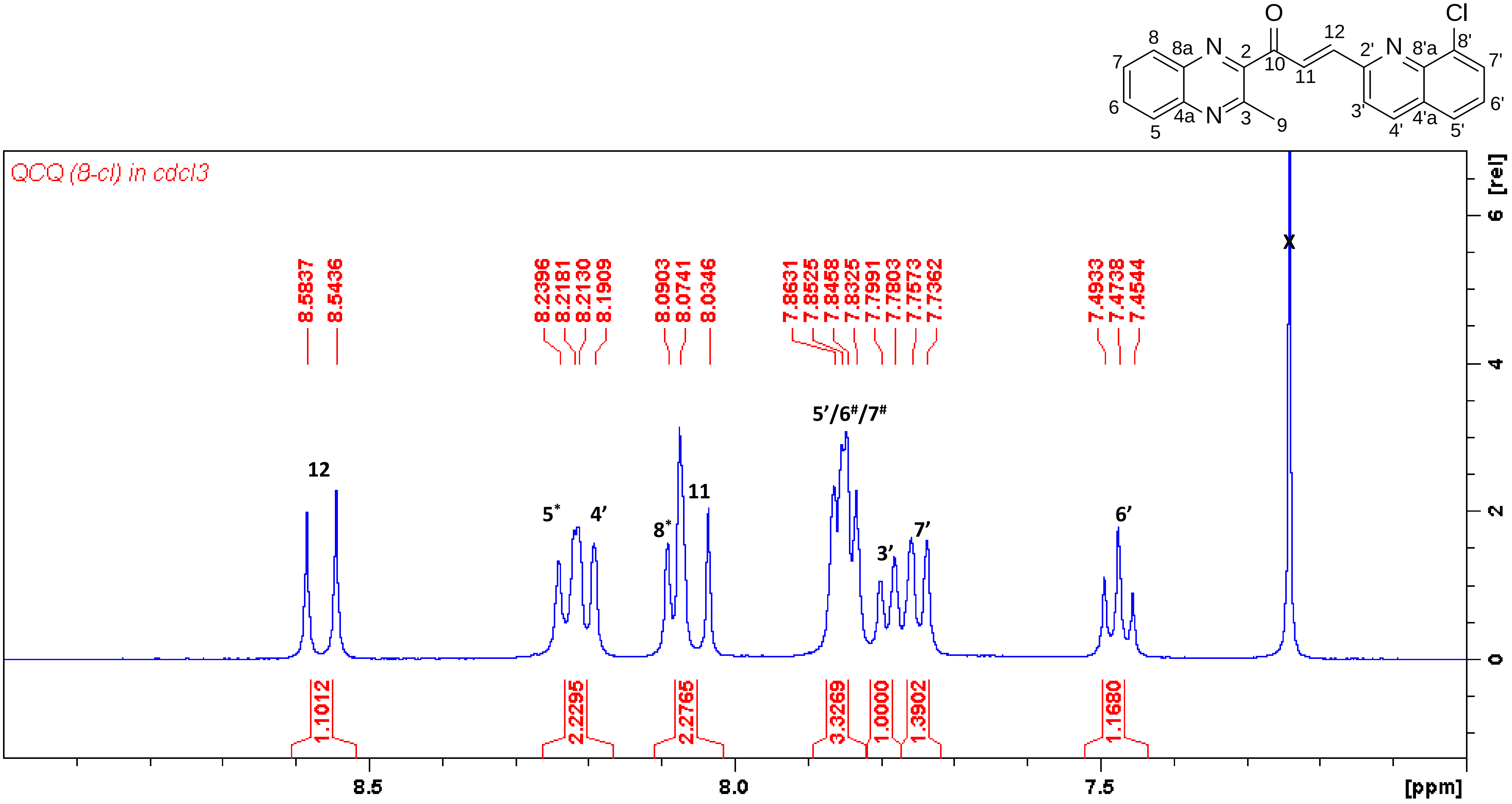

*, # Indicates assignments are interchangeable

Expanded ^{1}H NMR spectrum of **B7b**

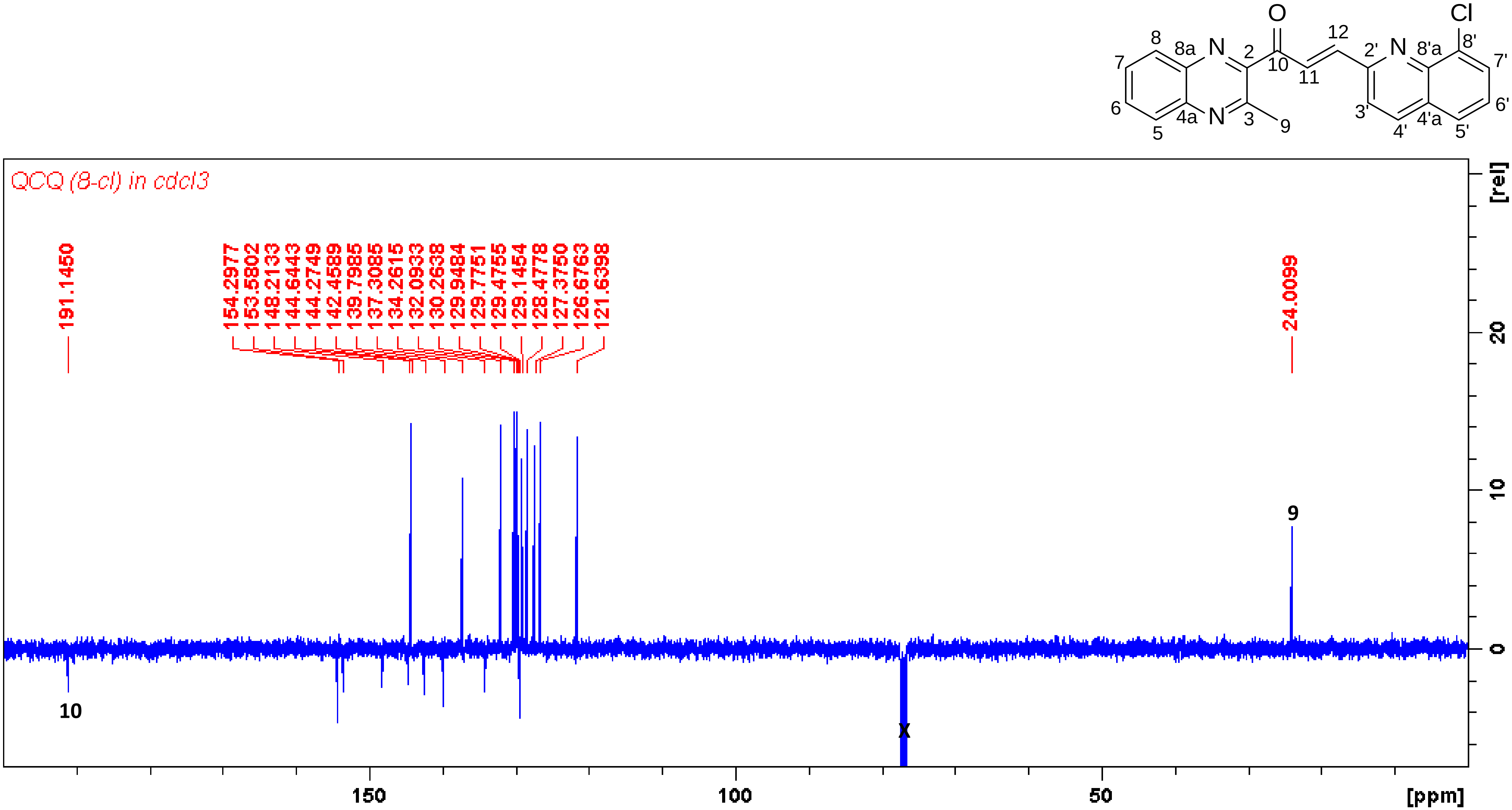

^{13}C NMR spectrum of **B7b**

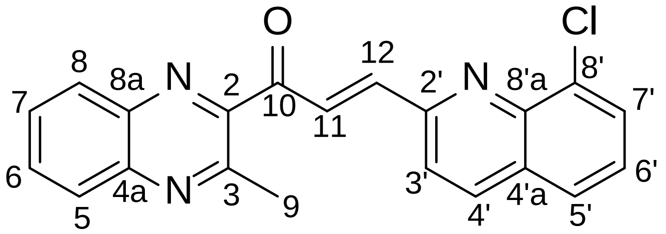

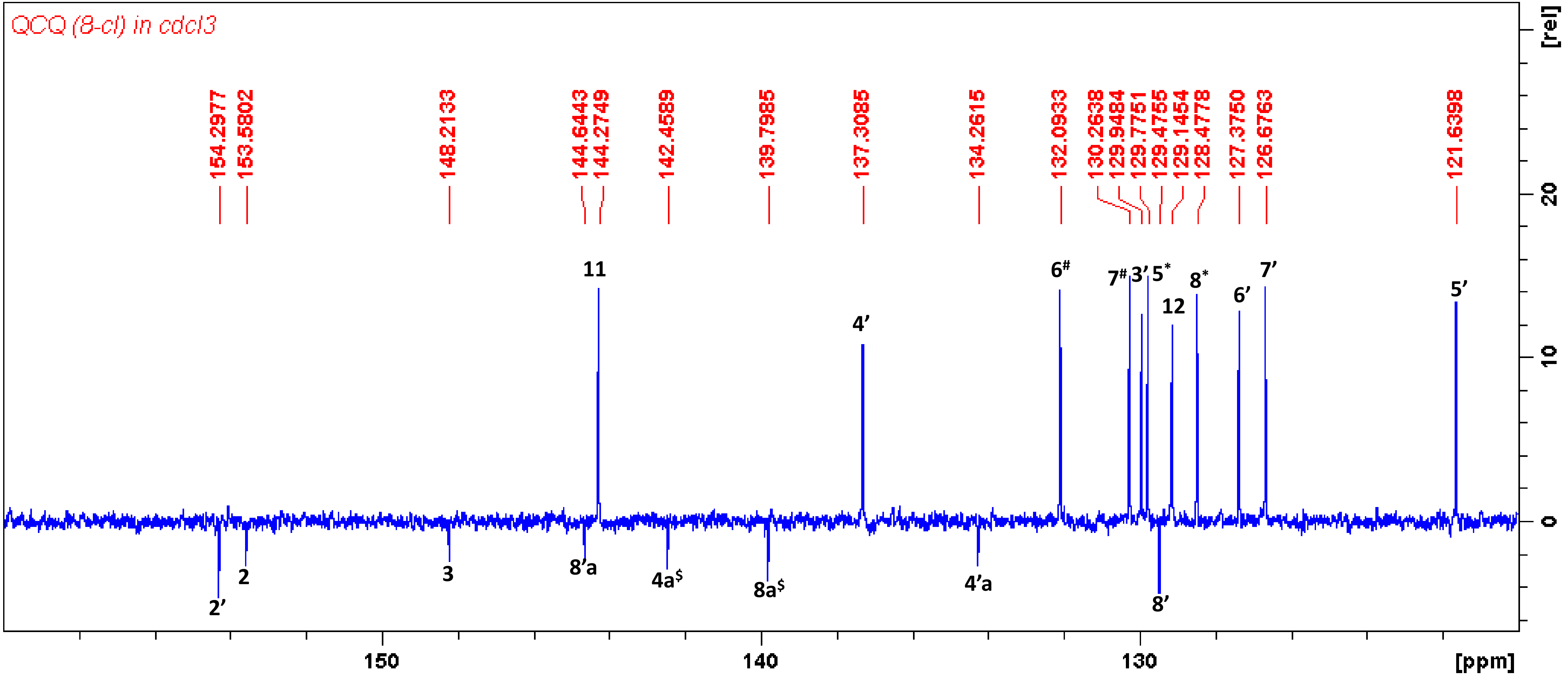

*, #, $ Indicates assignments are interchangeable

Expanded ^{13}C NMR spectrum of **B7b**

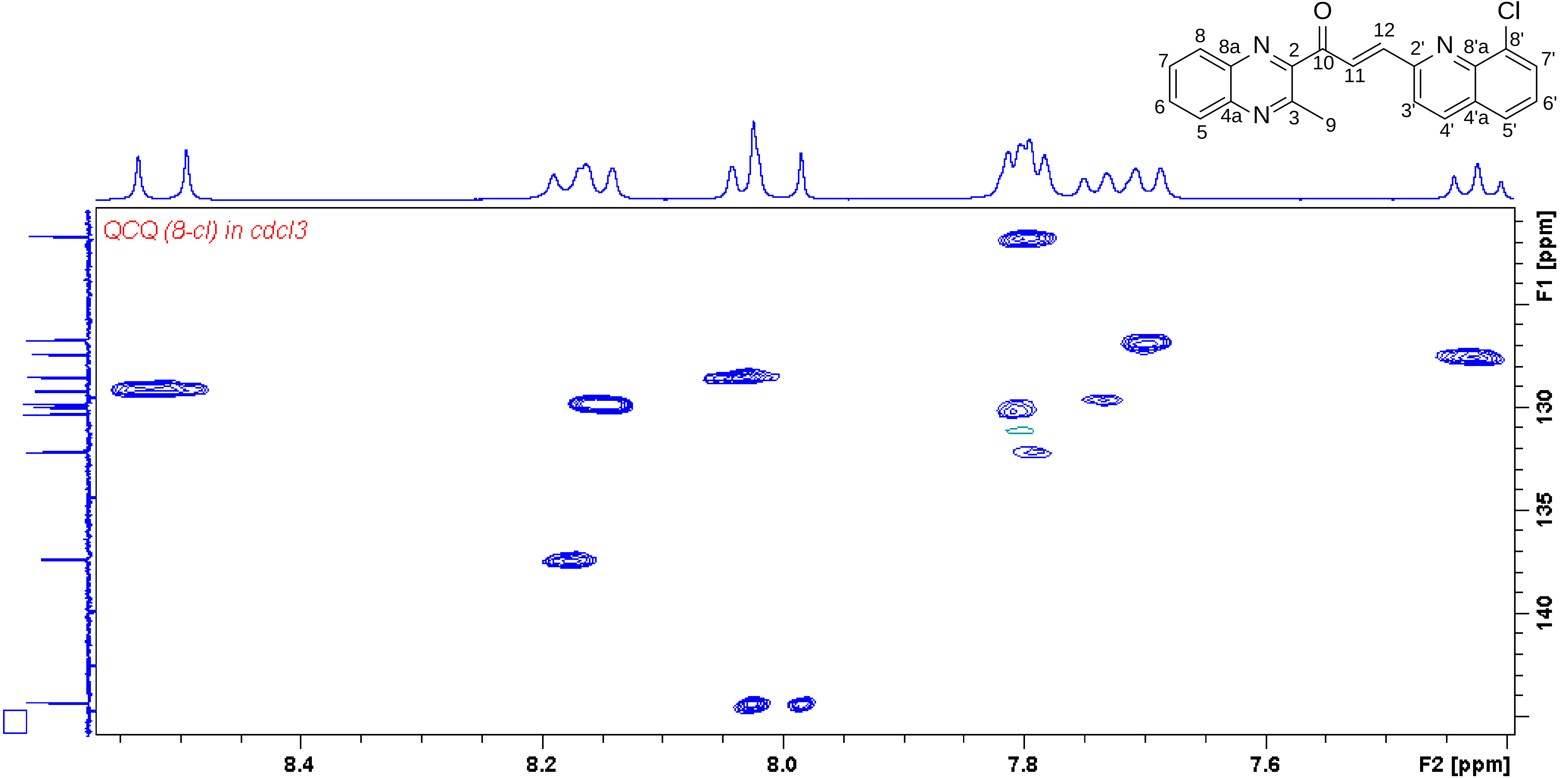

HSQC of **B7b**

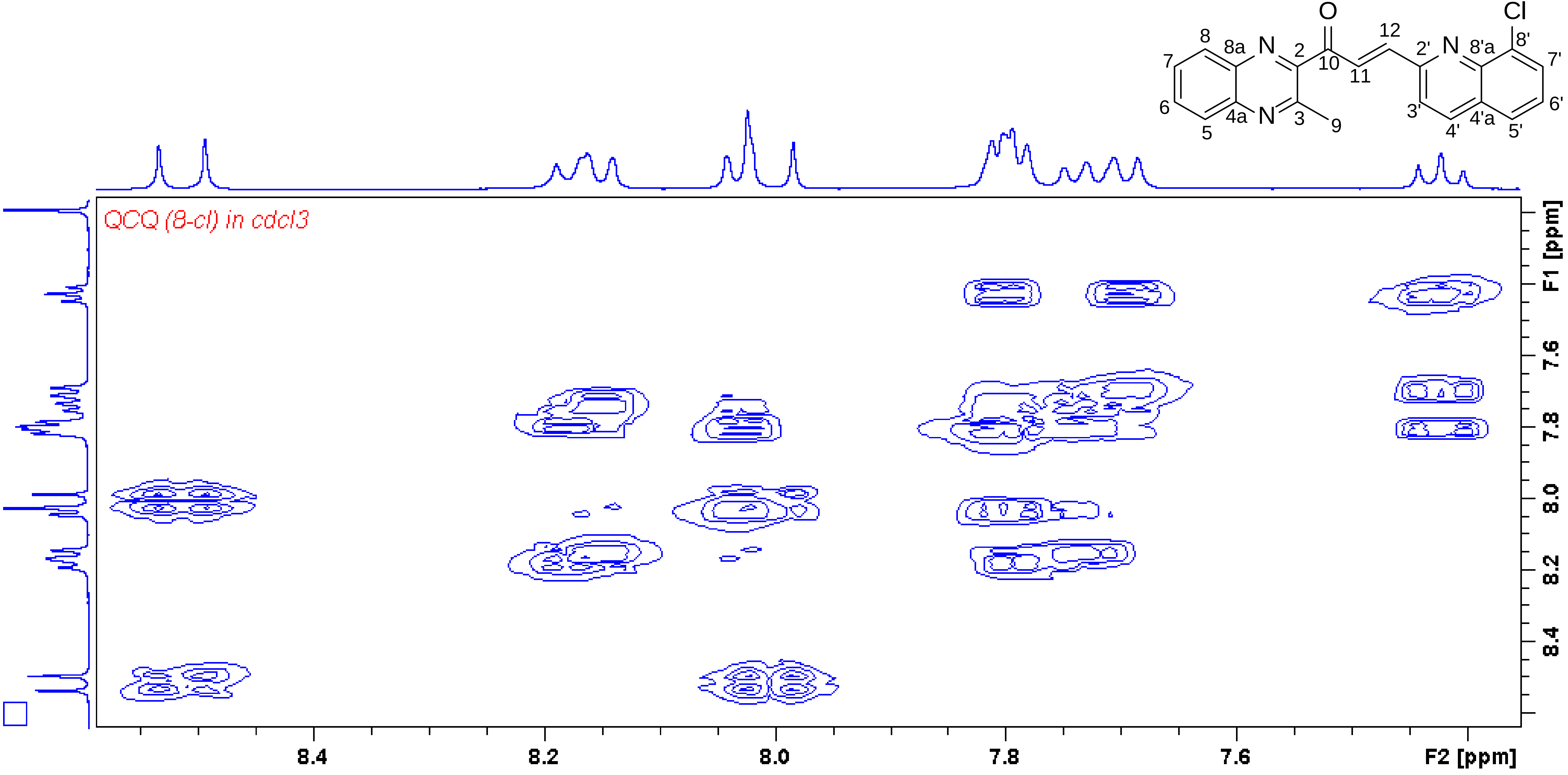
QCQ (8-cl) in cdcl3
F1 [ppm]
F2 [ppm]
8.4
8.2
8.0
7.8
7.6
O
Cl
N
N
N
2
3
4a
5
6
7
8
8a
9
10
11
12
2'
3'
4'
4'a
5'
6'
7'
8'
8'a

COSY of **B7b**

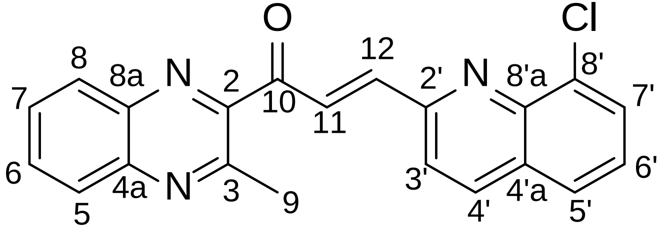

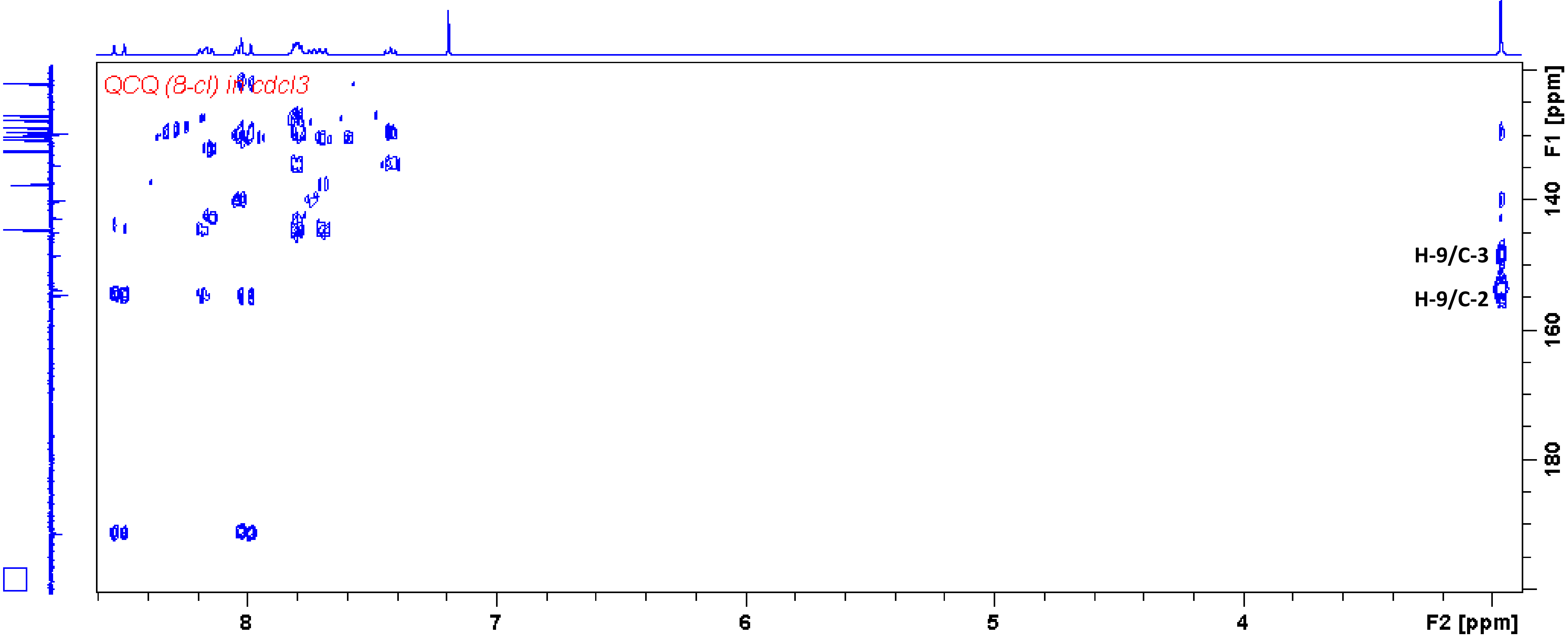

HMBC of **B7b**

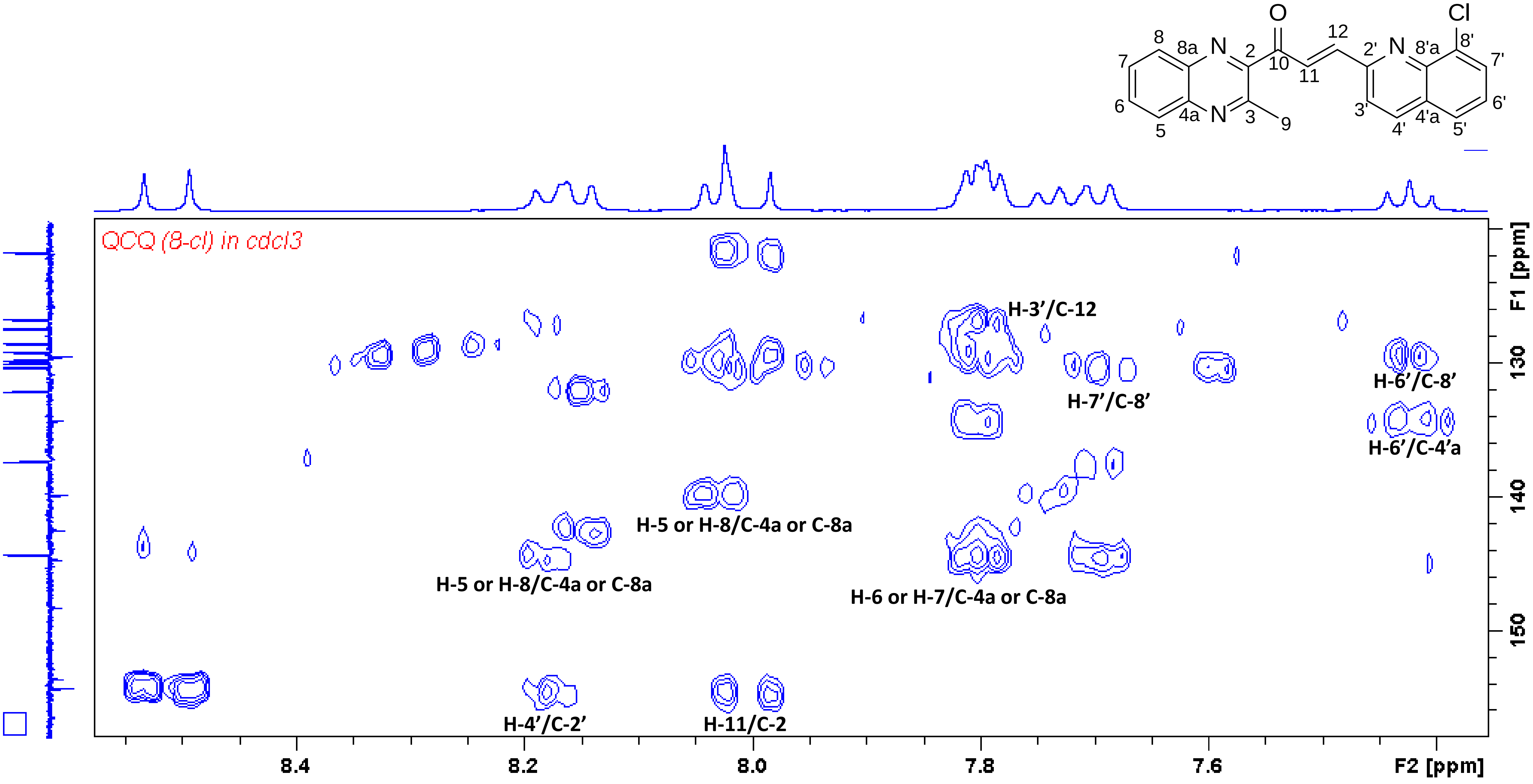

Expanded HMBC of **B7b**

Elemental Composition Report

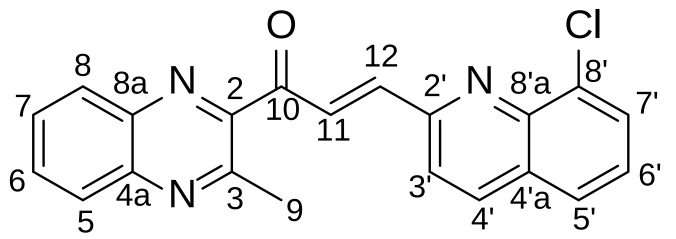

Single Mass Analysis

Tolerance = 5.0 PPM / DBE: min = -1.5, max = 100.0
Element prediction: Off
Number of isotope peaks used for i-FIT = 3

Monoisotopic Mass, Even Electron Ions
22 formula(e) evaluated with 1 results within limits (up to 20 closest results for each mass)
Elements Used:
C: 20-25 H: 10-20 N: 0-5 O: 1-5 Cl: 1-1
QCQ(8-Cl) 11 (0.338) Cm (1:61)
TOF MS AP+

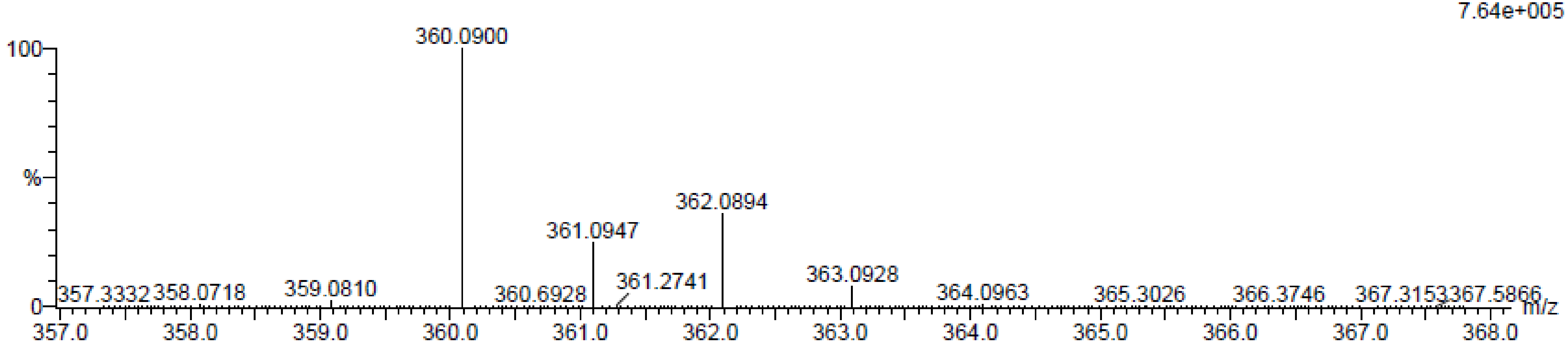

Minimum:				-1.5			
Maximum:		5.0	5.0	100.0			
Mass	Calc. Mass	mDa	PPM	DBE	i-FIT	i-FIT (Norm)	Formula
360.0900	360.0904	-0.4	-1.1	15.5	635.5	0.0	C21 H15 N3 O Cl

High resolution mass spectrum of **B7b**

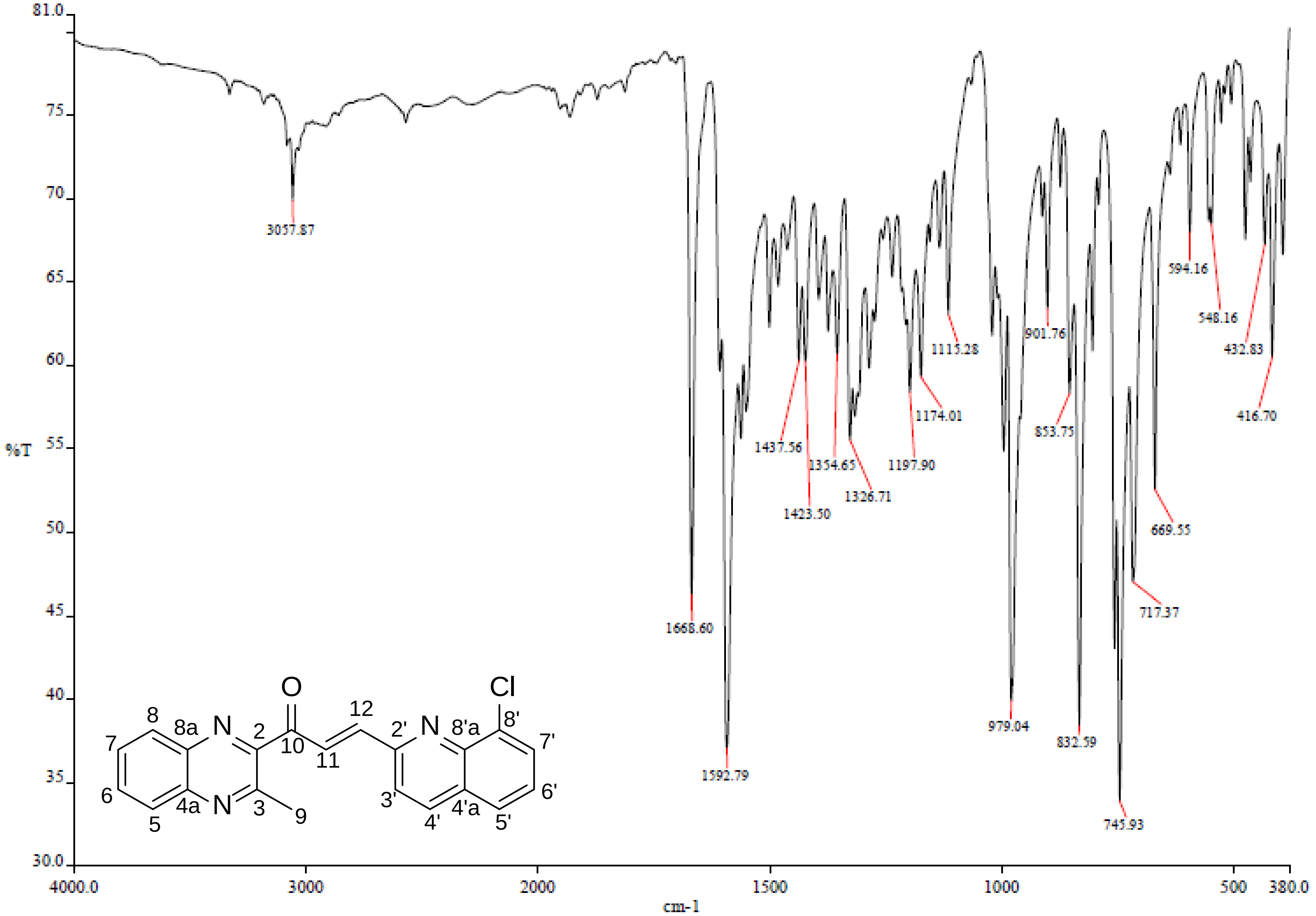

FTIR spectrum of **B7b**

Overlay Spectrum Graph Report

06/10/2017 12:03:01 PM

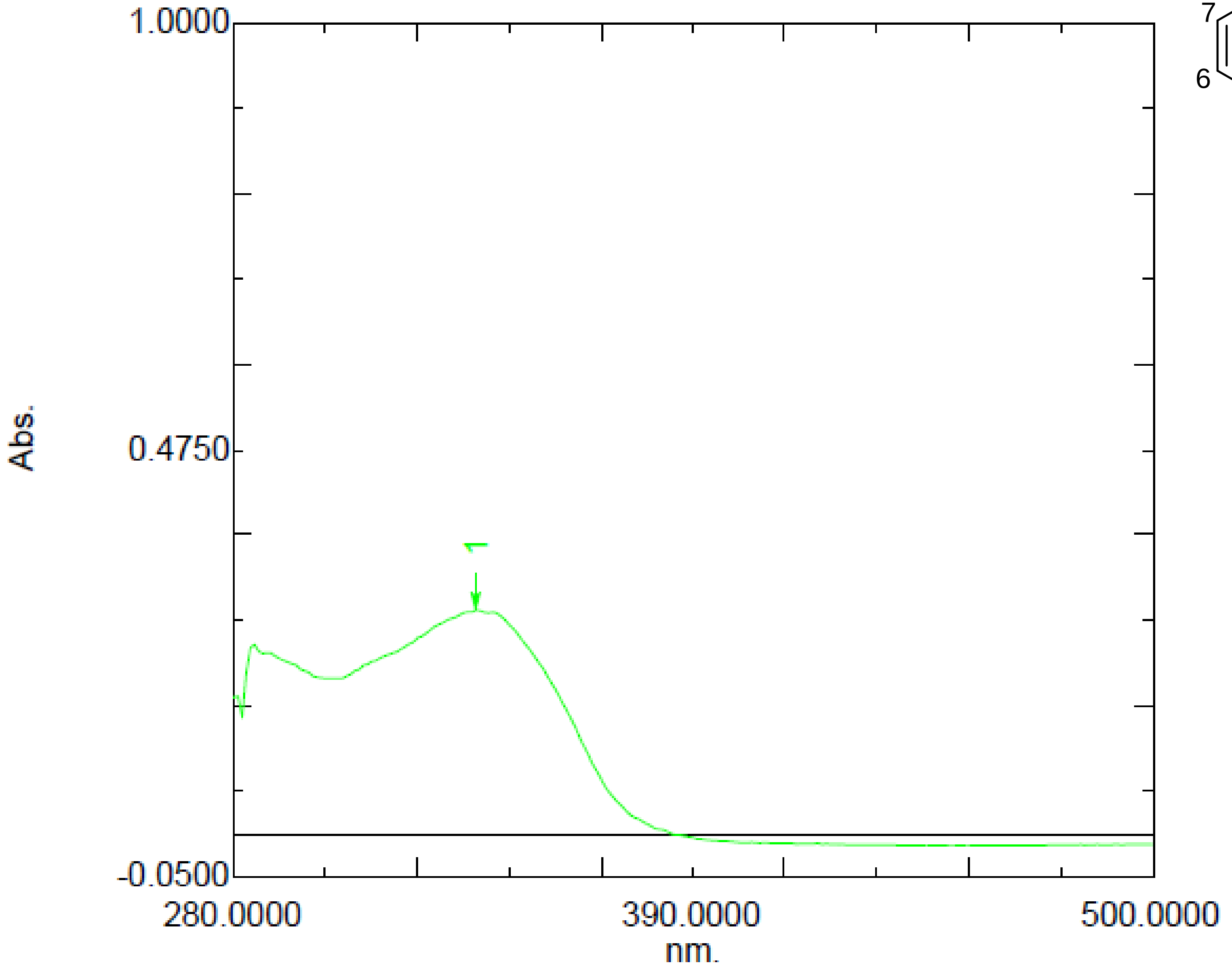

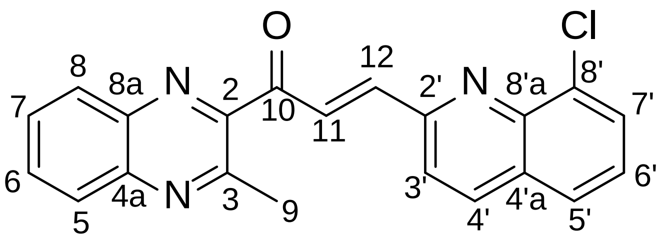

λ	absorbance	logε
338	0.2777	4.30

UV spectrum of **B7b**

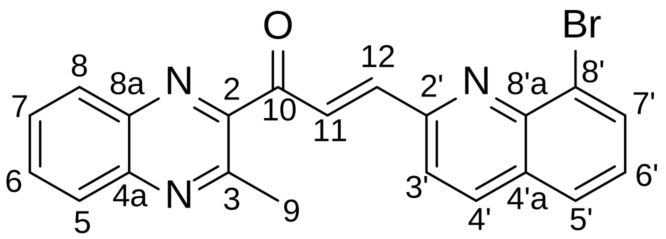

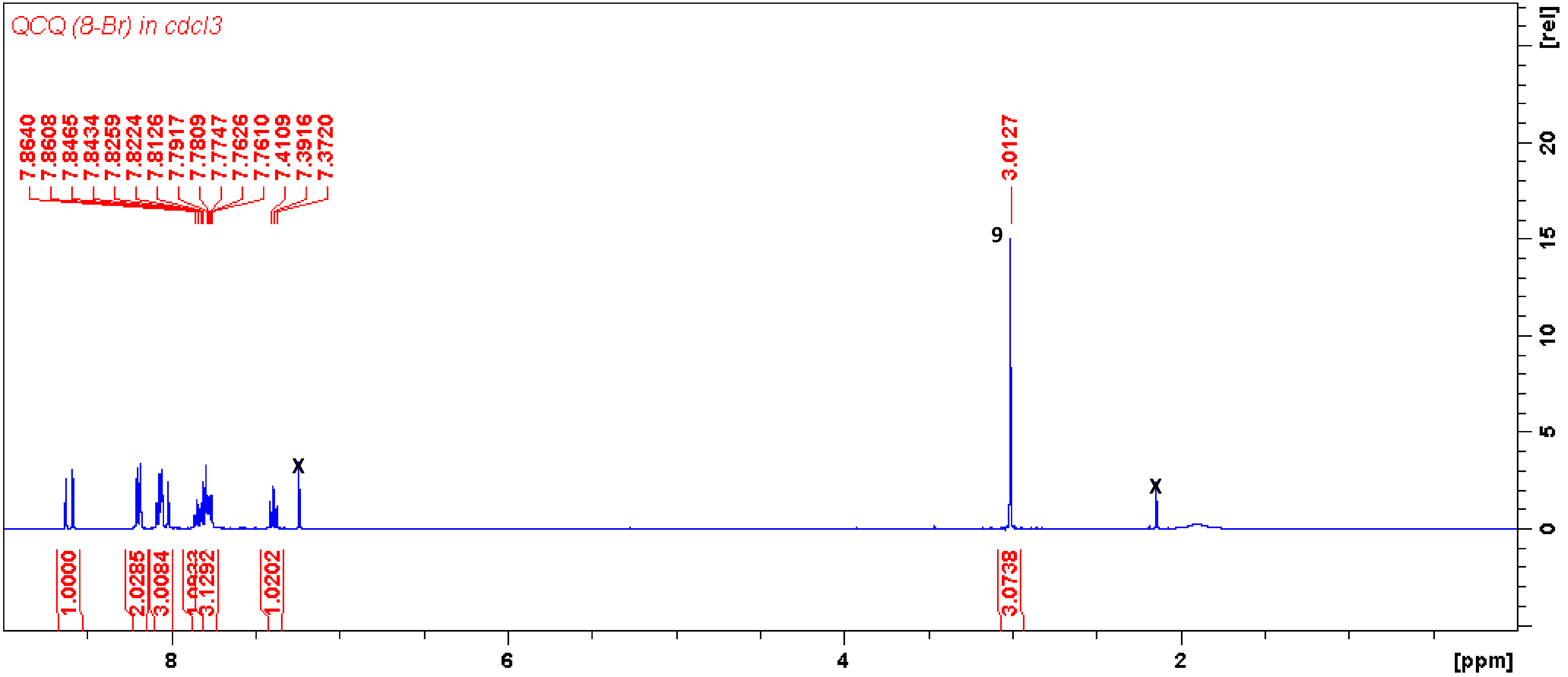

^{1}H NMR spectrum of **B7c**

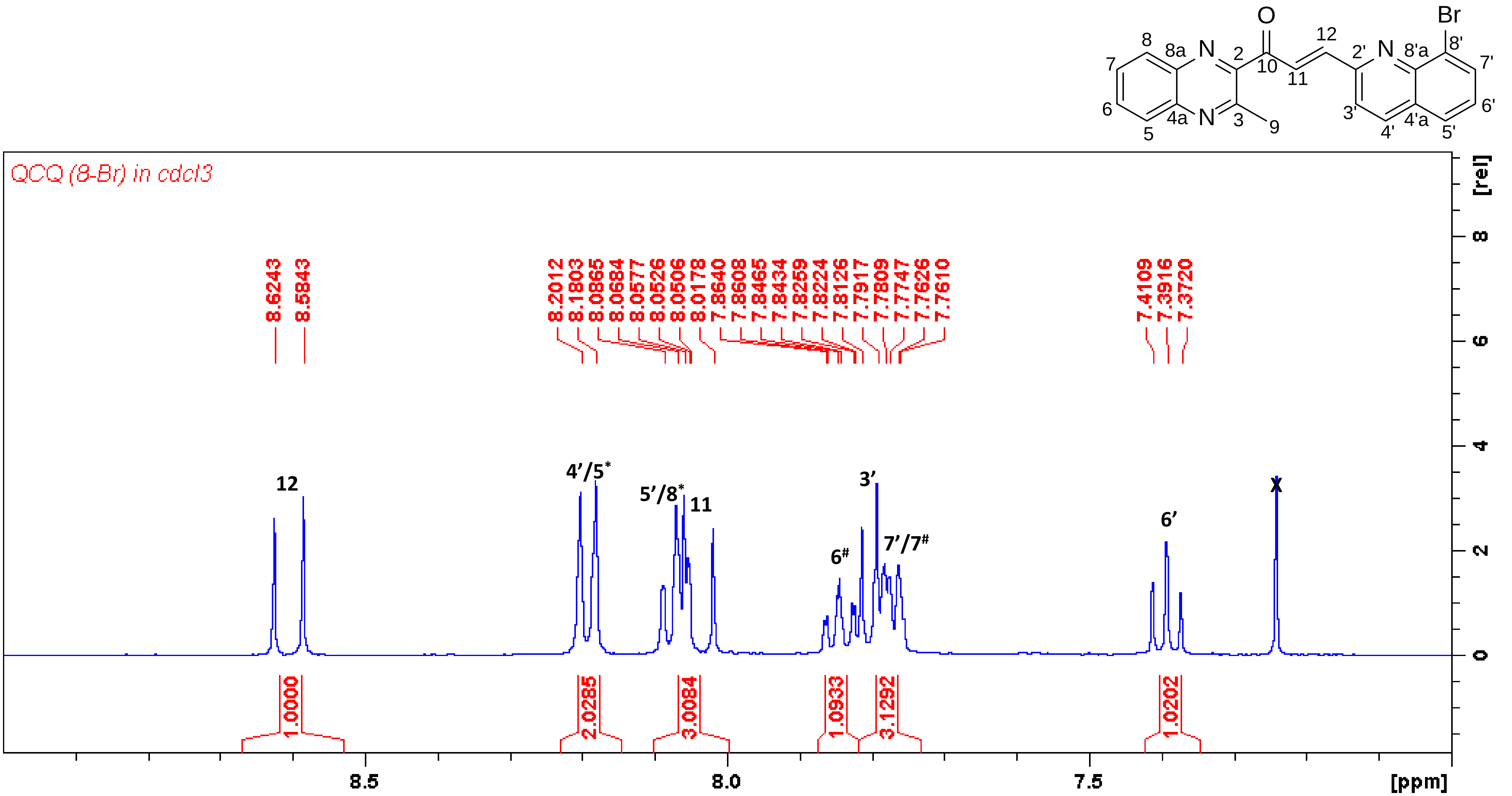

*, # Indicates assignments are interchangeable

Expanded ^{1}H NMR spectrum of **B7c**

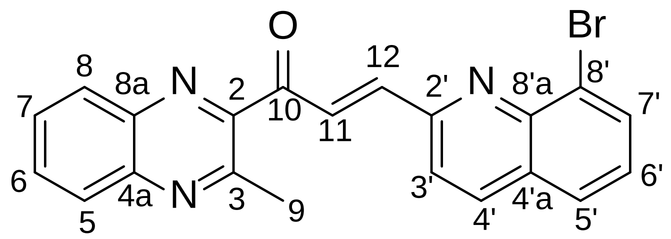

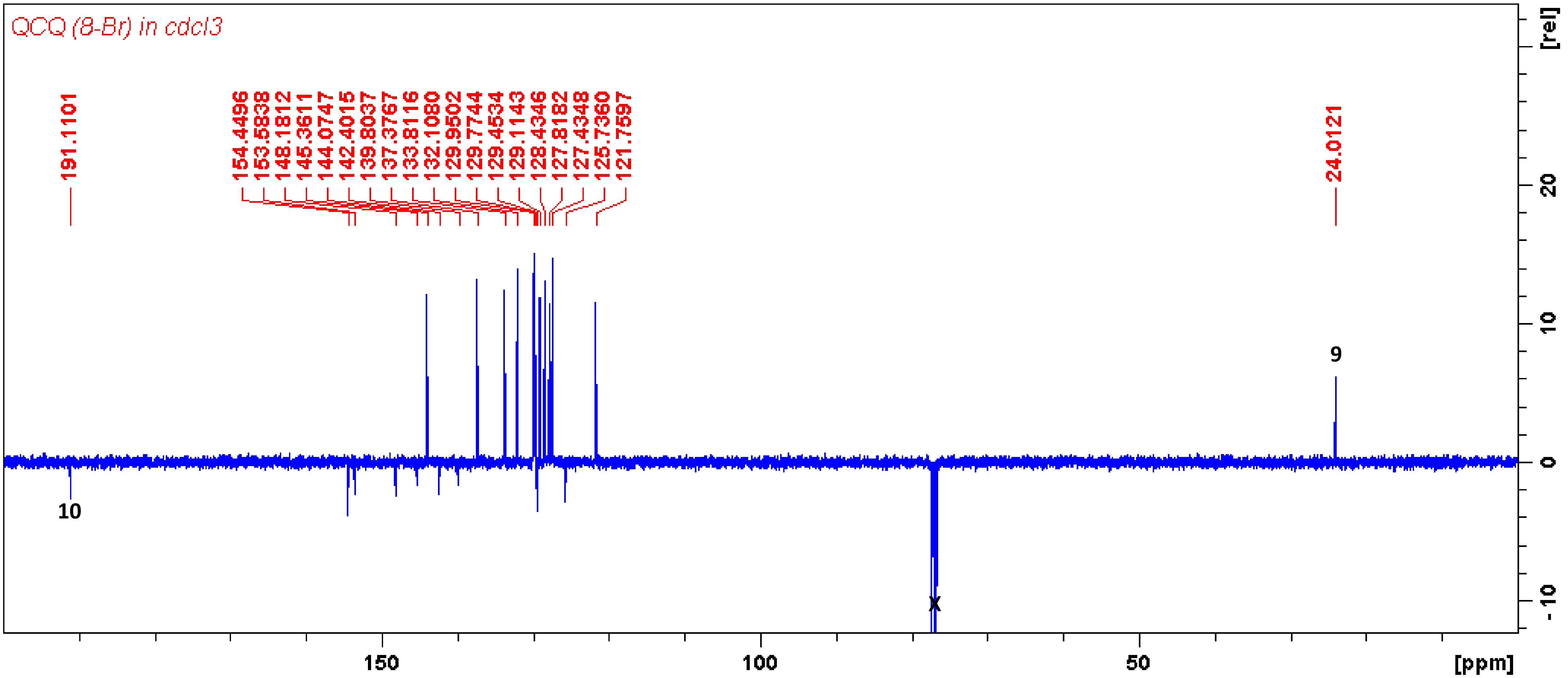

^{13}C NMR spectrum of **B7c**

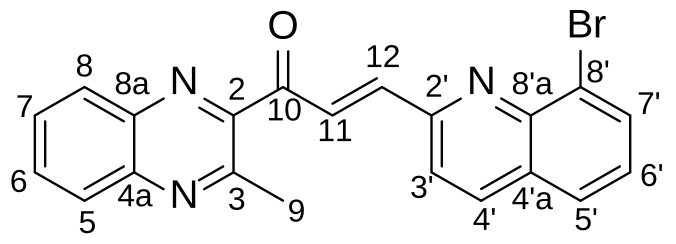

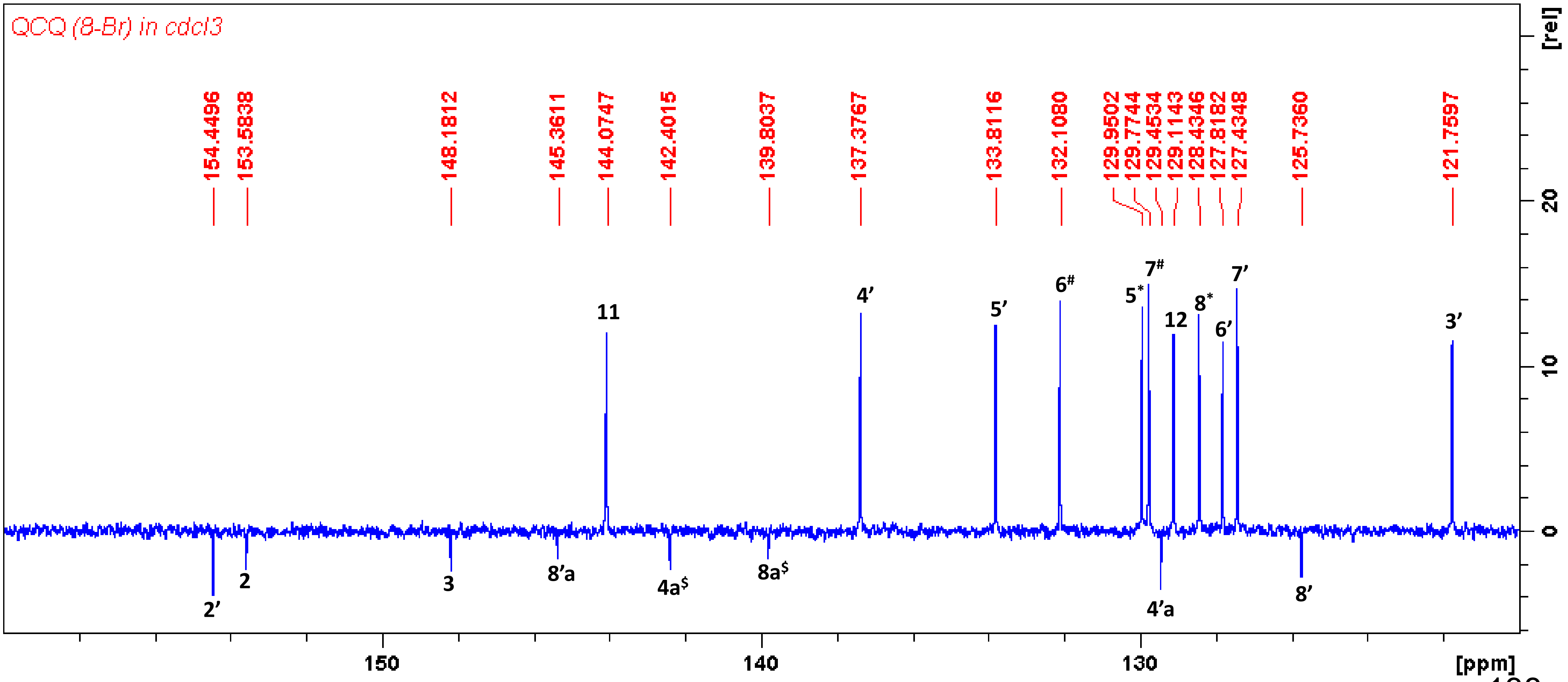

*, #, $ Indicates assignments are interchangeable

Expanded ^{13}C NMR spectrum of **B7c**

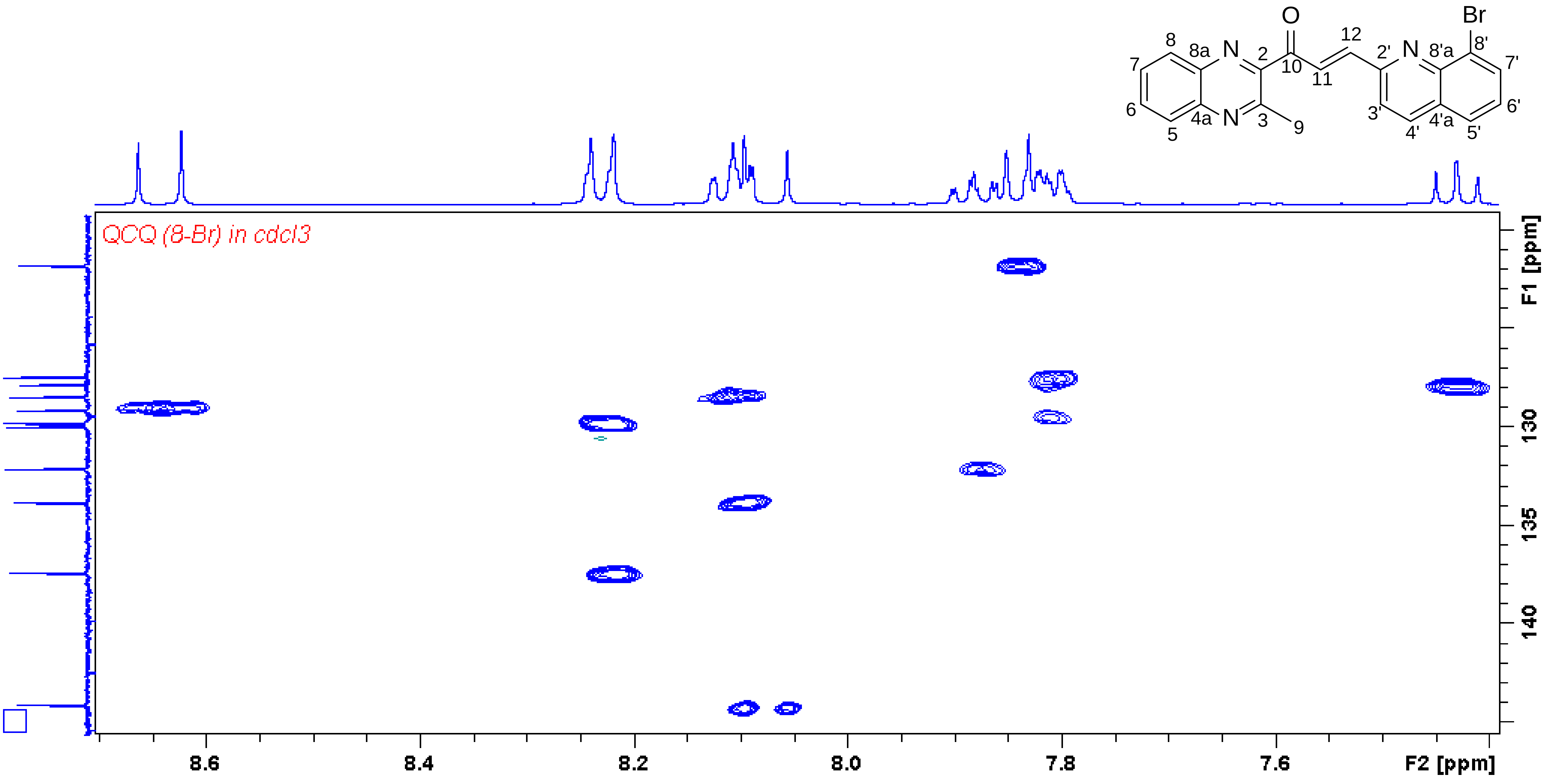

QCQ (8-Br) in cdcl3
F1 [ppm]
130
135
140
8.6
8.4
8.2
8.0
7.8
7.6
F2 [ppm]
O
Br
N
N
8
8a
7
6
5
4a
2
3
9
10
11
12
2'
3'
4'
4'a
5'
6'
7'
8'
8'a

HSQC of **B7c**

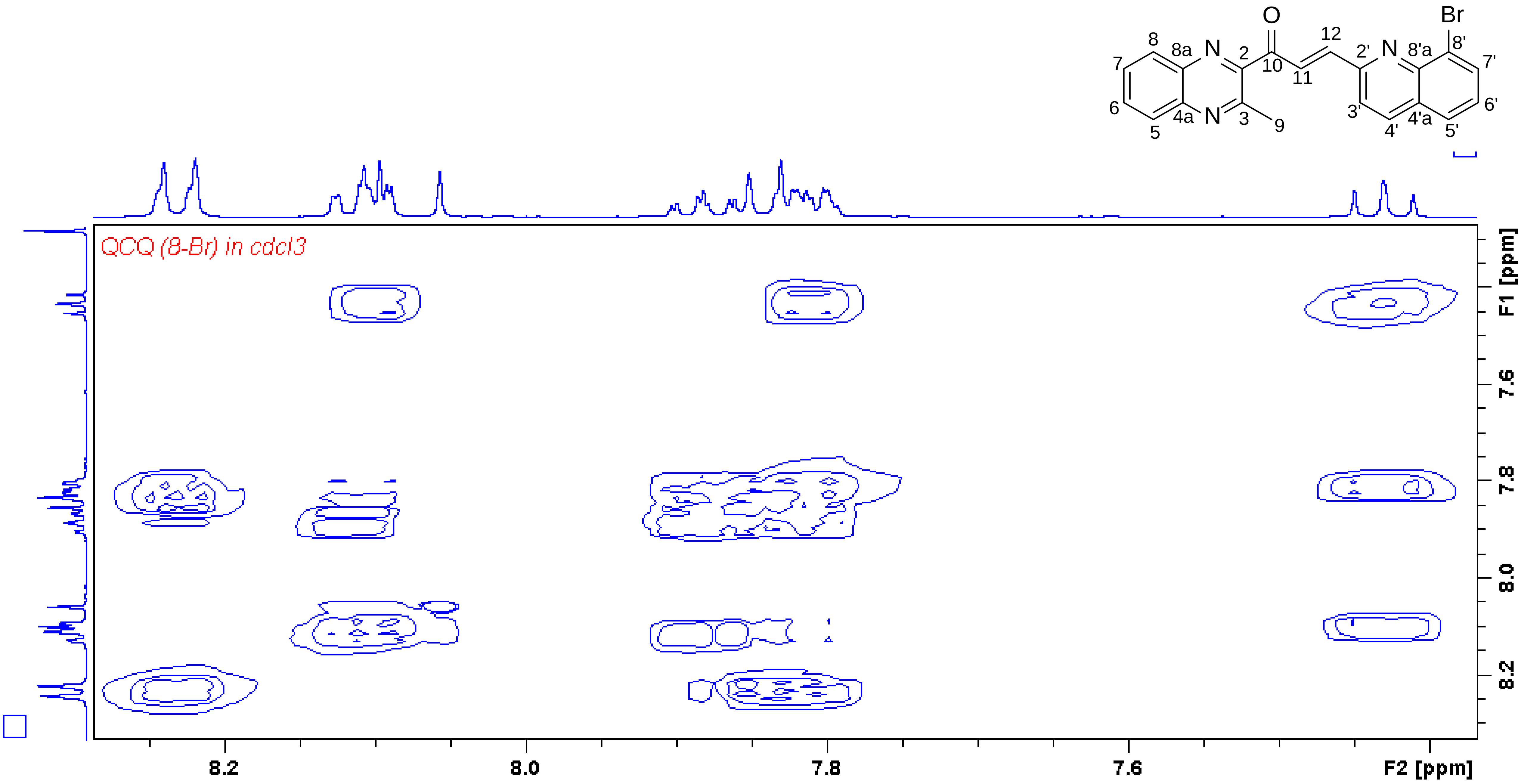

COSY of **B7c**

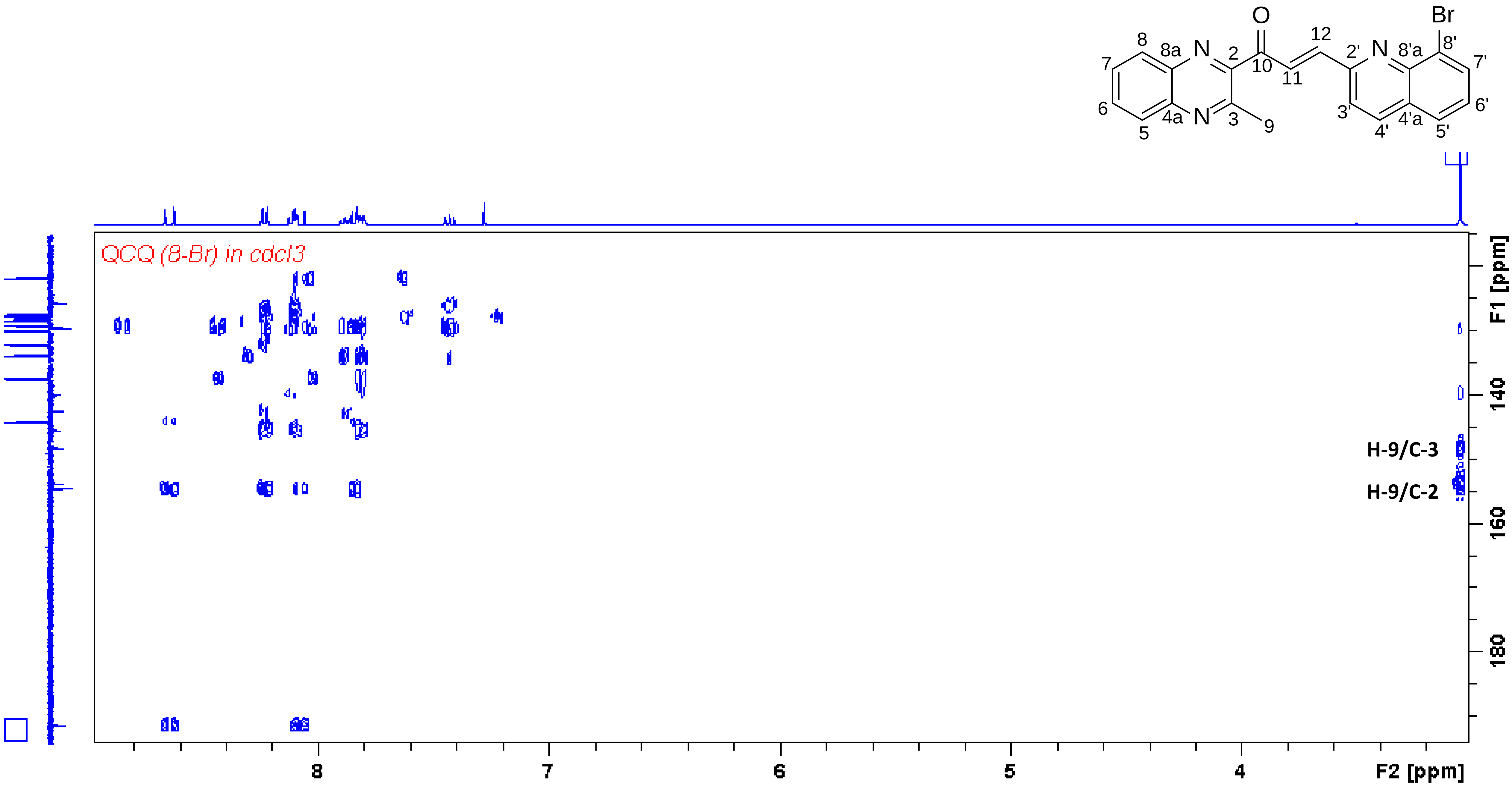
QCQ (8-Br) in cdcl3
H-9/C-3
H-9/C-2
F1 [ppm]
F2 [ppm]
8
7
6
5
4
140
160
180
O
Br
N
N
2
3
4a
5
6
7
8
8a
9
10
11
12
2'
3'
4'
4'a
5'
6'
7'
8'
8'a

HMBC of **B7c**

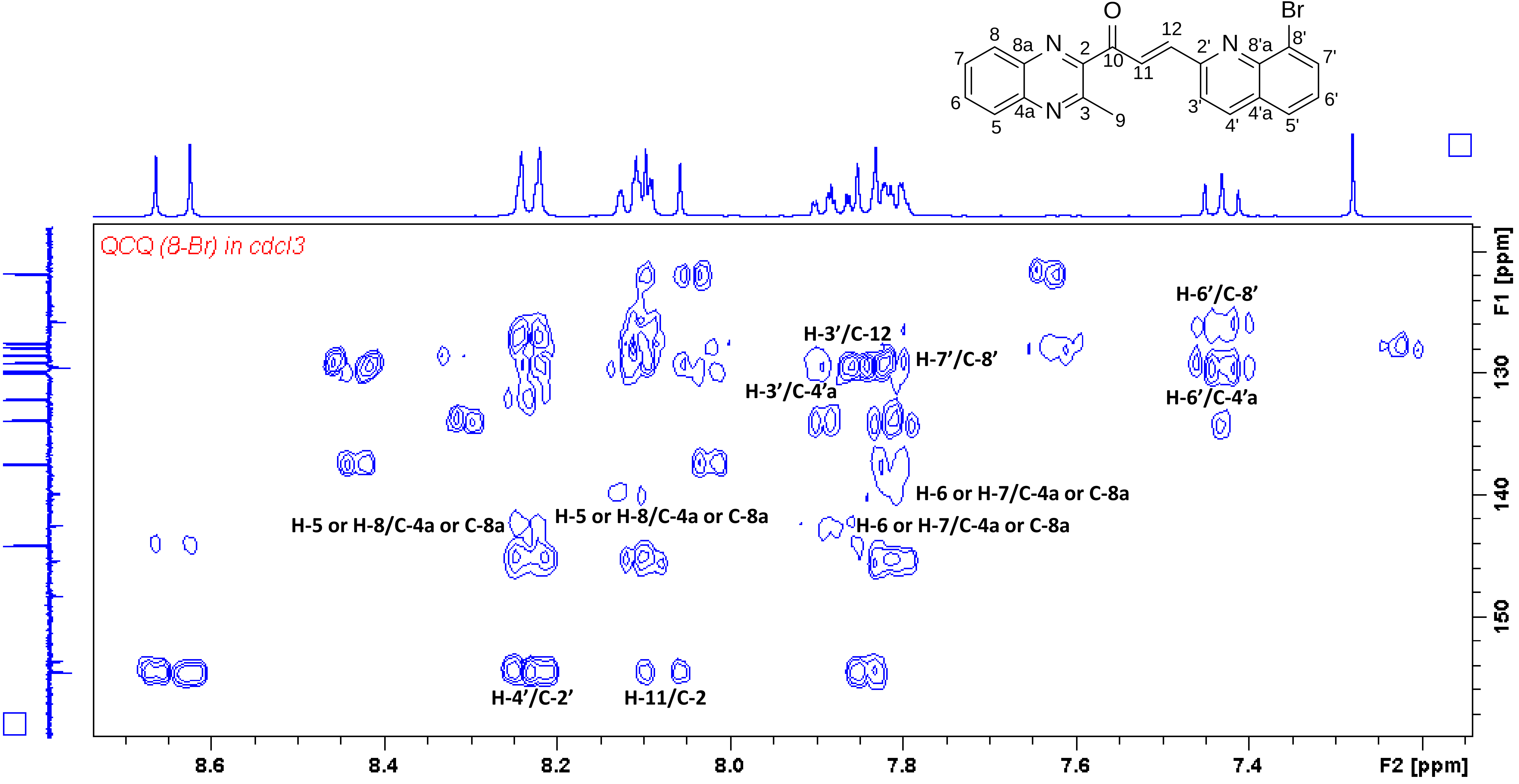

Expanded HMBC of **B7c**

Elemental Composition Report

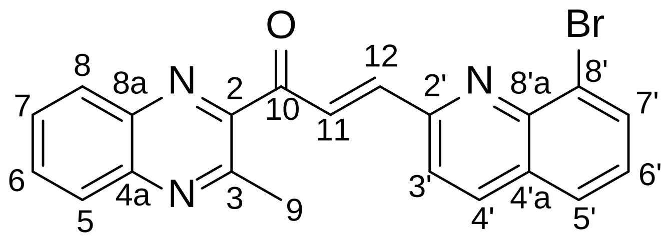

Single Mass Analysis

Tolerance = 5.0 PPM / DBE: min = -1.5, max = 100.0
Element prediction: Off
Number of isotope peaks used for i-FIT = 3

Monoisotopic Mass, Even Electron Ions
30 formula(e) evaluated with 1 results within limits (up to 20 closest results for each mass)
Elements Used:
C: 20-25 H: 10-15 N: 0-5 O: 1-5 Br: 0-1

QCQ(8-Br) 2 (0.034) Cm (1:61)
TOF MS AP+

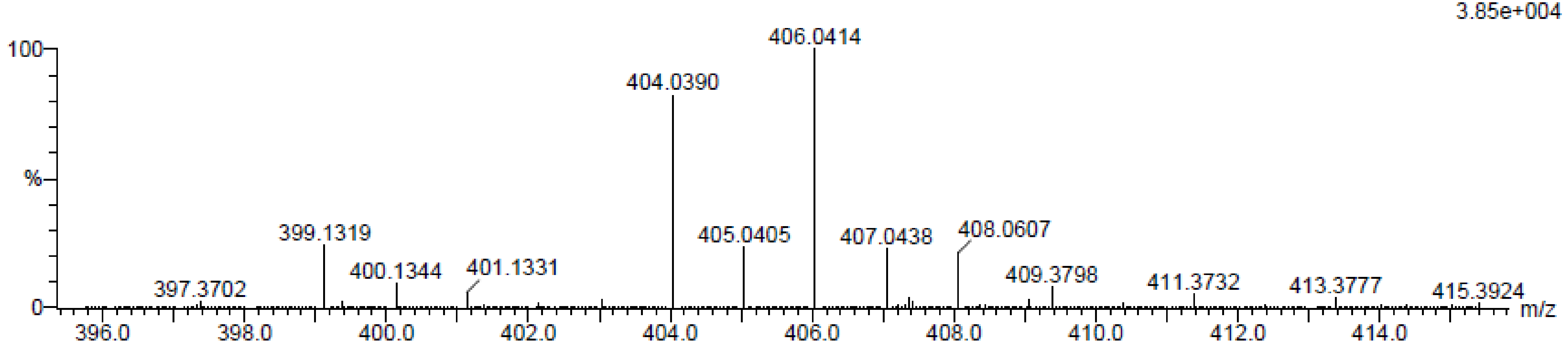

Minimum:				-1.5			
Maximum:		5.0	5.0	100.0			

Mass	Calc. Mass	mDa	PPM	DBE	i-FIT	i-FIT (Norm)	Formula
404.0390	404.0398	-0.8	-2.0	15.5	401.5	0.0	C21 H15 N3 O Br

High resolution mass spectrum of **B7c**

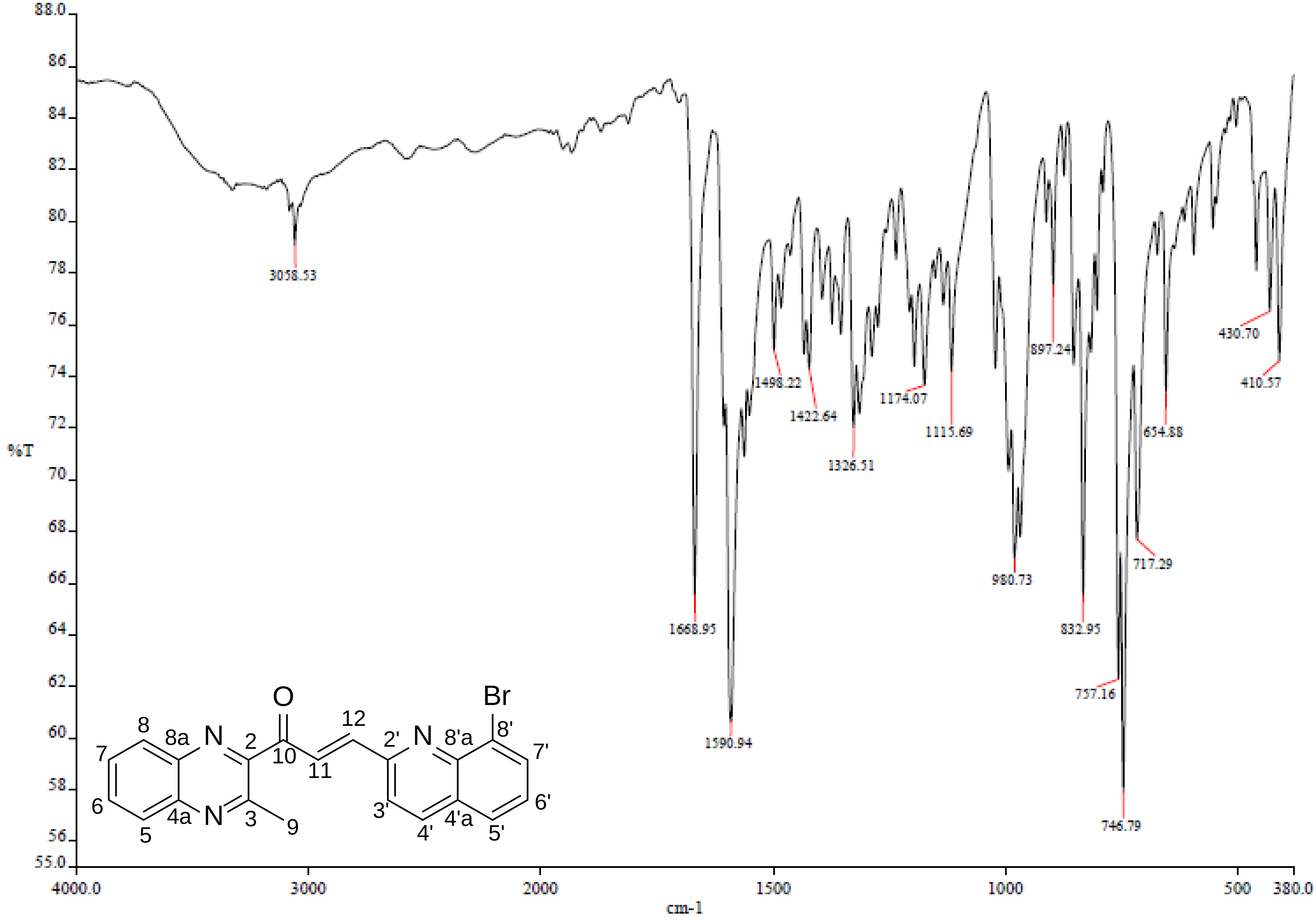

FTIR spectrum of **B7c**

Overlay Spectrum Graph Report

06/10/2017 12:01:40 PM

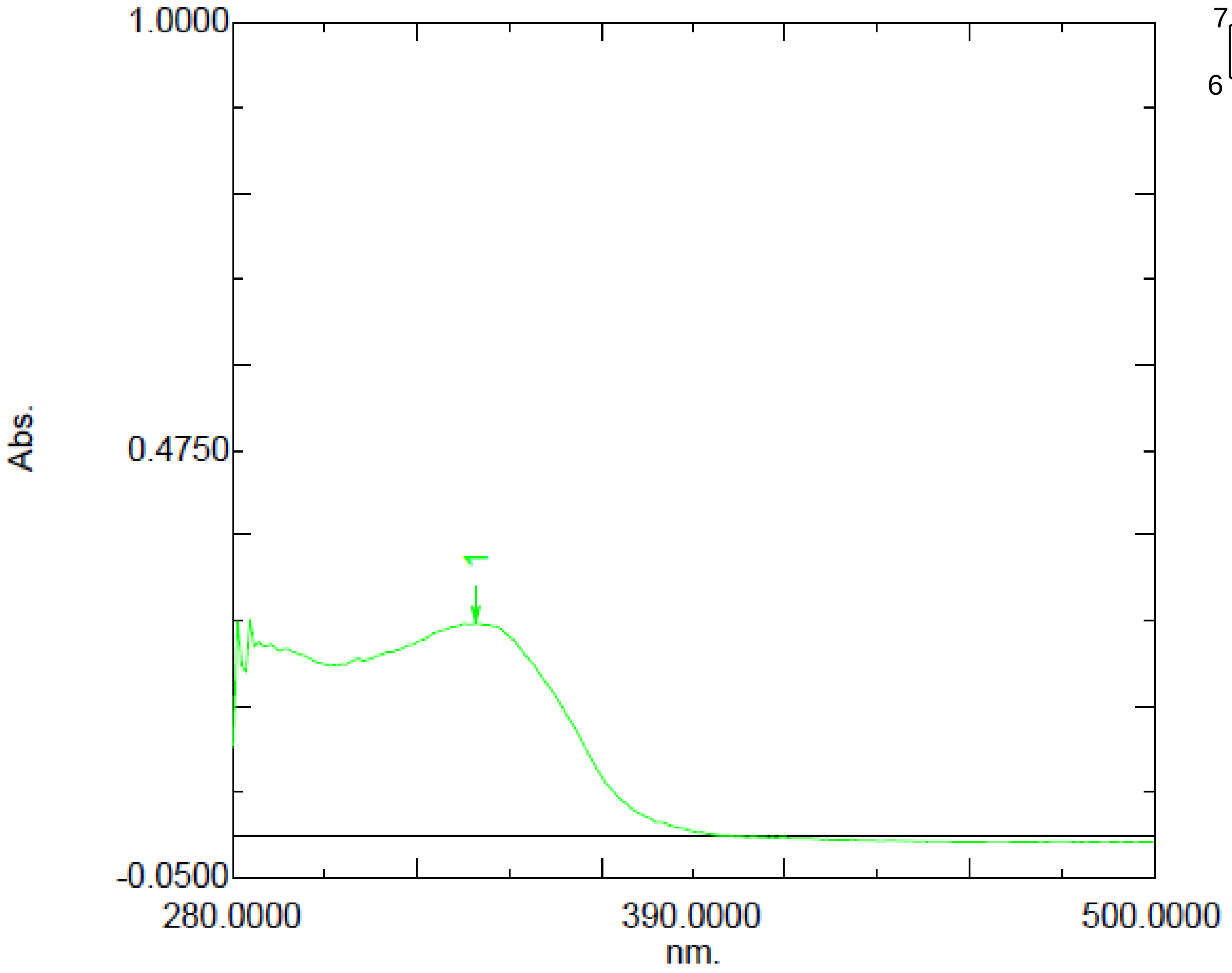

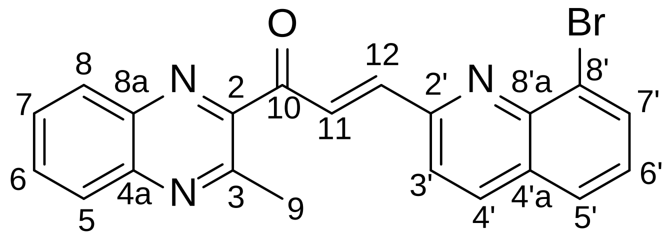

λ	absorbance	logε
341	0.2605	4.32

UV spectrum of **B7c**

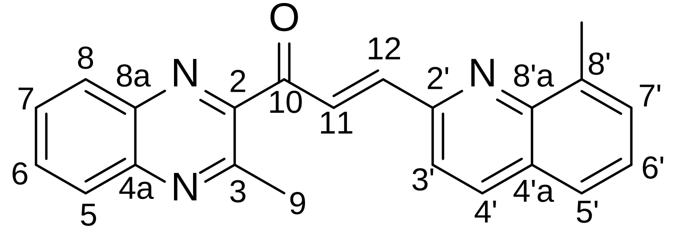

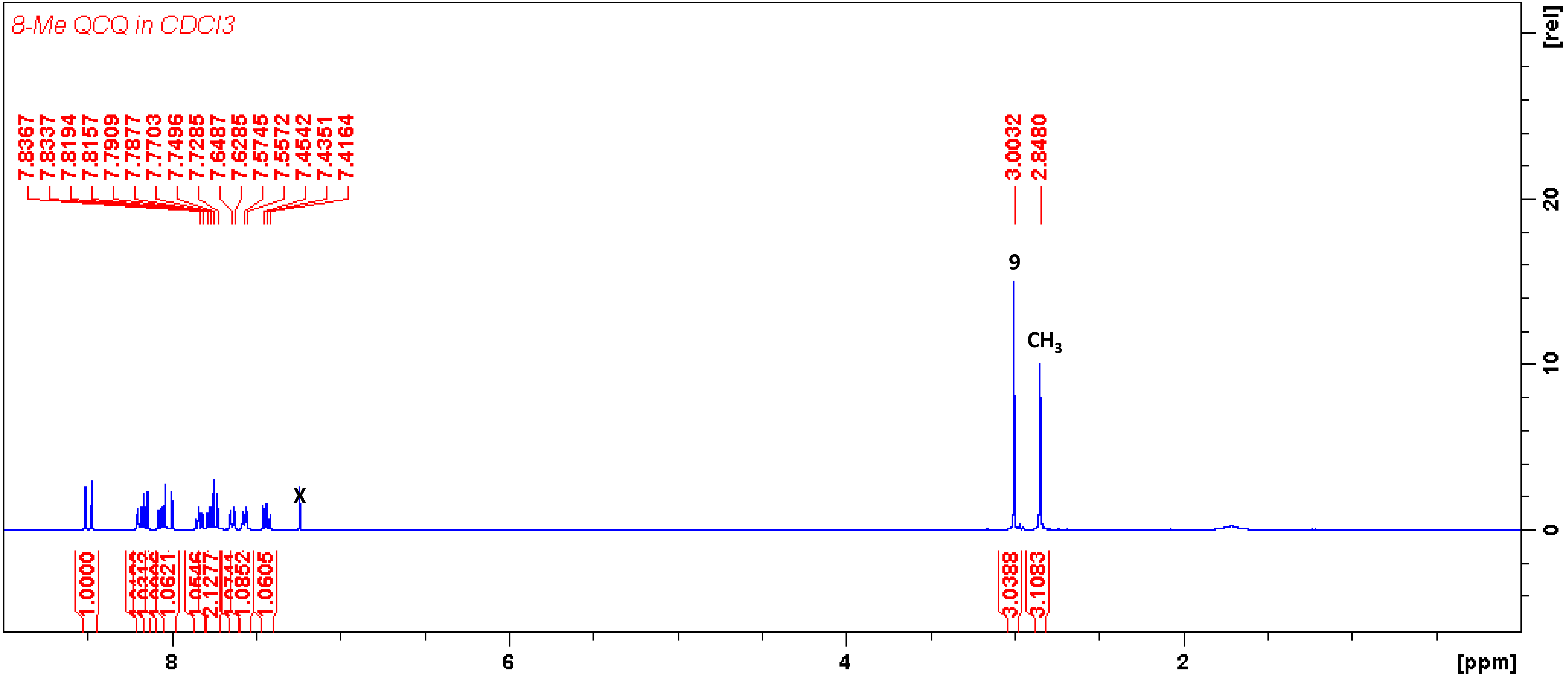

^{1}H NMR spectrum of **B7d**

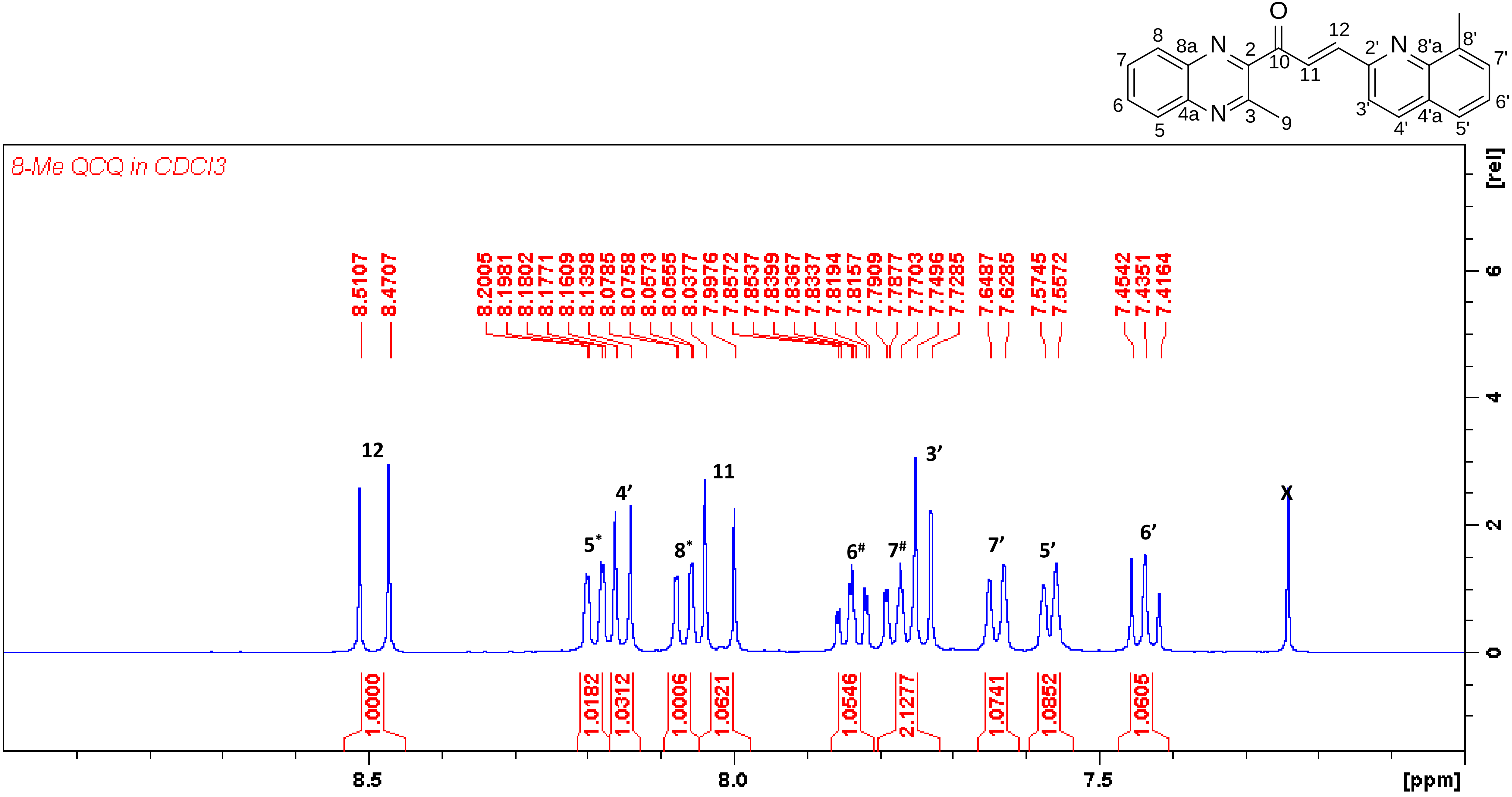

*, # Indicates assignments are interchangeable

Expanded ^{1}H NMR spectrum of **B7d**

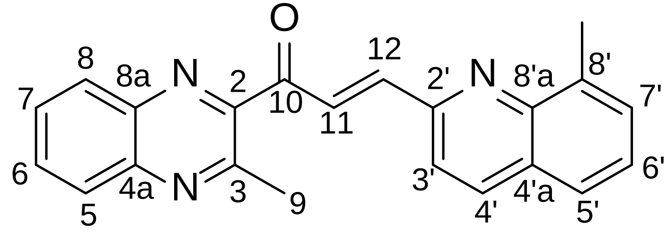

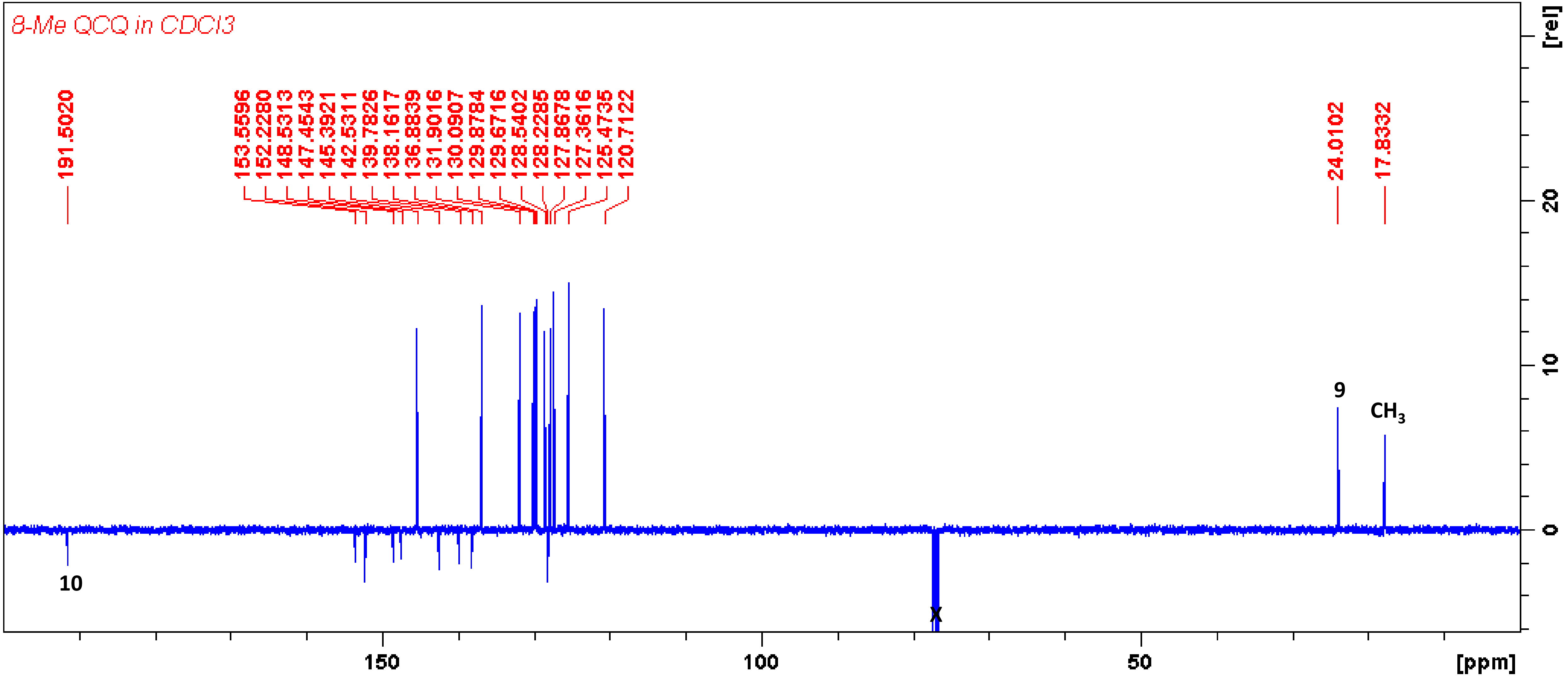

^{13}C NMR spectrum of **B7d**

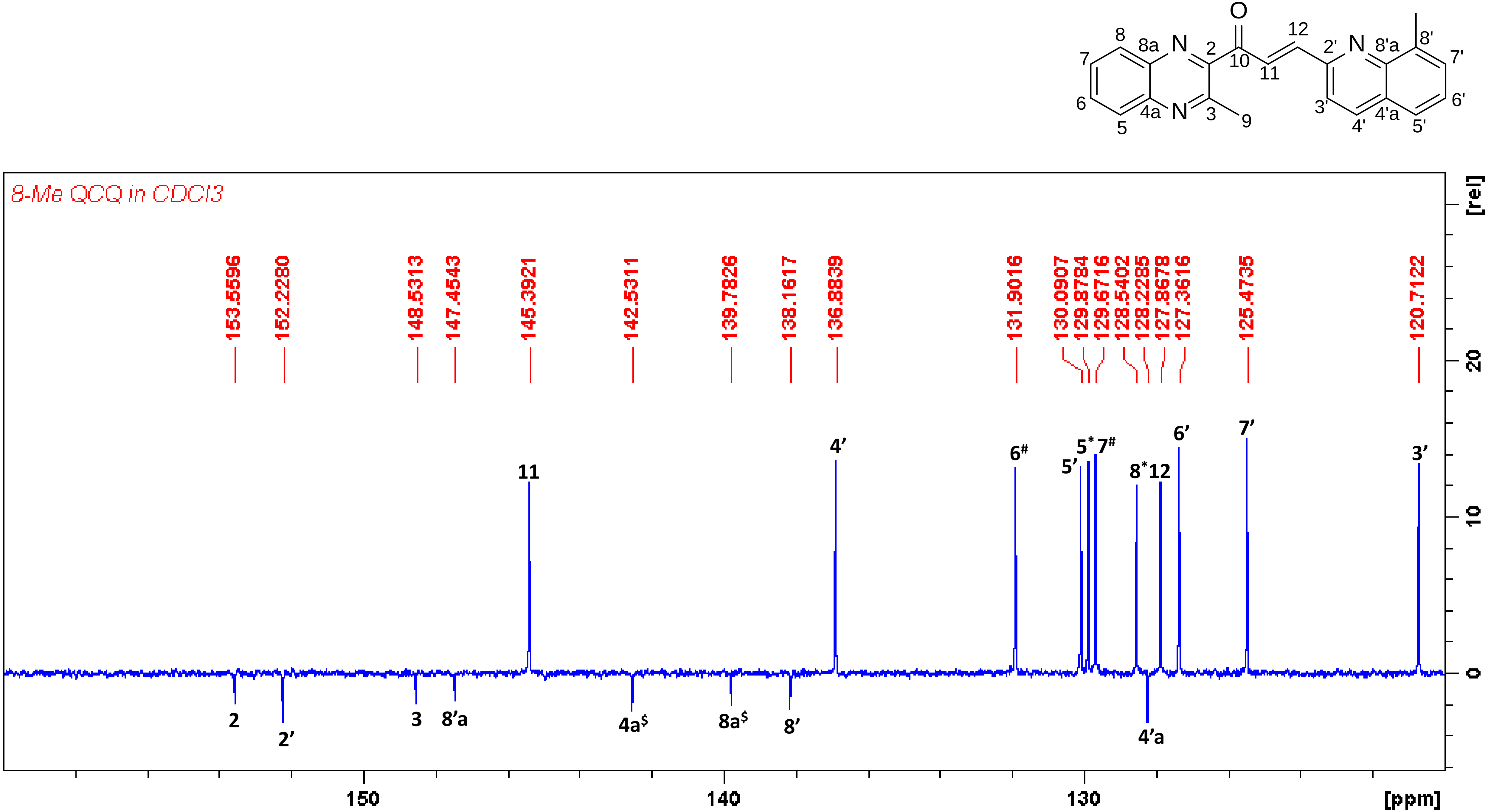

*, #, $ Indicates assignments are interchangeable

Expanded ^{13}C NMR spectrum of **B7d**

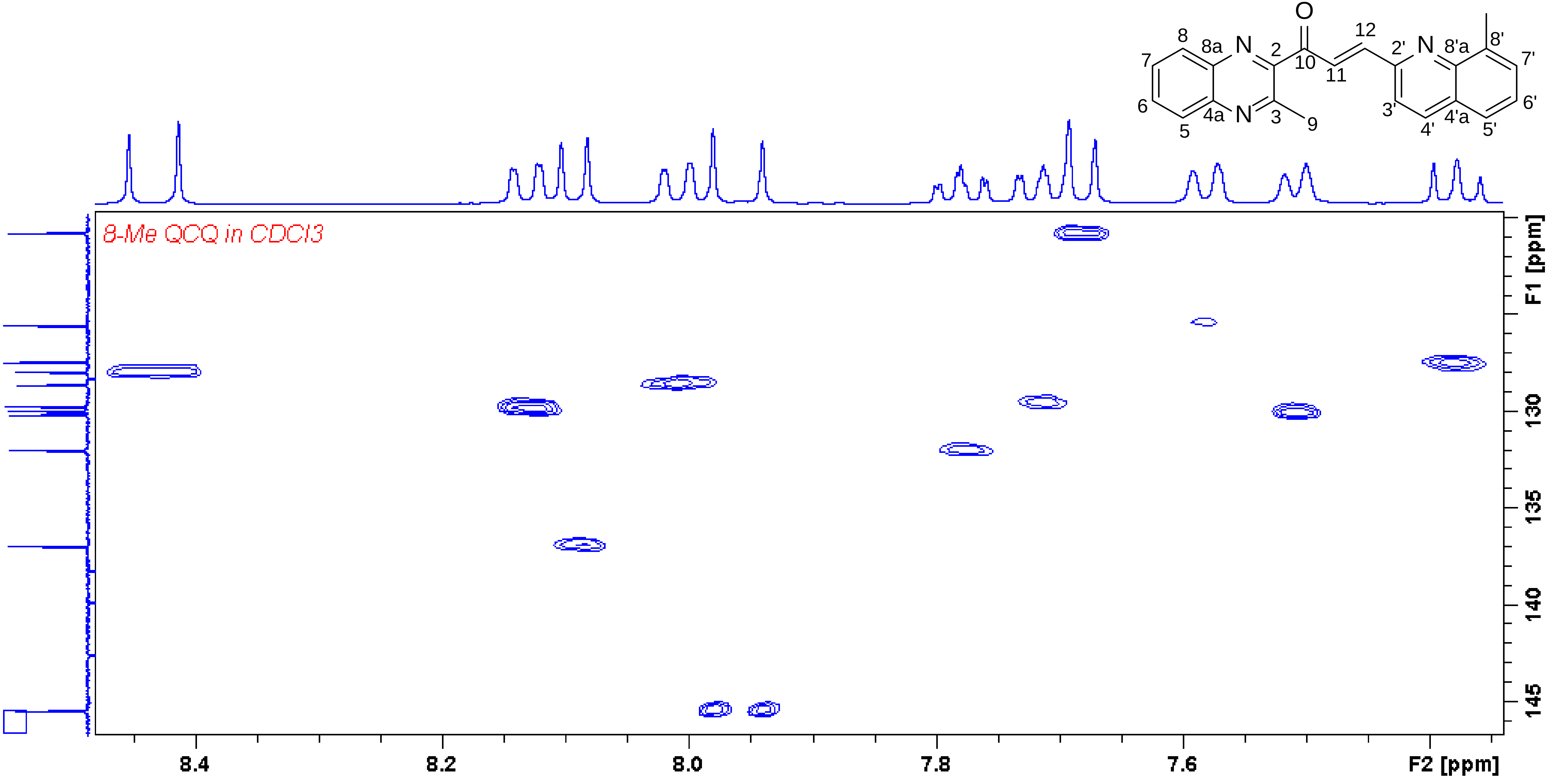

8-Me QCQ in CDCl3
F1 [ppm]
F2 [ppm]
8.4
8.2
8.0
7.8
7.6
130
135
140
145
O
N
N
N
8
8a
2
10
12
2'
8'a
8'
7'
7
11
6
4a
3
9
3'
4'
4'a
5'
6'
5

HSQC of **B7d**

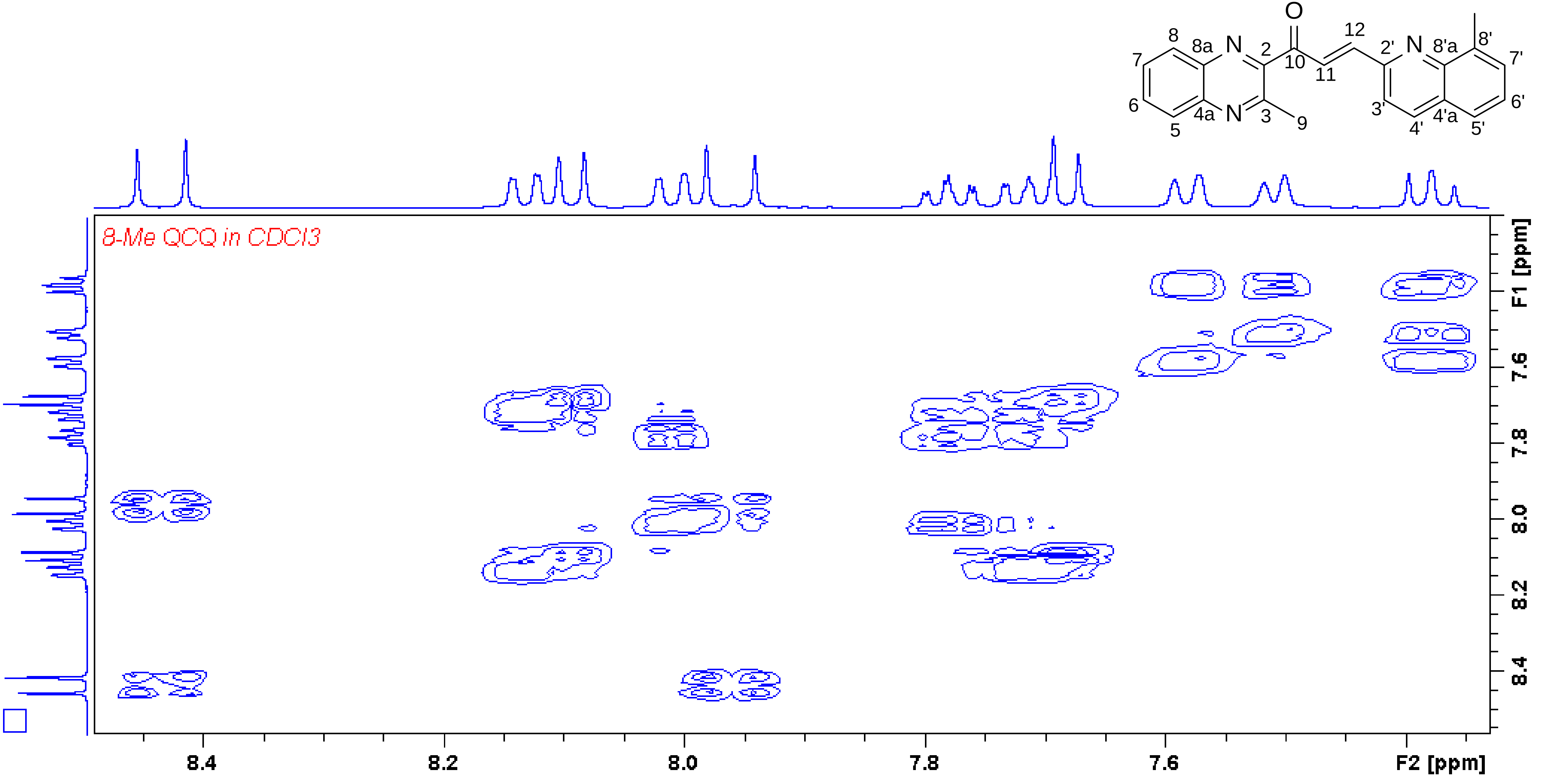

COSY of **B7d**

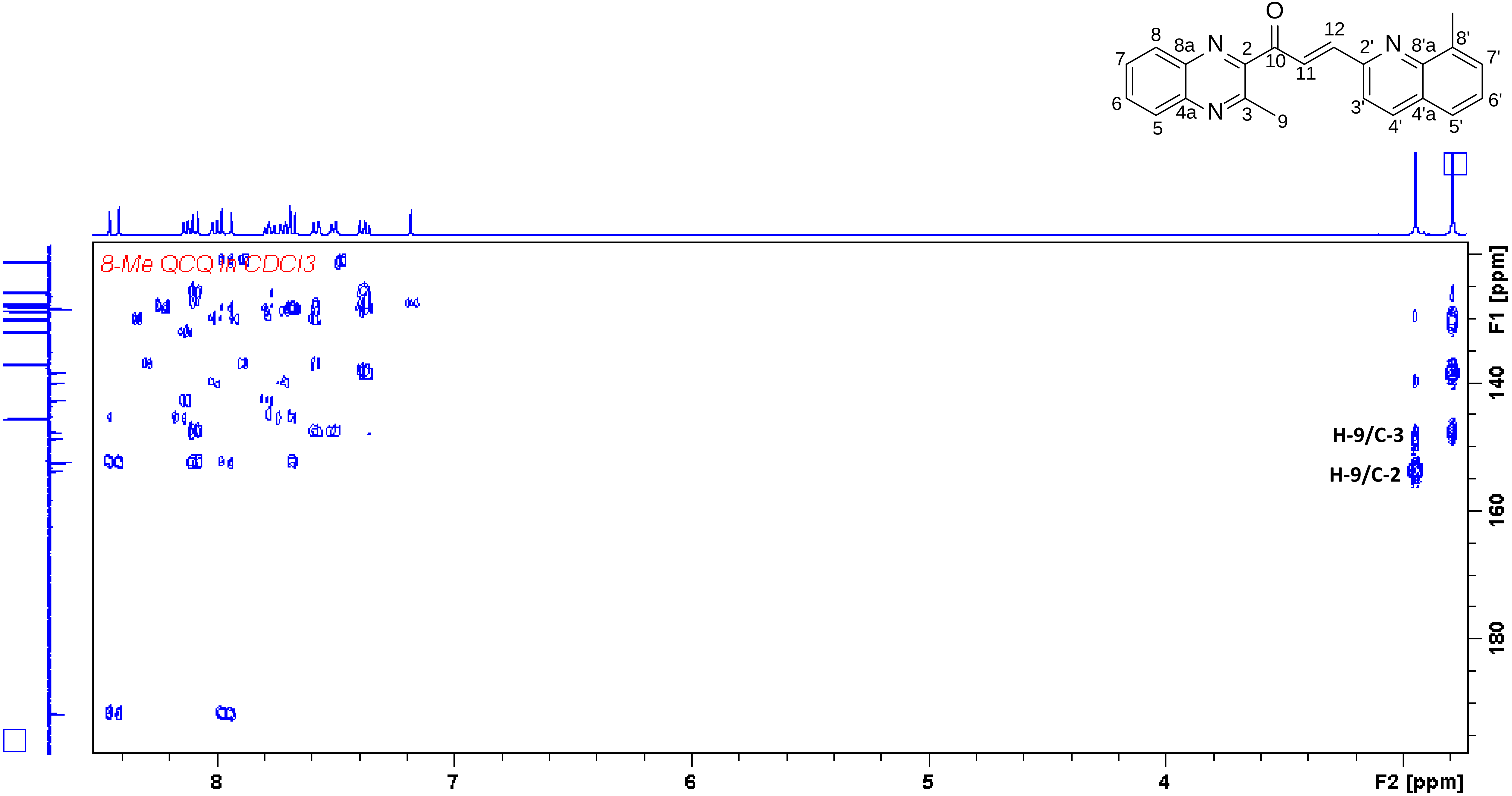
8-Me QCQ in CDCl3
H-9/C-3
H-9/C-2
F1 [ppm]
140
160
180
8
7
6
5
4
F2 [ppm]
O
N
N
8
8a
7
6
5
4a
2
3
9
10
11
12
2'
N
8'a
8'
7'
6'
5'
4'a
4'
3'

HMBC of **B7d**

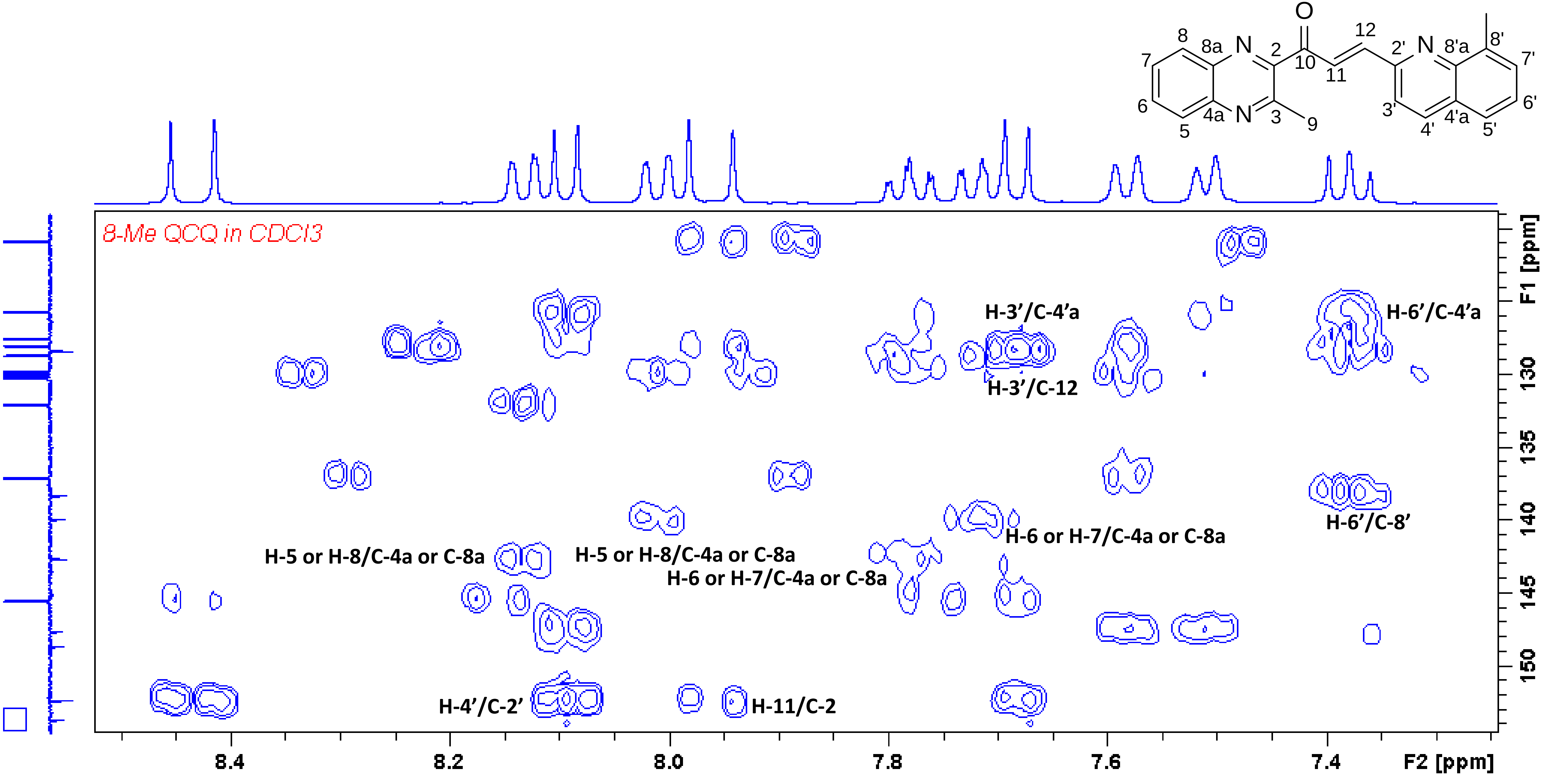

Expanded HMBC of **B7d**

Elemental Composition Report

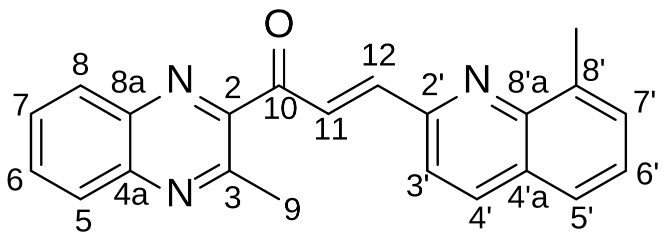

Single Mass Analysis

Tolerance = 5.0 PPM / DBE: min = -1.5, max = 100.0
Element prediction: Off
Number of isotope peaks used for i-FIT = 3

Monoisotopic Mass, Even Electron Ions
35 formula(e) evaluated with 1 results within limits (up to 20 closest results for each mass)
Elements Used:
C: 20-25 H: 15-20 N: 0-5 O: 0-5 Na: 0-1
QCQ (8-Me) 21 (0.675) Cm (1:61)
TOF MS ES+

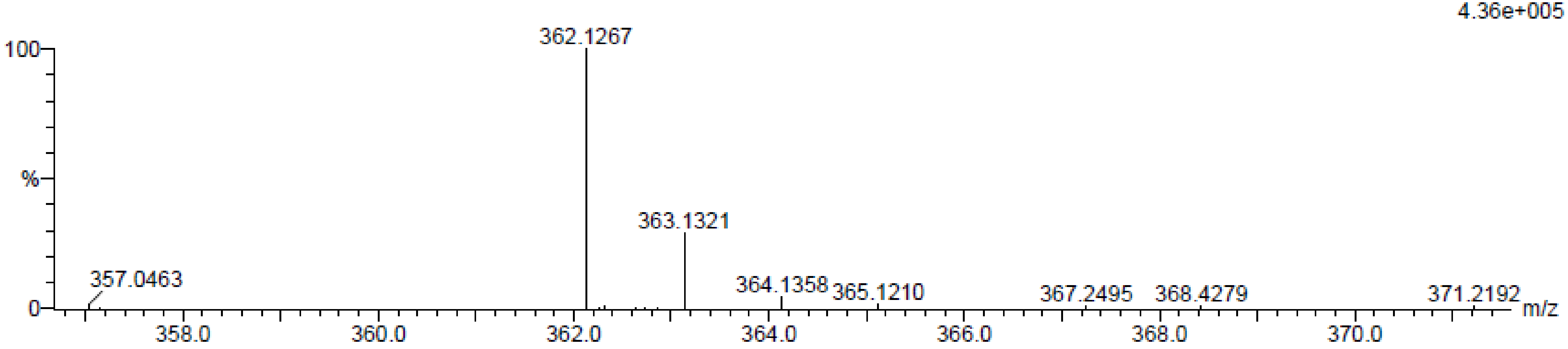

Minimum:				-1.5			
Maximum:		5.0	5.0	100.0			
Mass	Calc. Mass	mDa	PPM	DBE	i-FIT	i-FIT (Norm)	Formula
362.1267	362.1269	-0.2	-0.6	15.5	100.8	0.0	C22 H17 N3 O Na

High resolution mass spectrum of **B7d**

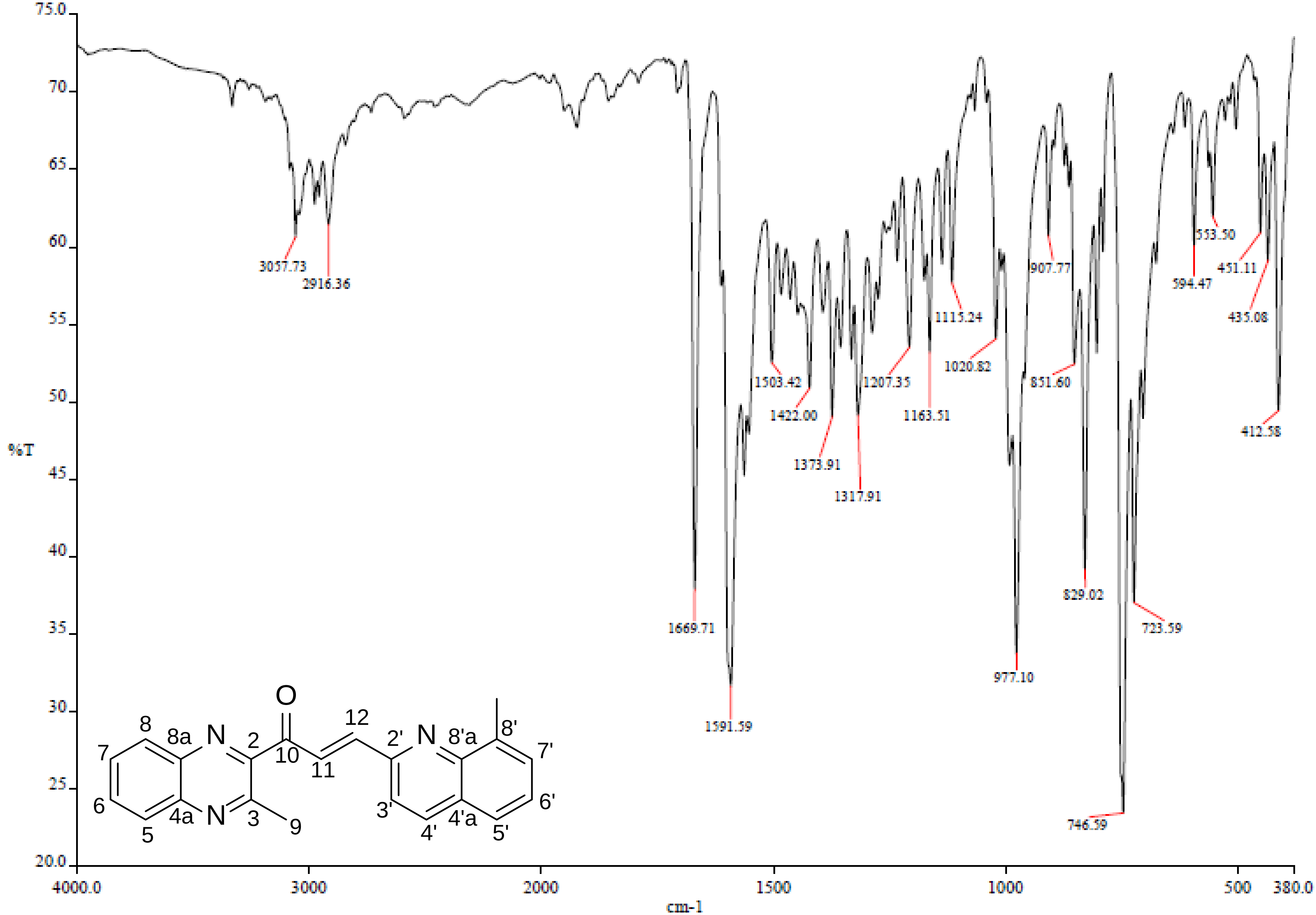

FTIR spectrum of **B7d**

Overlay Spectrum Graph Report

06/10/2017 12:02:17 PM

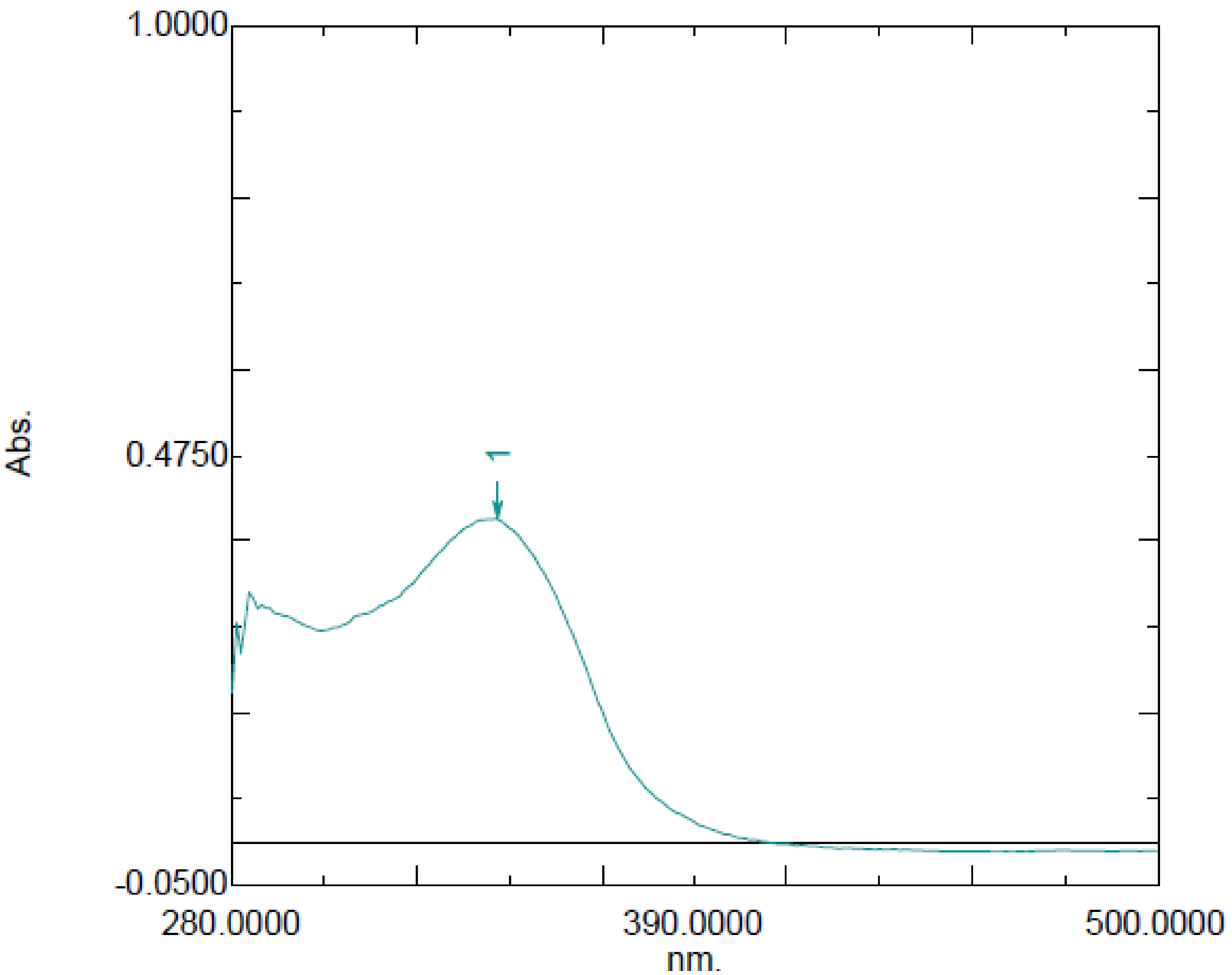

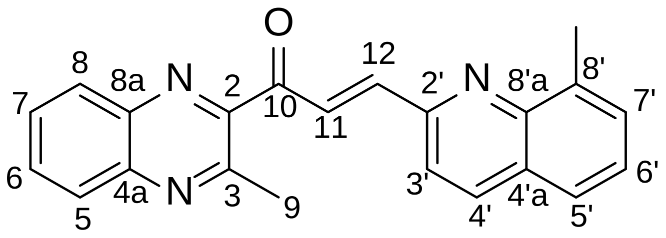

λ	absorbance	logε
343	0.3969	4.43

UV spectrum of **B7d**

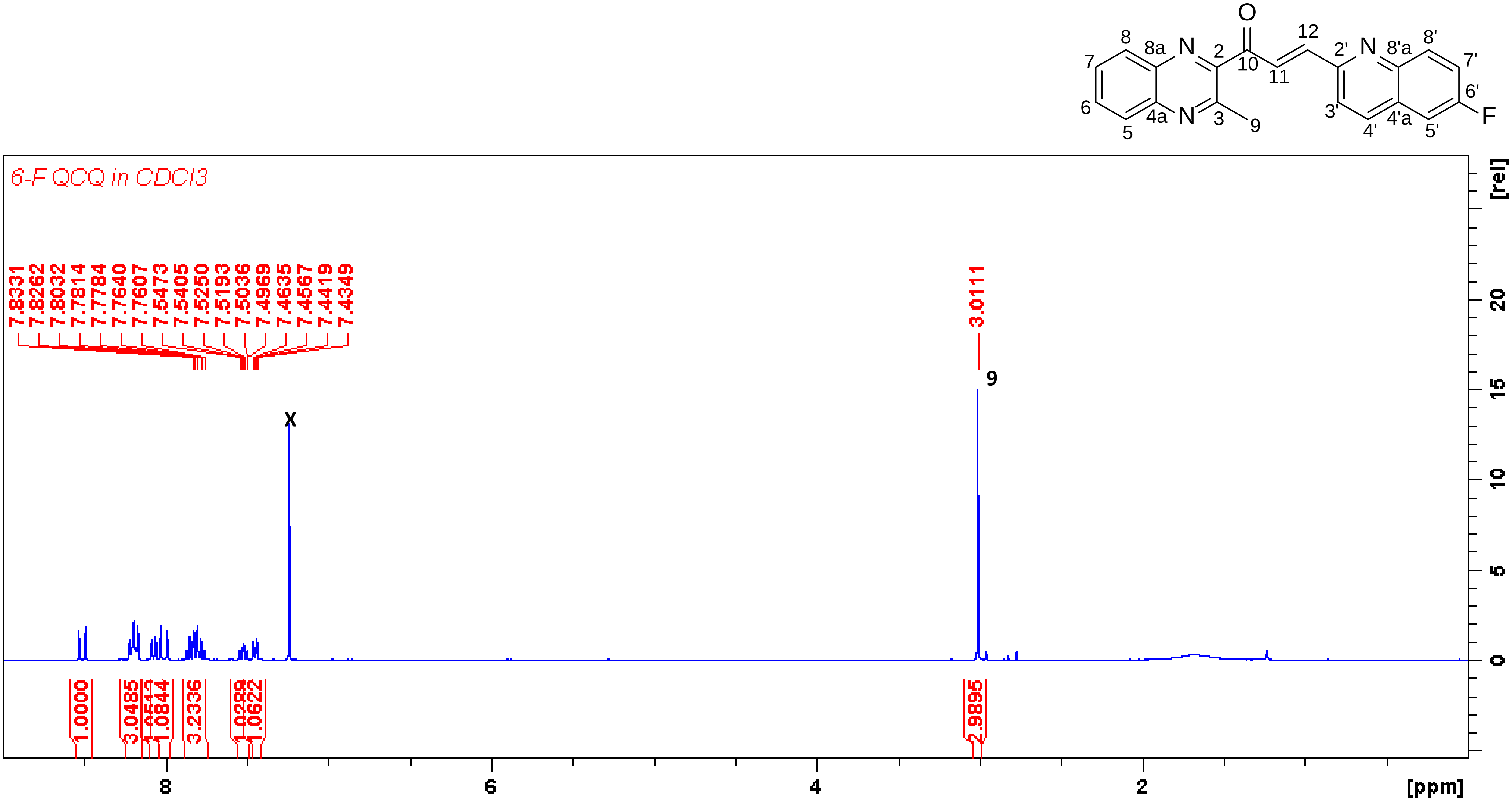

^{1}H NMR spectrum of **B7e**

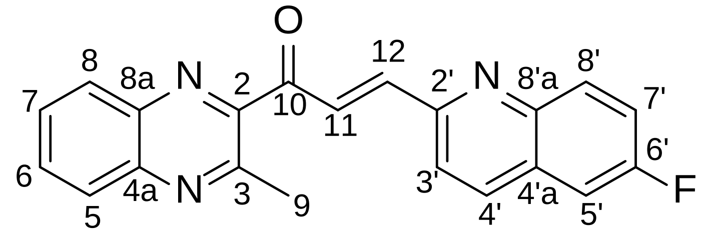

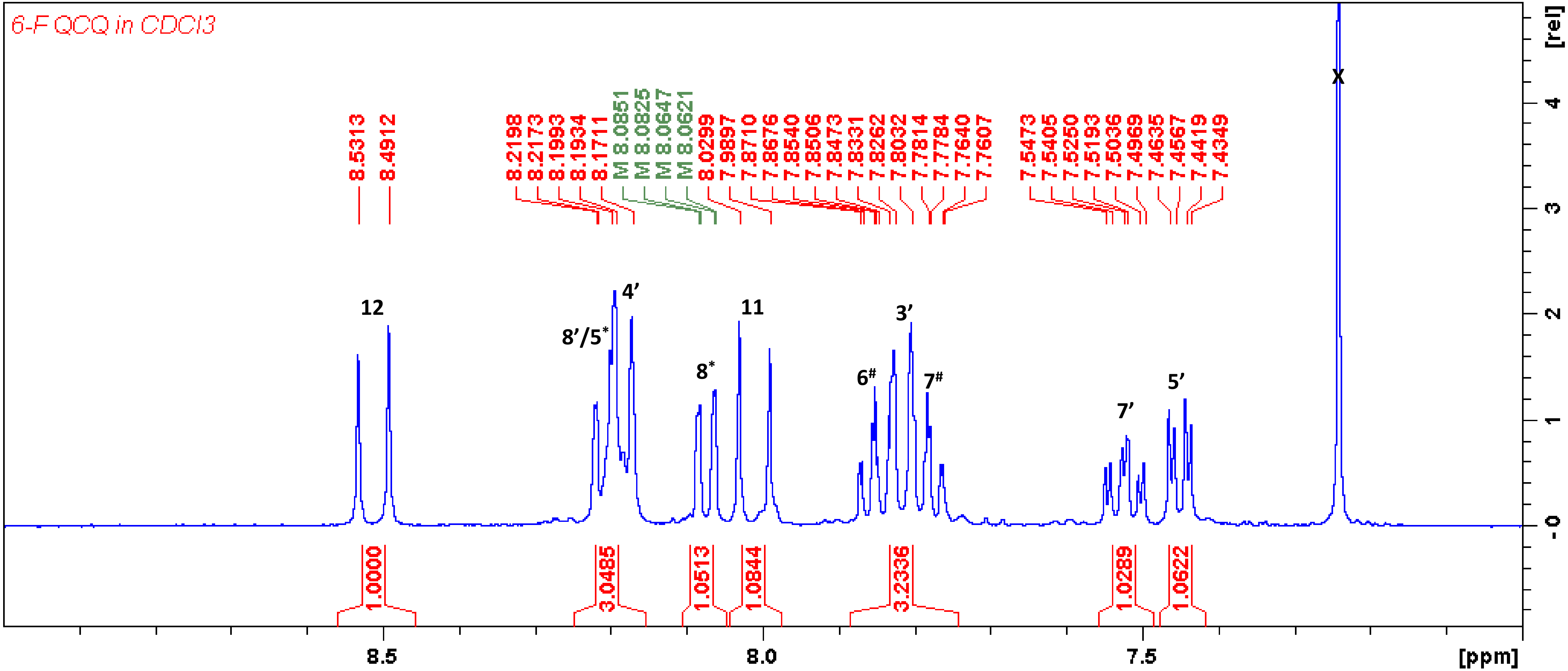

*, # Indicates assignments are interchangeable

Expanded ^{1}H NMR spectrum of **B7e**

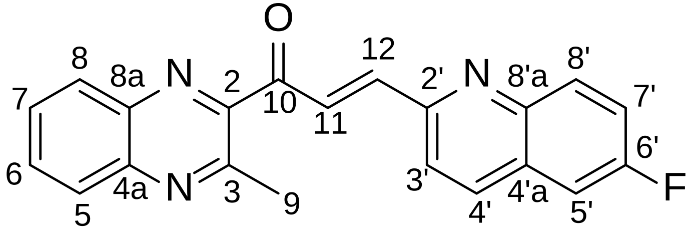

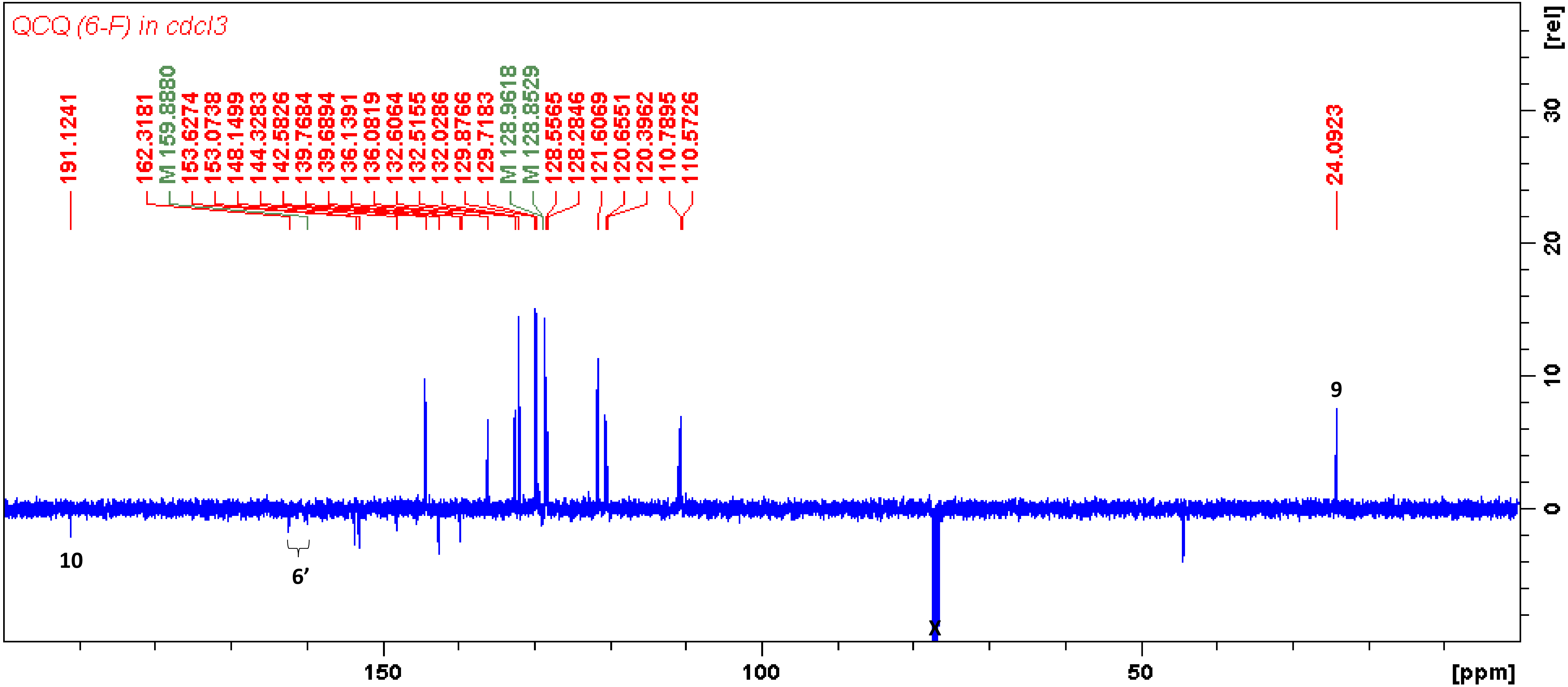

^{13}C NMR spectrum of **B7e**

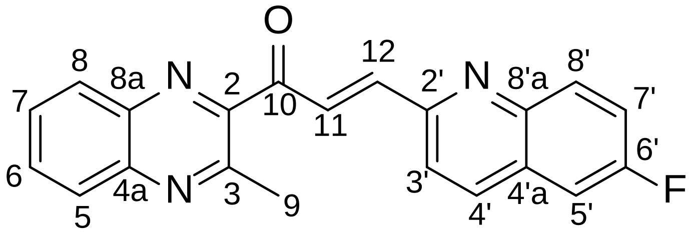

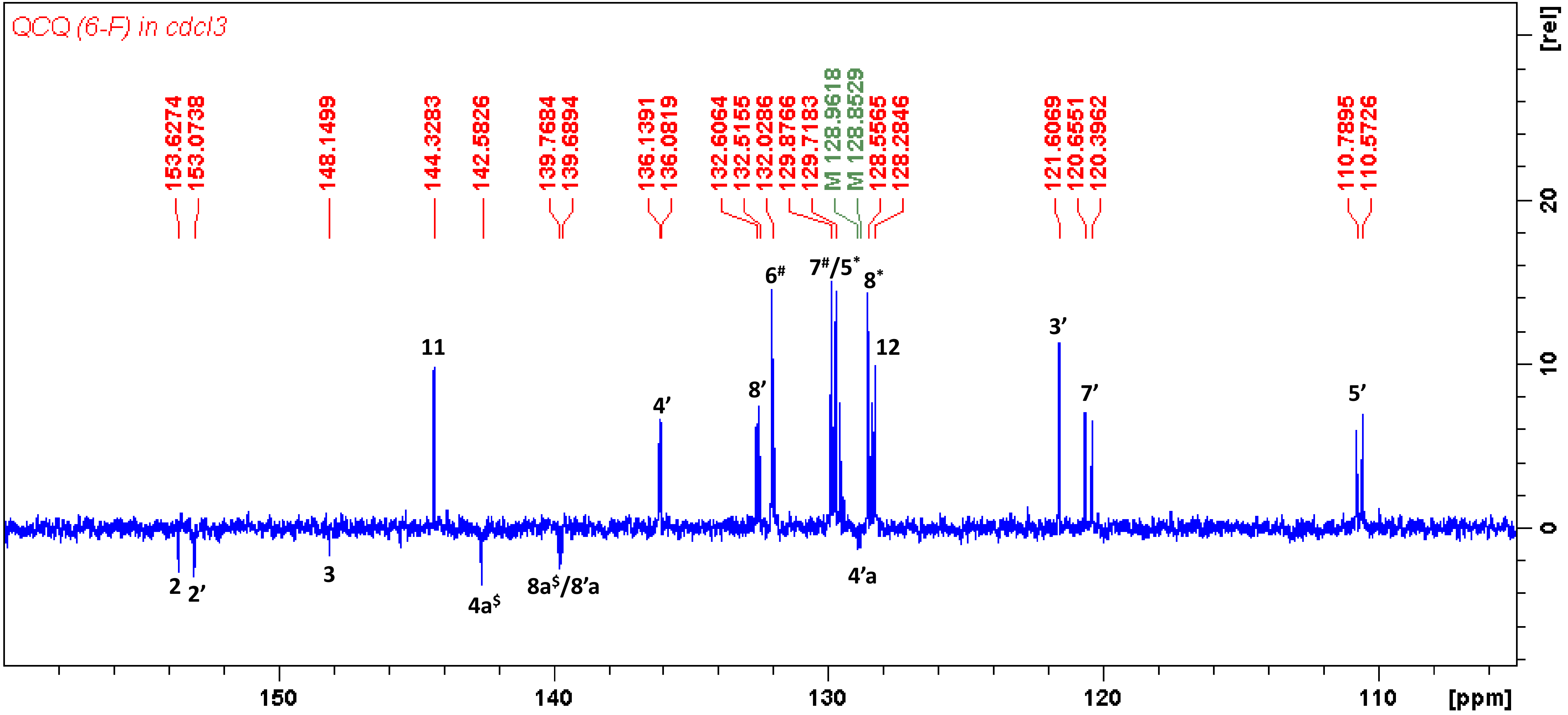

*, #, $ Indicates assignments are interchangeable

Expanded ^{13}C NMR spectrum of **B7e**

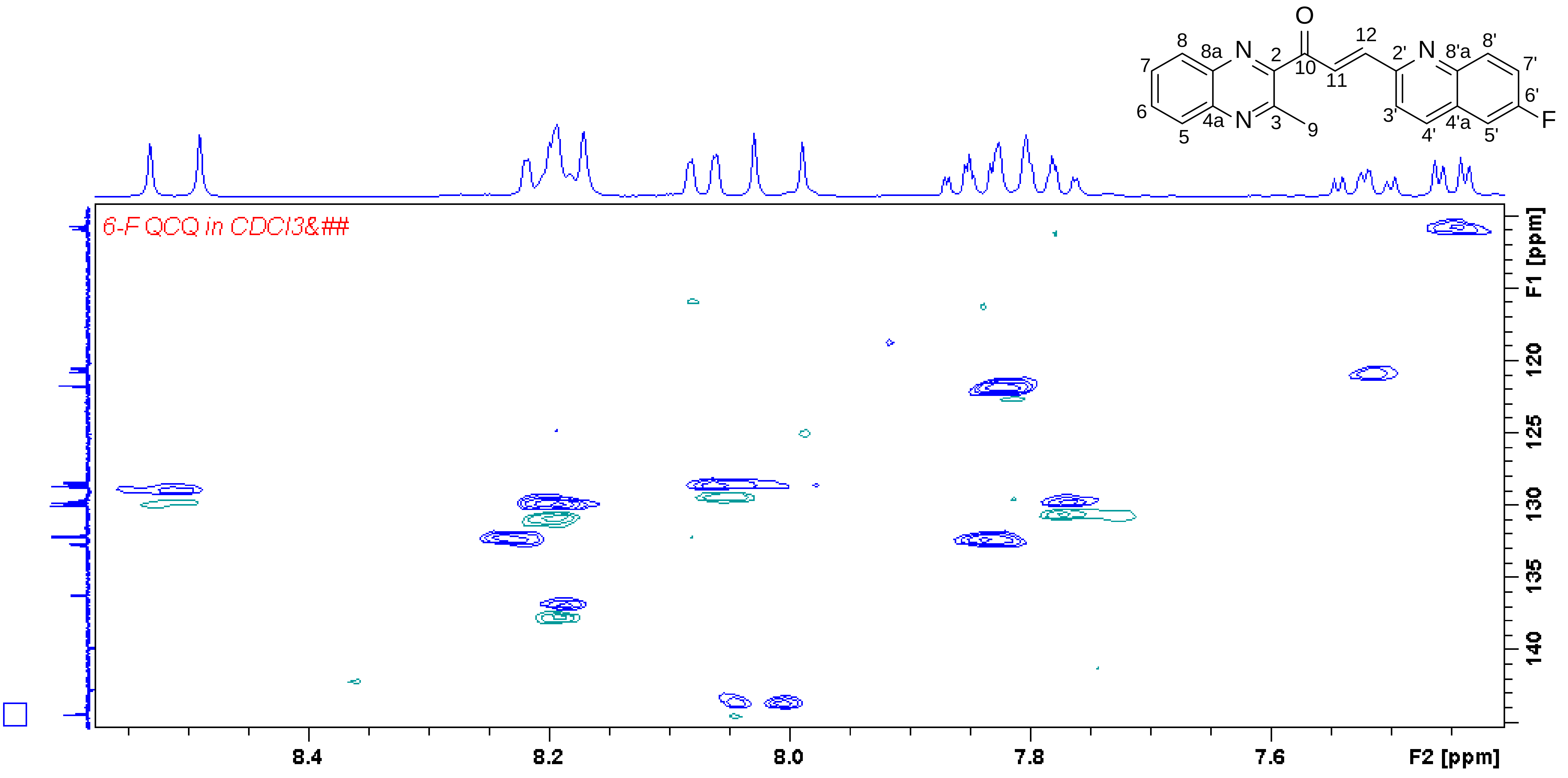
6-F QCQ in CDCl3&##
F1 [ppm]
F2 [ppm]
120
125
130
135
140
8.4
8.2
8.0
7.8
7.6
O
N
N
F
8
8a
2
10
11
12
2'
8'a
8'
7
7'
6
6'
4a
3
9
3'
4'
4'a
5'
5

HSQC of **B7e**

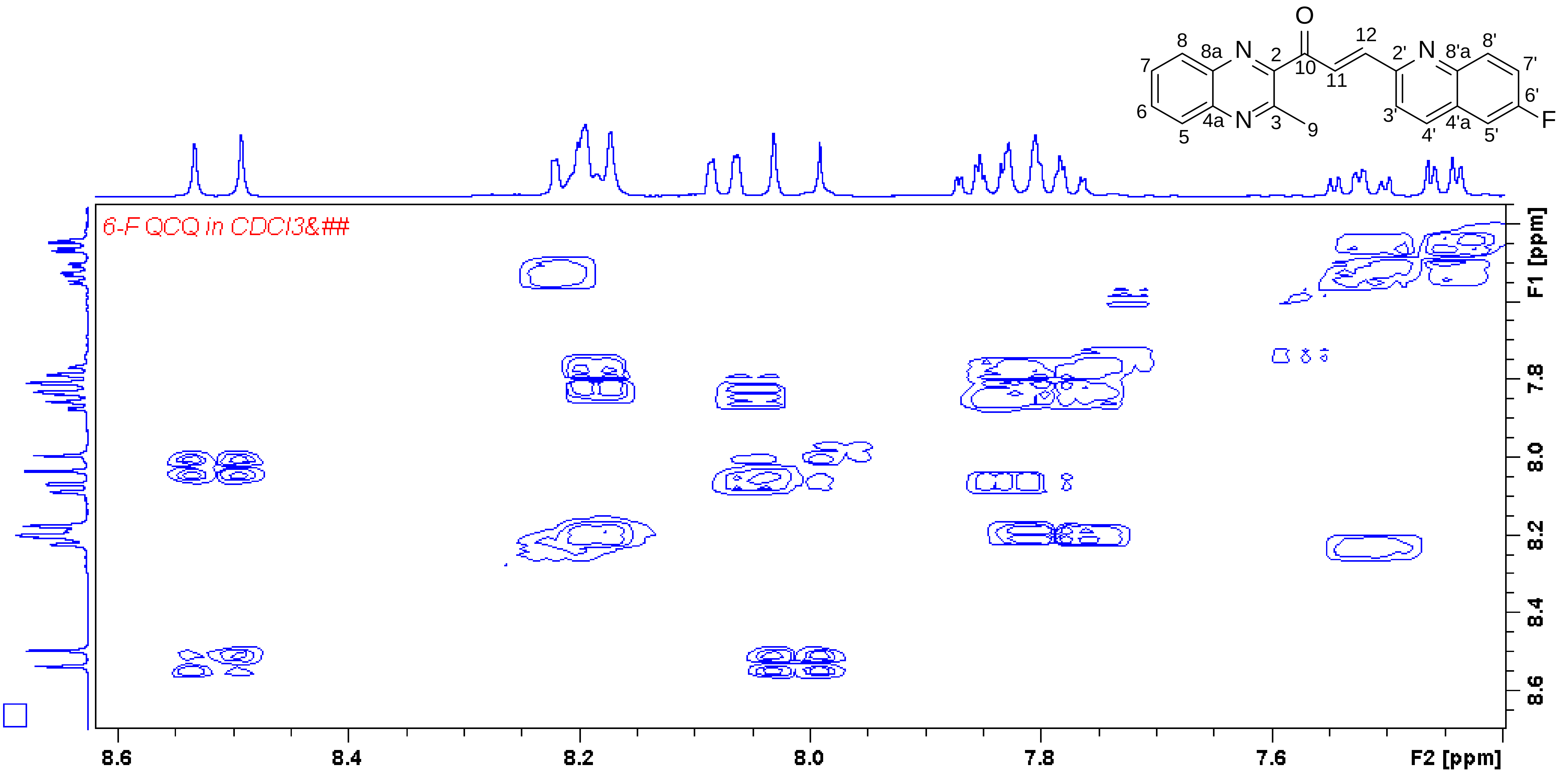

COSY of **B7e**

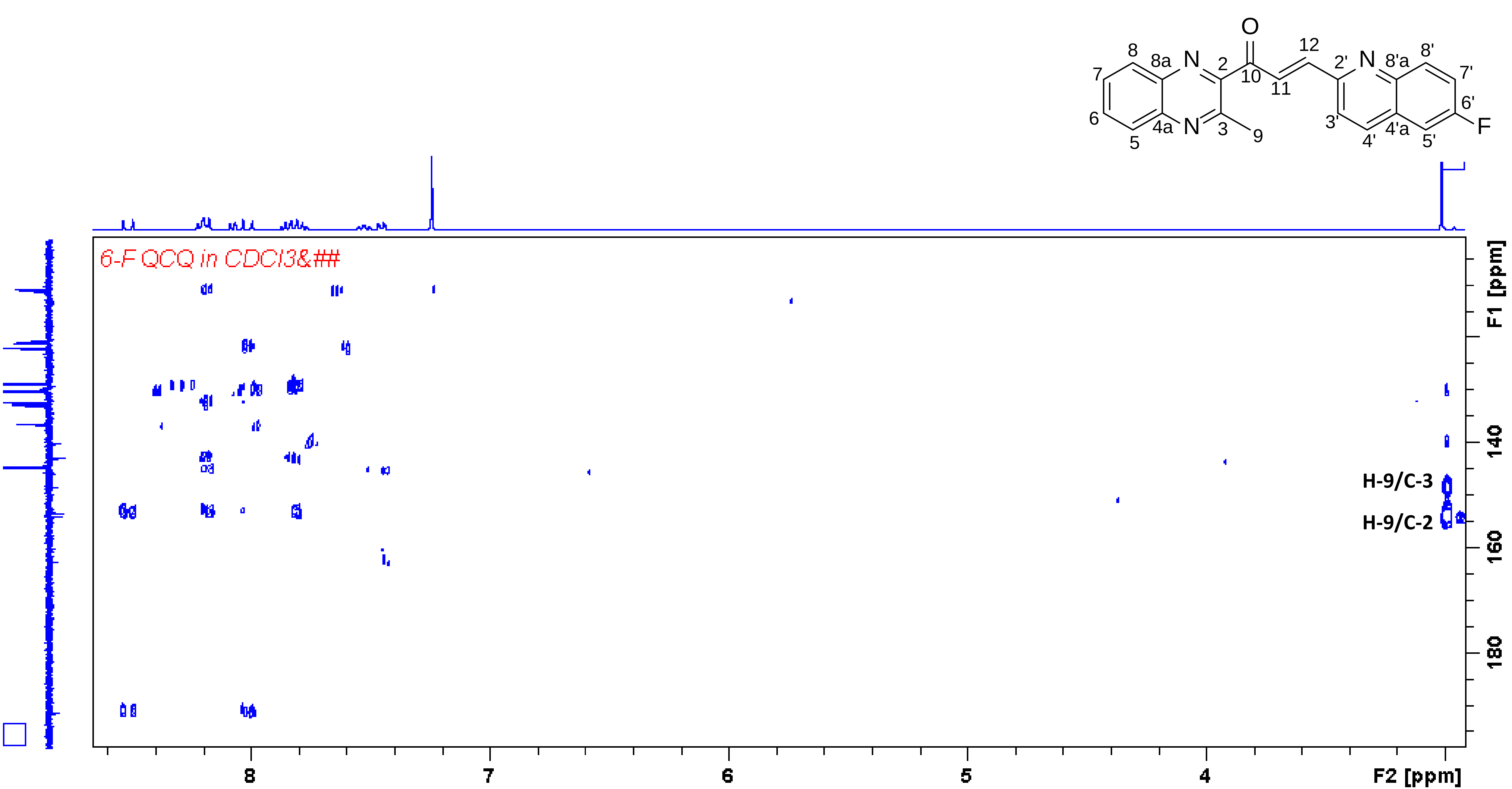

HMBC of **B7e**

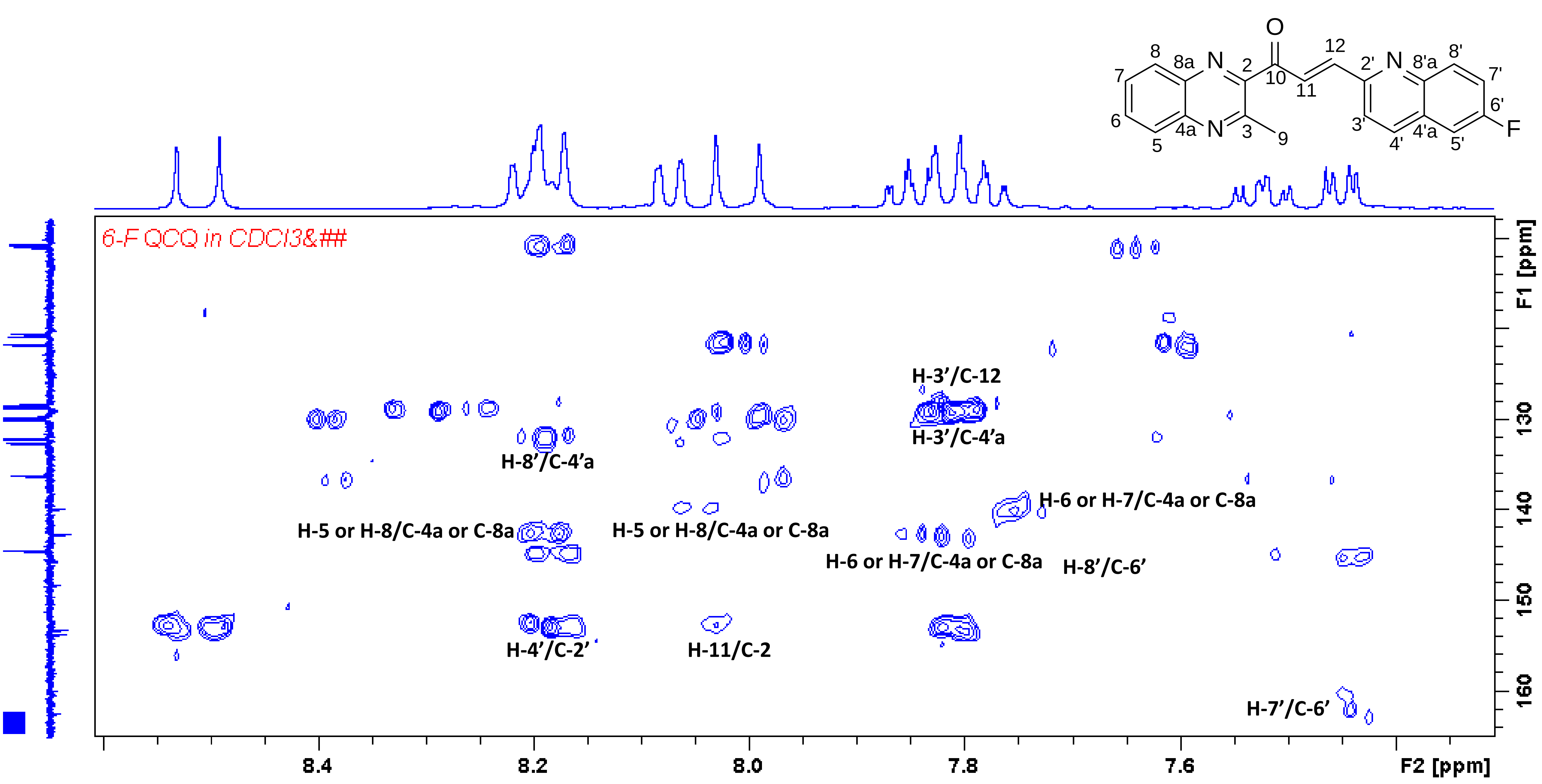

Expanded HMBC of **B7e**

Elemental Composition Report

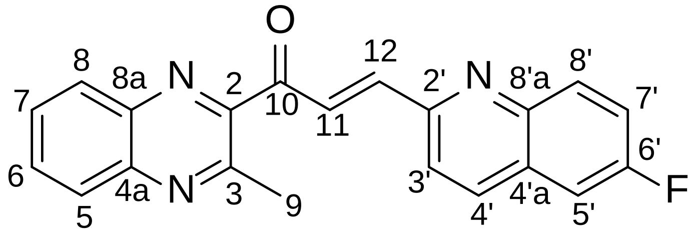

Single Mass Analysis

Tolerance = 5.0 PPM / DBE: min = -1.5, max = 100.0

Element prediction: Off

Number of isotope peaks used for i-FIT = 3

Monoisotopic Mass, Even Electron Ions

35 formula(e) evaluated with 1 results within limits (up to 20 closest results for each mass)

Elements Used:

C: 20-25 H: 10-15 N: 0-5 O: 1-5 F: 0-1

QCQ(6-F) 23 (0.742) Cm (1:61)

TOF MS AP+

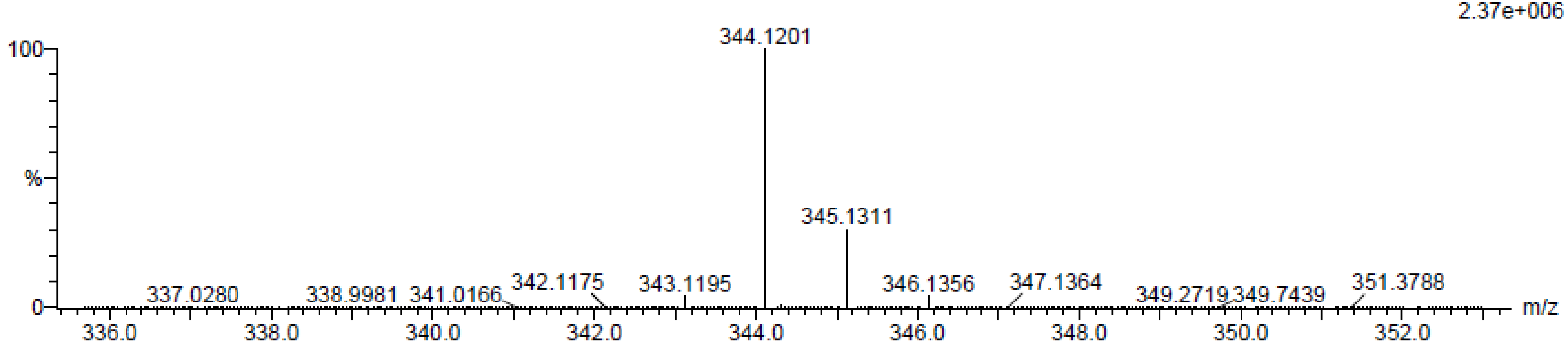

Minimum:				-1.5			
Maximum:		5.0	5.0	100.0			
Mass	Calc. Mass	mDa	PPM	DBE	i-FIT	i-FIT (Norm)	Formula
344.1201	344.1199	0.2	0.6	15.5	706.1	0.0	C21 H15 N3 O F

High resolution mass spectrum of **B7e**

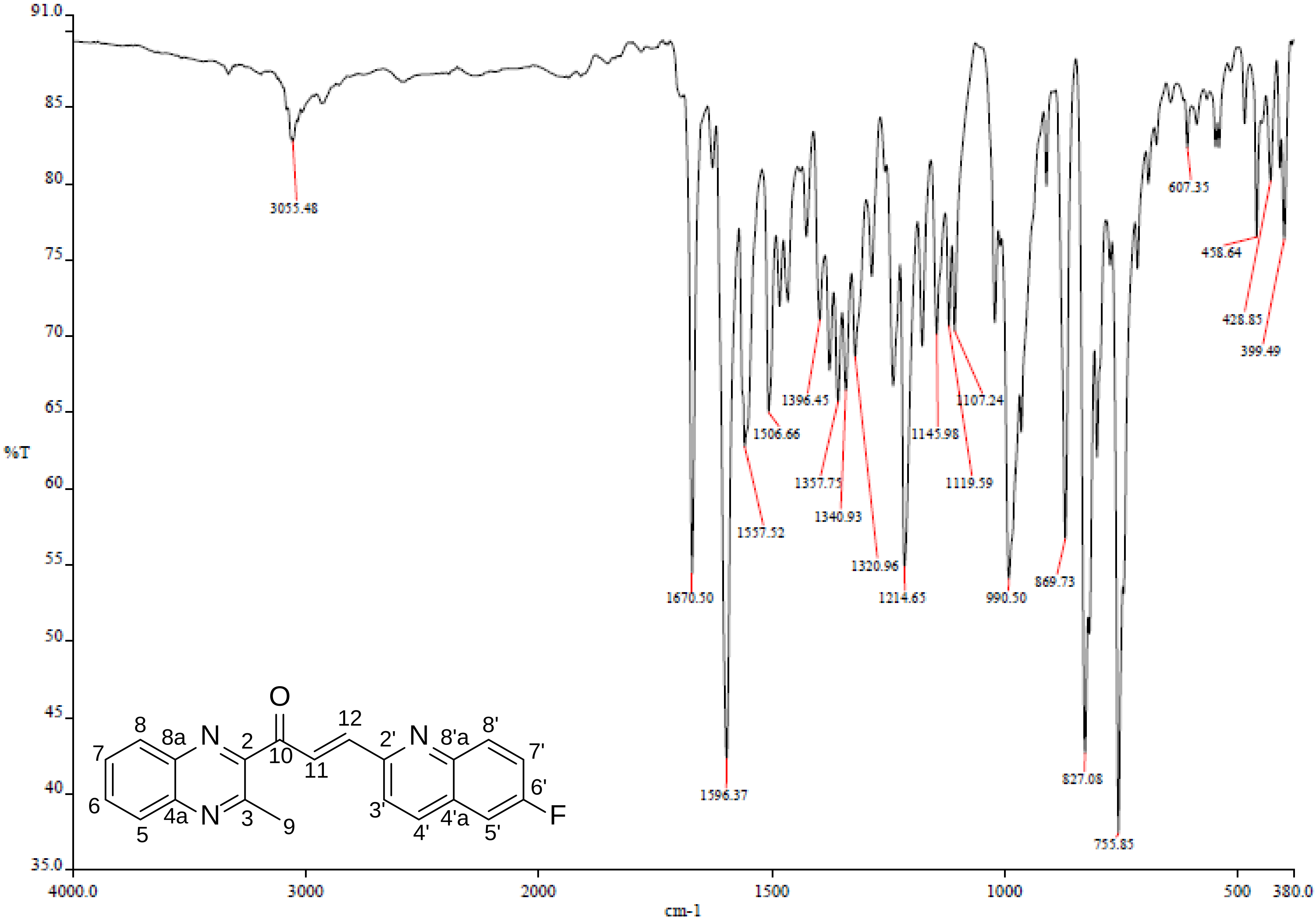

FTIR spectrum of **B7e**

Overlay Spectrum Graph Report

06/10/2017 12:00:23 PM

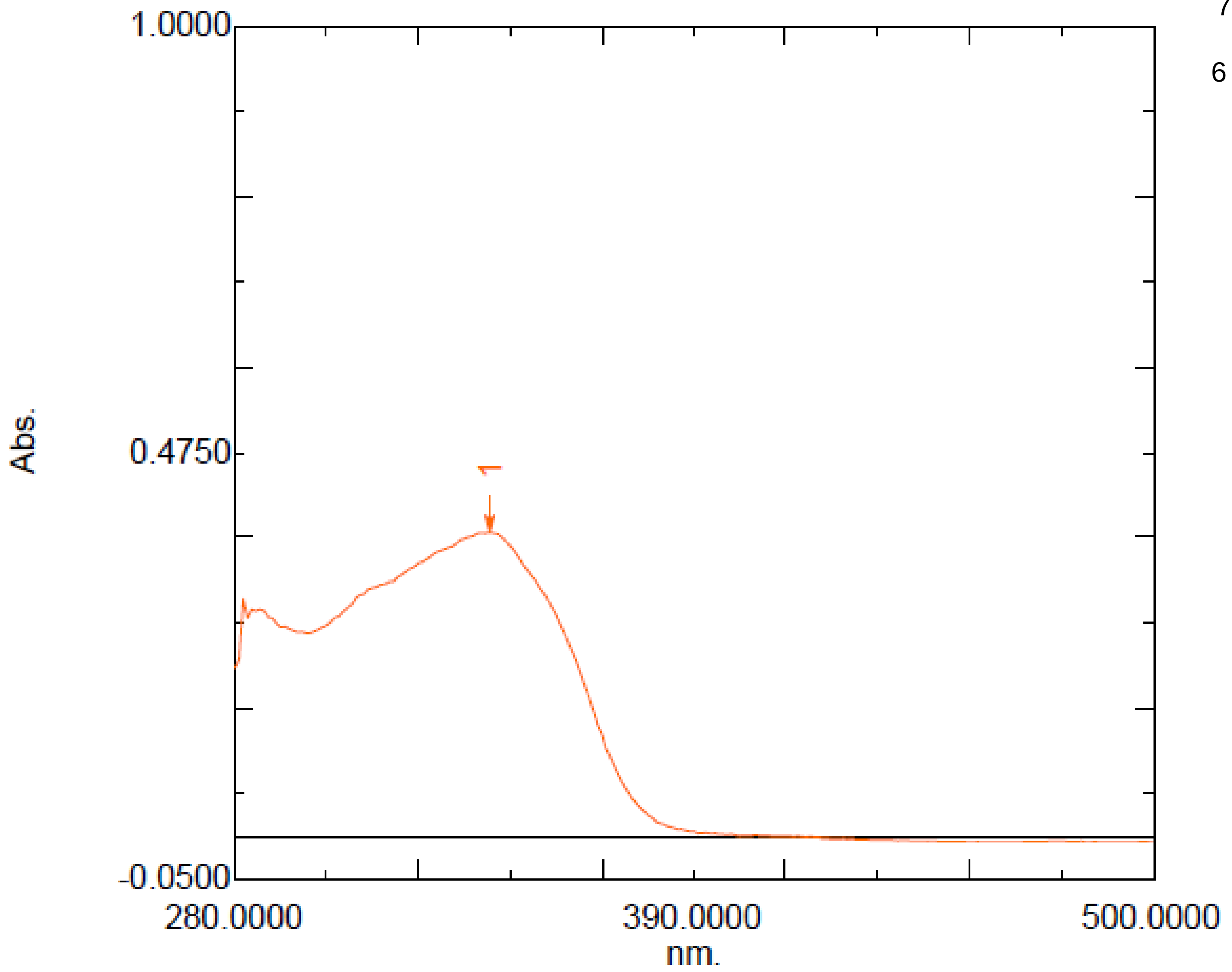

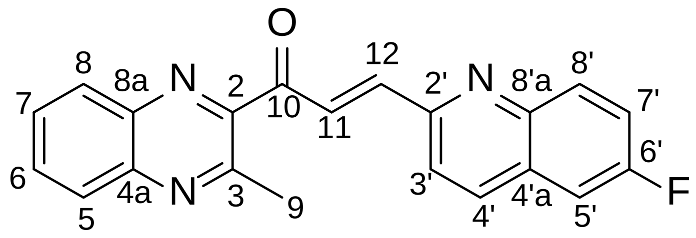

λ	absorbance	logε
339	0.3760	4.41

UV spectrum of **B7e**

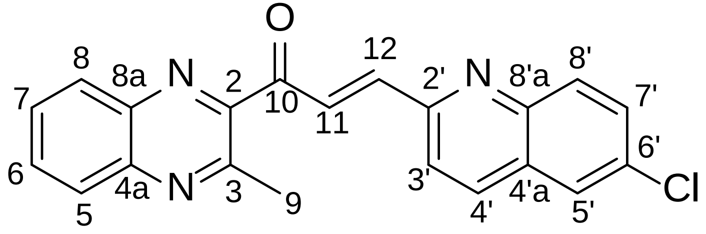

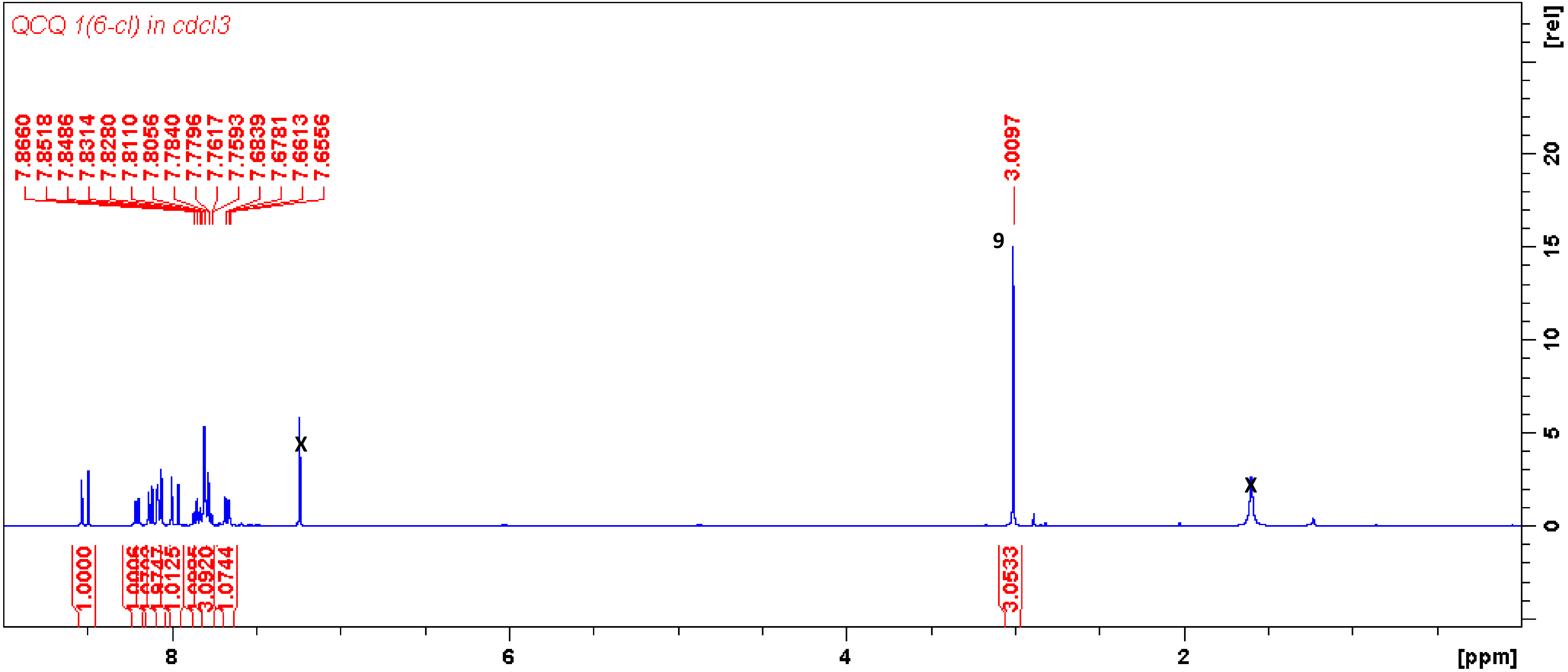

^{1}H NMR spectrum of **B7f**

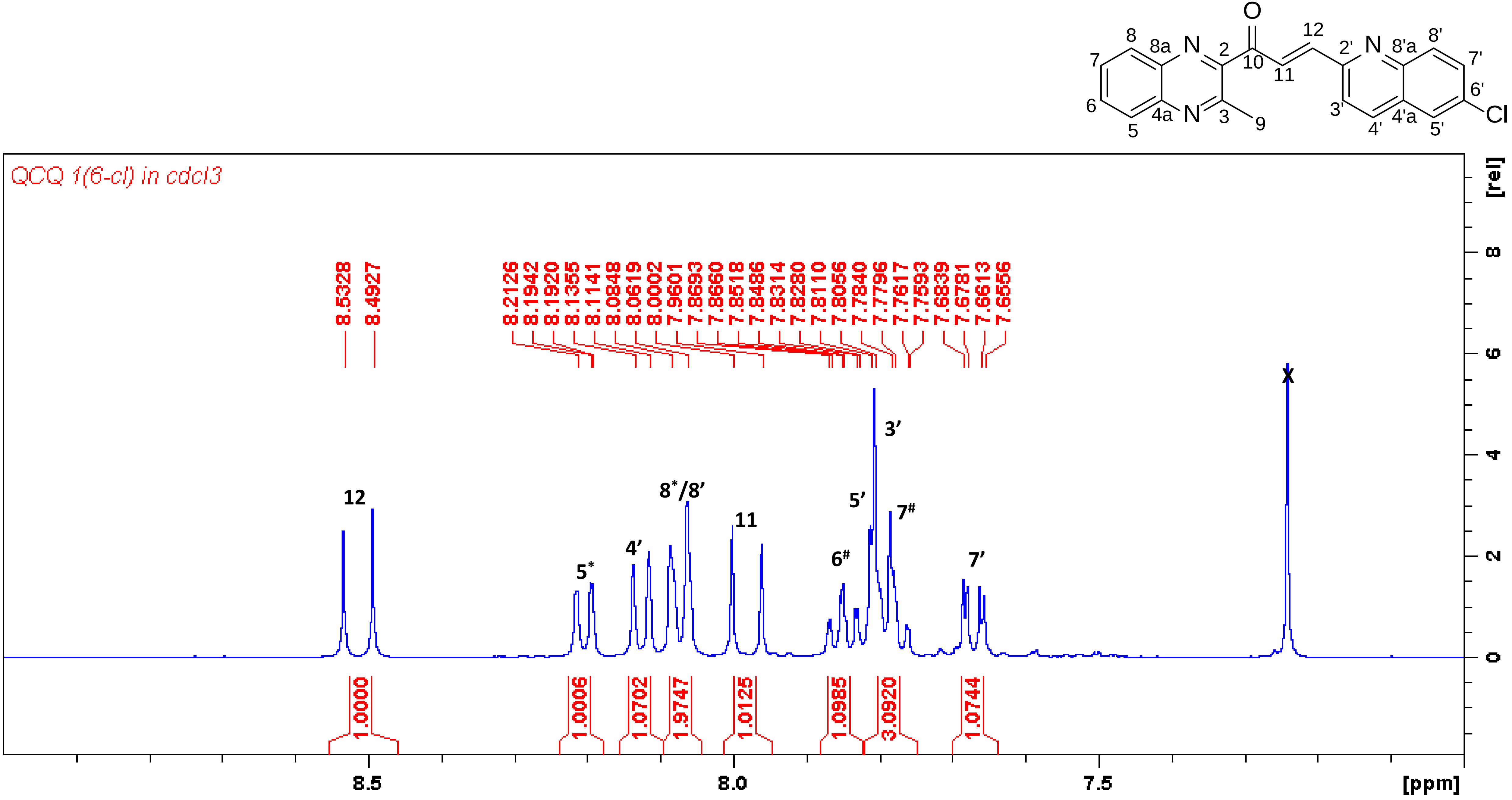

*, # Indicates assignments are interchangeable

Expanded ^{1}H NMR spectrum of **B7f**

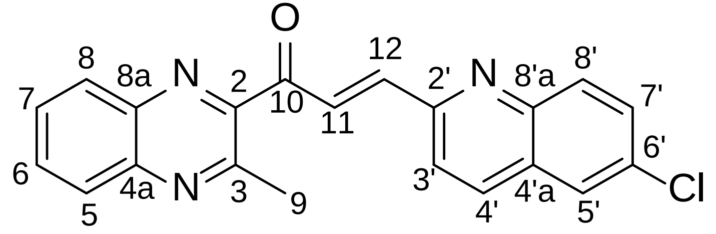

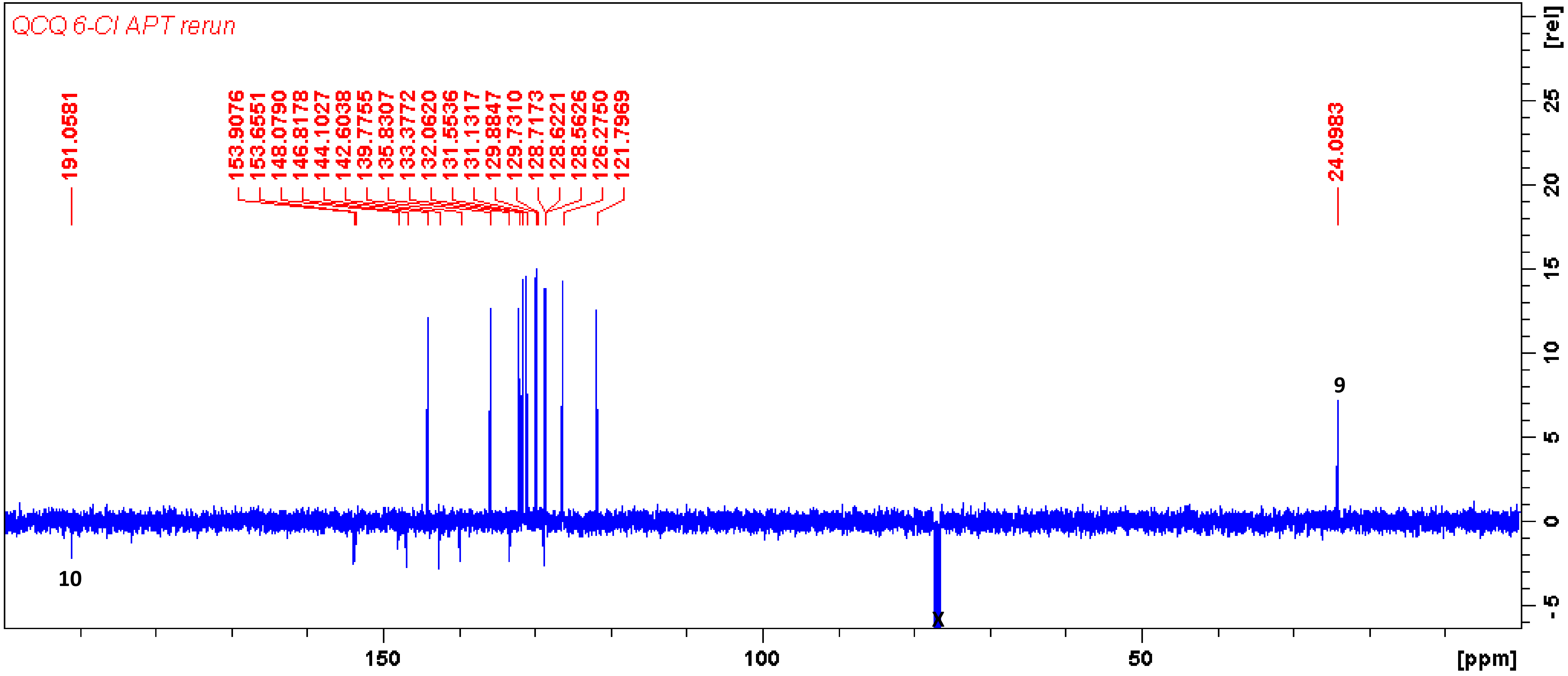

^{13}C NMR spectrum of **B7f**

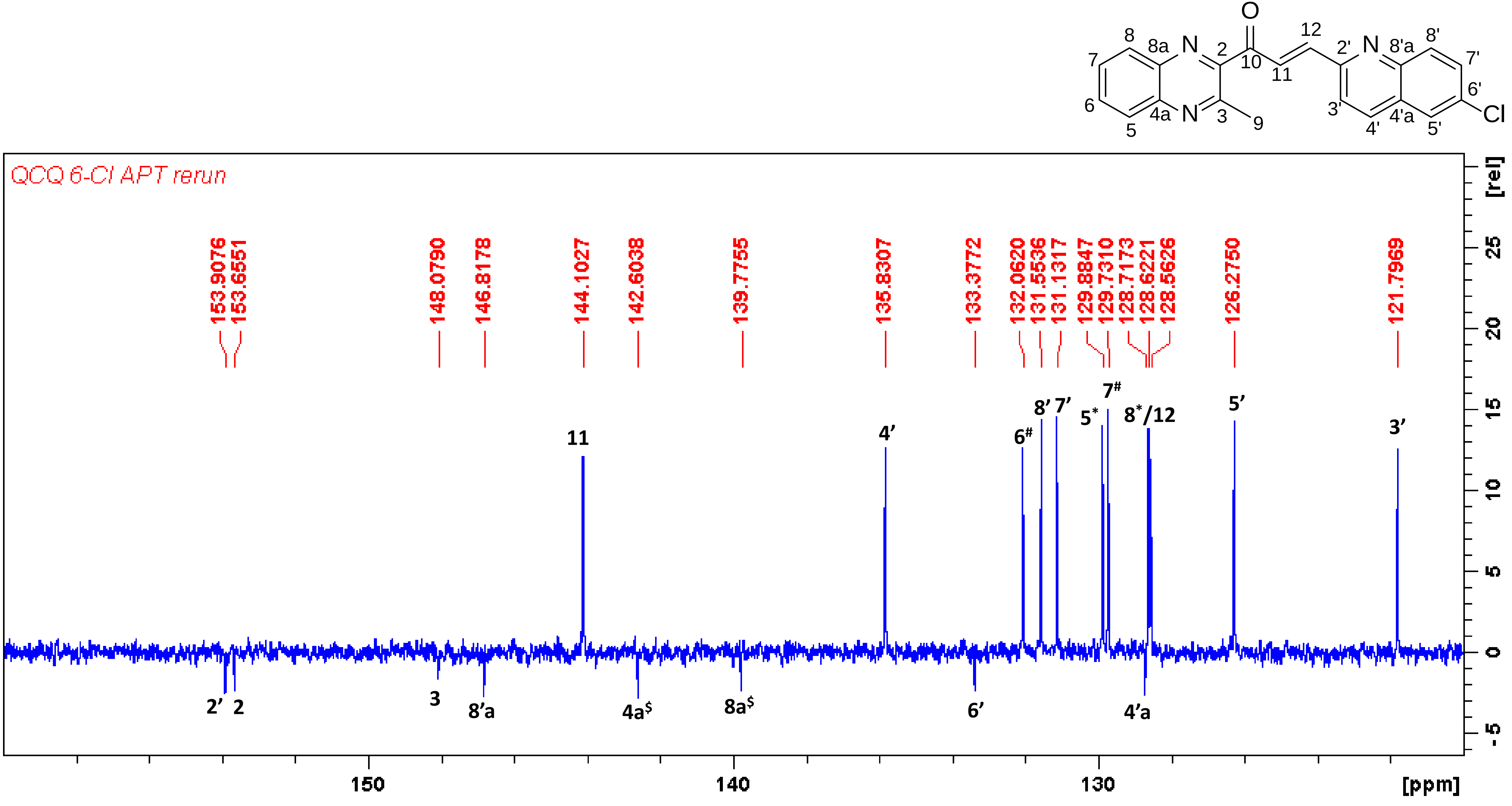

*, #, $ Indicates assignments are interchangeable

Expanded ^{13}C NMR spectrum of **B7f**

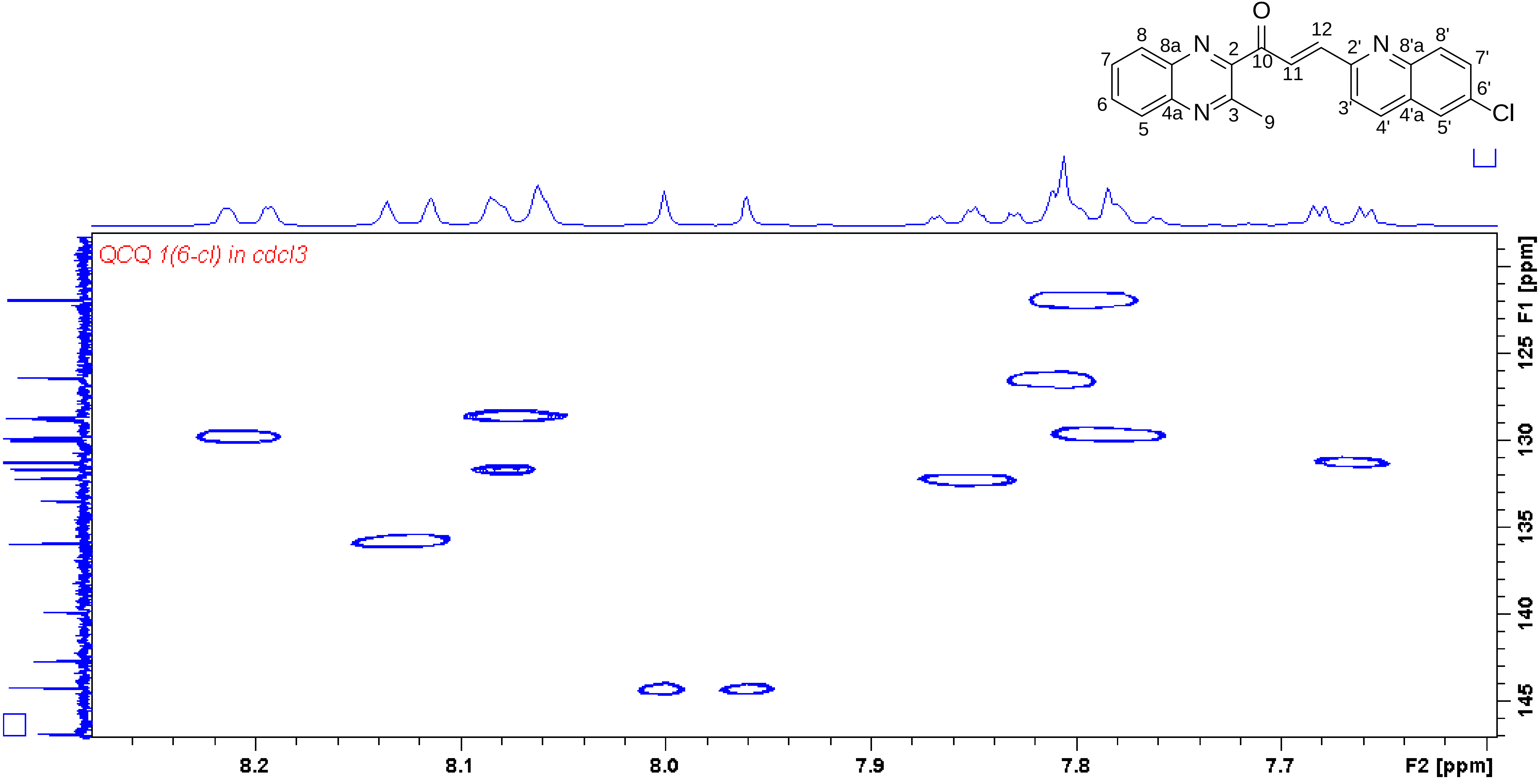
QCQ 1(6-cl) in cdcl3
F1 [ppm]
F2 [ppm]
8.2
8.1
8.0
7.9
7.8
7.7
125
130
135
140
145

HSQC of **B7f**

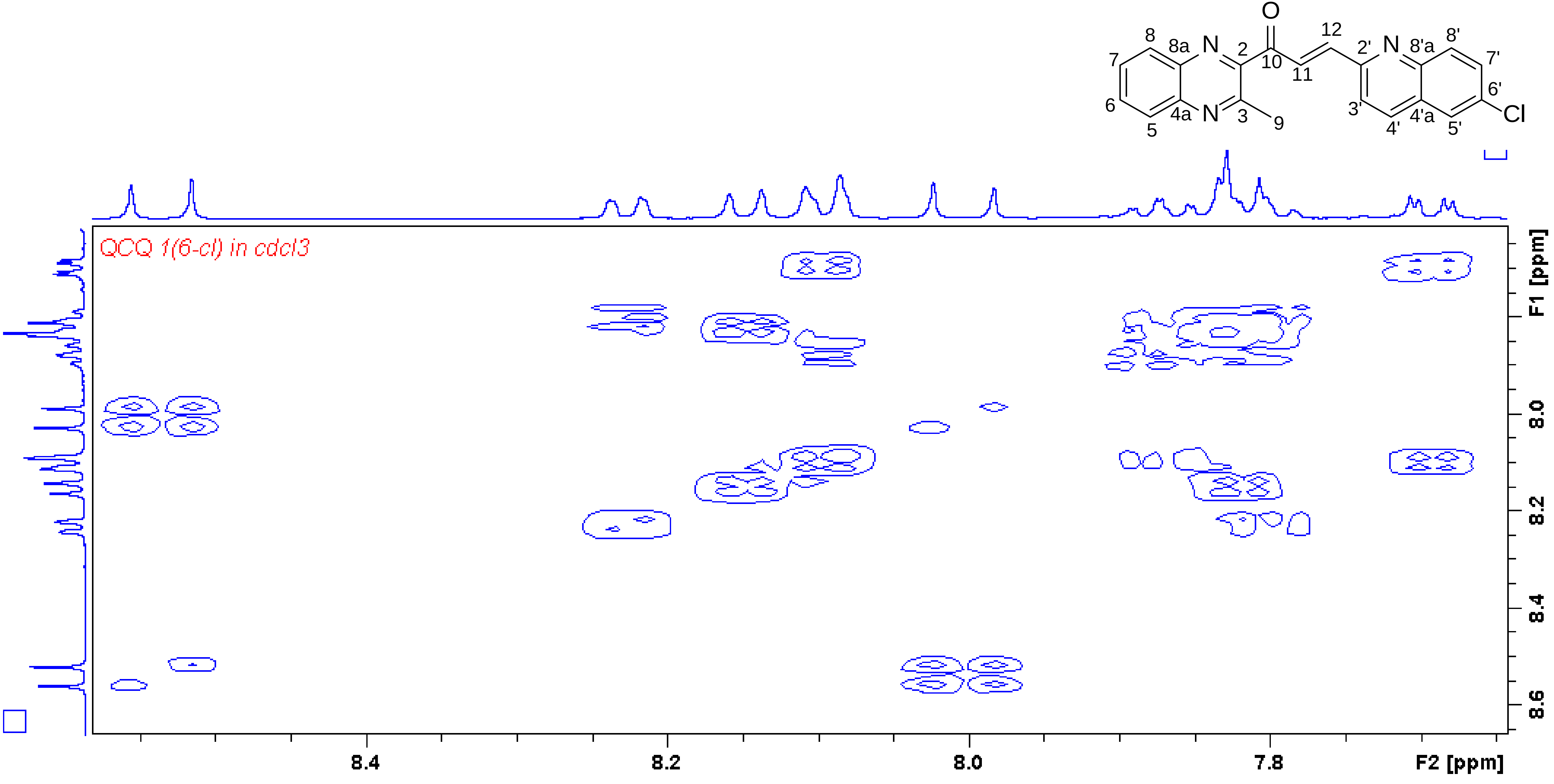

COSY of **B7f**

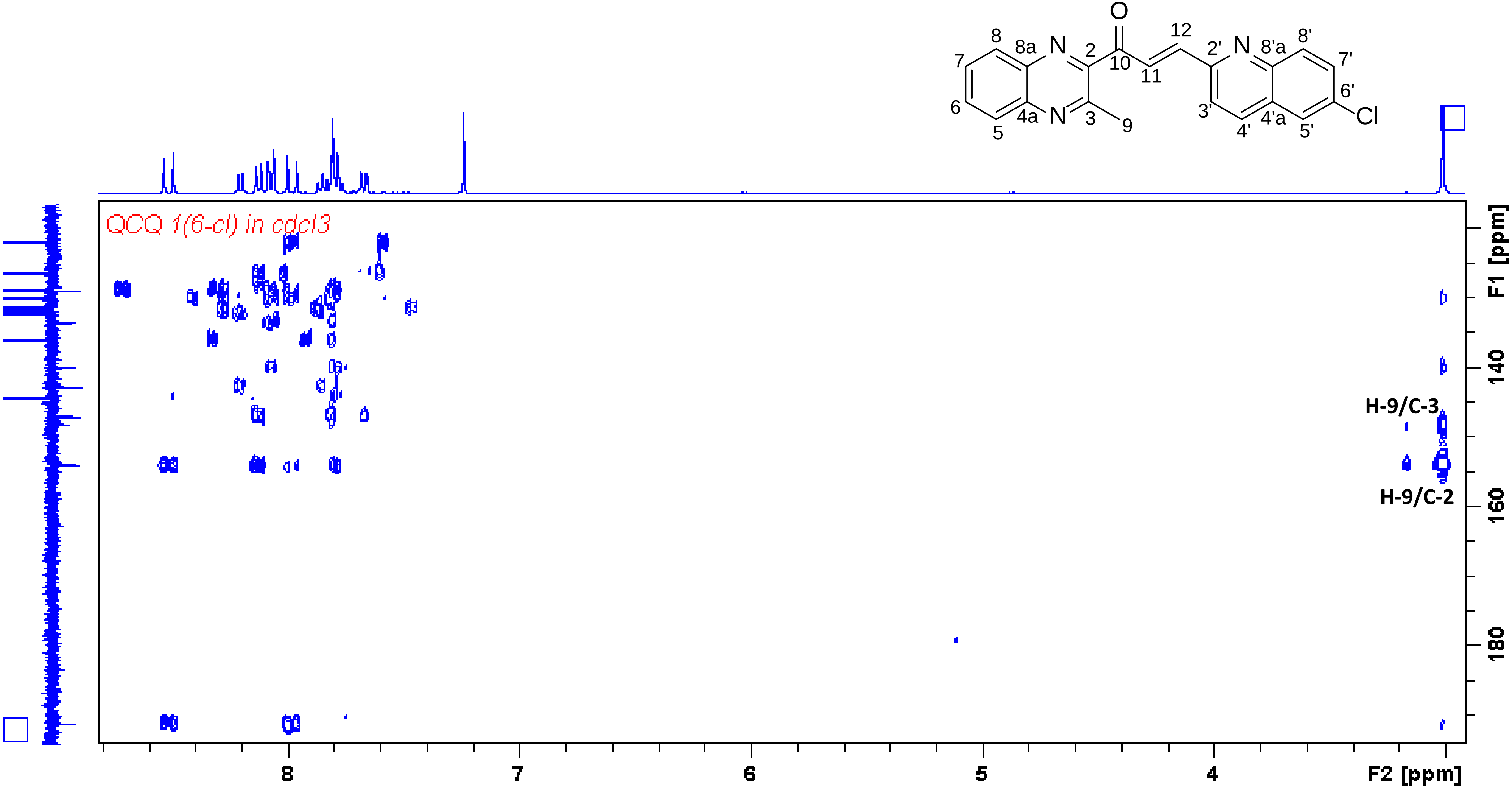

QCQ 1(6-cl) in cdcl3
H-9/C-3
H-9/C-2
F1 [ppm]
F2 [ppm]
140
160
180
8
7
6
5
4
O
N
N
N
Cl

HMBC of **B7f**

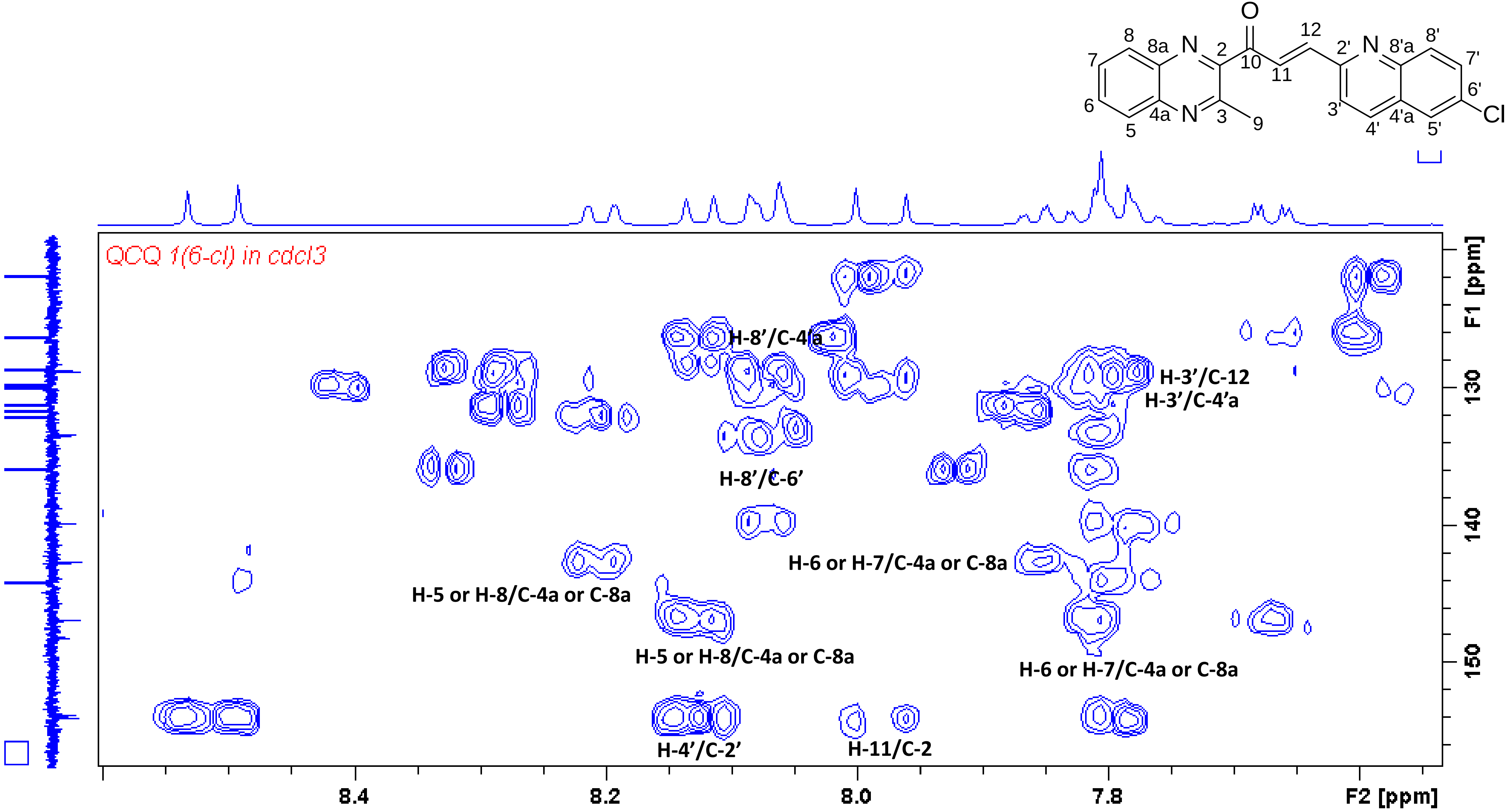

Expanded HMBC of **B7f**

Elemental Composition Report

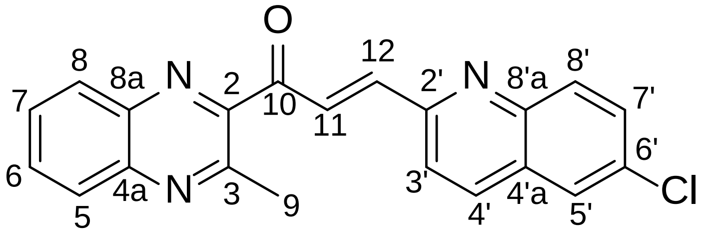

Single Mass Analysis

Tolerance = 5.0 PPM / DBE: min = -1.5, max = 100.0
Element prediction: Off
Number of isotope peaks used for i-FIT = 3

Monoisotopic Mass, Even Electron Ions
21 formula(e) evaluated with 1 results within limits (up to 20 closest results for each mass)
Elements Used:
C: 20-25 H: 10-15 N: 0-5 O: 0-5 Cl: 1-1
SSQCQ1 4 (0.102) Cm (1:61)
TOF MS AP+

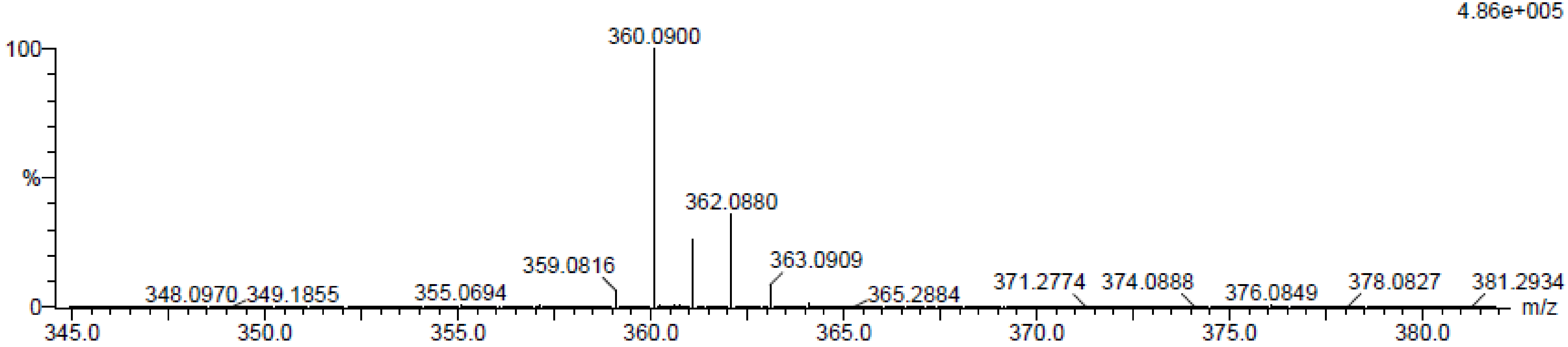

Minimum:				-1.5			
Maximum:		5.0	5.0	100.0			
Mass	Calc. Mass	mDa	PPM	DBE	i-FIT	i-FIT (Norm)	Formula
360.0900	360.0904	-0.4	-1.1	15.5	707.0	0.0	C21 H15 N3 O Cl

High resolution mass spectrum of **B7f**

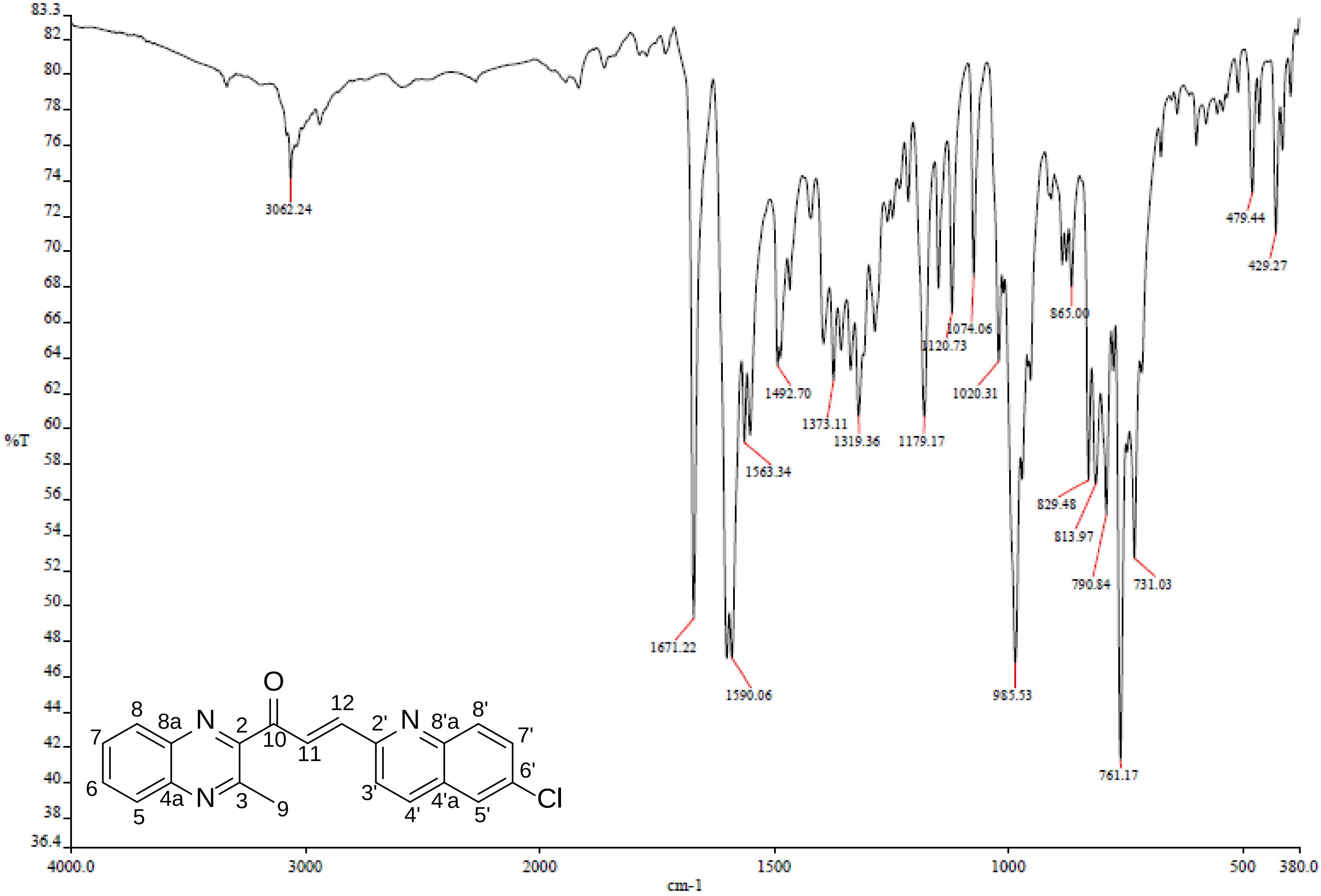

FTIR spectrum of **B7f**

Overlay Spectrum Graph Report

06/10/2017 11:59:31 AM

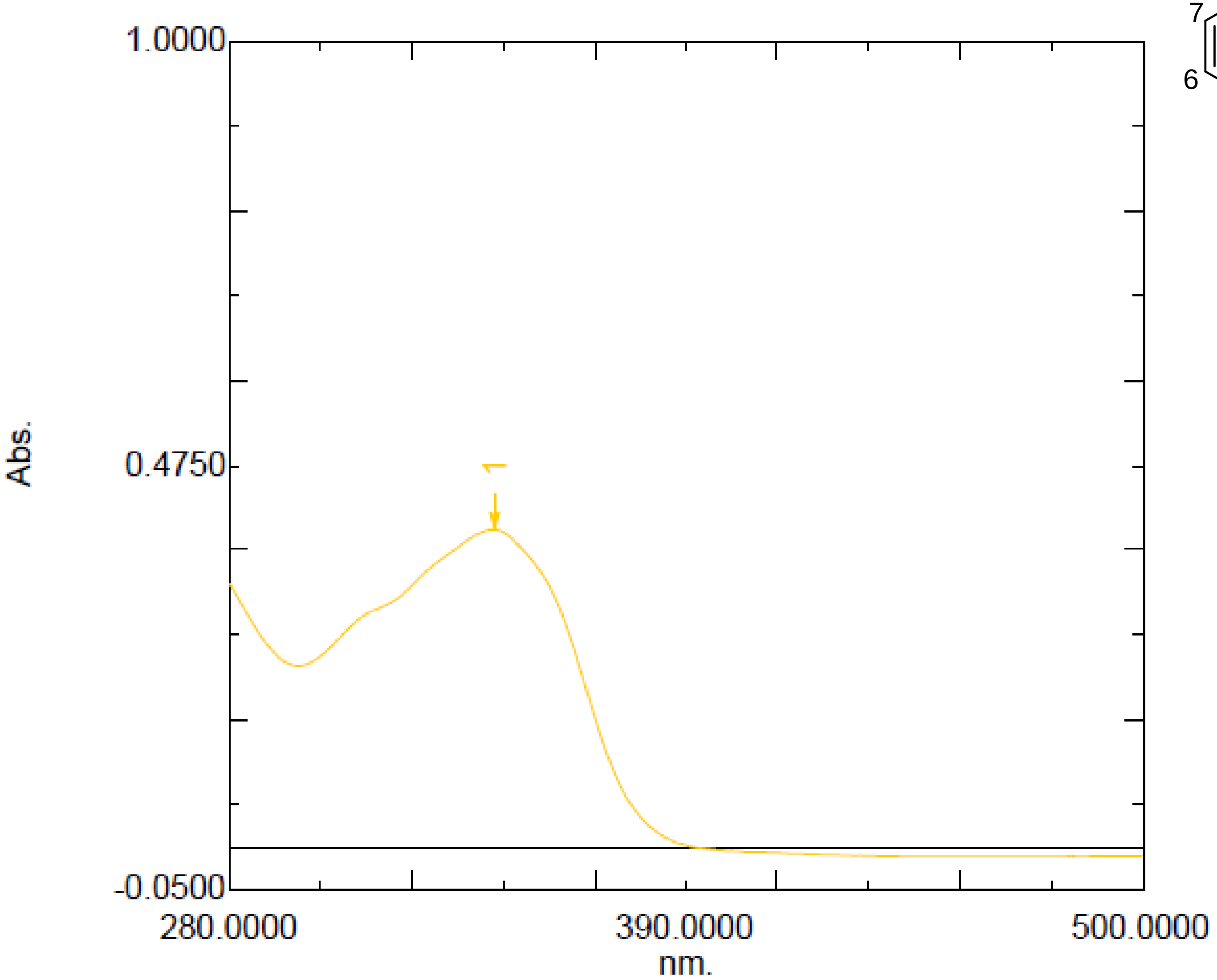

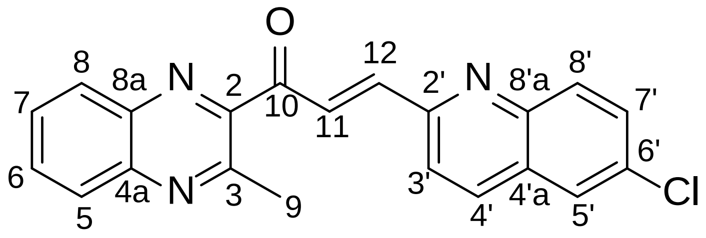

λ	absorbance	logε
344	0.3954	4.45

UV spectrum of **B7f**

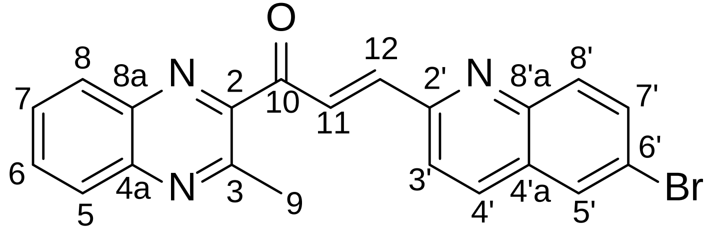

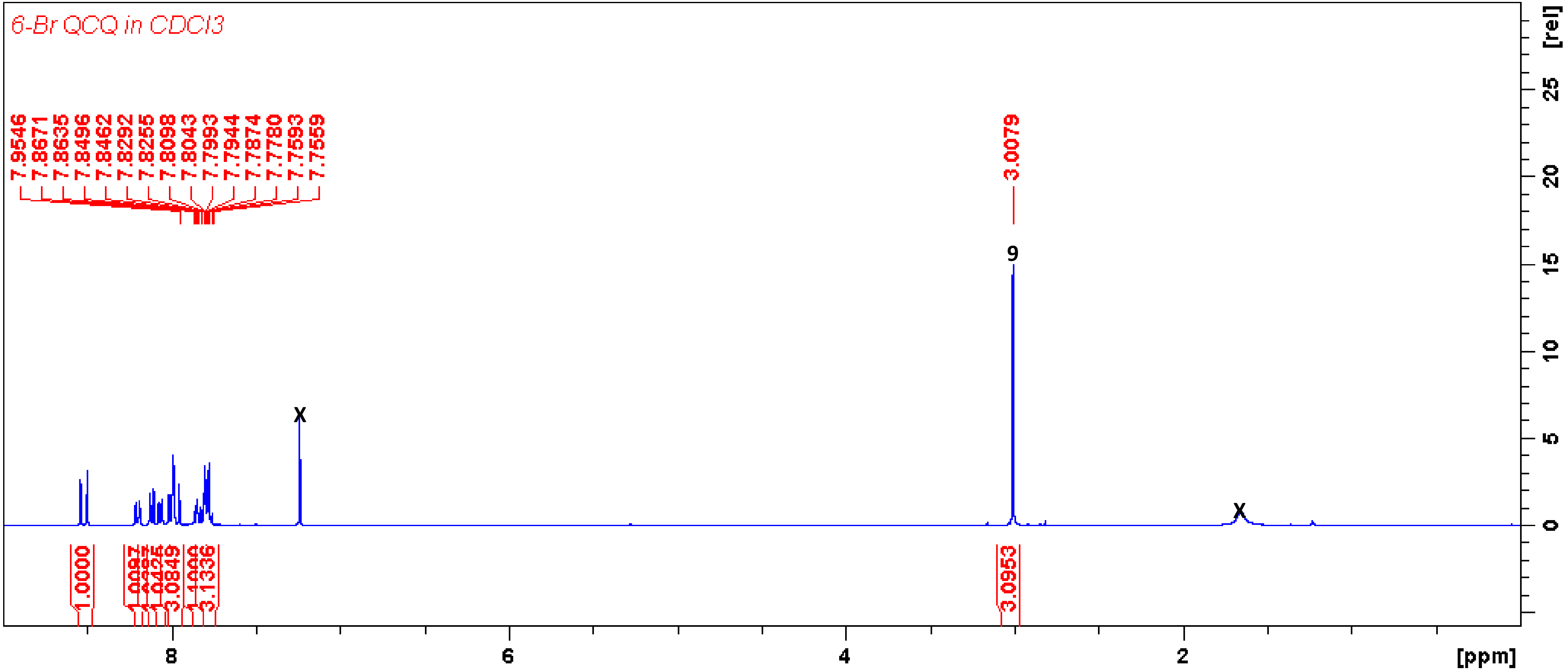

^{1}H NMR spectrum of **B7g**

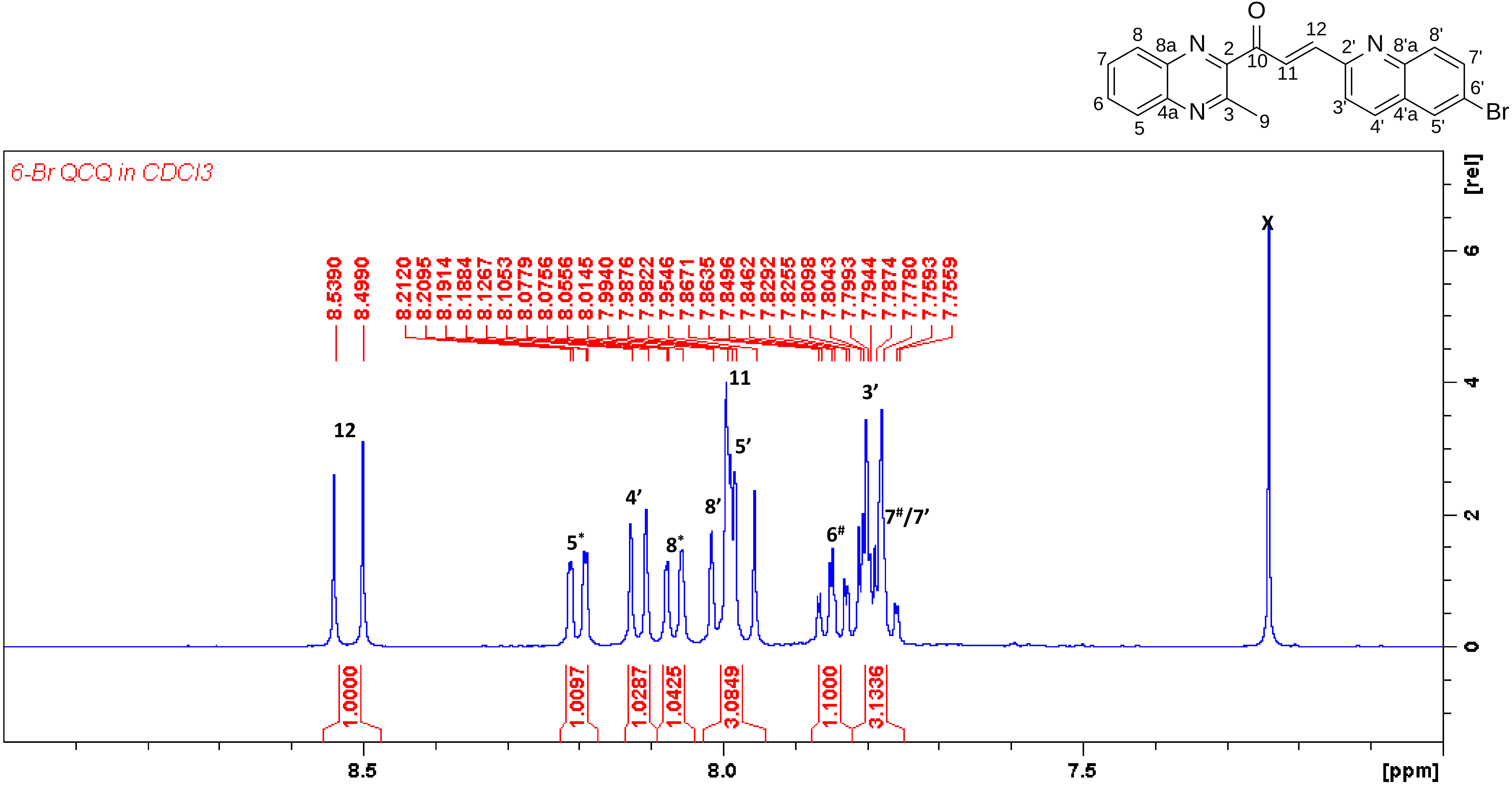

*, # Indicates assignments are interchangeable

Expanded ^{1}H NMR spectrum of **B7g**

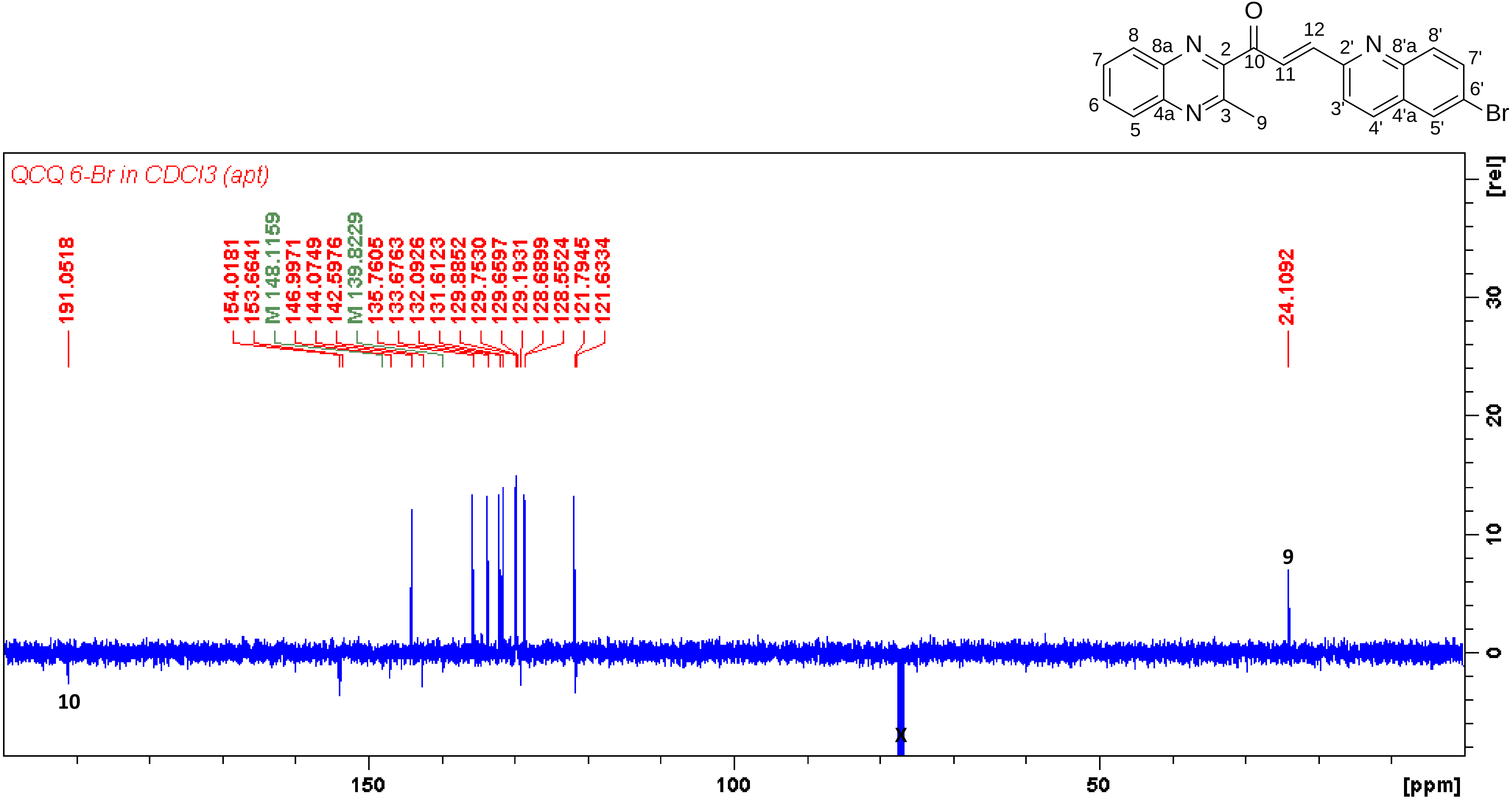

^{13}C NMR spectrum of **B7g**

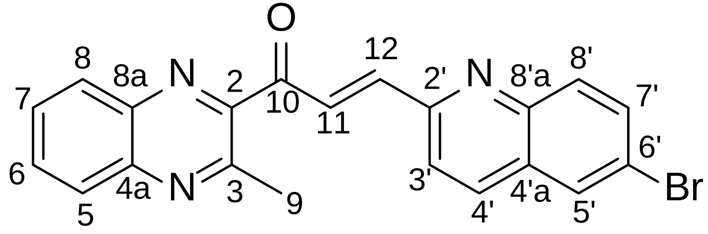

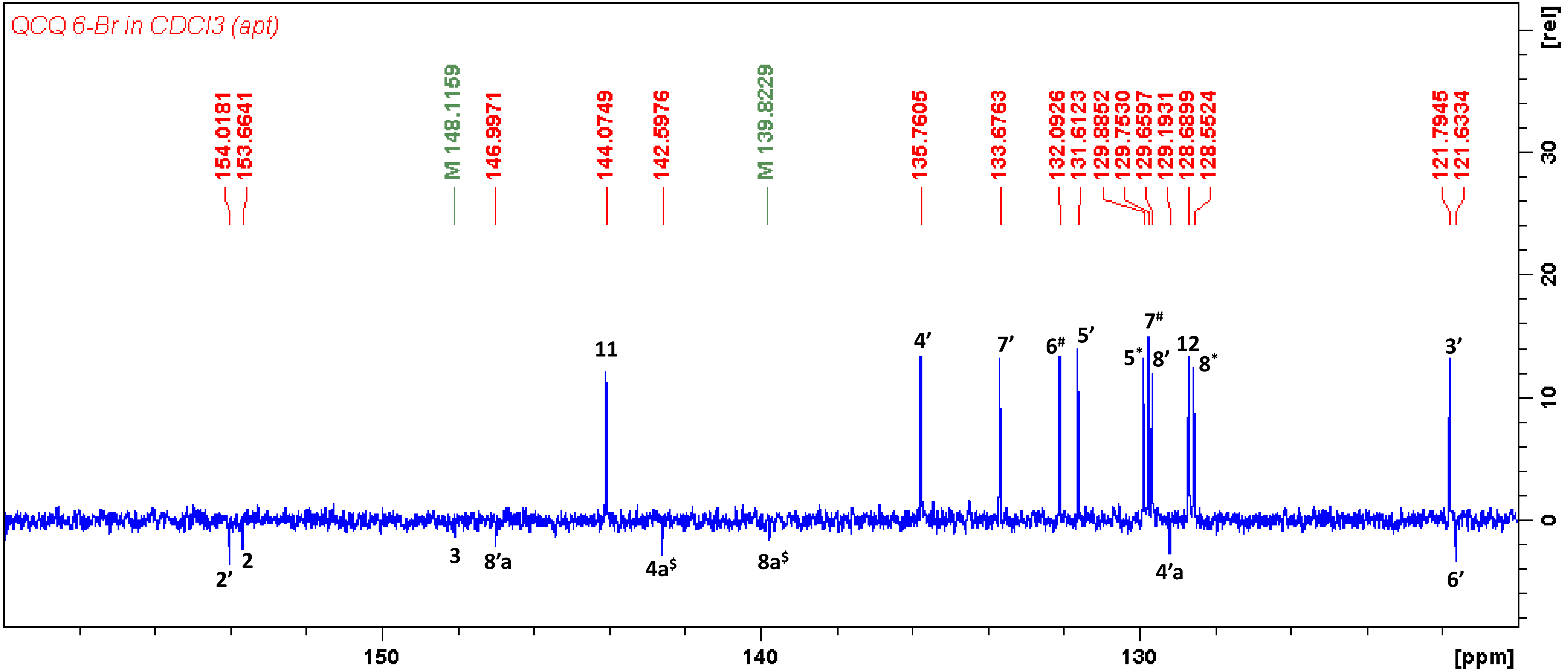

*, #, $ Indicates assignments are interchangeable

Expanded ^{13}C NMR spectrum of **B7g**

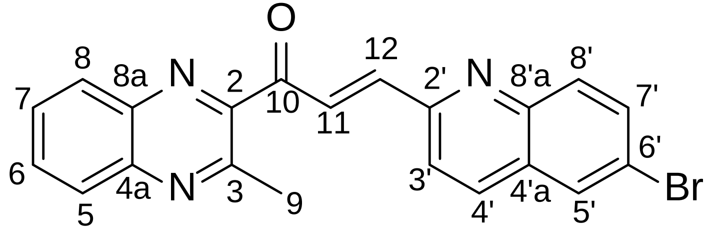
O
N
N
Br
8
8a
7
6
5
4a
2
3
9
10
11
12
2'
8'a
8'
7'
6'
5'
4'a
4'
3'

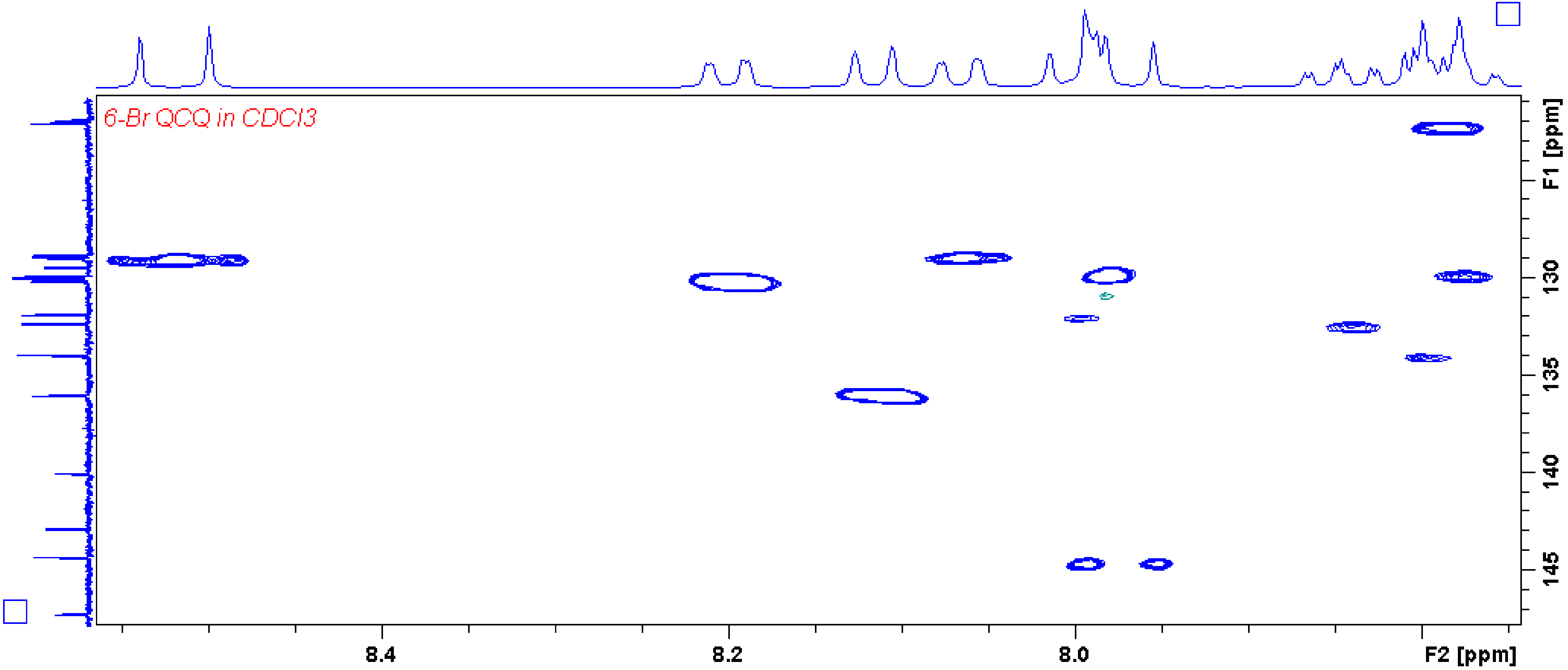
6-Br QCQ in CDCl3
F1 [ppm]
130
135
140
145
8.4
8.2
8.0
F2 [ppm]

HSQC of **B7g**

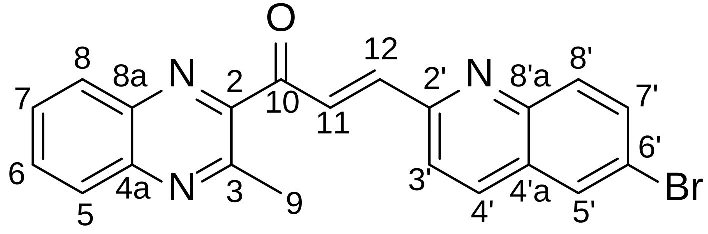
O
N
N
Br
8
7
6
5
8a
4a
2
3
9
10
11
12
2'
8'a
8'
7'
6'
5'
4'a
4'
3'

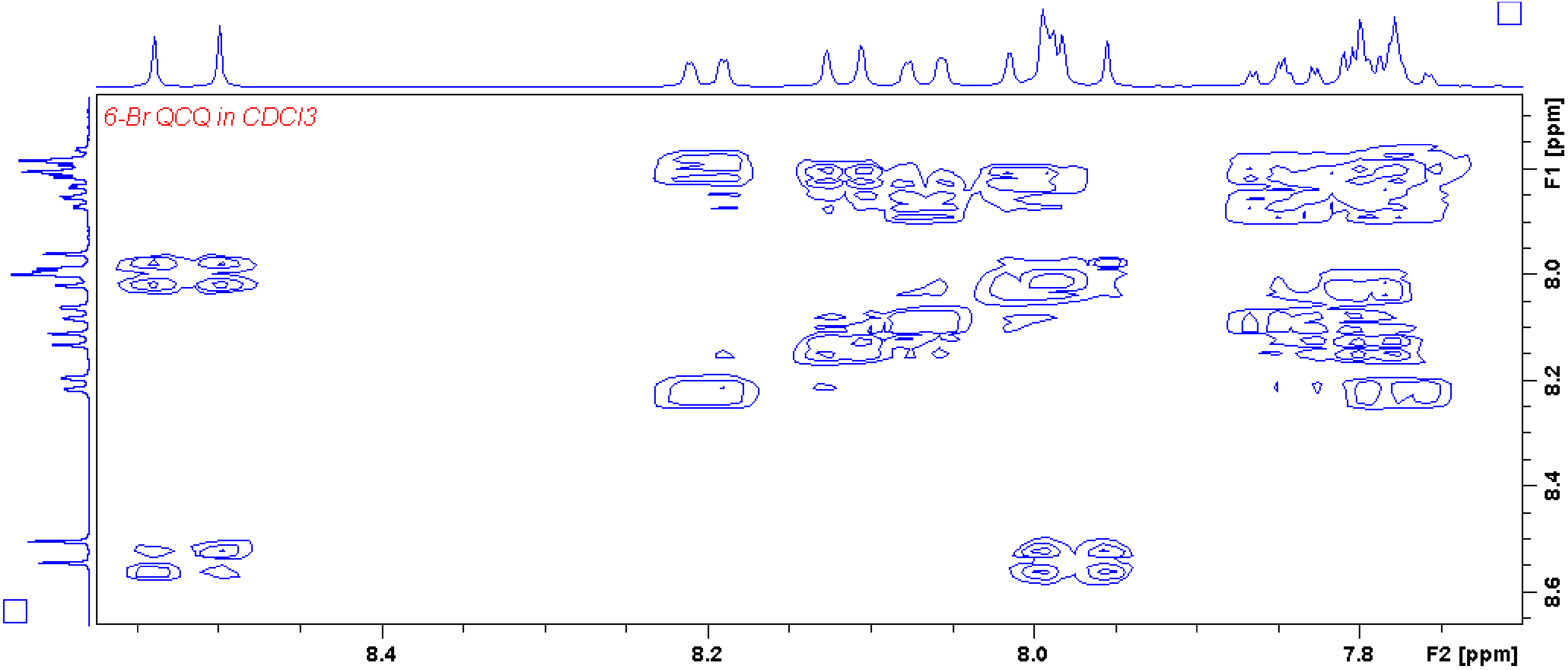
6-Br QCQ in CDCl3
F1 [ppm]
8.0
8.2
8.4
8.6
8.4
8.2
8.0
7.8
F2 [ppm]

COSY of **B7g**

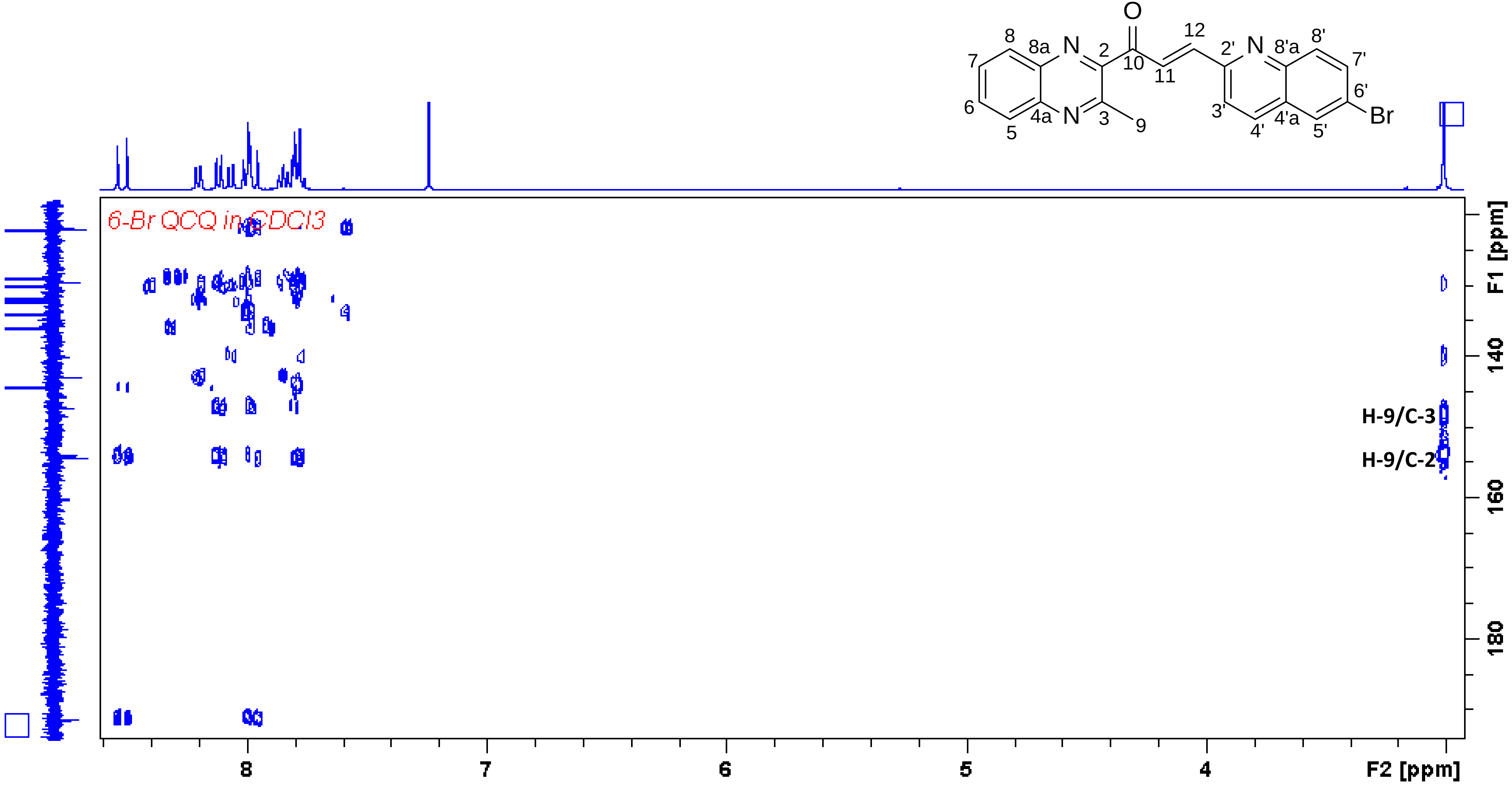

HMBC of **B7g**

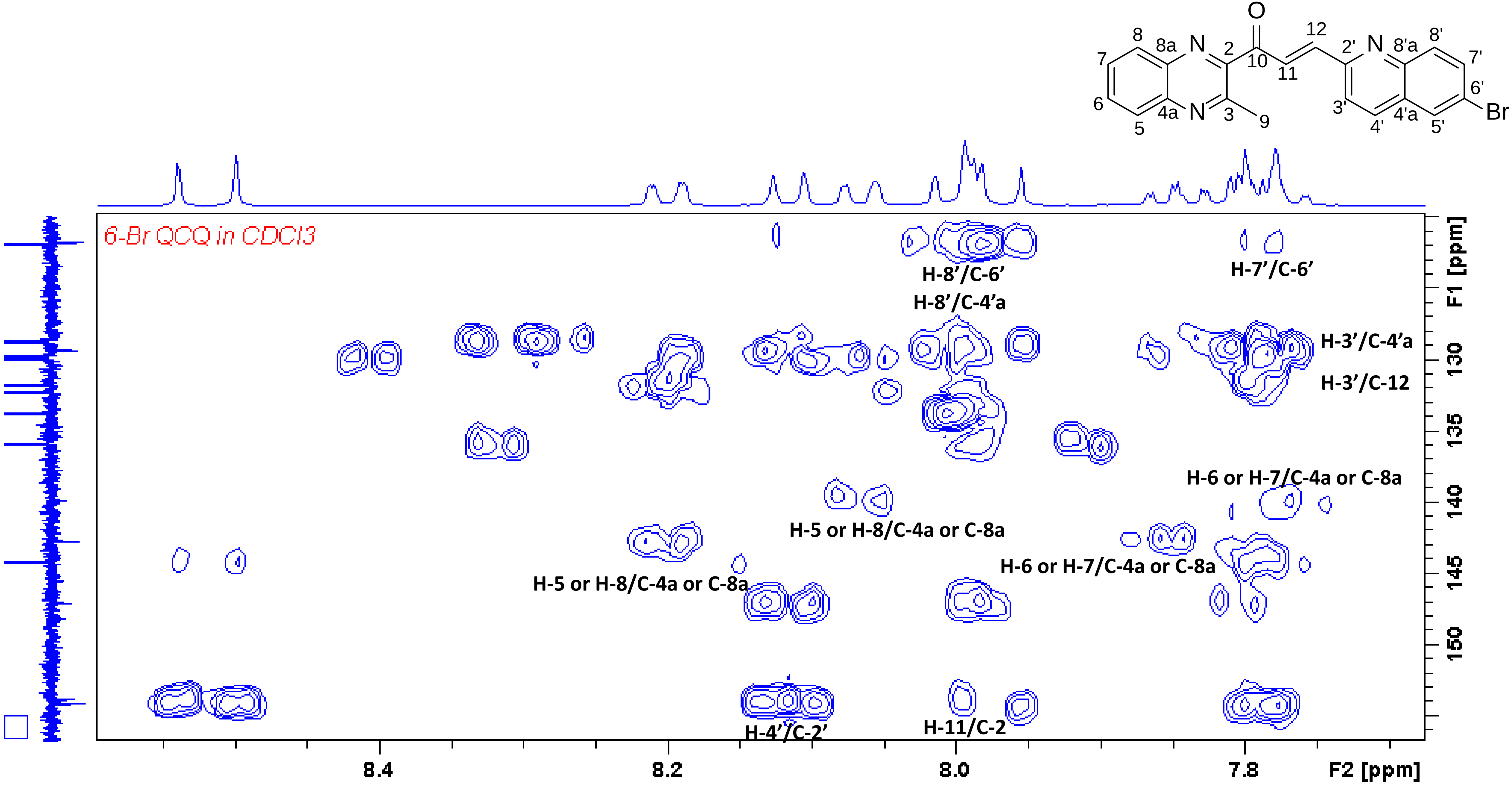

Expanded HMBC of **B7g**

Elemental Composition Report

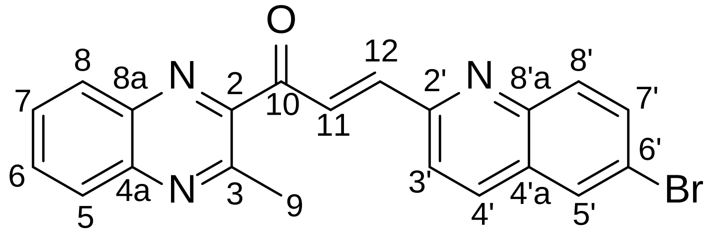

Single Mass Analysis

Tolerance = 5.0 PPM / DBE: min = -1.5, max = 100.0
Element prediction: Off
Number of isotope peaks used for i-FIT = 3

Monoisotopic Mass, Even Electron Ions
35 formula(e) evaluated with 1 results within limits (up to 20 closest results for each mass)
Elements Used:
C: 20-25 H: 10-15 N: 0-5 O: 0-5 Br: 0-1

QCQ(6-Br) 22 (0.709) Cm (1:61)
TOF MS AP+

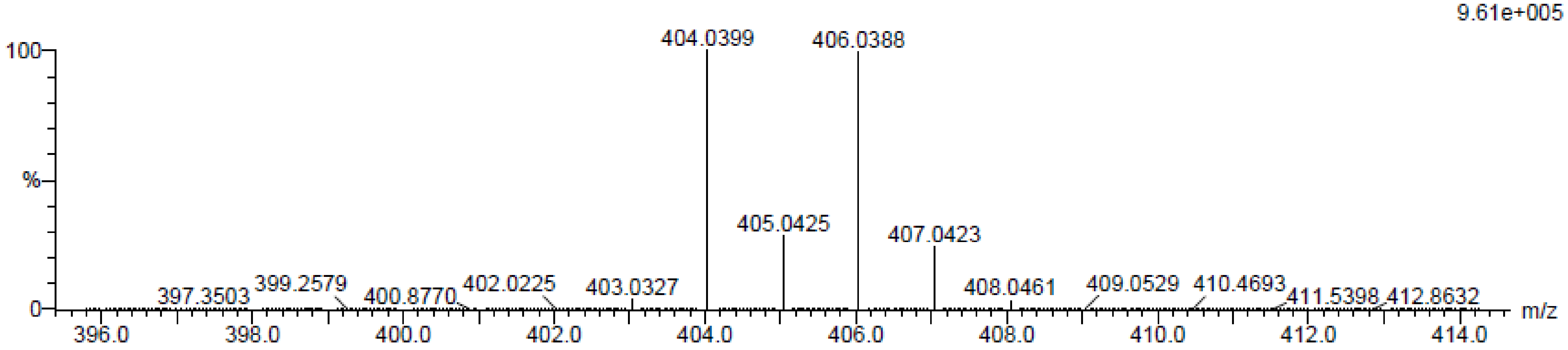

Mass	Calc. Mass	mDa	PPM	DBE	i-FIT	i-FIT (Norm)	Formula
Minimum:				-1.5			
Maximum:		5.0	5.0	100.0			
404.0399	404.0398	0.1	0.2	15.5	650.9	0.0	C21 H15 N3 O Br

High resolution mass spectrum of **B7g**

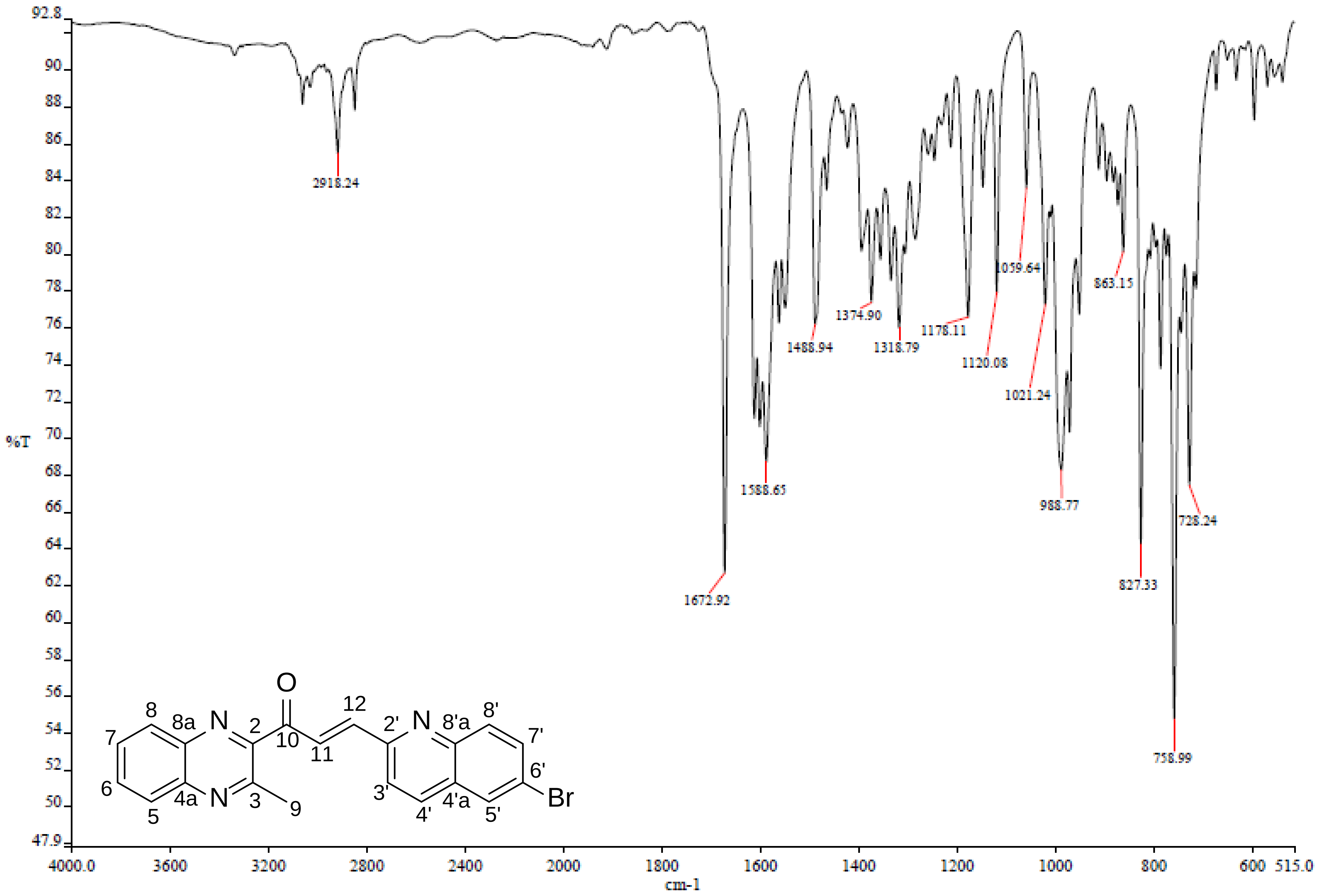

FTIR spectrum of **B7g**

Overlay Spectrum Graph Report

06/10/2017 11:58:02 AM

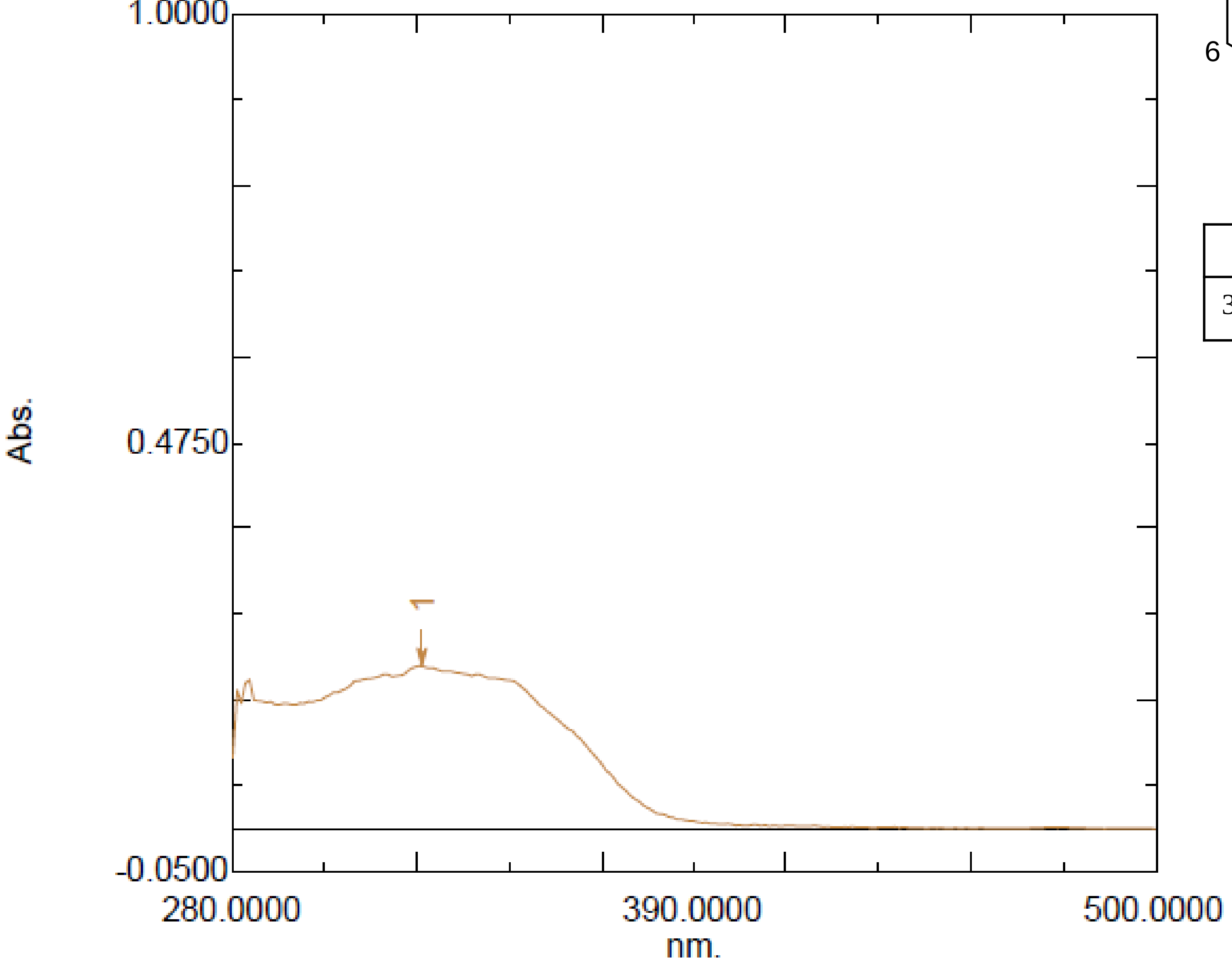

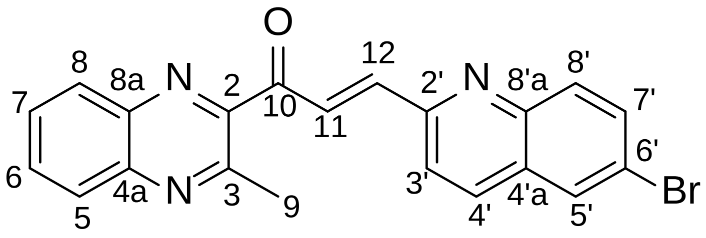

λ	absorbance	logε
325	0.2020	4.21

UV spectrum of **B7g**

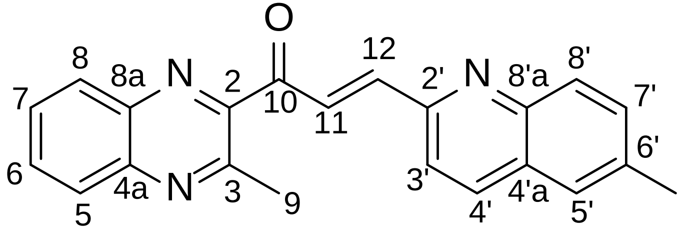

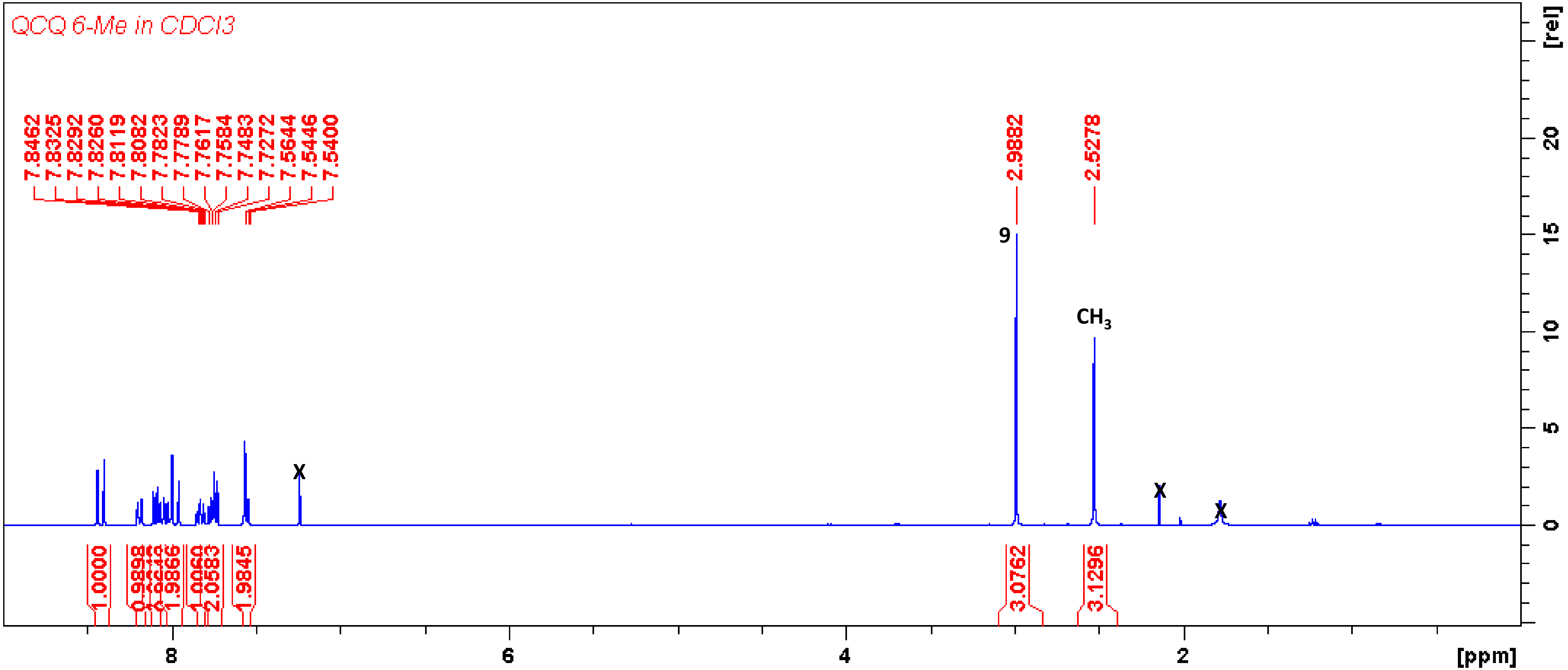

^{1}H NMR spectrum of **B7h**

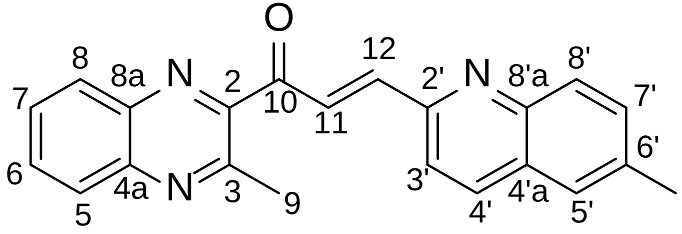

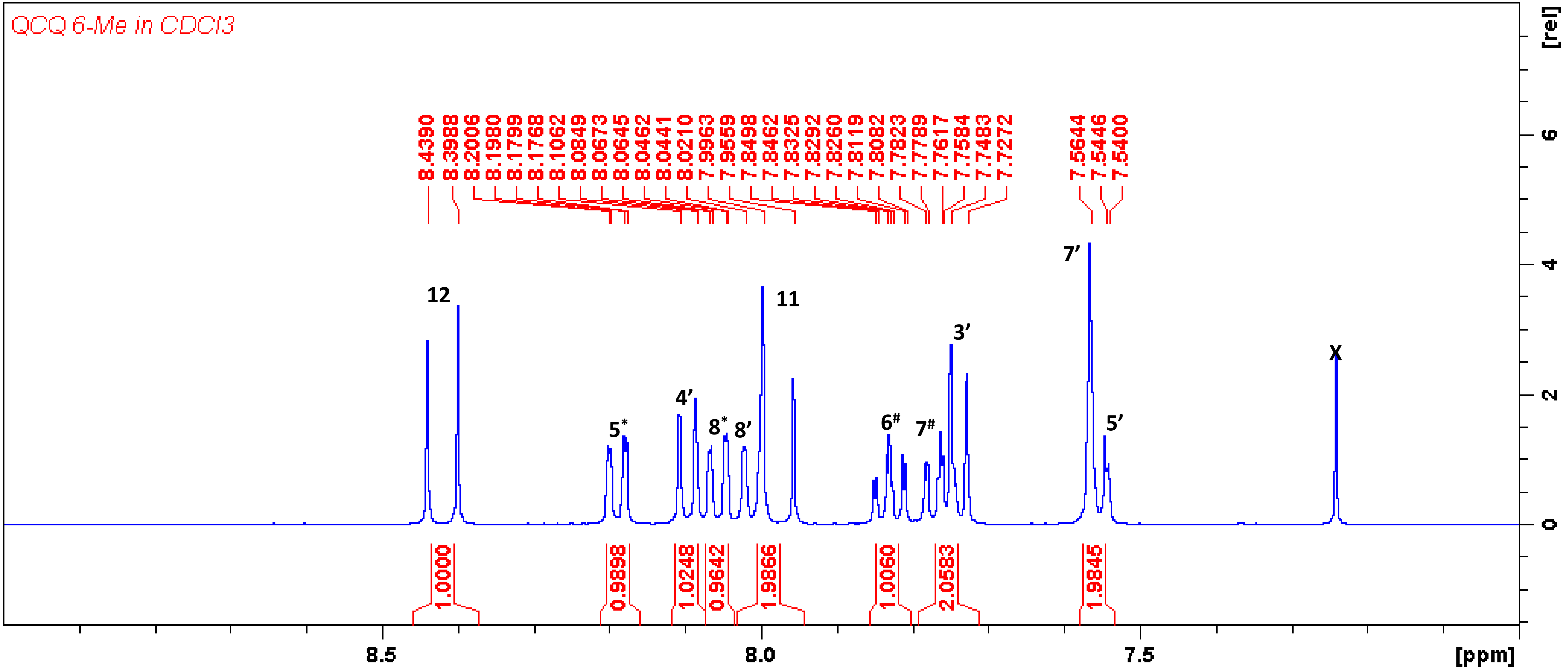

*, # Indicates assignments are interchangeable

Expanded ^{1}H NMR spectrum of **B7h**

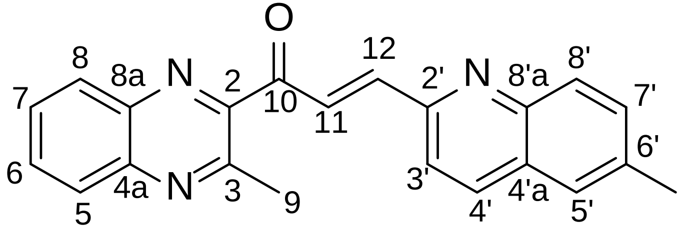

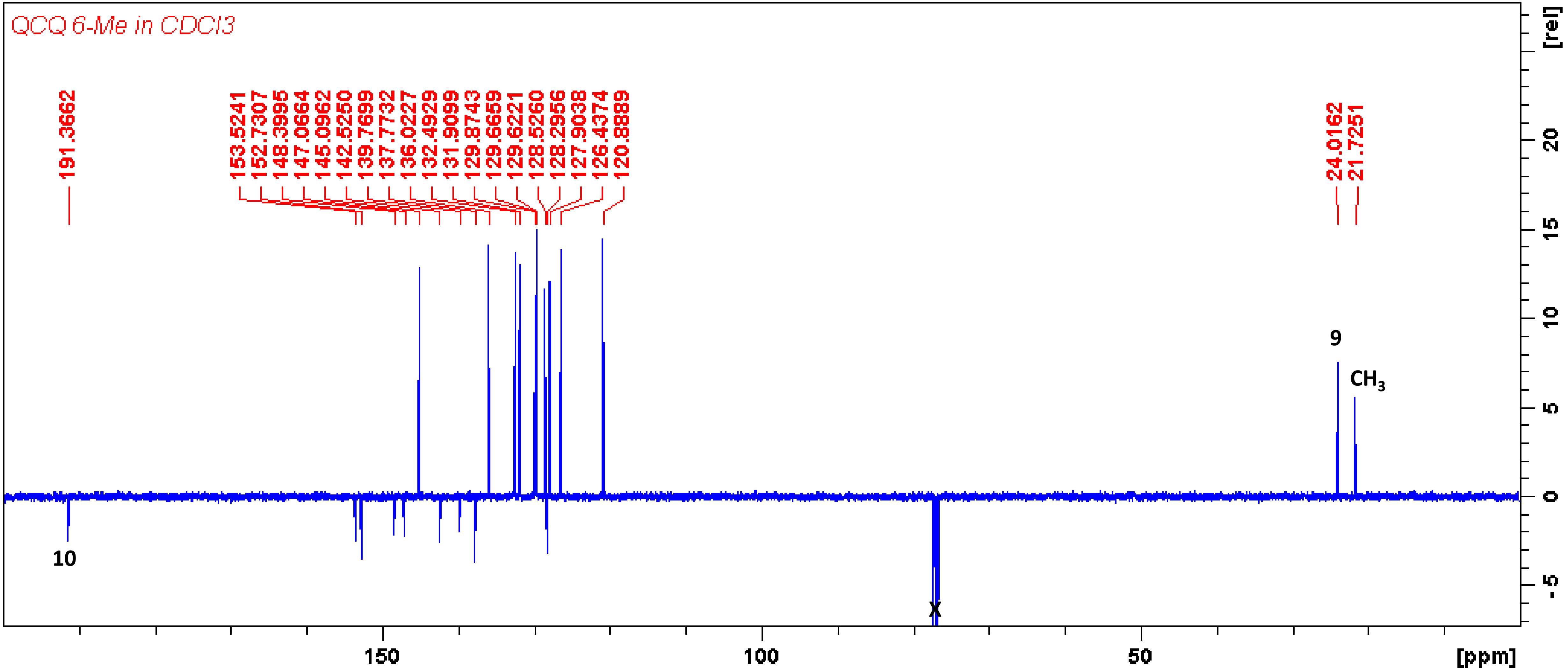

^{13}C NMR spectrum of **B7h**

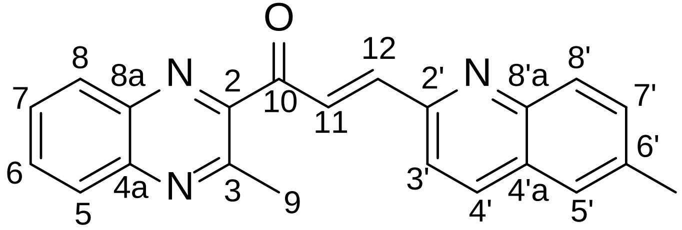

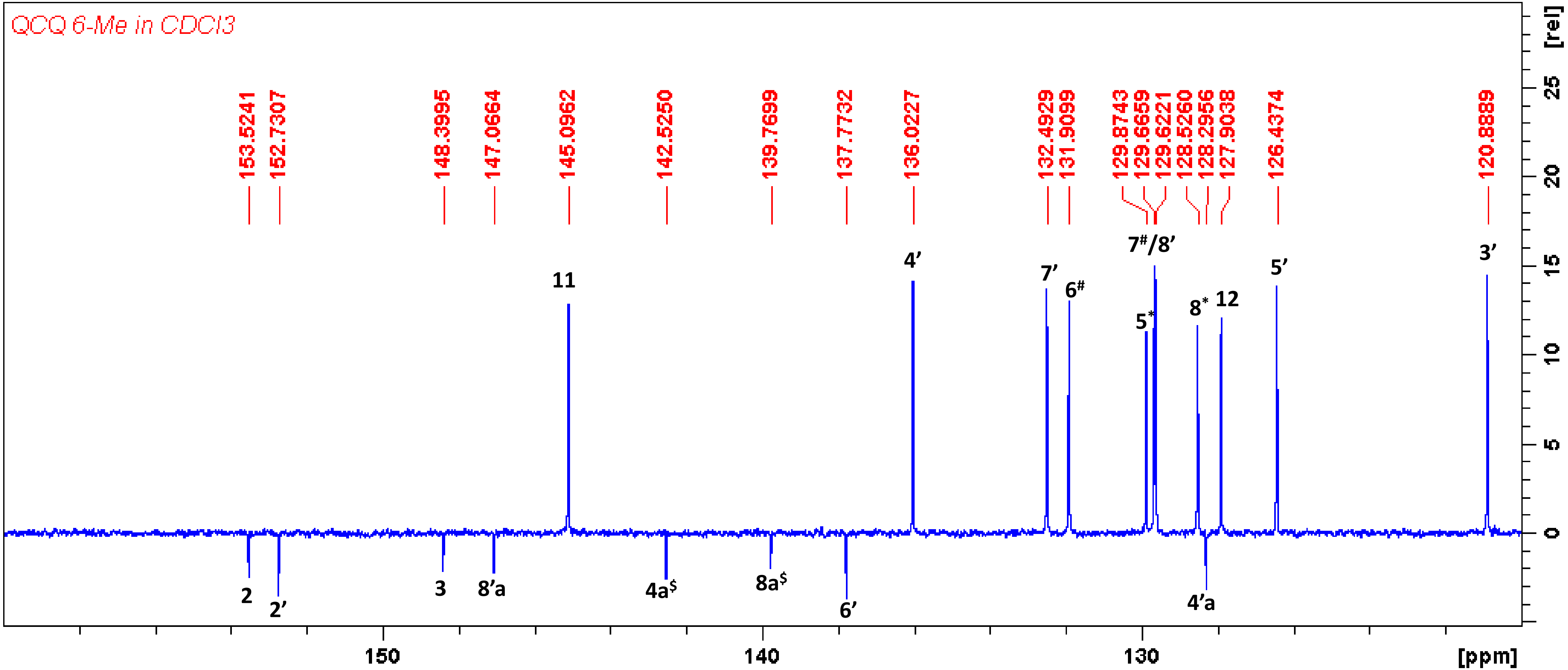

*, #, $ Indicates assignments are interchangeable

Expanded ^{13}C NMR spectrum of **B7h**

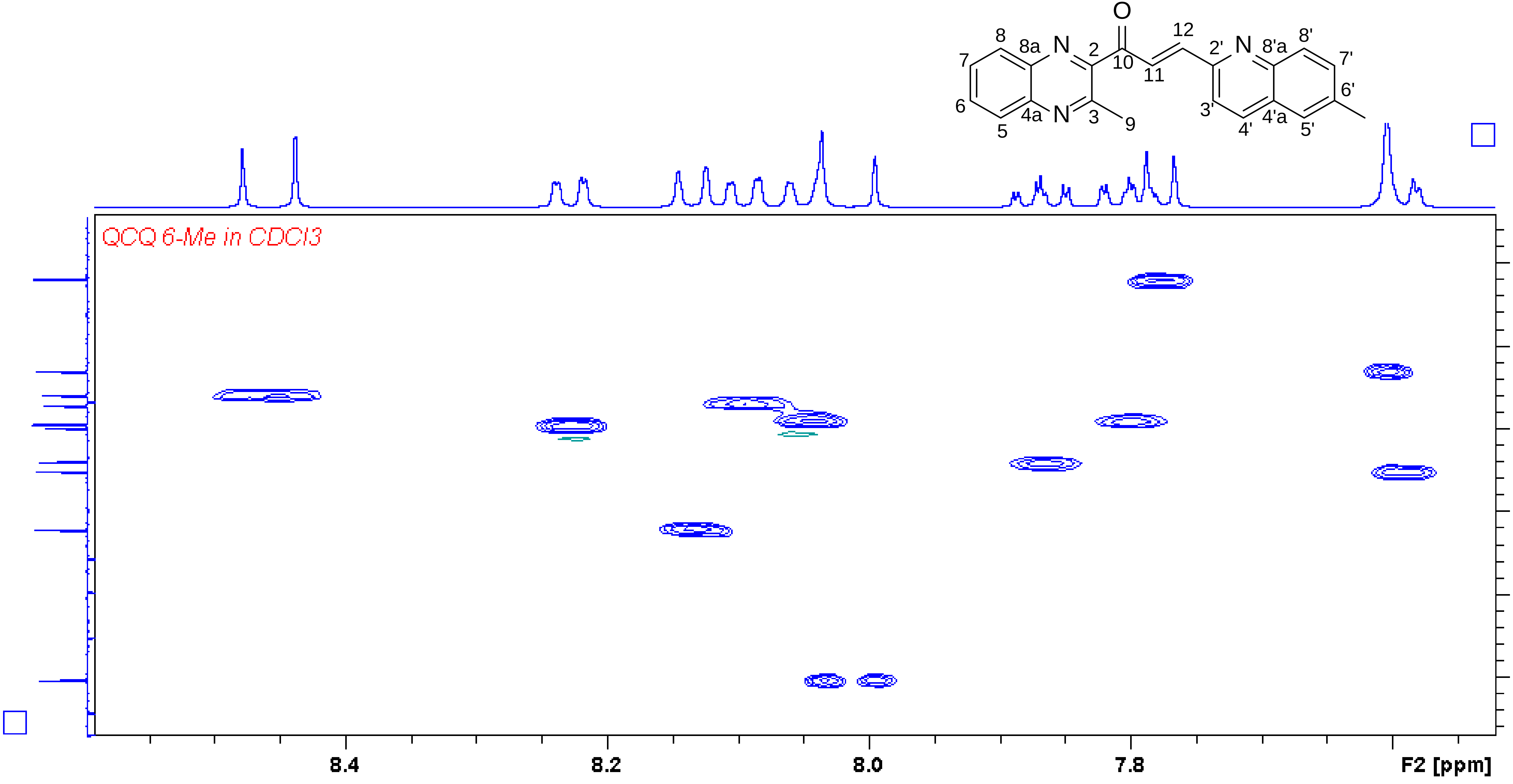

HSQC of **B7h**

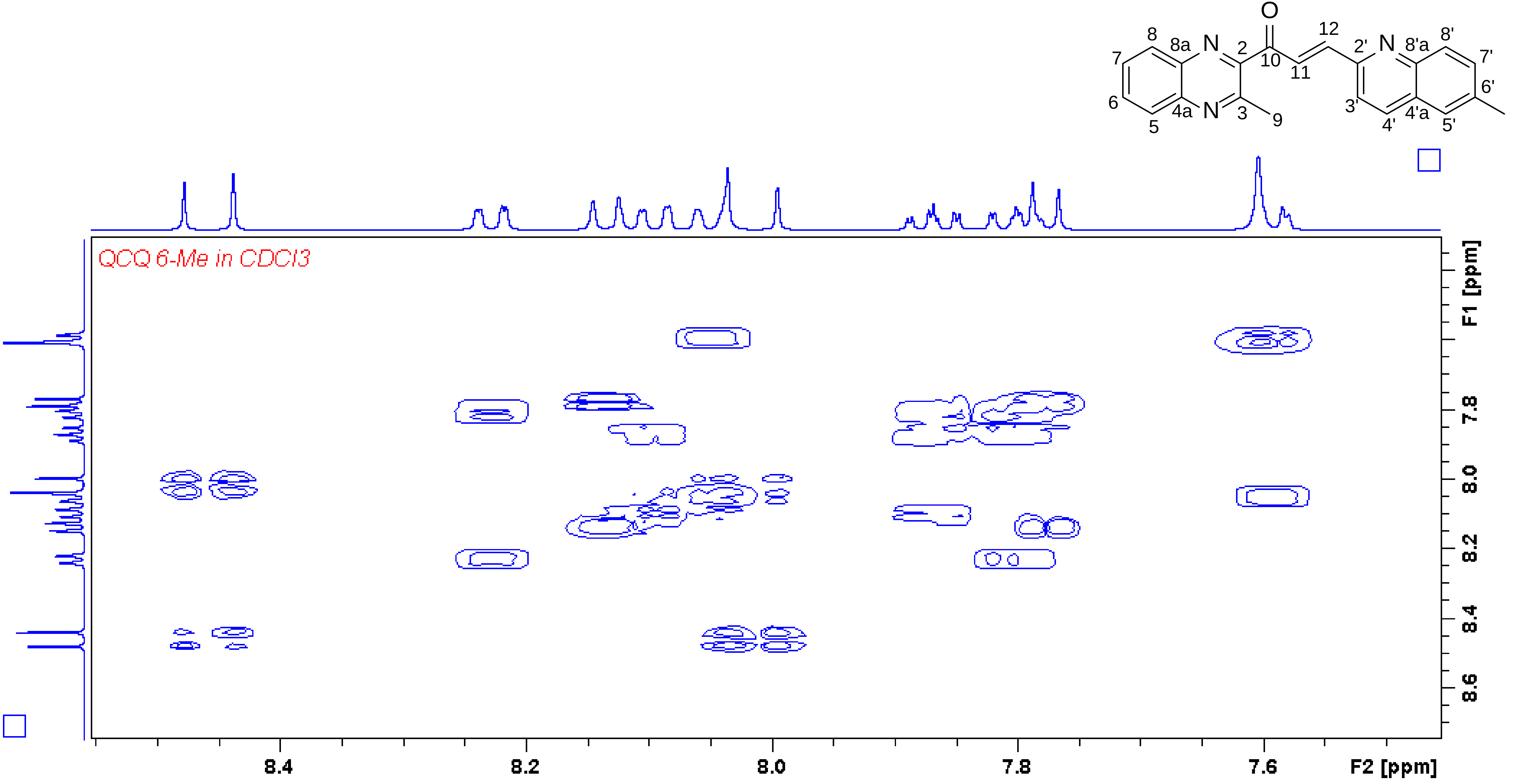
O
8
8a
N
2
12
2'
N
8'a
8'
7
10
11
7'
6'
6
4a
N
3
9
3'
4'
4'a
5'
5
QCQ 6-Me in CDCl3
F1 [ppm]
7.8
8.0
8.2
8.4
8.6
8.4
8.2
8.0
7.8
7.6
F2 [ppm]

COSY of **B7h**

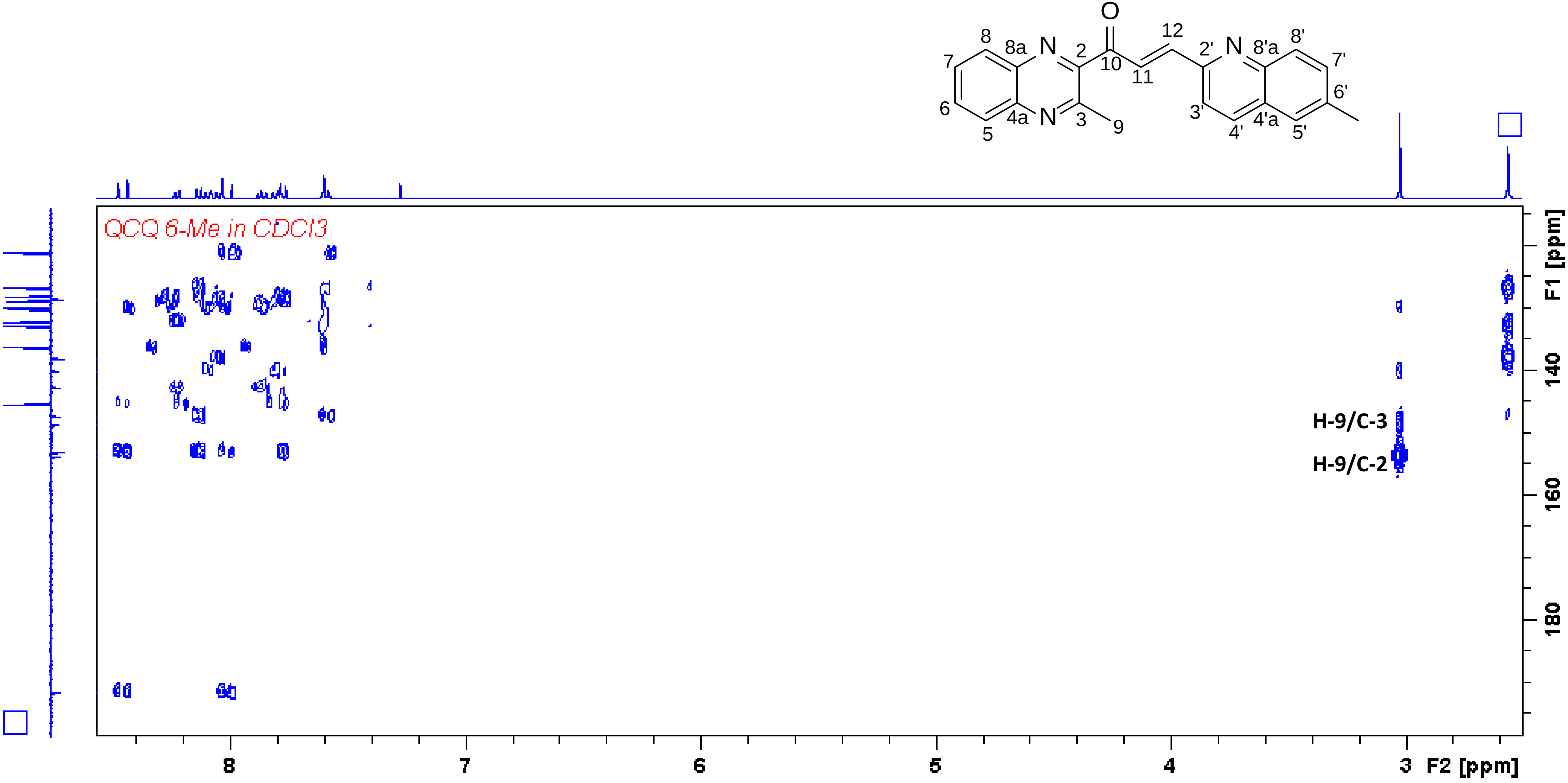
QCQ 6-Me in CDCl3
H-9/C-3
H-9/C-2
F1 [ppm]
F2 [ppm]
140
160
180
8
7
6
5
4
3
O
N
N
N
8
8a
7
6
5
4a
2
3
9
10
11
12
2'
3'
4'
4'a
5'
6'
7'
8'
8'a

HMBC of **B7h**

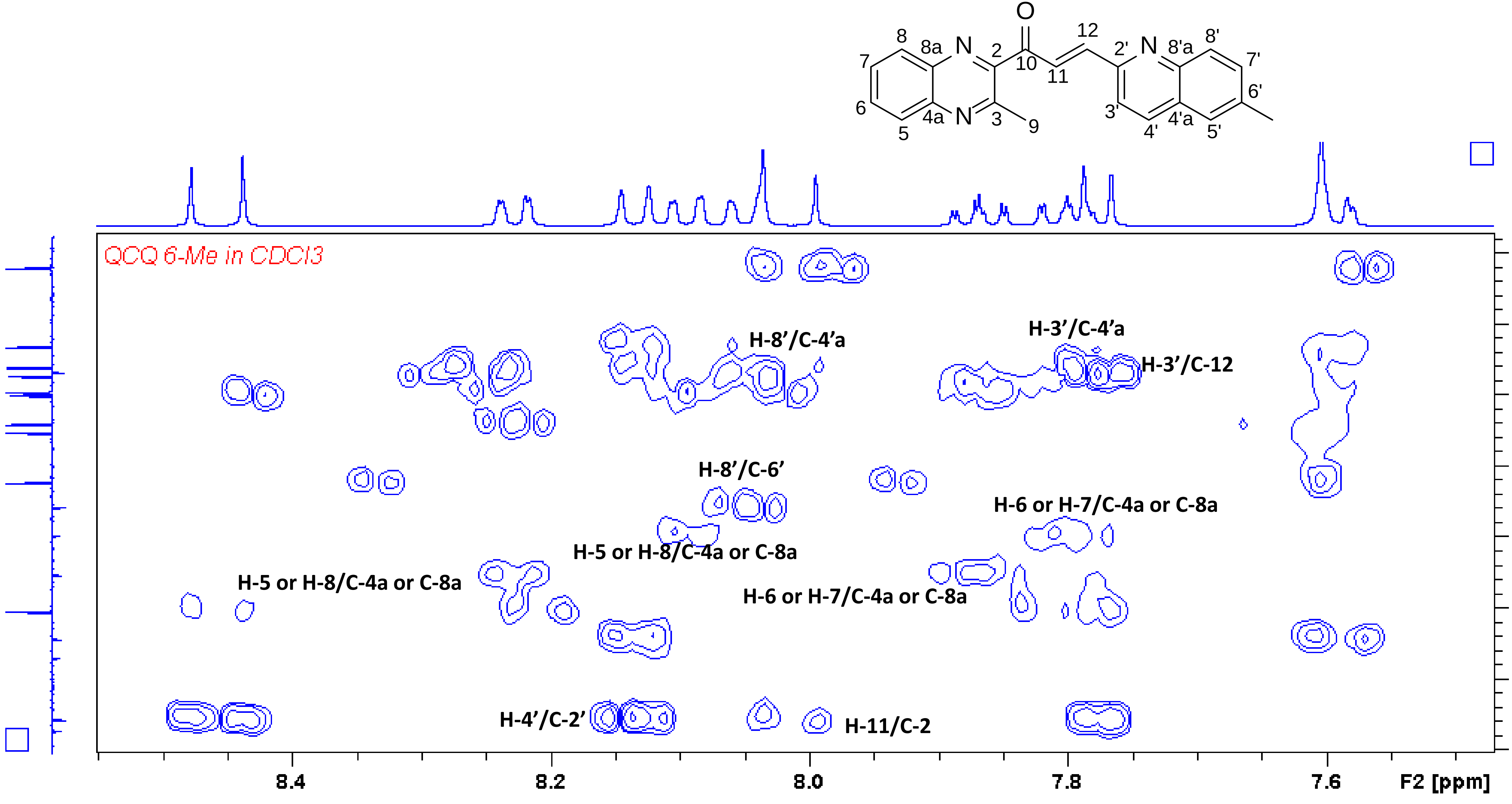

Expanded HMBC of **B7h**

Elemental Composition Report

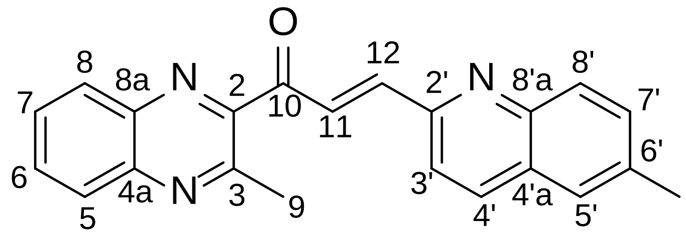

Single Mass Analysis

Tolerance = 5.0 PPM / DBE: min = -1.5, max = 100.0
Element prediction: Off
Number of isotope peaks used for i-FIT = 3

Monoisotopic Mass, Even Electron Ions
35 formula(e) evaluated with 1 results within limits (up to 20 closest results for each mass)
Elements Used:
C: 20-25 H: 15-20 N: 0-5 O: 0-5 Na: 0-1
QCQ (6-Me) 28 (0.910) Cm (1:61)
TOF MS ES+

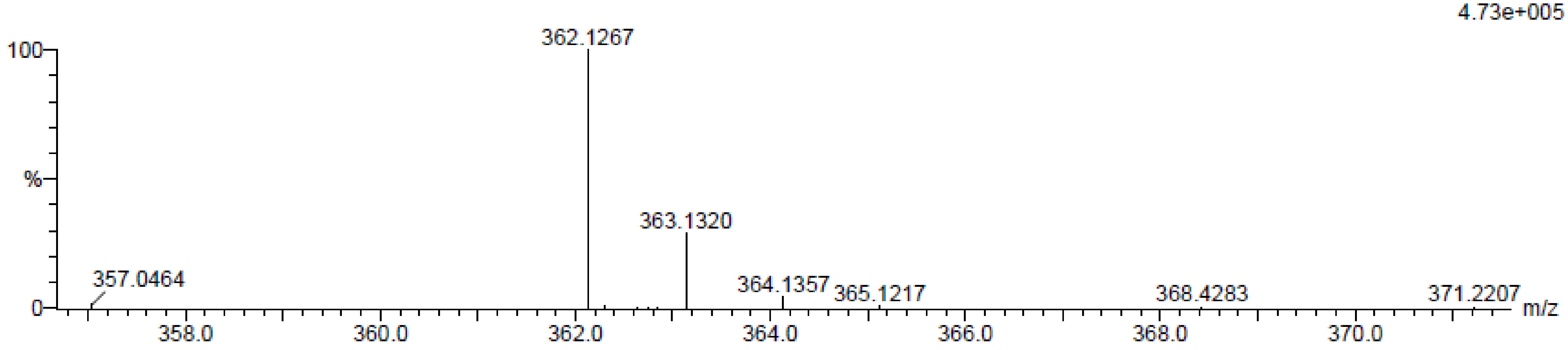

Minimum:				-1.5			
Maximum:		5.0	5.0	100.0			
Mass	Calc. Mass	mDa	PPM	DBE	i-FIT	i-FIT (Norm)	Formula
362.1267	362.1269	-0.2	-0.6	15.5	86.2	0.0	C22 H17 N3 O Na

High resolution mass spectrum of **B7h**

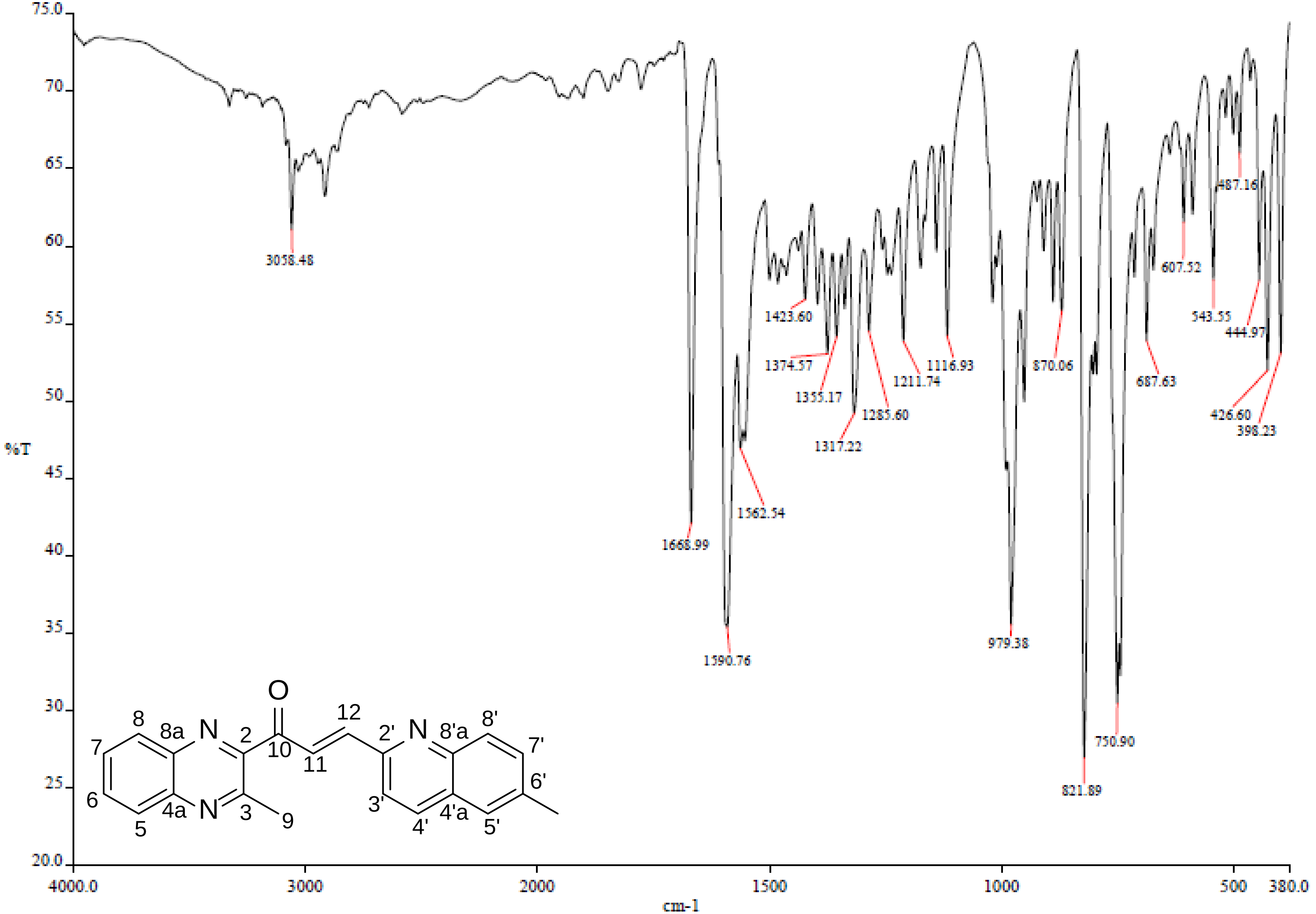

FTIR spectrum of **B7h**

Overlay Spectrum Graph Report

06/10/2017 11:58:48 AM

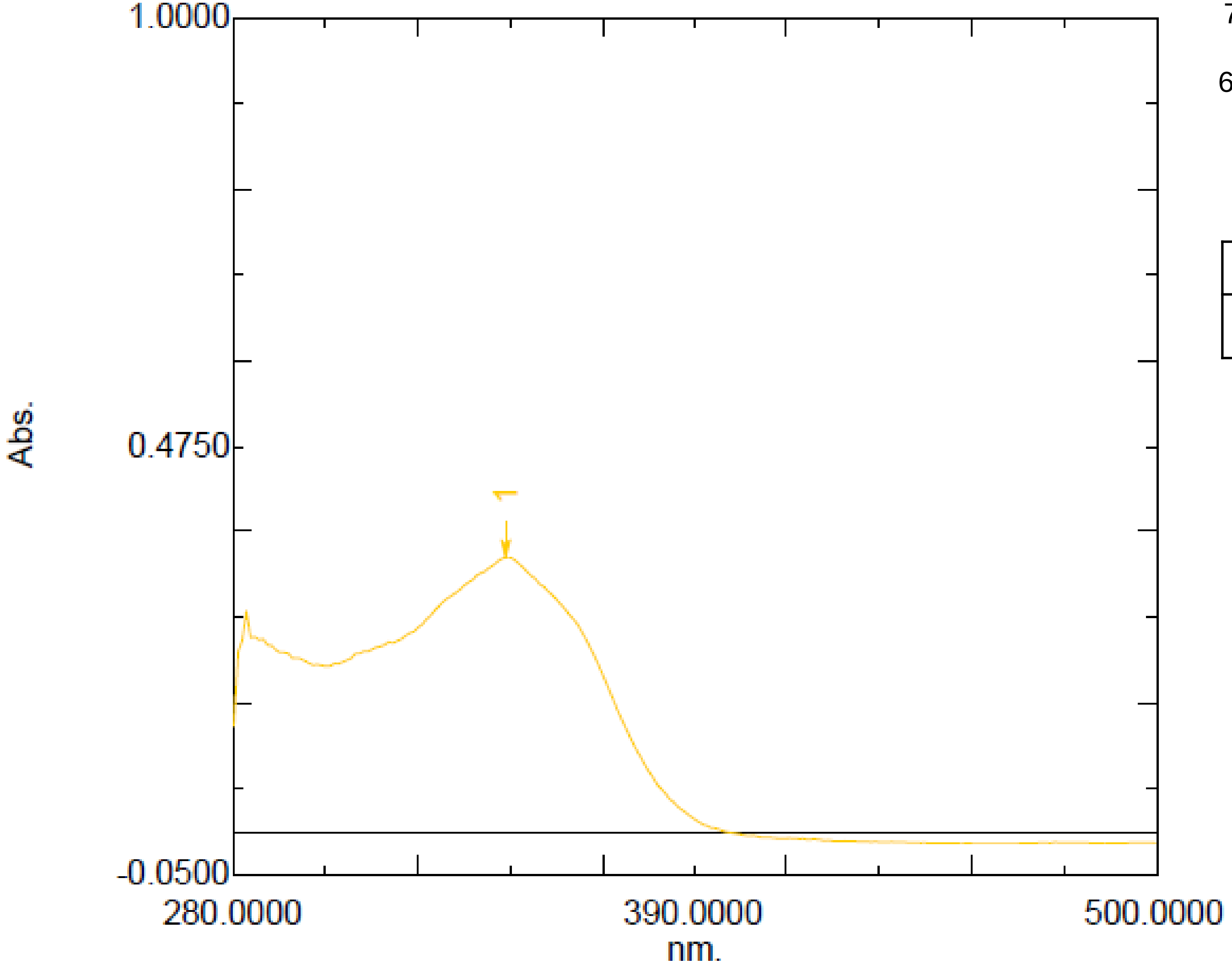

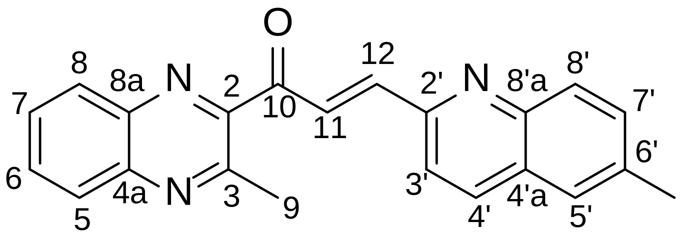

λ	absorbance	logε
345	0.3384	4.36

UV spectrum of **B7h**

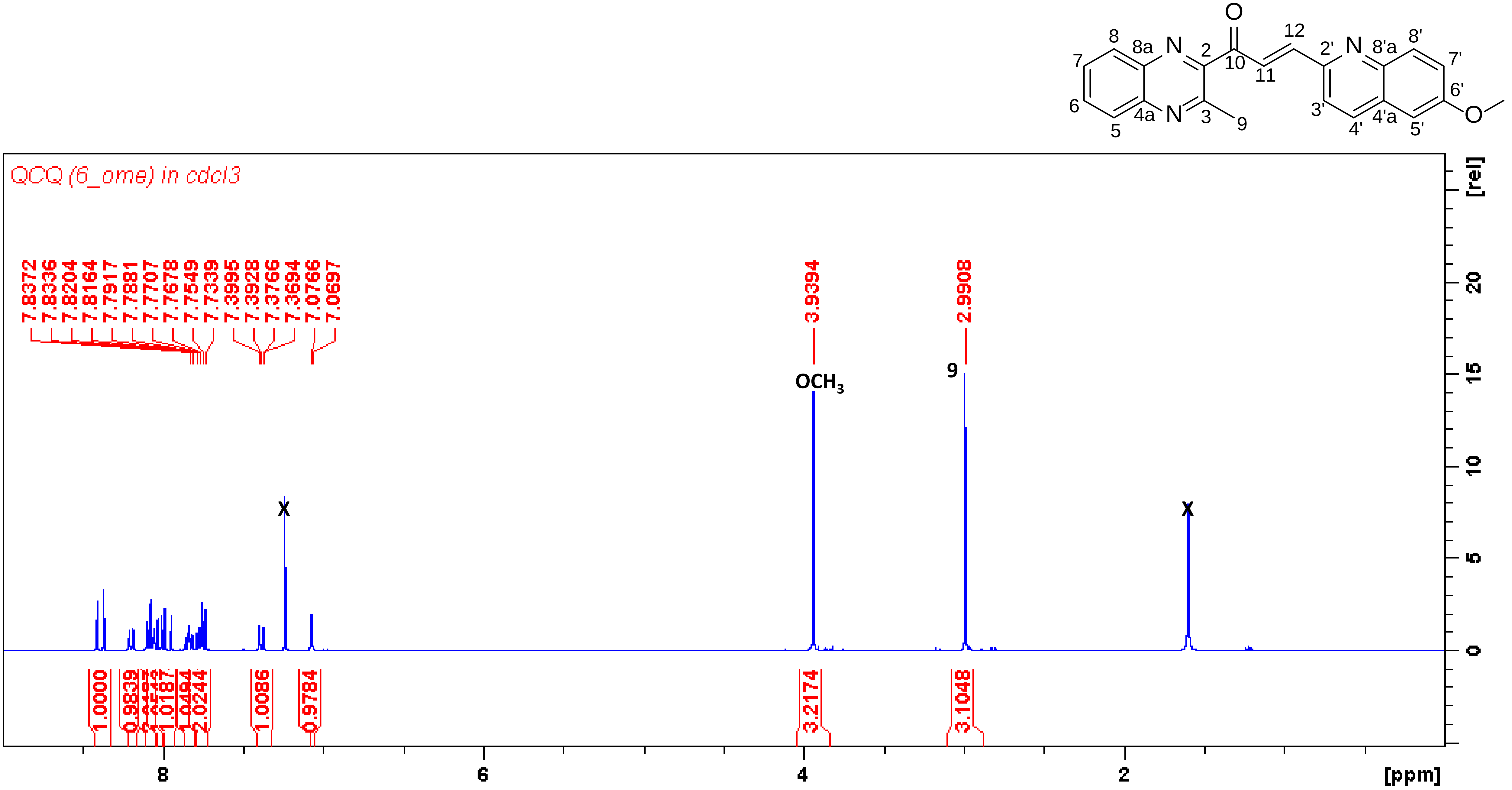

^{1}H NMR spectrum of **B7i**

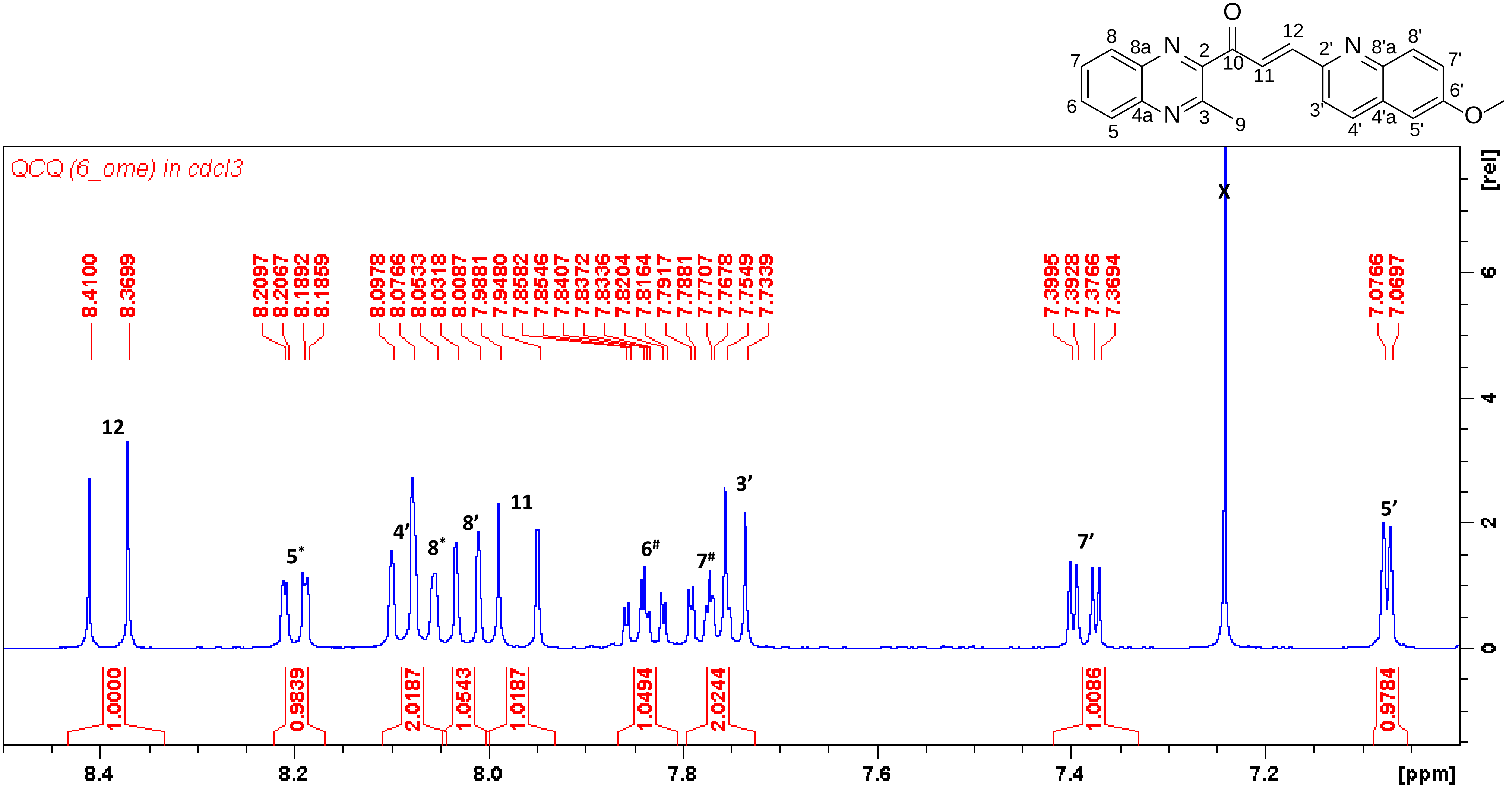

*, # Indicates assignments are interchangeable

Expanded ^{1}H NMR spectrum of **B7i**

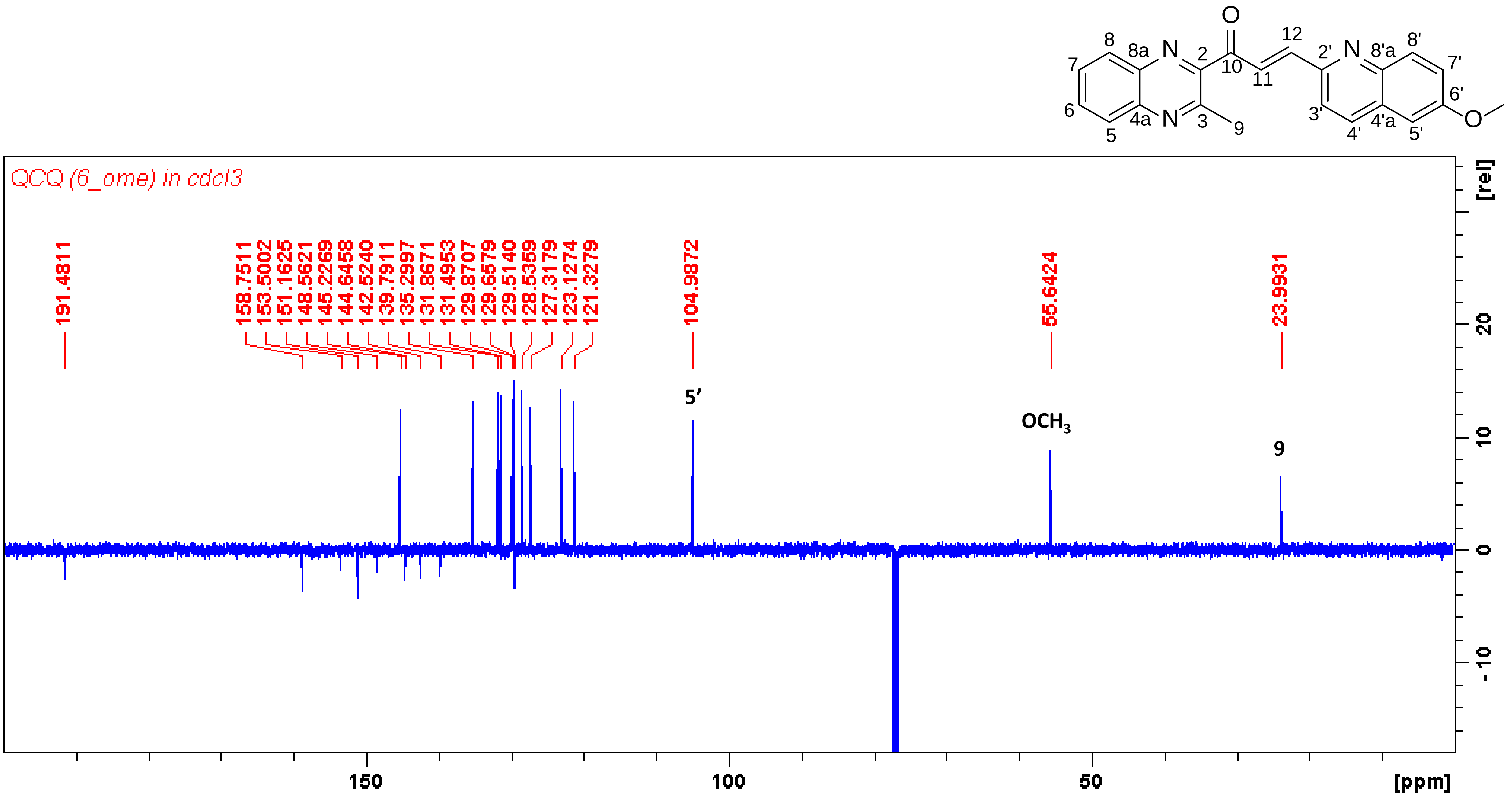

^{13}C NMR spectrum of **B7i**

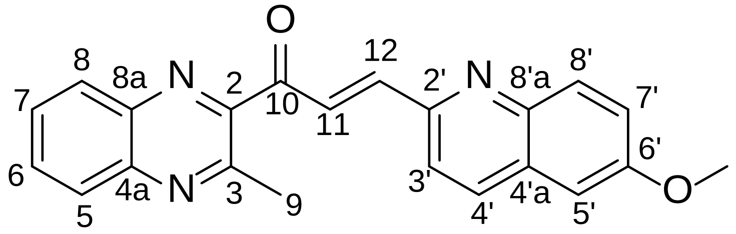

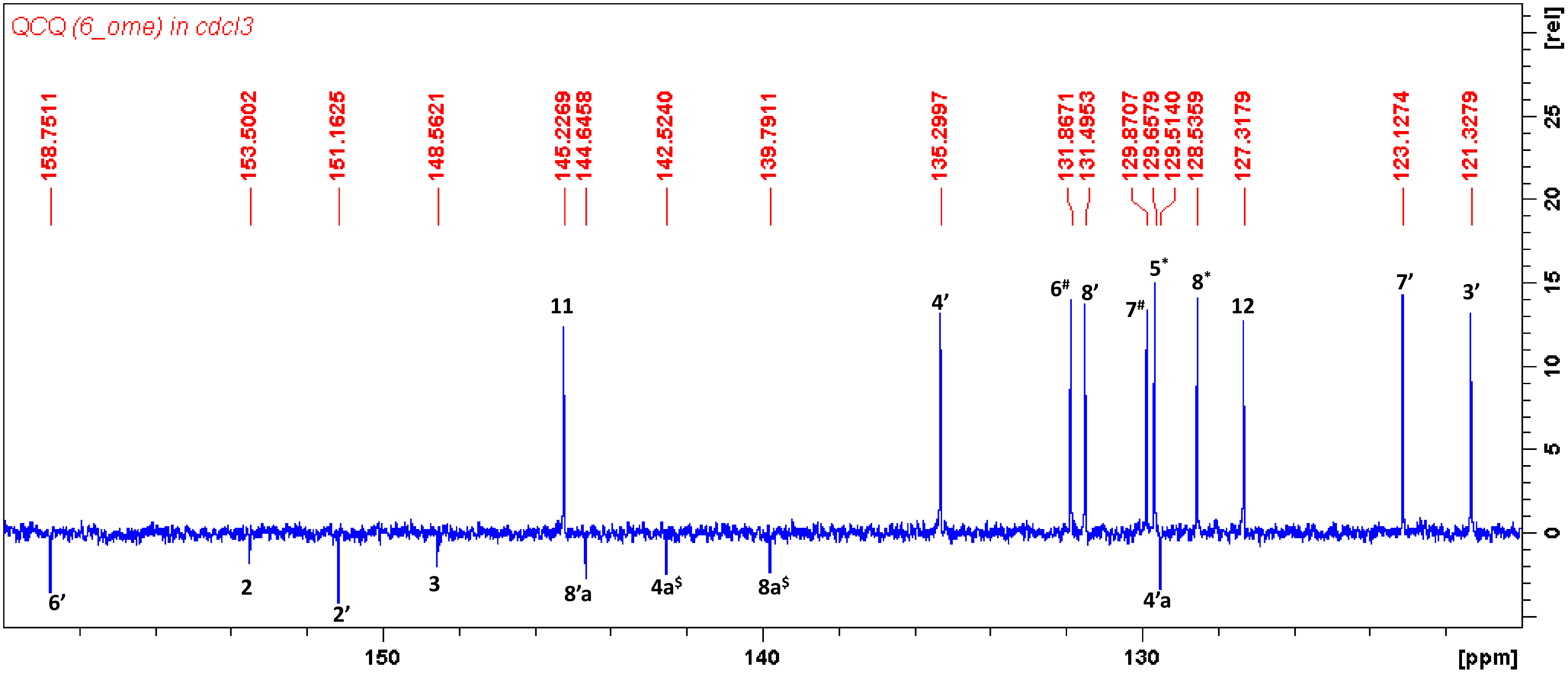

*, #, $ Indicates assignments are interchangeable

Expanded ^{13}C NMR spectrum of **B7i**

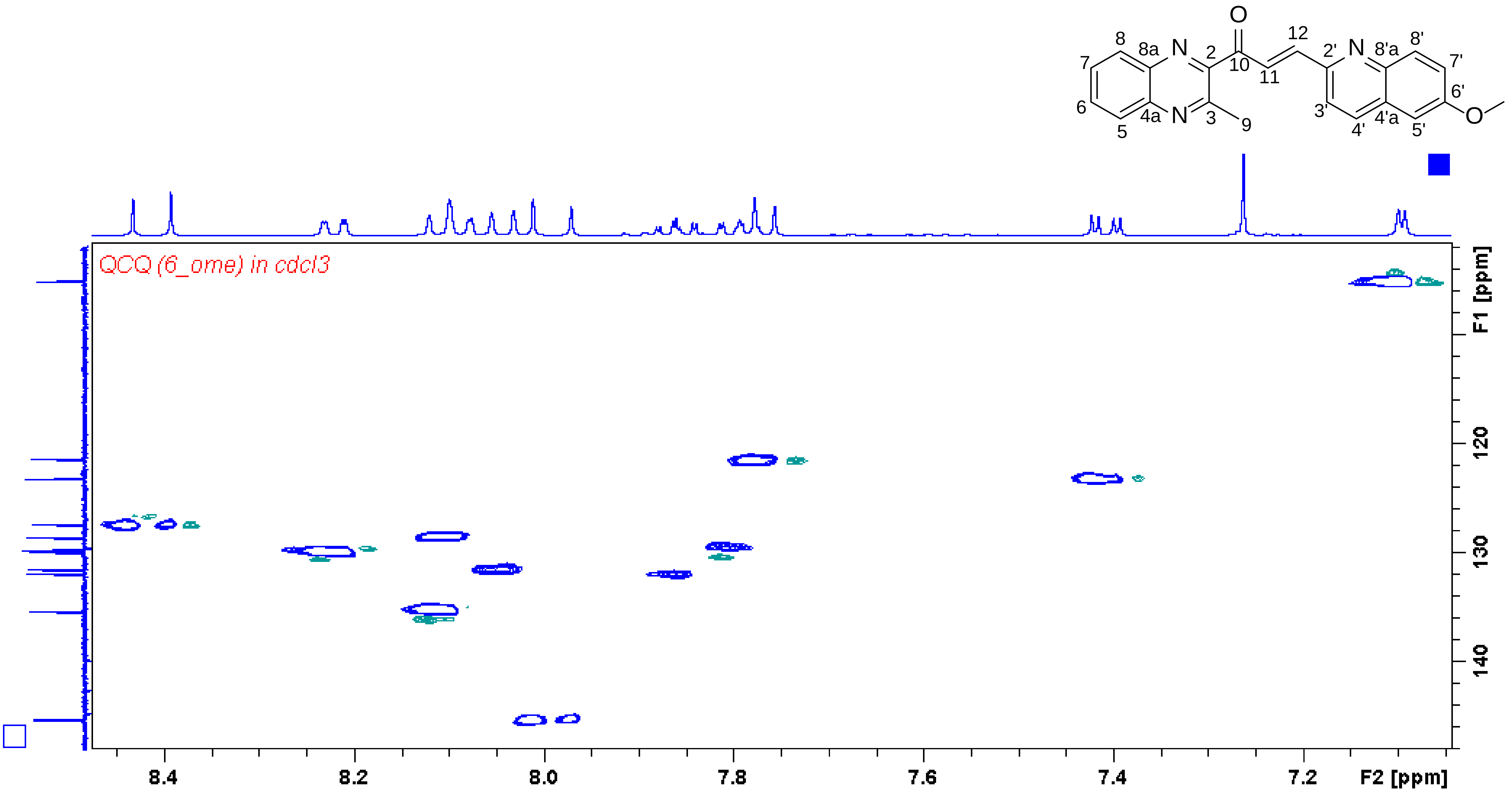

O
8
8a
N
2
12
2'
N
8'a
8'
7'
7
10
11
6'
6
4a
N
3
9
3'
4'
4'a
5'
O
5
QCQ (6_ome) in cdcl3
F1 [ppm]
120
130
140
8.4
8.2
8.0
7.8
7.6
7.4
7.2
F2 [ppm]

HSQC of **B7i**

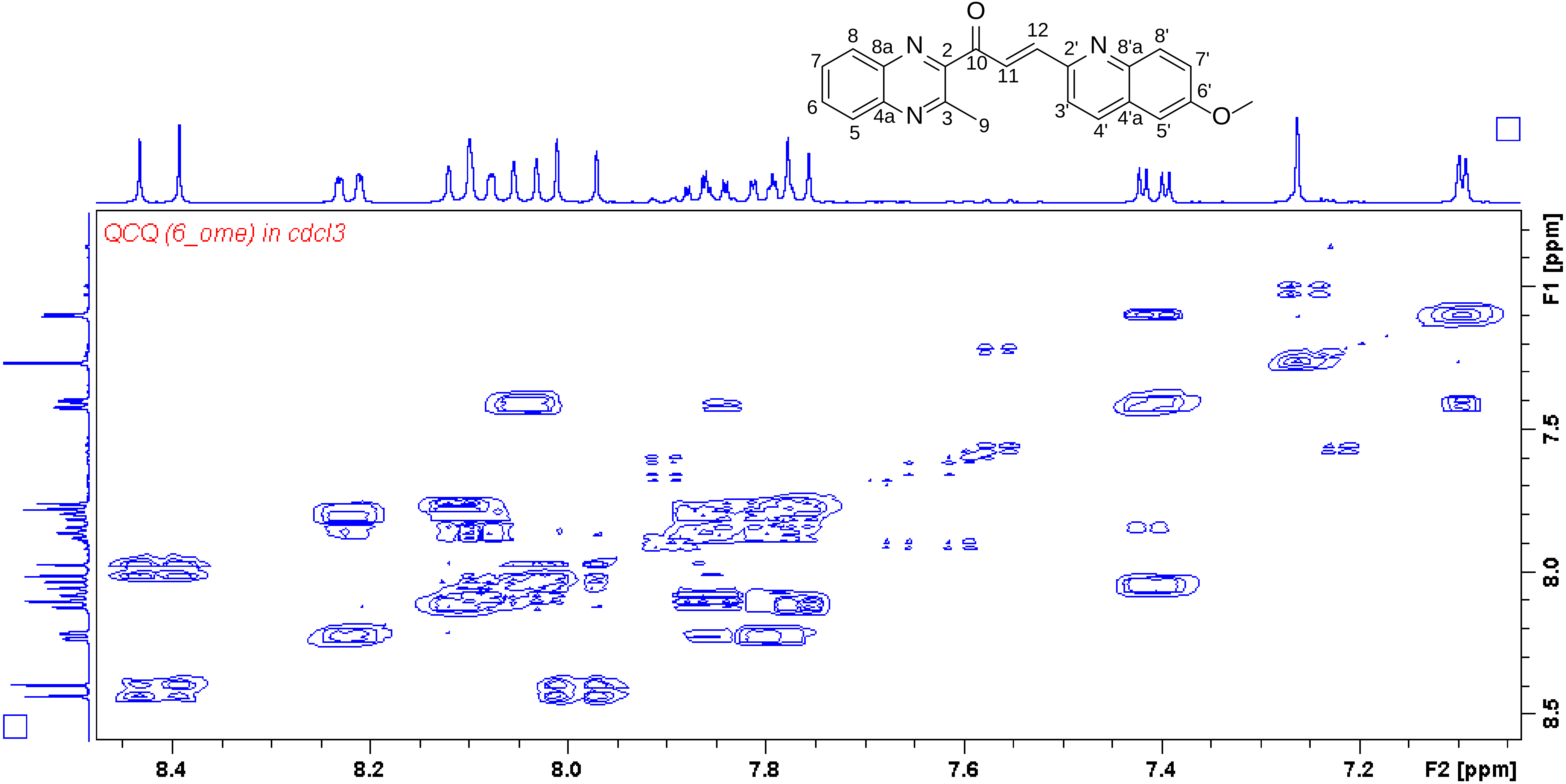

COSY of **B7i**

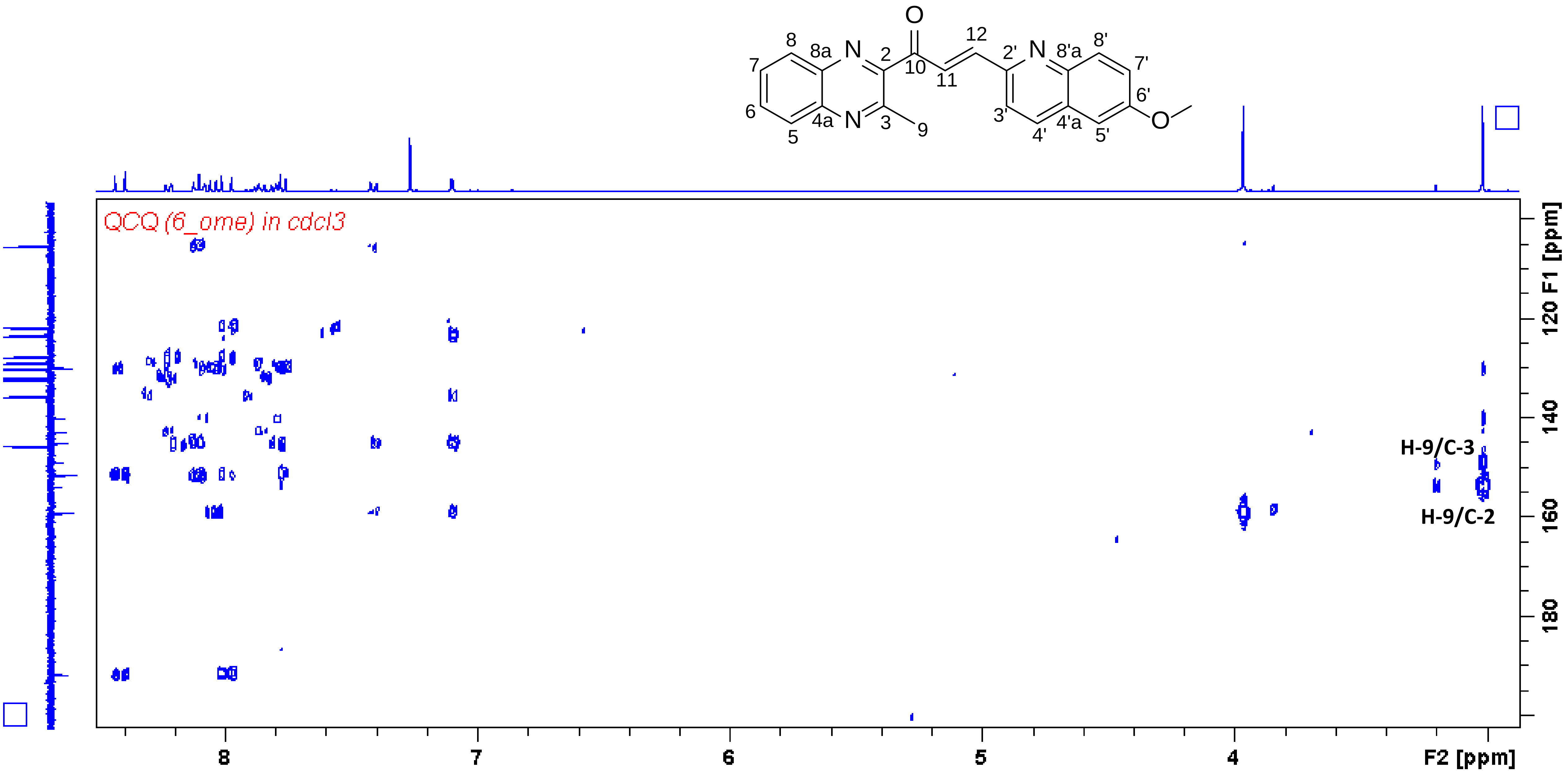

HMBC of **B7i**

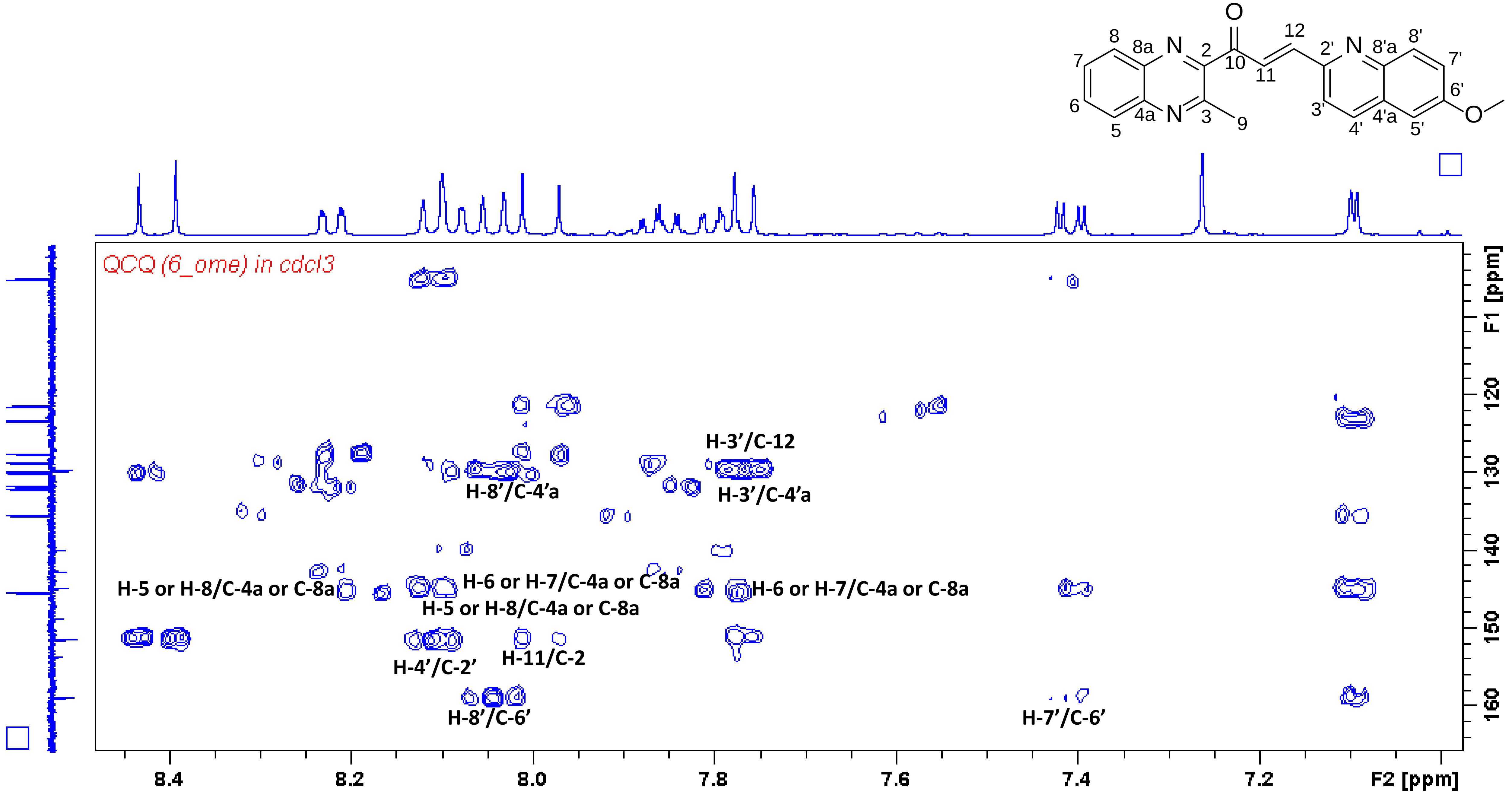

Expanded HMBC of **B7i**

Elemental Composition Report

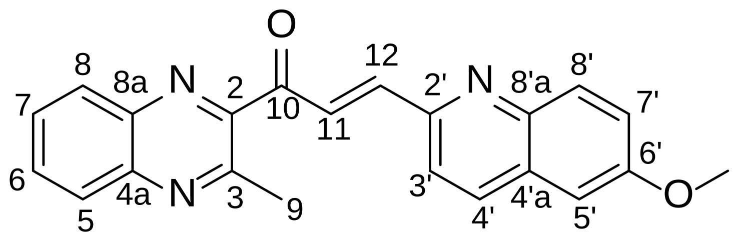

Single Mass Analysis

Tolerance = 5.0 PPM / DBE: min = -1.5, max = 100.0
Element prediction: Off
Number of isotope peaks used for i-FIT = 3

Monoisotopic Mass, Even Electron Ions
23 formula(e) evaluated with 1 results within limits (up to 20 closest results for each mass)
Elements Used:
C: 20-25 H: 10-20 N: 0-5 O: 1-5
QCQ(6-OCH3) 7 (0.202) Cm (1:61)
TOF MS AP+

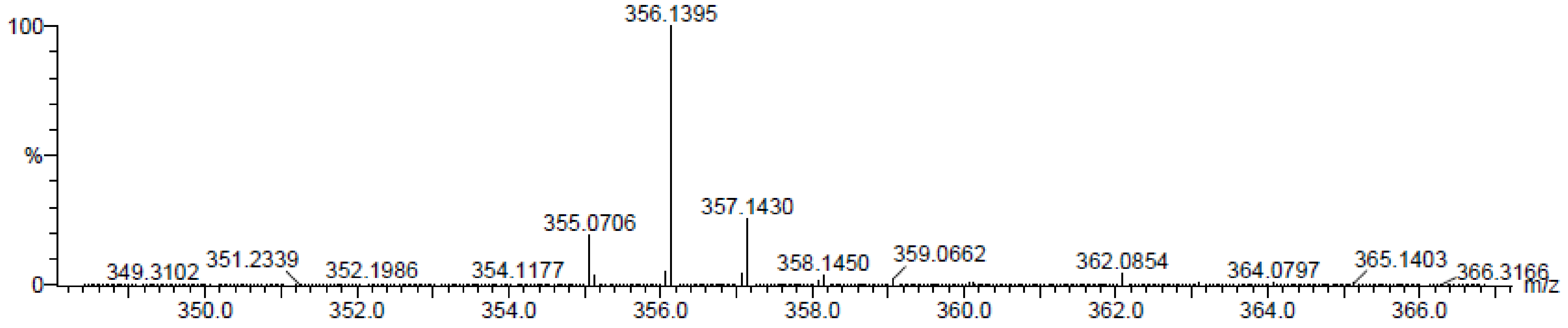

Minimum:				-1.5			
Maximum:		5.0	5.0	100.0			
Mass	Calc. Mass	mDa	PPM	DBE	i-FIT	i-FIT (Norm)	Formula
356.1395	356.1399	-0.4	-1.1	15.5	516.4	0.0	C22 H18 N3 O2

High resolution mass spectrum of **B7i**

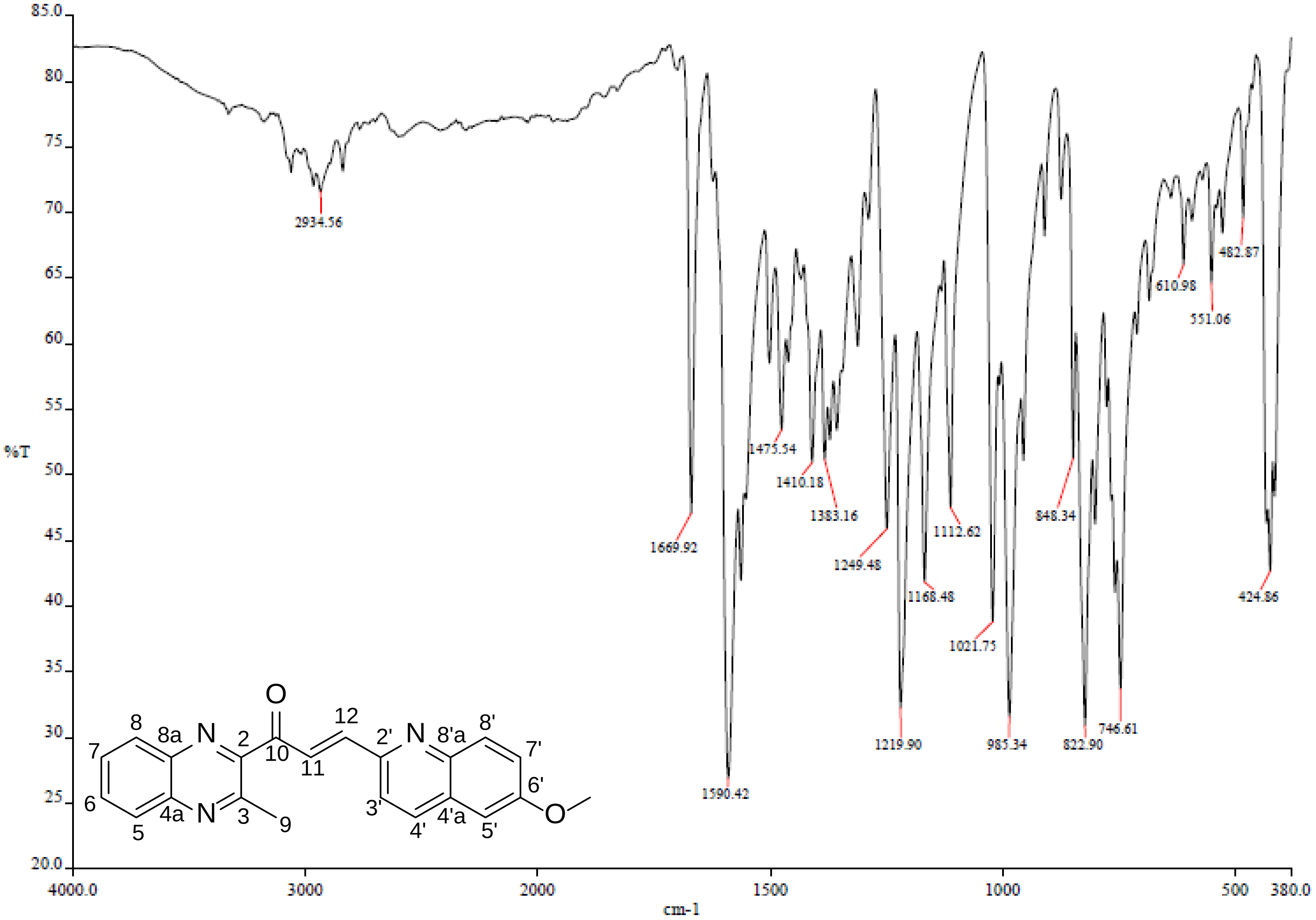

FTIR spectrum of **B7i**

Overlay Spectrum Graph Report

06/10/2017 12:01:02 PM

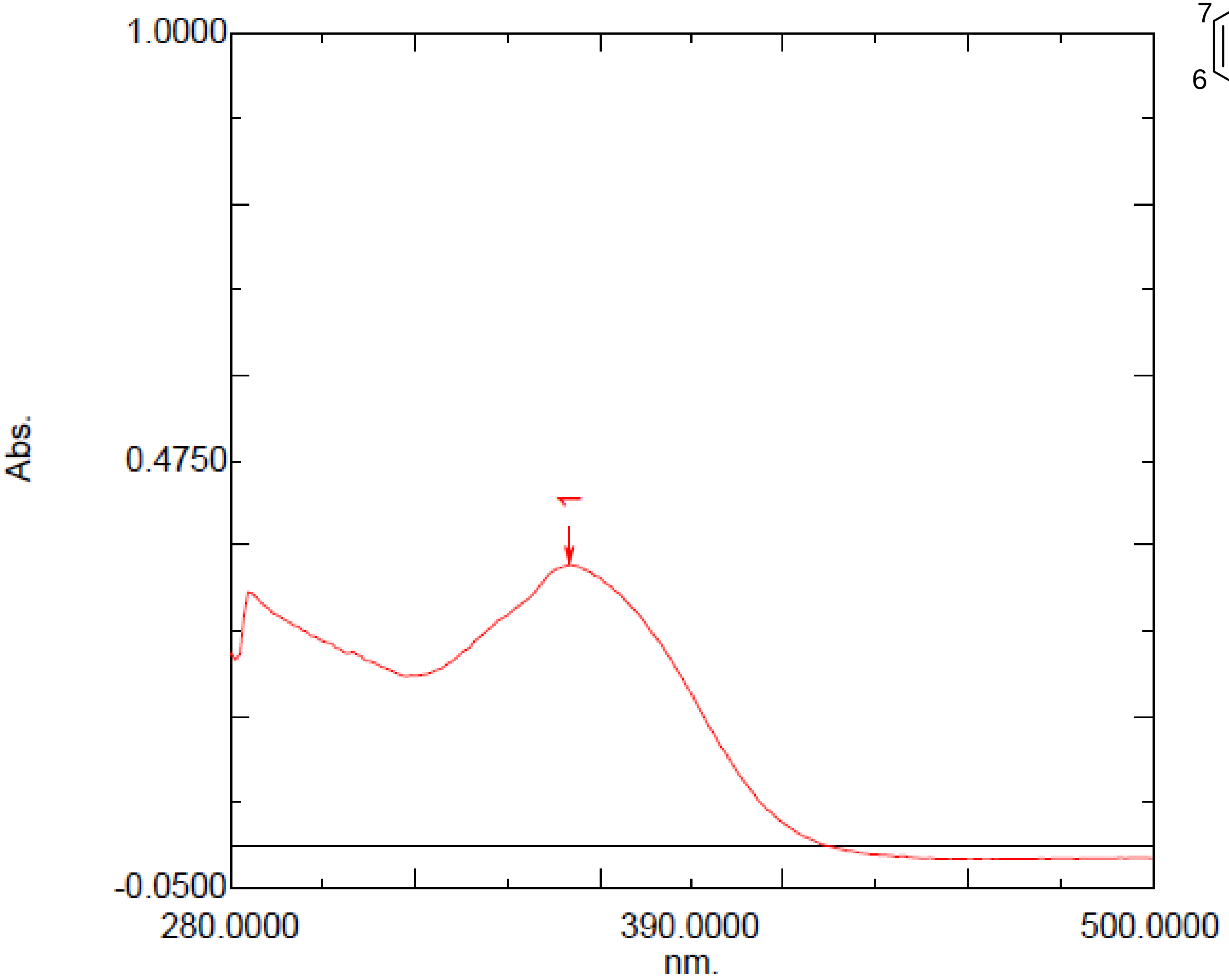

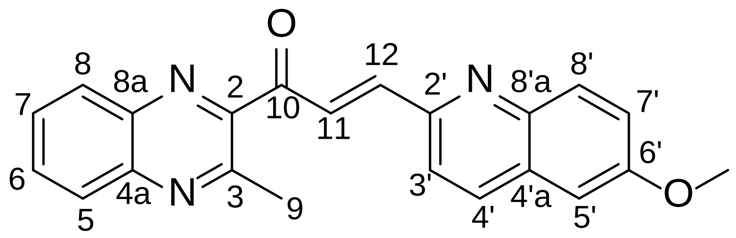

λ	absorbance	logε
361	0.3468	4.39

UV spectrum of **B7i**

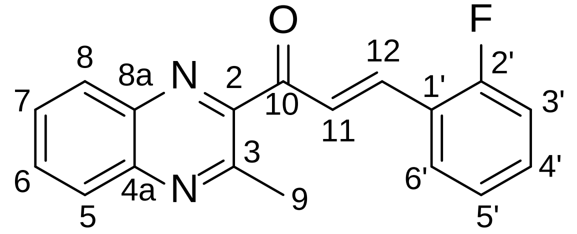

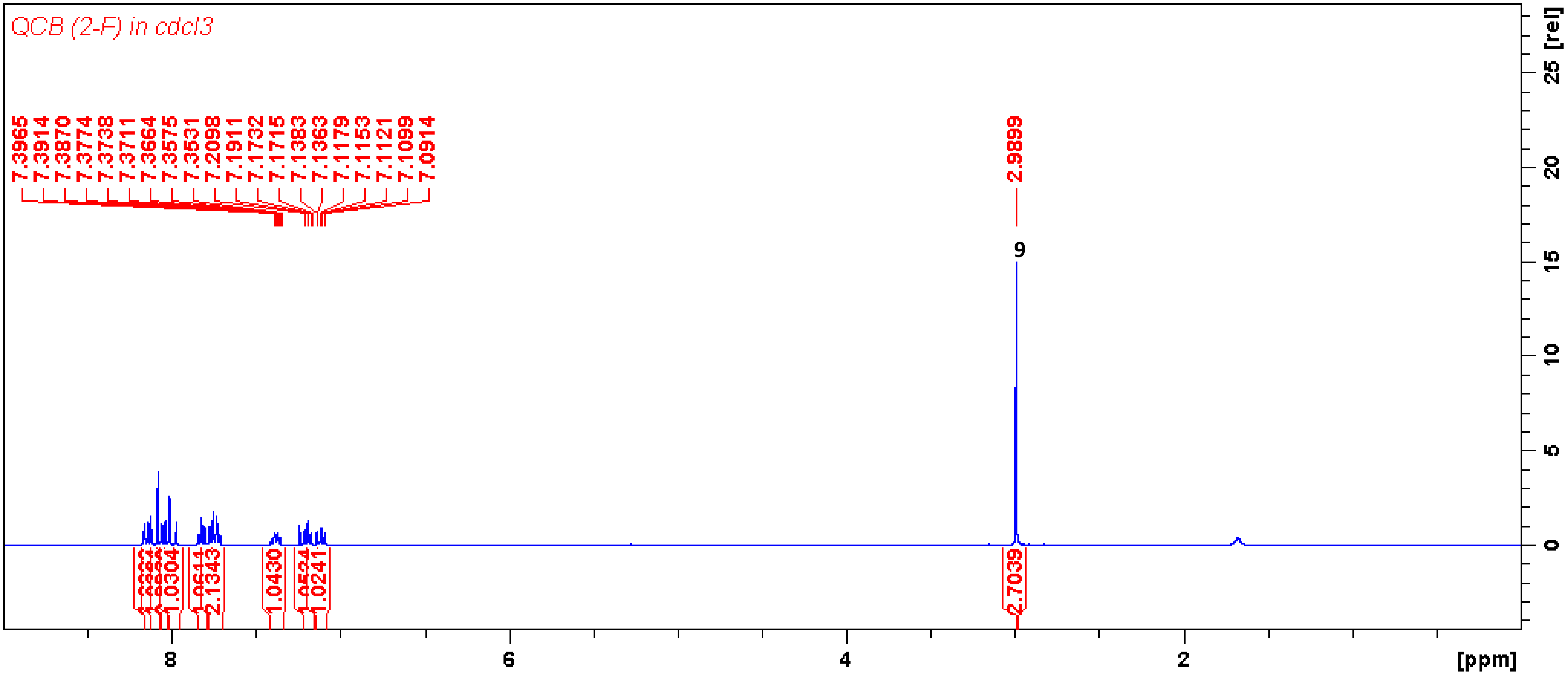

^1H NMR spectrum of **B10a**

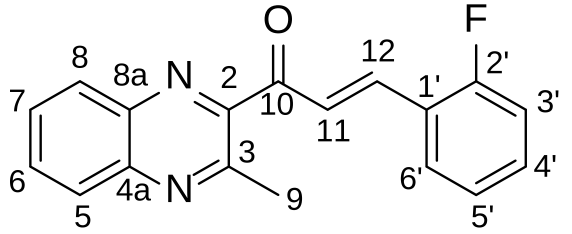

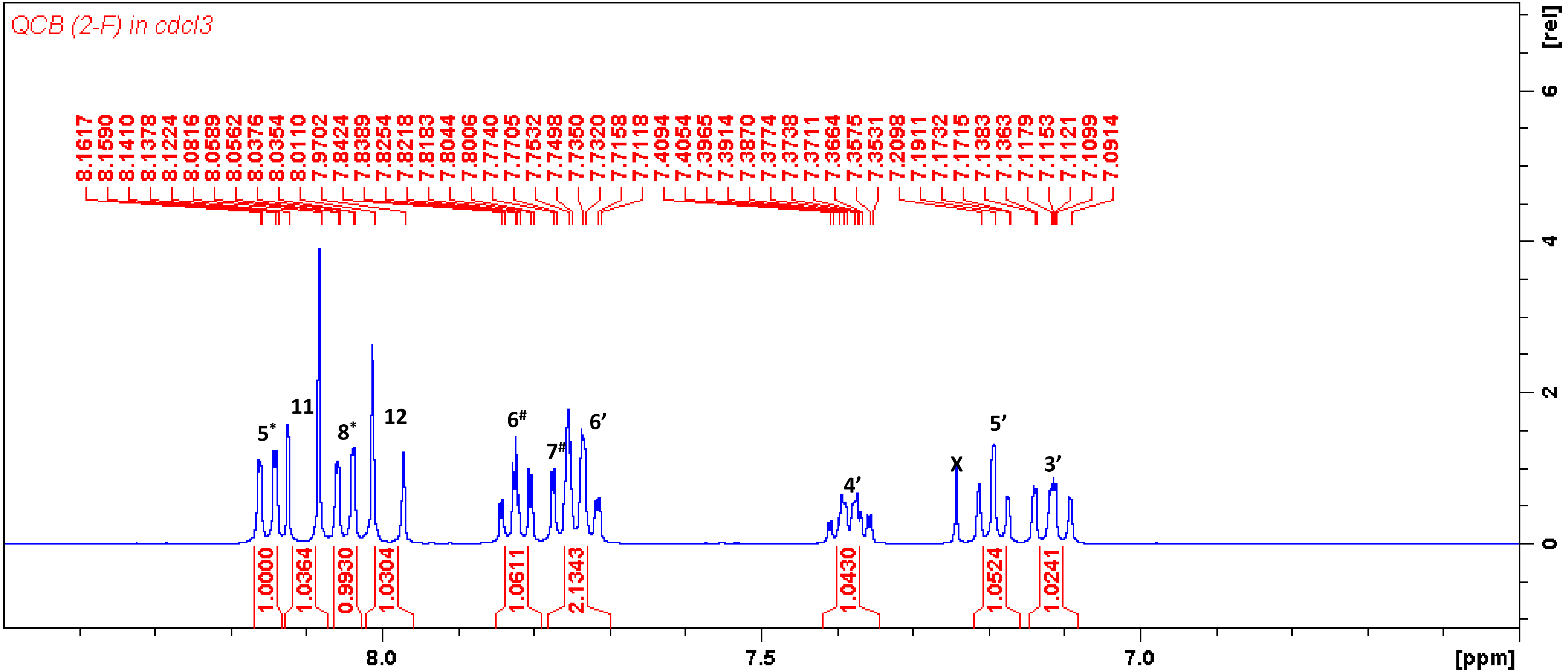

*, # Indicates assignments are interchangeable

Expanded ^{1}H NMR spectrum of **B10a**

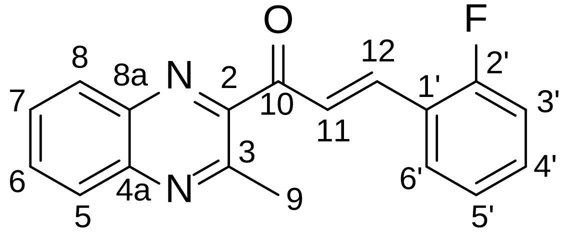

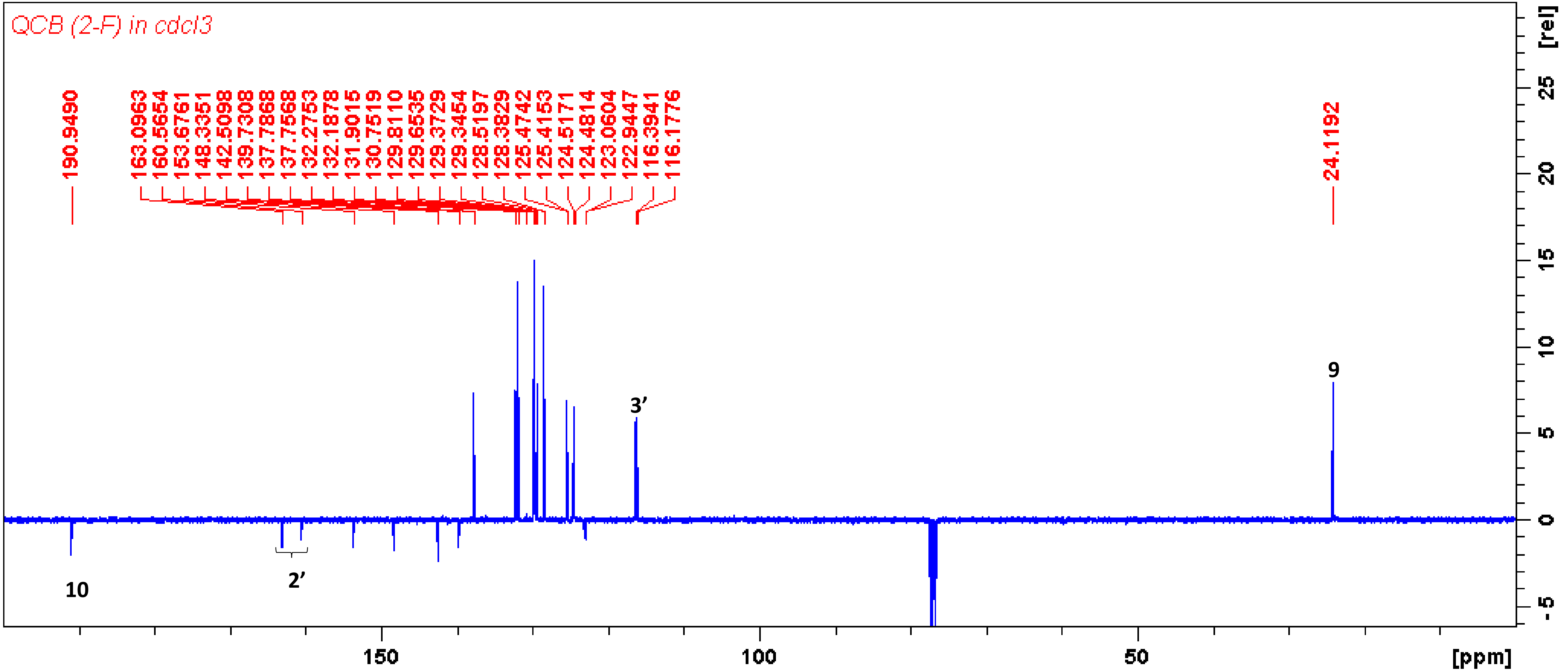

^{13}C NMR spectrum of **B10a**

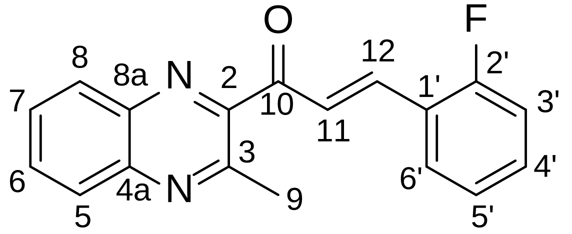

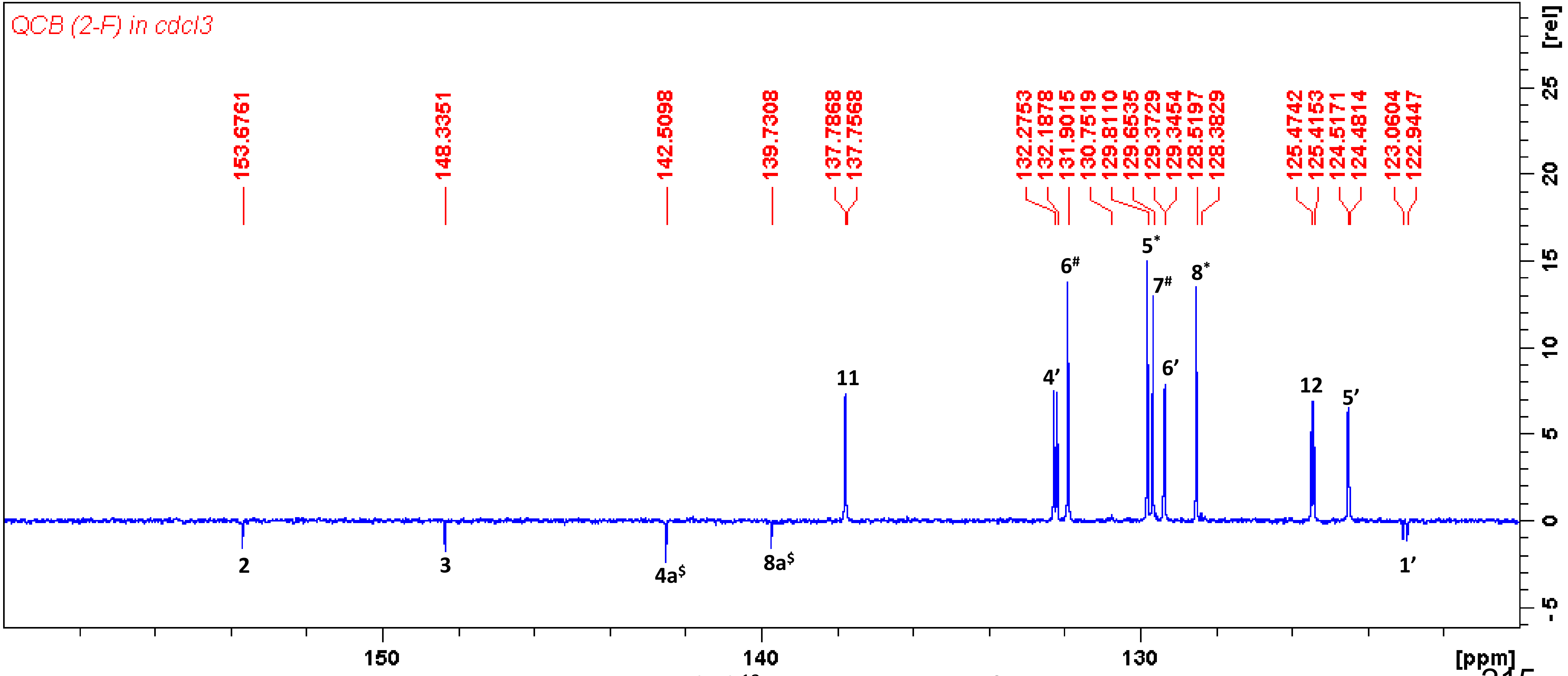

*, #, $ Indicates assignments are interchangeable

Expanded ^{13}C NMR spectrum of **B10a**

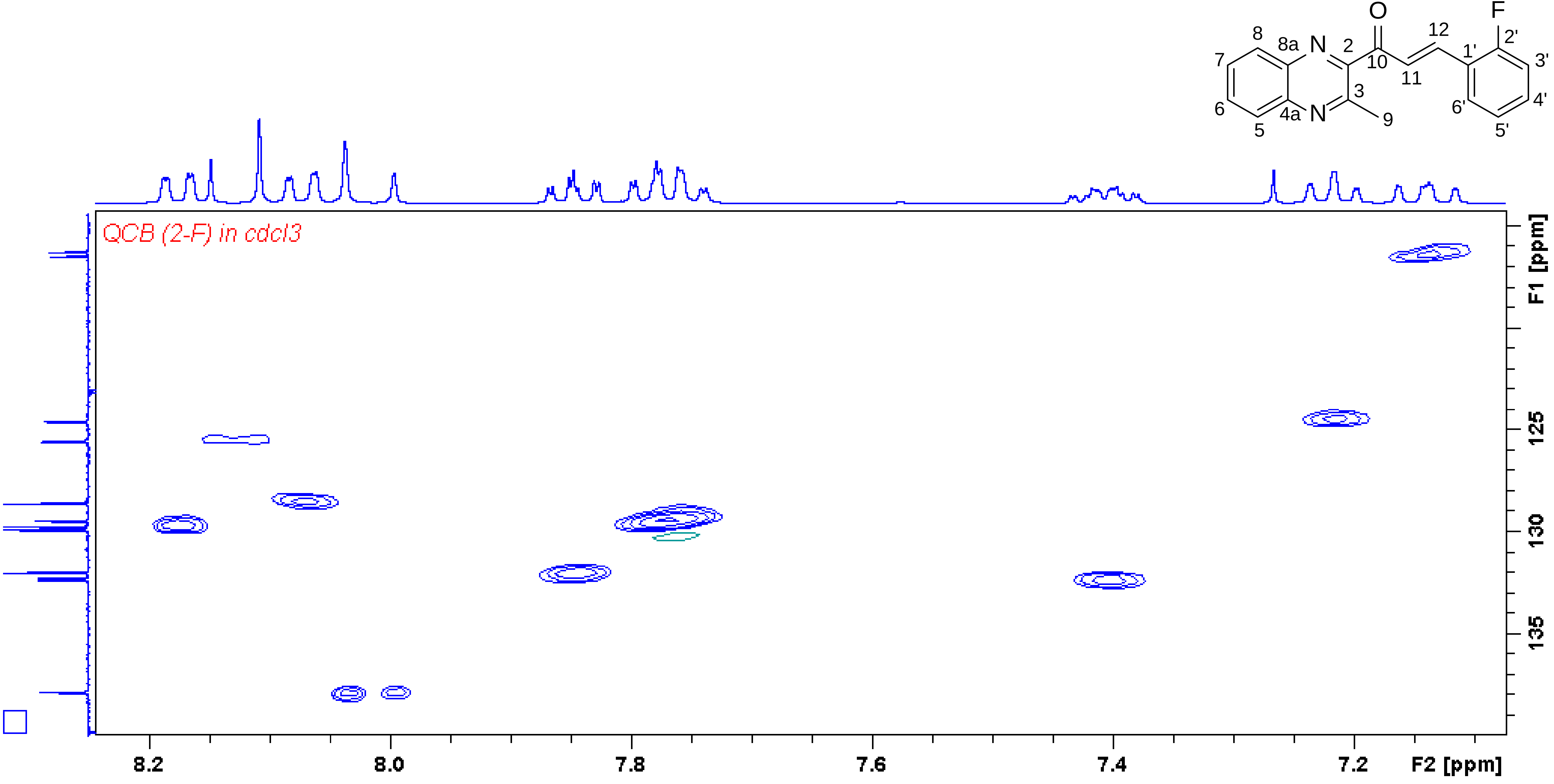

HSQC of **B10a**

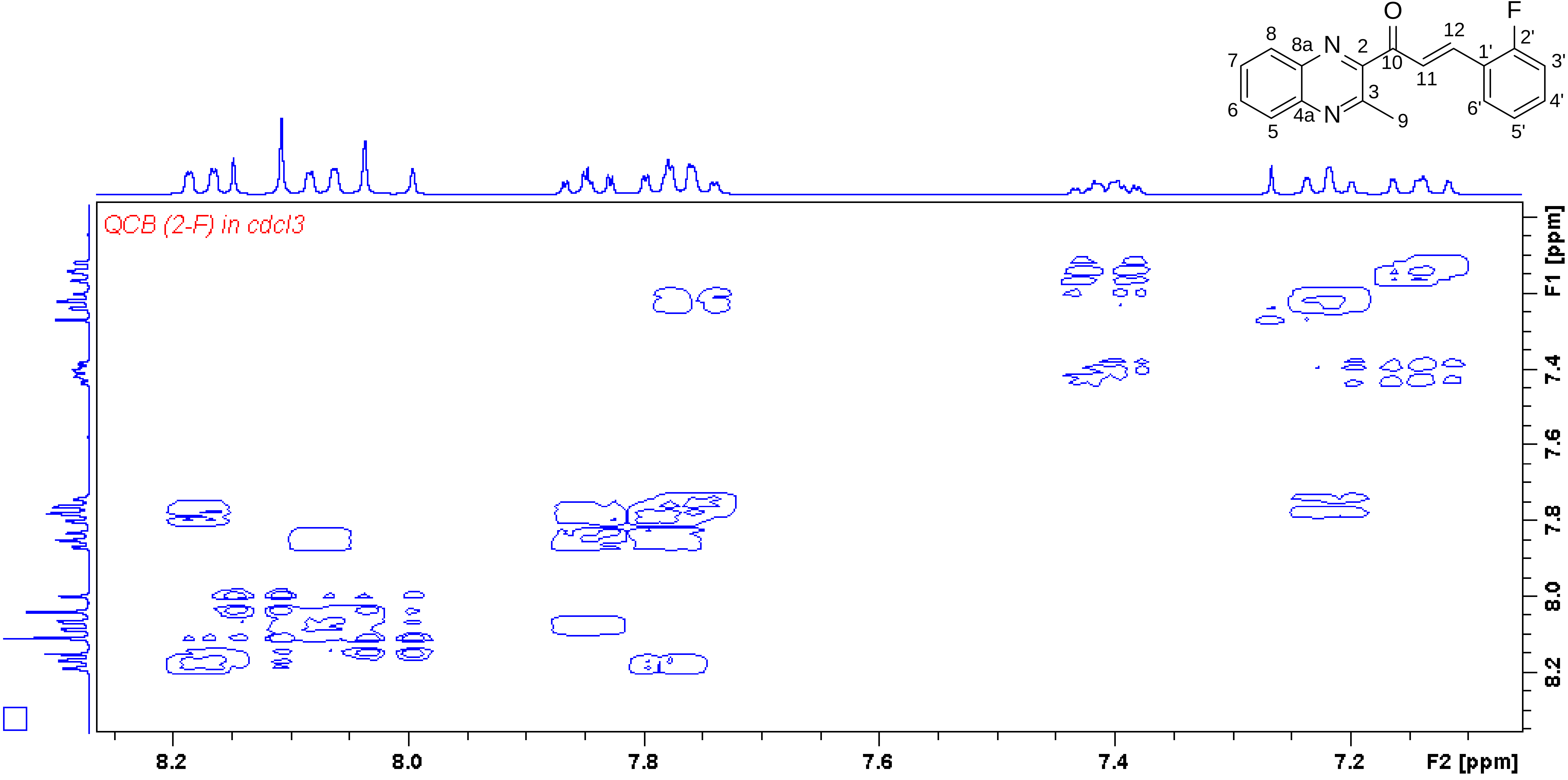

COSY of **B10a**

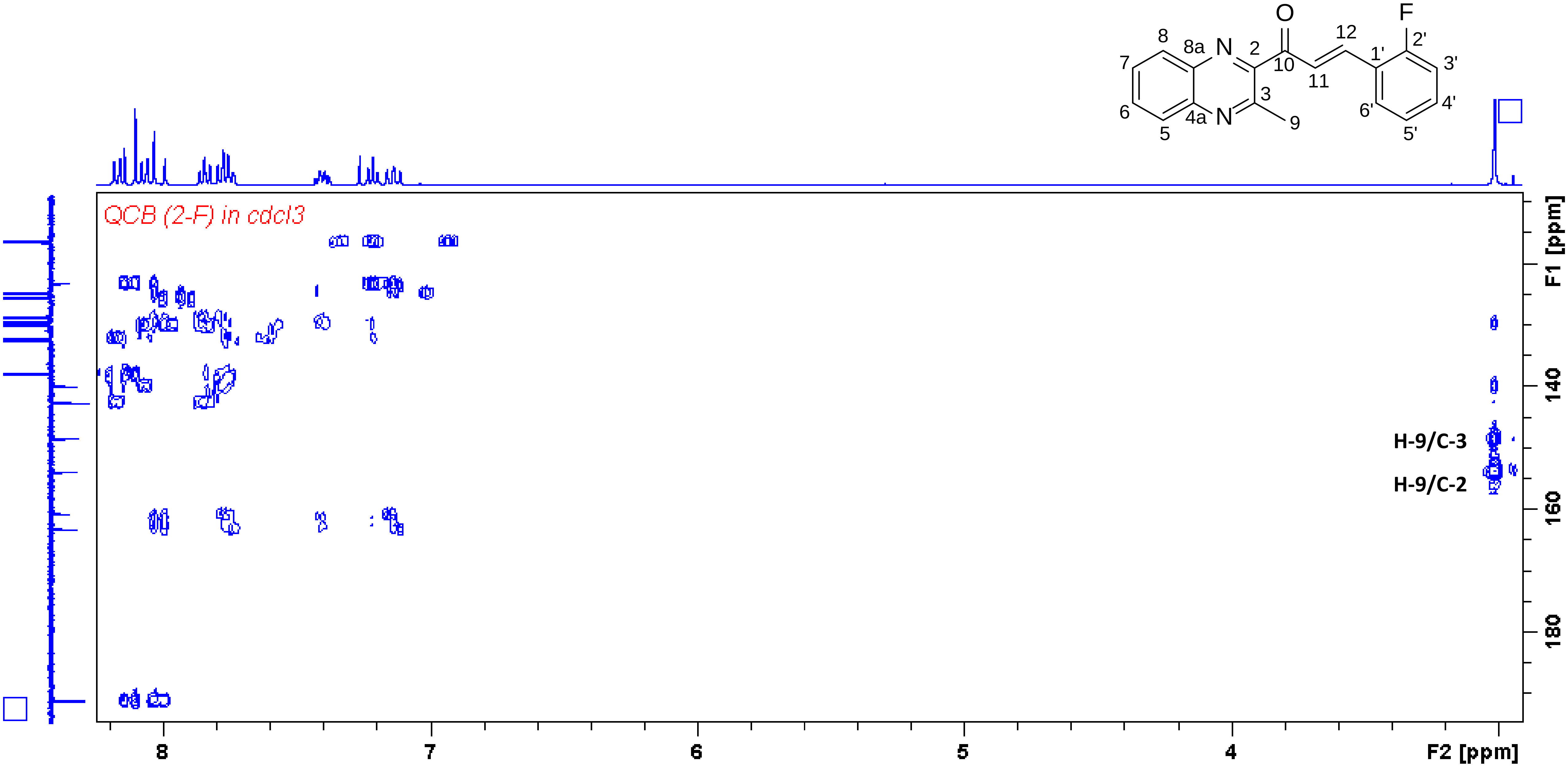

HMBC of **B10a**

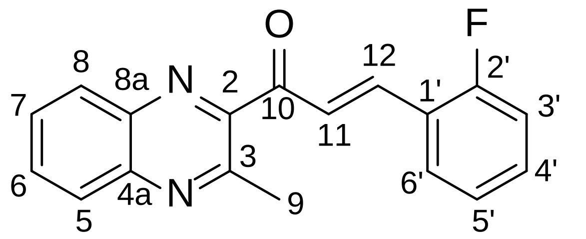

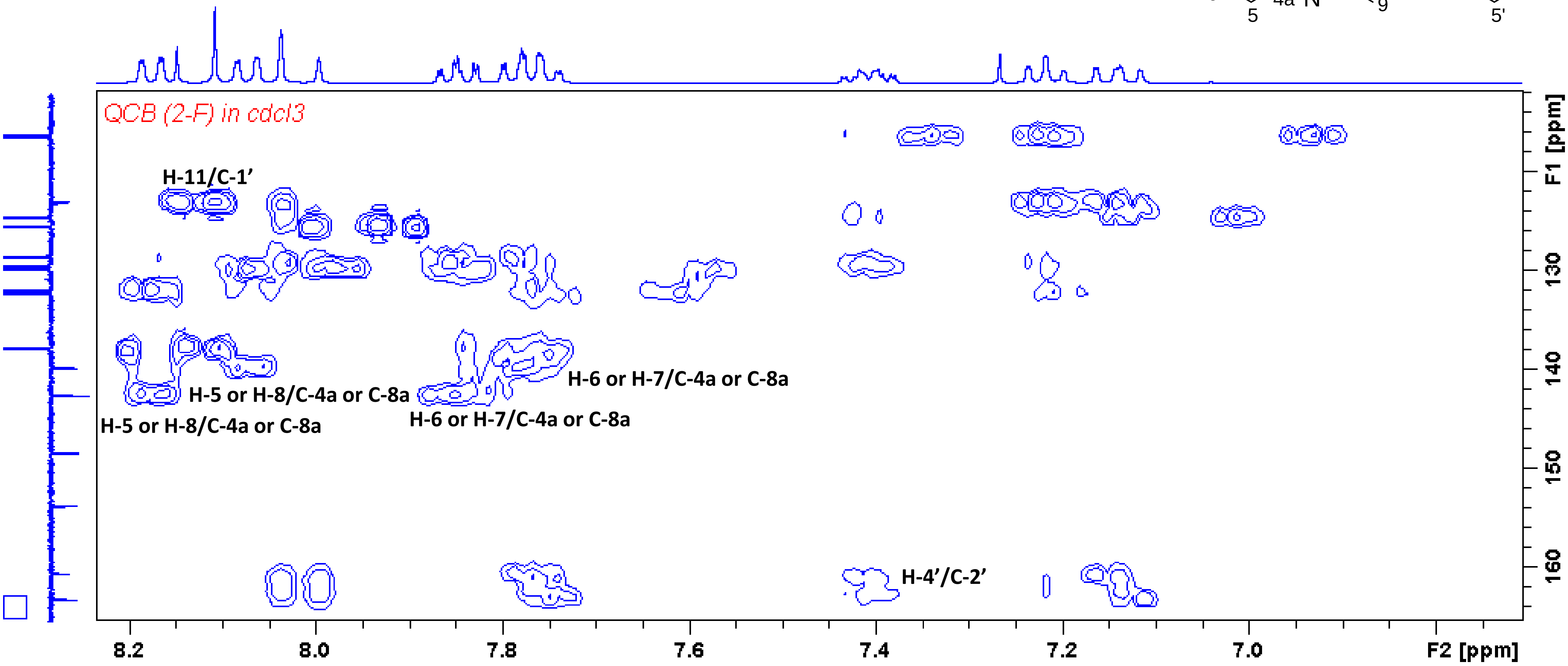

Expanded HMBC of **B10a**

Elemental Composition Report

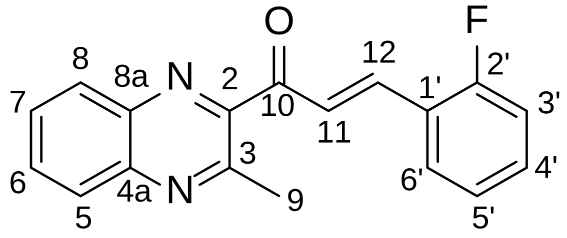

Single Mass Analysis

Tolerance = 5.0 PPM / DBE: min = -1.5, max = 100.0
Element prediction: Off
Number of isotope peaks used for i-FIT = 3

Monoisotopic Mass, Even Electron Ions
32 formula(e) evaluated with 1 results within limits (up to 20 closest results for each mass)
Elements Used:
C: 15-20 H: 10-15 N: 0-5 O: 1-5 F: 0-1
QCB(2-F) 57 (1.889) Cm (1:61)
TOF MS AP+

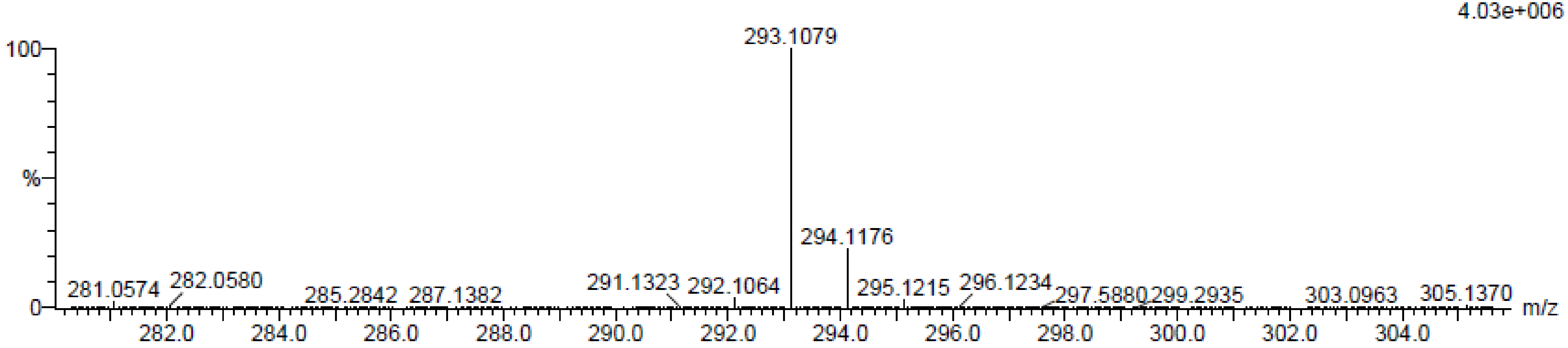

Minimum:				-1.5			
Maximum:		5.0	5.0	100.0			

Mass	Calc. Mass	mDa	PPM	DBE	i-FIT	i-FIT (Norm)	Formula
293.1079	293.1090	-1.1	-3.8	12.5	813.3	0.0	C18 H14 N2 O F

High resolution mass spectrum of **B10a**

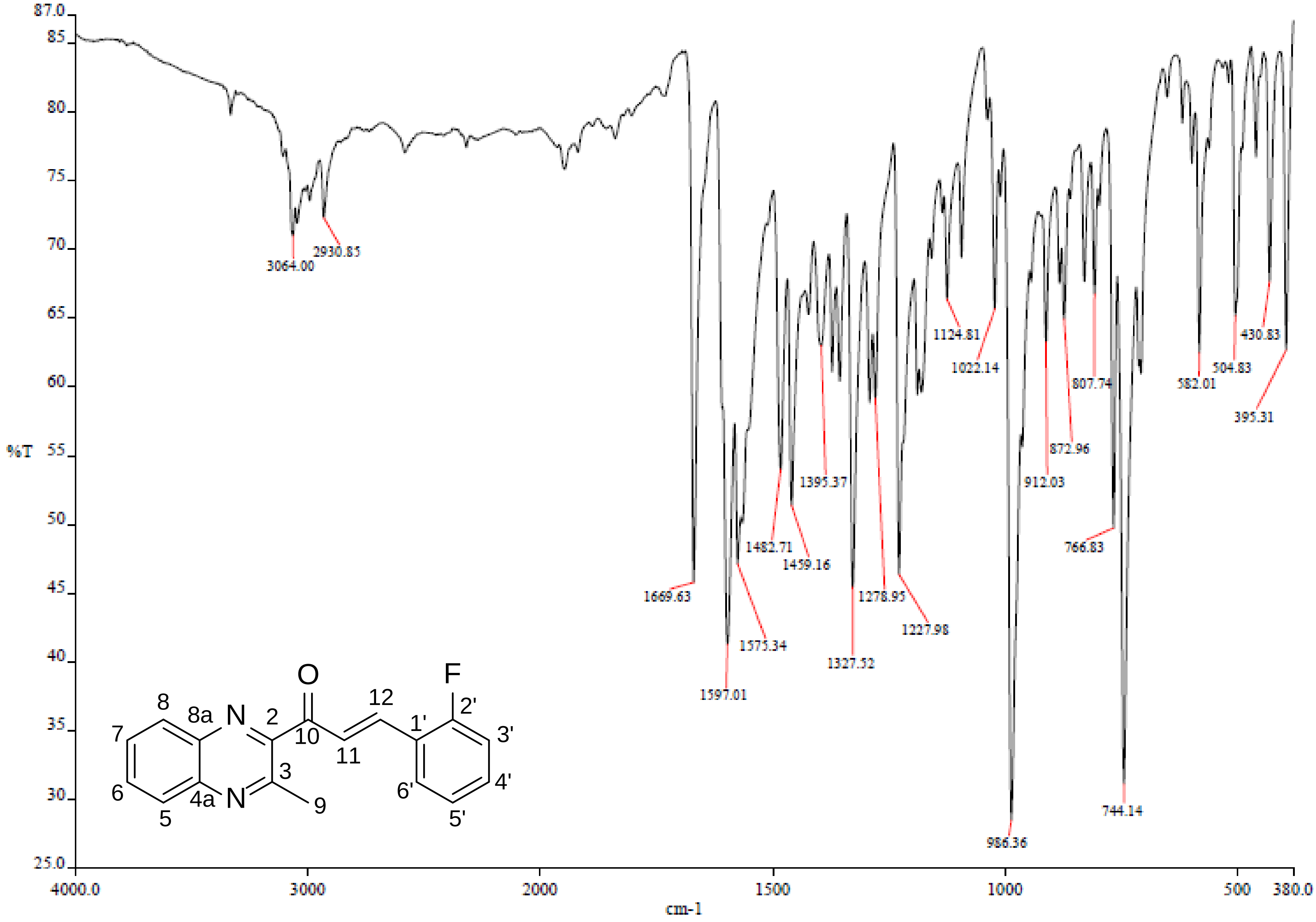

FTIR spectrum of **B10a**

Overlay Spectrum Graph Report

06/10/2017 11:41:50 AM

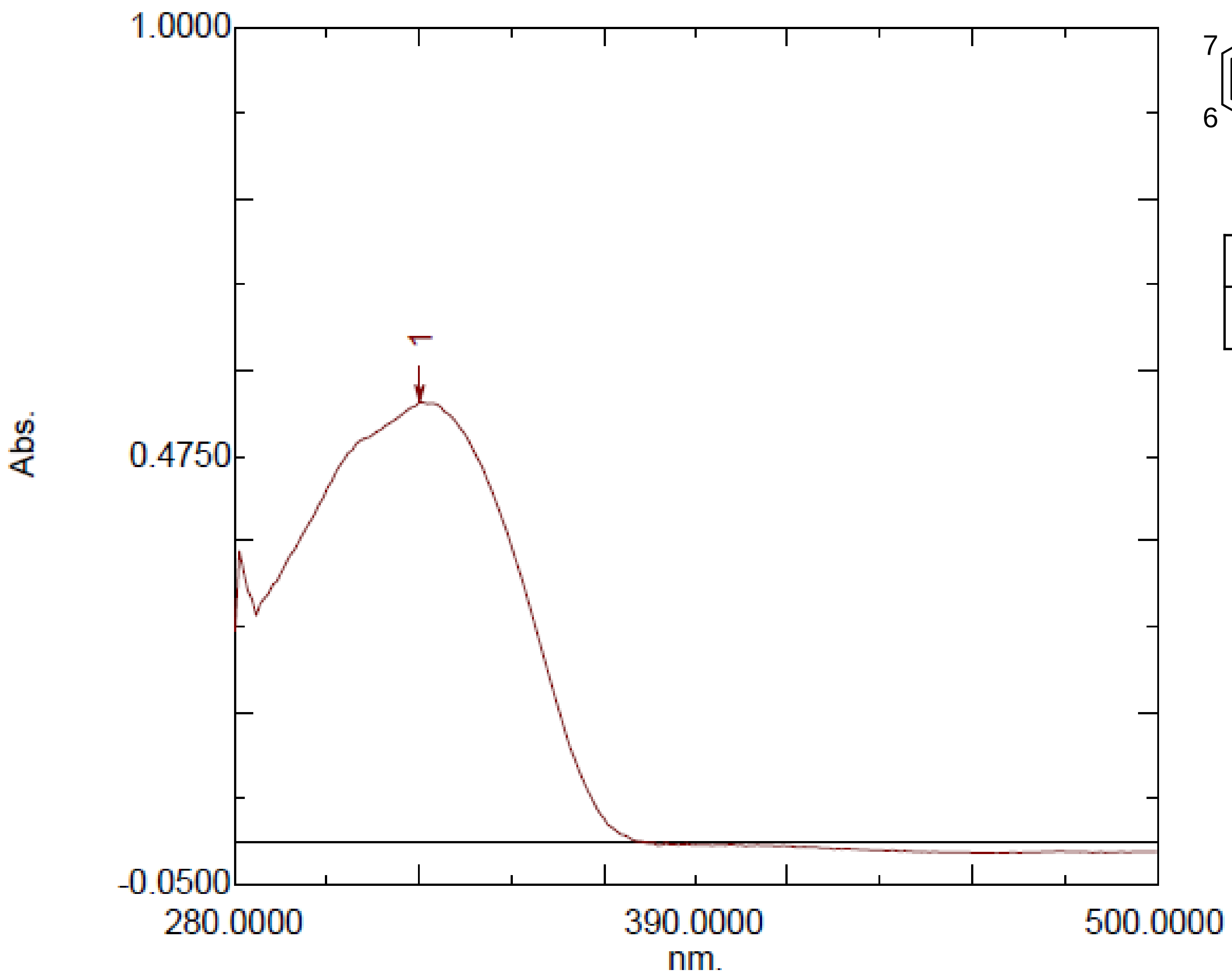

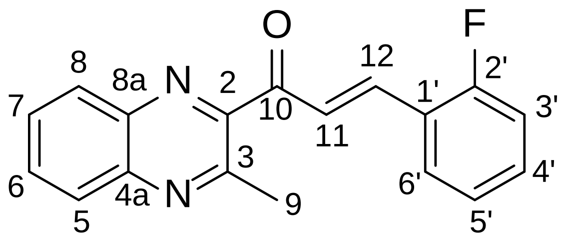

λ	absorbance	logε
324	0.5405	4.50

UV spectrum of **B10a**

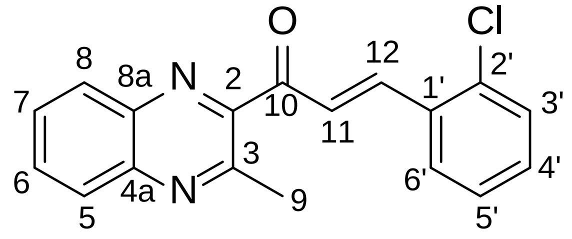

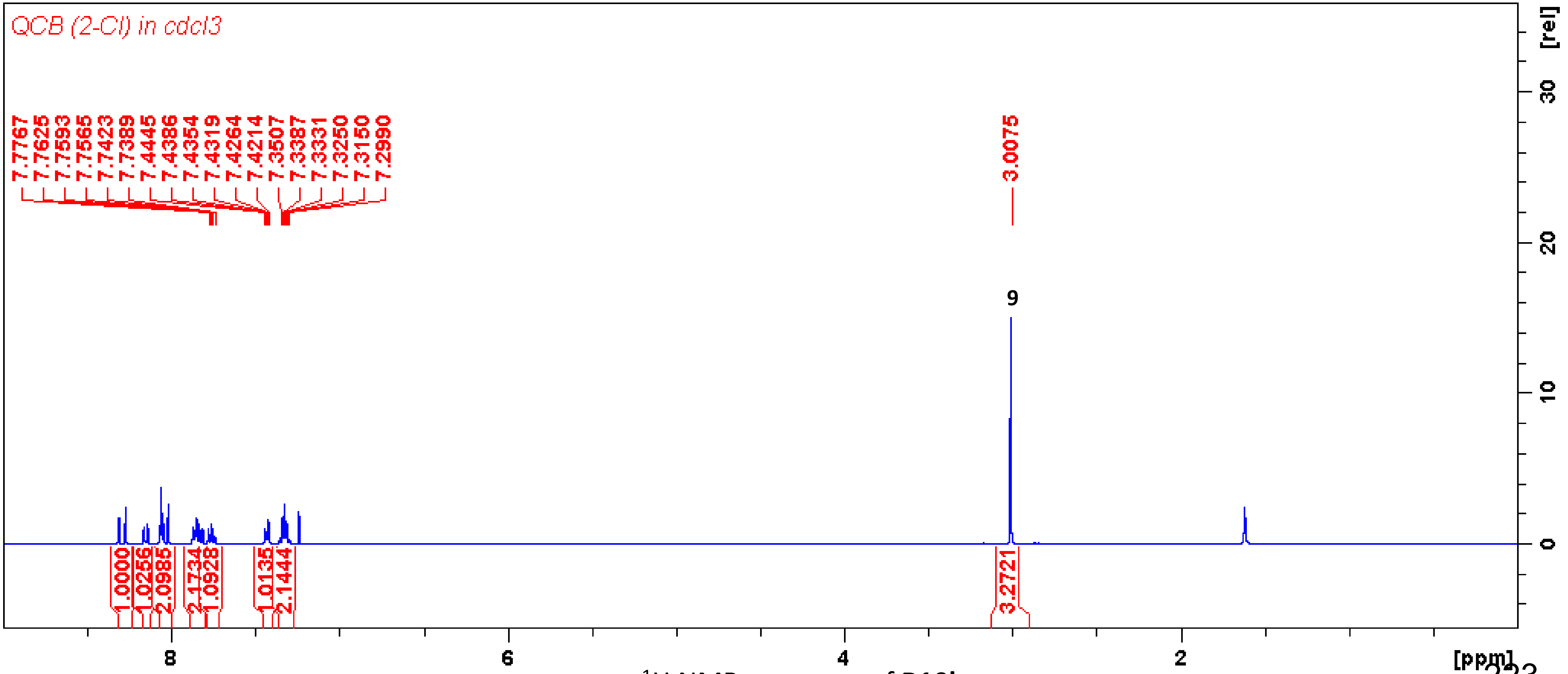

^{1}H NMR spectrum of **B10b**

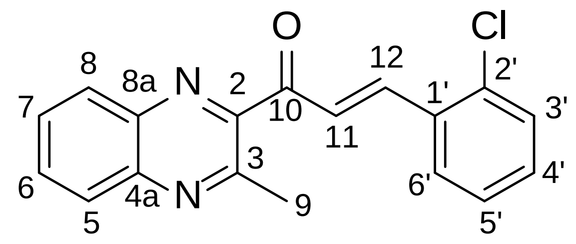

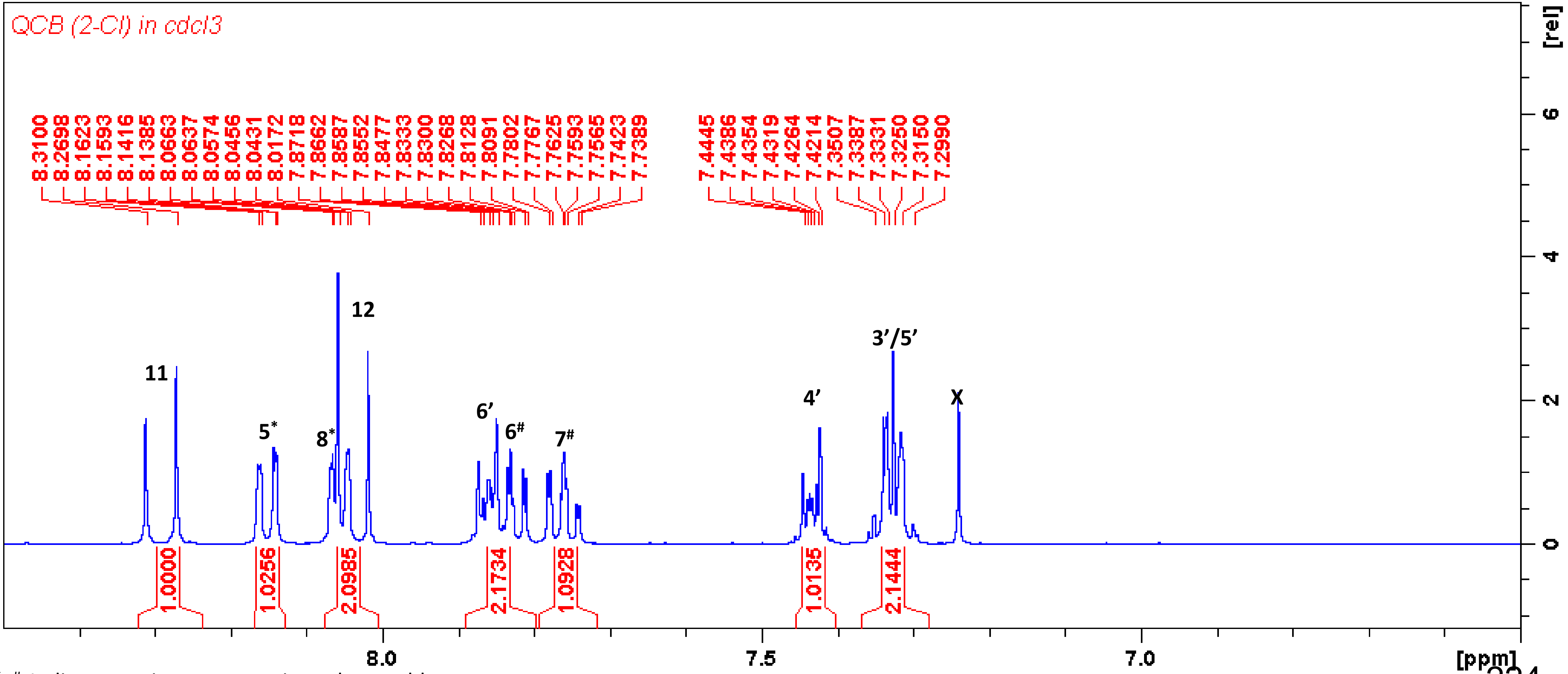

*, # Indicates assignments are interchangeable

Expanded ^1H NMR spectrum of **B10b**

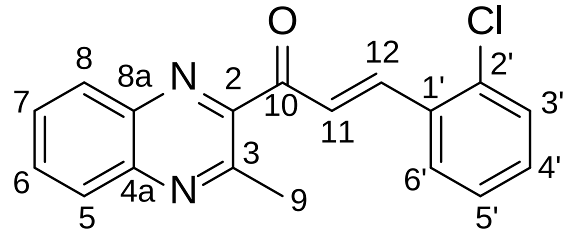

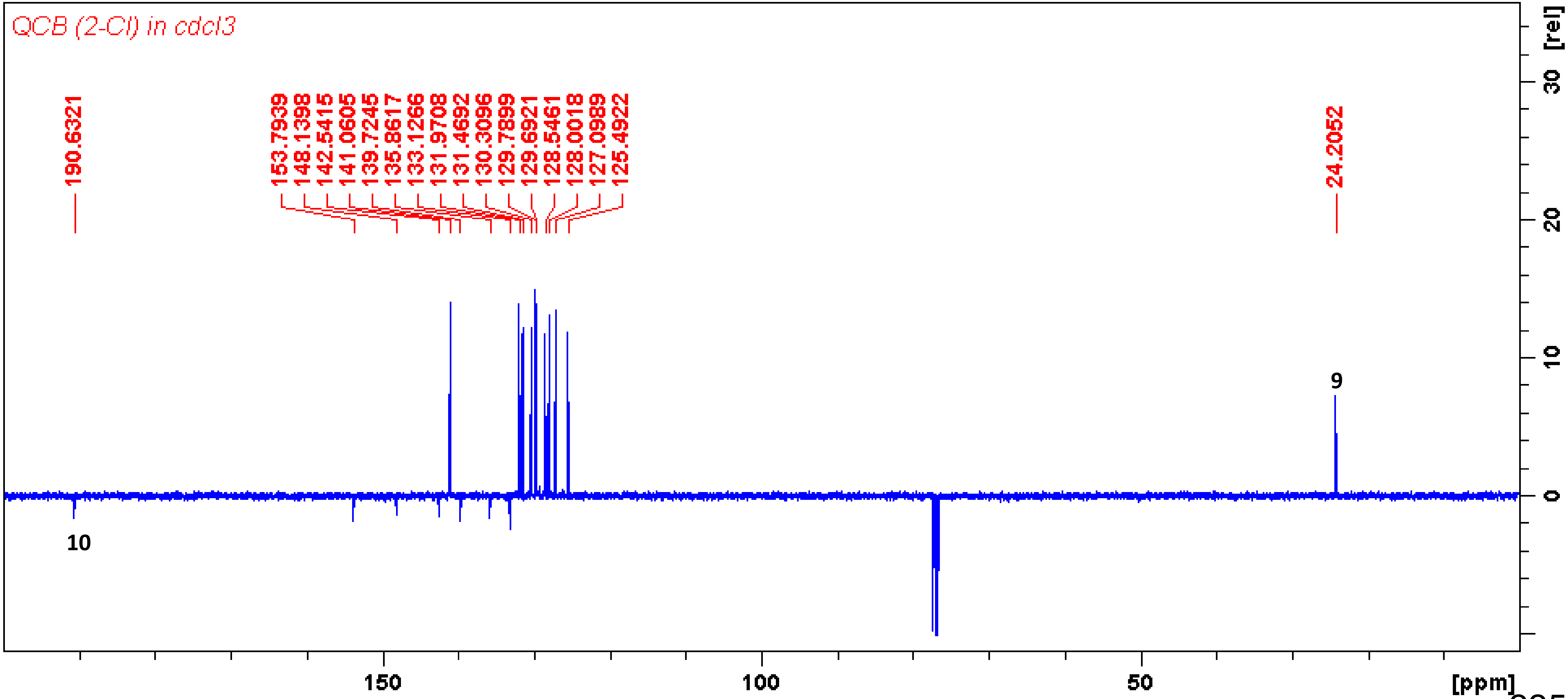

^{13}C NMR spectrum of **B10b**

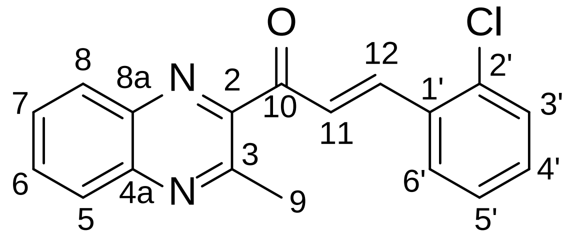

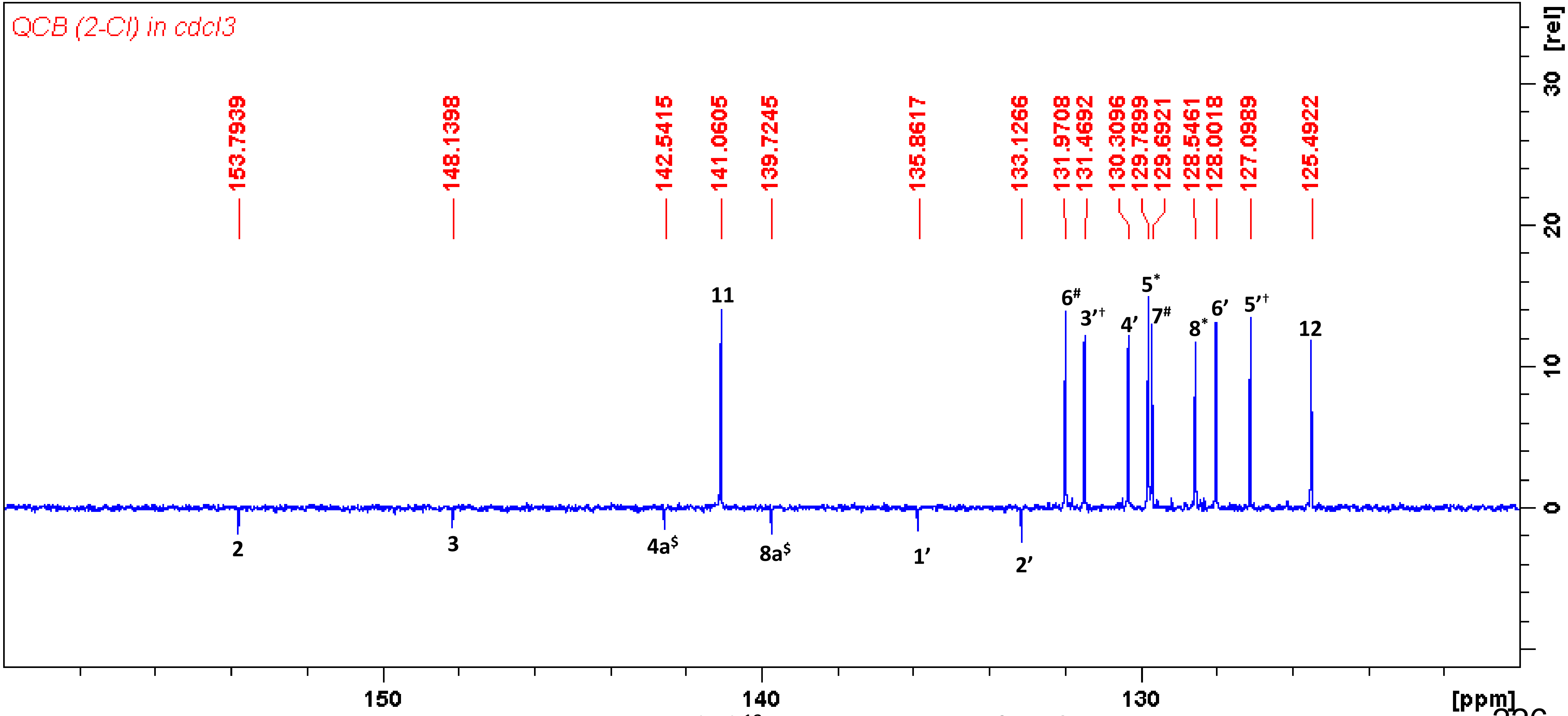

*, #, $, † Indicates assignments are interchangeable

Expanded ^{13}C NMR spectrum of **B10b**

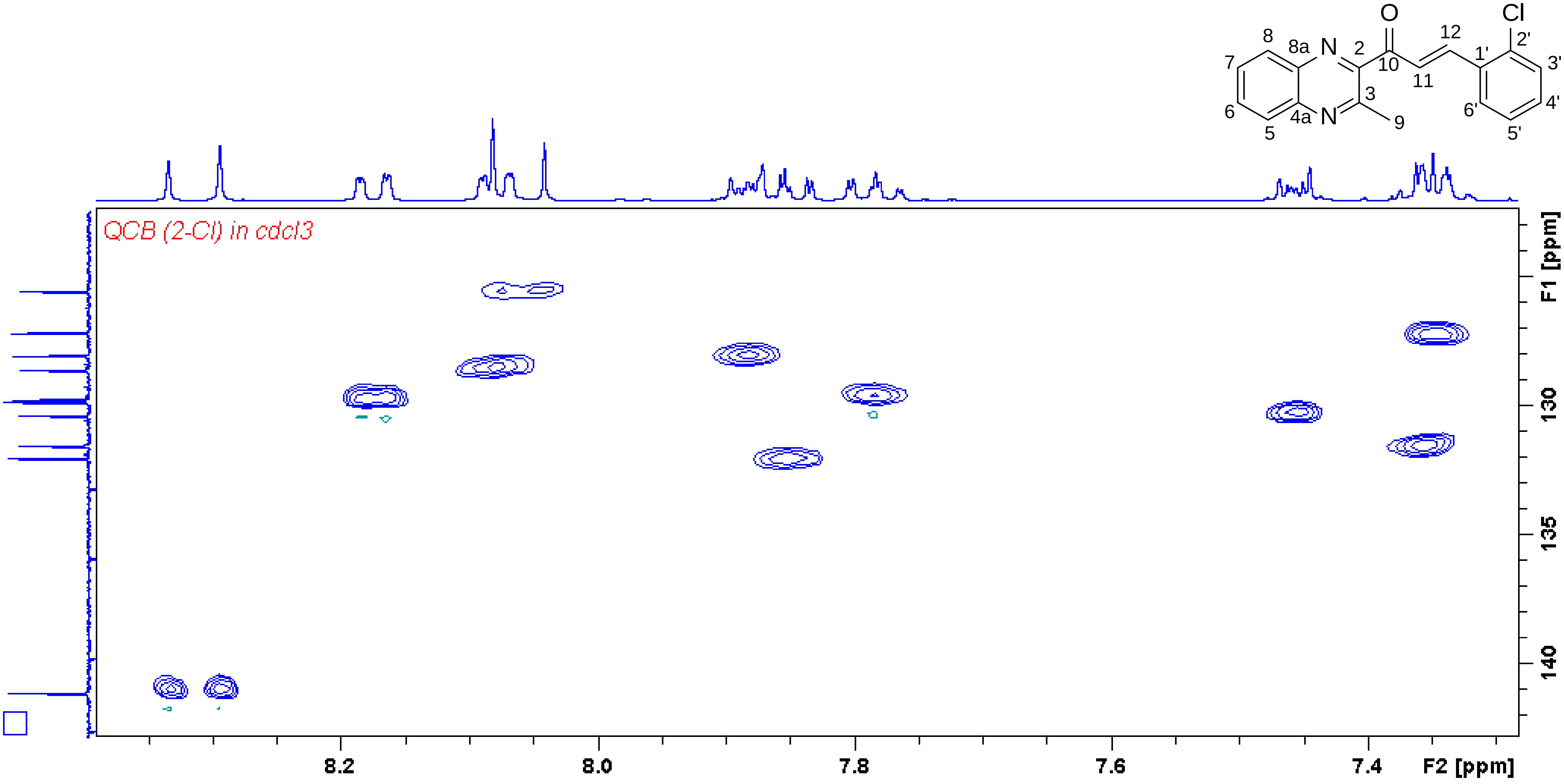

QCB (2-Cl) in cdcl3
O
Cl
N
N
2
3
4a
5
6
7
8
8a
9
10
11
12
1'
2'
3'
4'
5'
6'
F1 [ppm]
130
135
140
8.2
8.0
7.8
7.6
7.4
F2 [ppm]

HSQC of **B10b**

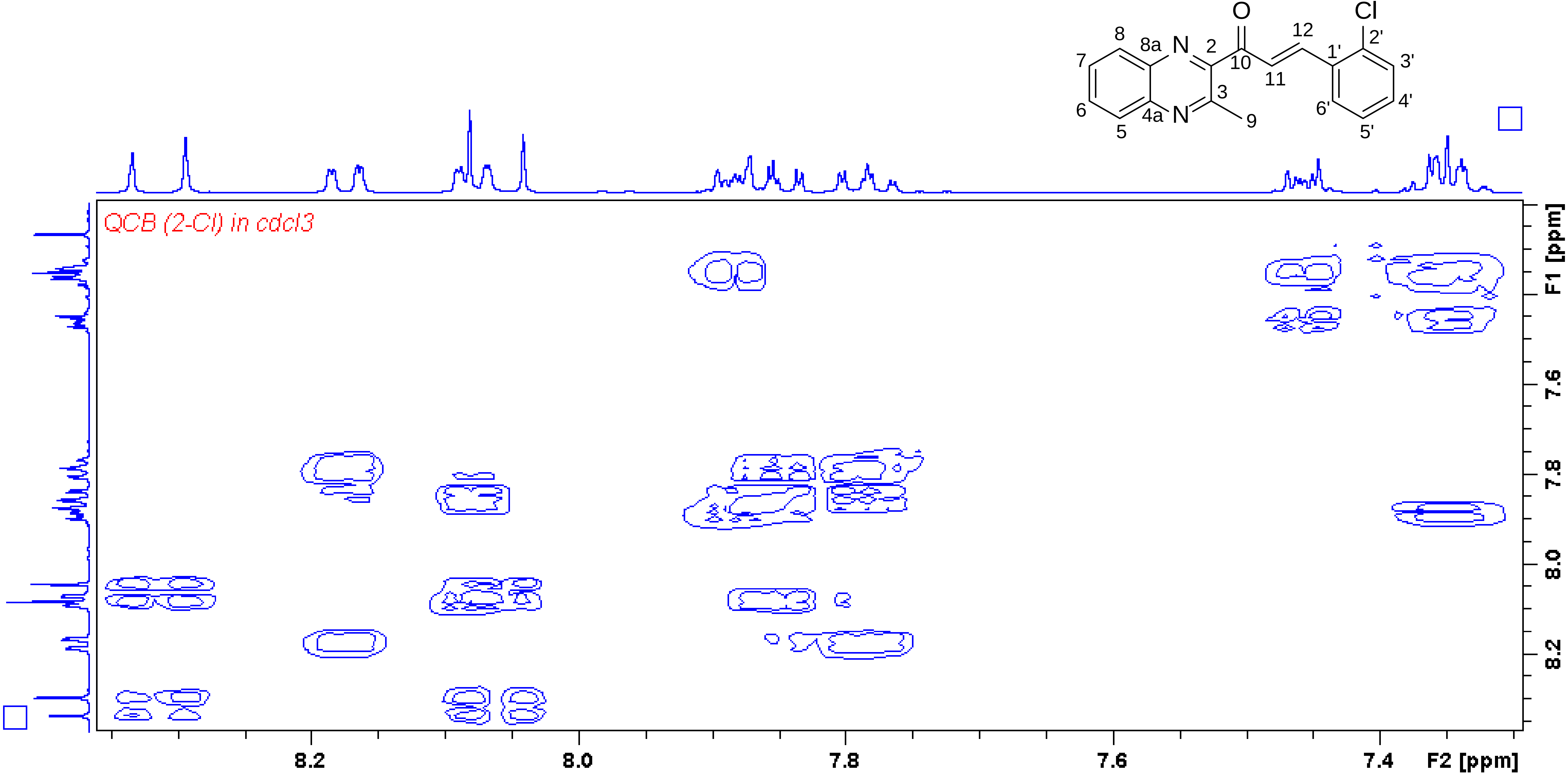

COSY of **B10b**

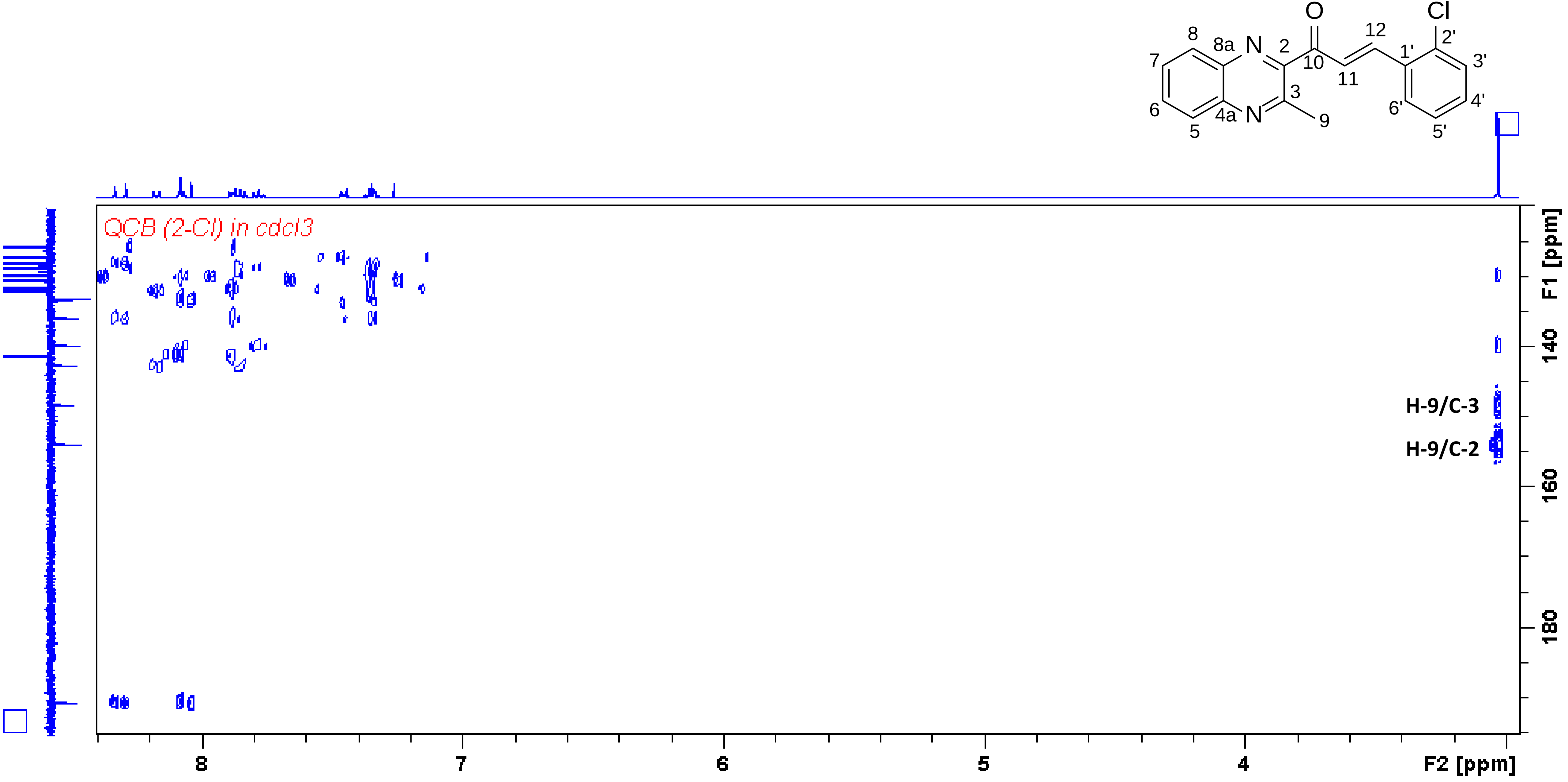

O
Cl
8
8a
N
2
12
2'
7
10
1'
3'
11
3
6
4a
N
9
6'
4'
5
5'
QCB (2-Cl) in cdcl3
H-9/C-3
H-9/C-2
F1 [ppm]
140
160
180
8
7
6
5
4
F2 [ppm]

HMBC of **B10b**

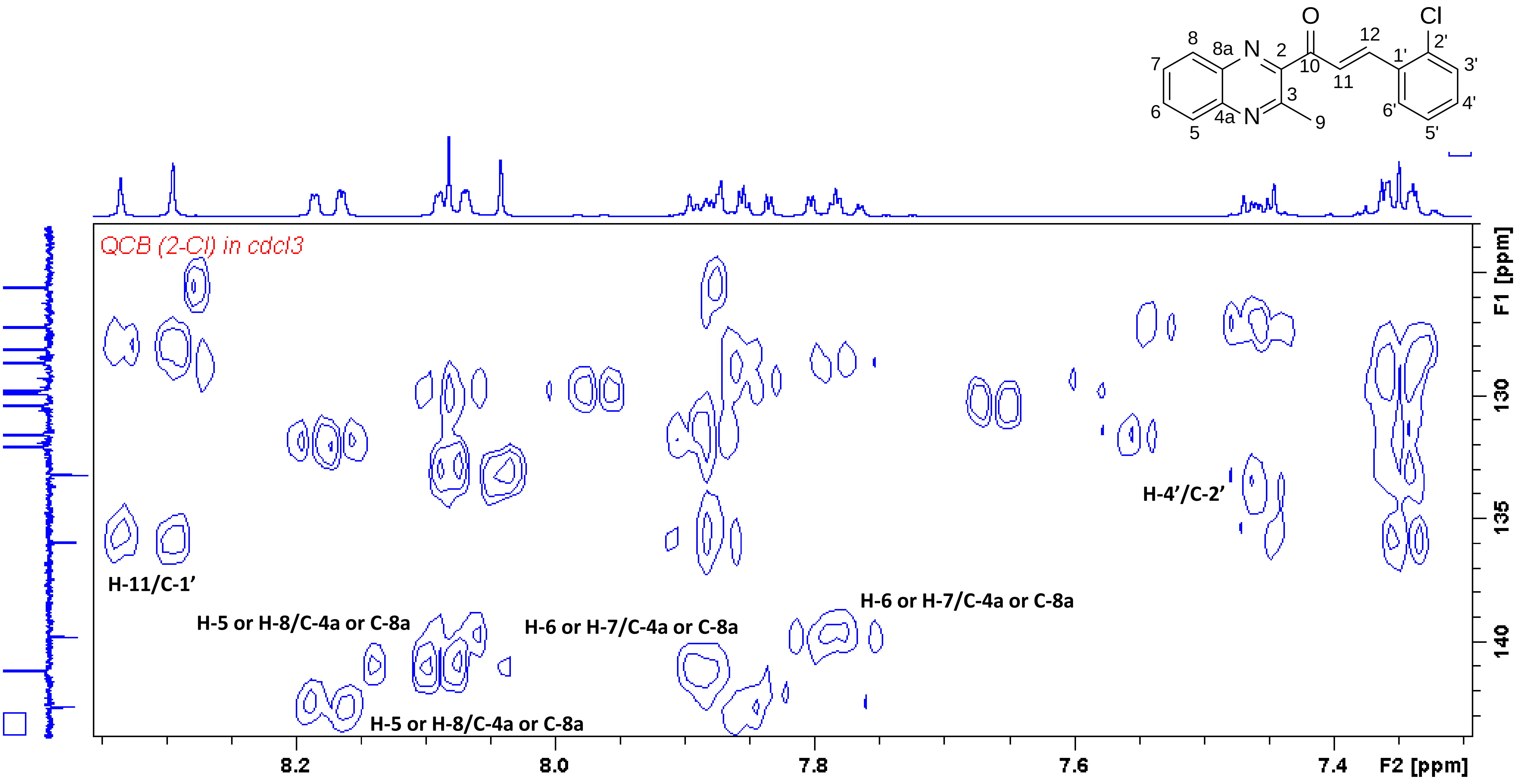

Expanded HMBC of **B10b**

Elemental Composition Report

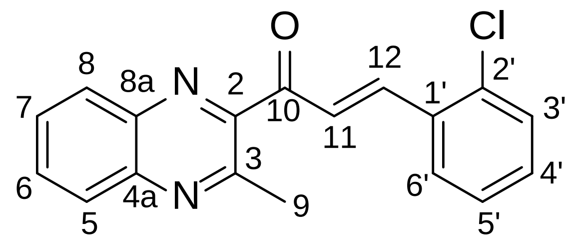

Single Mass Analysis

Tolerance = 5.0 PPM / DBE: min = -1.5, max = 100.0
Element prediction: Off
Number of isotope peaks used for i-FIT = 3

Monoisotopic Mass, Even Electron Ions
30 formula(e) evaluated with 1 results within limits (up to 20 closest results for each mass)
Elements Used:
C: 15-20 H: 10-15 N: 0-5 O: 1-5 Cl: 0-1
QCB(2-Cl) 35 (1.147) Cm (1:61)
TOF MS AP+

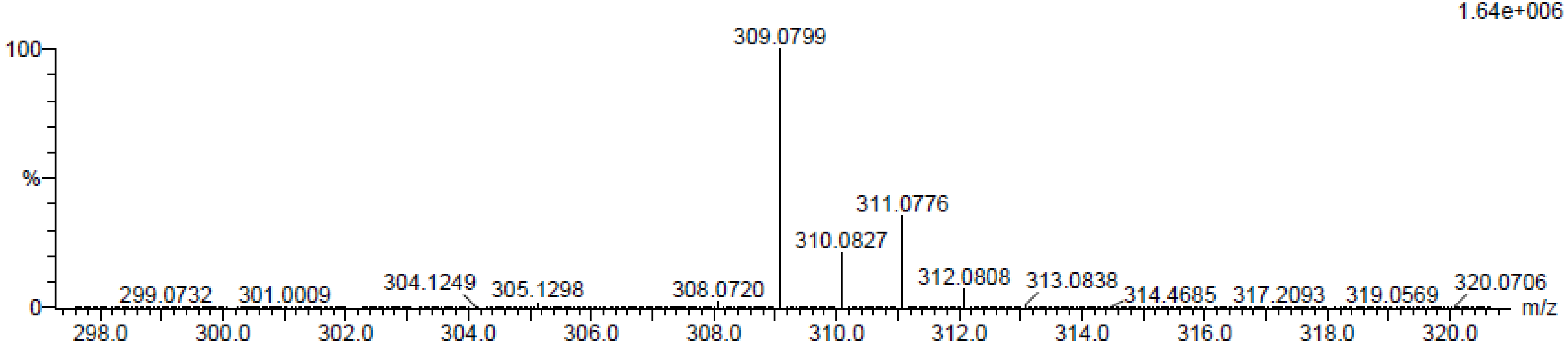

Minimum:				-1.5			
Maximum:		5.0	5.0	100.0			
Mass	Calc. Mass	mDa	PPM	DBE	i-FIT	i-FIT (Norm)	Formula
309.0799	309.0795	0.4	1.3	12.5	735.9	0.0	C18 H14 N2 O Cl

High resolution mass spectrum of **B10b**

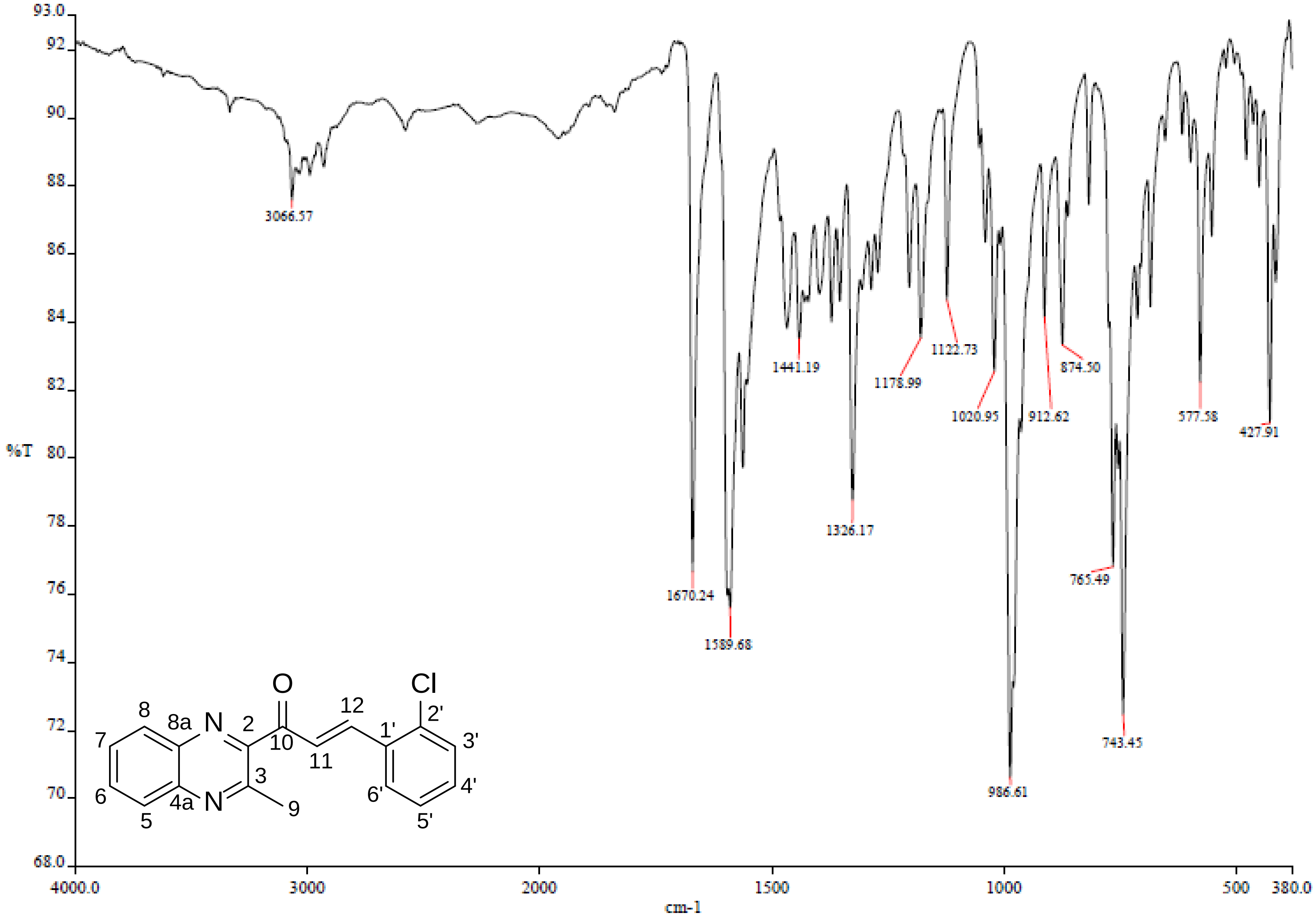

FTIR spectrum of **B10b**

Overlay Spectrum Graph Report

06/10/2017 11:40:39 AM

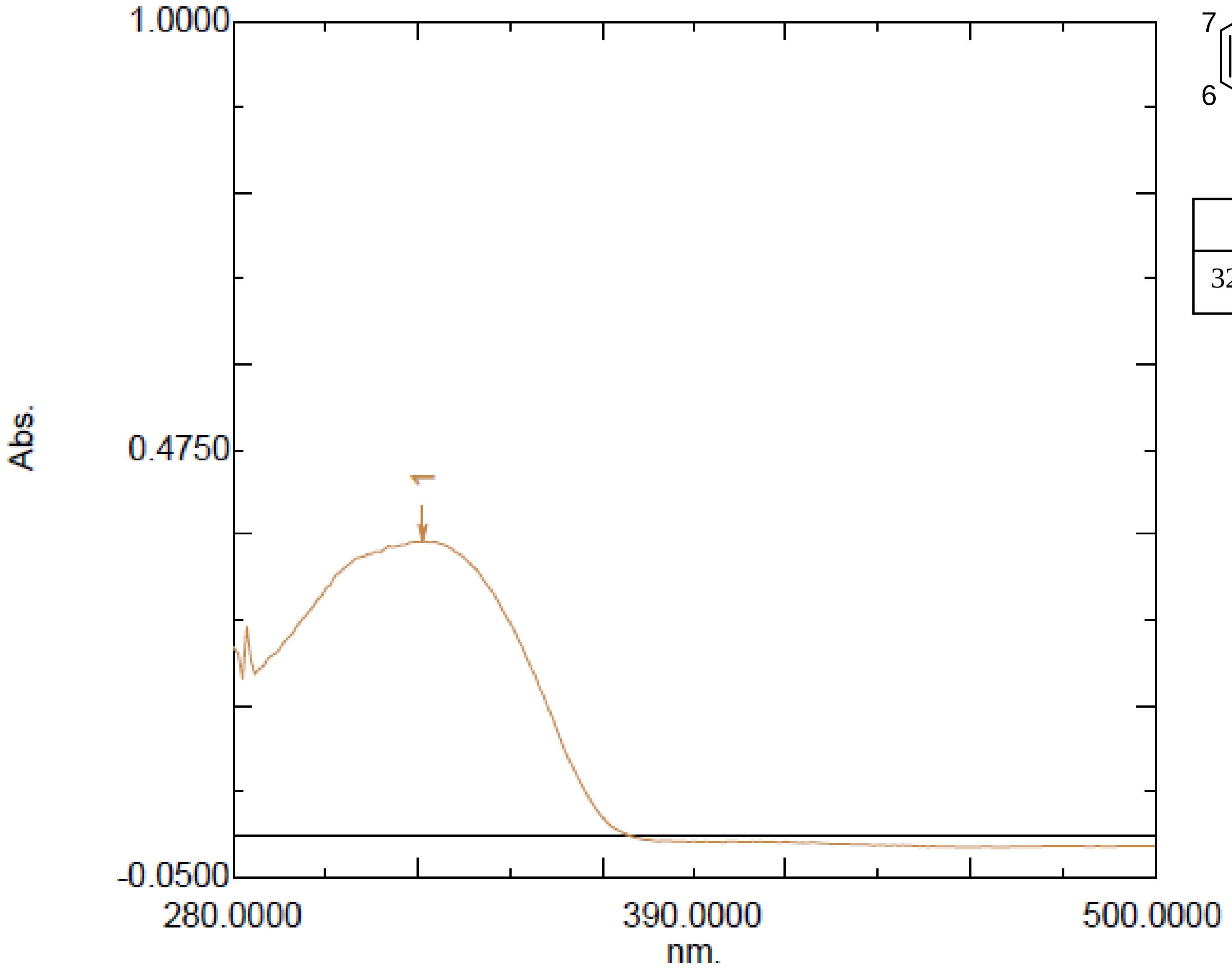

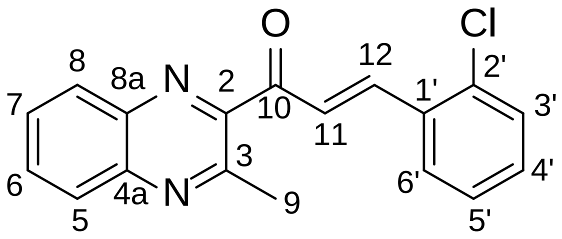

λ	absorbance	logε
325	0.3627	4.35

UV spectrum of **B10b**

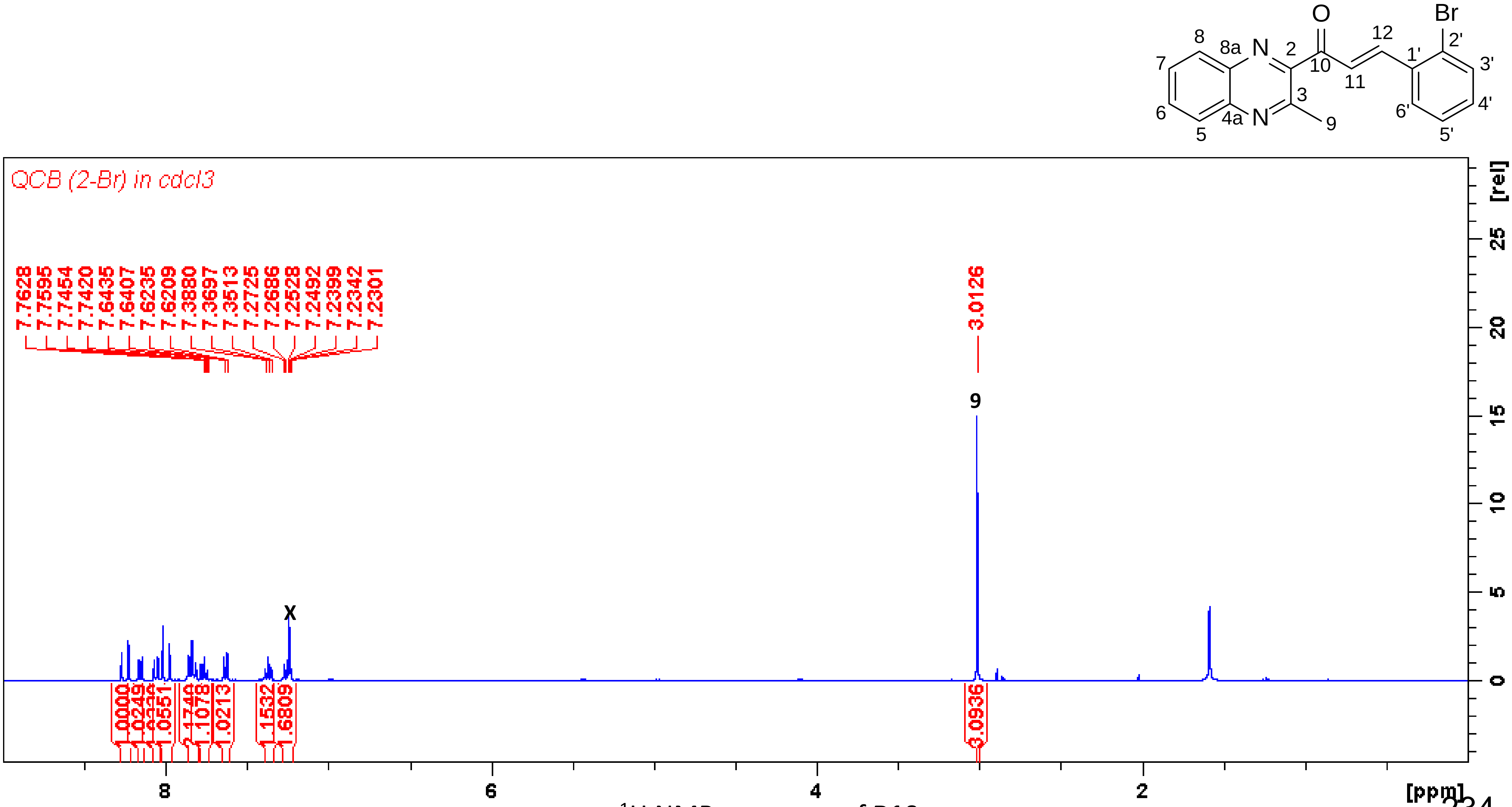

^{1}H NMR spectrum of **B10c**

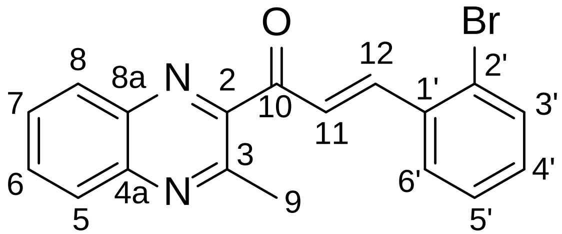

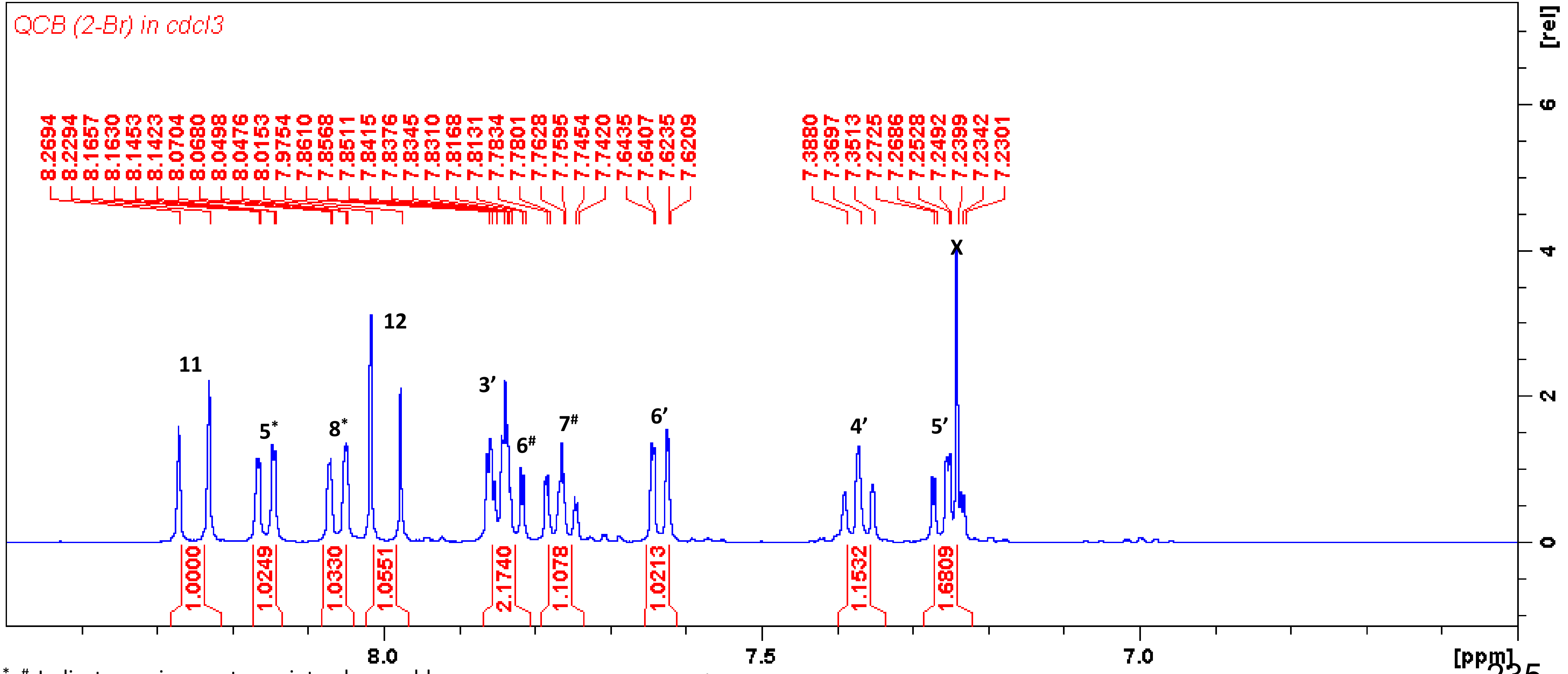

*, # Indicates assignments are interchangeable

Expanded ^{1}H NMR spectrum of **B10c**

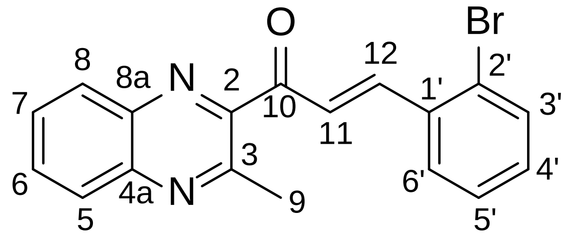

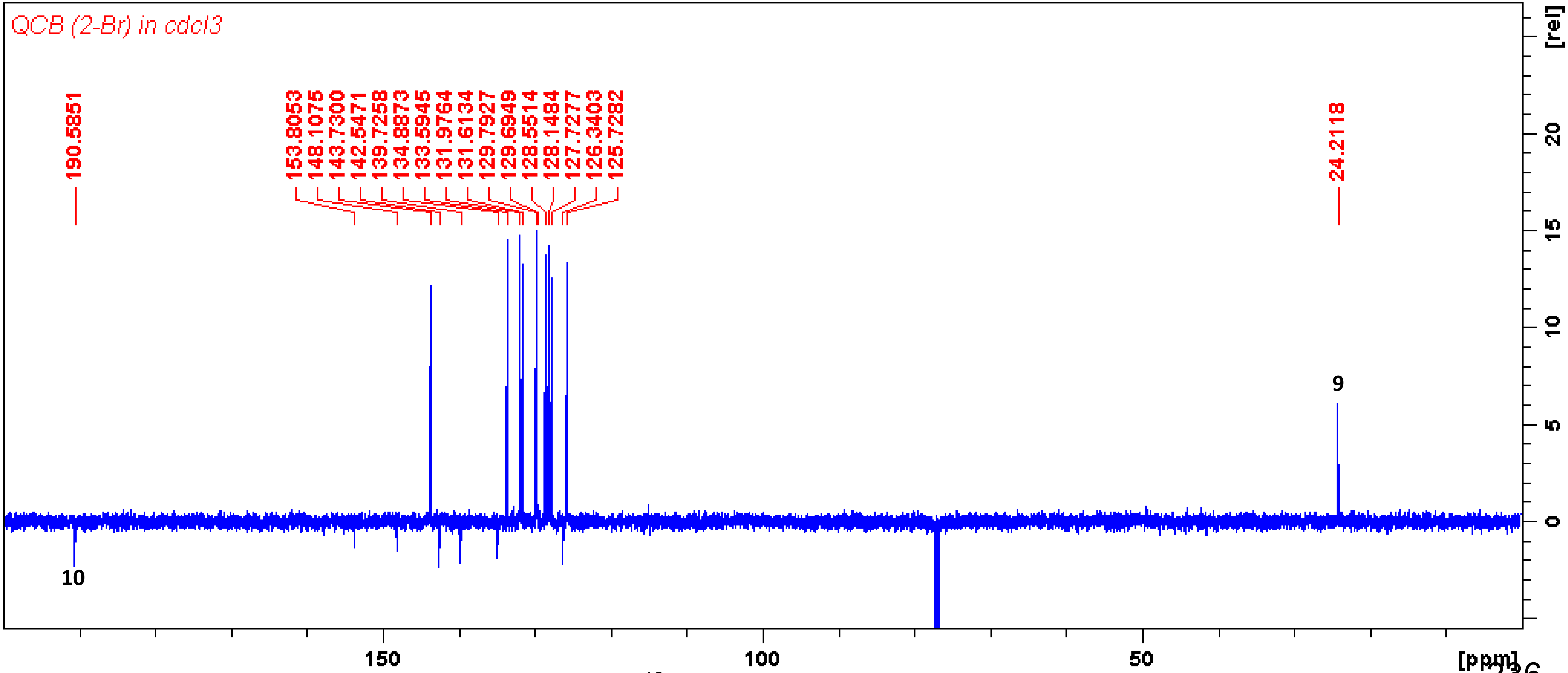

^{13}C NMR spectrum of **B10c**

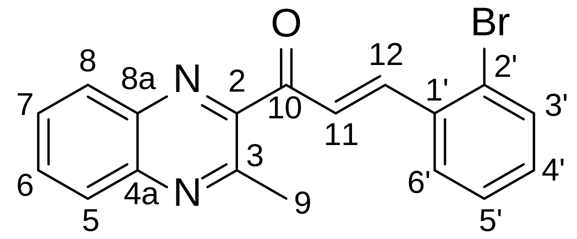

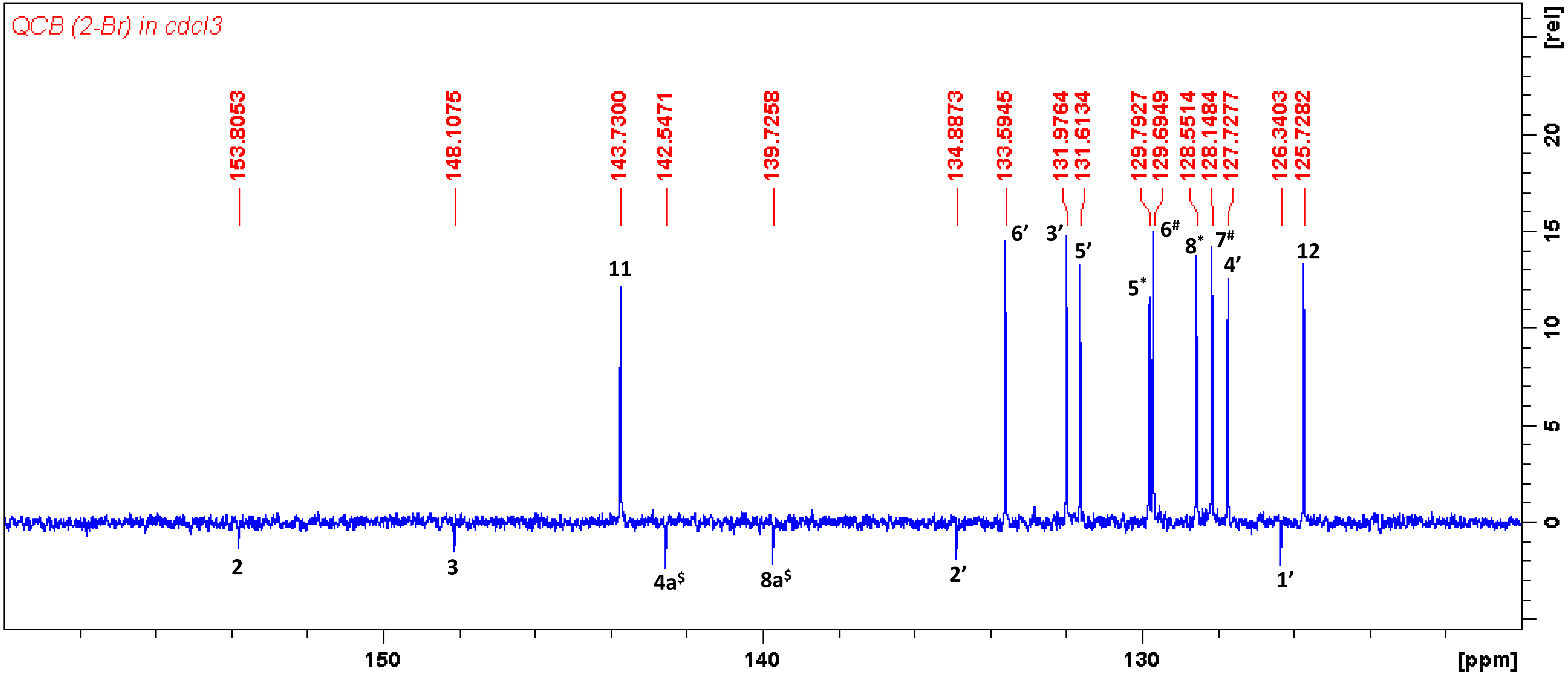

*, #, $ Indicates assignments are interchangeable

Expanded ^{13}C NMR spectrum of **B10c**

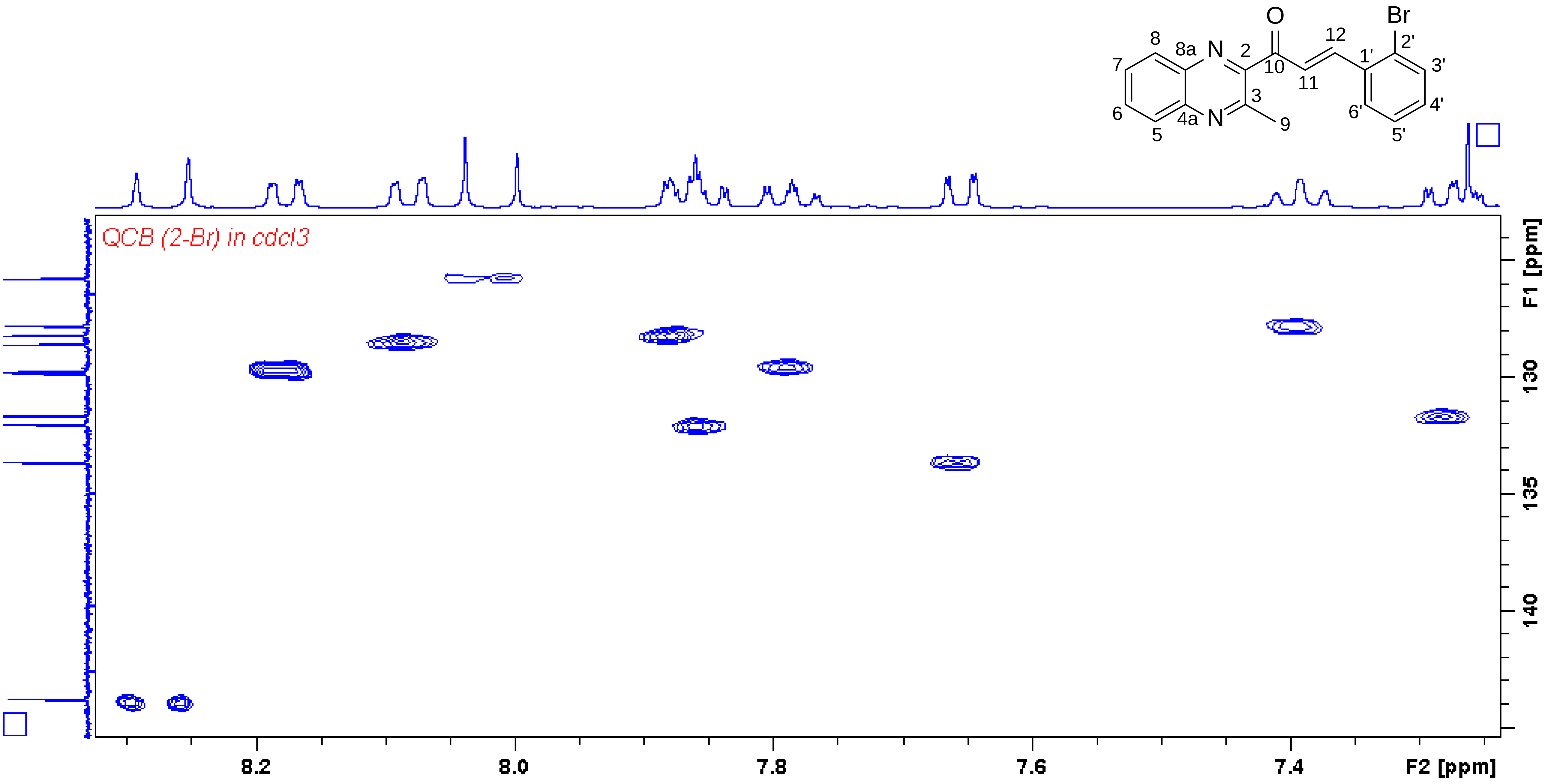
O
Br
8
8a
N
2
12
2'
7
10
1'
3'
11
3
6
6'
4'
4a
N
9
5
5'
QCB (2-Br) in cdcl3
F1 [ppm]
130
135
140
8.2
8.0
7.8
7.6
7.4
F2 [ppm]

HSQC of **B10c**

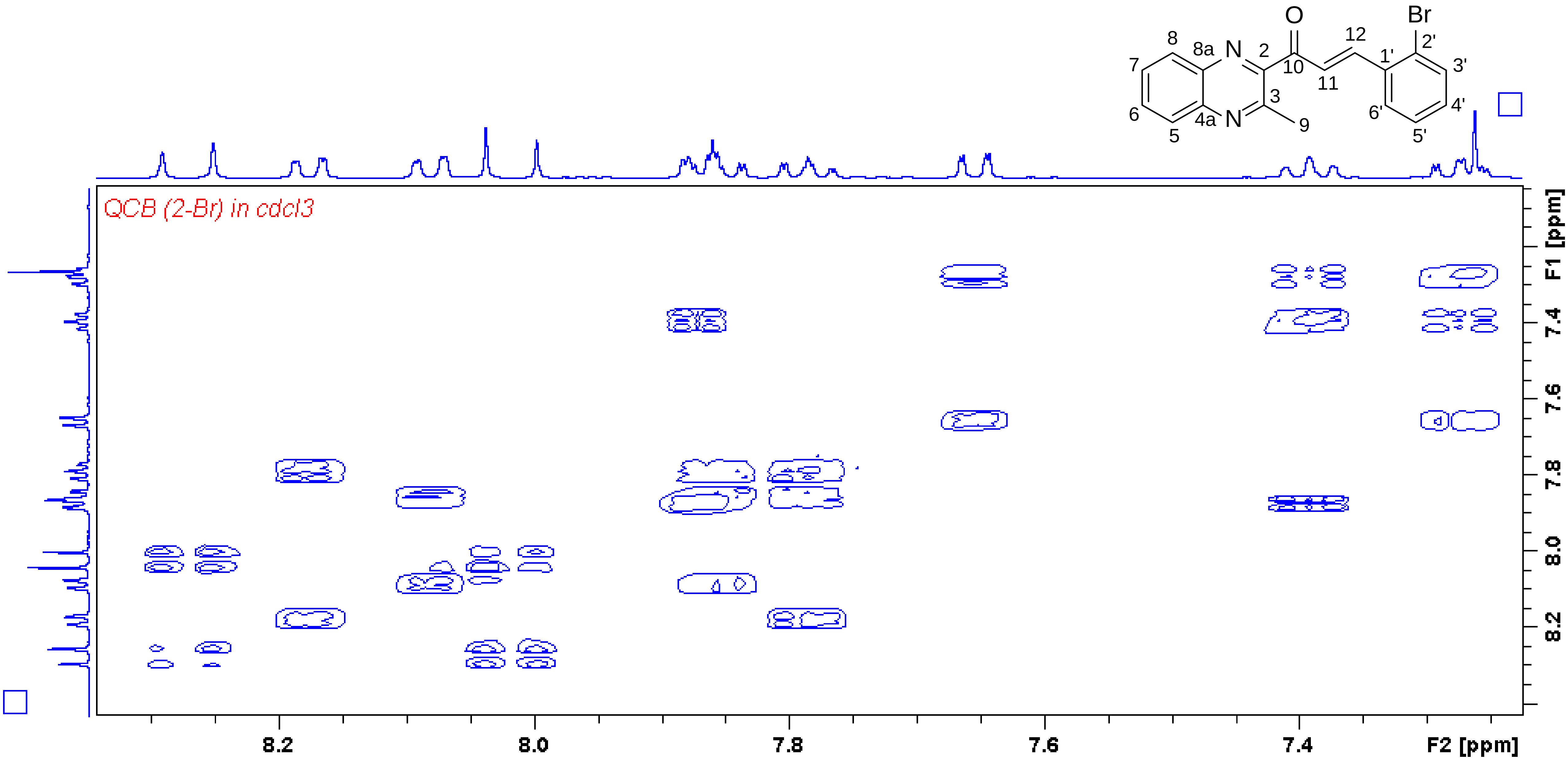

COSY of **B10c**

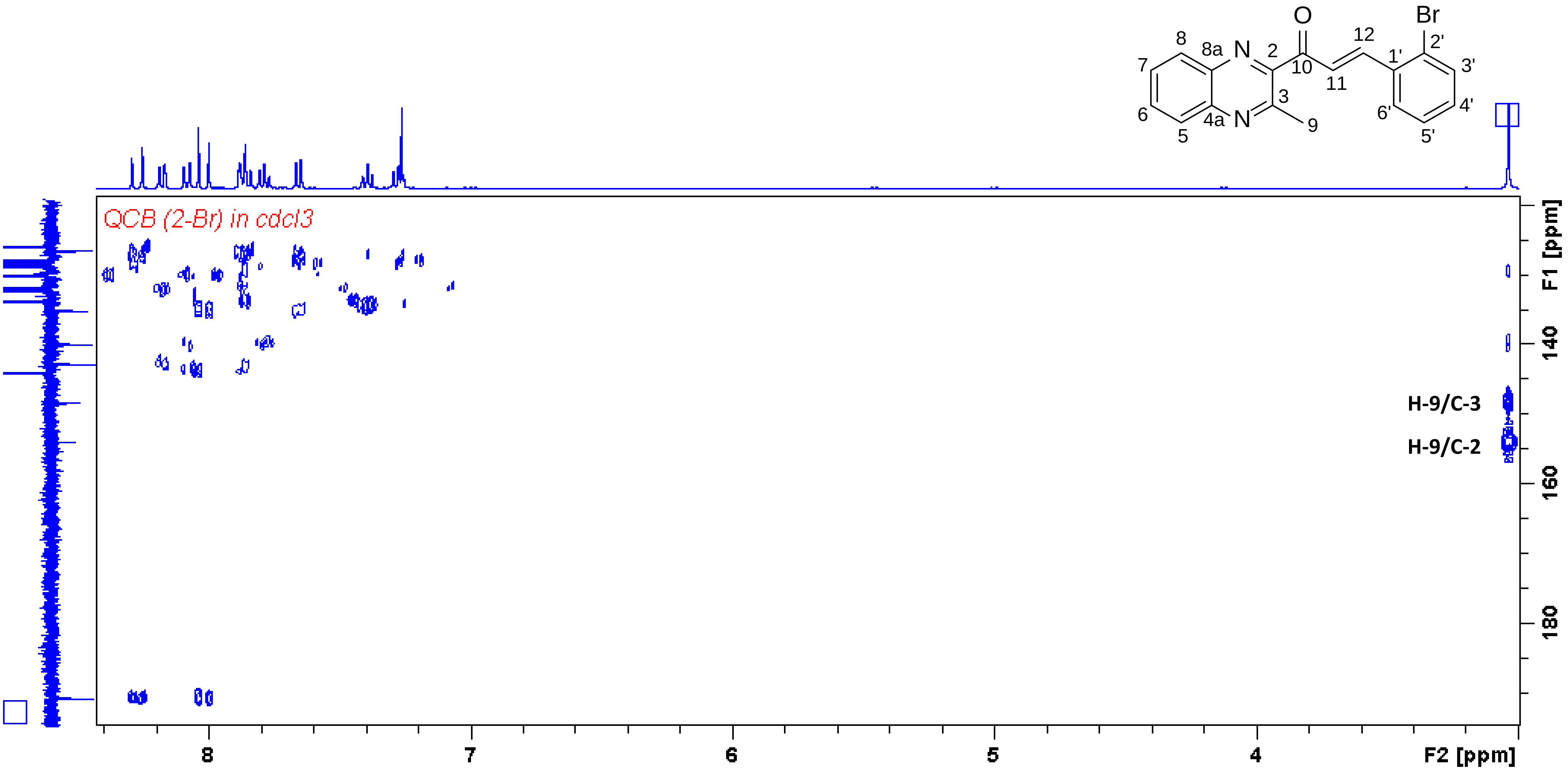
QCB (2-Br) in cdcl3
H-9/C-3
H-9/C-2
F1 [ppm]
F2 [ppm]
140
160
180
8
7
6
5
4
O
Br
N
N
8
7
6
5
8a
4a
2
3
9
10
11
12
1'
2'
3'
4'
5'
6'

HMBC of **B10c**

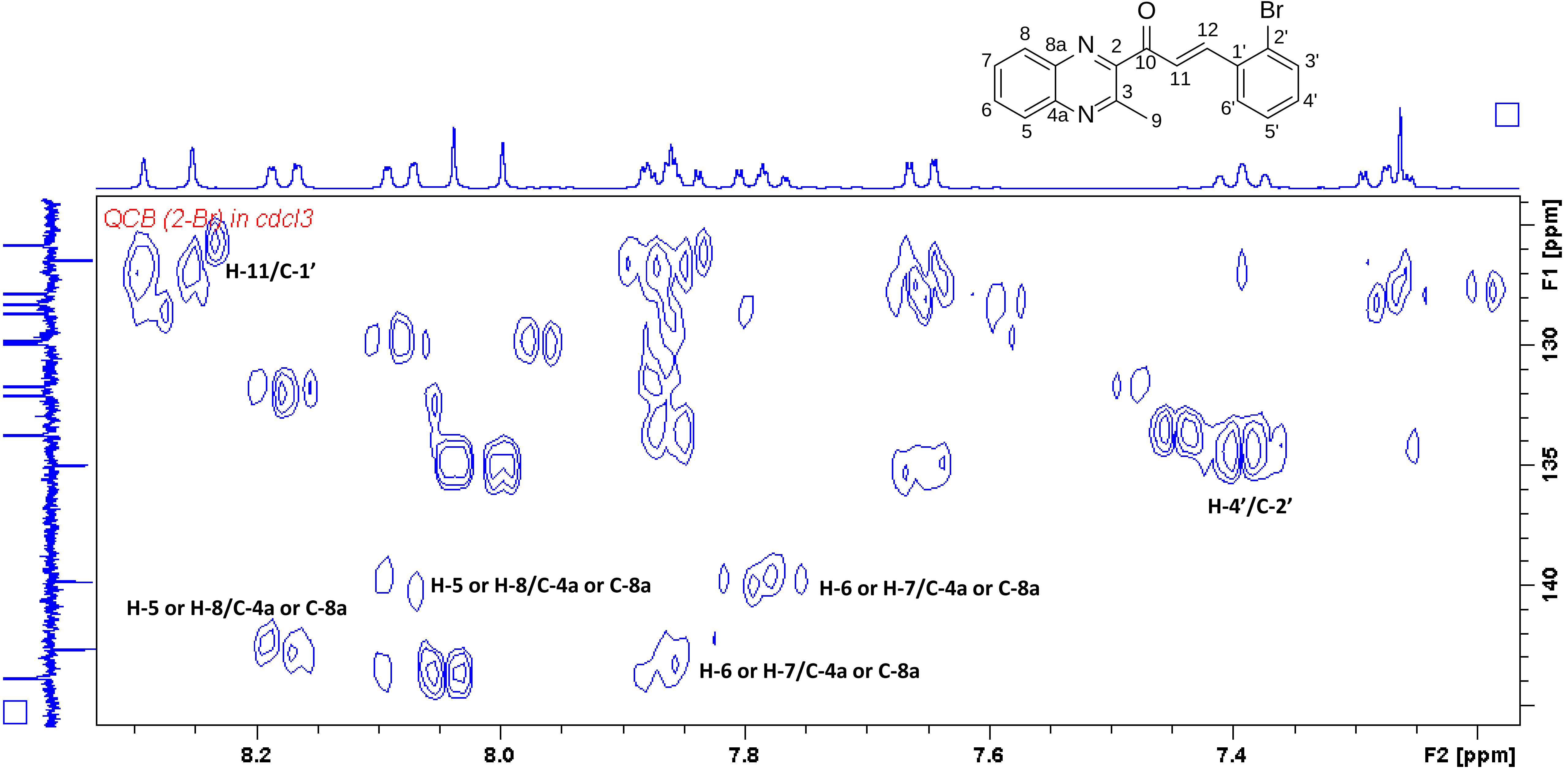

Expanded HMBC of **B10c**

Elemental Composition Report

Single Mass Analysis

Tolerance = 5.0 PPM / DBE: min = -1.5, max = 100.0
Element prediction: Off
Number of isotope peaks used for i-FIT = 2

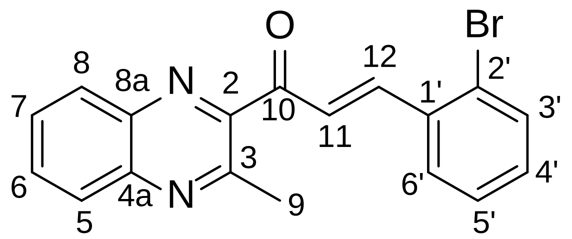

Monoisotopic Mass, Even Electron Ions
35 formula(e) evaluated with 1 results within limits (up to 20 best isotopic matches for each mass)
Elements Used:
C: 15-20 H: 10-15 N: 0-5 O: 0-5 Br: 0-1

QCB (2-Br) 58 (1.922) Cm (1:61)
TOF MS AP+

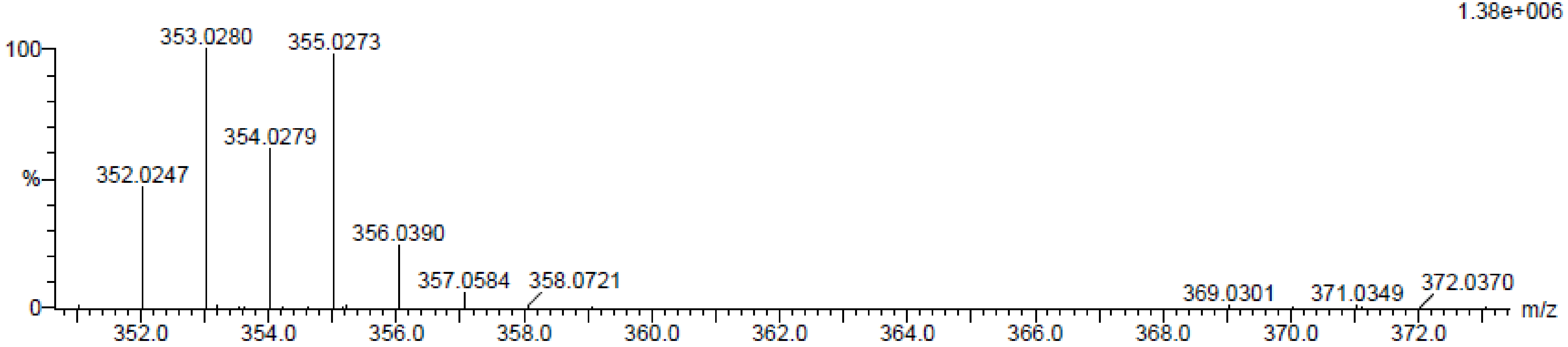

Mass	Calc. Mass	mDa	PPM	DBE	i-FIT	i-FIT (Norm)	Formula
Minimum:				-1.5			
Maximum:		5.0	5.0	100.0			
353.0280	353.0289	-0.9	-2.5	12.5	102.3	0.0	C18 H14 N2 O Br

High resolution mass spectrum of **B10c**

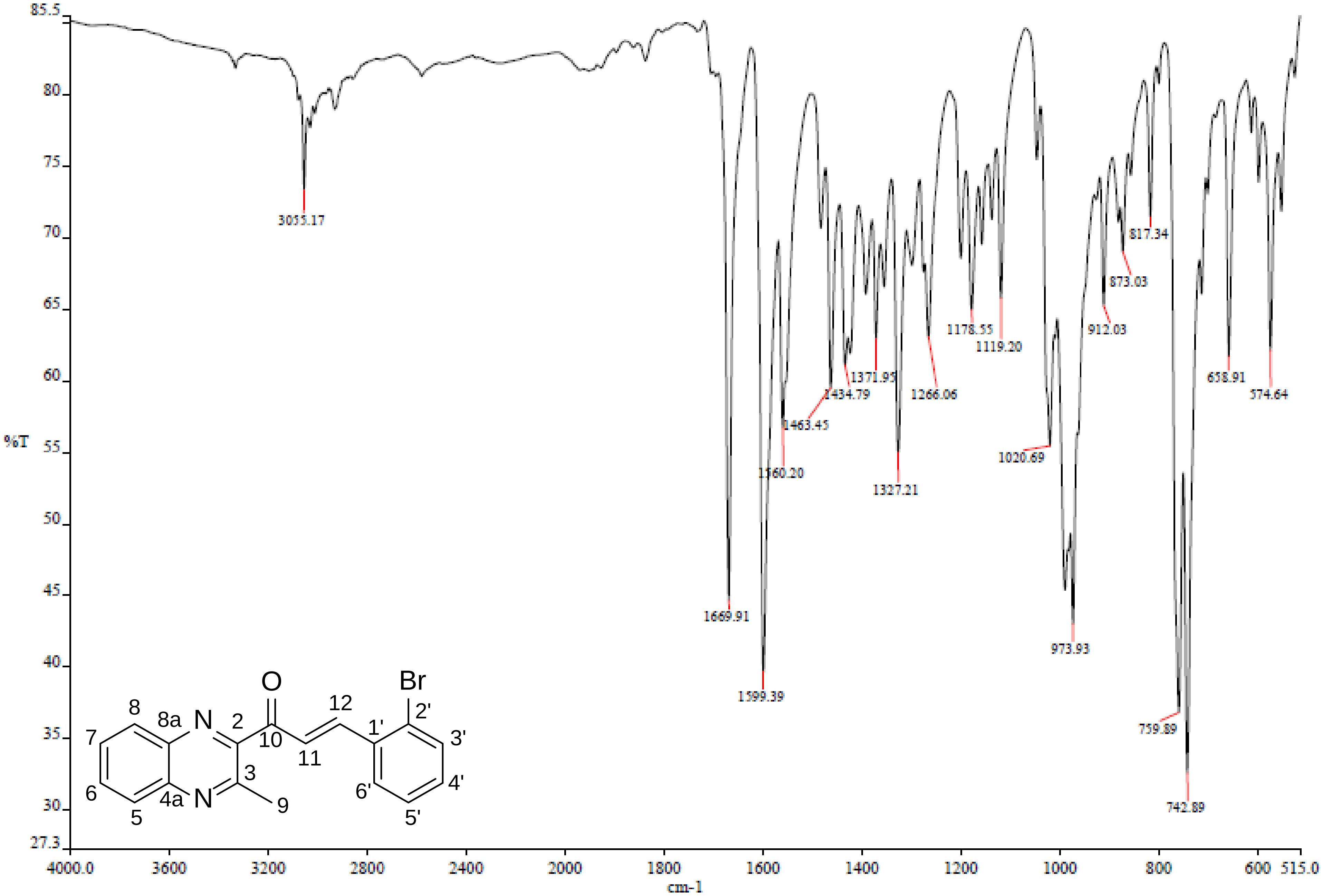

FTIR spectrum of **B10c**

Overlay Spectrum Graph Report

06/10/2017 11:39:33 AM

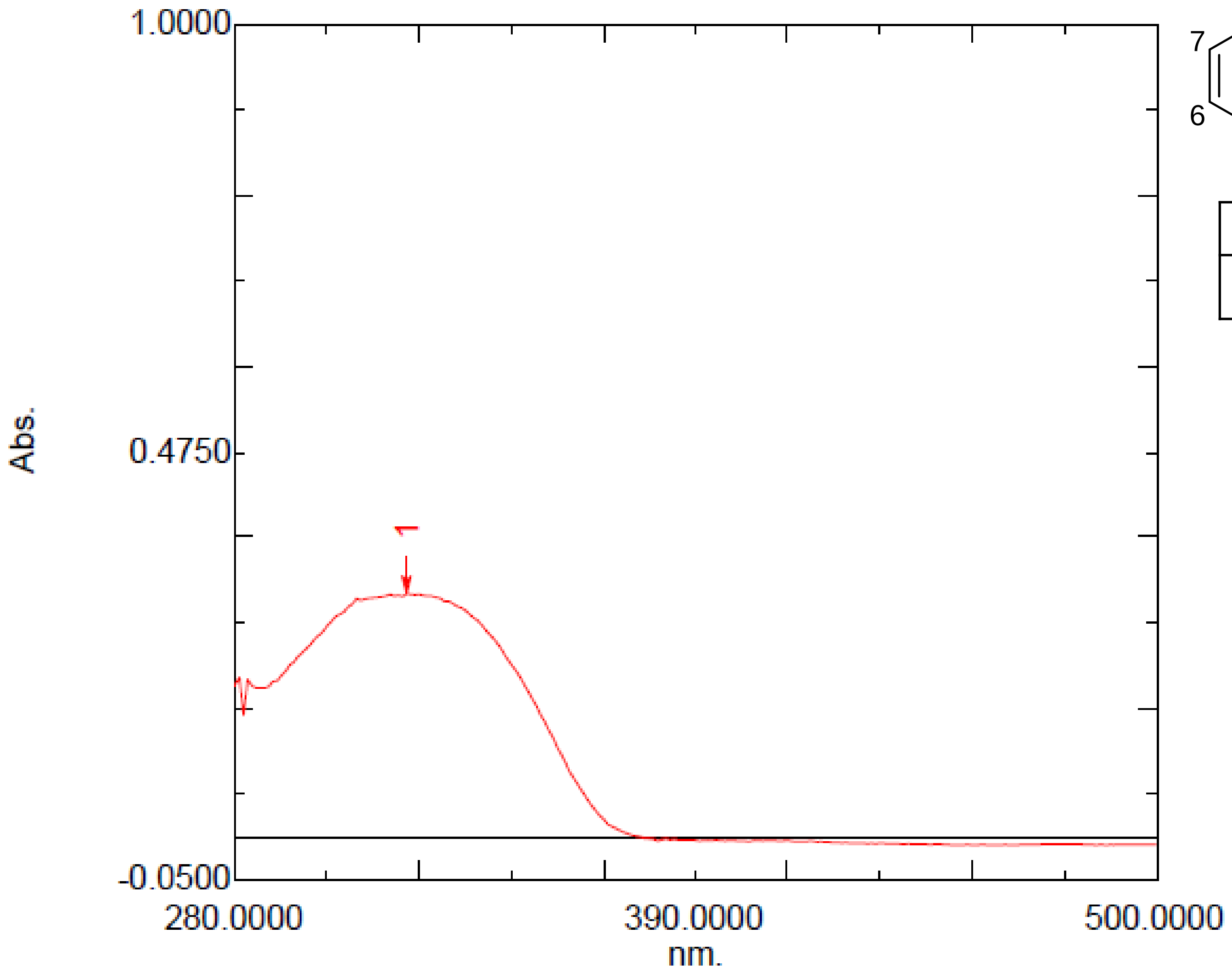

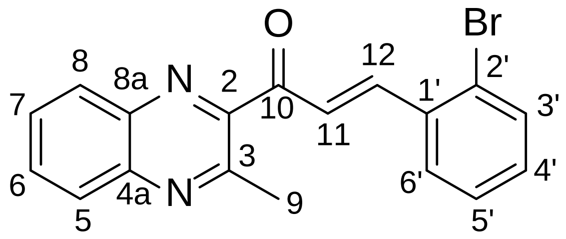

λ	absorbance	logε
321	0.3008	4.33

UV spectrum of **B10c**

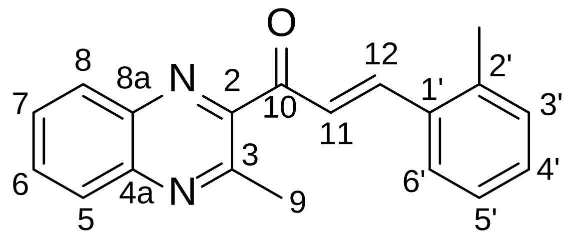

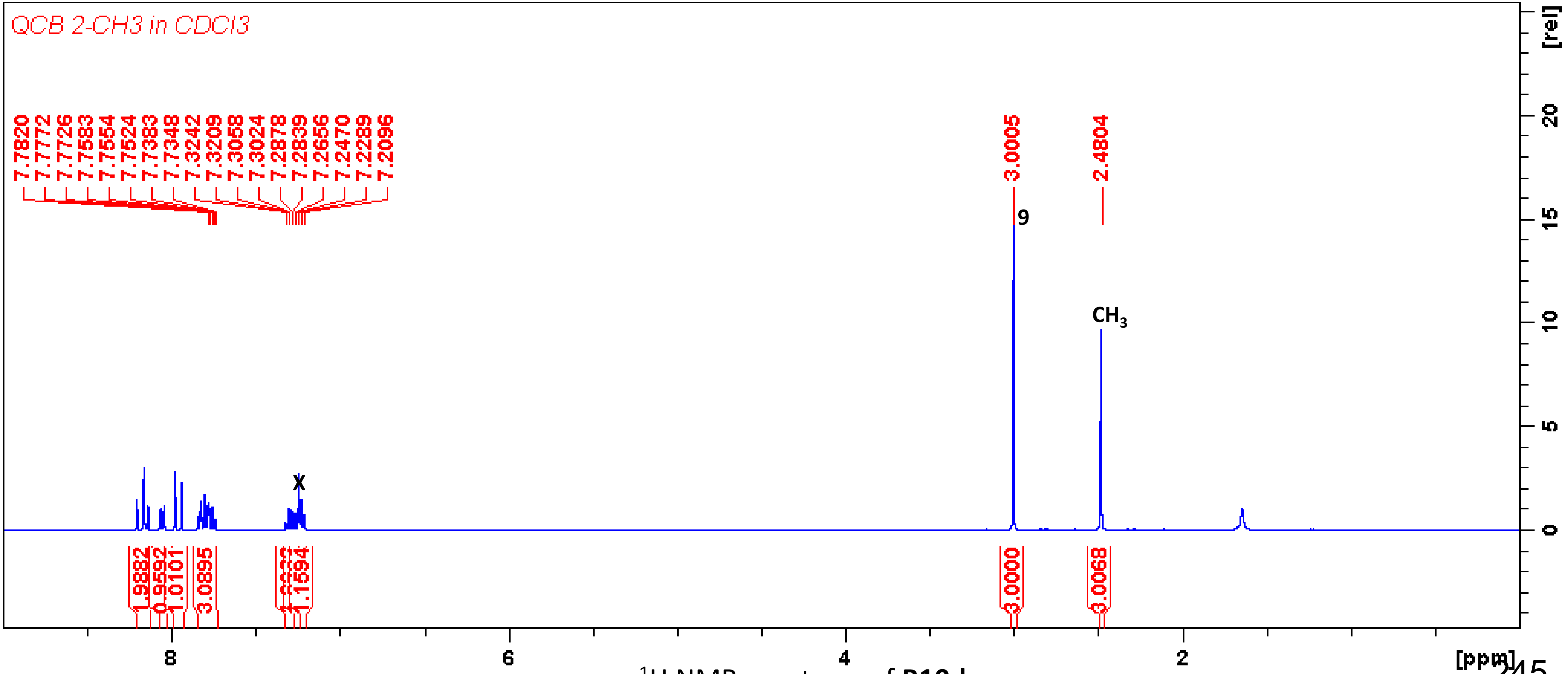

^{1}H NMR spectrum of **B10d**

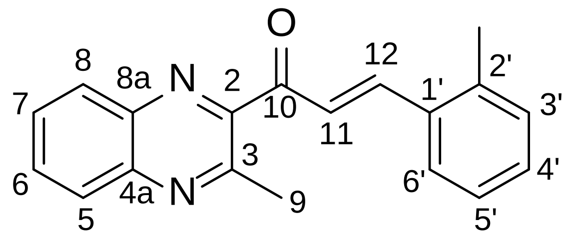

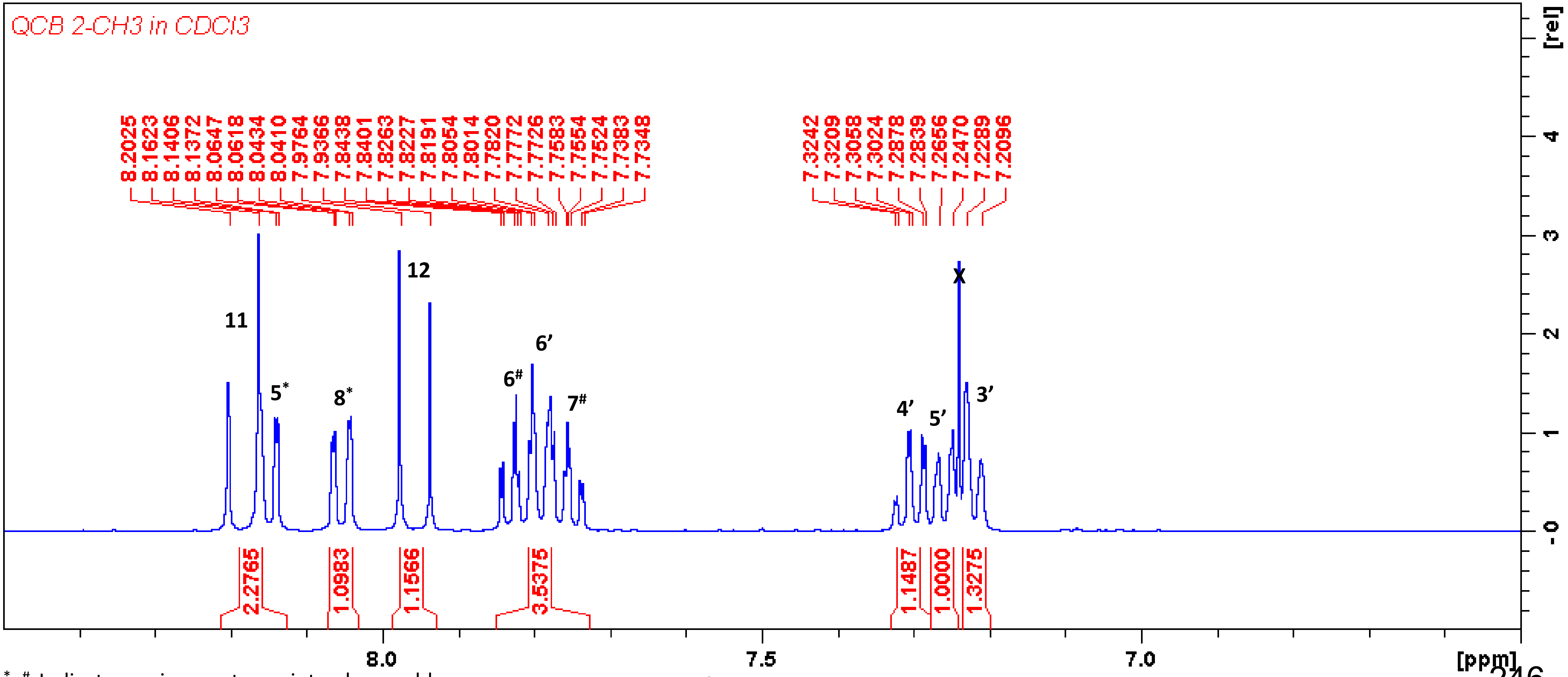

*, # Indicates assignments are interchangeable

Expanded ^{1}H NMR spectrum of **B10d**

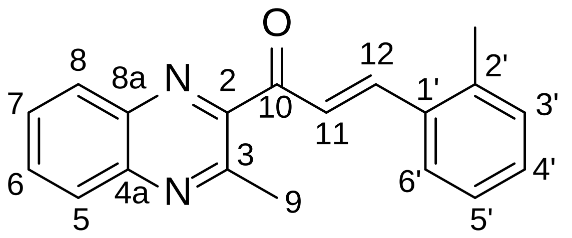

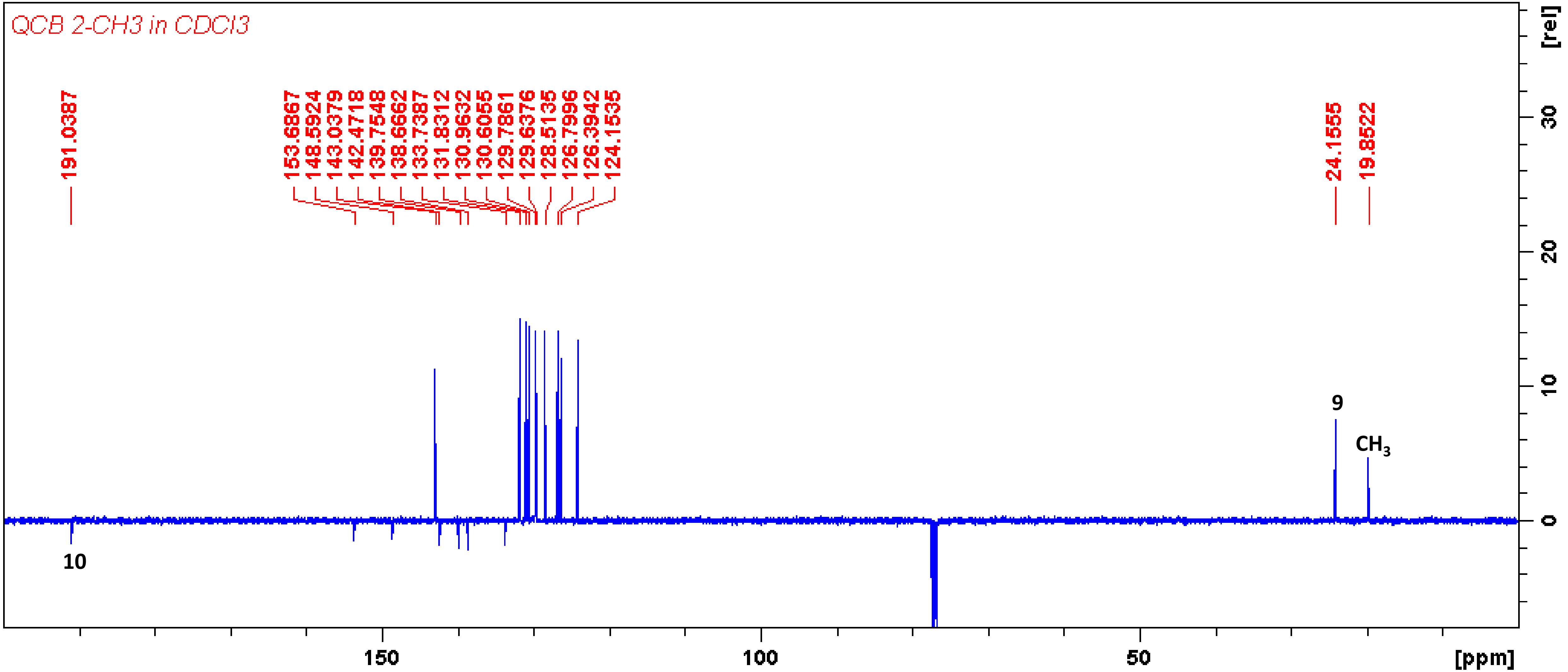

^{13}C NMR spectrum of **B10d**

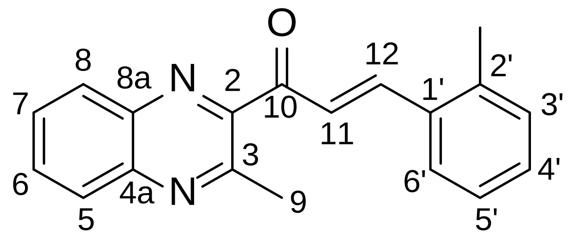

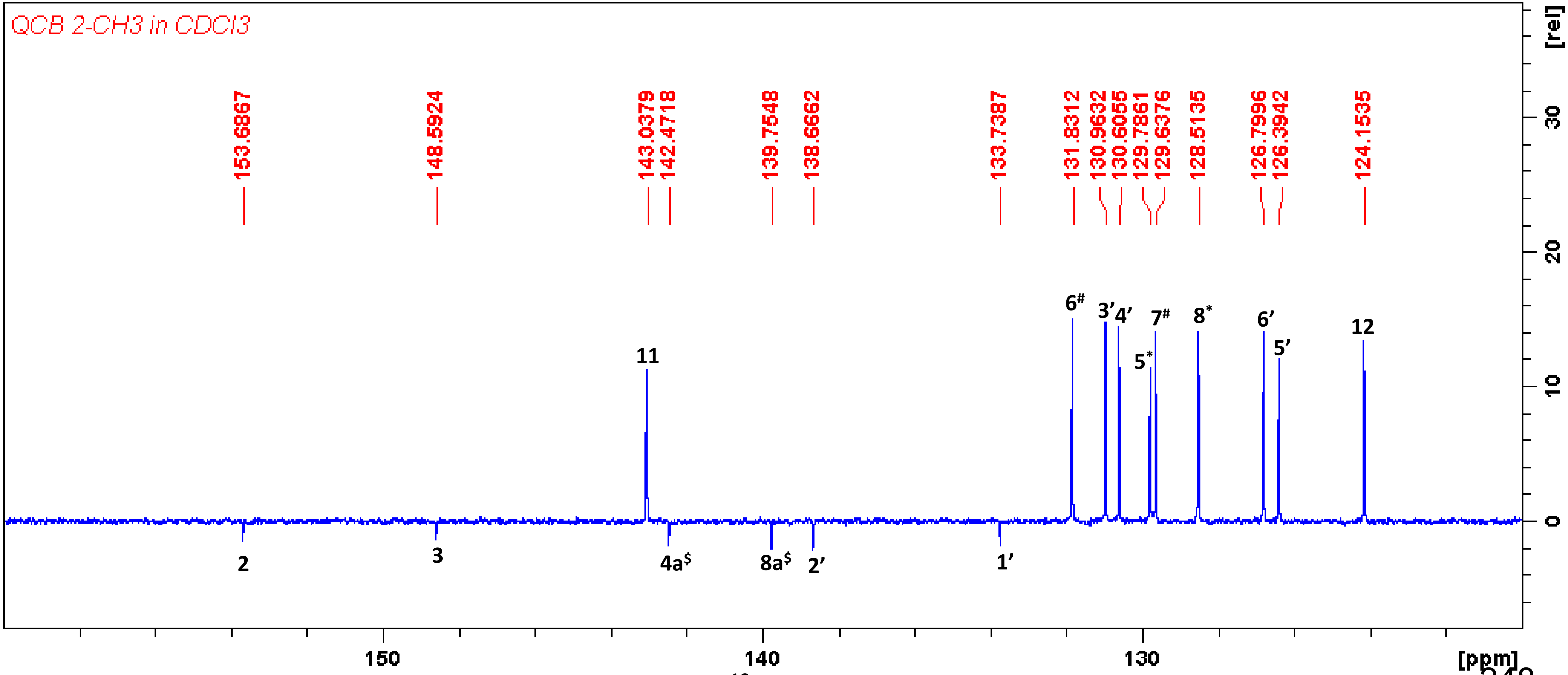

*, #, $ Indicates assignments are interchangeable

Expanded ^{13}C NMR spectrum of **B10d**

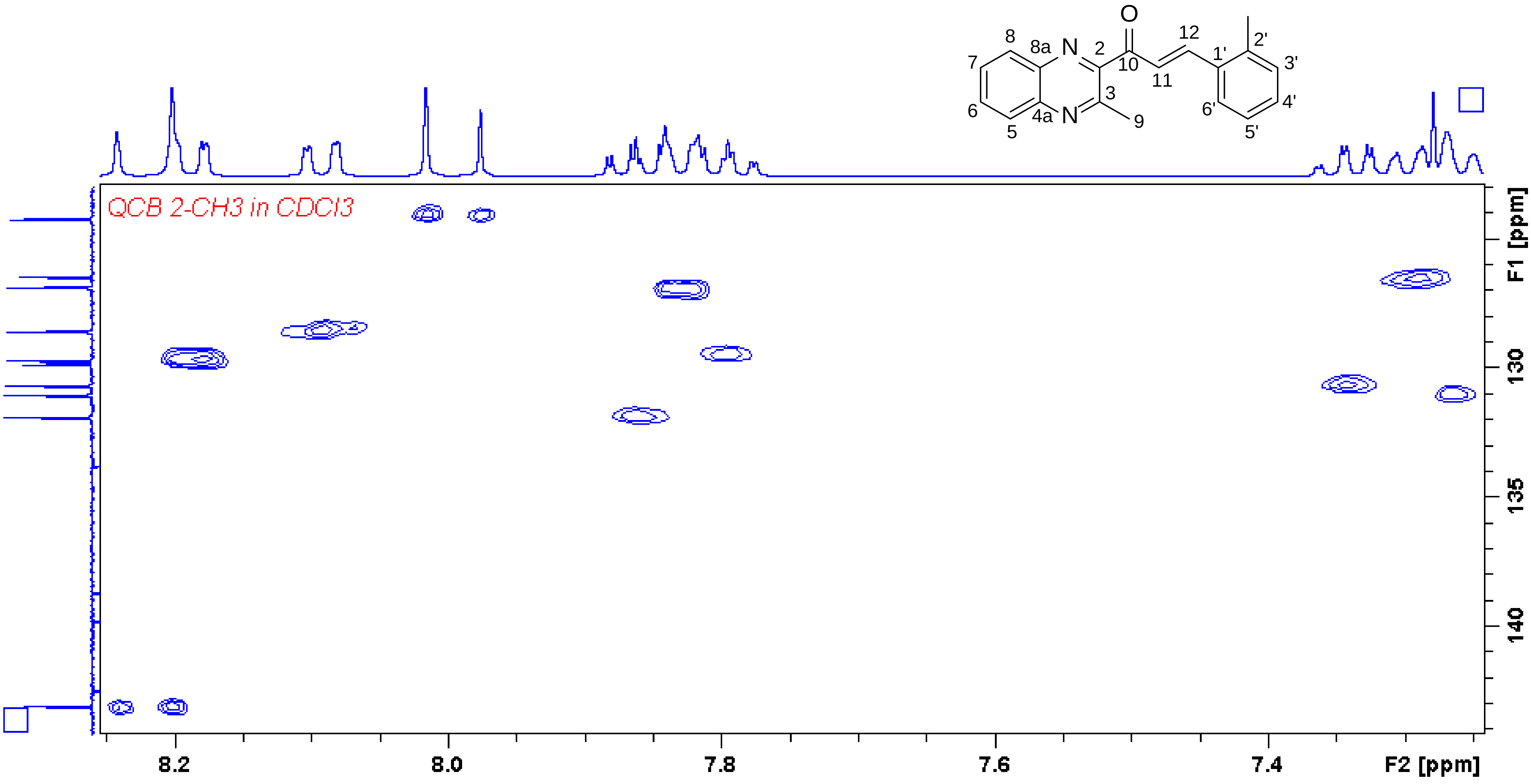

QCB 2-CH3 in CDCl3
8.2
8.0
7.8
7.6
7.4
F2 [ppm]
130
135
140
F1 [ppm]
O
N
N
2
3
4a
8a
5
6
7
8
9
10
11
12
1'
2'
3'
4'
5'
6'

HSQC of **B10d**

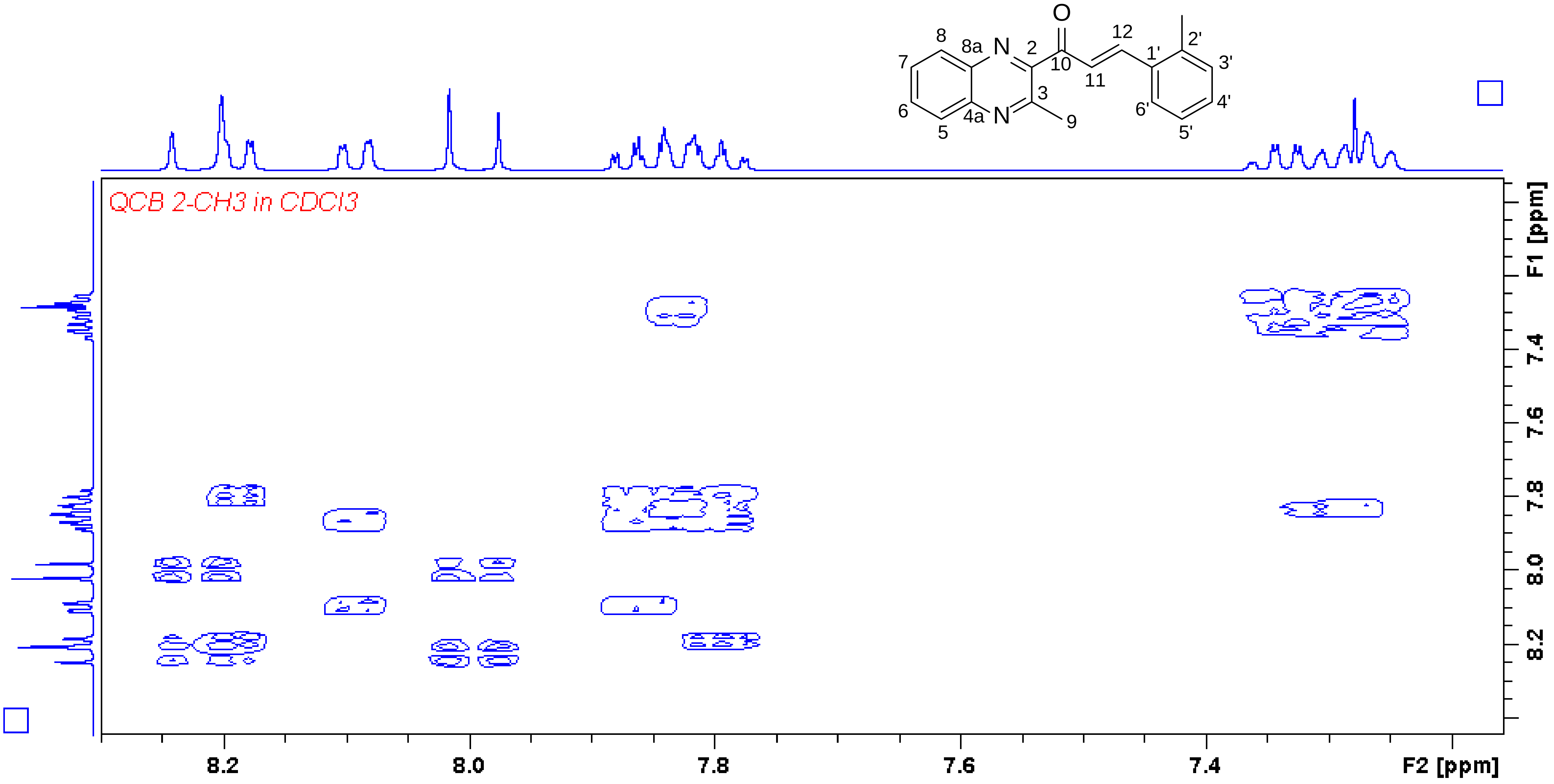

QCB 2-CH3 in CDCl3
F1 [ppm]
F2 [ppm]
8.2
8.0
7.8
7.6
7.4
O
N
N
8
8a
2
7
10
12
11
1'
2'
3'
4'
5'
6'
3
9
6
5
4a

COSY of **B10d**

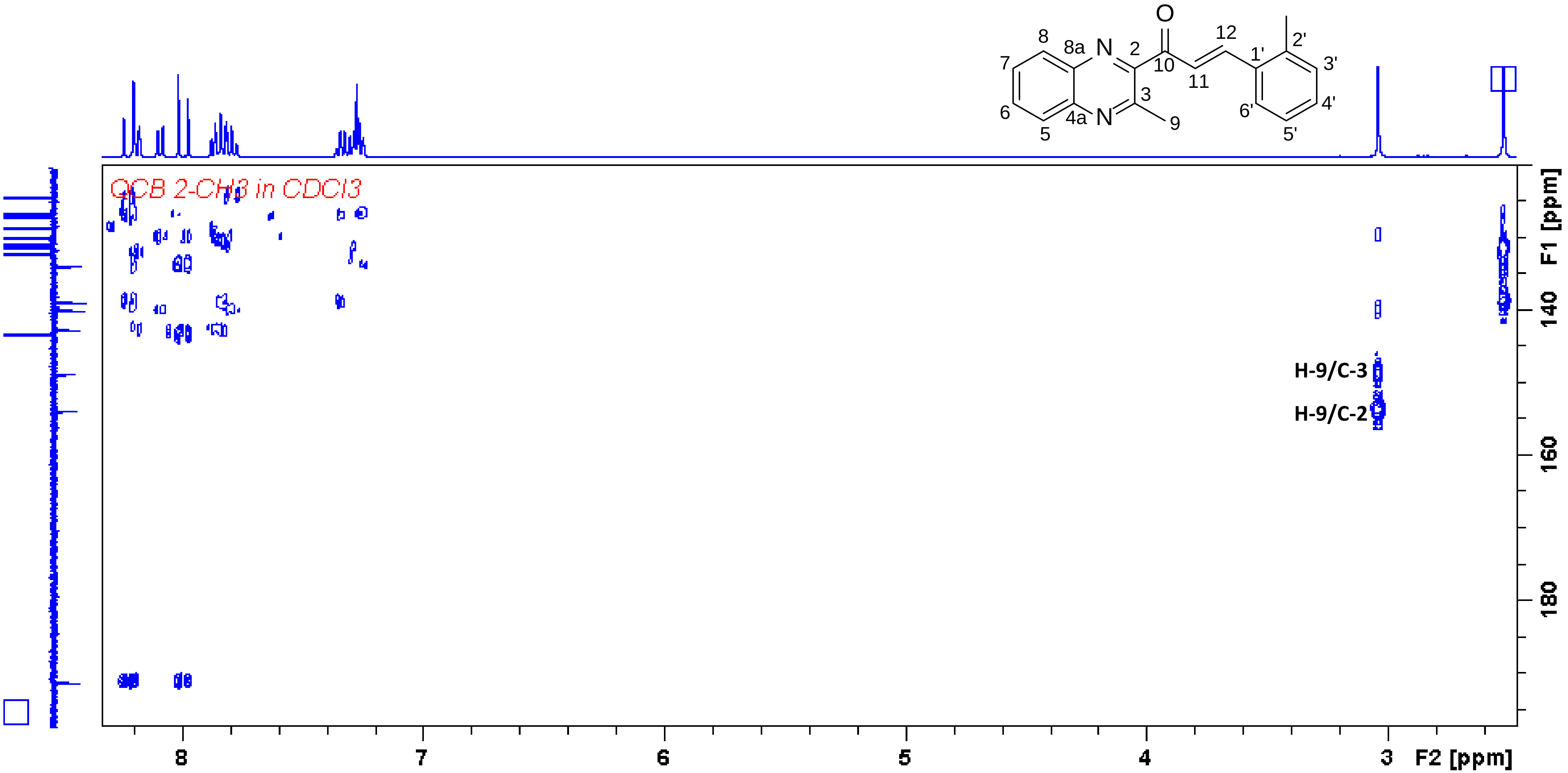

QCB 2-CH3 in CDCl3
O
8
8a
N
2
10
12
2'
1'
3'
7
11
3
6'
4'
6
4a
N
9
5
5'
H-9/C-3
H-9/C-2
F1 [ppm]
140
160
180
8
7
6
5
4
3
F2 [ppm]

HMBC of **B10d**

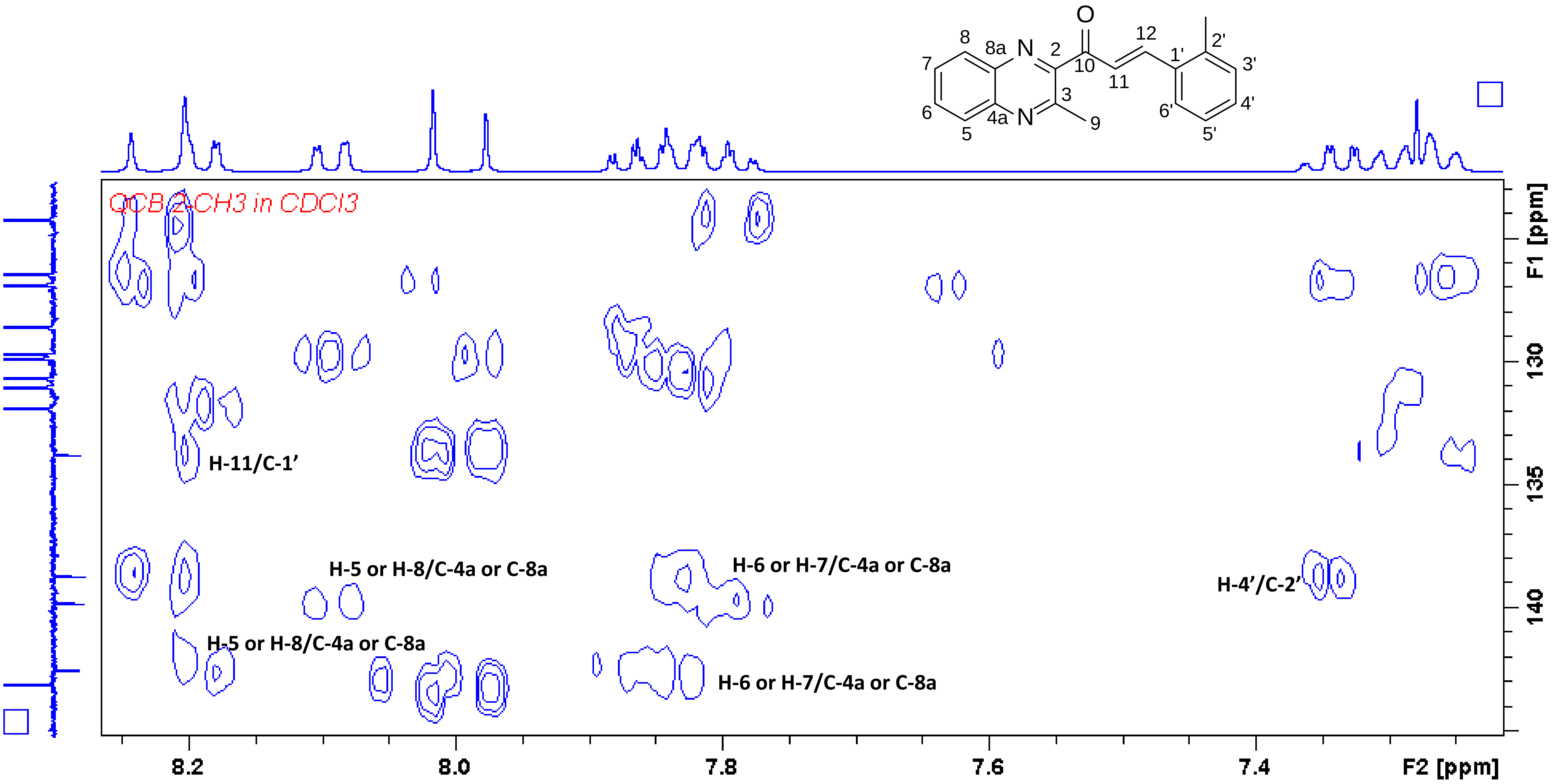

Expanded HMBC of **B10d**

Elemental Composition Report

Page 1

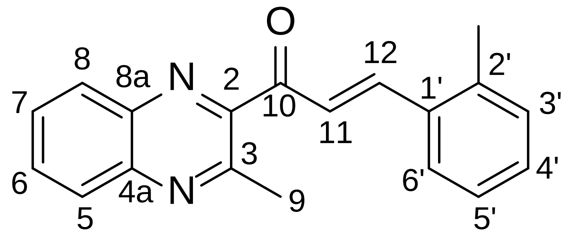

Single Mass Analysis

Tolerance = 5.0 PPM / DBE: min = -1.5, max = 100.0
Element prediction: Off
Number of isotope peaks used for i-FIT = 2

Monoisotopic Mass, Even Electron Ions
19 formula(e) evaluated with 1 results within limits (up to 20 best isotopic matches for each mass)
Elements Used:
C: 15-20 H: 15-20 N: 0-5 O: 0-5
QCB (2-Me) 50 (1.651) Cm (1:61)
TOF MS ES+

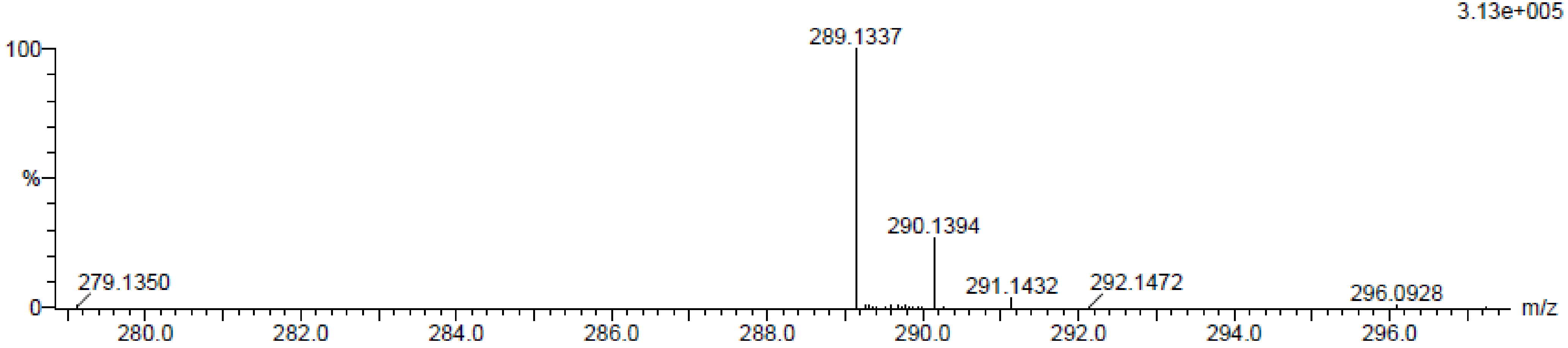

Minimum:				-1.5			
Maximum:		5.0	5.0	100.0			
Mass	Calc. Mass	mDa	PPM	DBE	i-FIT	i-FIT (Norm)	Formula
289.1337	289.1341	-0.4	-1.4	12.5	225.7	0.0	C19 H17 N2 O

High resolution mass spectrum of **B10d**

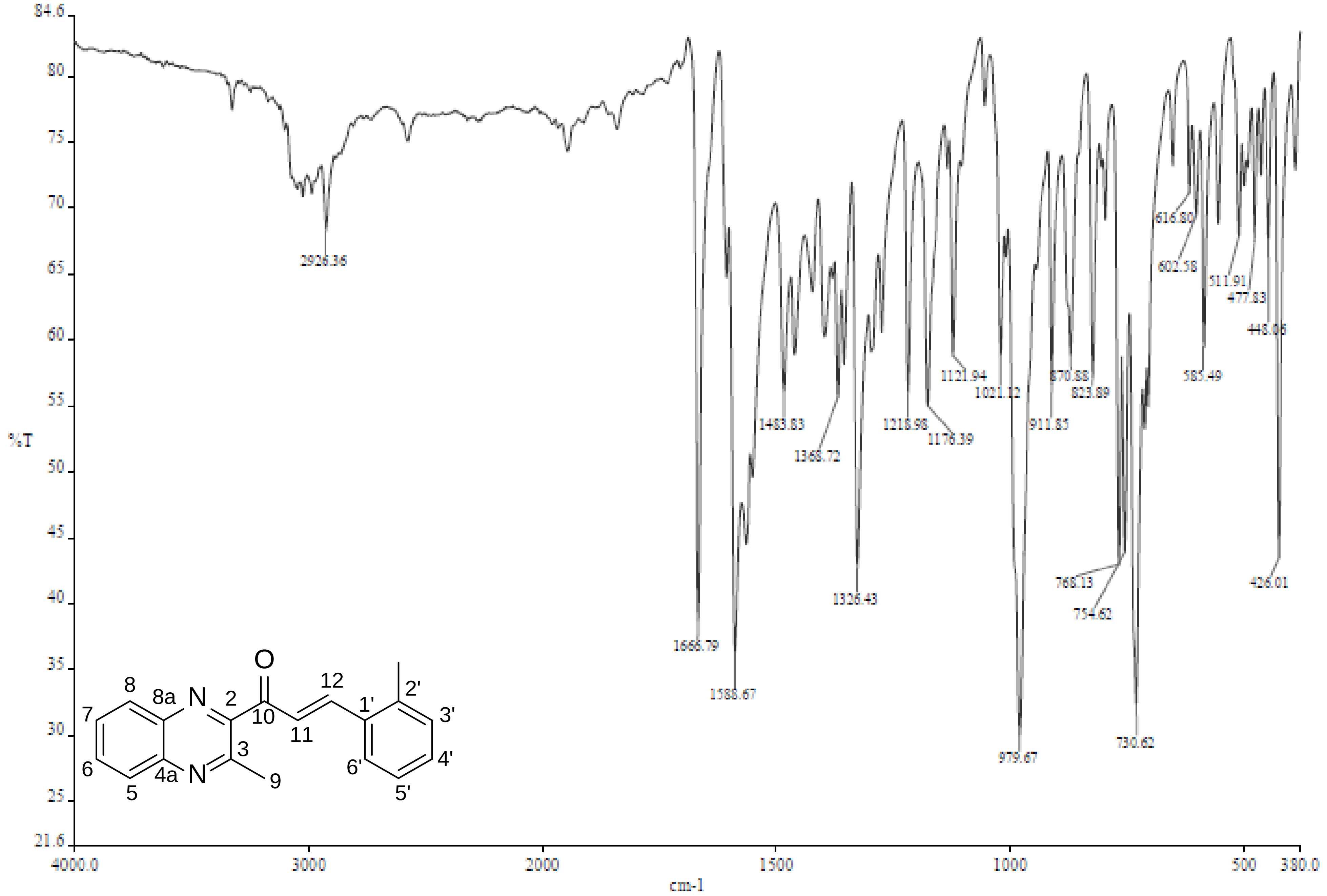

FTIR spectrum of **B10d**

Overlay Spectrum Graph Report

06/10/2017 11:40:02 AM

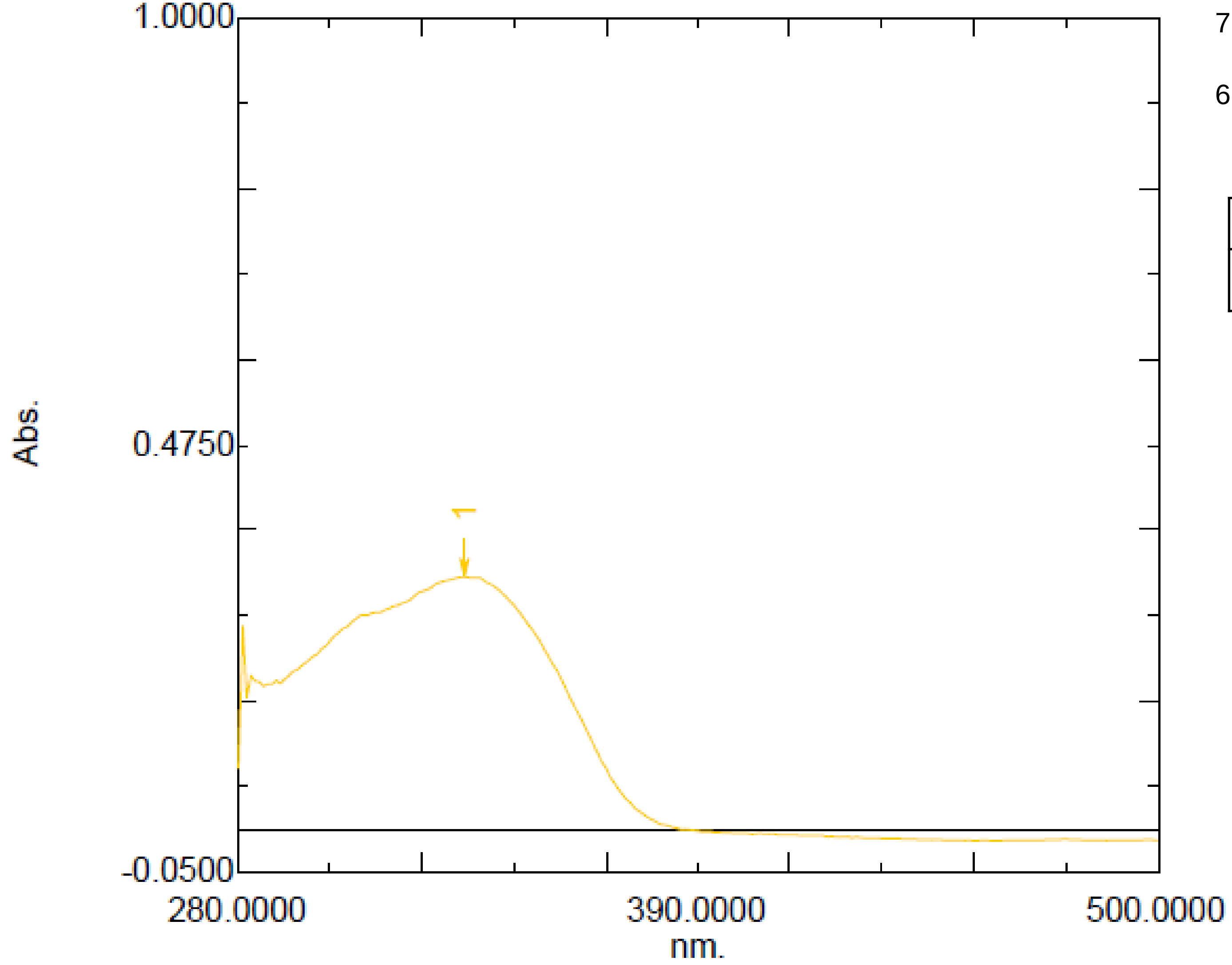

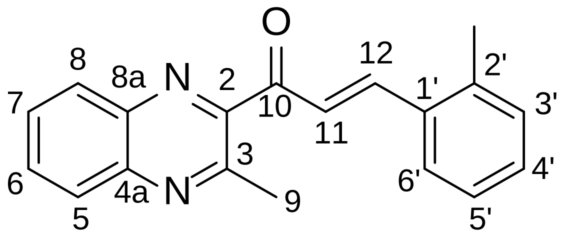

λ	absorbance	logε
334	0.3129	4.26

UV spectrum of **B10d**

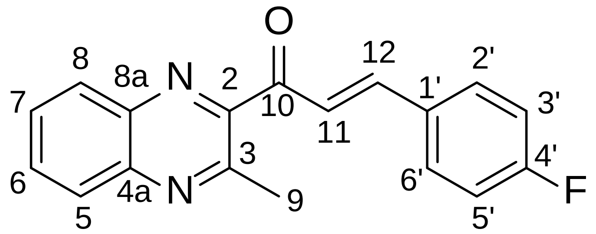

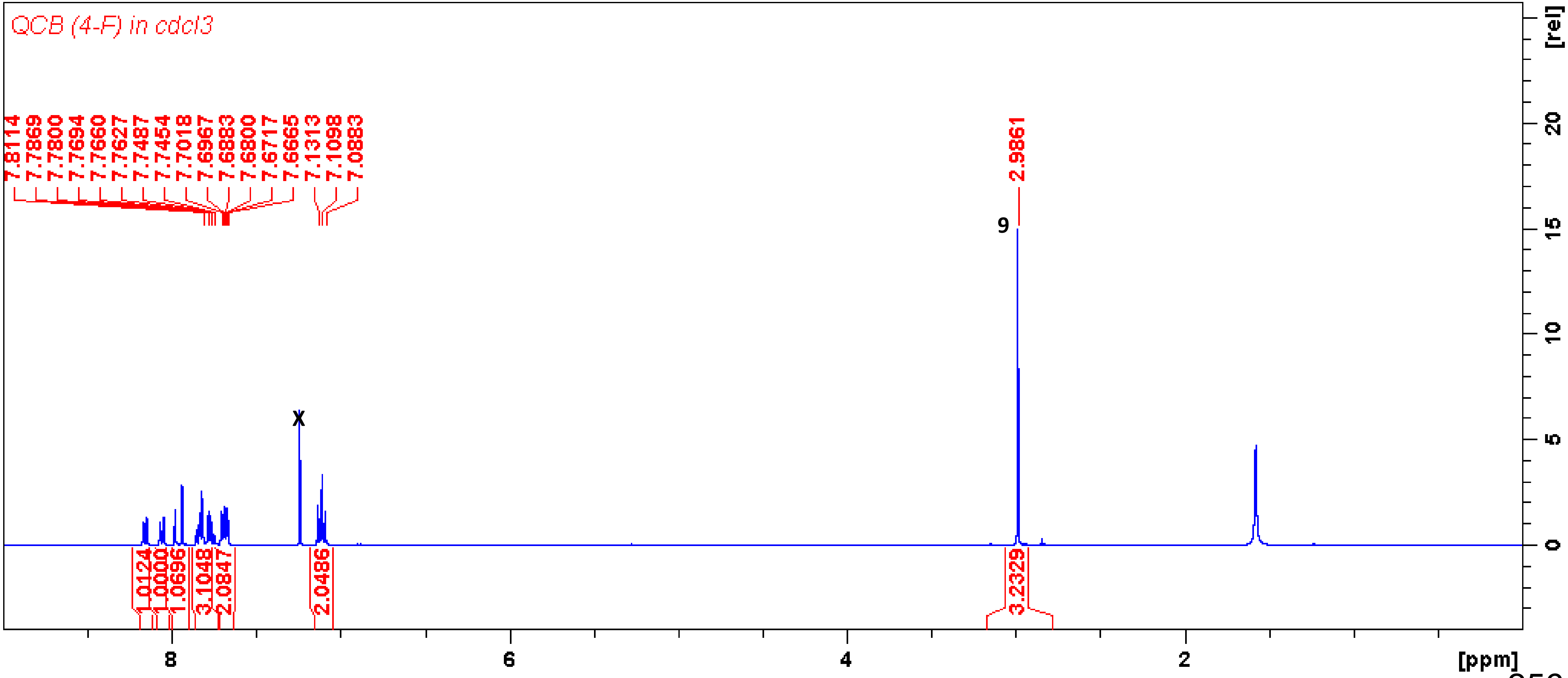

^{1}H NMR spectrum of **B10e**

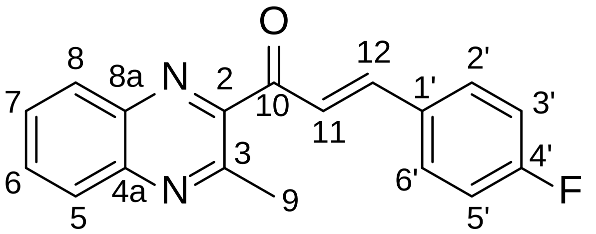

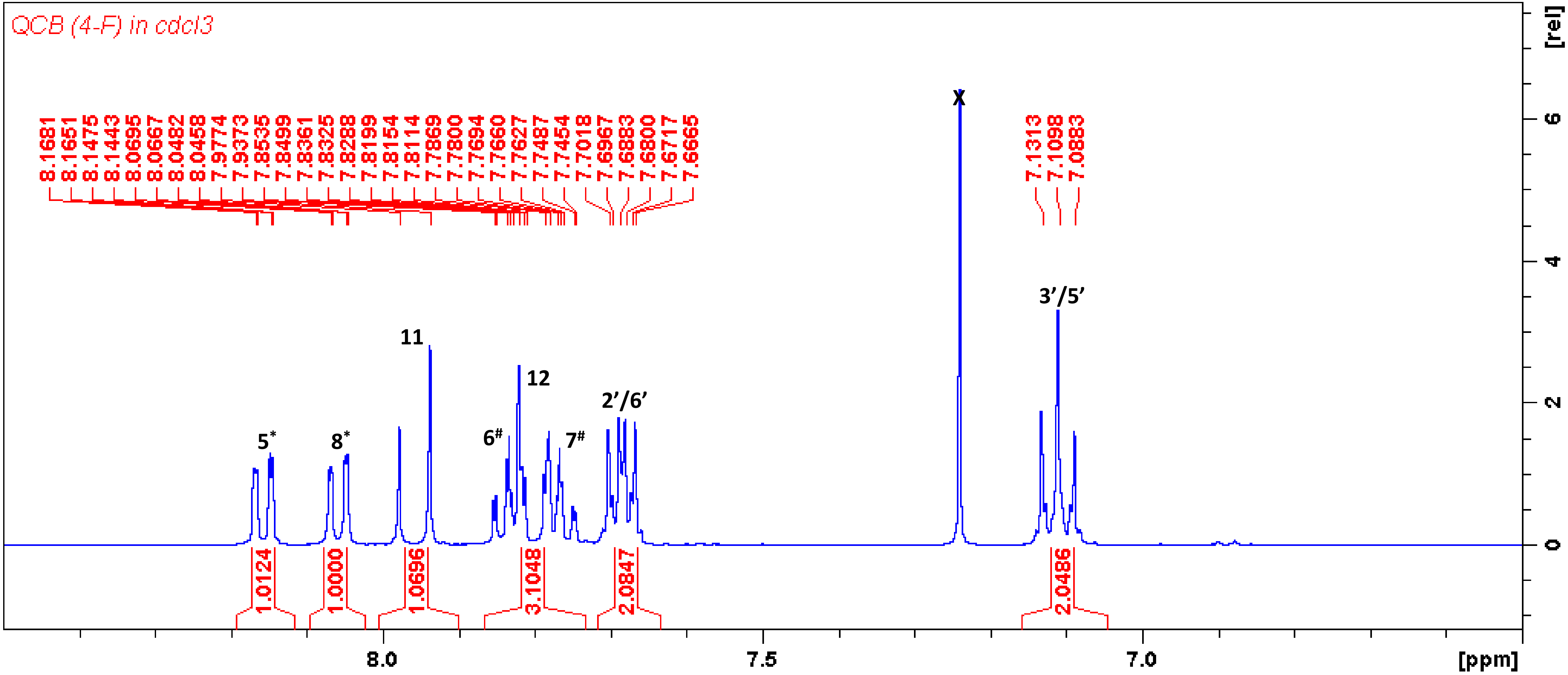

*, # Indicates assignments are interchangeable

Expanded ^{1}H NMR spectrum of **B10e**

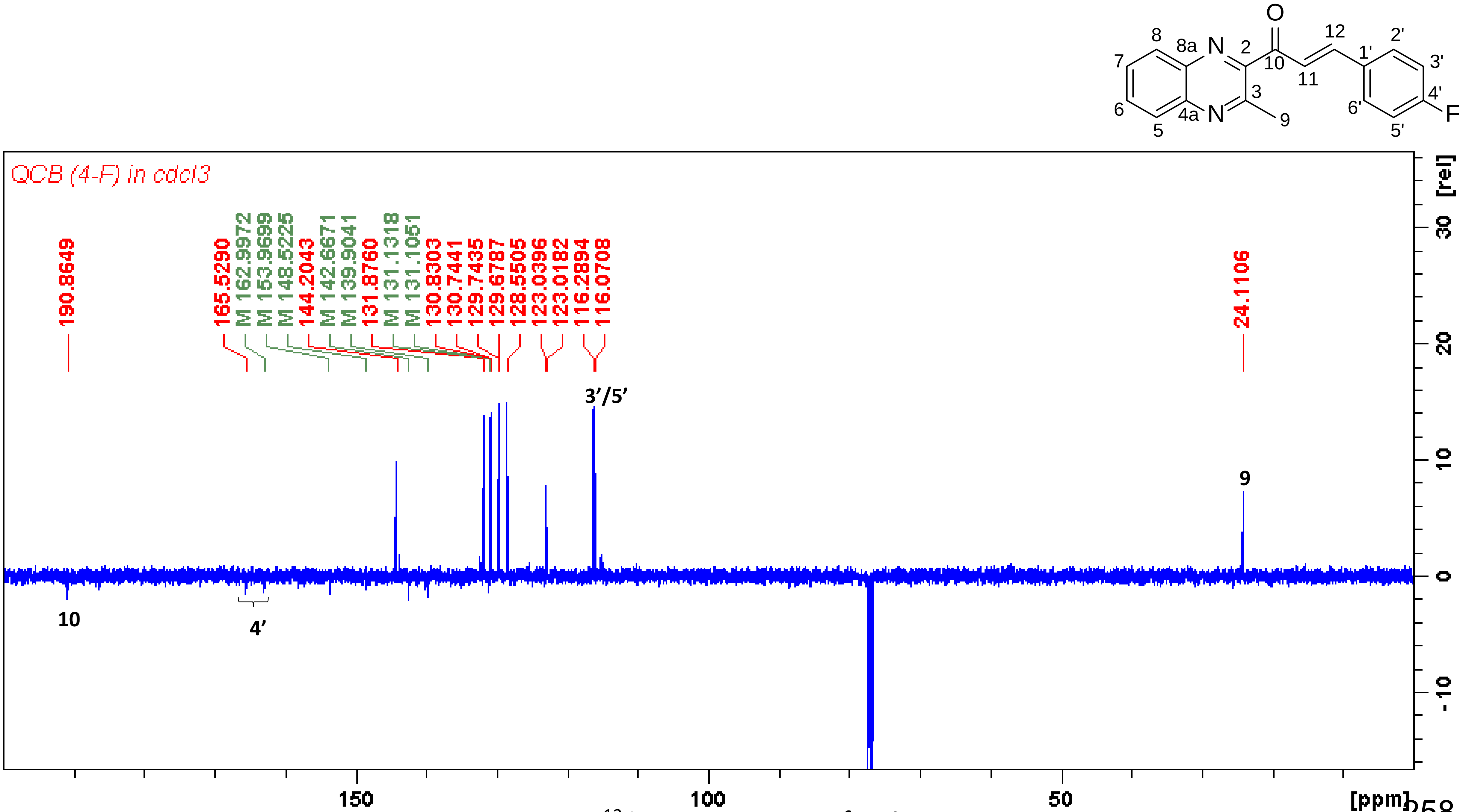

^{13}C NMR spectrum of **B10e**

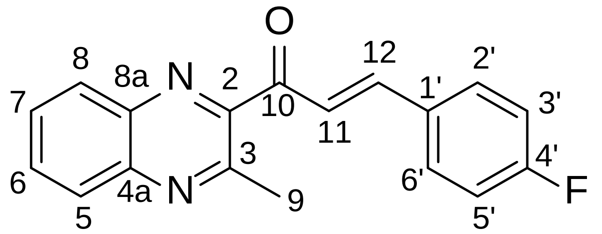

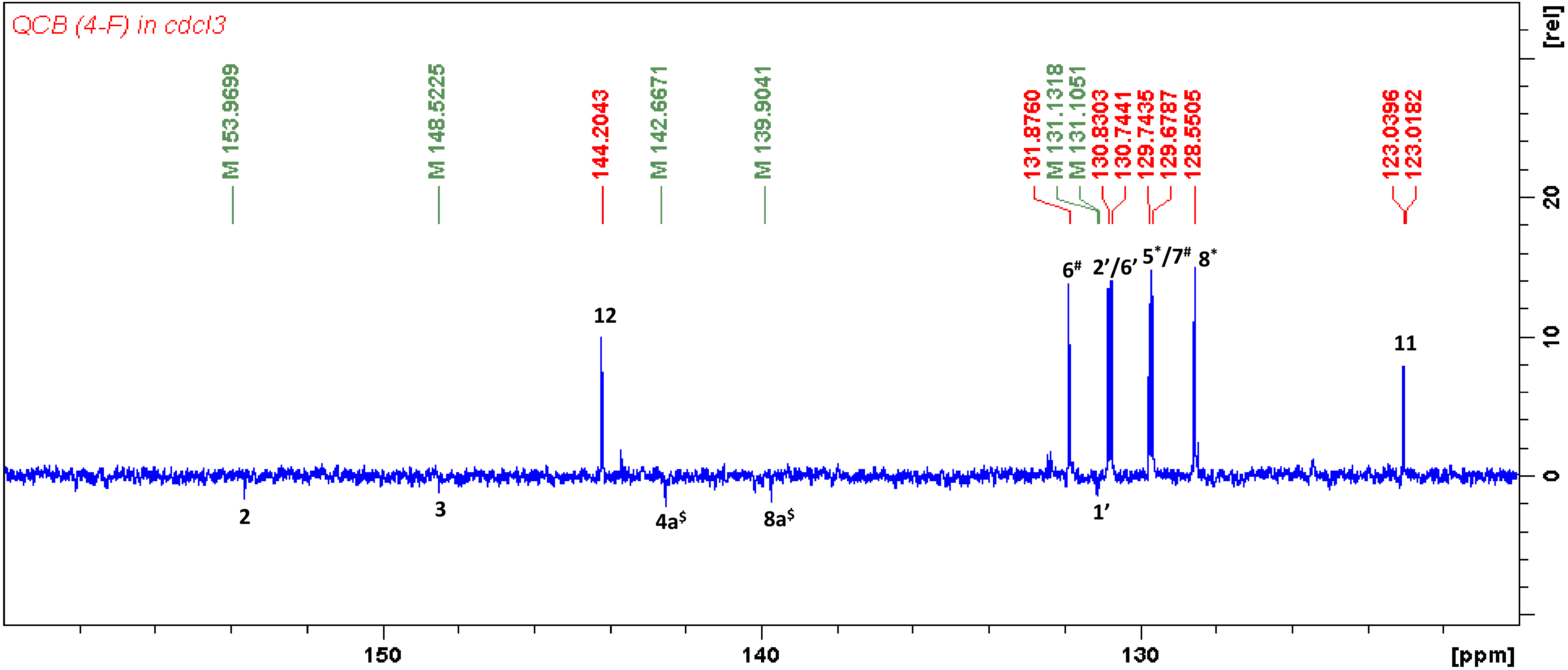

*, #, $ Indicates assignments are interchangeable

Expanded ^{13}C NMR spectrum of **B10e**

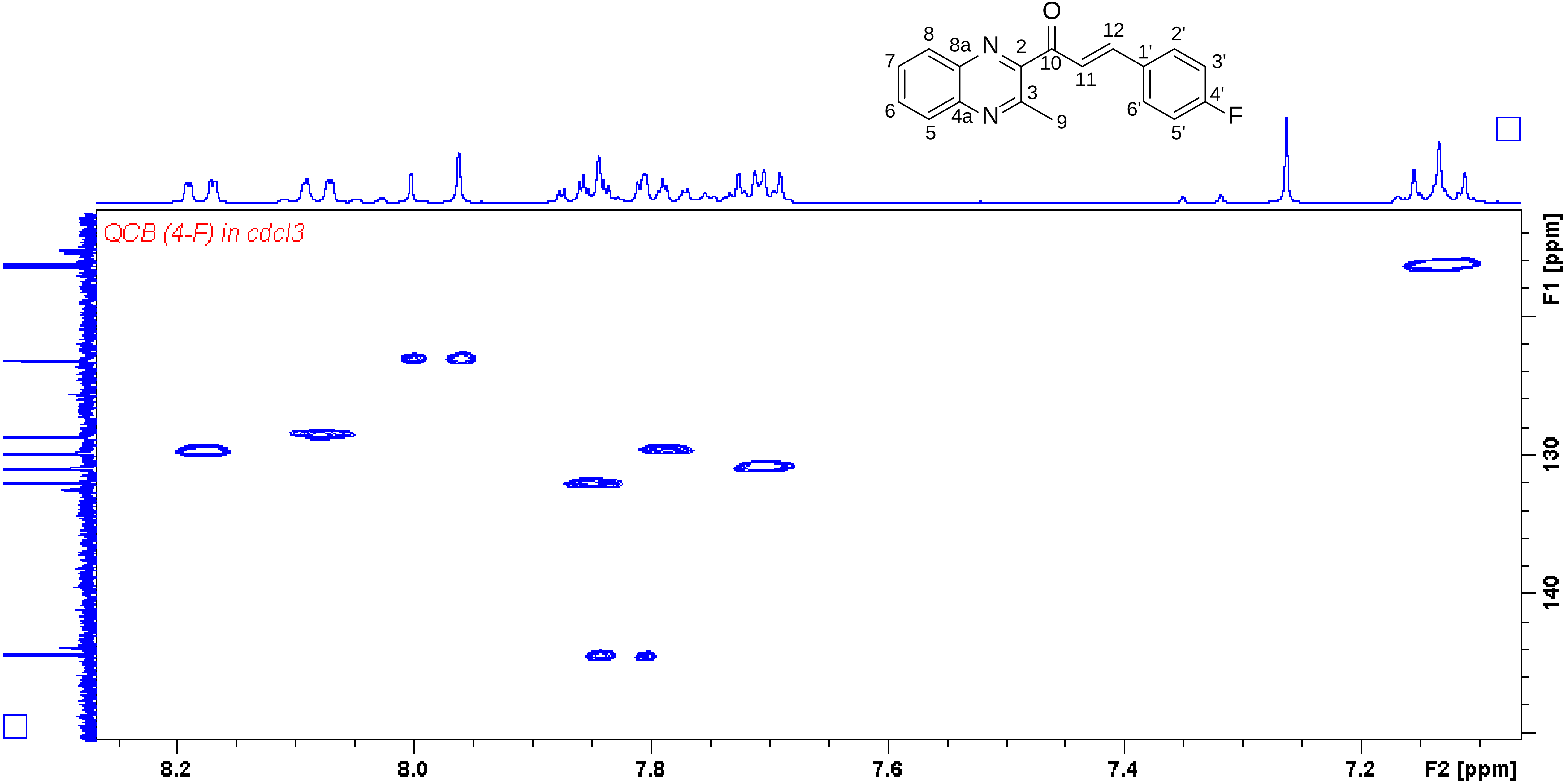

O
8
8a
N
2
12
2'
7
10
1'
3'
11
3
4'
6
6'
F
4a
N
9
5
5'
QCB (4-F) in cdcl3
F1 [ppm]
130
140
8.2
8.0
7.8
7.6
7.4
7.2
F2 [ppm]

HSQC of **B10e**

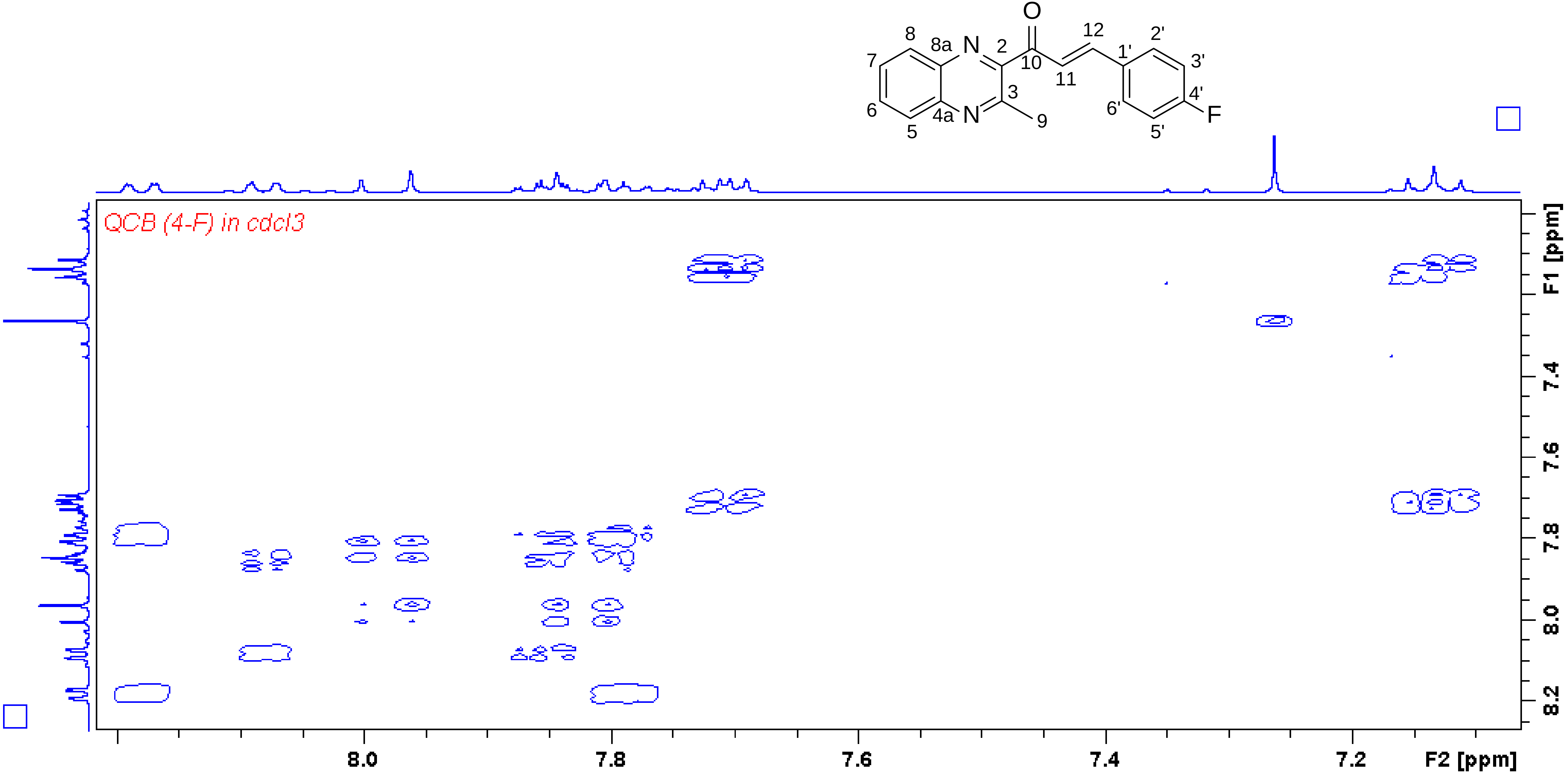

COSY of **B10e**

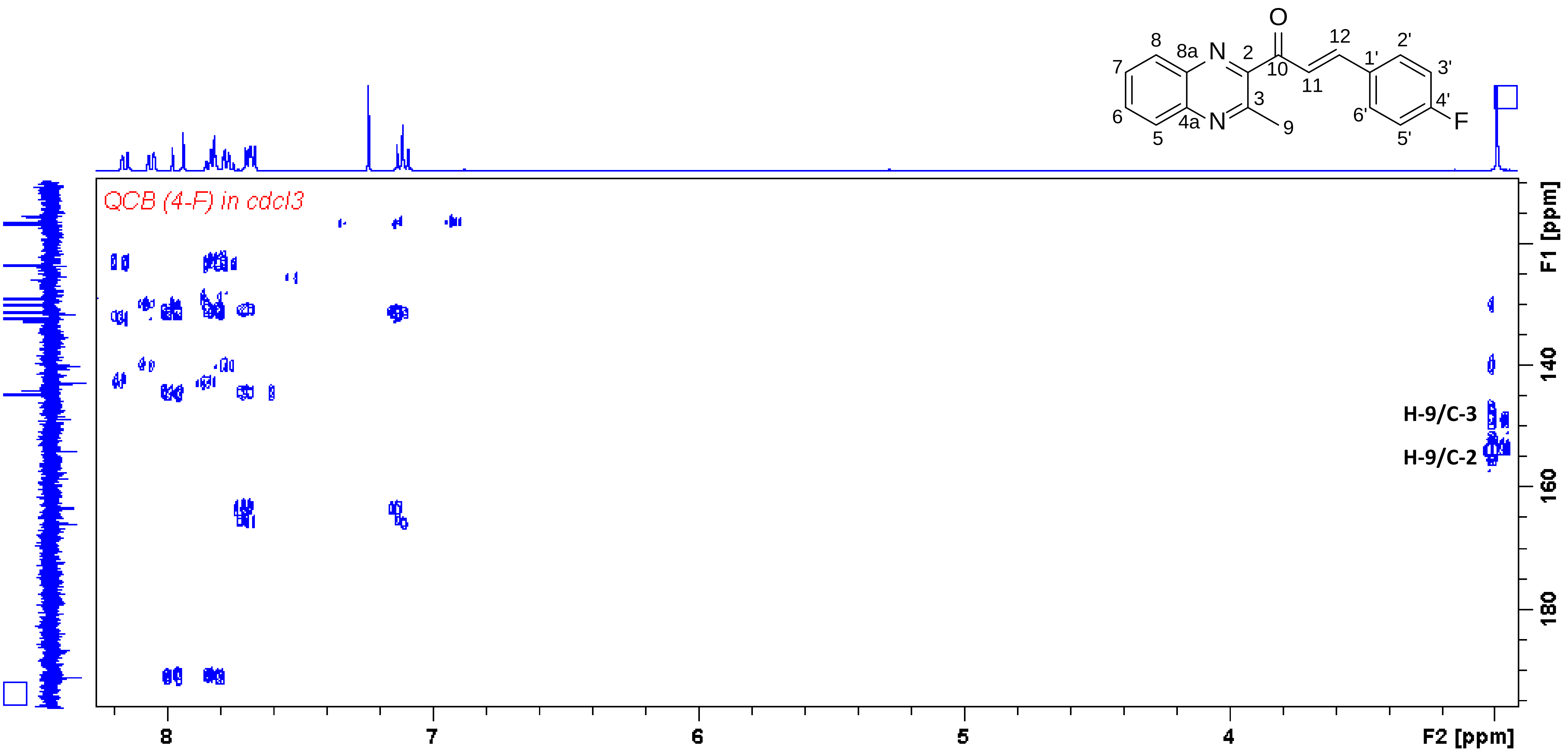
QCB (4-F) in cdcl3
H-9/C-3
H-9/C-2
F1 [ppm]
F2 [ppm]
O
N
N
F
8
8a
7
6
5
4a
2
3
9
10
11
12
1'
2'
3'
4'
5'
6'

HMBC of **B10e**

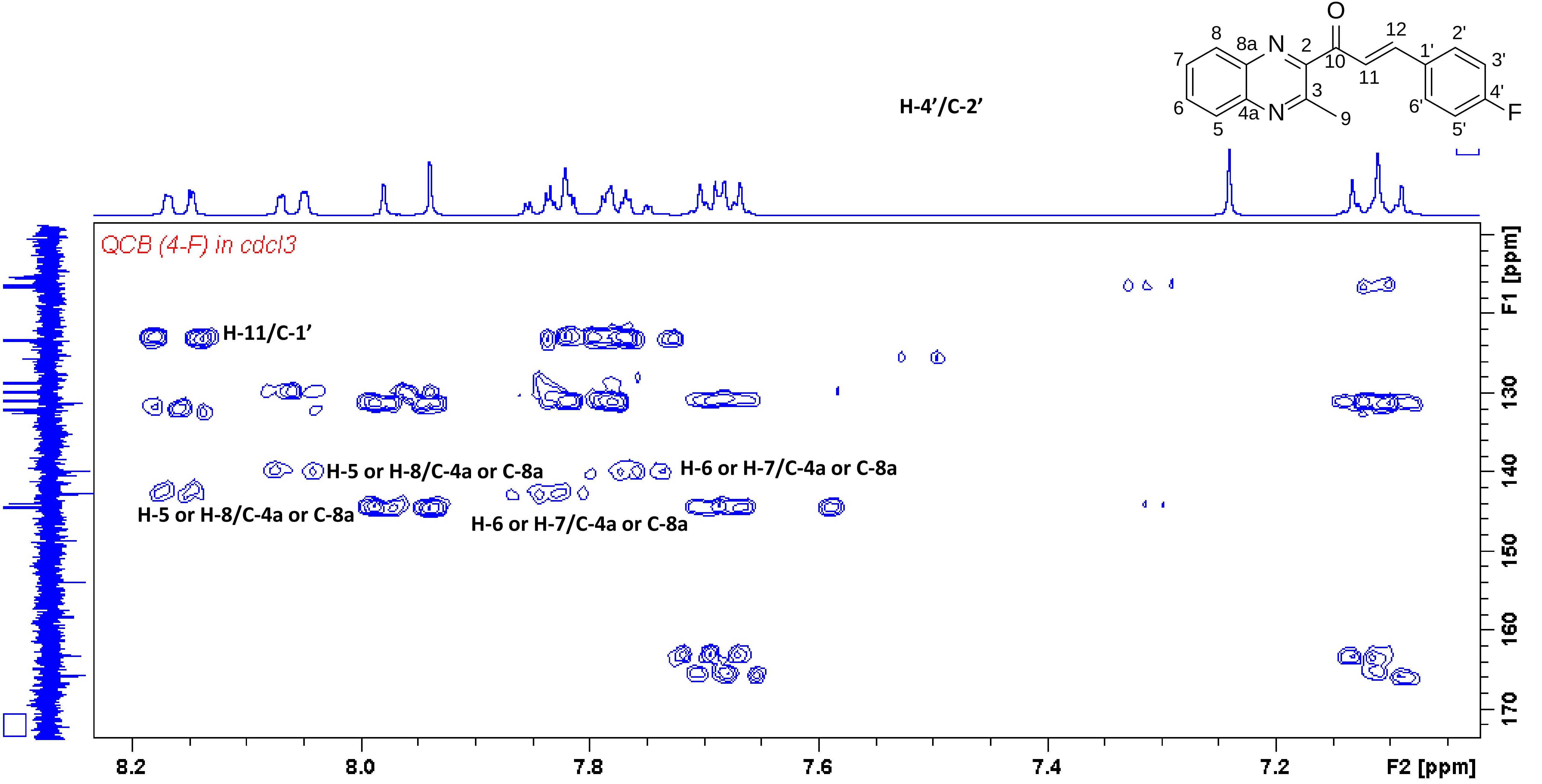

Expanded HMBC of **B10e**

Elemental Composition Report

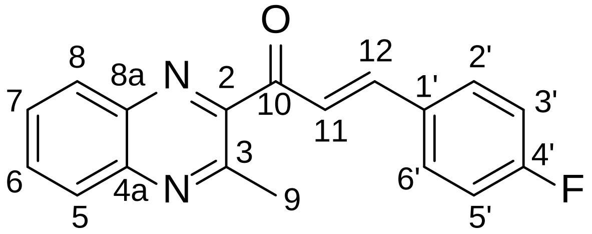

Single Mass Analysis

Tolerance = 5.0 PPM / DBE: min = -1.5, max = 100.0
Element prediction: Off
Number of isotope peaks used for i-FIT = 3

Monoisotopic Mass, Even Electron Ions
32 formula(e) evaluated with 1 results within limits (up to 20 closest results for each mass)
Elements Used:
C: 15-20 H: 10-15 N: 0-5 O: 1-5 F: 0-1
QCB(4-F) 28 (0.911) Cm (1:61)
TOF MS AP+

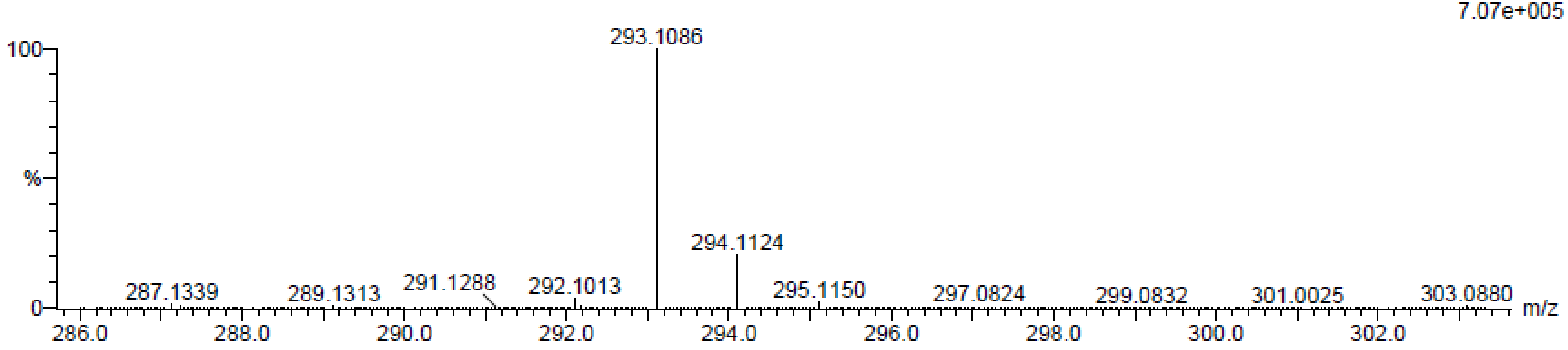

Minimum:				-1.5			
Maximum:		5.0	5.0	100.0			
Mass	Calc. Mass	mDa	PPM	DBE	i-FIT	i-FIT (Norm)	Formula
293.1086	293.1090	-0.4	-1.4	12.5	659.2	0.0	C18 H14 N2 O F

High resolution mass spectrum of **B10e**

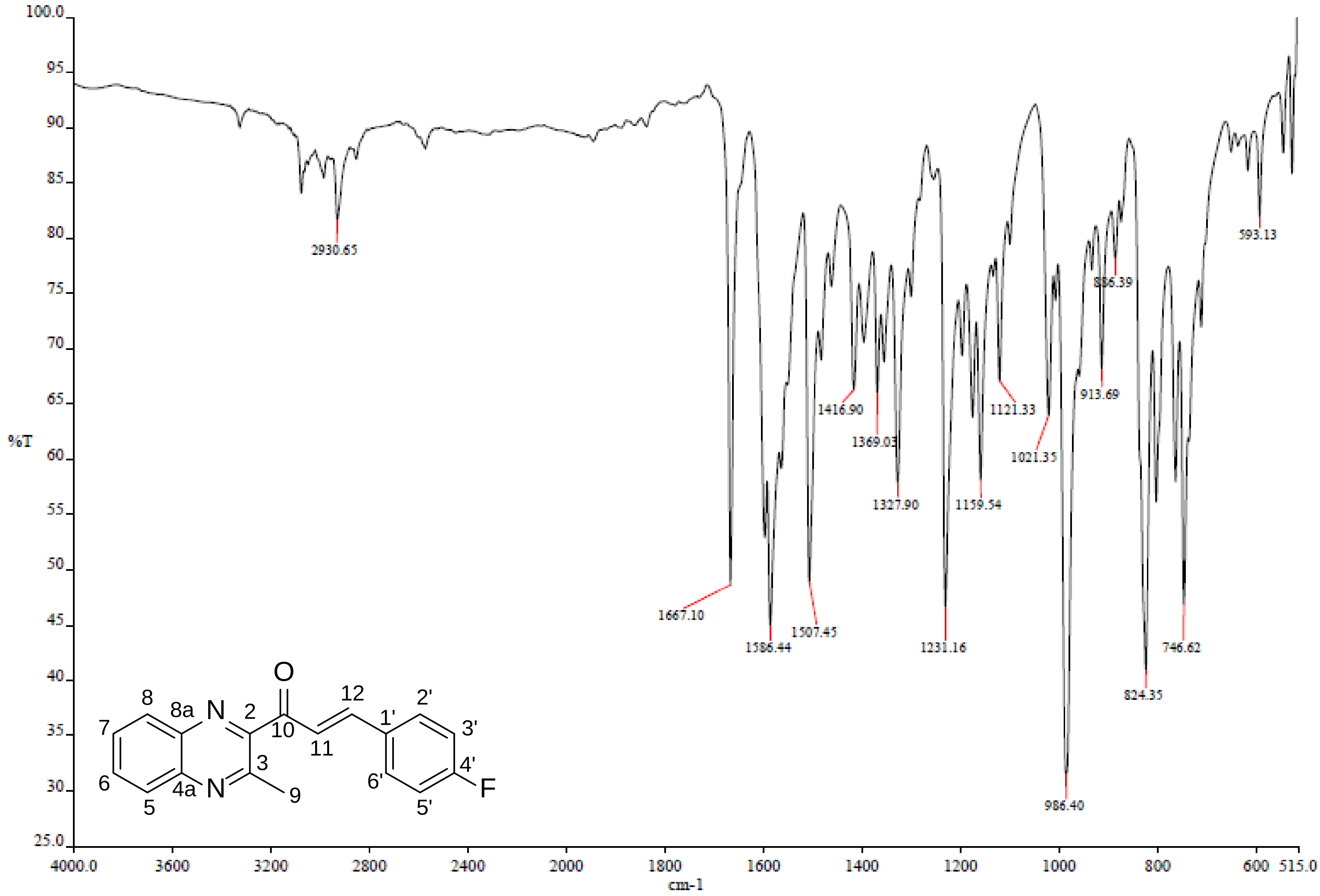

FTIR spectrum of **B10e**

Overlay Spectrum Graph Report

06/10/2017 11:45:37 AM

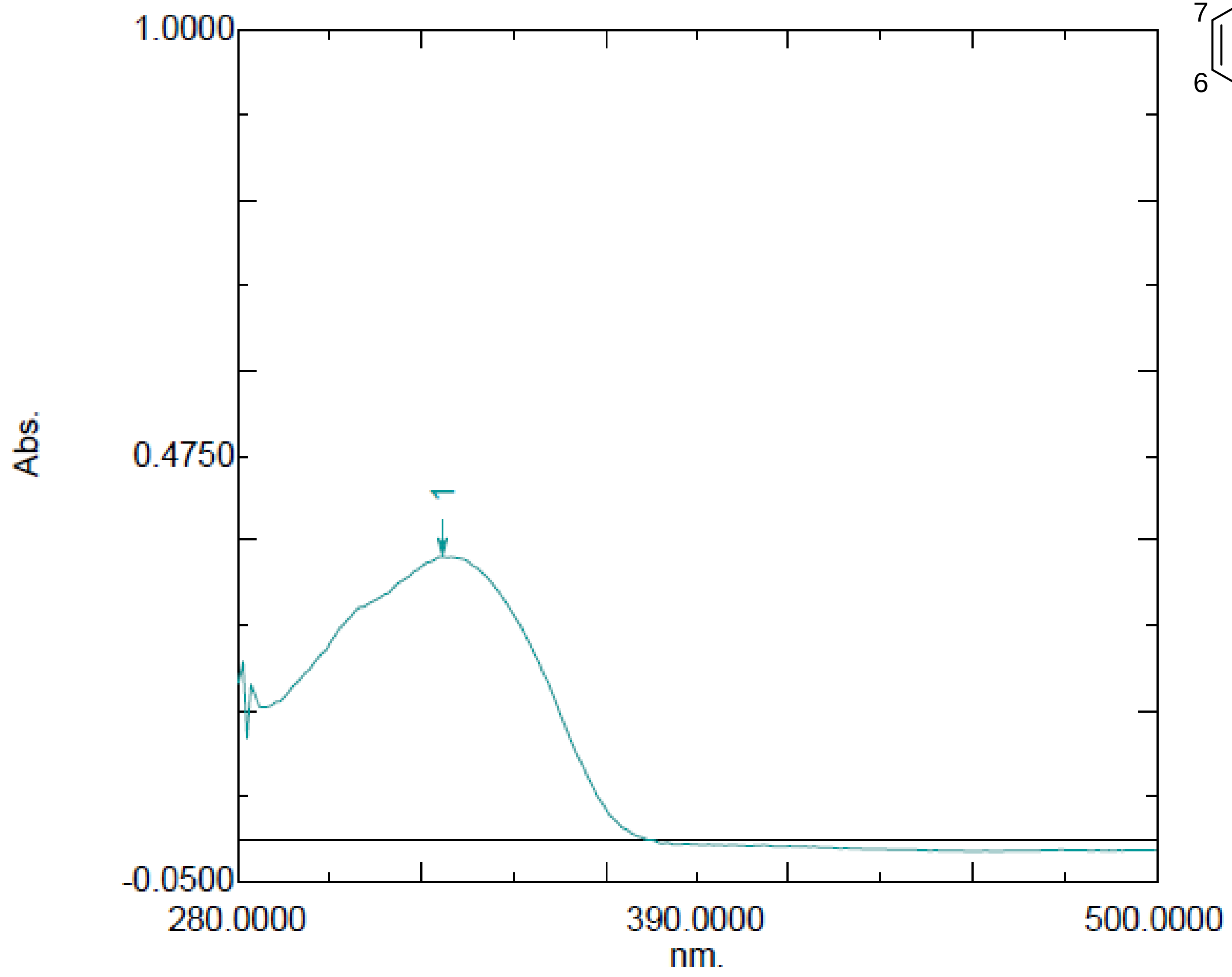

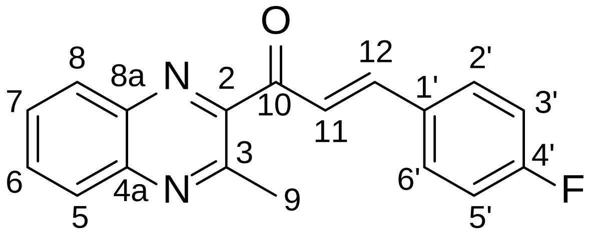

λ	absorbance	logε
329	0.3502	4.31

UV spectrum of **B10e**

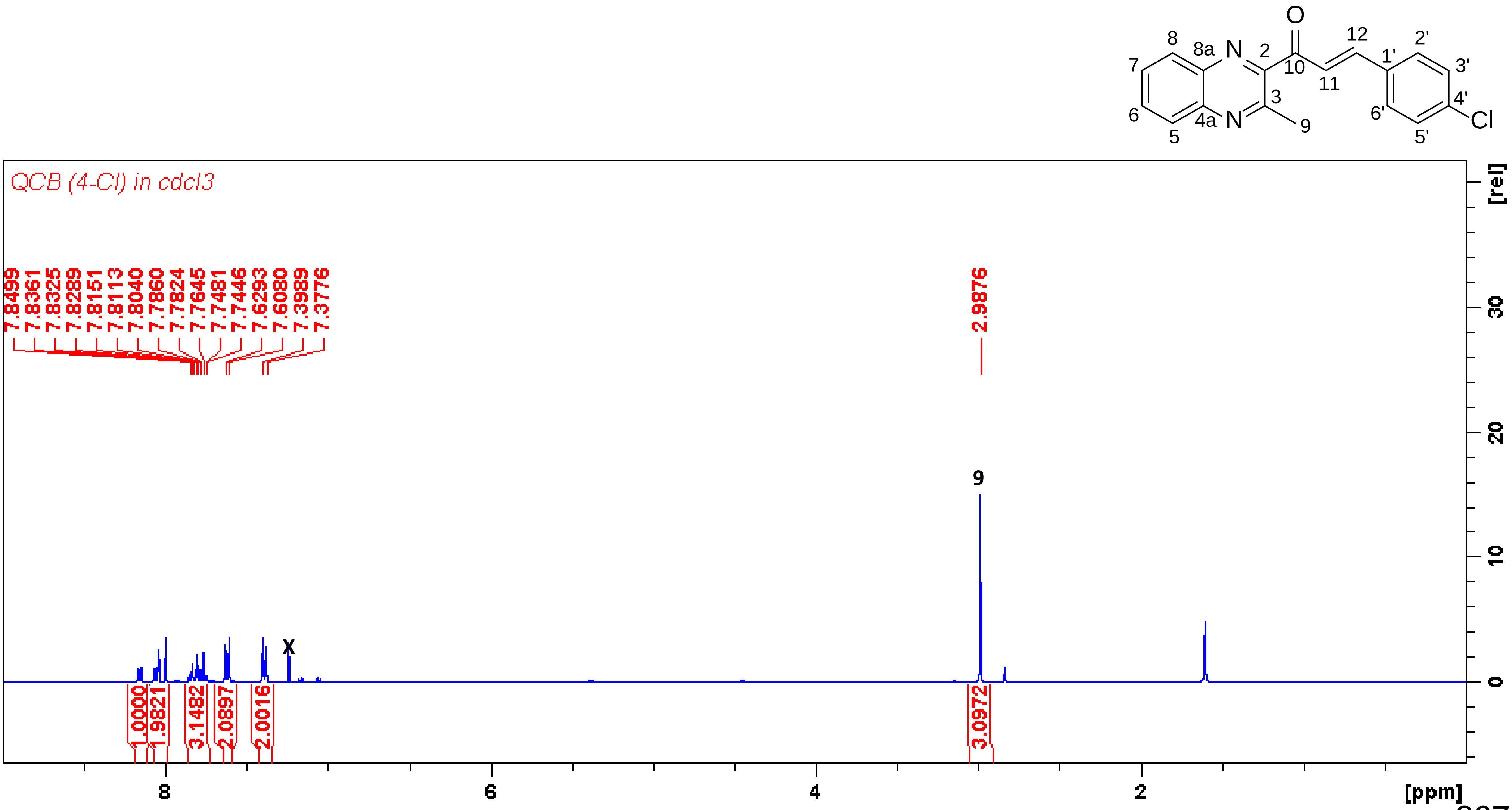

^{1}H NMR spectrum of **B10f**

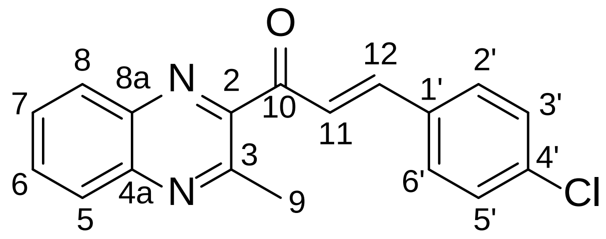

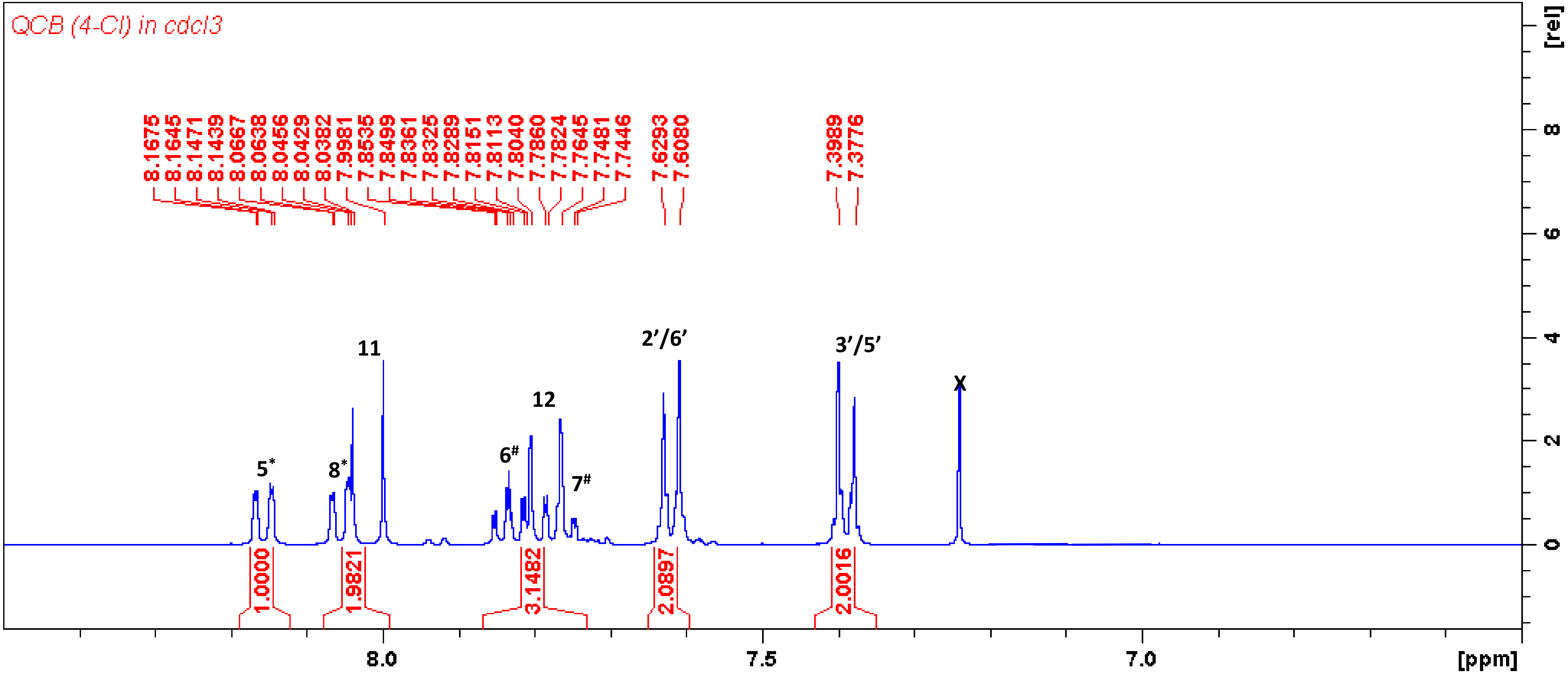

*, # Indicates assignments are interchangeable

Expanded ^{1}H NMR spectrum of **B10f**

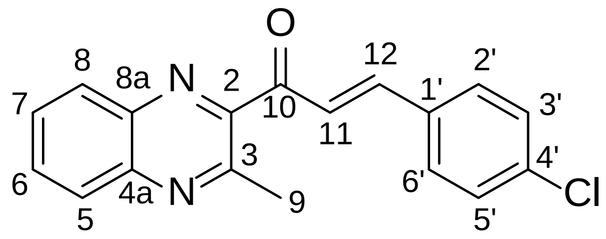

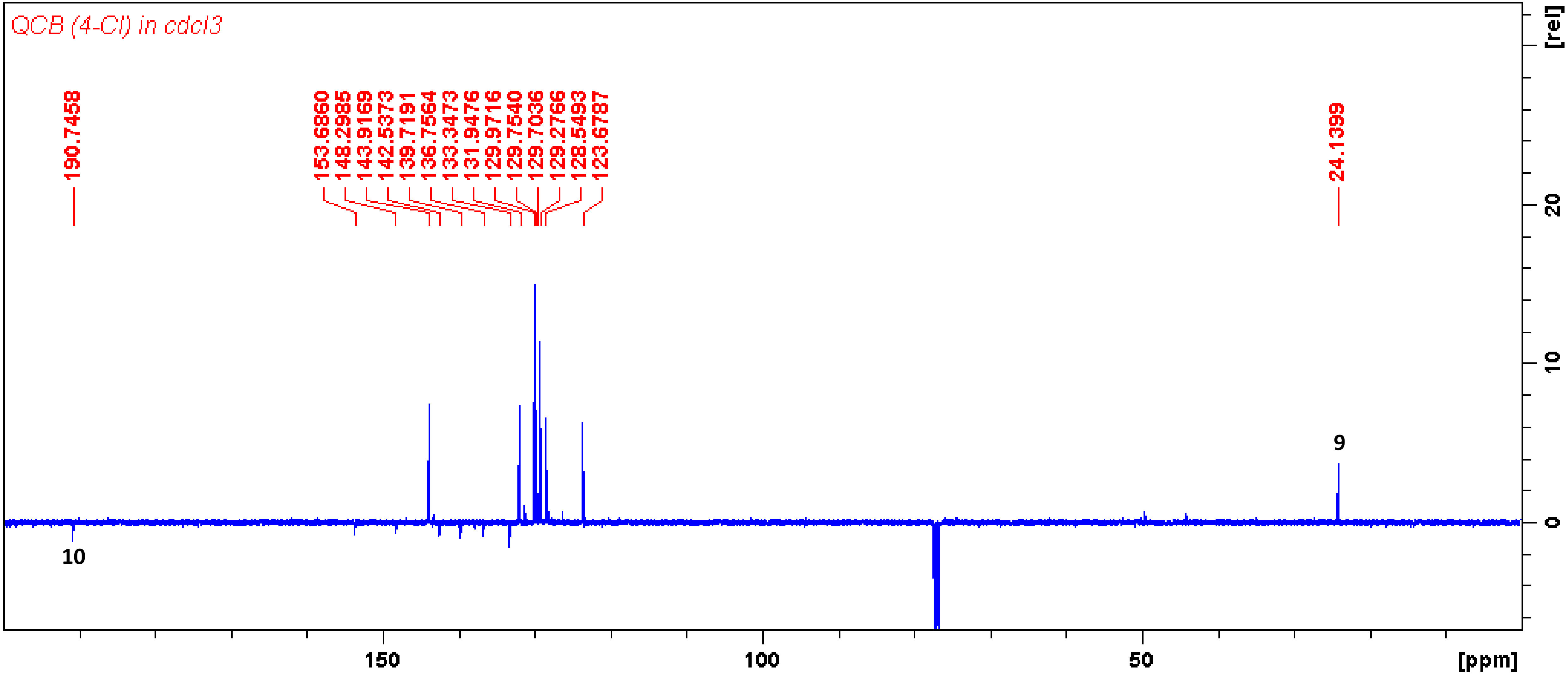

^{13}C NMR spectrum of **B10f**

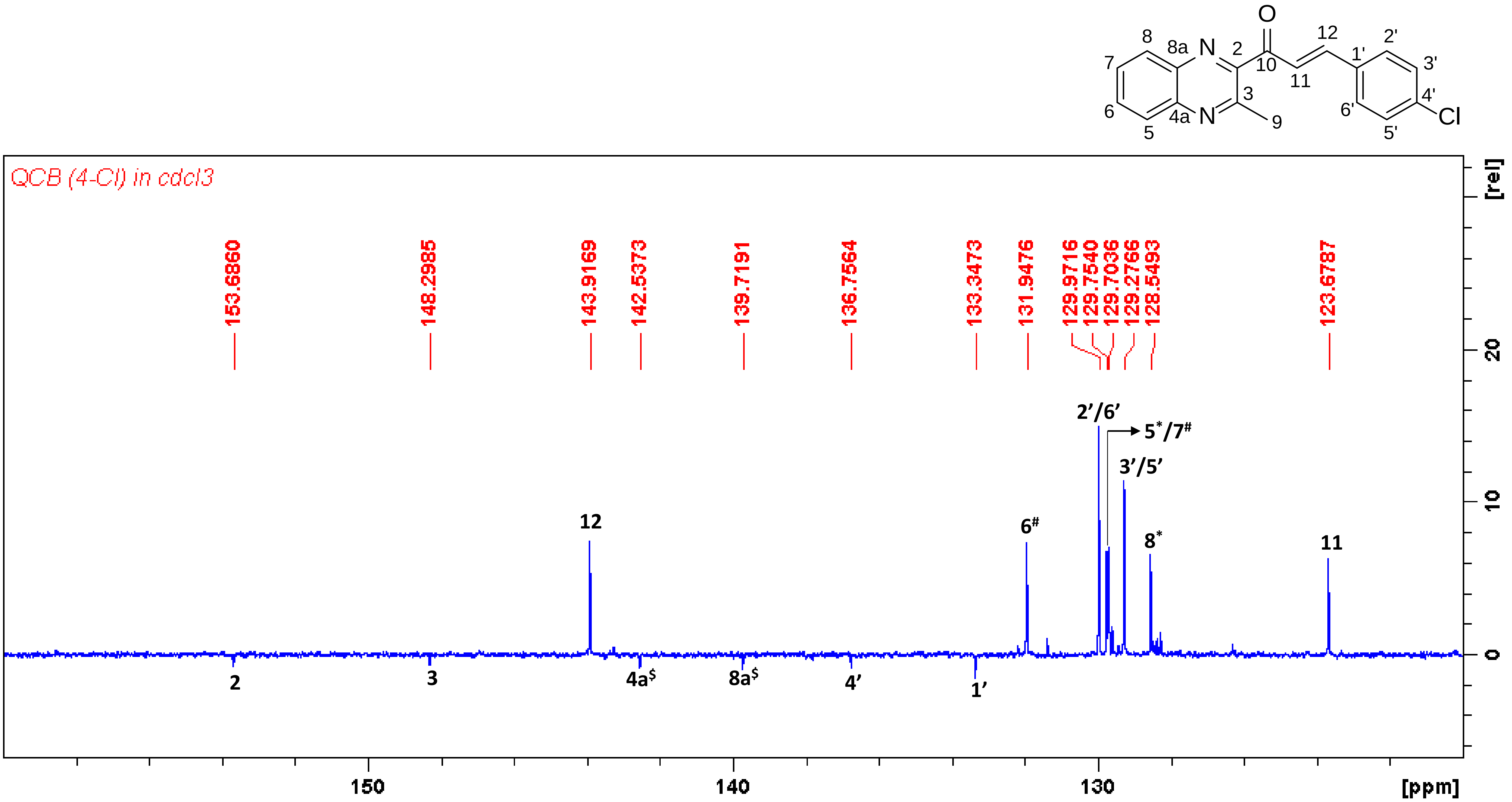

*, #, $ Indicates assignments are interchangeable

Expanded ^{13}C NMR spectrum of **B10f**

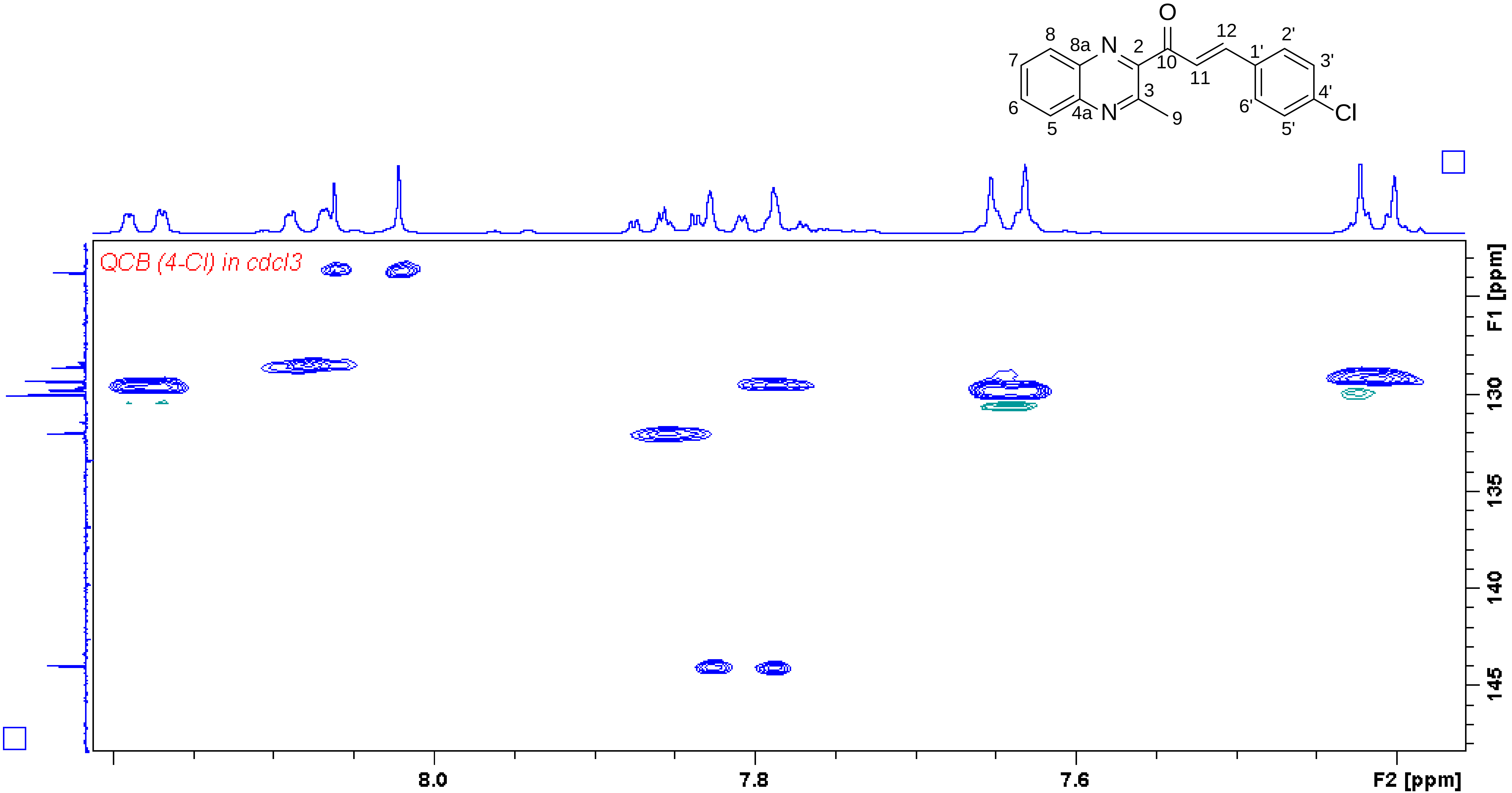

QCB (4-Cl) in cdcl3
F1 [ppm]
130
135
140
145
8.0
7.8
7.6
F2 [ppm]
O
N
Cl
2
3
4a
5
6
7
8
8a
9
10
11
12
1'
2'
3'
4'
5'
6'

HSQC of **B10f**

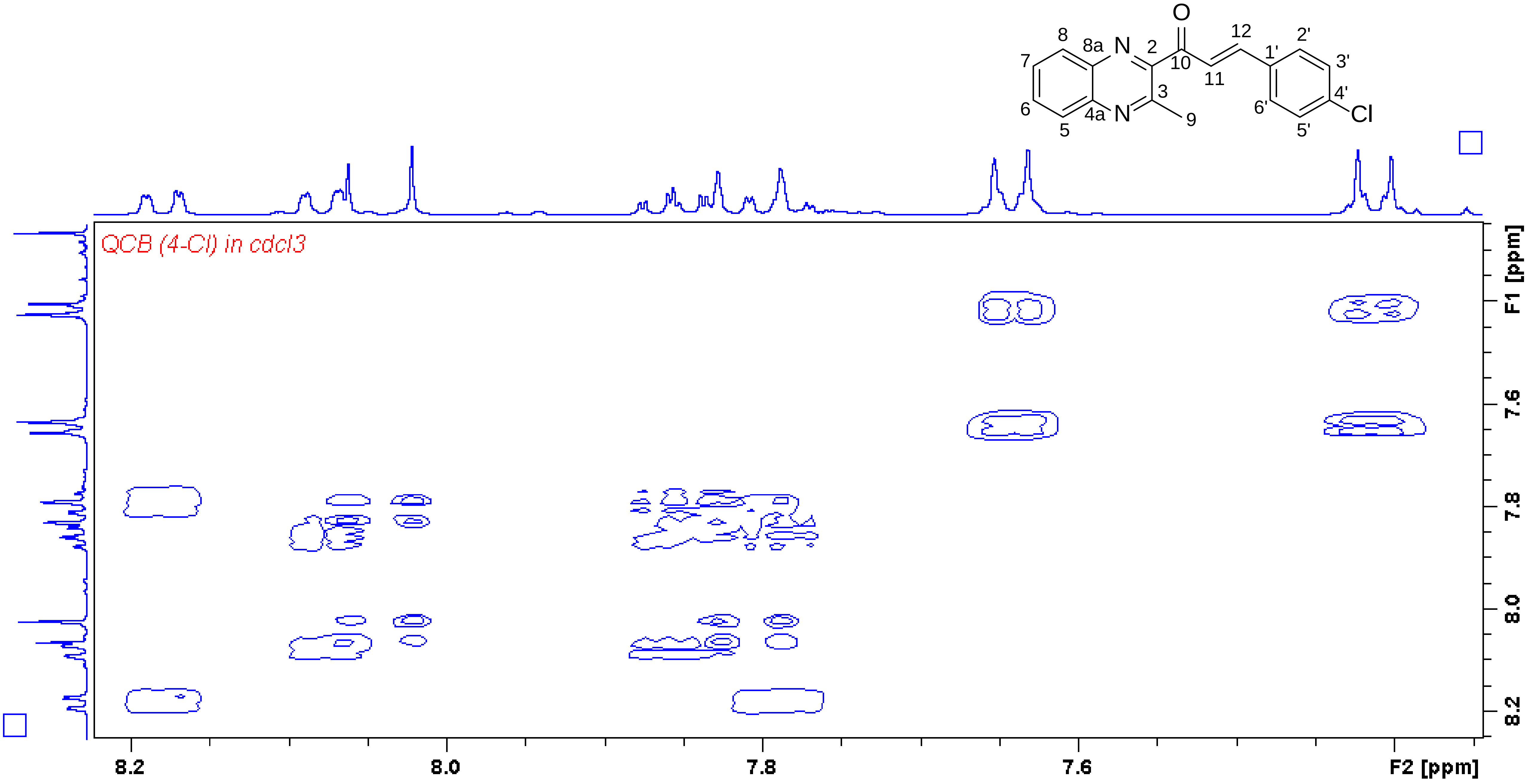
QCB (4-Cl) in cdcl3
F1 [ppm]
F2 [ppm]
8.2
8.0
7.8
7.6
O
N
N
Cl
2
3
4a
5
6
7
8
8a
9
10
11
12
1'
2'
3'
4'
5'
6'

COSY of **B10f**

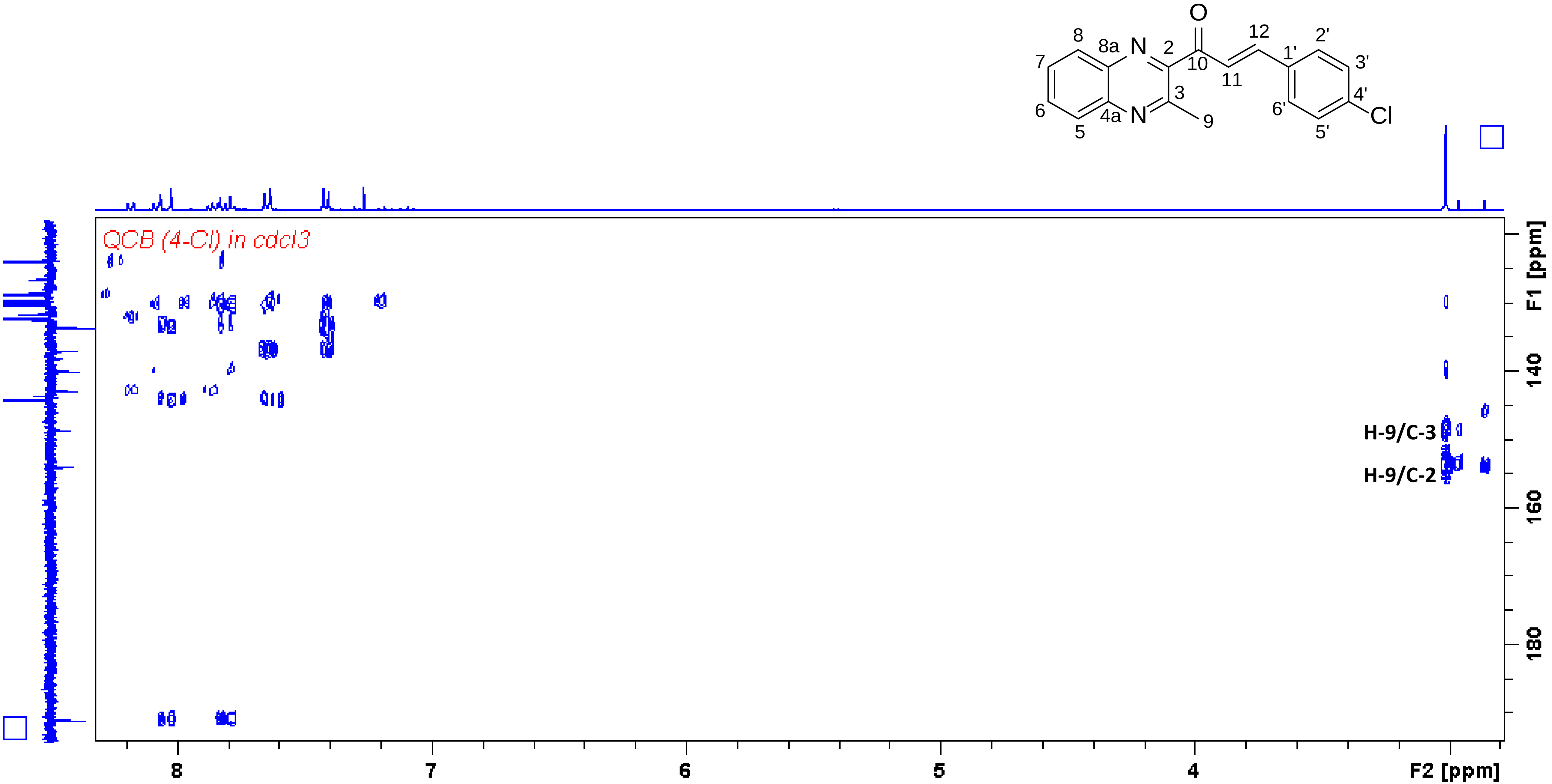

HMBC of **B10f**

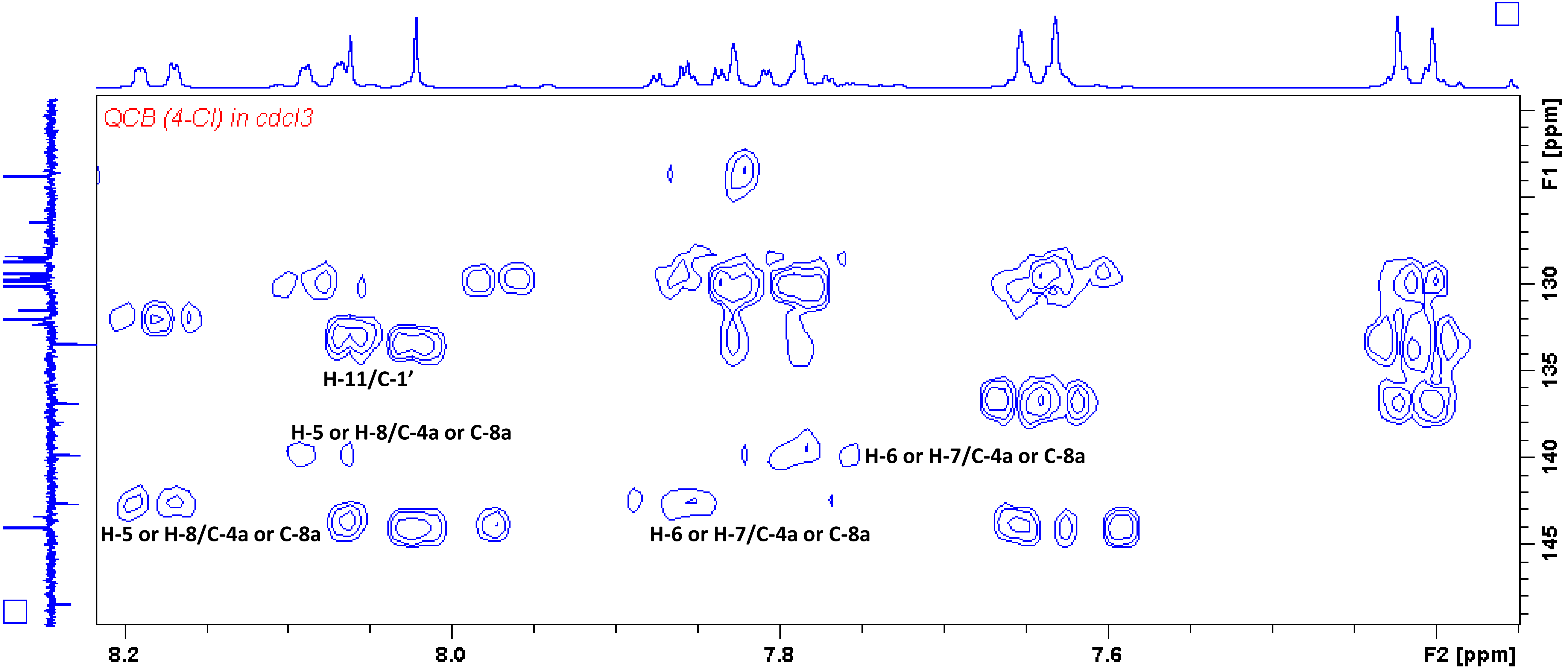

Expanded HMBC of **B10f**

Elemental Composition Report

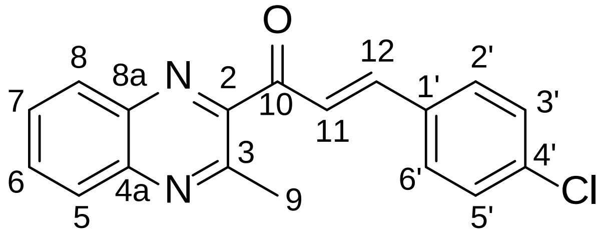

Single Mass Analysis

Tolerance = 5.0 PPM / DBE: min = -1.5, max = 100.0
Element prediction: Off
Number of isotope peaks used for i-FIT = 3

Monoisotopic Mass, Even Electron Ions
30 formula(e) evaluated with 1 results within limits (up to 20 closest results for each mass)
Elements Used:
C: 15-20 H: 10-15 N: 0-5 O: 1-5 Cl: 0-1
QCB(4-Cl) 59 (1.990) Cm (1:60)
TOF MS AP+

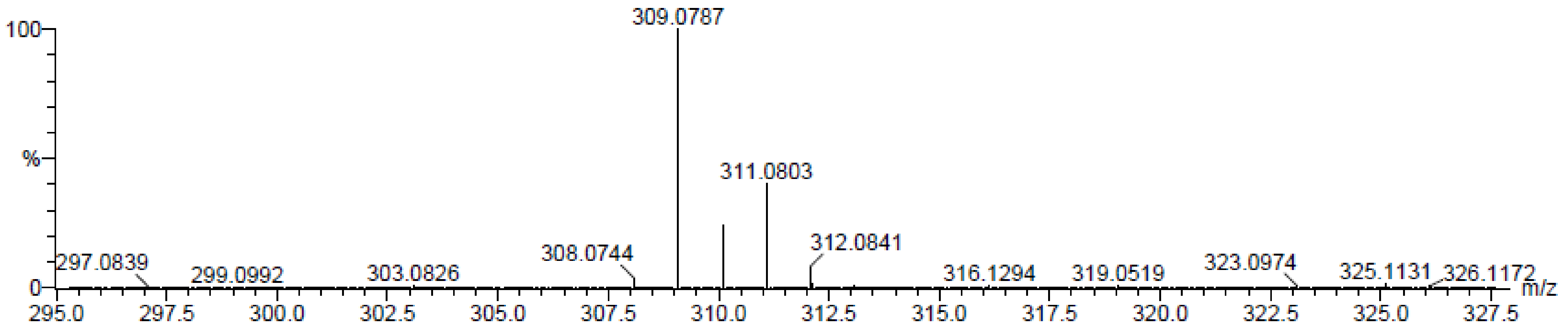

Minimum:				-1.5			
Maximum:		5.0	5.0	100.0			
Mass	Calc. Mass	mDa	PPM	DBE	i-FIT	i-FIT (Norm)	Formula
309.0787	309.0795	-0.8	-2.6	12.5	683.3	0.0	C18 H14 N2 O Cl

High resolution mass spectrum of **B10f**

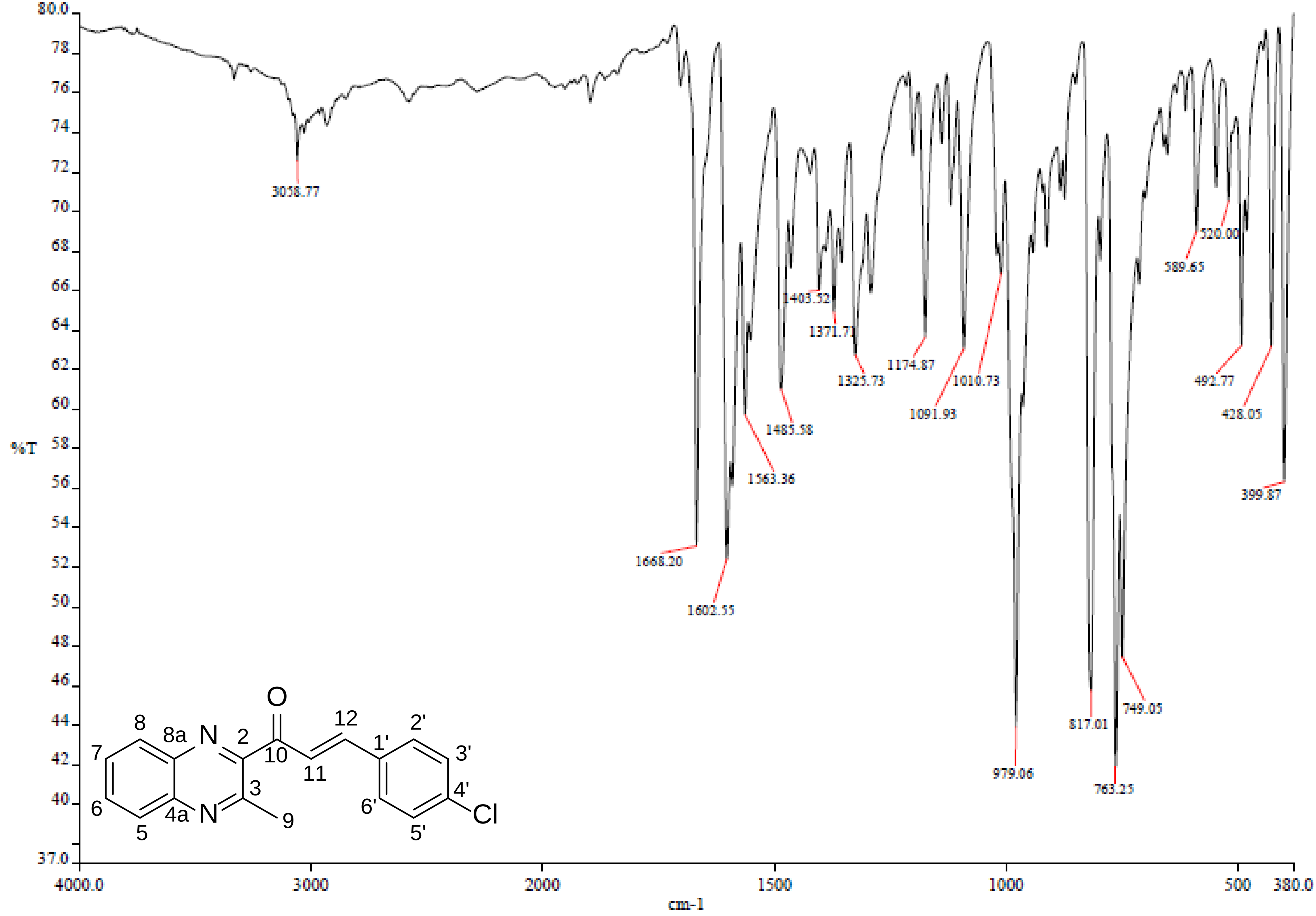

FTIR spectrum of **B10f**

Overlay Spectrum Graph Report

06/10/2017 11:44:50 AM

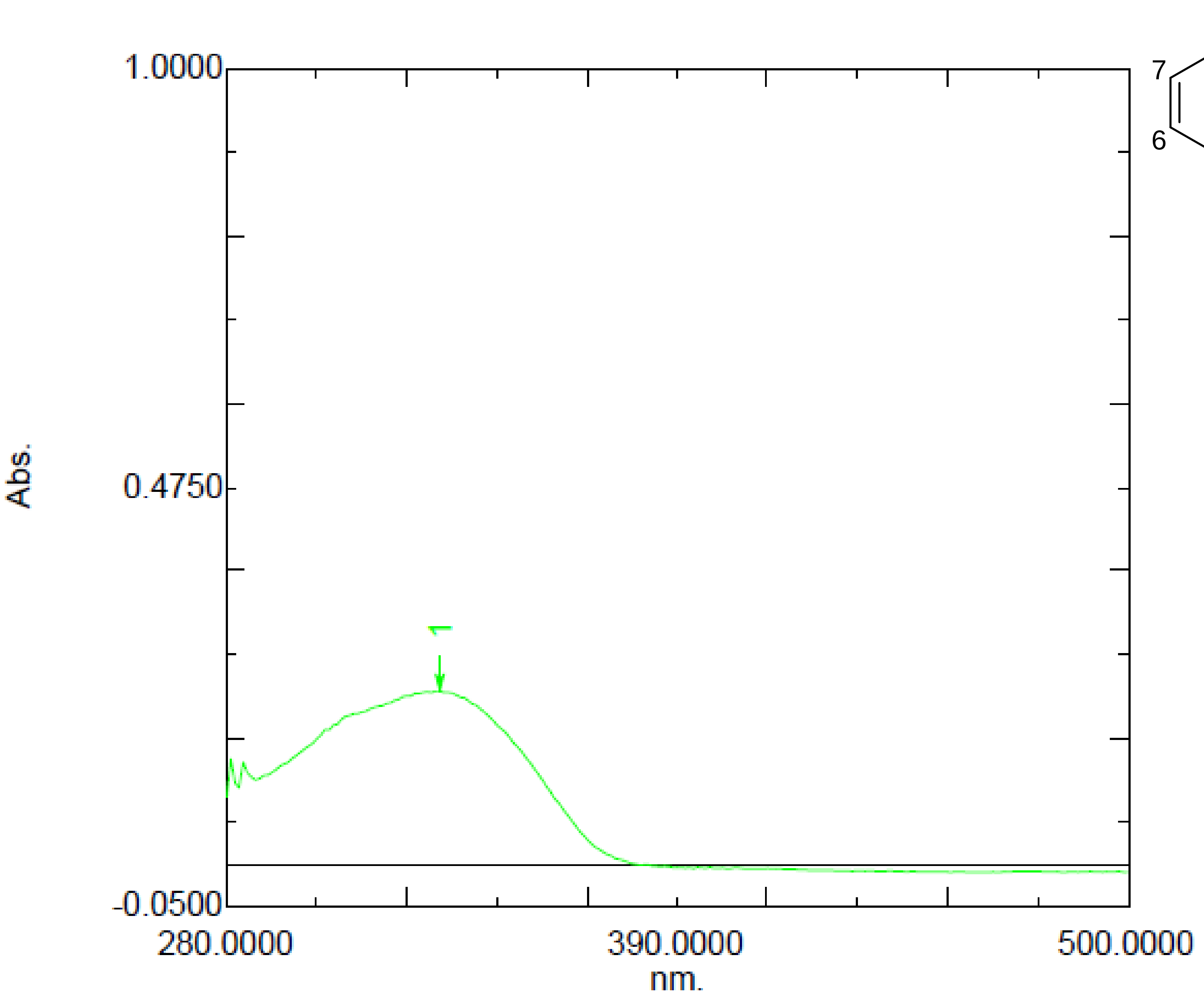

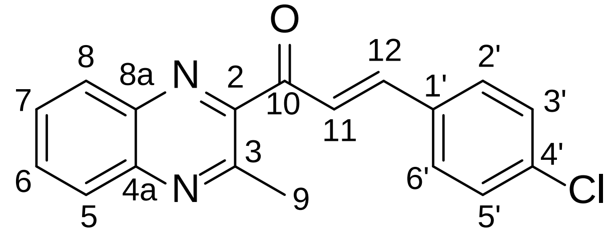

λ	absorbance	logε
331	0.2194	4.13

UV spectrum of **B10f**

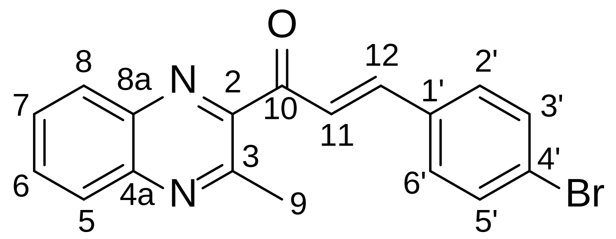

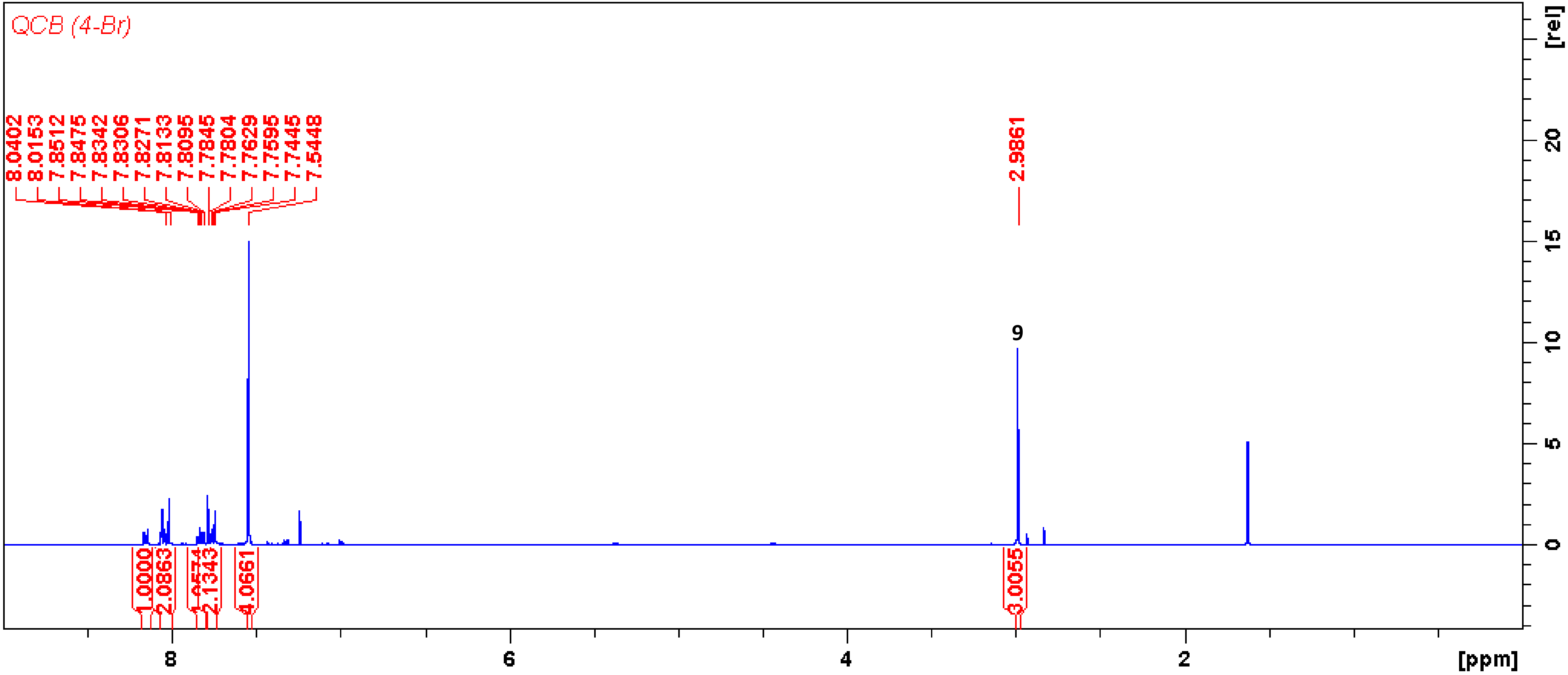

^{1}H NMR spectrum of **B10g**

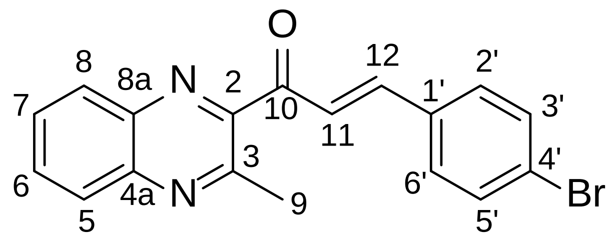

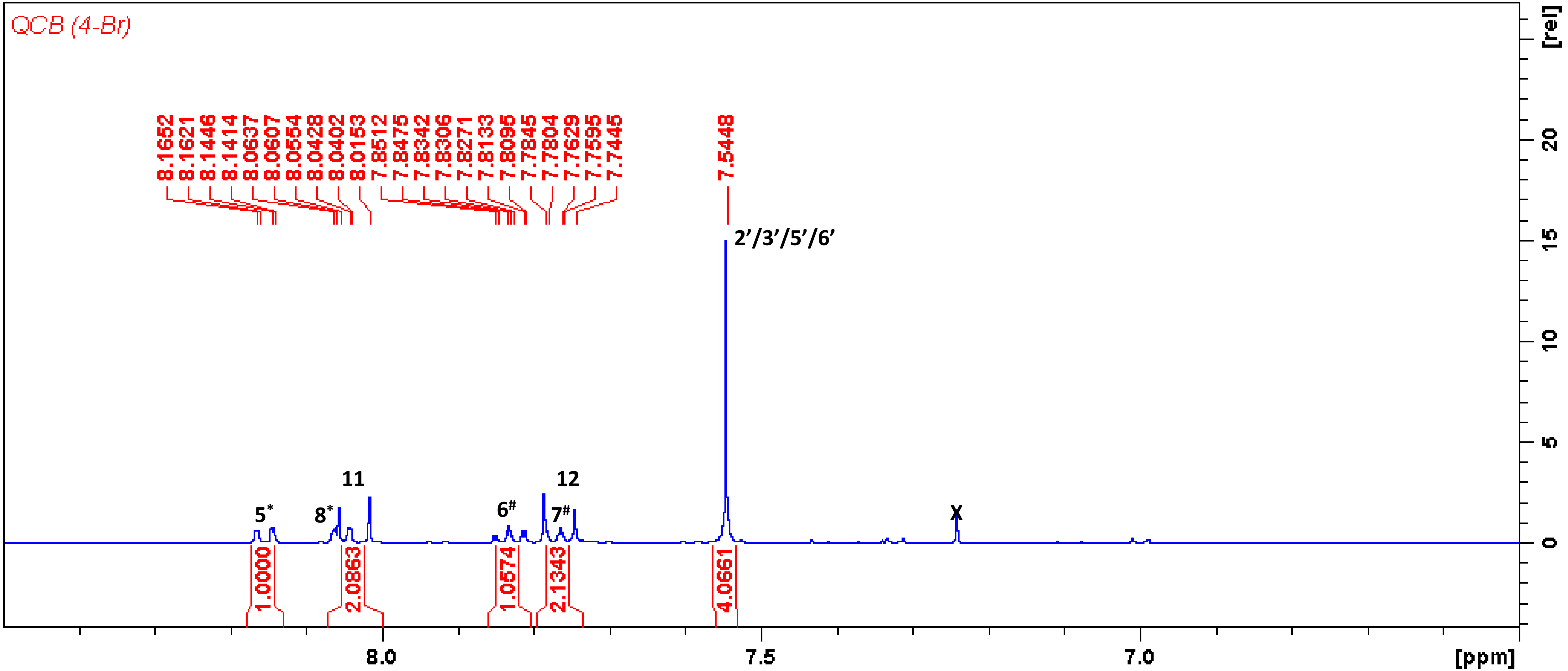

*, # Indicates assignments are interchangeable

Expanded ¹H NMR spectrum of **B10g**

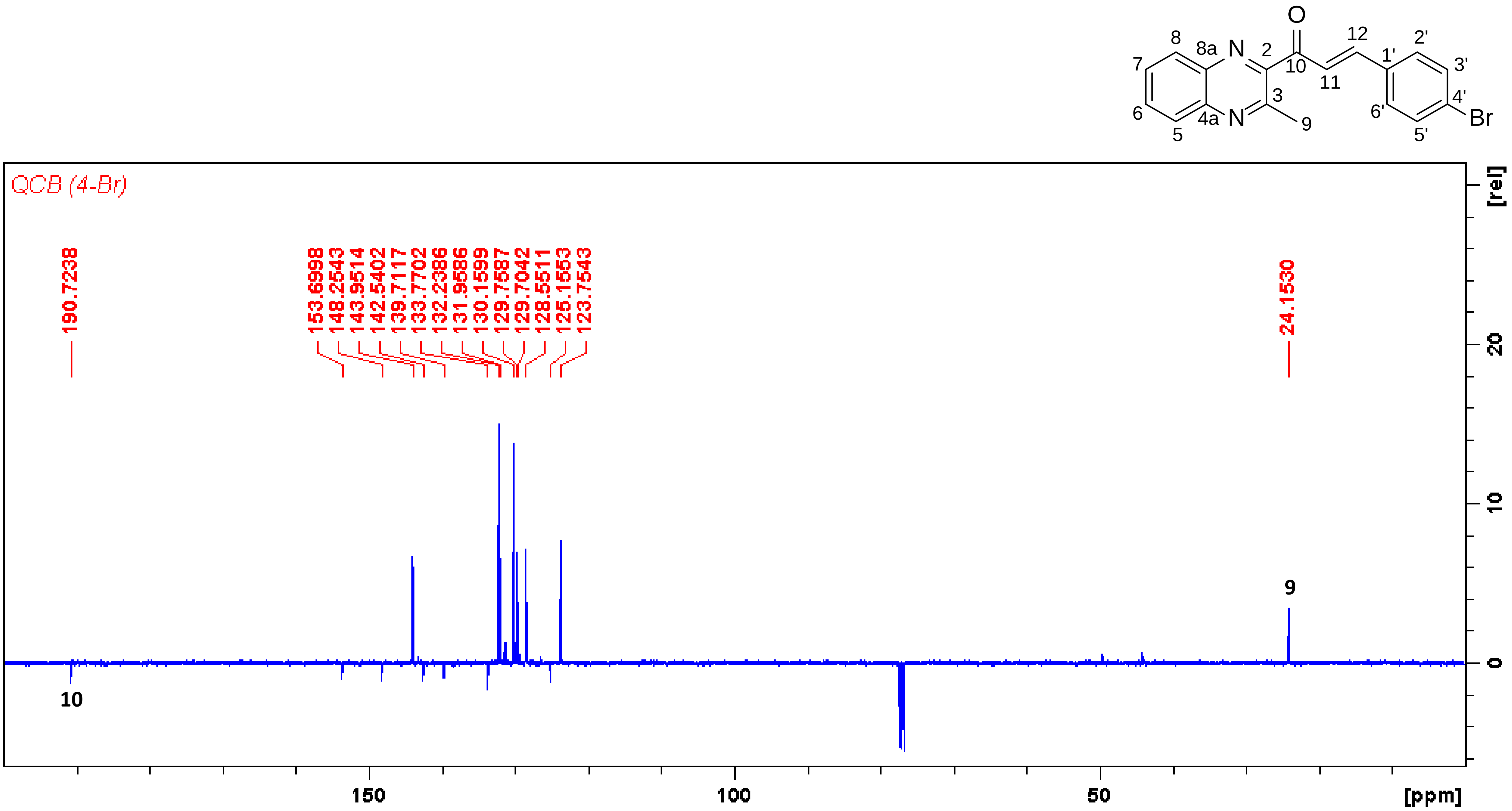

^{13}C NMR spectrum of **B10g**

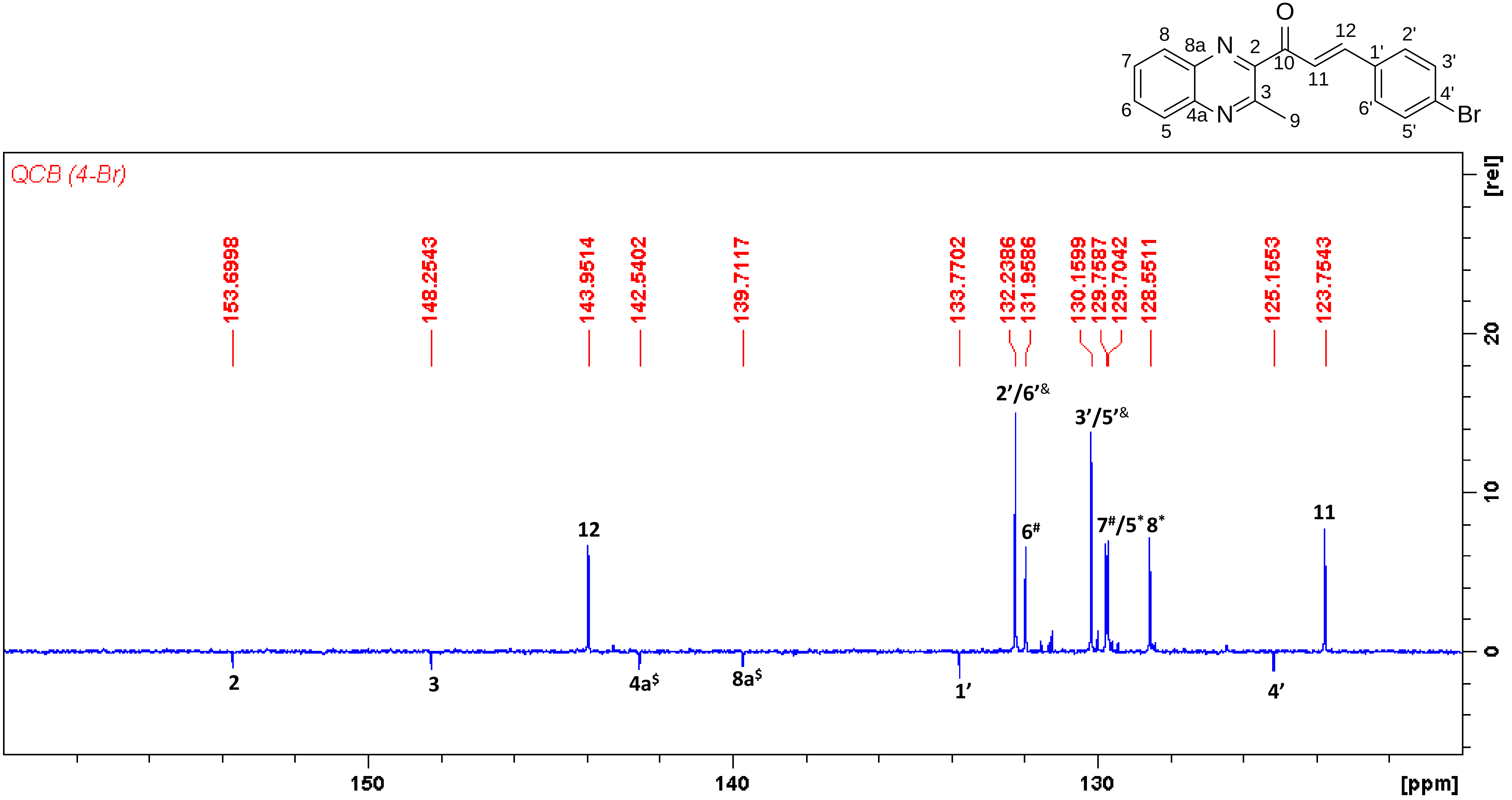

*, #, $, & Indicates assignments are interchangeable

Expanded ^{13}C NMR spectrum of **B10g**

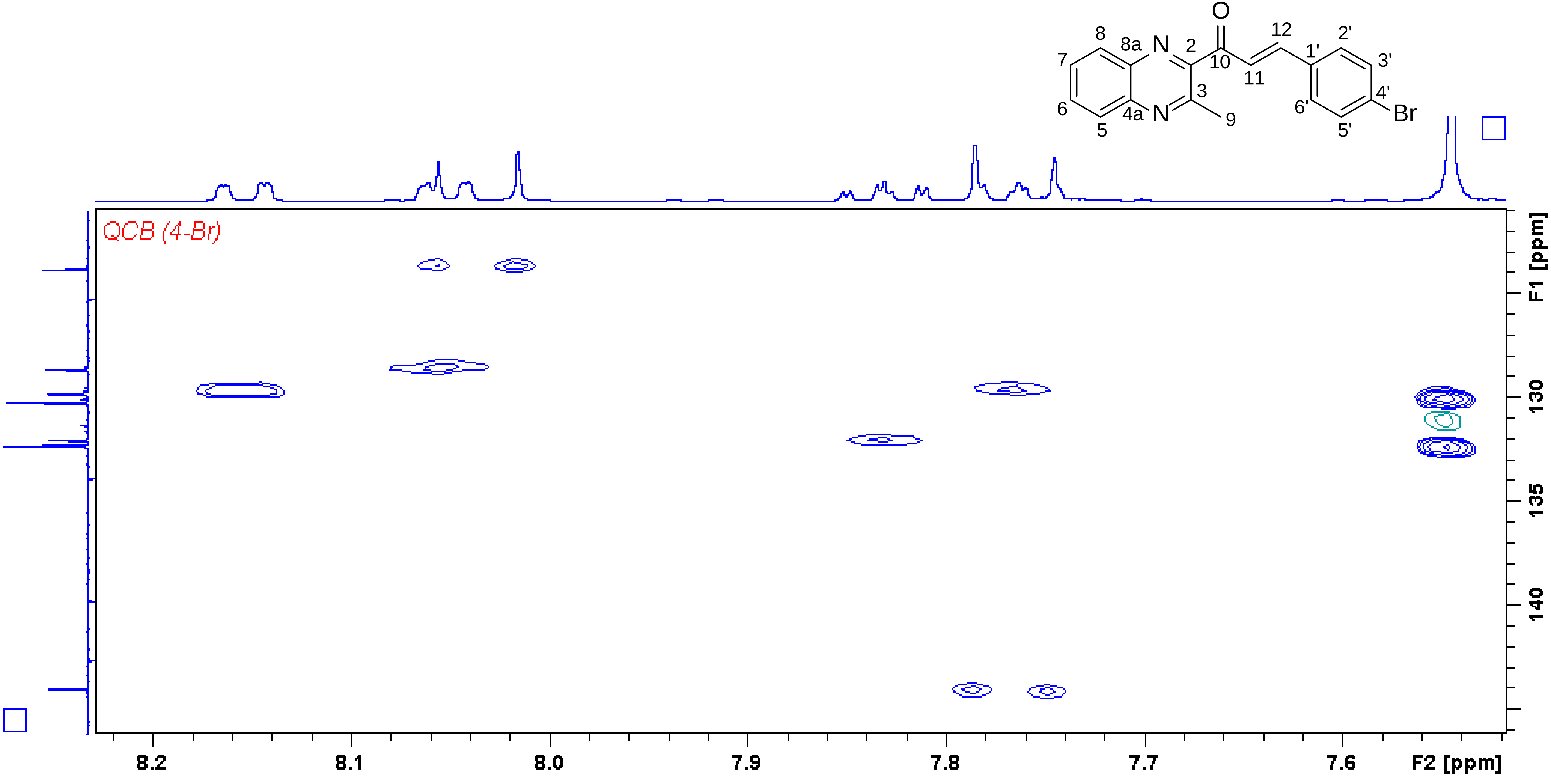
QCB (4-Br)
O
N
N
8
8a
2
12
2'
7
10
1'
3'
11
3
4'
6
4a
6'
Br
9
5
5'
8.2
8.1
8.0
7.9
7.8
7.7
7.6
F2 [ppm]
F1 [ppm]
130
135
140

HSQC of **B10g**

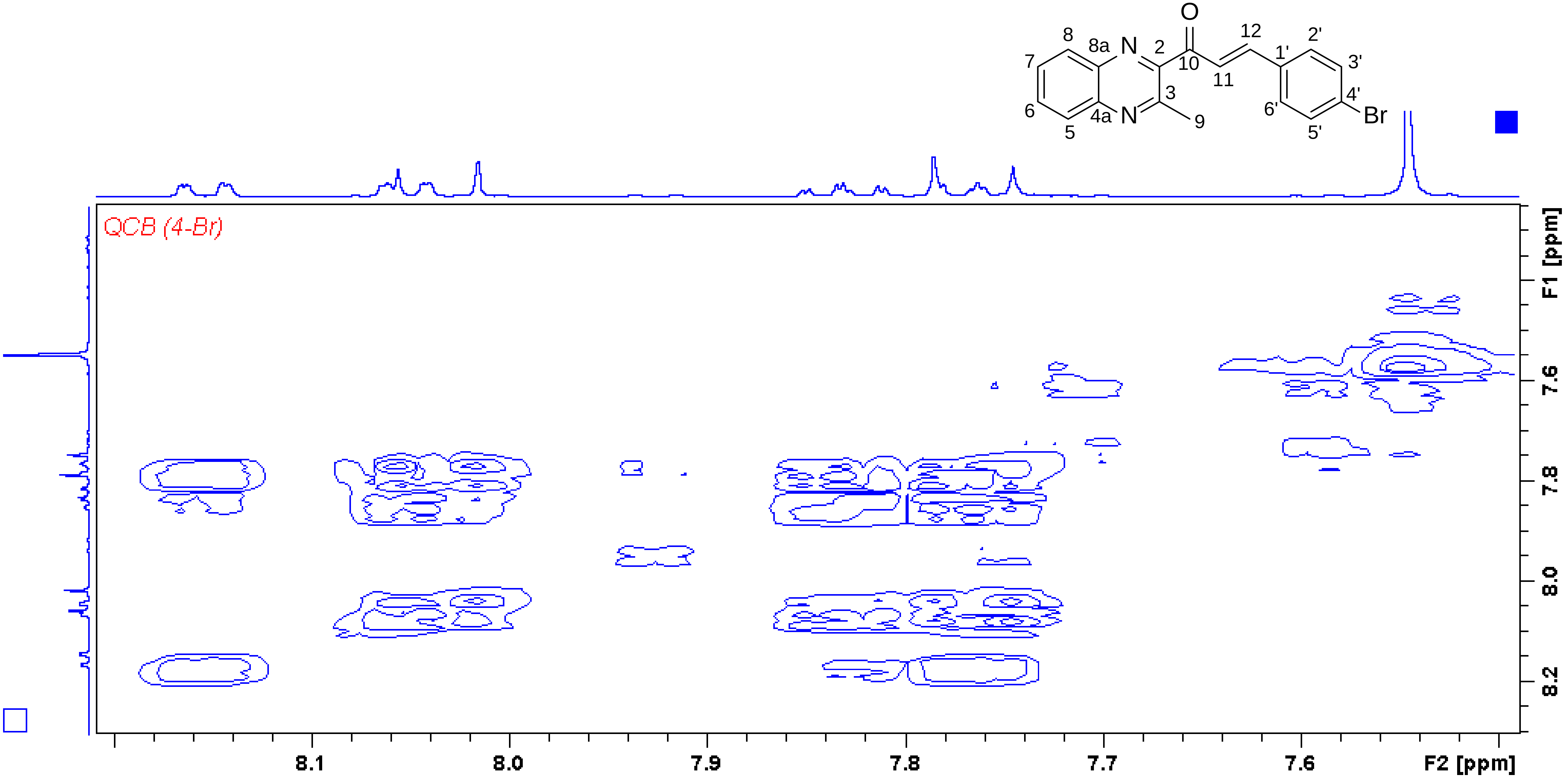
QCB (4-Br)
O
N
N
Br
8
8a
2
7
10
12
2'
1'
3'
11
3
4'
6
4a
9
6'
5
5'
8.1
8.0
7.9
7.8
7.7
7.6
F2 [ppm]
F1 [ppm]
7.6
7.8
8.0
8.2

COSY of **B10g**

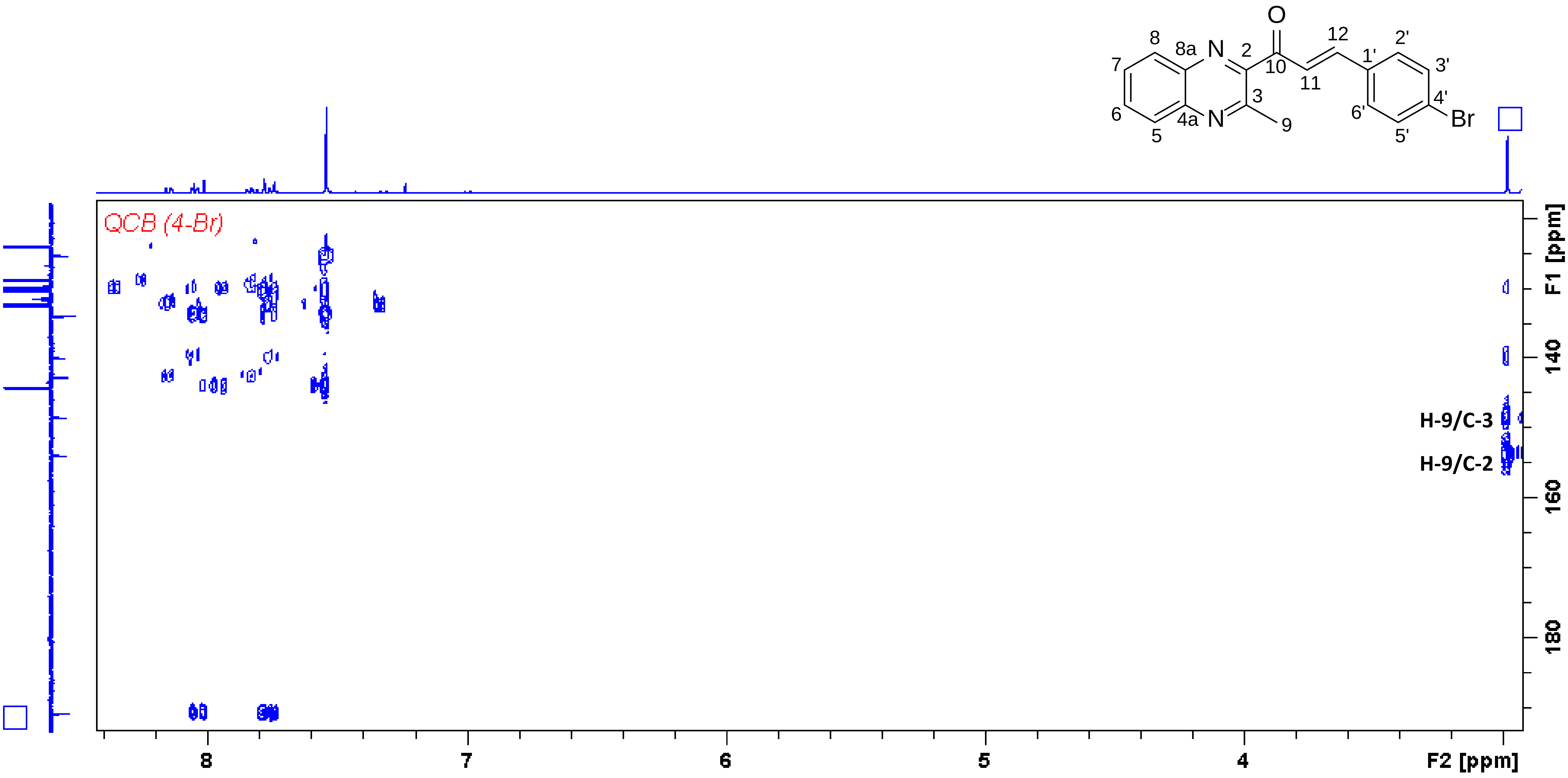

O
8
8a
N
2
12
2'
7
10
1'
3'
11
3
4'
6
6'
Br
4a
N
9
5
5'
QCB (4-Br)
H-9/C-3
H-9/C-2
F1 [ppm]
140
160
180
8
7
6
5
4
F2 [ppm]

HMBC of **B10g**

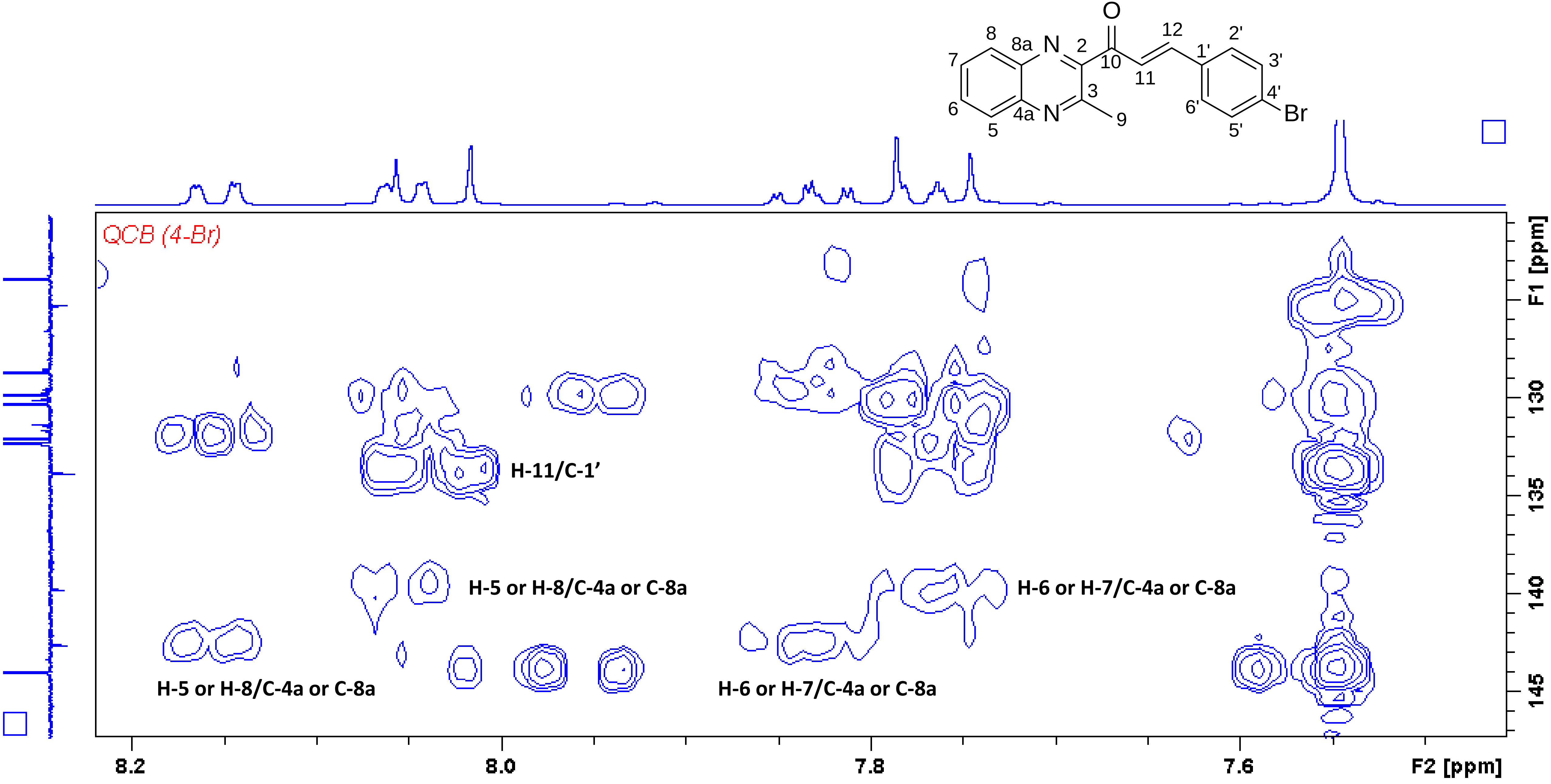

Expandedd HMBC of **B10g**

Elemental Composition Report

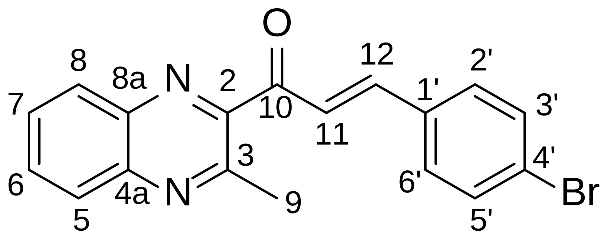

Single Mass Analysis

Tolerance = 5.0 PPM / DBE: min = -1.5, max = 100.0
Element prediction: Off
Number of isotope peaks used for i-FIT = 3

Monoisotopic Mass, Even Electron Ions
29 formula(e) evaluated with 1 results within limits (up to 20 closest results for each mass)
Elements Used:
C: 15-20 H: 10-15 N: 0-5 O: 1-5 Br: 0-1

QCB(4-Br) 1 (0.034) Cm (1:60)
TOF MS AP+

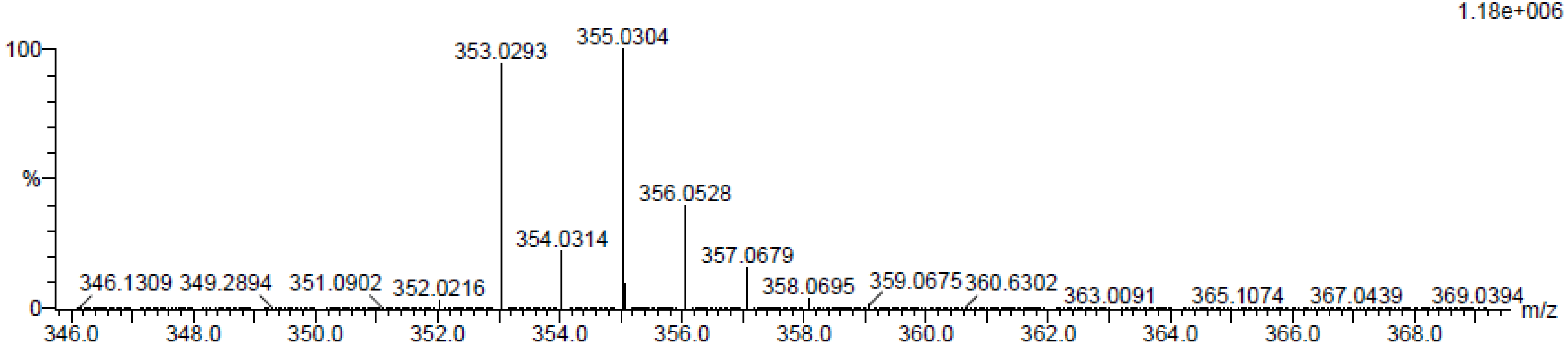

Minimum:				-1.5			
Maximum:		5.0	5.0	100.0			
Mass	Calc. Mass	mDa	PPM	DBE	i-FIT	i-FIT (Norm)	Formula
353.0293	353.0289	0.4	1.1	12.5	730.0	0.0	C18 H14 N2 O Br

High resolution mass spectrum of **B10g**

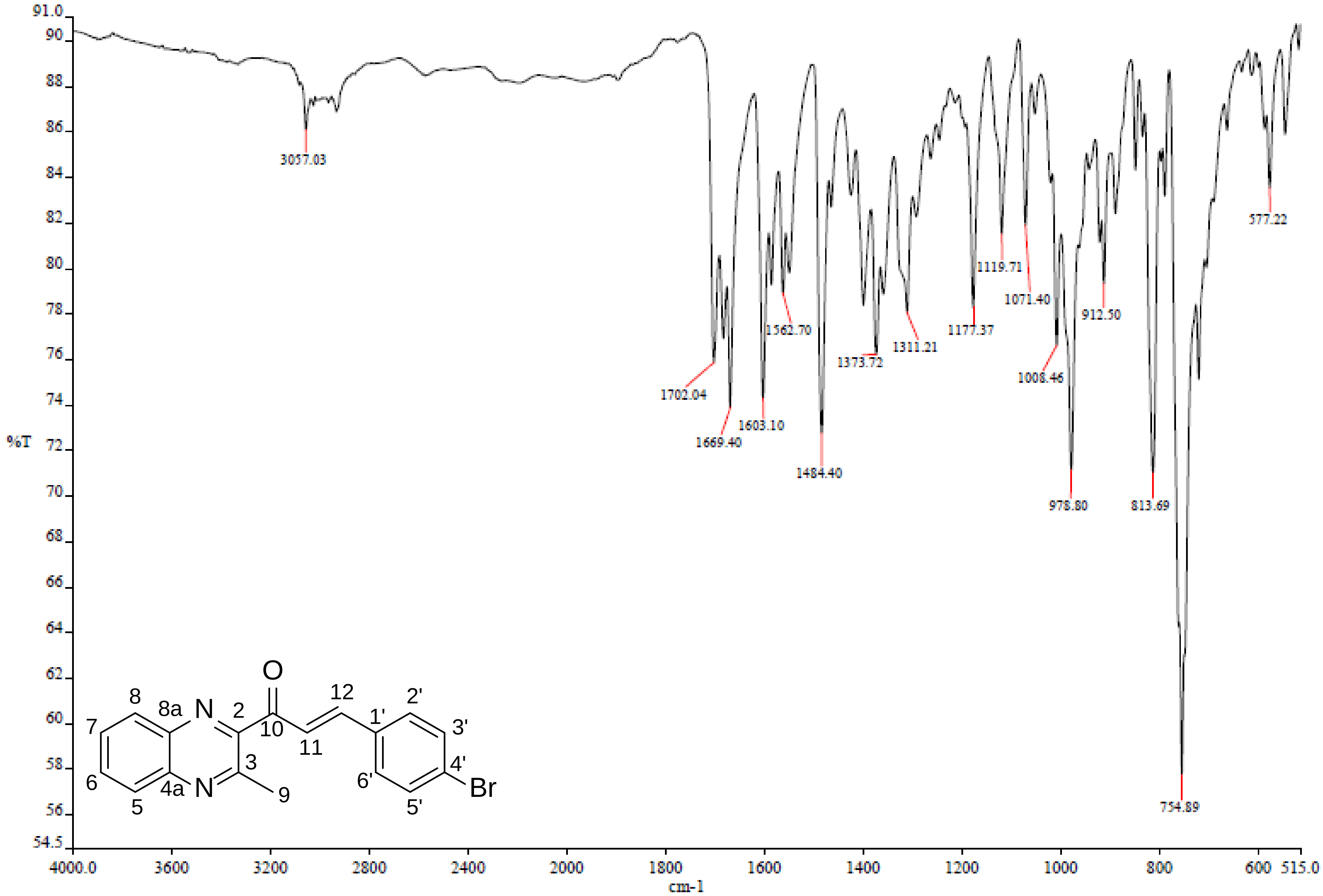

FTIR spectrum of **B10g**

Overlay Spectrum Graph Report

06/10/2017 11:43:27 AM

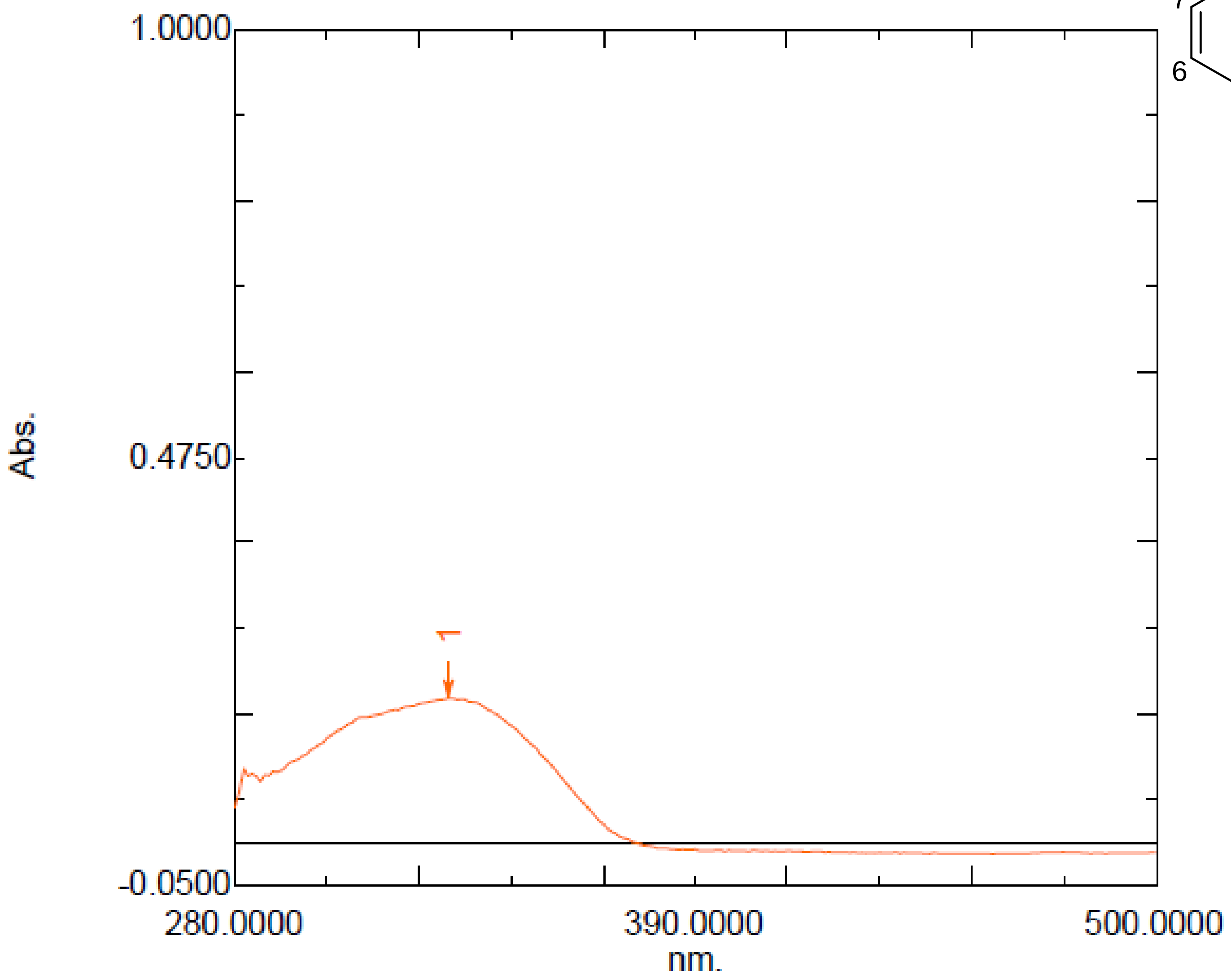

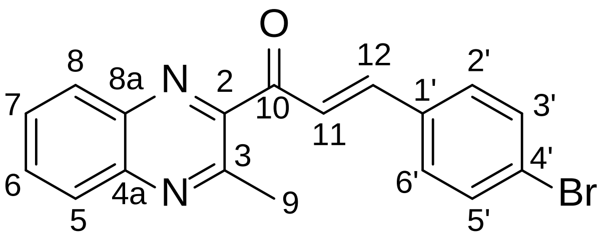

λ	absorbance	logε
331	0.1795	4.10

UV spectrum of **B10g**

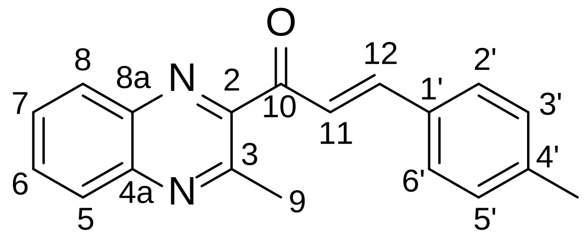

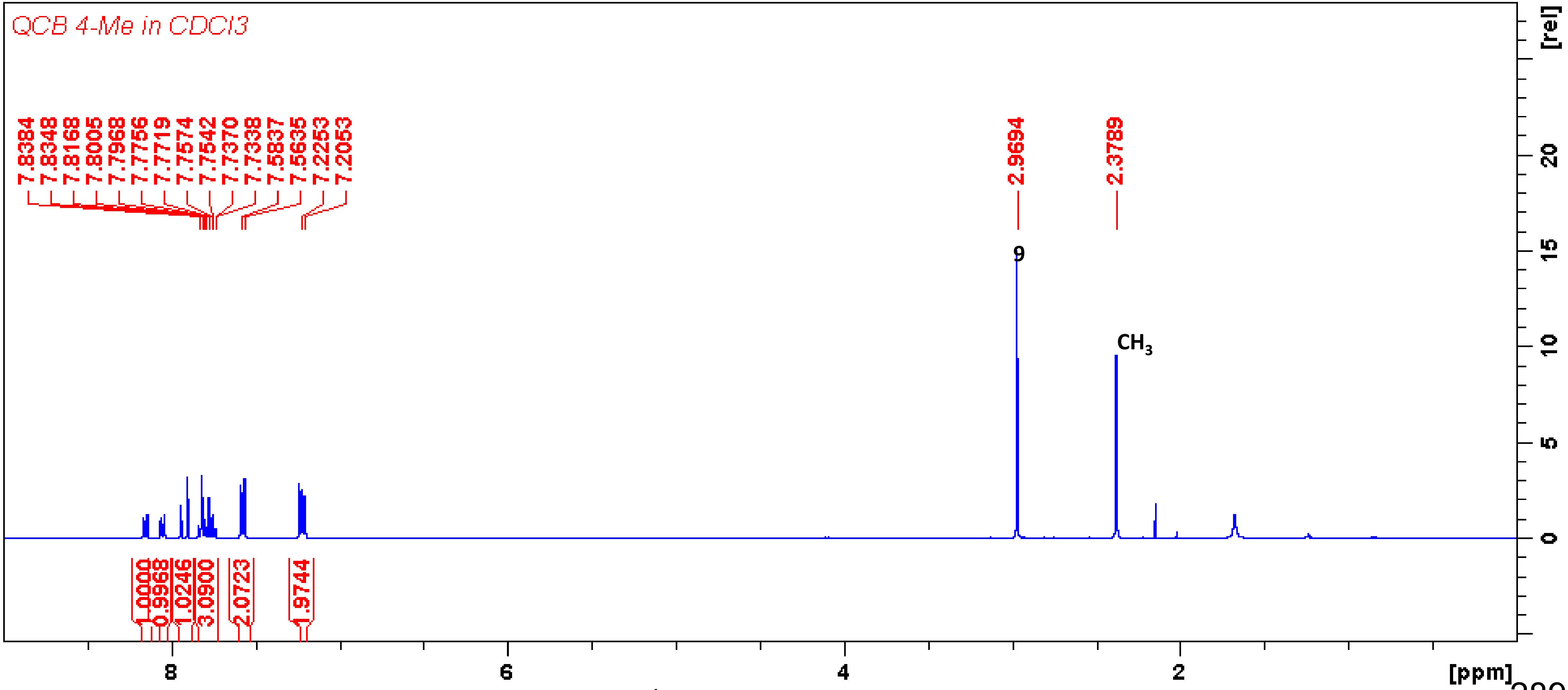

^{1}H NMR spectrum of **B10h**

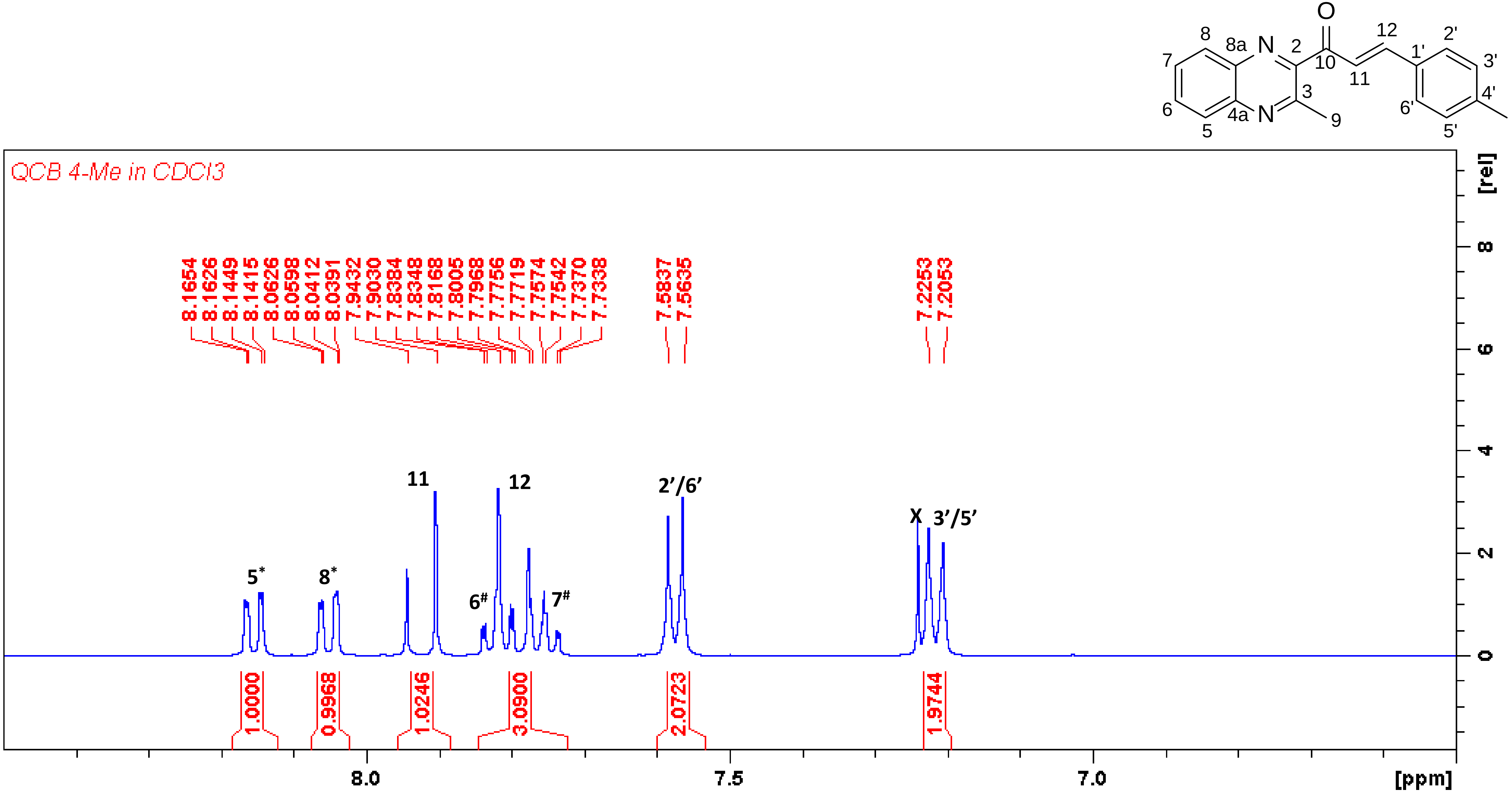

*, # Indicates assignments are interchangeable

Expanded [1]H NMR spectrum of **B10h**

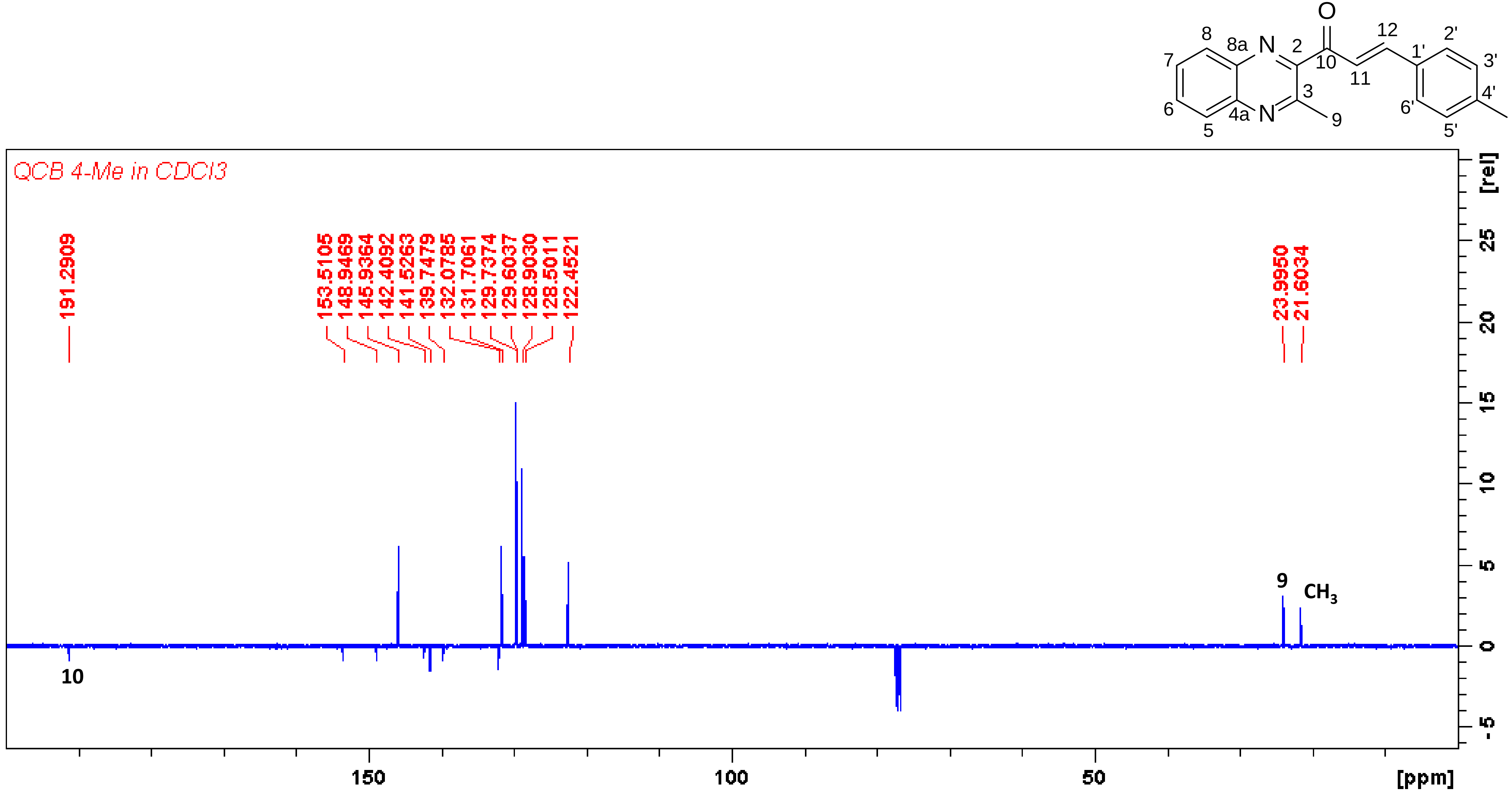

^{13}C NMR spectrum of **B10h**

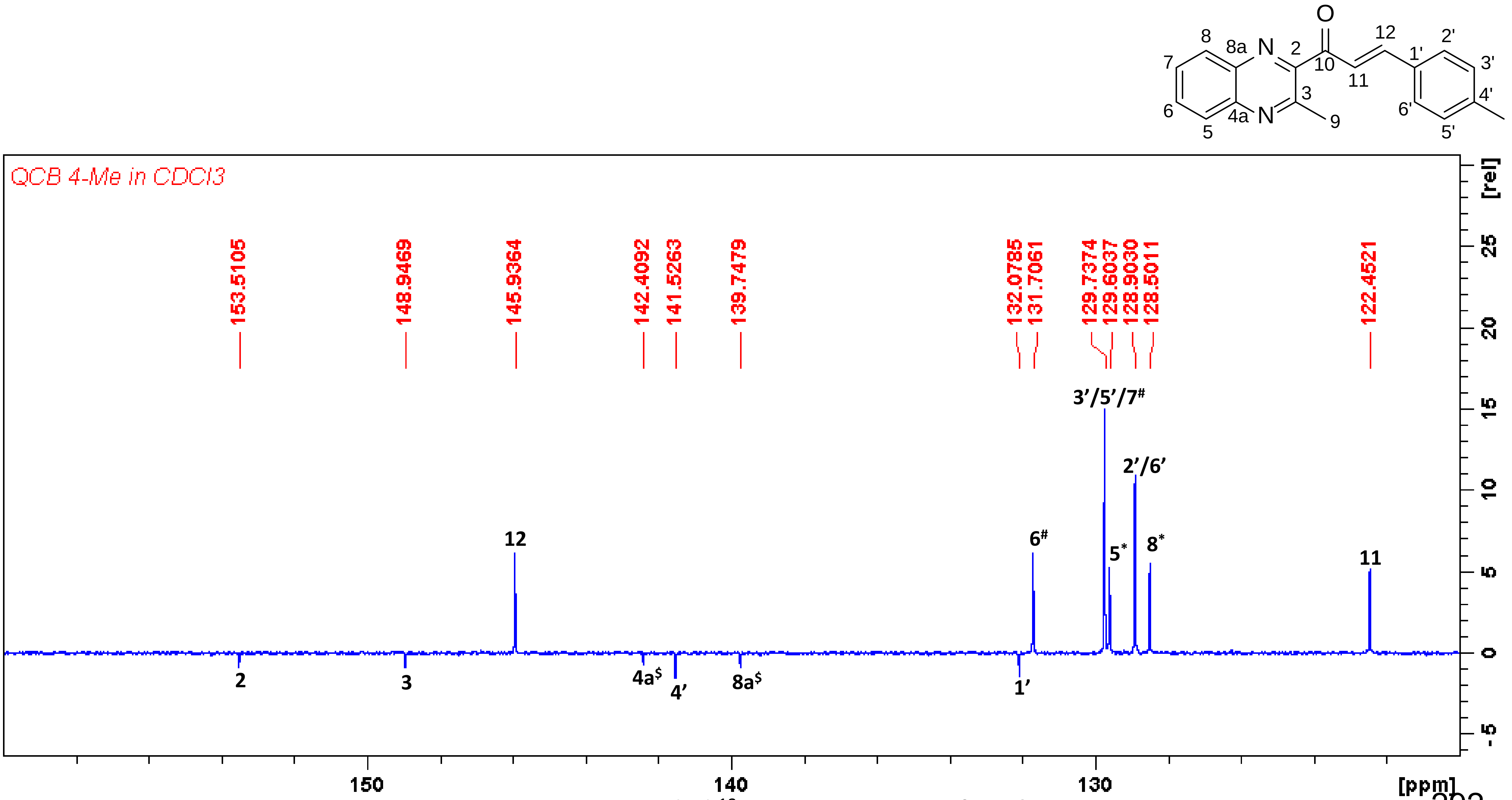

*, #, $ indicates assignments are interchangeable

Expanded ^{13}C NMR spectrum of **B10h**

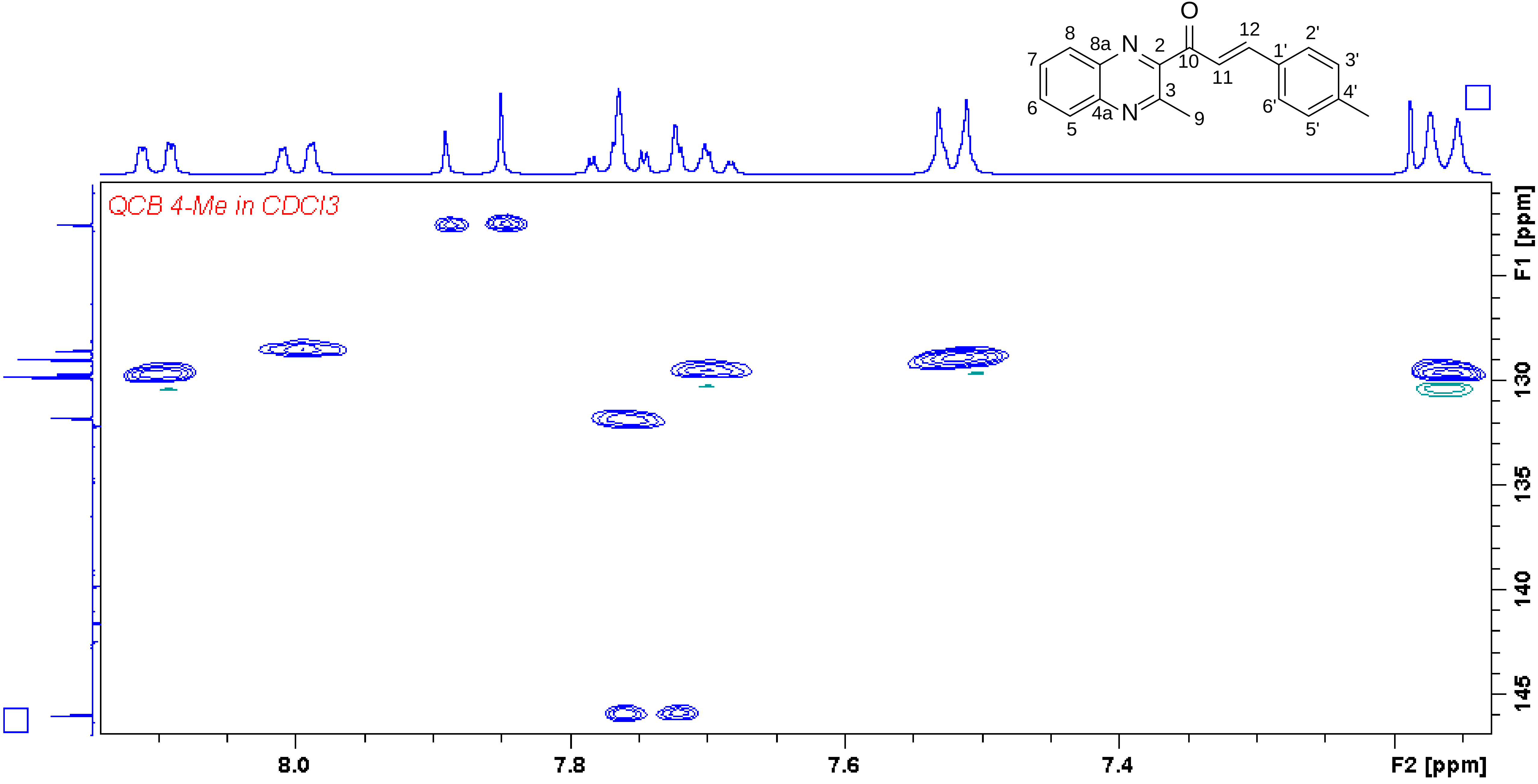

HSQC of **B10h**

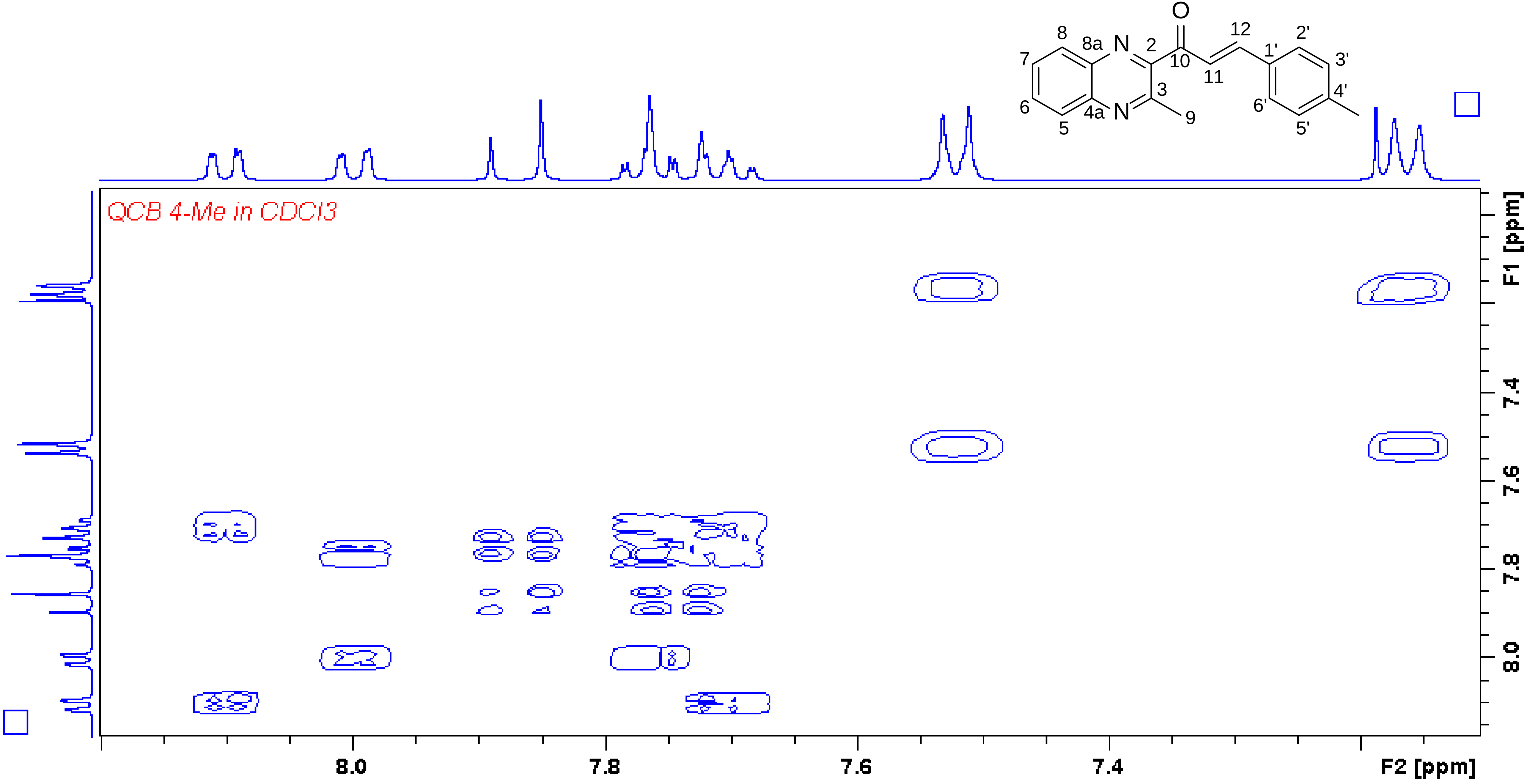
QCB 4-Me in CDCl3
F1 [ppm]
F2 [ppm]
8.0
7.8
7.6
7.4
O
N
N
2
3
4a
5
6
7
8
8a
9
10
11
12
1'
2'
3'
4'
5'
6'

COSY of **B10h**

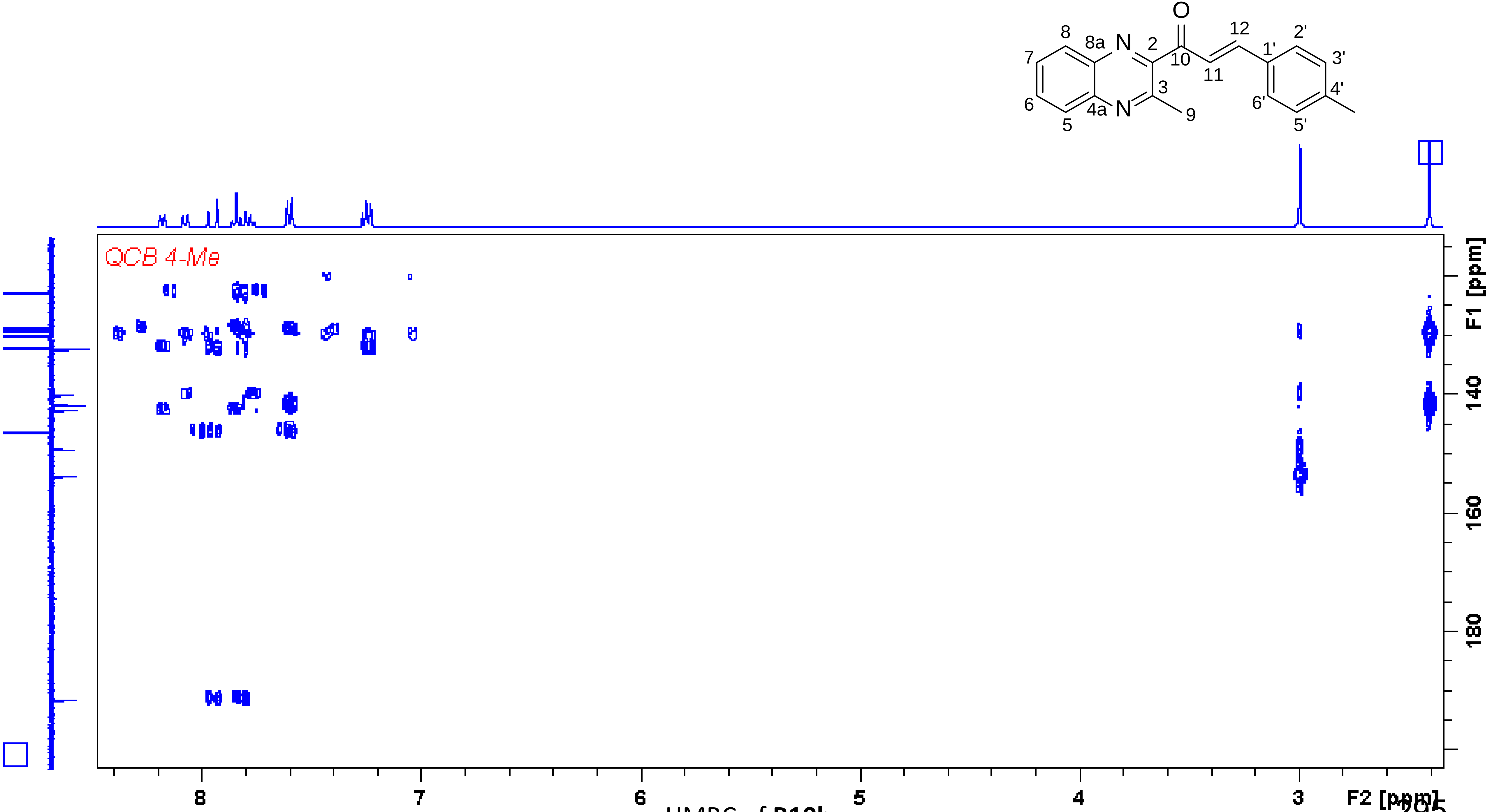

O
8
8a
N
2
12
2'
7
10
11
1'
3'
3
4'
6
6'
4a
N
9
5
5'
QCB 4-Me
F1 [ppm]
140
160
180
8
7
6
5
4
3
F2 [ppm]

HMBC of **B10h**

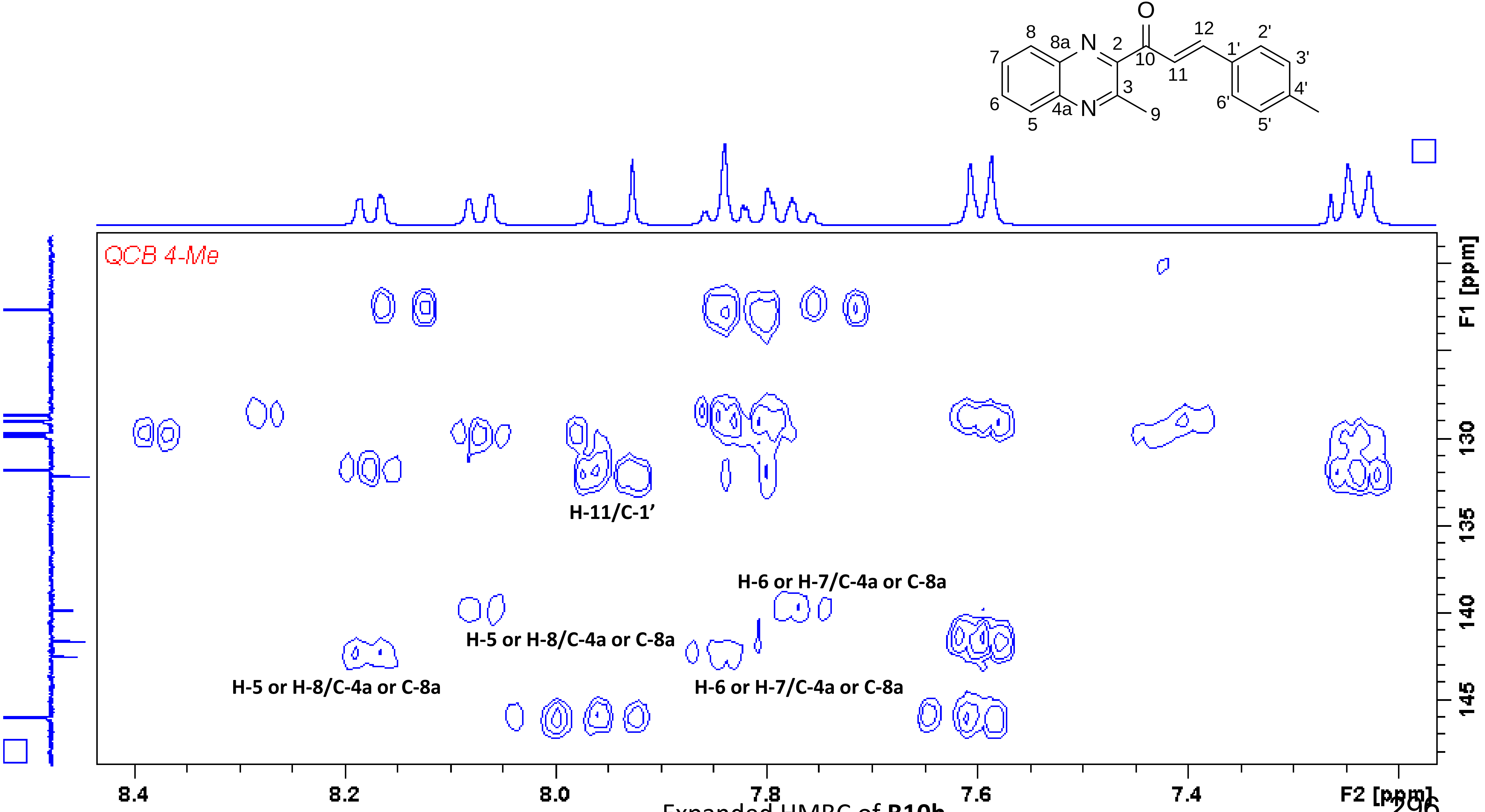

Expanded HMBC of **B10h**

Elemental Composition Report

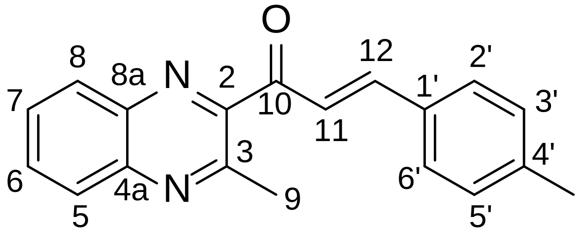

Single Mass Analysis

Tolerance = 5.0 PPM / DBE: min = -1.5, max = 100.0
Element prediction: Off
Number of isotope peaks used for i-FIT = 3

Monoisotopic Mass, Even Electron Ions
11 formula(e) evaluated with 1 results within limits (up to 20 closest results for each mass)
Elements Used:
C: 15-20 H: 15-20 N: 0-5 O: 0-2 Na: 0-1
QCB (4-Me) 10 (0.304) Cm (1:61)
TOF MS ES+

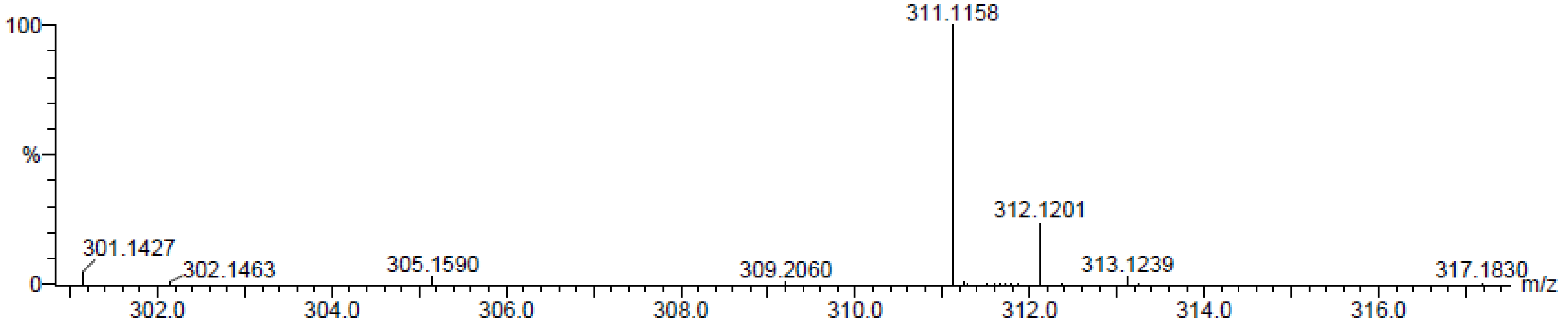

Minimum:				-1.5			
Maximum:		5.0	5.0	100.0			
Mass	Calc. Mass	mDa	PPM	DBE	i-FIT	i-FIT (Norm)	Formula
311.1158	311.1160	-0.2	-0.6	12.5	163.0	0.0	C19 H16 N2 O Na

High resolution mass spectrum of **B10h**

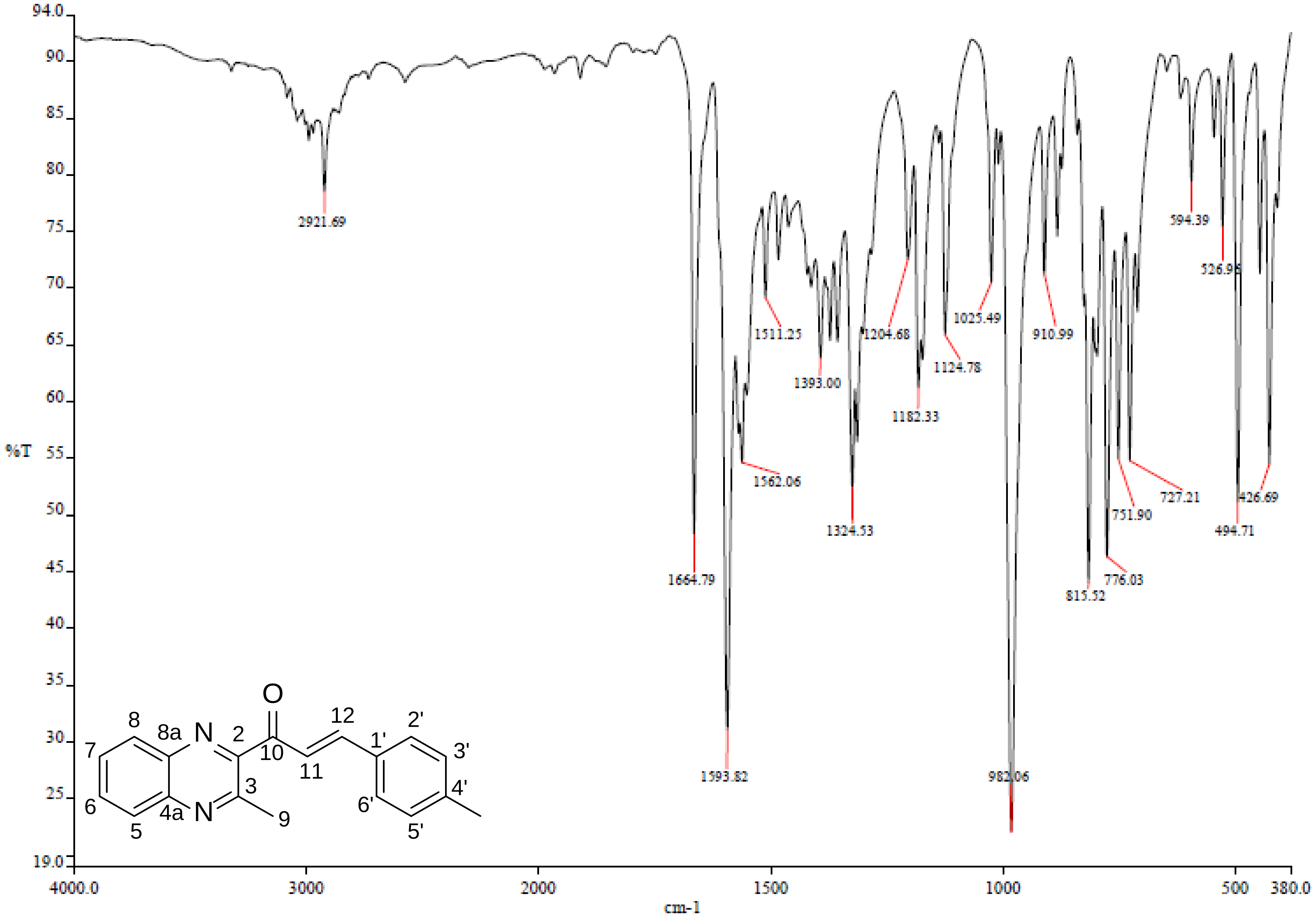

FTIR spectrum of **B10h**

Overlay Spectrum Graph Report

06/10/2017 11:44:06 AM

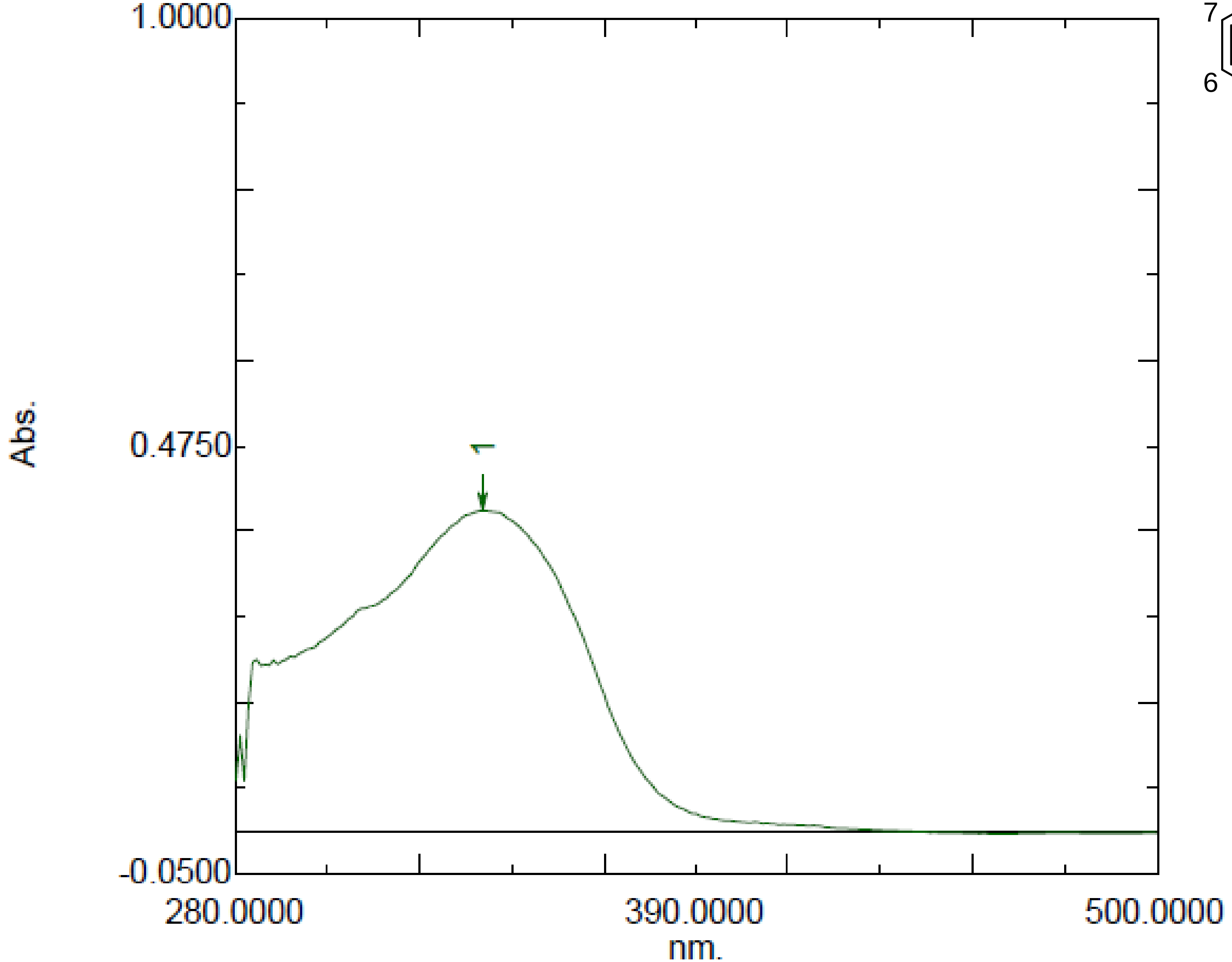

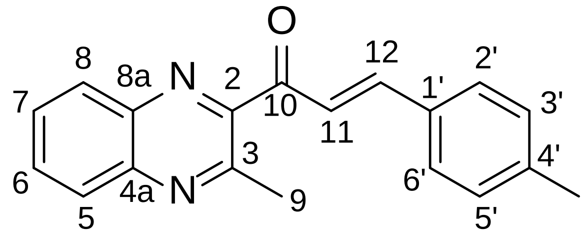

λ	absorbance	logε
339	0.3954	4.36

UV spectrum of **B10h**

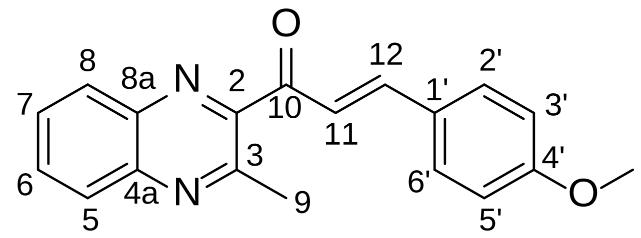

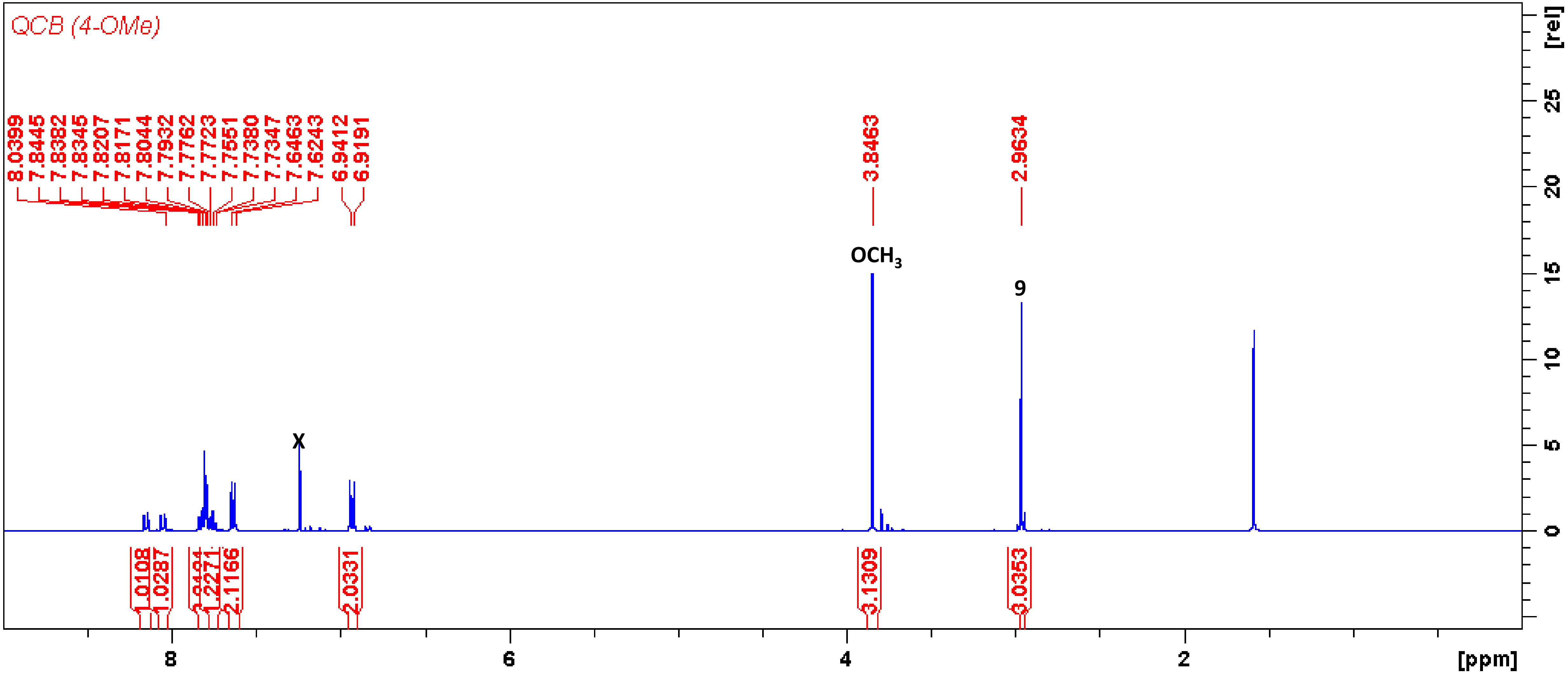

^{1}H NMR spectrum of **B10i**

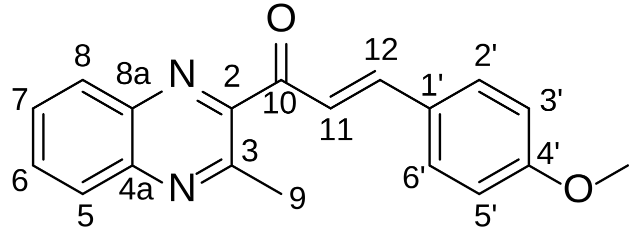

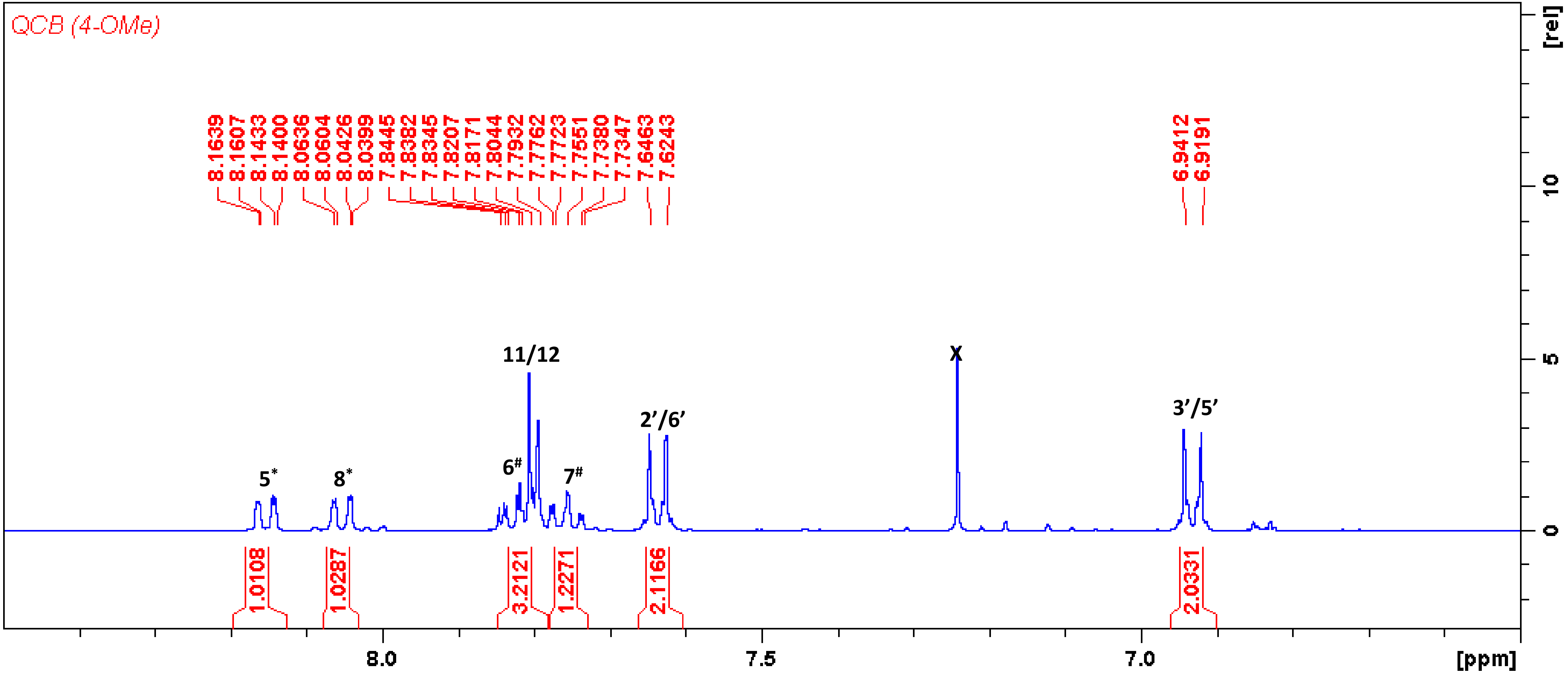

*, # Indicates assignments are interchangeable

Expanded ^{1}H NMR spectrum of **B10i**

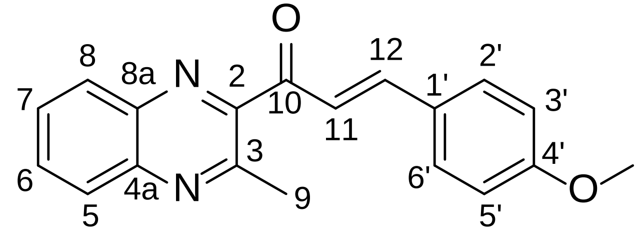

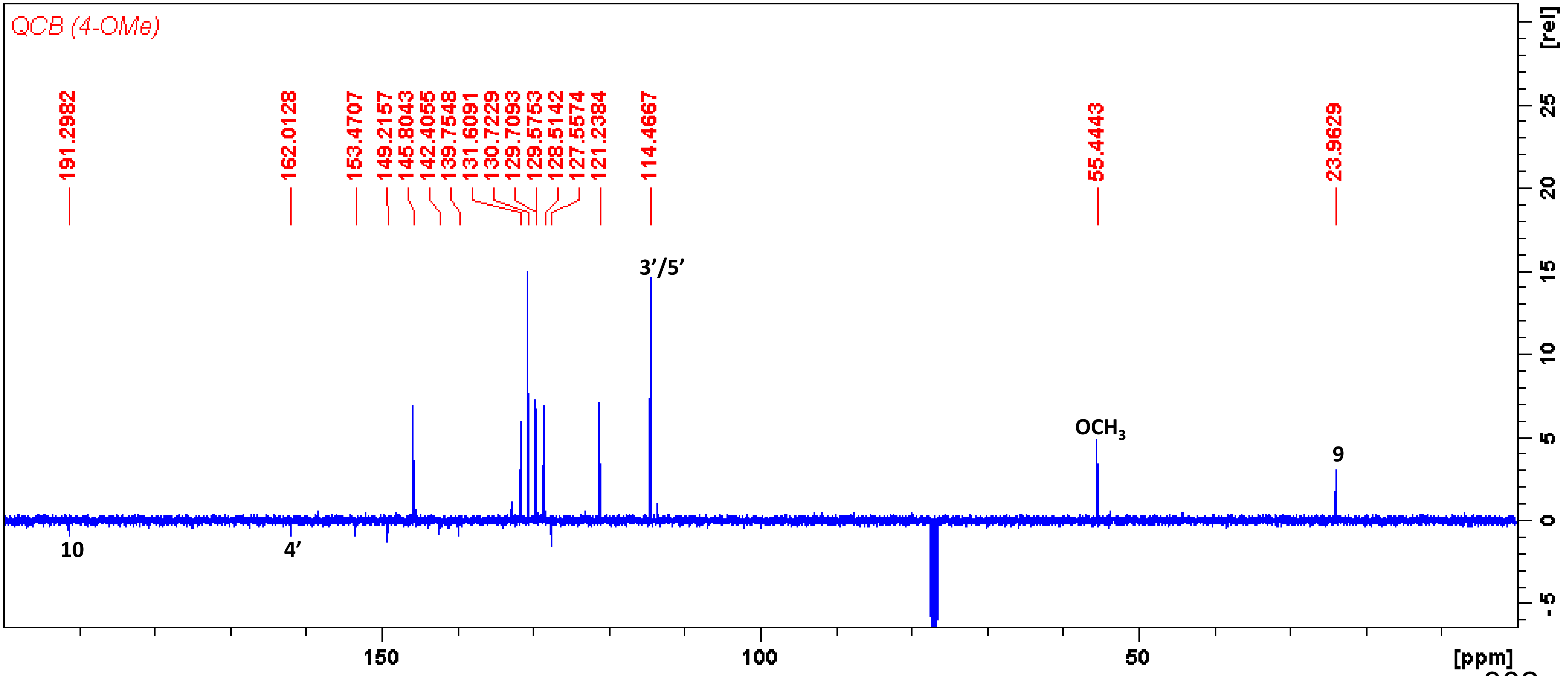

^{13}C NMR spectrum of **B10i**

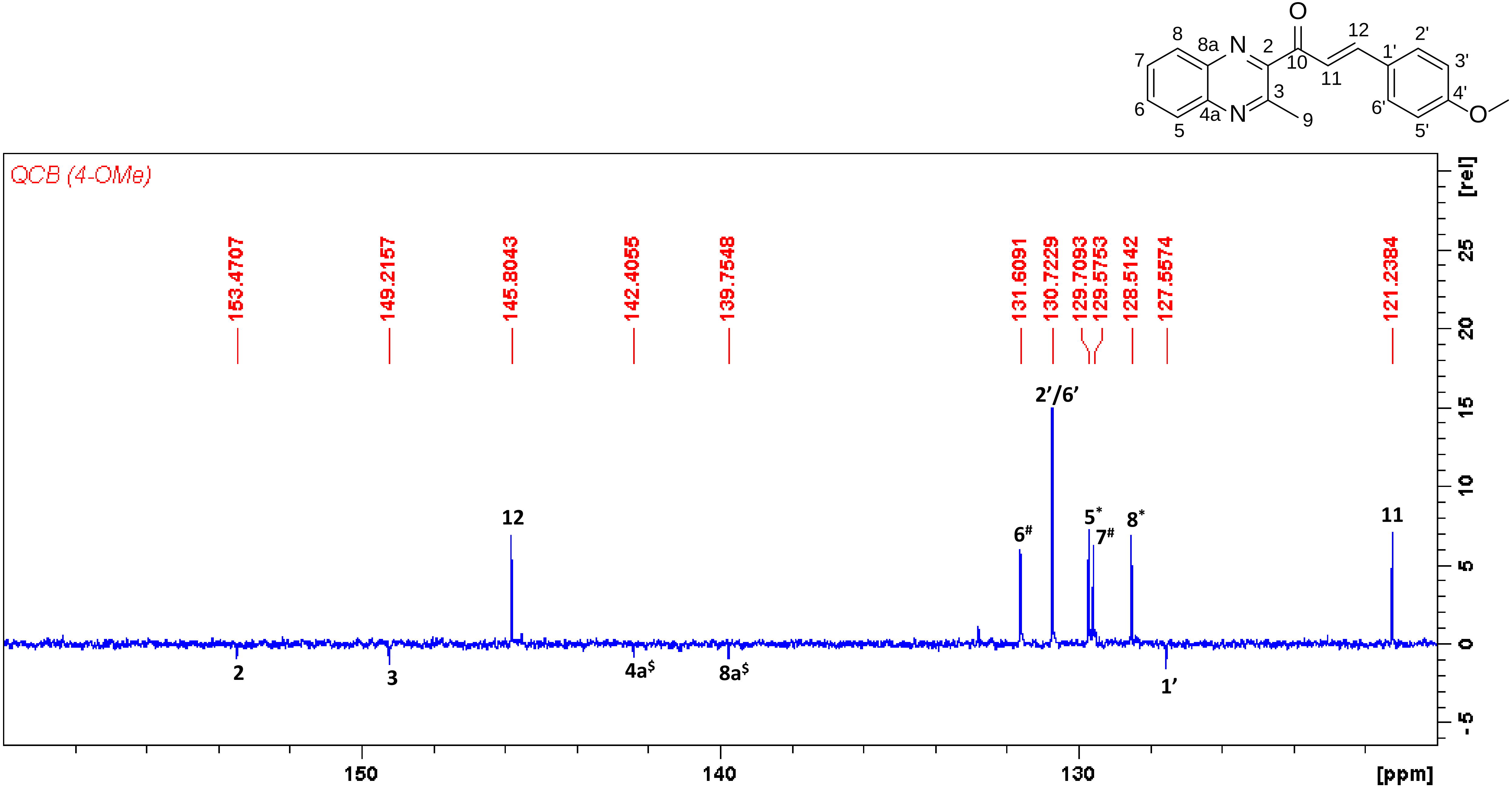

*, #, $ Indicates assignments are interchangeable

Expanded ^{13}C NMR spectrum of **B10i**

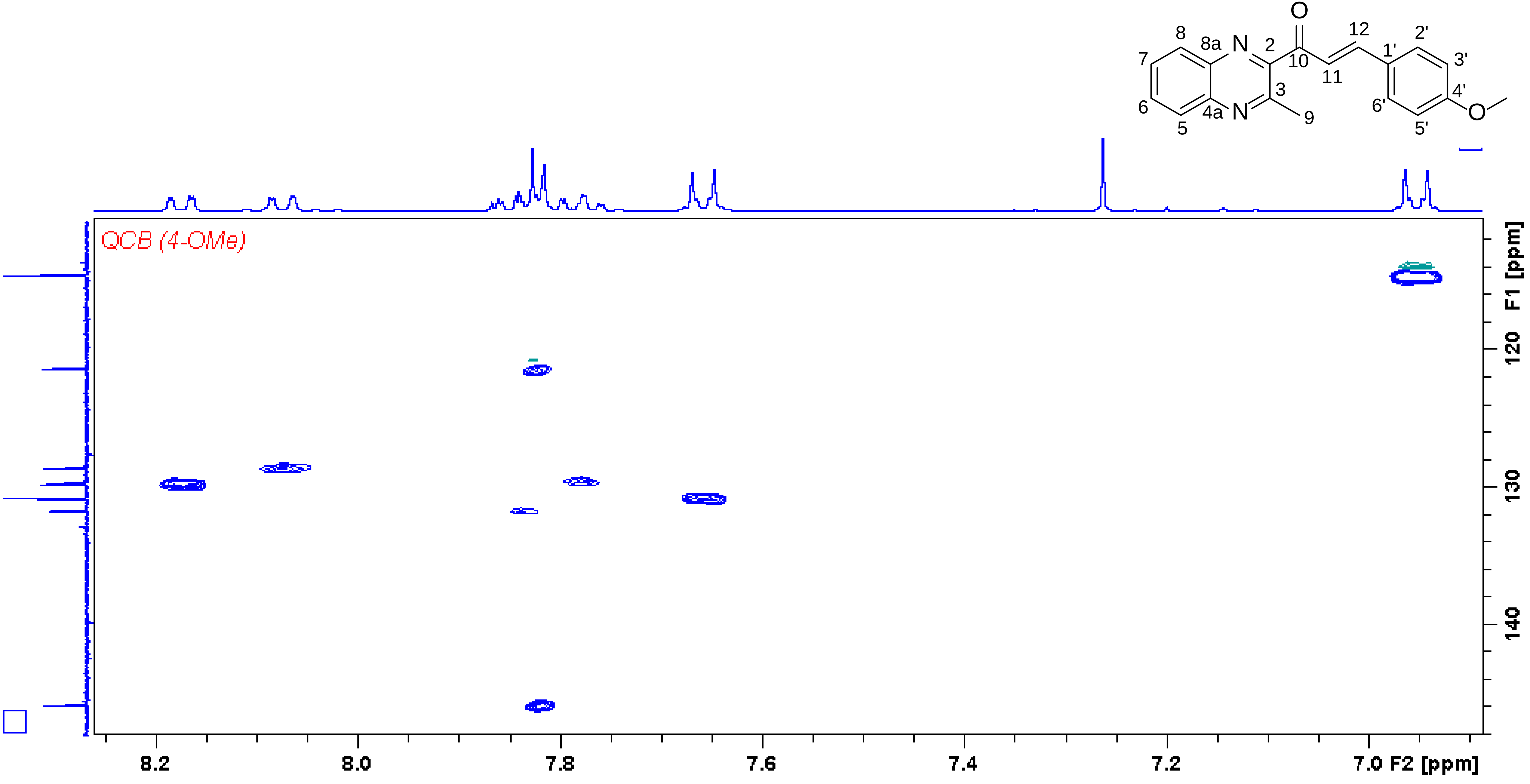
QCB (4-OMe)
F1 [ppm]
F2 [ppm]
8.2
8.0
7.8
7.6
7.4
7.2
7.0
120
130
140
O
N
N
8
8a
2
12
2'
7
10
11
1'
3'
3
4'
6
4a
9
6'
5
5'
O

HSQC of **B10i**

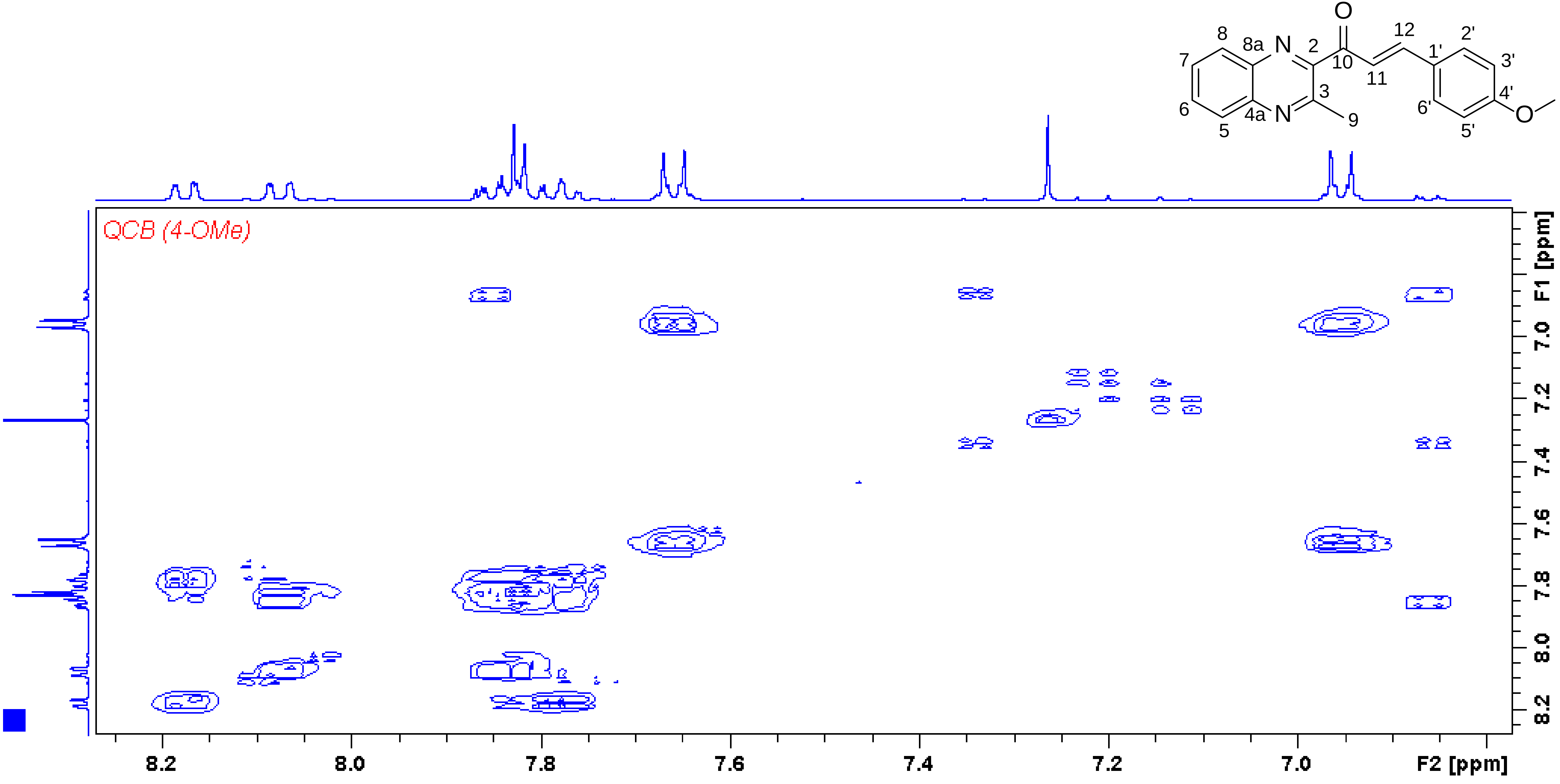

COSY of **B10i**

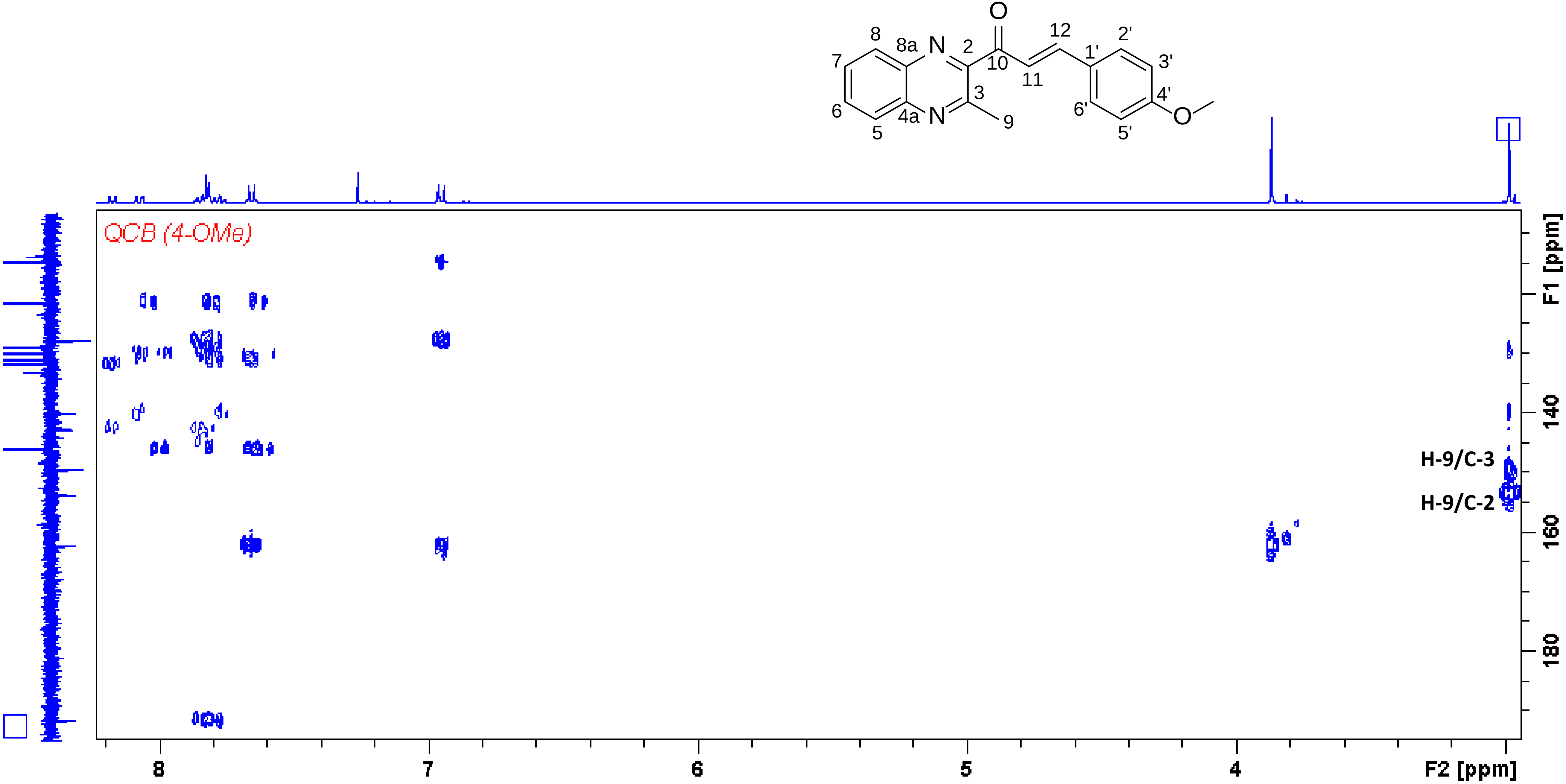

O
8
8a
N
2
12
2'
7
10
1'
3'
11
3
4'
6
4a
N
9
6'
O
5
5'
QCB (4-OMe)
F1 [ppm]
140
160
180
H-9/C-3
H-9/C-2
8
7
6
5
4
F2 [ppm]

HMBC of **B10i**

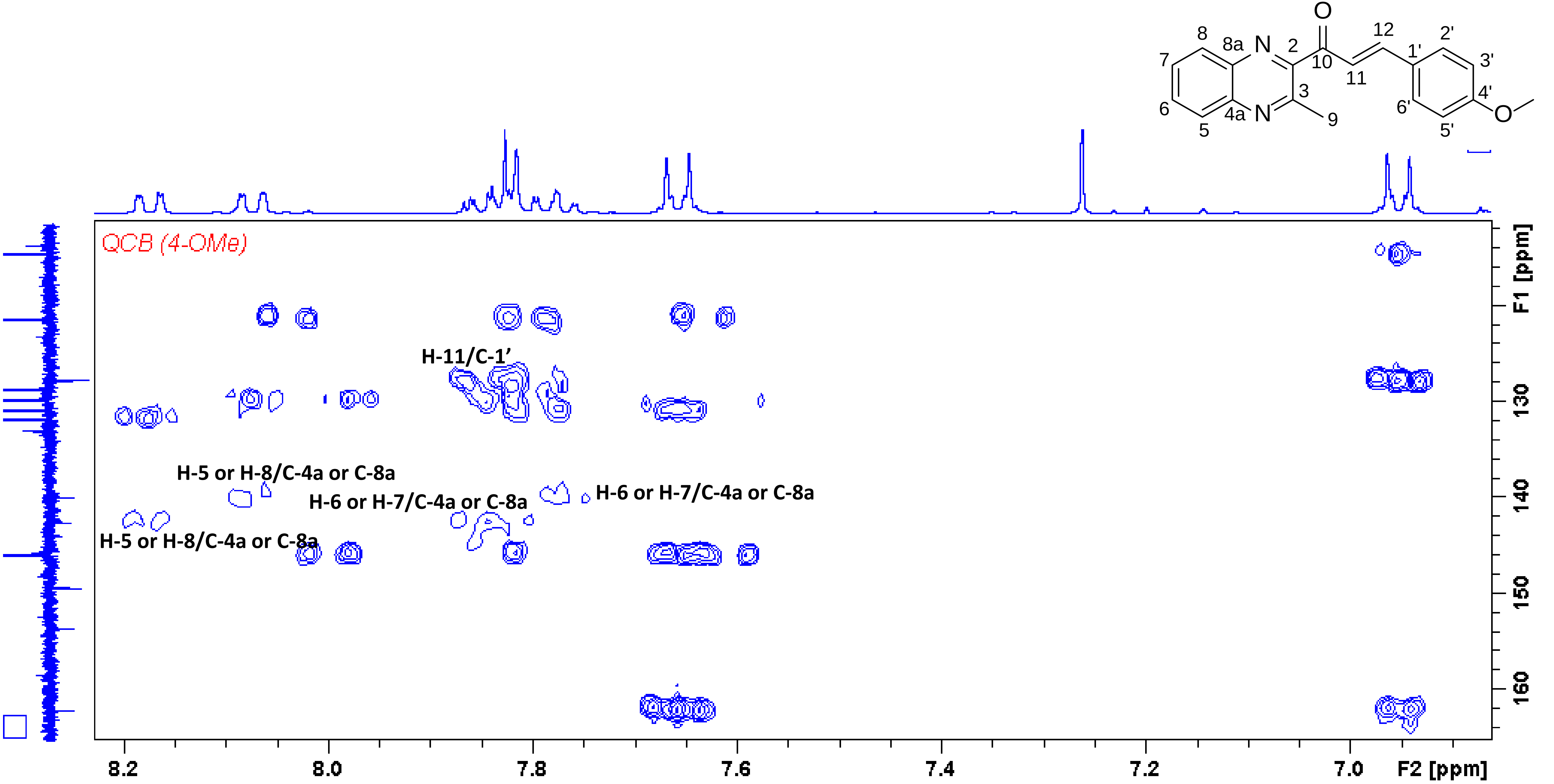

Expanded HMBC of **B10i**

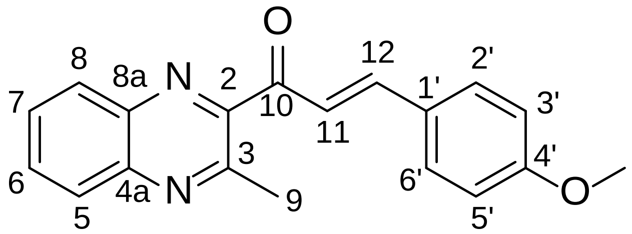

Single Mass Analysis

Tolerance = 5.0 PPM / DBE: min = -1.5, max = 100.0
Element prediction: Off
Number of isotope peaks used for i-FIT = 3

Monoisotopic Mass, Even Electron Ions
20 formula(e) evaluated with 1 results within limits (up to 20 closest results for each mass)
Elements Used:
C: 15-20 H: 10-20 N: 0-5 O: 1-5
QCB(4-OCH3) 2 (0.034) Cm (1:61)
TOF MS AP+

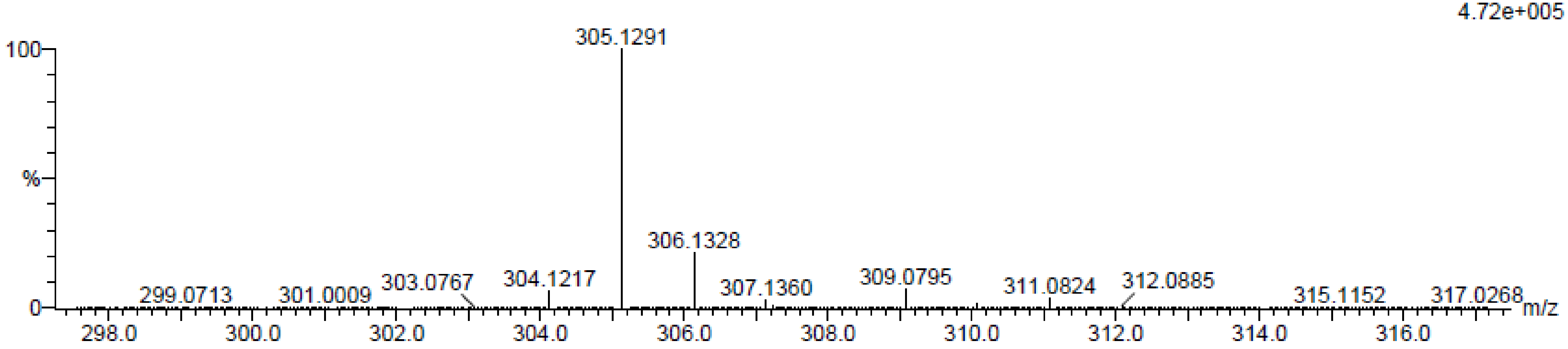

Minimum:				-1.5			
Maximum:		5.0	5.0	100.0			
Mass	Calc. Mass	mDa	PPM	DBE	i-FIT	i-FIT (Norm)	Formula
305.1291	305.1290	0.1	0.3	12.5	689.1	0.0	C19 H17 N2 O2

High resolution mass spectrum of **B10i**

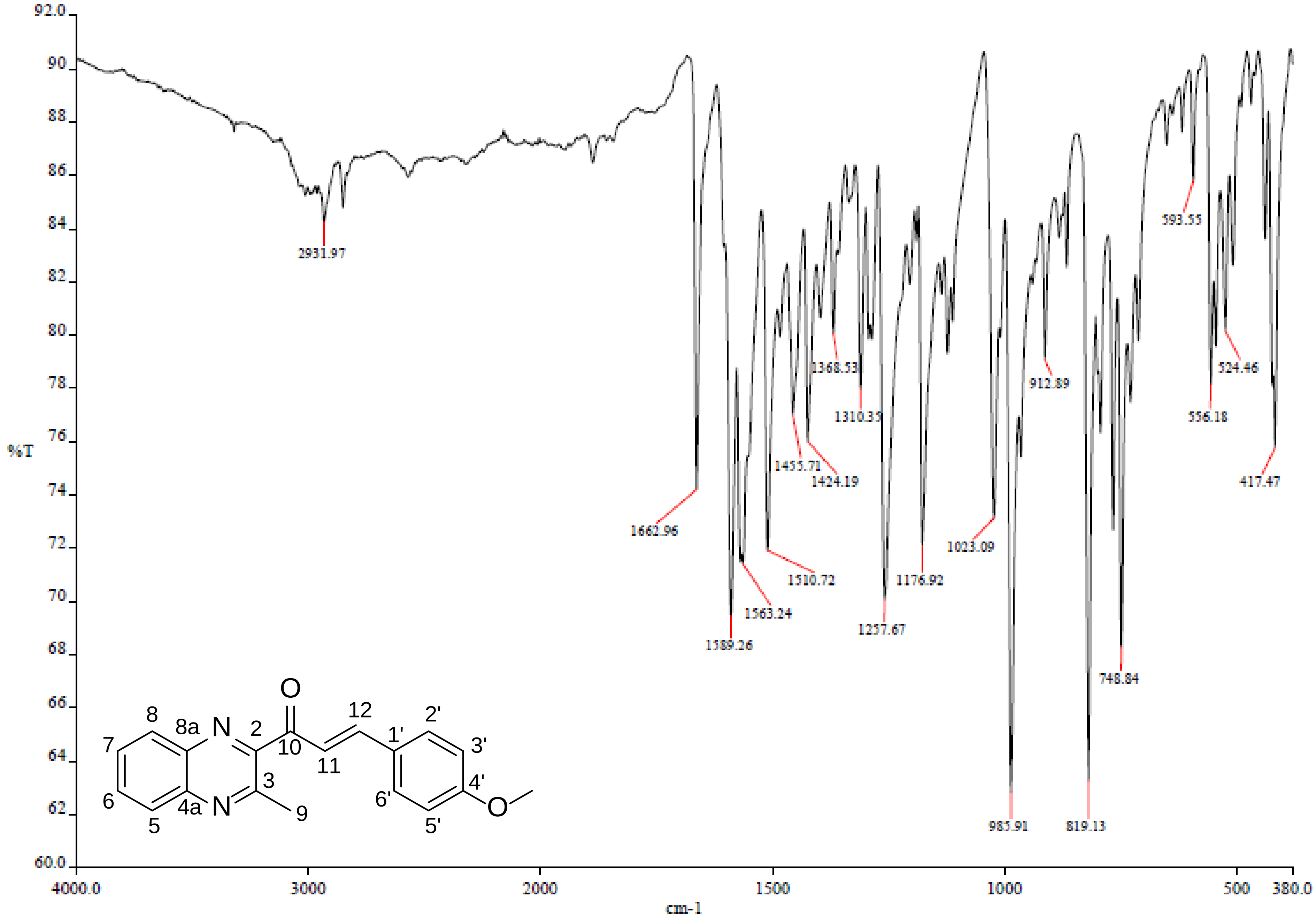

FTIR spectrum of **B10i**

Overlay Spectrum Graph Report

10/04/2018 03:53:51 PM

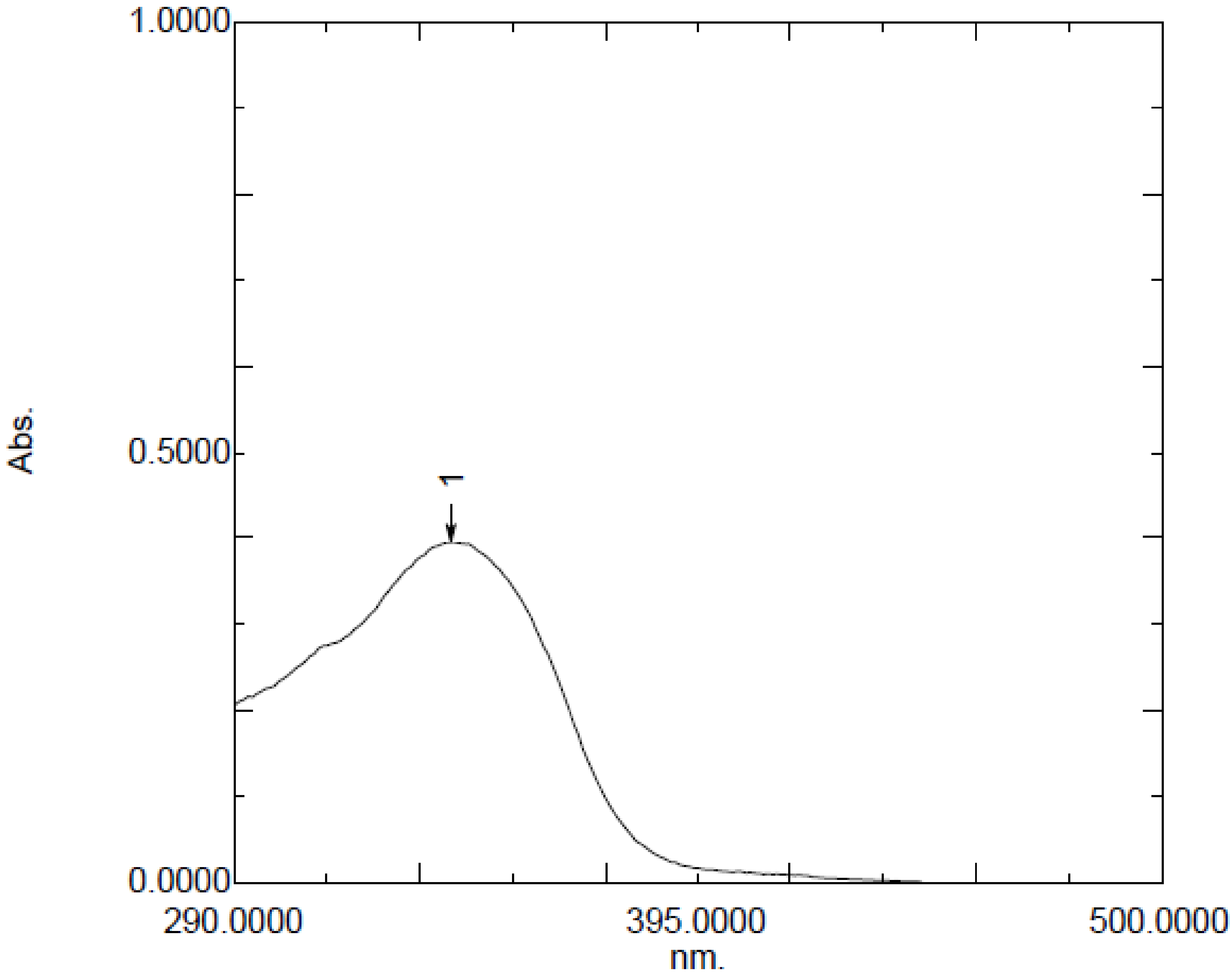

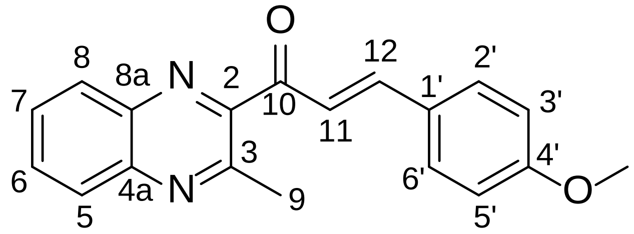

λ	absorbance	logε
339	0.4157	4.20

UV spectrum of **B10i**

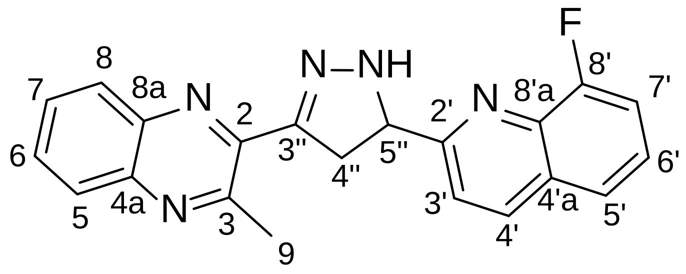

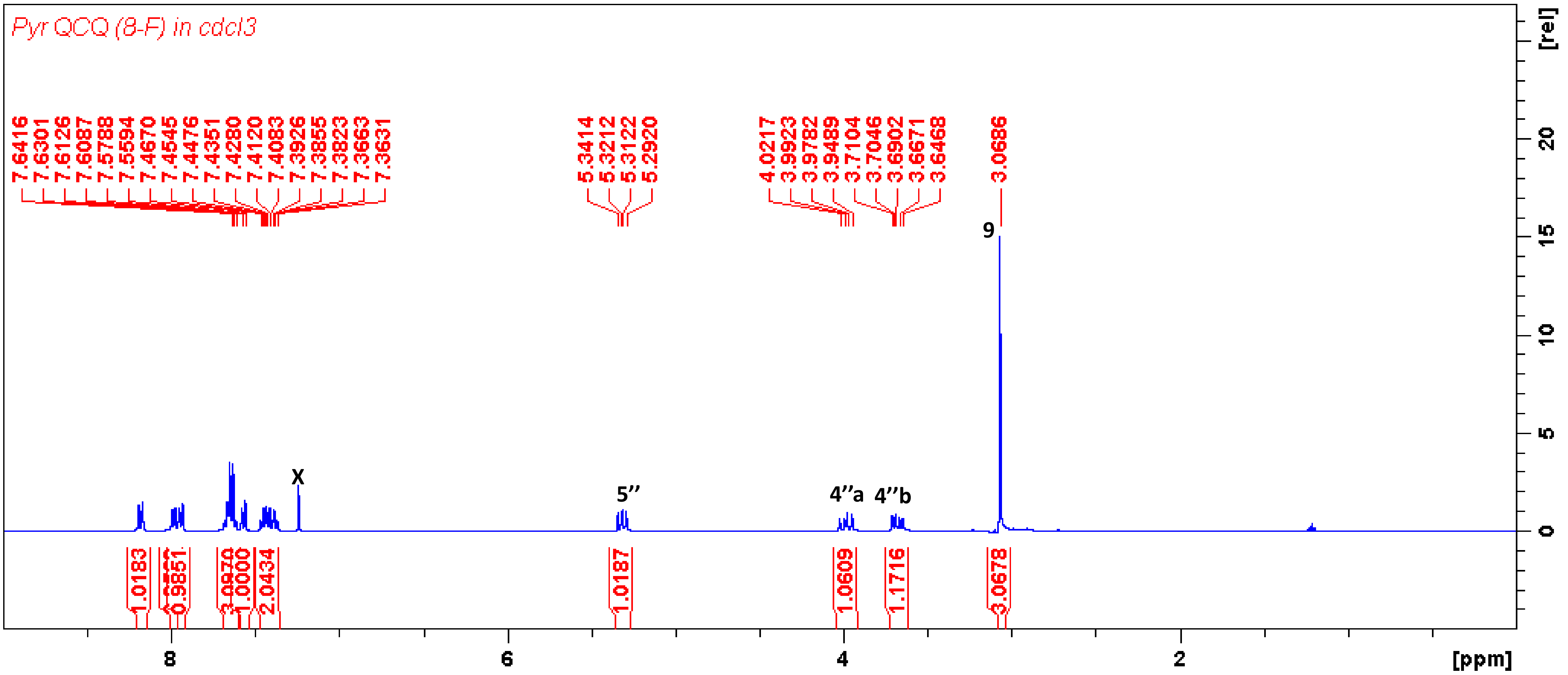

^{1}H NMR spectrum of **B8a**

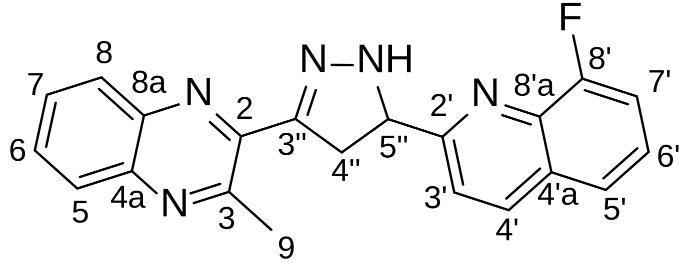

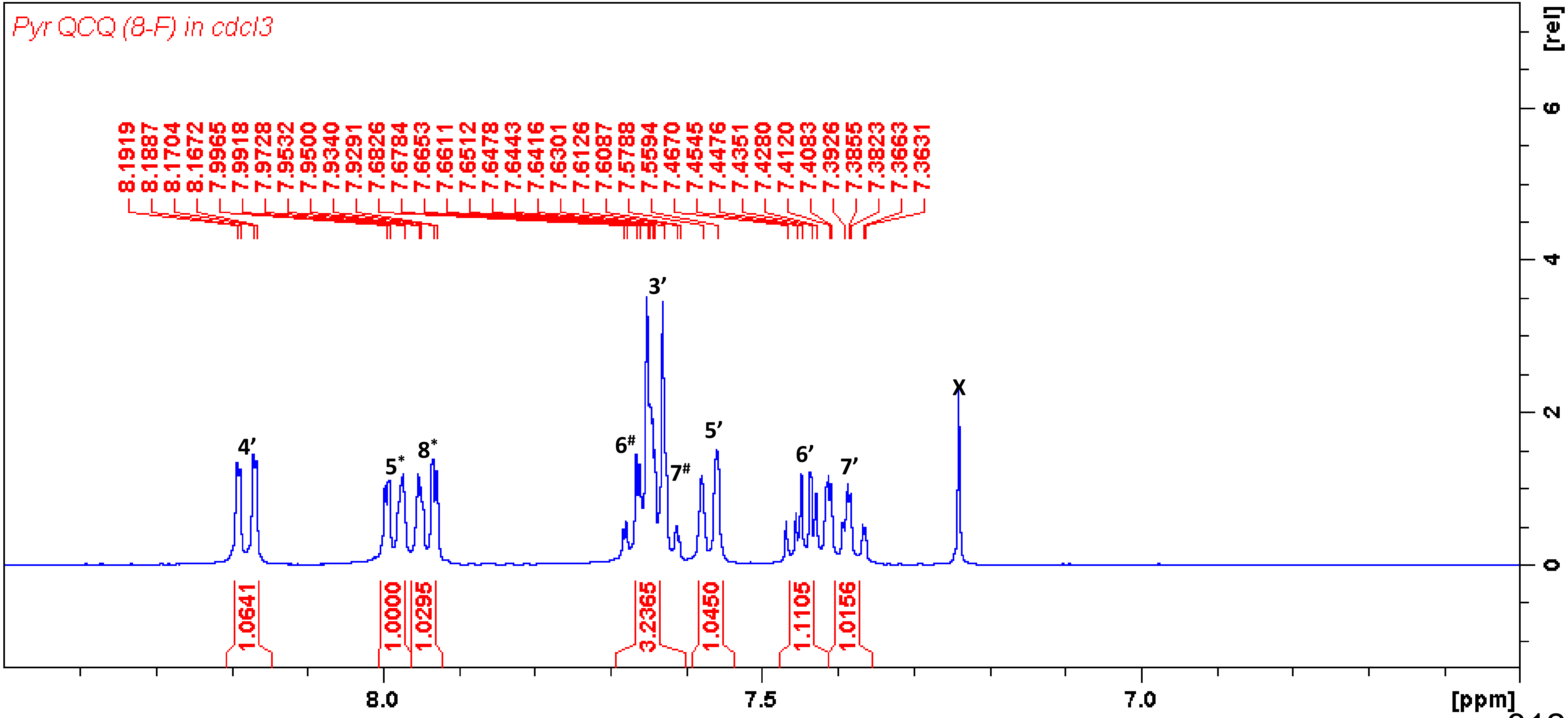

*, # Indicates assignments are interchangeable

Expanded ^{1}H NMR spectrum of **B8a**

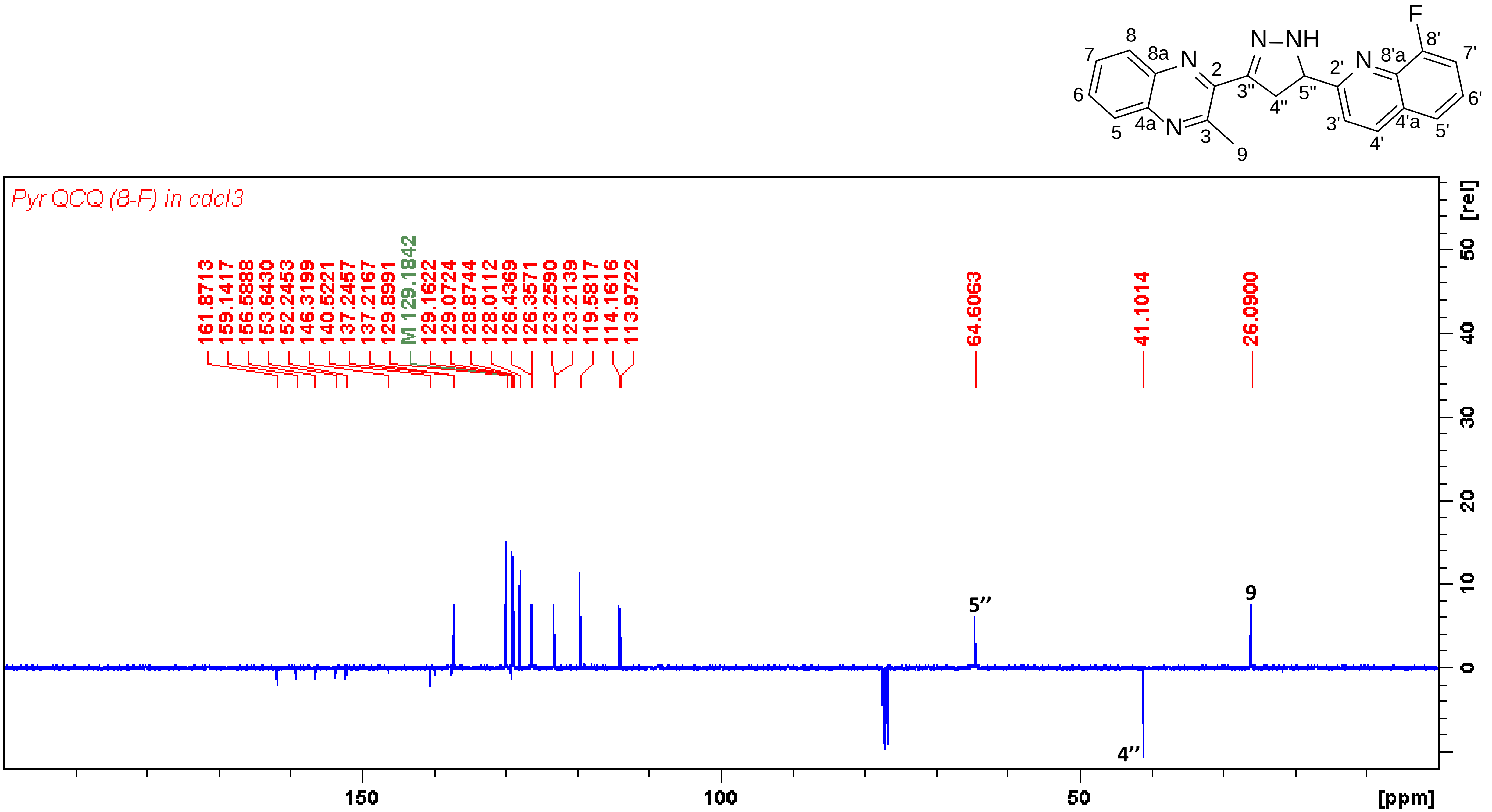

^{13}C NMR spectrum of **B8a**

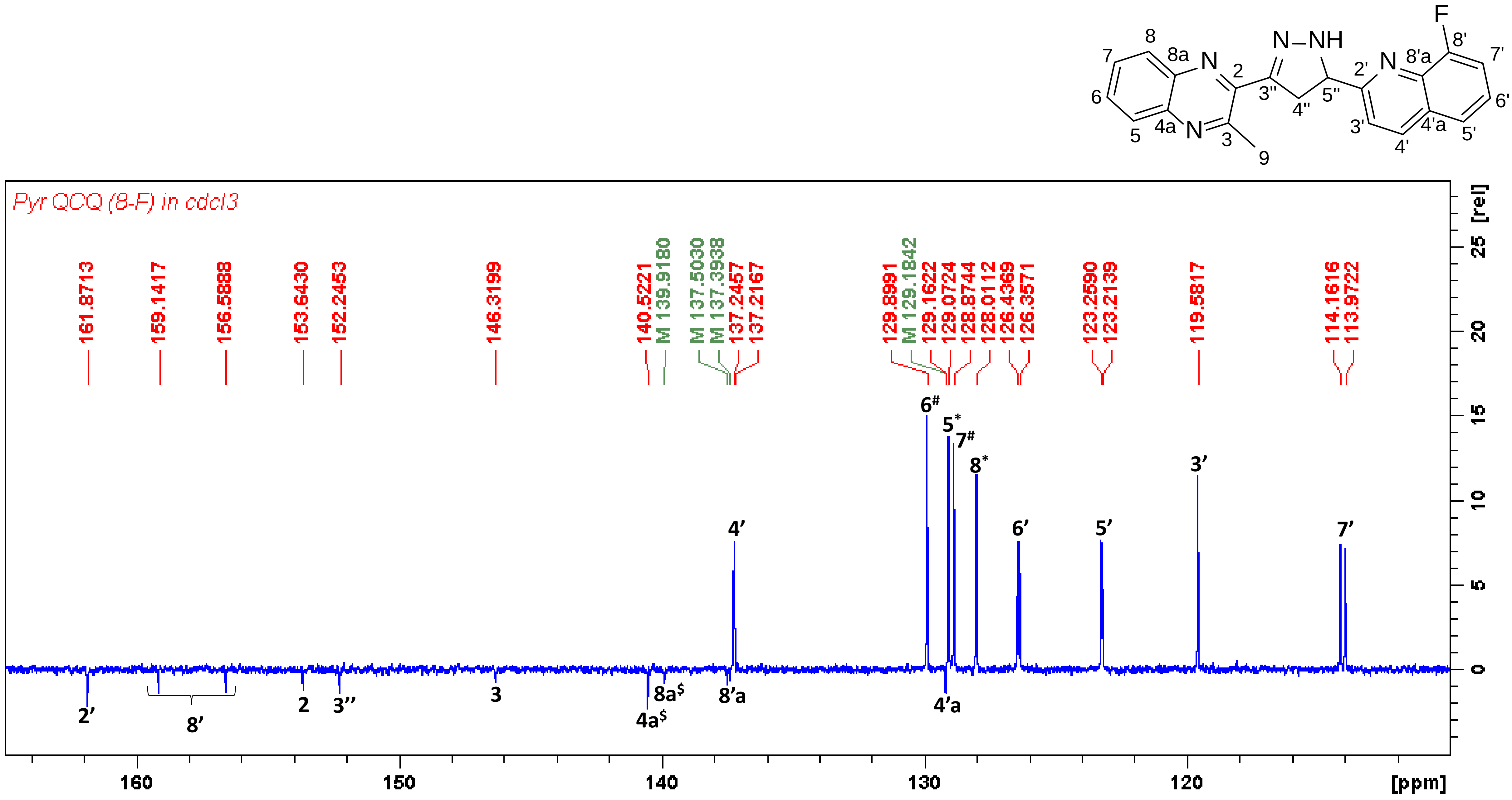

*, #, $ Indicates assignments are interchangeable

Expanded ^{13}C NMR spectrum of **B8a**

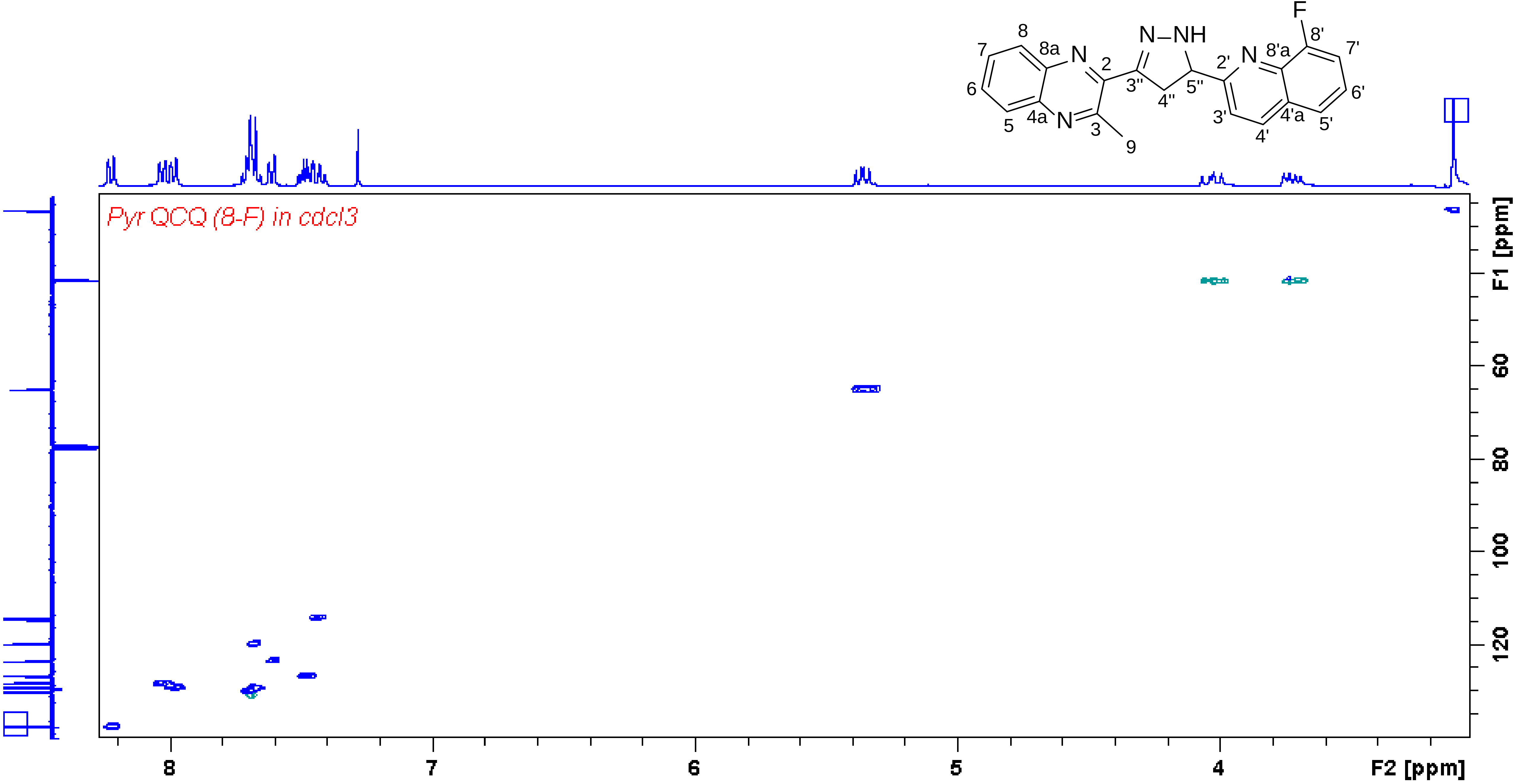

HSQC of **B8a**

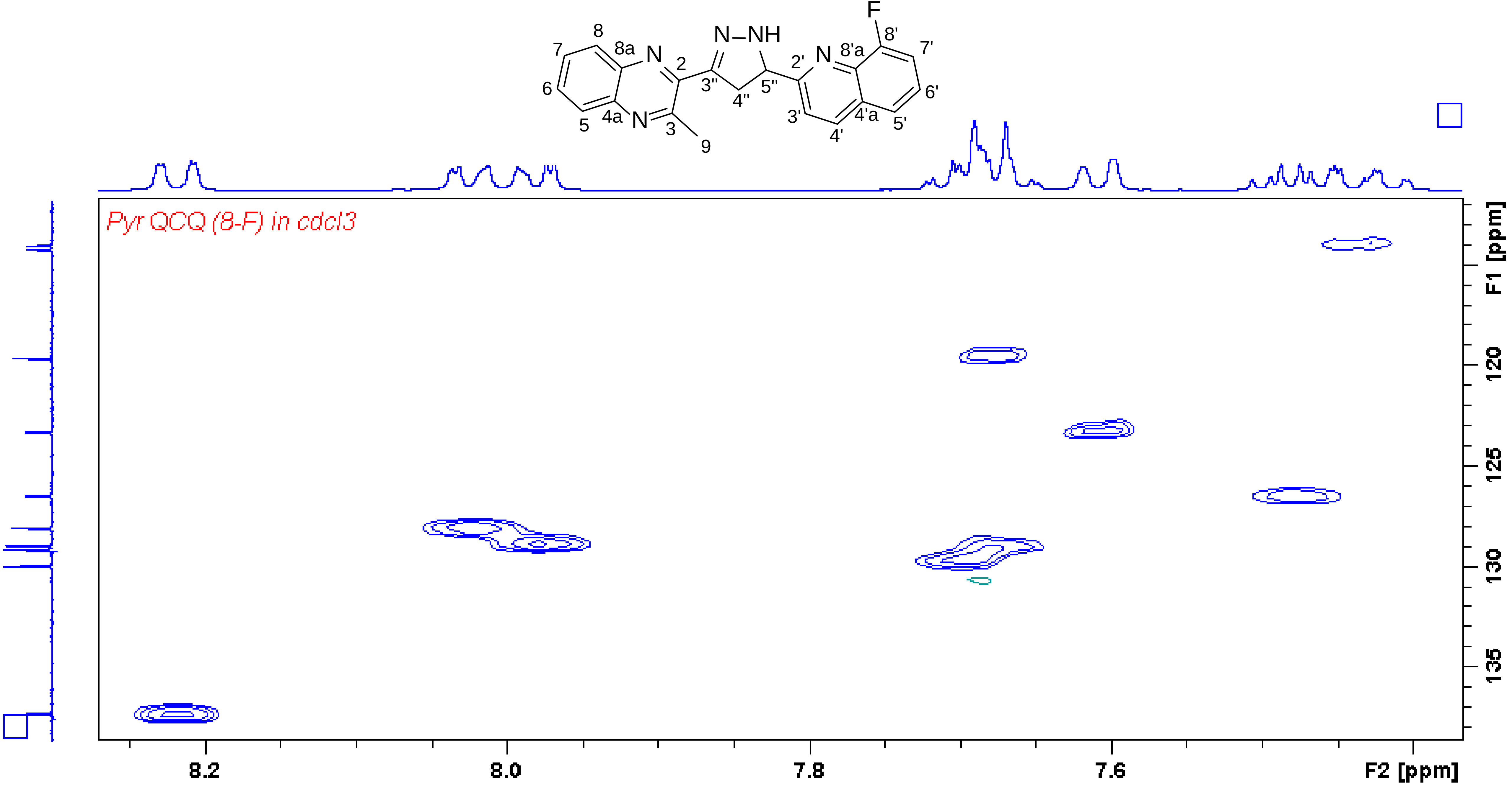

Expanded HSQC of **B8a**

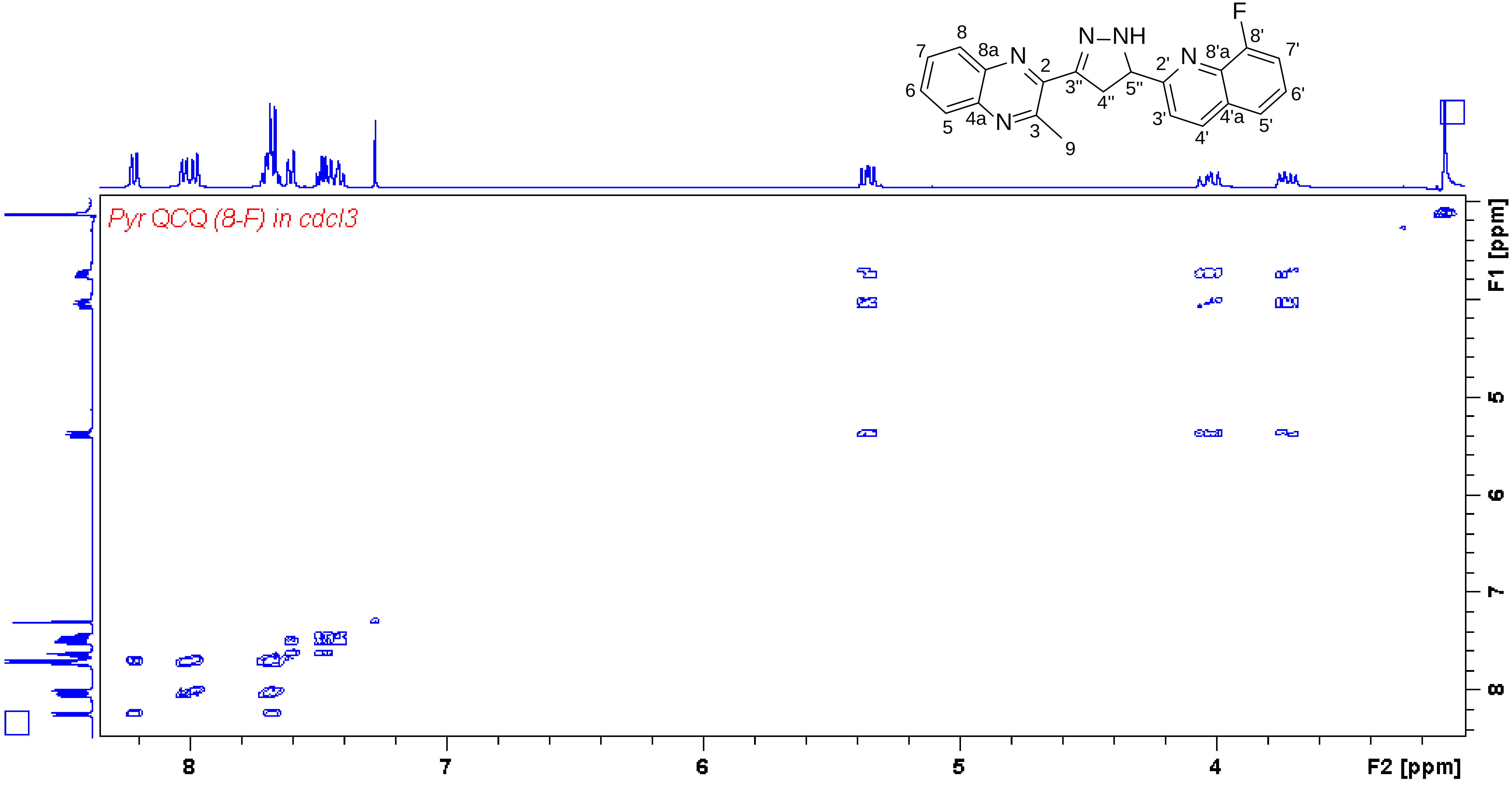

COSY of **B8a**

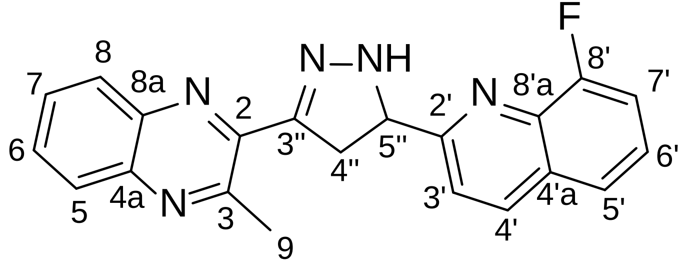

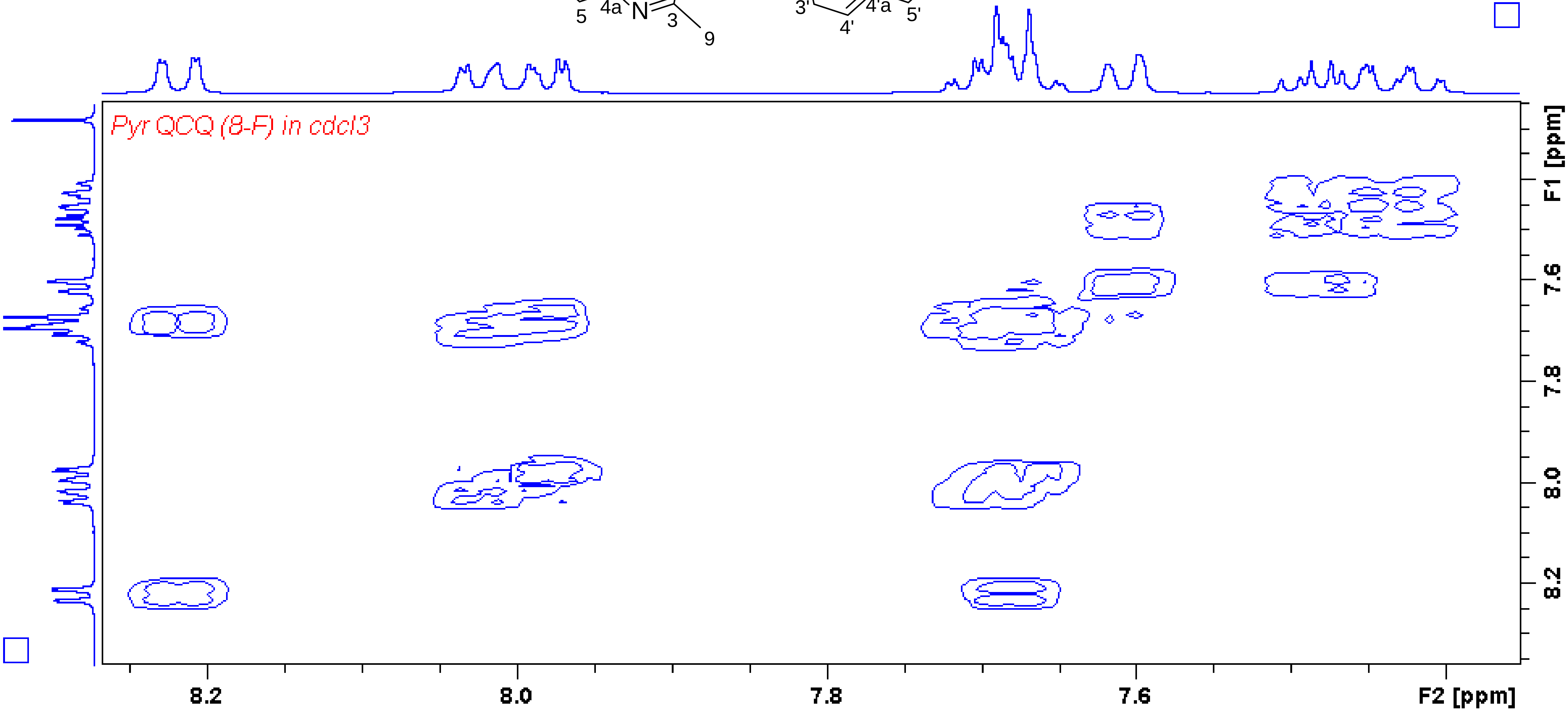

Expanded COSY of **B8a**

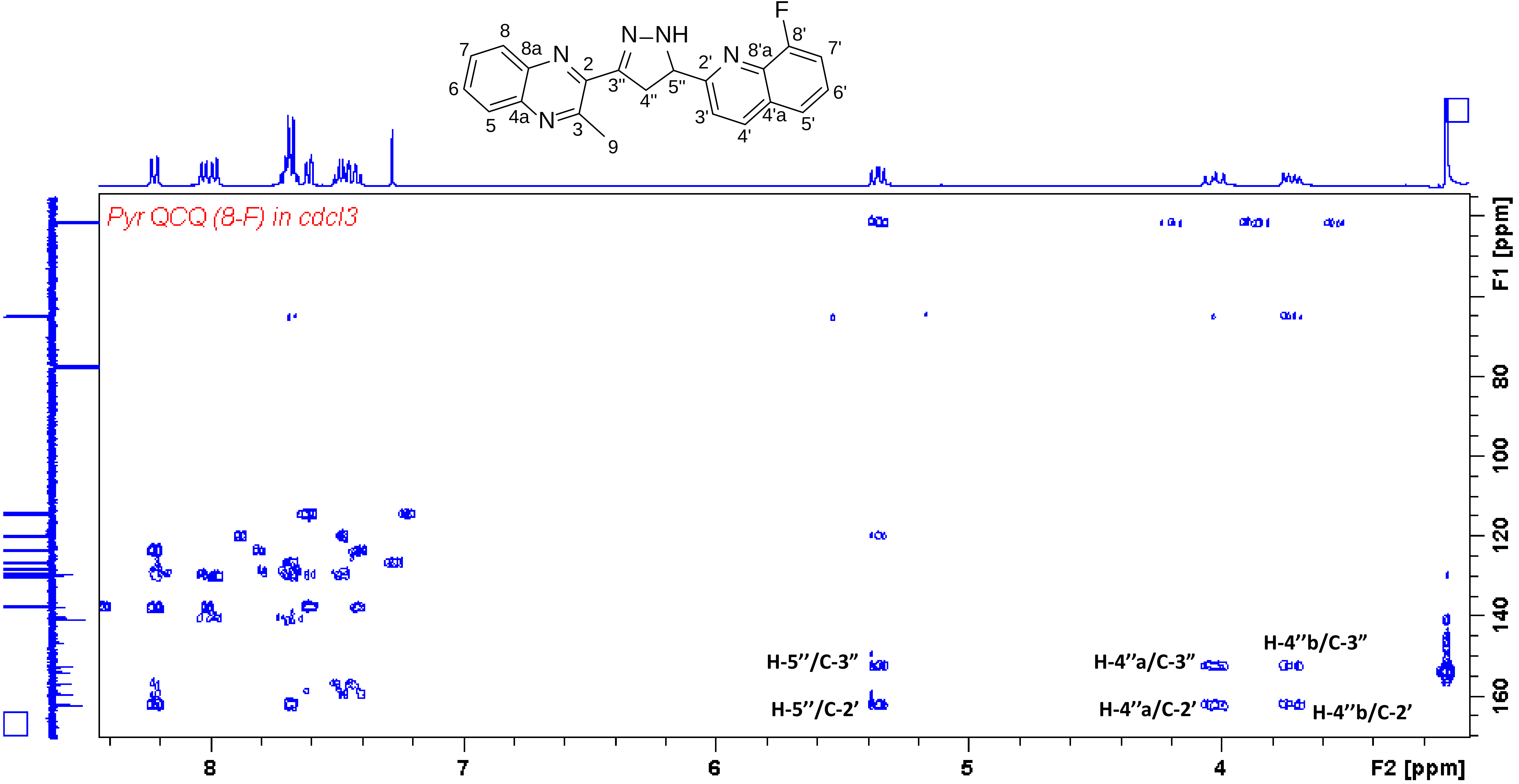
Pyr QCQ (8-F) in cdcl3
H-5''/C-3''
H-5''/C-2'
H-4''a/C-3''
H-4''b/C-3''
H-4''a/C-2'
H-4''b/C-2'
F1 [ppm]
F2 [ppm]

HMBC of **B8a**

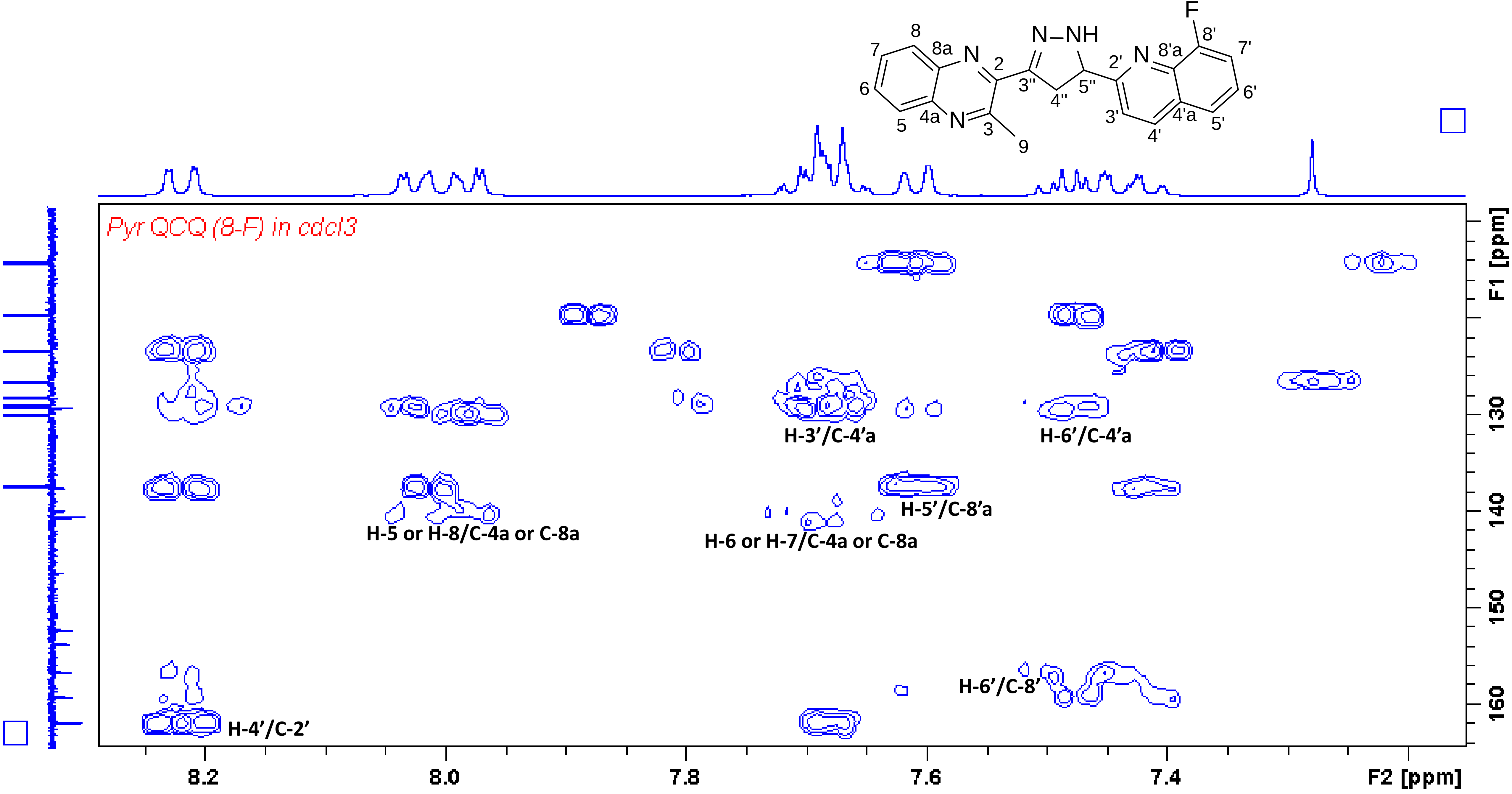

Expanded HMBC of **B8a**

Elemental Composition Report

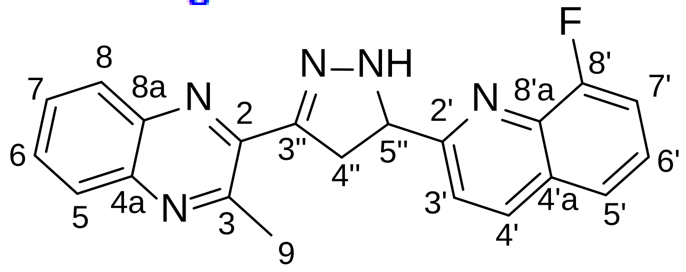

Single Mass Analysis

Tolerance = 5.0 PPM / DBE: min = -1.5, max = 100.0
Element prediction: Off
Number of isotope peaks used for i-FIT = 3

Monoisotopic Mass, Even Electron Ions
8 formula(e) evaluated with 1 results within limits (up to 20 closest results for each mass)
Elements Used:
C: 20-25 H: 15-20 N: 0-5 F: 0-1 Na: 0-1
Py-QCQ 8-F 53 (1.753) Cm (1:61)
TOF MS ES+

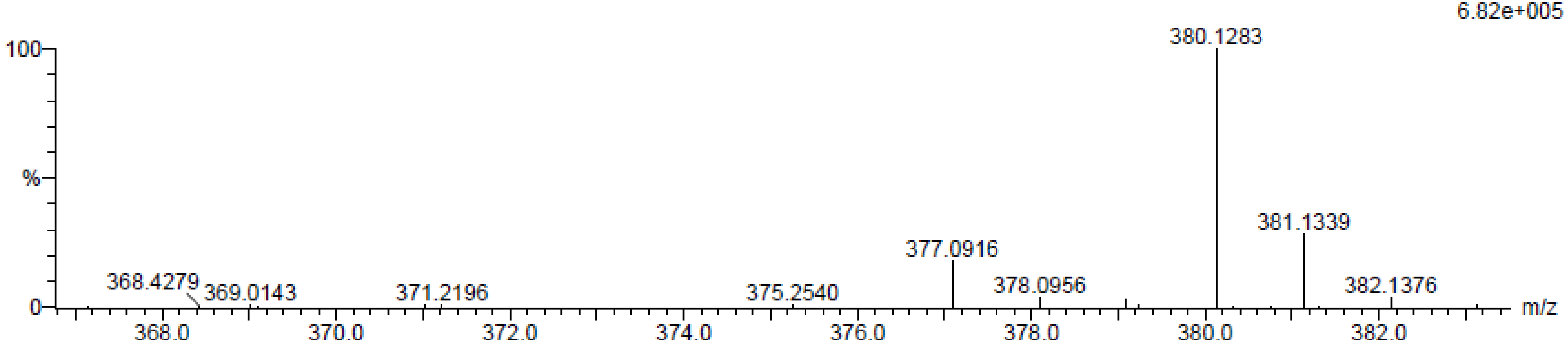

Minimum:				-1.5			
Maximum:		5.0	5.0	100.0			
Mass	Calc. Mass	mDa	PPM	DBE	i-FIT	i-FIT (Norm)	Formula
380.1283	380.1287	-0.4	-1.1	15.5	75.2	0.0	C21 H16 N5 F Na

High resolution mass spectrum of **B8a**

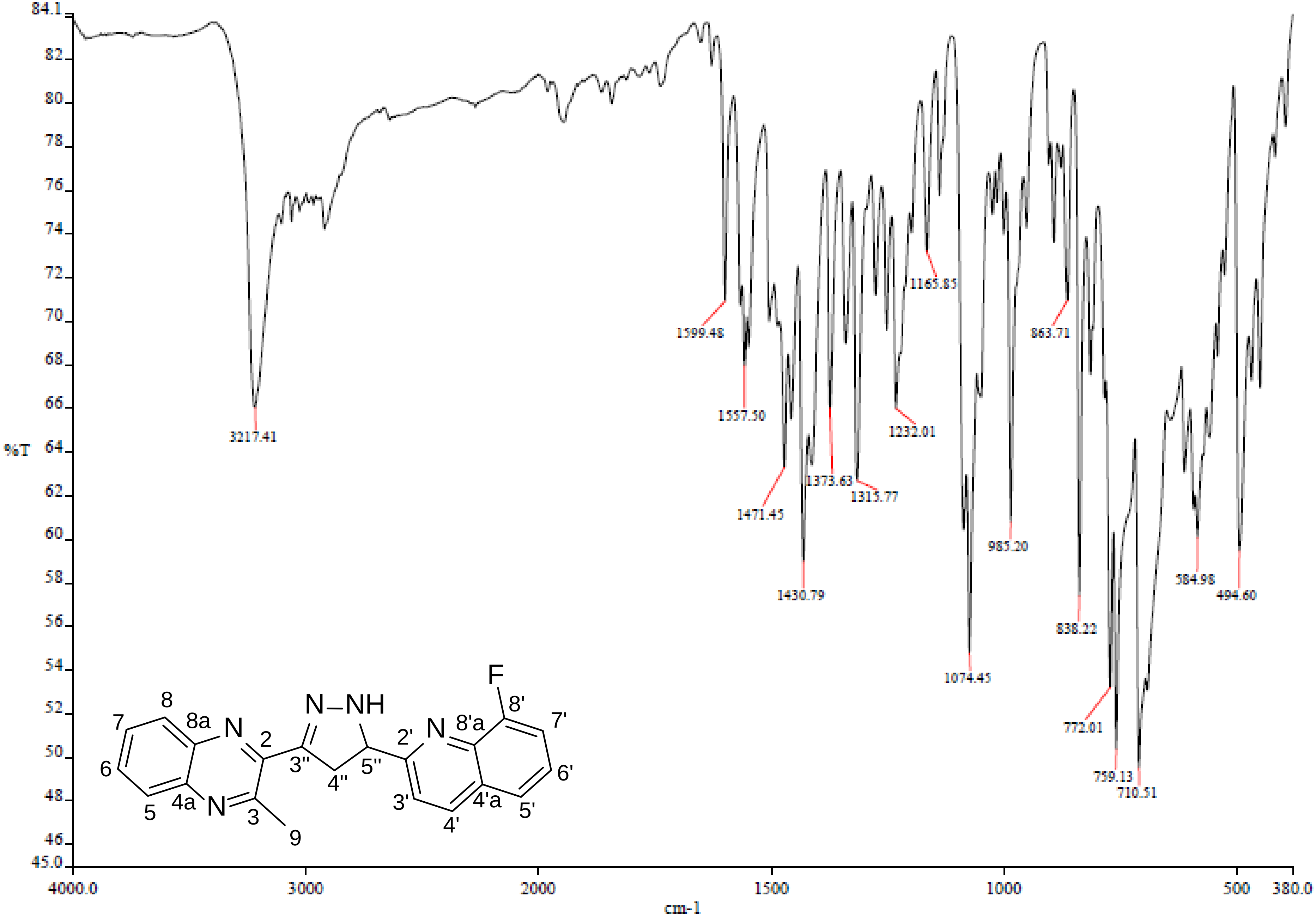

FTIR spectrum of **B8a**

Overlay Spectrum Graph Report

06/10/2017 12:11:47 PM

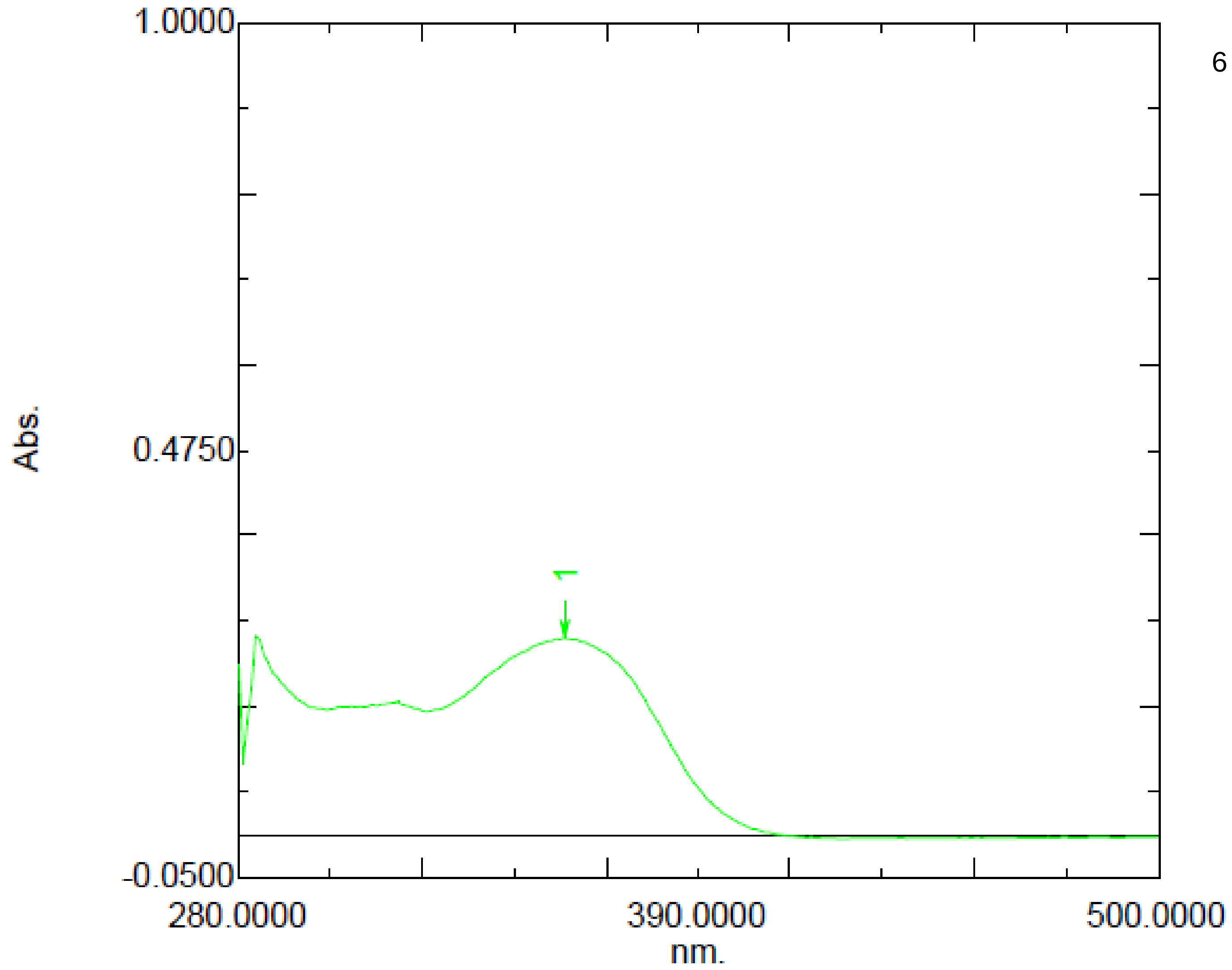

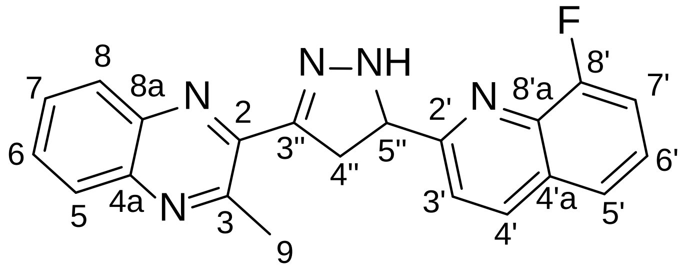

λ	absorbance	logε
358	0.2440	4.24

UV spectrum of **B8a**

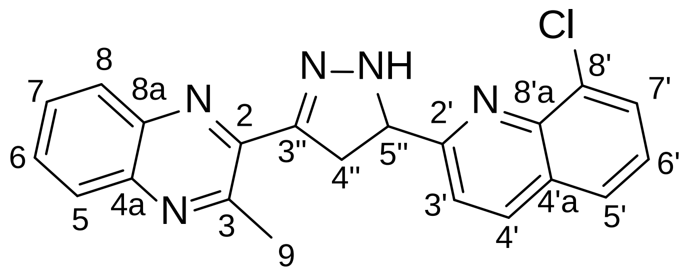

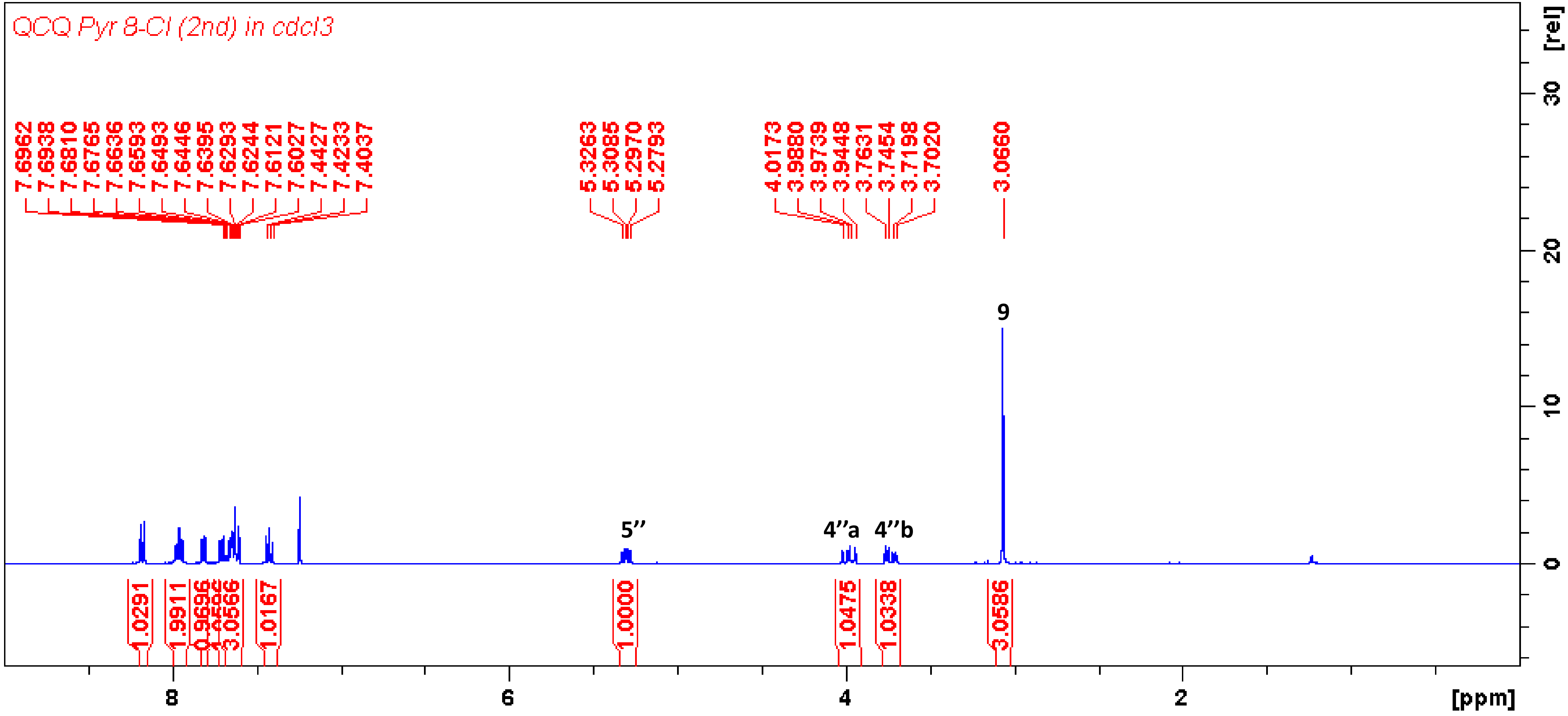

^{1}H NMR spectrum of **B8b**

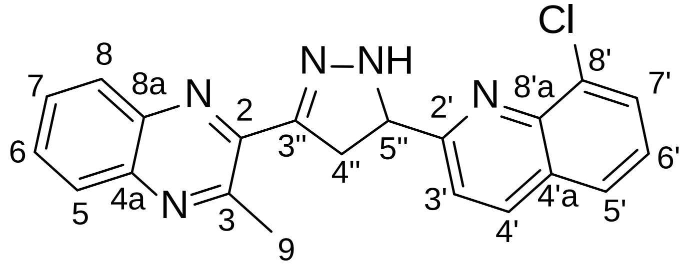

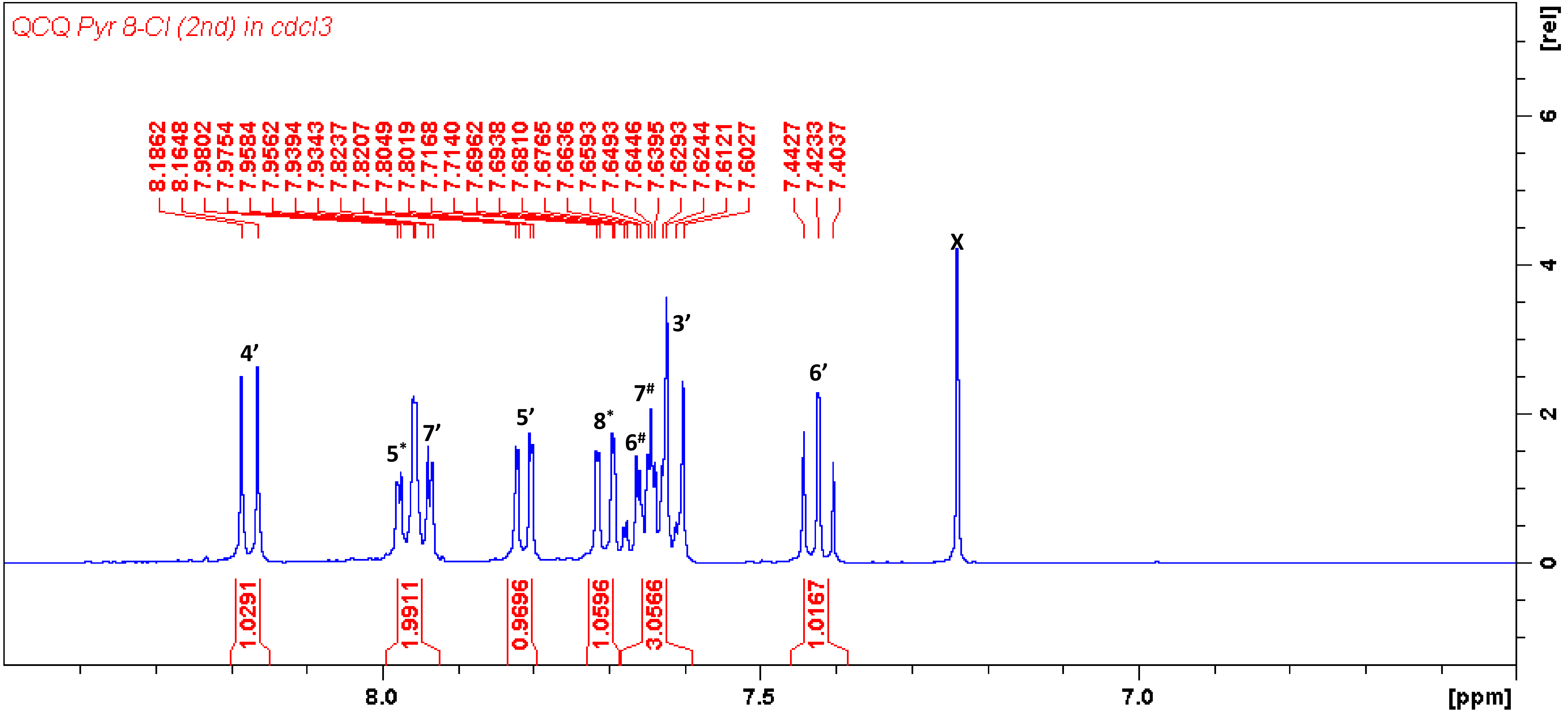

*, # Indicates assignments are interchangeable

Expanded ^{1}H NMR spectrum of **B8b**

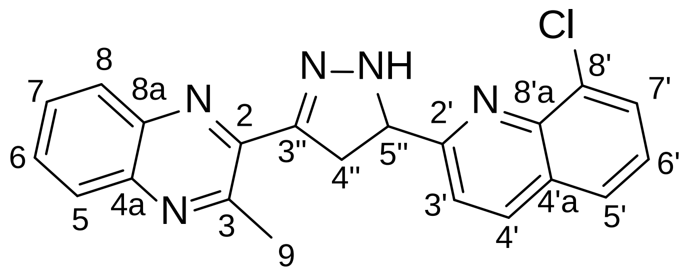

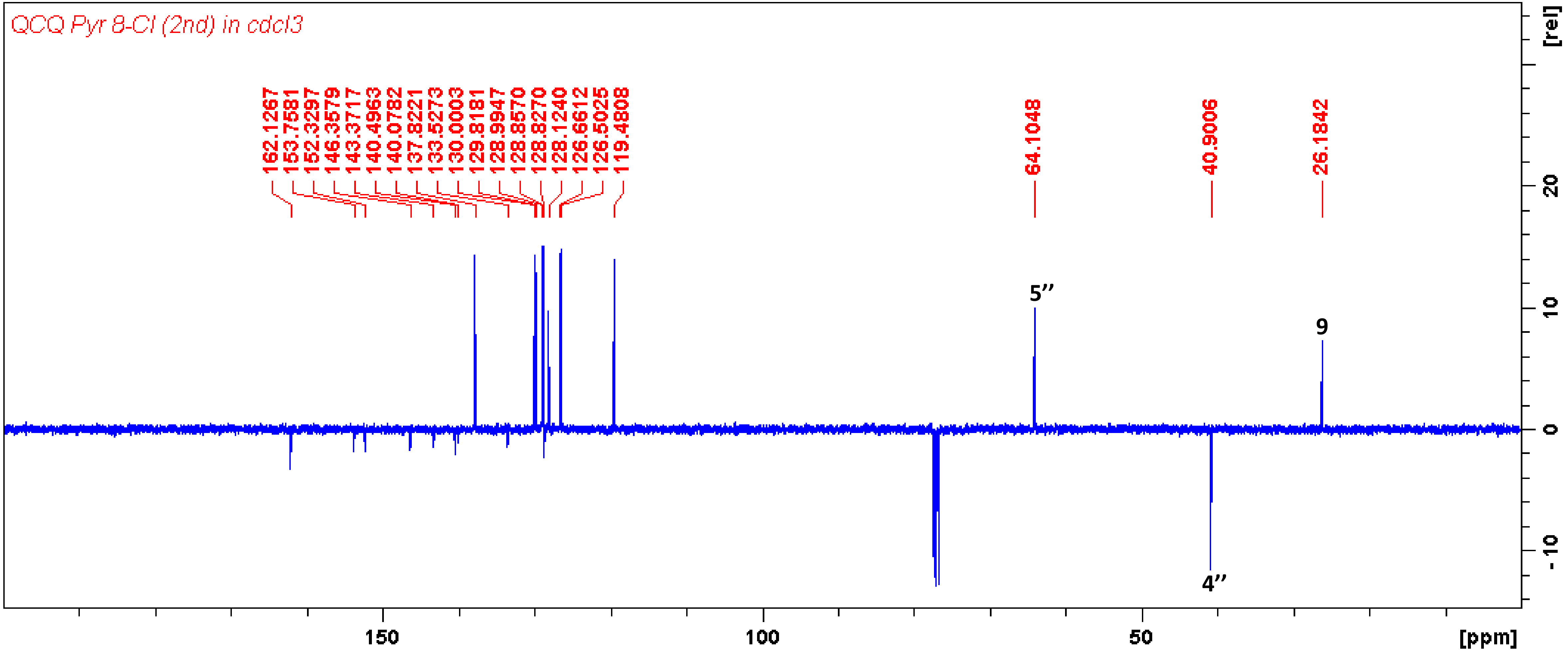

^{13}C NMR spectrum of **B8b**

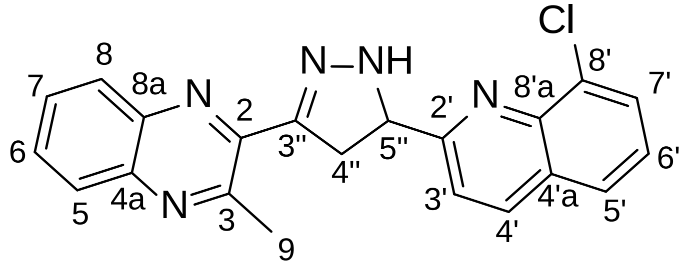

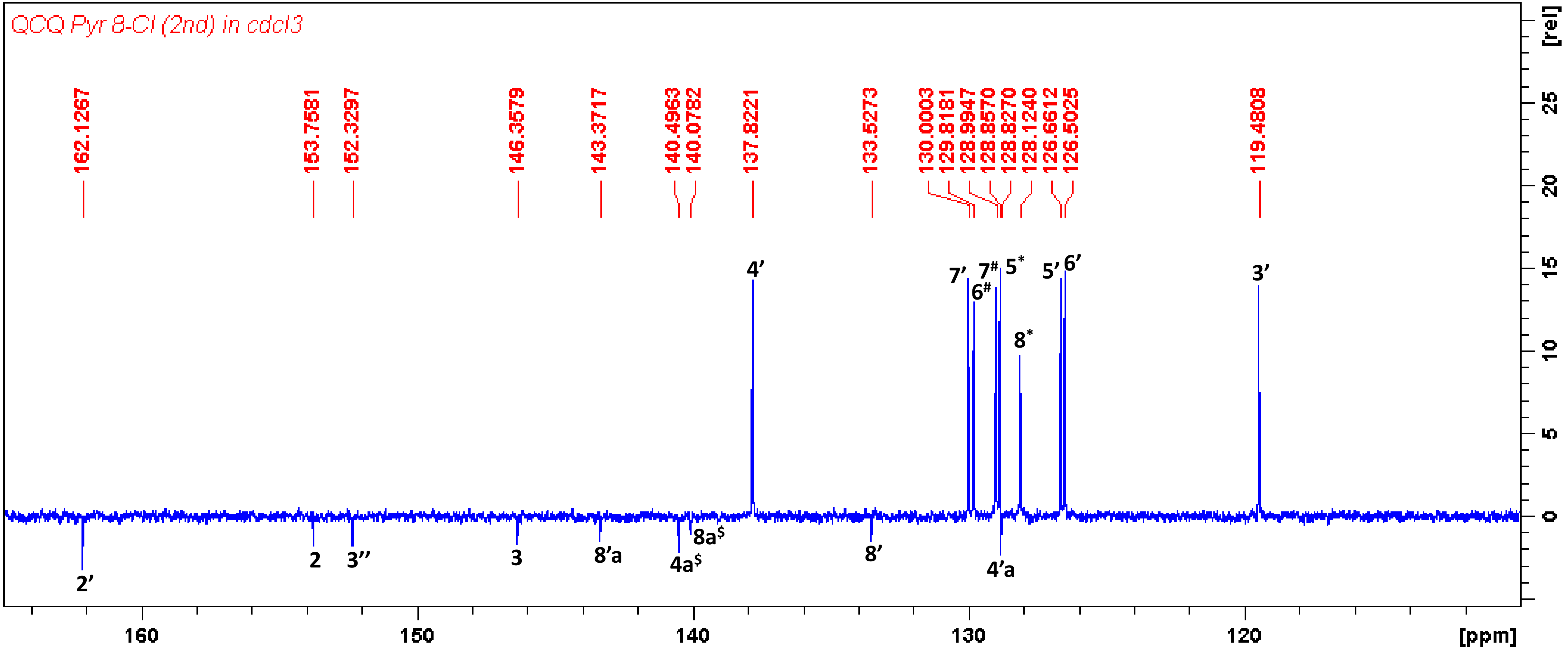

*, #, $ Indicates assignments are interchangeable

Expanded ^{13}C NMR spectrum of **B8b**

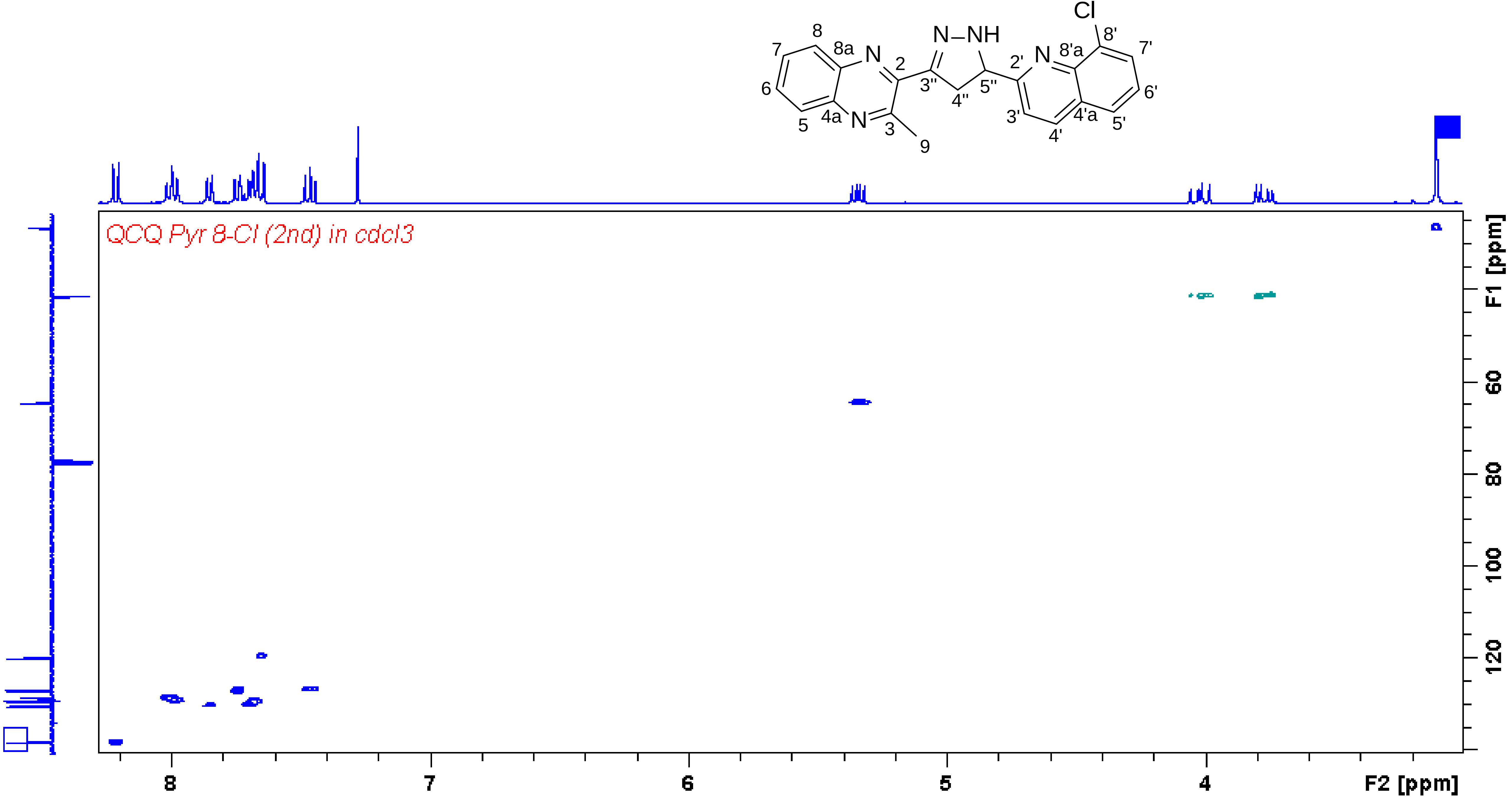

QCQ Pyr 8-Cl (2nd) in cdcl3
F1 [ppm]
F2 [ppm]
8
7
6
5
4
60
80
100
120
Cl
N–NH
N
8a
2
3''
4''
5''
2'
8'a
8'
7'
6'
5'
4'a
4'
3'
3
9
4a
5
6
7
8

HSQC of **B8b**

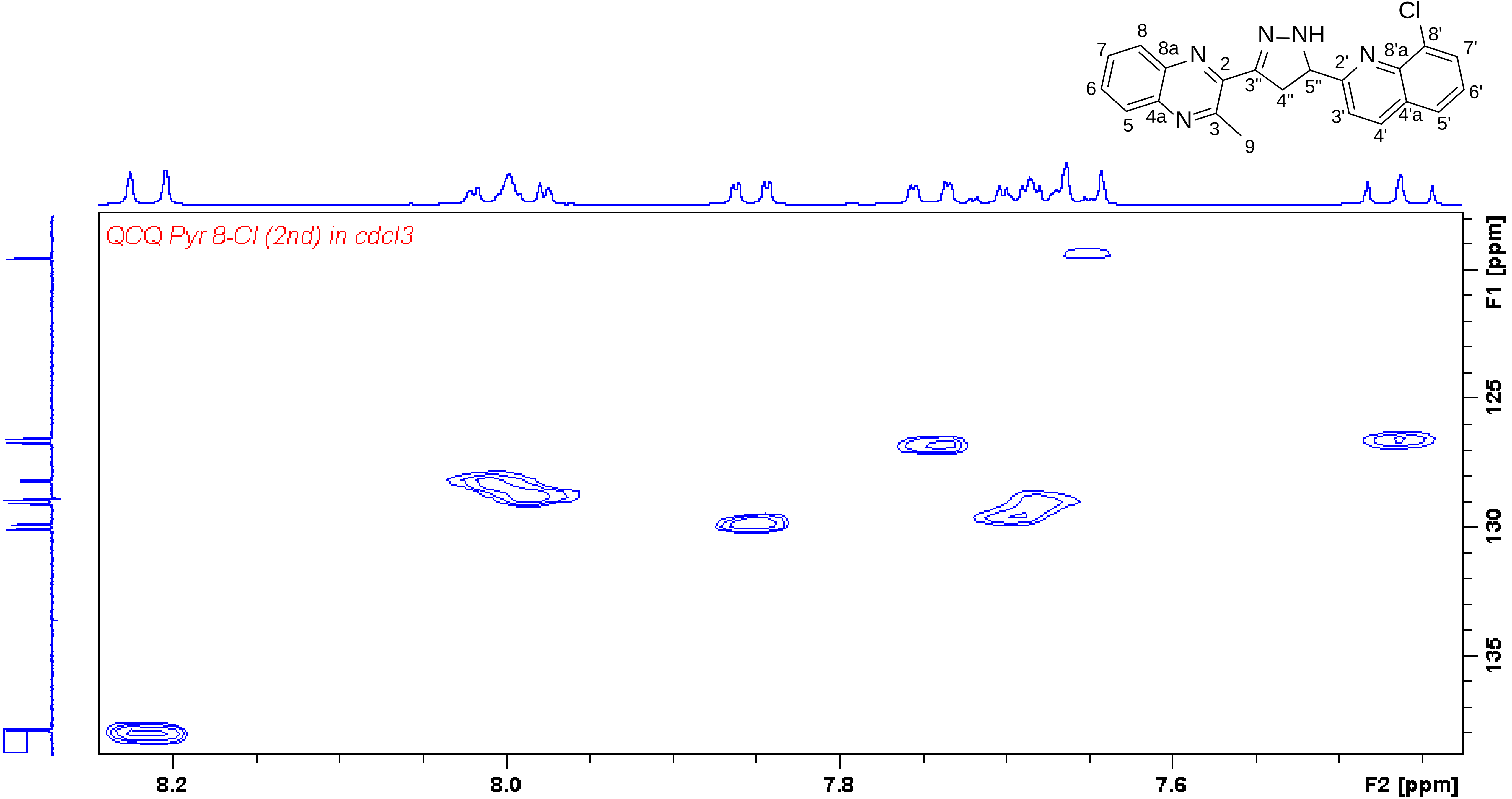

Expanded HSQC of **B8b**

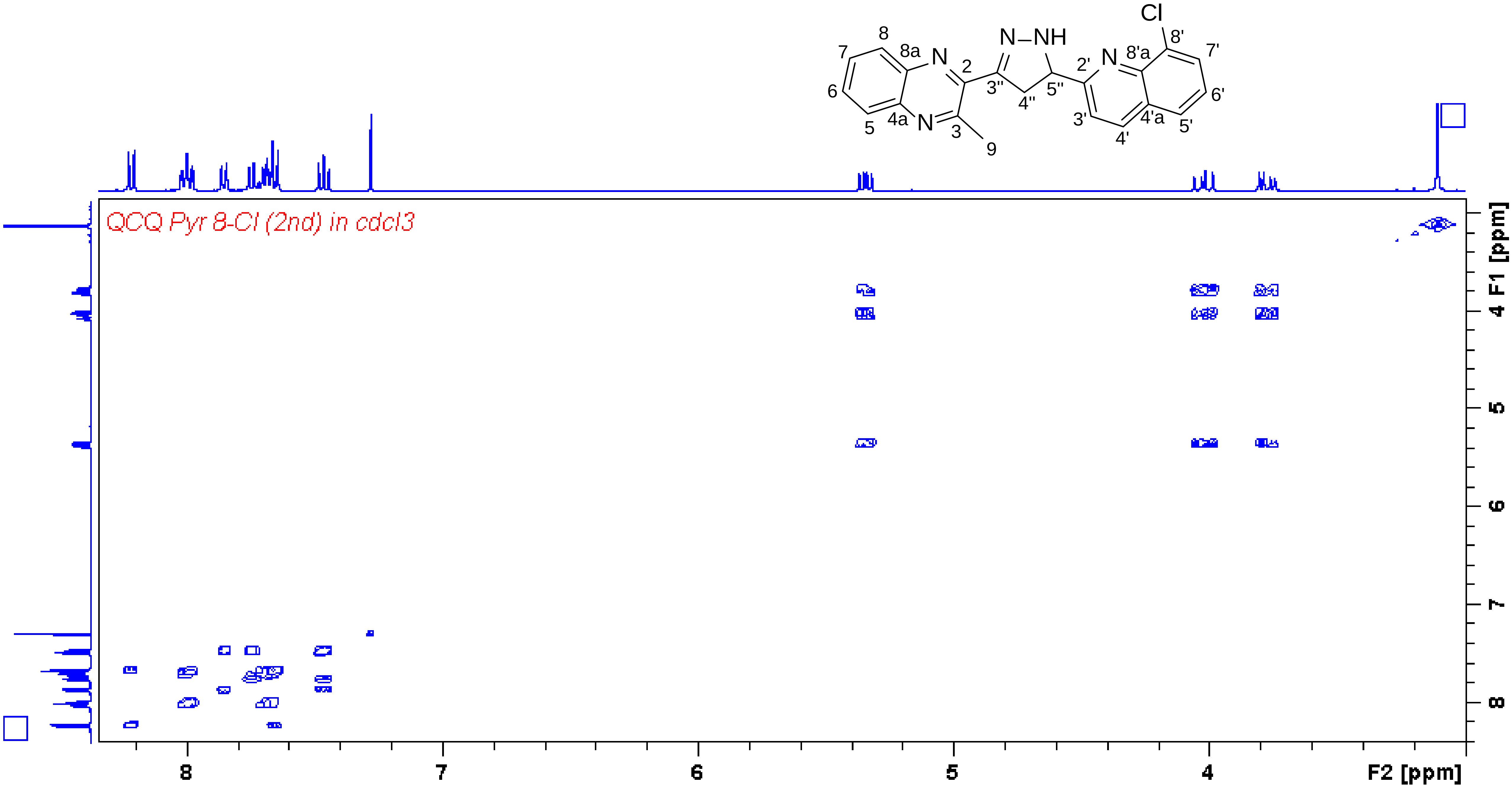

COSY of **B8b**

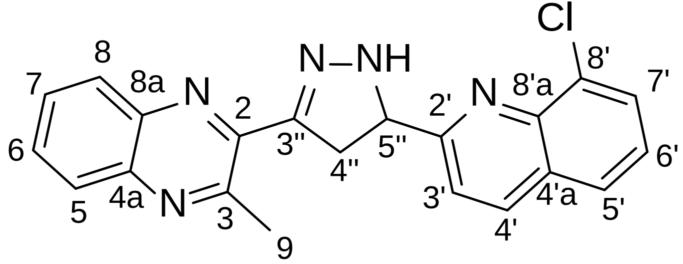

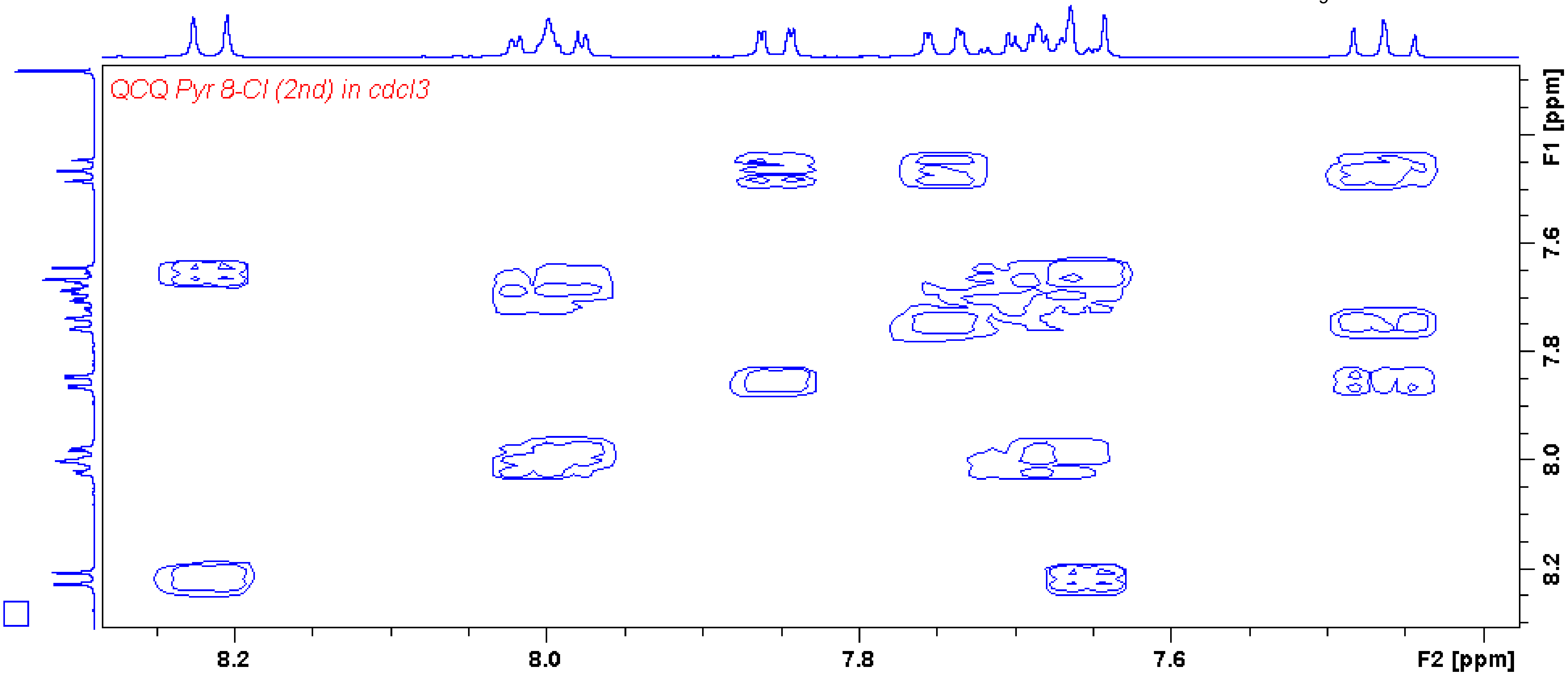

Expanded COSY of **B8b**

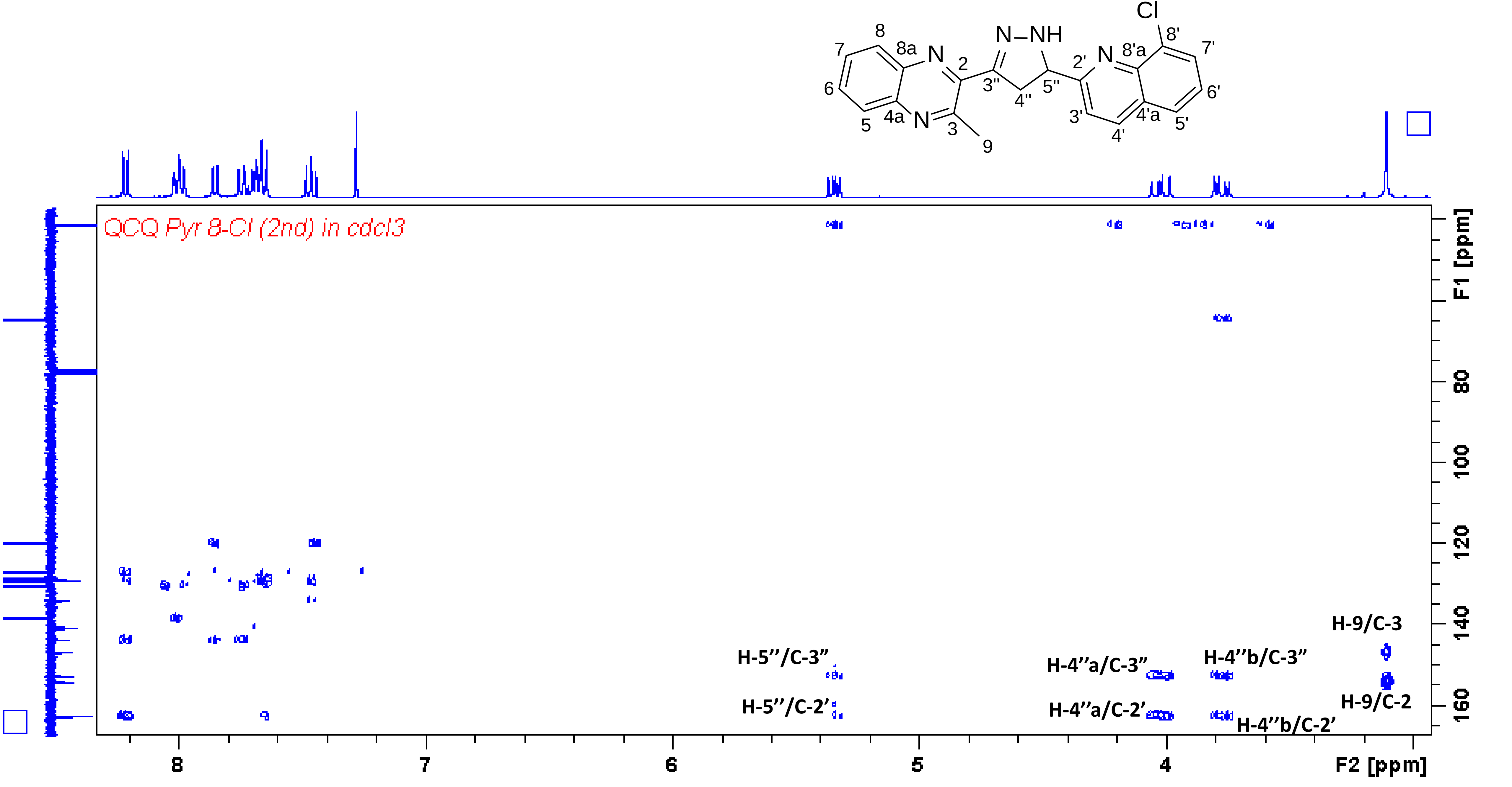
QCQ Pyr 8-Cl (2nd) in cdcl3
H-9/C-3
H-5''/C-3''
H-4''a/C-3''
H-4''b/C-3''
H-9/C-2
H-5''/C-2'
H-4''a/C-2'
H-4''b/C-2'
F1 [ppm]
F2 [ppm]

HMBC of **B8b**

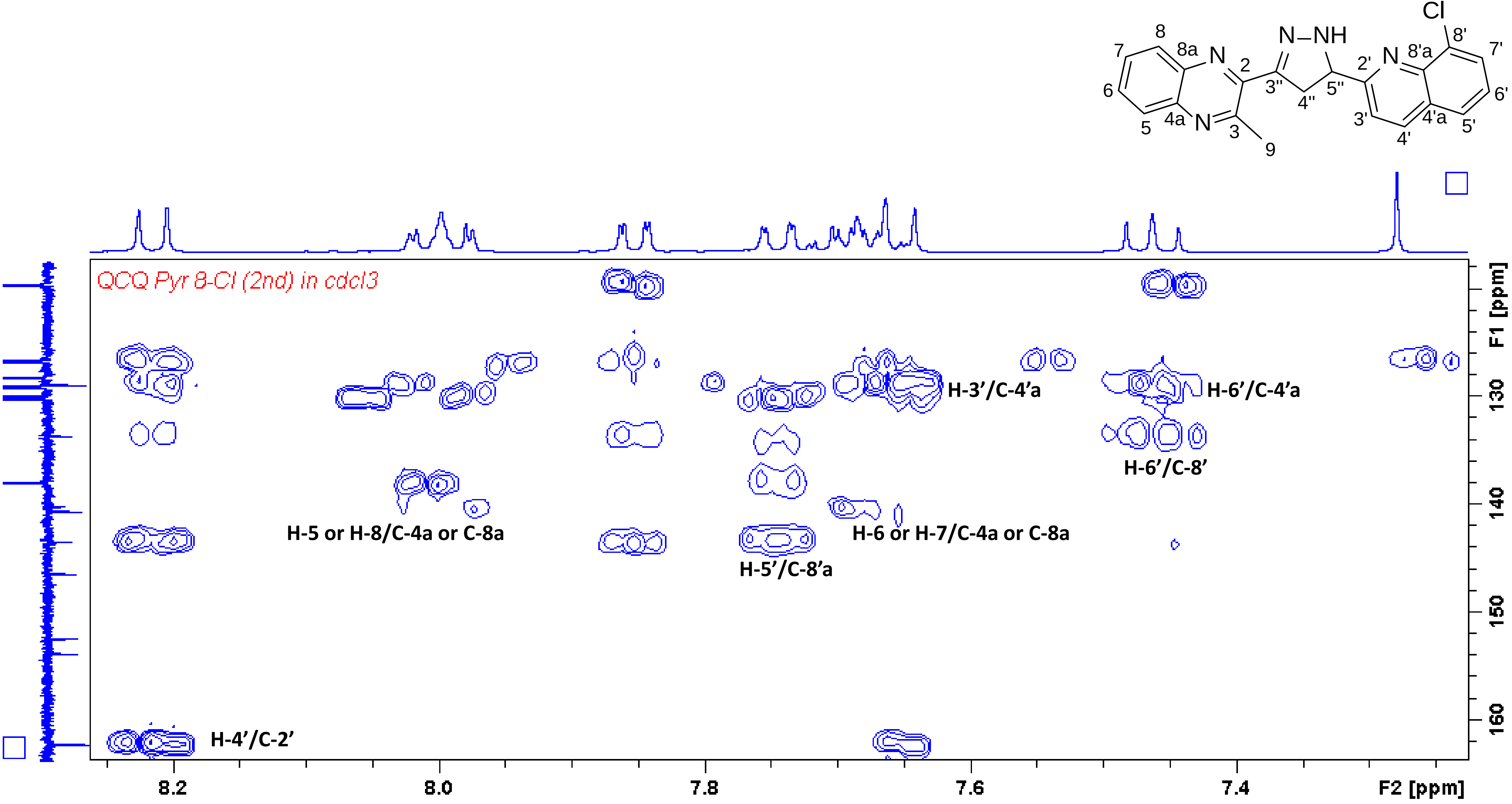

Expanded HMBC of **B8b**

Elemental Composition Report

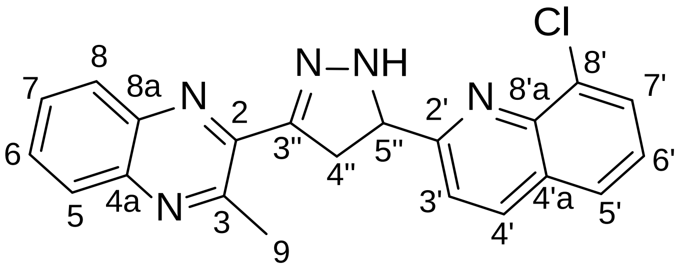

Single Mass Analysis

Tolerance = 5.0 PPM / DBE: min = -1.5, max = 100.0
Element prediction: Off
Number of isotope peaks used for i-FIT = 3

Monoisotopic Mass, Even Electron Ions
11 formula(e) evaluated with 1 results within limits (up to 20 closest results for each mass)
Elements Used:
C: 20-25 H: 15-20 N: 0-5 Na: 0-1 Cl: 0-1
Py-QCQ 8-Cl 25 (0.809) Cm (1:61)
TOF MS ES+

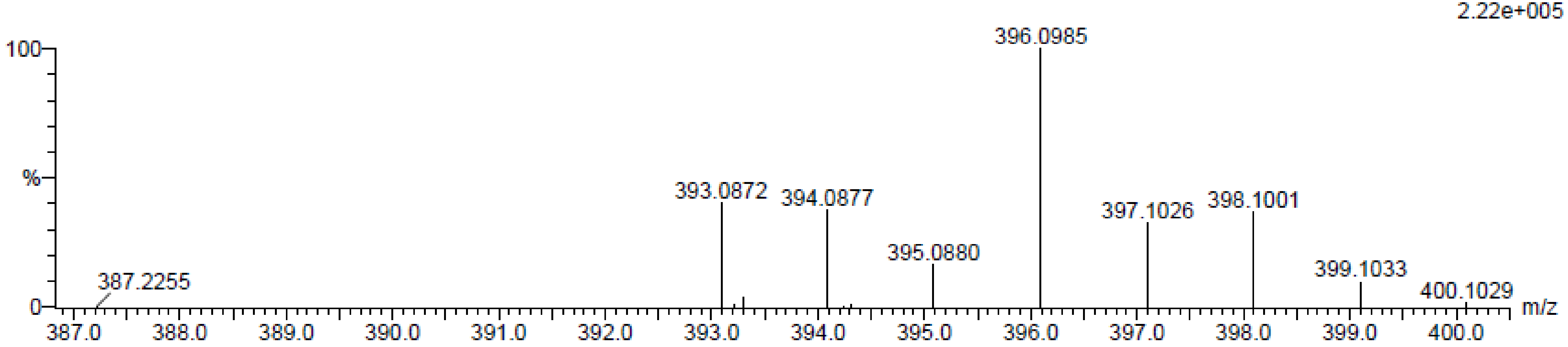

Minimum:				-1.5			
Maximum:		5.0	5.0	100.0			
Mass	Calc. Mass	mDa	PPM	DBE	i-FIT	i-FIT (Norm)	Formula
396.0985	396.0992	-0.7	-1.8	15.5	29.1	0.0	C21 H16 N5 Na Cl

High resolution mass spectrum of **B8b**

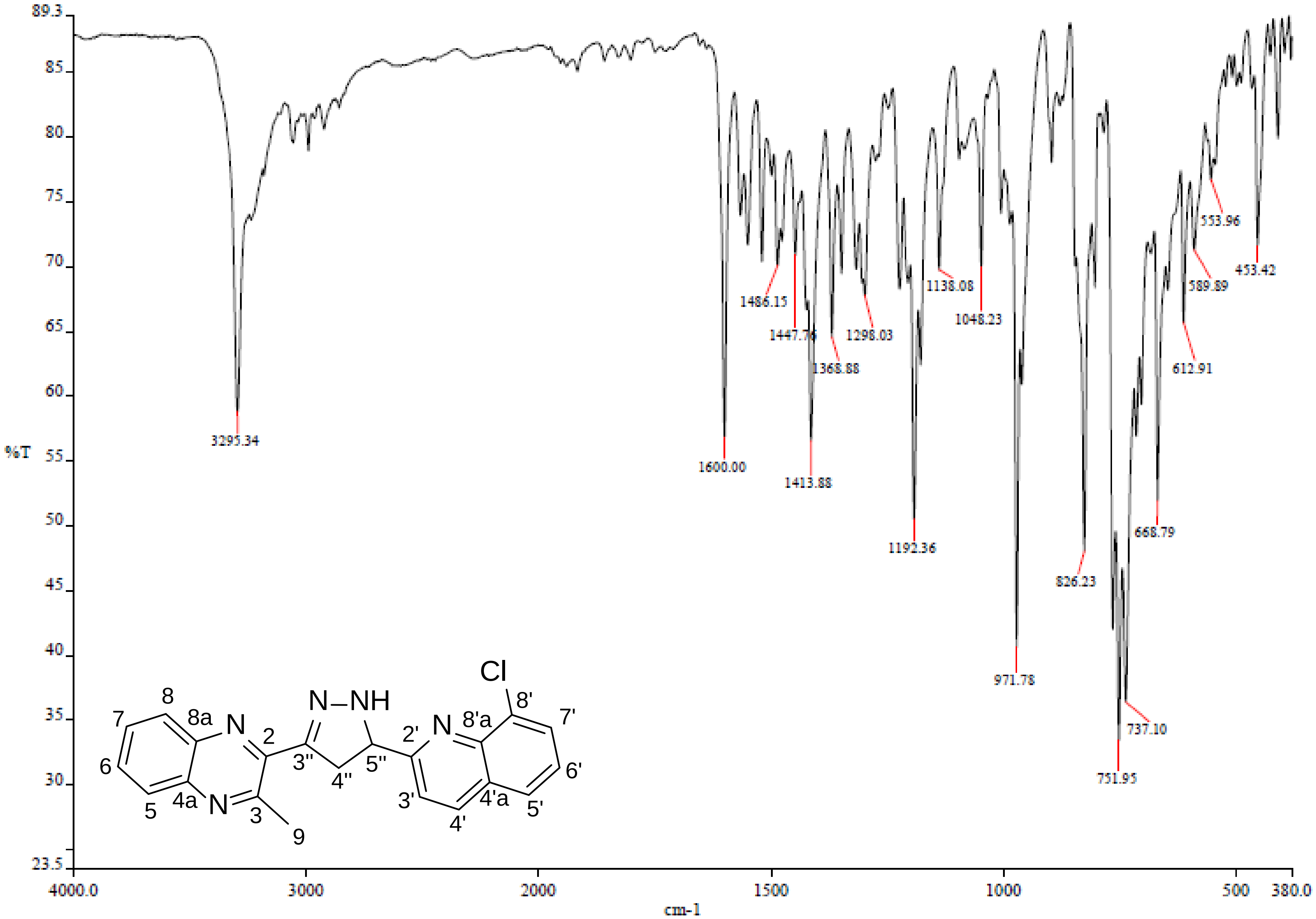

FTIR spectrum of **B8b**

Overlay Spectrum Graph Report

06/10/2017 12:10:36 PM

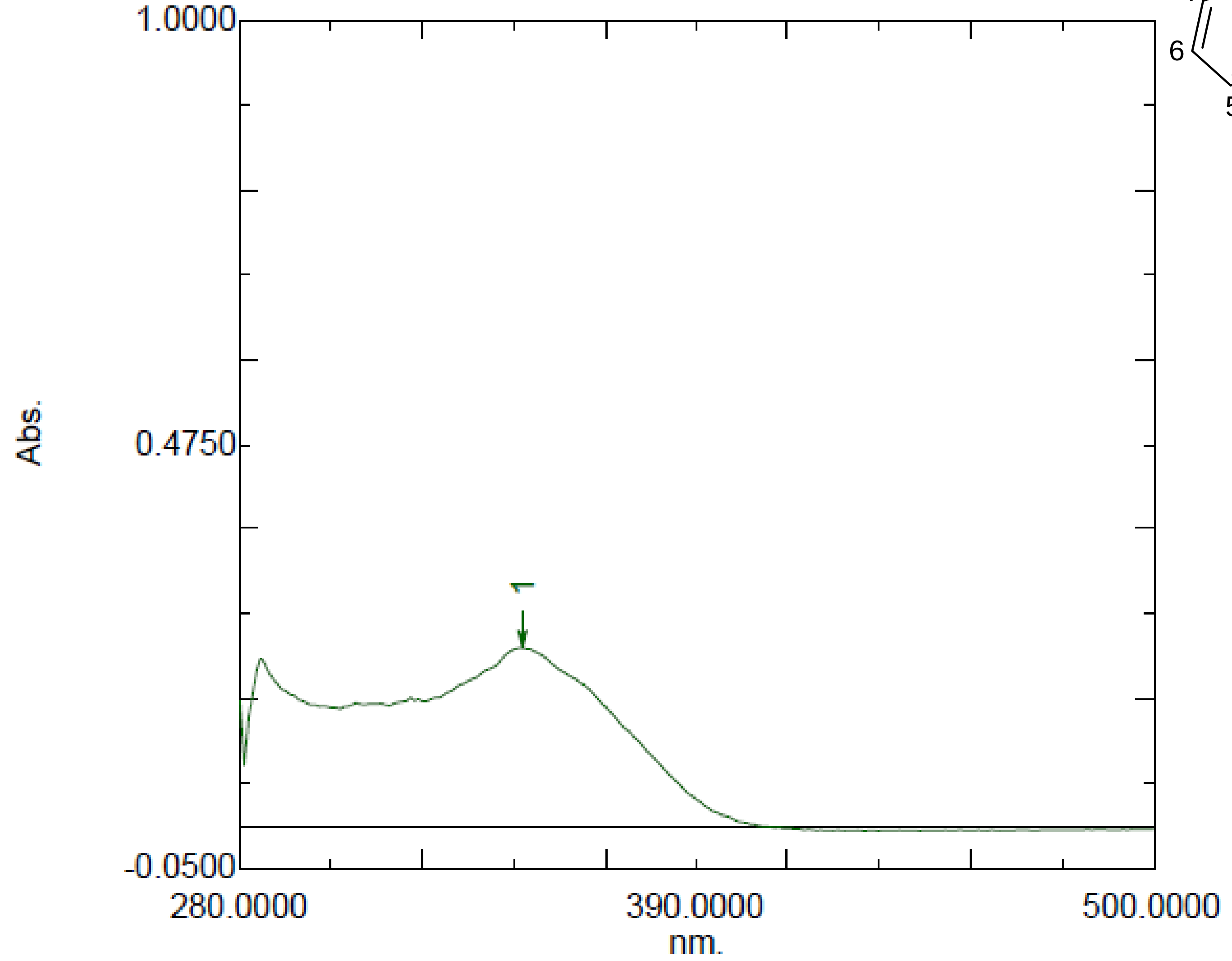

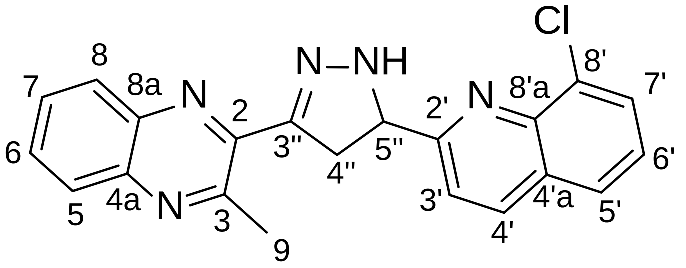

λ	absorbance	logε
348	0.2231	4.22

UV spectrum of **B8b**

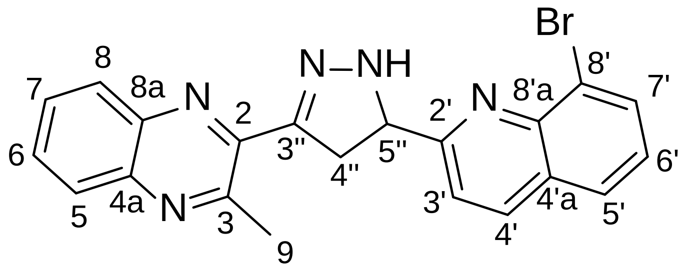

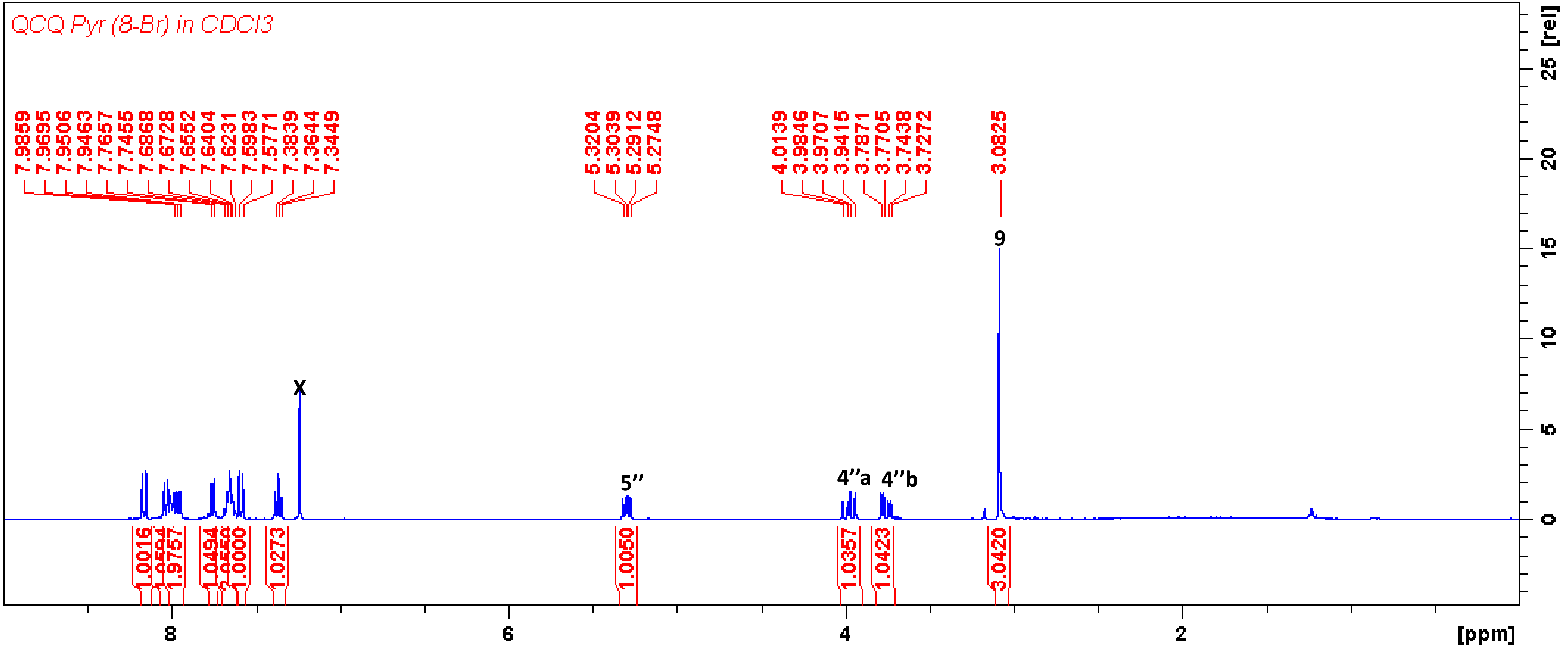

^{1}H NMR spectrum of **B8c**

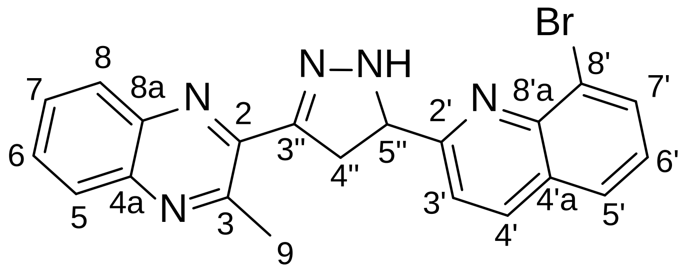

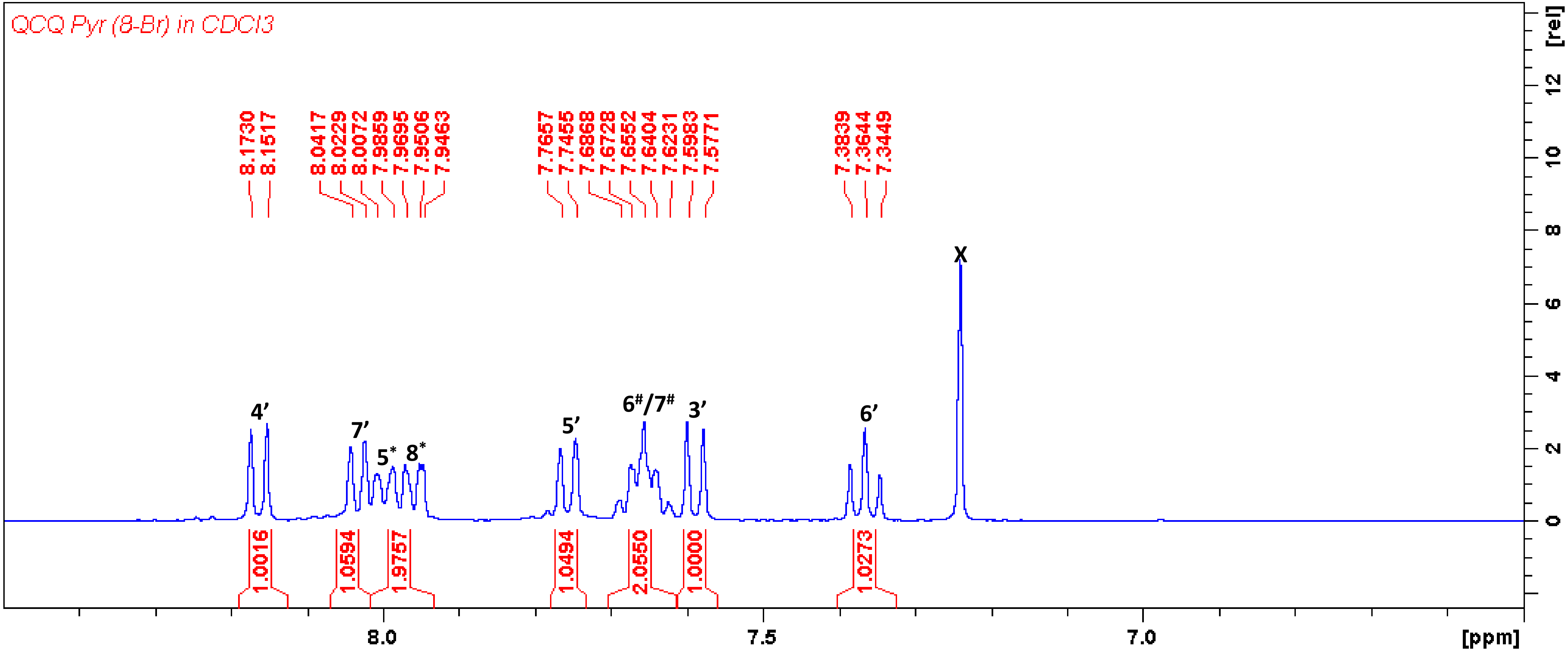

*, # Indicates assignments are interchangeable

Expanded ^{1}H NMR spectrum of **B8c**

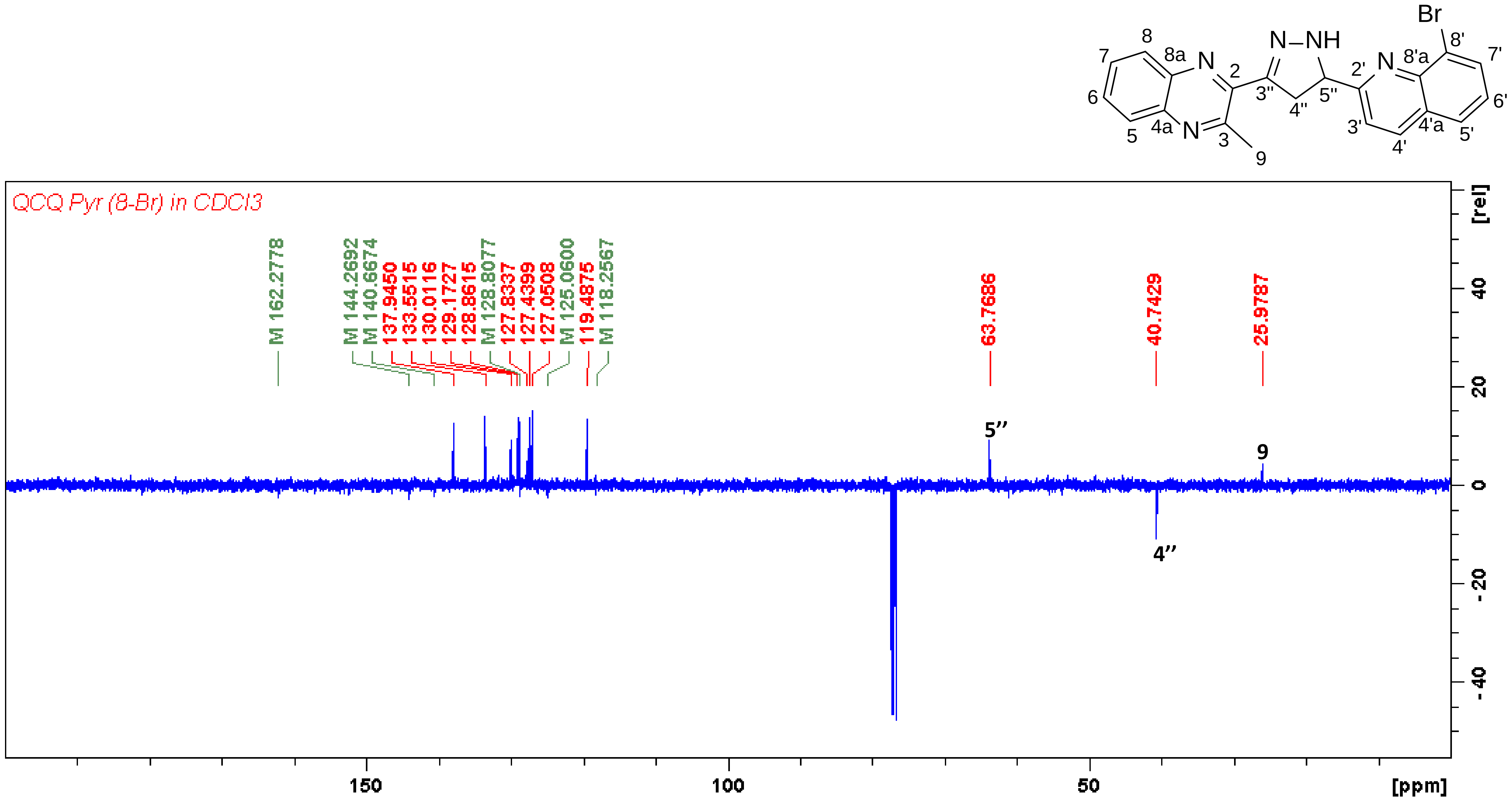

^{13}C NMR spectrum of **B8c**

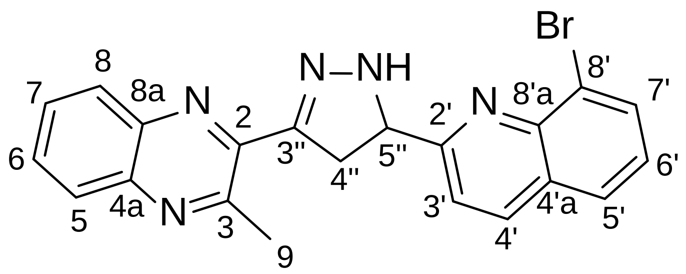

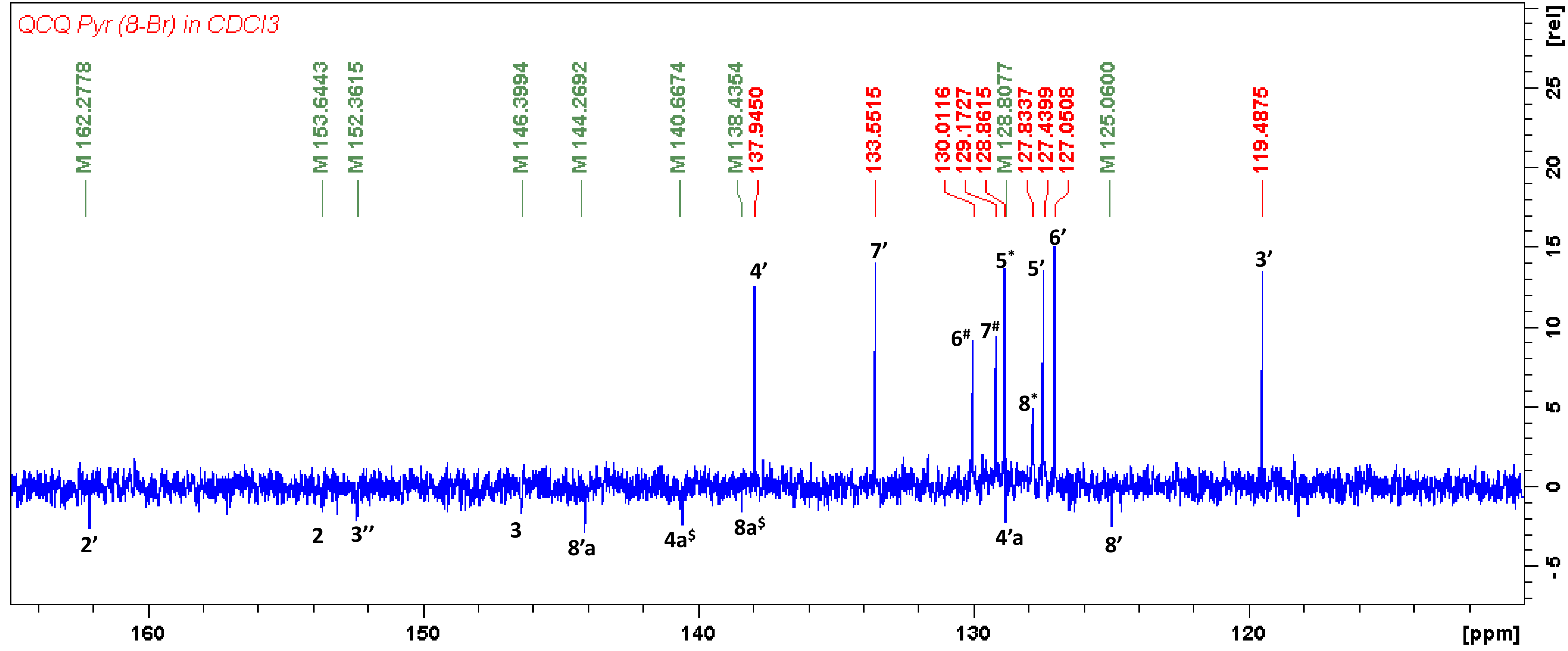

*, #, $ Indicates assignments are interchangeable

Expanded ^{13}C NMR spectrum of **B8c**

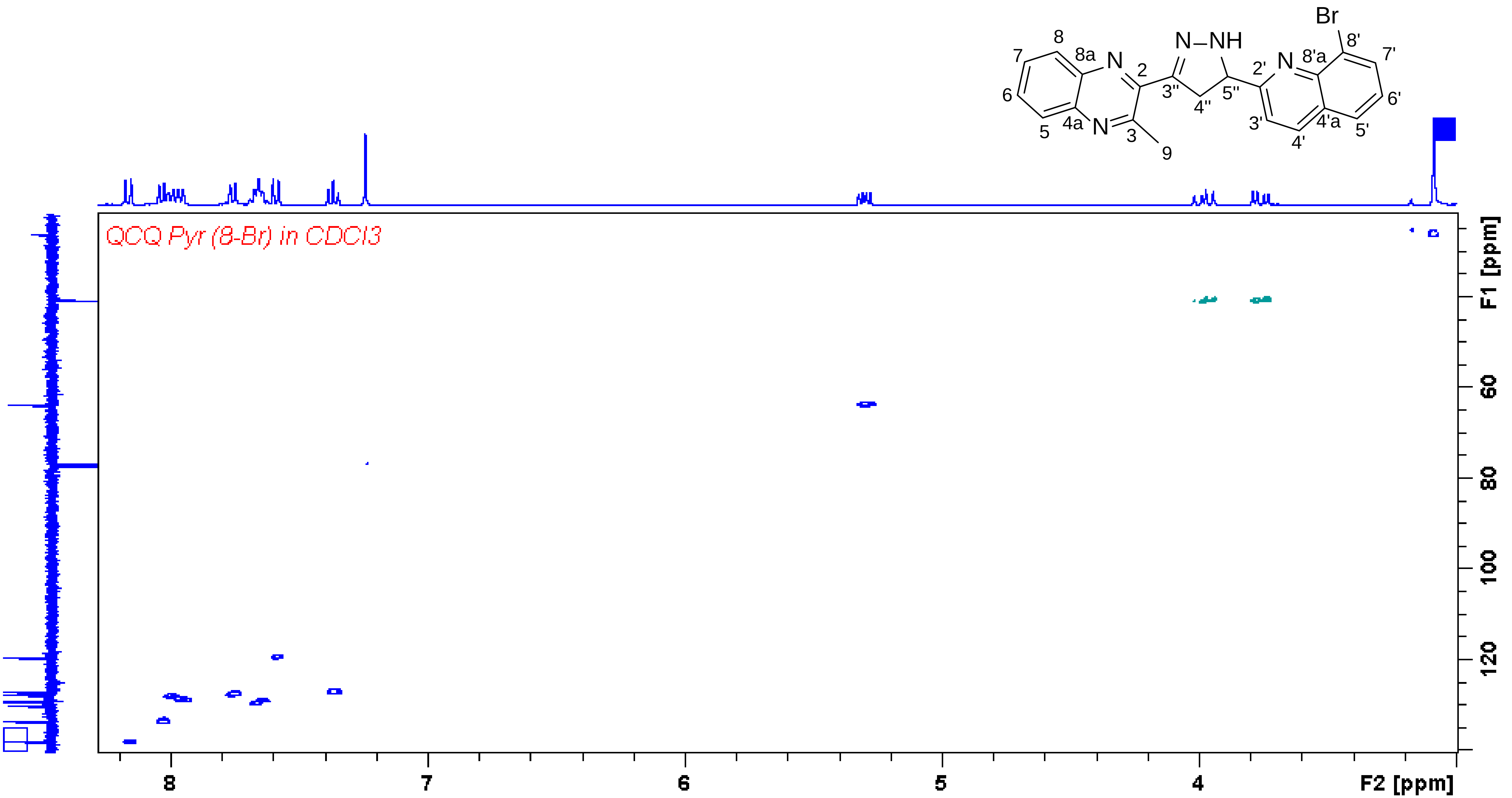
QCQ Pyr (8-Br) in CDCl3
F1 [ppm]
F2 [ppm]
Br
N–NH
N
N
8
7
6
5
4a
8a
2
3
9
3''
4''
5''
2'
3'
4'
4'a
5'
6'
7'
8'
8'a

HSQC of **B8c**

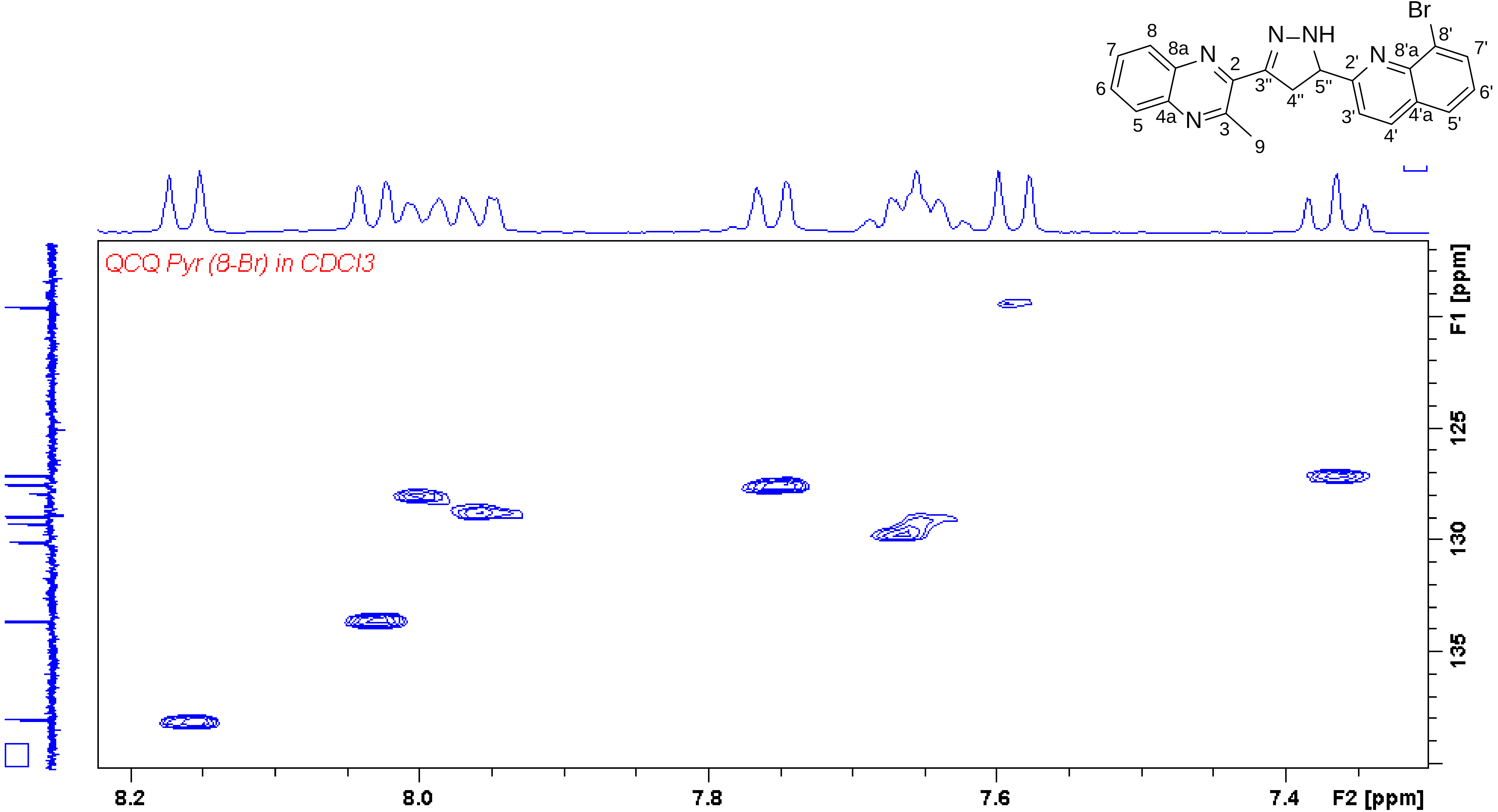

Expanded HSQC of **B8c**

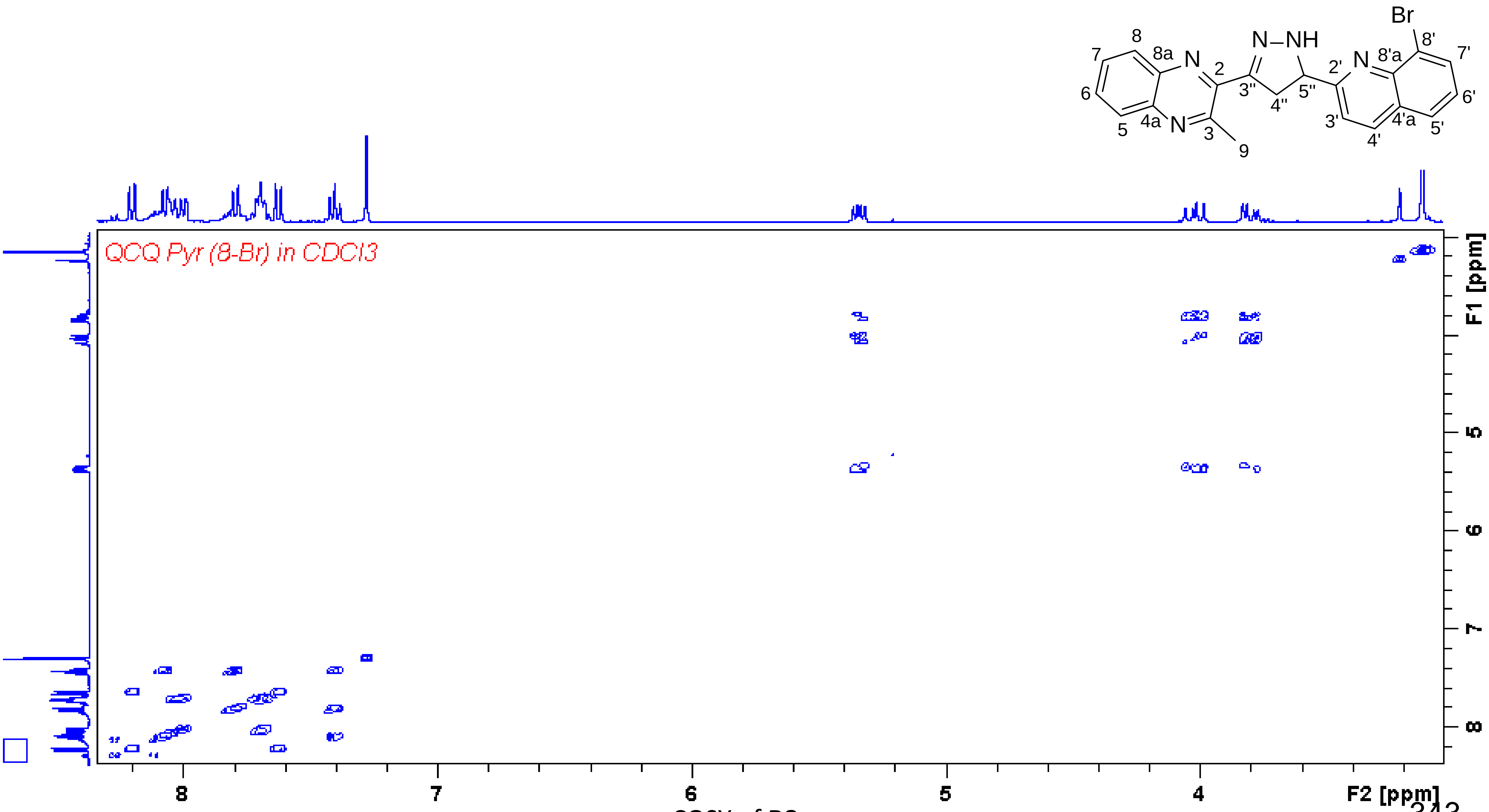
QCQ Pyr (8-Br) in CDCl3
F1 [ppm]
F2 [ppm]
Br
N–NH
N
8
7
6
5
4a
8a
2
3
9
3''
4''
5''
2'
3'
4'
4'a
5'
6'
7'
8'
8'a

COSY of **B8c**

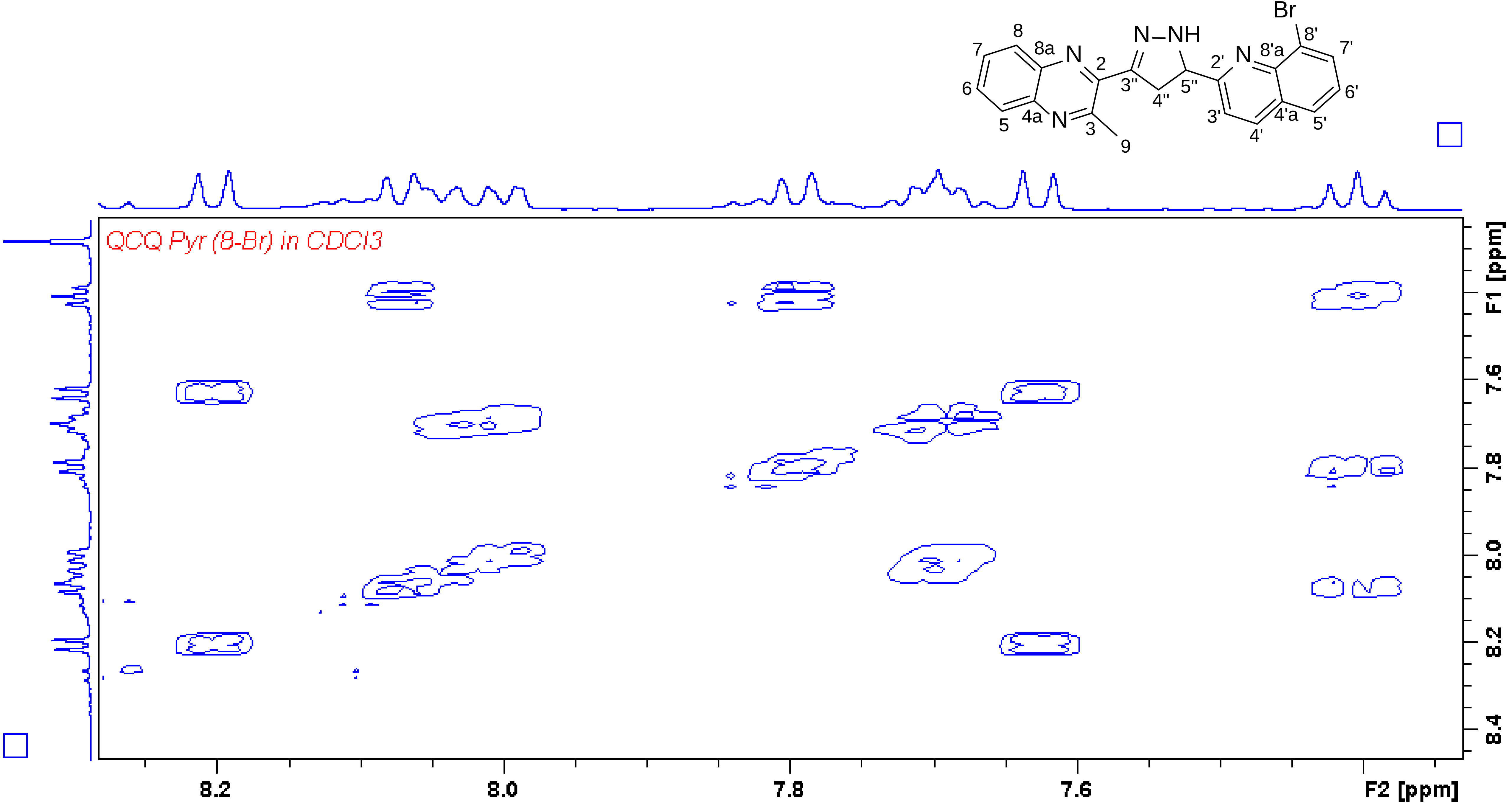

Expanded COSY of **B8c**

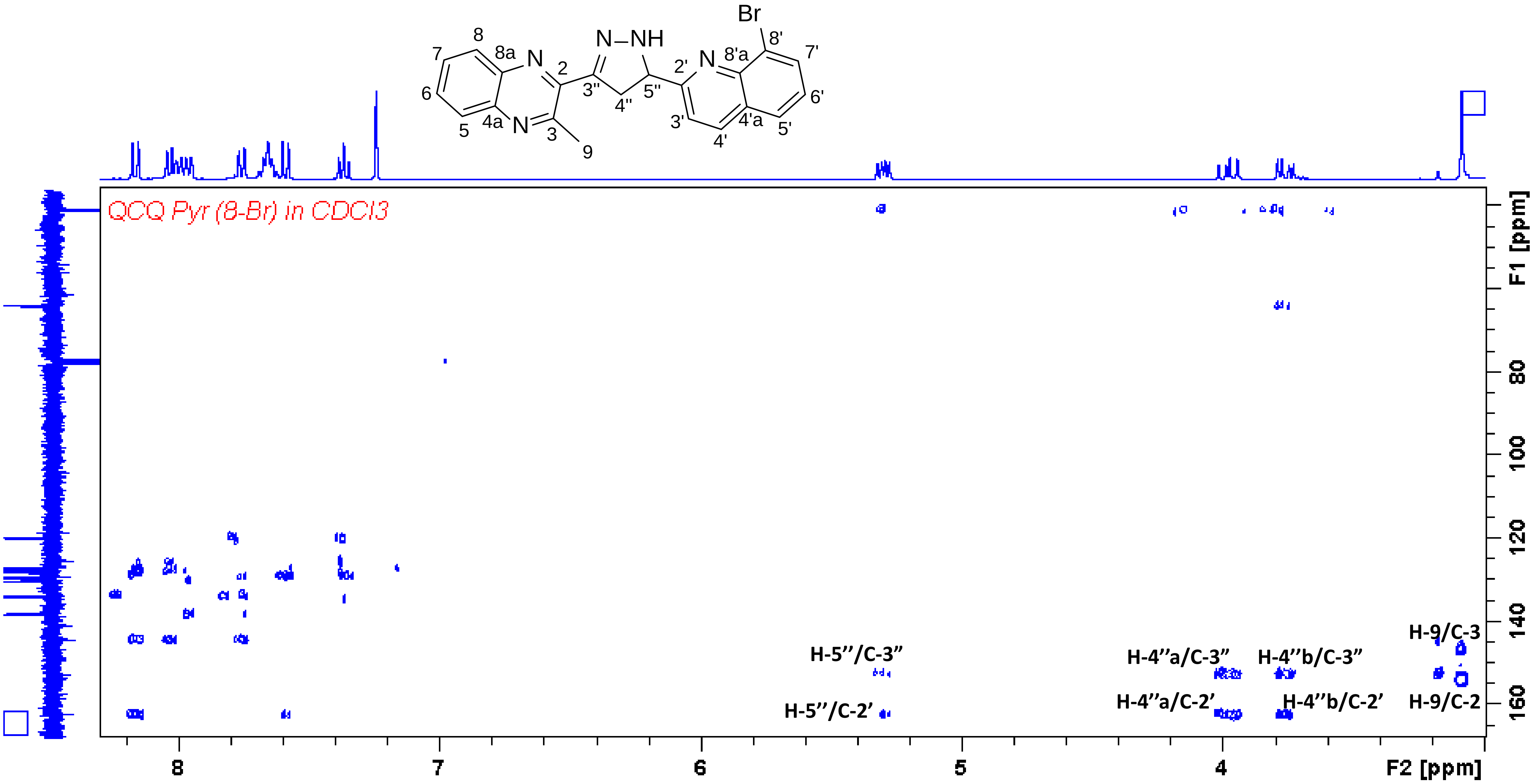

Br
8'
7'
N
8'a
N–NH
2'
8
8a
N
2
3''
5''
7
6'
6
4a
N
3
4''
3'
4'a
5'
5
9
4'
QCQ Pyr (8-Br) in CDCl3
H-5''/C-3''
H-4''a/C-3''
H-4''b/C-3''
H-9/C-3
H-5''/C-2'
H-4''a/C-2'
H-4''b/C-2'
H-9/C-2
F1 [ppm]
F2 [ppm]

HMBC of **B8c**

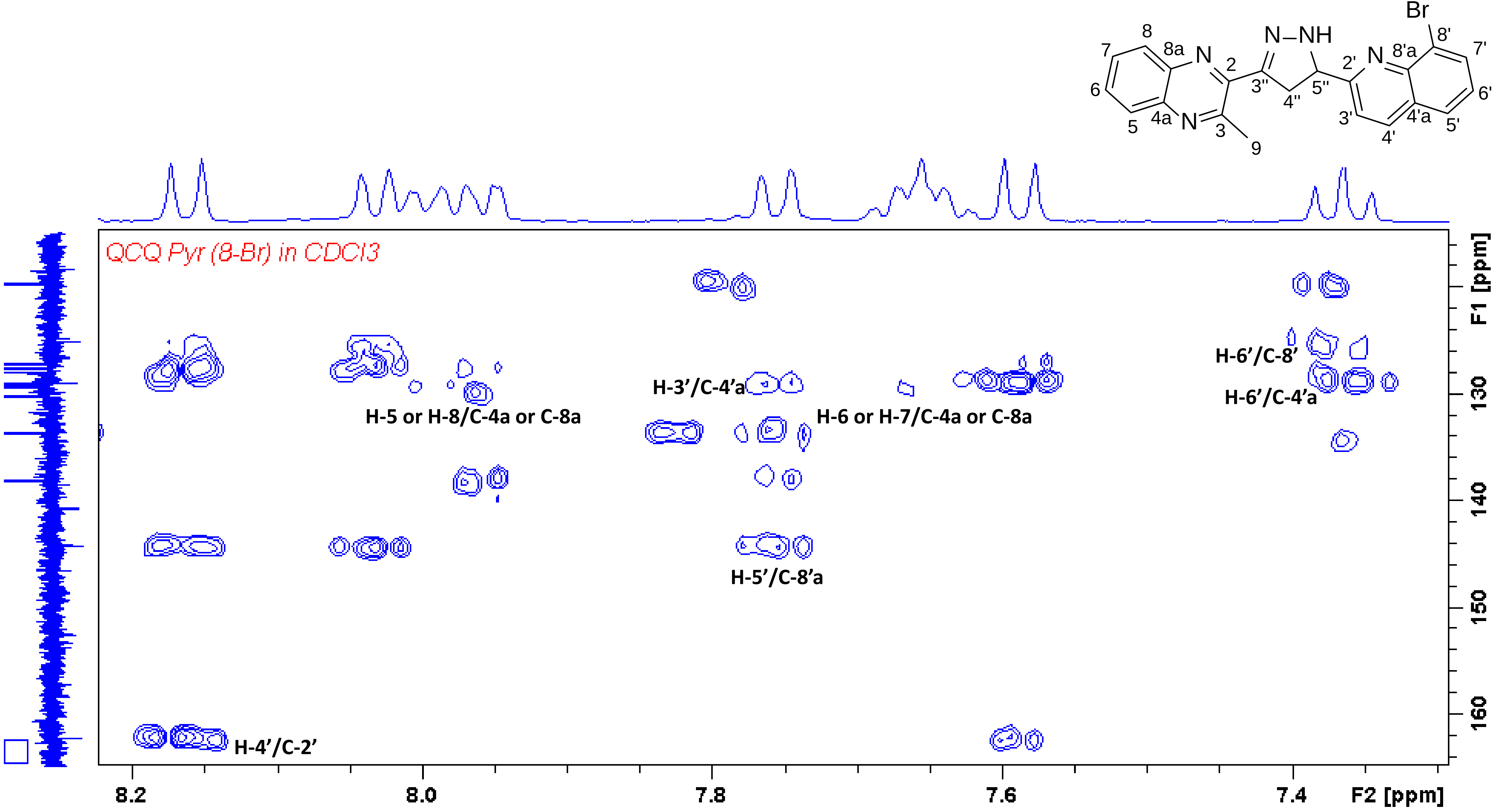

Expanded HMBC of **B8c**

Elemental Composition Report **Page 1**

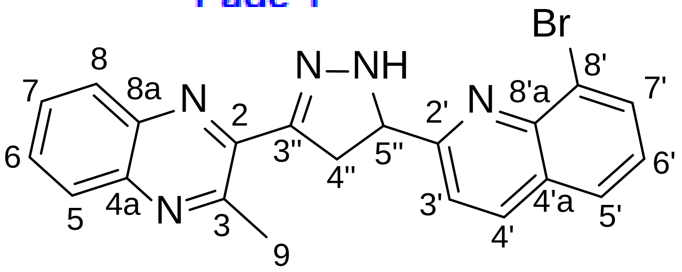

Single Mass Analysis
Tolerance = 5.0 PPM / DBE: min = -1.5, max = 100.0
Element prediction: Off
Number of isotope peaks used for i-FIT = 3

Monoisotopic Mass, Even Electron Ions
15 formula(e) evaluated with 1 results within limits (up to 20 closest results for each mass)
Elements Used:
C: 20-25 H: 15-20 N: 0-5 Na: 0-1 Br: 0-1

Py-QCQ 8-Br 17 (0.539) Cm (1:61)
TOF MS ES+

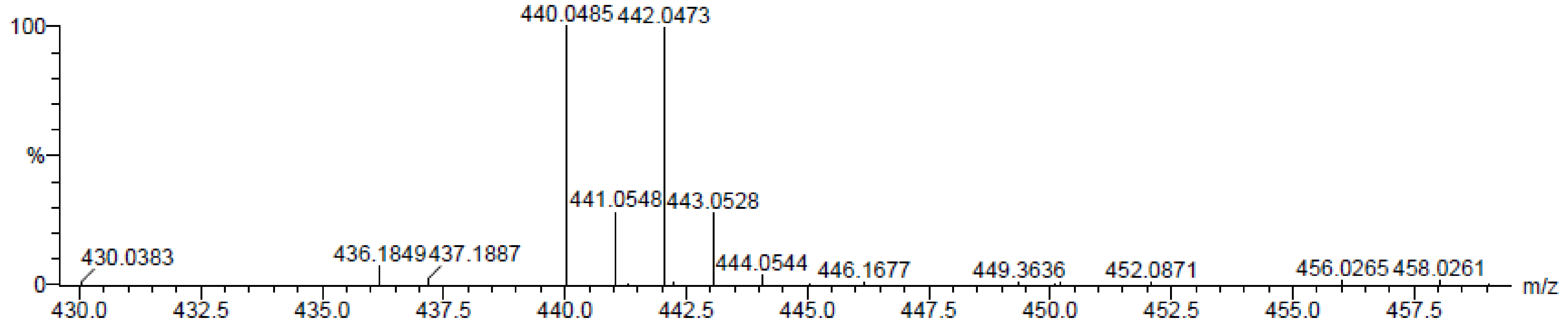

Minimum:				-1.5			
Maximum:		5.0	5.0	100.0			
Mass	Calc. Mass	mDa	PPM	DBE	i-FIT	i-FIT (Norm)	Formula
440.0485	440.0487	-0.2	-0.5	15.5	61.0	0.0	C21 H16 N5 Na Br

High resolution mass spectrum of **B8c**

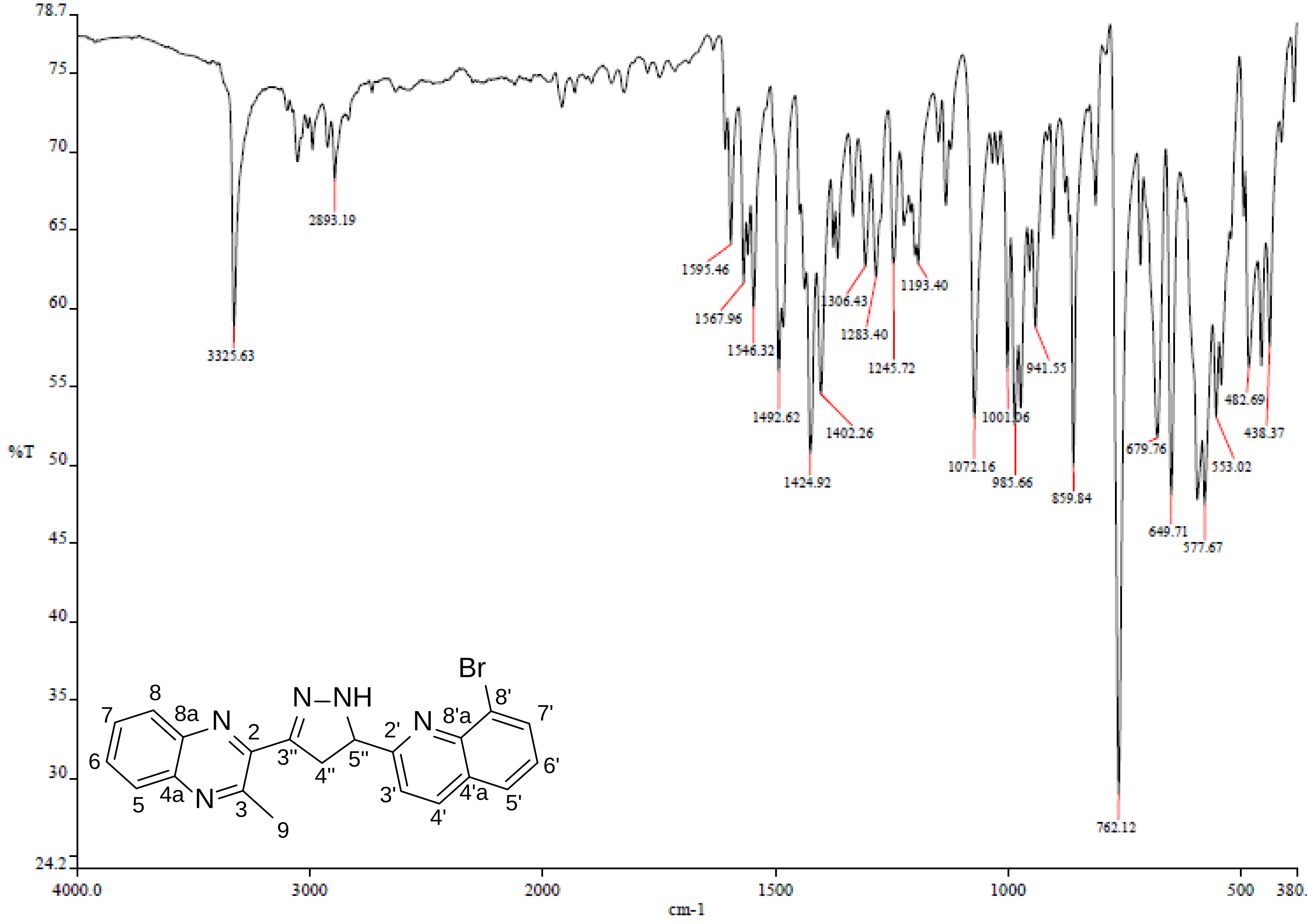

FTIR spectrum of **B8c**

Overlay Spectrum Graph Report

06/10/2017 12:08:26 PM

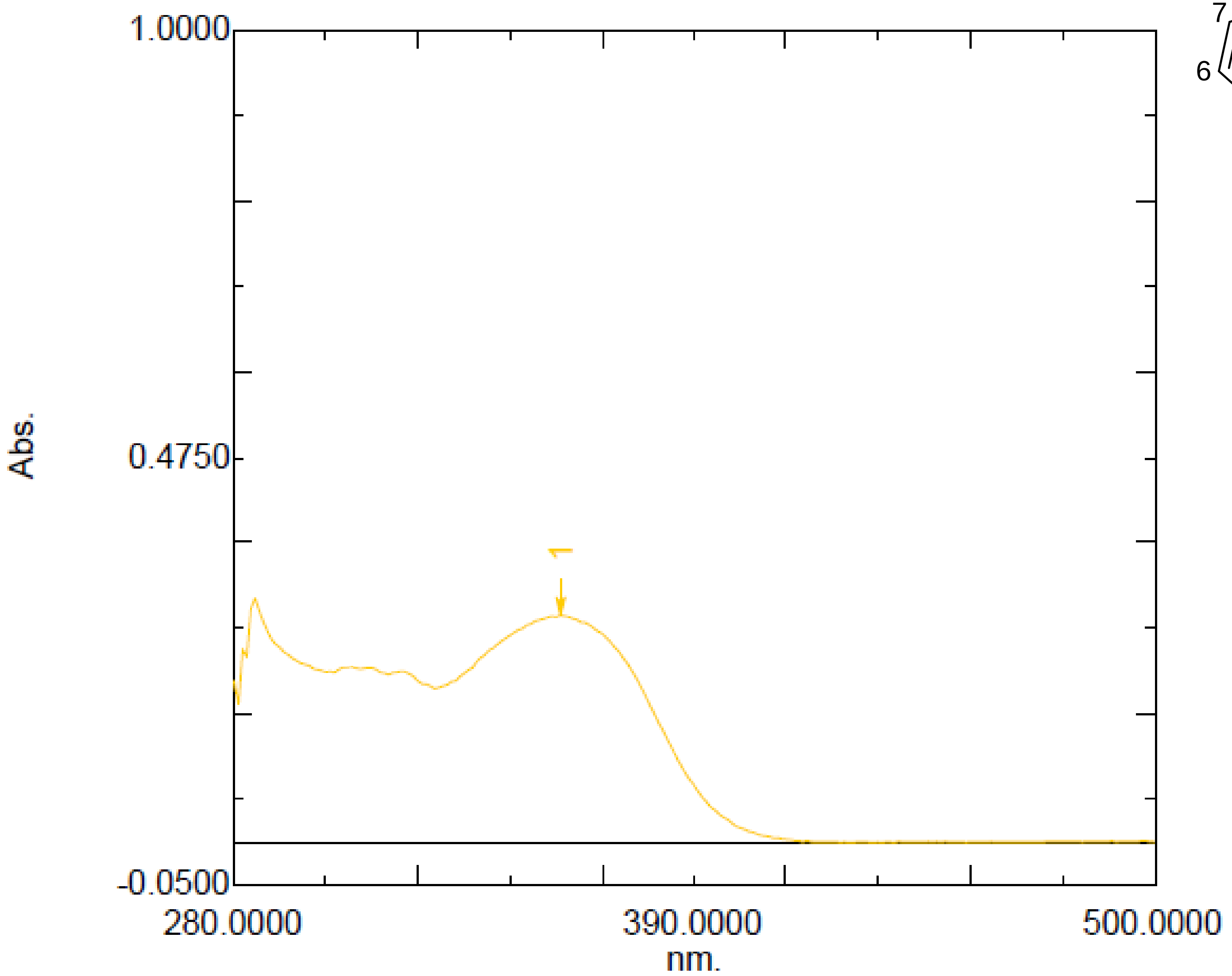

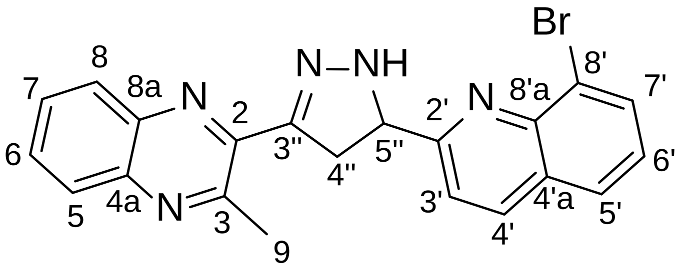

λ	absorbance	logε
359	0.2798	4.37

UV spectrum of **B8c**

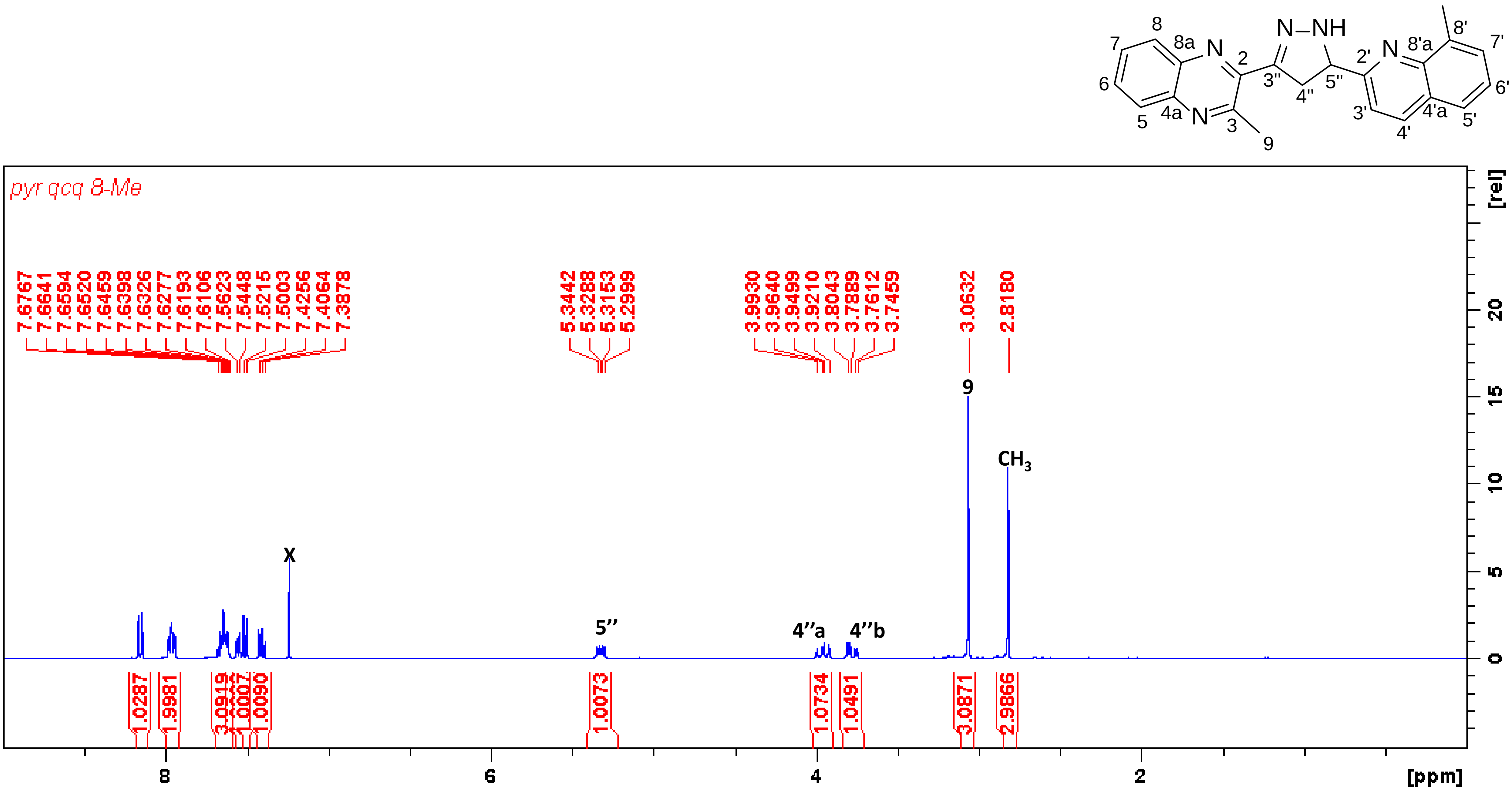

^{1}H NMR spectrum of **B8d**

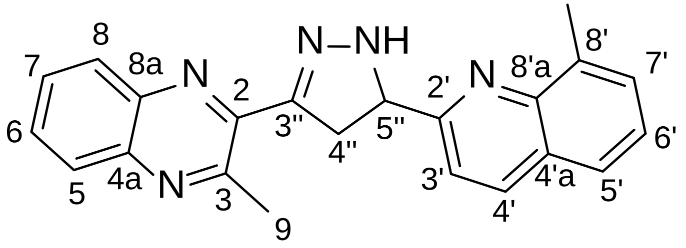

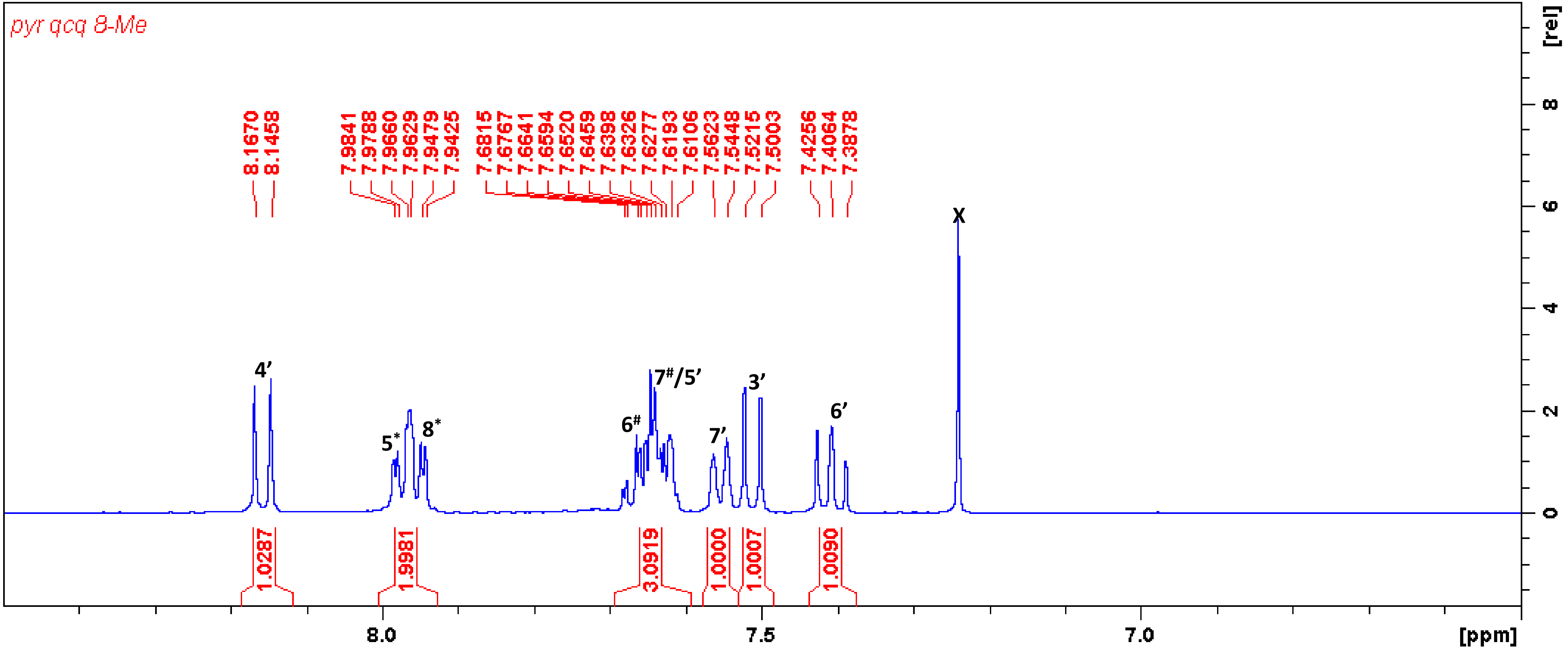

*, # Indicates assignments are interchangeable

Expanded ^{1}H NMR spectrum of **B8d**

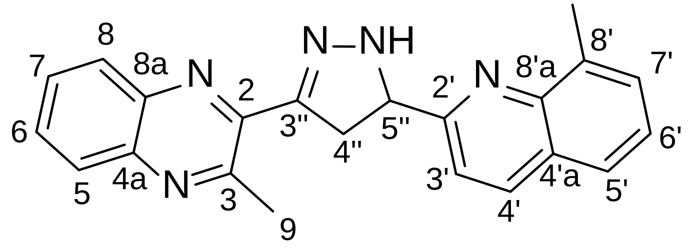

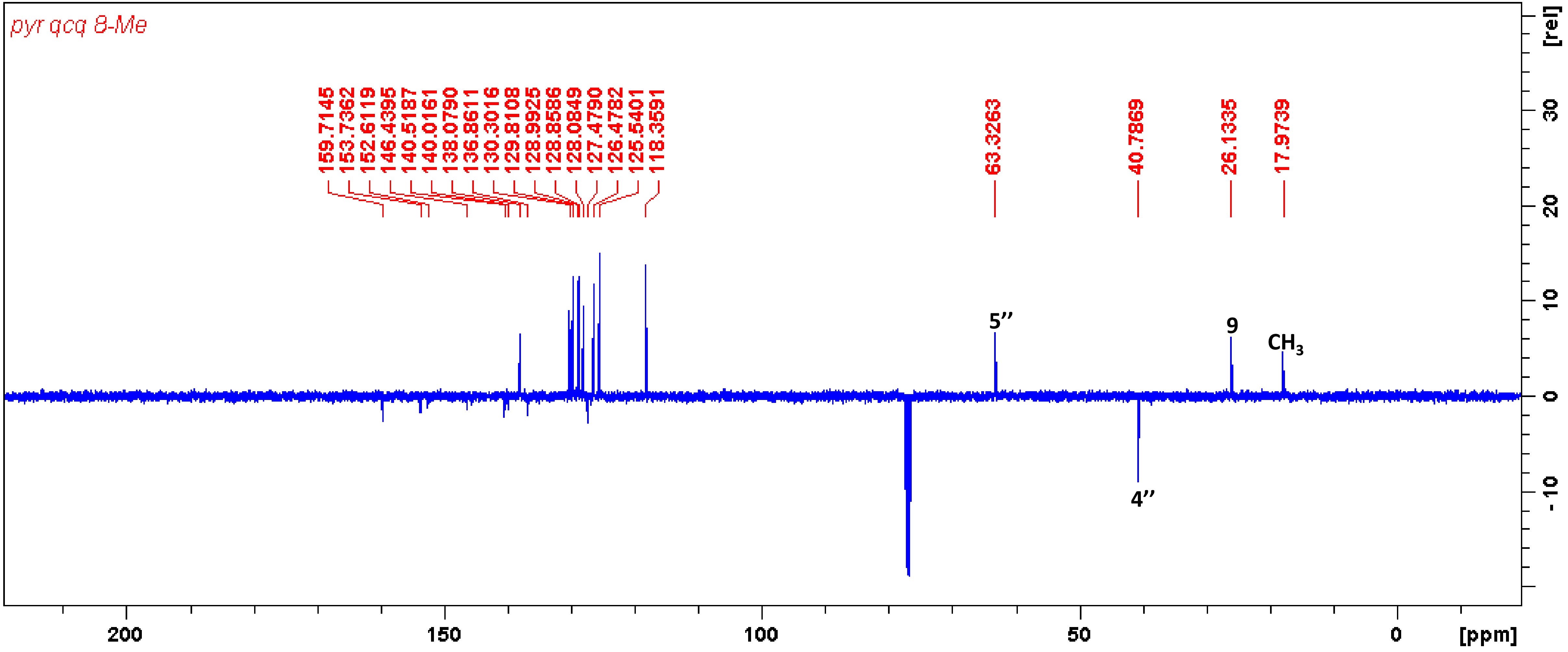

^{13}C NMR spectrum of **B8d**

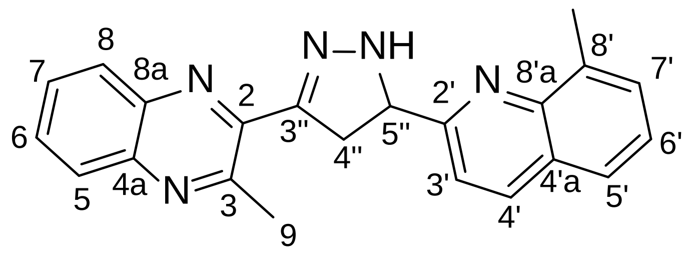

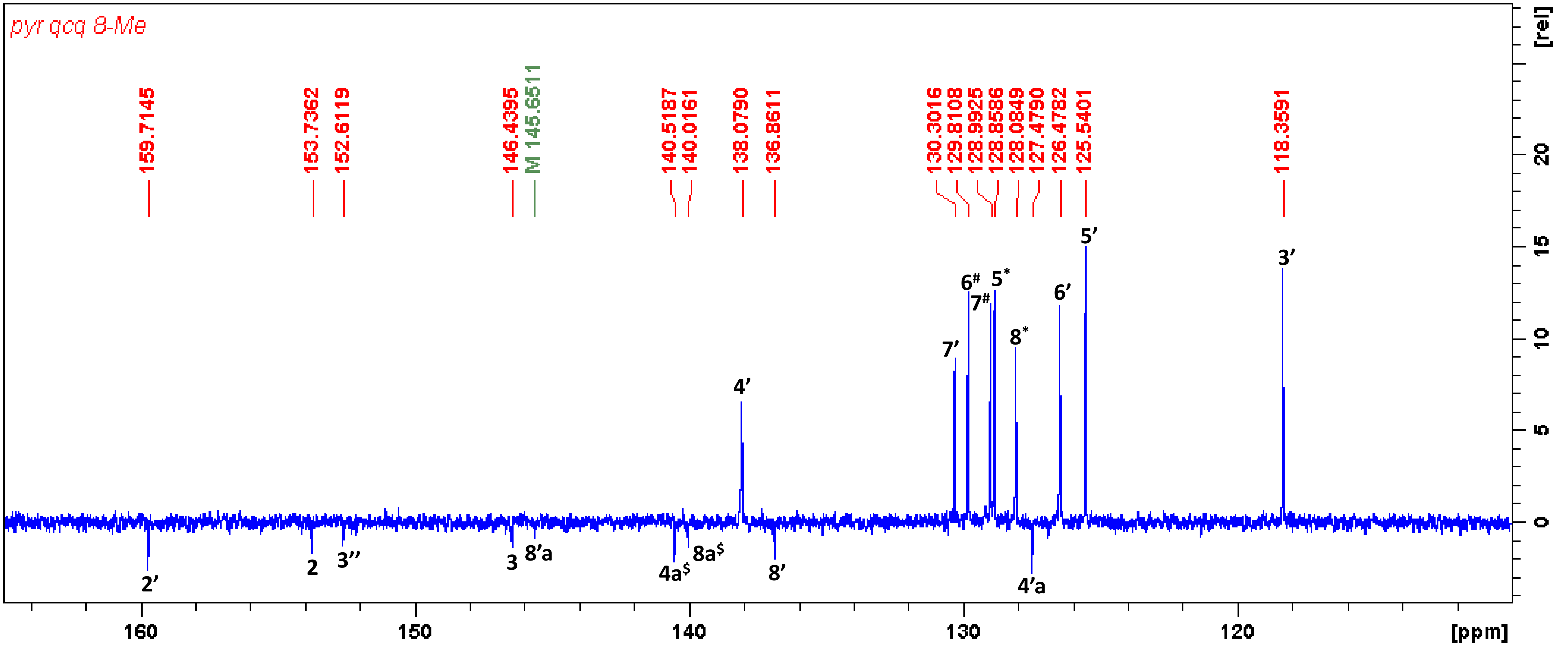

*, #, $ Indicates assignments are interchangeable

Expanded ^{13}C NMR spectrum of **B8d**

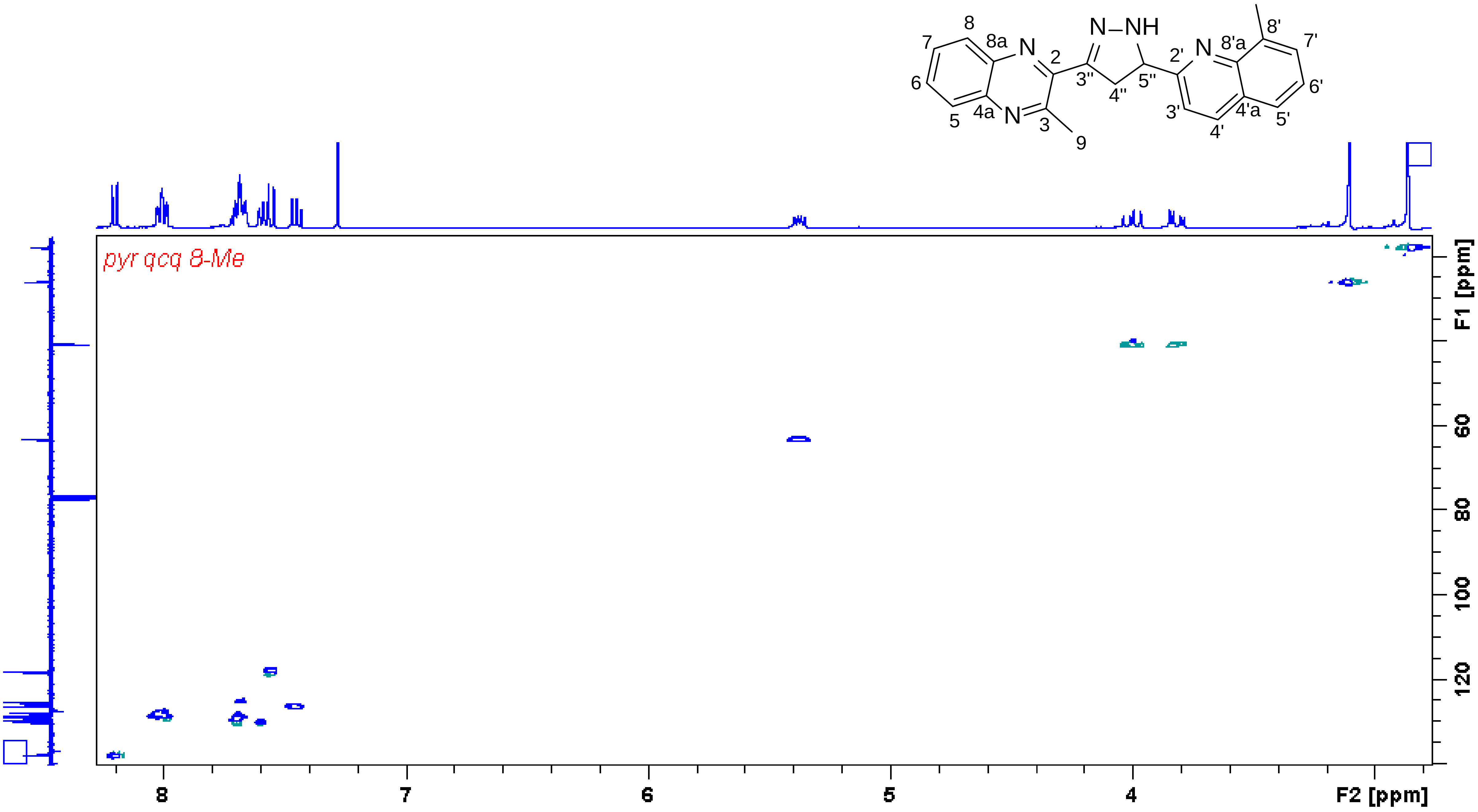
pyr qcq 8-Me
F1 [ppm]
F2 [ppm]
N–NH
N
N
N
8
7
6
5
4a
8a
2
3
9
3''
4''
5''
2'
8'a
8'
7'
6'
5'
4'a
4'
3'

HSQC of **B8d**

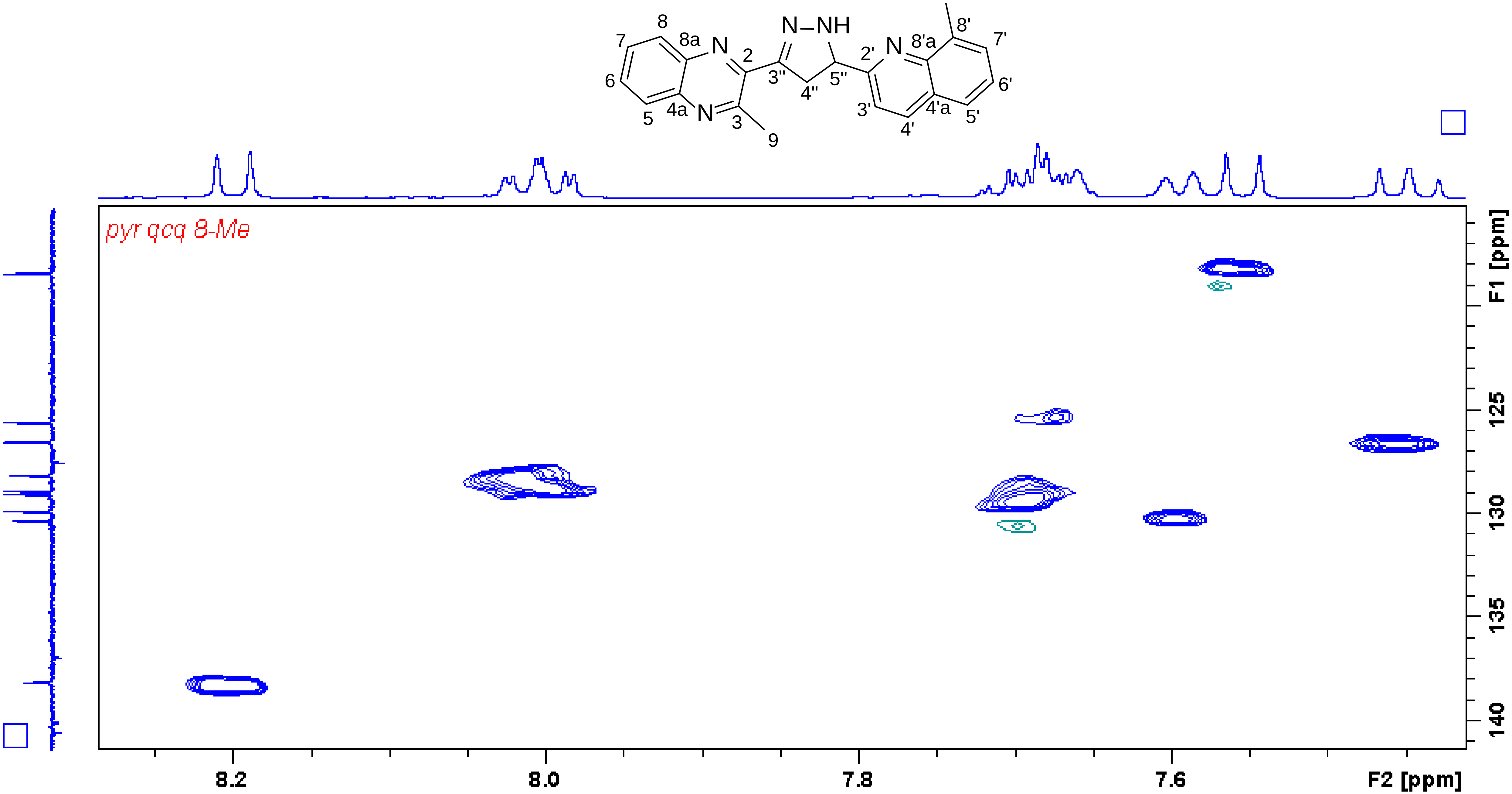

Expanded HSQC of **B8d**

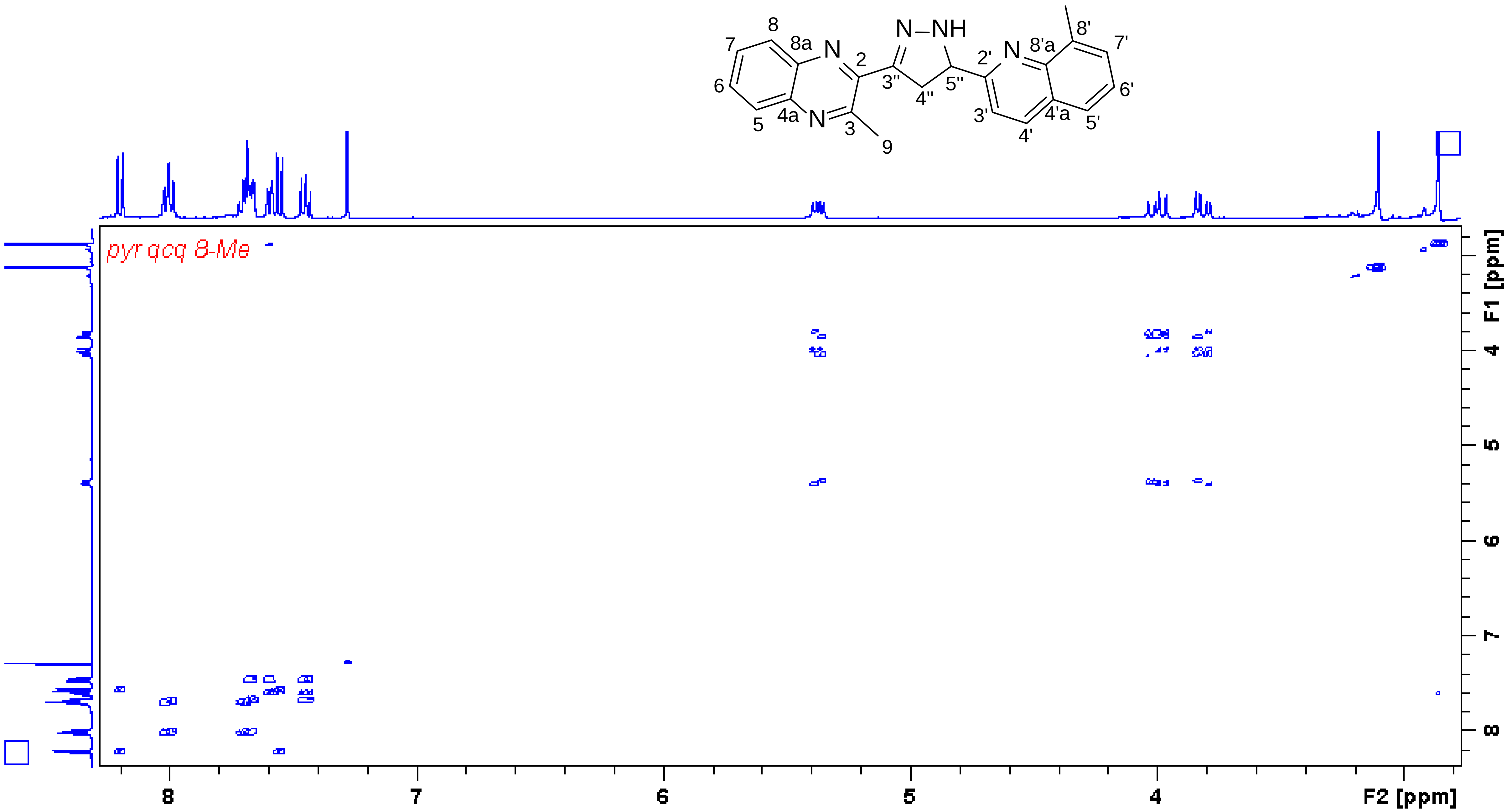
8
7
8a
N
2
N–NH
N
8'a
8'
7'
6
3''
5''
2'
6'
4''
5
4a
N
3
9
3'
4'
4'a
5'
pyr qcq 8-Me
F1 [ppm]
F2 [ppm]
8
7
6
5
4

COSY of **B8d**

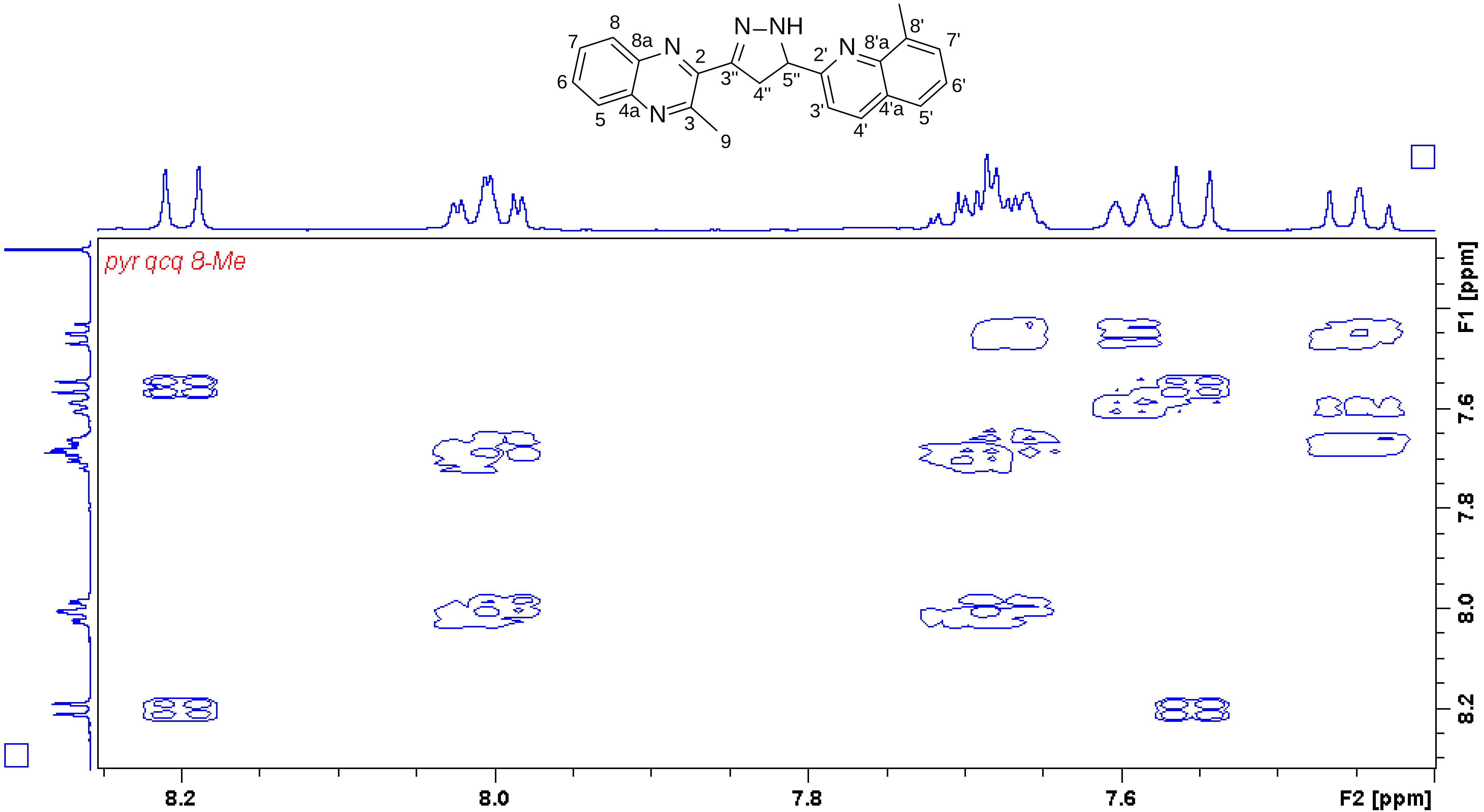

Expanded COSY of **B8d**

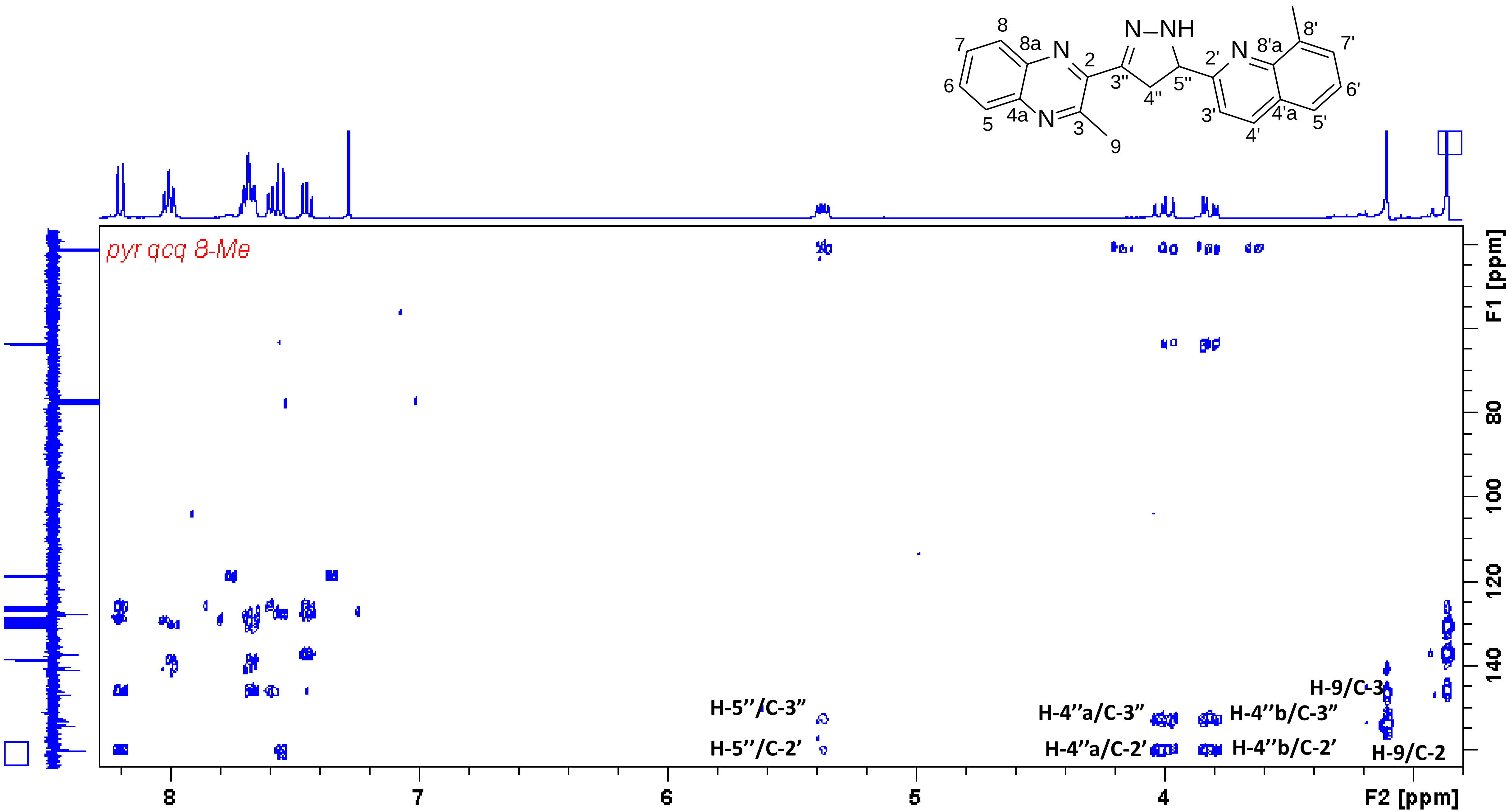

pyr qcq 8-Me
H-5''/C-3''
H-5''/C-2'
H-4''a/C-3''
H-4''b/C-3''
H-4''a/C-2'
H-4''b/C-2'
H-9/C-3
H-9/C-2
F1 [ppm]
F2 [ppm]

HMBC of **B8d**

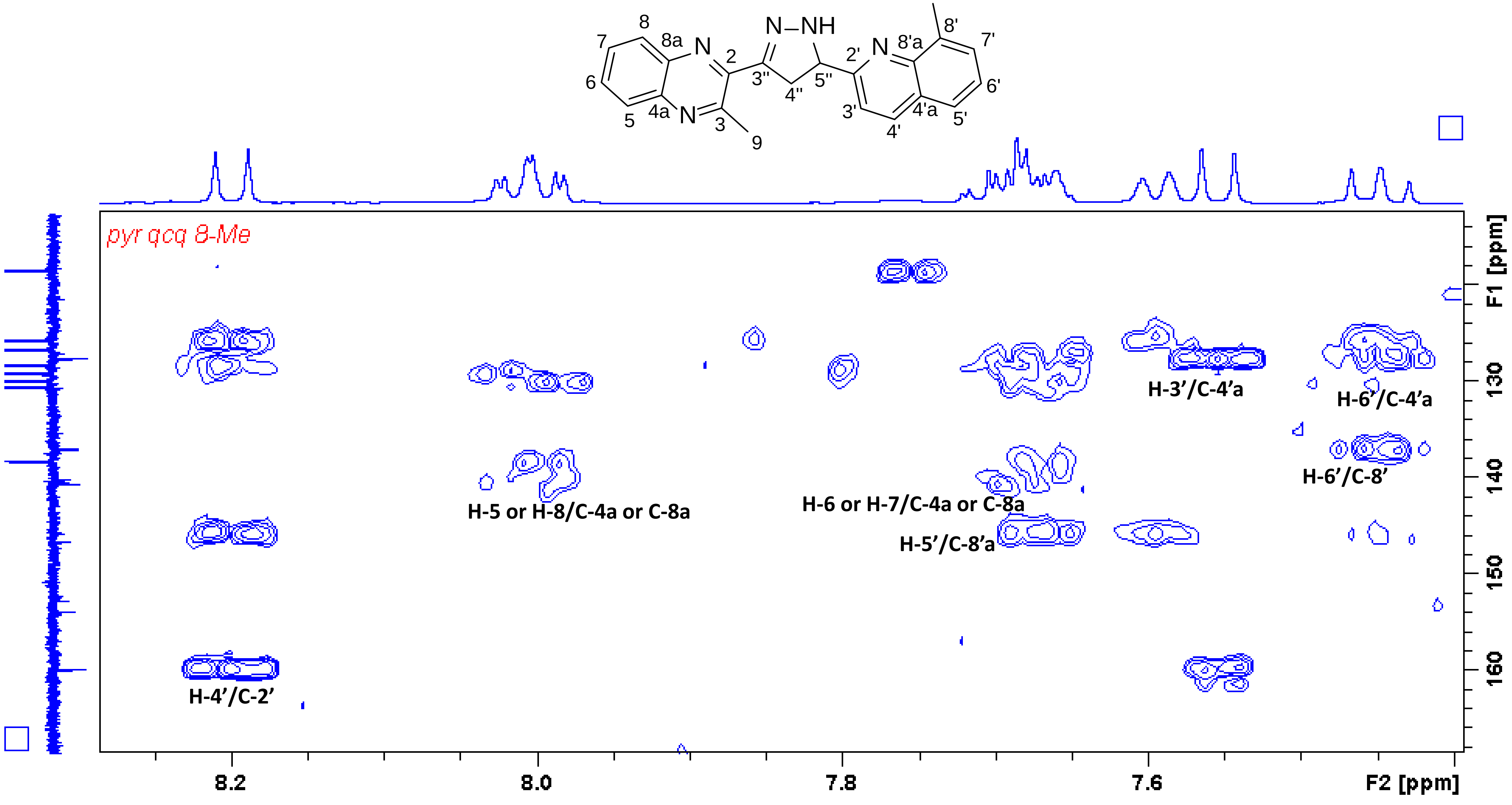

Expanded HMBC of **B8d**

Elemental Composition Report

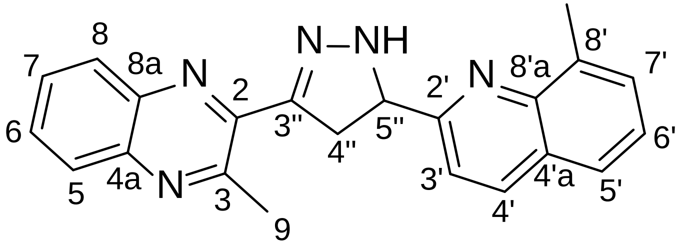

Single Mass Analysis

Tolerance = 5.0 PPM / DBE: min = -1.5, max = 100.0
Element prediction: Off
Number of isotope peaks used for i-FIT = 3

Monoisotopic Mass, Even Electron Ions
4 formula(e) evaluated with 1 results within limits (up to 20 closest results for each mass)
Elements Used:
C: 20-25 H: 15-20 N: 0-5 Na: 0-1
Py-QCQ 8-Me 28 (0.911) Cm (1:61)
TOF MS ES+

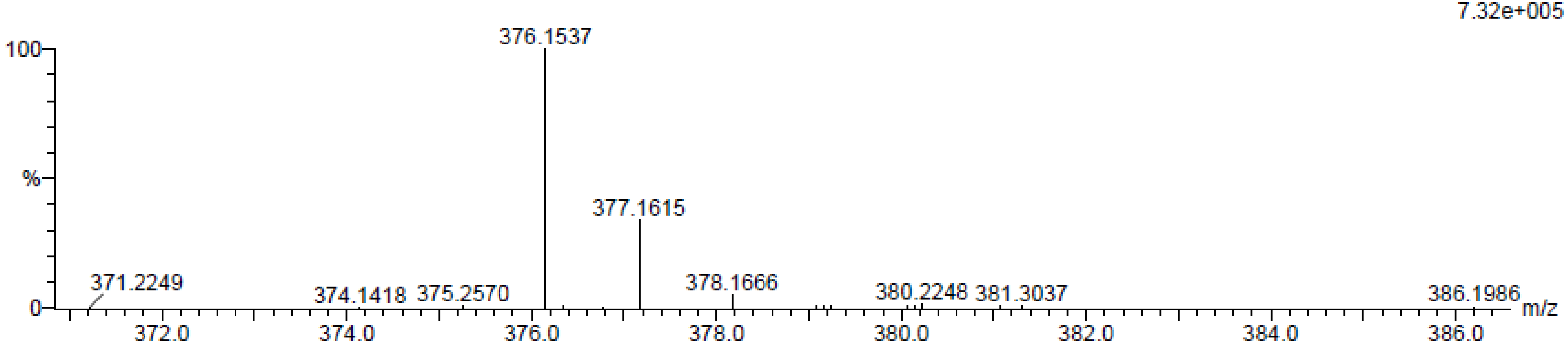

Minimum:				-1.5			
Maximum:		5.0	5.0	100.0			
Mass	Calc. Mass	mDa	PPM	DBE	i-FIT	i-FIT (Norm)	Formula
376.1537	376.1538	-0.1	-0.3	15.5	68.2	0.0	C22 H19 N5 Na

High resolution mass spectrum of **B8d**

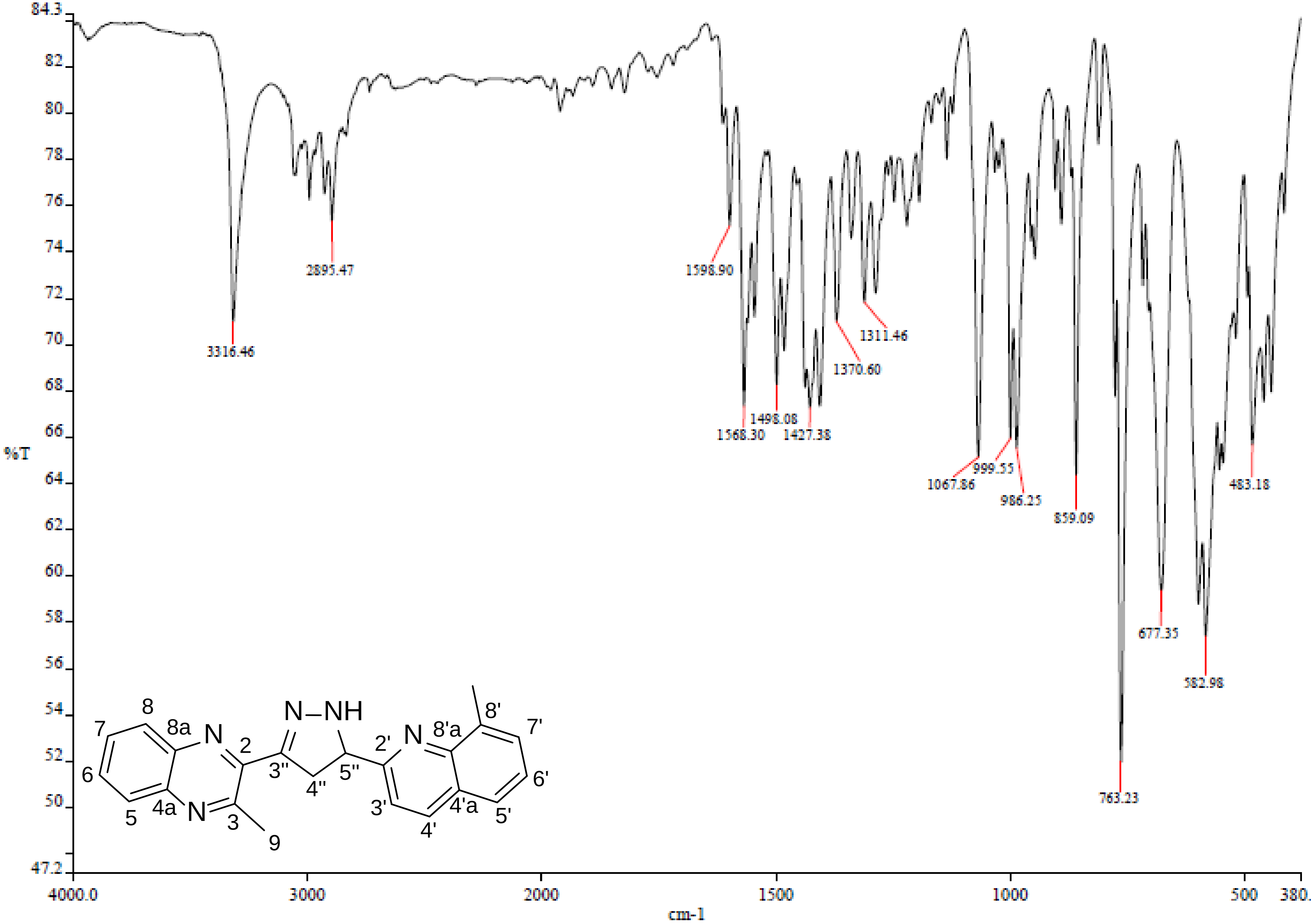

FTIR spectrum of **B8d**

Overlay Spectrum Graph Report

06/10/2017 12:09:42 PM

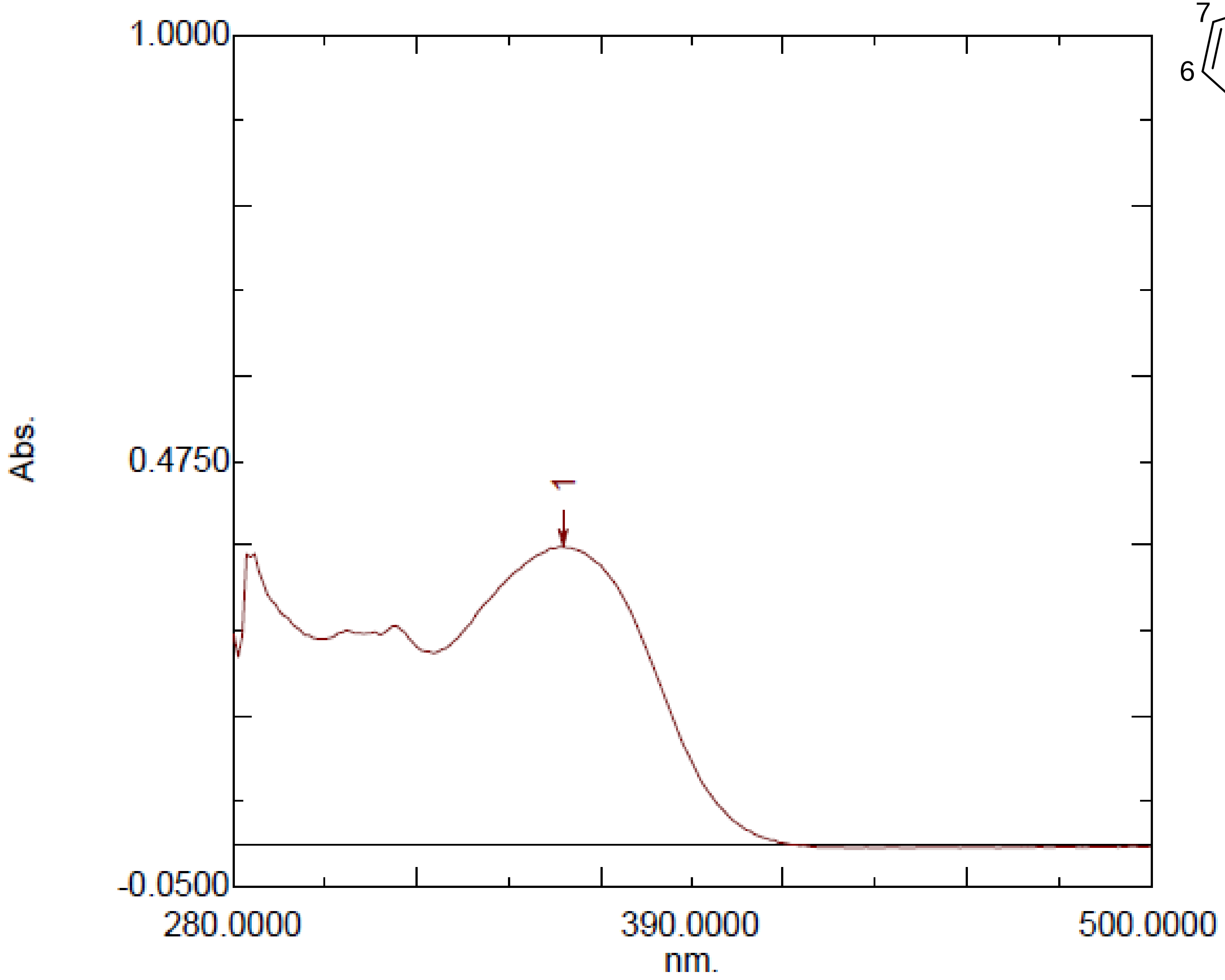

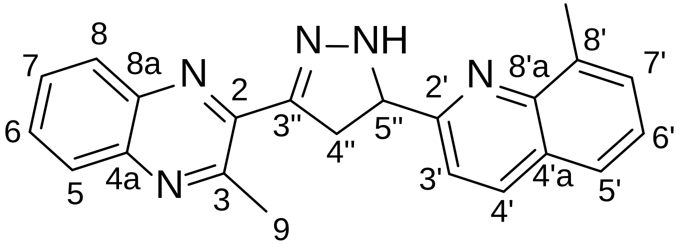

λ	absorbance	logε
358	0.3686	4.42

UV spectrum of **B8d**

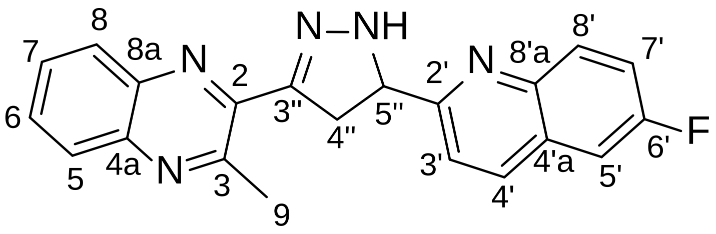

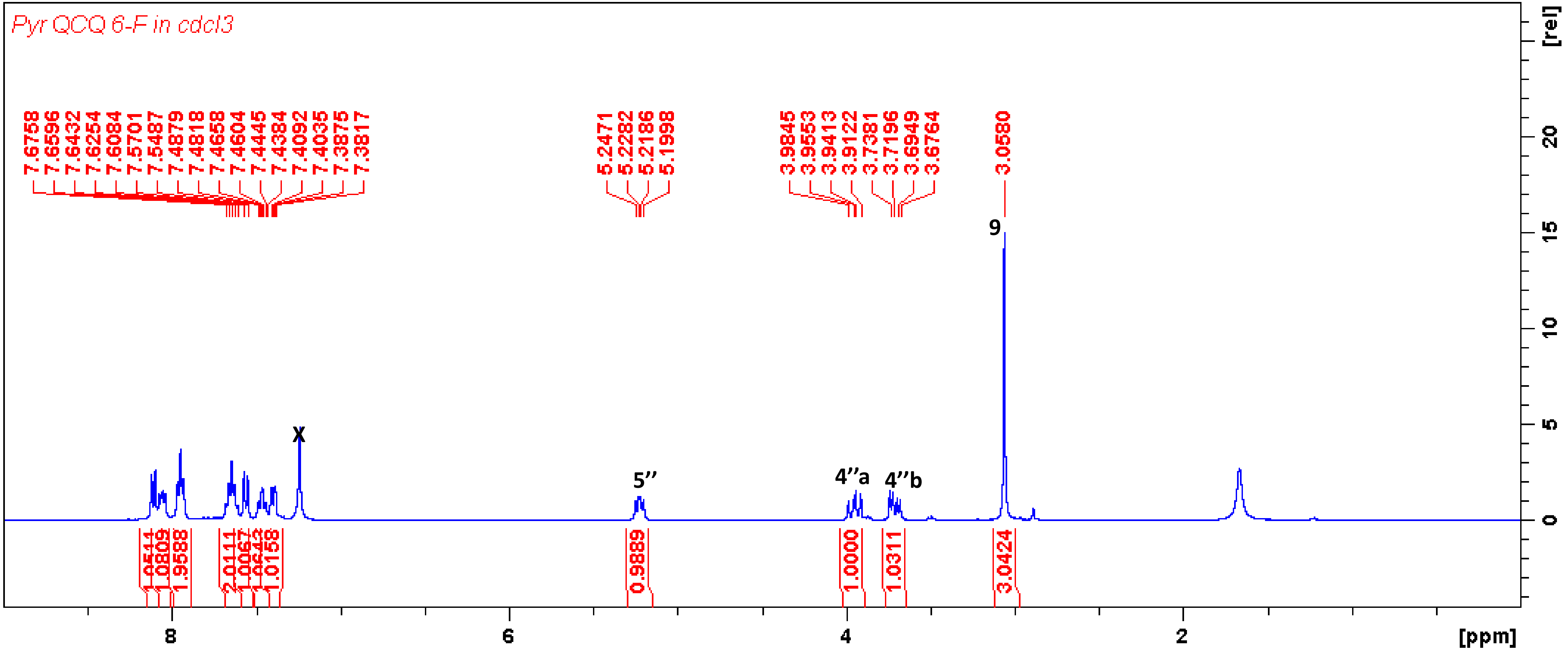

^{1}H NMR spectrum of **B8e**

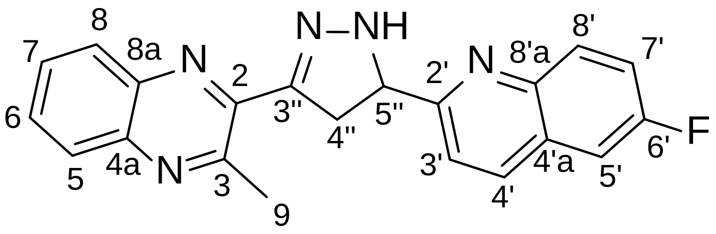

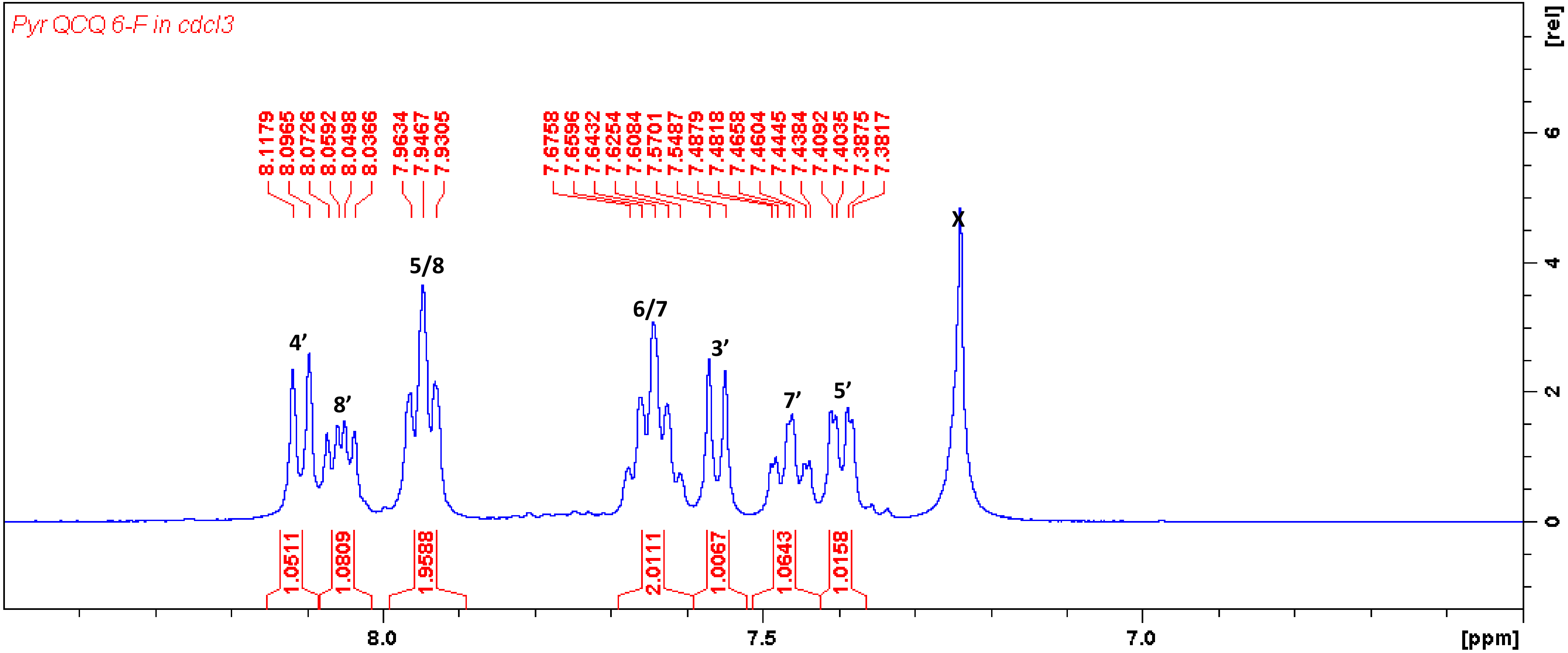

Expanded ^{1}H NMR spectrum of **B8e**

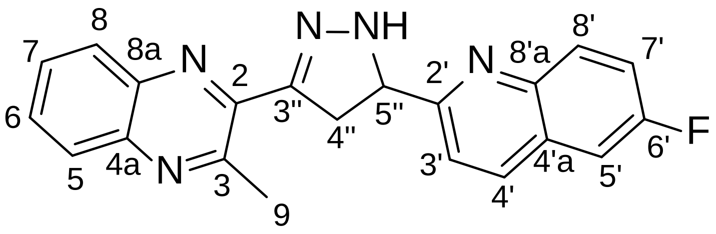

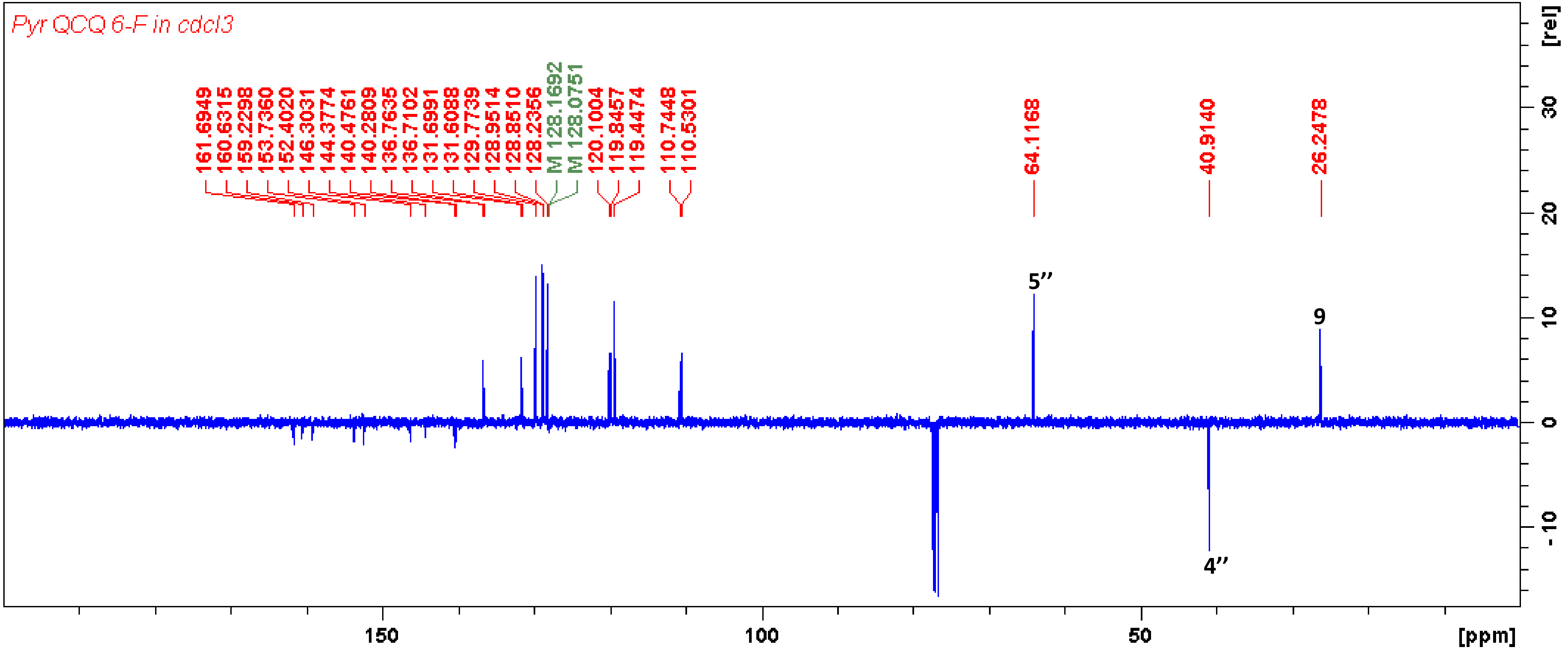

^{13}C NMR spectrum of **B8e**

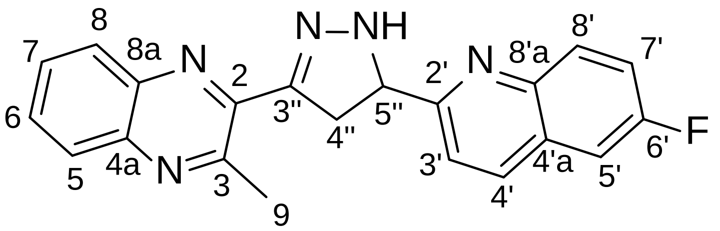

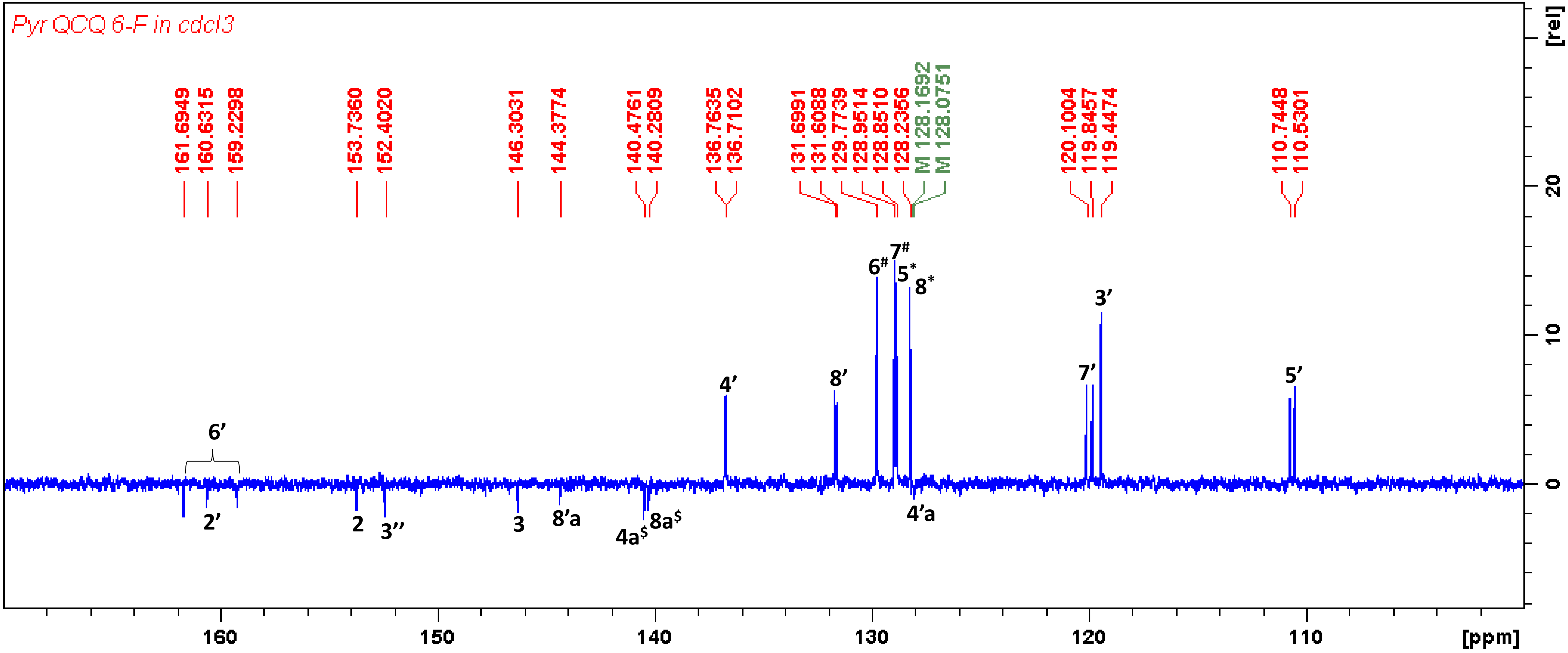

*, #, $ Indicates assignments are interchangeable

Expanded ^{13}C NMR spectrum of **B8e**

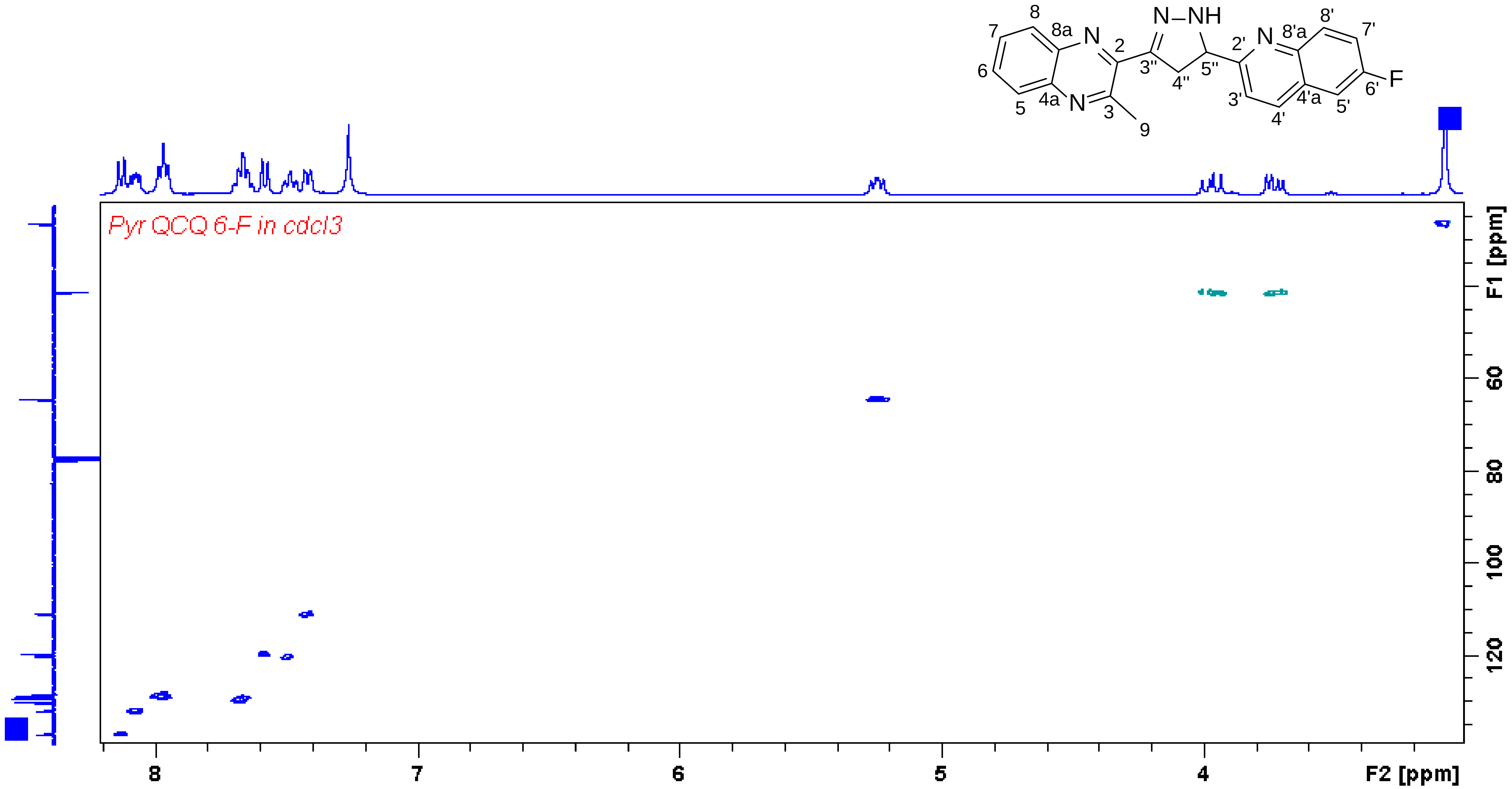

HSQC of **B8e**

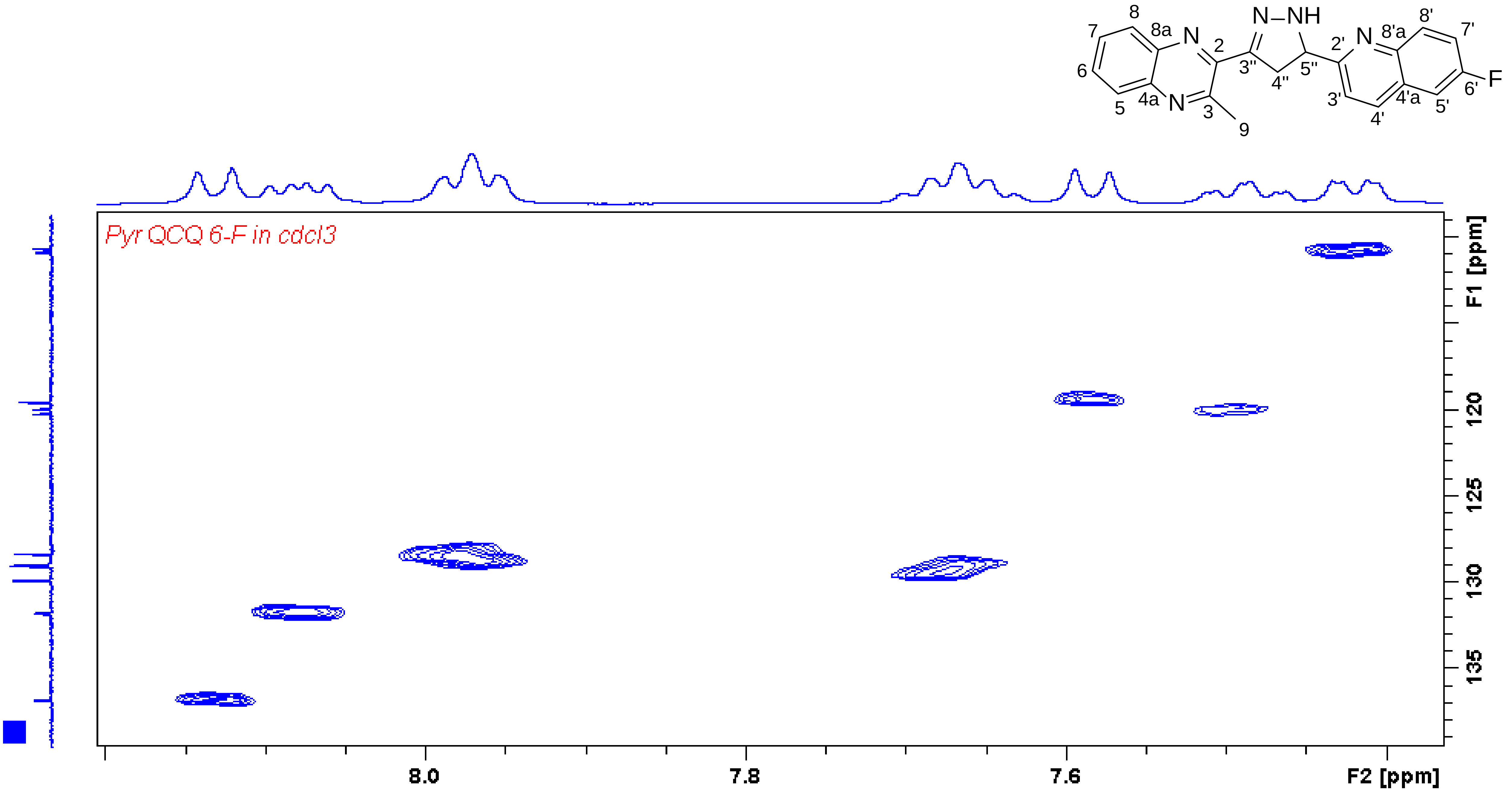

Expanded HSQC of **B8e**

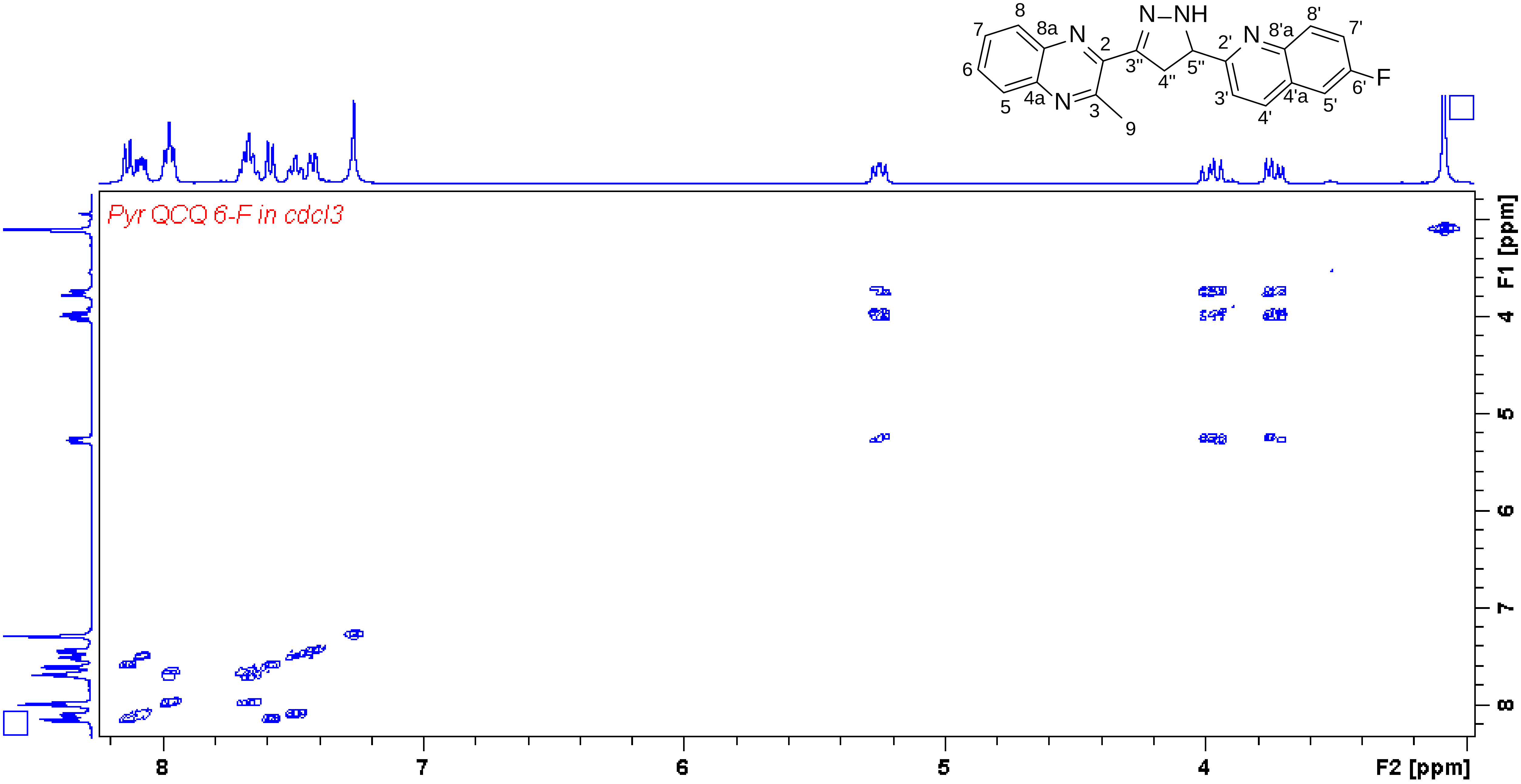
Pyr QCQ 6-F in cdcl3
F1 [ppm]
F2 [ppm]
8
7
6
5
4
N
N
N–NH
N
F
2
3
9
4a
5
6
7
8
8a
3''
4''
5''
2'
3'
4'
4'a
5'
6'
7'
8'
8'a

COSY of **B8e**

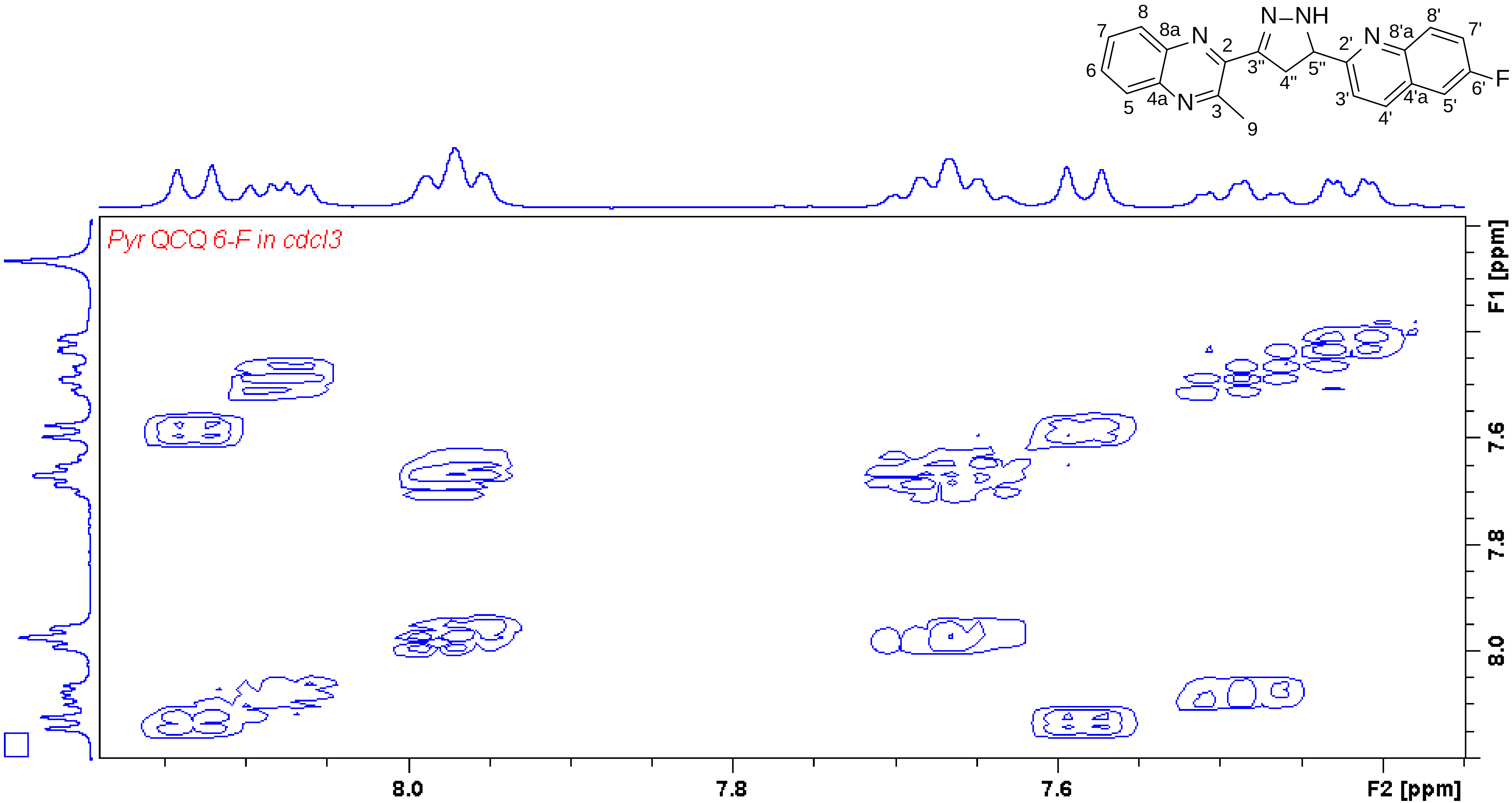

Expanded COSY of **B8e**

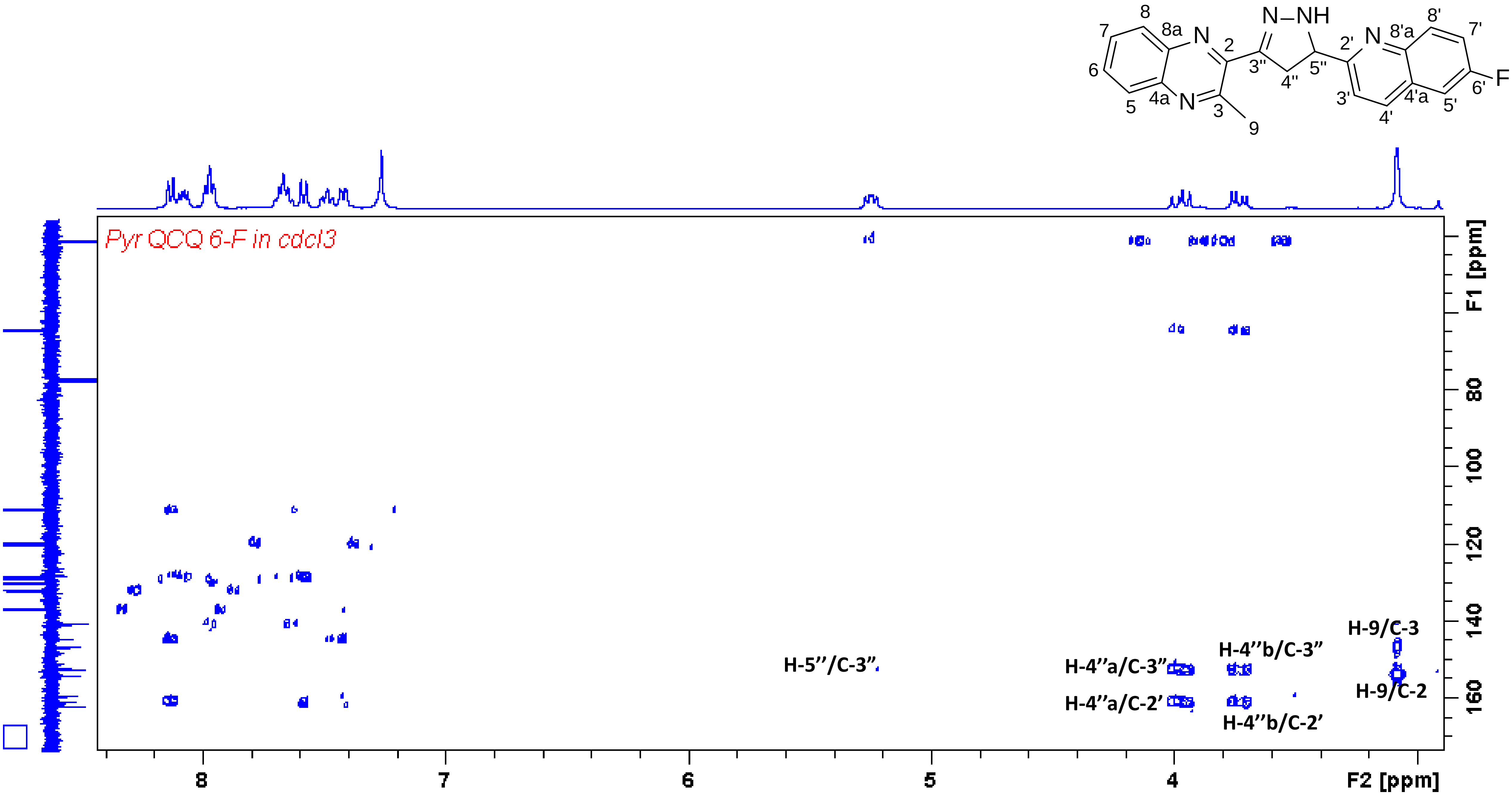

8
7
6
5
8a
4a
N
N
2
3
9
N–NH
3''
4''
5''
2'
N
8'a
8'
7'
6'
F
3'
4'
4'a
5'
Pyr QCQ 6-F in cdcl3
H-5''/C-3''
H-4''a/C-3''
H-4''b/C-3''
H-4''a/C-2'
H-4''b/C-2'
H-9/C-3
H-9/C-2
F1 [ppm]
80
100
120
140
160
8
7
6
5
4
F2 [ppm]

HMBC of **B8e**

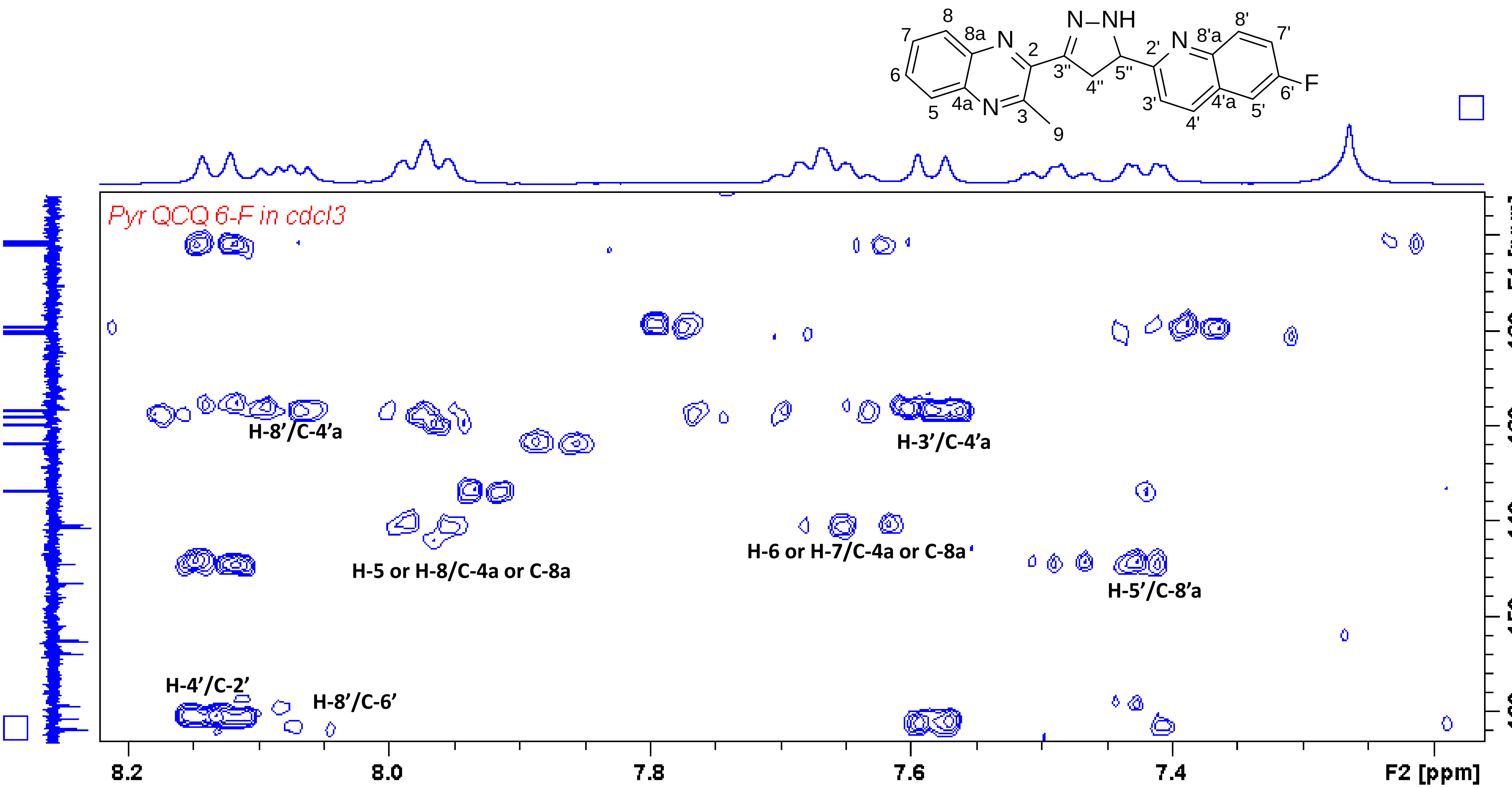

Expanded HMBC of **B8e**

Elemental Composition Report

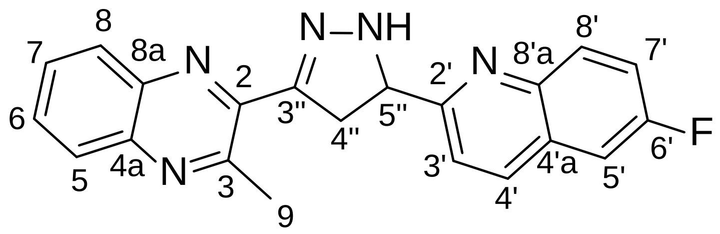

Single Mass Analysis

Tolerance = 5.0 PPM / DBE: min = -1.5, max = 100.0
Element prediction: Off
Number of isotope peaks used for i-FIT = 3

Monoisotopic Mass, Even Electron Ions
8 formula(e) evaluated with 1 results within limits (up to 20 closest results for each mass)
Elements Used:
C: 20-25 H: 15-20 N: 0-5 F: 0-1 Na: 0-1
Py-QCQ 6-F 2 (0.034) Cm (1:61)
TOF MS ES+

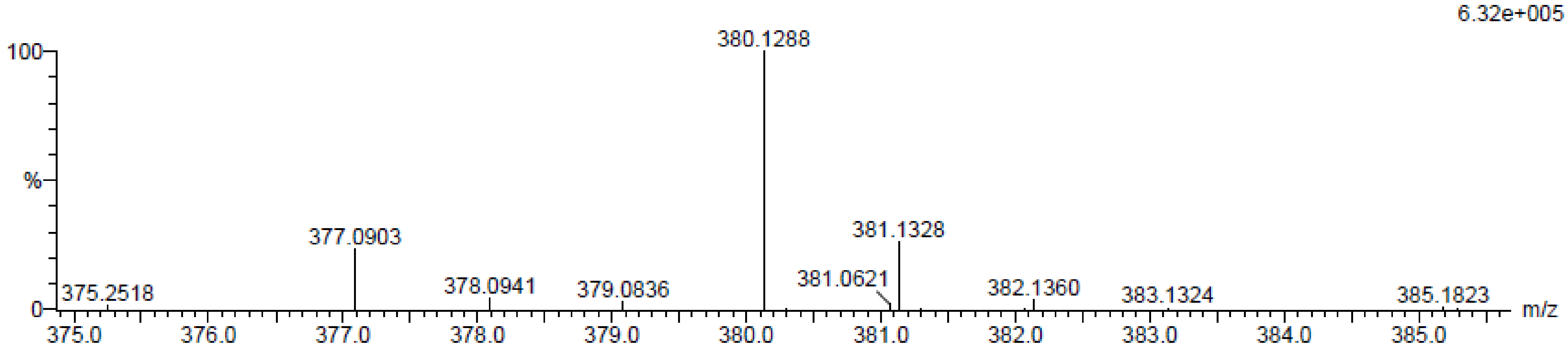

Minimum:				-1.5			
Maximum:		5.0	5.0	100.0			
Mass	Calc. Mass	mDa	PPM	DBE	i-FIT	i-FIT (Norm)	Formula
380.1288	380.1287	0.1	0.3	15.5	85.7	0.0	C21 H16 N5 F Na

High resolution mass spectrum of **B8e**

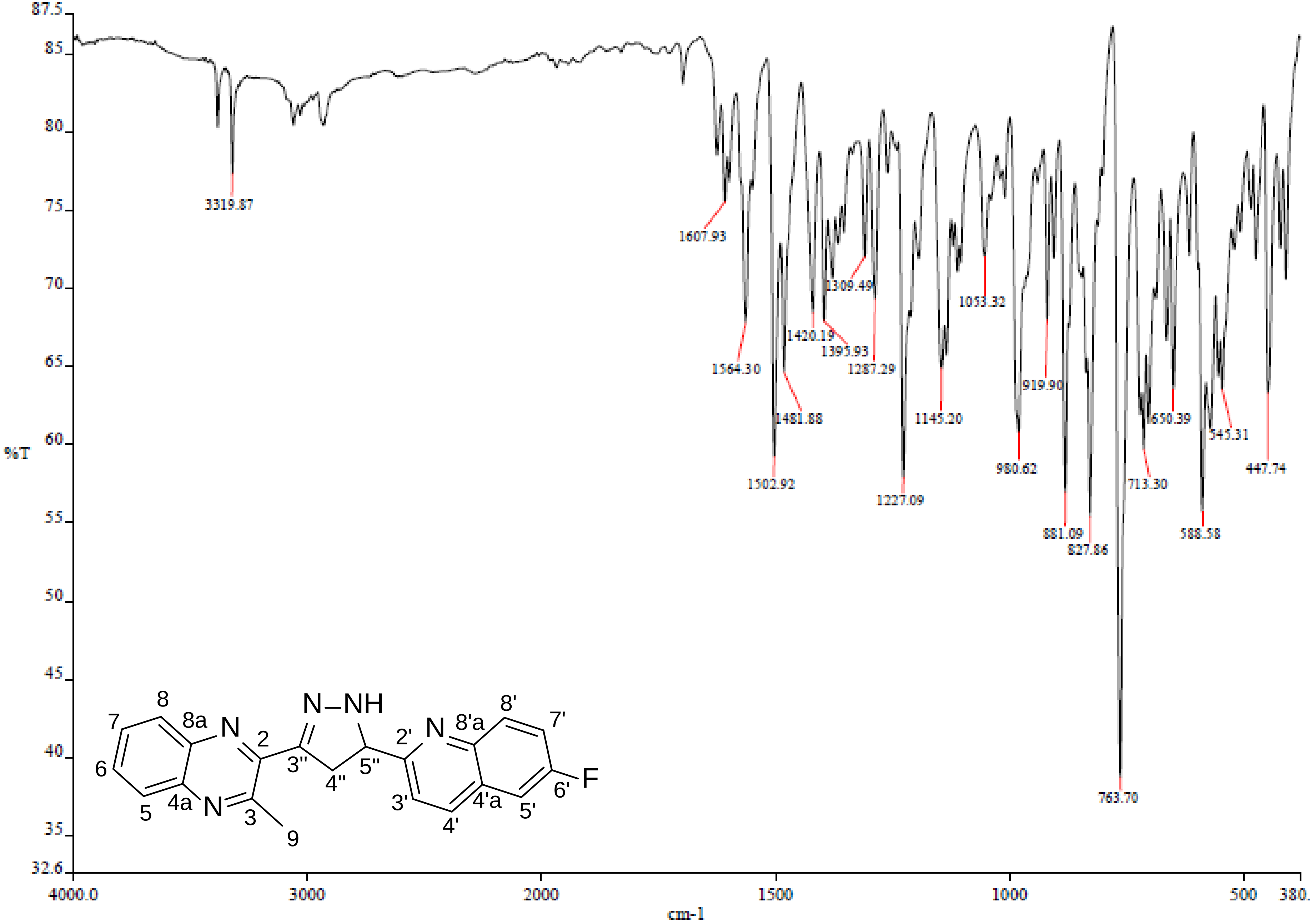

FTIR spectrum of **B8e**

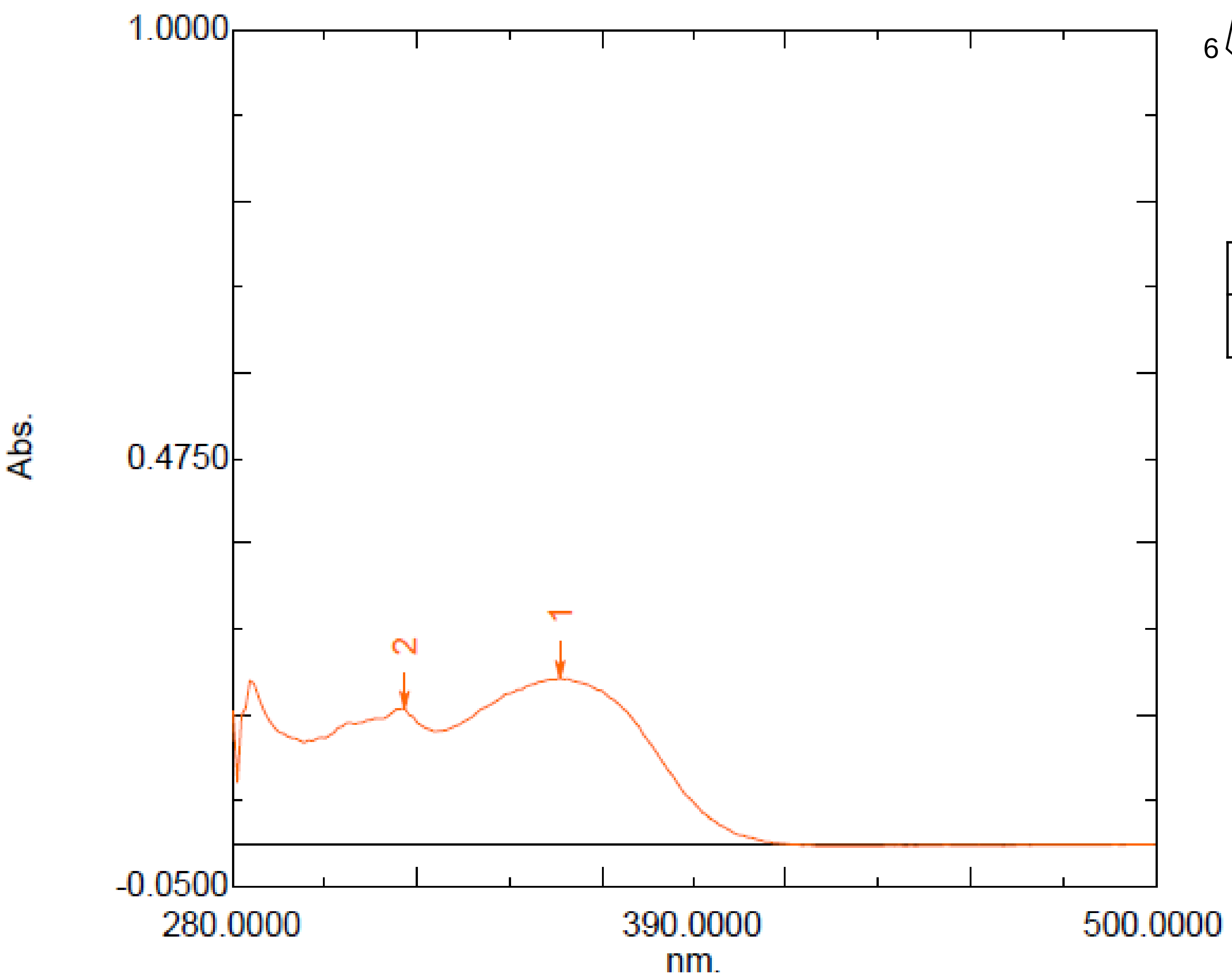

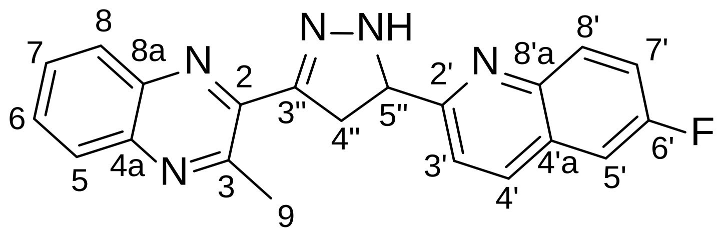

λ	absorbance	logε
358	0.2051	4.17

UV spectrum of **B8e**

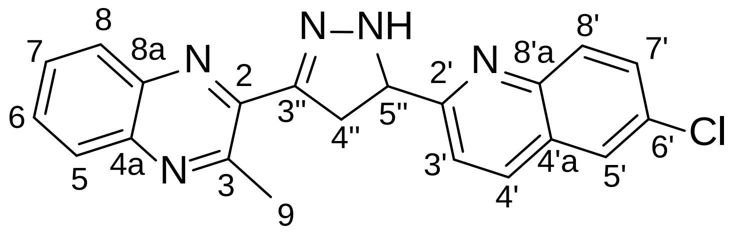

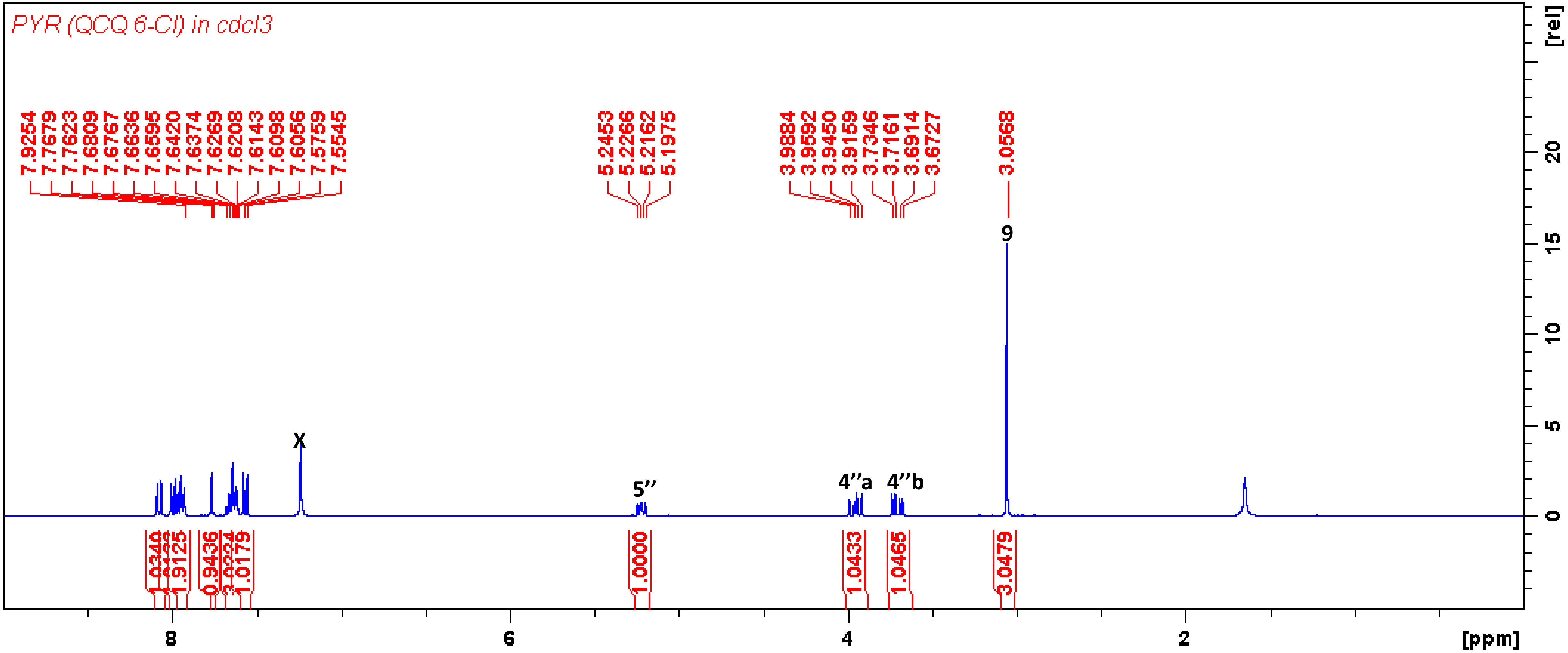

^{1}H NMR spectrum of **B8f**

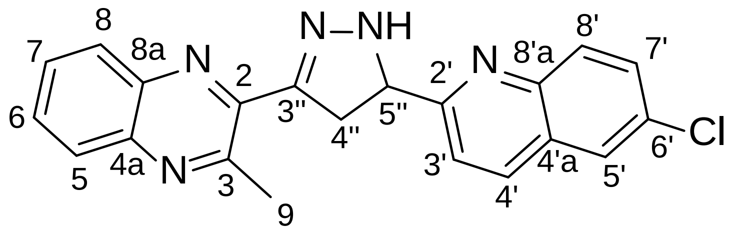

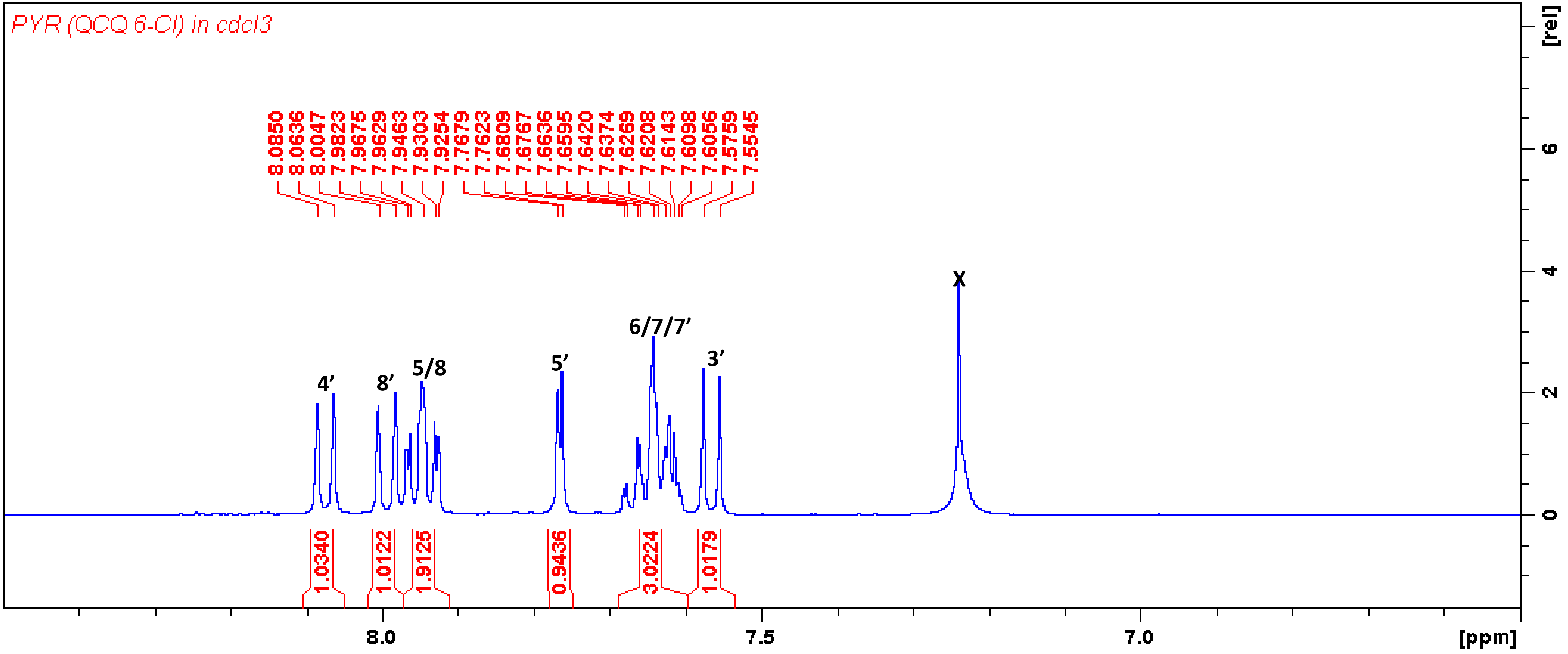

Expanded ^{1}H NMR spectrum of **B8f**

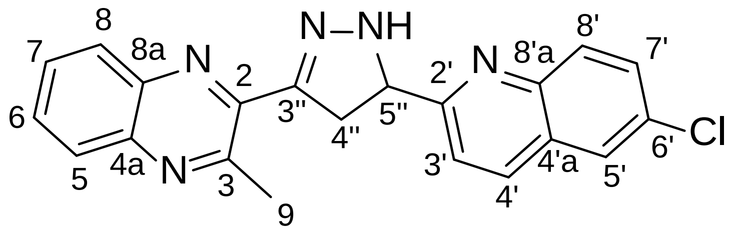

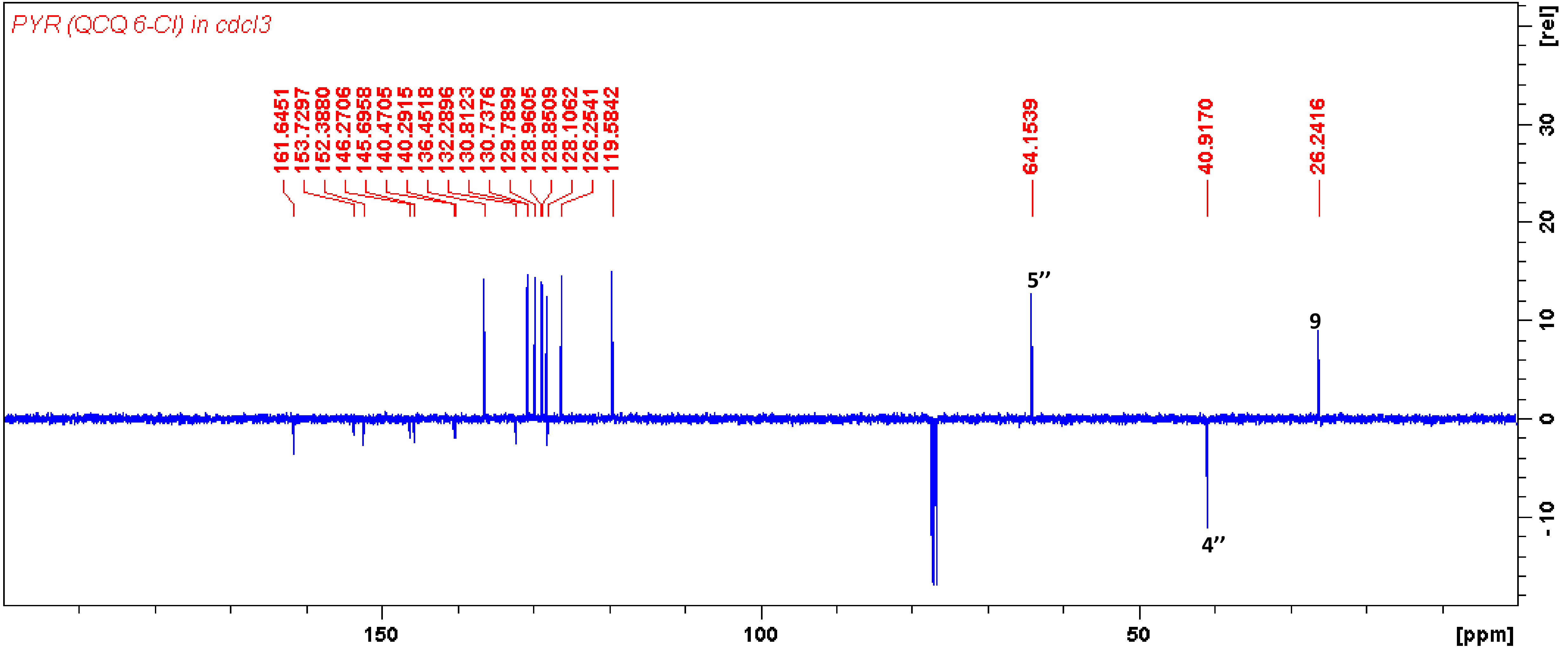

^{13}C NMR spectrum of **B8f**

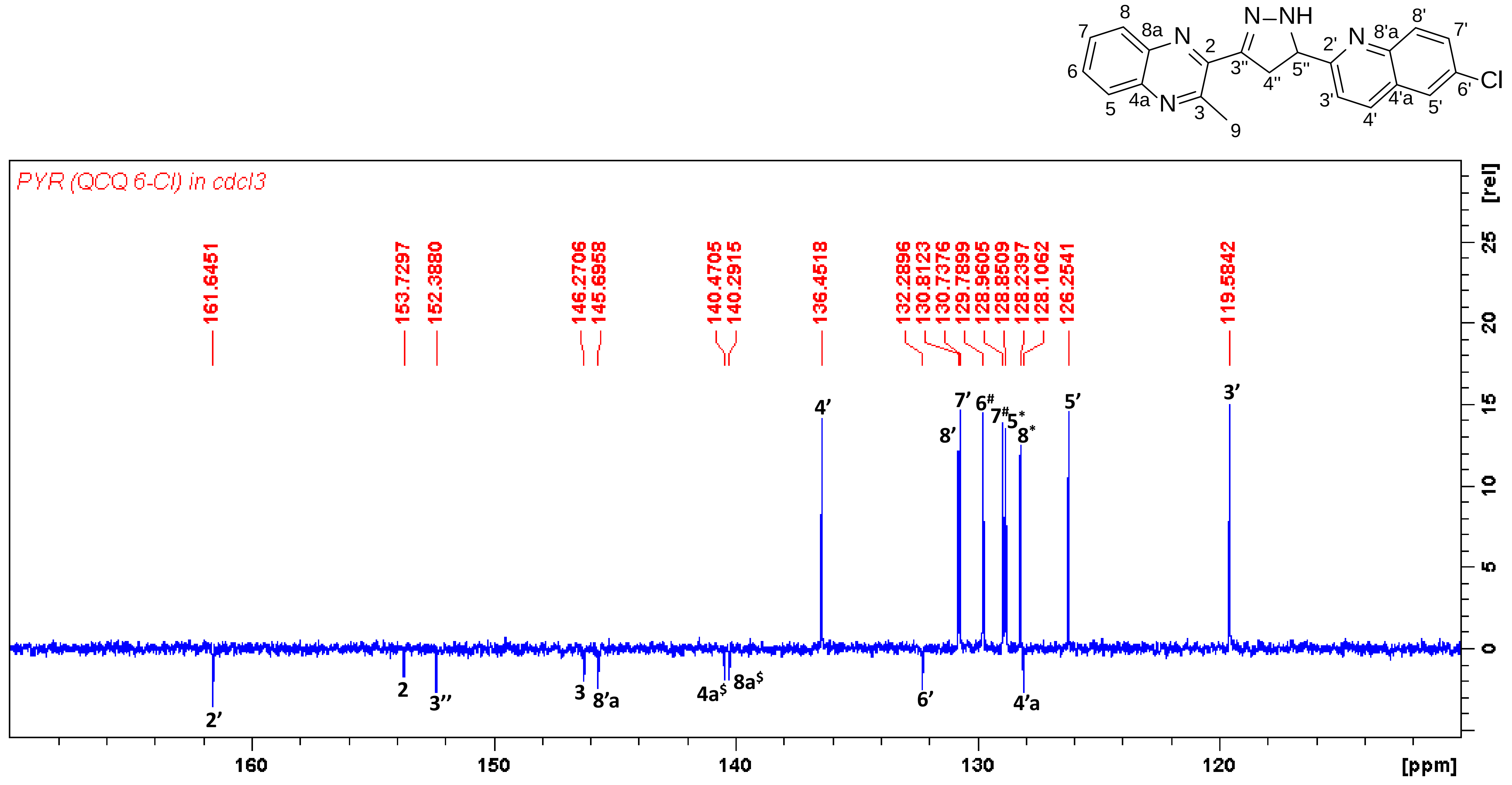

*, #, $ Indicates assignments are interchangeable

Expanded ^{13}C NMR spectrum of **B8f**

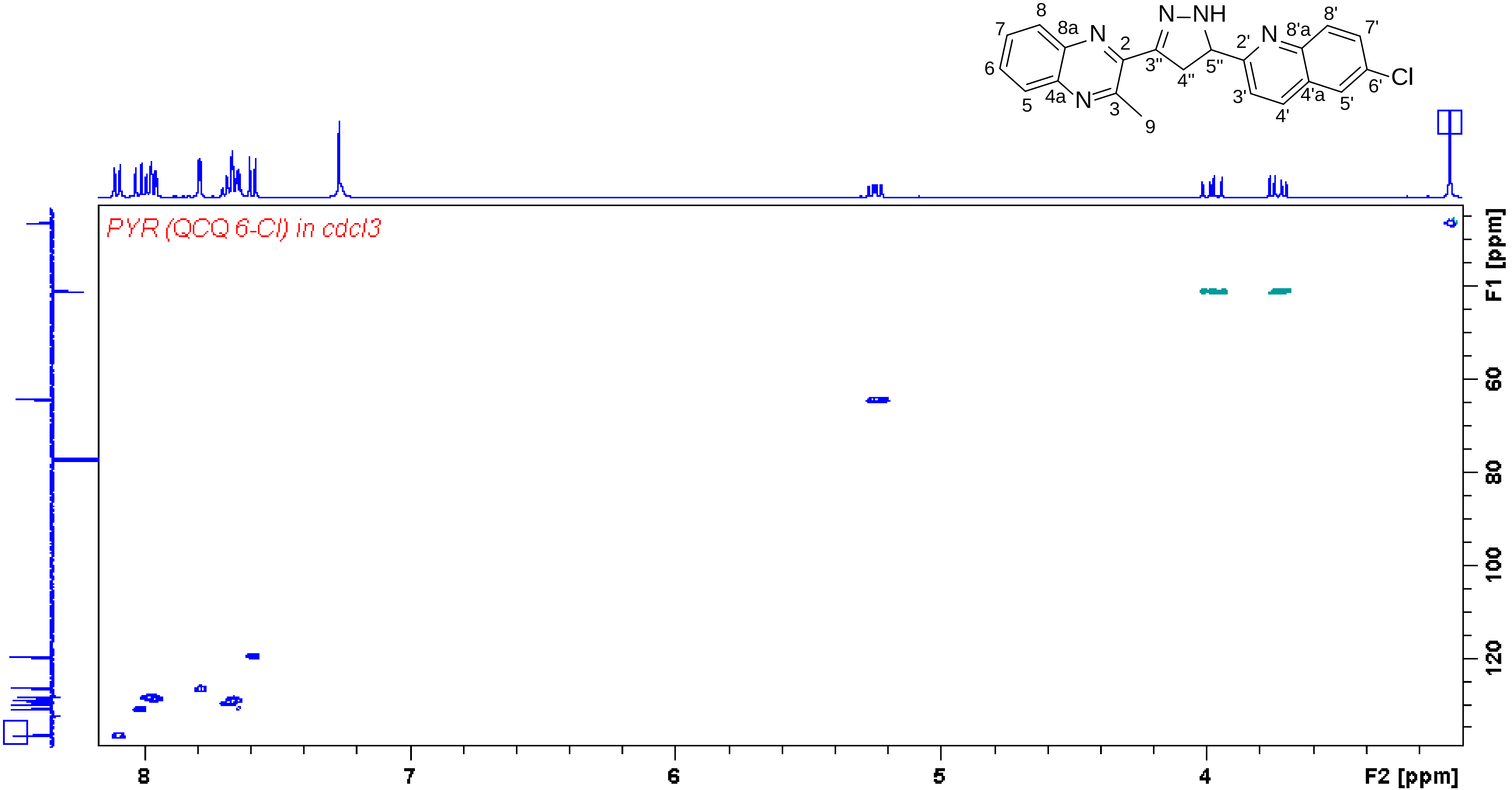

HSQC of **B8f**

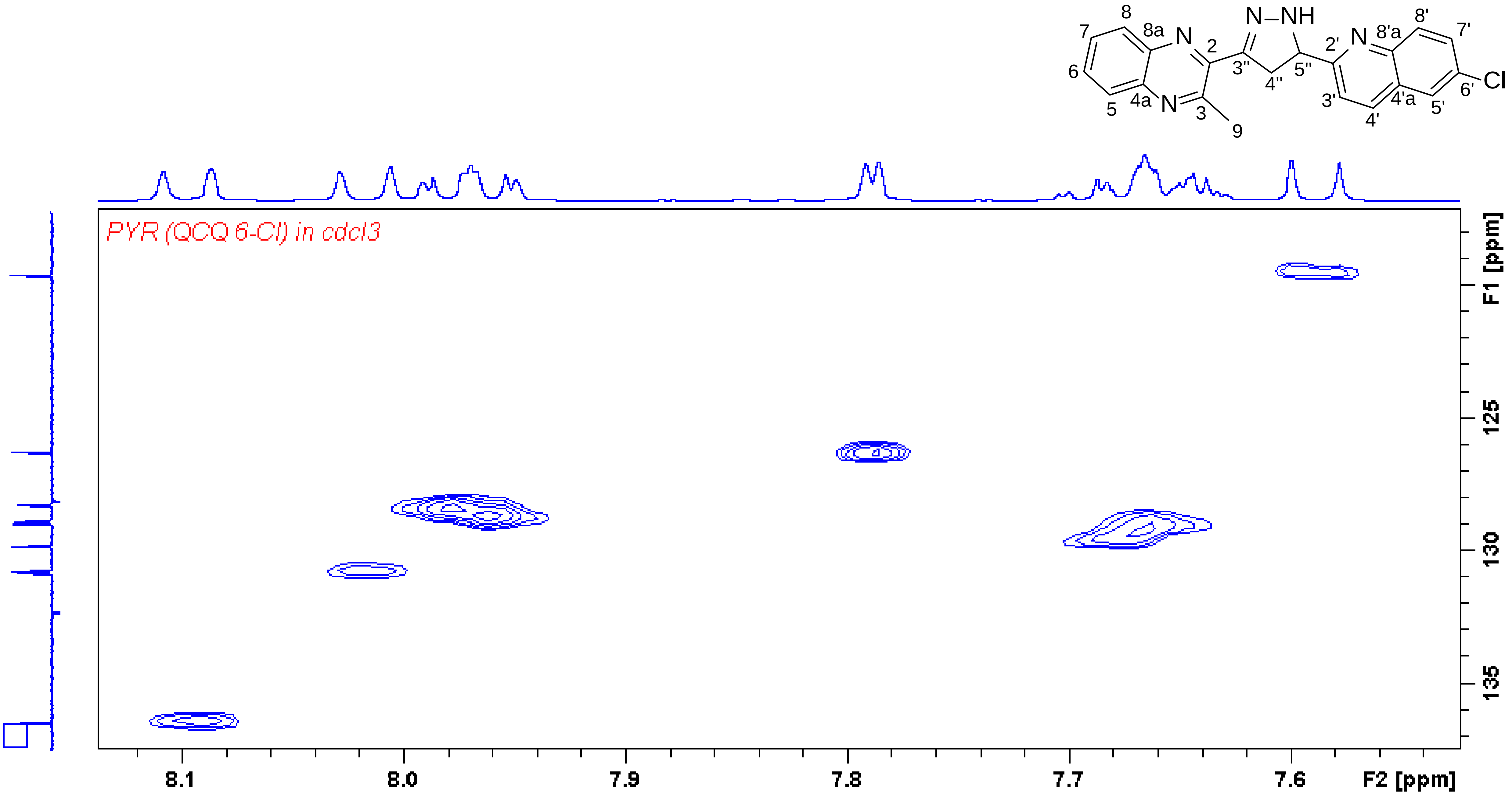

Expanded HSQC of **B8f**

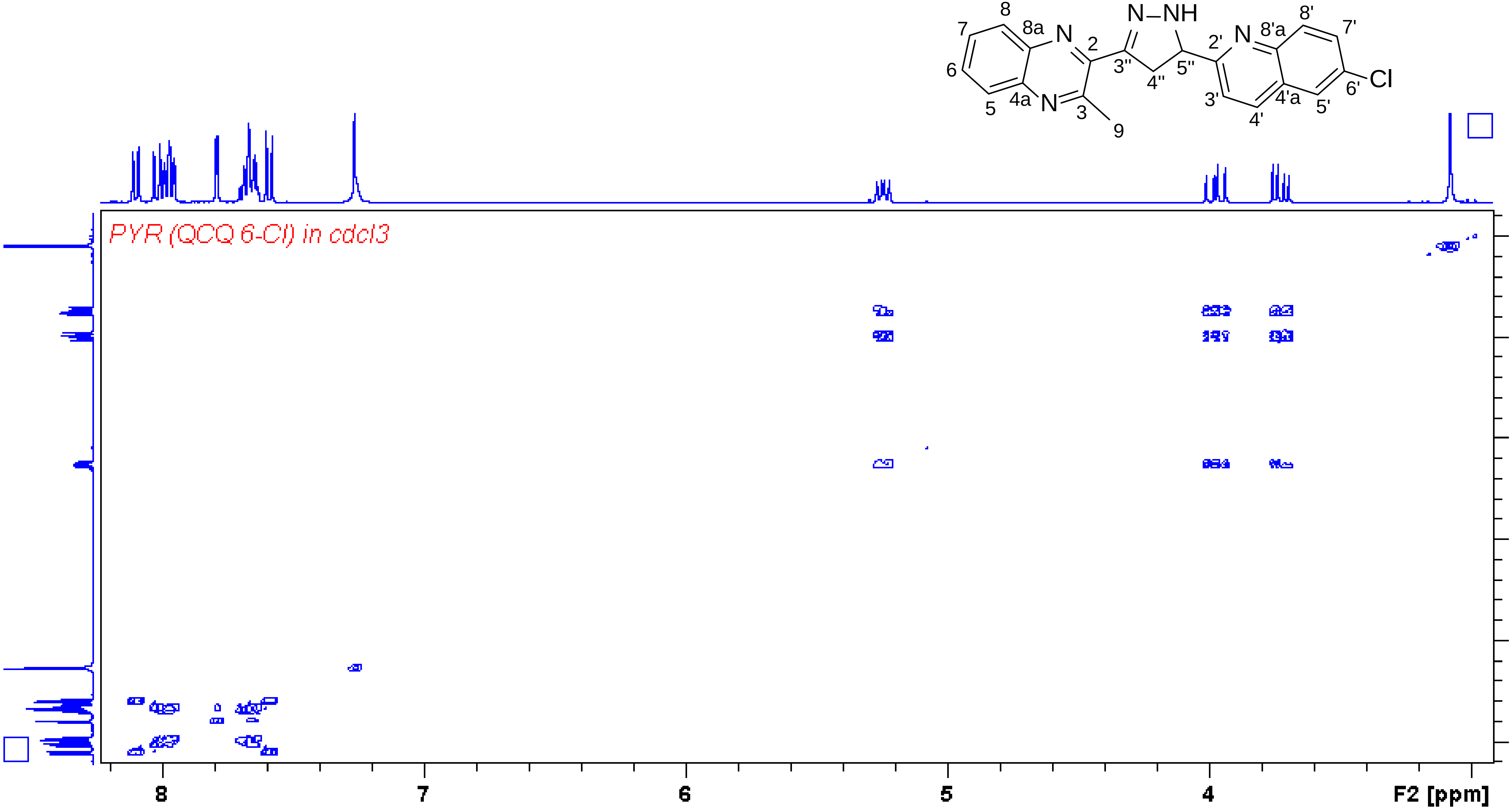
PYR (QCQ 6-Cl) in cdcl3
F1 [ppm]
F2 [ppm]
N–NH
Cl
8'a
8a
4a
4'a
2'
3'
4'
5'
6'
7'
8'
3''
4''
5''
9

COSY of **B8f**

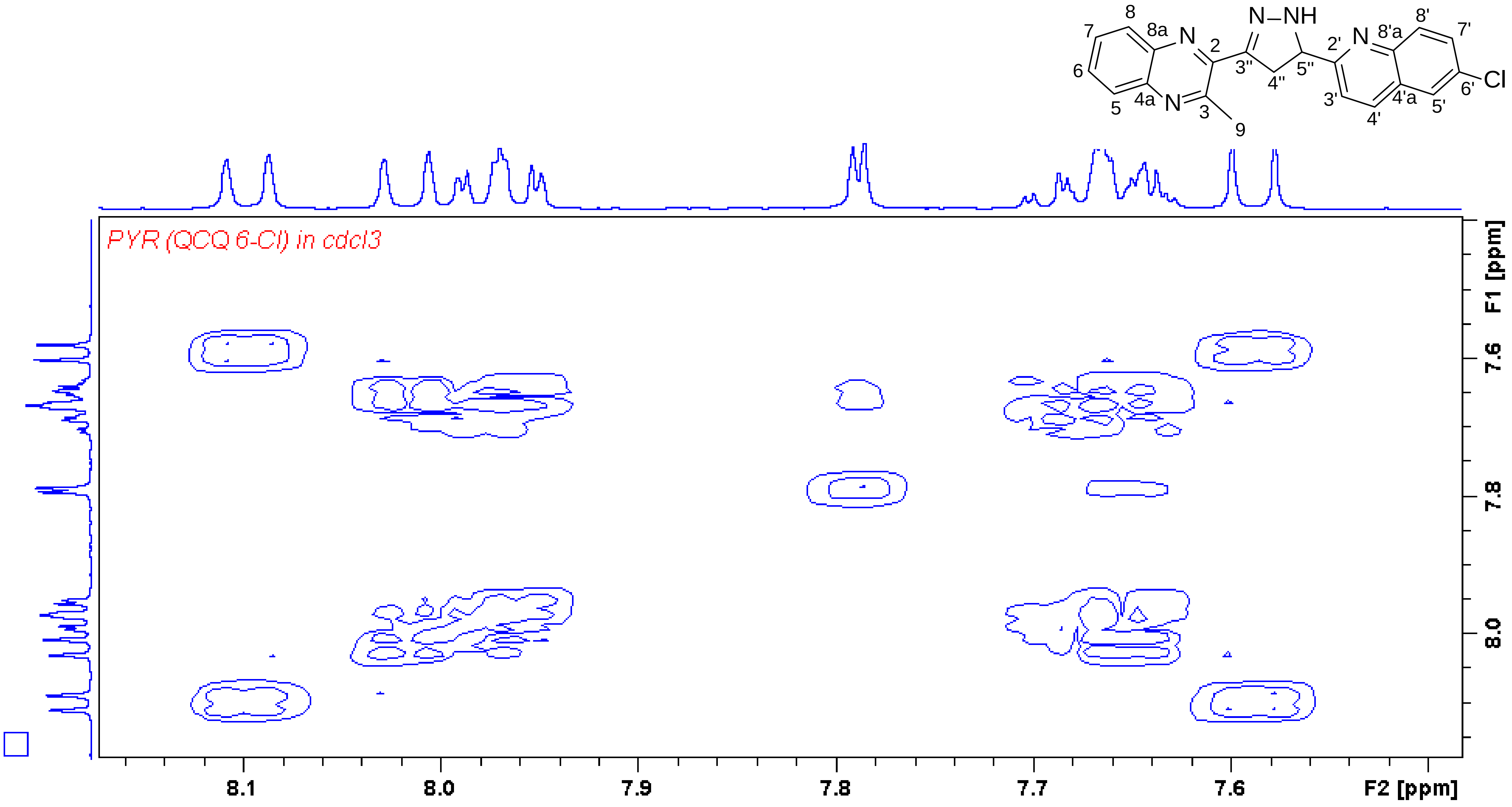

Expanded COSY of **B8f**

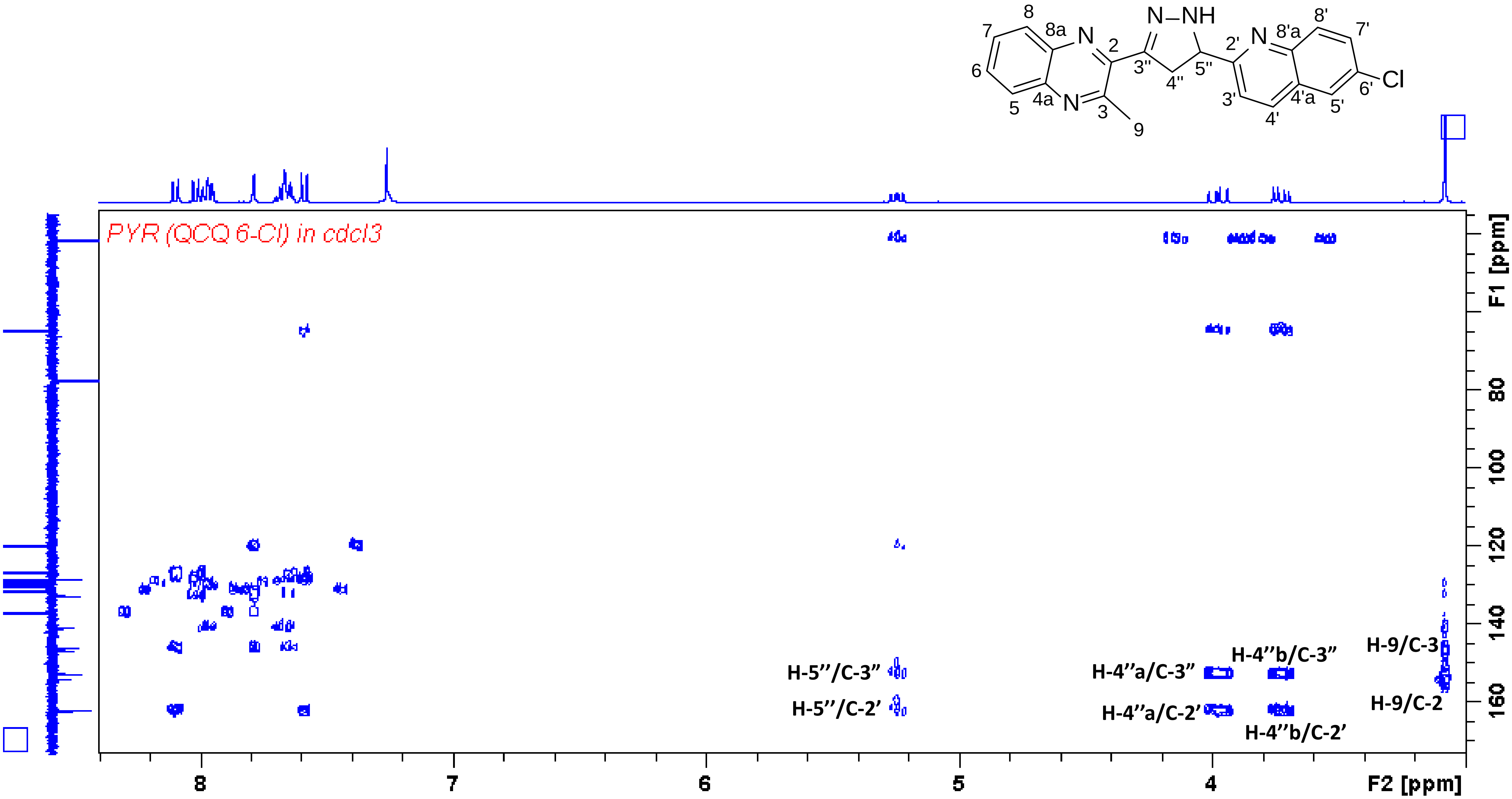

PYR (QCQ 6-Cl) in cdcl3
H-5''/C-3''
H-5''/C-2'
H-4''a/C-3''
H-4''b/C-3''
H-4''a/C-2'
H-4''b/C-2'
H-9/C-3
H-9/C-2
F1 [ppm]
F2 [ppm]

HMBC of **B8f**

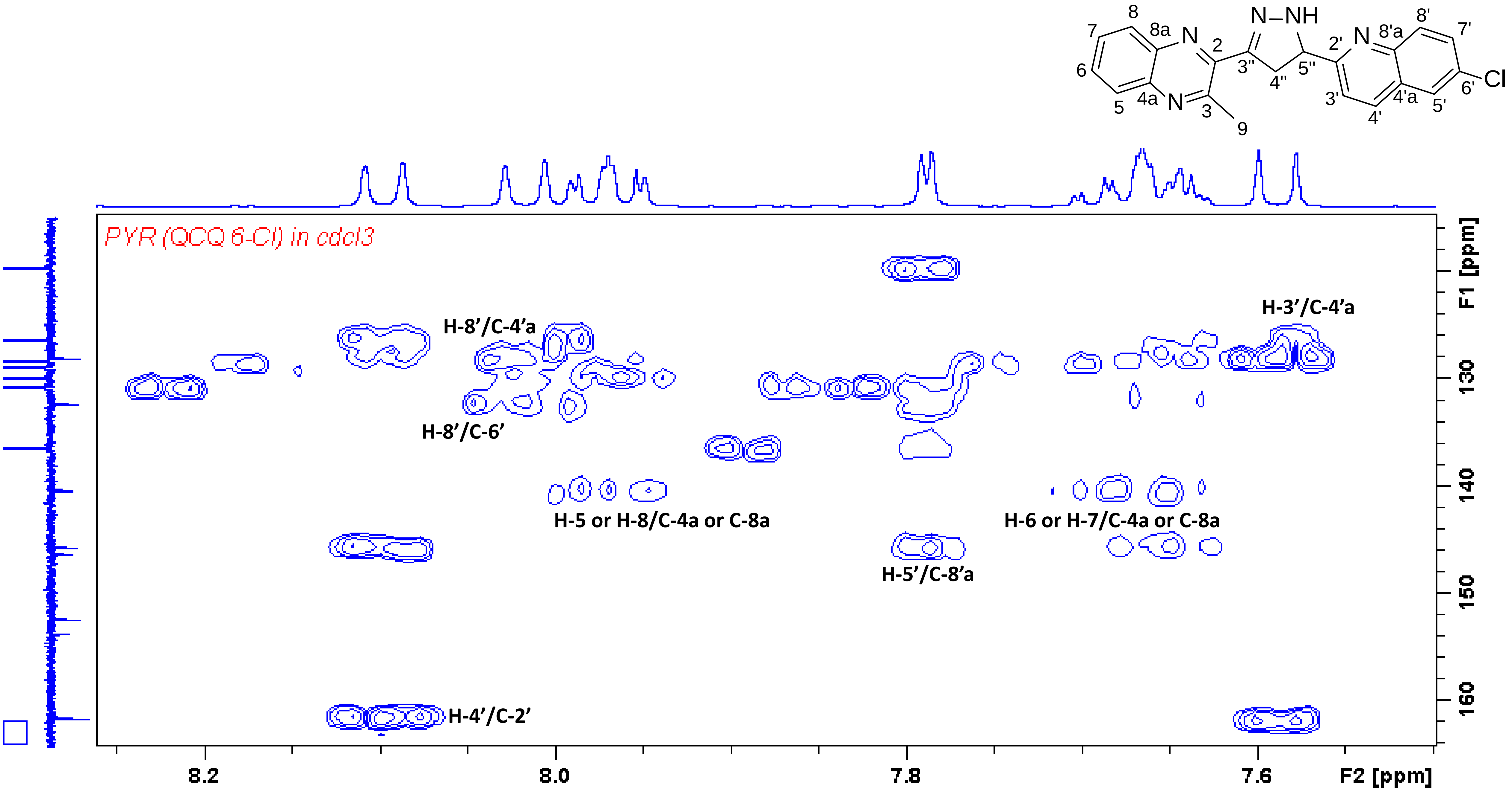

Expanded HMBC of **B8f**

Elemental Composition Report

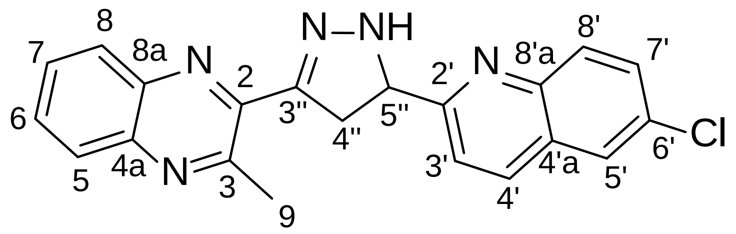

Single Mass Analysis

Tolerance = 5.0 PPM / DBE: min = -1.5, max = 100.0
Element prediction: Off
Number of isotope peaks used for i-FIT = 3

Monoisotopic Mass, Even Electron Ions
11 formula(e) evaluated with 1 results within limits (up to 20 closest results for each mass)
Elements Used:
C: 20-25 H: 15-20 N: 0-5 Na: 0-1 Cl: 0-1
Py-QCQ 6-Cl 42 (1.383) Cm (1:61)
TOF MS ES+

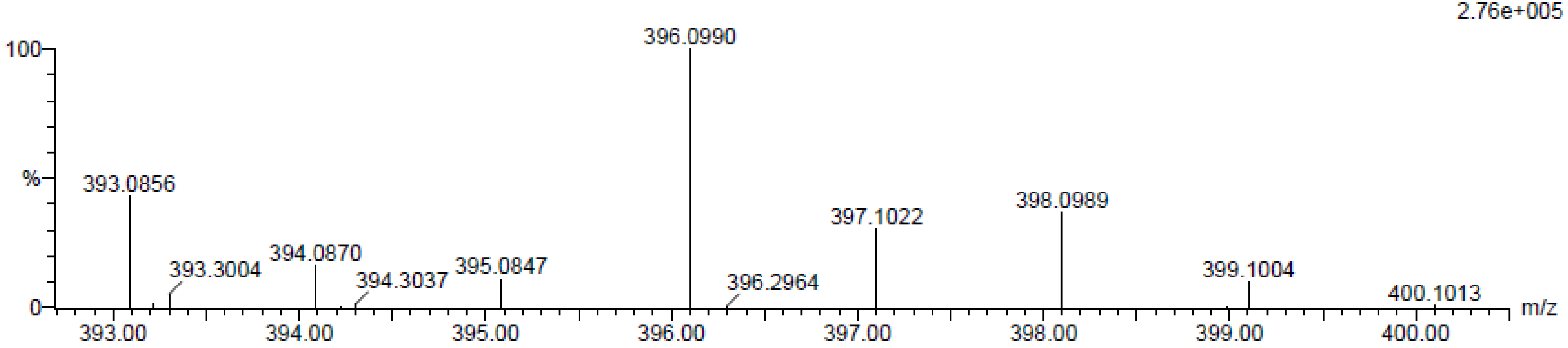

Minimum:				-1.5			
Maximum:		5.0	5.0	100.0			

Mass	Calc. Mass	mDa	PPM	DBE	i-FIT	i-FIT (Norm)	Formula
396.0990	396.0992	-0.2	-0.5	15.5	40.0	0.0	C21 H16 N5 Na Cl

High resolution mass spectrum of **B8f**

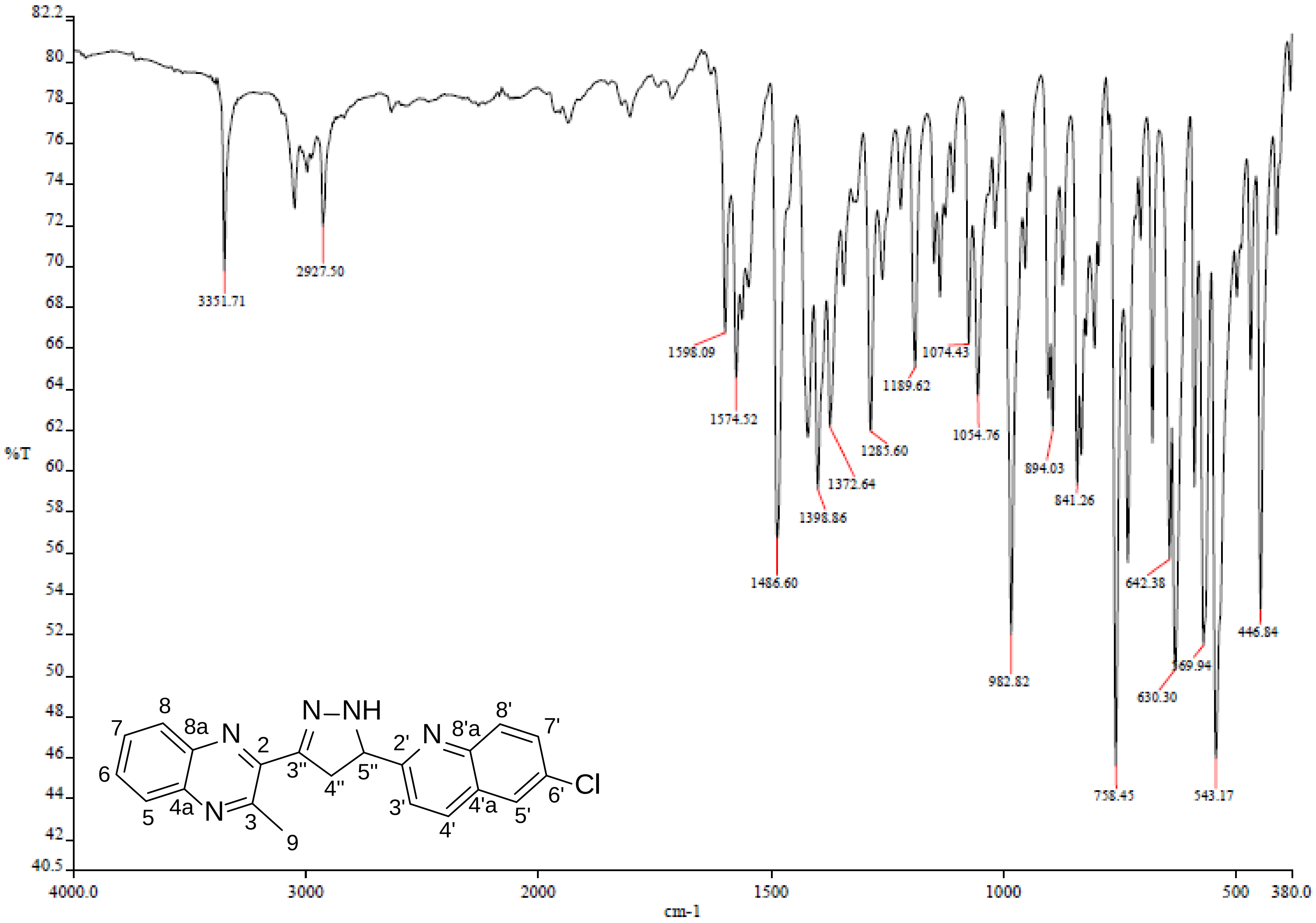

FTIR spectrum of **B8f**

Overlay Spectrum Graph Report

06/10/2017 12:06:52 PM

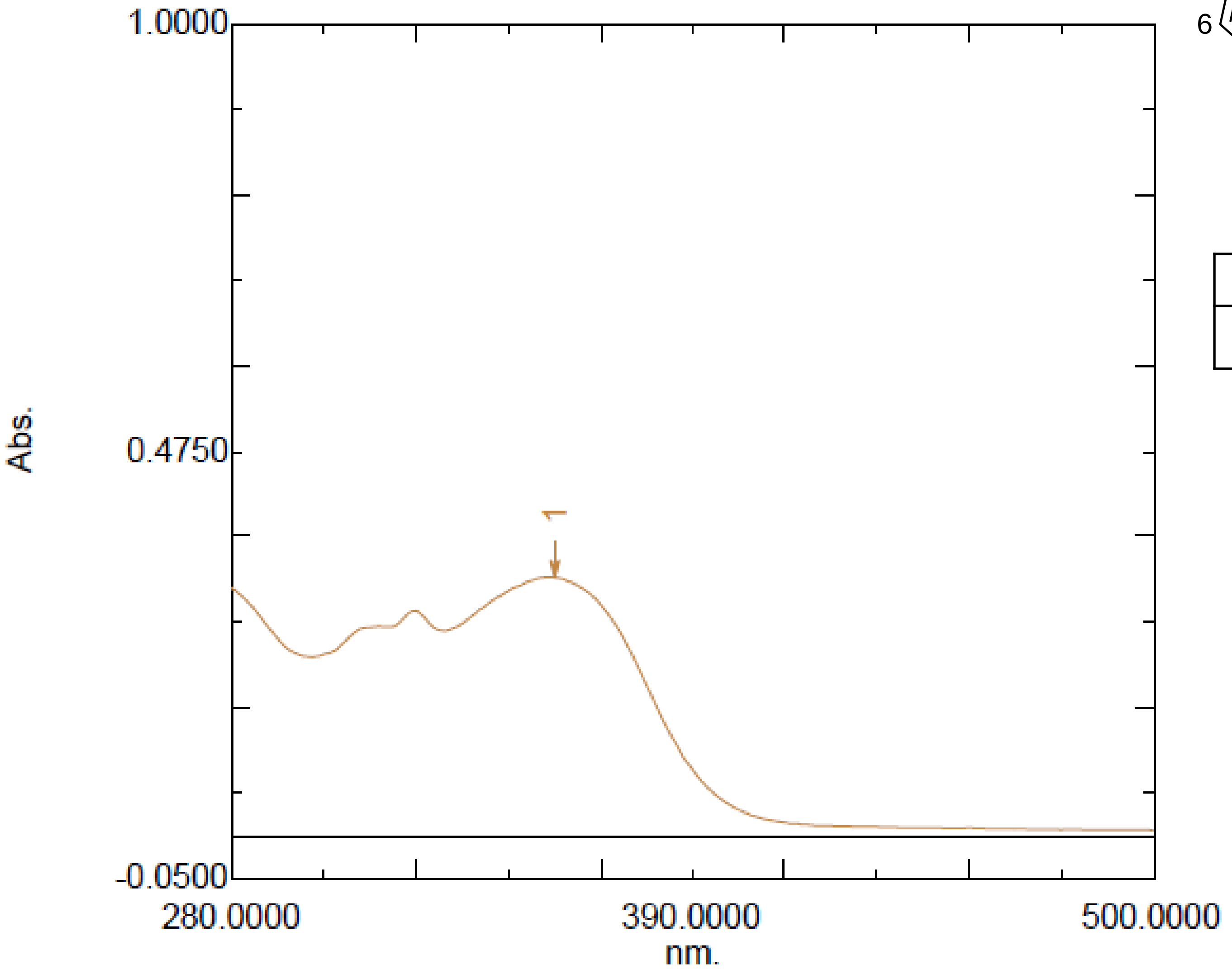

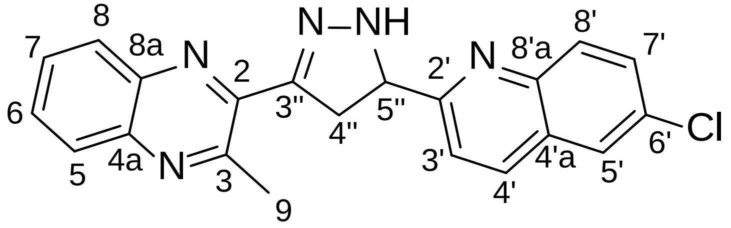

λ	absorbance	logε
356	0.3197	4.38

UV spectrum of **B8f**

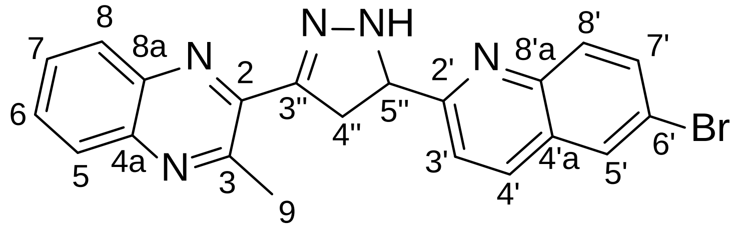

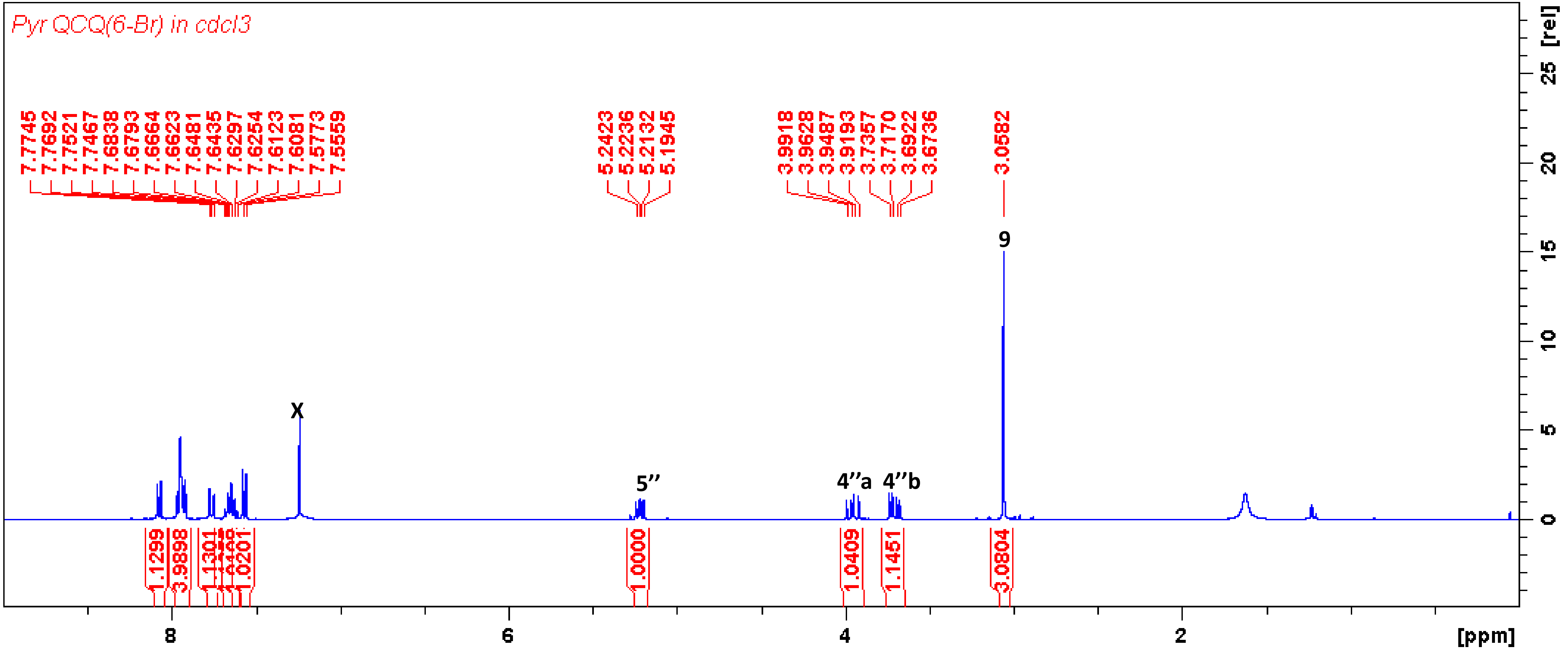

^{1}H NMR spectrum of **B8g**

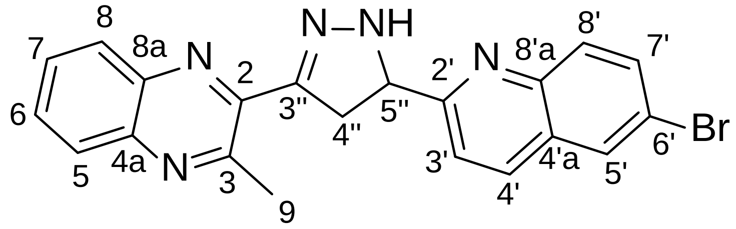

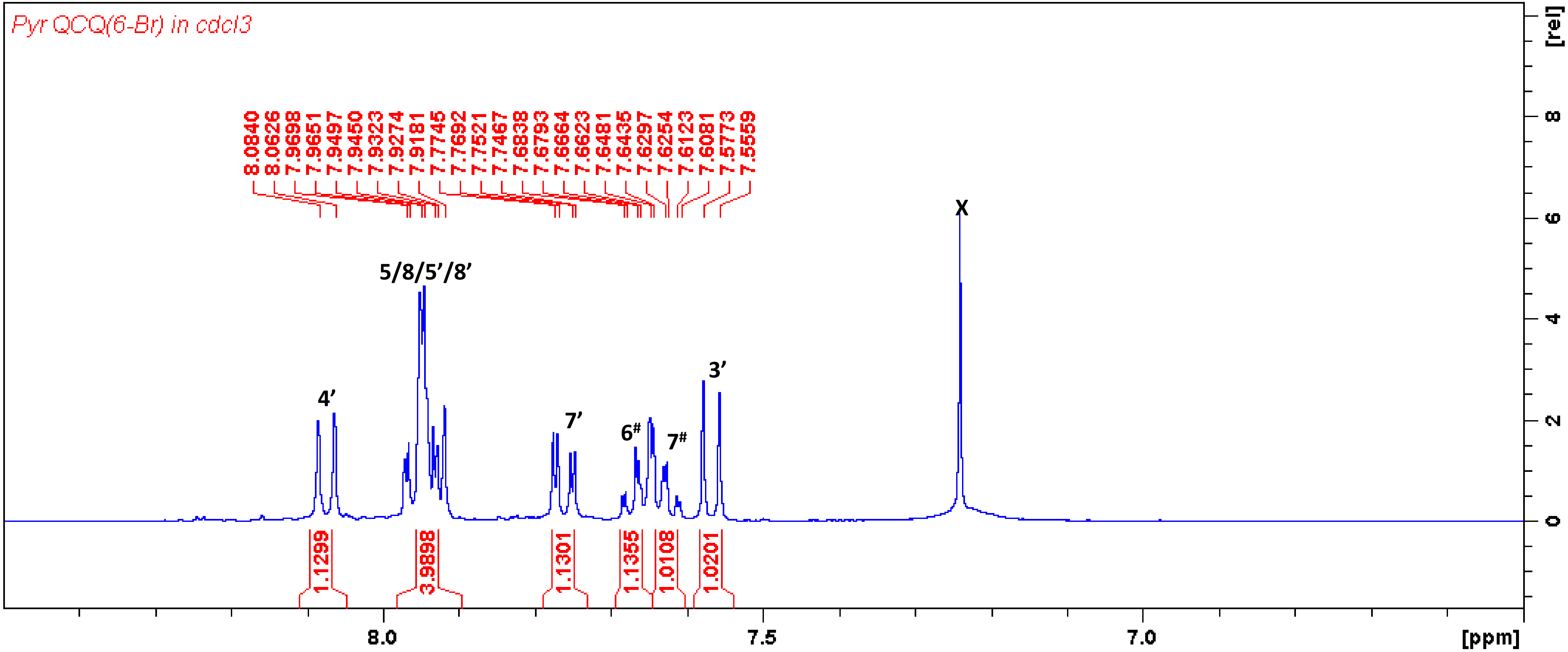

# Indicates assignments are interchangeable

Expanded ^{1}H NMR spectrum of **B8g**

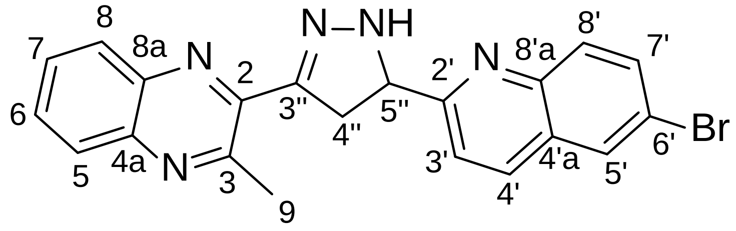

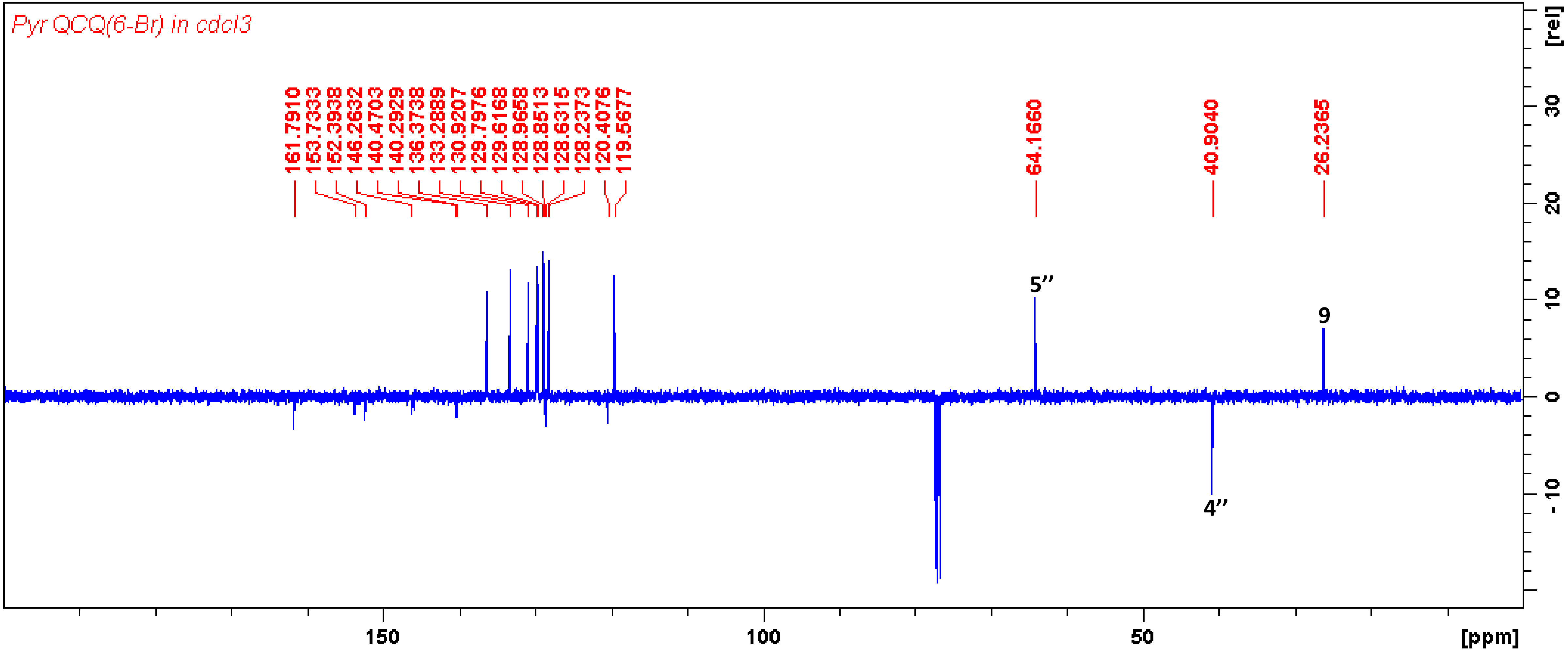

^{13}C NMR spectrum of **B8g**

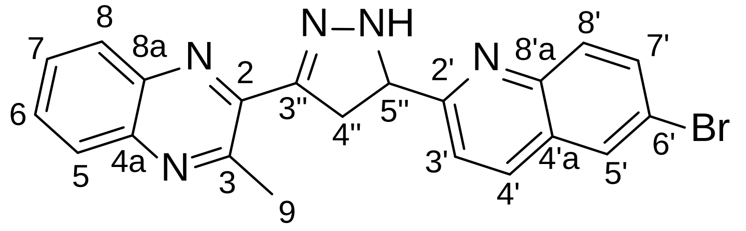

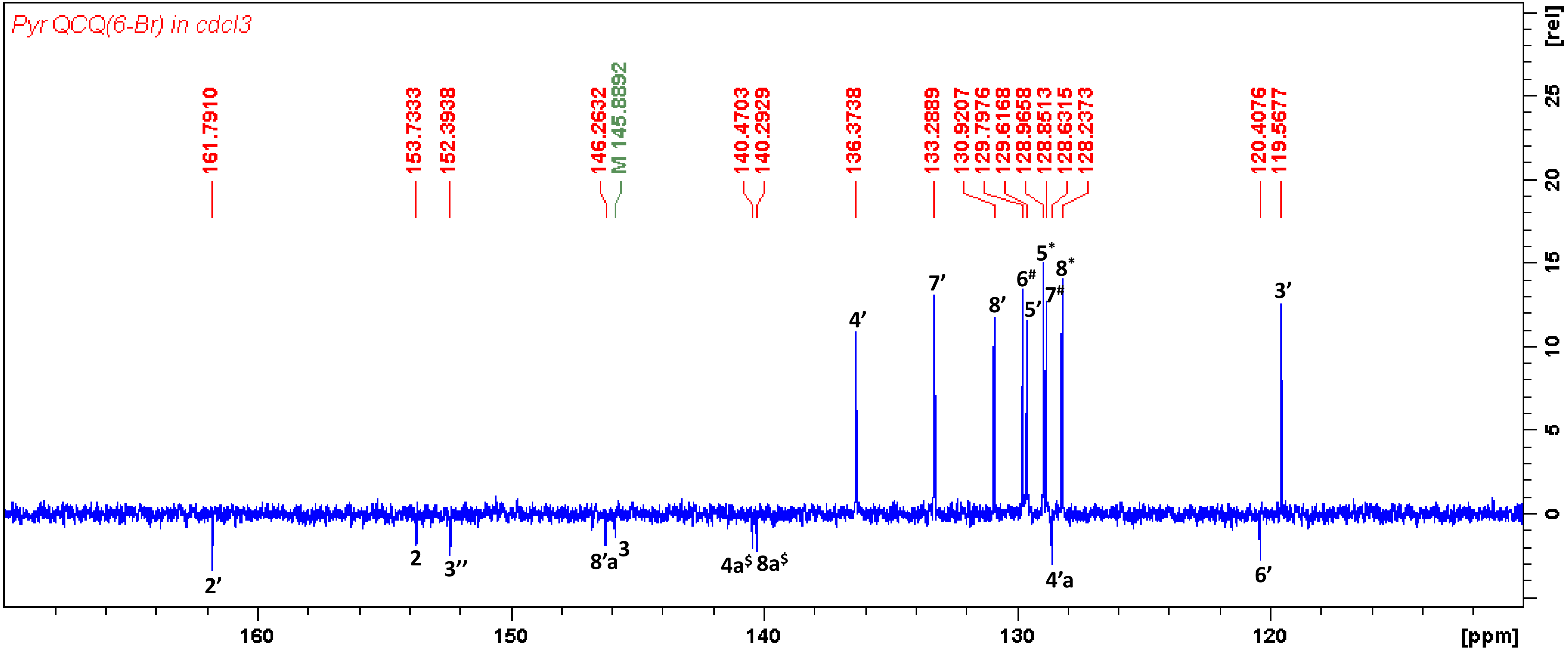

*, #, $ Indicates assignments are interchangeable

Expanded ^{13}C NMR spectrum of **B8g**

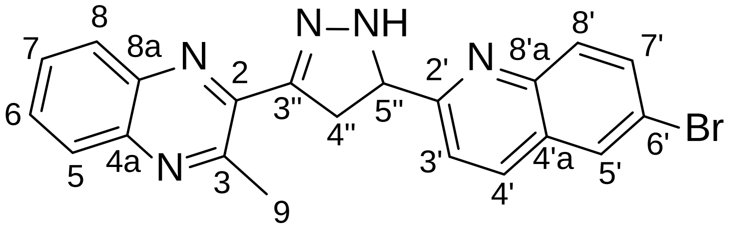

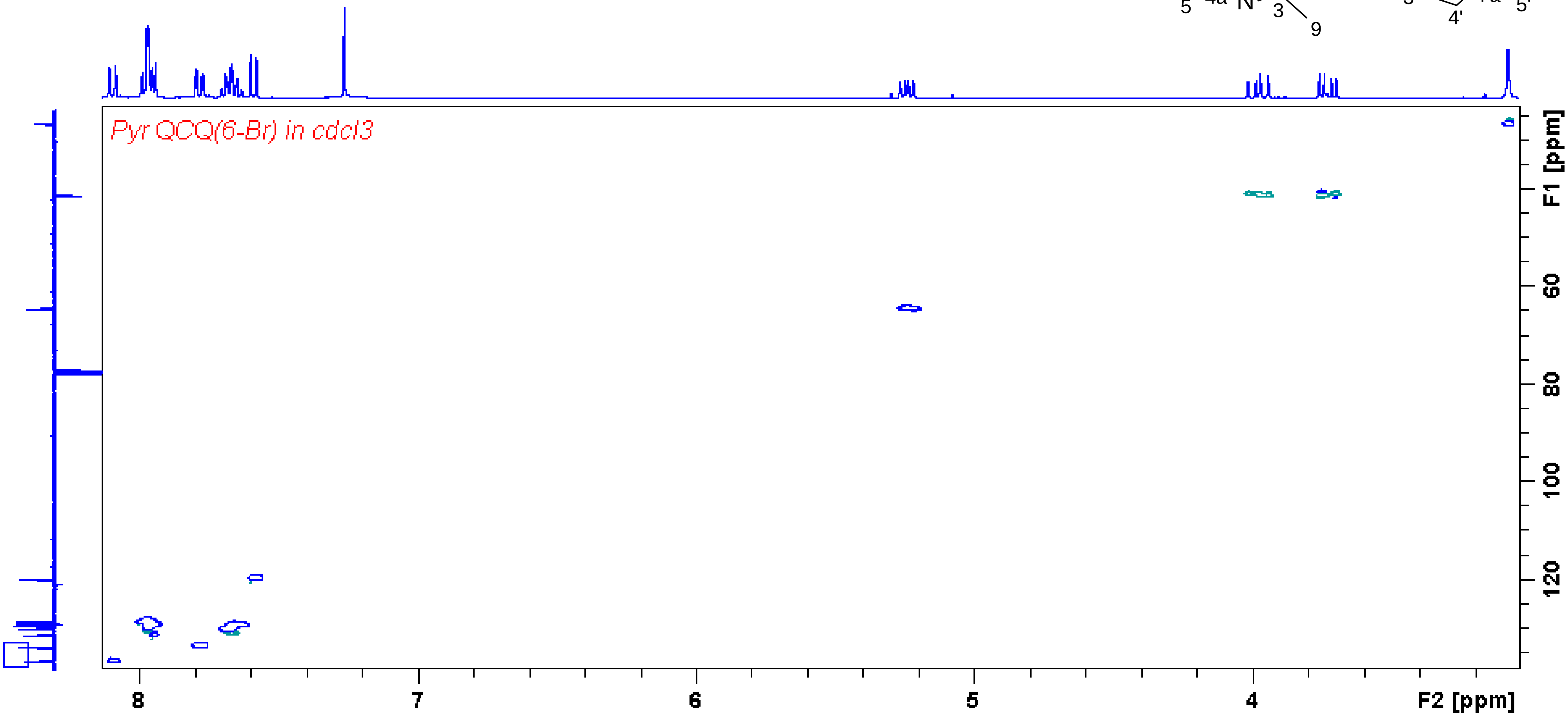

HSQC of **B8g**

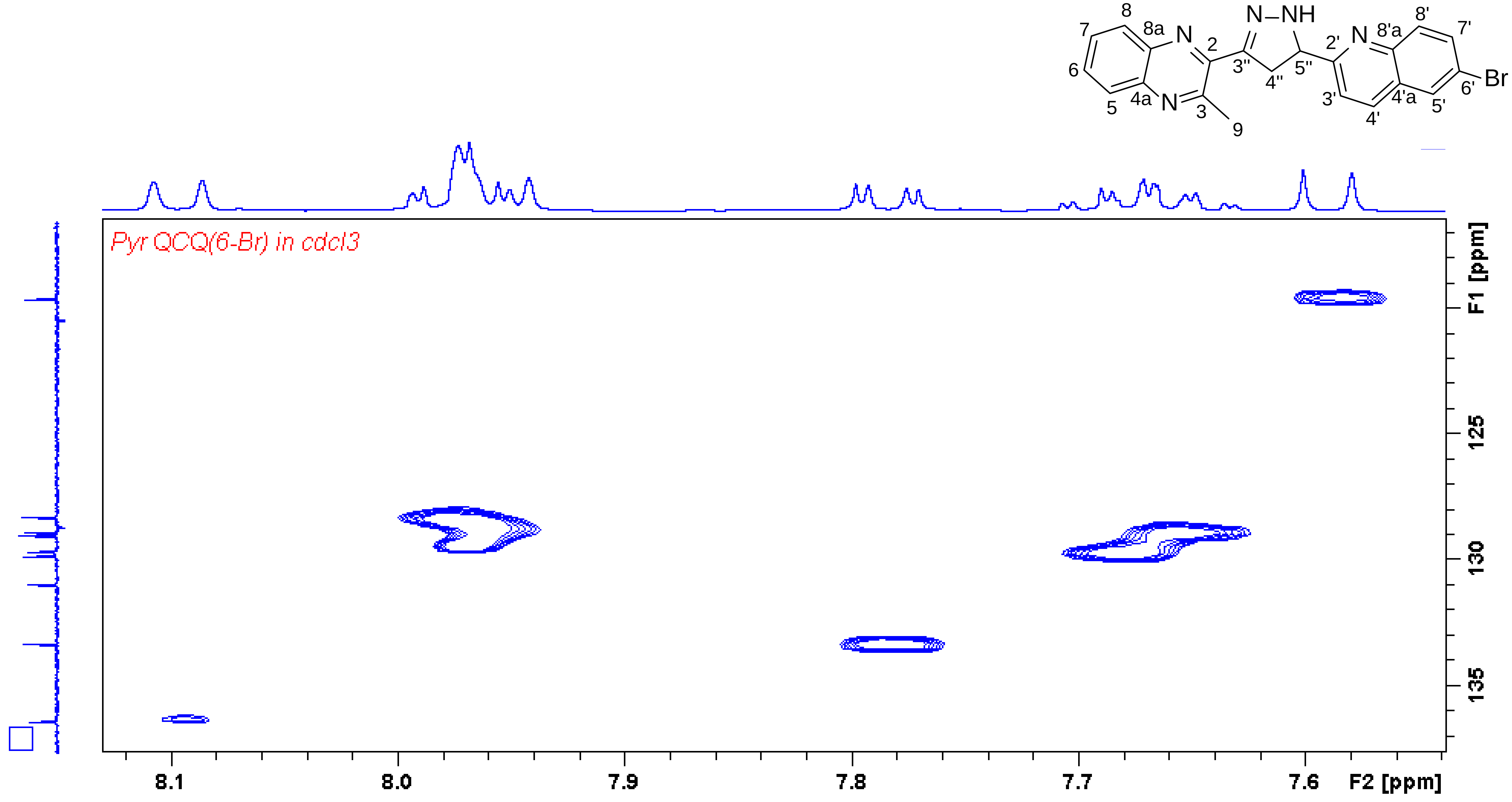

Expanded HSQC of **B8g**

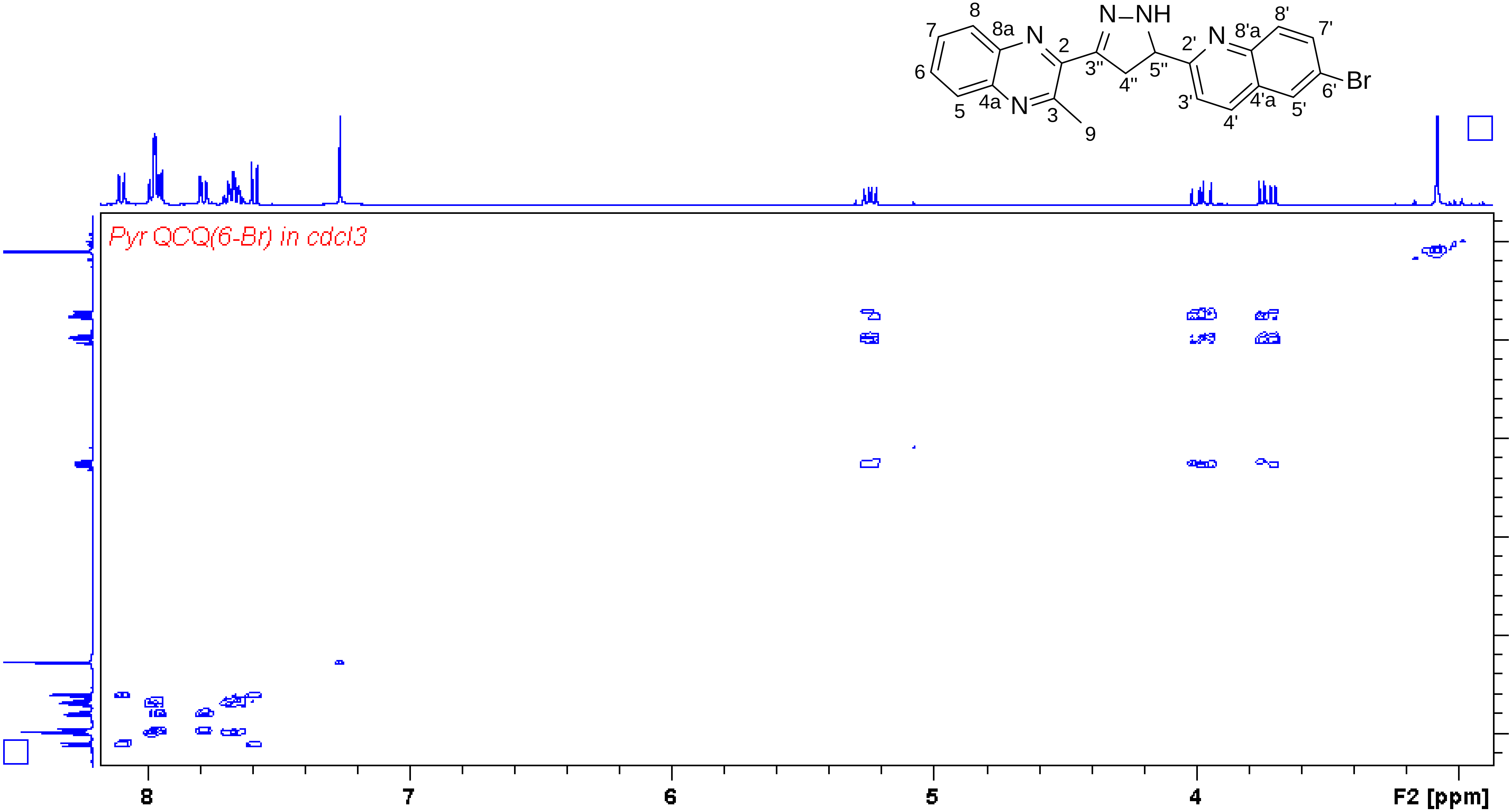

COSY of **B8g**

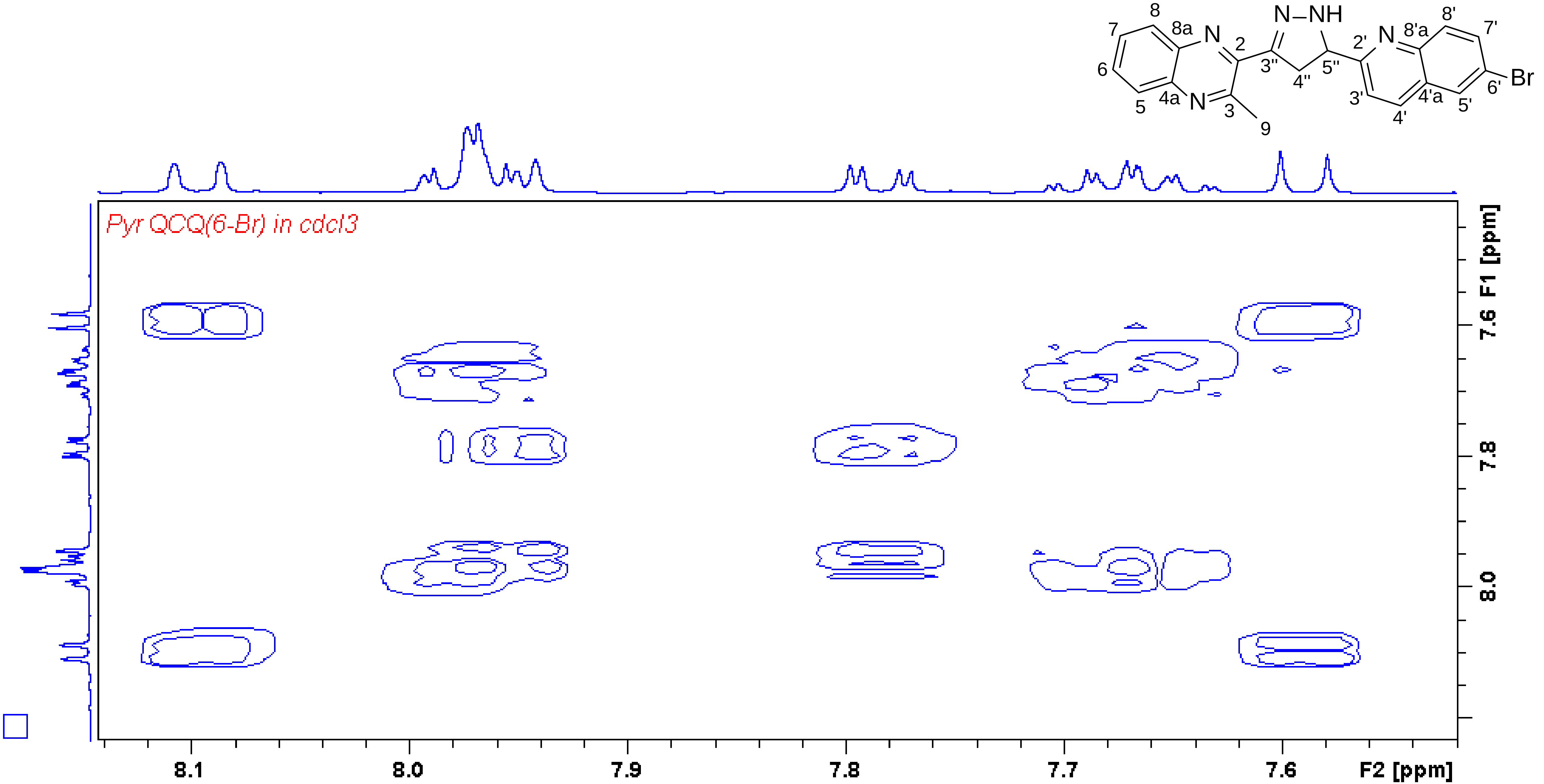

Expanded COSY of **B8g**

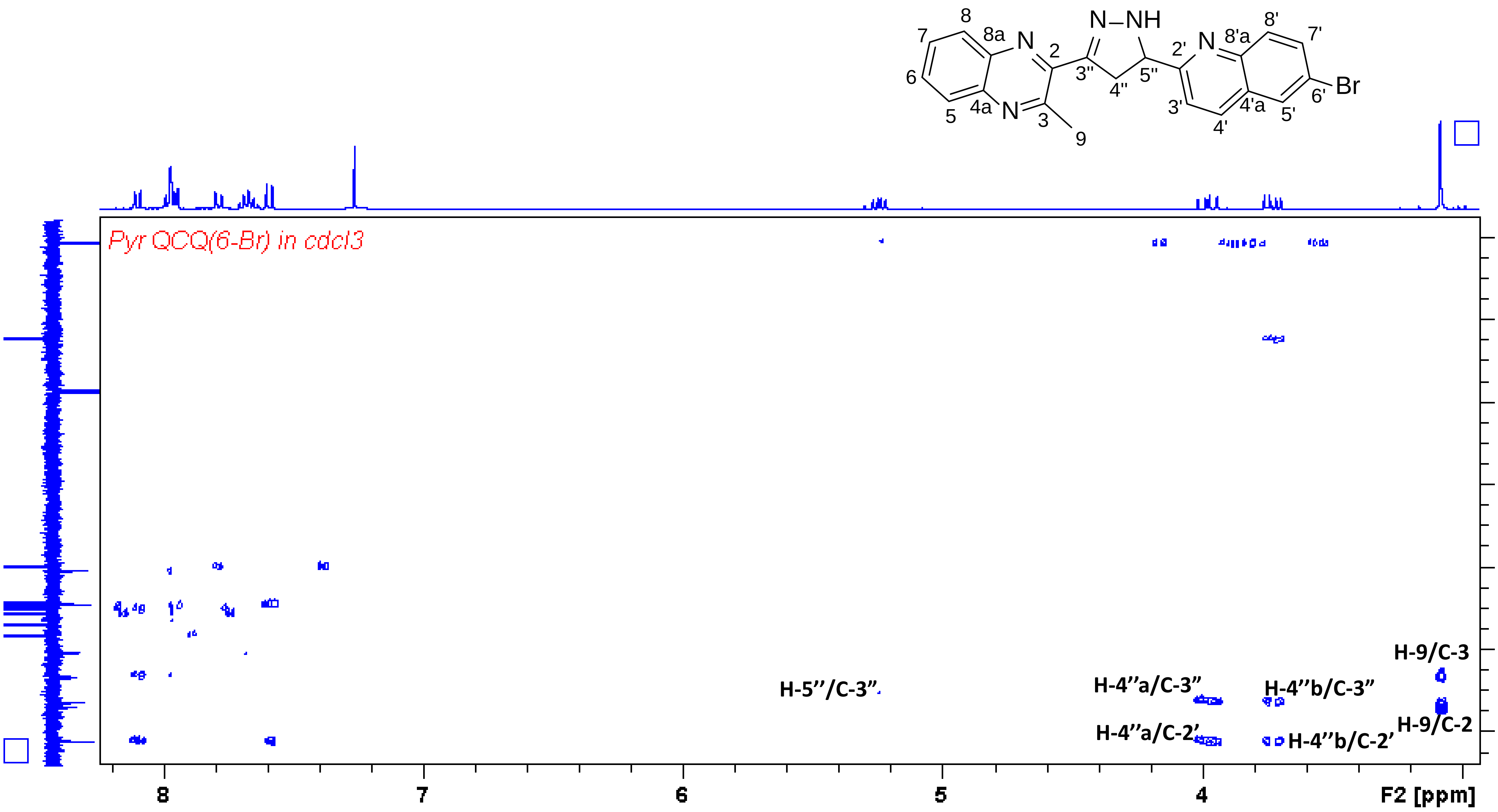
Pyr QCQ(6-Br) in cdcl3
H-9/C-3
H-5''/C-3''
H-4''a/C-3''
H-4''b/C-3''
H-4''a/C-2'
H-4''b/C-2'
H-9/C-2
F1 [ppm]
F2 [ppm]

HMBC of **B8g**

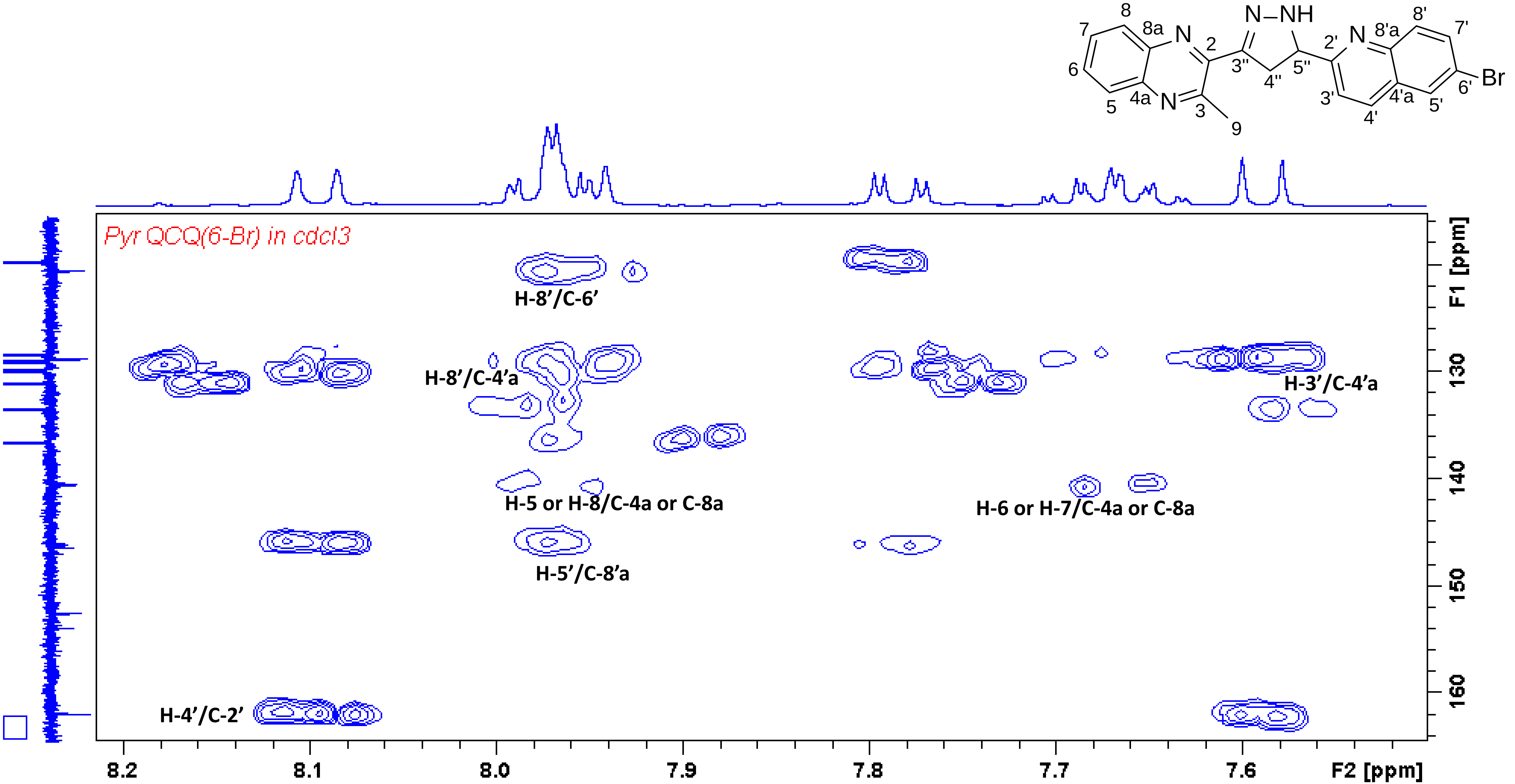

Expanded HMBC of **B8g**

Elemental Composition Report

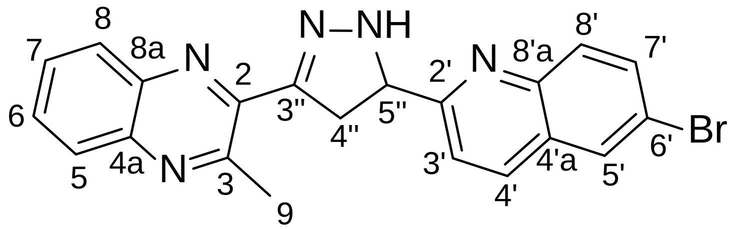

Single Mass Analysis

Tolerance = 5.0 PPM / DBE: min = -1.5, max = 100.0
Element prediction: Off
Number of isotope peaks used for i-FIT = 3

Monoisotopic Mass, Even Electron Ions
15 formula(e) evaluated with 1 results within limits (up to 20 closest results for each mass)
Elements Used:
C: 20-25 H: 15-20 N: 0-5 Na: 0-1 Br: 0-1

Py-QCQ 6-Br 2 (0.034) Cm (1:61)
TOF MS ES+

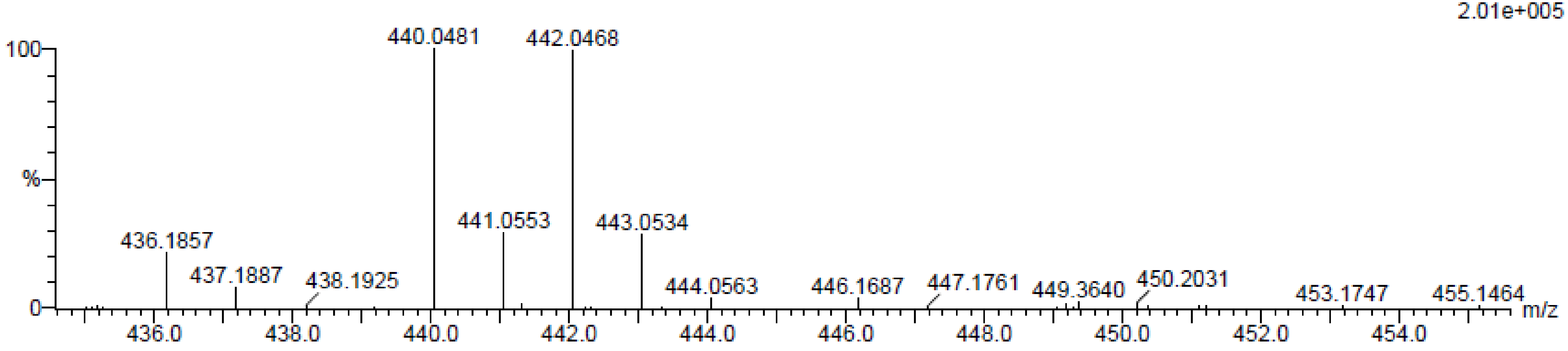

Minimum:				-1.5			
Maximum:		5.0	5.0	100.0			
Mass	Calc. Mass	mDa	PPM	DBE	i-FIT	i-FIT (Norm)	Formula
440.0481	440.0487	-0.6	-1.4	15.5	70.6	0.0	C21 H16 N5 Na Br

High resolution mass spectrum of **B8g**

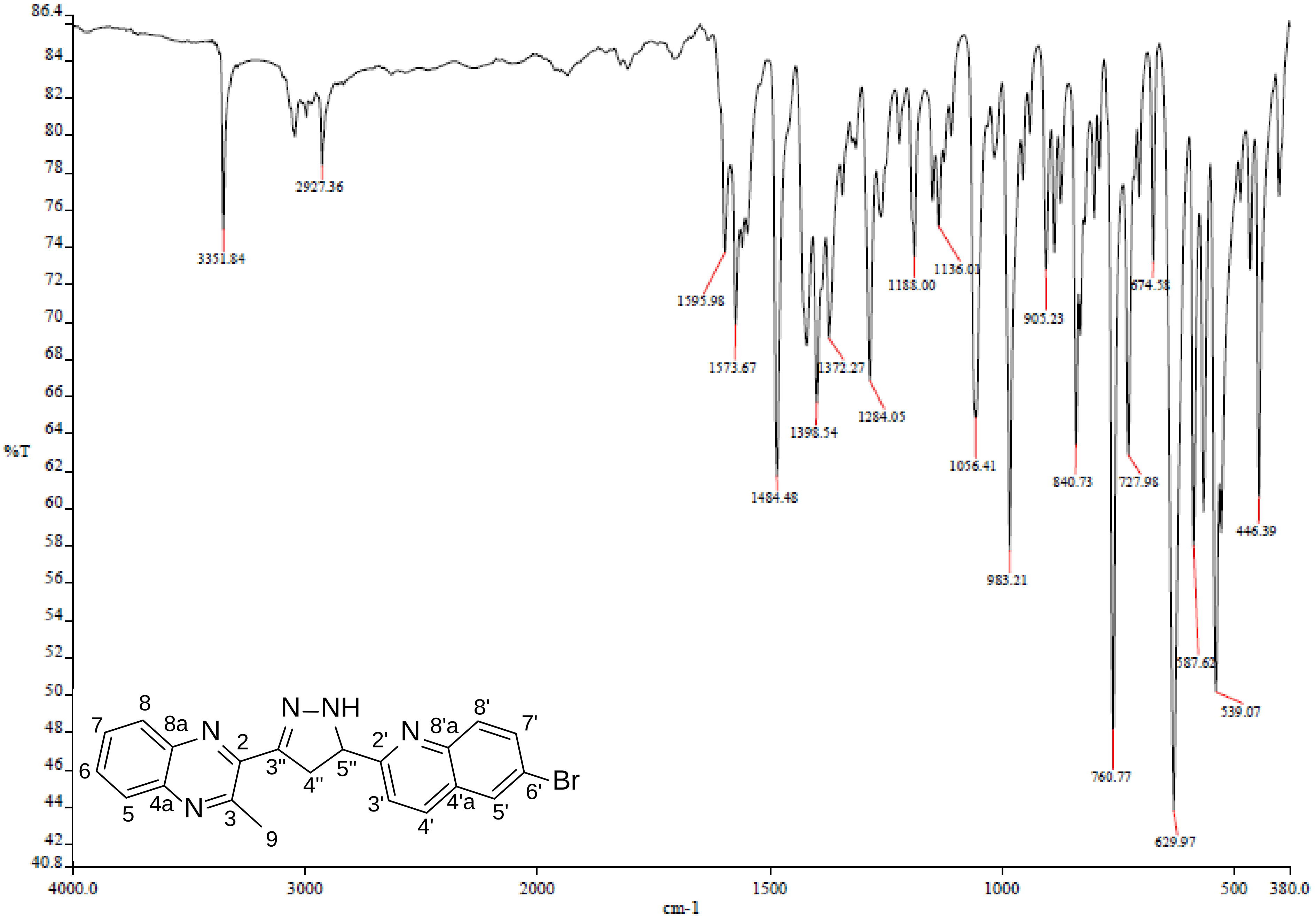

FTIR spectrum of **B8g**

Overlay Spectrum Graph Report

06/10/2017 12:05:34 PM

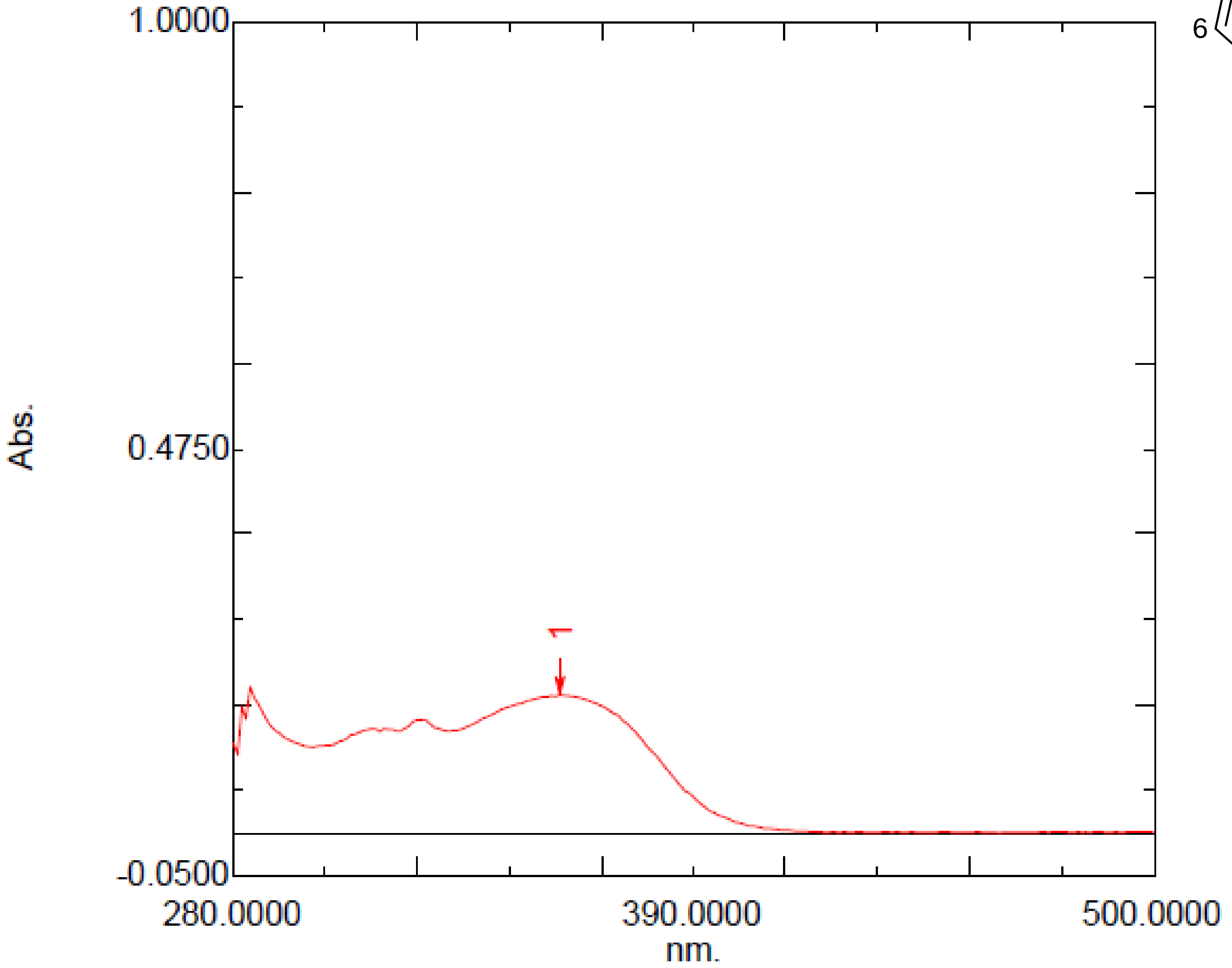

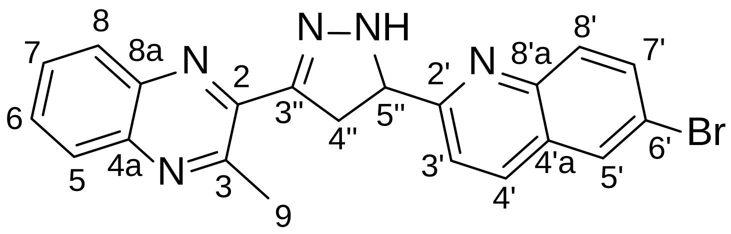

λ	absorbance	logε
358	0.1720	4.16

UV spectrum of **B8g**

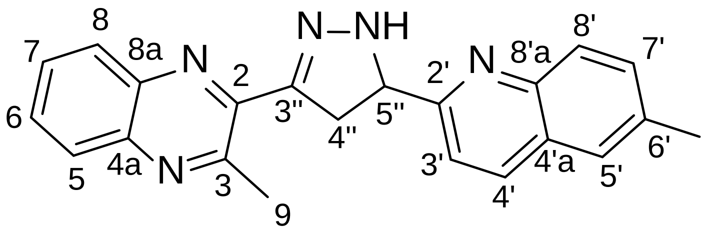

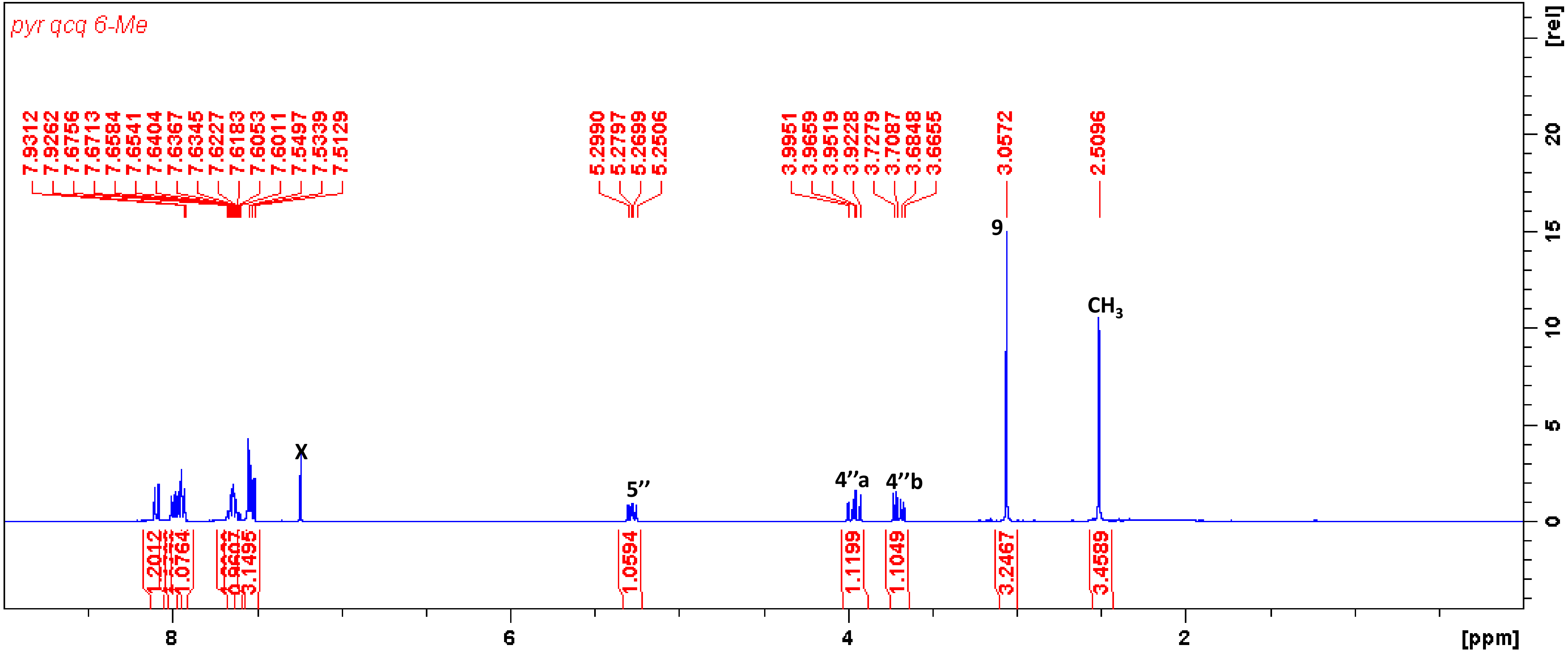

^{1}H NMR spectrum of **B8h**

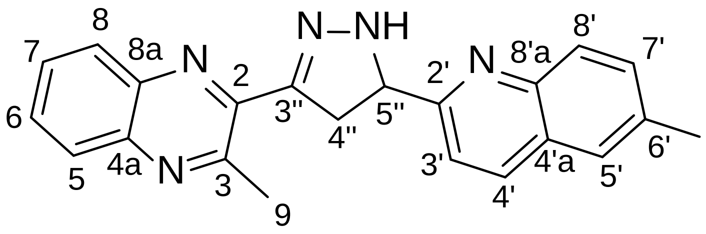

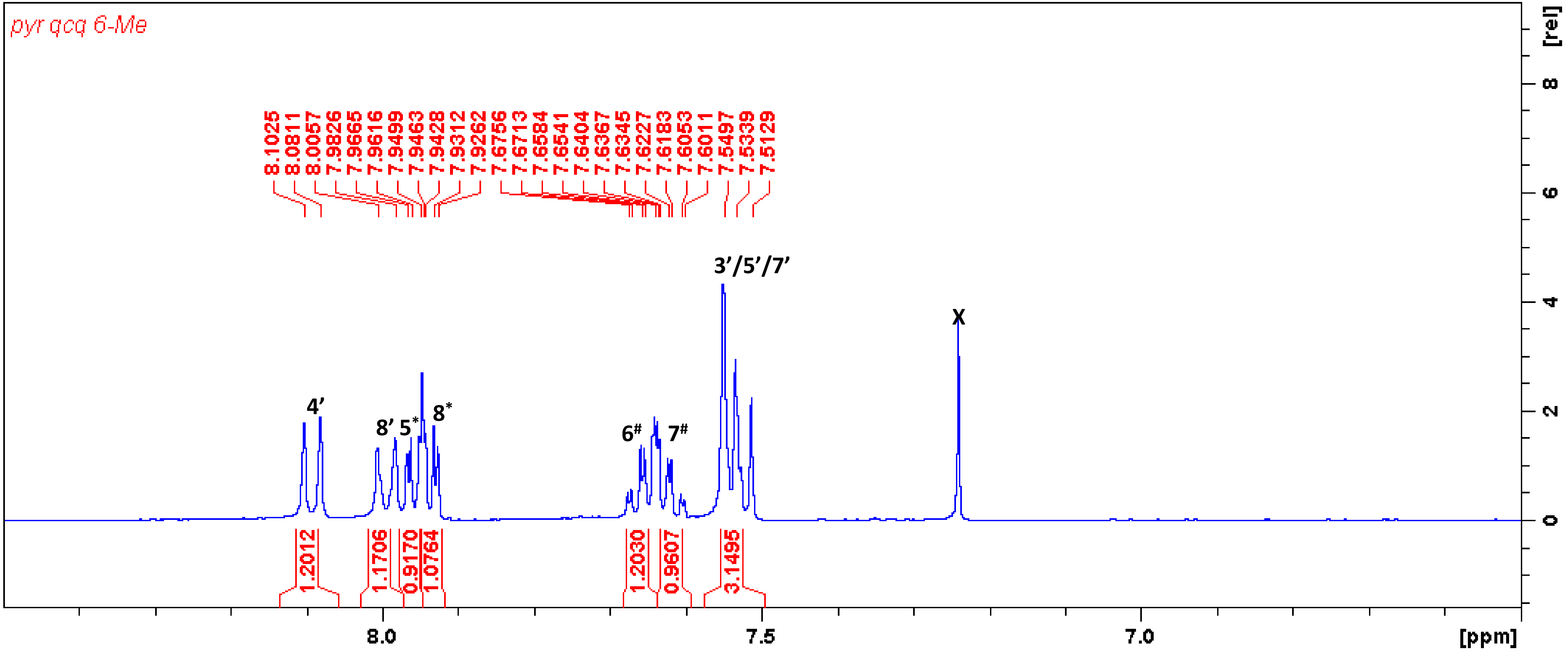

*, # Indicates assignments are interchangeable

Expanded ^{1}H NMR spectrum of **B8h**

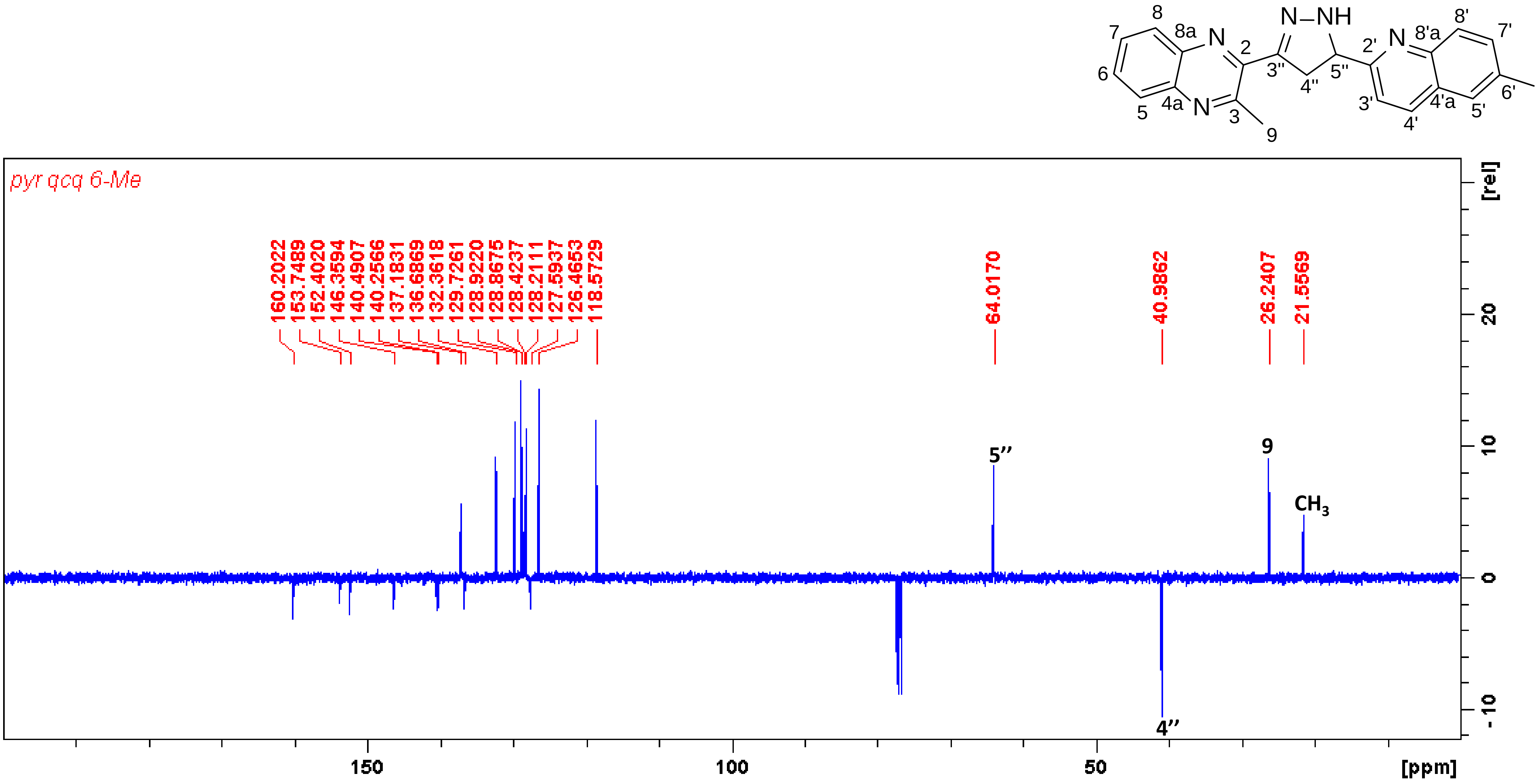

^{13}C NMR spectrum of **B8h**

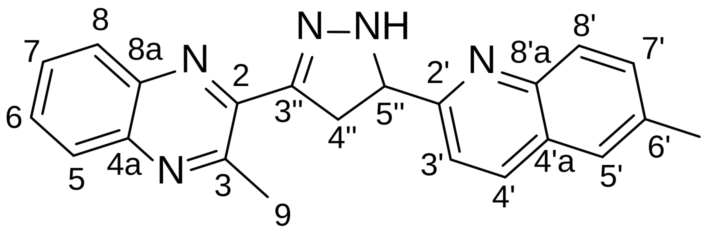

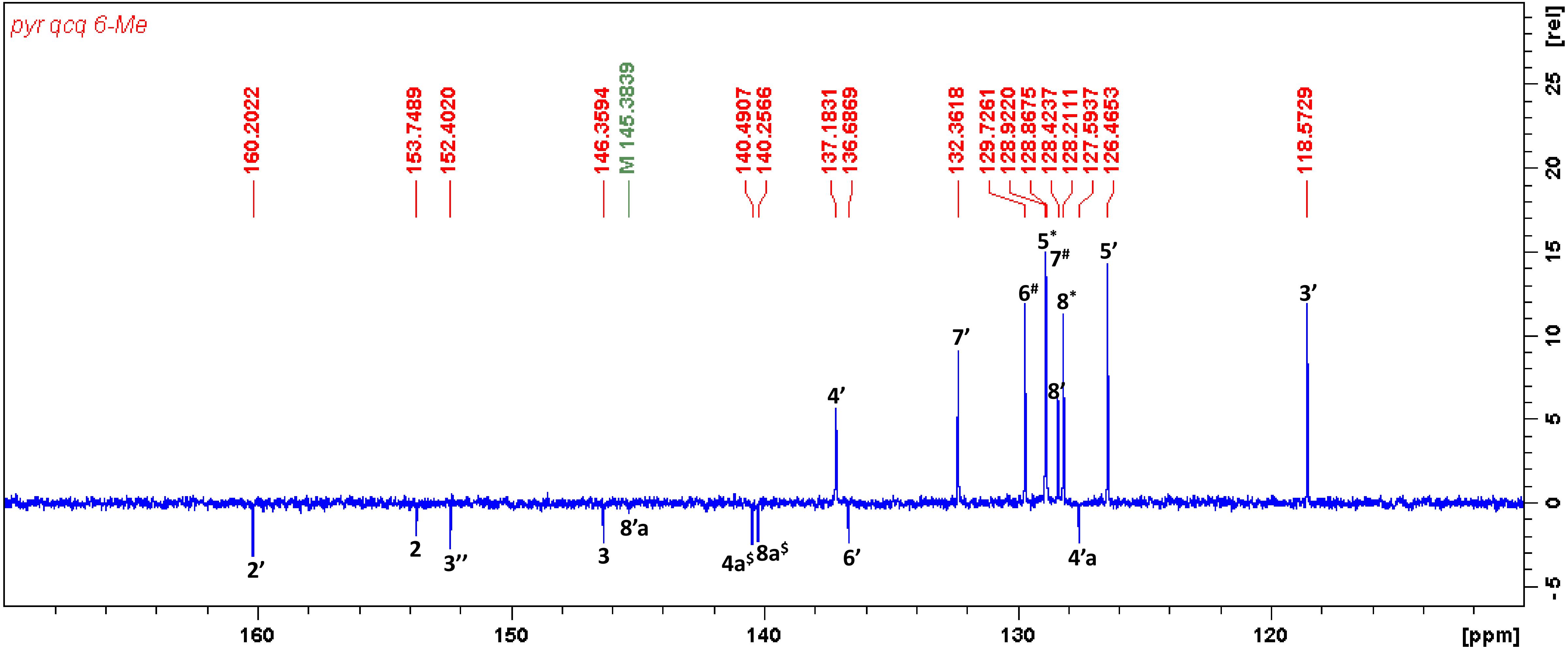

*, #, $ Indicates assignments are interchangeable

Expanded ^{13}C NMR spectrum of **B8h**

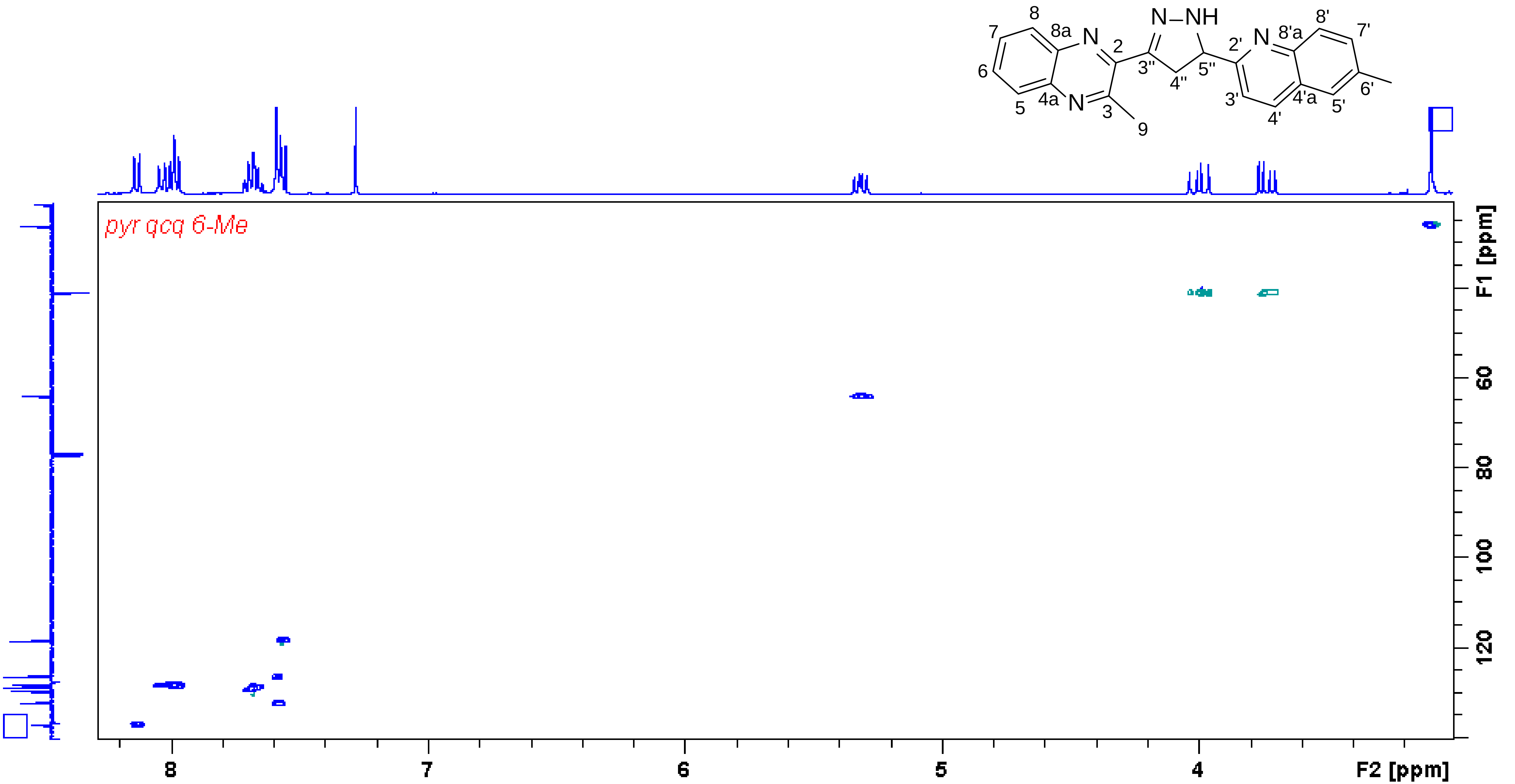

pyr qcq 6-Me
F1 [ppm]
F2 [ppm]
8
7
6
5
4
60
80
100
120
N
N–NH
N
2
3
3''
4''
5''
2'
3'
4'
4a
4'a
5
5'
6
6'
7
7'
8
8'
8a
8'a
9

HSQC of **B8h**

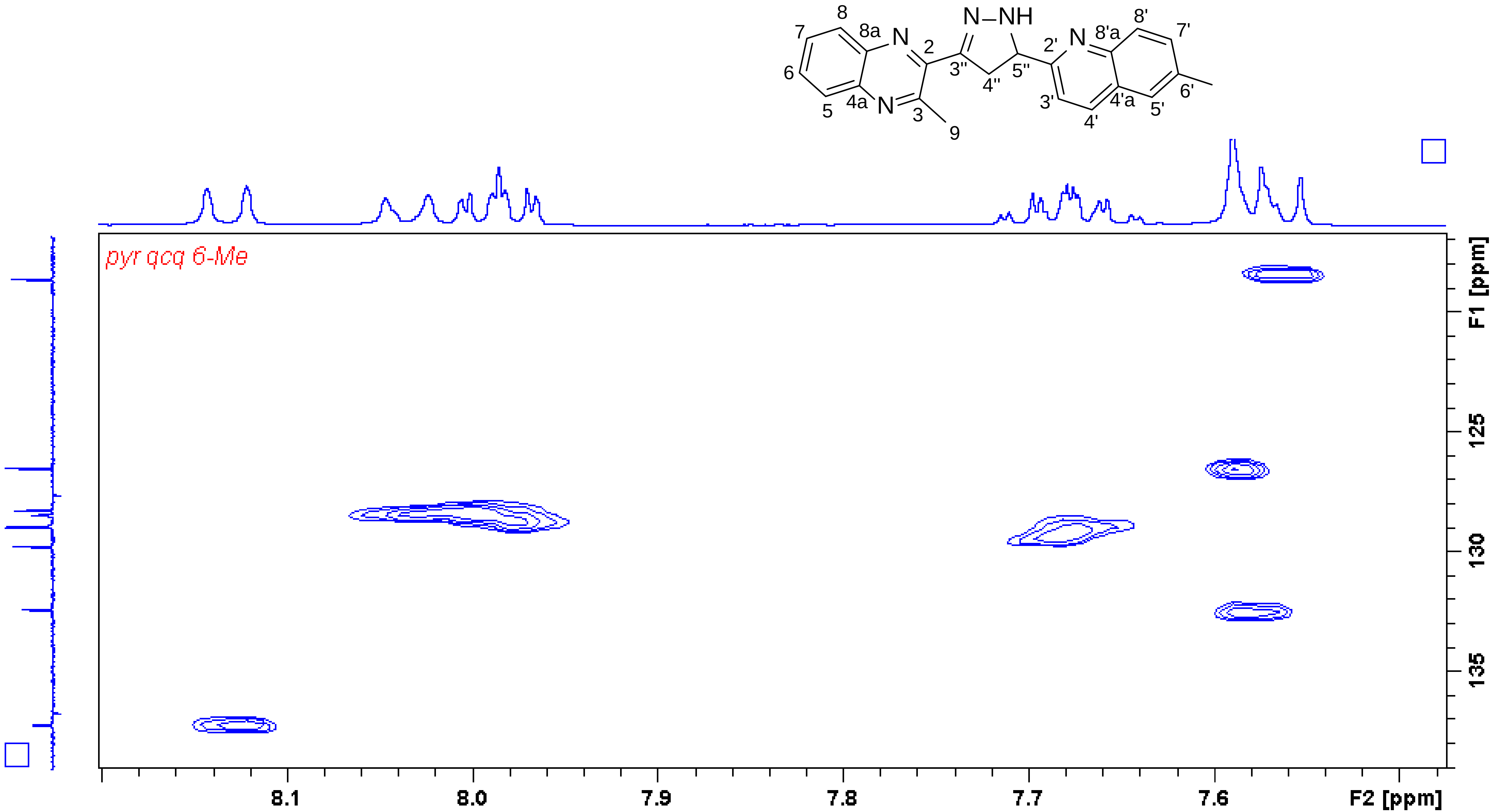

Expanded HSQC of **B8h**

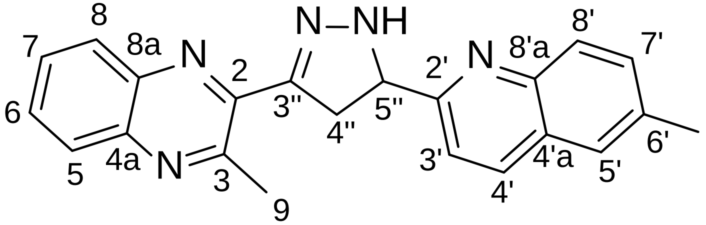

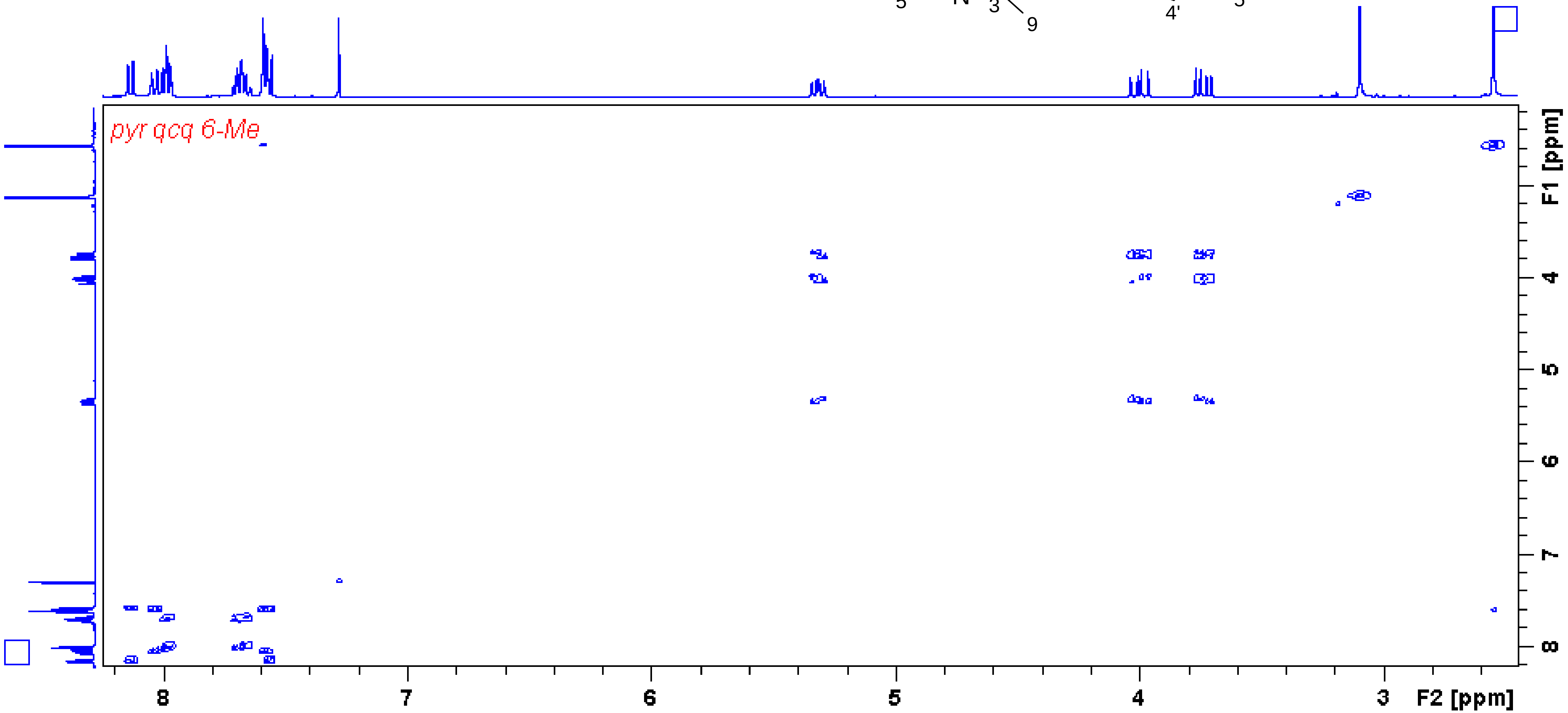

COSY of **B8h**

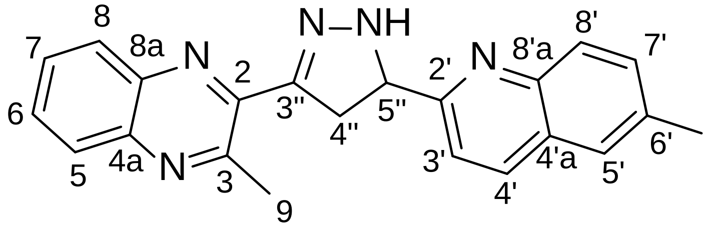

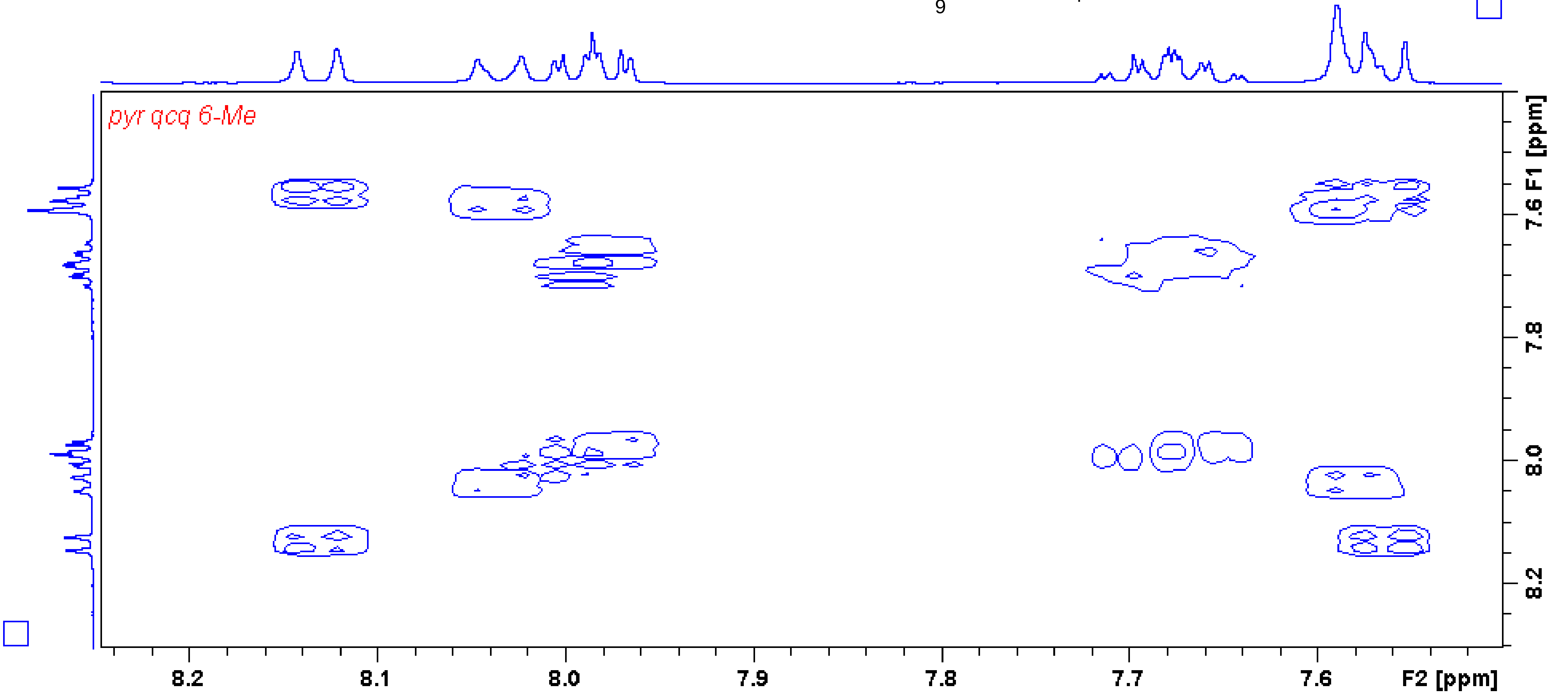

Expanded COSY of **B8h**

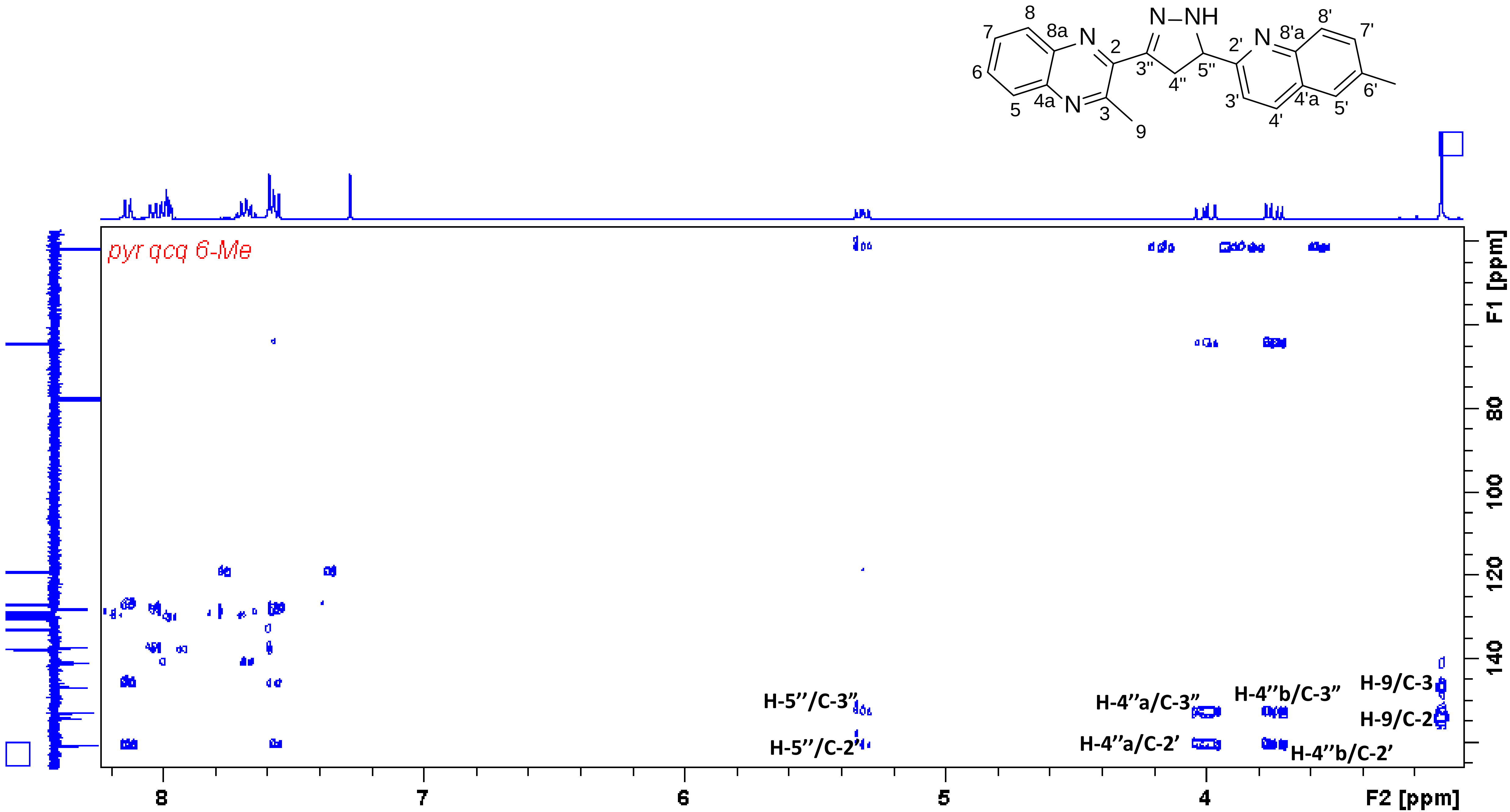

pyr qcq 6-Me
H-5''/C-3''
H-5''/C-2'
H-4''a/C-3''
H-4''b/C-3''
H-4''a/C-2'
H-4''b/C-2'
H-9/C-3
H-9/C-2
F1 [ppm]
F2 [ppm]

HMBC of **B8h**

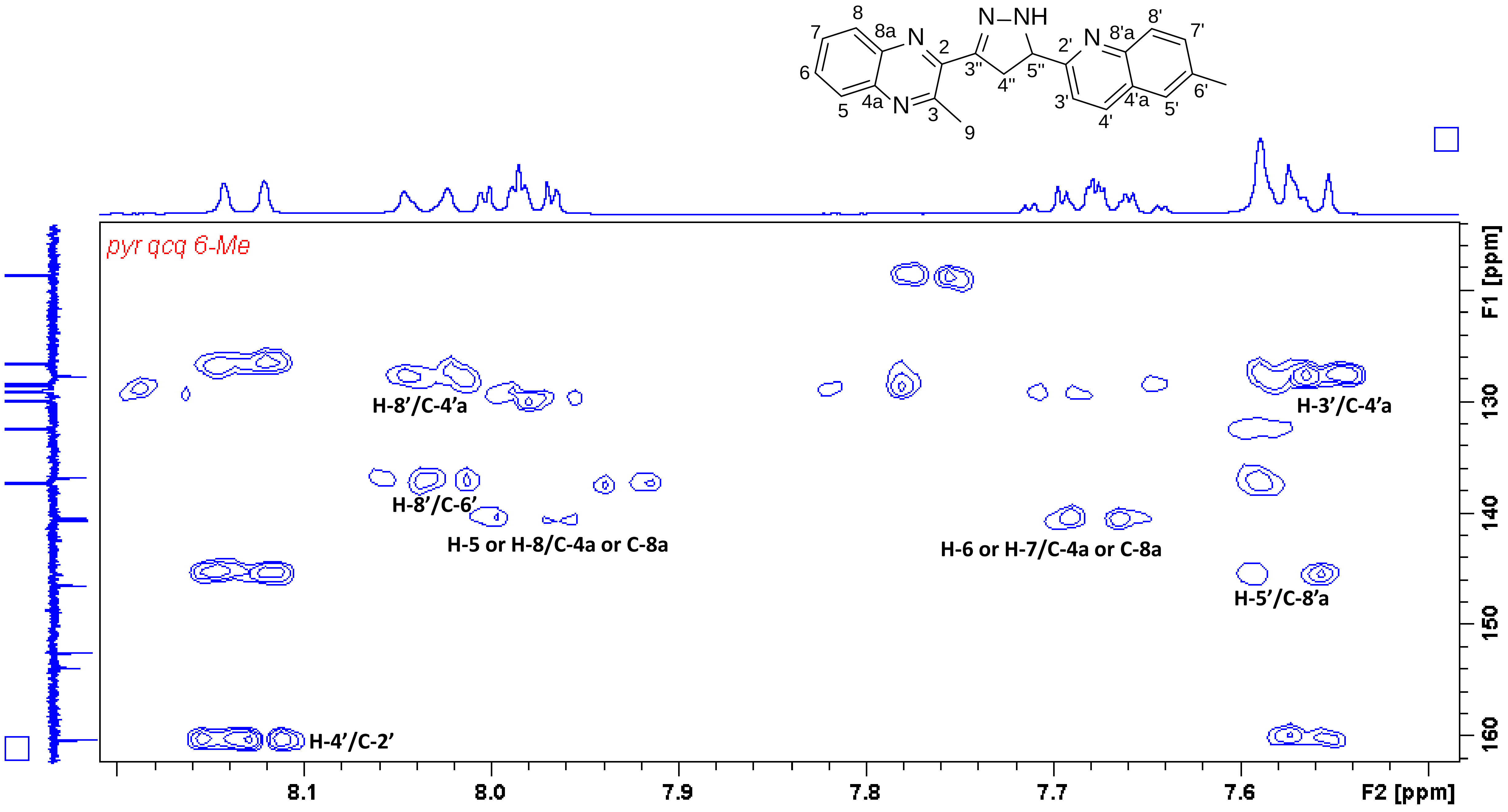

Expanded HMBC of **B8h**

Elemental Composition Report

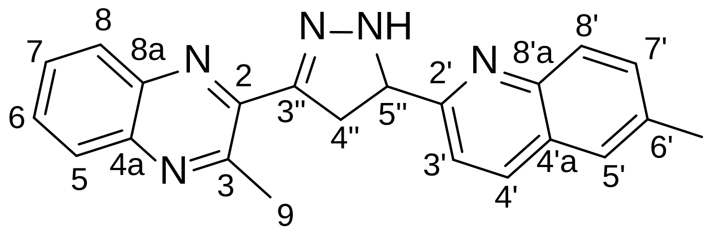

Single Mass Analysis

Tolerance = 5.0 PPM / DBE: min = -1.5, max = 100.0
Element prediction: Off
Number of isotope peaks used for i-FIT = 3

Monoisotopic Mass, Even Electron Ions
4 formula(e) evaluated with 1 results within limits (up to 20 closest results for each mass)
Elements Used:
C: 20-25 H: 15-20 N: 0-5 Na: 0-1
Py-QCQ 6-Me 58 (1.922) Cm (1:61)
TOF MS ES+

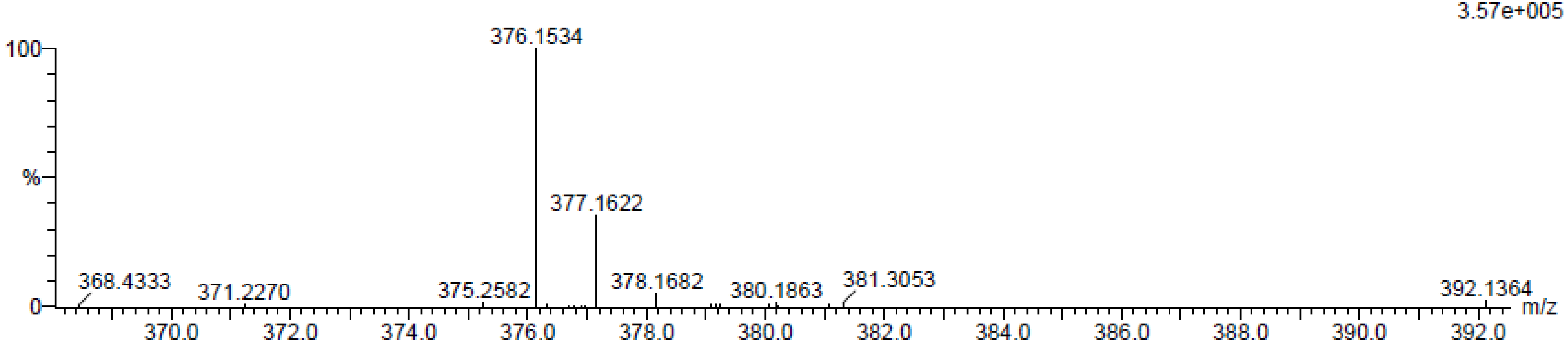

Minimum:				-1.5			
Maximum:		5.0	5.0	100.0			
Mass	Calc. Mass	mDa	PPM	DBE	i-FIT	i-FIT (Norm)	Formula
376.1534	376.1538	-0.4	-1.1	15.5	107.4	0.0	C22 H19 N5 Na

High resolution mass spectrum of **B8h**

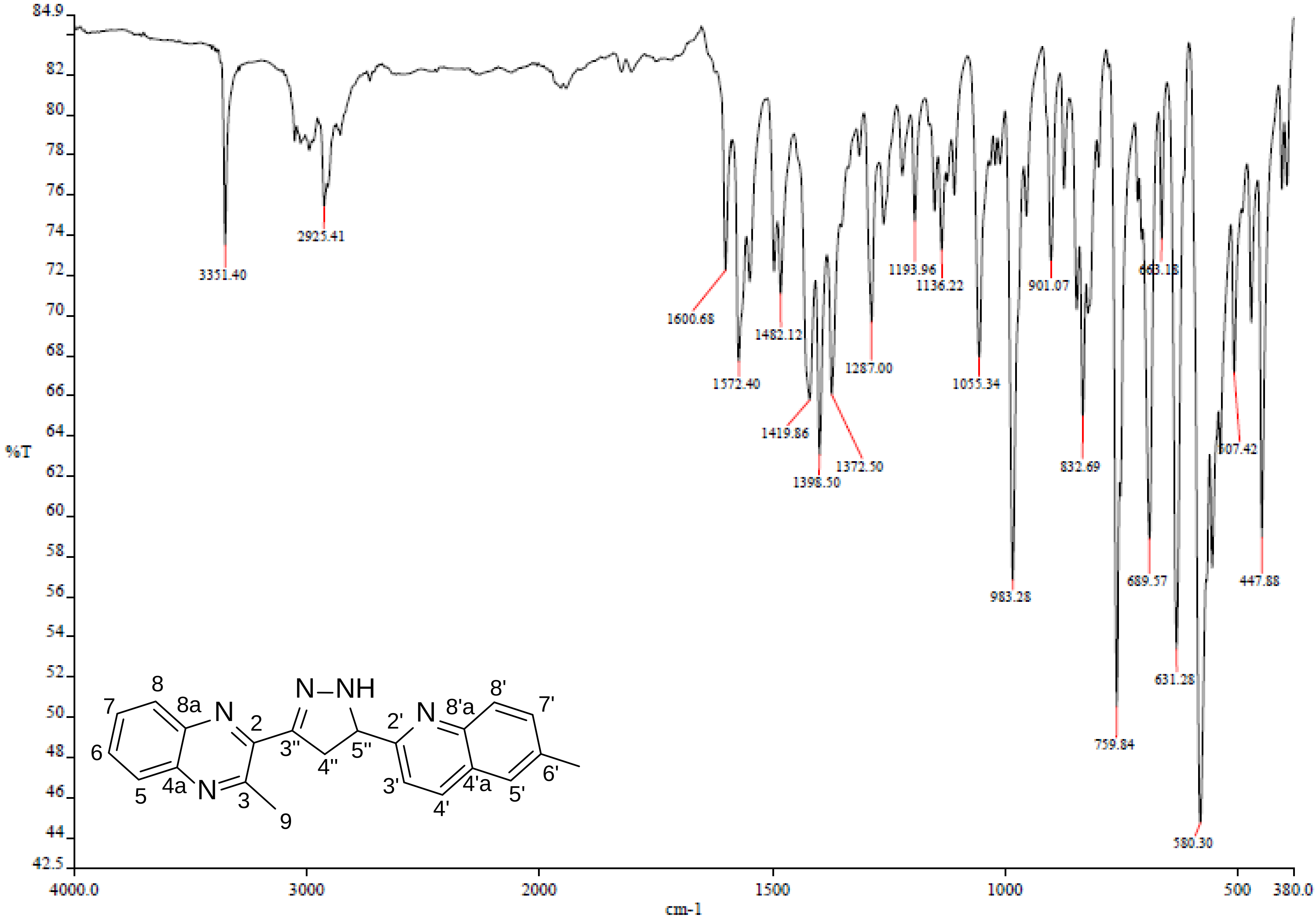

FTIR spectrum of **B8h**

Overlay Spectrum Graph Report

06/10/2017 12:06:16 PM

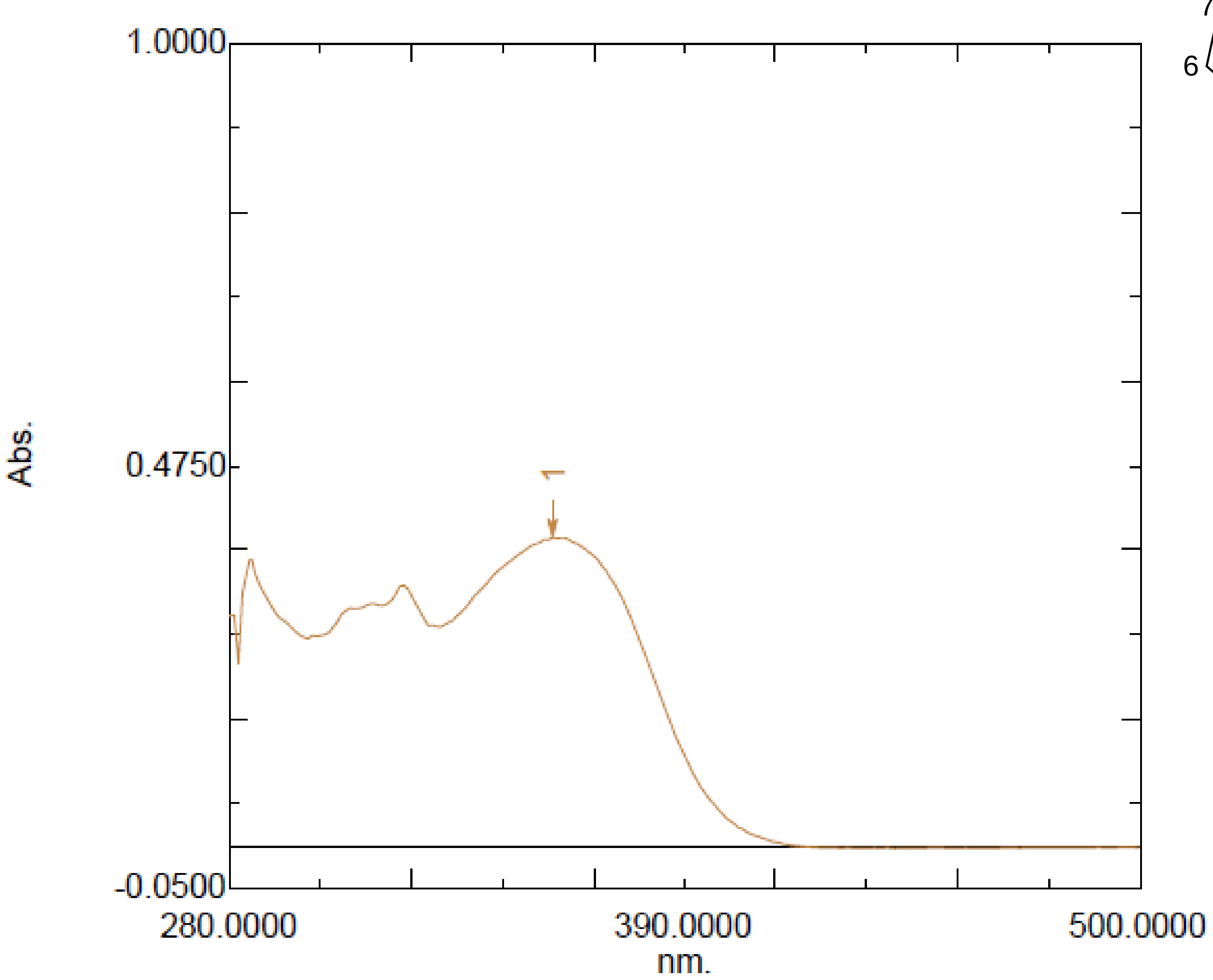

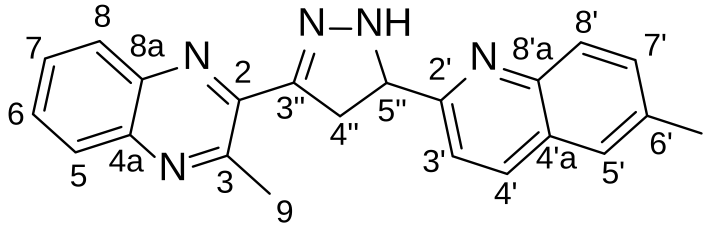

λ	absorbance	logε
358	0.3859	4.44

UV spectrum of **B8h**

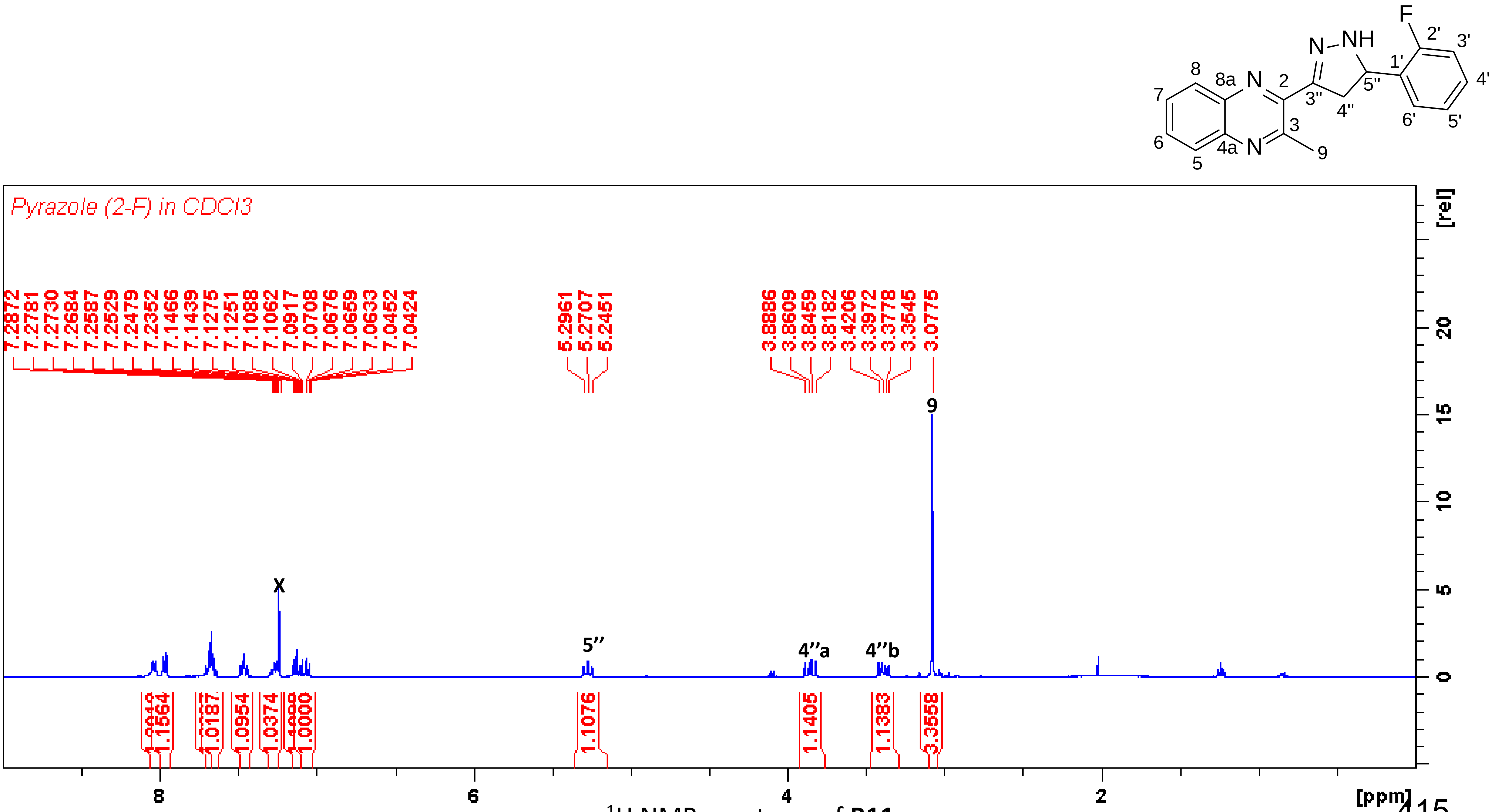

^{1}H NMR spectrum of **B11a**

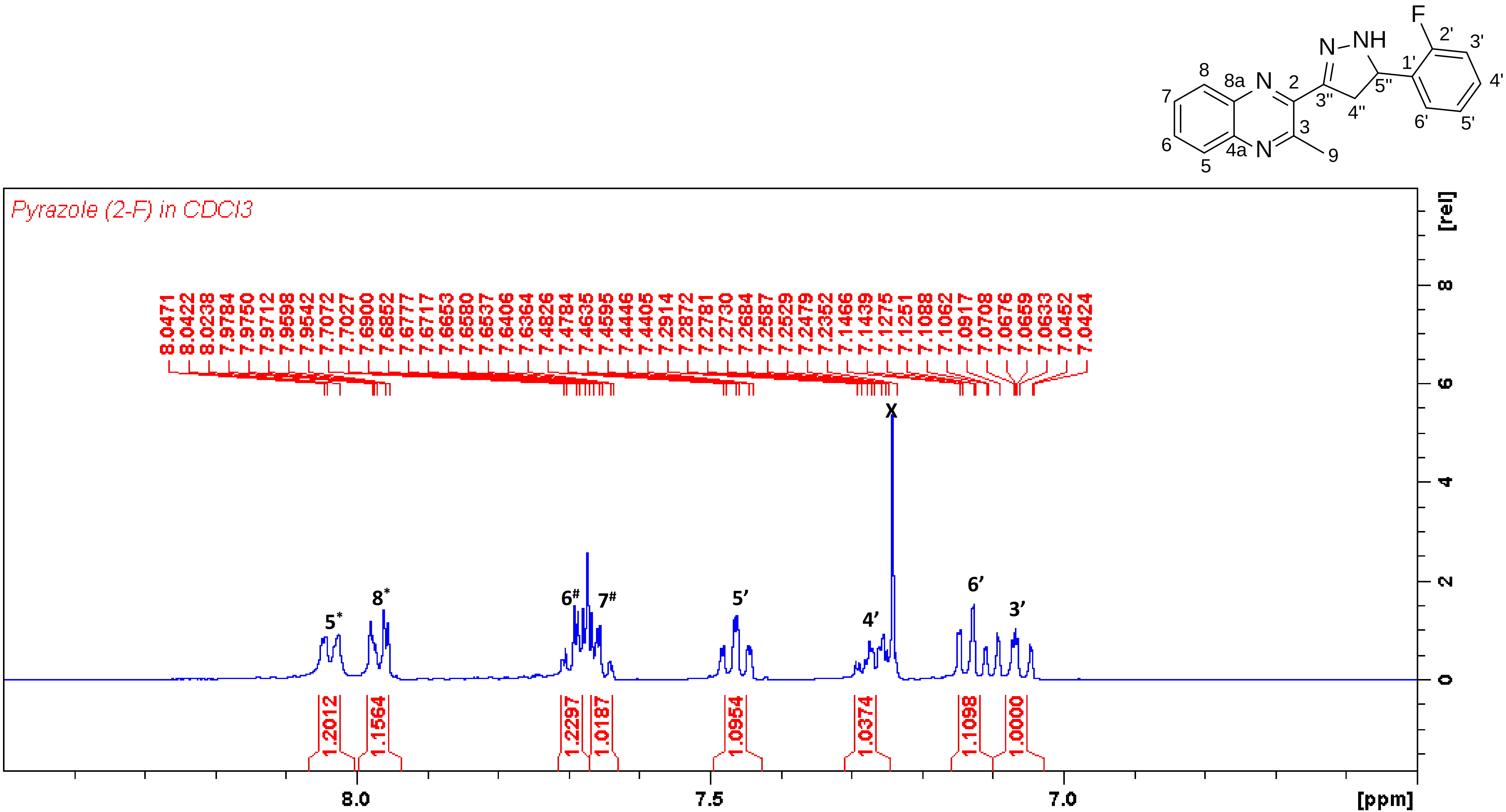

*, # Indicates assignments are interchangeable

Expanded ^{1}H NMR spectrum of **B11a**

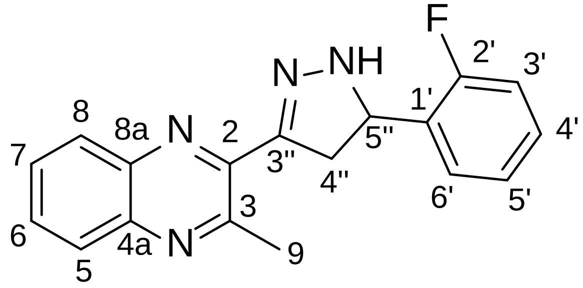

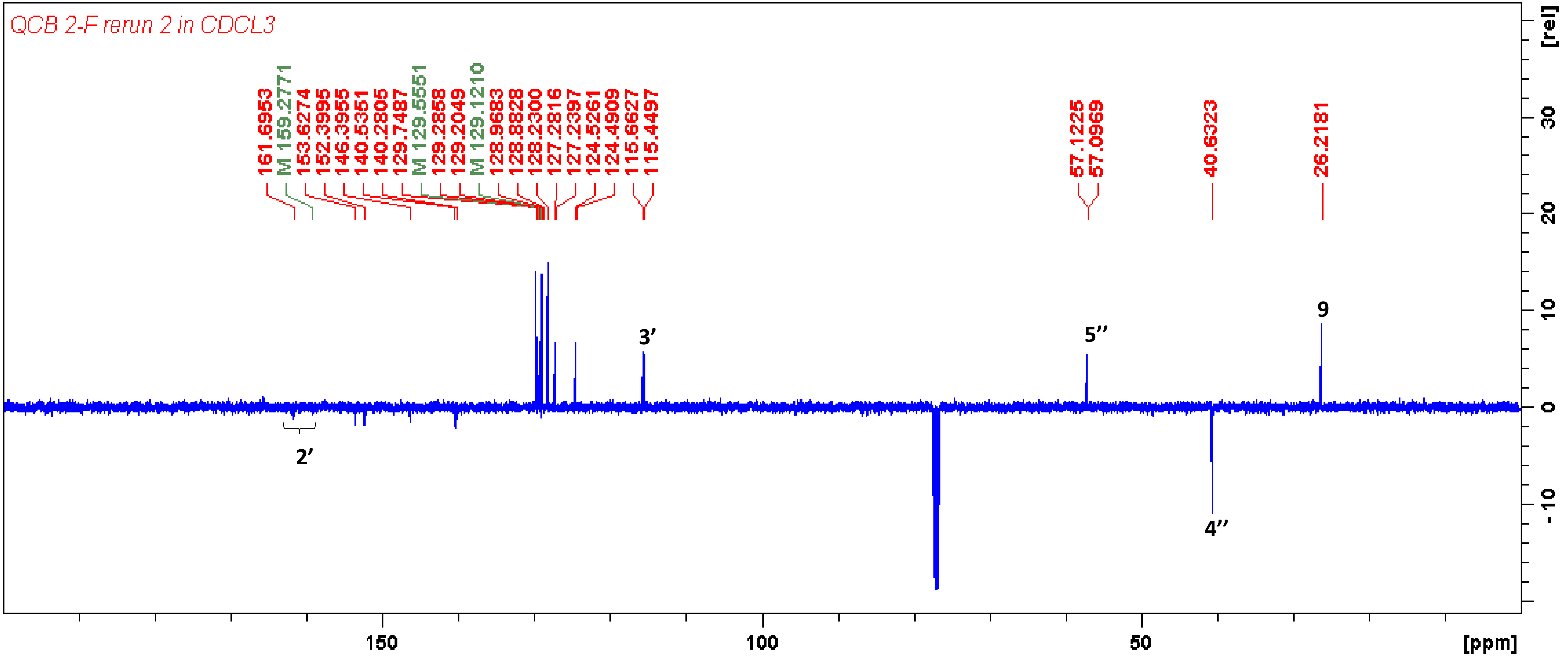

^{13}C NMR spectrum of **B11a**

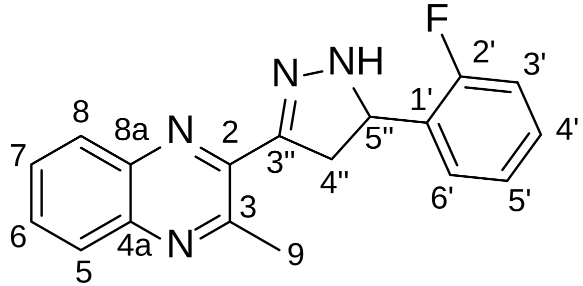

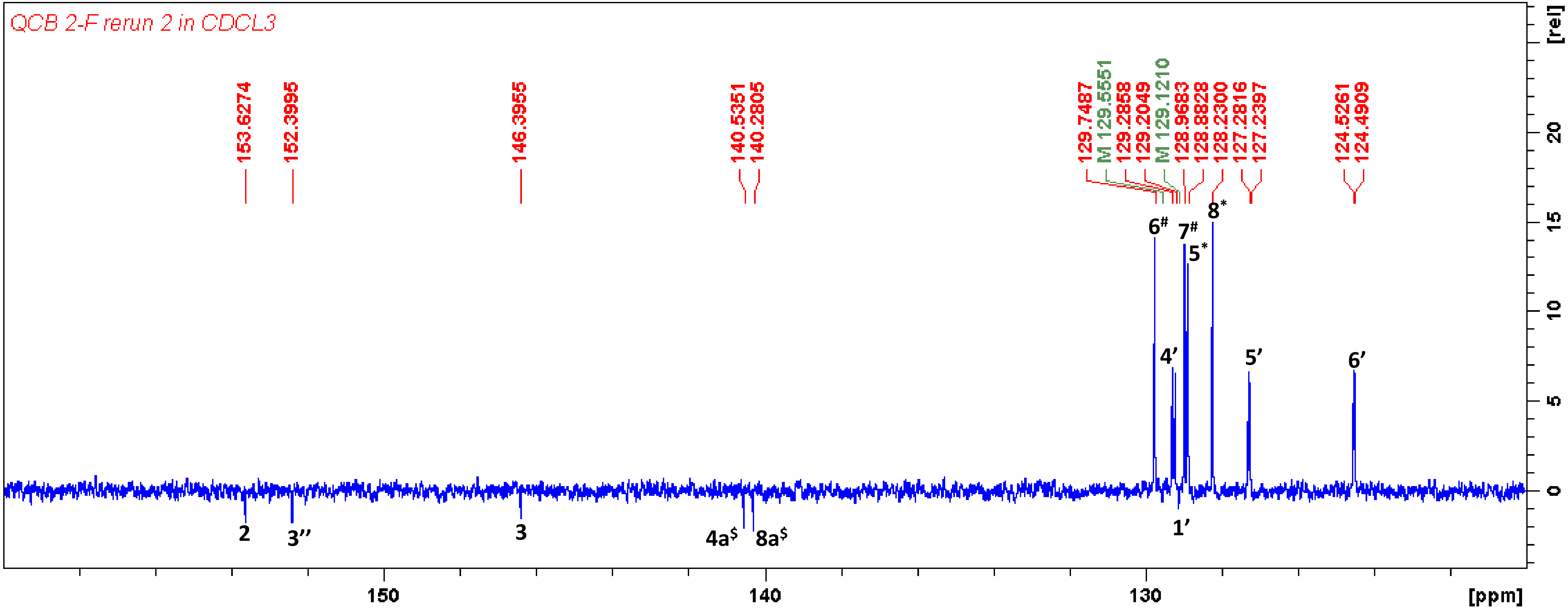

*, #, $ Indicates assignments are interchangeable

Expanded ^{13}C NMR spectrum of **B11a**

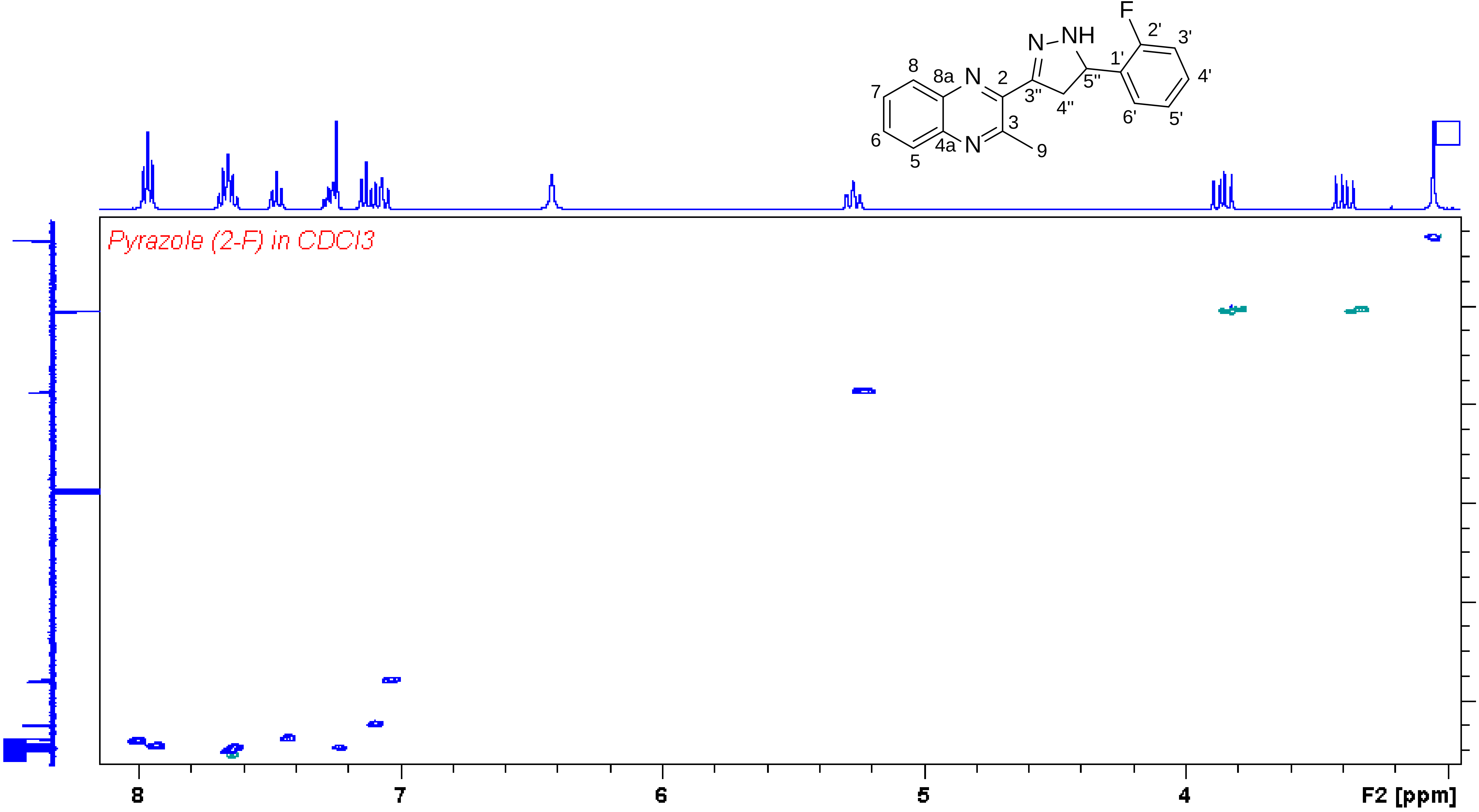

HSQC of **B11a**

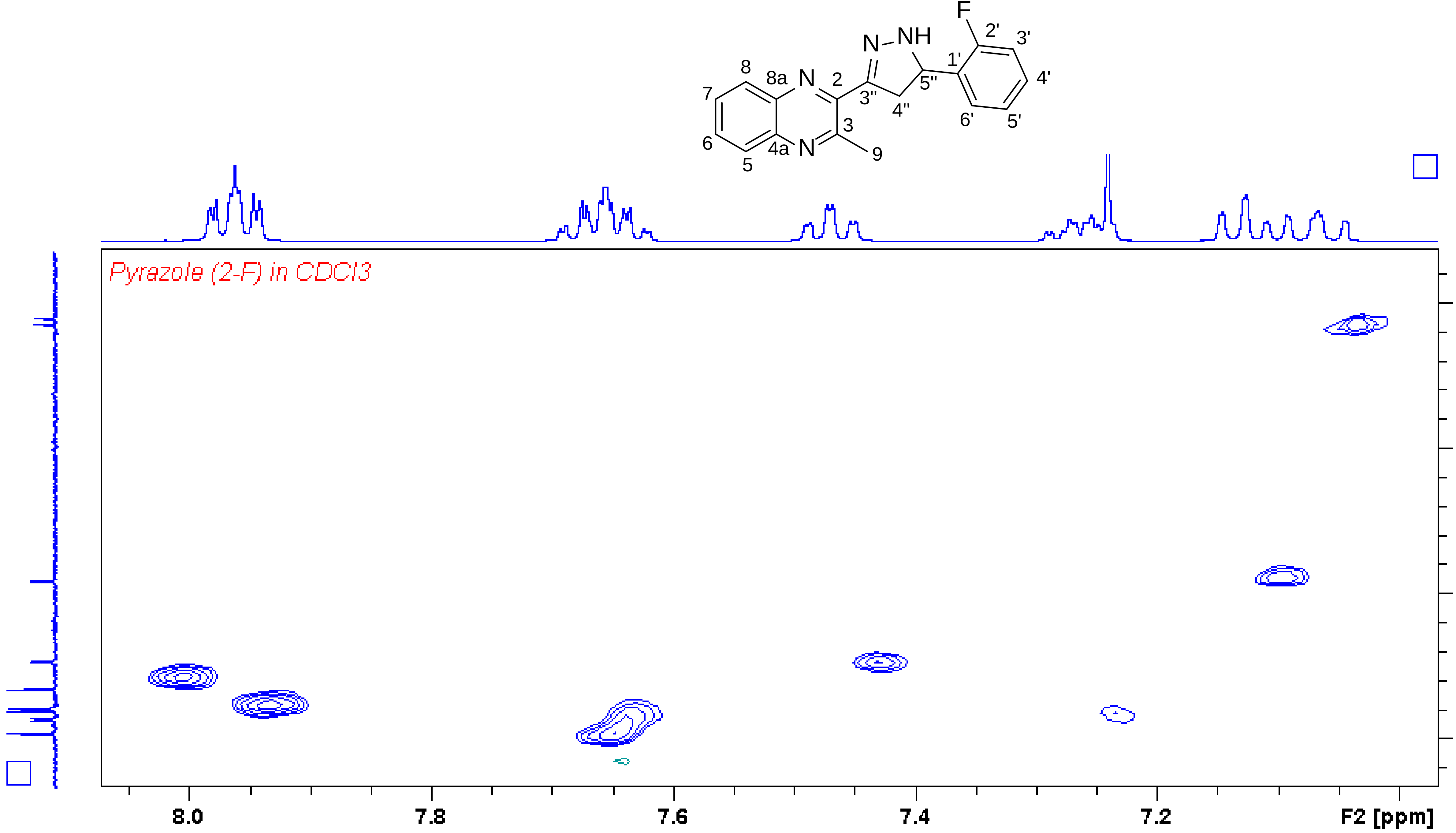

Expanded HSQC of **B11a**

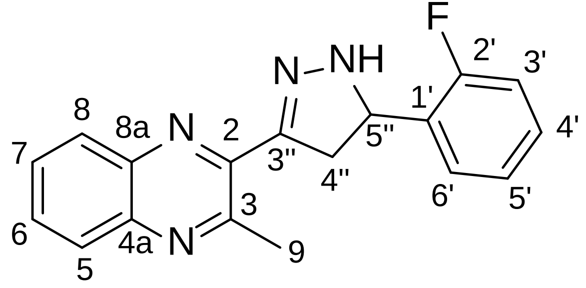

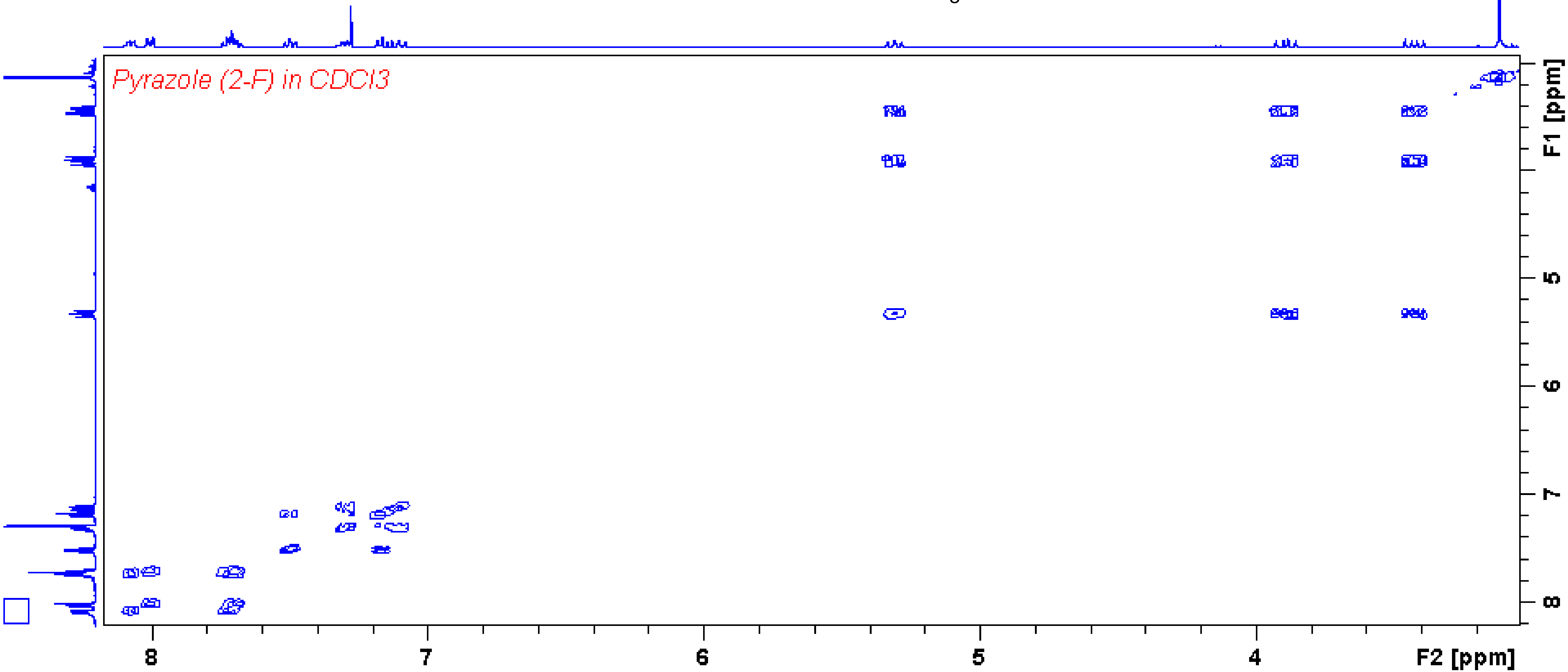

COSY of **B11a**

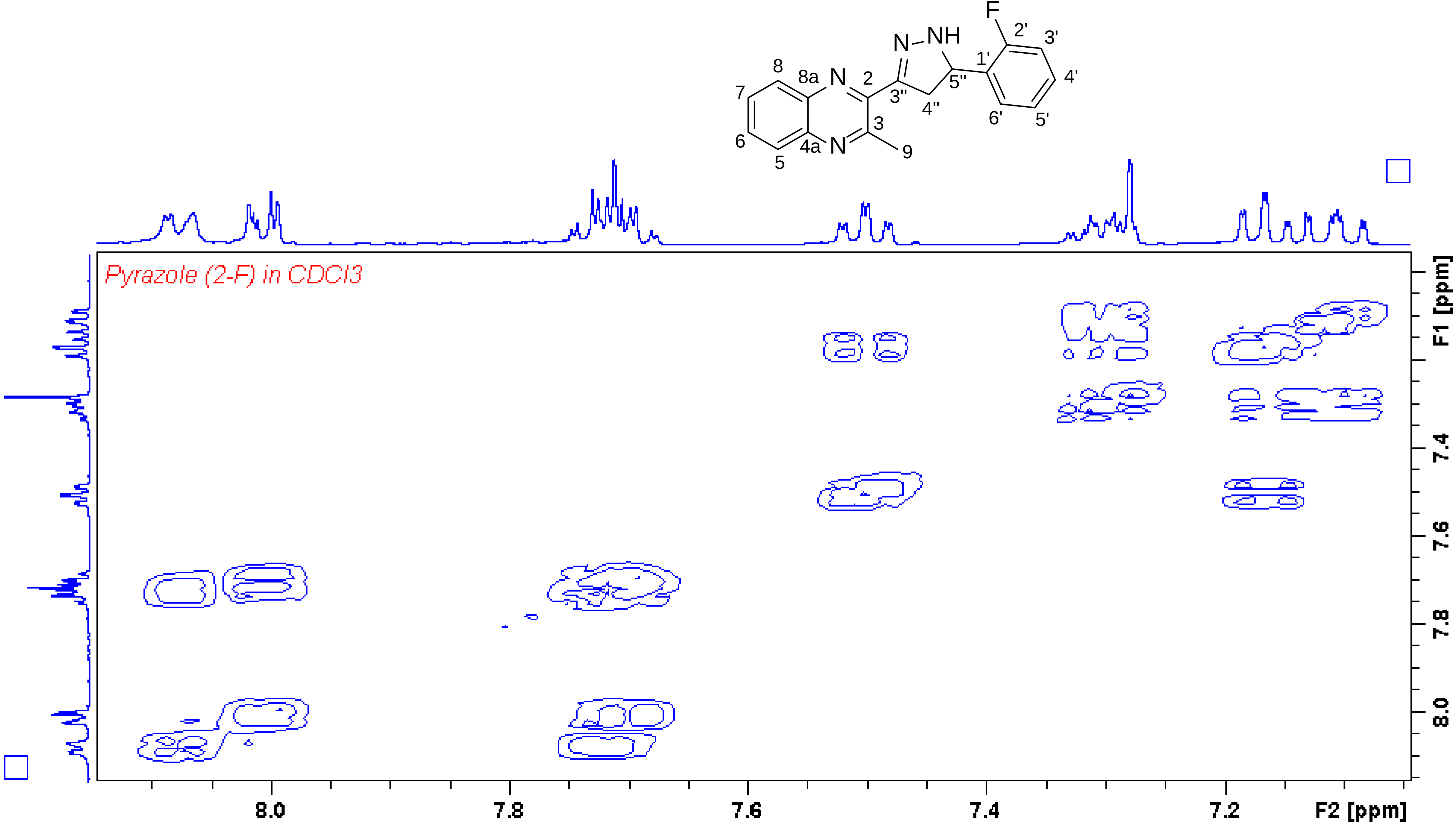

Expanded COSY of **B11a**

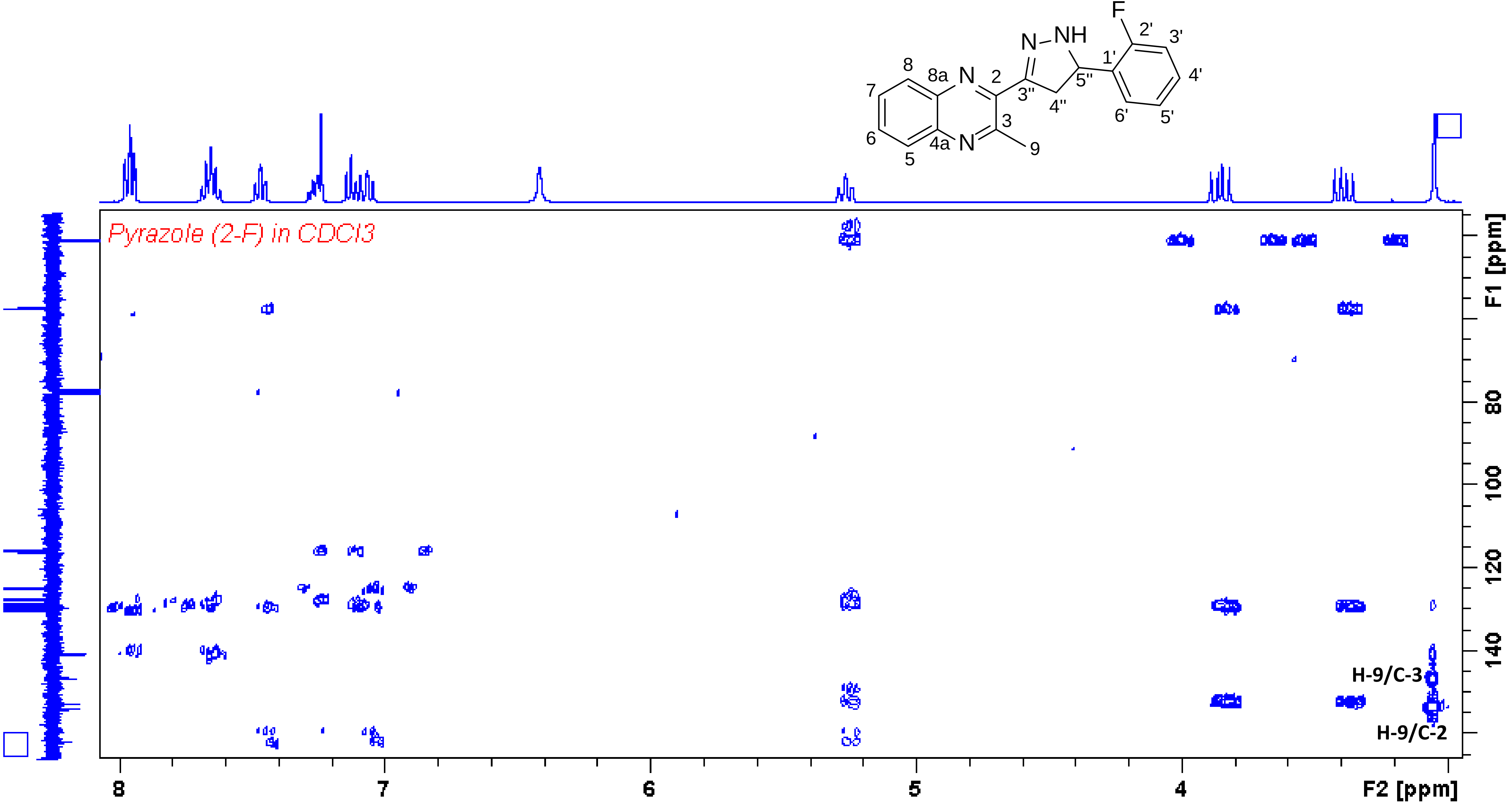

F
N
NH
2'
3'
1'
4'
8
8a
2
7
5''
3''
4''
6'
5'
3
6
4a
9
5
Pyrazole (2-F) in CDCl3
H-9/C-3
H-9/C-2
F1 [ppm]
F2 [ppm]
8
7
6
5
4
80
100
120
140

HMBC of **B11a**

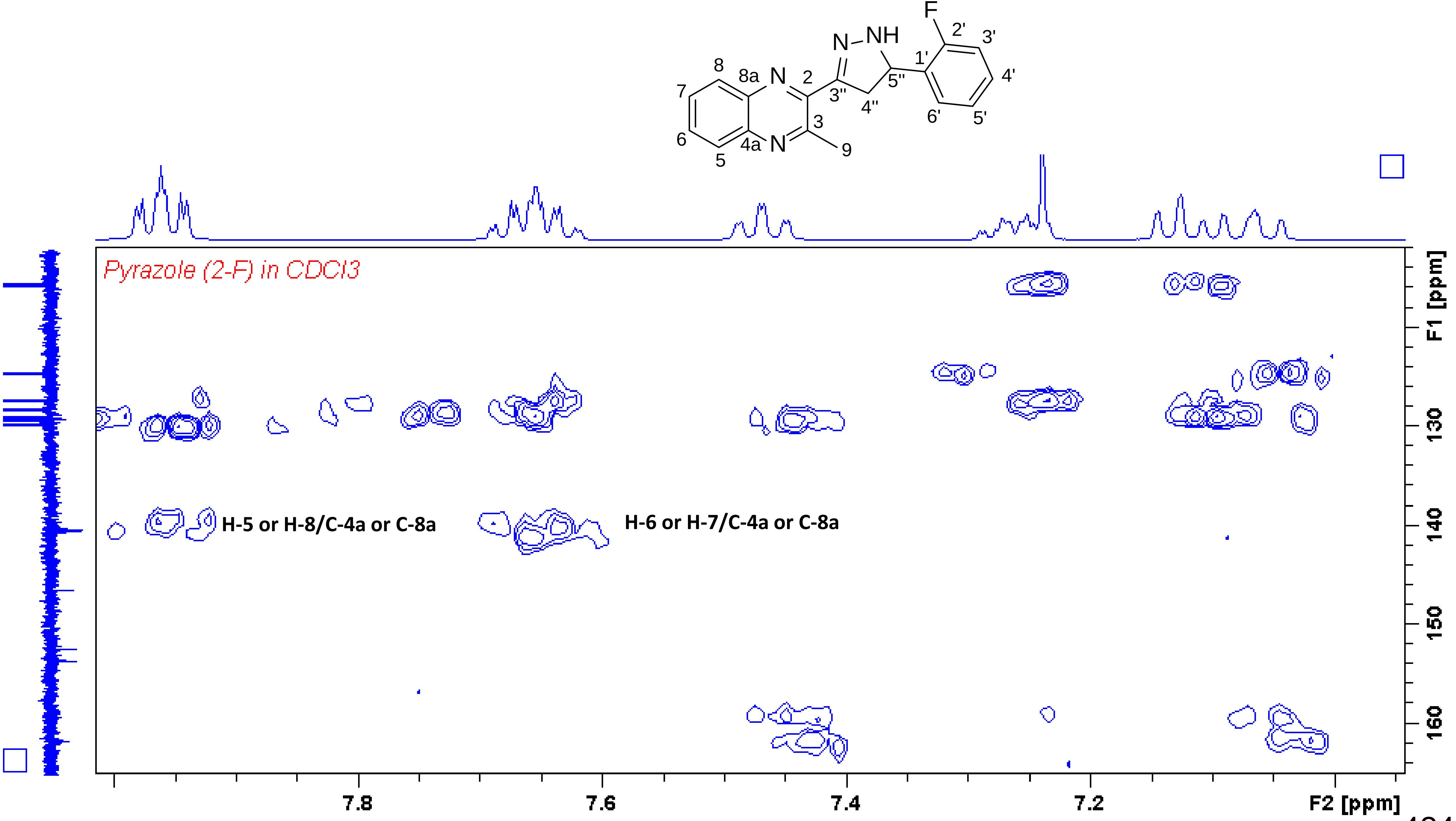

Expanded HMBC of **B11a**

Elemental Composition Report

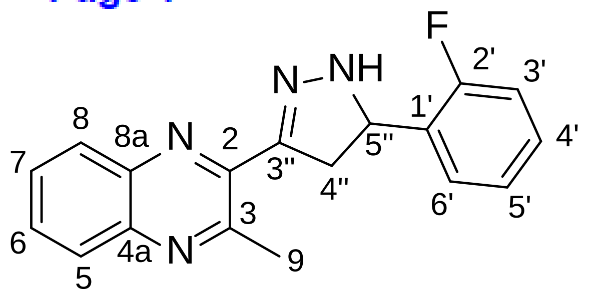

Single Mass Analysis

Tolerance = 5.0 PPM / DBE: min = -1.5, max = 100.0
Element prediction: Off
Number of isotope peaks used for i-FIT = 3

Monoisotopic Mass, Even Electron Ions
9 formula(e) evaluated with 1 results within limits (up to 20 closest results for each mass)
Elements Used:
C: 15-20 H: 15-20 N: 0-5 F: 0-1 Na: 0-1
Py-QCB 2-F 7 (0.203) Cm (1:61)
TOF MS ES+

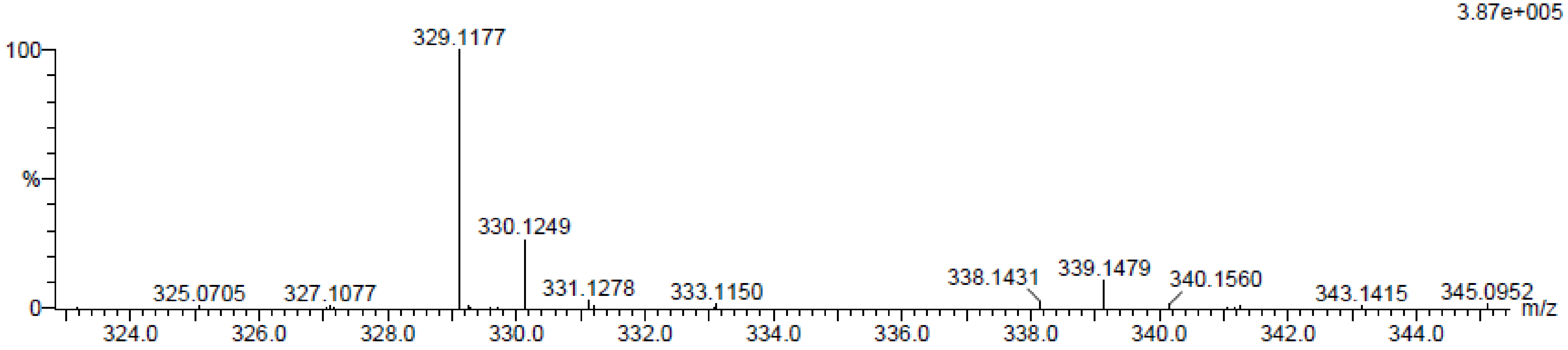

Minimum:				-1.5			
Maximum:		5.0	5.0	100.0			
Mass	Calc. Mass	mDa	PPM	DBE	i-FIT	i-FIT (Norm)	Formula
329.1177	329.1178	-0.1	-0.3	12.5	104.8	0.0	C18 H15 N4 F Na

High resolution mass spectrum of **B11a**

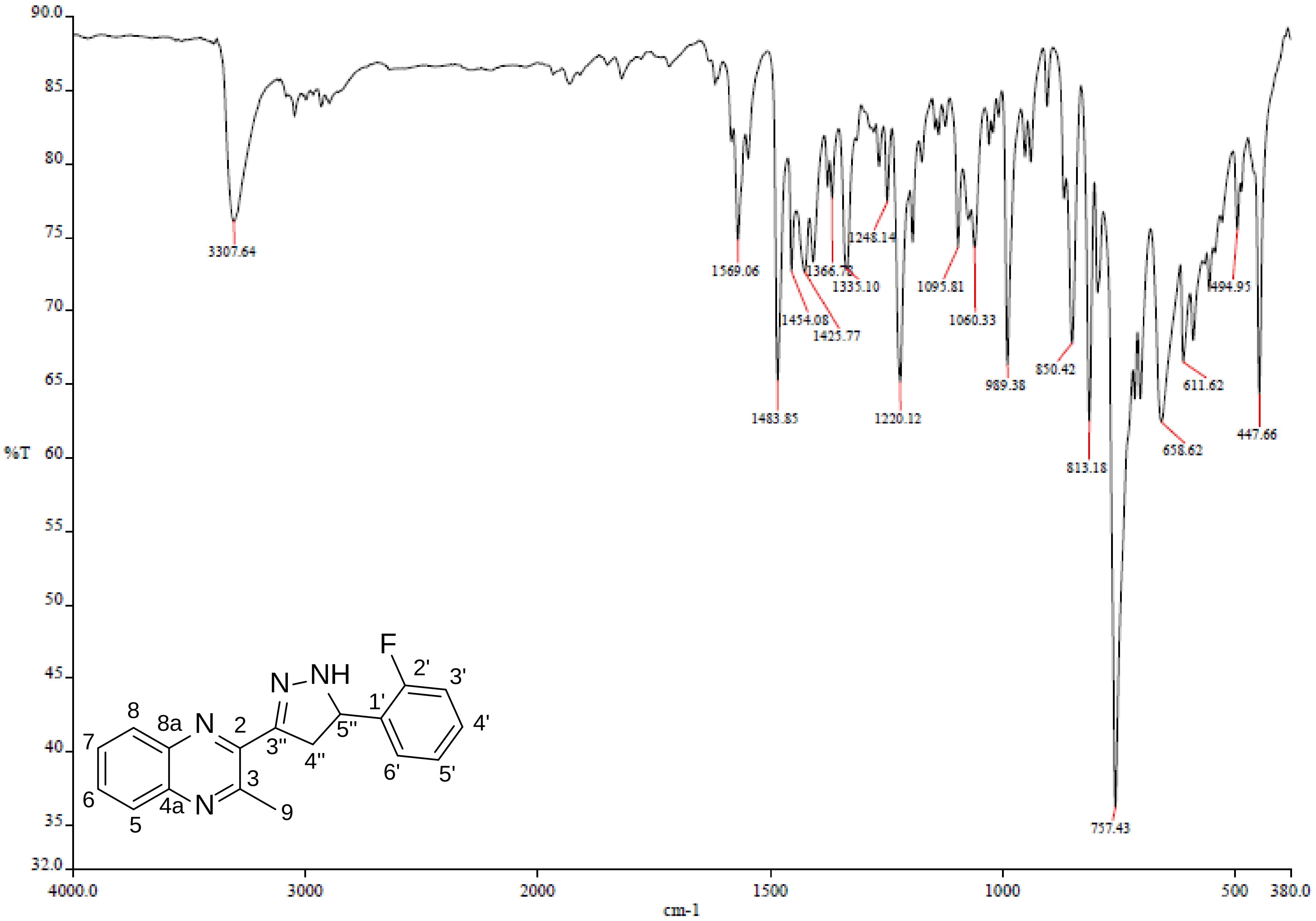

FTIR spectrum of **B11a**

Overlay Spectrum Graph Report

06/10/2017 11:50:06 AM

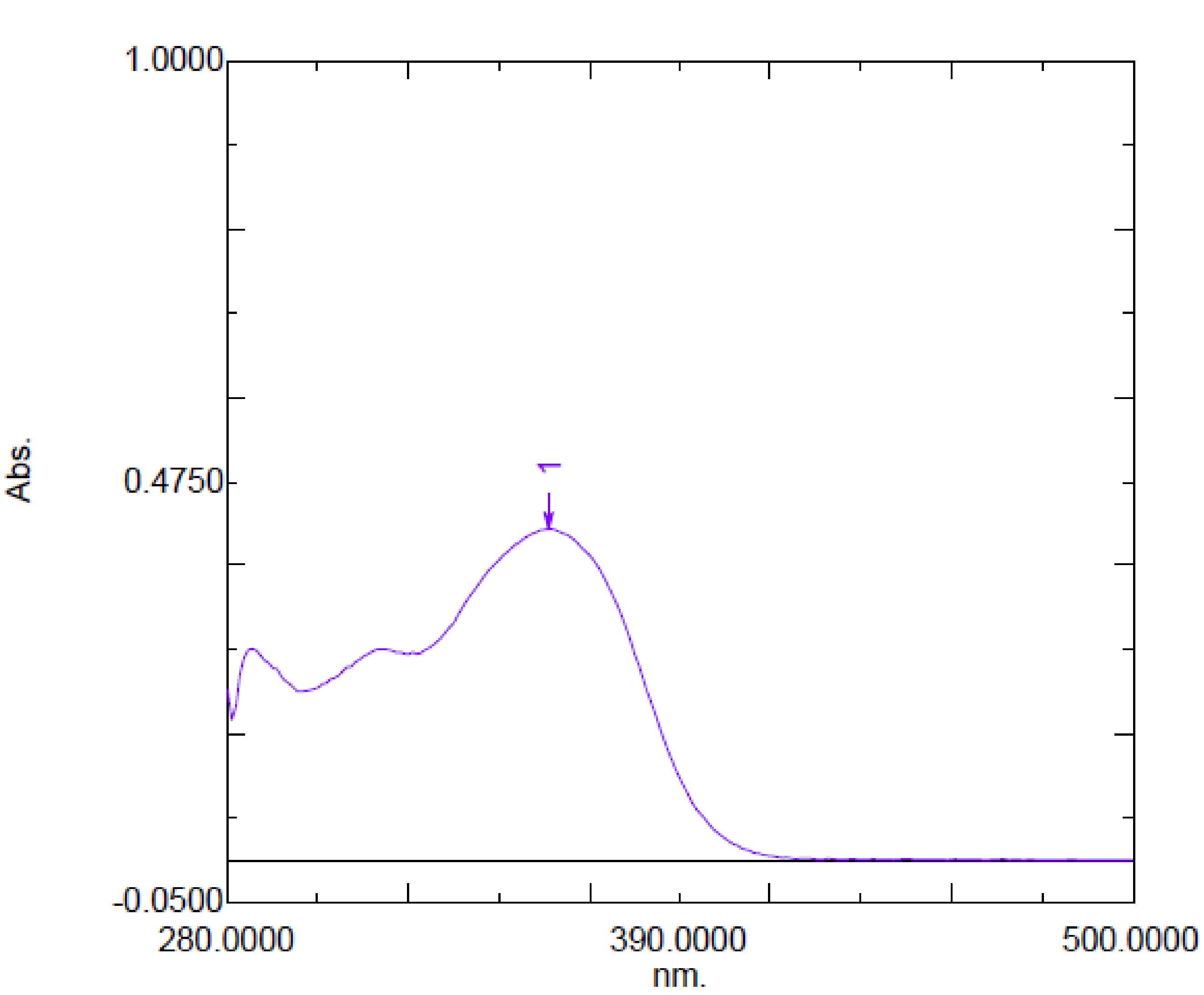

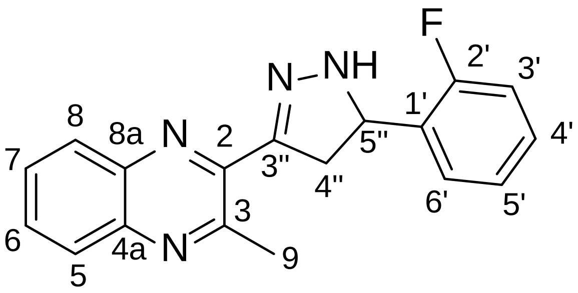

λ	absorbance	logε
358	0.4157	4.41

UV spectrum of **B11a**

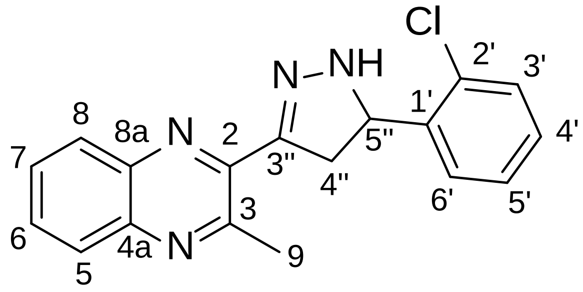

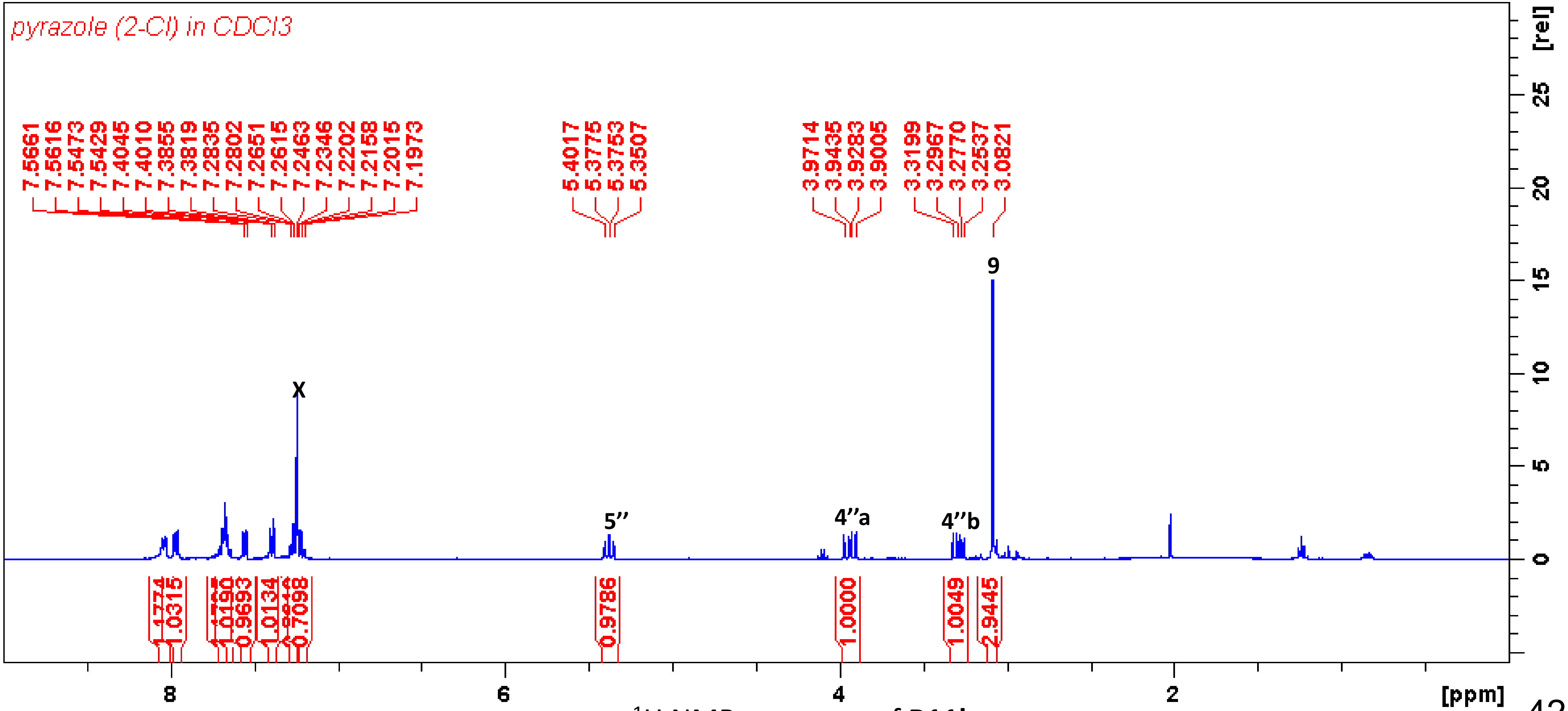

^{1}H NMR spectrum of **B11b**

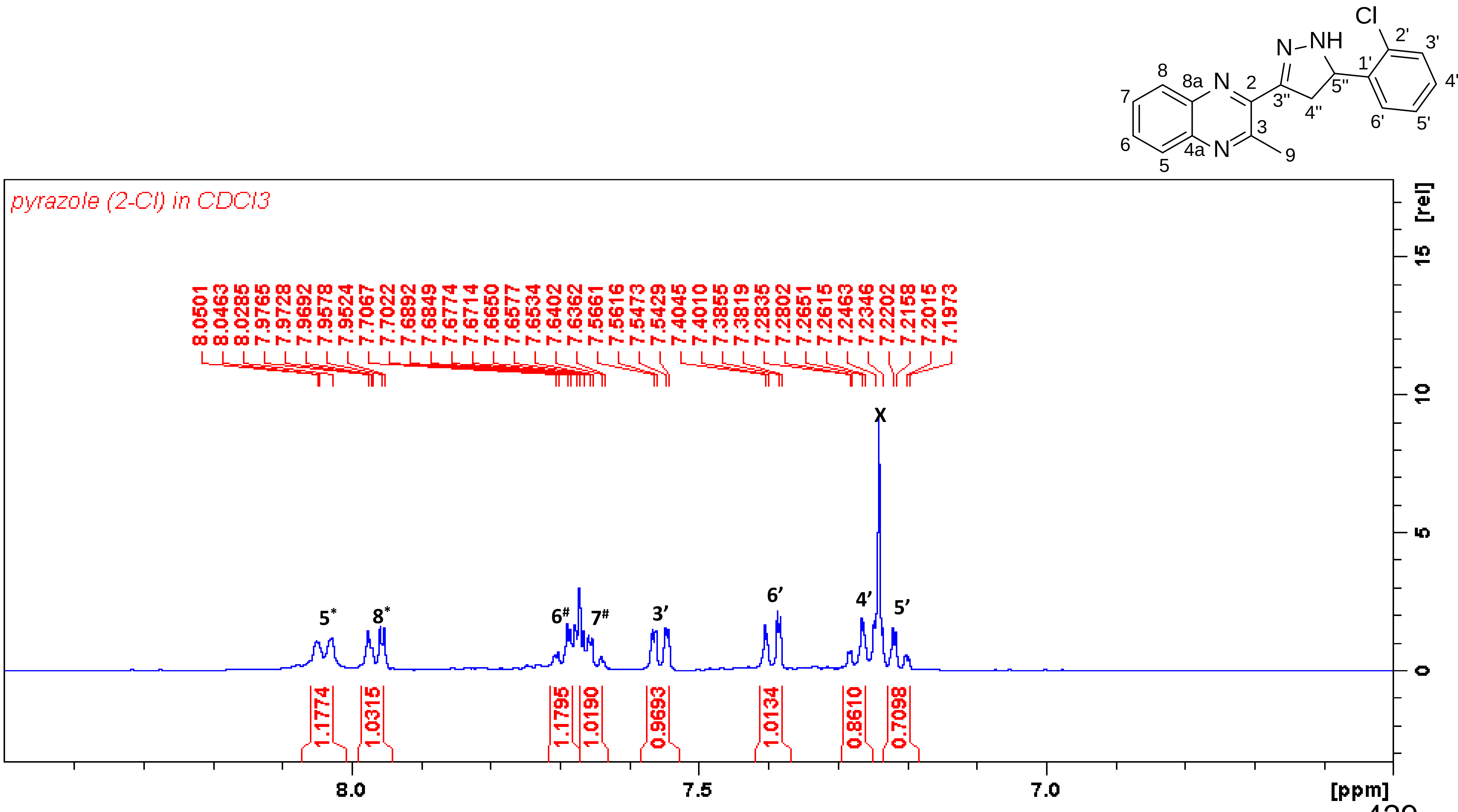

*, # Indicates assignments are interchangeable

Expanded ^{1}H NMR spectrum of **B11b**

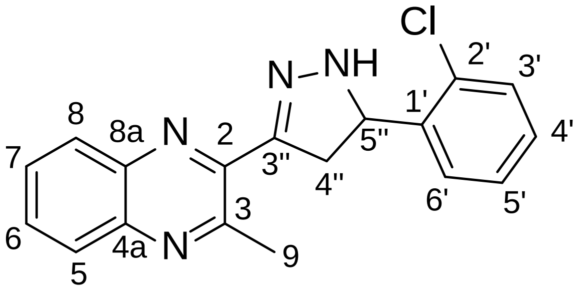

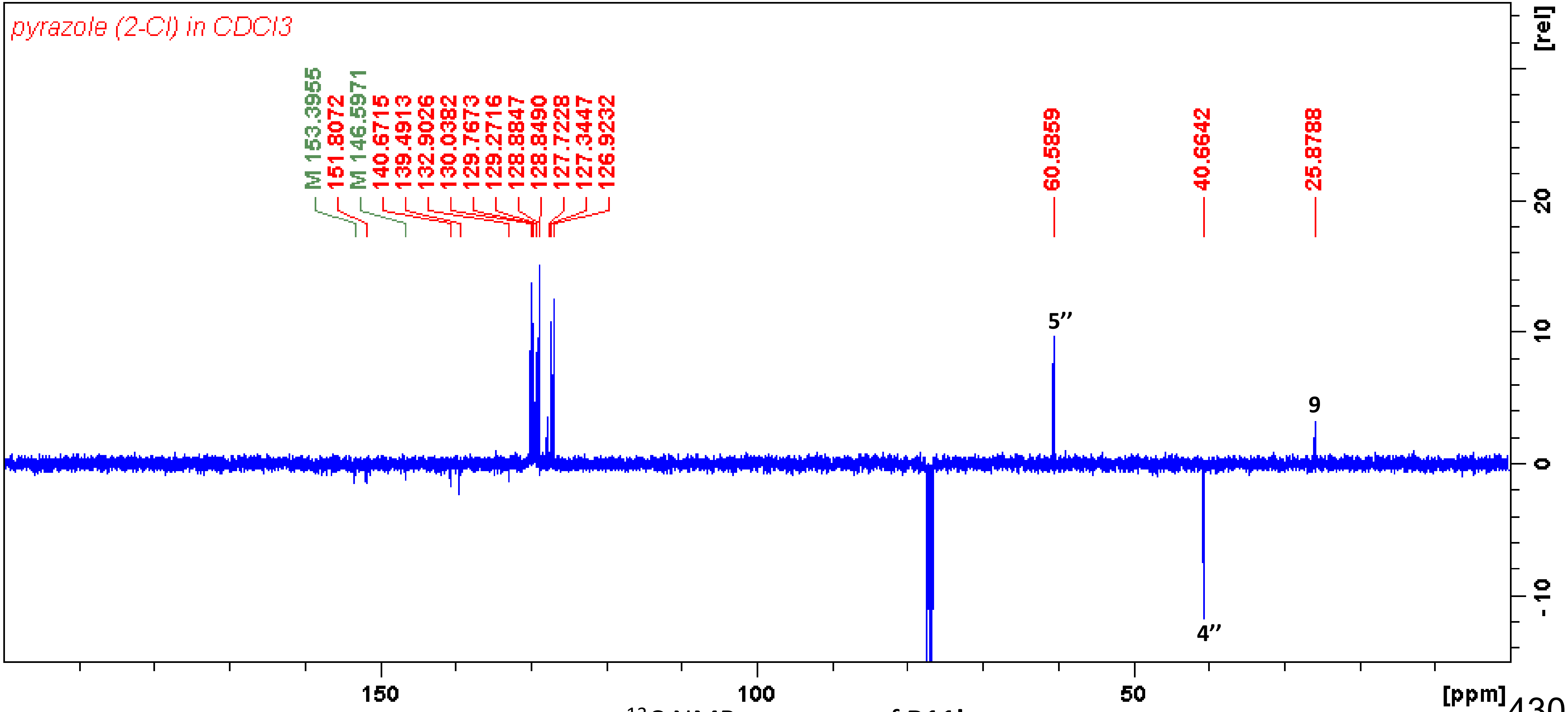

^{13}C NMR spectrum of **B11b**

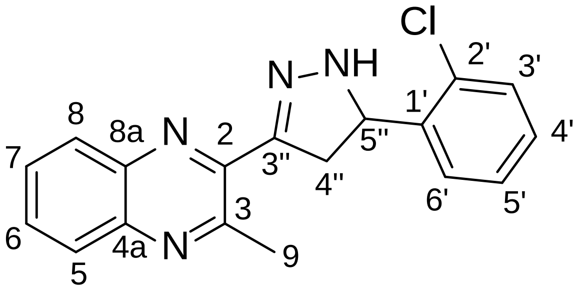

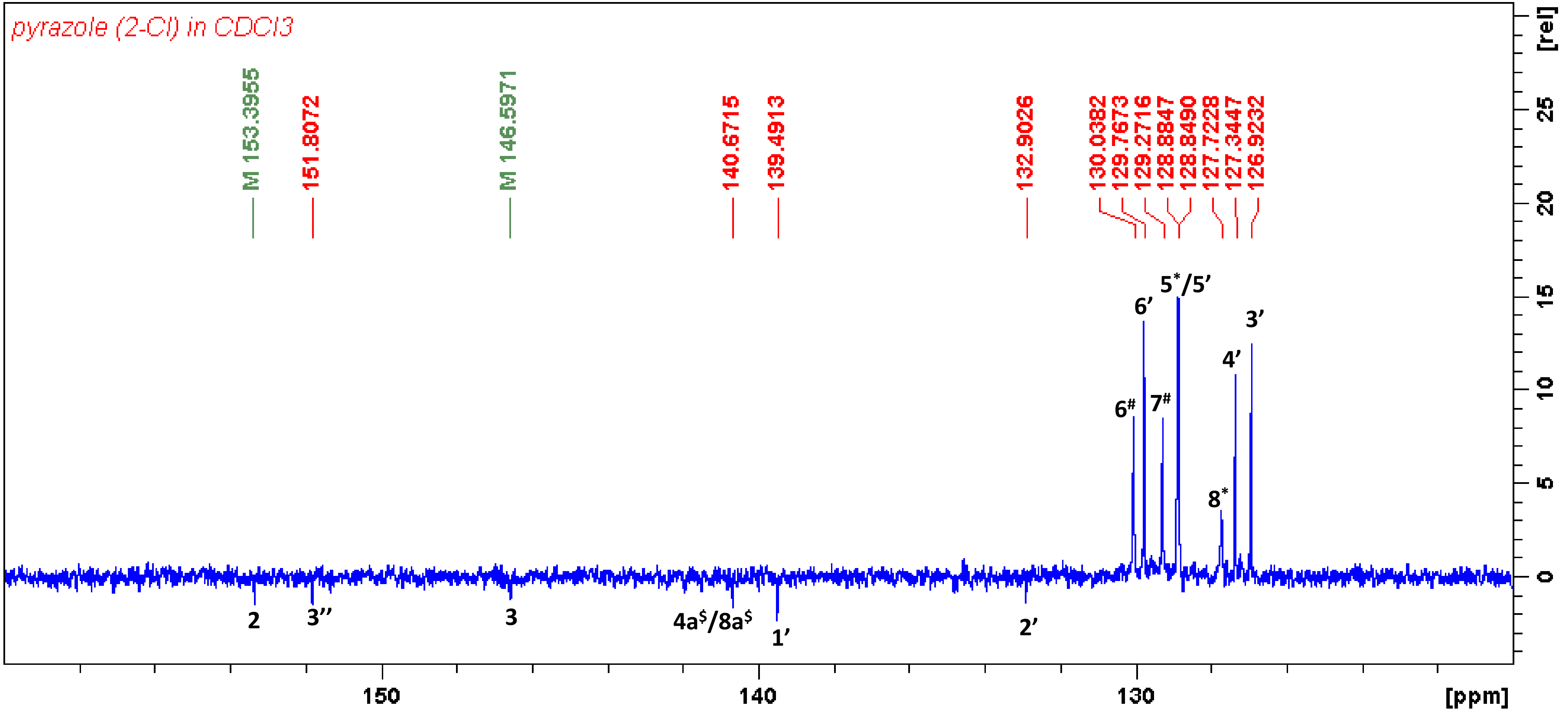

*, #, $ Indicates assignments are interchangeable

Expanded ^{13}C NMR spectrum of **B11b**

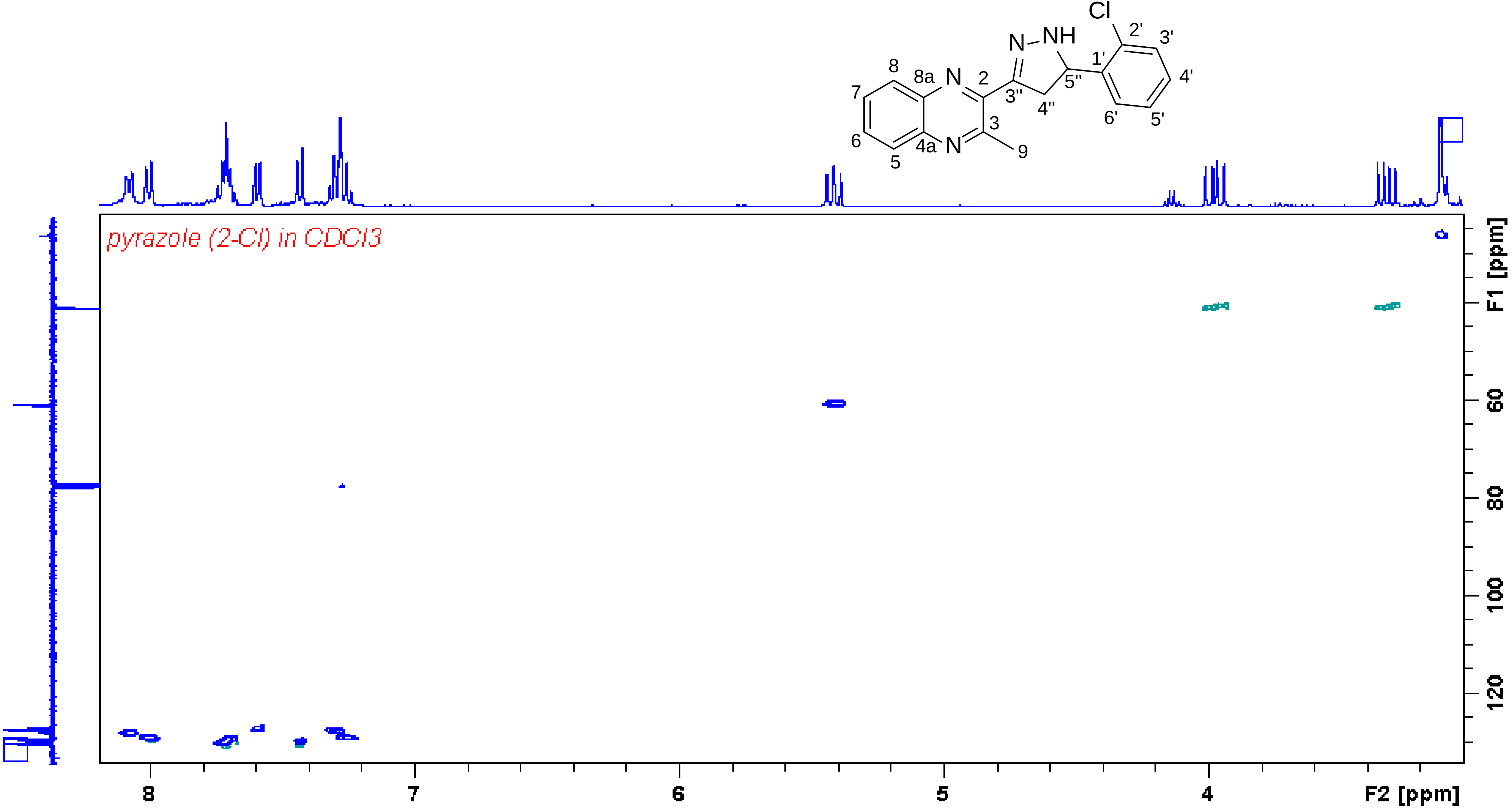
pyrazole (2-Cl) in CDCl3
F1 [ppm]
60
80
100
120
8
7
6
5
4
F2 [ppm]
Cl
NH
N
2'
3'
1'
4'
5''
8
8a
N
2
3''
7
4''
6'
5'
3
6
4a
N
9
5

HSQC of **B11b**

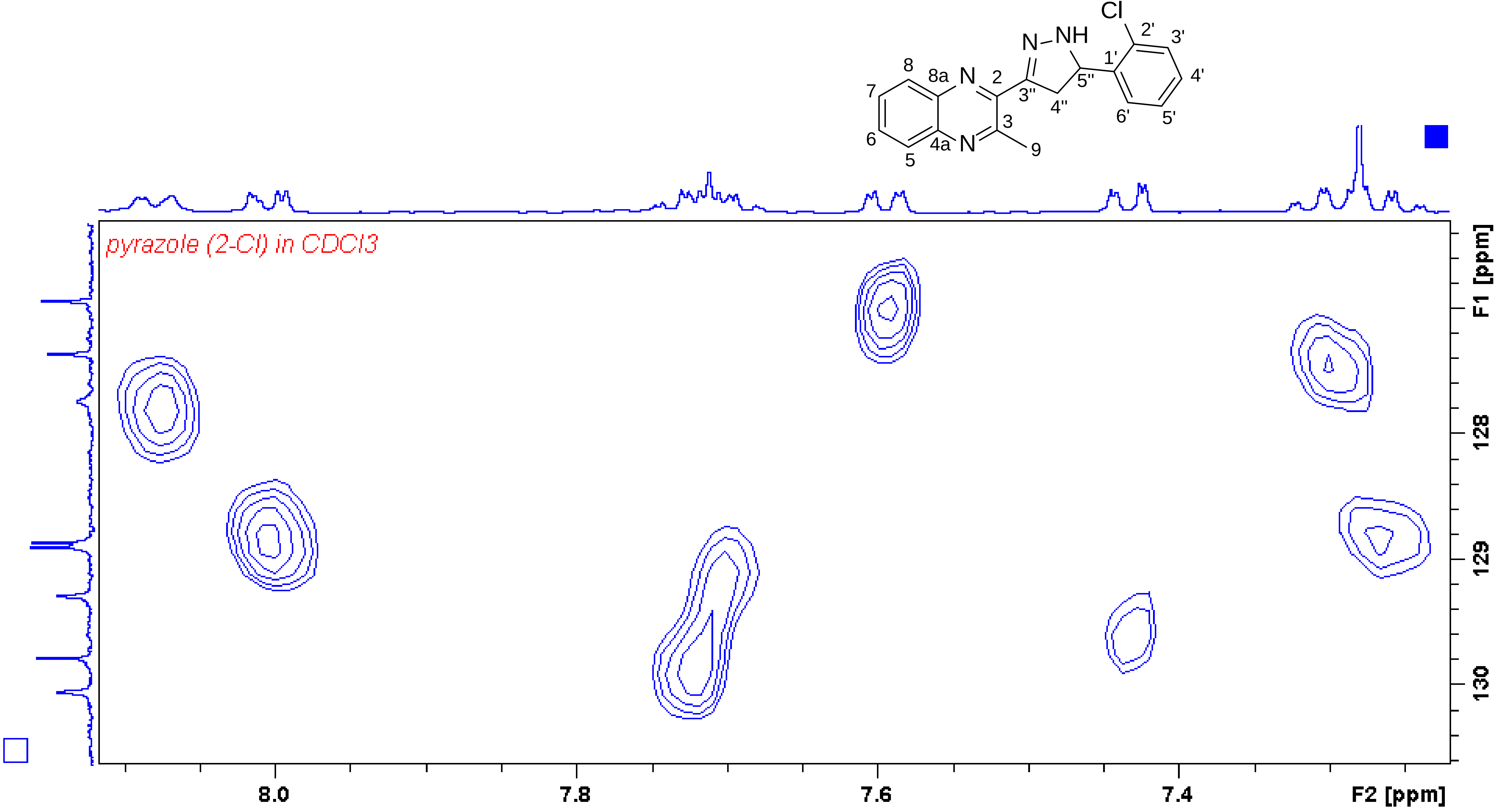

Expanded HSQC of **B11b**

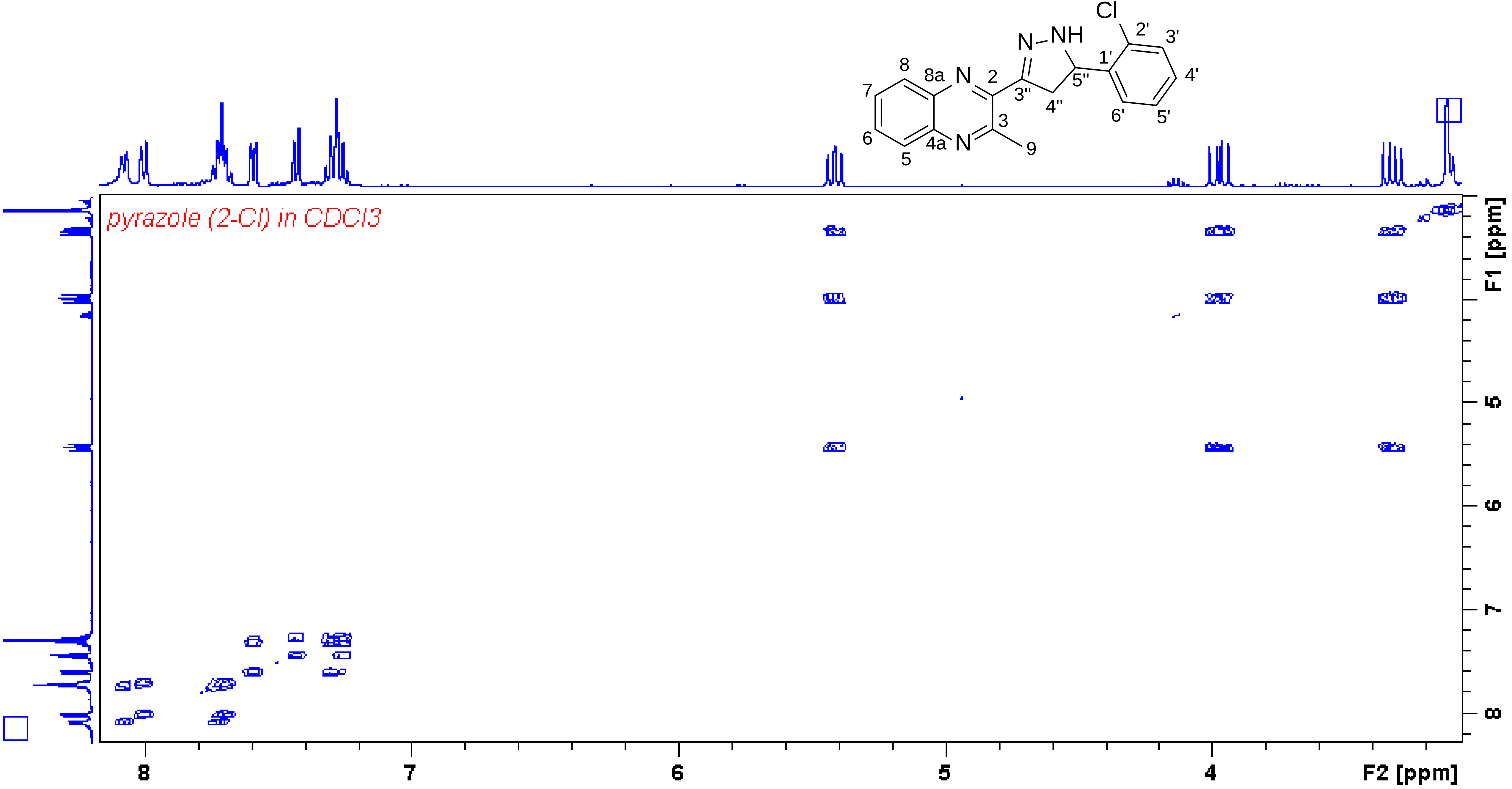

COSY of **B11b**

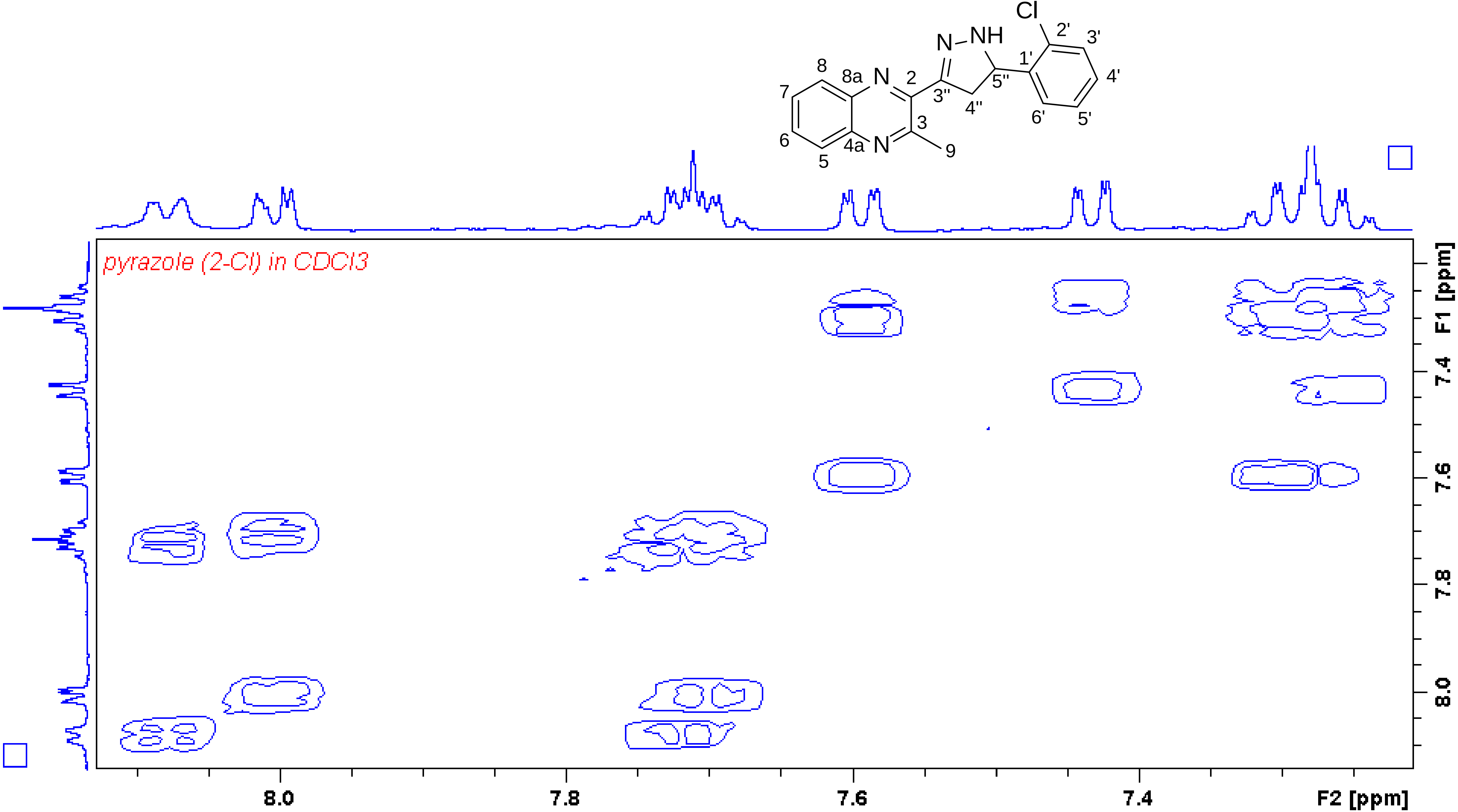

Expanded COSY of **B11b**

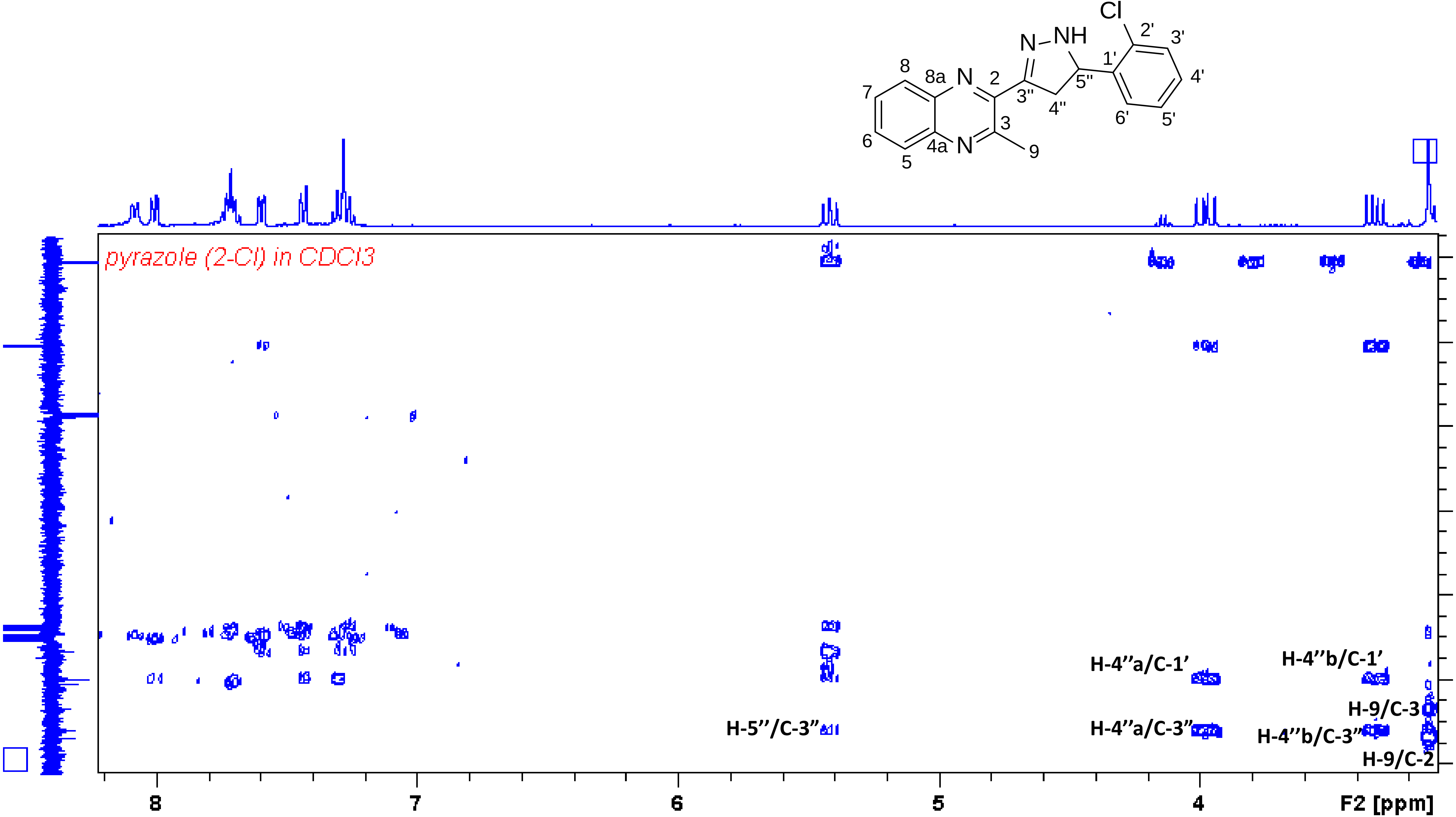

Cl
2'
3'
N
NH
1'
8
8a
N
2
4'
7
5''
3''
4''
6'
5'
3
6
4a
N
9
5
pyrazole (2-Cl) in CDCl3
F1 [ppm]
80
100
120
140
H-4''a/C-1'
H-4''b/C-1'
H-9/C-3
H-5''/C-3''
H-4''a/C-3''
H-4''b/C-3''
H-9/C-2
8
7
6
5
4
F2 [ppm]

HMBC of **B11b**

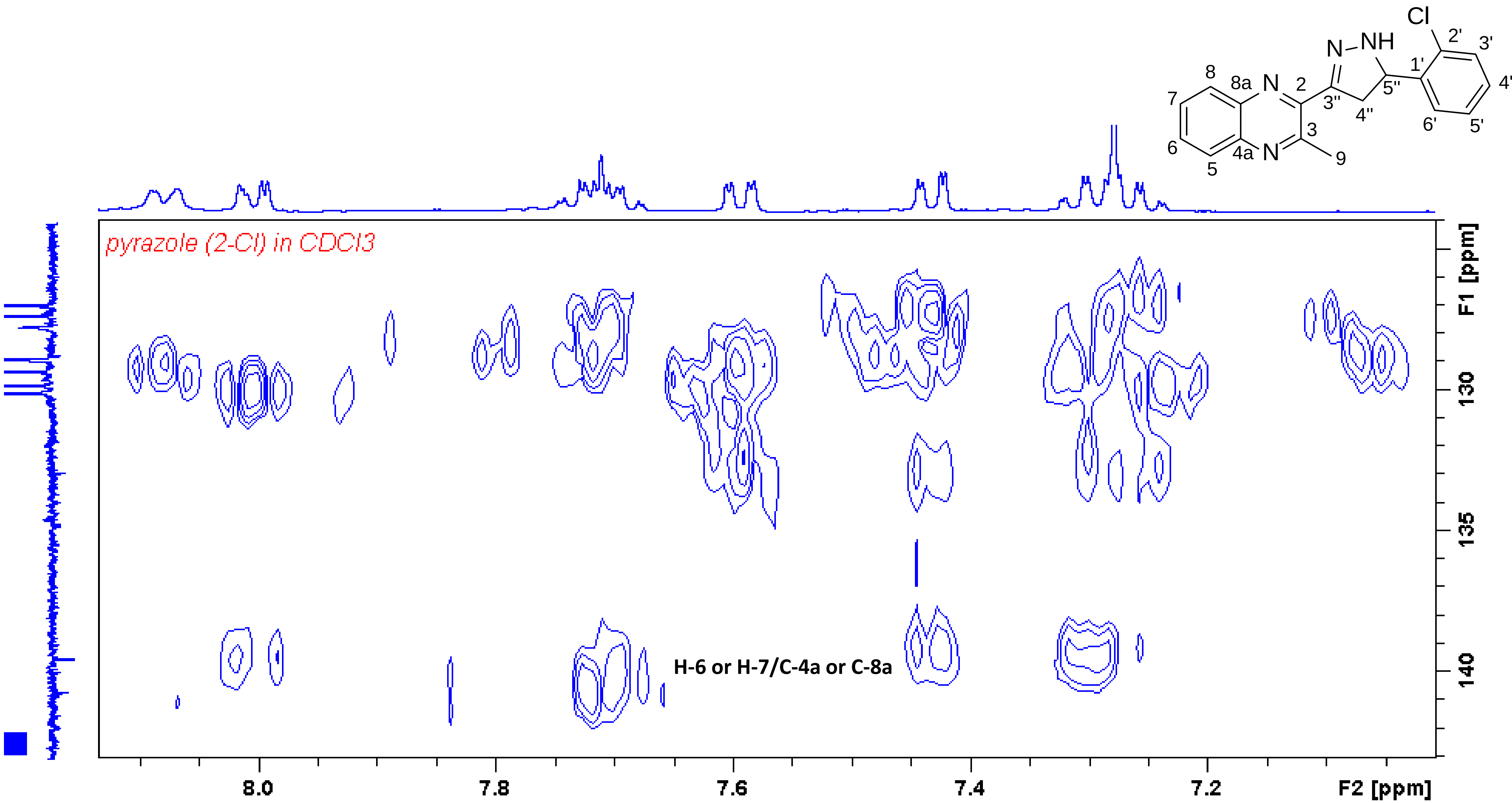

Expanded HMBC of **B11b**

Elemental Composition Report

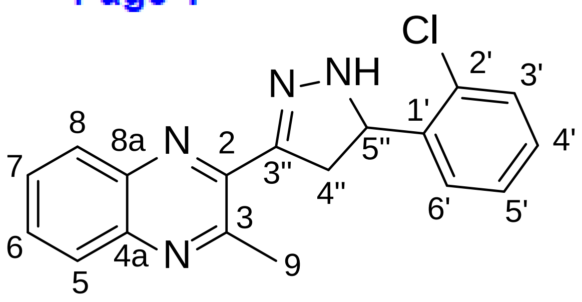

Single Mass Analysis

Tolerance = 5.0 PPM / DBE: min = -1.5, max = 100.0
Element prediction: Off
Number of isotope peaks used for i-FIT = 3

Monoisotopic Mass, Even Electron Ions
10 formula(e) evaluated with 1 results within limits (up to 20 closest results for each mass)
Elements Used:
C: 15-20 H: 15-20 N: 0-5 Na: 0-1 Cl: 0-1
Py-QCB 2-Cl 17 (0.540) Cm (1:61)
TOF MS ES+

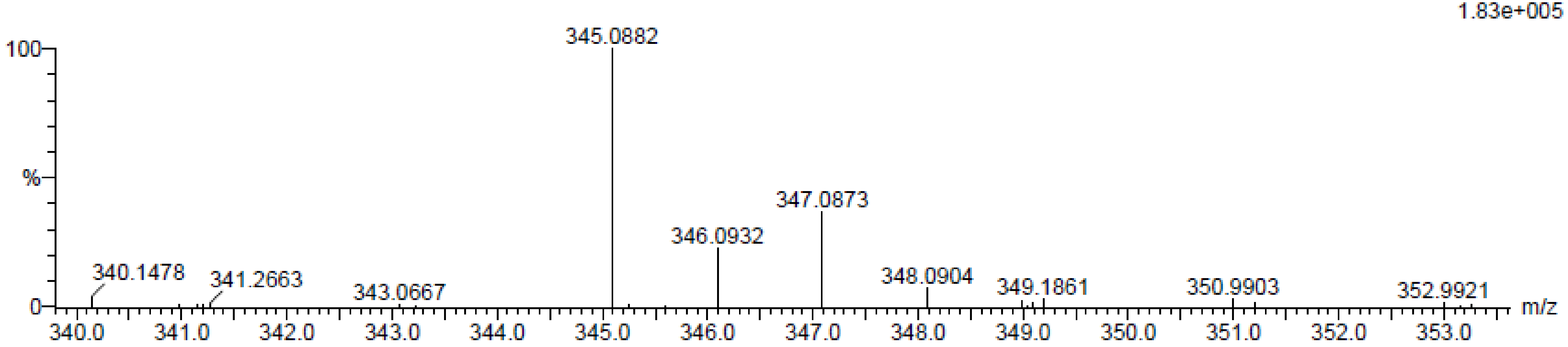

Minimum:				-1.5			
Maximum:		5.0	5.0	100.0			
Mass	Calc. Mass	mDa	PPM	DBE	i-FIT	i-FIT (Norm)	Formula
345.0882	345.0883	-0.1	-0.3	12.5	47.9	0.0	C18 H15 N4 Na Cl

High resolution mass spectrum of **B11b**

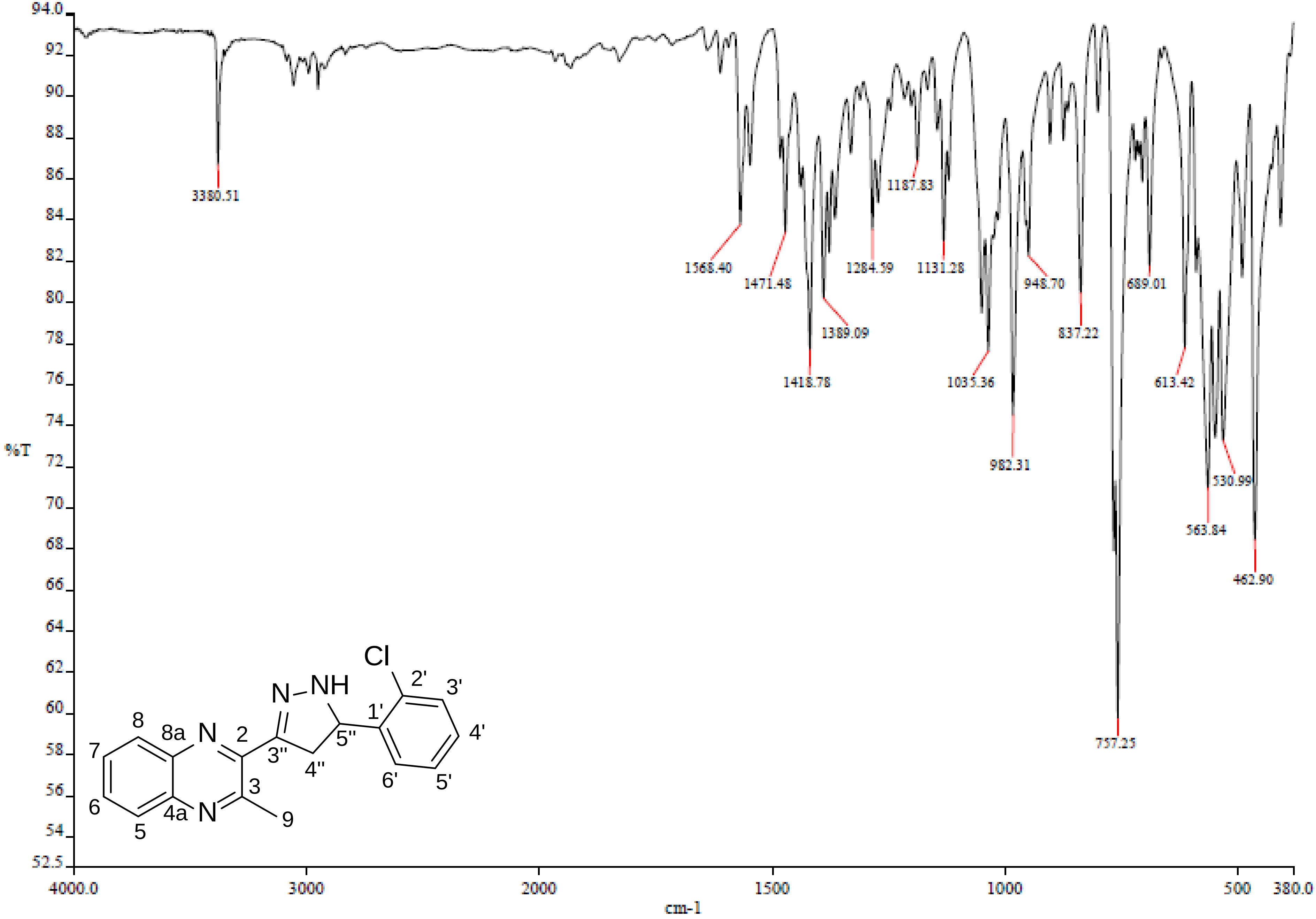

FTIR spectrum of **B11b**

Overlay Spectrum Graph Report

06/10/2017 11:49:22 AM

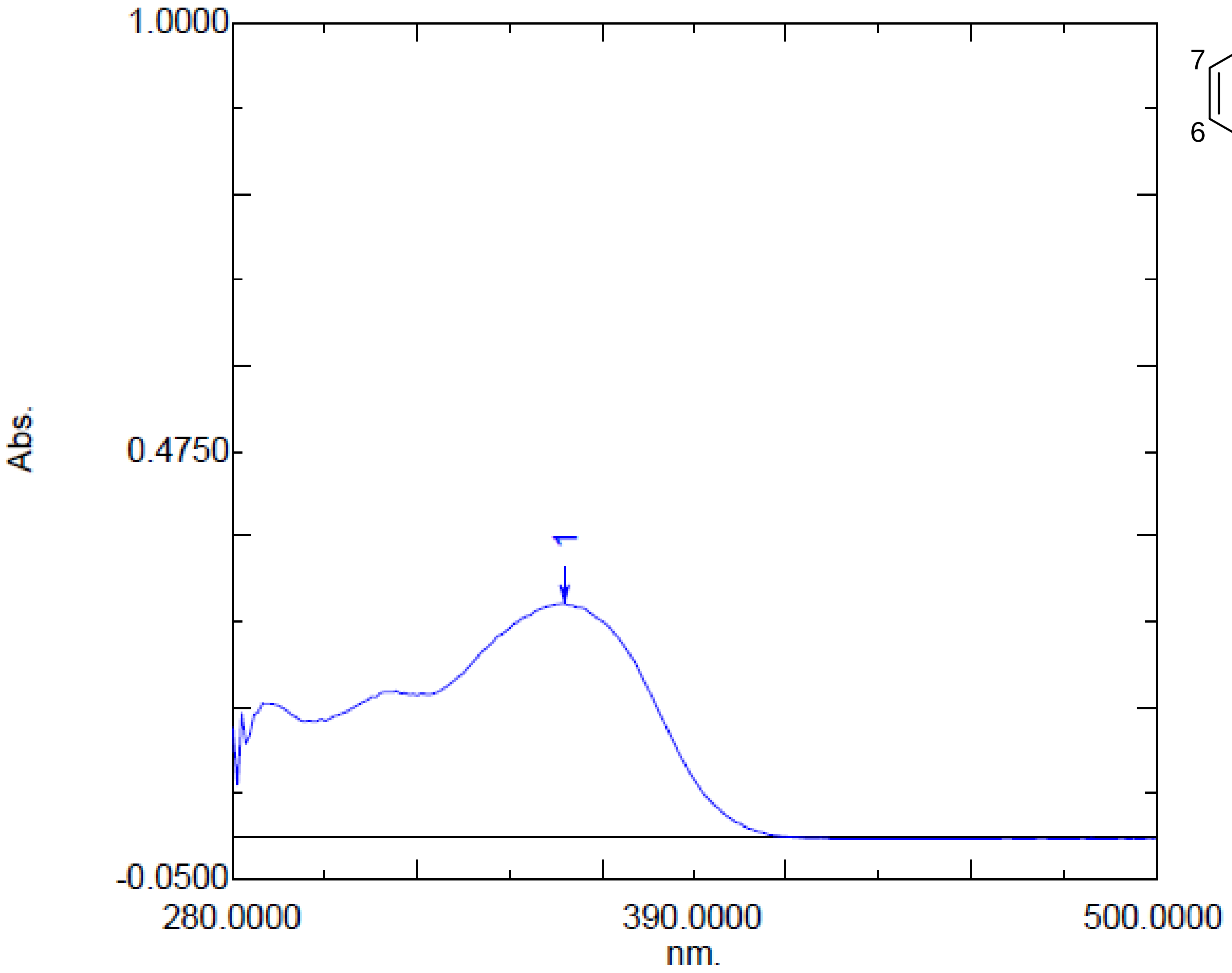

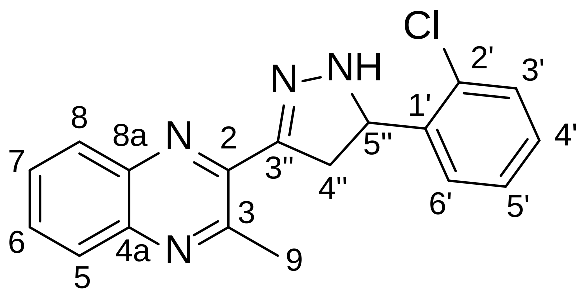

λ	absorbance	logε
359	0.2879	4.27

UV spectrum of **B11b**

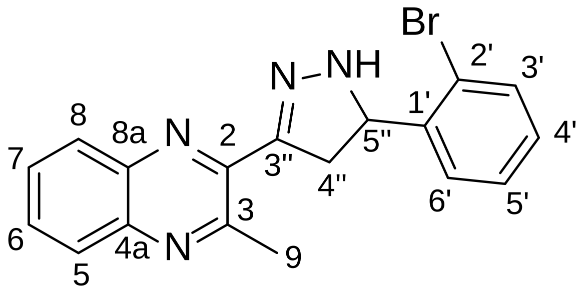

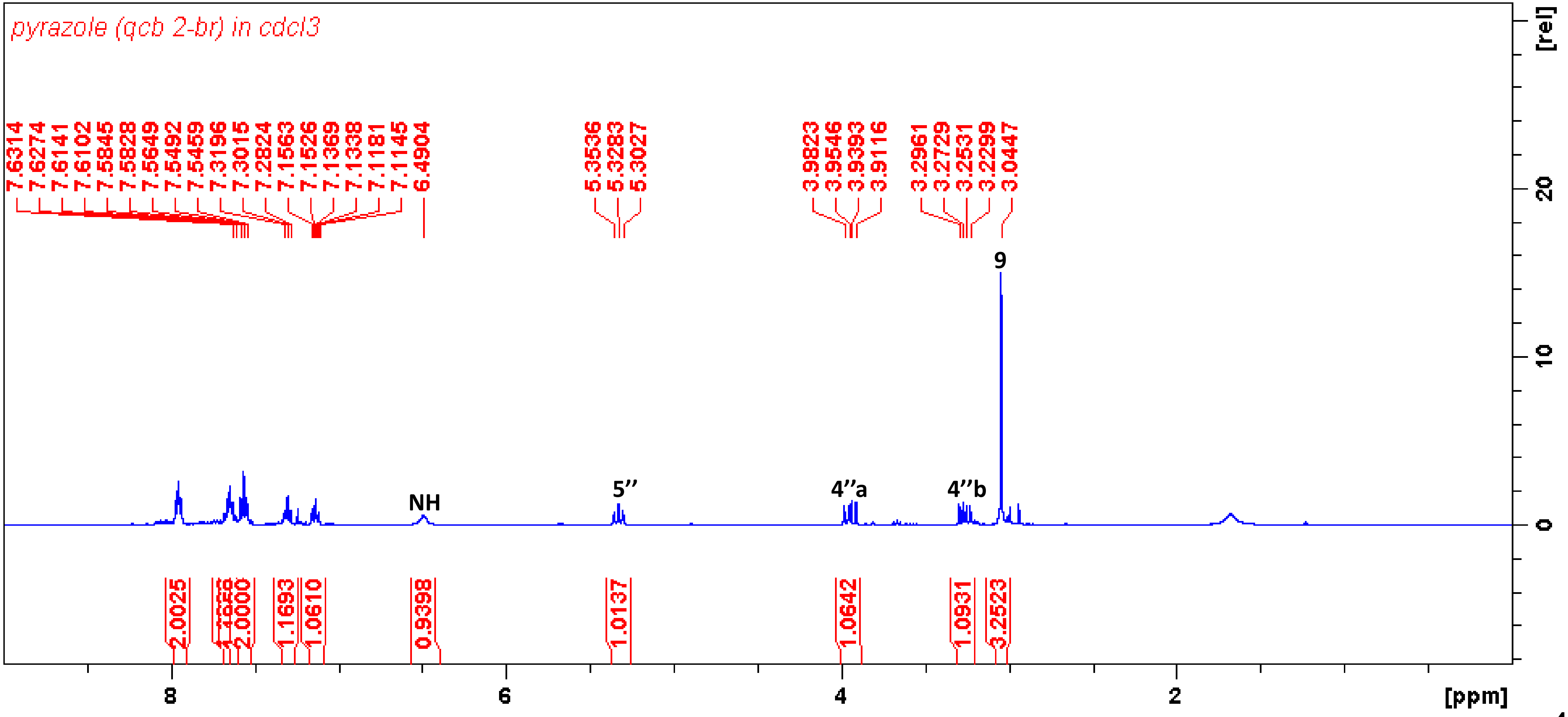

^{1}H NMR spectrum of **B11c**

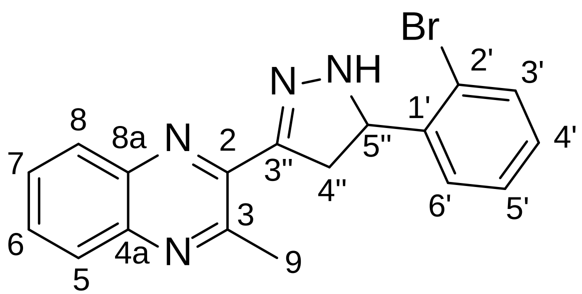

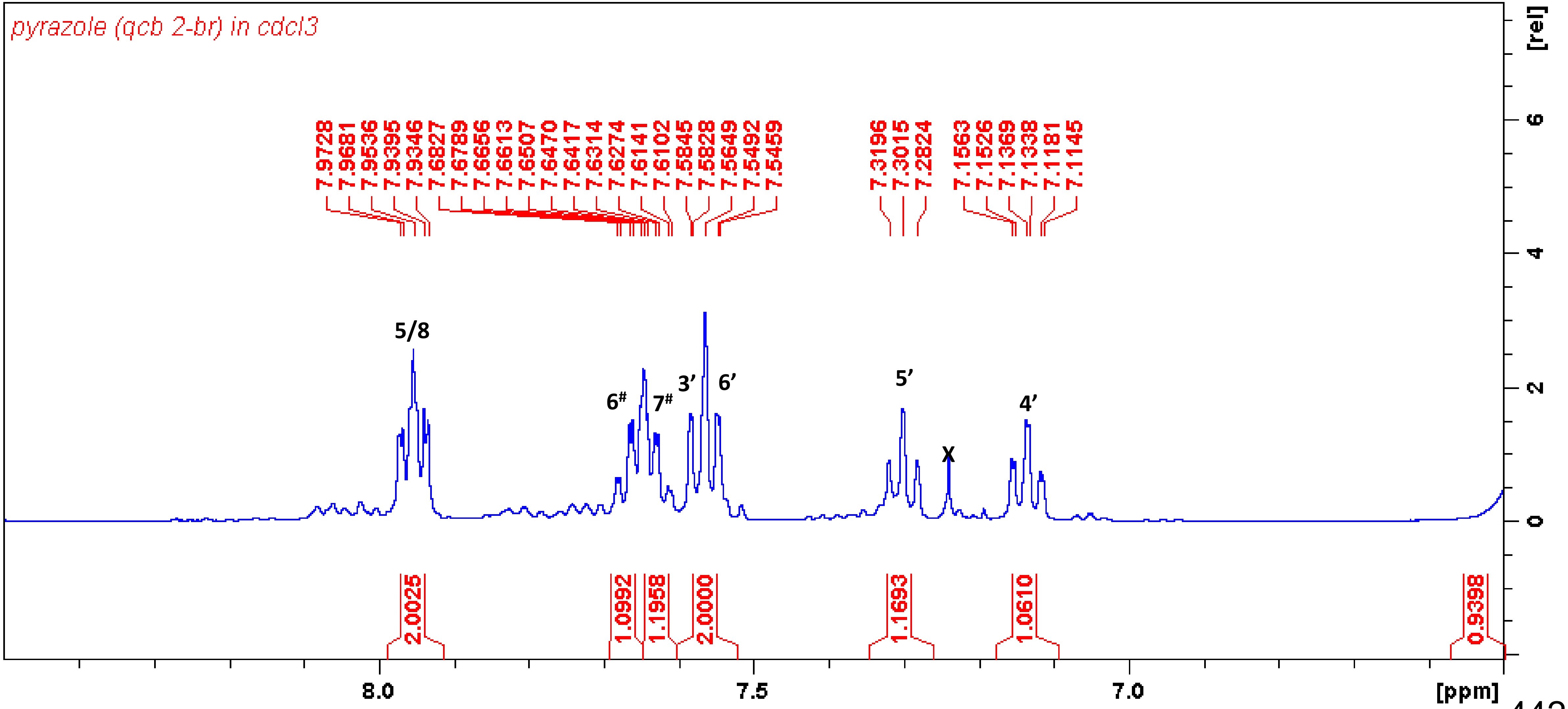

*, # Indicates assignments are interchangeable

Expanded ^{1}H NMR spectrum of **B11c**

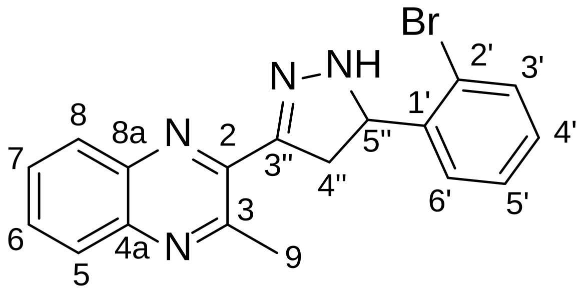

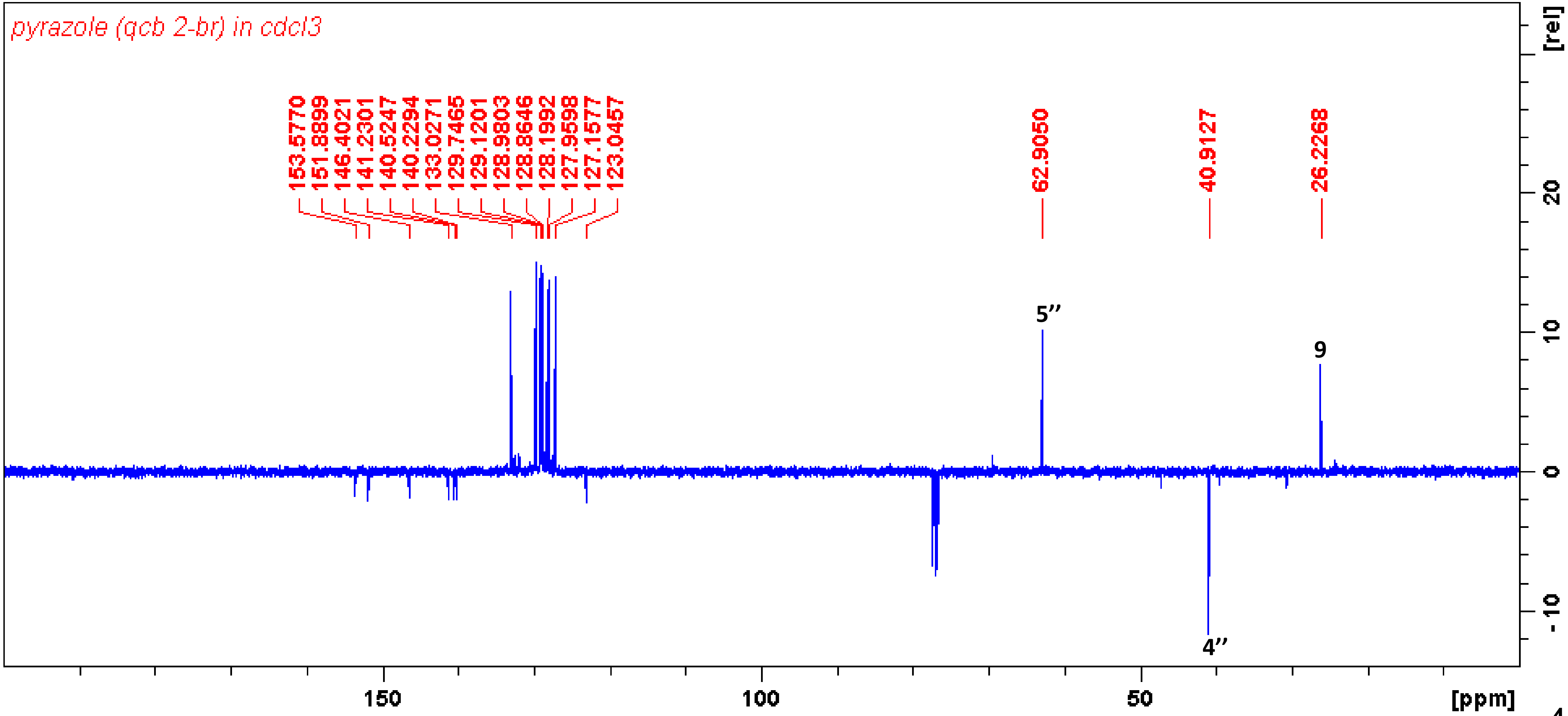

^{13}C NMR spectrum of **B11c**

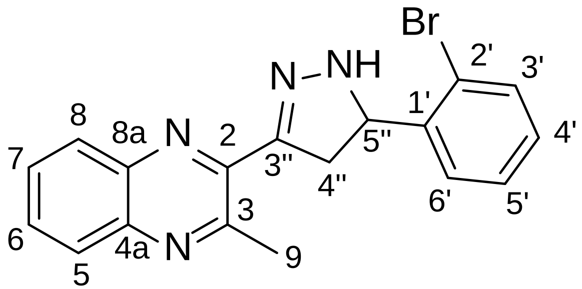

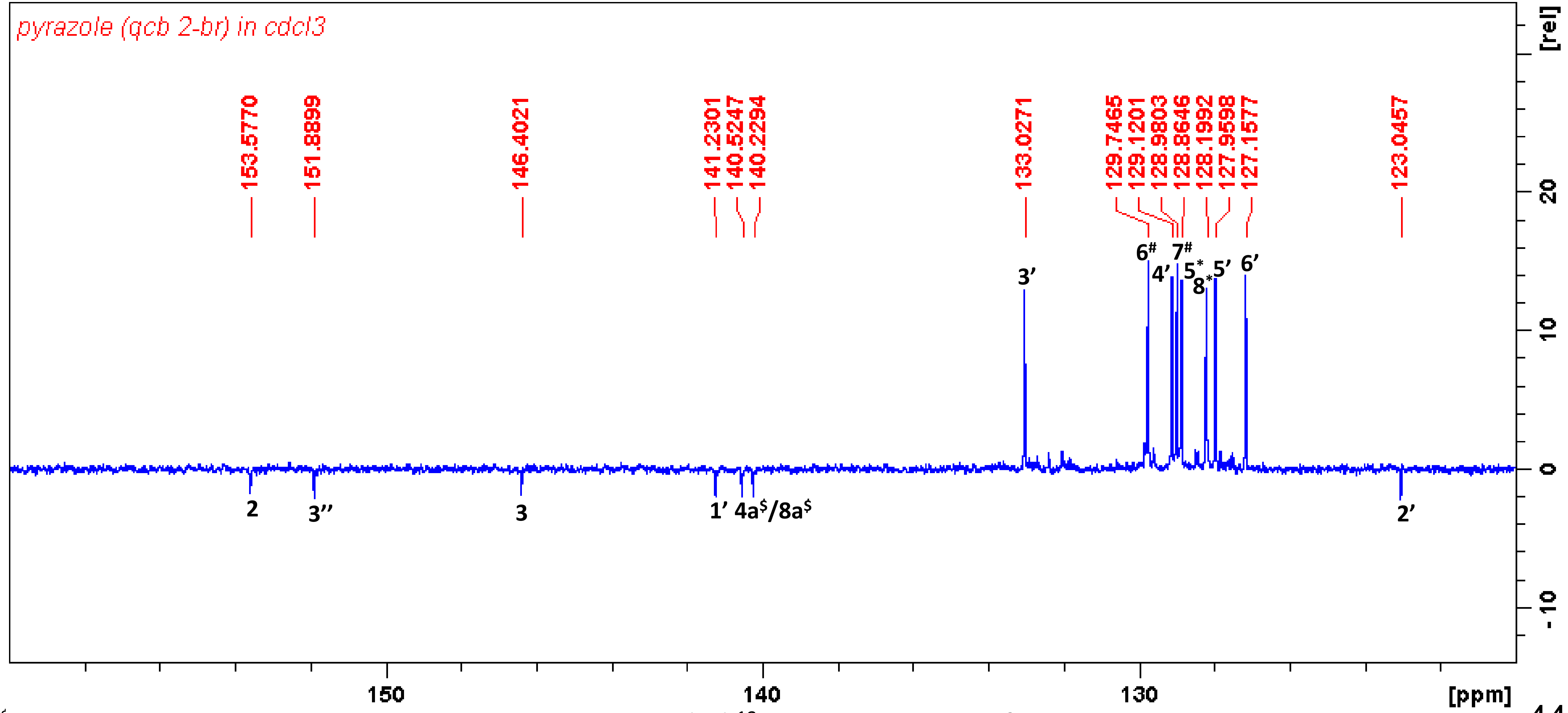

*, #, $ Indicates assignments are interchangeable

Expanded ^{13}C NMR spectrum of **B11c**

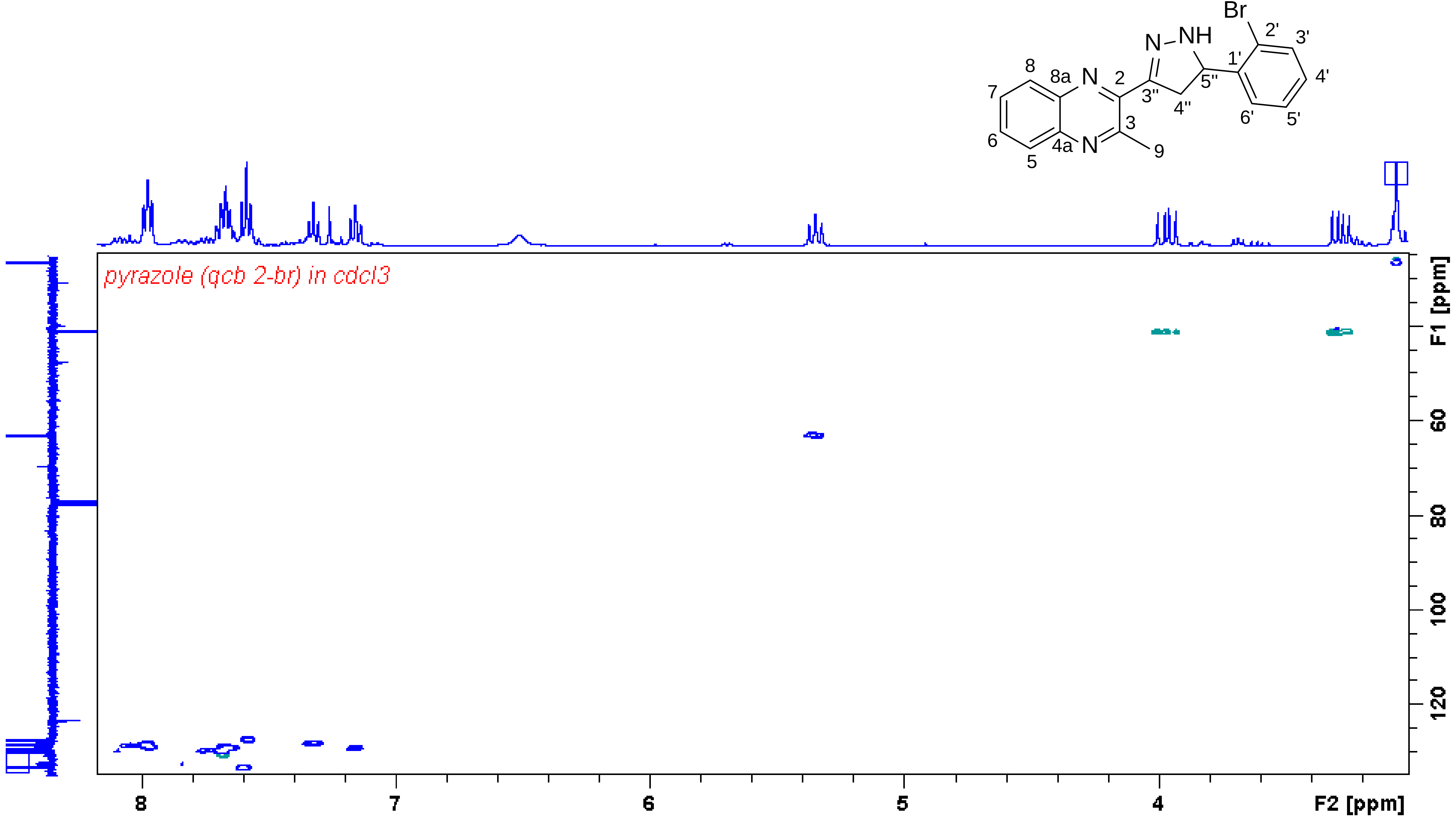
Br
2'
3'
N
NH
8
8a
N
2
1'
4'
7
3''
5''
4''
3
6'
5'
6
4a
N
9
5
pyrazole (qcb 2-br) in cdcl3
F1 [ppm]
60
80
100
120
8
7
6
5
4
F2 [ppm]

HSQC of **B11c**

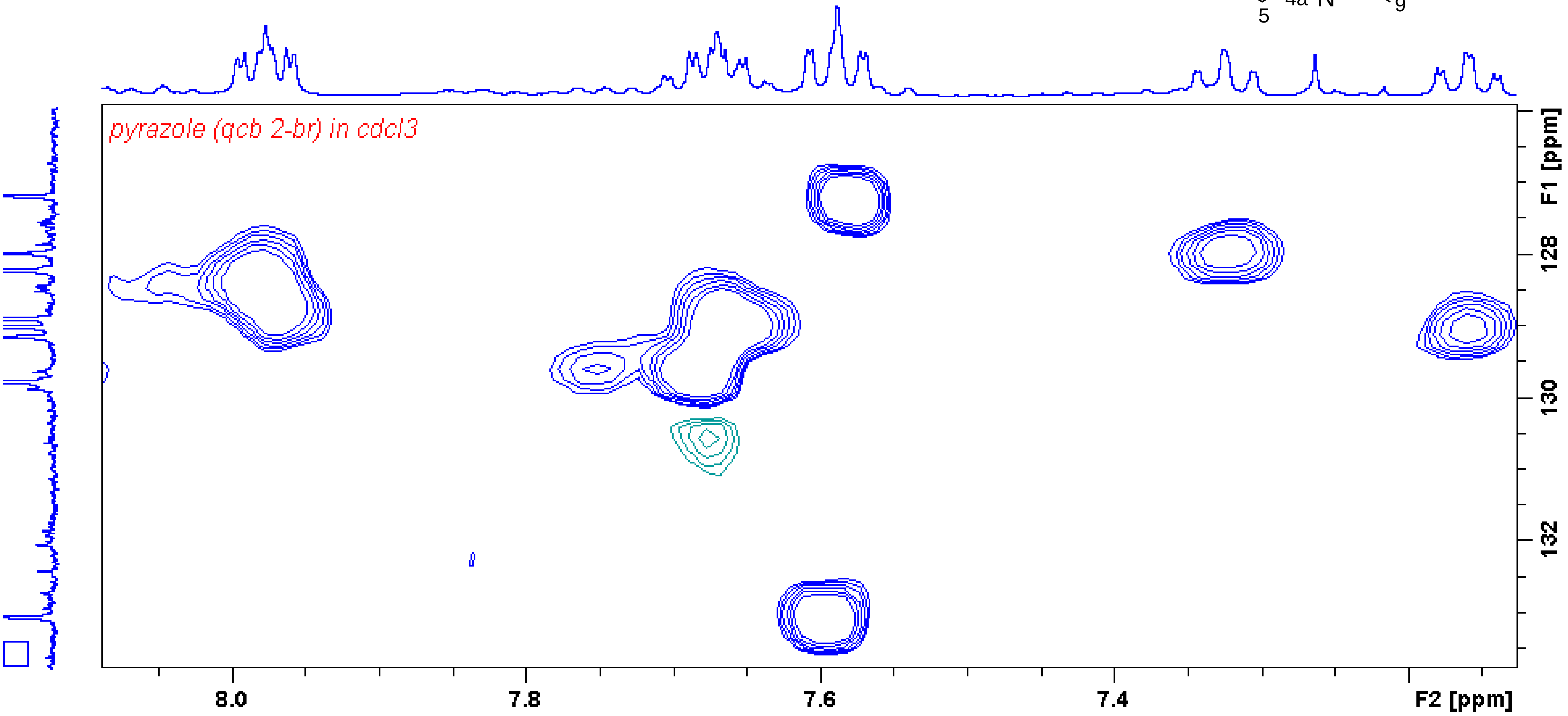

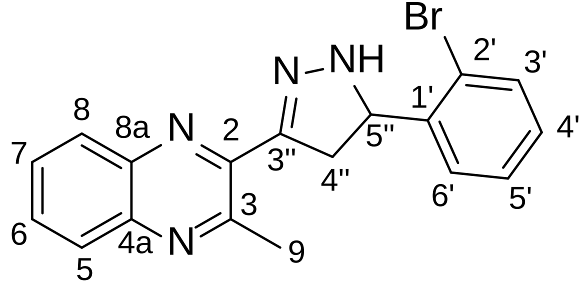

Expanded HSQC of **B11c**

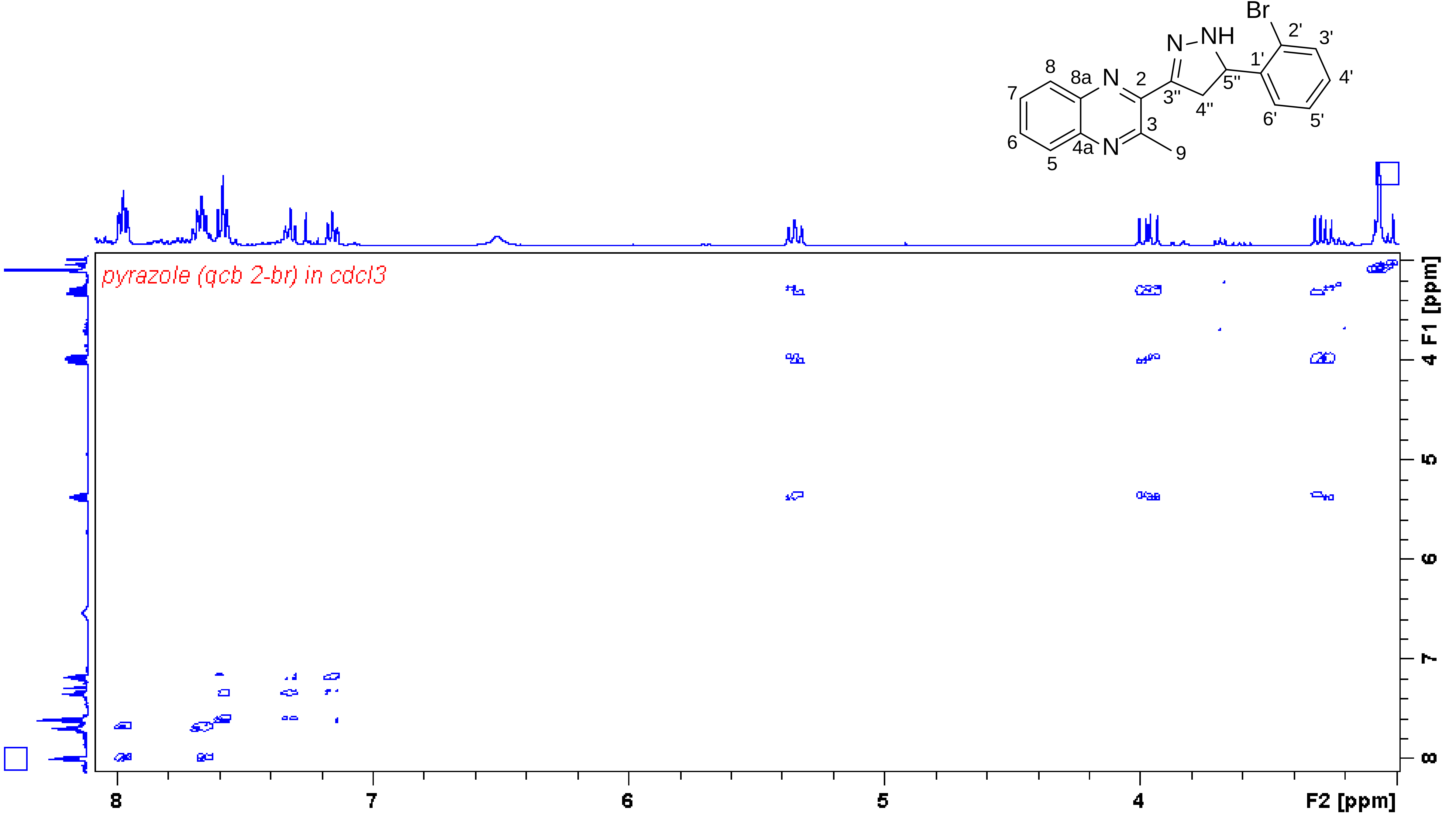
pyrazole (qcb 2-br) in cdcl3
F1 [ppm]
F2 [ppm]
Br
2'
3'
N
NH
1'
8
8a
N
2
3''
5''
4'
7
4''
6
3
6'
5'
4a
N
9
5

COSY of **B11c**

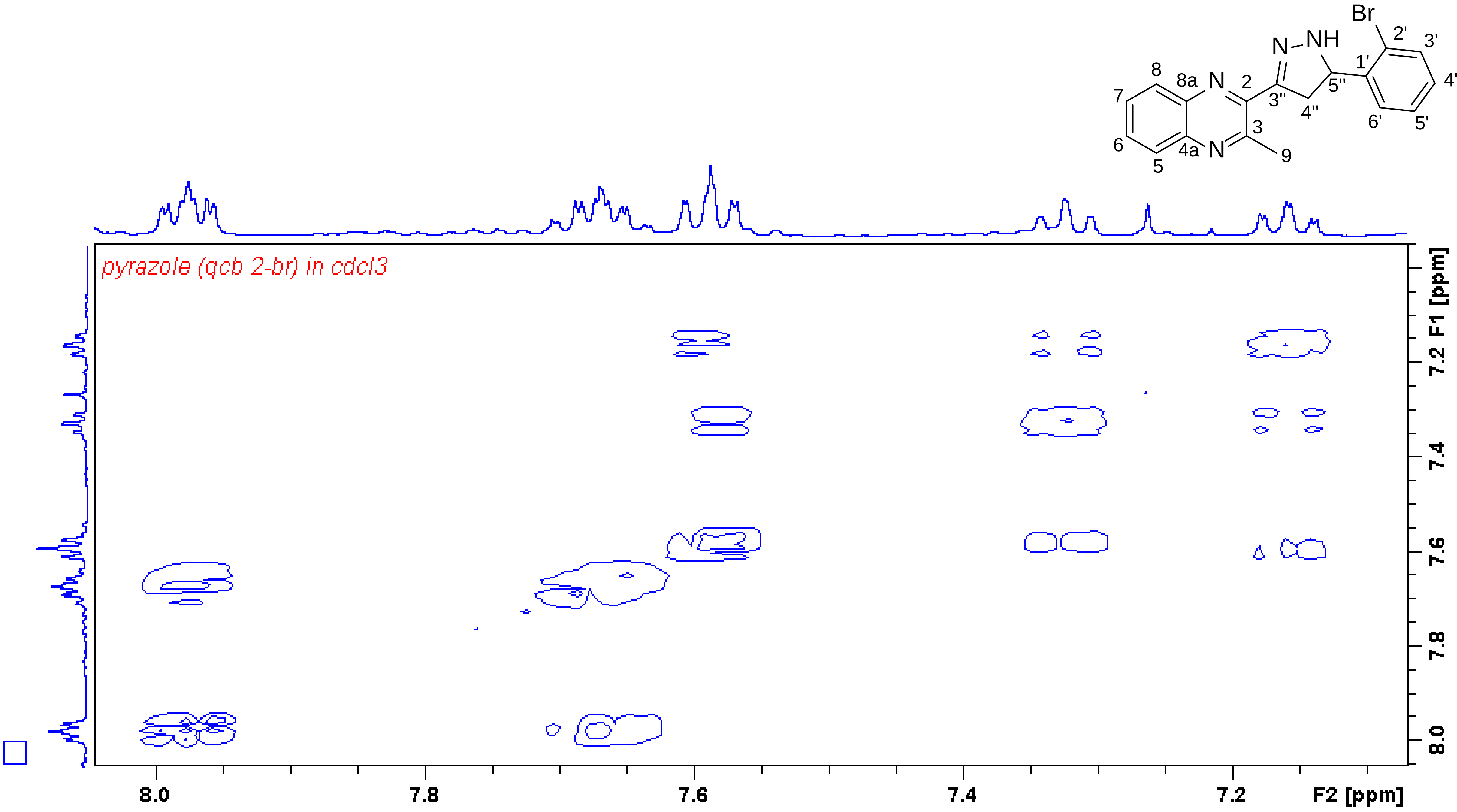

Expanded COSY of **B11c**

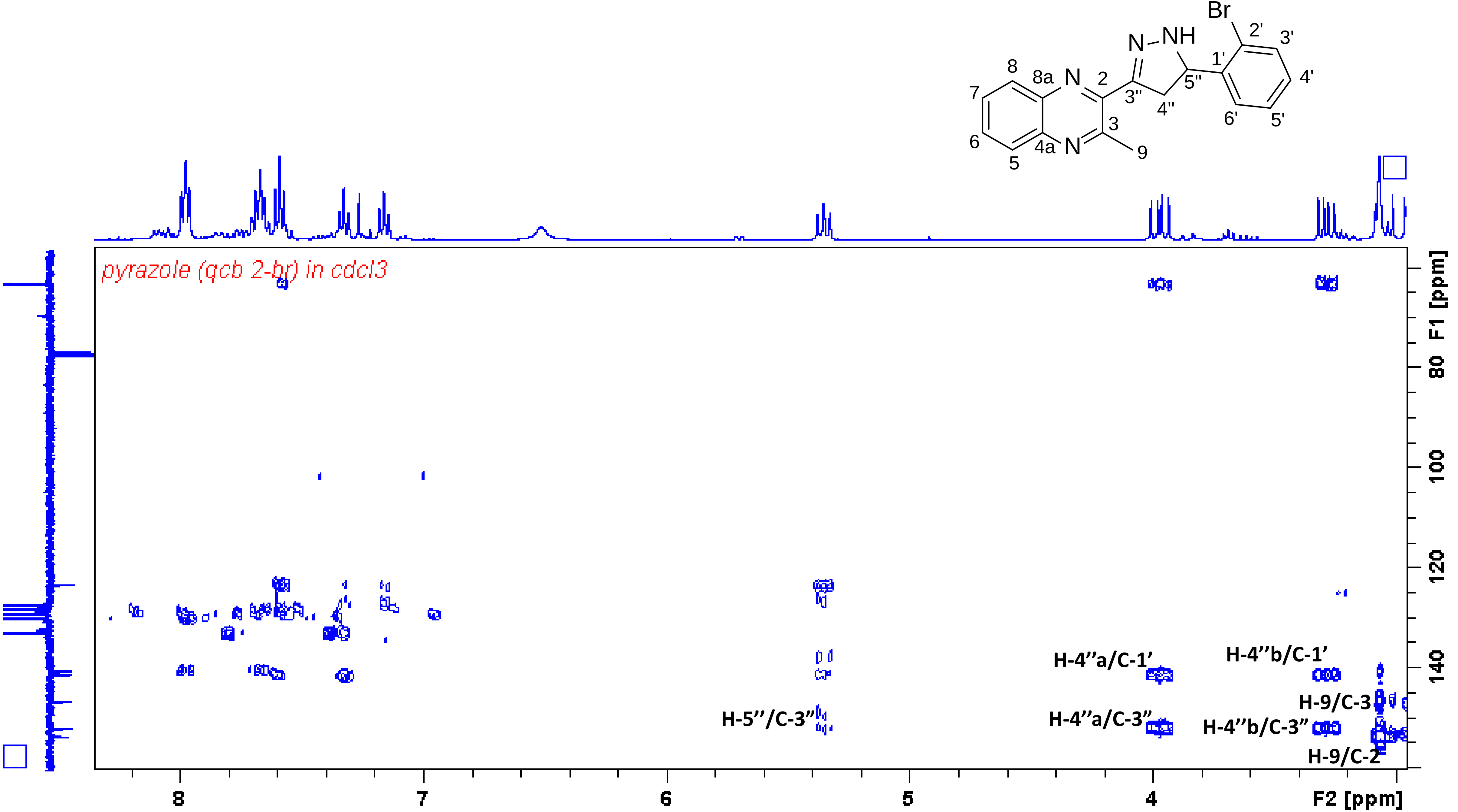

Br
pyrazole (qcb 2-br) in cdcl3
H-4''a/C-1'
H-4''b/C-1'
H-9/C-3
H-5''/C-3''
H-4''a/C-3''
H-4''b/C-3''
H-9/C-2
F1 [ppm]
F2 [ppm]

HMBC of **B11c**

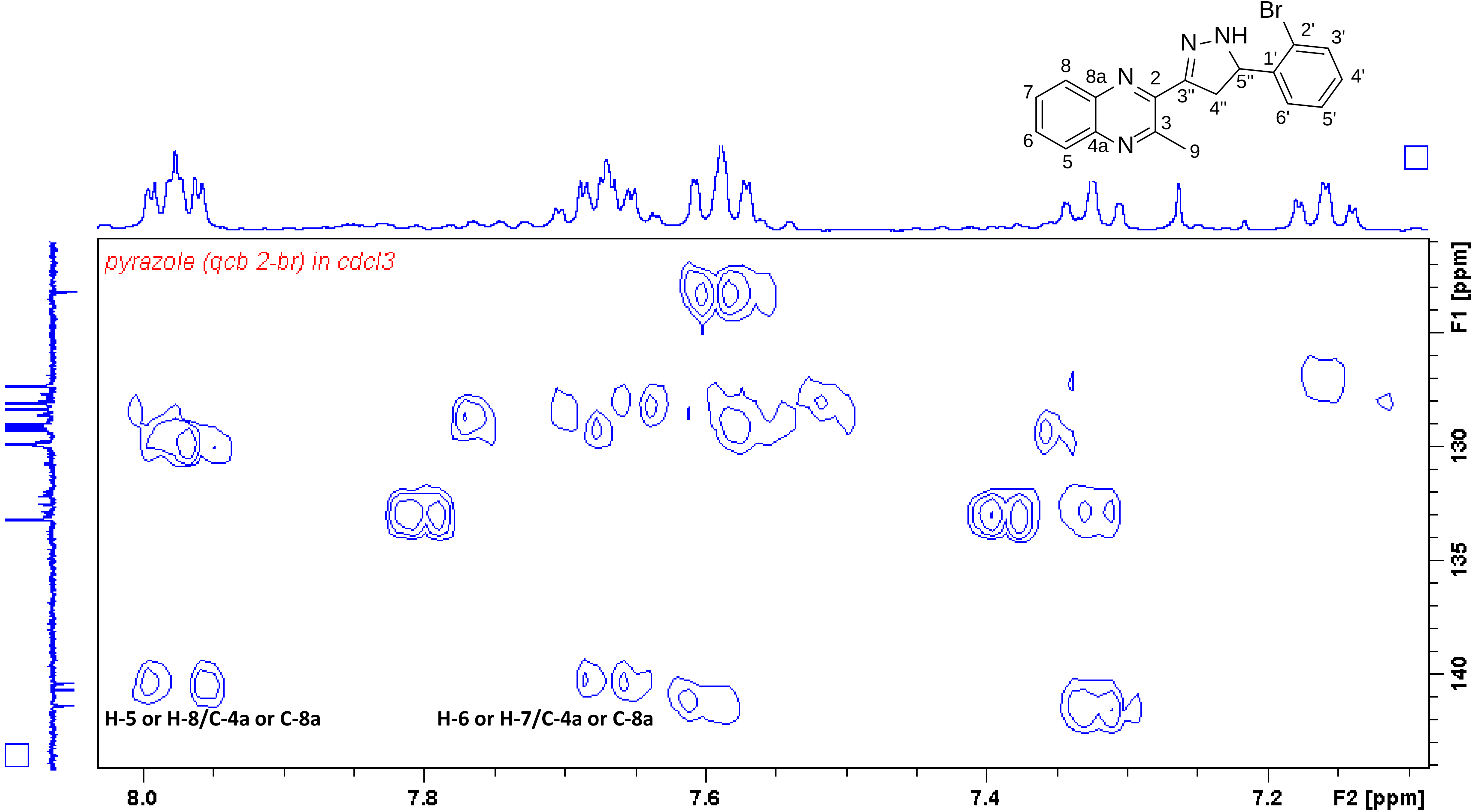

Expanded HMBC of **B11c**

Elemental Composition Report

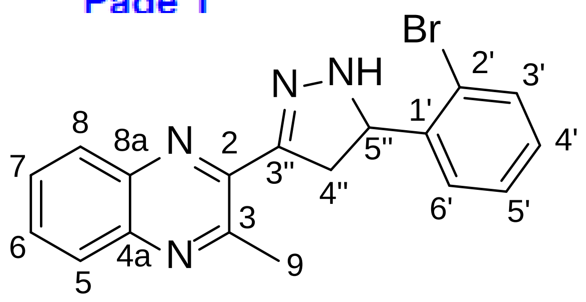

Single Mass Analysis

Tolerance = 5.0 PPM / DBE: min = -1.5, max = 100.0
Element prediction: Off
Number of isotope peaks used for i-FIT = 3

Monoisotopic Mass, Even Electron Ions
8 formula(e) evaluated with 1 results within limits (up to 20 closest results for each mass)
Elements Used:
C: 15-20 H: 15-20 N: 0-5 Br: 0-1

Py-QCB 2-Br 19 (0.605) Cm (1:61)
TOF MS ES+

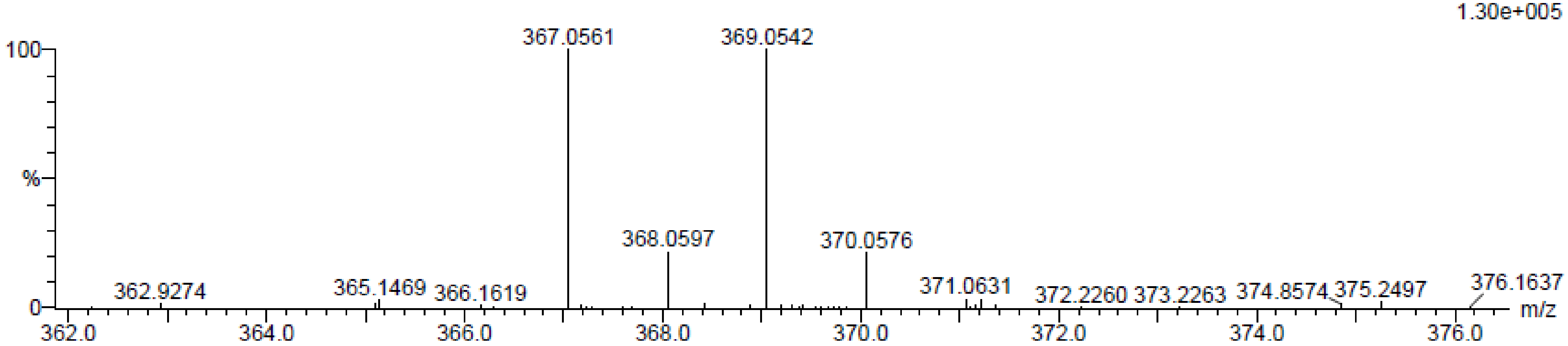

Minimum:				-1.5			
Maximum:		5.0	5.0	100.0			
Mass	Calc. Mass	mDa	PPM	DBE	i-FIT	i-FIT (Norm)	Formula
367.0561	367.0558	0.3	0.8	12.5	169.6	0.0	C18 H16 N4 Br

High resolution mass spectrum of **B11c**

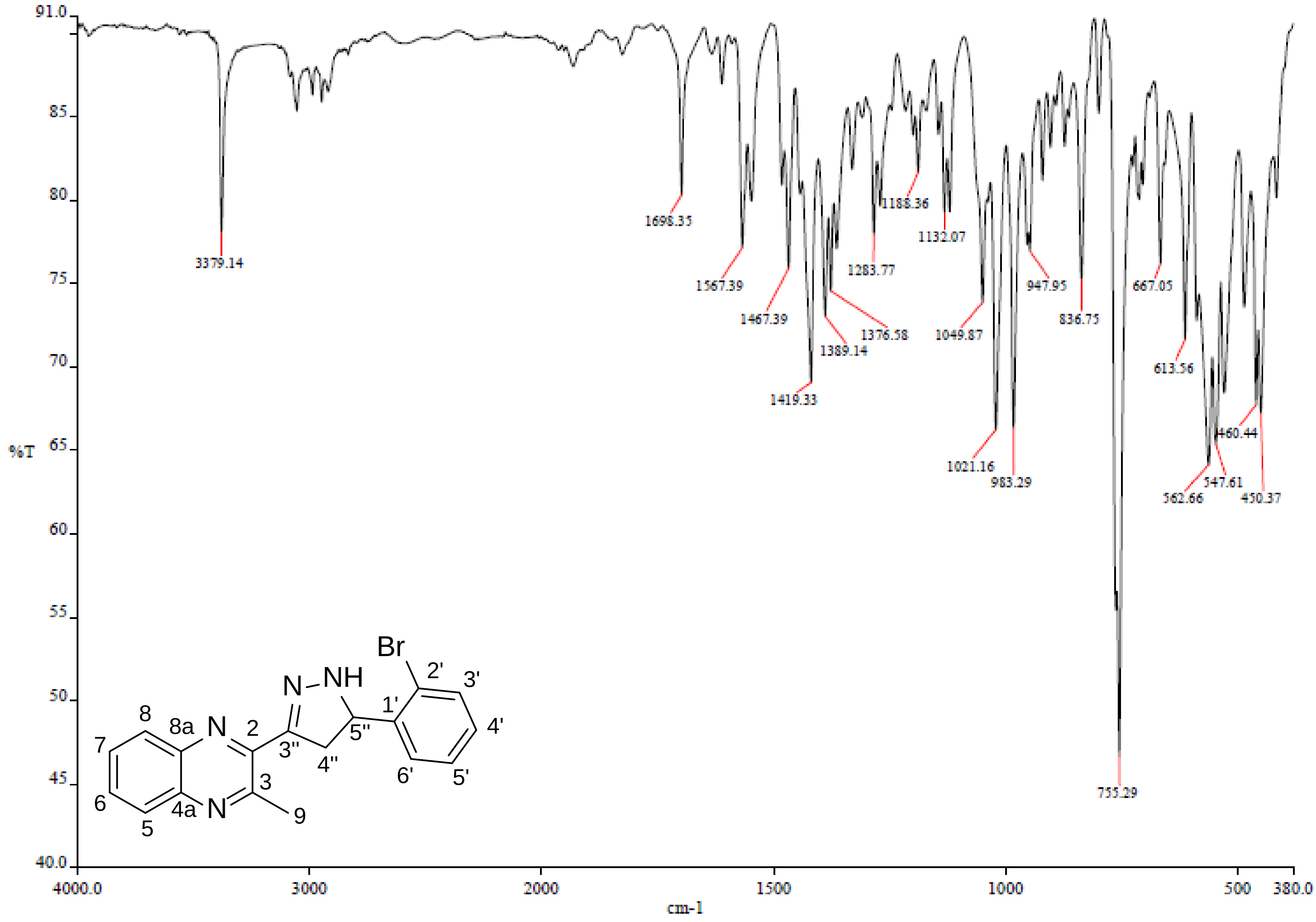

FTIR spectrum of **B11c**

Overlay Spectrum Graph Report

06/10/2017 11:47:52 AM

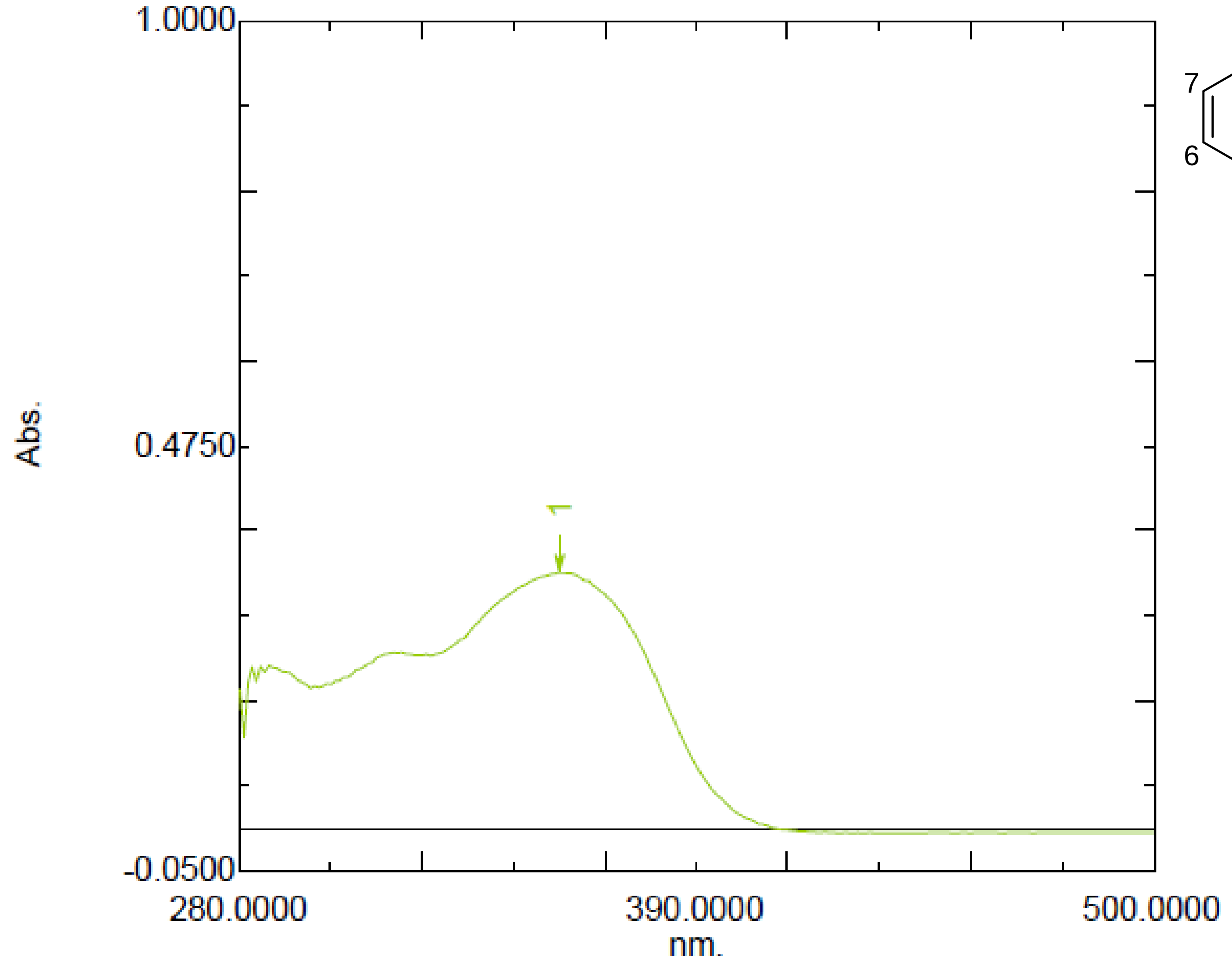

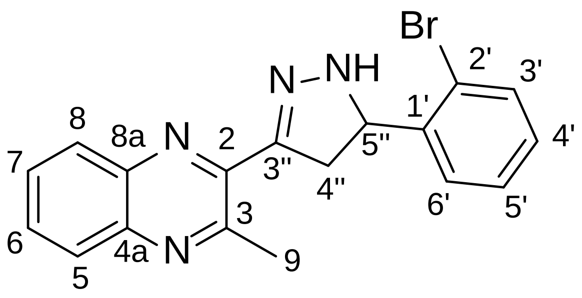

λ	absorbance	logε
357	0.3185	4.37

UV spectrum of **B11c**

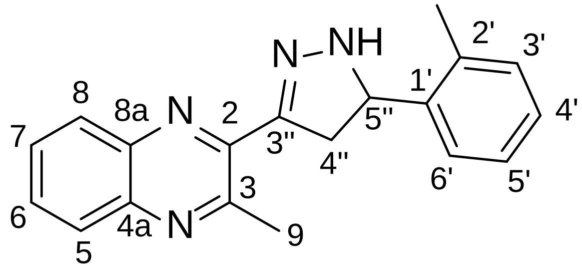

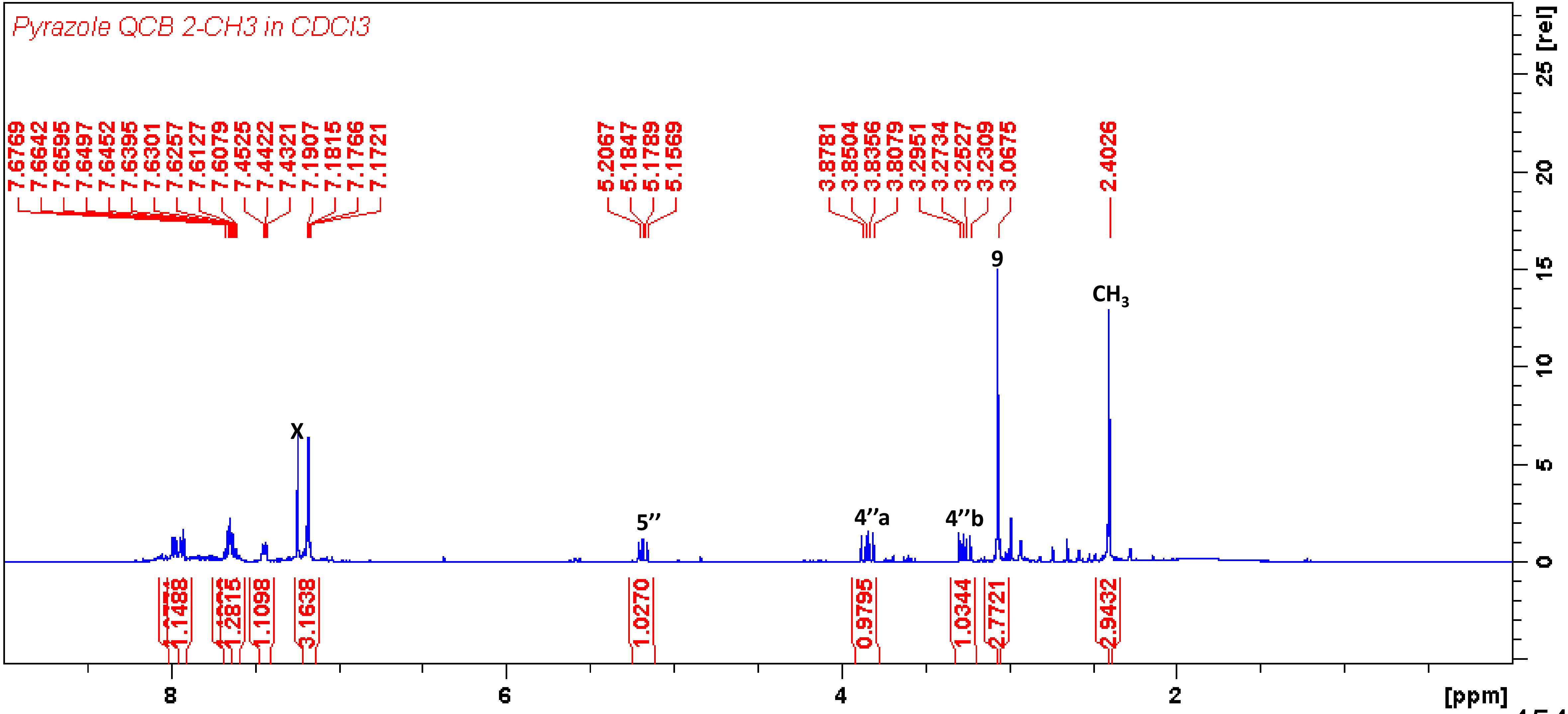

^{1}H NMR spectrum of **B11d**

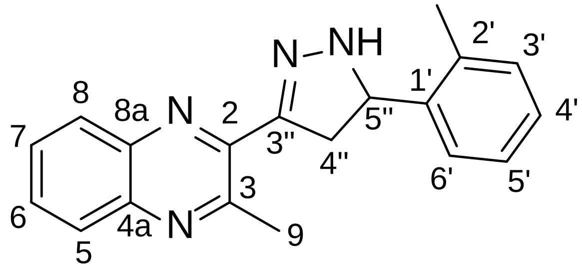

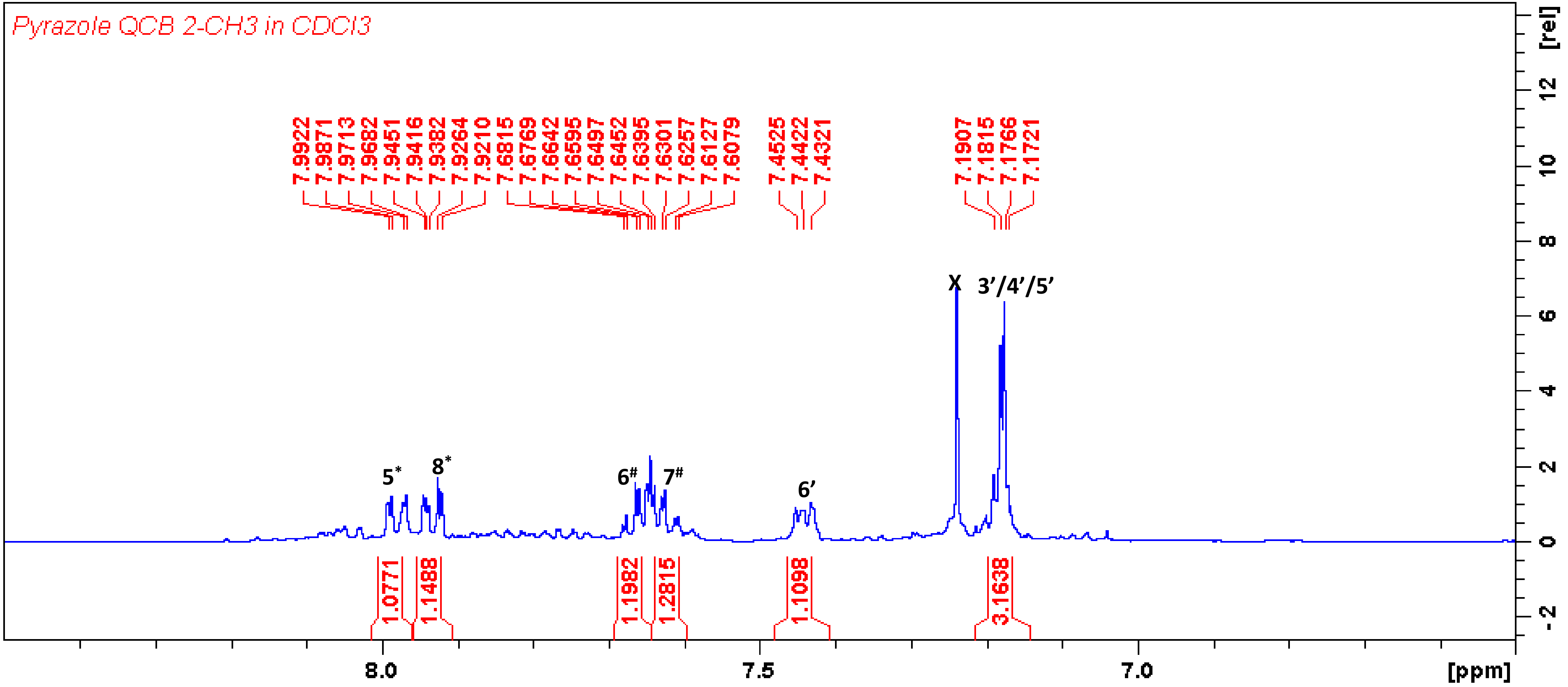

*, # Indicates assignments are interchangeable

Expanded ^{1}H NMR spectrum of **B11d**

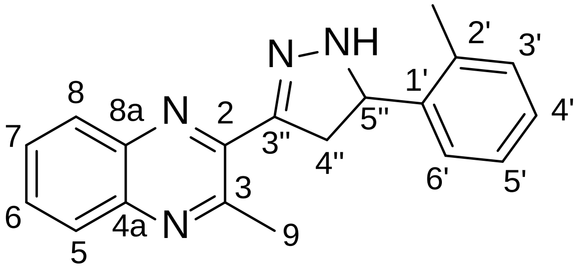

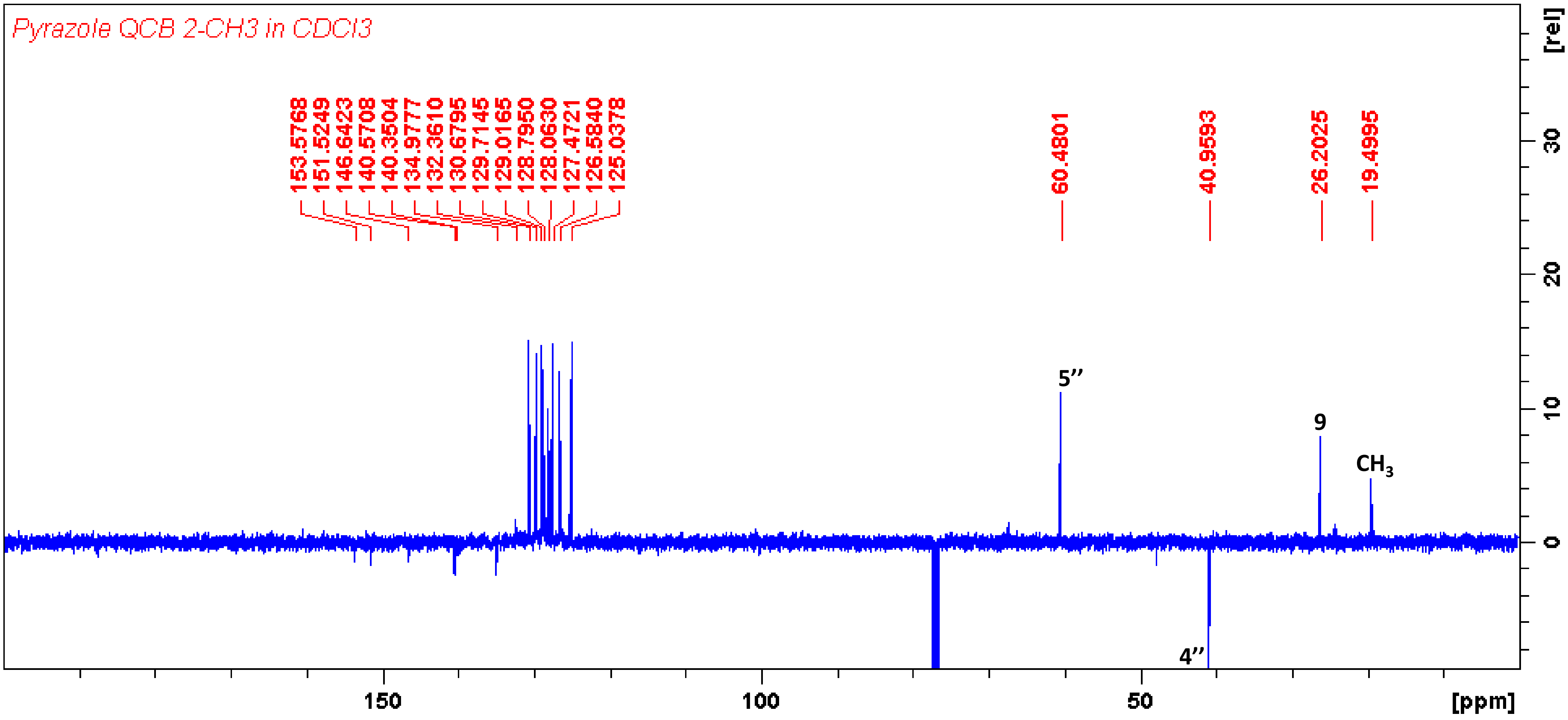

^{13}C NMR spectrum of **B11d**

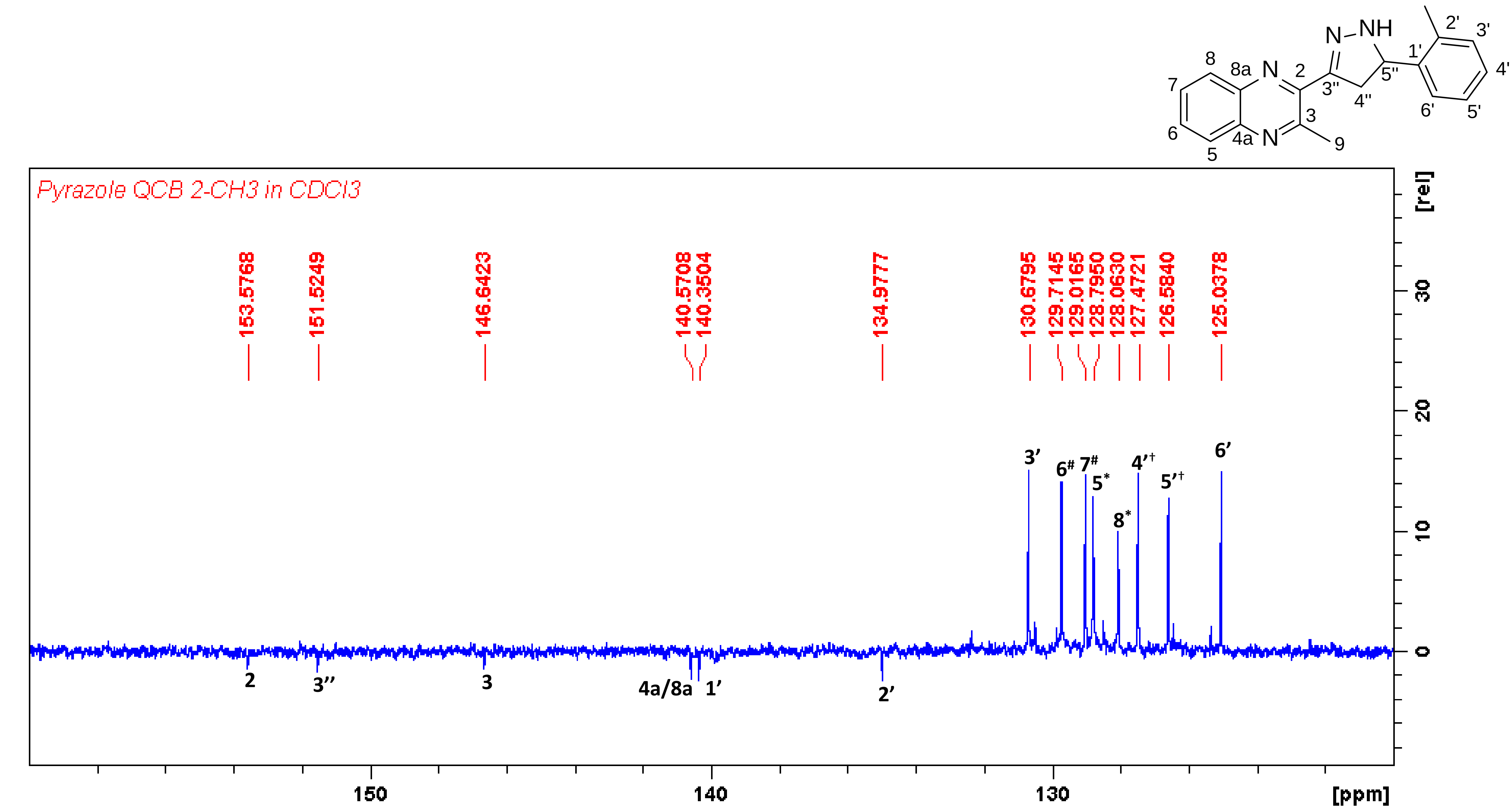

*, #, $, † Indicates assignments are interchangeable

Expanded ^{13}C NMR spectrum of **B11d**

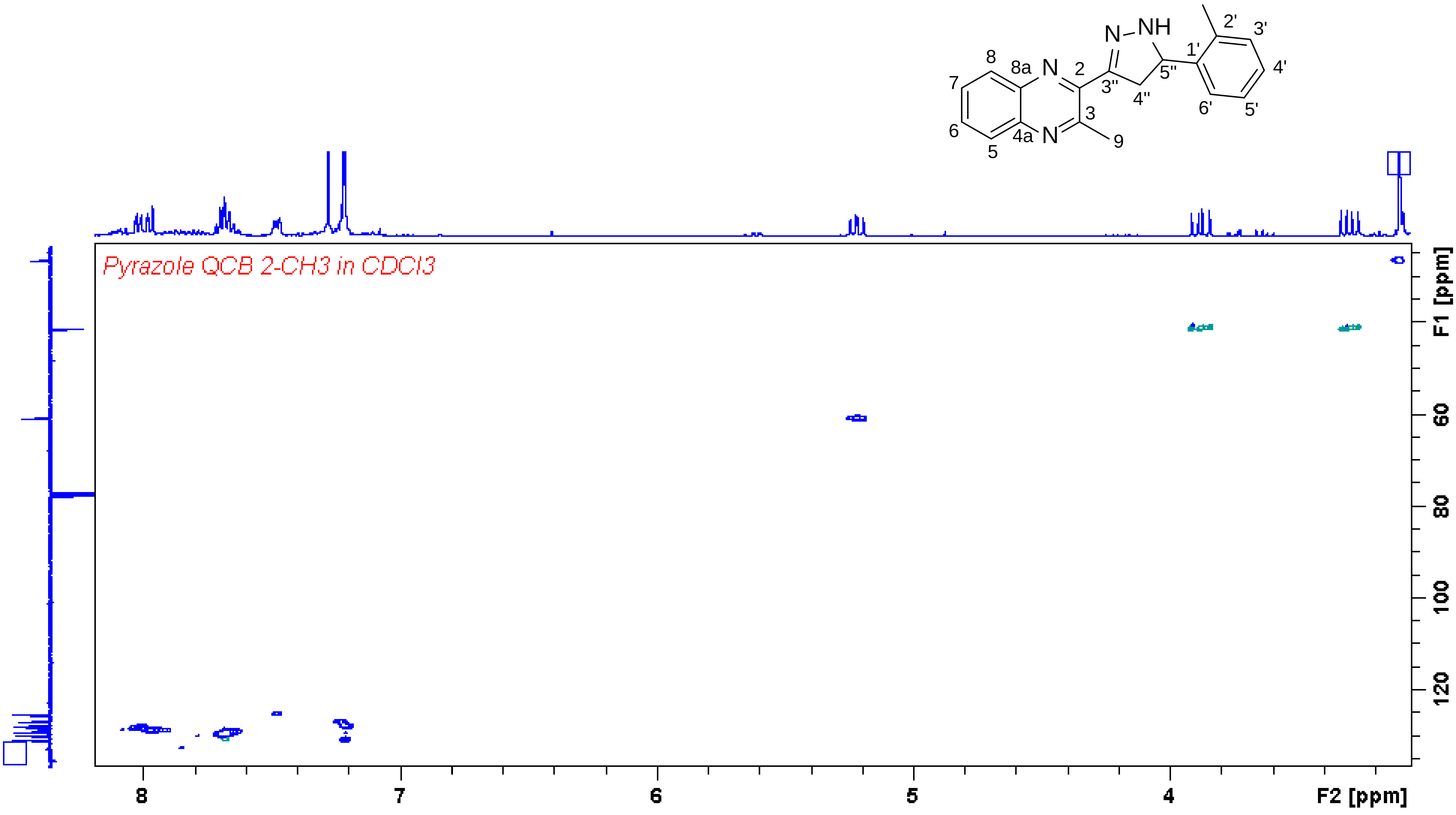
Pyrazole QCB 2-CH3 in CDCl3
N
NH
N
N
8
8a
2
2'
3'
1'
4'
5''
3''
7
4''
6'
5'
3
6
4a
9
5
8
7
6
5
4
F2 [ppm]
60
80
100
120
F1 [ppm]

HSQC of **B11d**

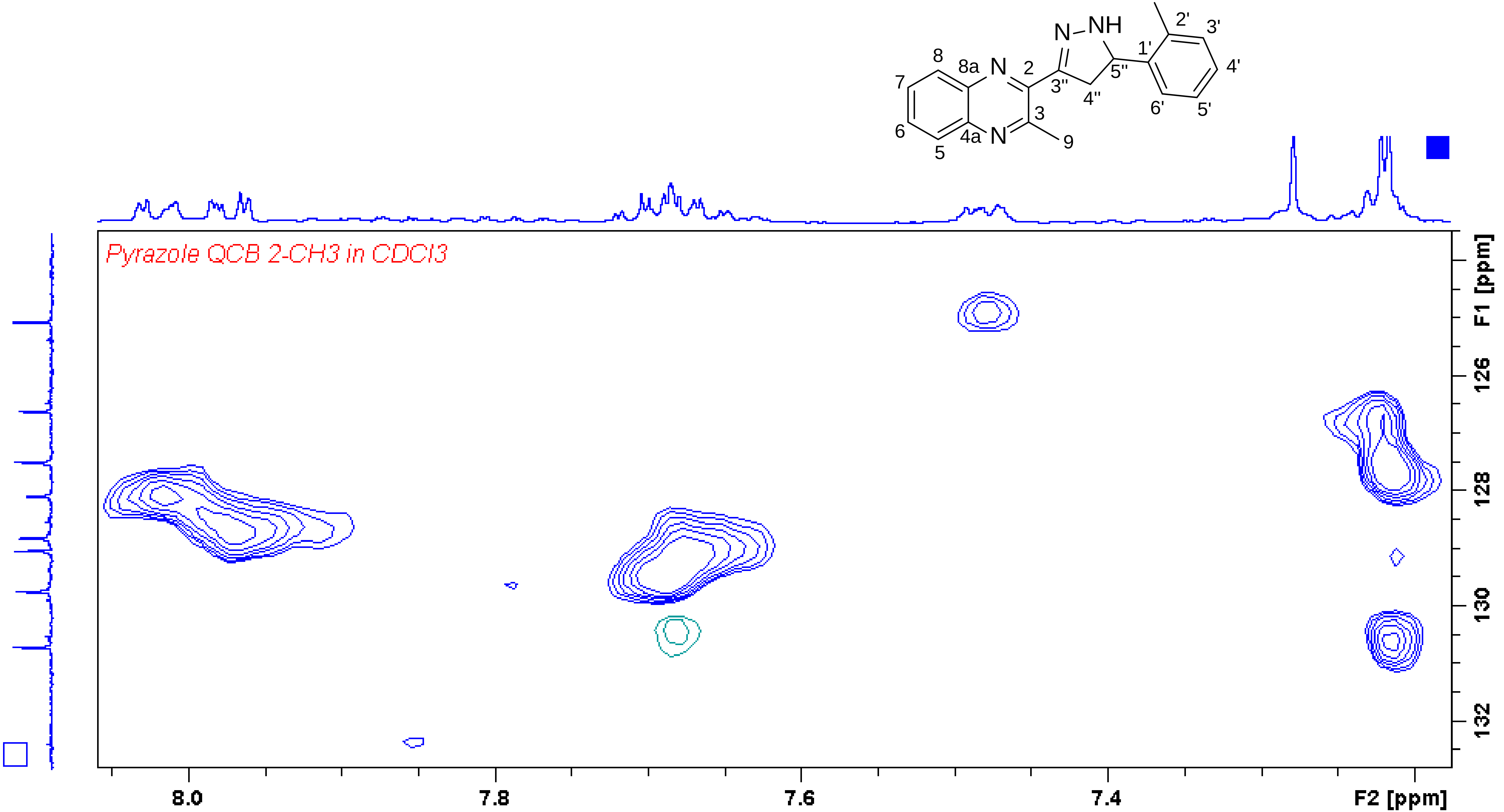

Expanded HSQC of **B11d**

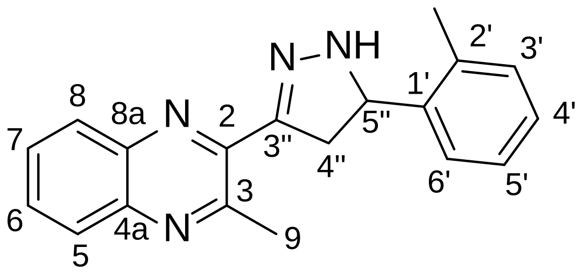

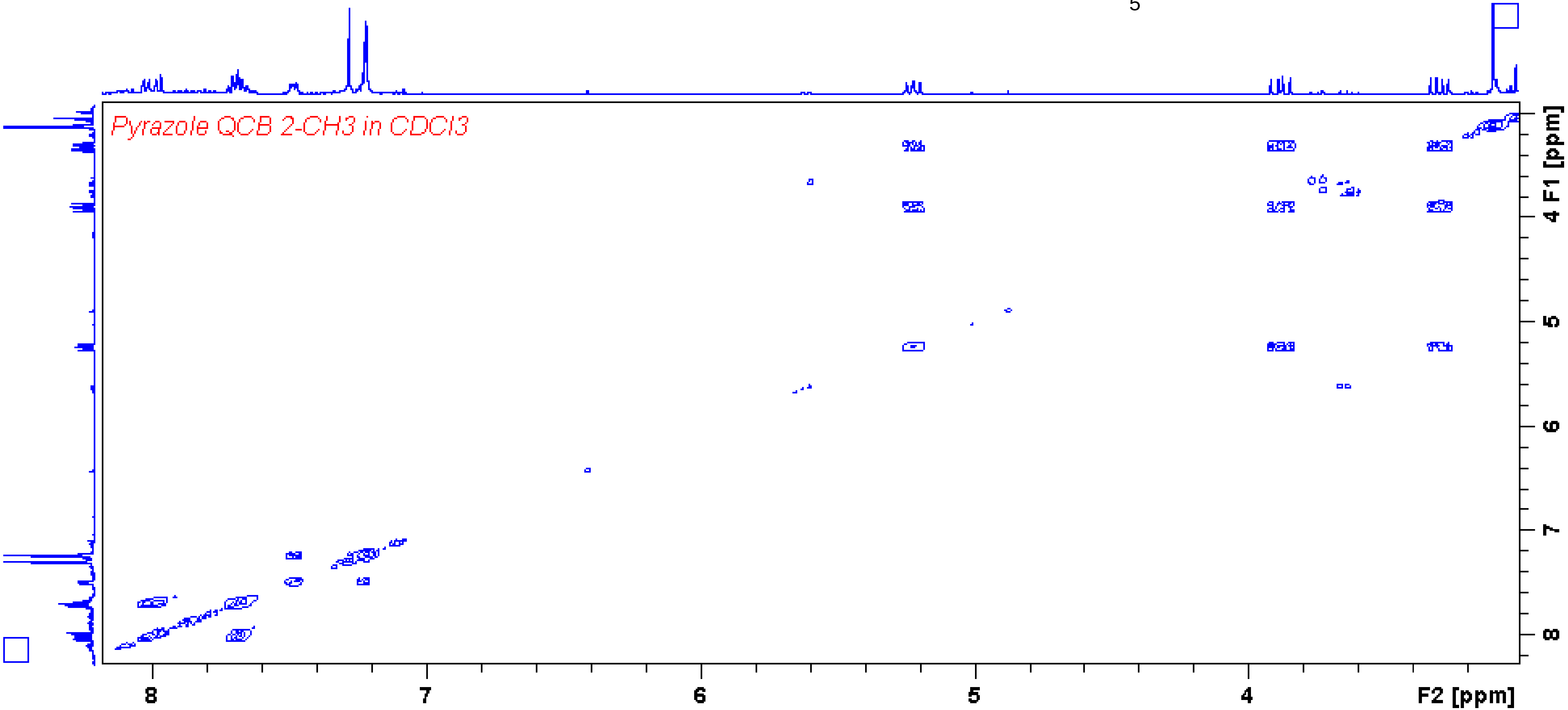

COSY of **B11d**

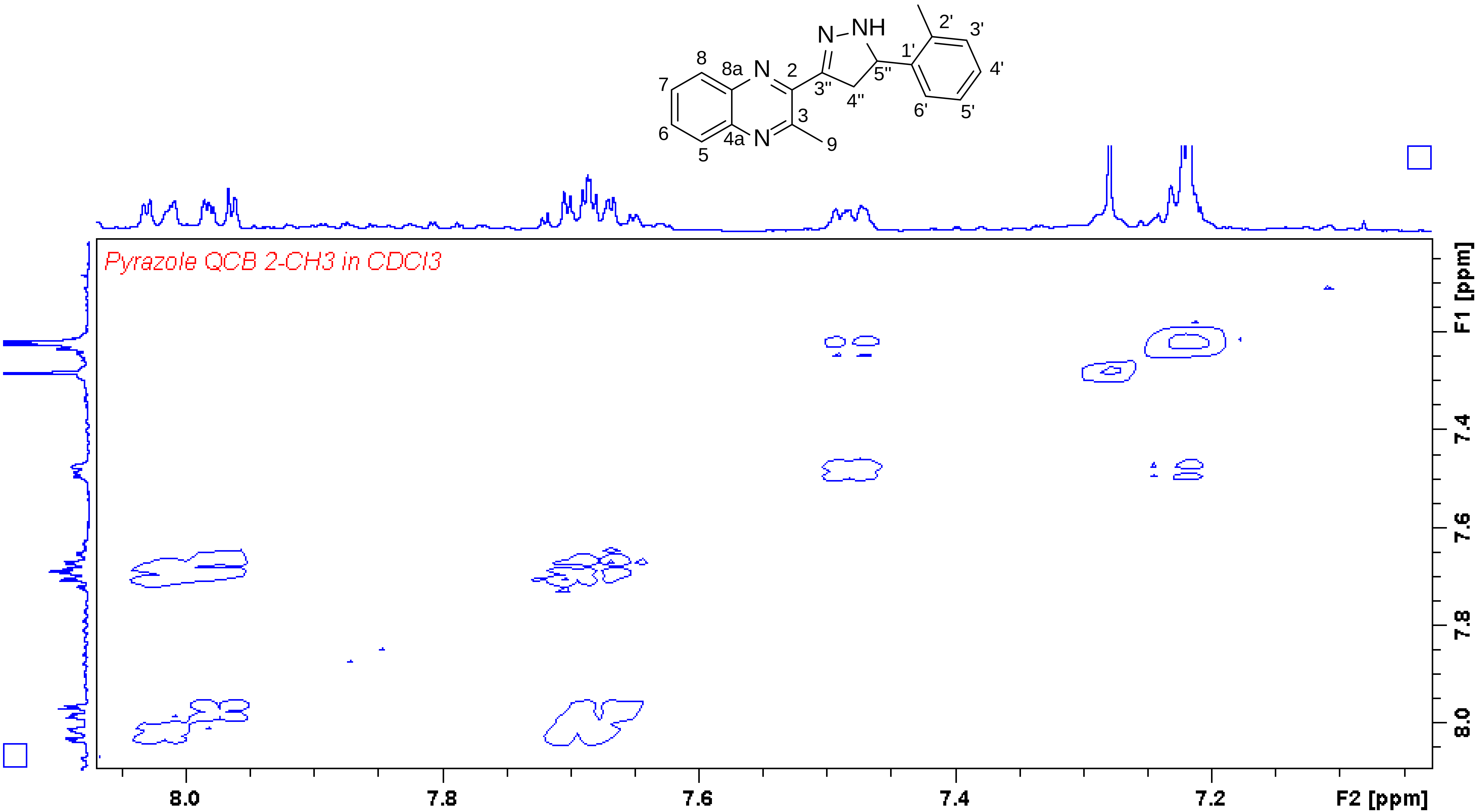

Expanded COSY of **B11d**

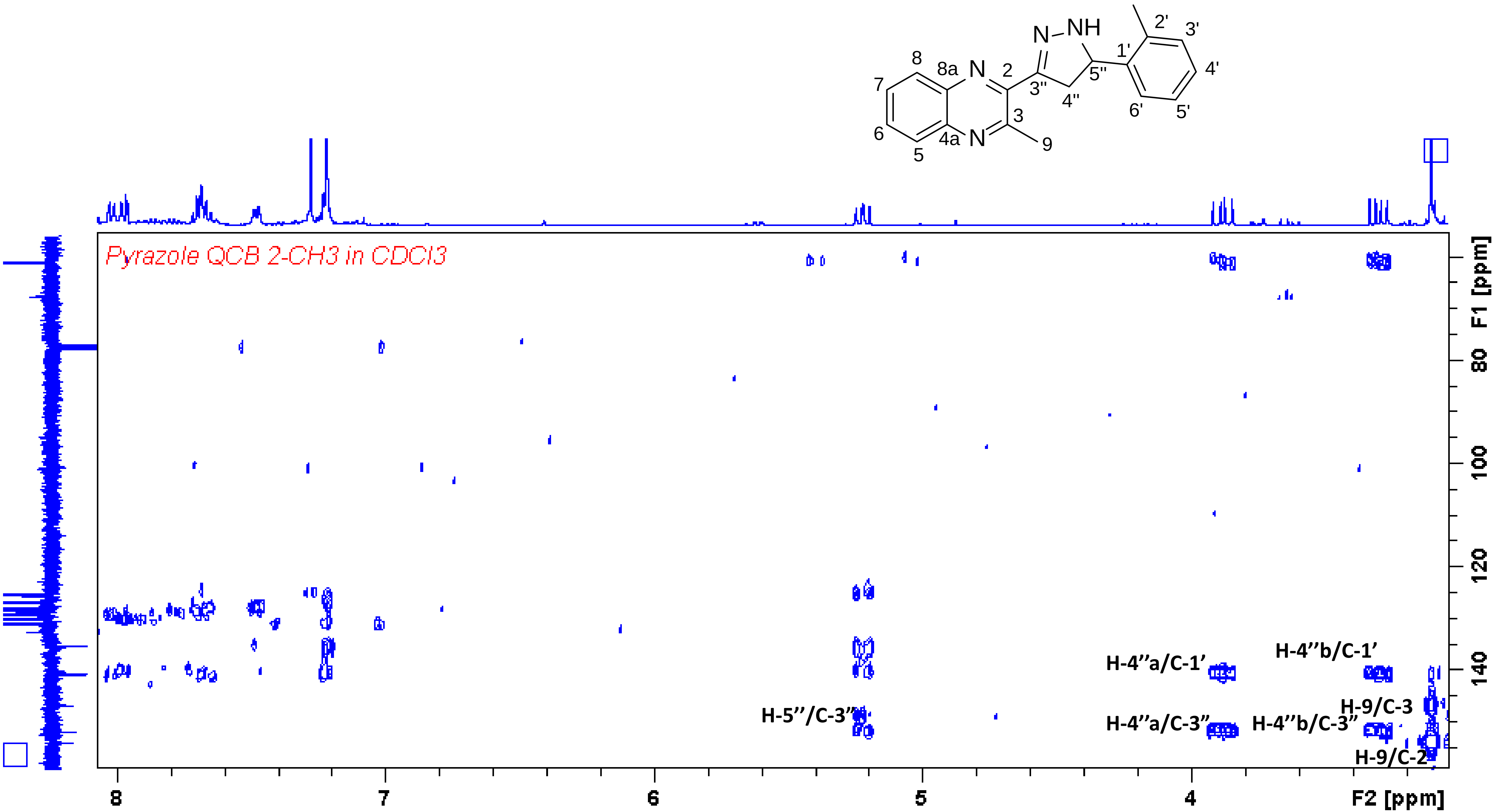

Pyrazole QCB 2-CH3 in CDCl3
H-4''a/C-1'
H-4''b/C-1'
H-5''/C-3''
H-4''a/C-3''
H-4''b/C-3''
H-9/C-3
H-9/C-2
F1 [ppm]
F2 [ppm]

HMBC of **B11d**

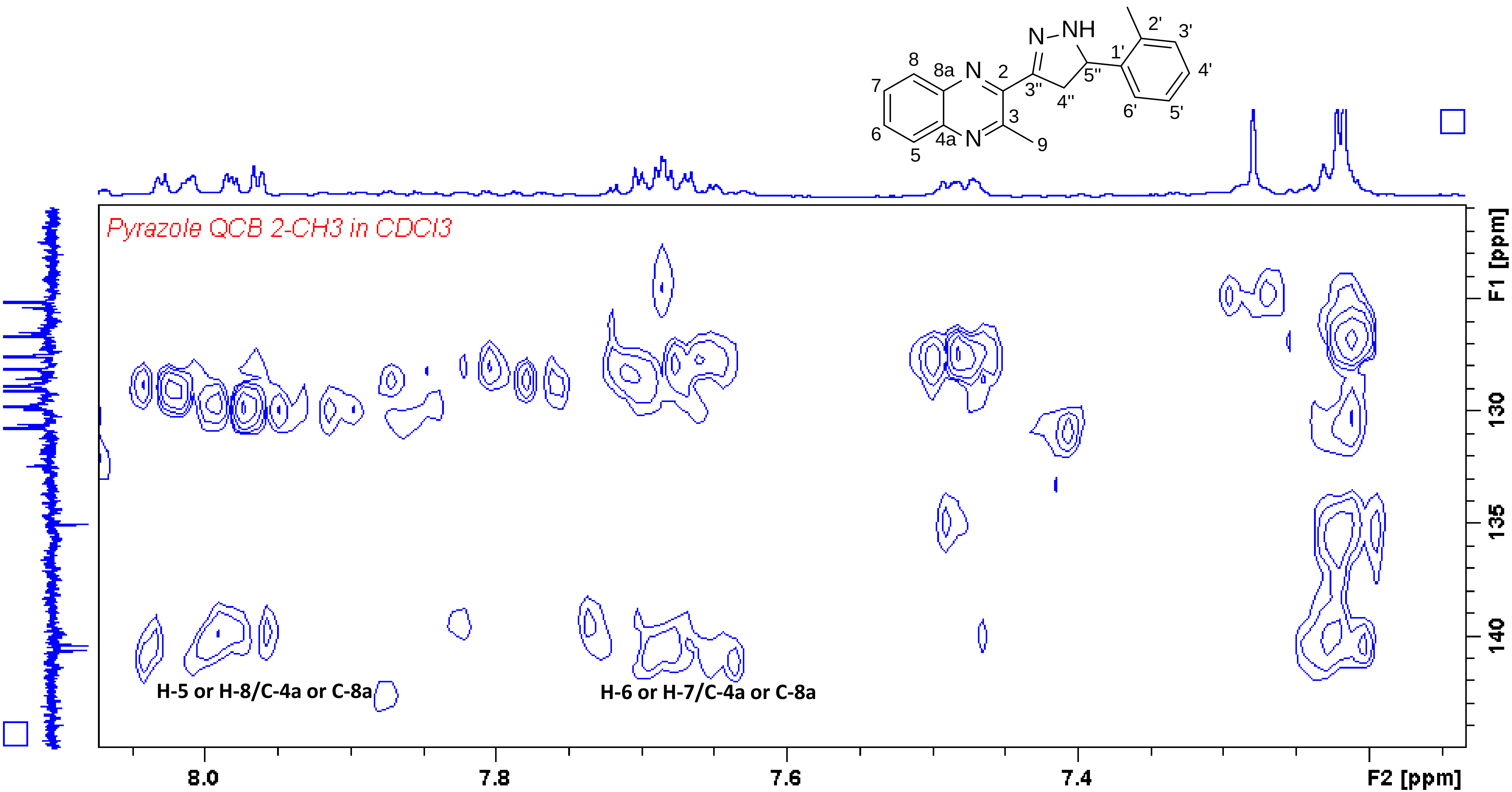

Expanded HMBC of **B11d**

Elemental Composition Report

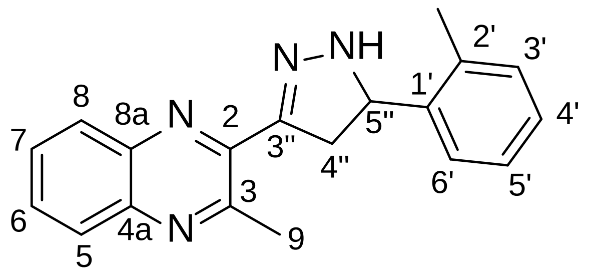

Single Mass Analysis

Tolerance = 50.0 PPM / DBE: min = -1.5, max = 100.0
Element prediction: Off
Number of isotope peaks used for i-FIT = 2

Monoisotopic Mass, Even Electron Ions
3 formula(e) evaluated with 1 results within limits (up to 20 best isotopic matches for each mass)
Elements Used:
C: 15-20 H: 15-20 N: 0-5
Py-QCB 2-Me 50 (1.653) Cm (1:61)
TOF MS ES+

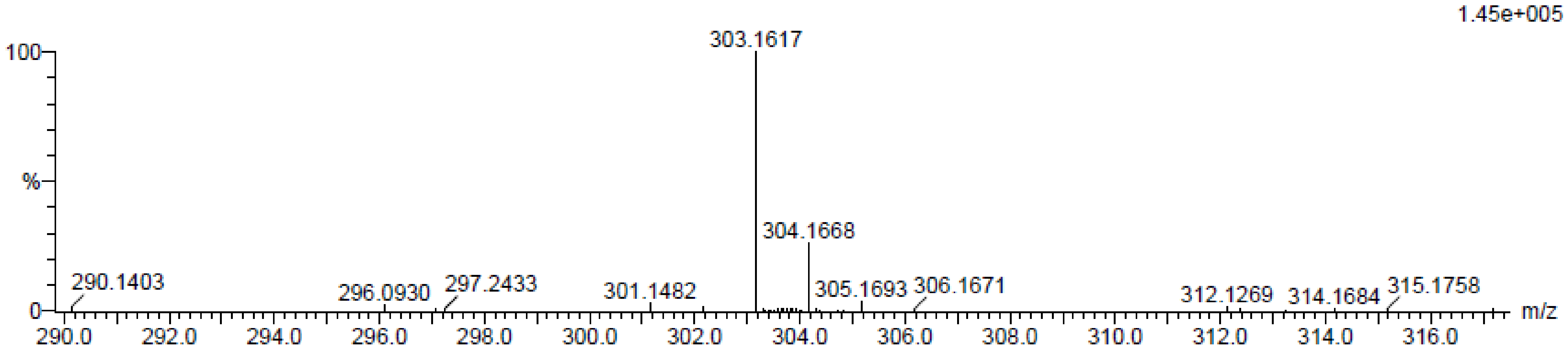

Minimum:				-1.5			
Maximum:		5.0	50.0	100.0			
Mass	Calc. Mass	mDa	PPM	DBE	i-FIT	i-FIT (Norm)	Formula
303.1617	303.1610	0.7	2.3	12.5	228.6	0.0	C19 H19 N4

High resolution mass spectrum of **B11d**

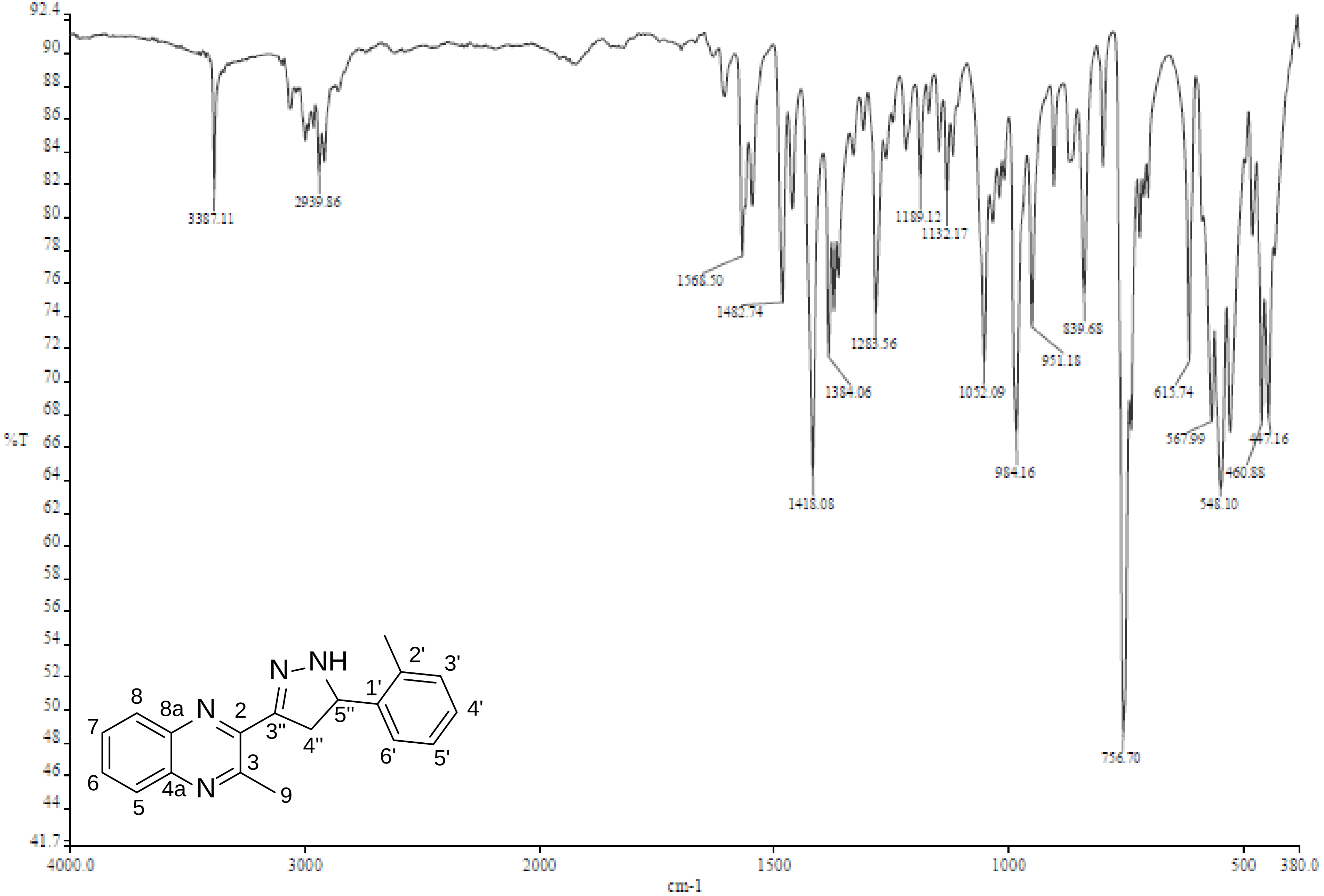

FTIR spectrum of **B11d**

Overlay Spectrum Graph Report

06/10/2017 11:48:37 AM

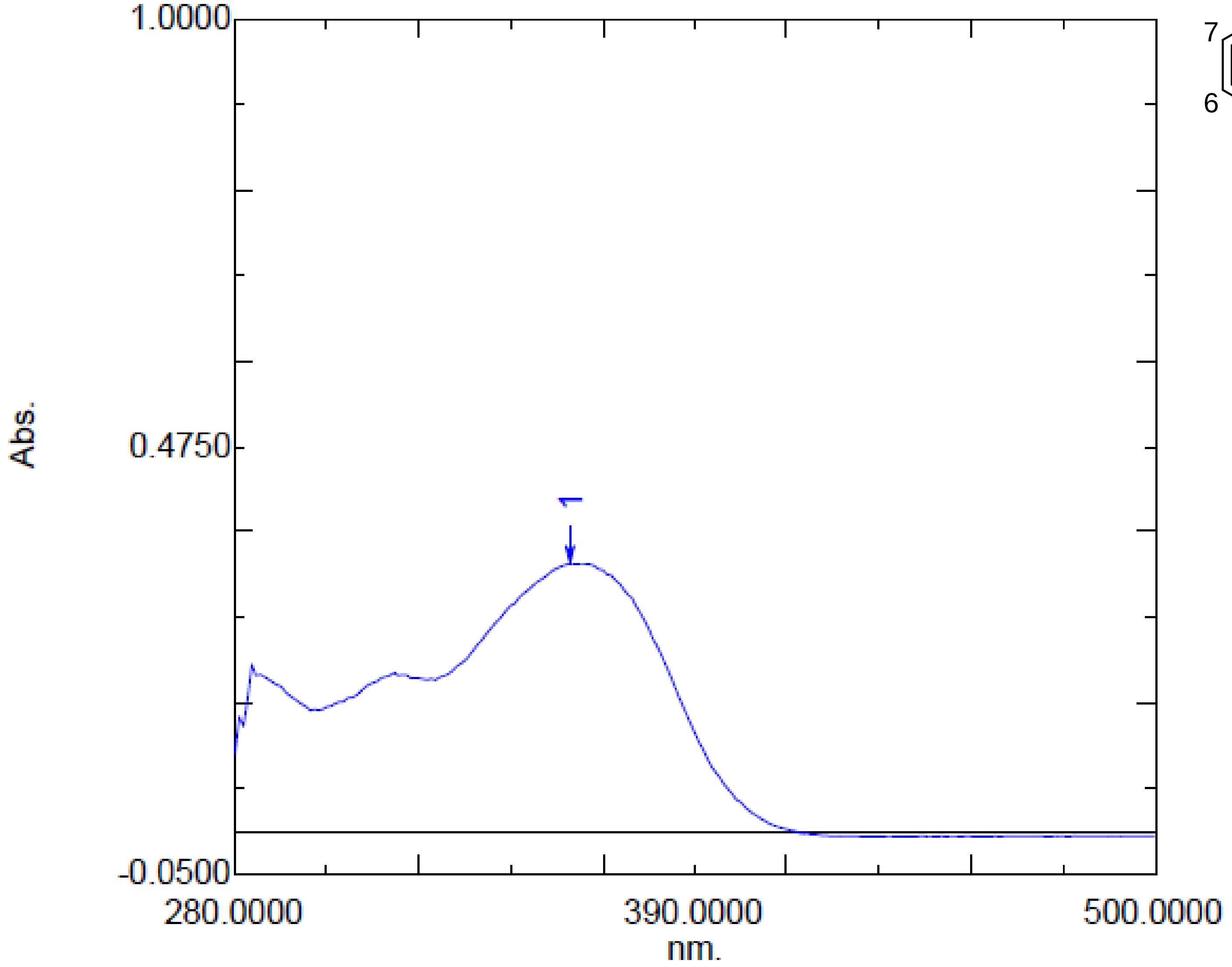

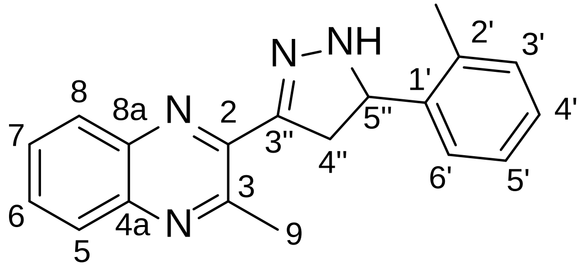

λ	absorbance	logε
360	0.3311	4.30

UV spectrum of **B11d**

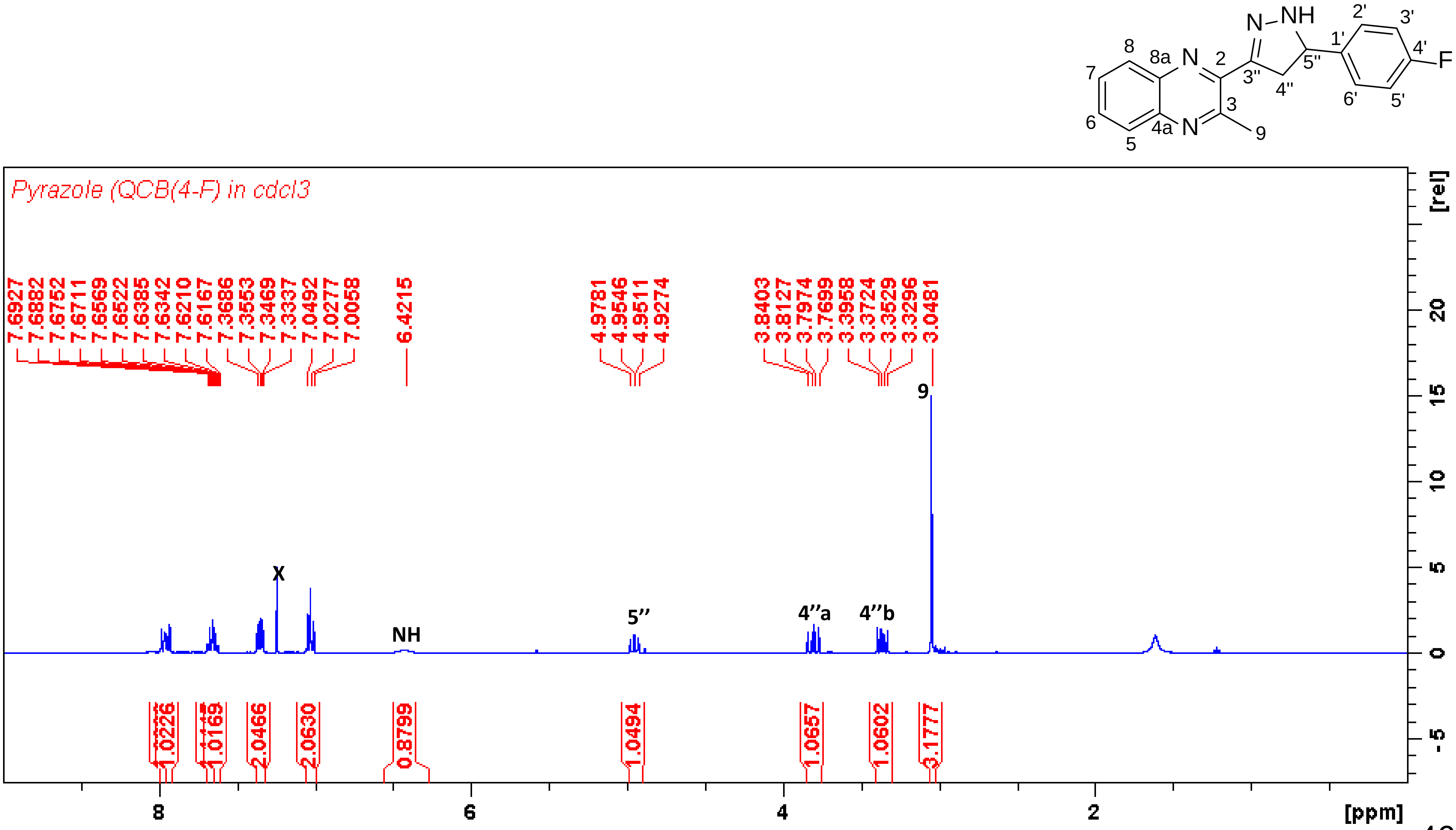

^{1}H NMR spectrum of **B11e**

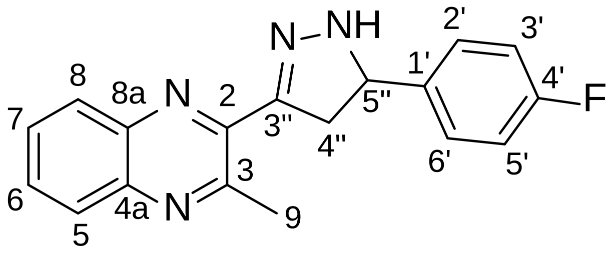

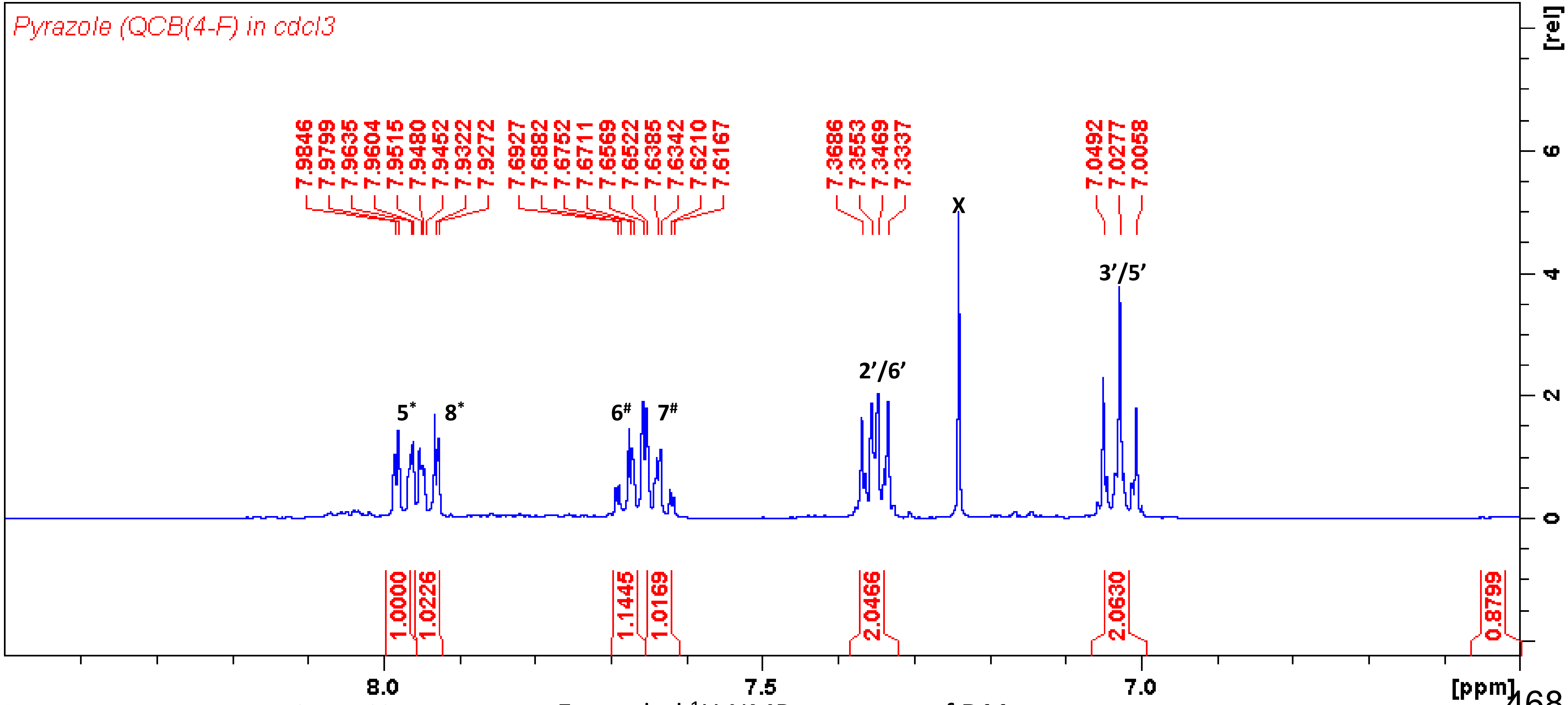

*, # Indicates assignments are interchangeable

Expanded ^{1}H NMR spectrum of **B11e**

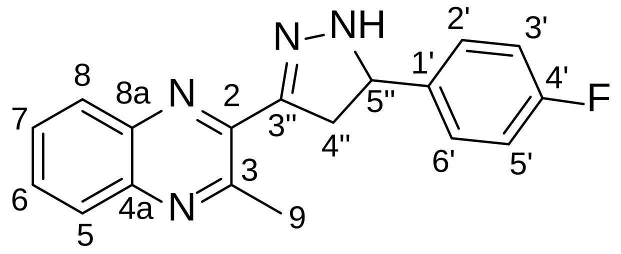

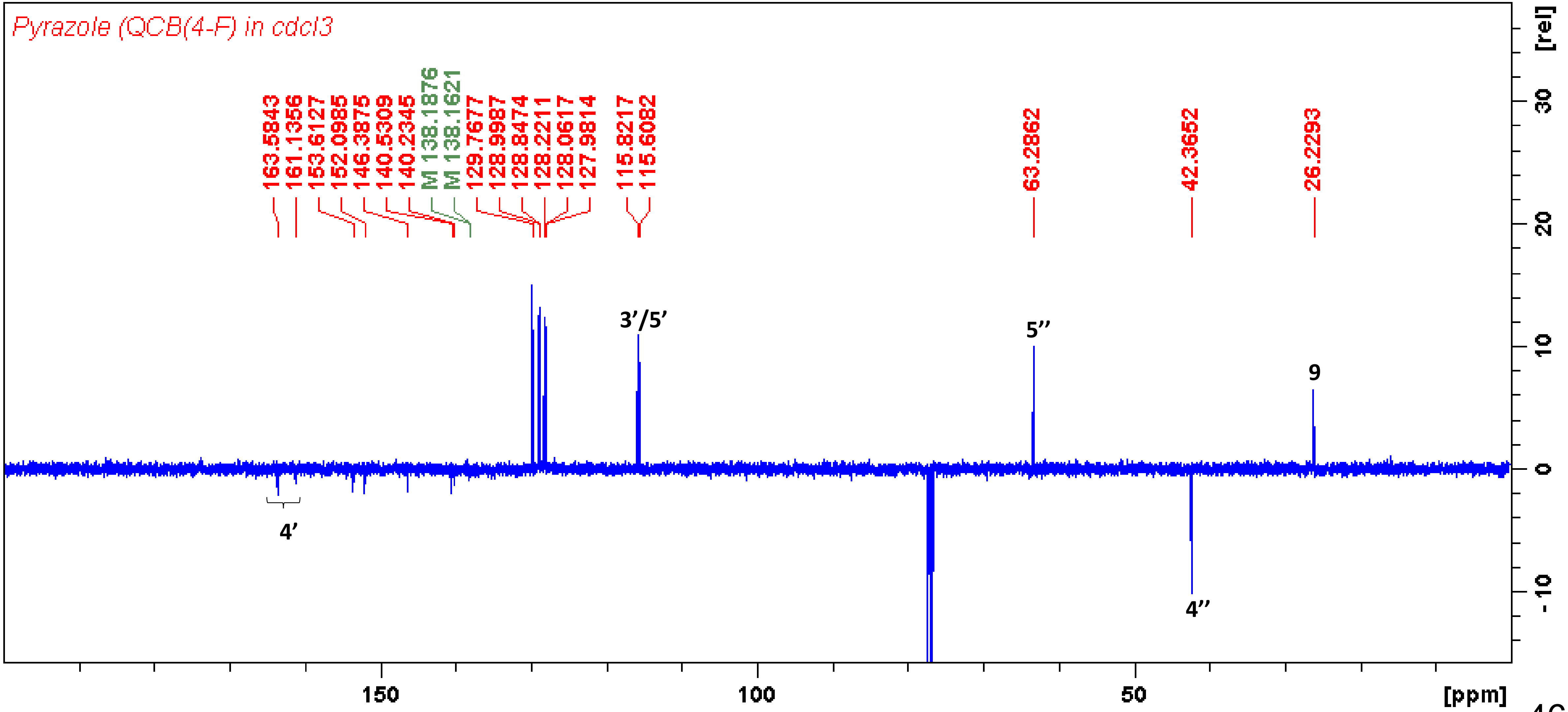

^{13}C NMR spectrum of **B11e**

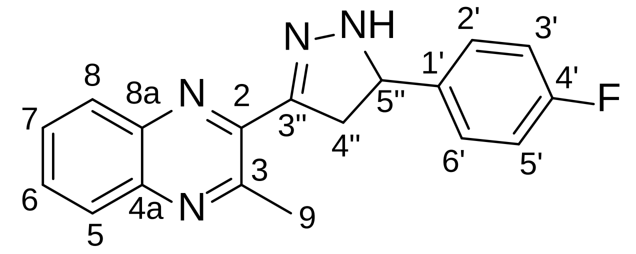

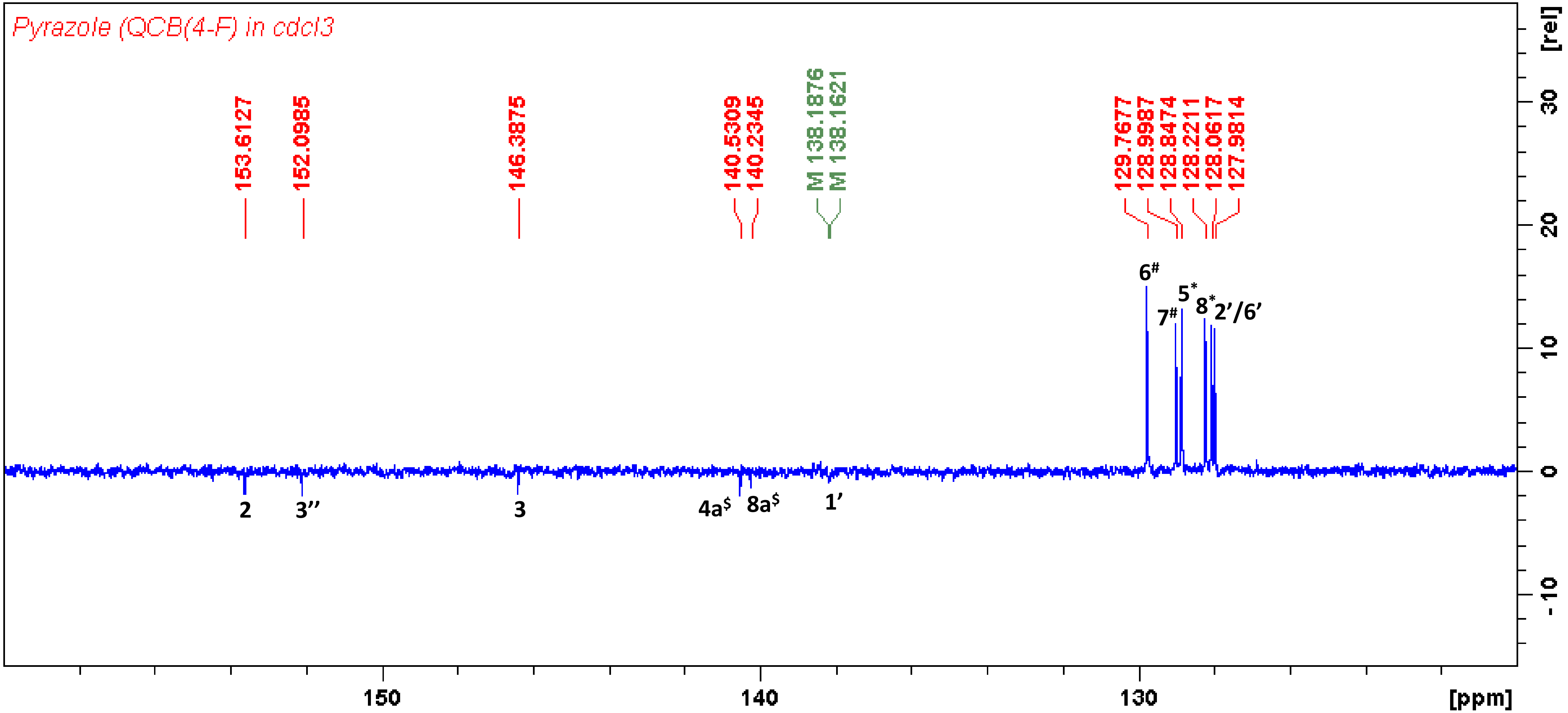

*, #, $ Indicates assignments are interchangeable

Expanded ^{13}C NMR spectrum of **B11e**

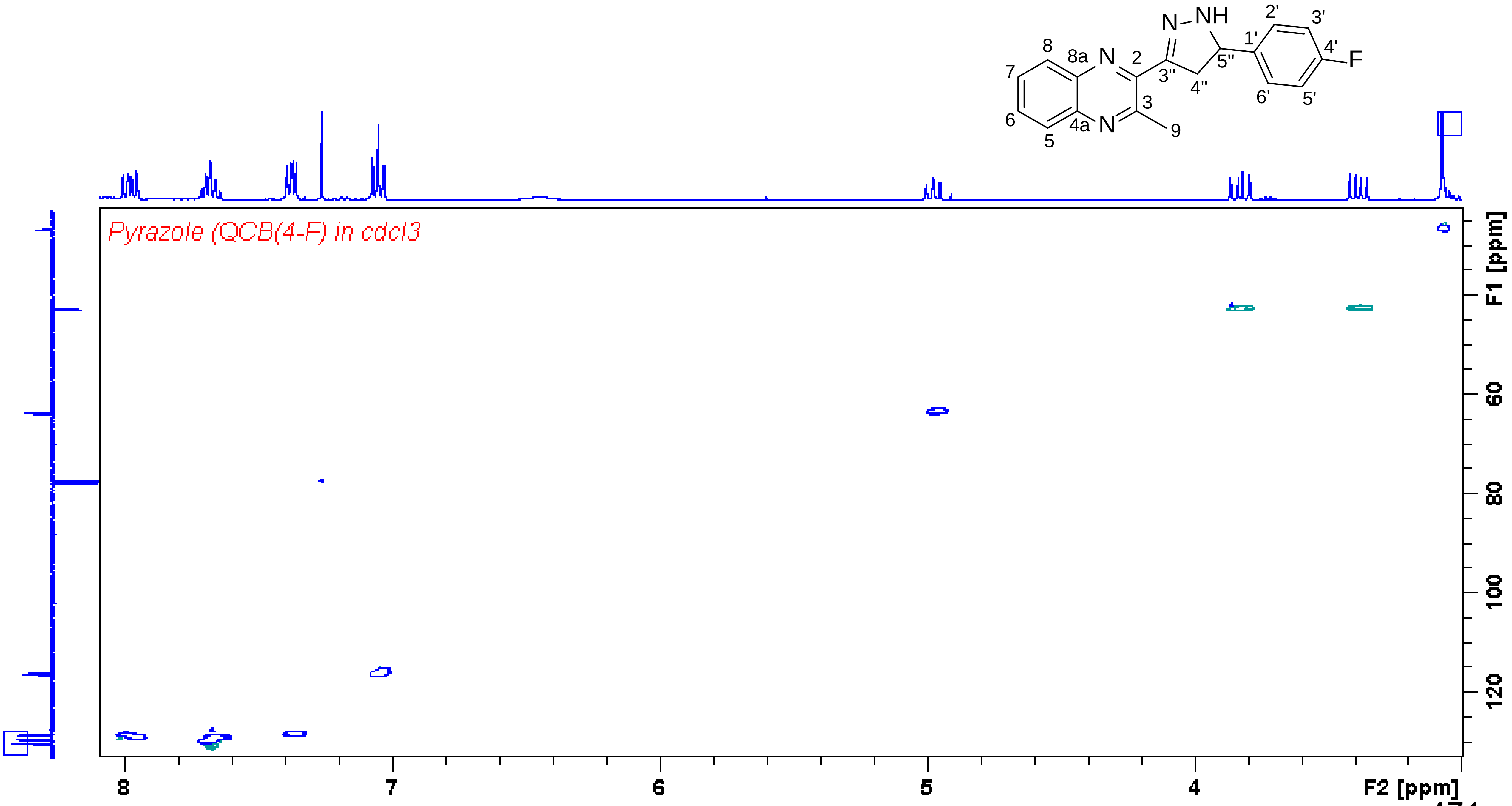
Pyrazole (QCB(4-F) in cdcl3
F1 [ppm]
F2 [ppm]
8
7
6
5
4
60
80
100
120
N
NH
F
8
8a
2
2'
3'
1'
4'
5''
3''
4''
7
6
5
4a
3
9
6'
5'

HSQC of **B11e**

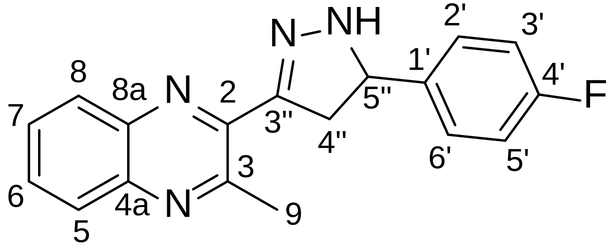

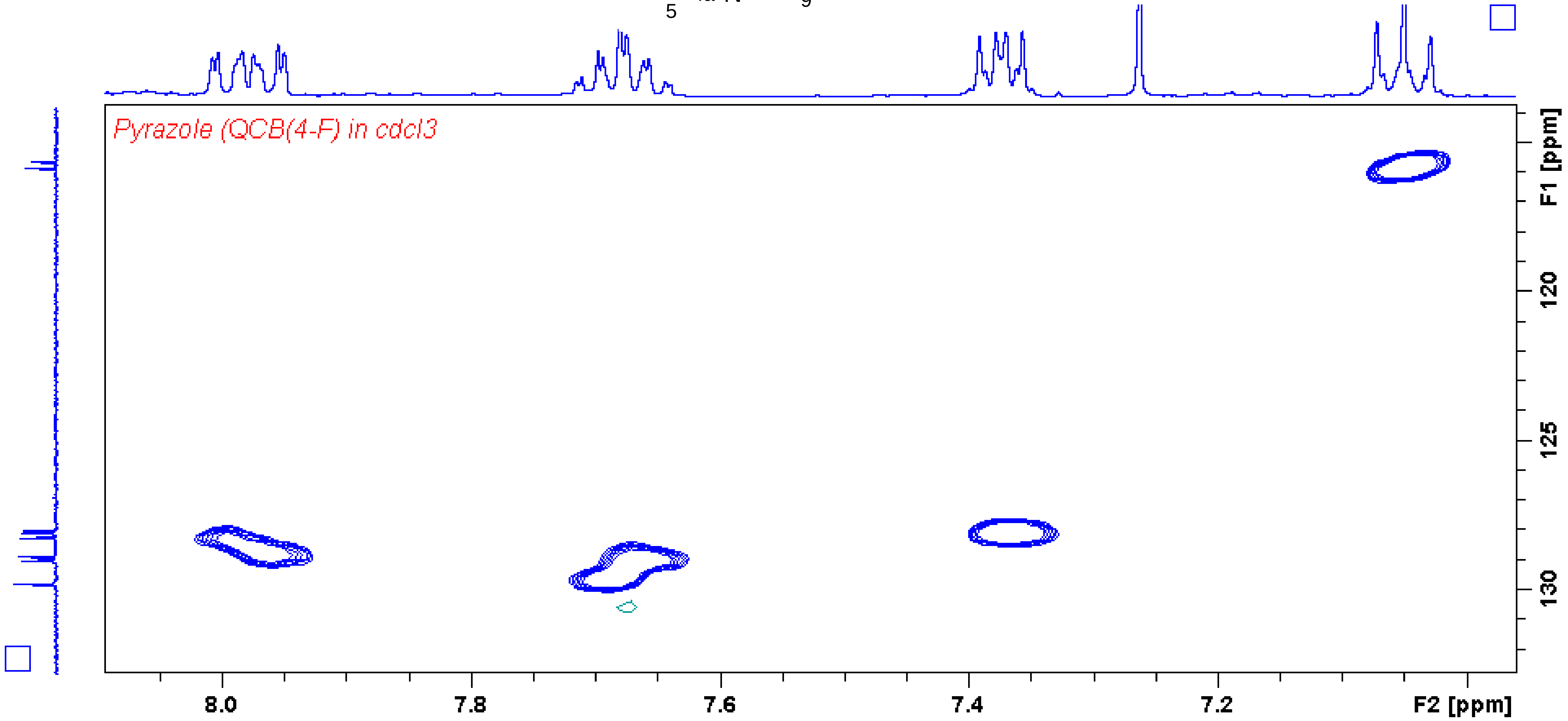

Expanded HSQC of **B11e**

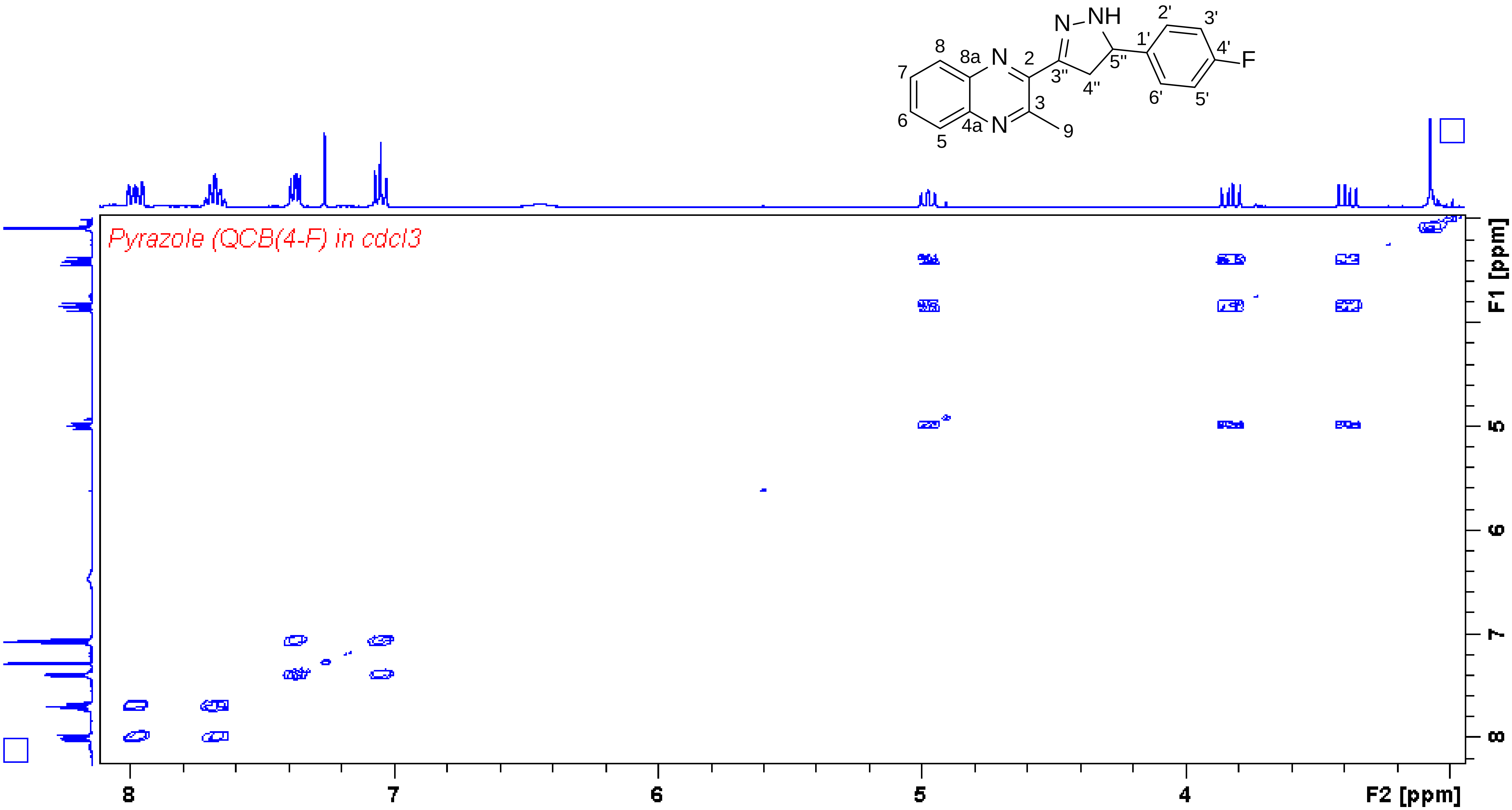

N
NH
2'
3'
8
1'
4'
F
8a
N
2
5''
7
3''
4''
3
6'
5'
6
4a
N
9
5
Pyrazole (QCB(4-F) in cdcl3
F1 [ppm]
F2 [ppm]
8
7
6
5
4

COSY of **B11e**

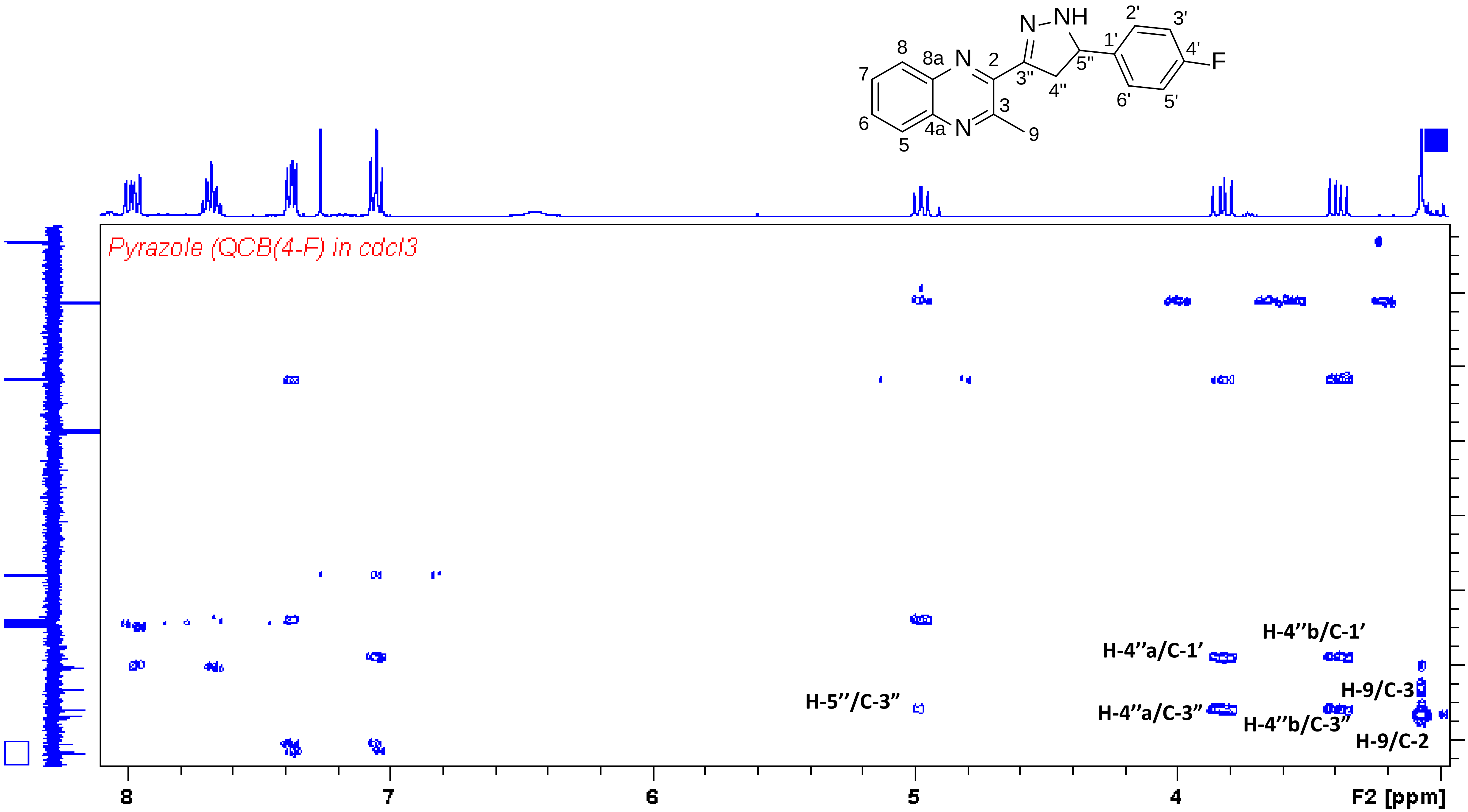
Pyrazole (QCB(4-F) in cdcl3
H-4''b/C-1'
H-4''a/C-1'
H-9/C-3
H-5''/C-3''
H-4''a/C-3''
H-4''b/C-3''
H-9/C-2
F2 [ppm]
F1 [ppm]

HMBC of **B11e**

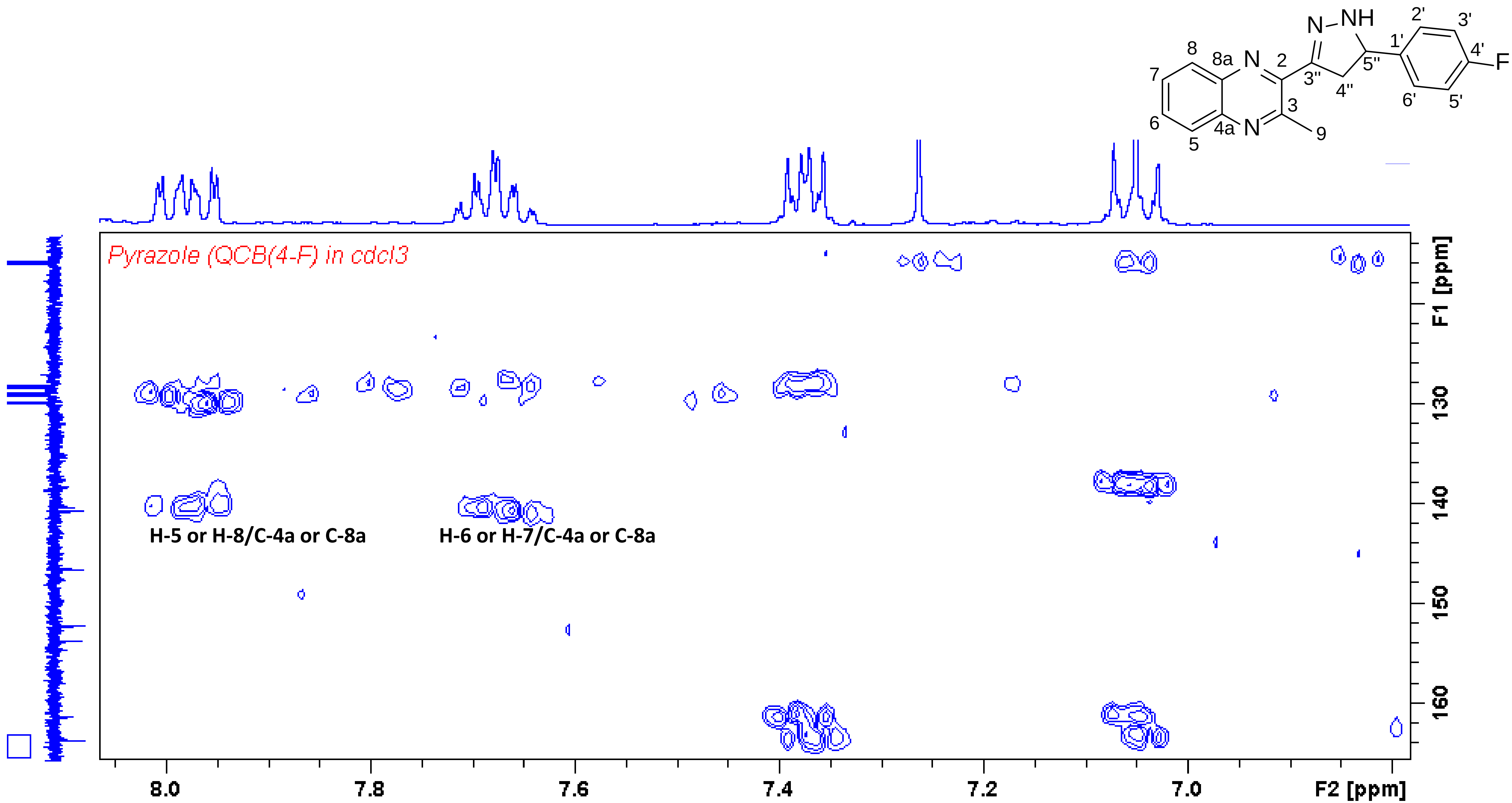

Expanded HMBC of **B11e**

Elemental Composition Report

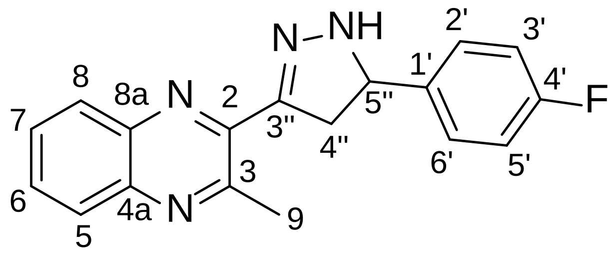

Single Mass Analysis

Tolerance = 5.0 PPM / DBE: min = -1.5, max = 100.0
Element prediction: Off
Number of isotope peaks used for i-FIT = 3

Monoisotopic Mass, Even Electron Ions
9 formula(e) evaluated with 1 results within limits (up to 20 closest results for each mass)
Elements Used:
C: 15-20 H: 15-20 N: 0-5 F: 0-1 Na: 0-1
Py-QCB 4-F 16 (0.506) Cm (1:61)
TOF MS ES+

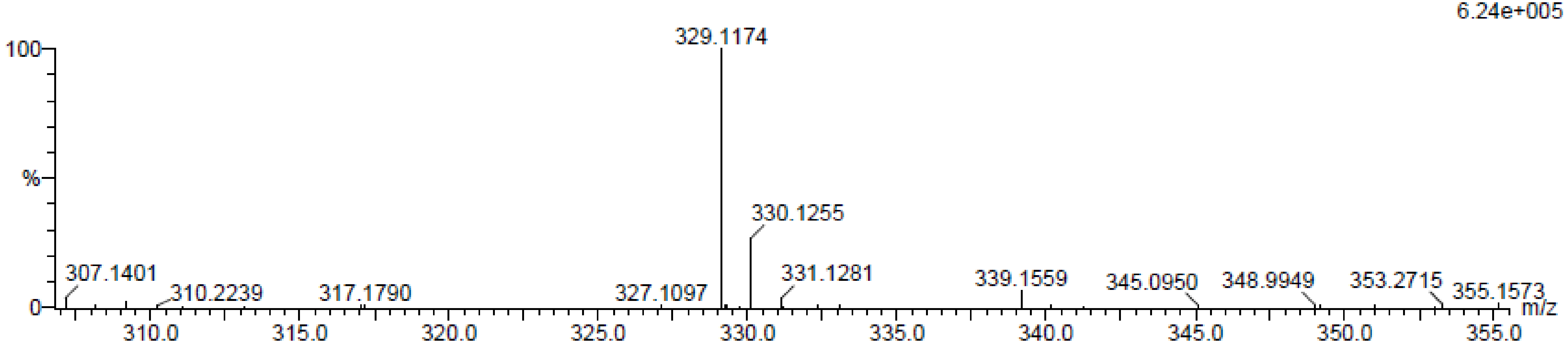

Minimum:				-1.5			
Maximum:		5.0	5.0	100.0			
Mass	Calc. Mass	mDa	PPM	DBE	i-FIT	i-FIT (Norm)	Formula
329.1174	329.1178	-0.4	-1.2	12.5	96.8	0.0	C18 H15 N4 F Na

High resolution mass spectrum of **B11e**

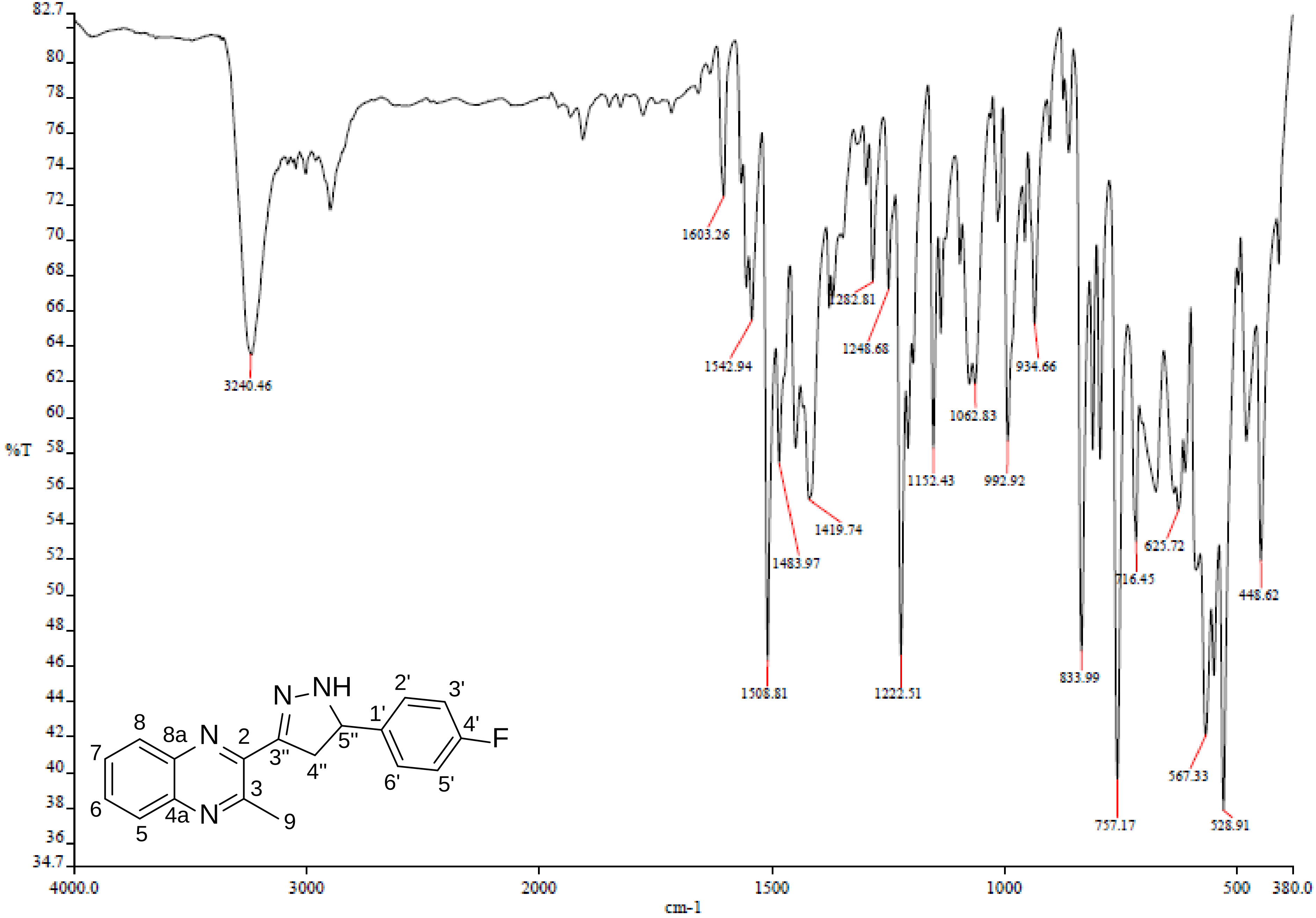

FTIR spectrum of **B11e**

Overlay Spectrum Graph Report

06/10/2017 11:54:57 AM

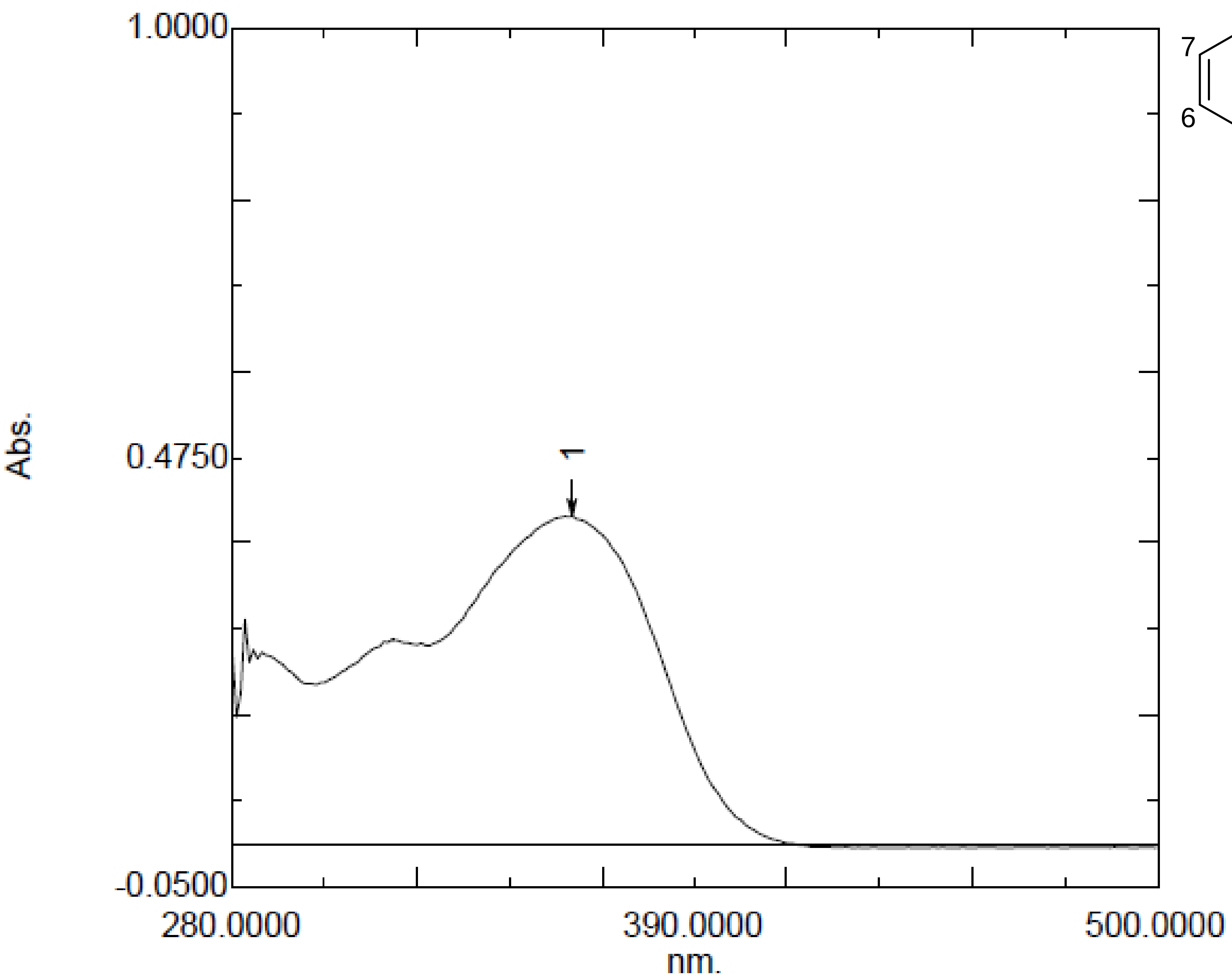

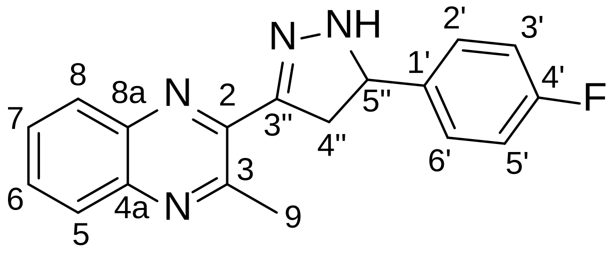

λ	absorbance	logε
361	0.4029	4.39

UV spectrum of **B11e**

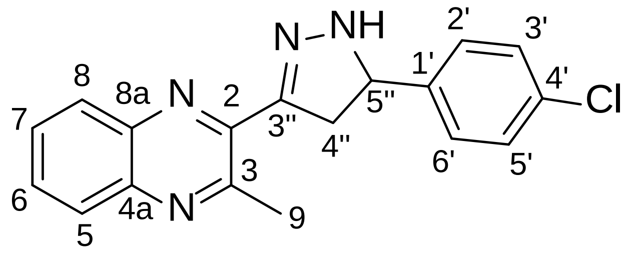

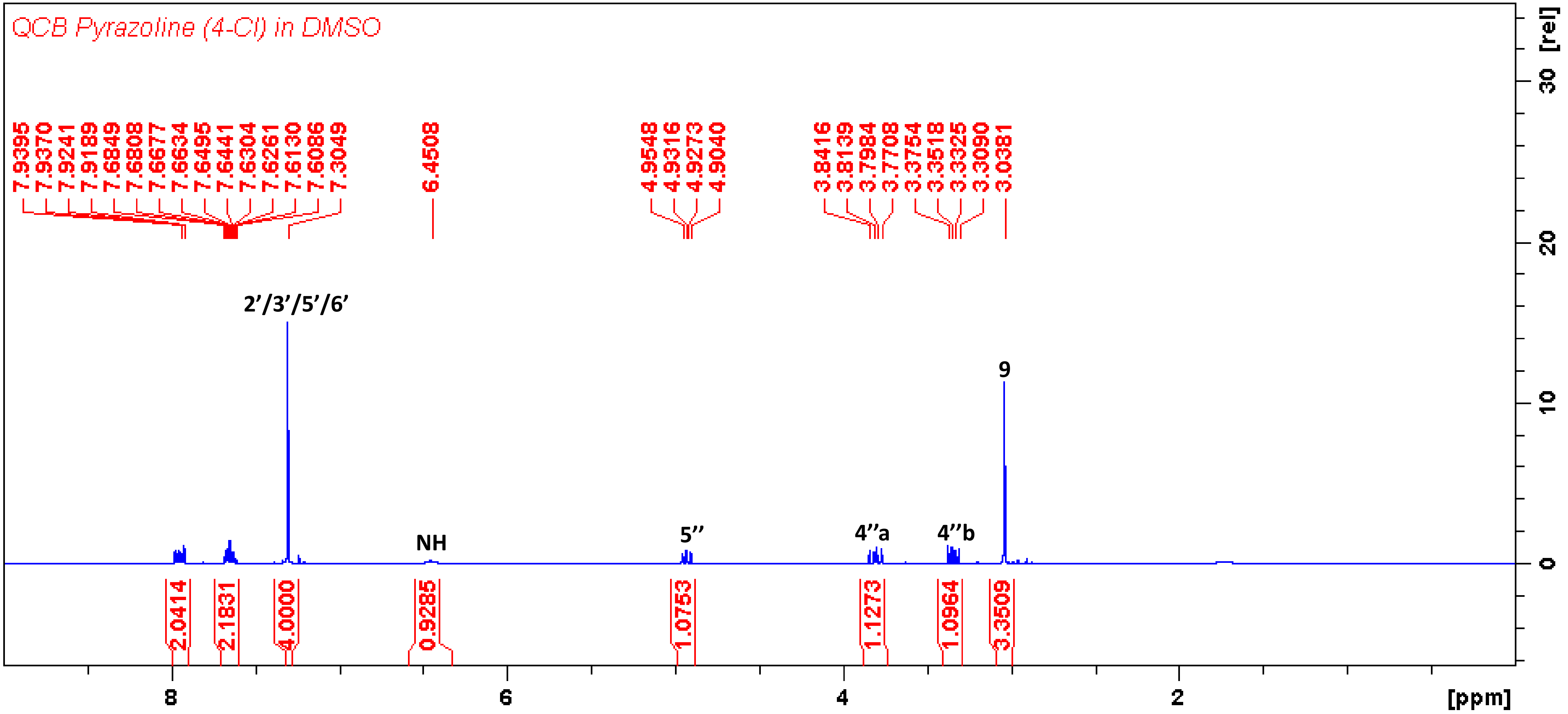

^{1}H NMR spectrum of **B11f**

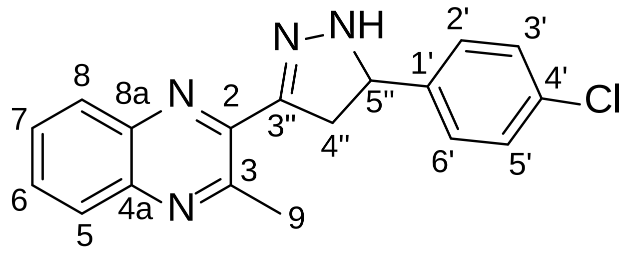

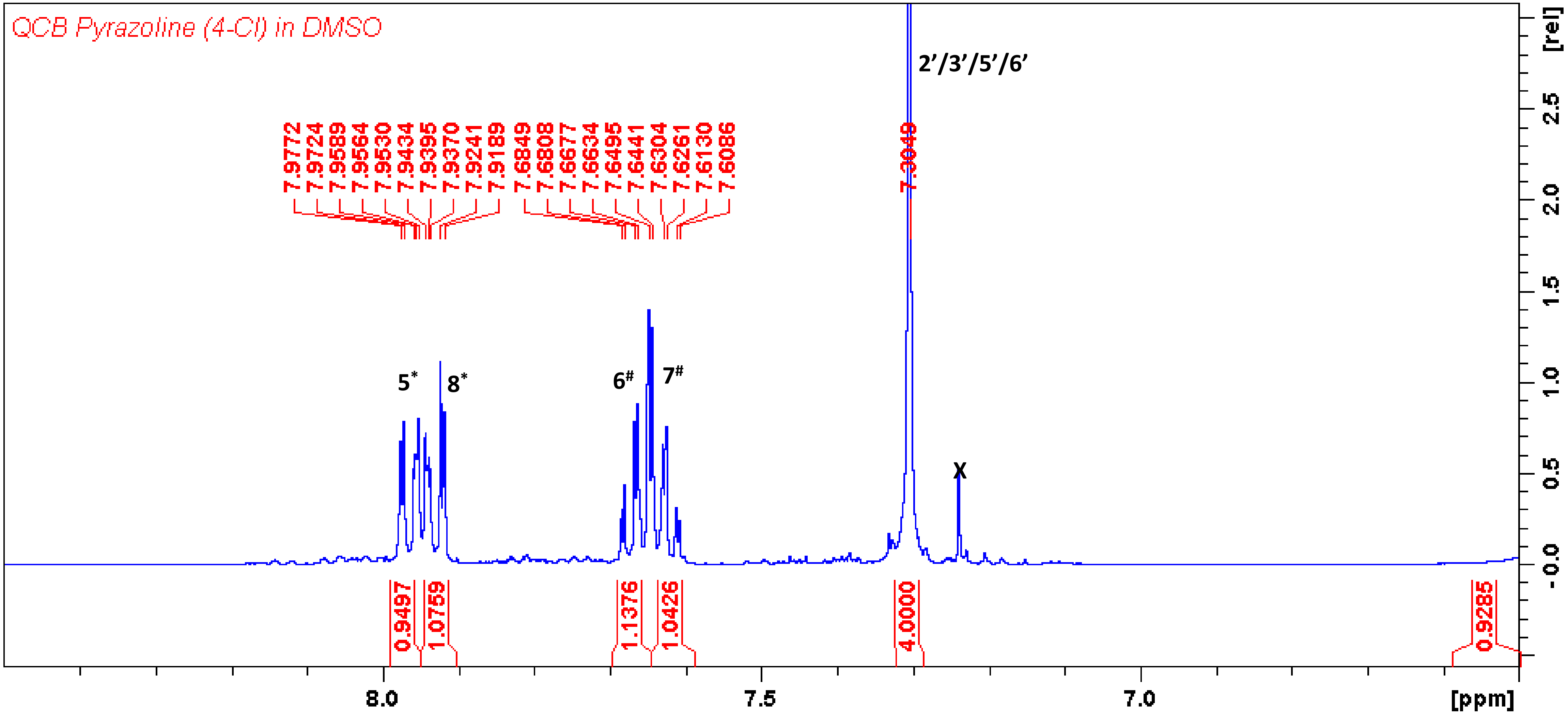

*, # Indicates assignments are interchangeable

Expanded ^{1}H NMR spectrum of **B11f**

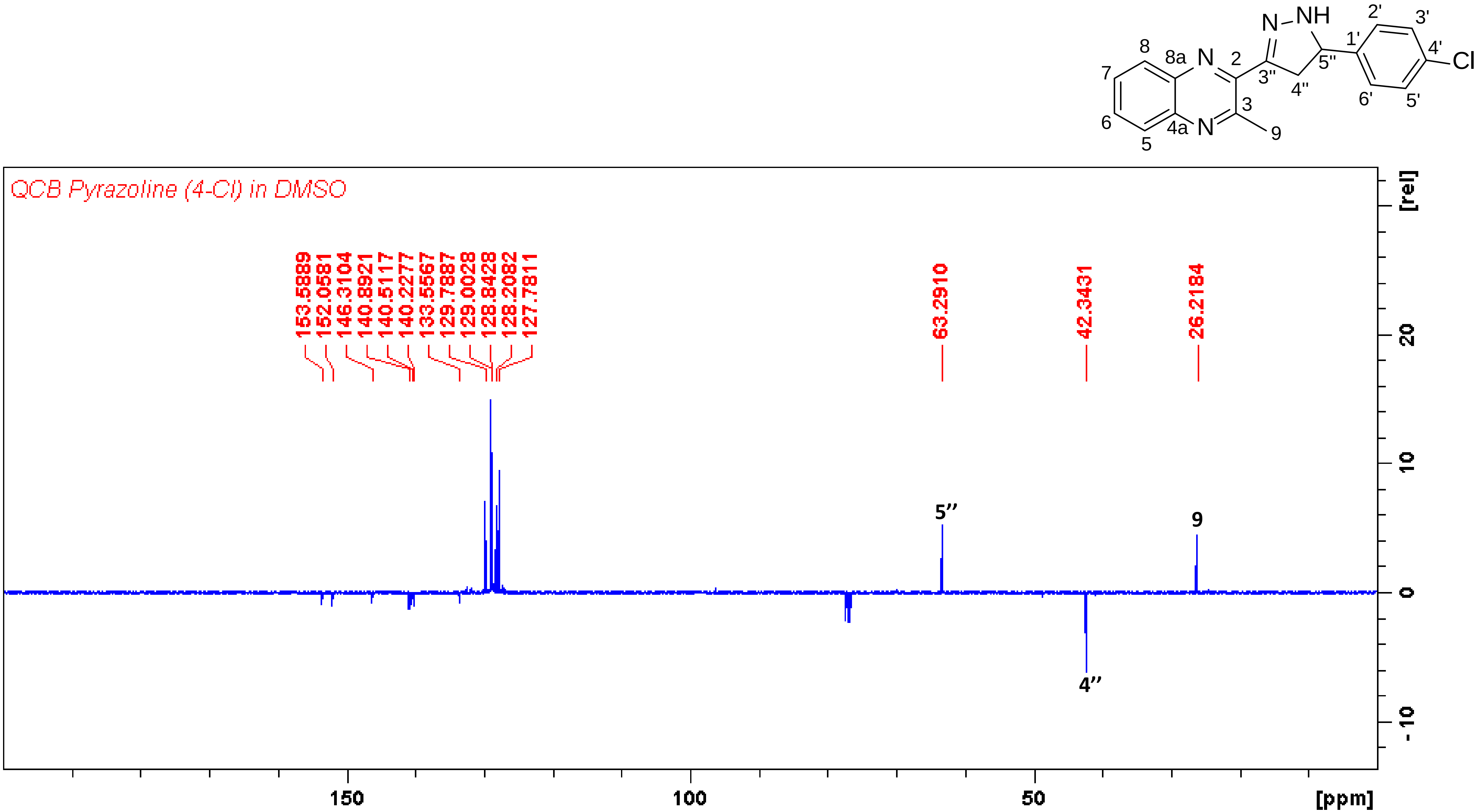

^{13}C NMR spectrum of **B11f**

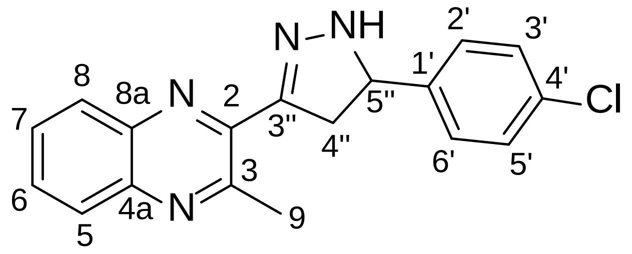

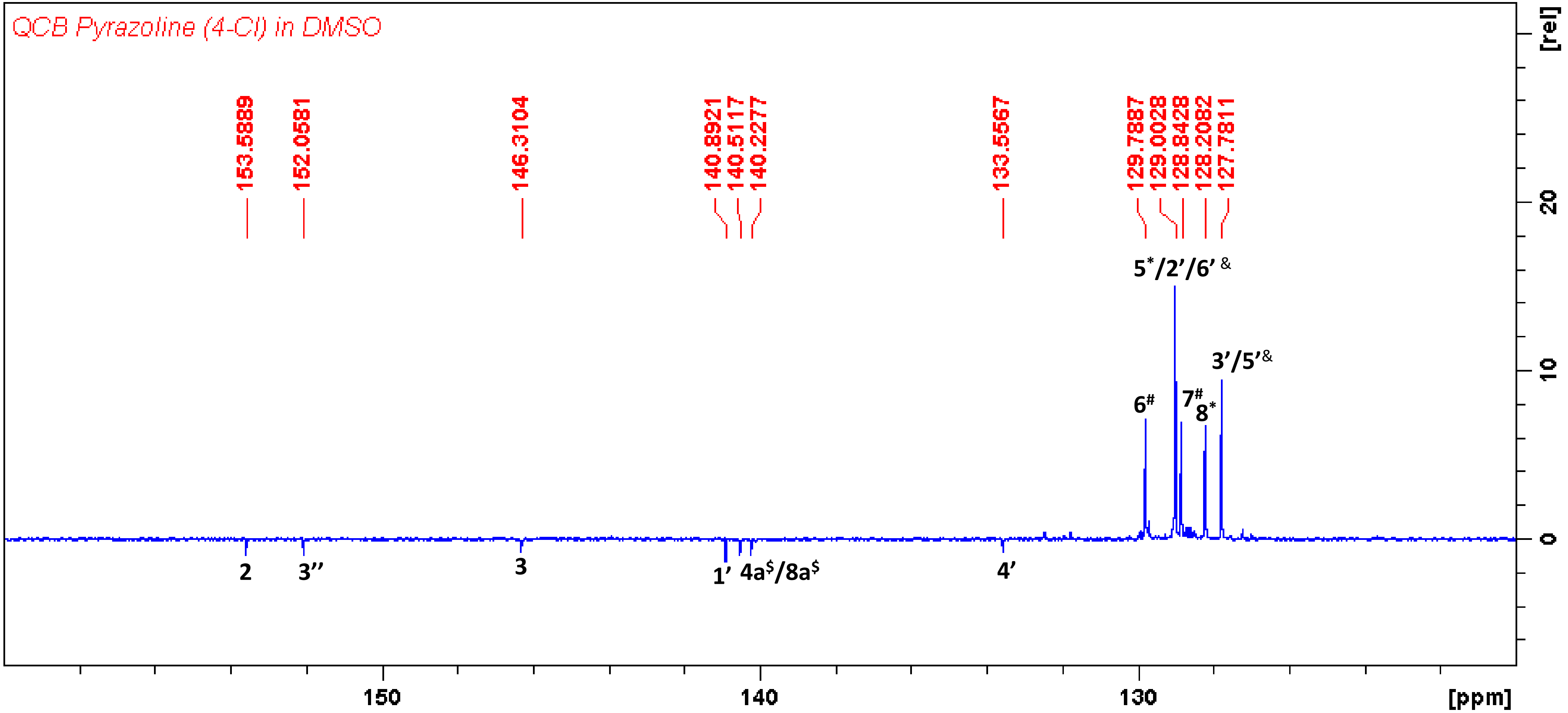

*, #, $, & Indicates assignments are interchangeable

Expanded ^{13}C NMR spectrum of **B11f**

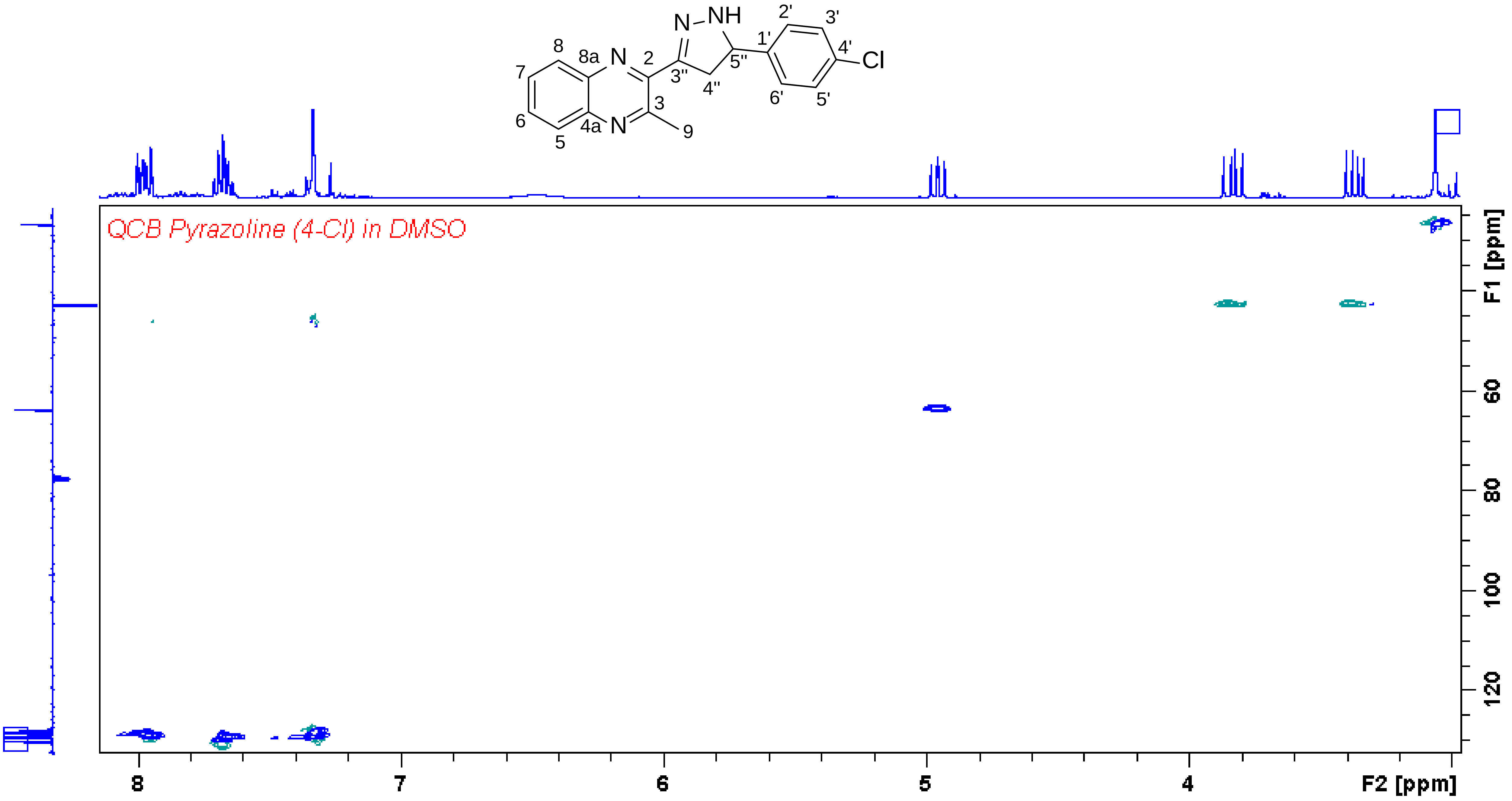

HSQC of **B11f**

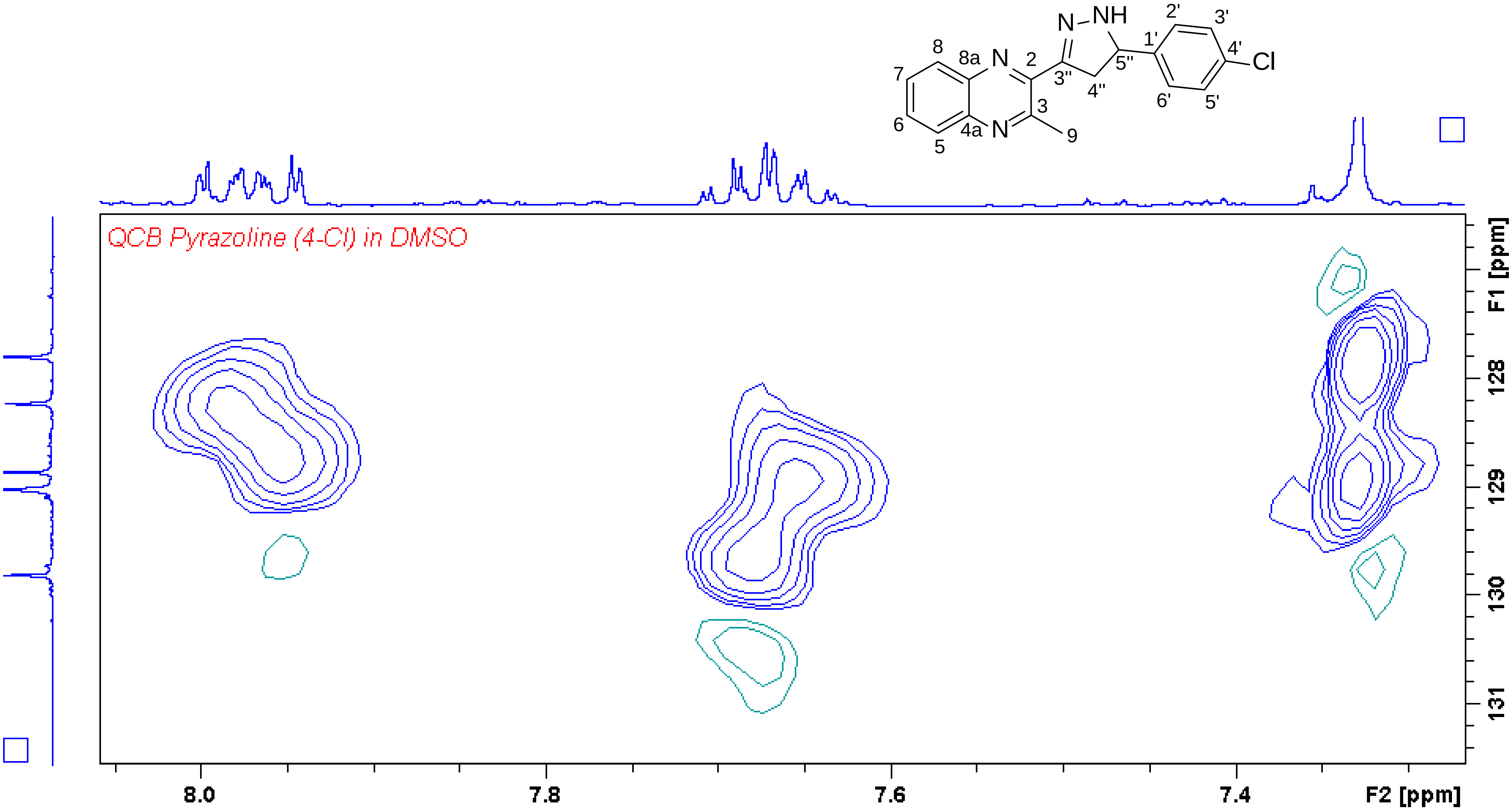

Expanded HSQC of **B11f**

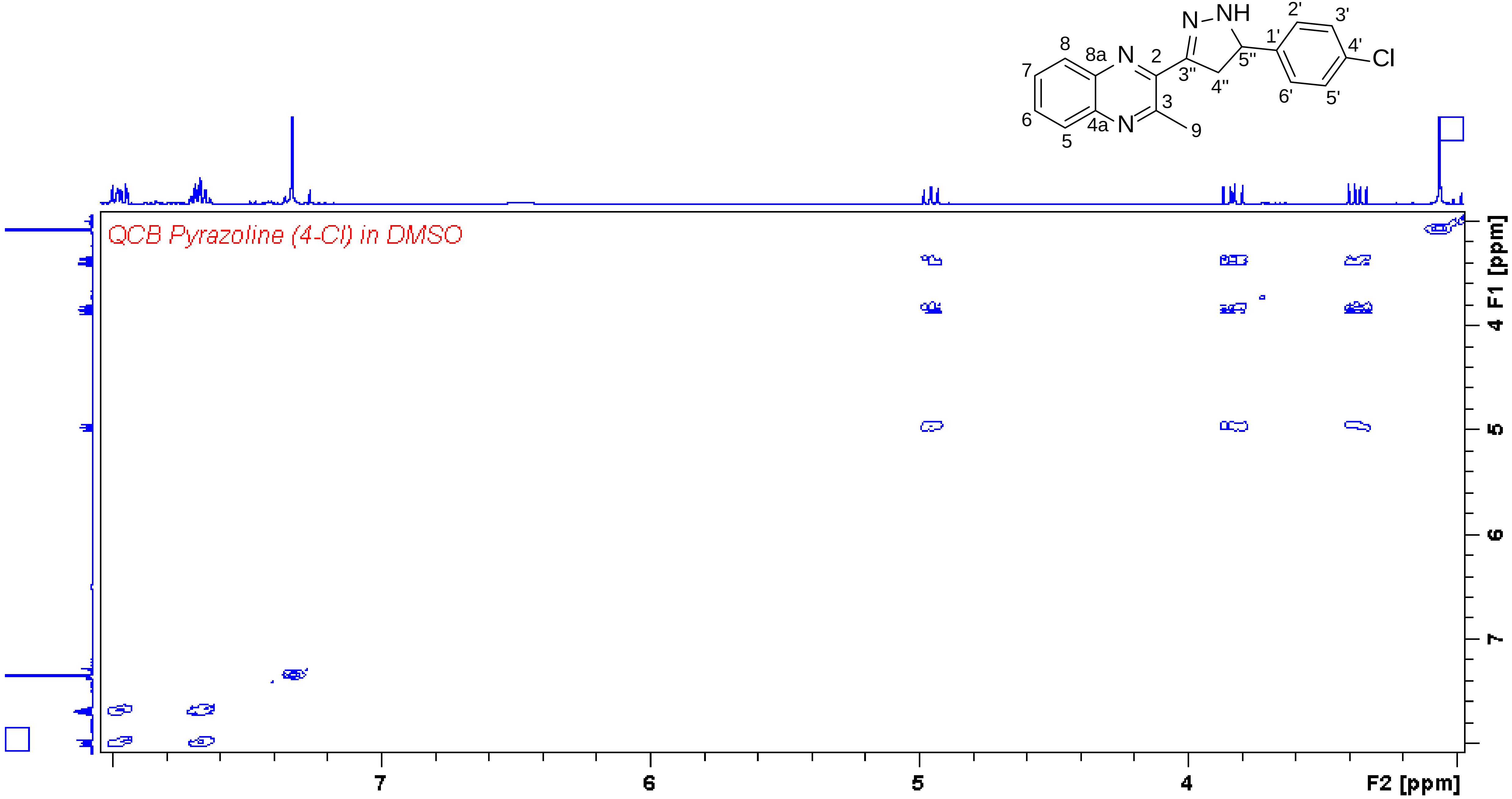
QCB Pyrazoline (4-Cl) in DMSO
F1 [ppm]
F2 [ppm]
7
6
5
4
N
NH
N
N
Cl
8
8a
7
6
5
4a
2
3
9
3''
4''
5''
1'
2'
3'
4'
5'
6'

COSY of **B11f**

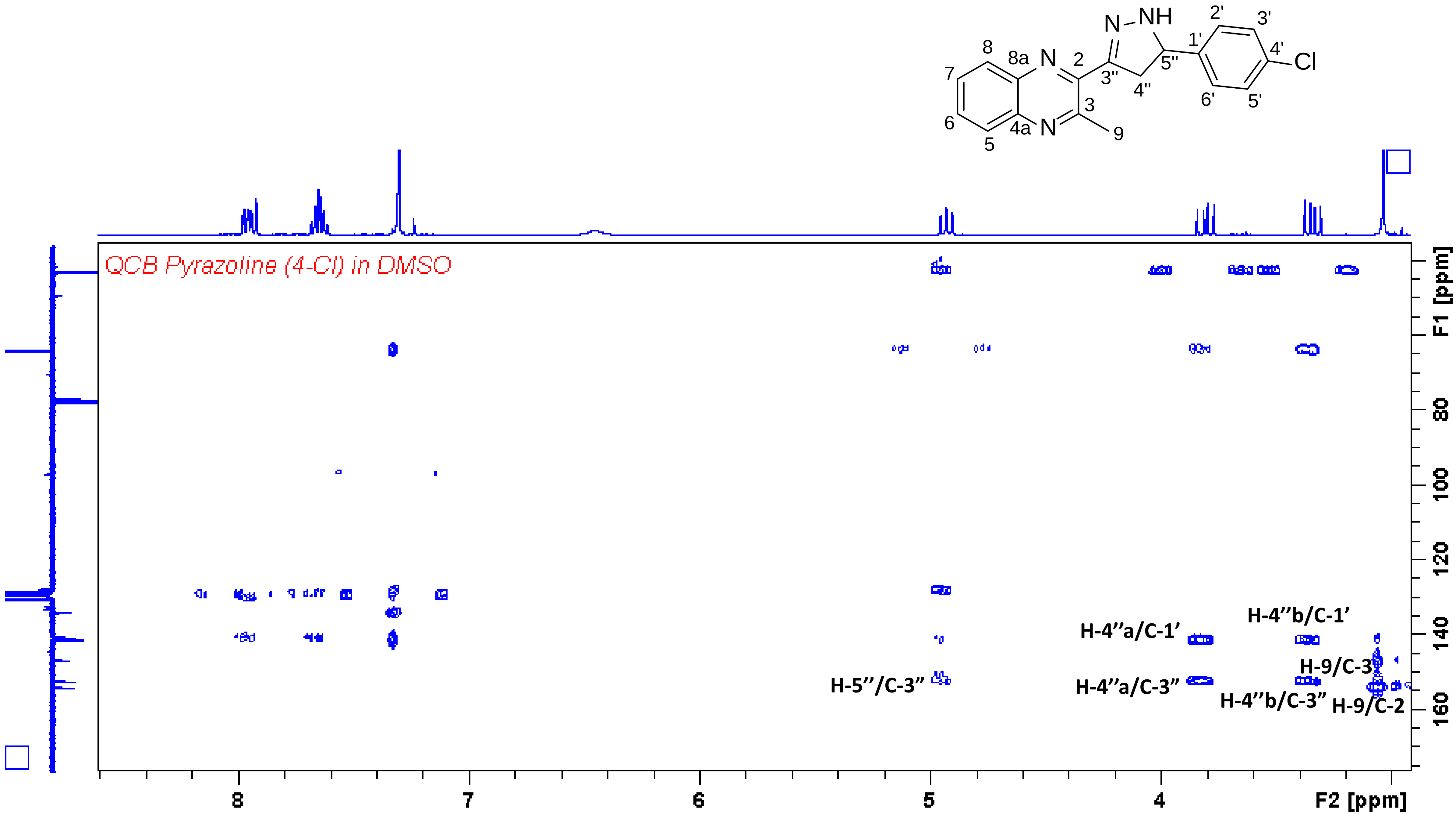
N
NH
2'
3'
8
8a
N
2
1'
4'
Cl
7
3''
5''
4''
6'
5'
6
3
4a
N
9
5
QCB Pyrazoline (4-Cl) in DMSO
H-4''b/C-1'
H-4''a/C-1'
H-9/C-3
H-5''/C-3''
H-4''a/C-3''
H-4''b/C-3''
H-9/C-2
F1 [ppm]
F2 [ppm]

HMBC of **B11f**

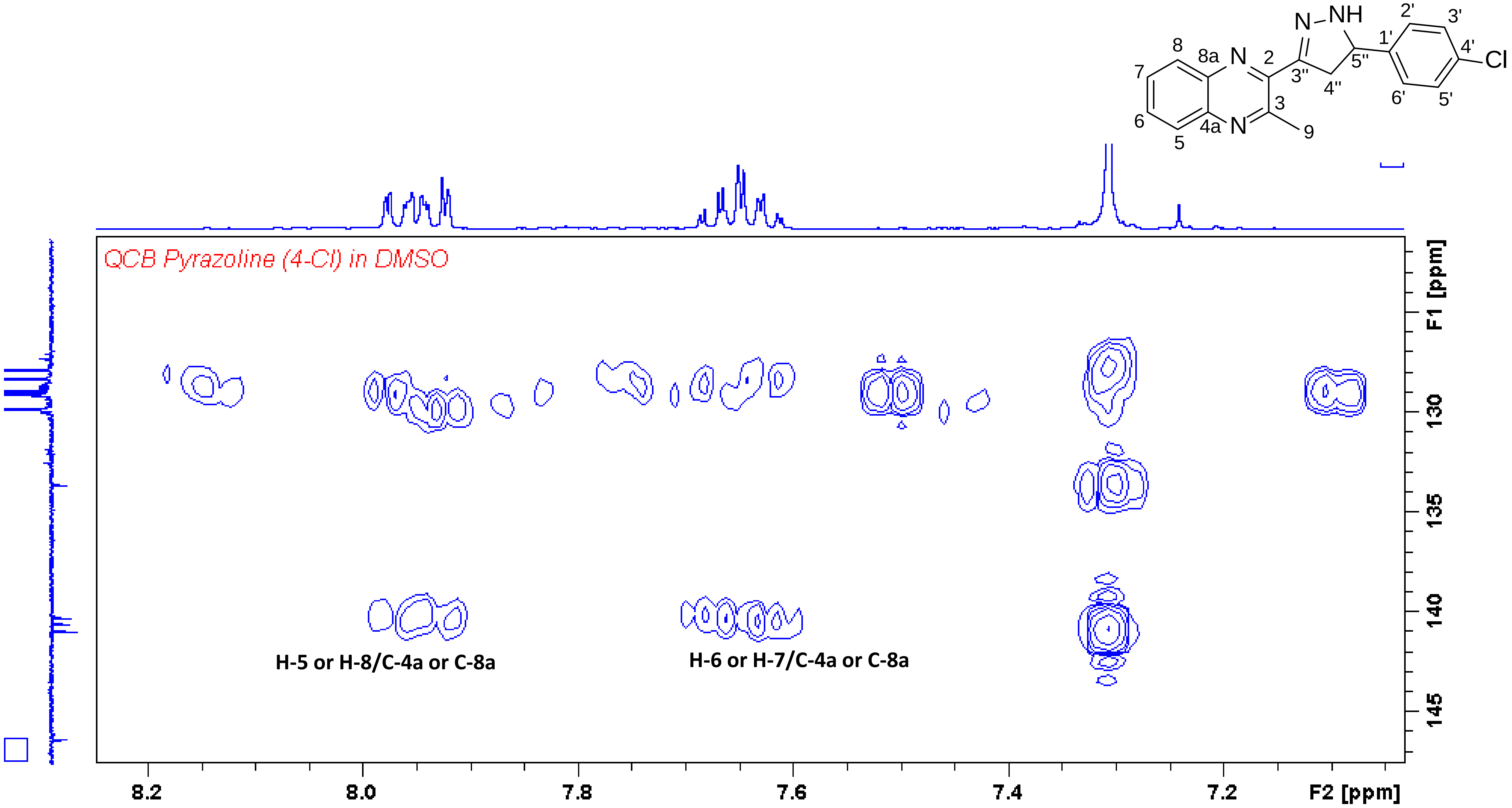

Expanded HMBC of **B11f**

Elemental Composition Report

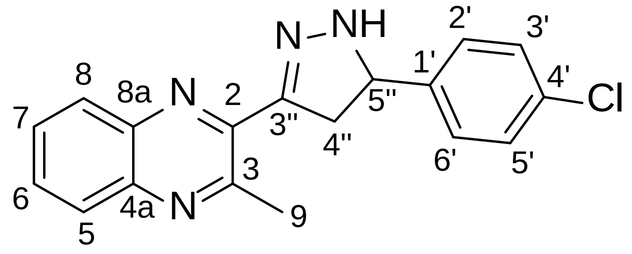

Single Mass Analysis

Tolerance = 5.0 PPM / DBE: min = -1.5, max = 100.0
Element prediction: Off
Number of isotope peaks used for i-FIT = 3

Monoisotopic Mass, Even Electron Ions
10 formula(e) evaluated with 1 results within limits (up to 20 closest results for each mass)
Elements Used:
C: 15-20 H: 15-20 N: 0-5 Na: 0-1 Cl: 0-1
Py-QCB 4-Cl 53 (1.754) Cm (1:61)
TOF MS ES+

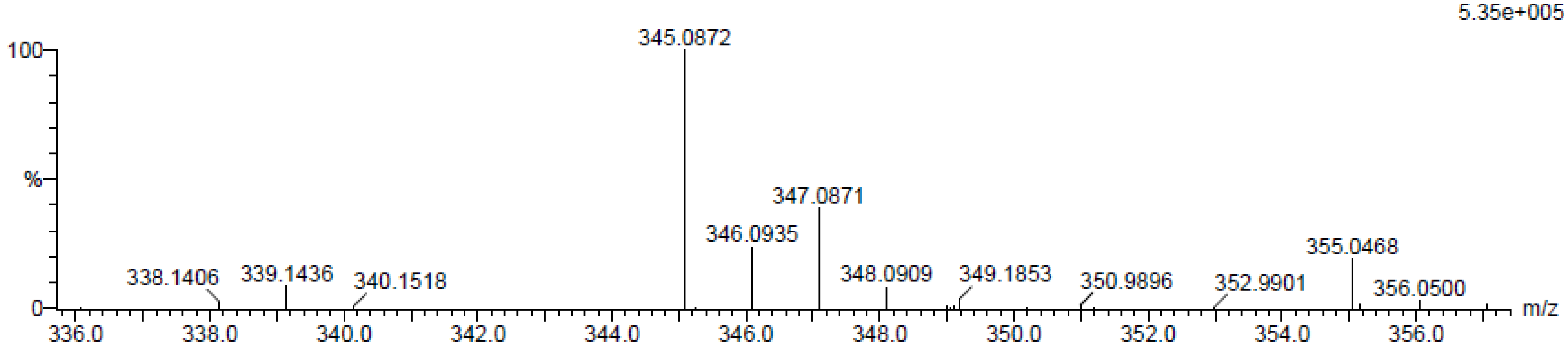

Minimum:				-1.5			
Maximum:		5.0	5.0	100.0			
Mass	Calc. Mass	mDa	PPM	DBE	i-FIT	i-FIT (Norm)	Formula
345.0872	345.0883	-1.1	-3.2	12.5	44.7	0.0	C18 H15 N4 Na Cl

High resolution mass spectrum of **B11f**

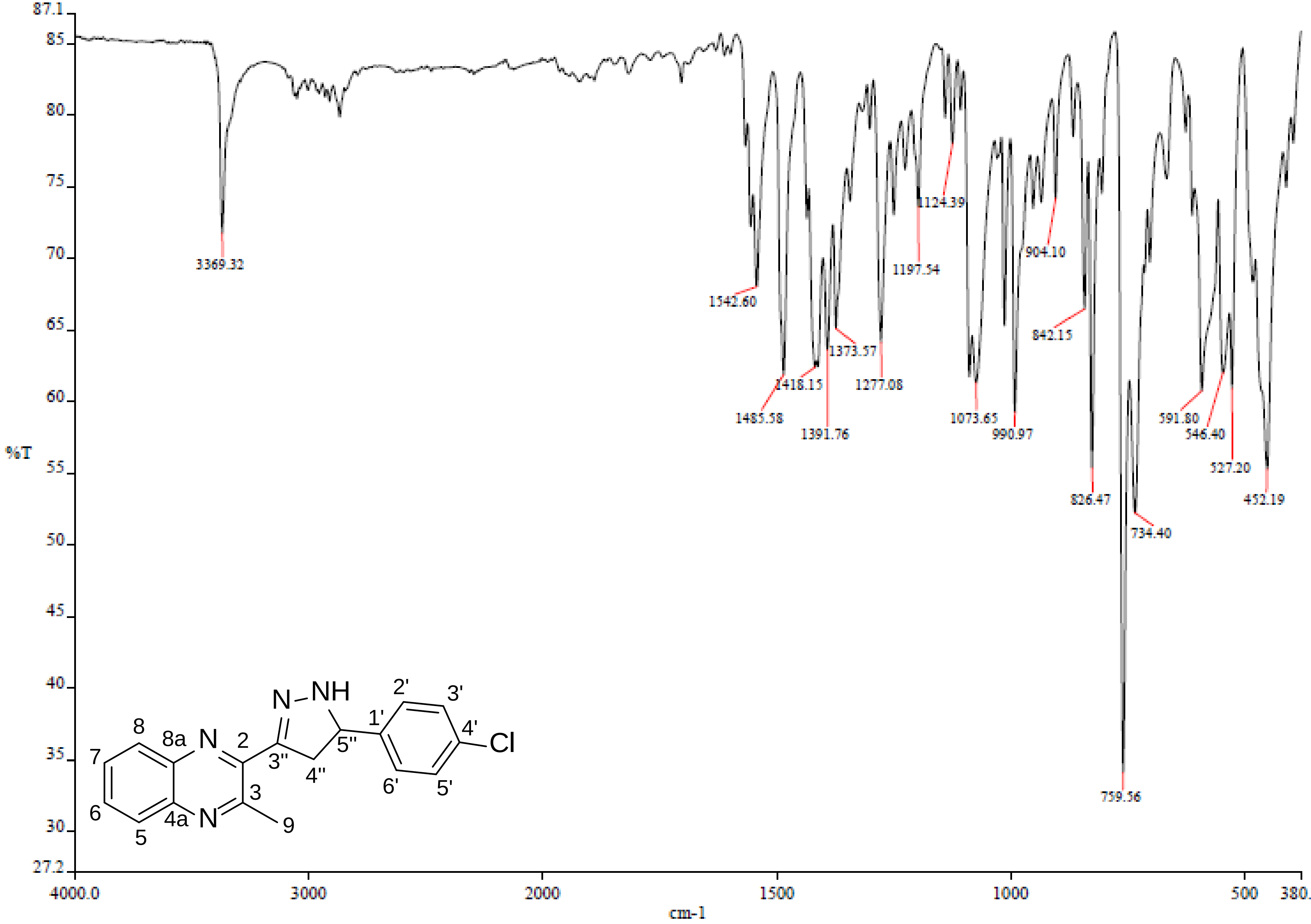

FTIR spectrum of **B11f**

Overlay Spectrum Graph Report

06/10/2017 11:52:43 AM

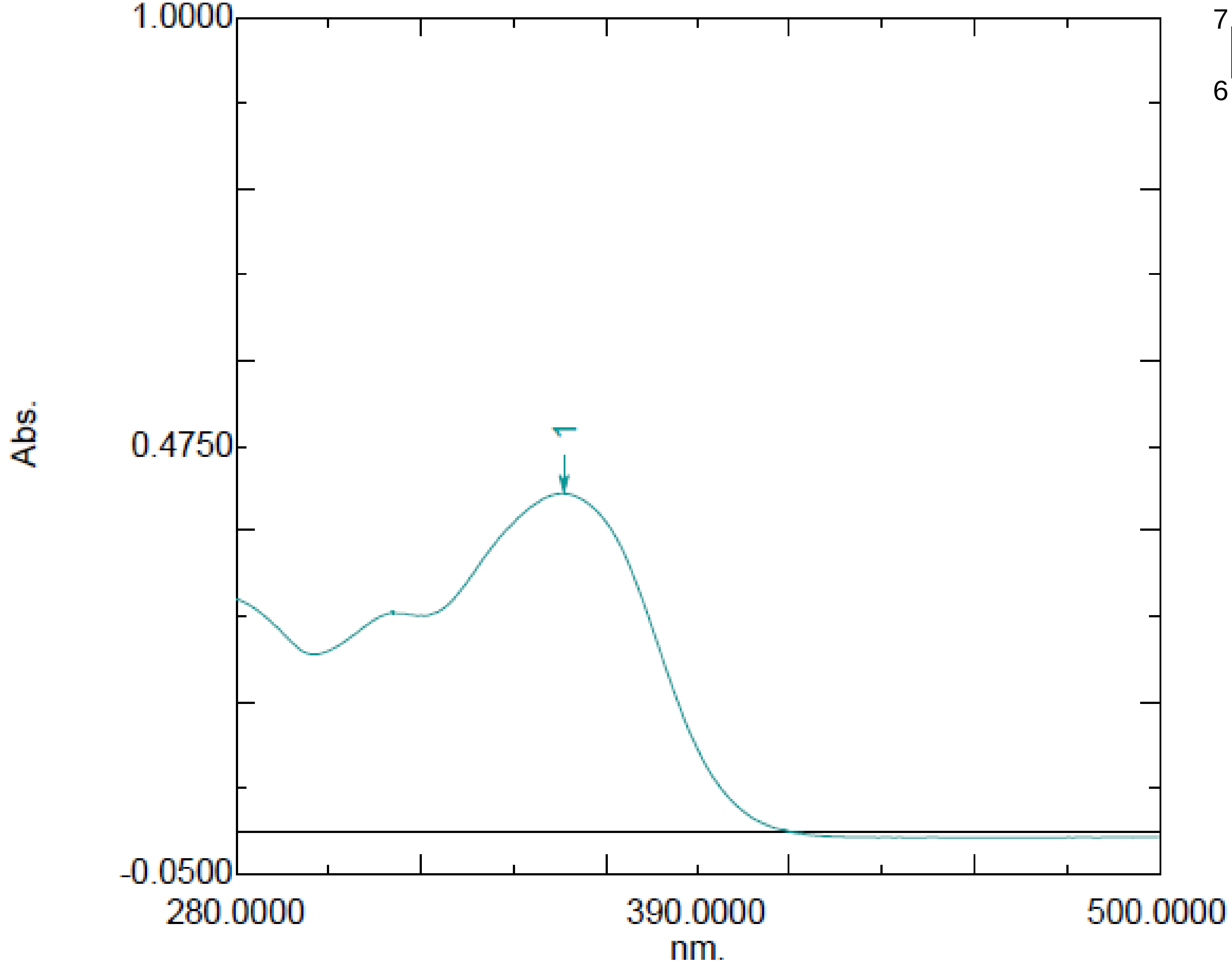

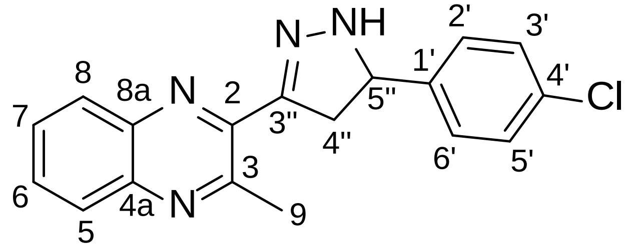

λ	absorbance	logε
358	0.4164	4.43

UV spectrum of **B11f**

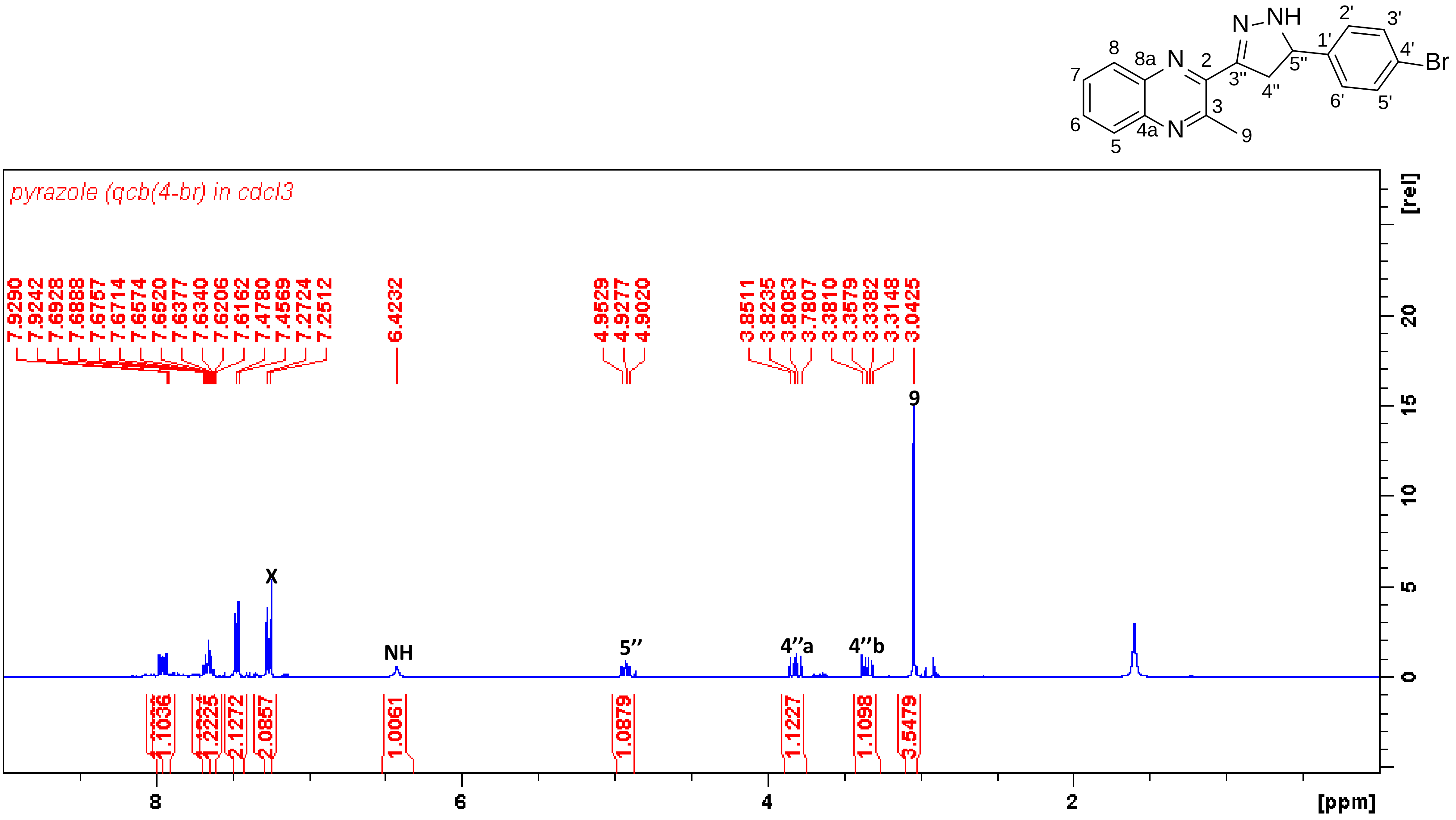

^{1}H NMR spectrum of **B11g**

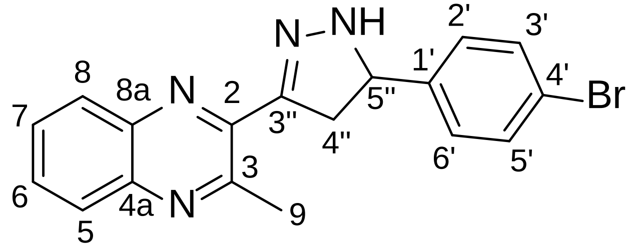

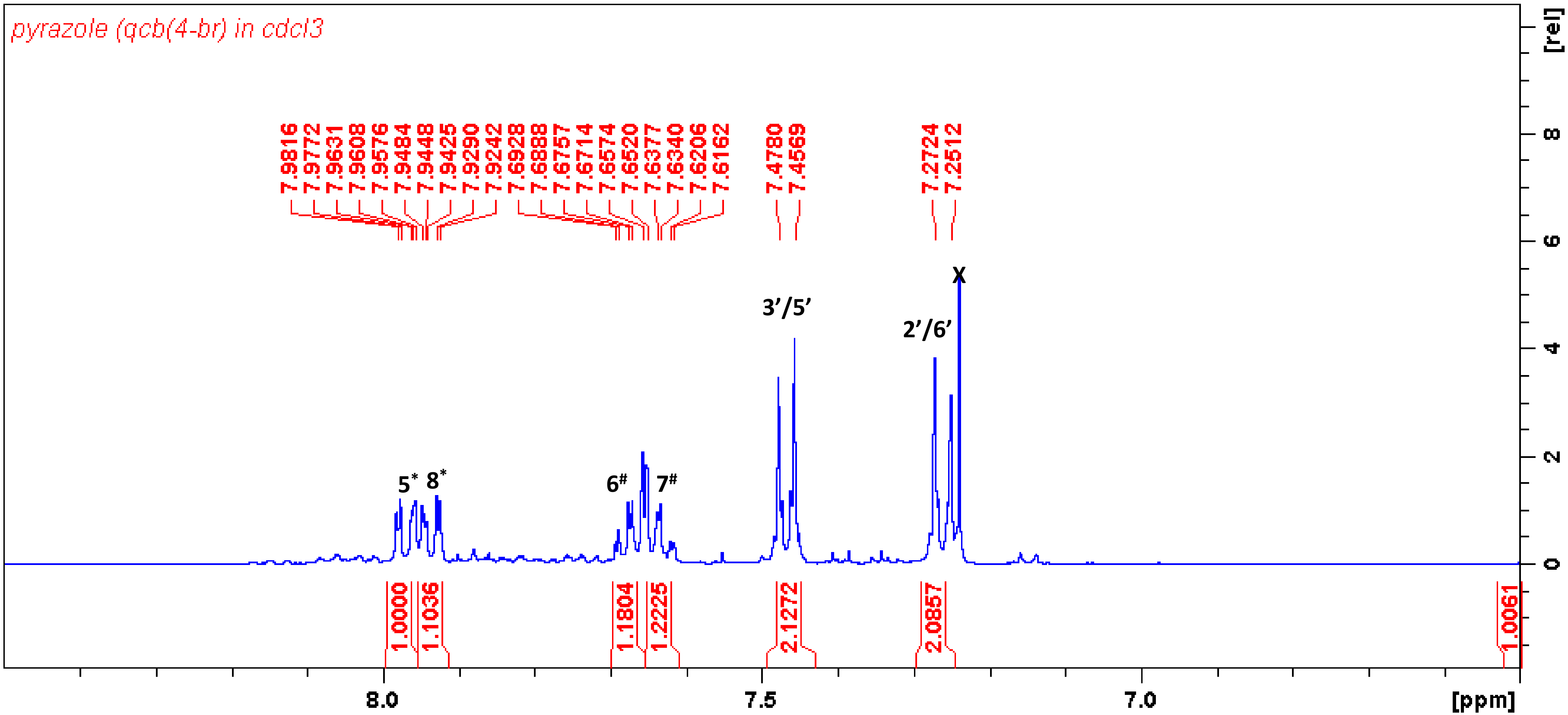

*, # Indicates assignments are interchangeable

Expanded ^{1}H NMR spectrum of **B11g**

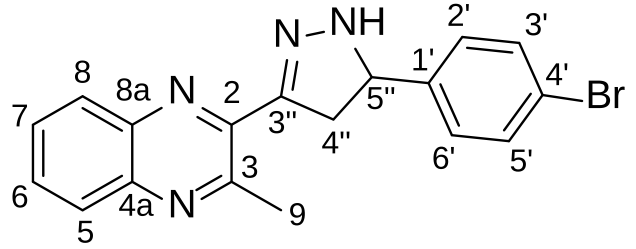

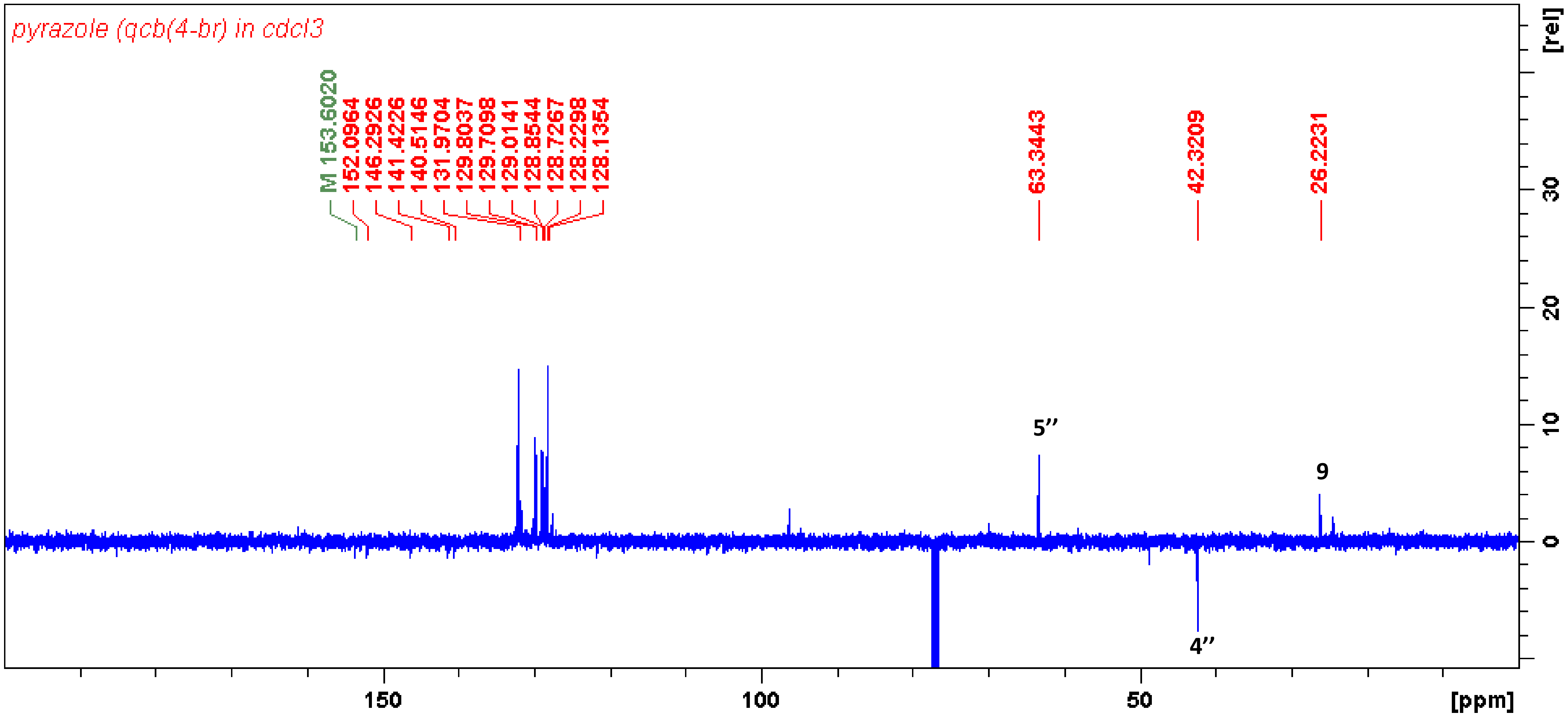

^{13}C NMR spectrum of **B11g**

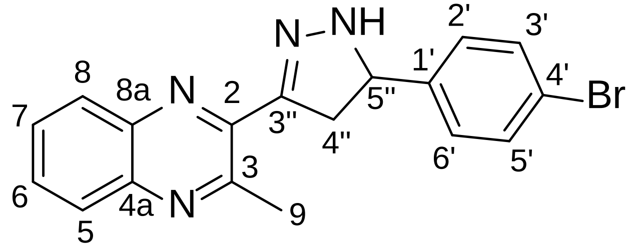

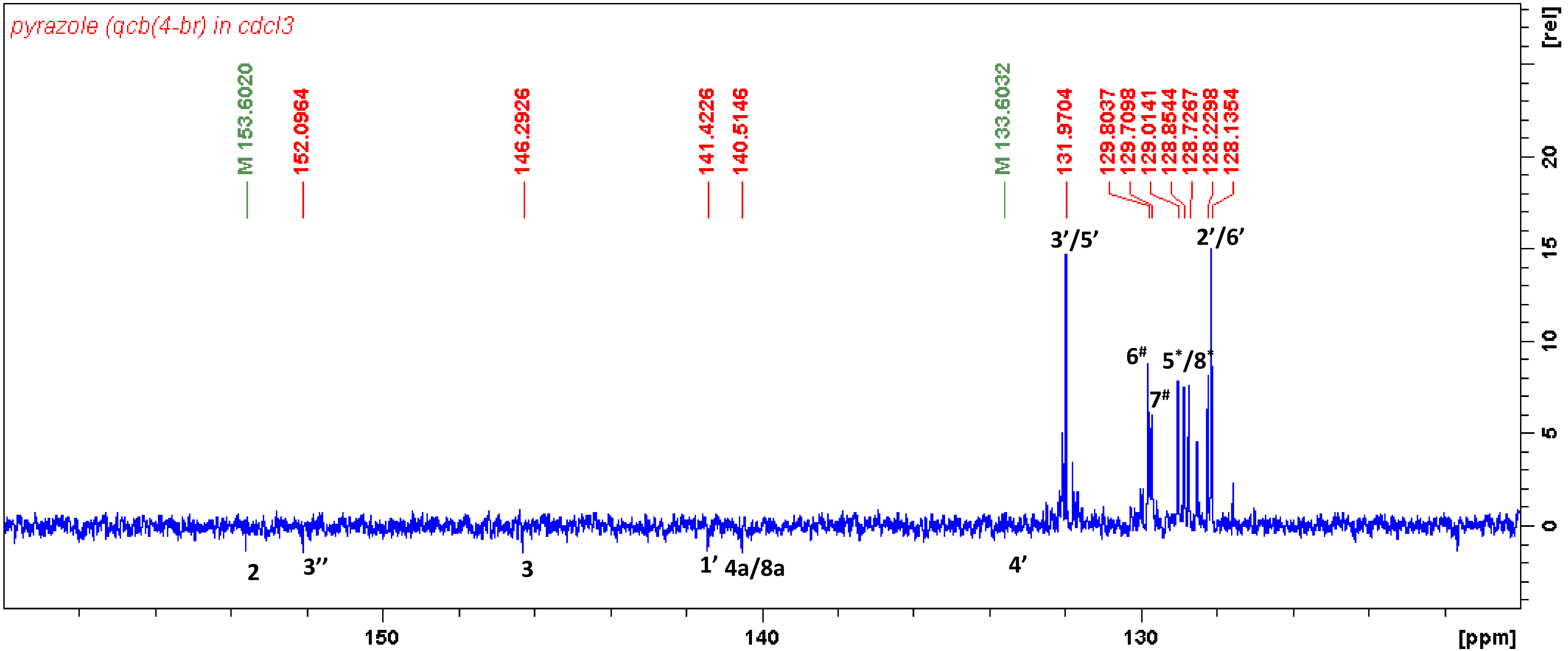

*, #, $ Indicates assignments are interchangeable

Expanded ^{13}C NMR spectrum of **B11g**

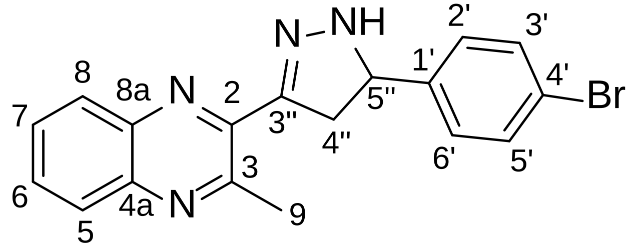

N
NH
2'
3'
8
8a
N
2
1'
4'
Br
7
3''
5''
4''
3
6'
5'
6
4a
N
9
5

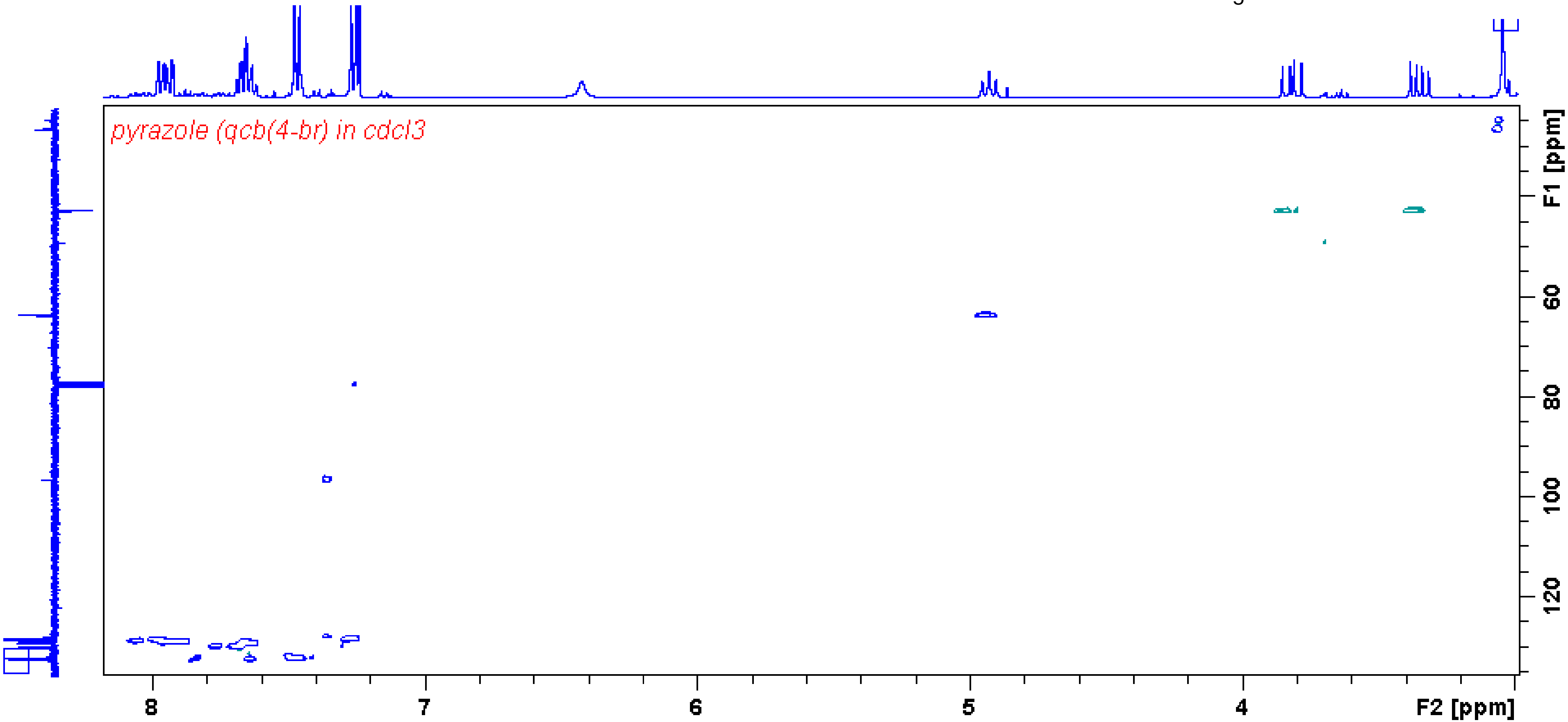

pyrazole (qcb(4-br) in cdcl3
F1 [ppm]
60
80
100
120
8
7
6
5
4
F2 [ppm]

HSQC of **B11g**

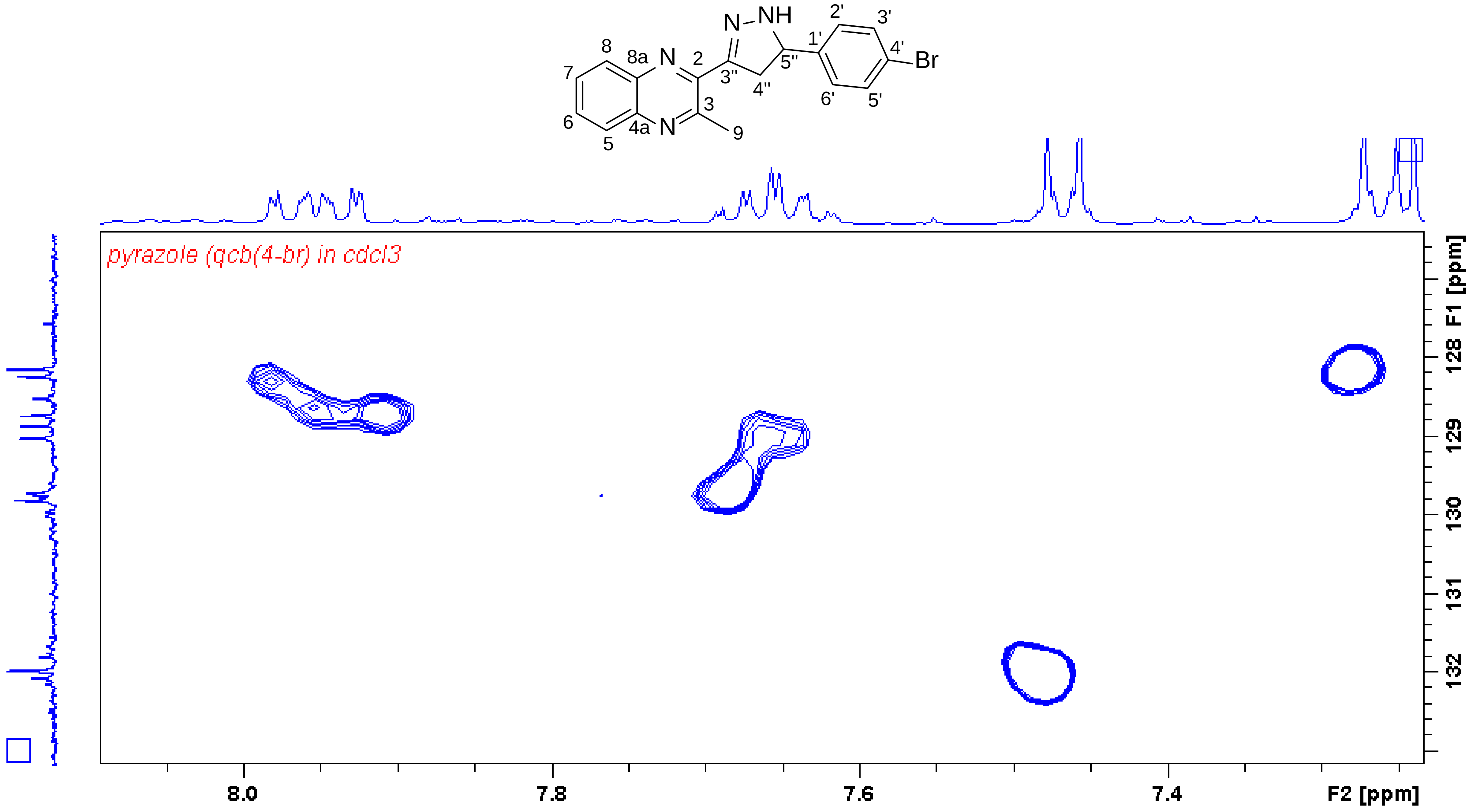

Expanded HSQC of **B11g**

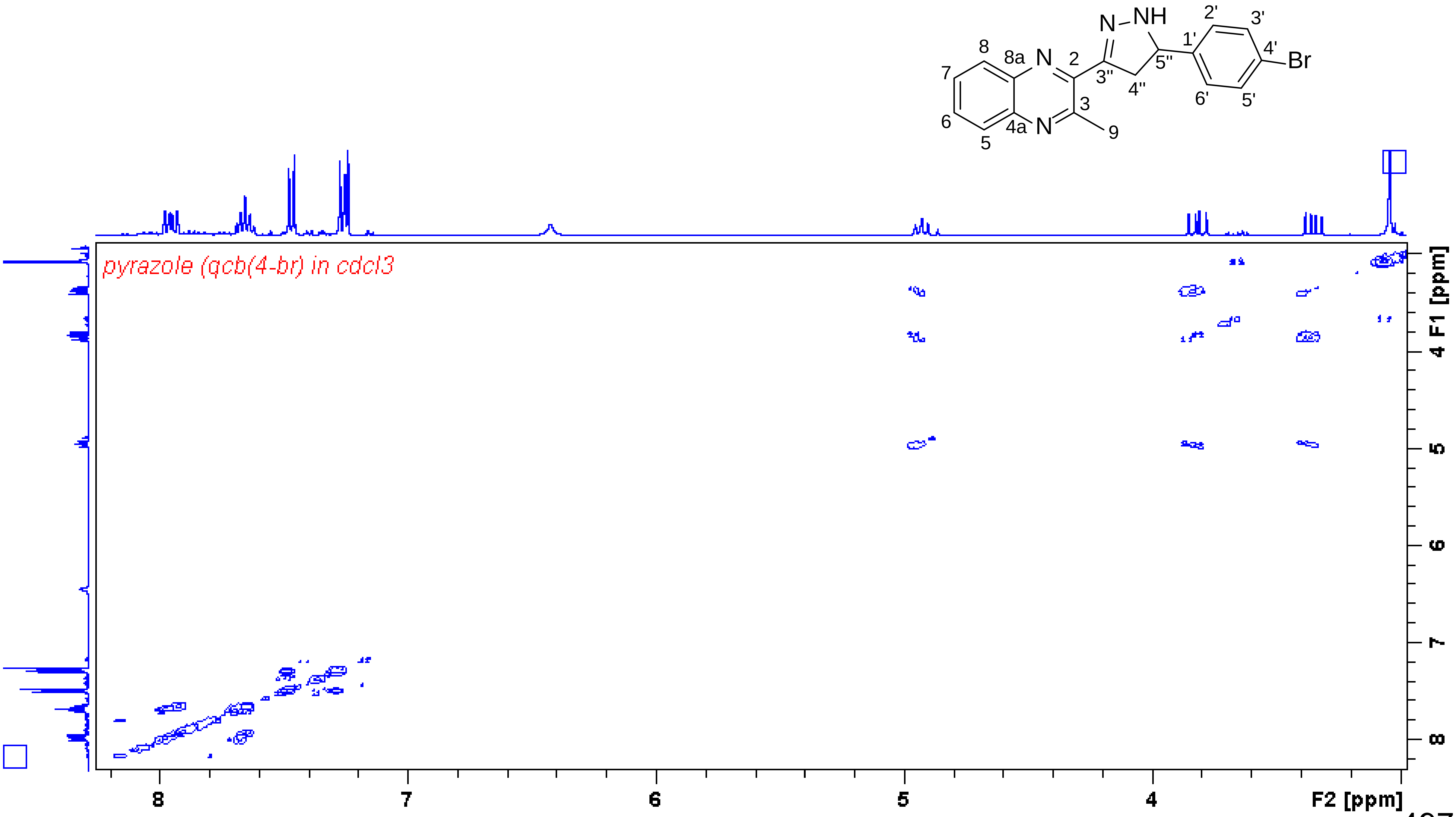
pyrazole (qcb(4-br) in cdcl3
F1 [ppm]
F2 [ppm]
N
NH
N
N
Br
2
3
8
8a
7
6
5
4a
3''
4''
5''
1'
2'
3'
4'
5'
6'
9

COSY of **B11g**

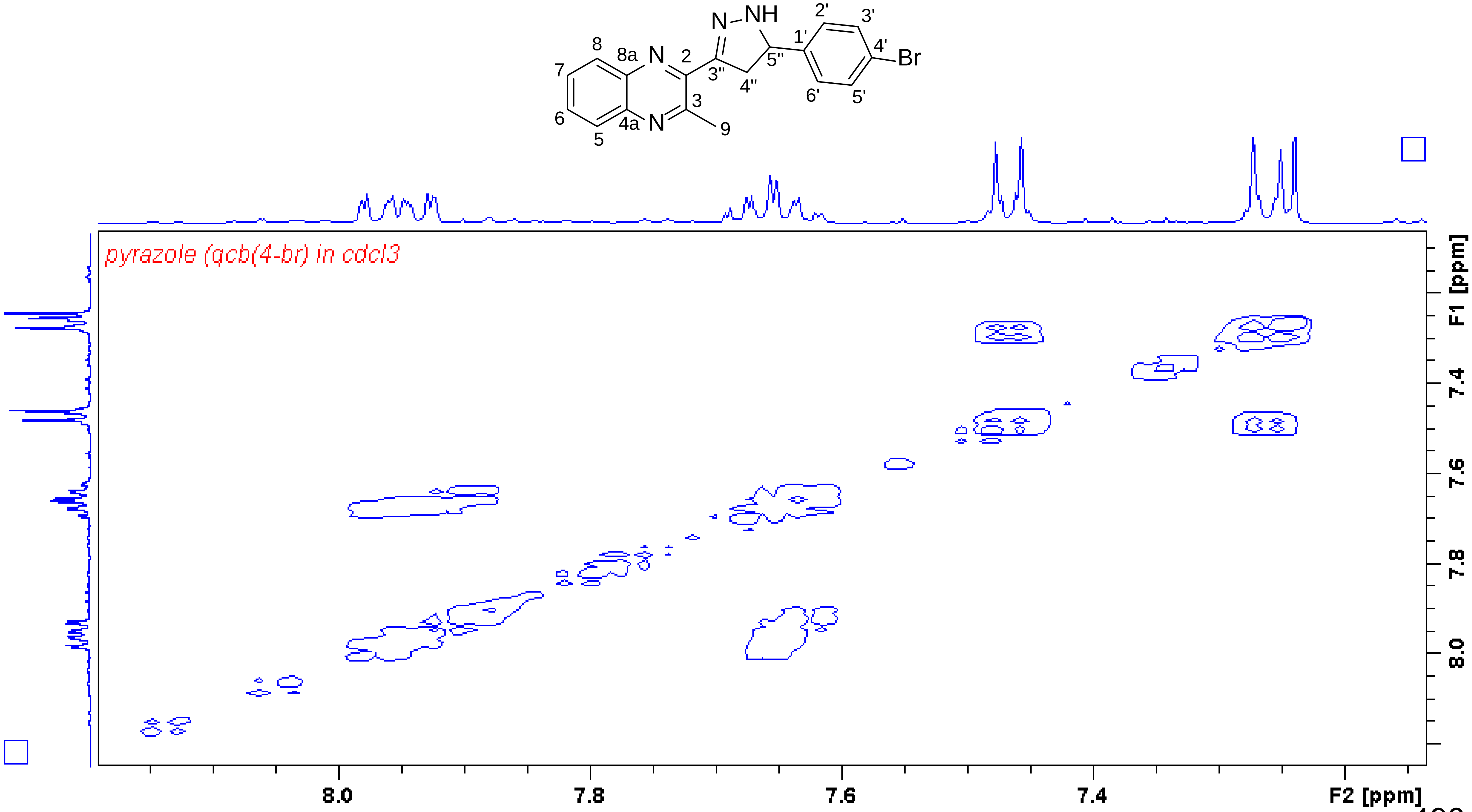

Expanded COSY of **B11g**

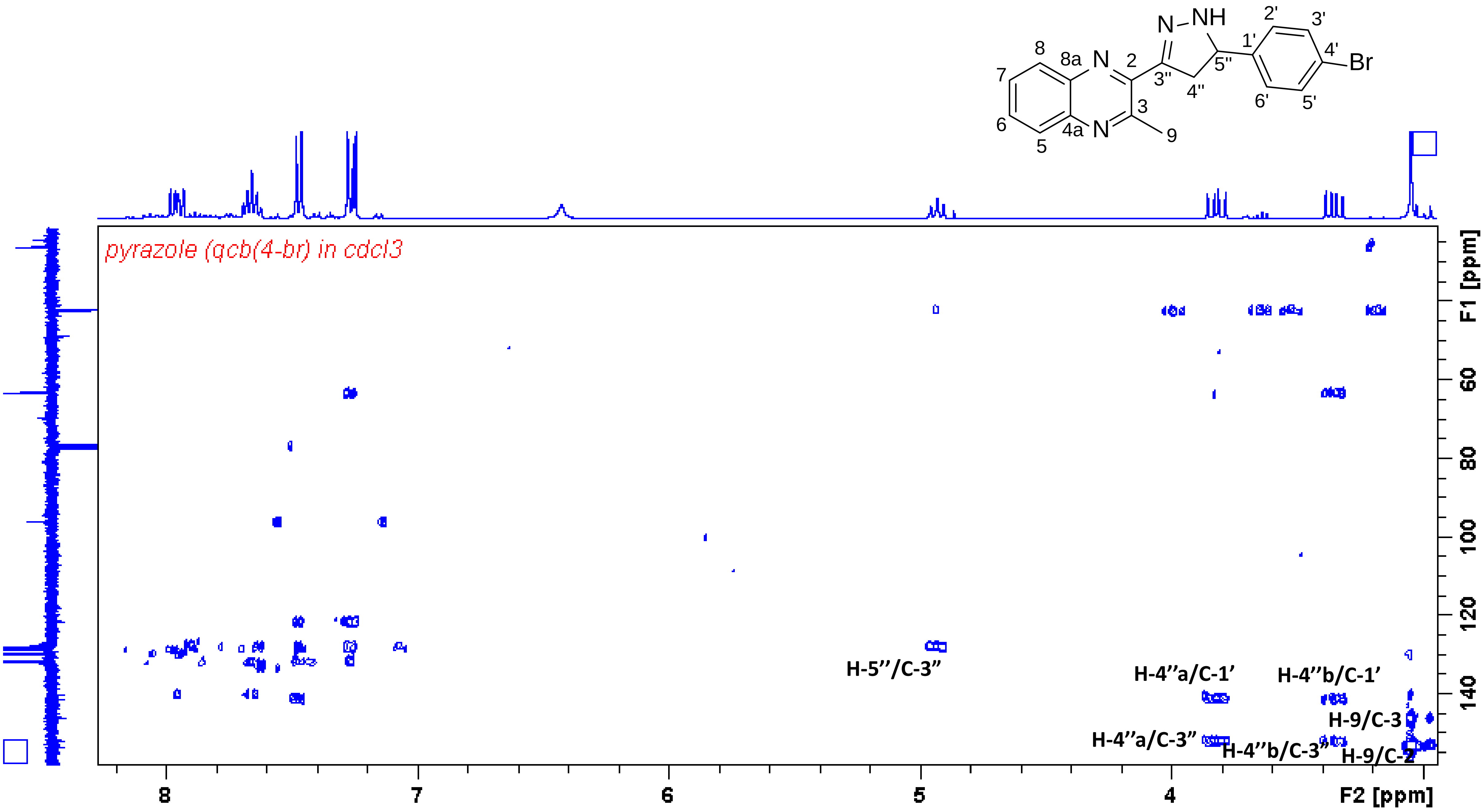

N
NH
2'
3'
8
8a
2
1'
4'
Br
7
3''
5''
4''
6'
5'
3
6
4a
N
9
5
pyrazole (qcb(4-br) in cdcl3
H-5''/C-3''
H-4''a/C-1'
H-4''b/C-1'
H-9/C-3
H-4''a/C-3''
H-4''b/C-3''
H-9/C-2
F1 [ppm]
F2 [ppm]

HMBC of **B11g**

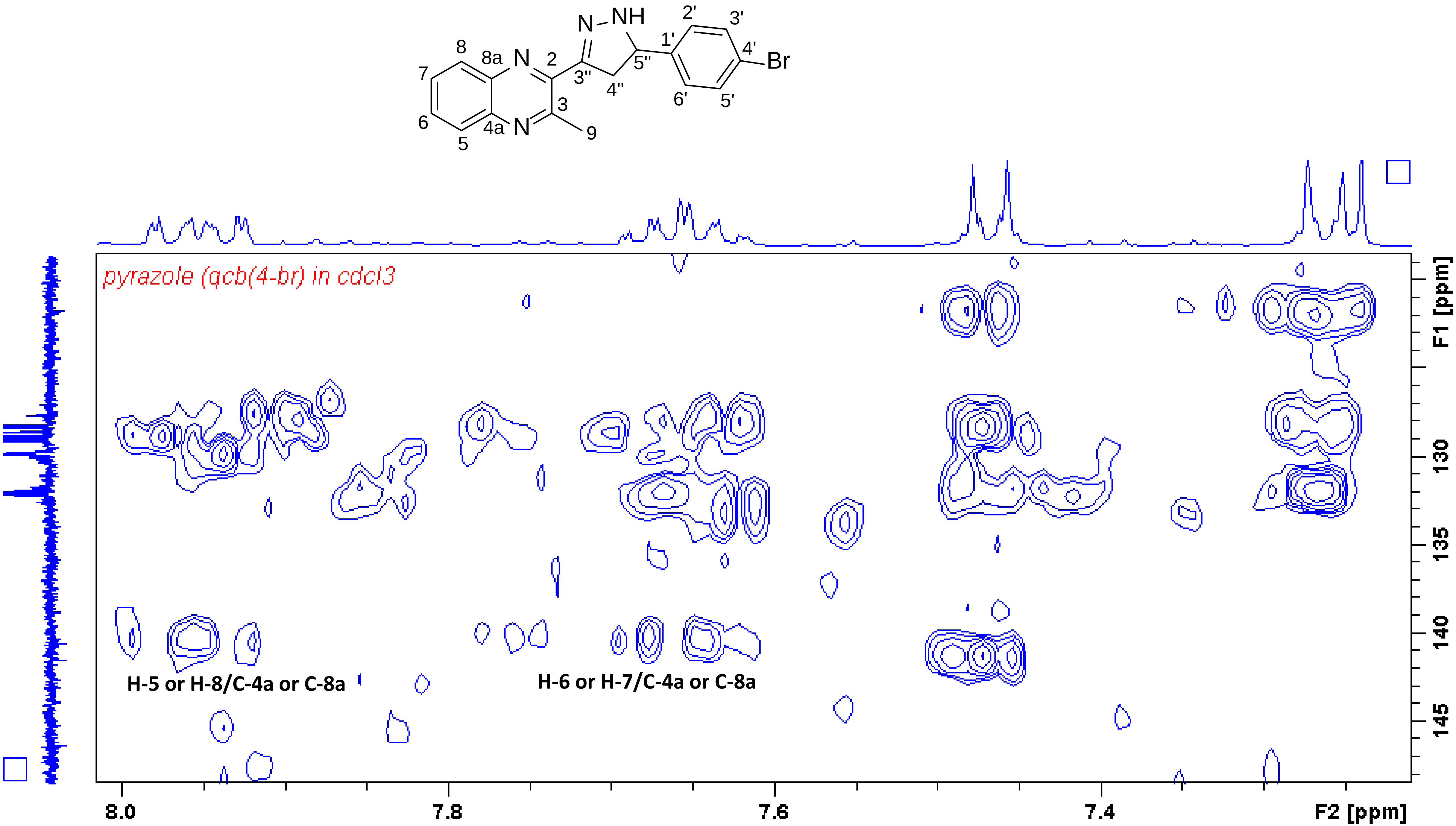

Expanded HMBC of **B11g**

Elemental Composition Report

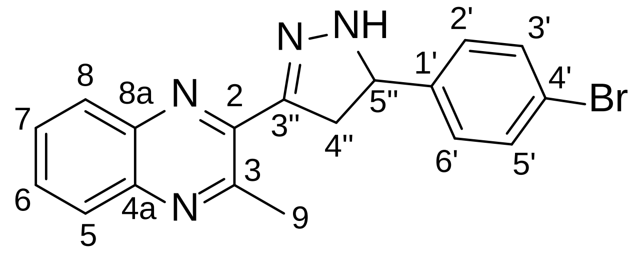

Single Mass Analysis

Tolerance = 5.0 PPM / DBE: min = -1.5, max = 100.0
Element prediction: Off
Number of isotope peaks used for i-FIT = 3

Monoisotopic Mass, Even Electron Ions
15 formula(e) evaluated with 1 results within limits (up to 20 closest results for each mass)
Elements Used:
C: 15-20 H: 15-20 N: 0-5 Na: 0-1 Br: 0-1

Py-QCB 4-Br 45 (1.484) Cm (1:61)
TOF MS ES+

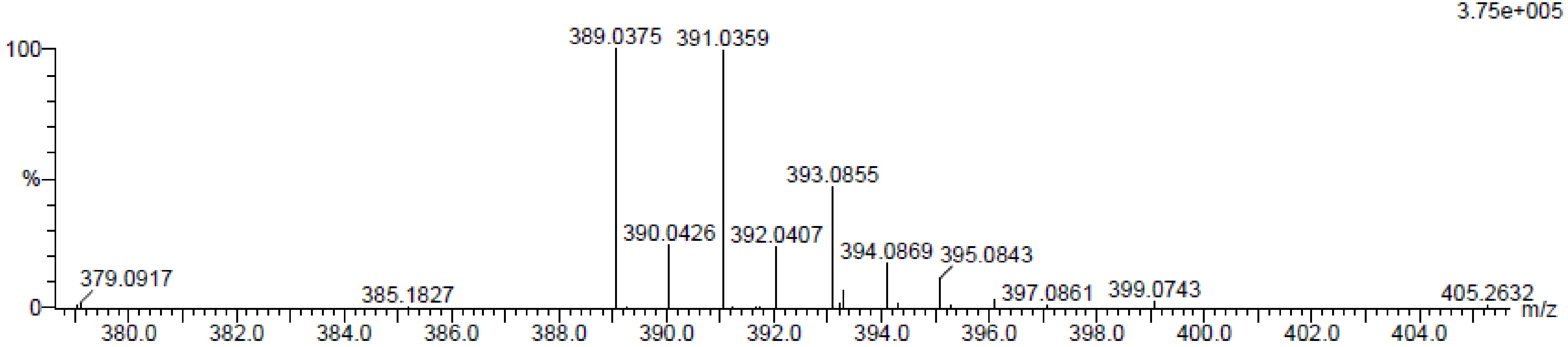

Minimum:				-1.5			
Maximum:		5.0	5.0	100.0			
Mass	Calc. Mass	mDa	PPM	DBE	i-FIT	i-FIT (Norm)	Formula
389.0375	389.0378	-0.3	-0.8	12.5	55.4	0.0	C18 H15 N4 Na Br

High resolution mass spectrum of **B11g**

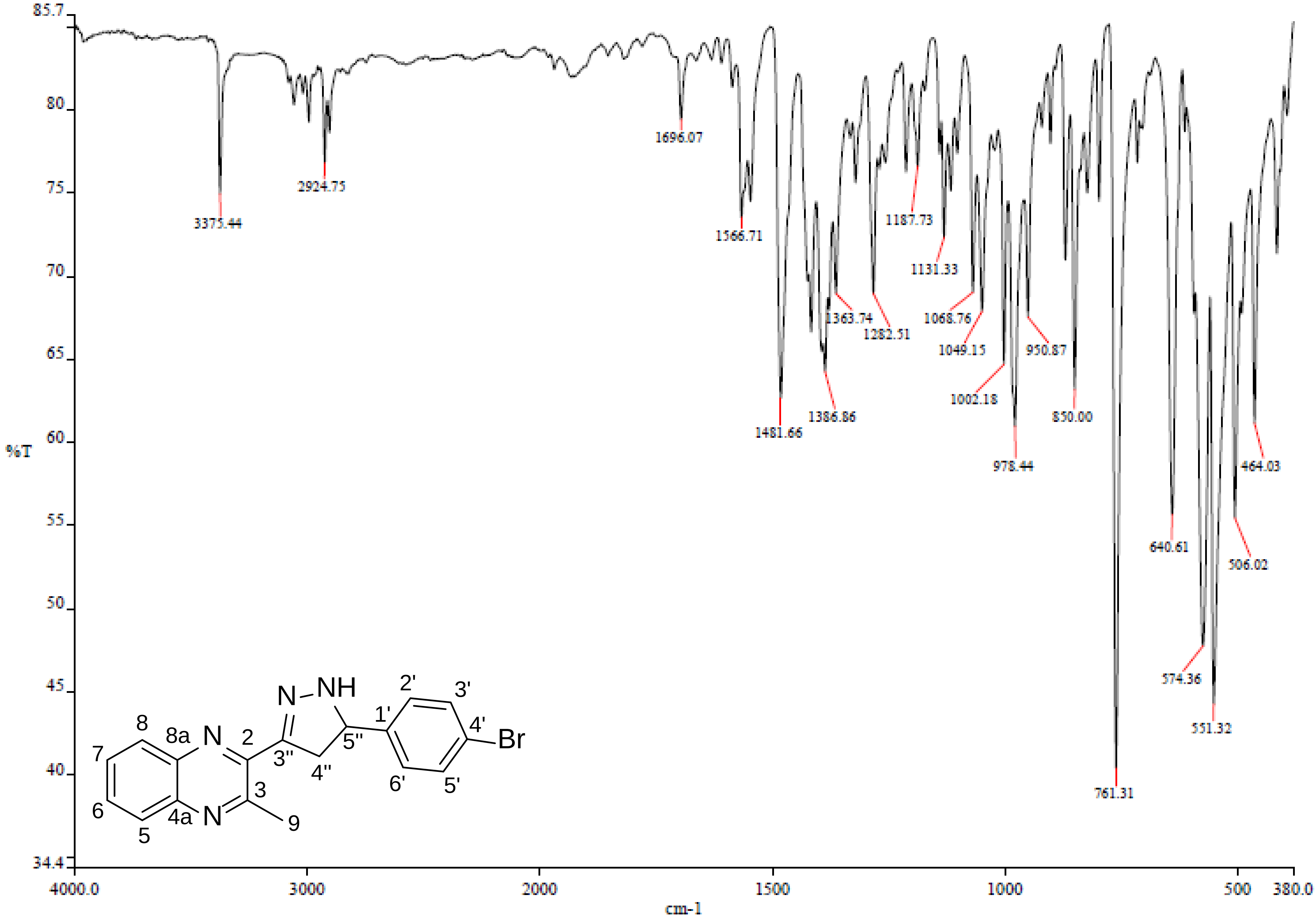

FTIR spectrum of **B11g**

Overlay Spectrum Graph Report

06/10/2017 11:50:56 AM

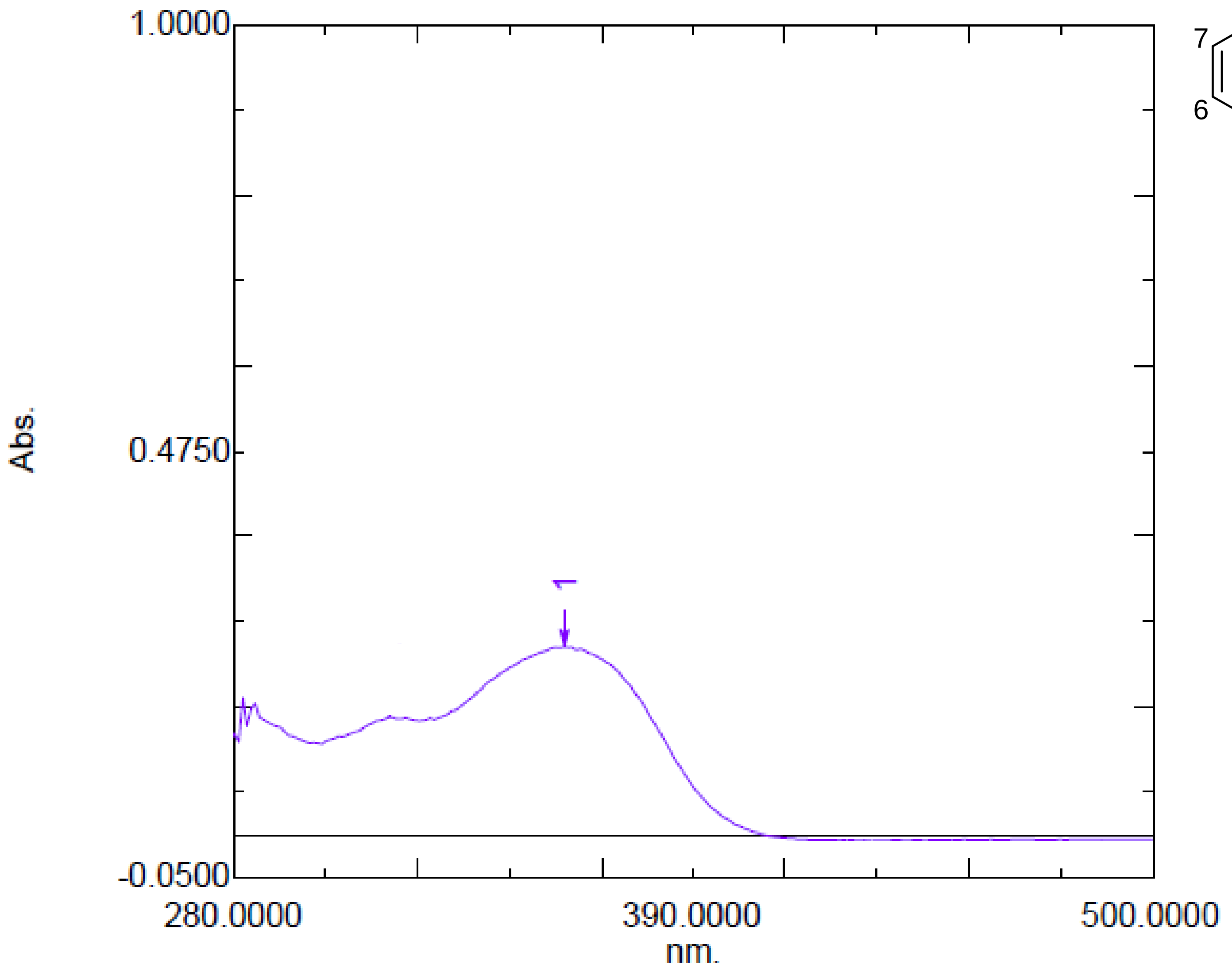

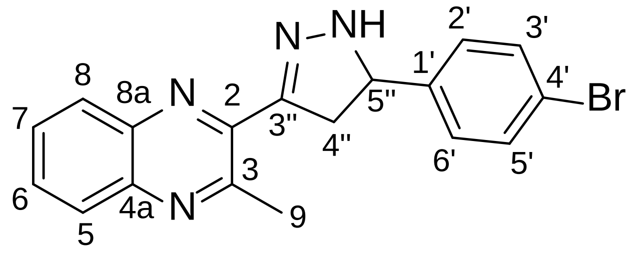

λ	absorbance	logε
359	0.2336	4.23

UV spectrum of **B11g**

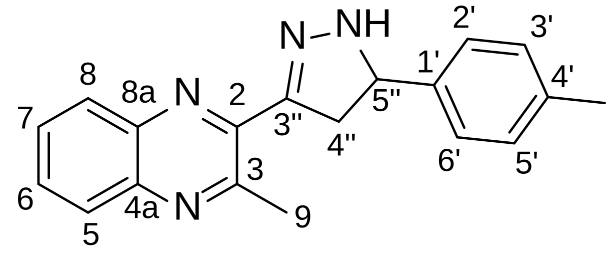

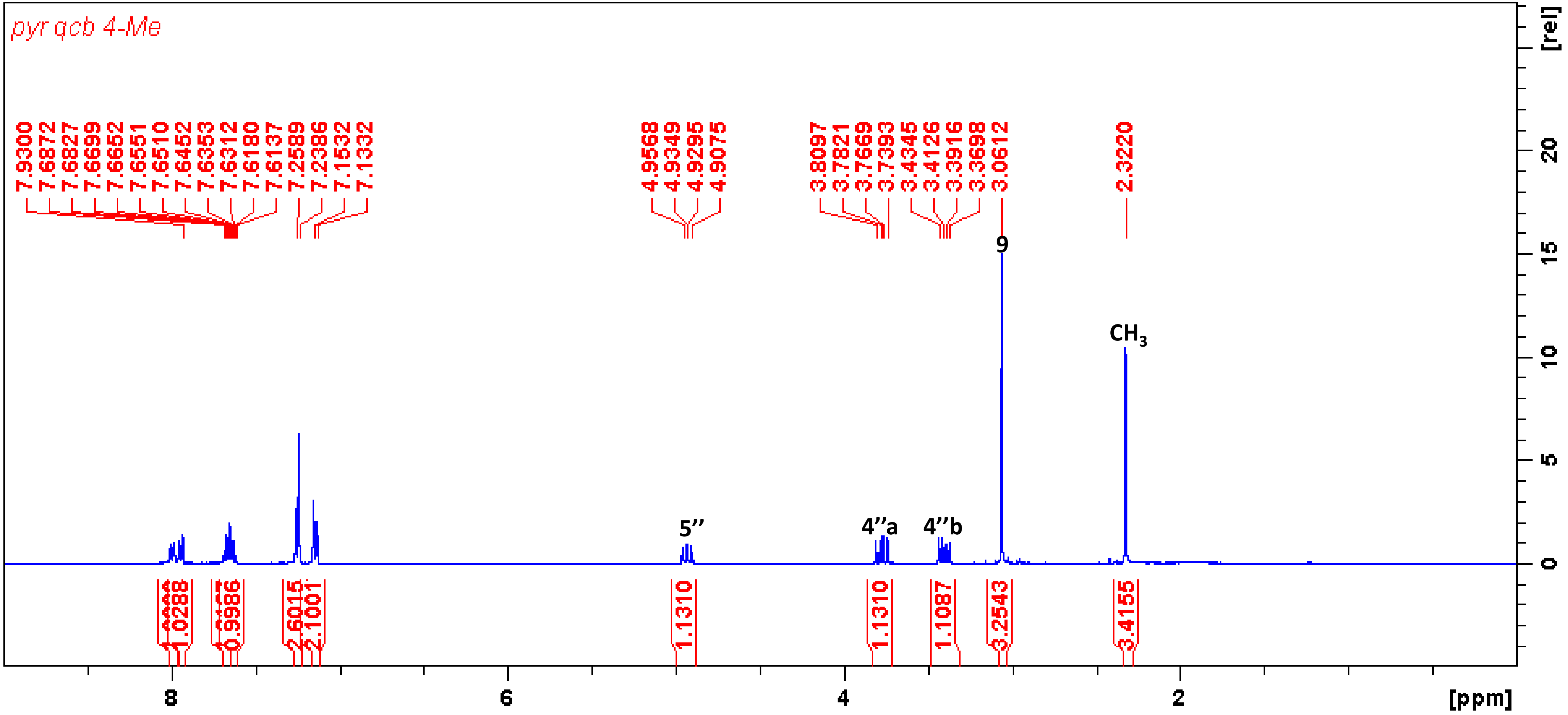

^{1}H NMR spectrum of **B11h**

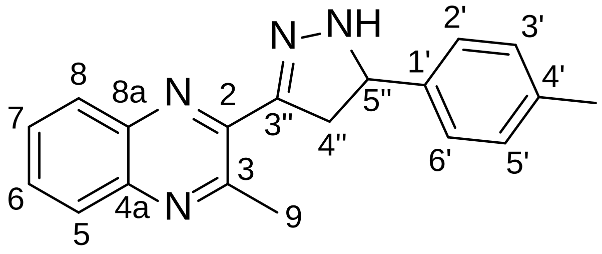

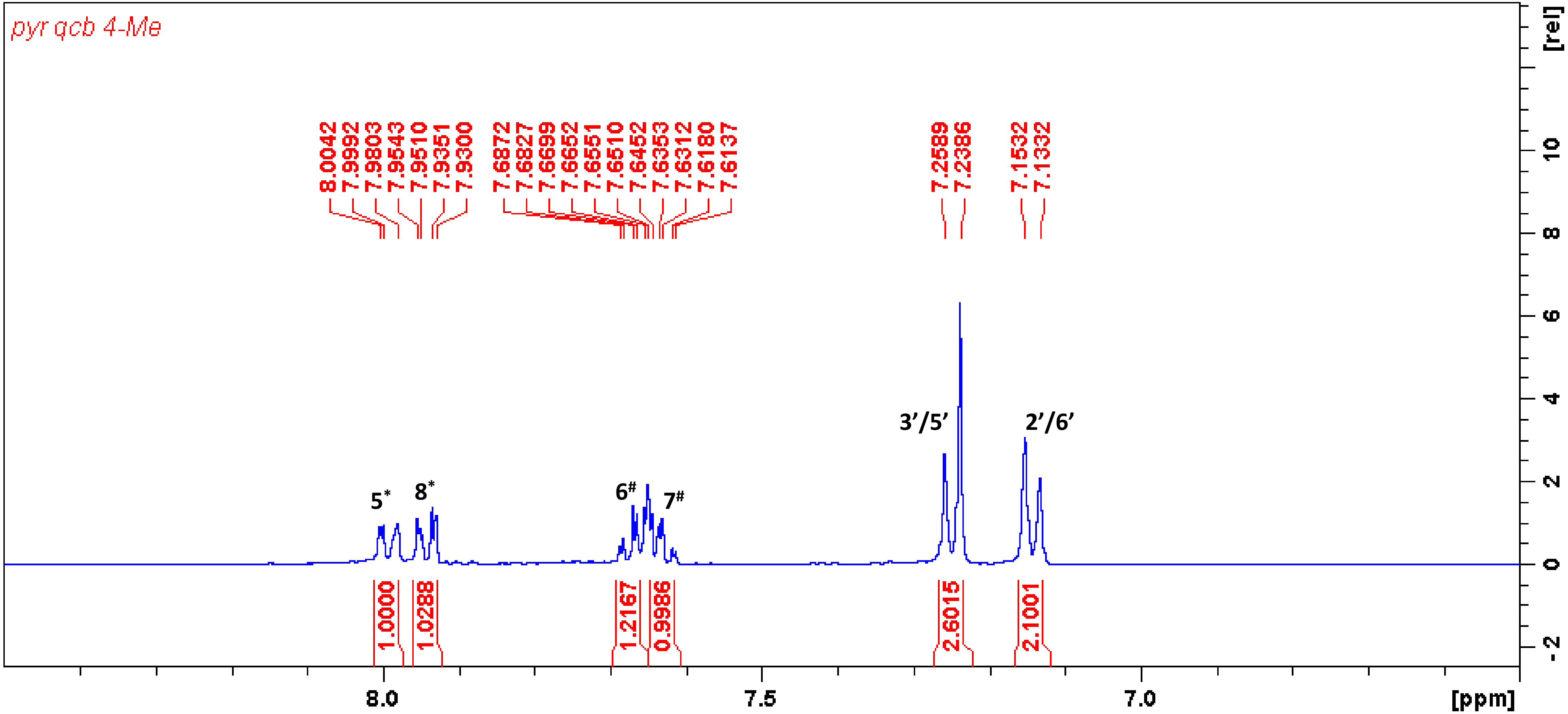

*, # Indicates assignments are interchangeable

Expanded ^{1}H NMR spectrum of **B11h**

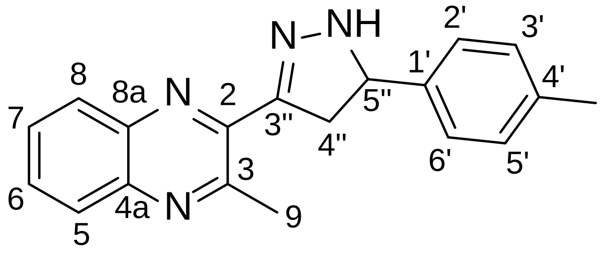

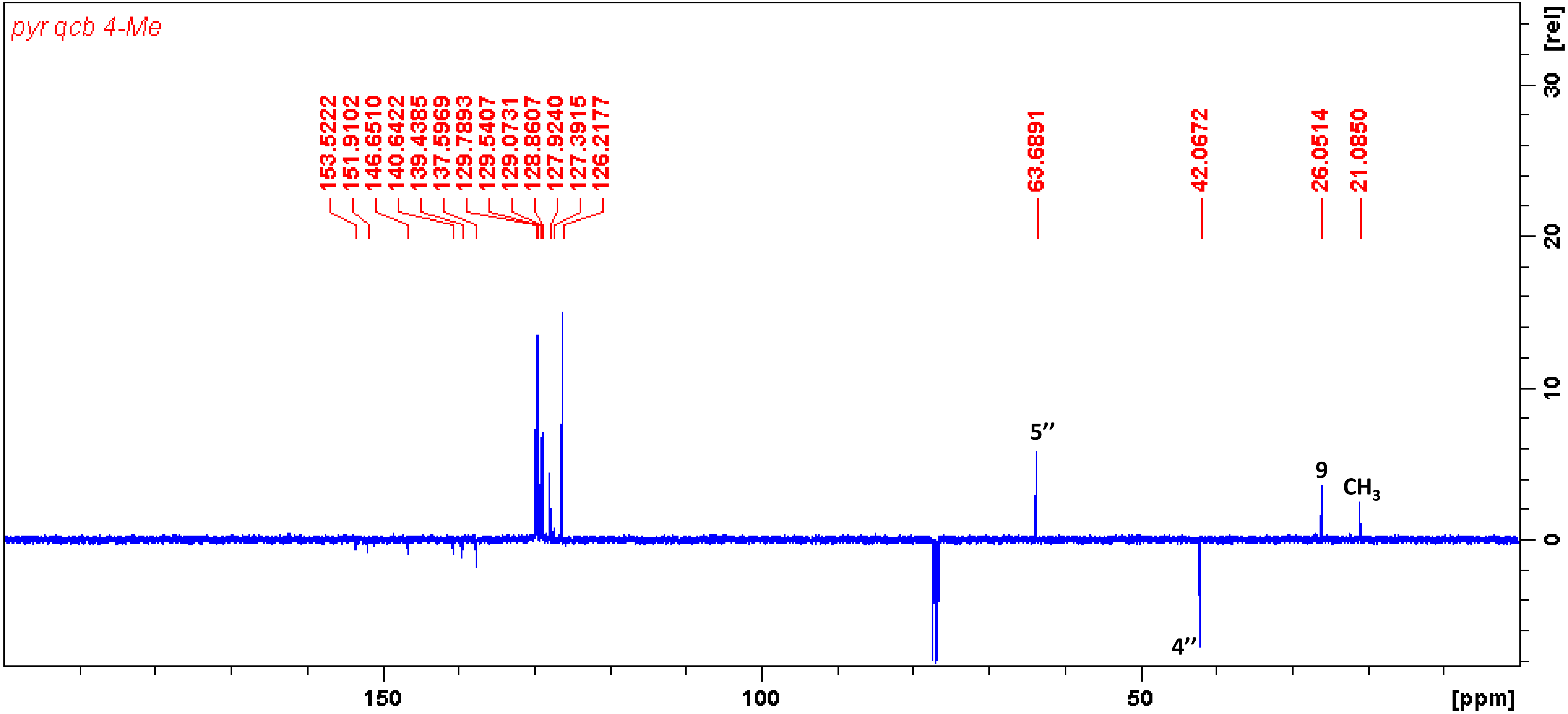

^{13}C NMR spectrum of **B11h**

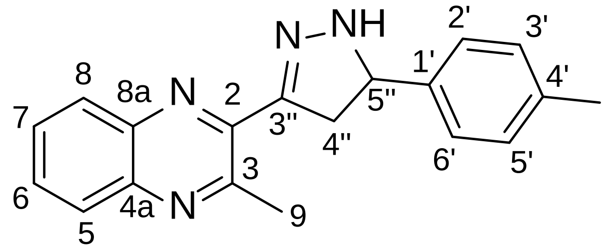

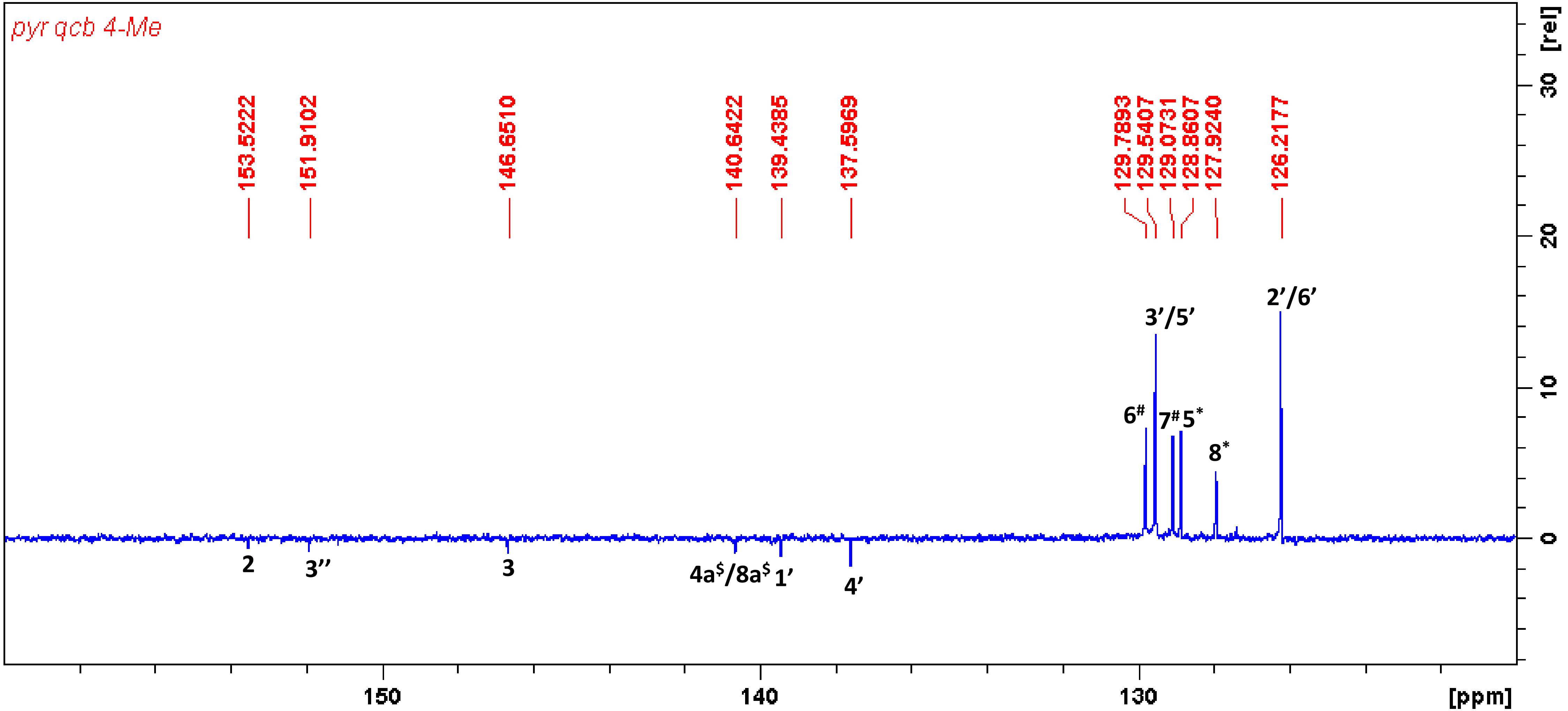

*, #, $ Indicates assignments are interchangeable

Expanded ^{13}C NMR spectrum of **B11h**

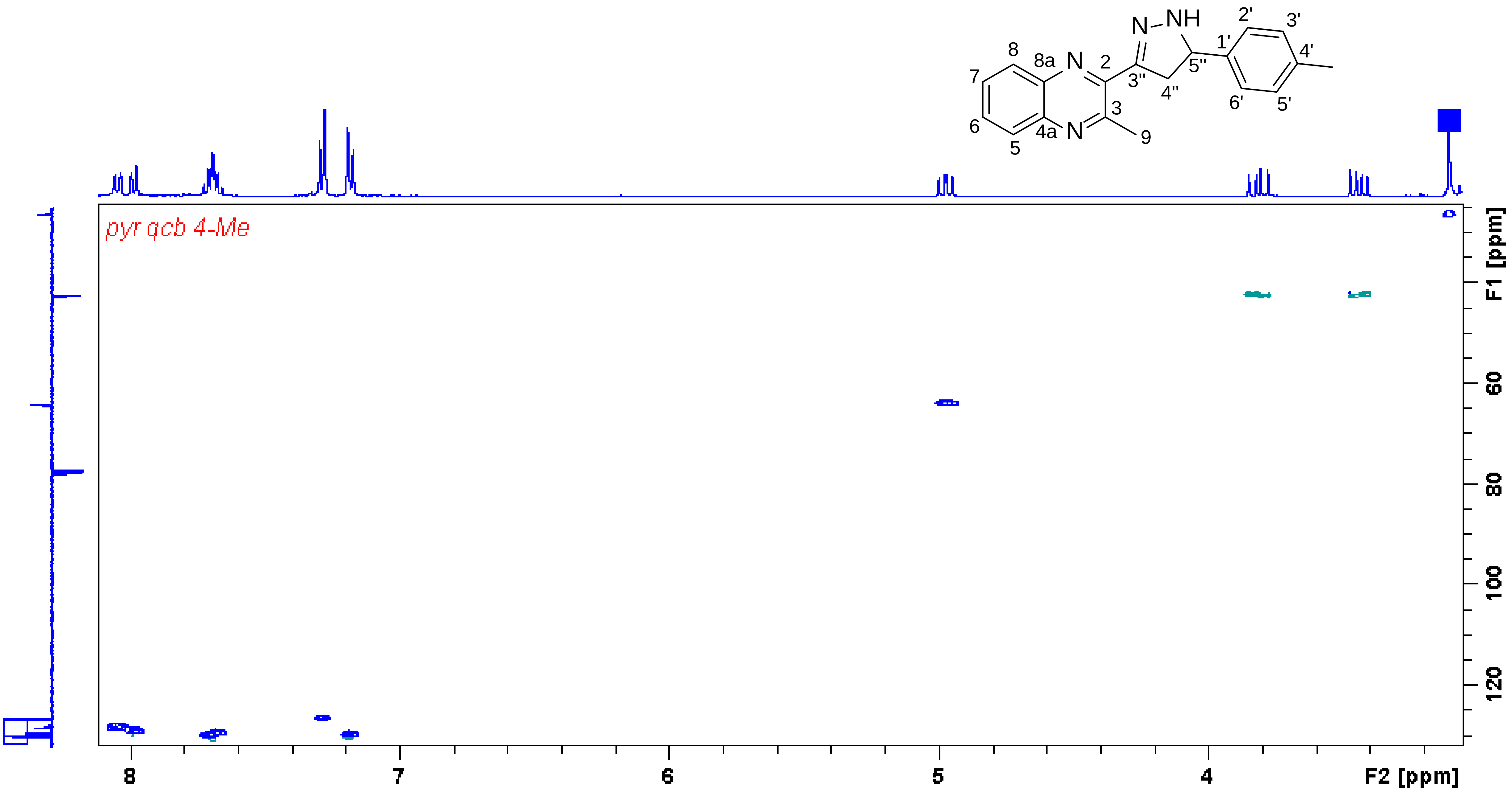
pyr qcb 4-Me
F1 [ppm]
60
80
100
120
8
7
6
5
4
F2 [ppm]
N
NH
2'
3'
1'
4'
8
8a
N
2
3''
5''
7
4''
6'
5'
3
6
4a
N
9
5

HSQC of **B11h**

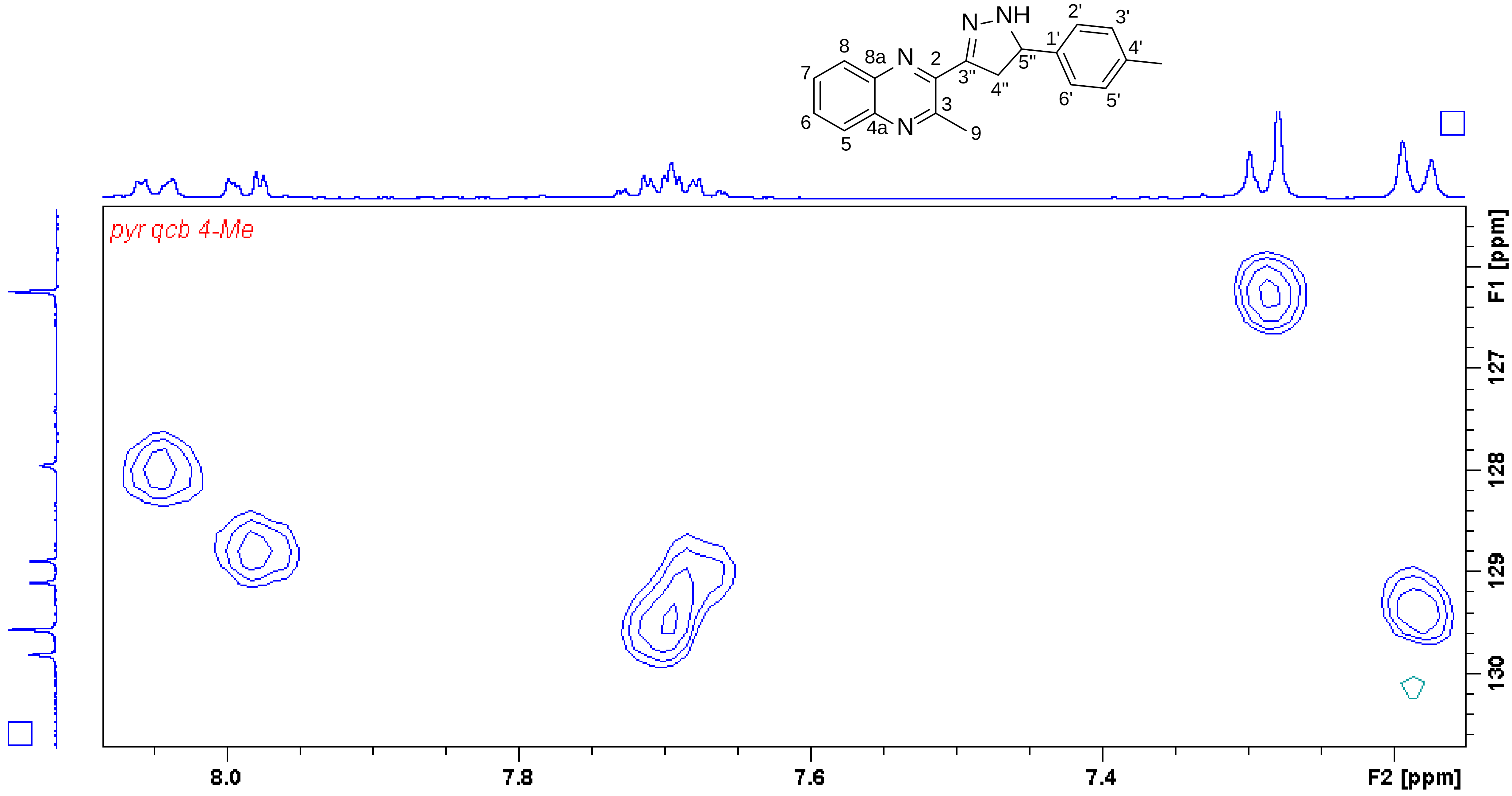

Expanded HSQC of **B11h**

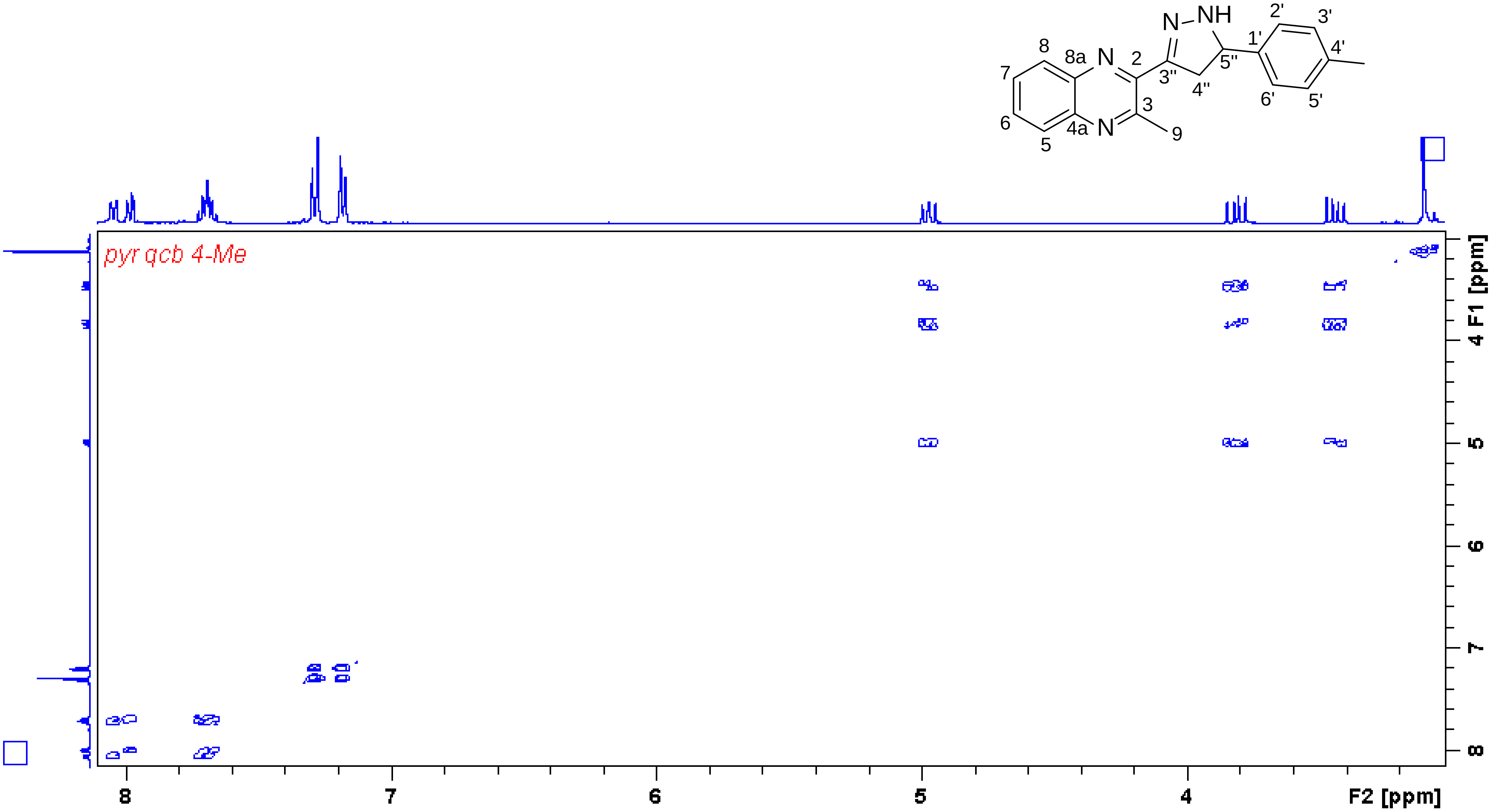

COSY of **B11h**

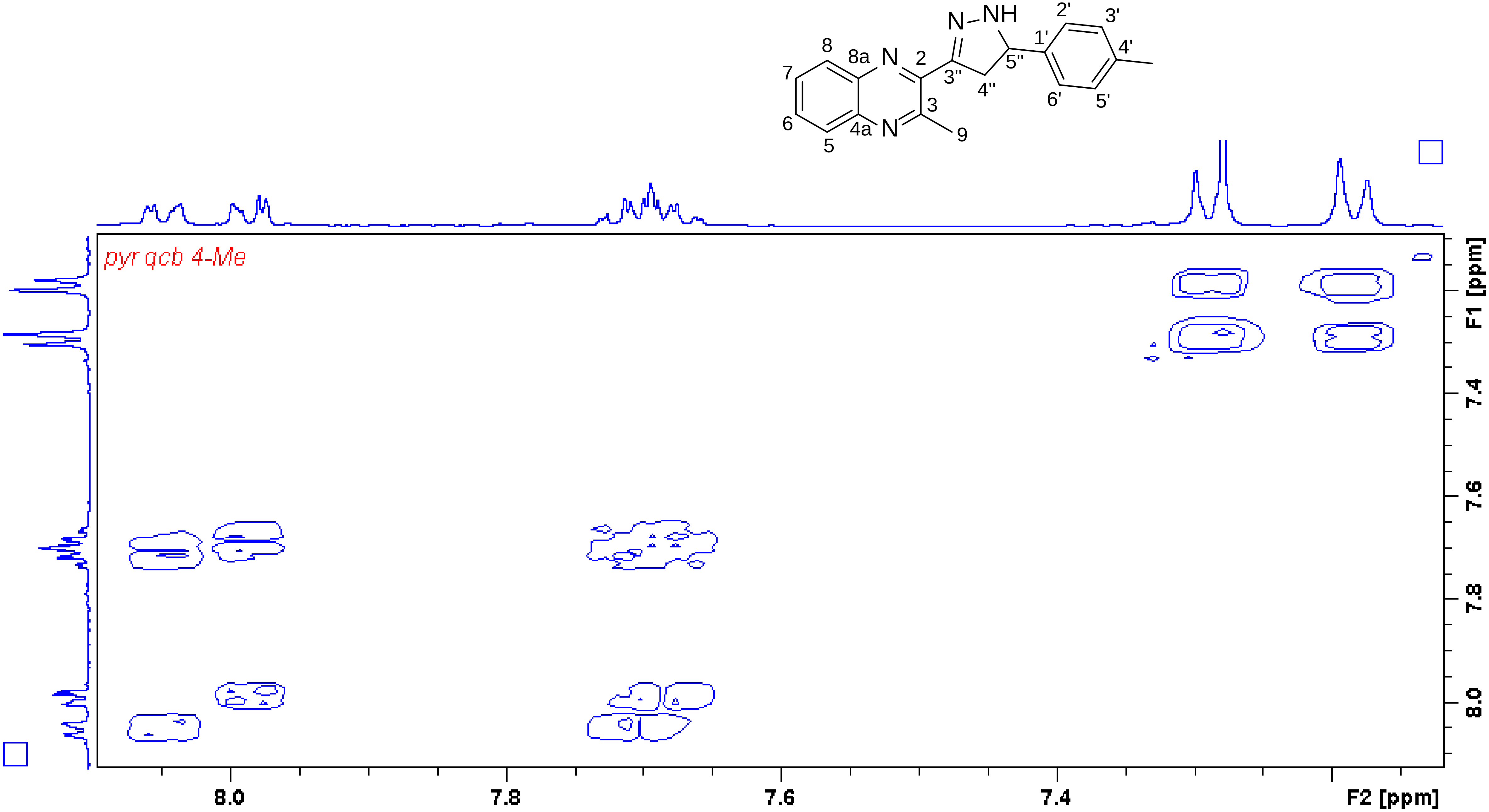

Expanded COSY of **B11h**

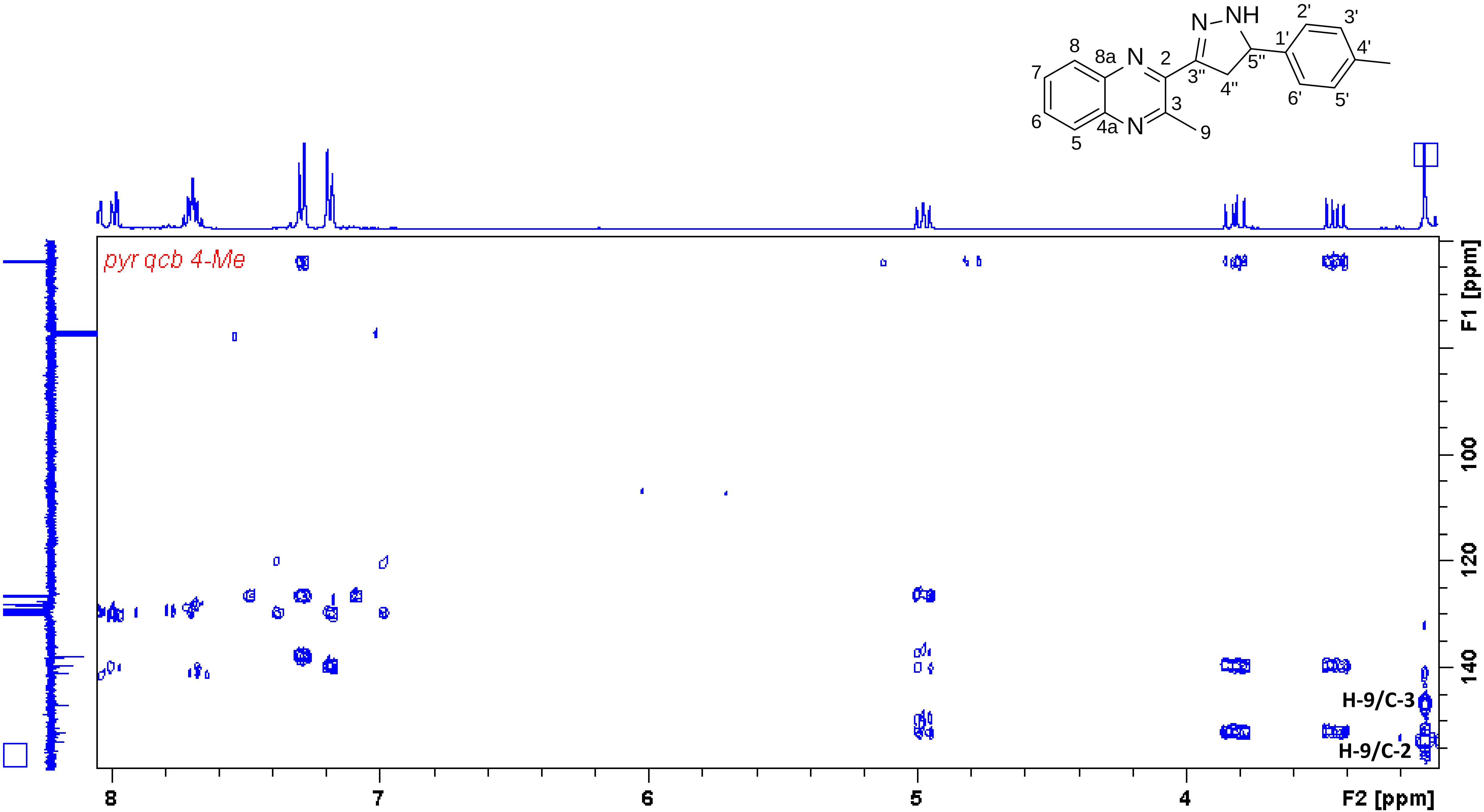

HMBC of **B11h**

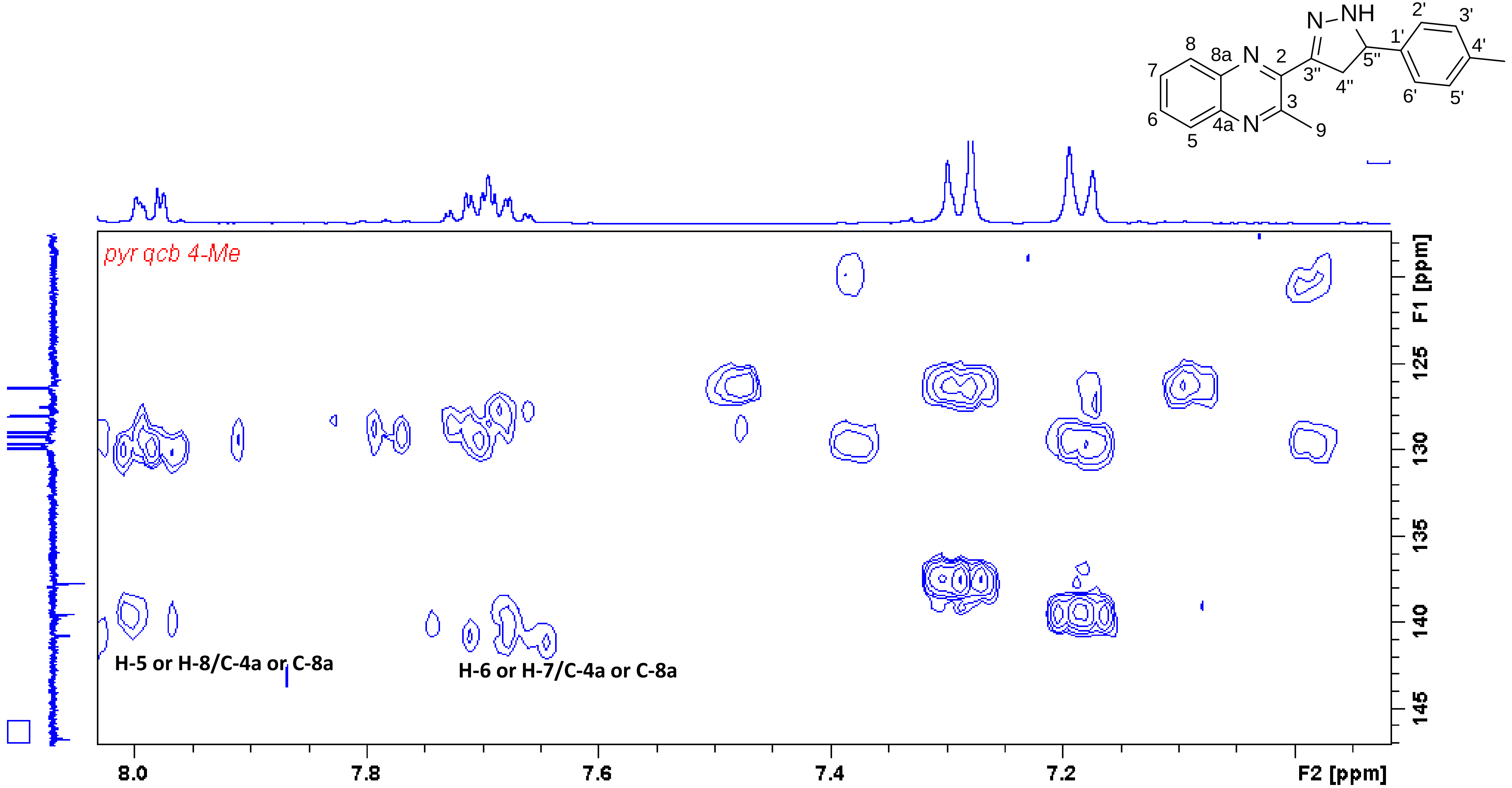

Expanded HMBC of **B11h**

Elemental Composition Report

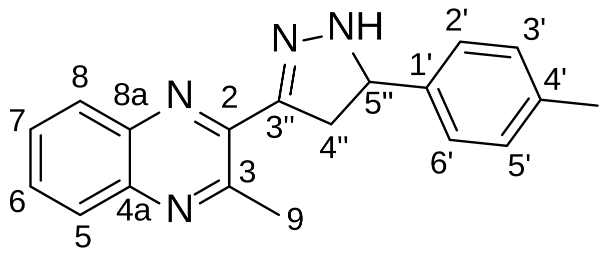

Single Mass Analysis

Tolerance = 5.0 PPM / DBE: min = -1.5, max = 100.0
Element prediction: Off
Number of isotope peaks used for i-FIT = 3

Monoisotopic Mass, Even Electron Ions
6 formula(e) evaluated with 1 results within limits (up to 20 closest results for each mass)
Elements Used:
C: 15-20 H: 15-20 N: 0-5 Na: 0-1
Py-QCB 4-Me 2 (0.034)
TOF MS ES+

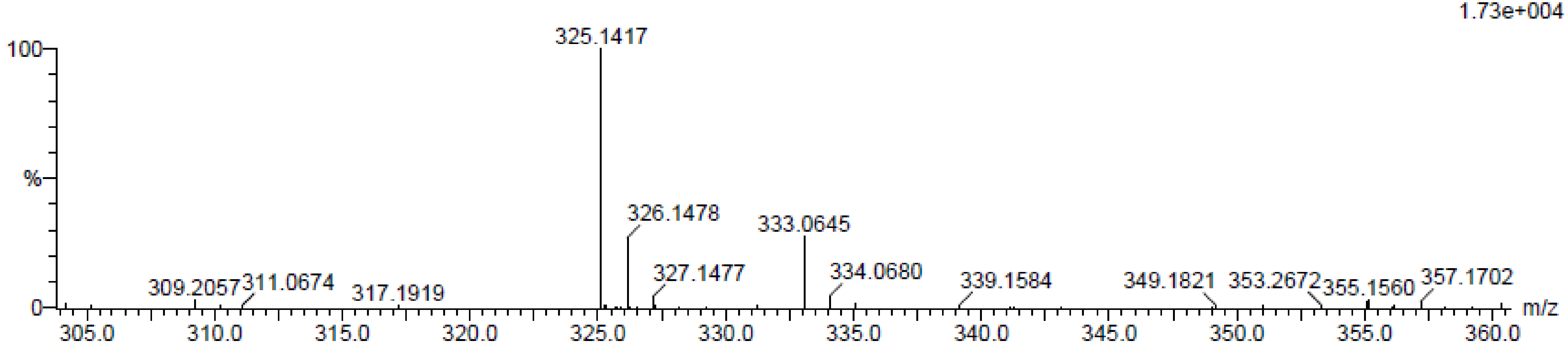

Minimum:				-1.5			
Maximum:		5.0	5.0	100.0			
Mass	Calc. Mass	mDa	PPM	DBE	i-FIT	i-FIT (Norm)	Formula
325.1417	325.1429	-1.2	-3.7	12.5	89.3	0.0	C19 H18 N4 Na

High resolution mass spectrum of **B11h**

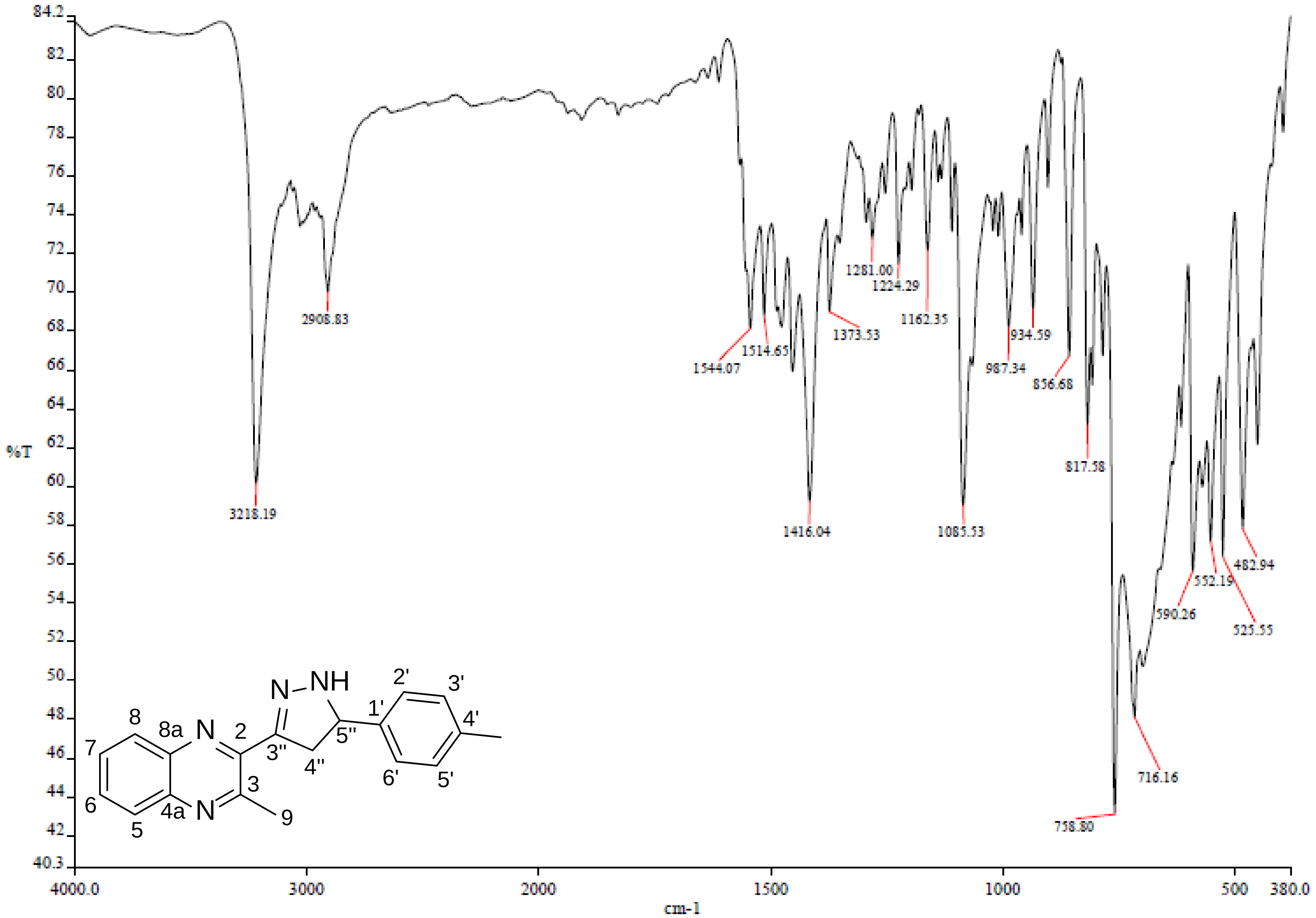

FTIR spectrum of **B11h**

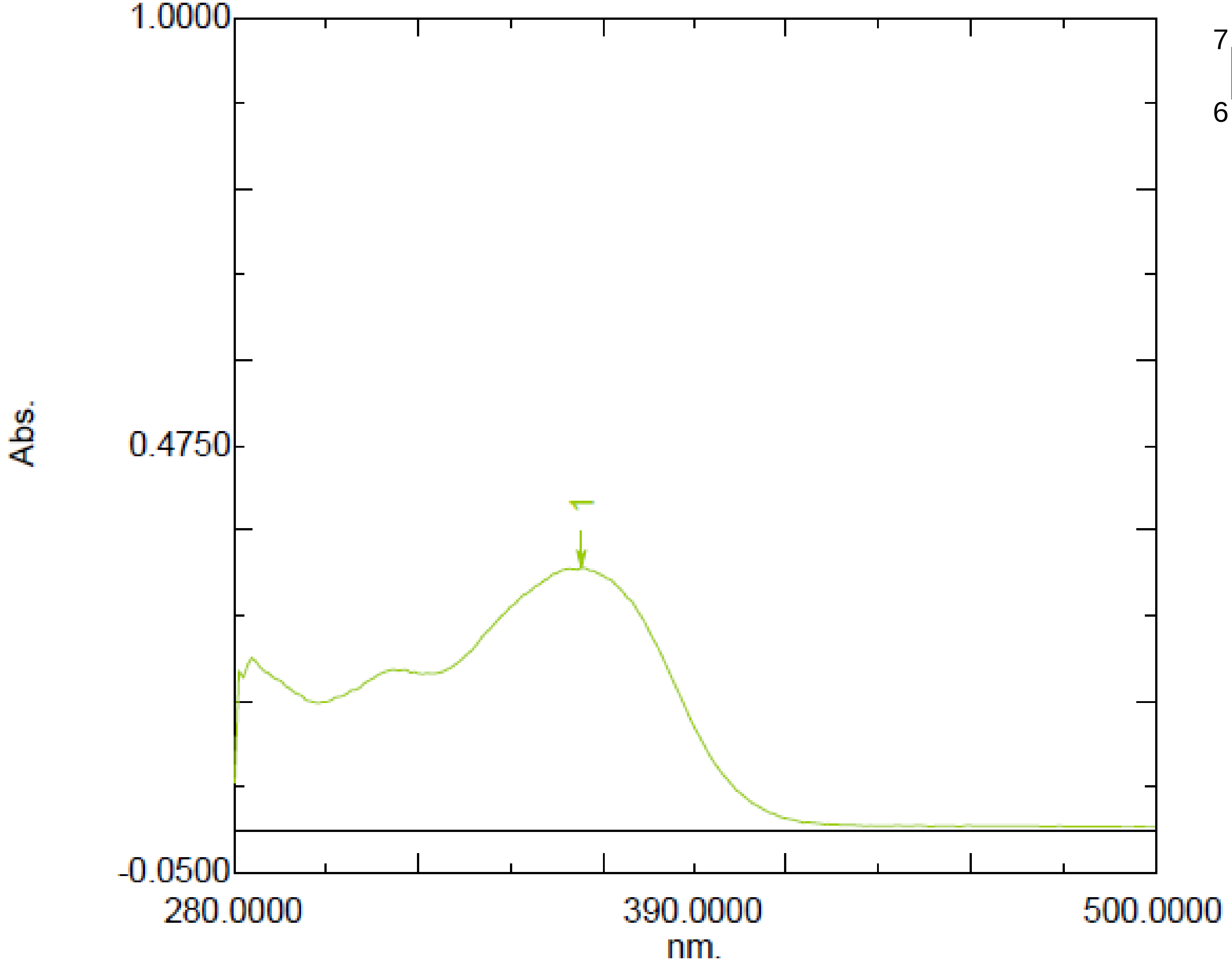

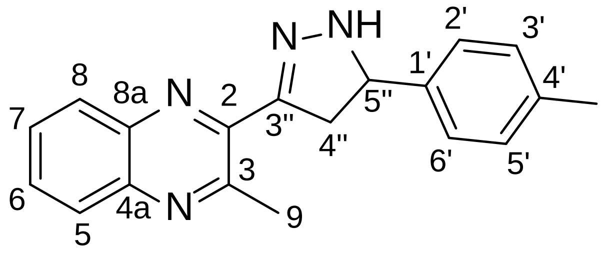

λ	absorbance	logε
360	0.3230	4.29

UV spectrum of **B11h**

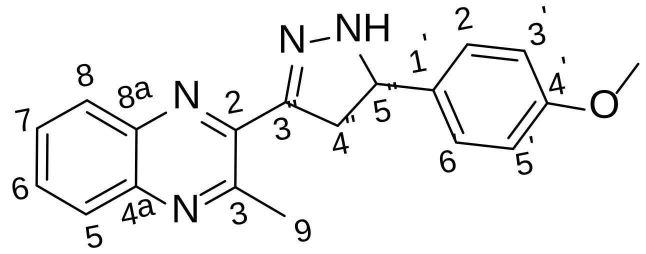

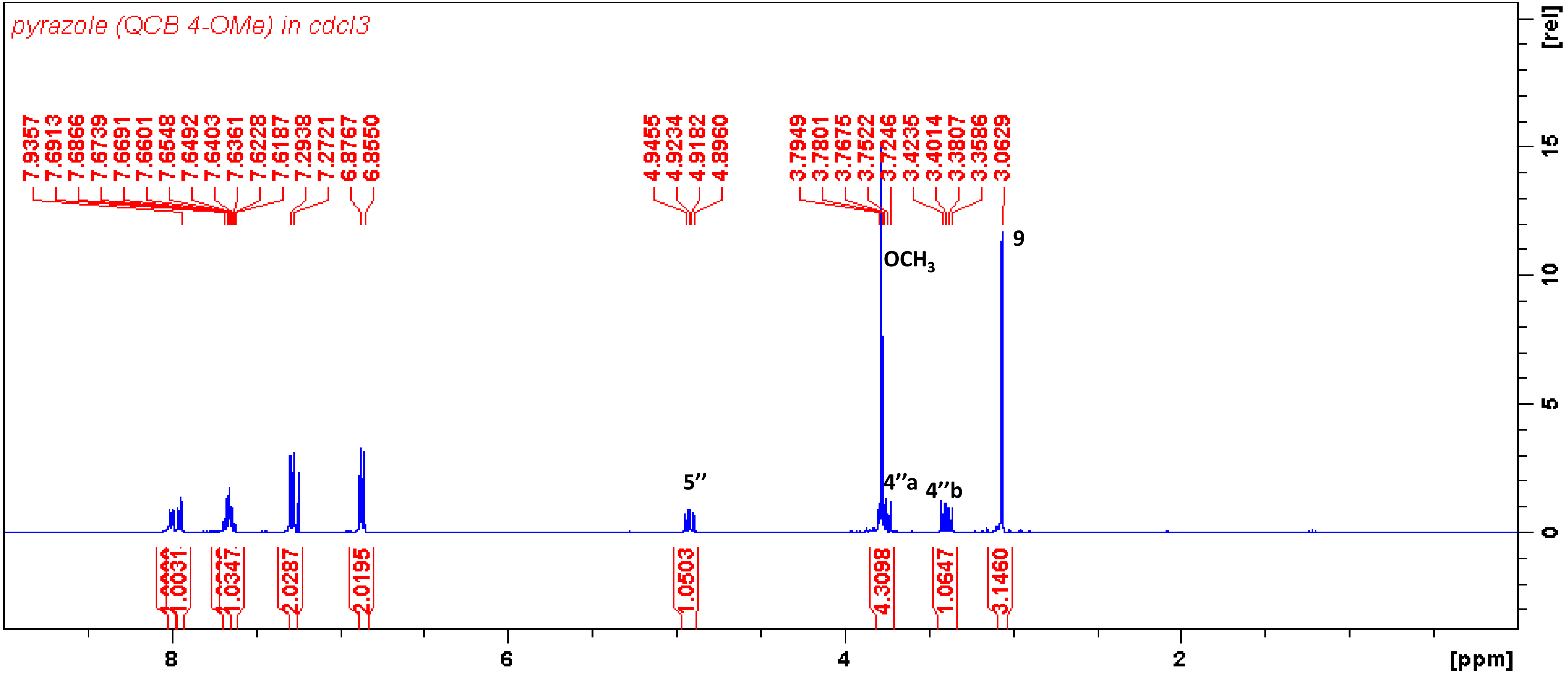

^{1}H NMR spectrum of **B11i**

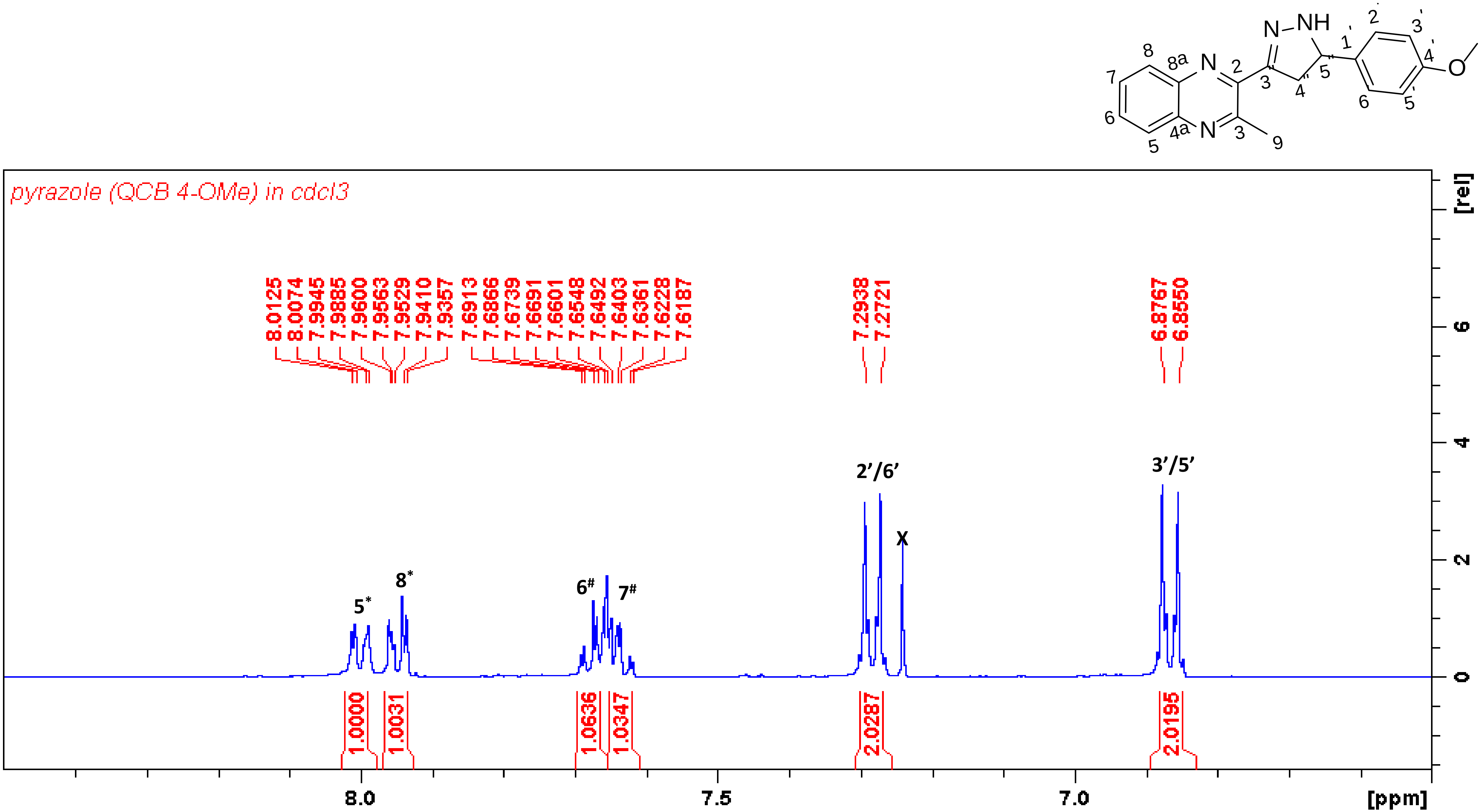

*, # Indicates assignments are interchangeable

Expanded ^{1}H NMR spectrum of **B11i**

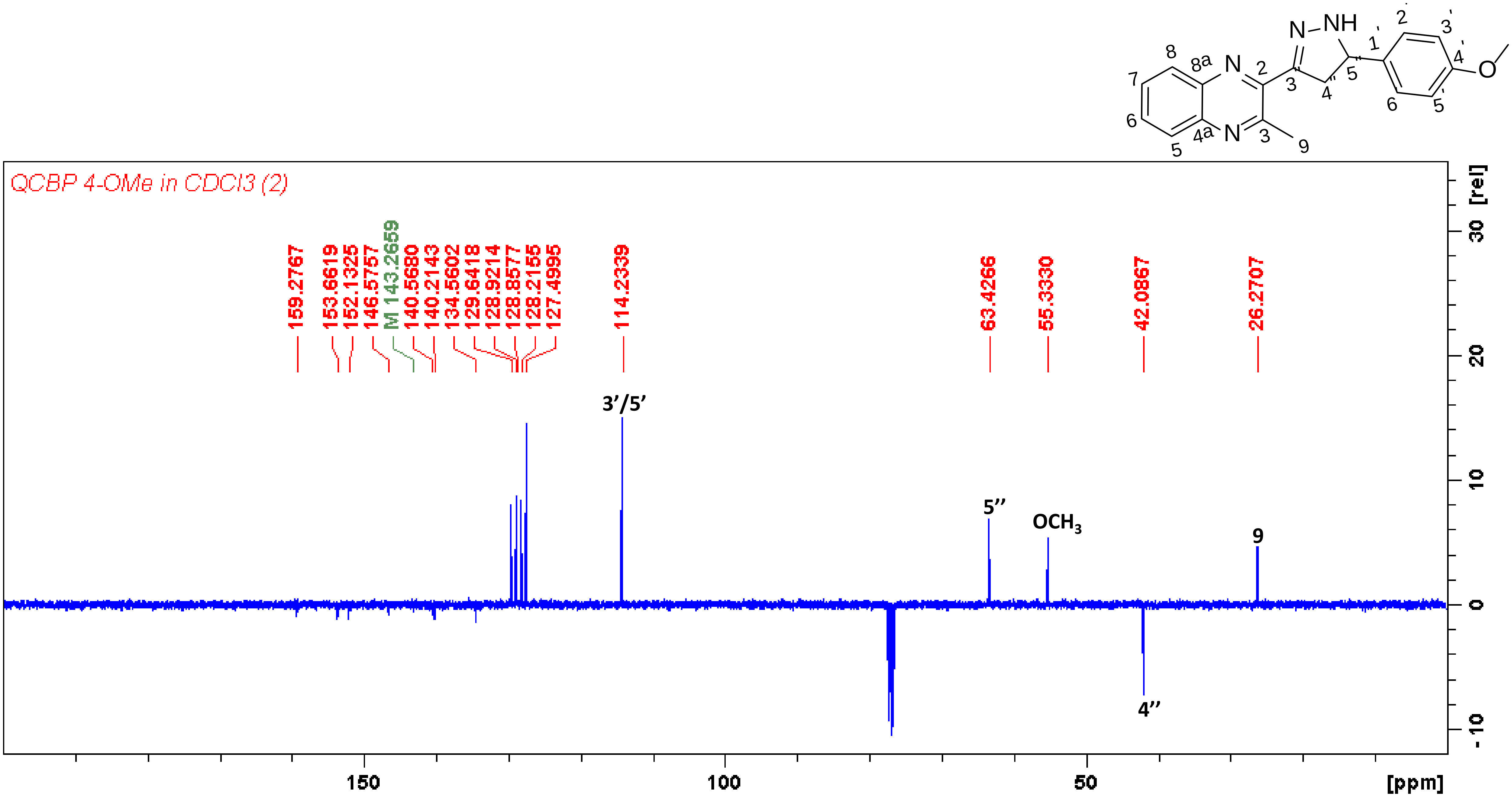

^{13}C NMR spectrum of **B11i**

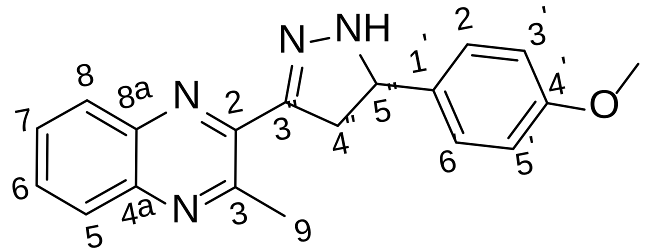

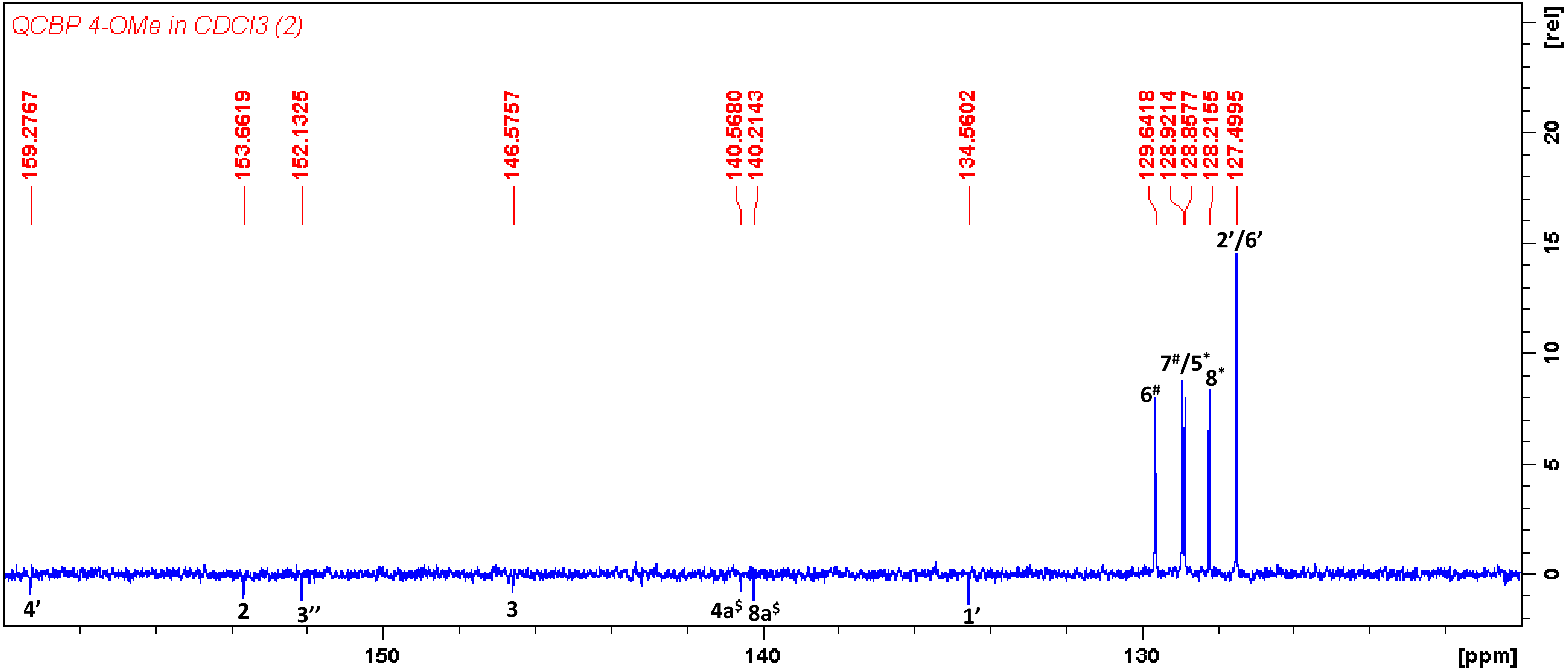

*, #, $ Indicates assignments are interchangeable

Expanded ^{13}C NMR spectrum of **B11i**

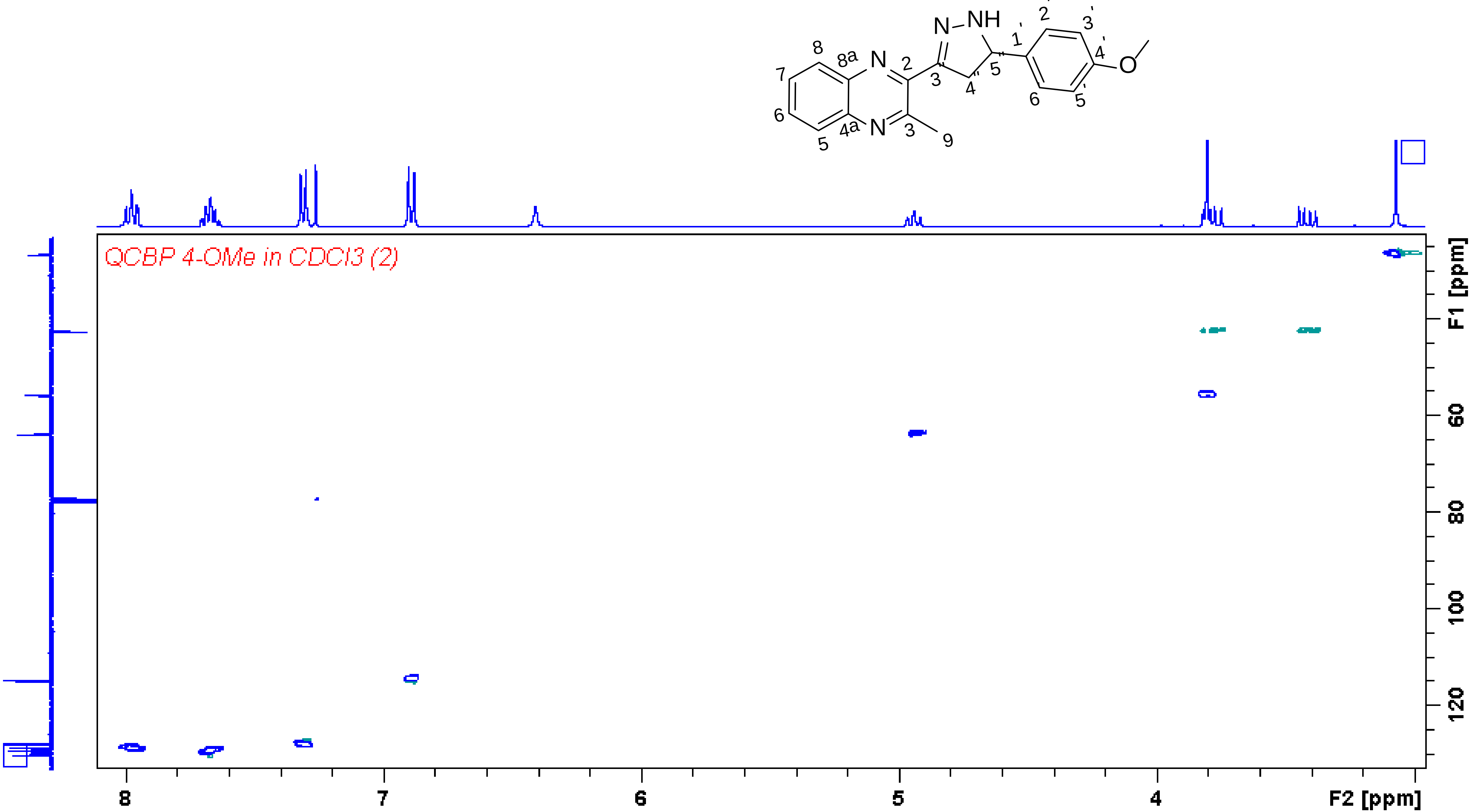

HSQC of **B11i**

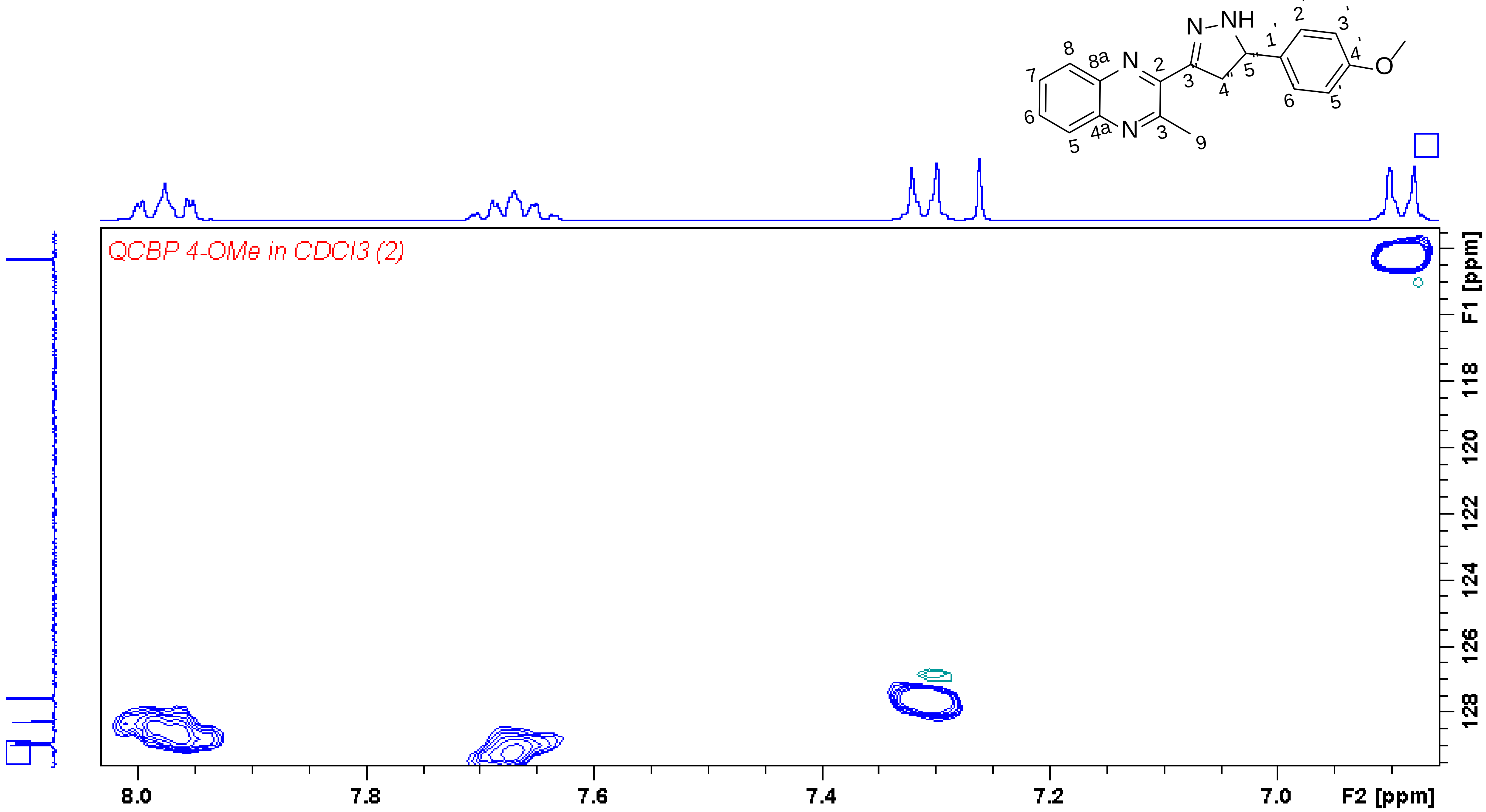

Expanded HSQC of **B11i**

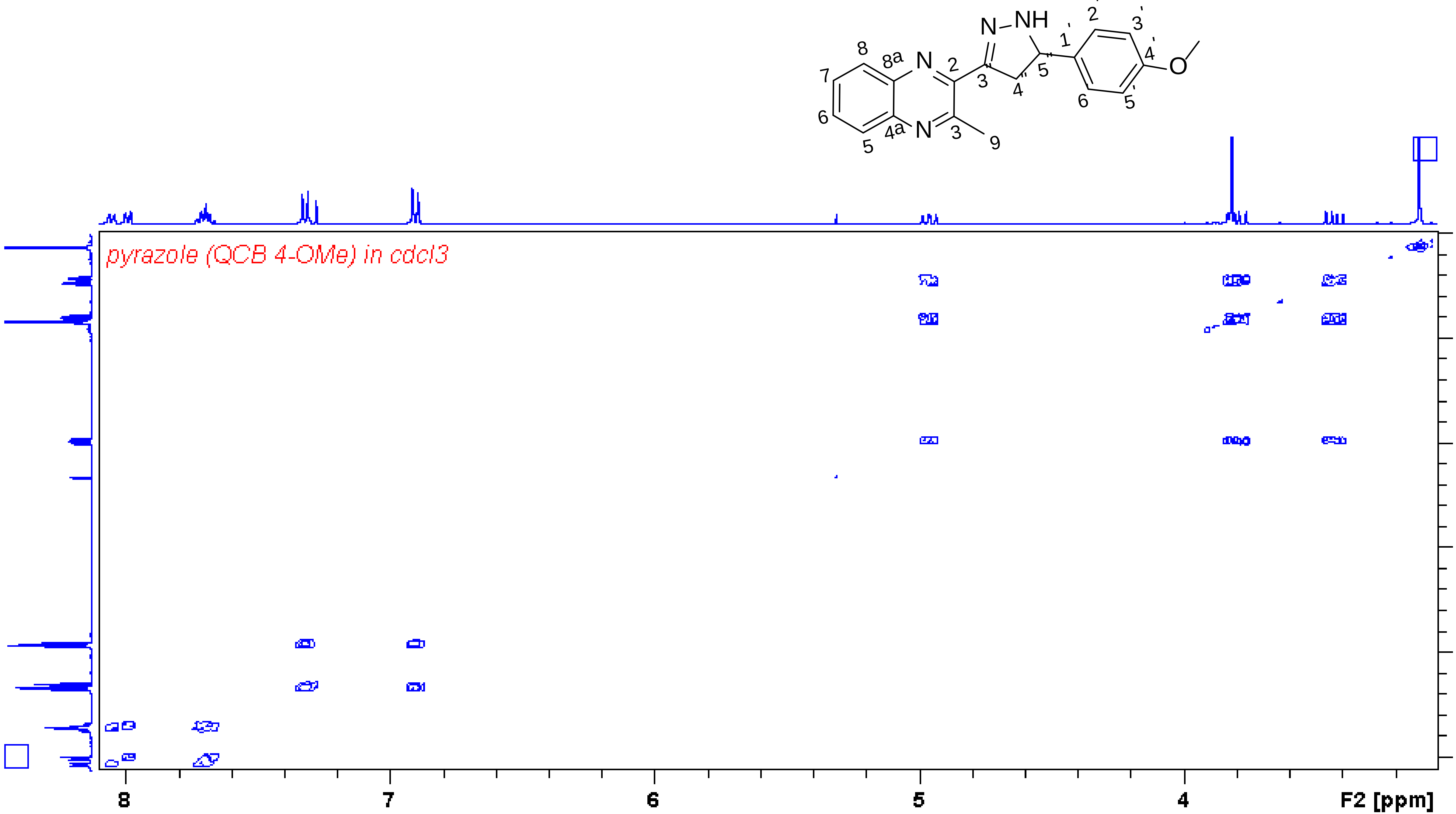

COSY of **B11i**

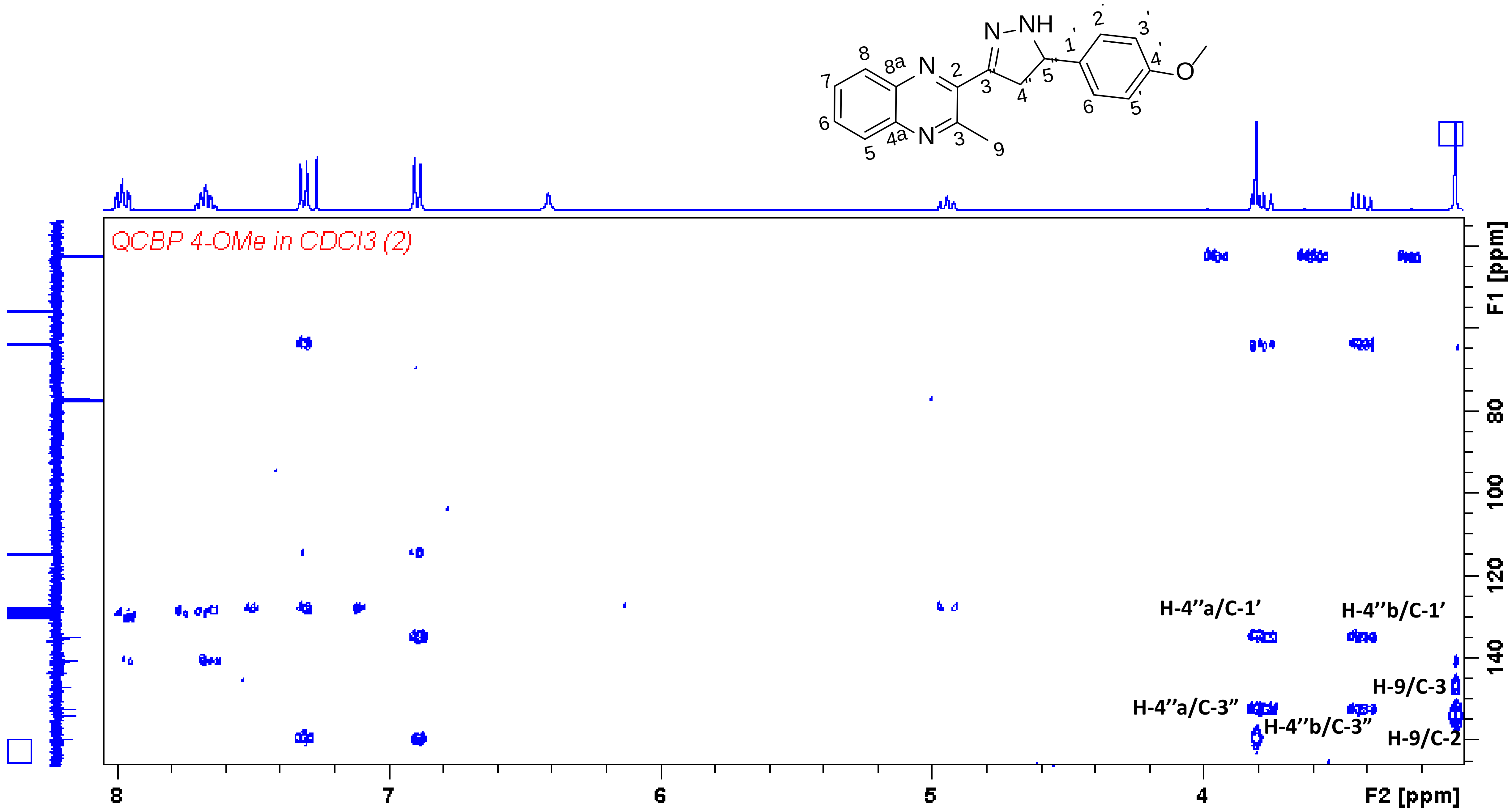
QCBP 4-OMe in CDCl3 (2)
H-4''a/C-1'
H-4''b/C-1'
H-9/C-3
H-4''a/C-3''
H-4''b/C-3''
H-9/C-2
F1 [ppm]
F2 [ppm]

HMBC of **B11i**

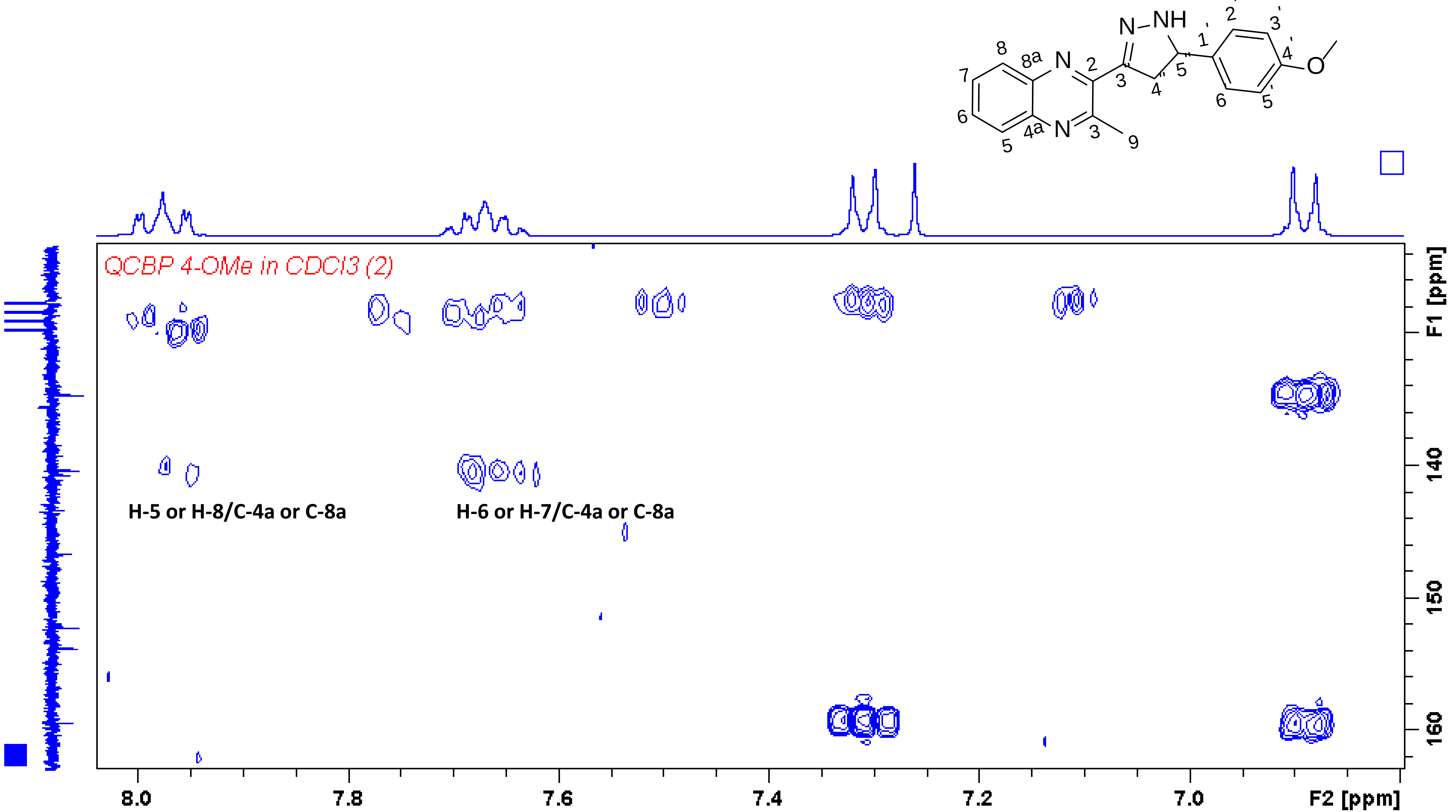

Expanded HMBC of **B11i**

Elemental Composition Report

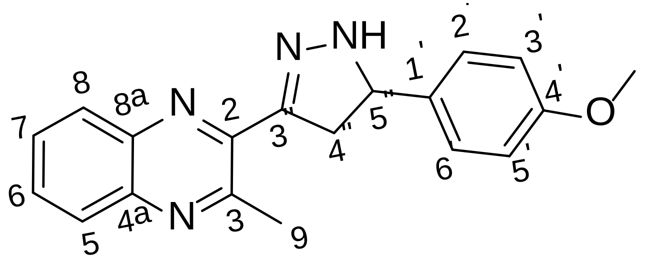

Single Mass Analysis

Tolerance = 5.0 PPM / DBE: min = -1.5, max = 100.0
Element prediction: Off
Number of isotope peaks used for i-FIT = 3

Monoisotopic Mass, Even Electron Ions
30 formula(e) evaluated with 1 results within limits (up to 20 closest results for each mass)
Elements Used:
C: 15-20 H: 15-20 N: 0-5 O: 0-5 Na: 0-1
Py-QCB 4-OMe 9 (0.270) Cm (1:61)
TOF MS ES+

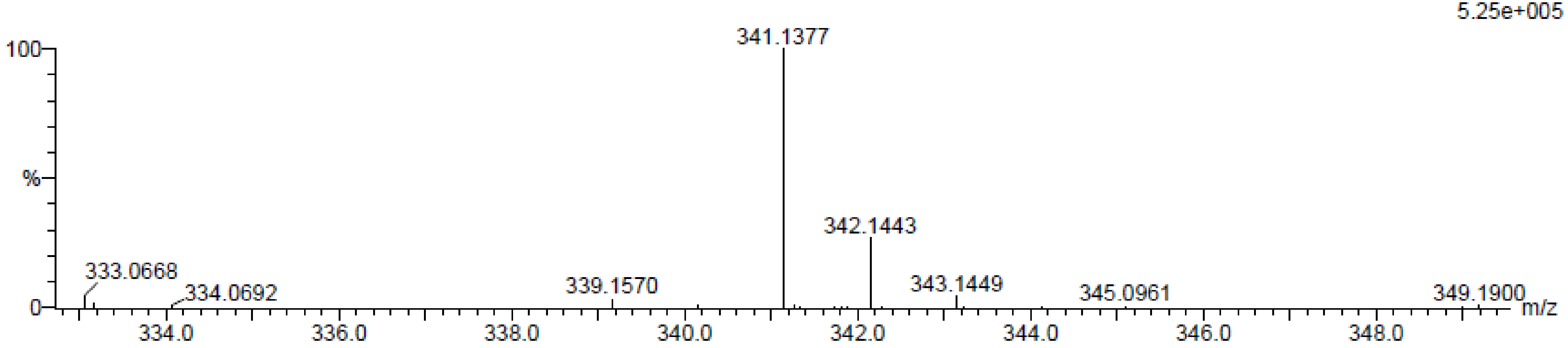

Minimum:				-1.5			
Maximum:		5.0	5.0	100.0			
Mass	Calc. Mass	mDa	PPM	DBE	i-FIT	i-FIT (Norm)	Formula
341.1377	341.1378	-0.1	-0.3	12.5	137.6	0.0	C19 H18 N4 O Na

High resolution mass spectrum of **B11i**

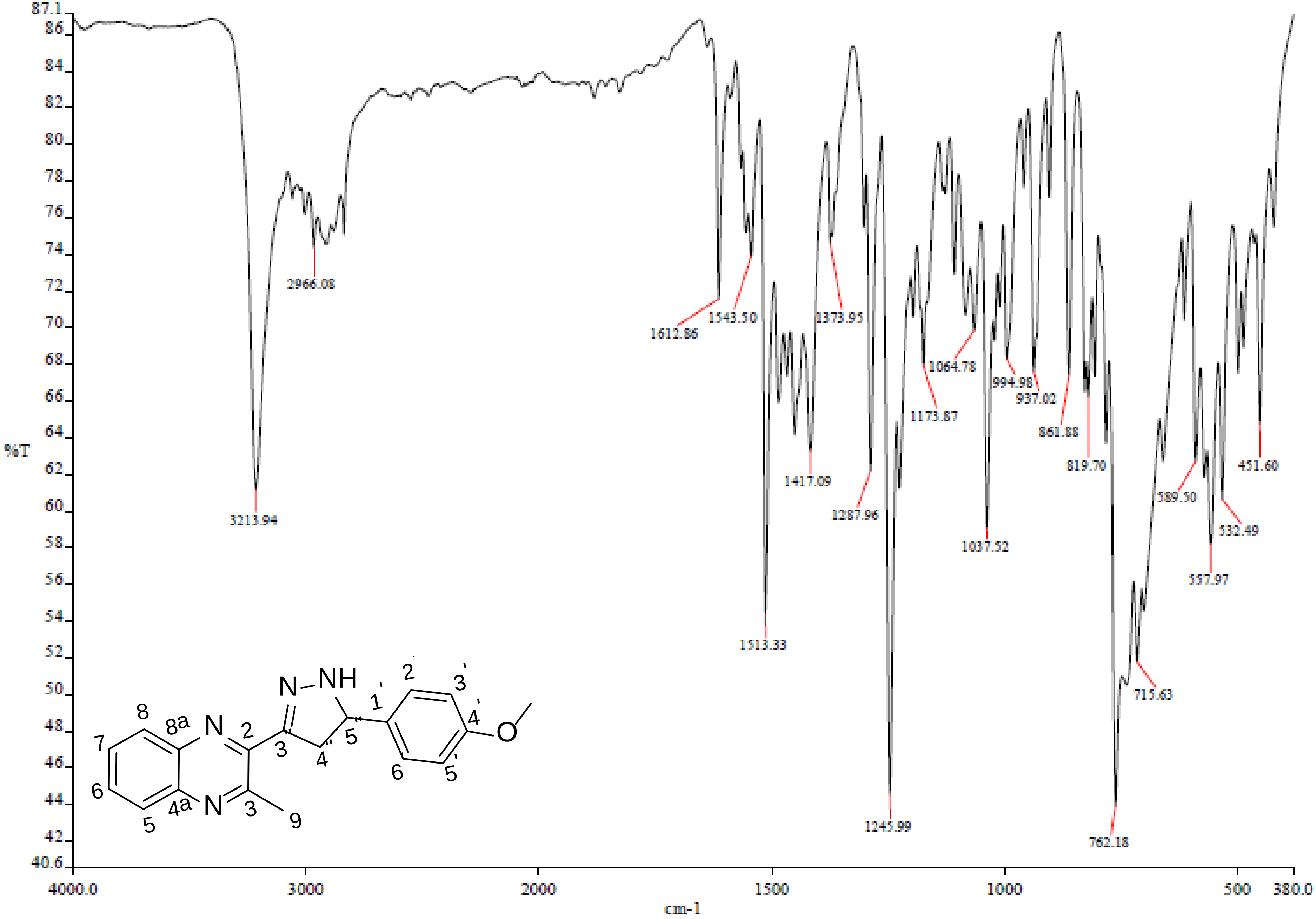

FTIR spectrum of **B11i**

Overlay Spectrum Graph Report

06/10/2017 11:55:56 AM

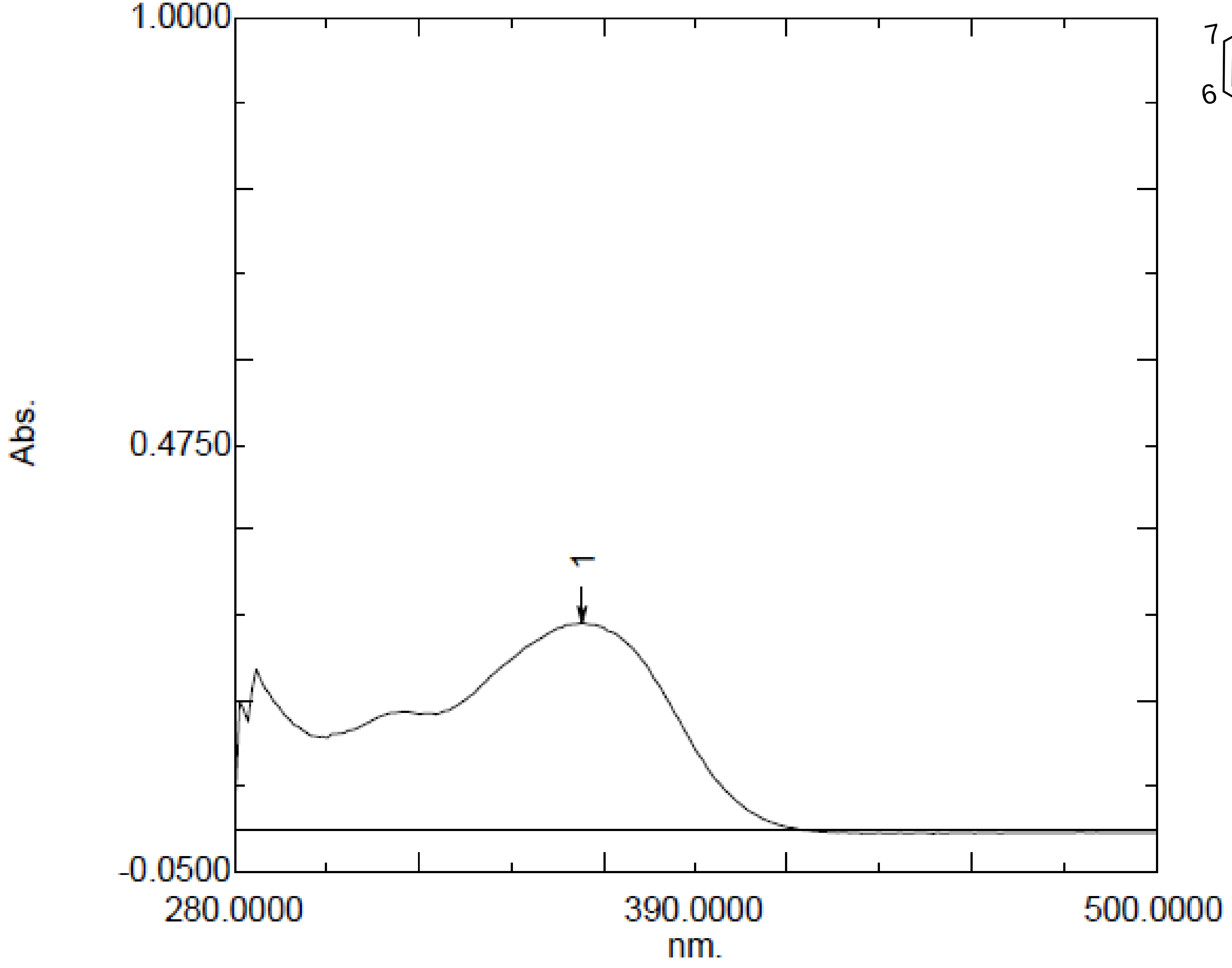

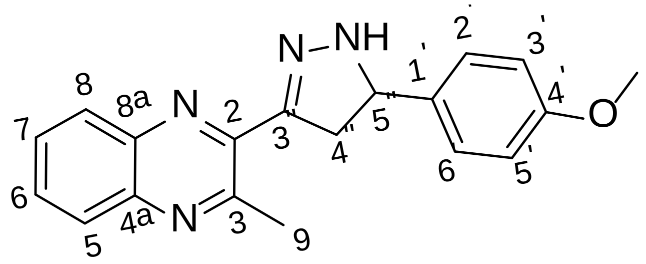

λ	absorbance	logε
363	0.2557	4.21

UV spectrum of **B11i**

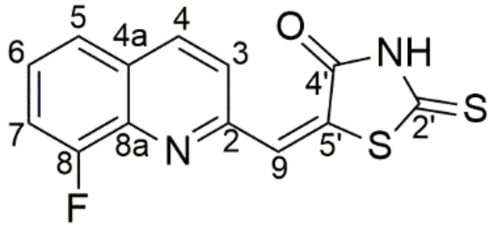

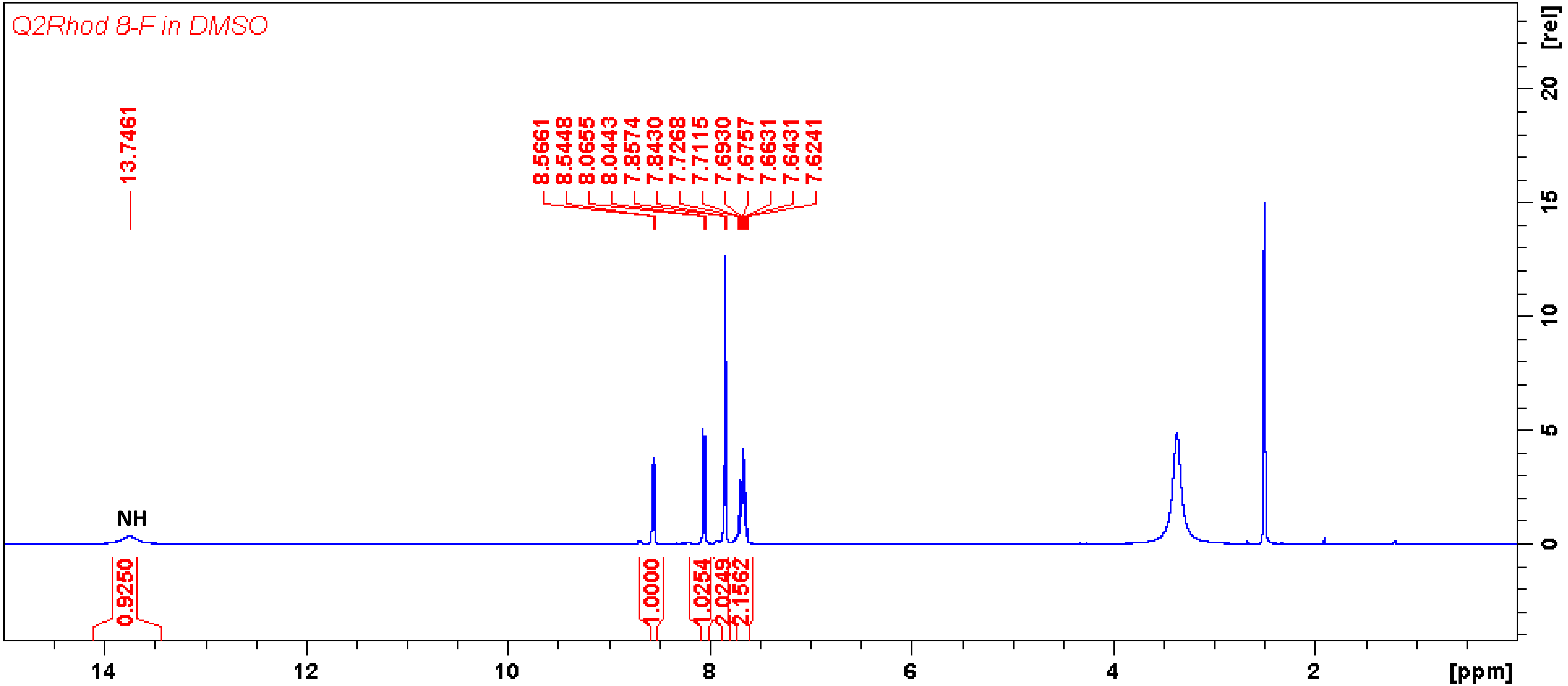

^{1}H NMR spectrum of **C5a**

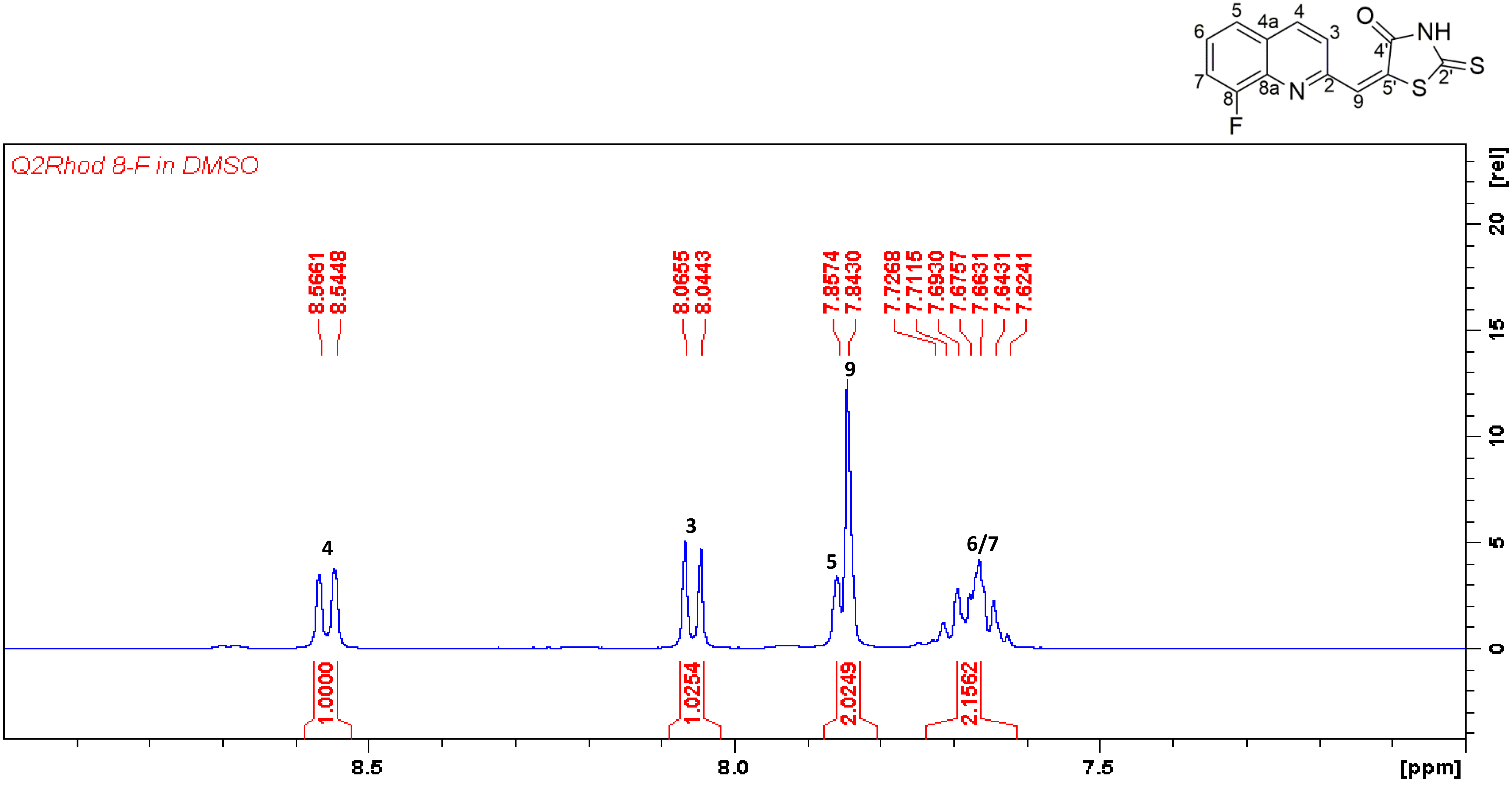

Expanded ^{1}H NMR spectrum of **C5a**

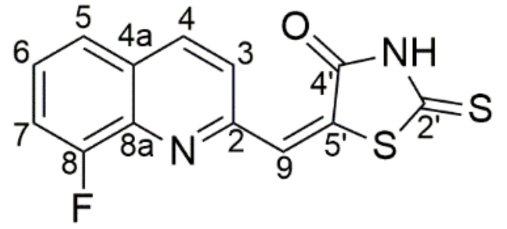

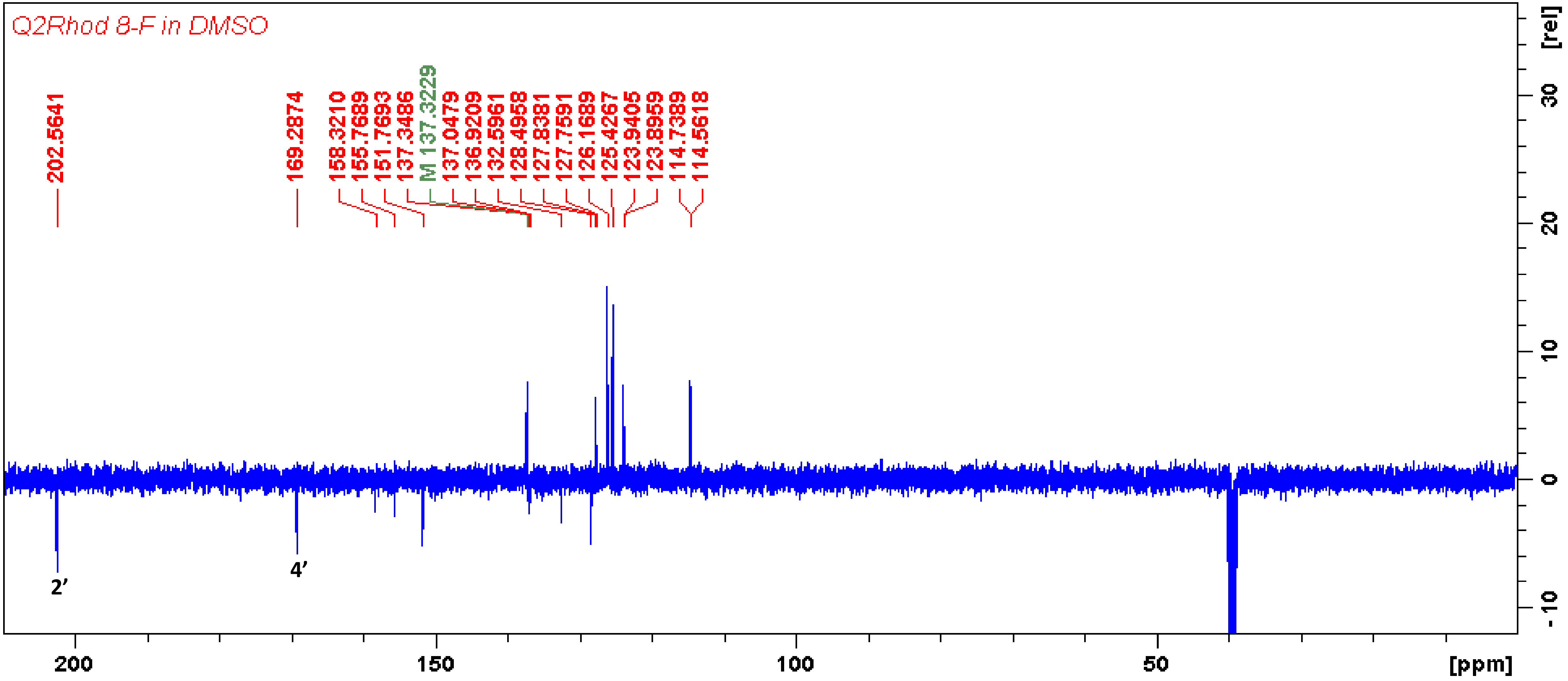

^{13}C NMR spectrum of **C5a**

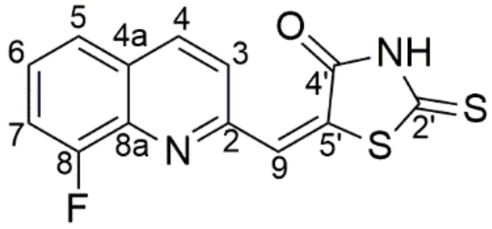

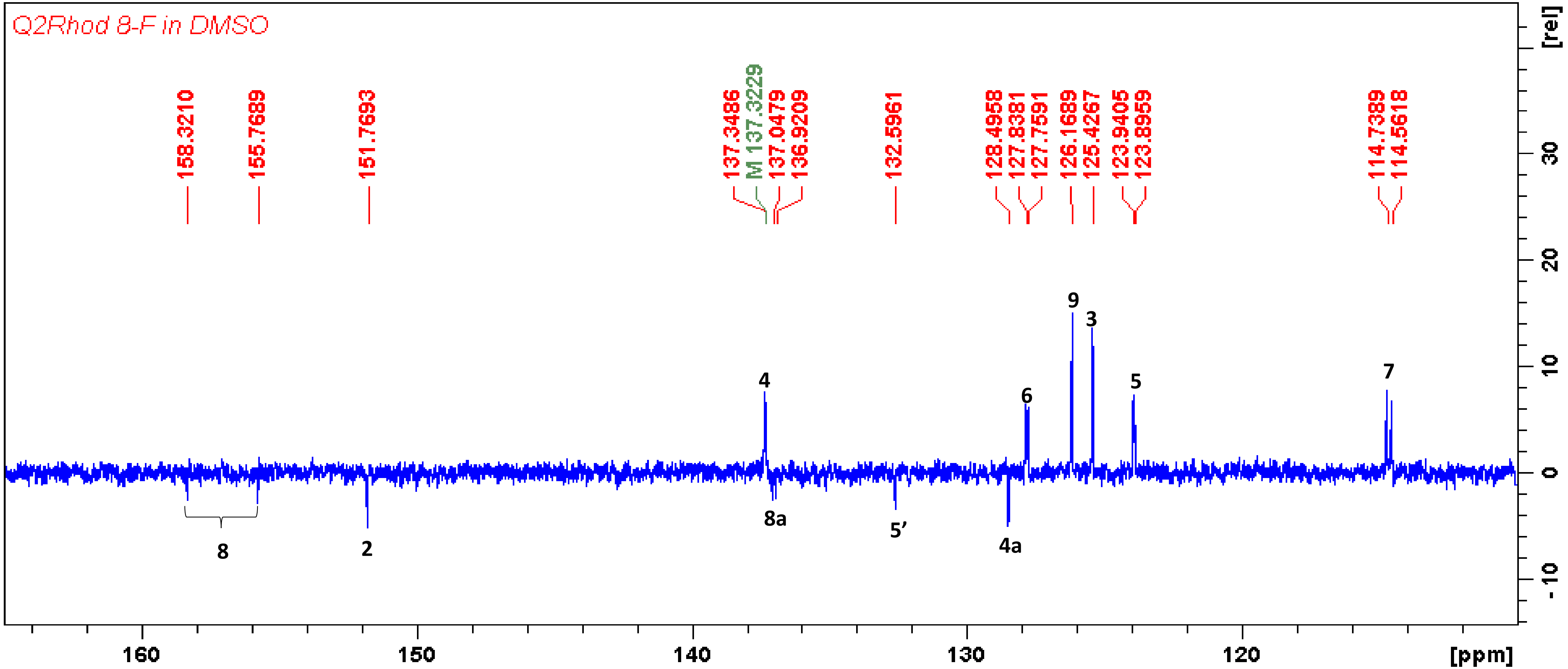

Expanded ^{13}C NMR spectrum of **C5a**

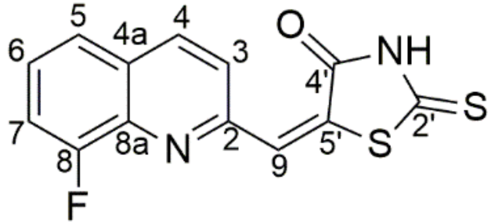
5
4a
4
3
O
NH
6
4'
S
2'
7
8
8a
N
2
5'
S
9
F

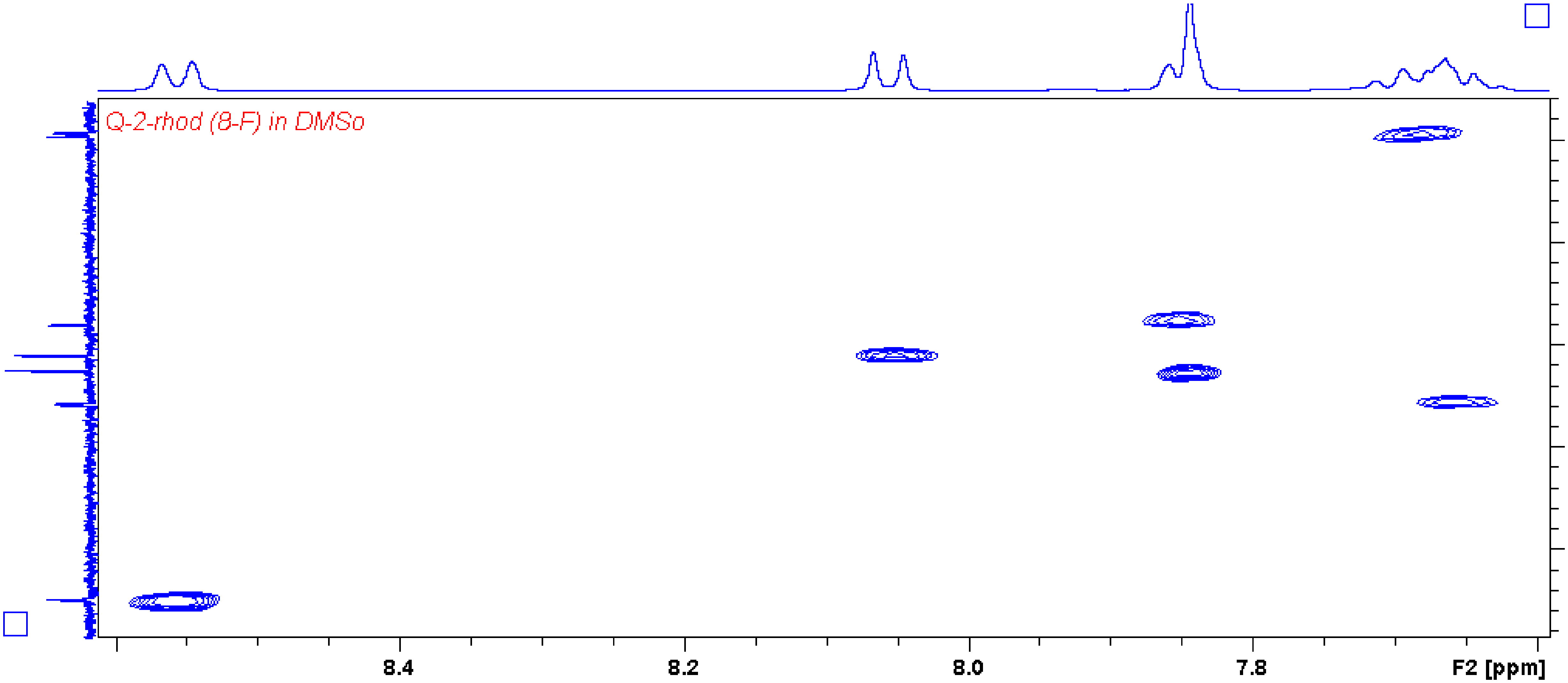
Q-2-rhod (8-F) in DMSo
F1 [ppm]
120
125
130
135
8.4
8.2
8.0
7.8
F2 [ppm]

HSQC of **C5a**

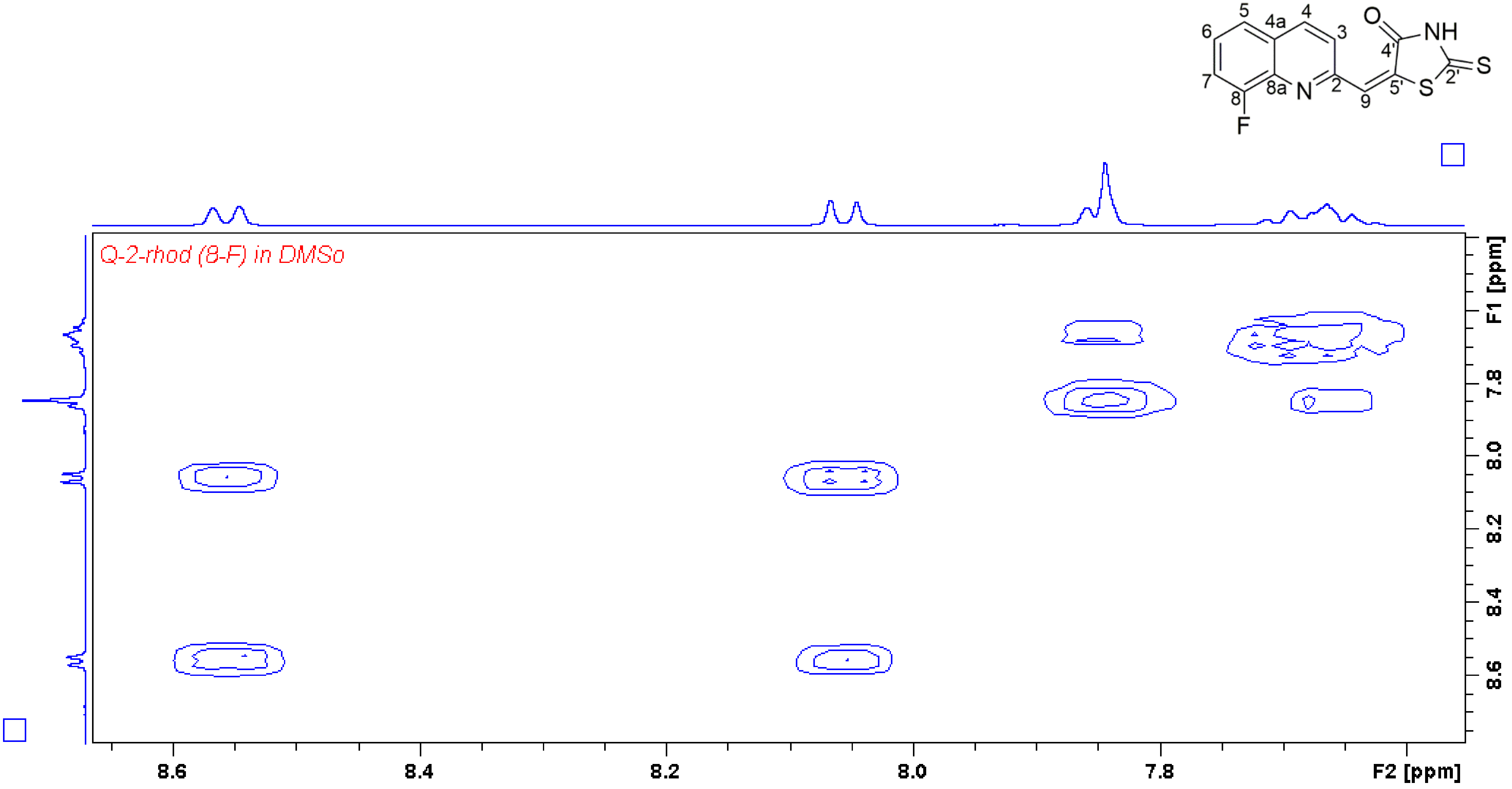

COSY of **C5a**

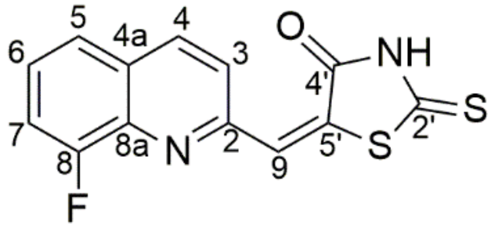

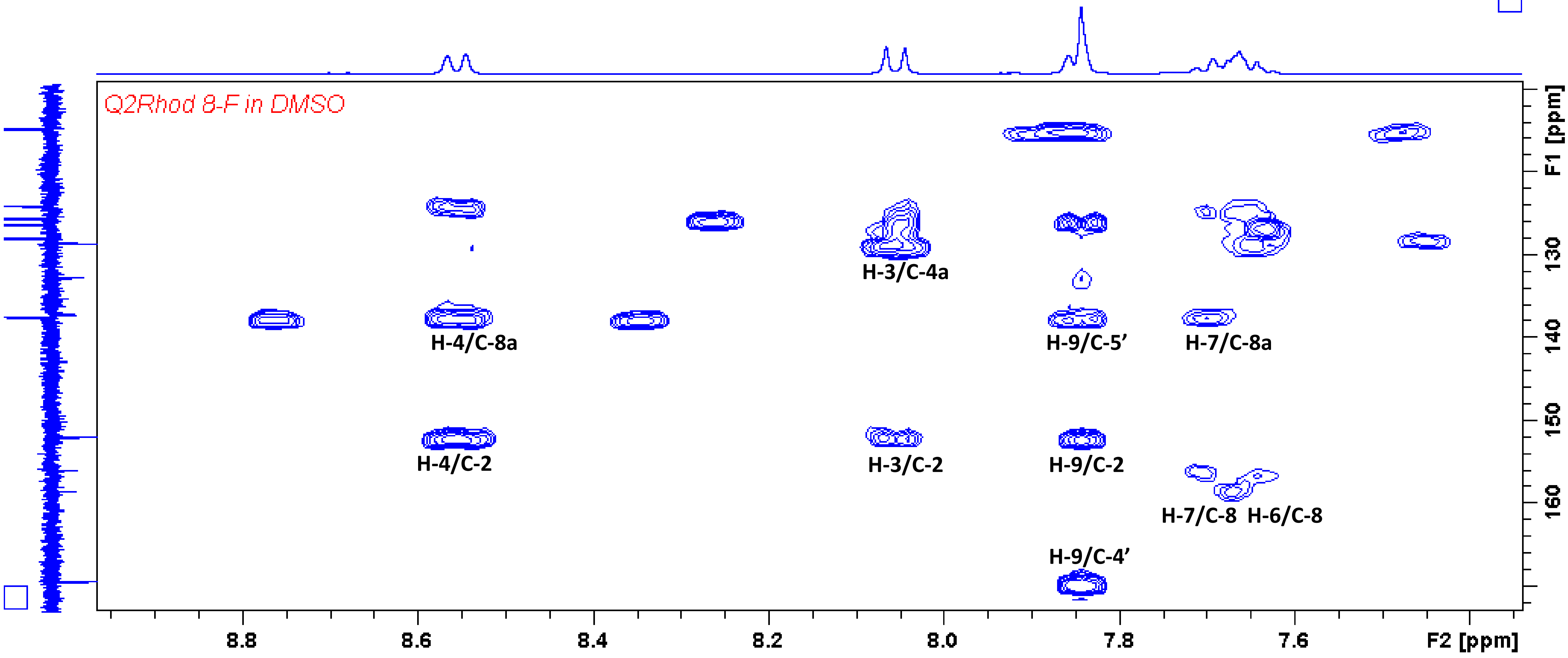
Q2Rhod 8-F in DMSO
H-3/C-4a
H-4/C-8a
H-9/C-5’
H-7/C-8a
H-4/C-2
H-3/C-2
H-9/C-2
H-7/C-8
H-6/C-8
H-9/C-4’
F1 [ppm]
F2 [ppm]
8.8
8.6
8.4
8.2
8.0
7.8
7.6
130
140
150
160

HMBC of **C5a**

Elemental Composition Report

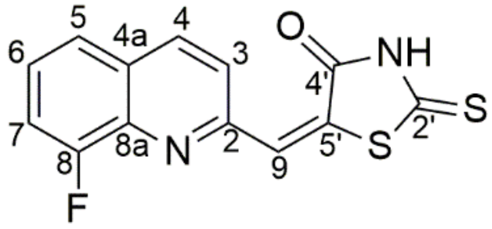

Single Mass Analysis

Tolerance = 5.0 PPM / DBE: min = -1.5, max = 100.0
Element prediction: Off
Number of isotope peaks used for i-FIT = 2

Monoisotopic Mass, Even Electron Ions
54 formula(e) evaluated with 1 results within limits (up to 20 best isotopic matches for each mass)
Elements Used:
C: 10-15 H: 5-10 N: 0-5 O: 0-5 F: 1-1 S: 0-2
Q2R (8-F) 3 (0.068) Cm (1:61)
TOF MS ES-

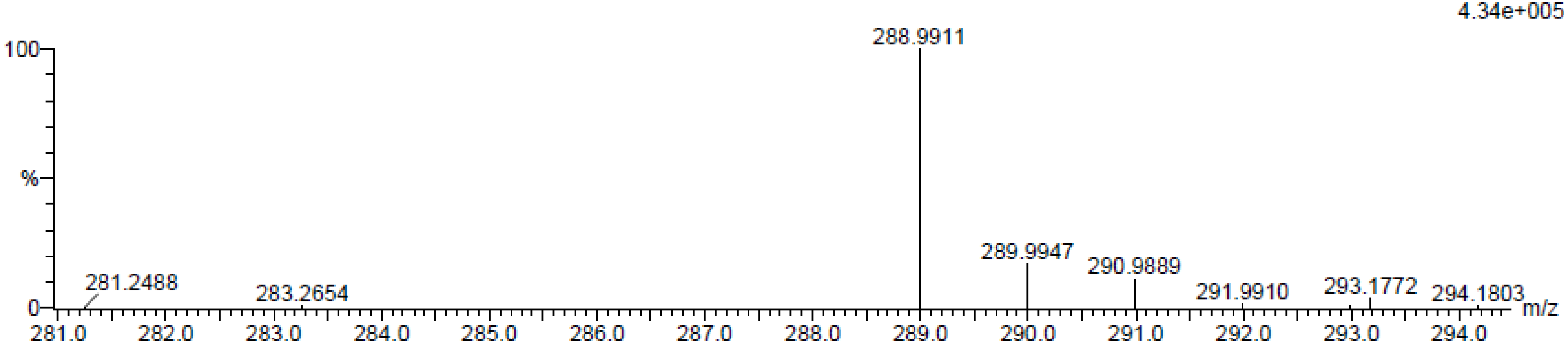

Minimum:				-1.5			
Maximum:		5.0	5.0	100.0			
Mass	Calc. Mass	mDa	PPM	DBE	i-FIT	i-FIT (Norm)	Formula
288.9911	288.9906	0.5	1.7	11.5	10.9	0.0	C13 H6 N2 O F S2

High resolution mass spectrum of **C5a**

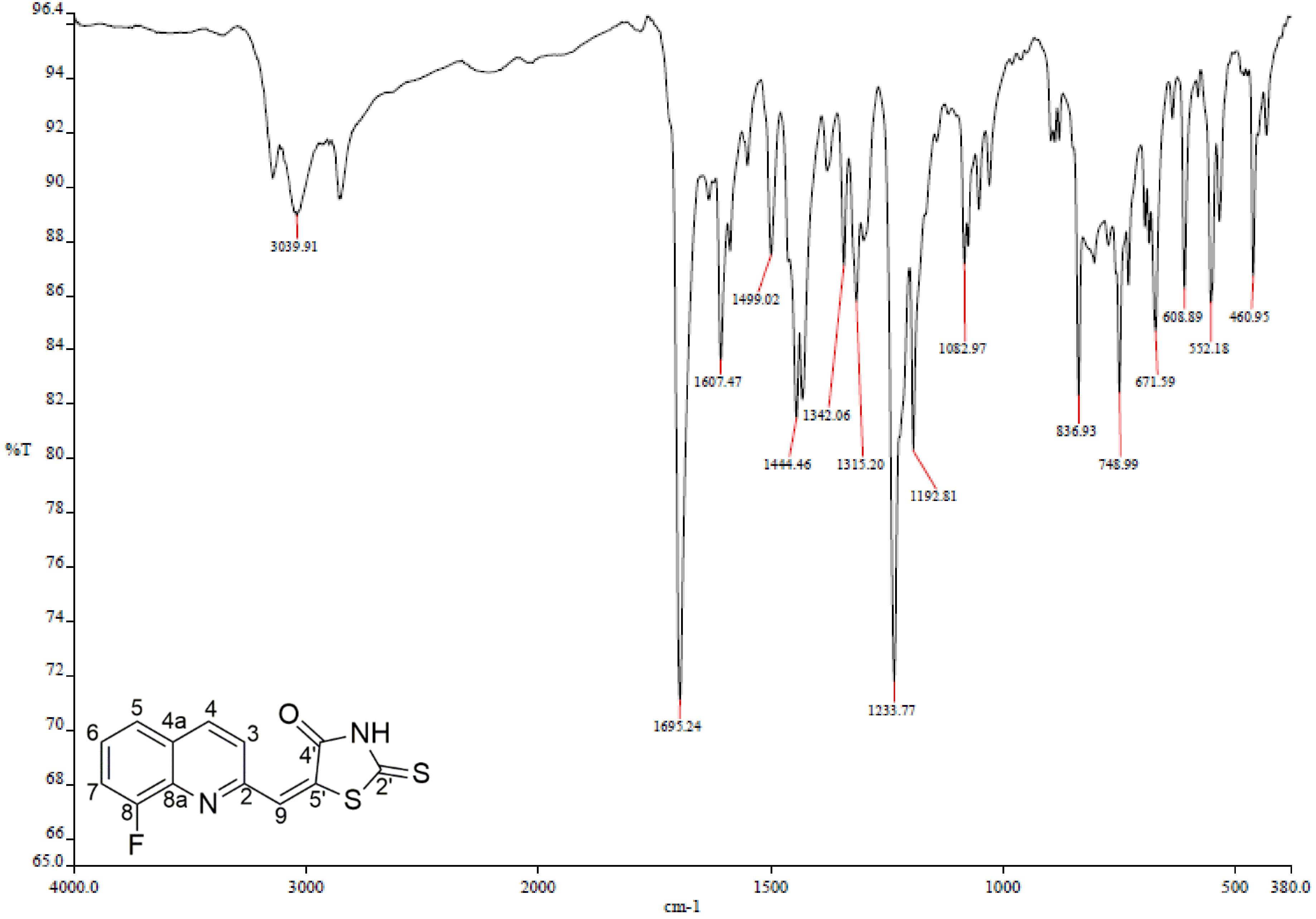

FTIR spectrum of **C5a**

Overlay Spectrum Graph Report

06/10/2017 11:27:15 AM

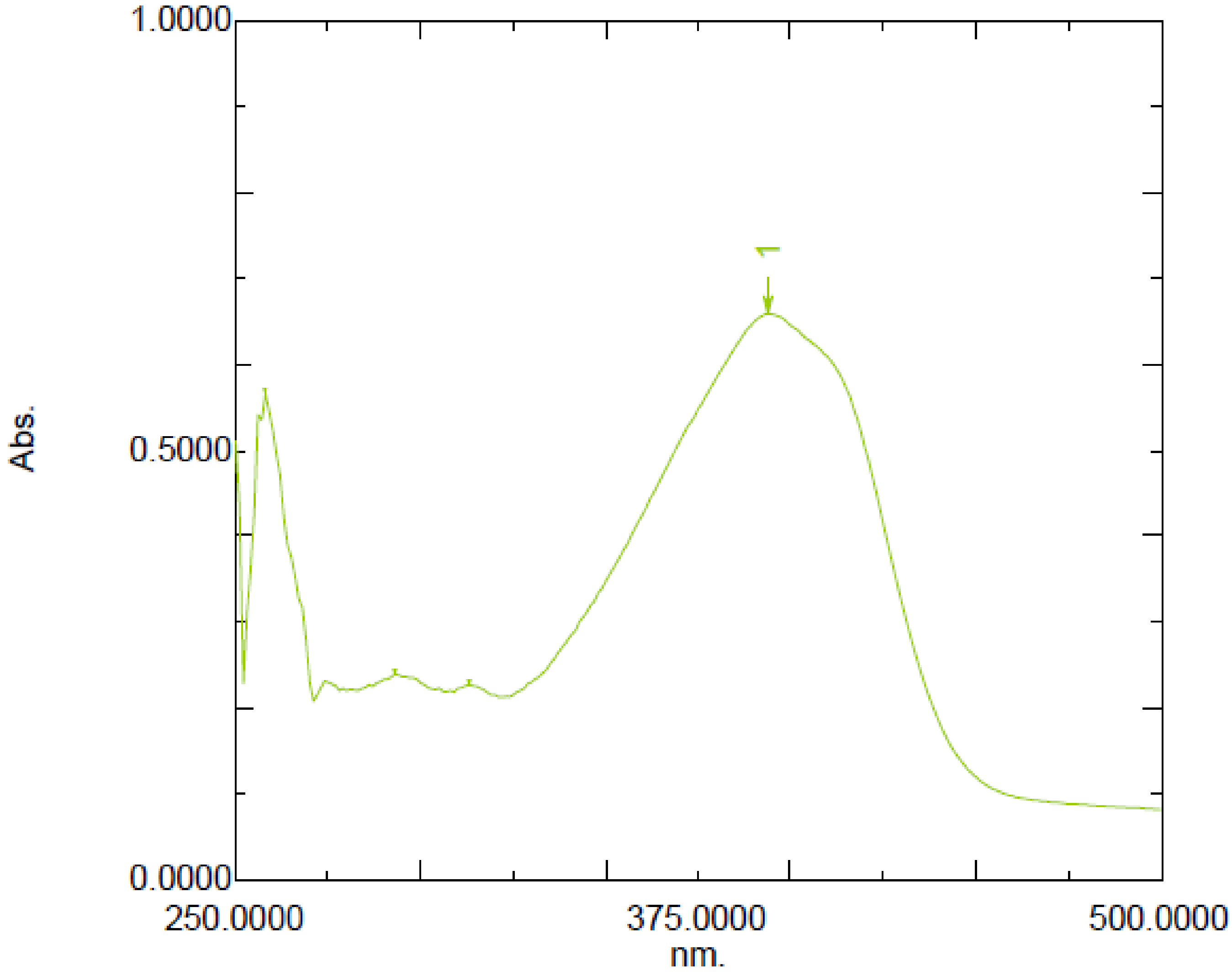

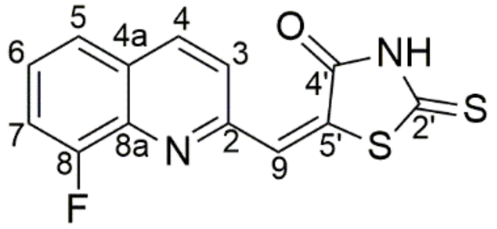

λ	absorbance	logε
394	0.659	4.58

UV spectrum of **C5a**

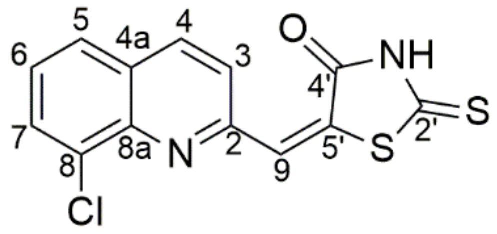

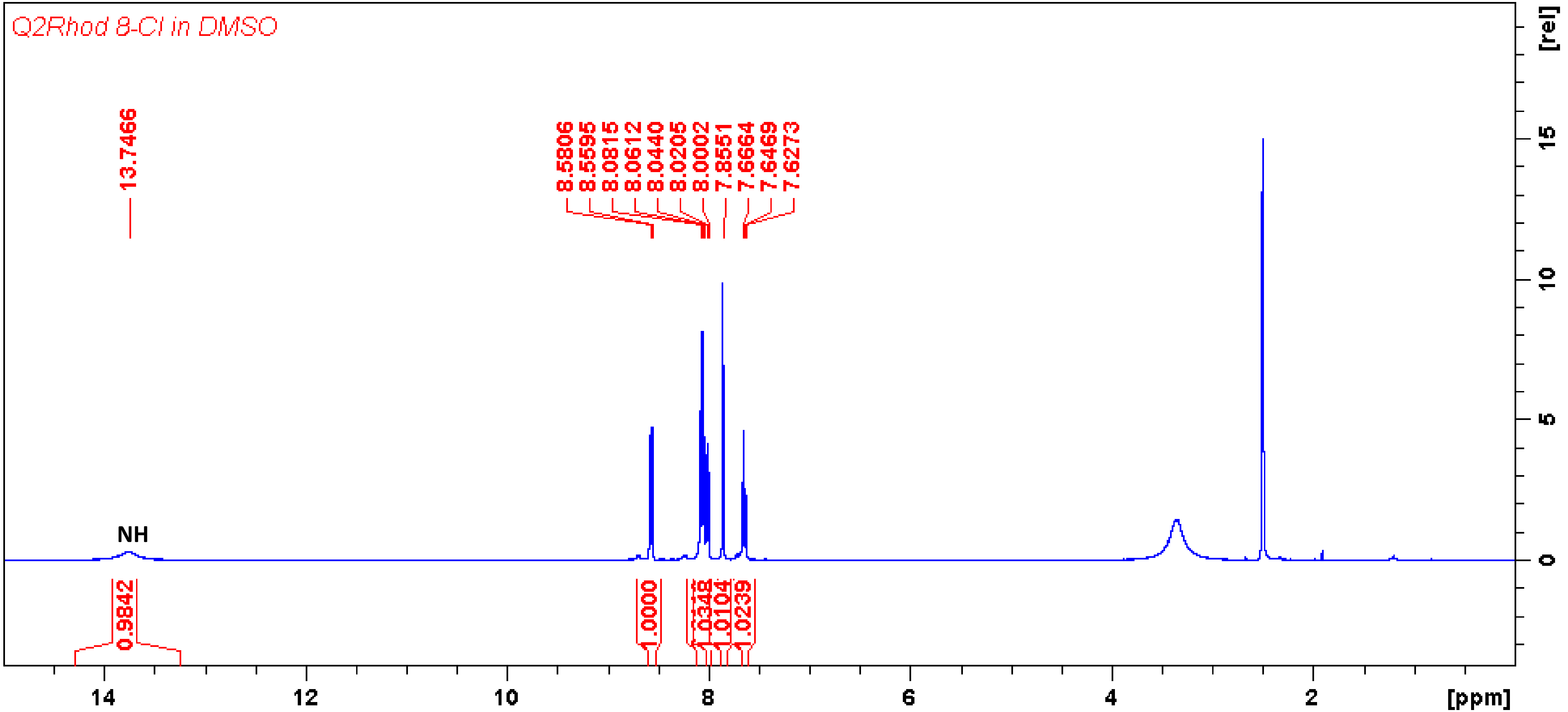

^{1}H NMR spectrum of **C5b**

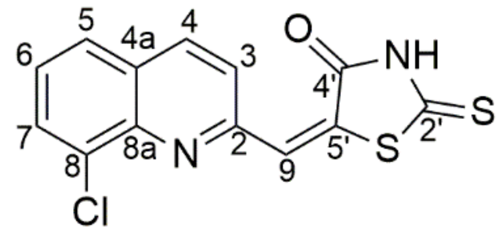

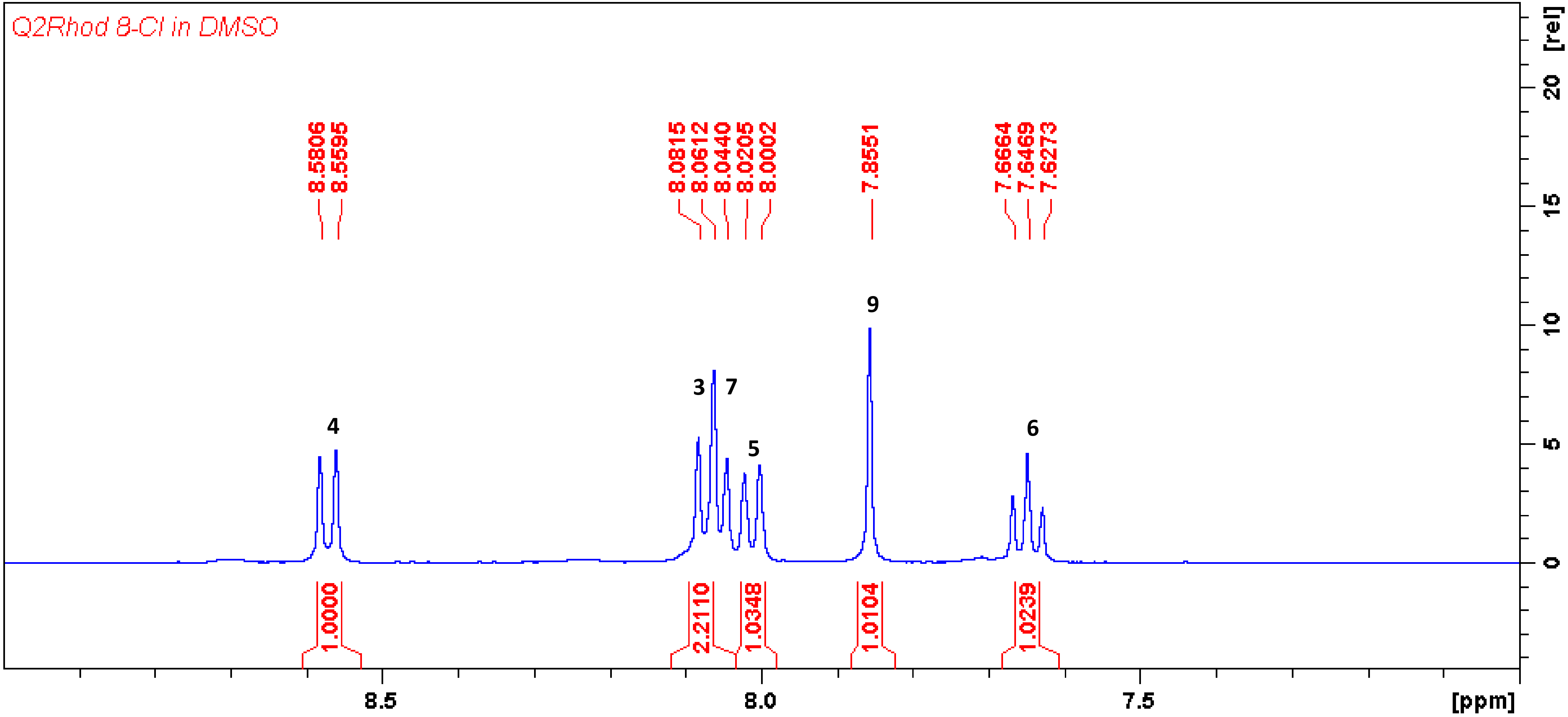

Expanded ^{1}H NMR spectrum of **C5b**

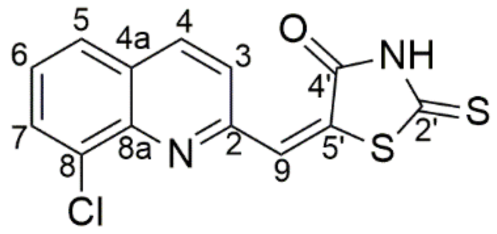

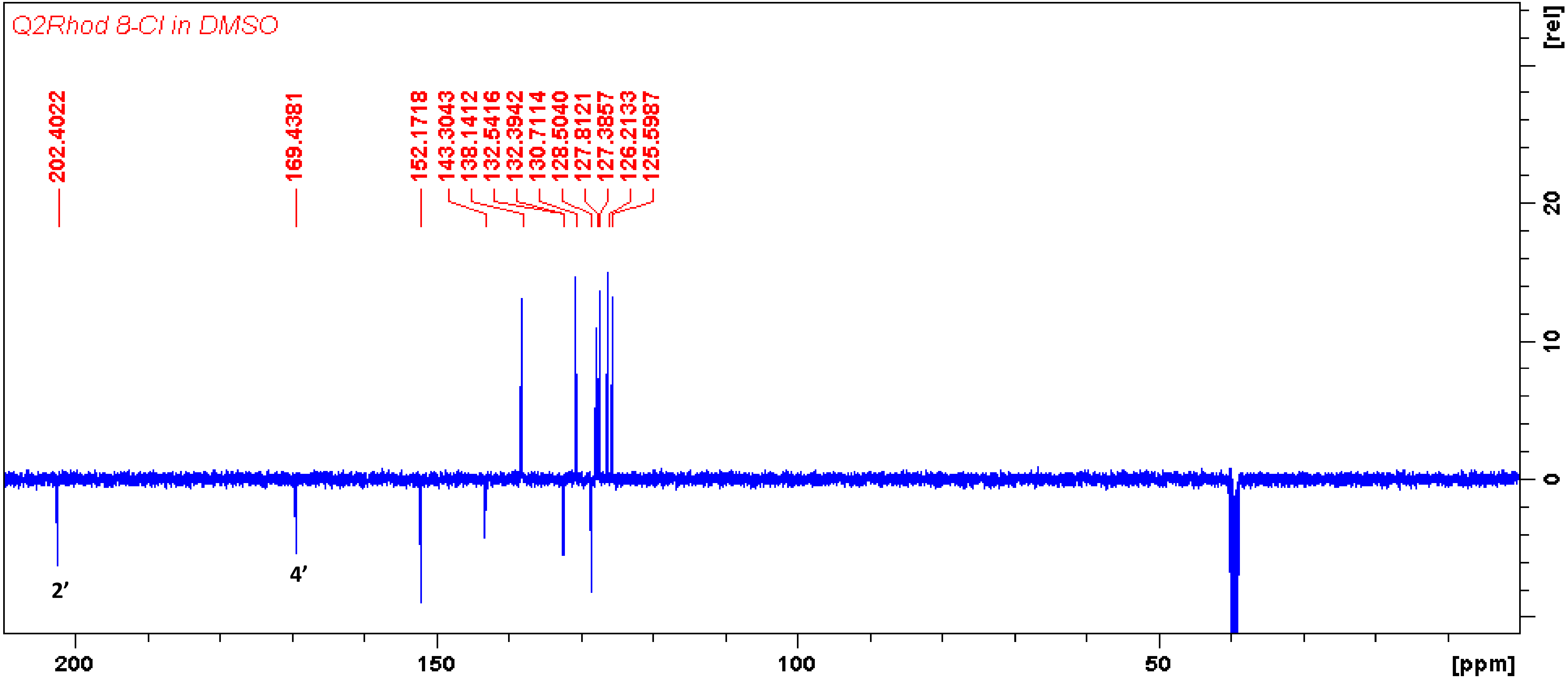

^{13}C NMR spectrum of **C5b**

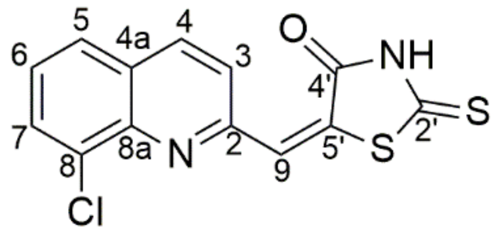

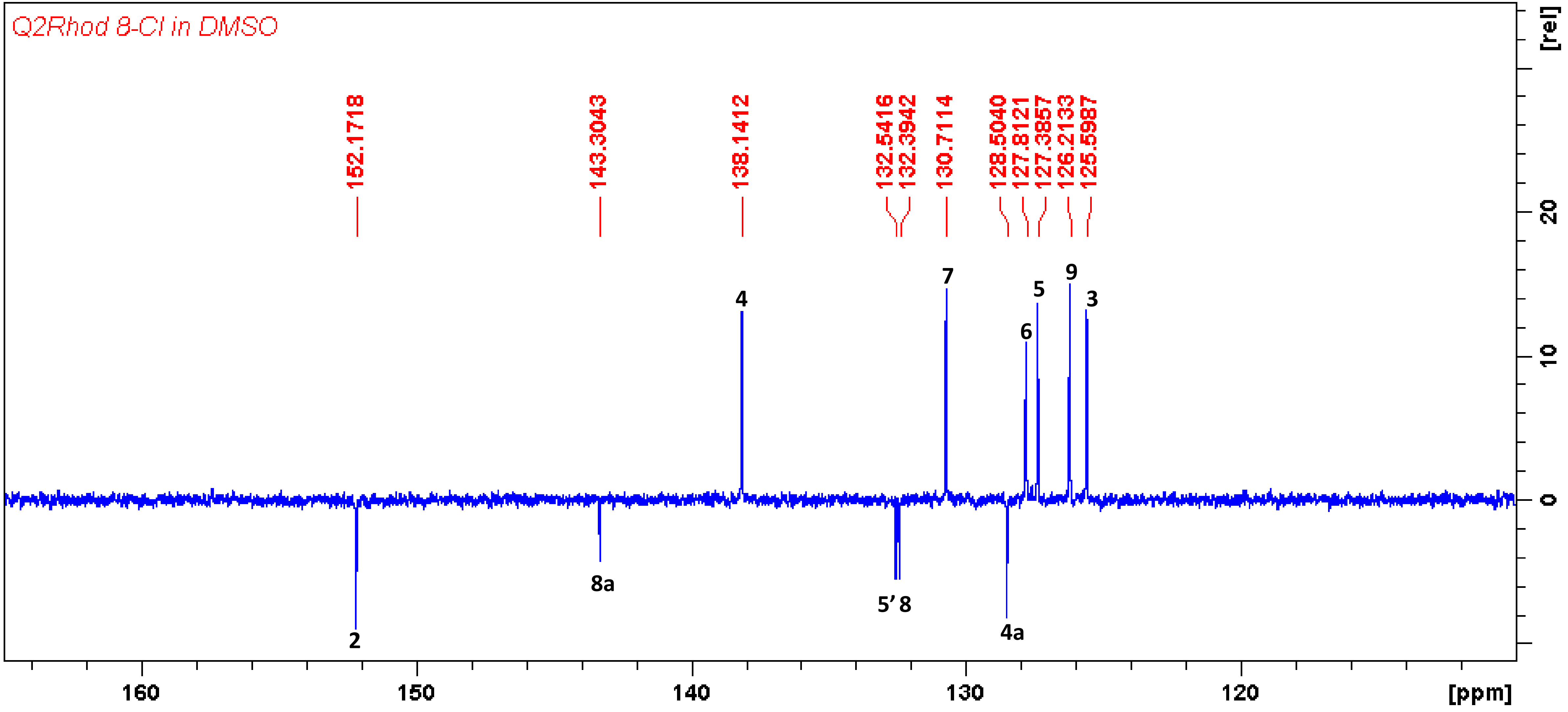

Expanded ^{13}C NMR spectrum of **C5b**

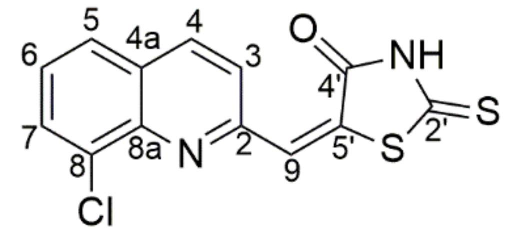

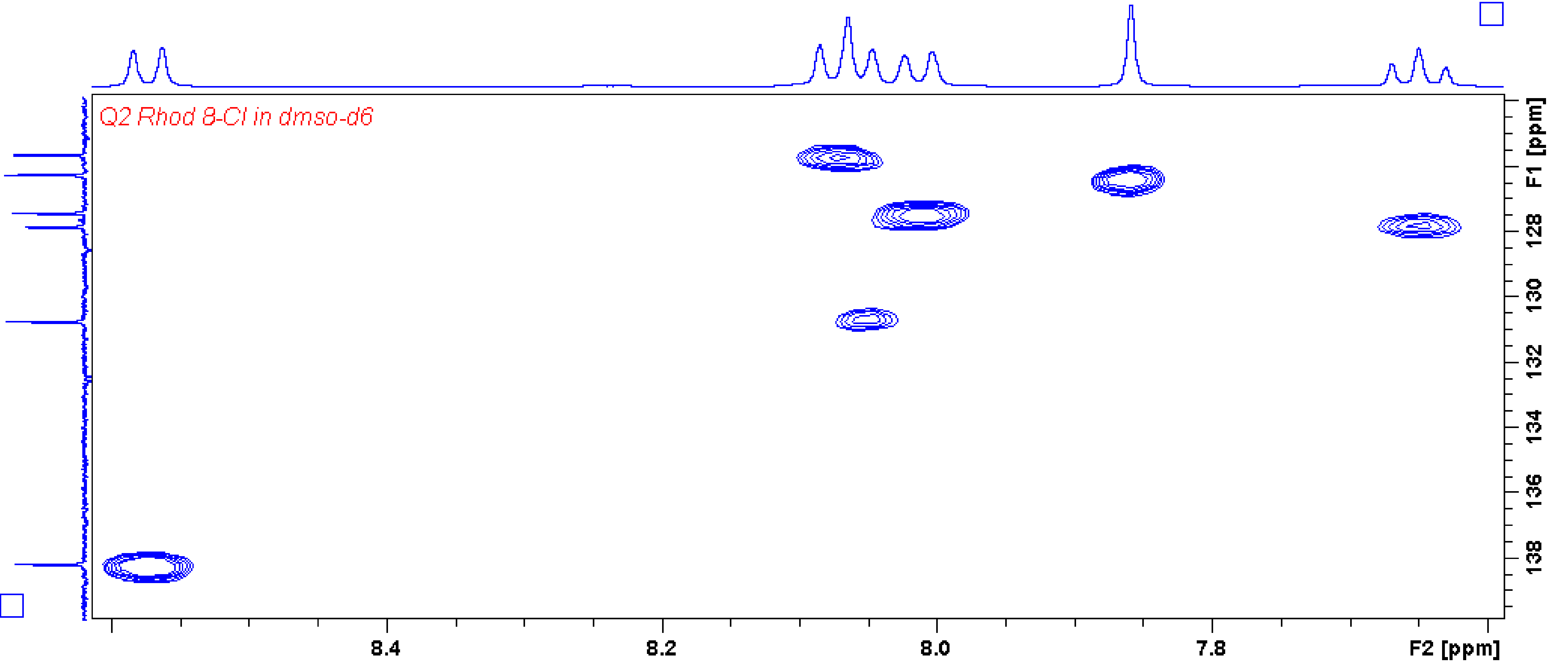
Q2 Rhod 8-Cl in dmso-d6
F1 [ppm]
F2 [ppm]
8.4
8.2
8.0
7.8
128
130
132
134
136
138

HSQC of **C5b**

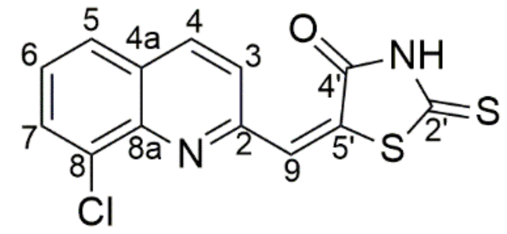
O
NH
S
S
N
Cl
5
4a
4
3
6
7
8
8a
2
9
4'
5'
2'

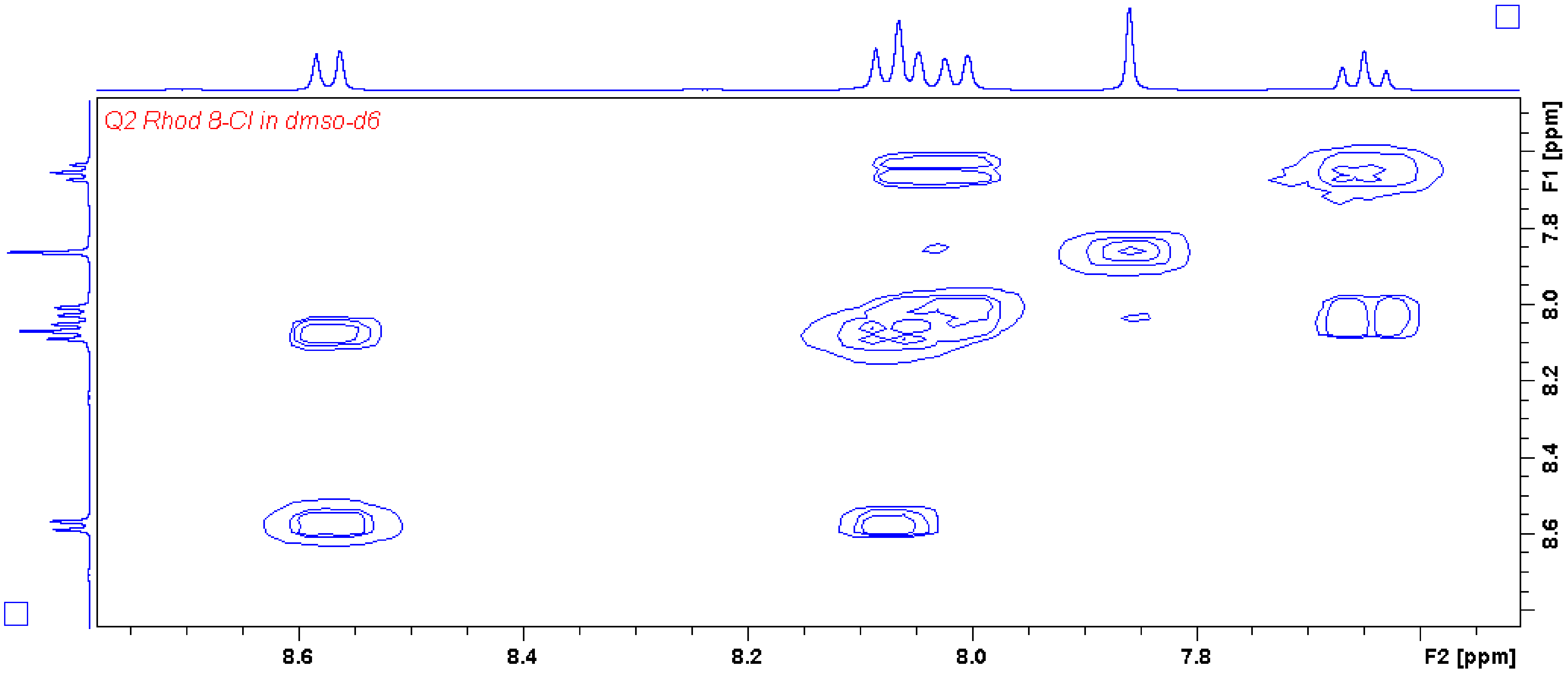
Q2 Rhod 8-Cl in dmso-d6
F1 [ppm]
7.8
8.0
8.2
8.4
8.6
F2 [ppm]

COSY of **C5b**

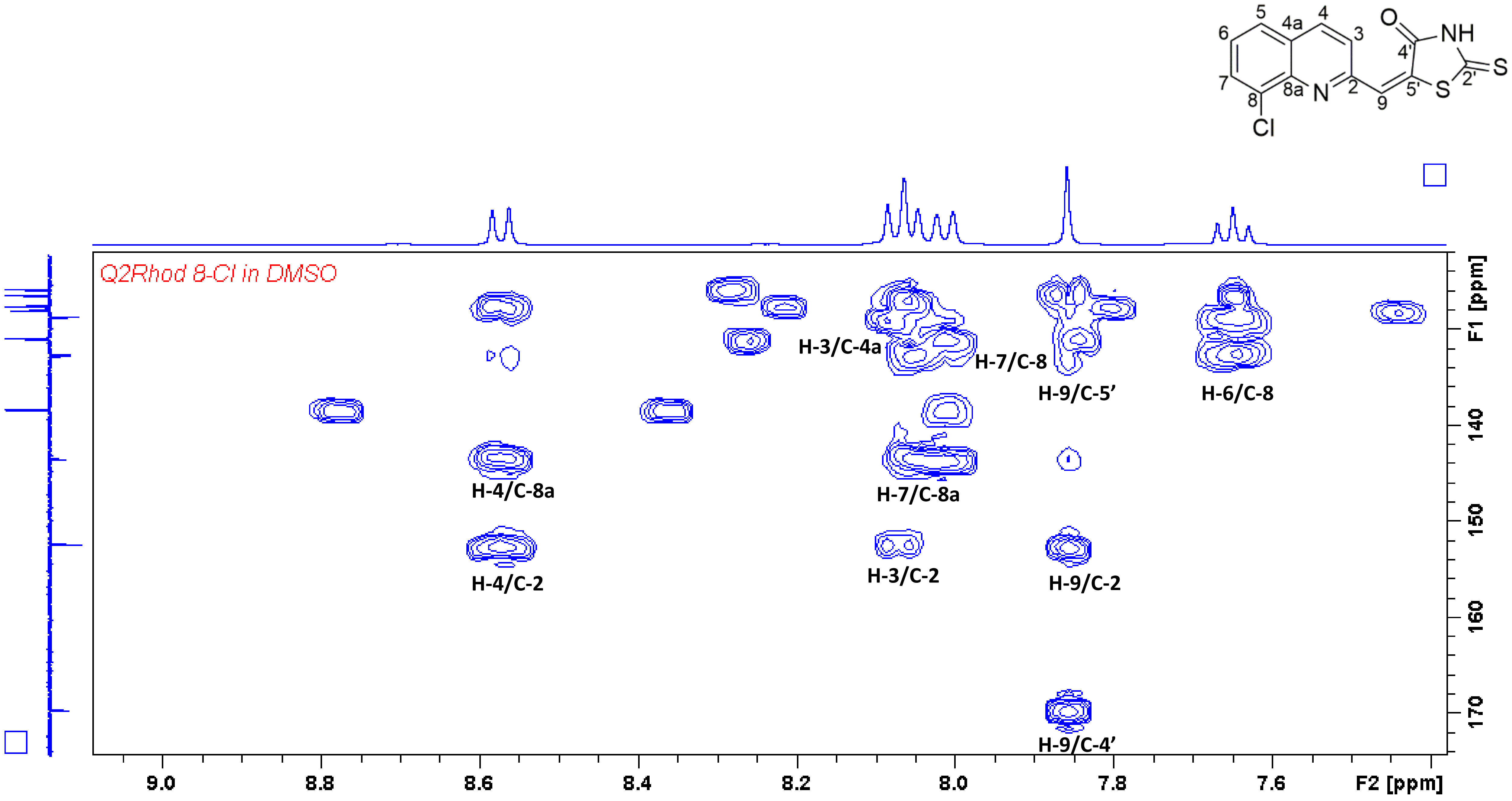

Q2Rhod 8-Cl in DMSO
H-3/C-4a
H-7/C-8
H-9/C-5'
H-6/C-8
H-4/C-8a
H-7/C-8a
H-4/C-2
H-3/C-2
H-9/C-2
H-9/C-4'
F1 [ppm]
F2 [ppm]

HMBC of **C5b**

Elemental Composition Report

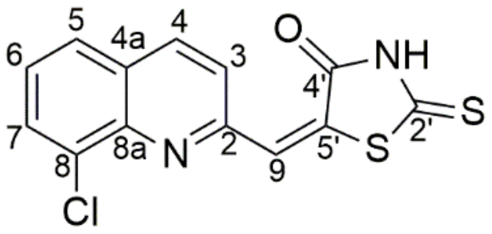

Single Mass Analysis

Tolerance = 5.0 PPM / DBE: min = -1.5, max = 100.0
Element prediction: Off
Number of isotope peaks used for i-FIT = 2

Monoisotopic Mass, Even Electron Ions
110 formula(e) evaluated with 1 results within limits (up to 20 best isotopic matches for each mass)
Elements Used:
C: 10-15 H: 5-10 N: 0-5 O: 0-5 S: 0-2 Cl: 0-1
Q2R (8-Cl) 52 (1.720) Cm (1:61)
TOF MS ES-

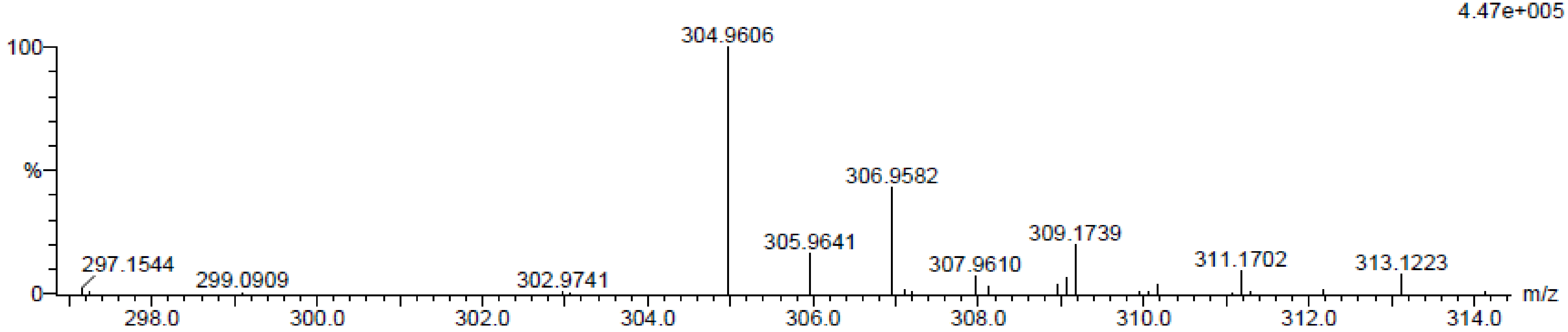

Minimum:				-1.5			
Maximum:		5.0	5.0	100.0			
Mass	Calc. Mass	mDa	PPM	DBE	i-FIT	i-FIT (Norm)	Formula
304.9606	304.9610	-0.4	-1.3	11.5	12.9	0.0	C13 H6 N2 O S2 Cl

High resolution mass spectrum of **C5b**

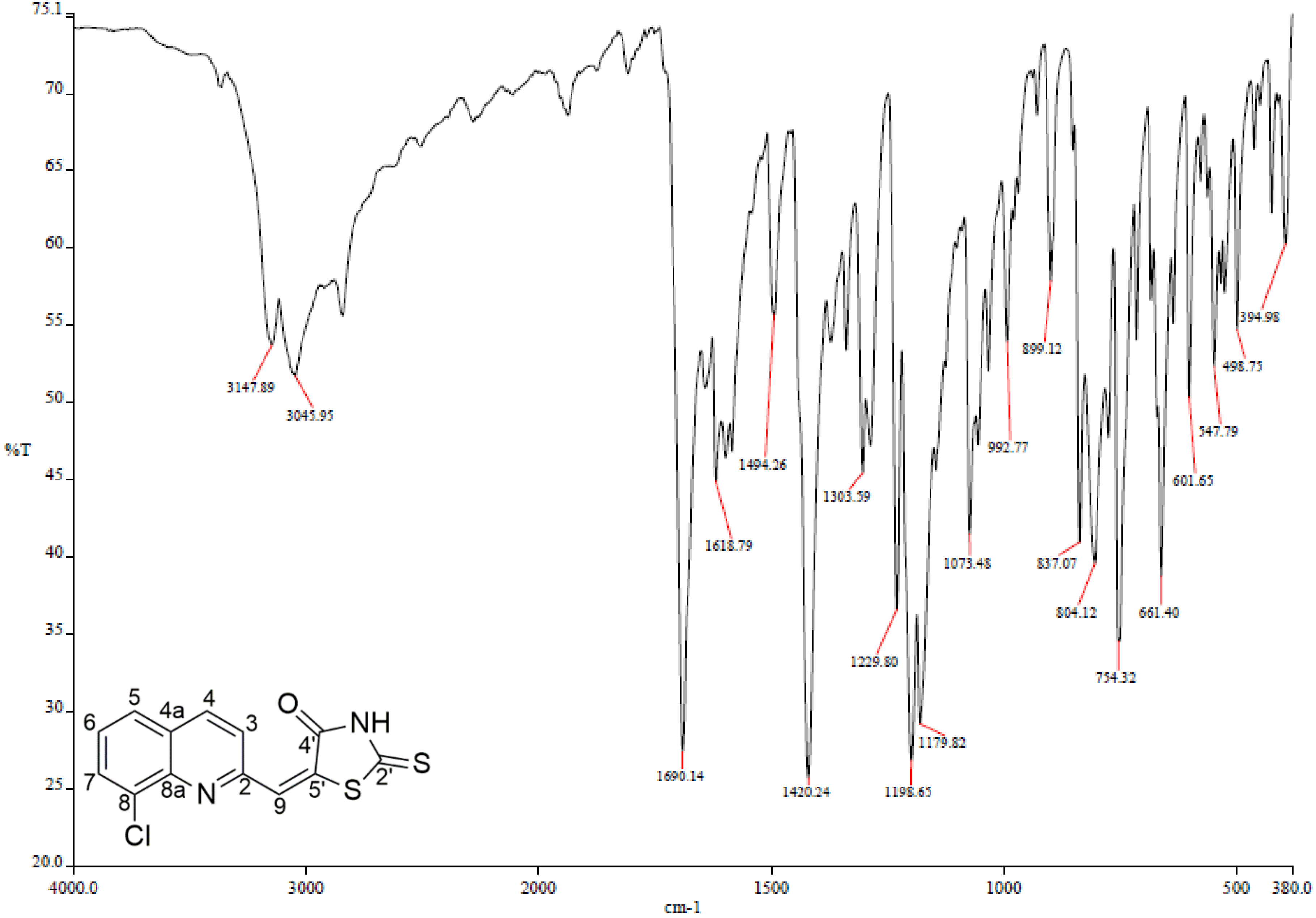

FTIR spectrum of **C5b**

Overlay Spectrum Graph Report

06/10/2017 11:28:23 AM

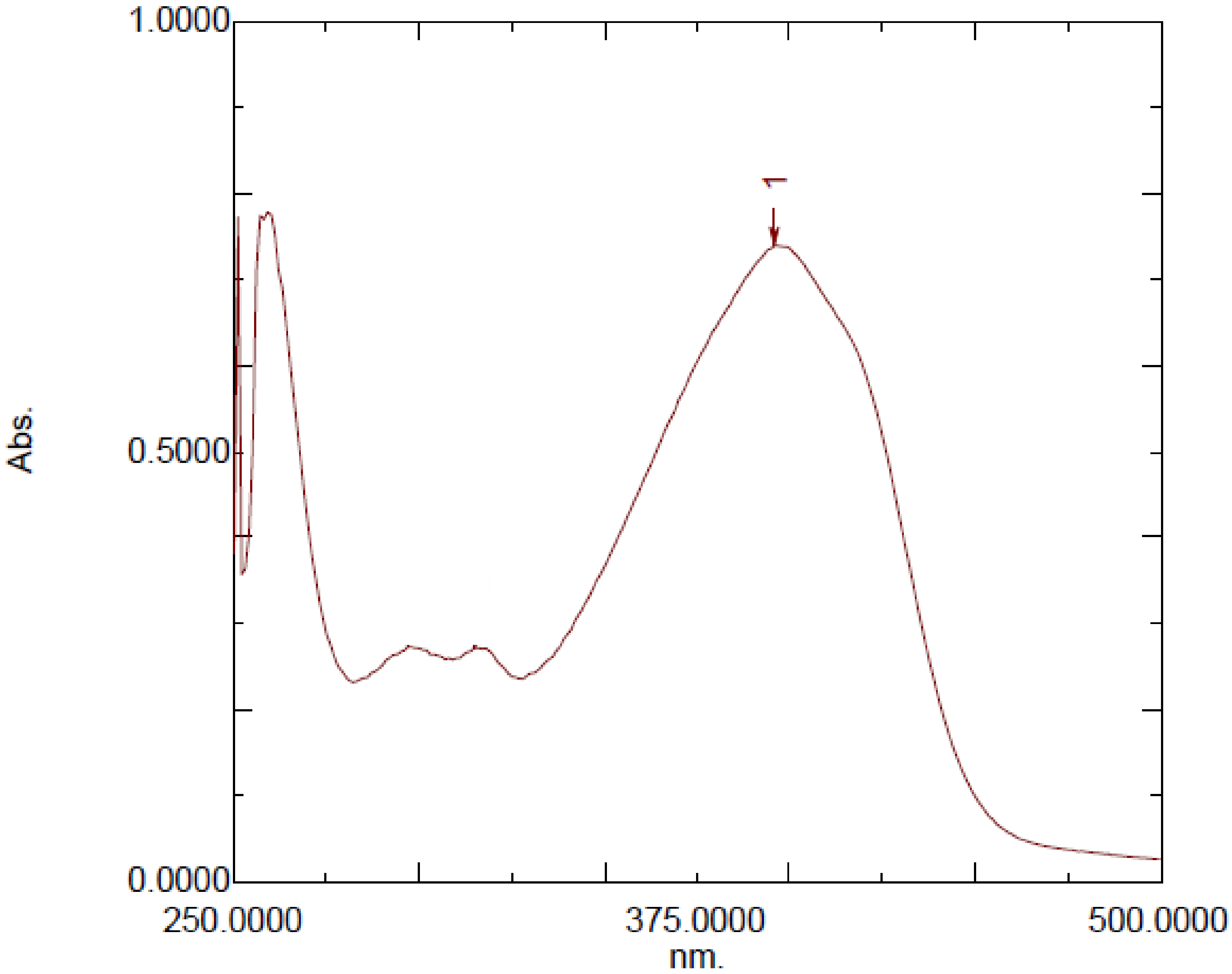

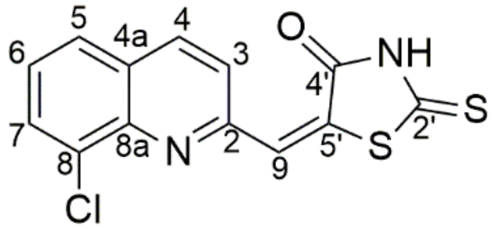

λ	absorbance	logε
396	0.740	4.66

UV spectrum of **C5b**

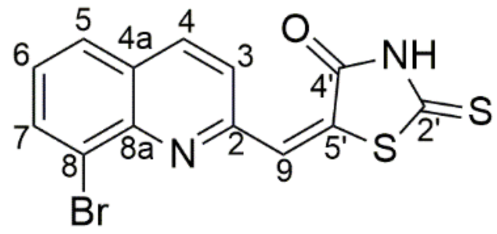

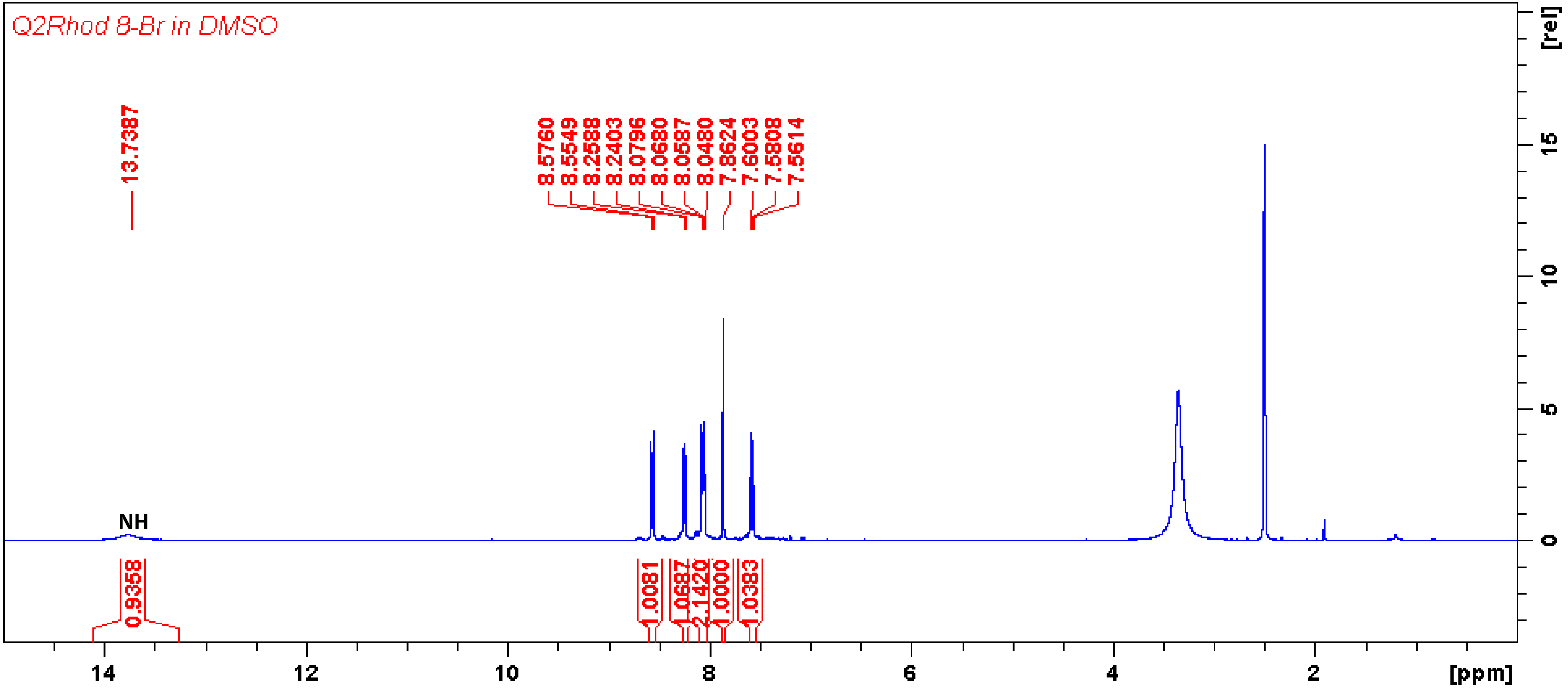

[1]H NMR spectrum of **C5c**

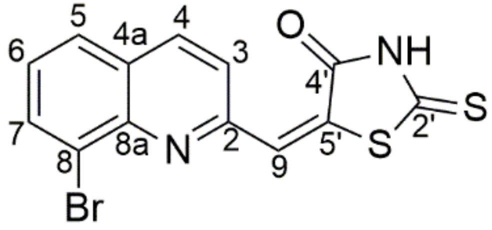

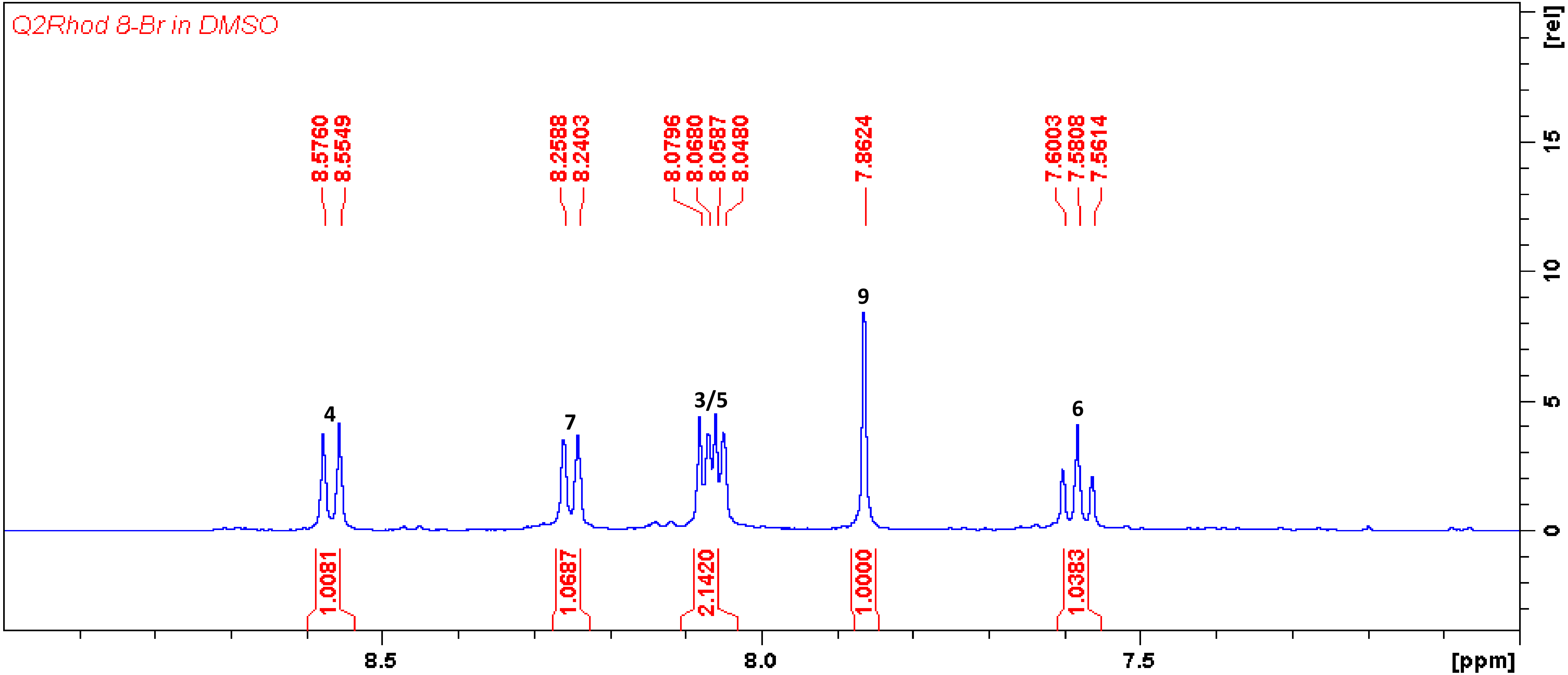

Expanded ^{1}H NMR spectrum of **C5c**

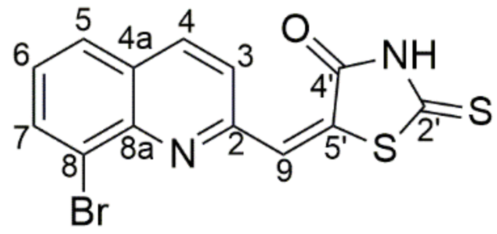

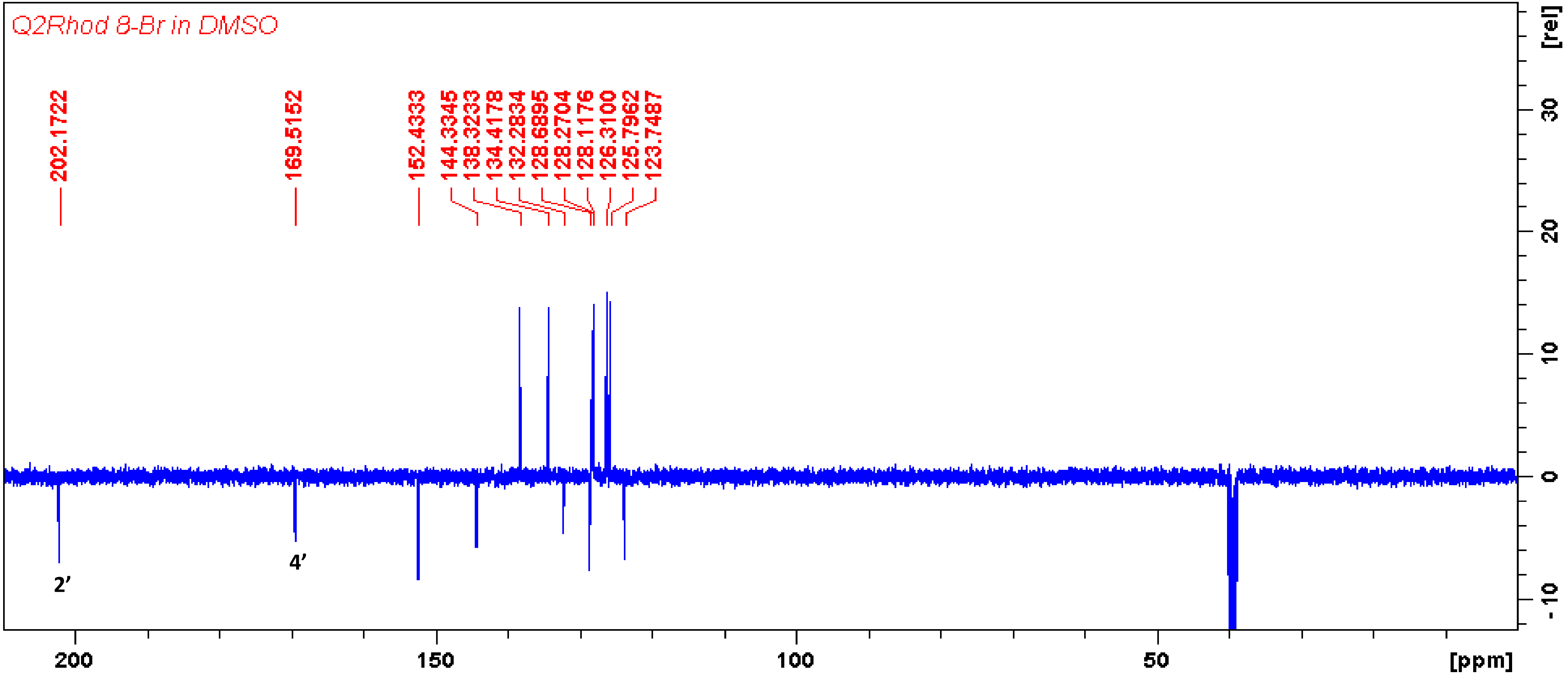

^{13}C NMR spectrum of **C5c**

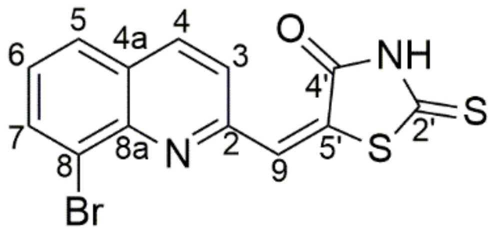

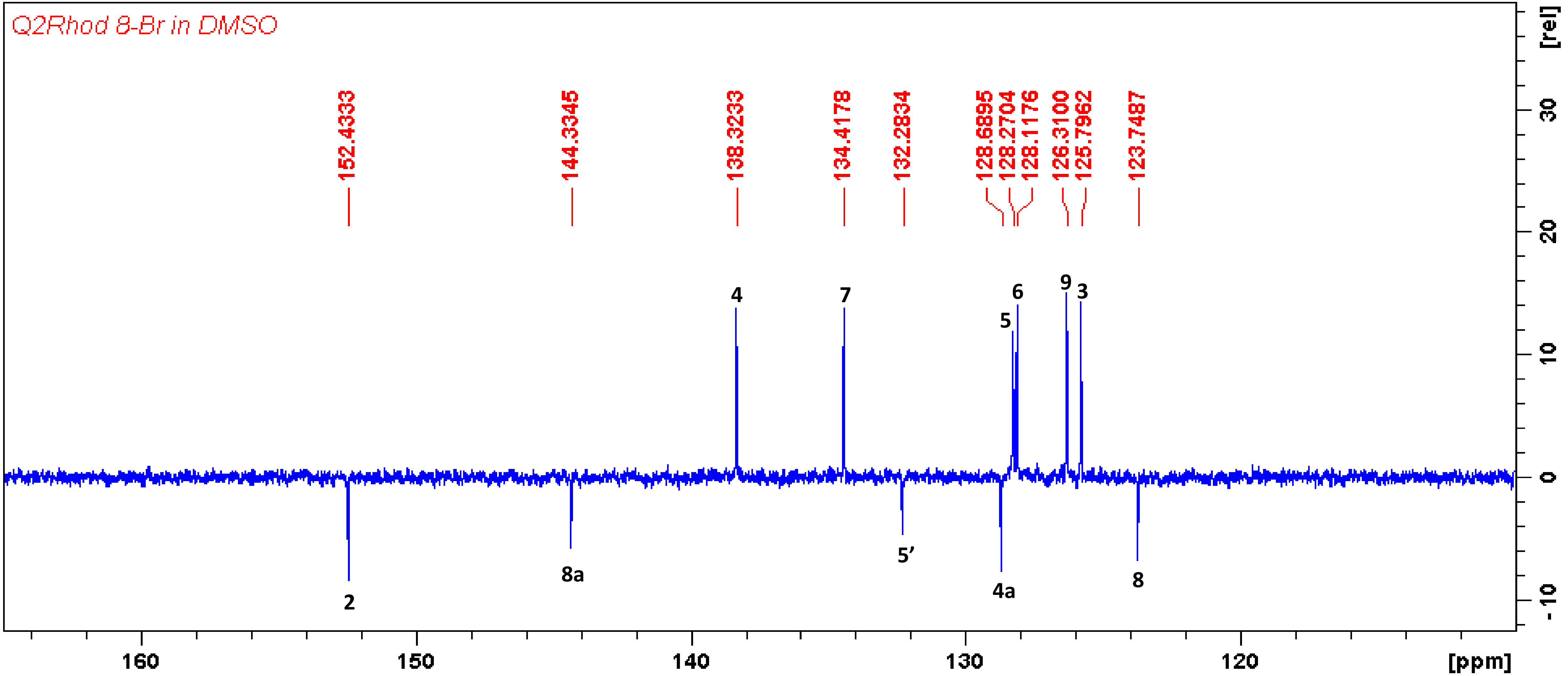

Expanded ^{13}C NMR spectrum of **C5c**

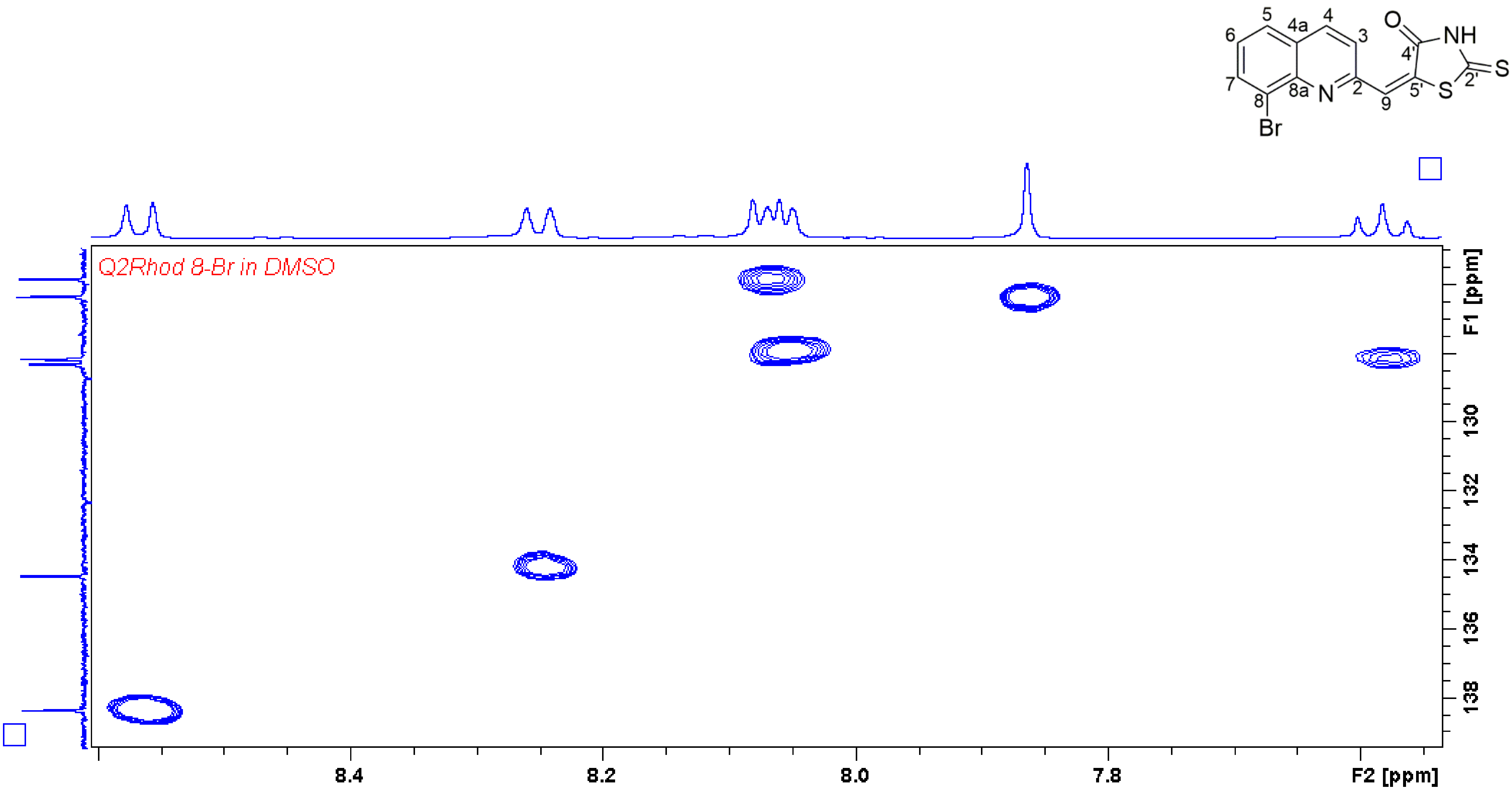

HSQC of **C5c**

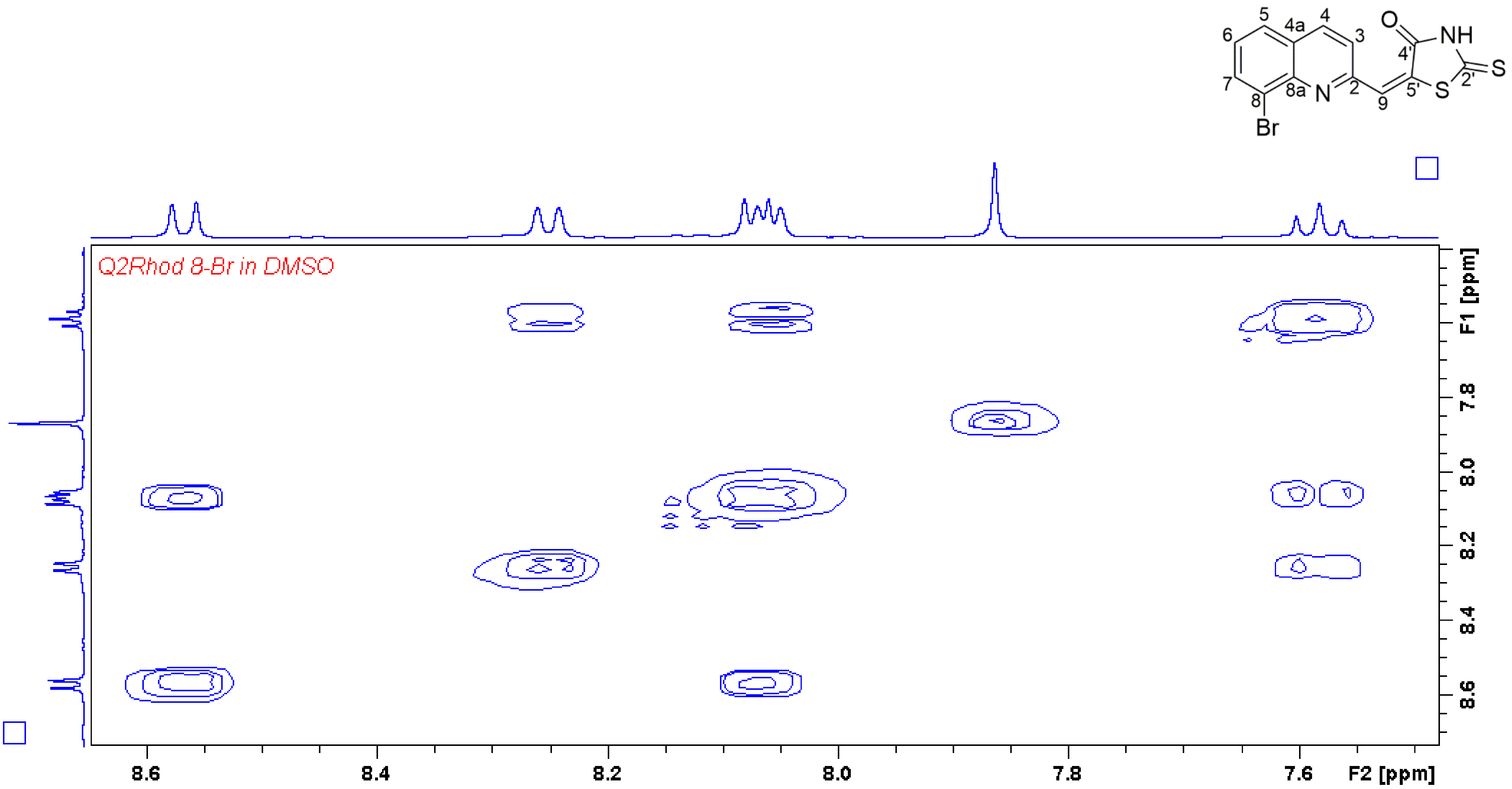
Q2Rhod 8-Br in DMSO
F1 [ppm]
F2 [ppm]
8.6
8.4
8.2
8.0
7.8
7.6
O
NH
S
S
N
Br
4'
2'
5'
9
2
3
4
4a
5
6
7
8
8a

COSY of **C5c**

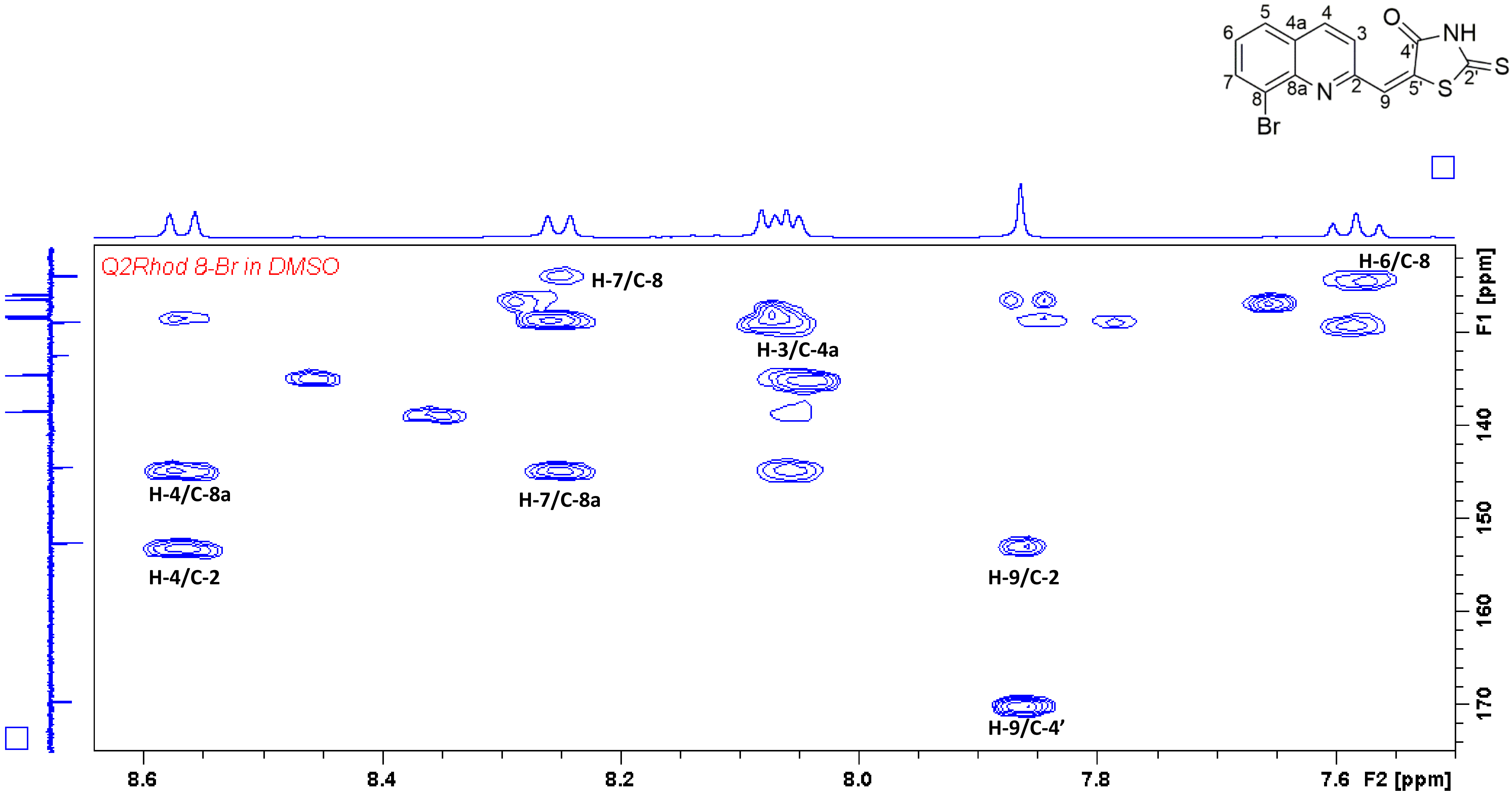
Q2Rhod 8-Br in DMSO
H-7/C-8
H-6/C-8
H-3/C-4a
H-4/C-8a
H-7/C-8a
H-4/C-2
H-9/C-2
H-9/C-4'
F1 [ppm]
F2 [ppm]
8.6
8.4
8.2
8.0
7.8
7.6
140
150
160
170
Br
NH
O
S
N

HMBC of **C5c**

Elemental Composition Report

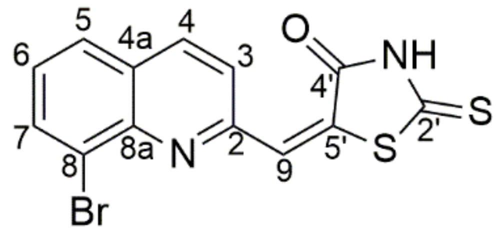

Single Mass Analysis

Tolerance = 5.0 PPM / DBE: min = -1.5, max = 100.0
Element prediction: Off
Number of isotope peaks used for i-FIT = 2

Monoisotopic Mass, Even Electron Ions
130 formula(e) evaluated with 1 results within limits (up to 20 best isotopic matches for each mass)
Elements Used:
C: 10-15 H: 5-10 N: 0-5 O: 0-5 S: 0-2 Br: 0-1

Q2R (8-Br) 55 (1.821) Cm (1:61)
TOF MS ES-

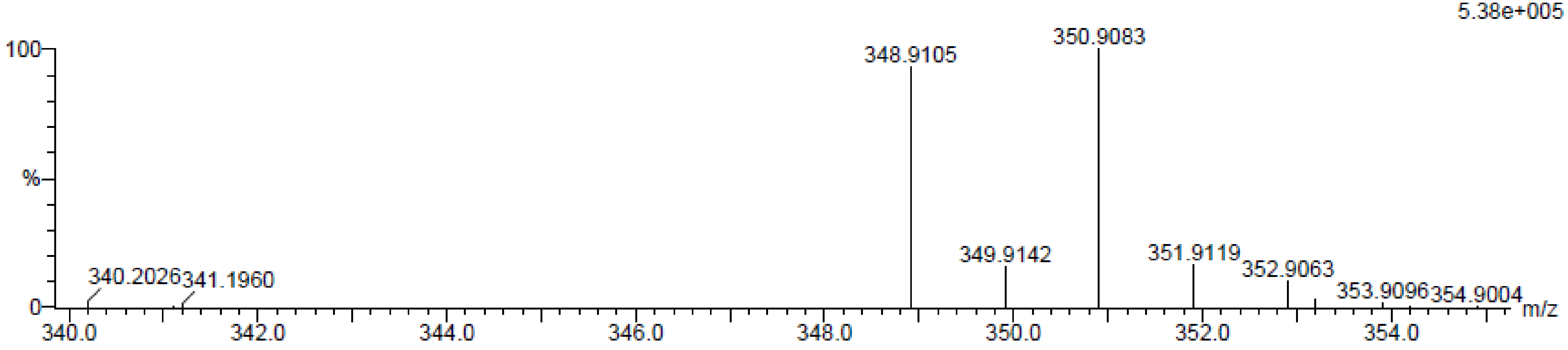

Minimum:				-1.5			
Maximum:		5.0	5.0	100.0			
Mass	Calc. Mass	mDa	PPM	DBE	i-FIT	i-FIT (Norm)	Formula
348.9105	348.9105	0.0	0.0	11.5	11.8	0.0	C13 H6 N2 O S2 Br

High resolution mass spectrum of **C5c**

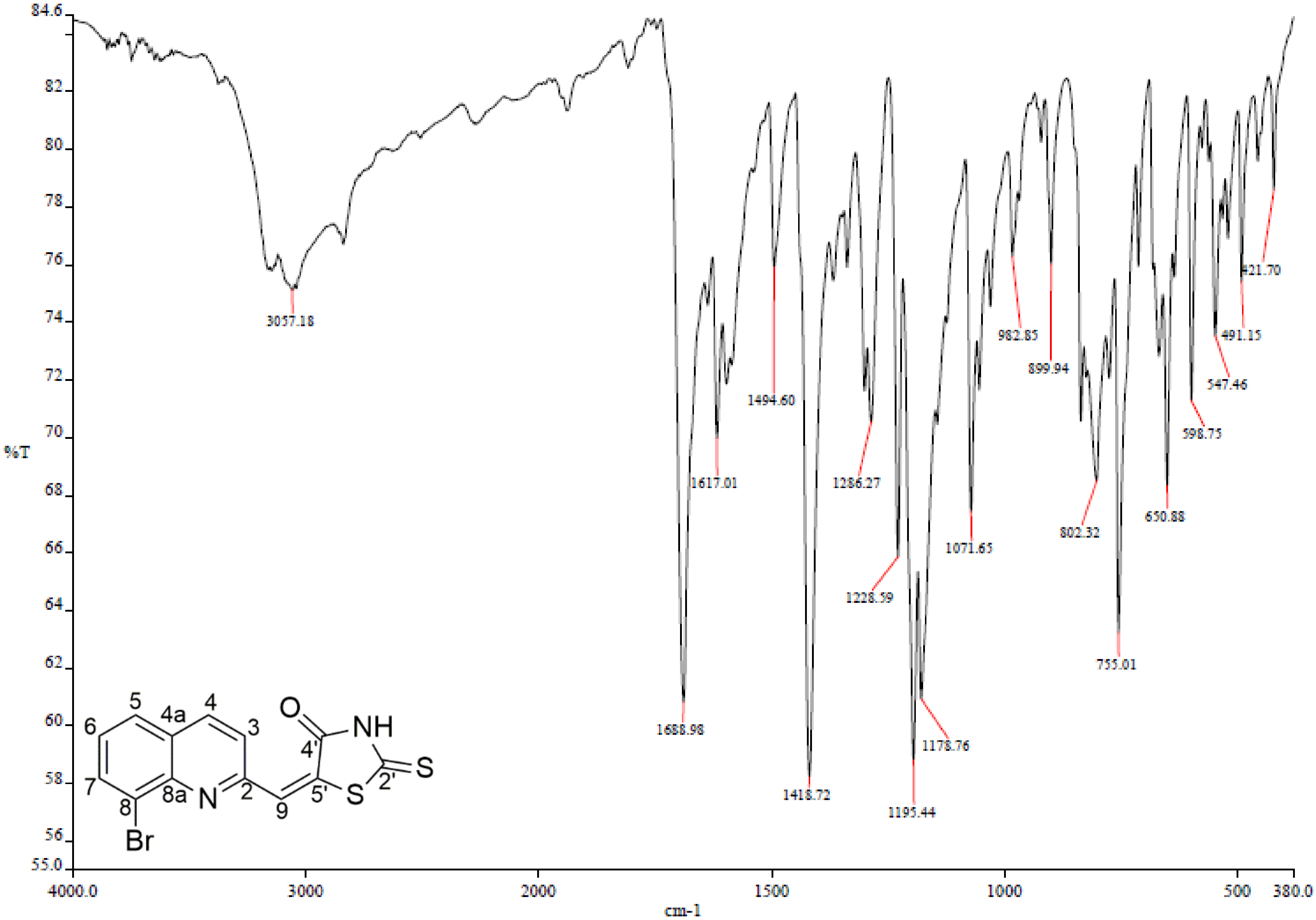

FTIR spectrum of **C5c**

Overlay Spectrum Graph Report

06/10/2017 11:30:22 AM

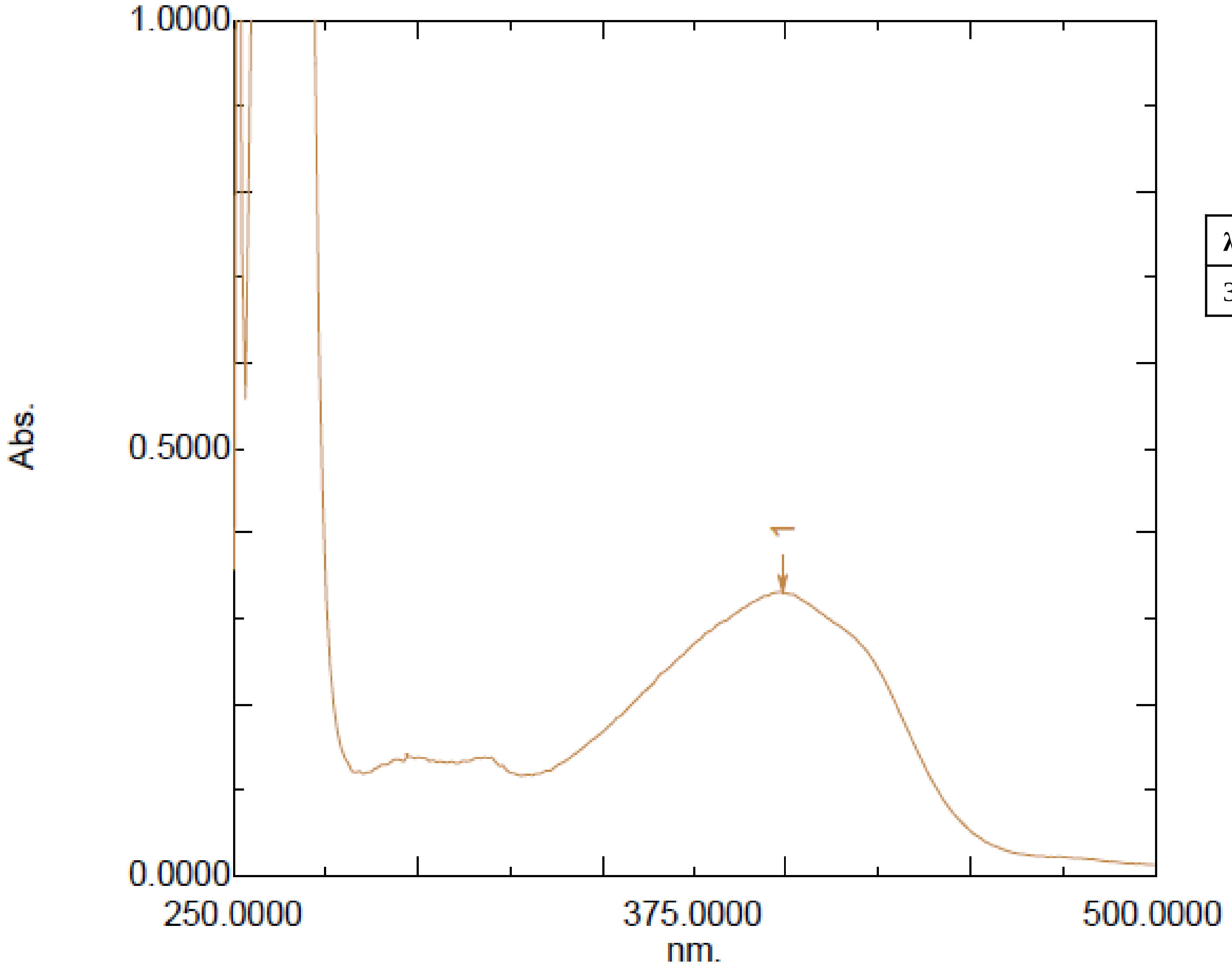

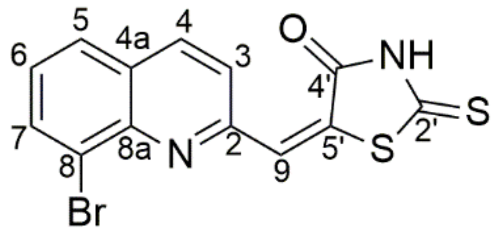

λ	absorbance	logε
398	0.331	4.37

UV spectrum of **C5c**

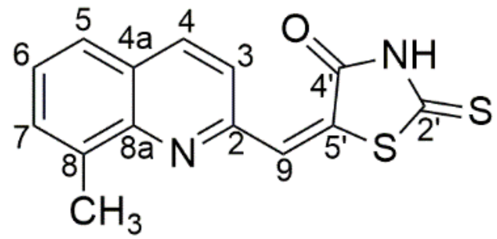

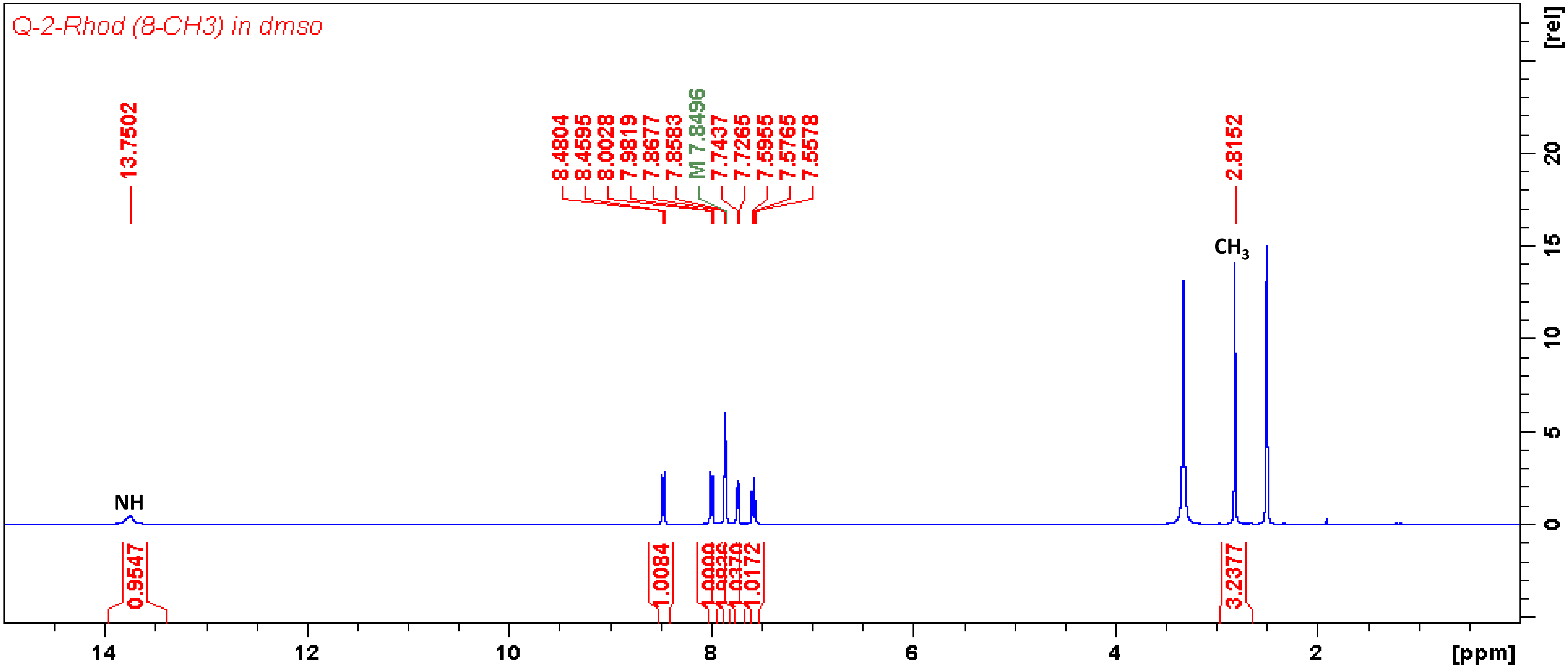

^{1}H NMR spectrum of **C5d**

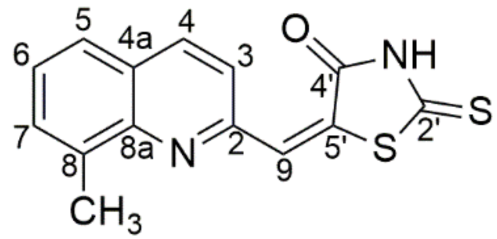

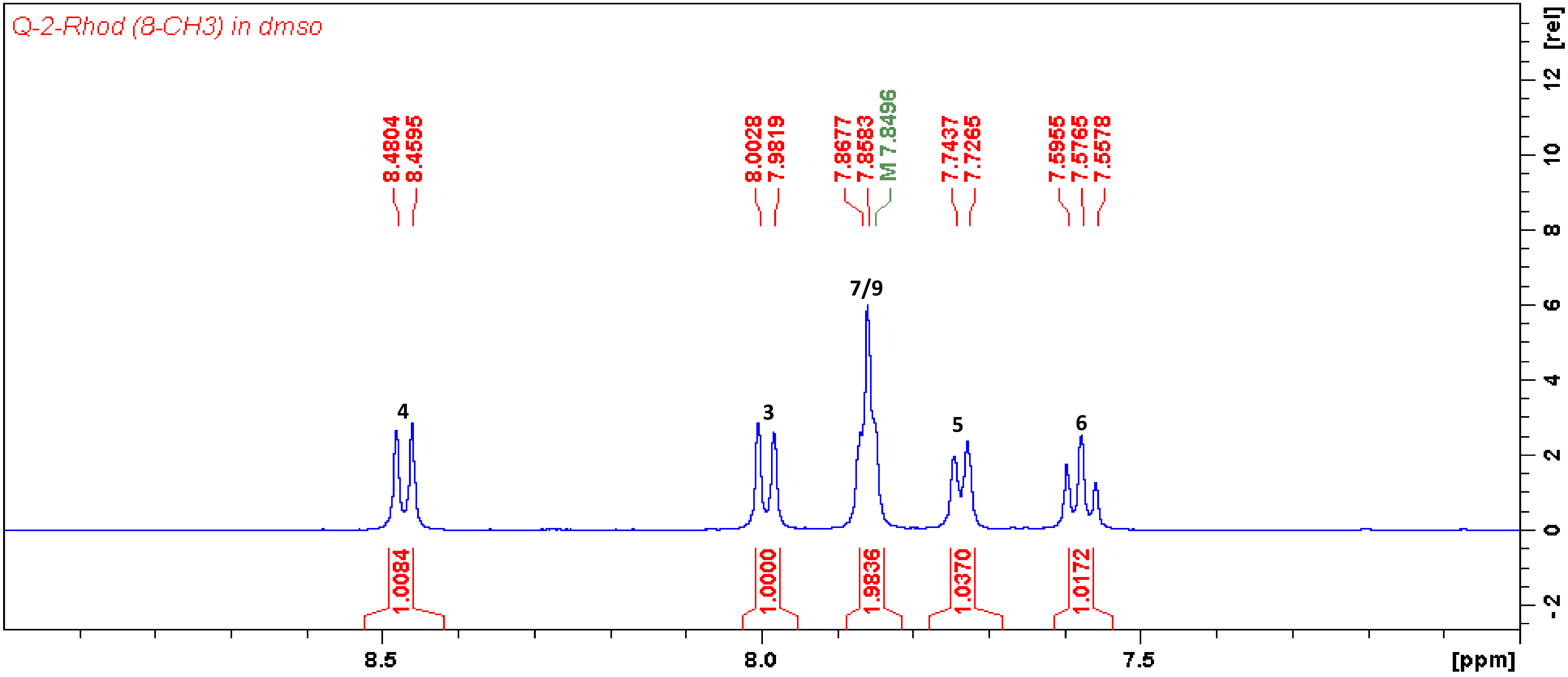

Expanded ^{1}H NMR spectrum of **C5d**

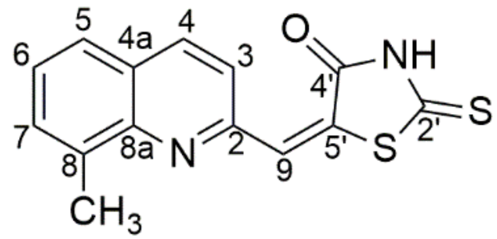

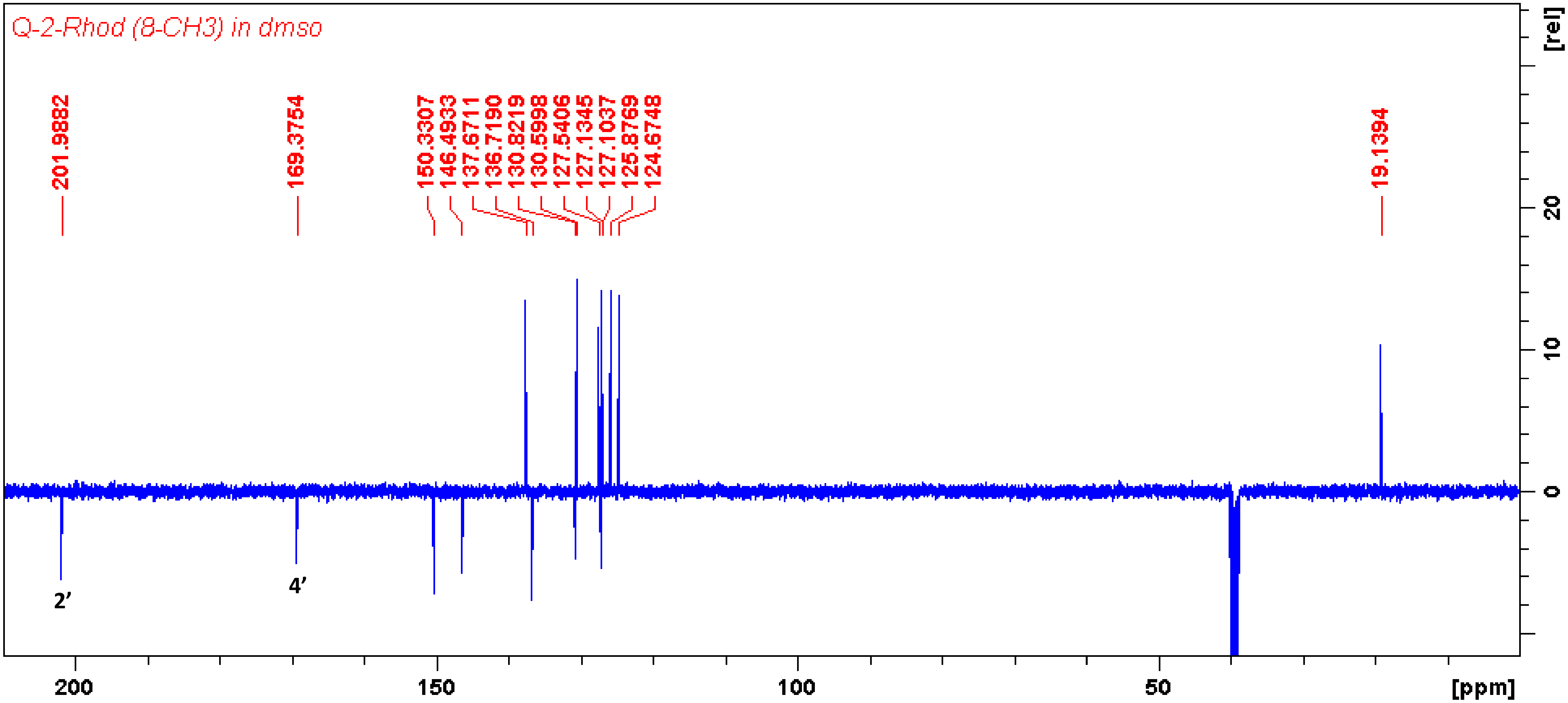

^{13}C NMR spectrum of **C5d**

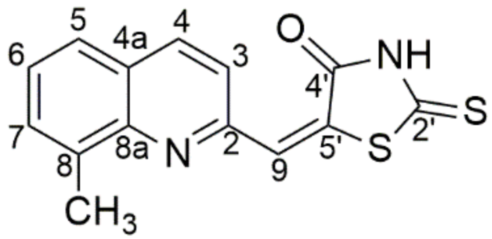

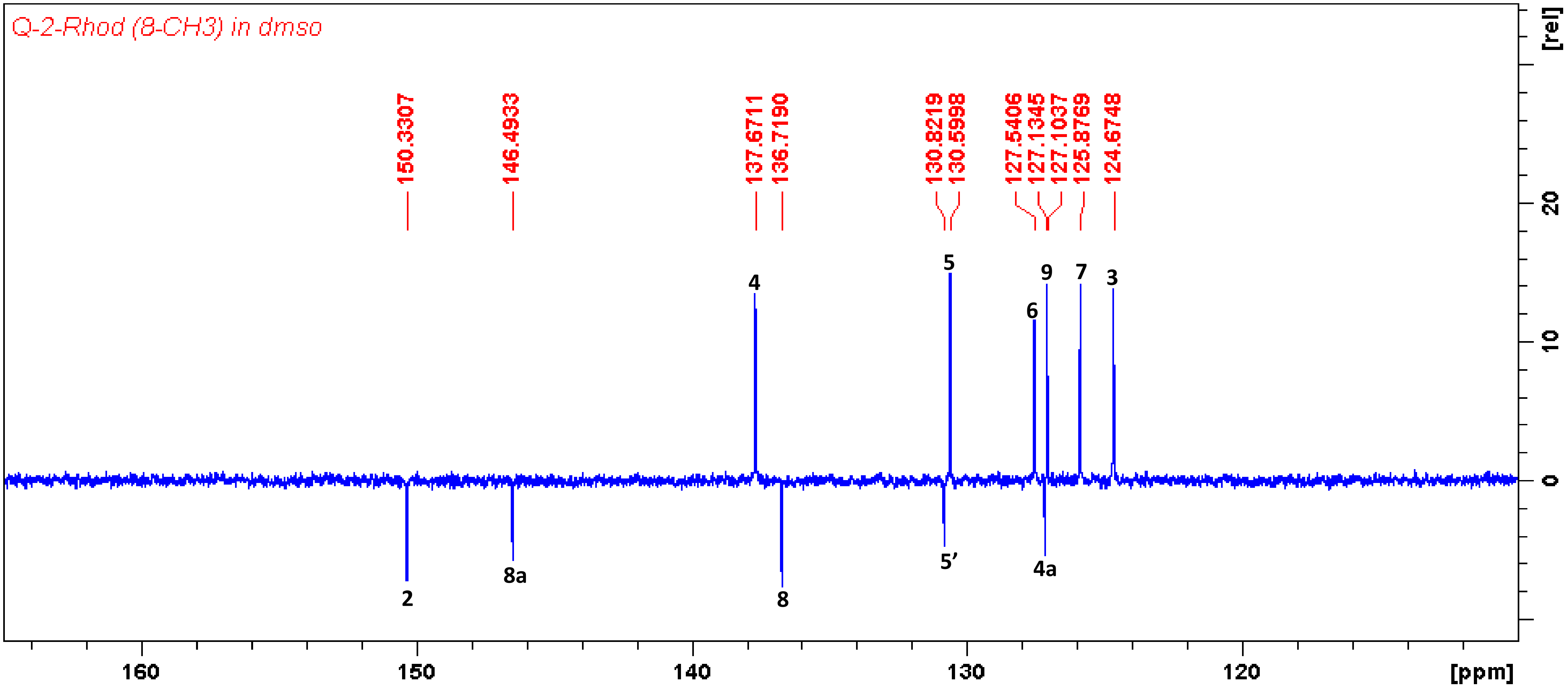

Expanded ^{13}C NMR spectrum of **C5d**

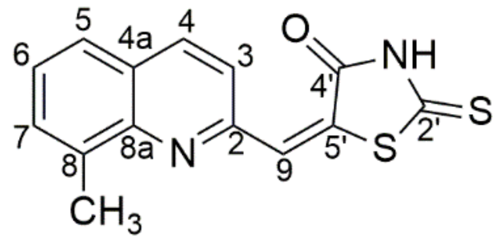

O
NH
S
S
N
CH3
5
4a
4
3
6
7
8
8a
2
9
4'
5'
2'

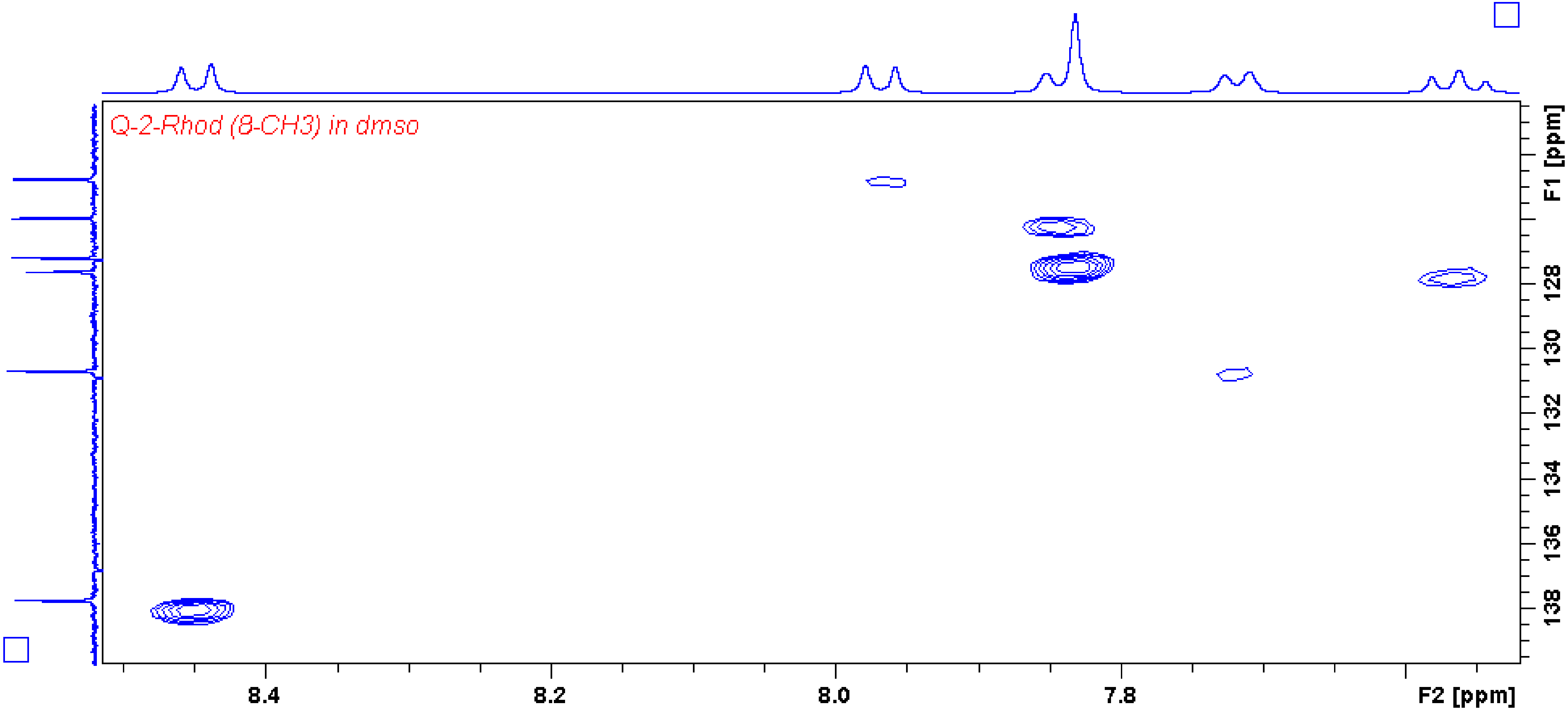

Q-2-Rhod (8-CH3) in dmso
F1 [ppm]
128
130
132
134
136
138
8.4
8.2
8.0
7.8
F2 [ppm]

HSQC of **C5d**

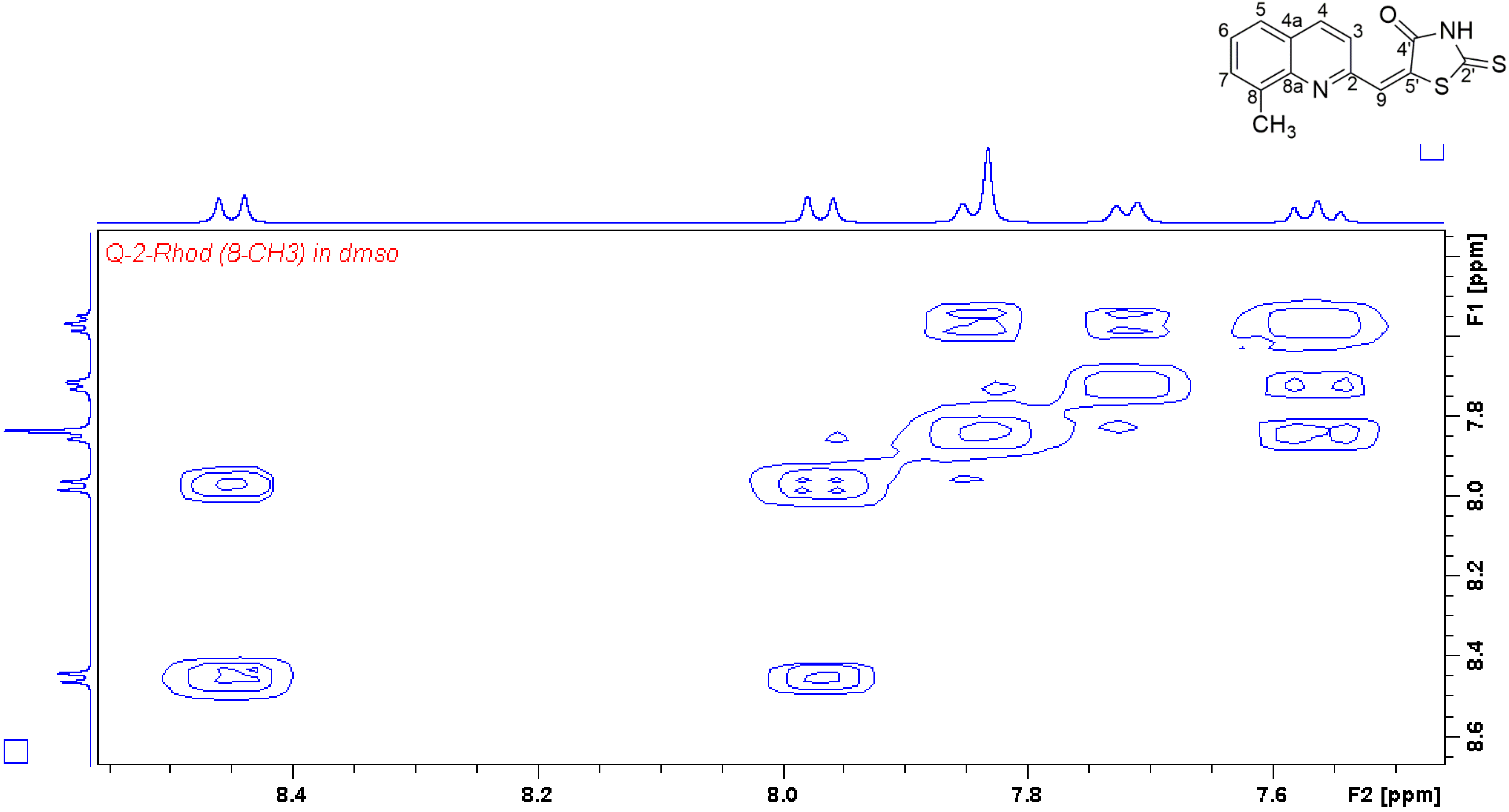
Q-2-Rhod (8-CH3) in dmso
F1 [ppm]
F2 [ppm]
8.4
8.2
8.0
7.8
7.6
8.6
5
4a
4
3
6
7
8
8a
N
2
9
5'
4'
2'
O
NH
S
S
CH3

COSY of **C5d**

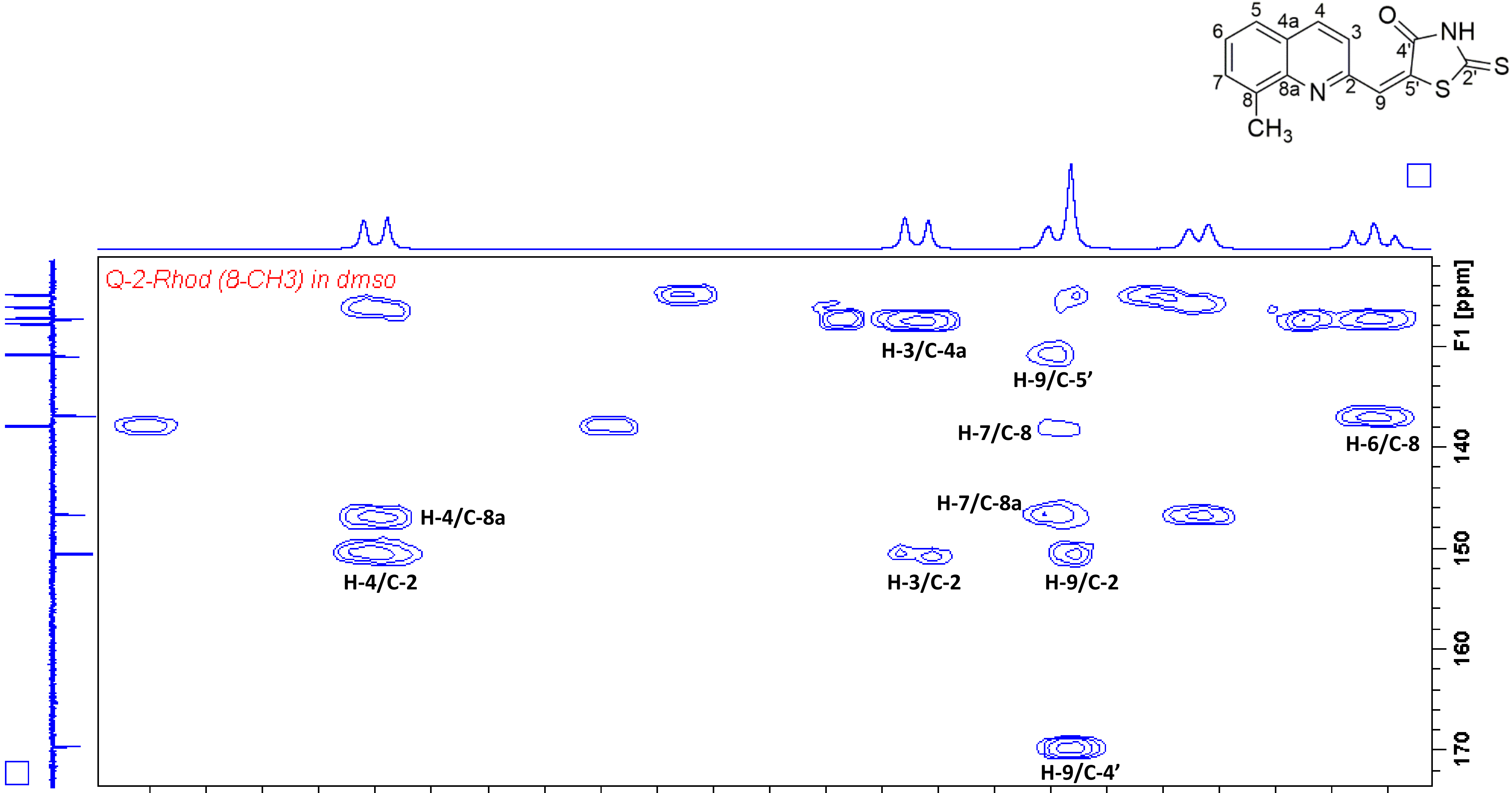

5
4a
4
3
6
7
8
8a
N
2
9
5'
S
2'
S
4'
O
NH
CH3
Q-2-Rhod (8-CH3) in dmso
H-3/C-4a
H-9/C-5'
H-7/C-8
H-6/C-8
H-7/C-8a
H-4/C-8a
H-4/C-2
H-3/C-2
H-9/C-2
H-9/C-4'
F1 [ppm]
140
150
160
170
8.6
8.4
8.2
8.0
7.8
F2 [ppm]

HMBC of **C5d**

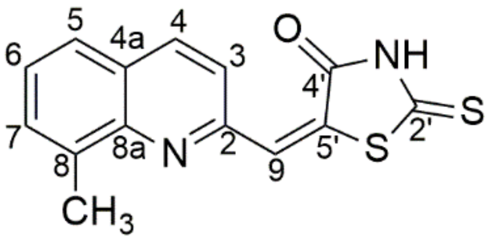

Elemental Composition Report

Single Mass Analysis

Tolerance = 5.0 PPM / DBE: min = -1.5, max = 100.0
Element prediction: Off
Number of isotope peaks used for i-FIT = 2

Monoisotopic Mass, Even Electron Ions
51 formula(e) evaluated with 1 results within limits (up to 20 best isotopic matches for each mass)
Elements Used:
C: 10-15 H: 5-10 N: 0-5 O: 0-5 S: 0-2
Q2R (8-CH3) 16 (0.505) Cm (1:61)
TOF MS ES-

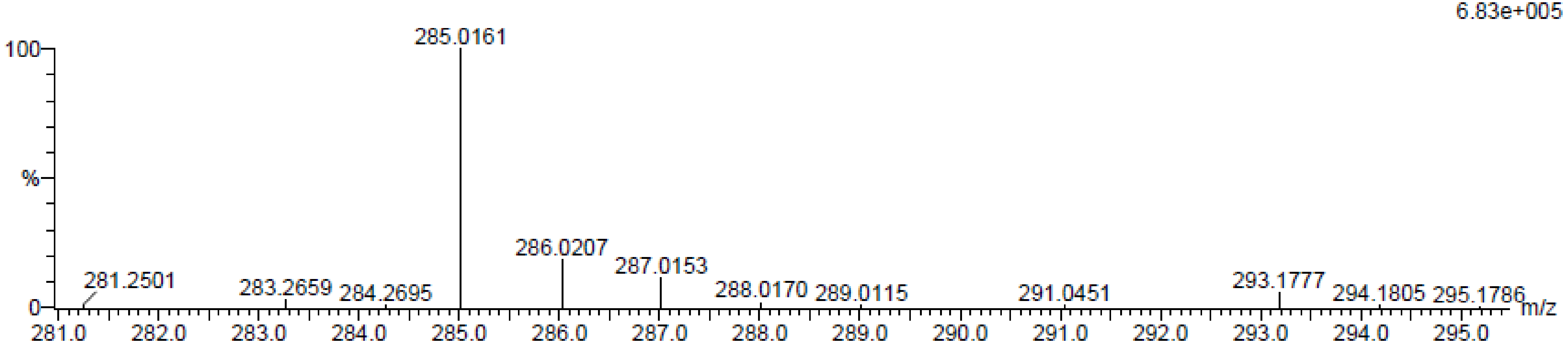

Minimum:				-1.5			
Maximum:		5.0	5.0	100.0			
Mass	Calc. Mass	mDa	PPM	DBE	i-FIT	i-FIT (Norm)	Formula
285.0161	285.0156	0.5	1.8	11.5	17.8	0.0	C14 H9 N2 O S2

High resolution mass spectrum of **C5d**

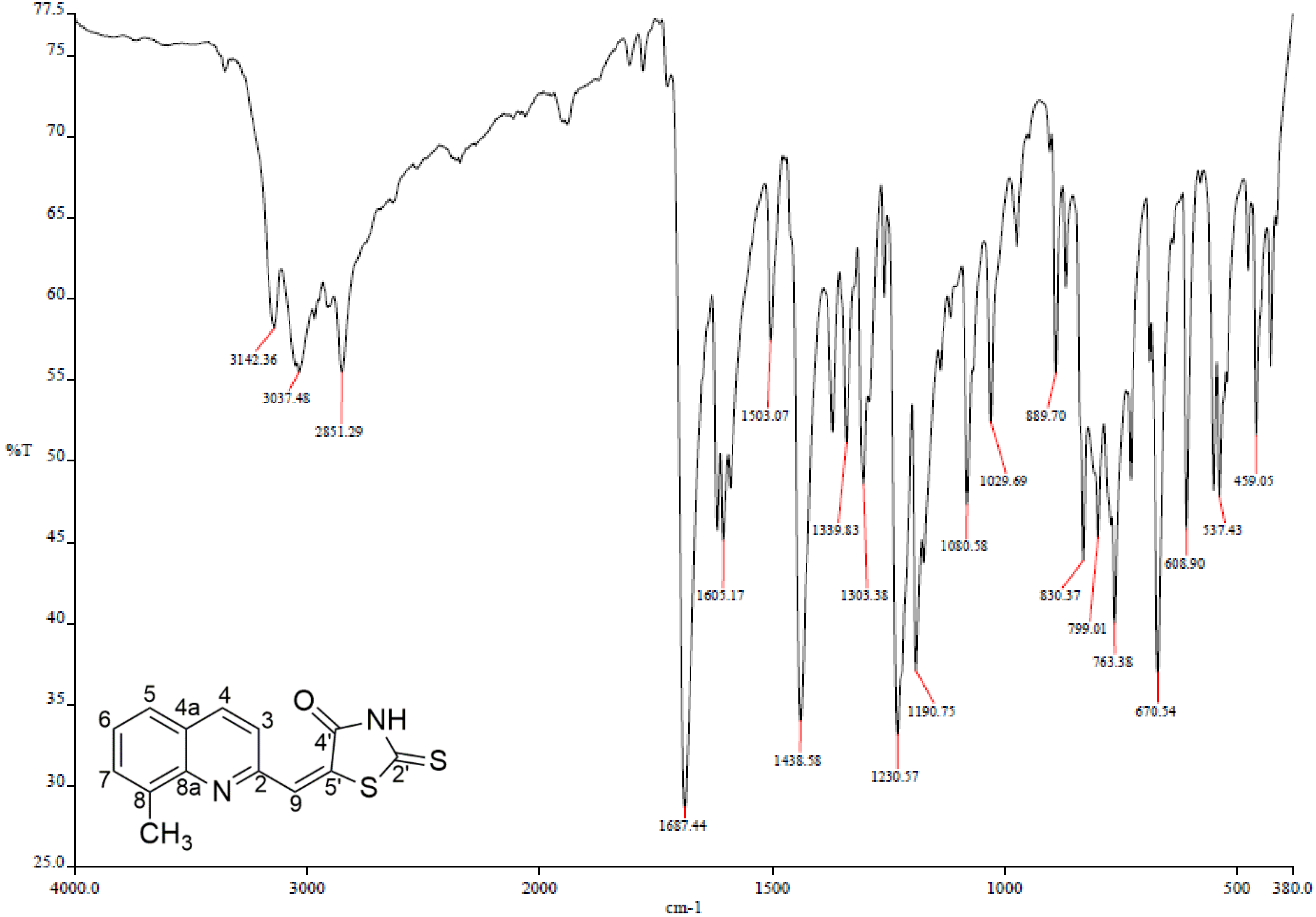

FTIR spectrum of **C5d**

Overlay Spectrum Graph Report

06/10/2017 11:28:58 AM

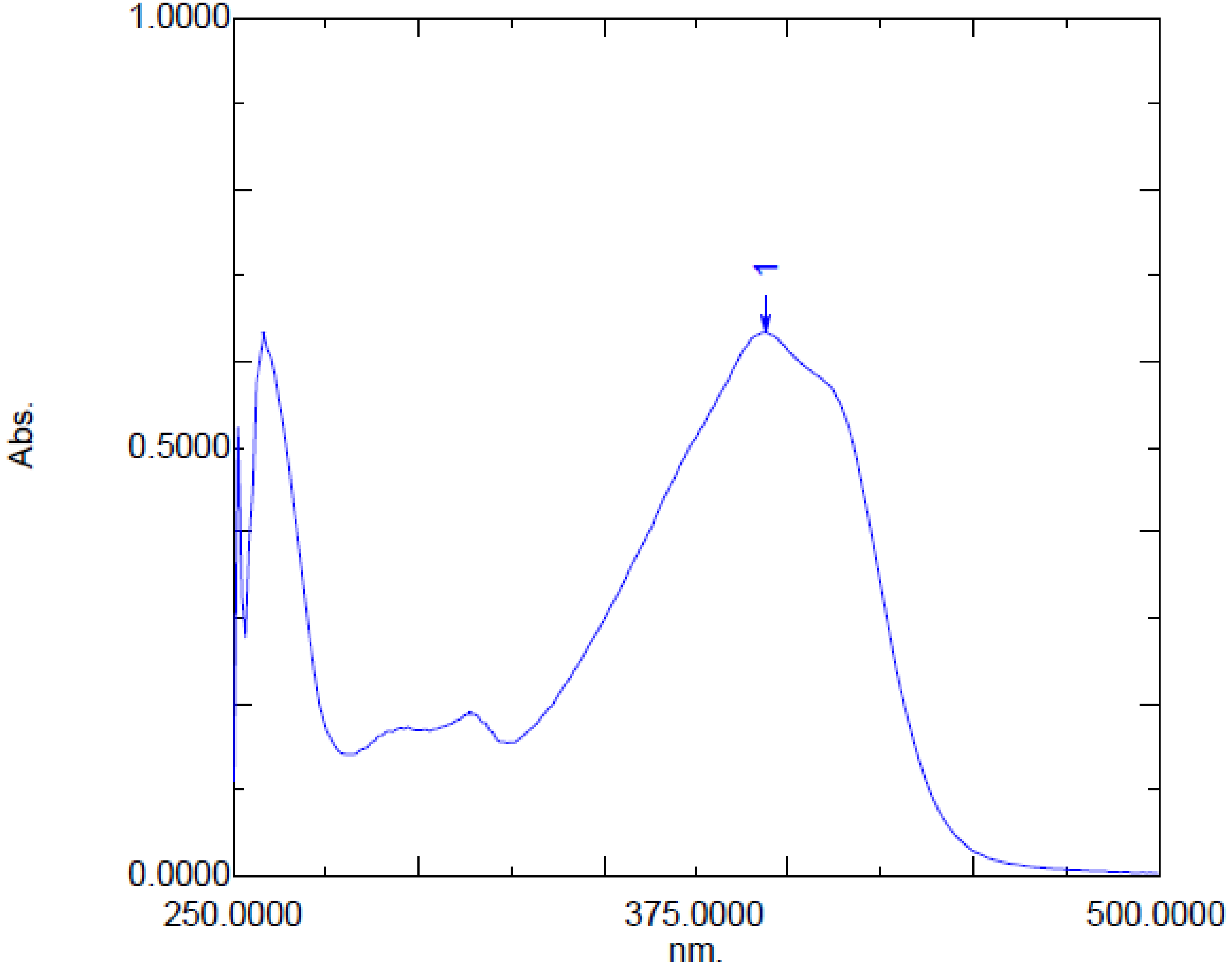

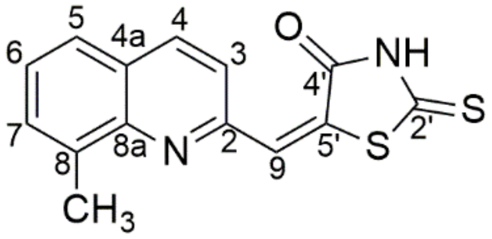

λ	absorbance	logε
394	0.634	4.56

UV spectrum of **C5d**

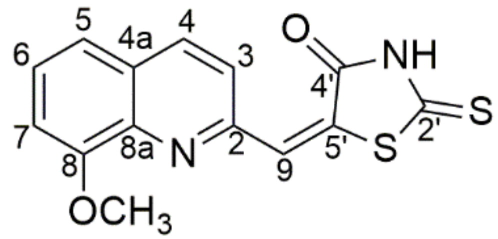

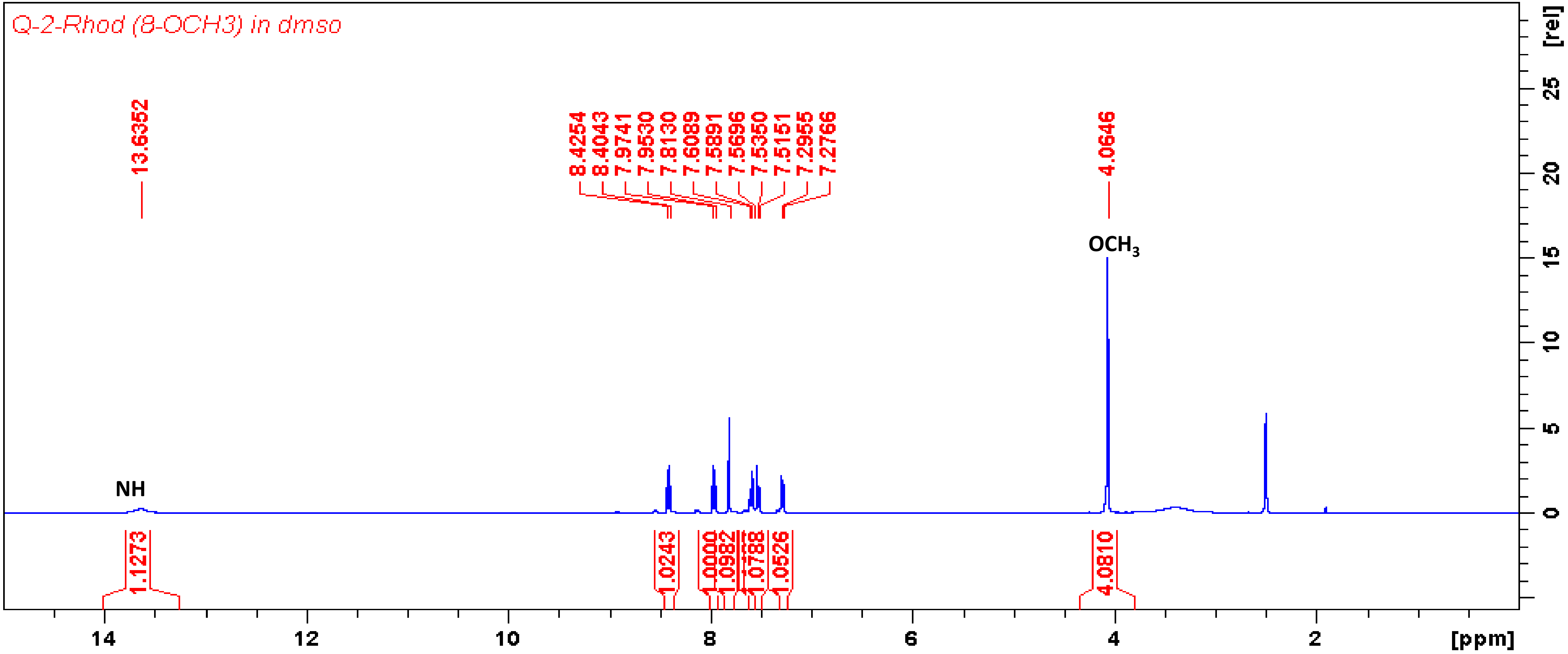

^{1}H NMR spectrum of **C5e**

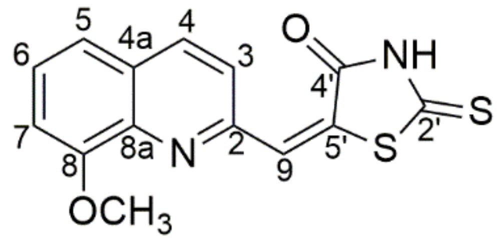

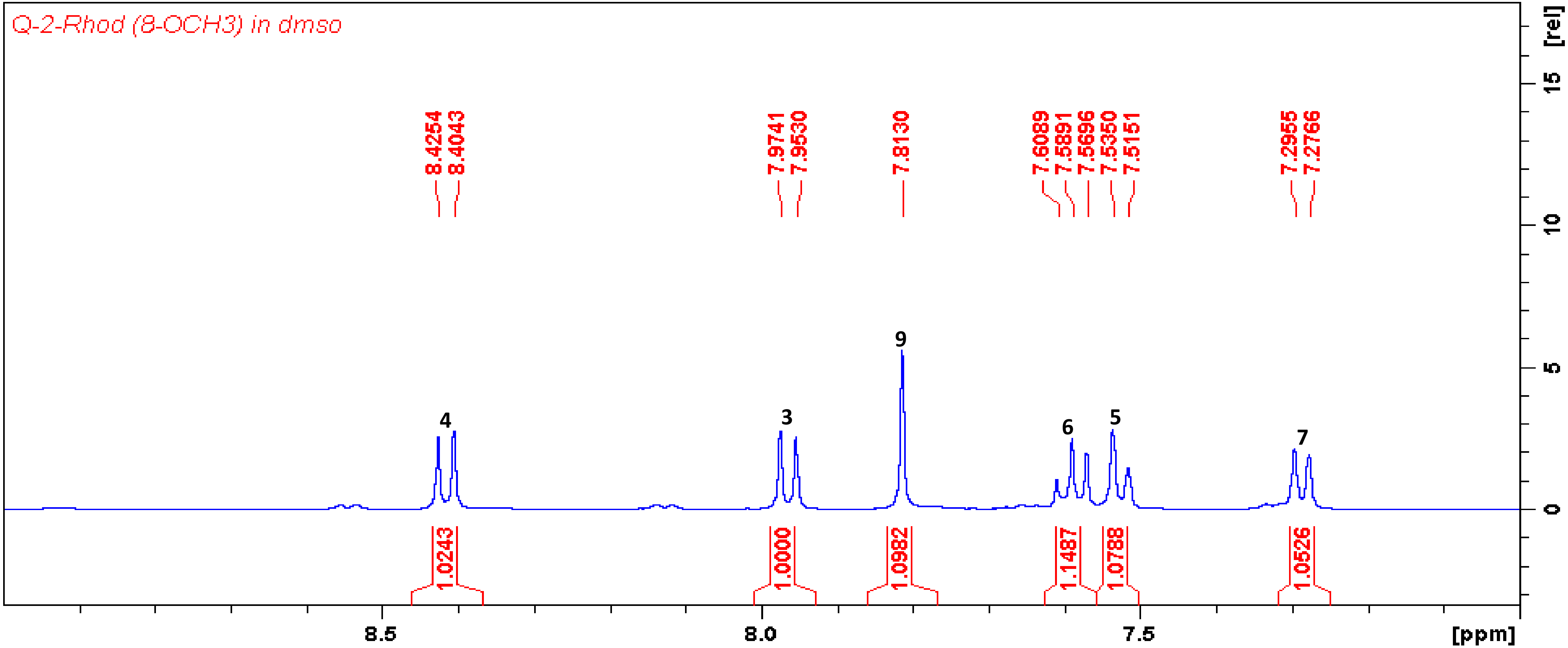

Expanded ^{1}H NMR spectrum of **C5e**

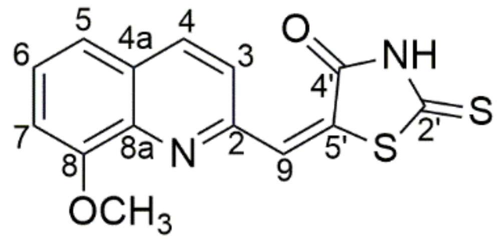

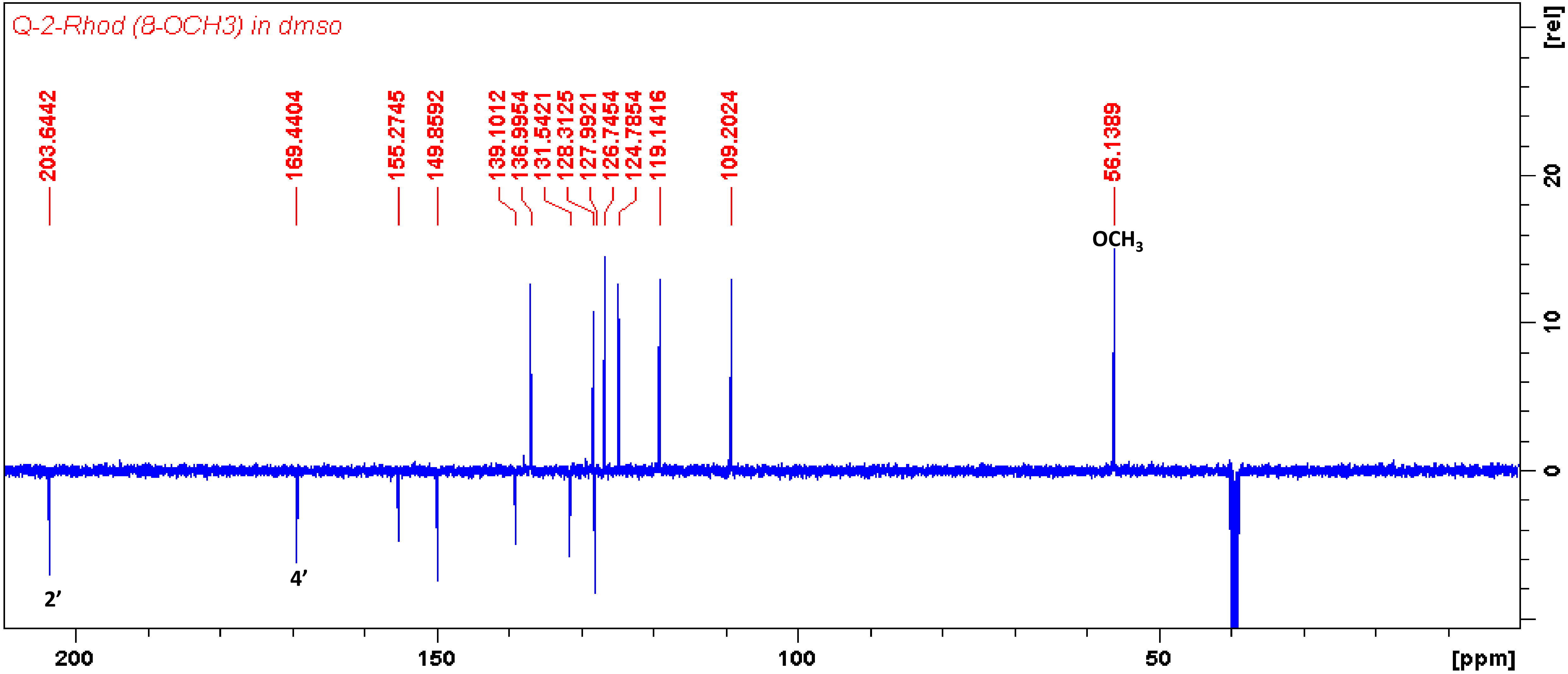

^{13}C NMR spectrum of **C5e**

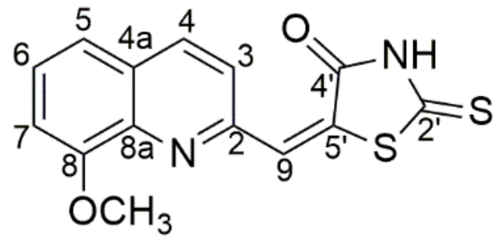

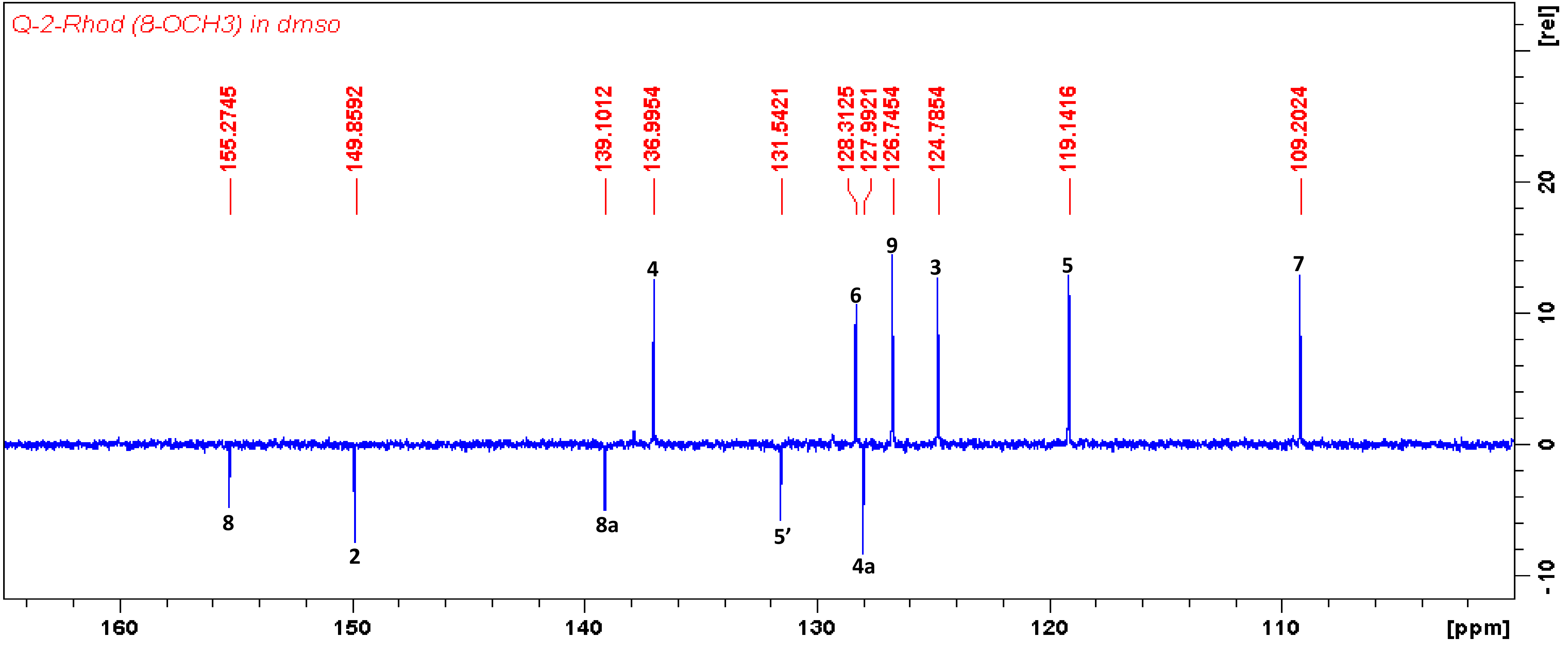

Expanded ^{13}C NMR spectrum of **C5e**

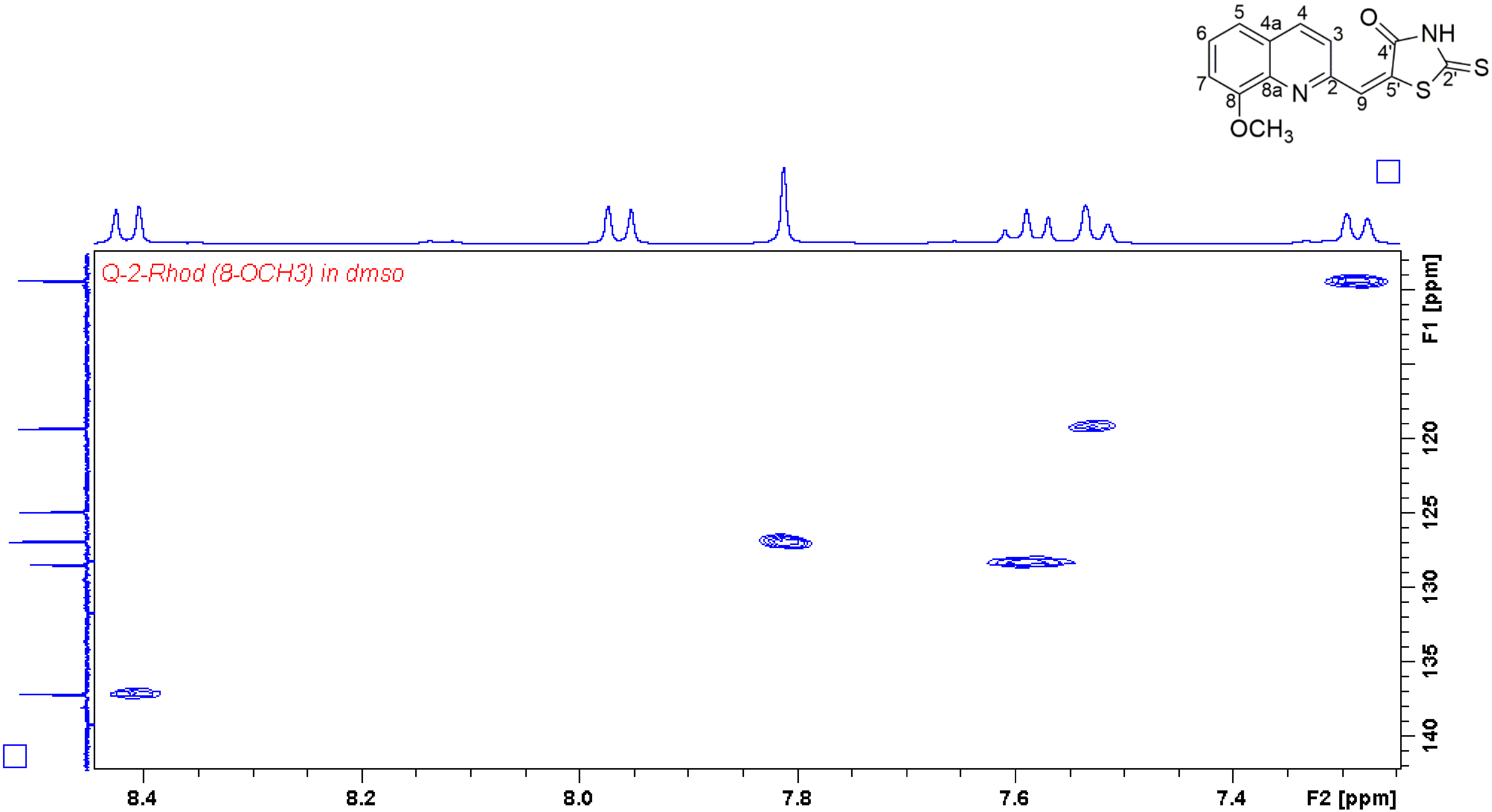
Q-2-Rhod (8-OCH3) in dmso
F1 [ppm]
F2 [ppm]
8.4
8.2
8.0
7.8
7.6
7.4
120
125
130
135
140
NH
O
S
OCH3

HSQC of **C5e**

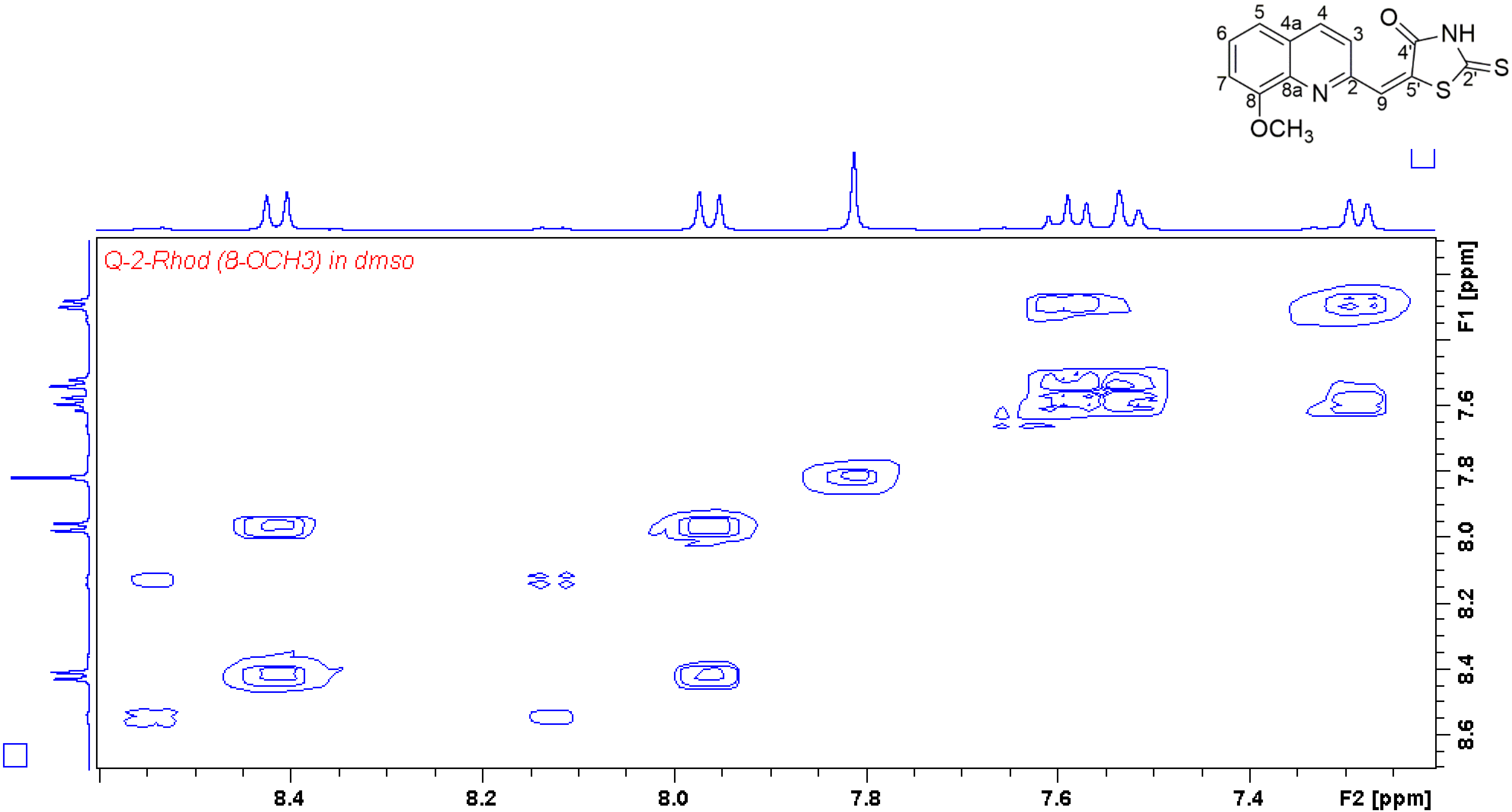

COSY of **C5e**

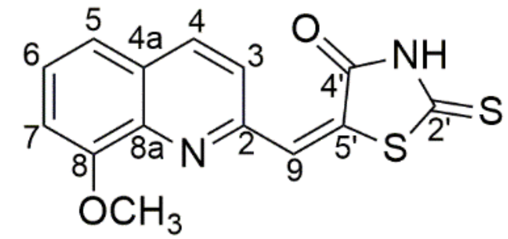

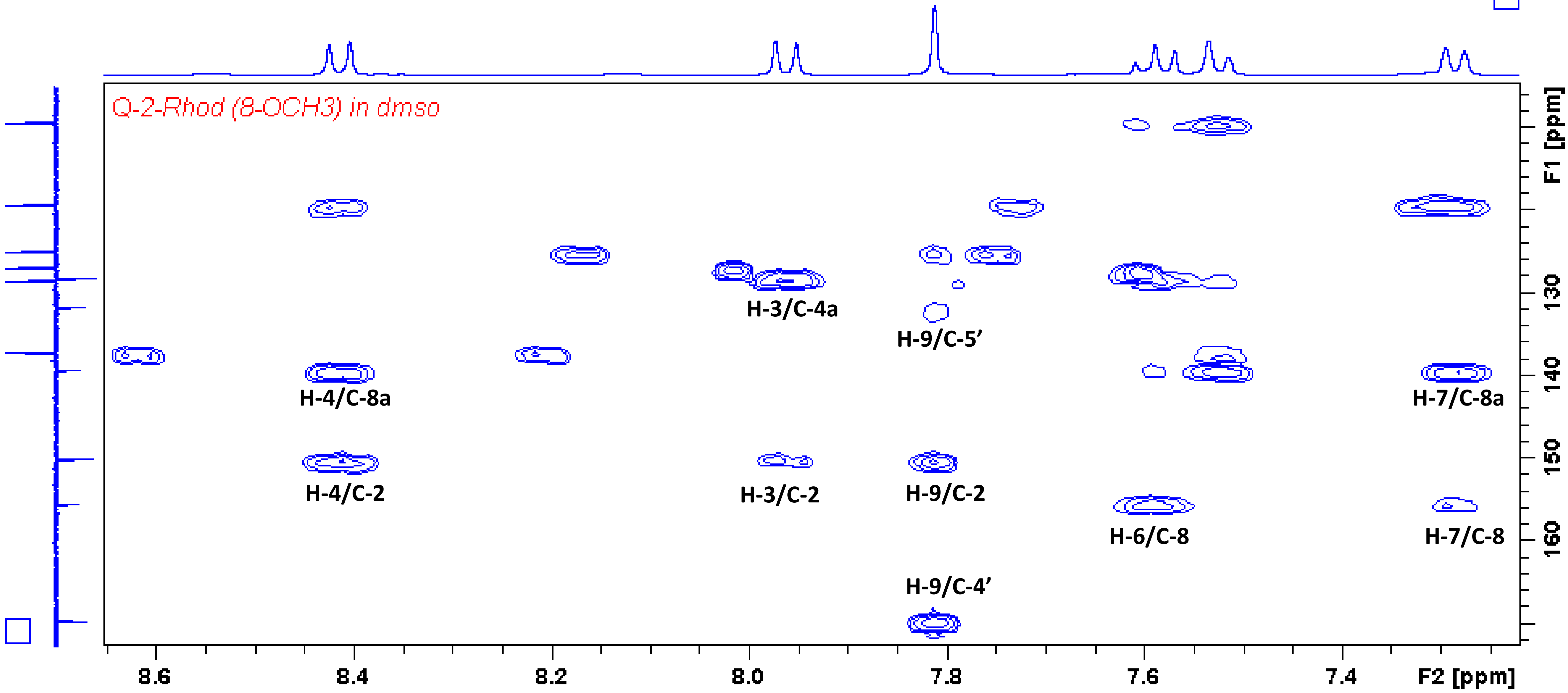
Q-2-Rhod (8-OCH3) in dmso
H-3/C-4a
H-9/C-5’
H-4/C-8a
H-7/C-8a
H-4/C-2
H-3/C-2
H-9/C-2
H-6/C-8
H-7/C-8
H-9/C-4’
F1 [ppm]
F2 [ppm]

HMBC of **C5e**

Elemental Composition Report

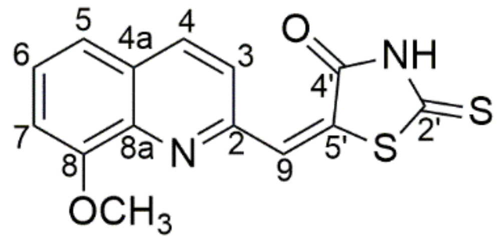

Single Mass Analysis

Tolerance = 5.0 PPM / DBE: min = -1.5, max = 100.0
Element prediction: Off
Number of isotope peaks used for i-FIT = 2

Monoisotopic Mass, Even Electron Ions
51 formula(e) evaluated with 1 results within limits (up to 20 best isotopic matches for each mass)
Elements Used:
C: 10-15 H: 5-10 N: 0-5 O: 0-5 S: 0-2
Q2R (8-OCH3) 54 (1.788) Cm (1:61)
TOF MS ES-

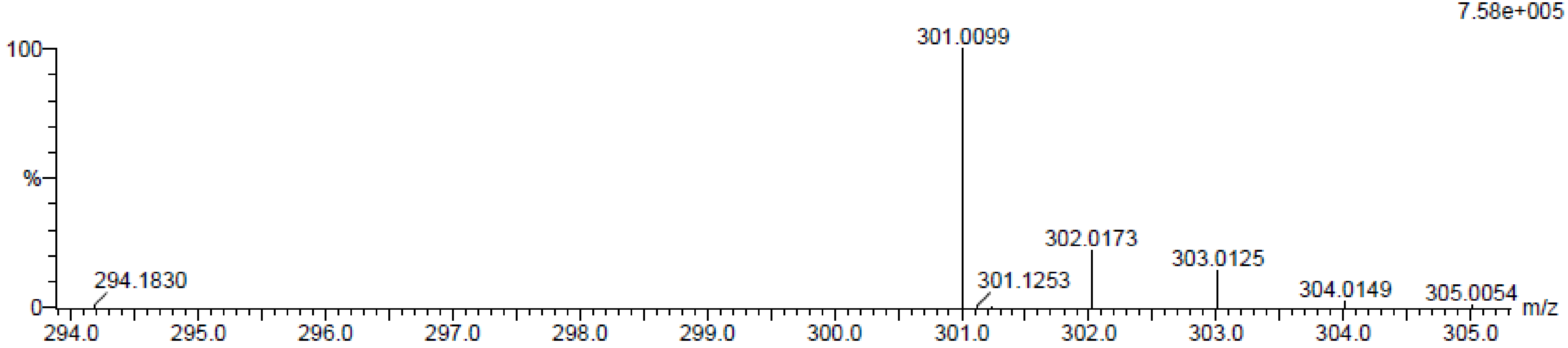

Minimum:				-1.5			
Maximum:		5.0	5.0	100.0			
Mass	Calc. Mass	mDa	PPM	DBE	i-FIT	i-FIT (Norm)	Formula
301.0099	301.0105	-0.6	-2.0	11.5	59.1	0.0	C14 H9 N2 O2 S2

High resolution mass spectrum of **C5e**

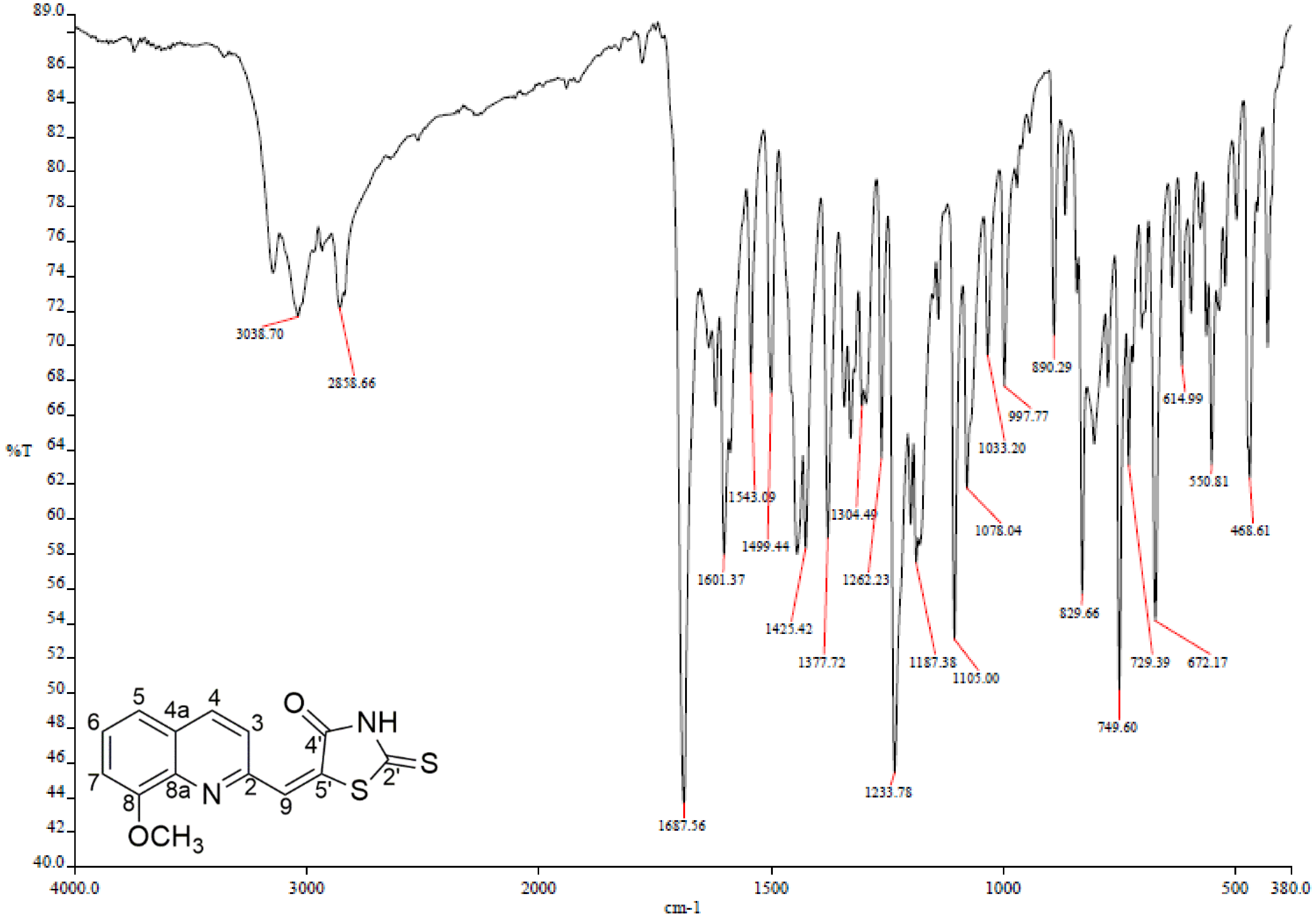

FTIR spectrum of **C5e**

Overlay Spectrum Graph Report

06/10/2017 11:25:30 AM

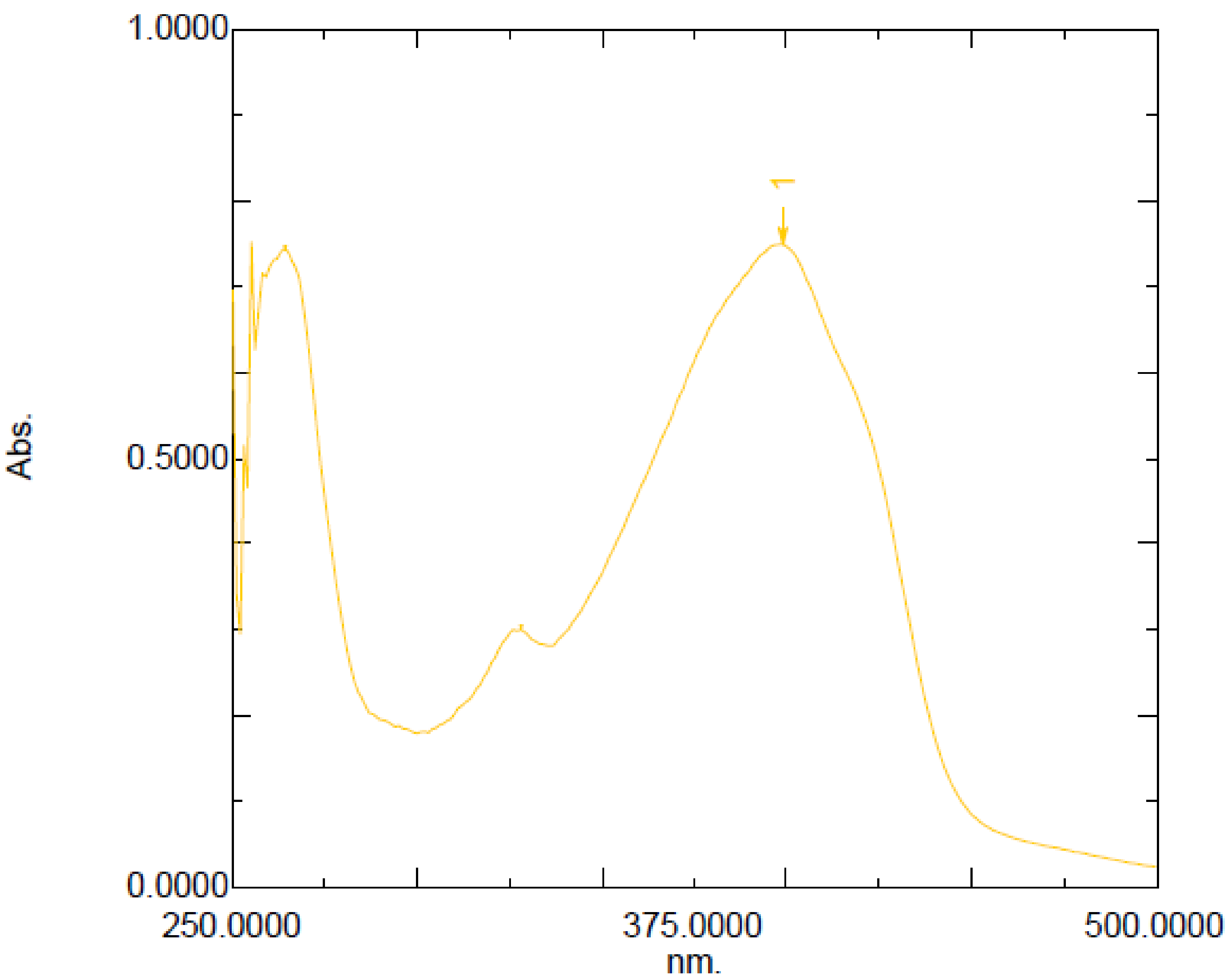

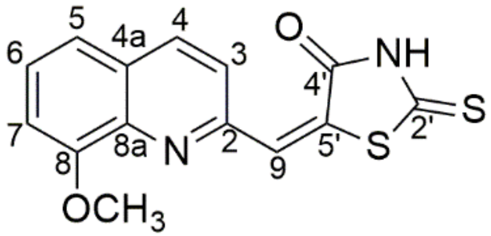

λ	absorbance	logε
399	0.749	4.66

UV spectrum of **C5e**

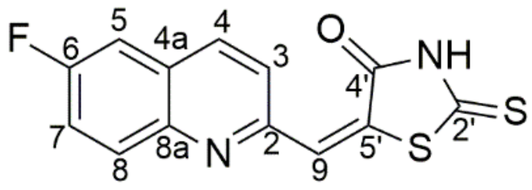

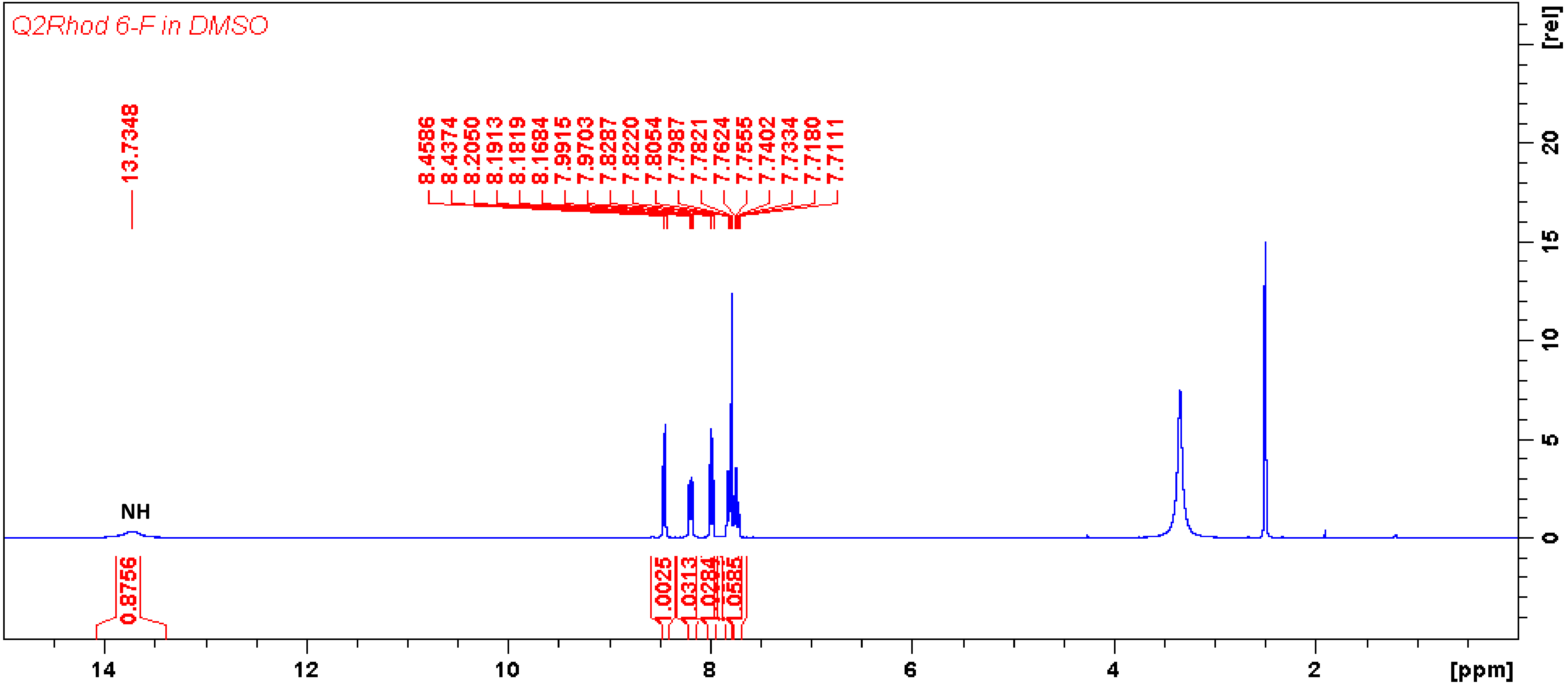

^{1}H NMR spectrum of **C5f**

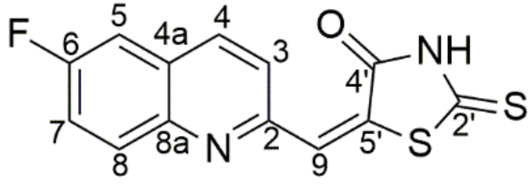

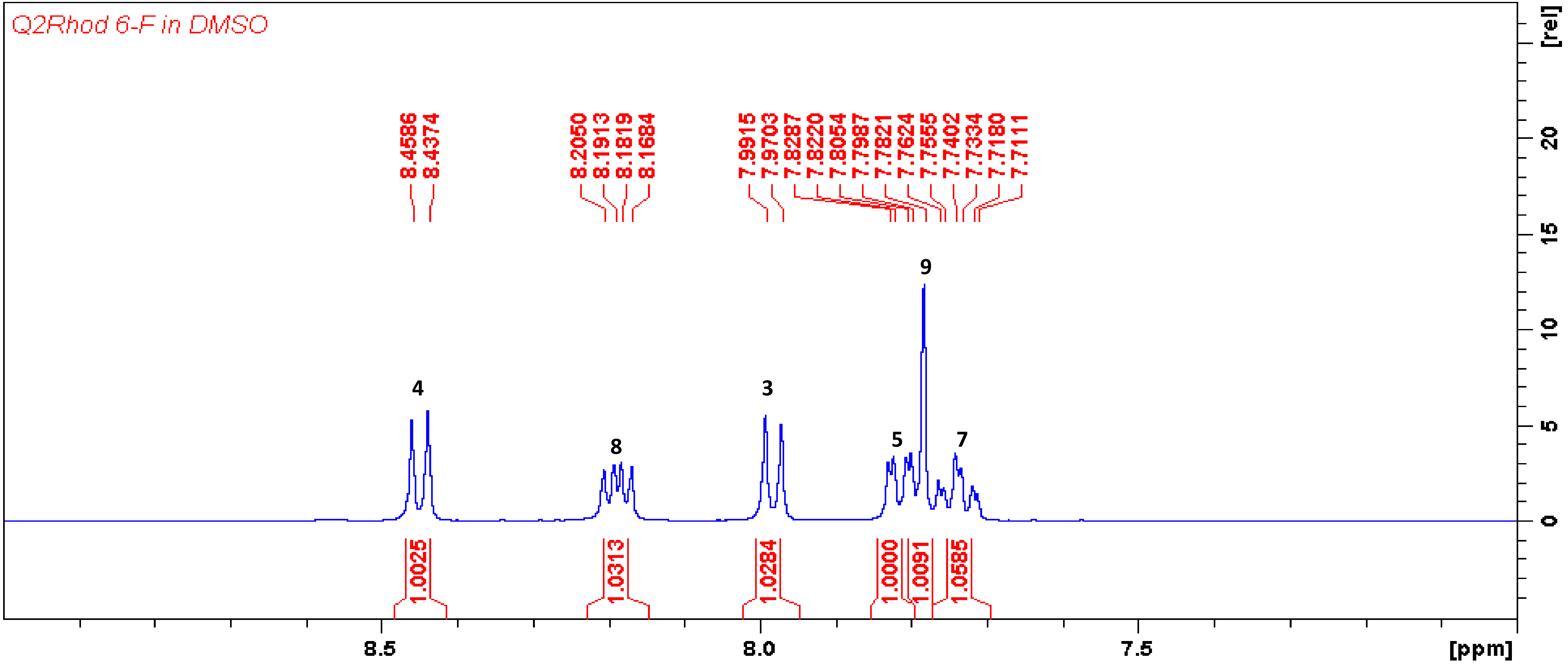

Expanded ^{1}H NMR spectrum of **C5f**

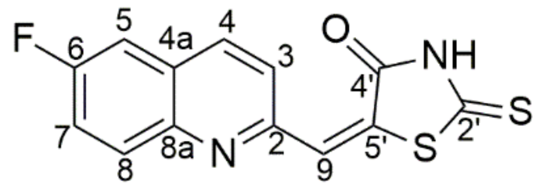

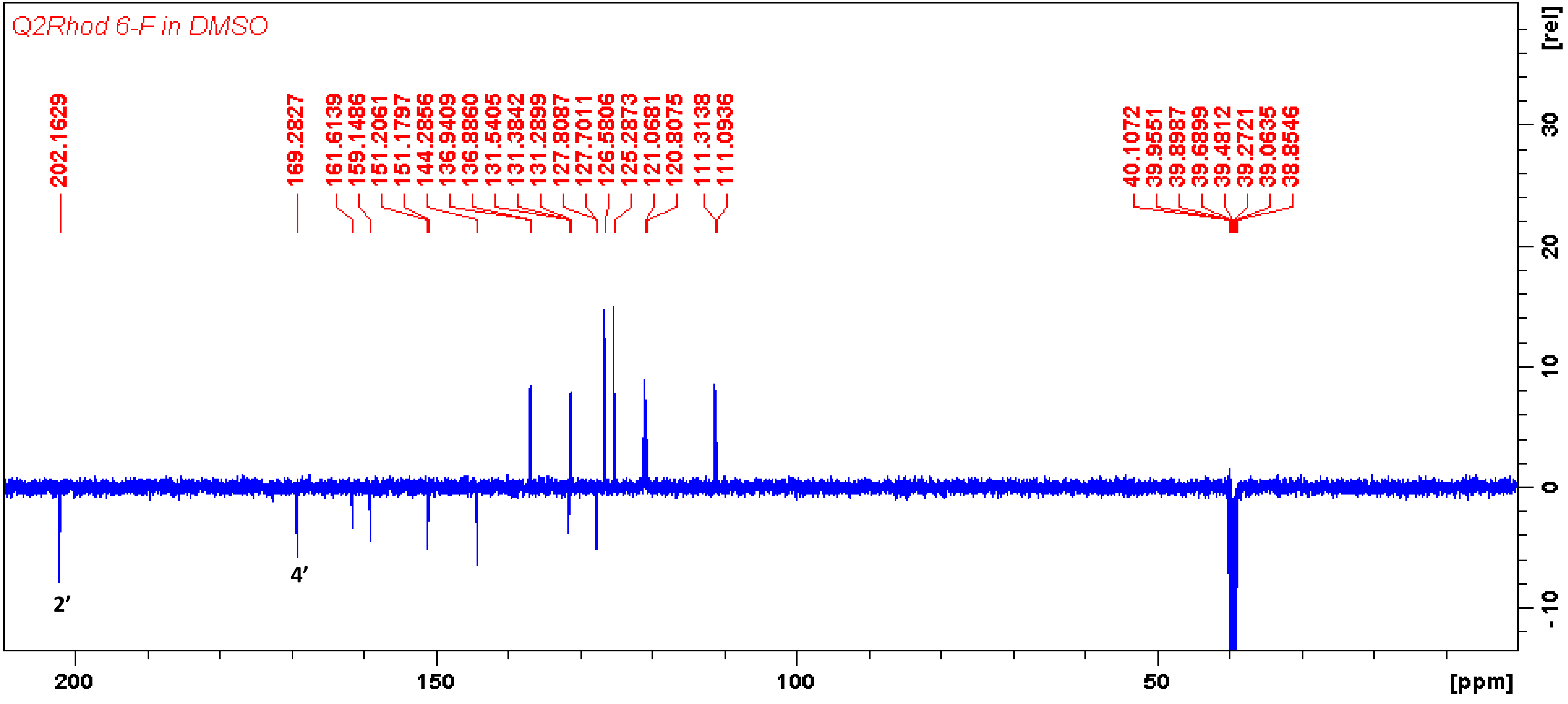

^{13}C NMR spectrum of **C5f**

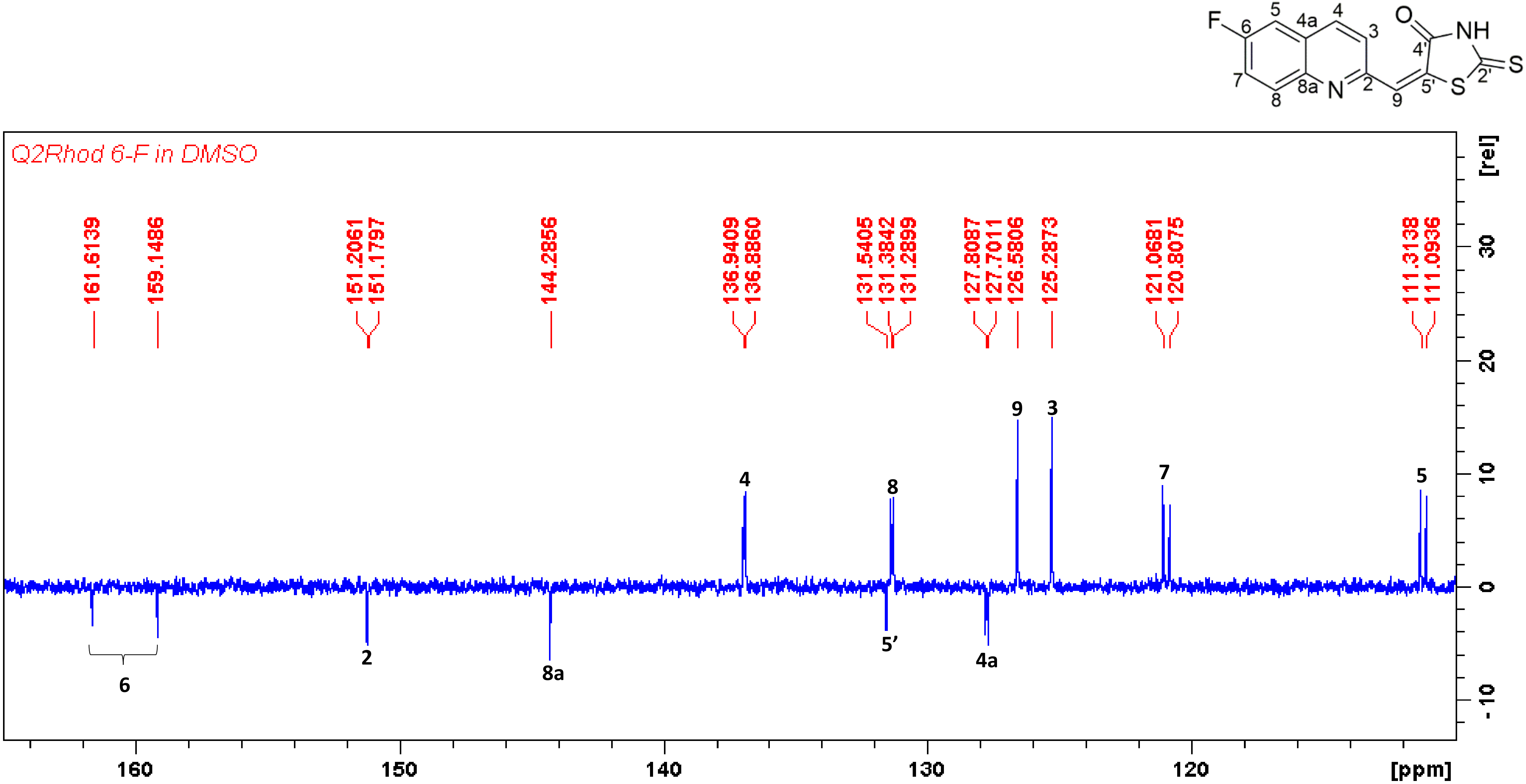

Expanded ^{13}C NMR spectrum of **C5f**

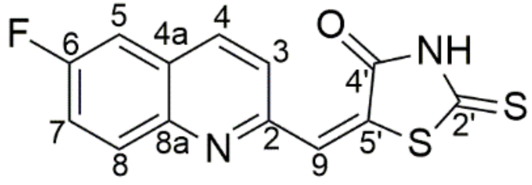

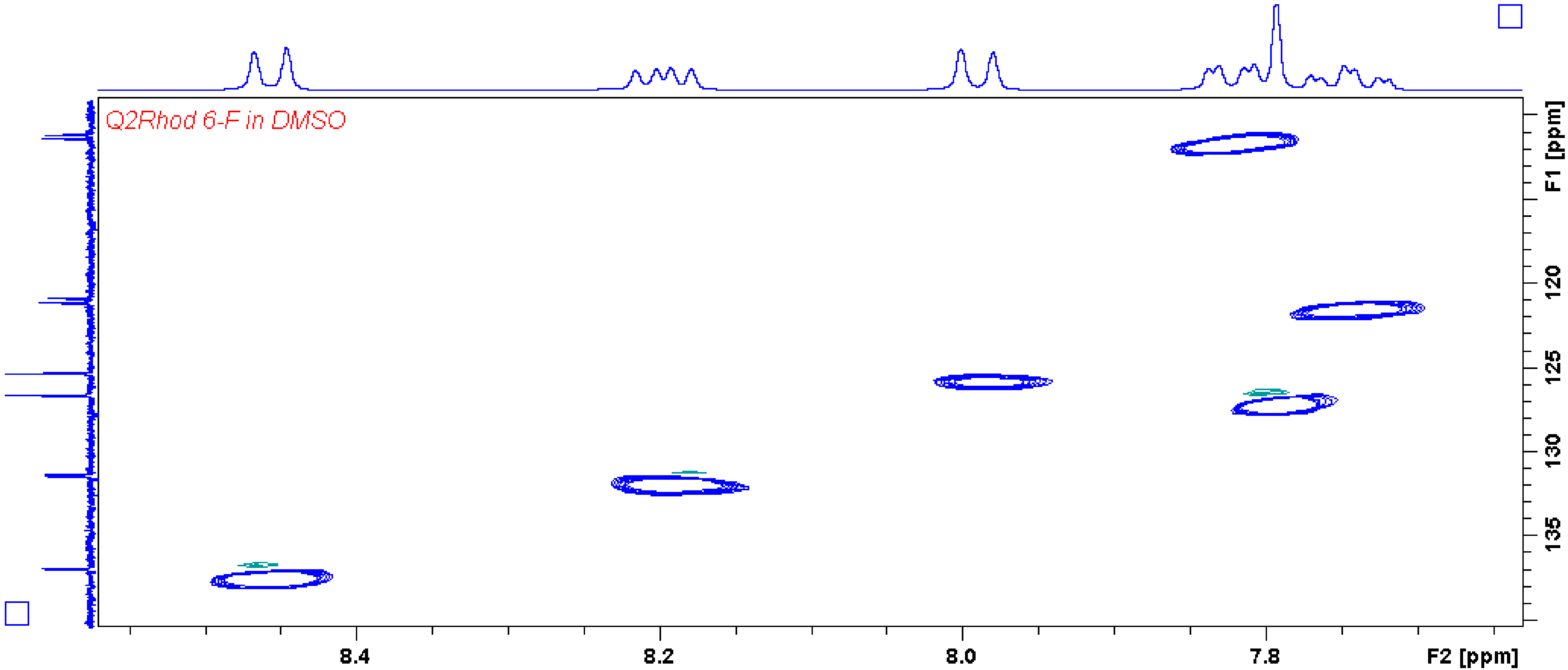

HSQC of **C5f**

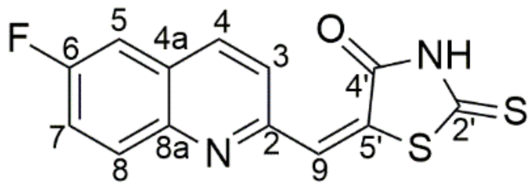
F
6
5
4a
4
3
O
NH
4'
S
2'
5'
S
2
9
N
8a
8
7

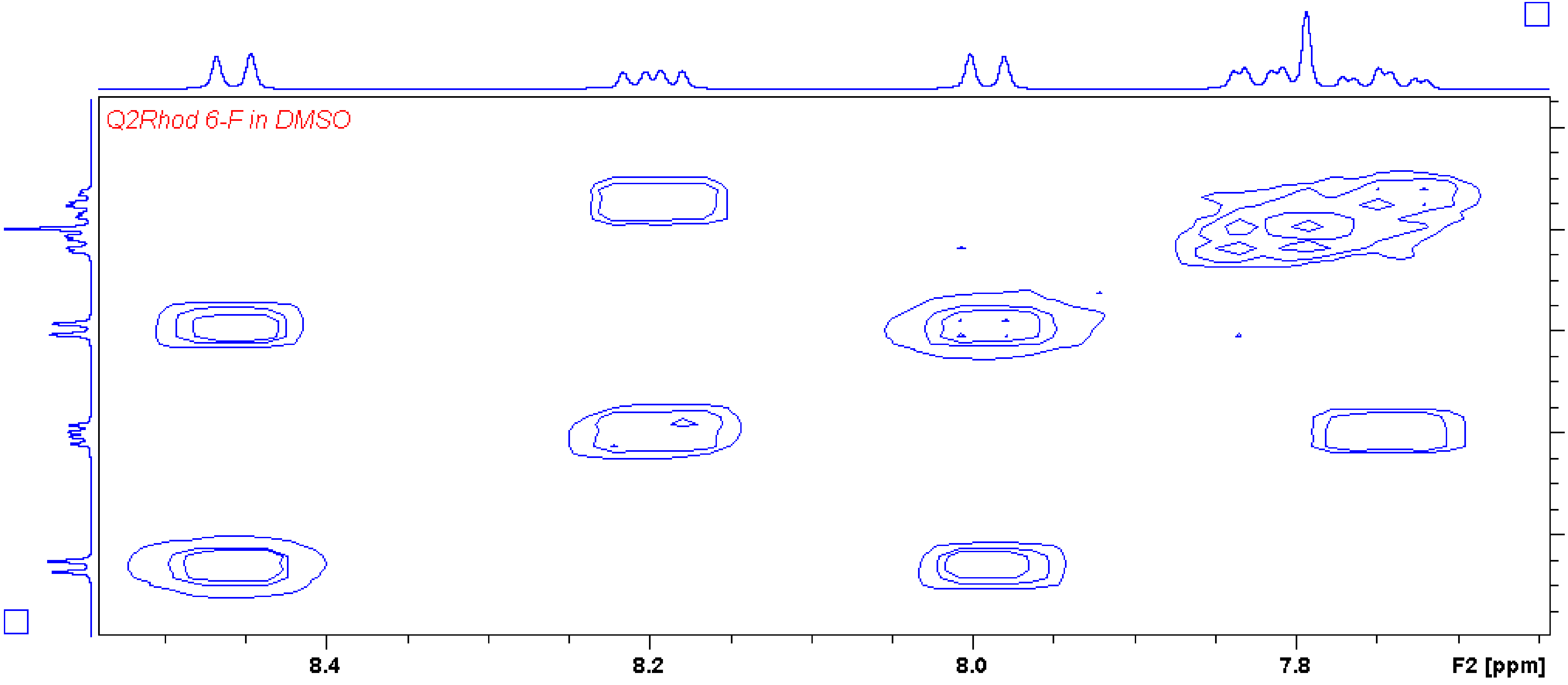
Q2Rhod 6-F in DMSO
7.8
8.0
8.2
8.4
F1 [ppm]
8.4
8.2
8.0
7.8
F2 [ppm]

COSY of **C5f**

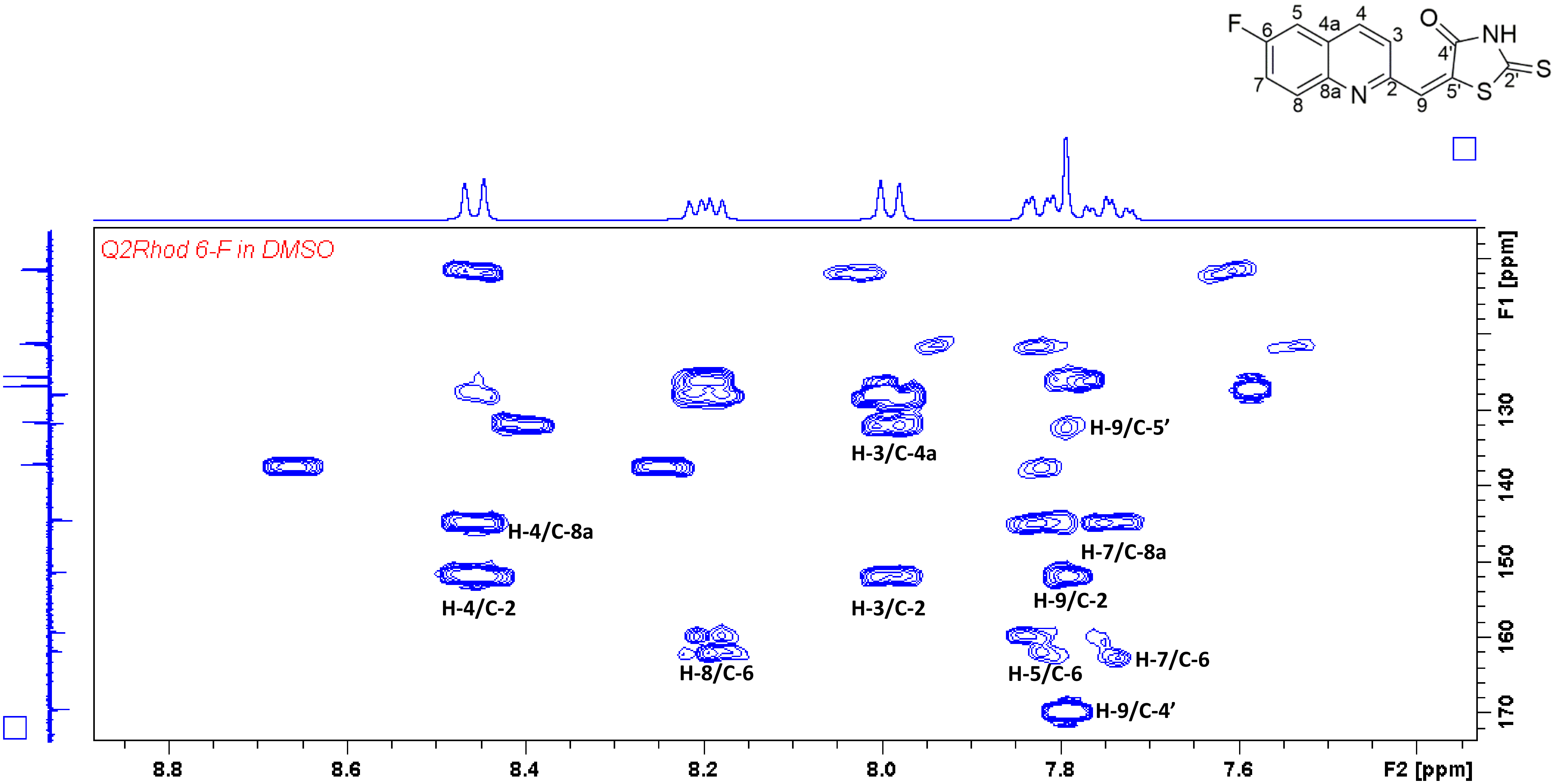

F
6
5
4a
4
3
O
NH
4'
S
2'
5'
S
2
9
N
8a
8
7
Q2Rhod 6-F in DMSO
H-4/C-8a
H-4/C-2
H-8/C-6
H-3/C-4a
H-3/C-2
H-9/C-5'
H-7/C-8a
H-9/C-2
H-5/C-6
H-7/C-6
H-9/C-4'
F1 [ppm]
130
140
150
160
170
8.8
8.6
8.4
8.2
8.0
7.8
7.6
F2 [ppm]

HMBC of **C5f**

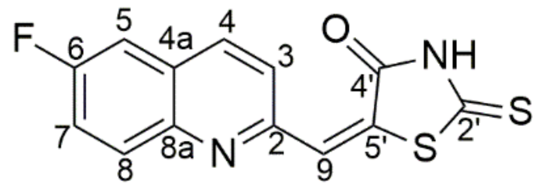

Elemental Composition Report

Single Mass Analysis
Tolerance = 5.0 PPM / DBE: min = -1.5, max = 100.0
Element prediction: Off
Number of isotope peaks used for i-FIT = 2

Monoisotopic Mass, Even Electron Ions
54 formula(e) evaluated with 1 results within limits (up to 20 best isotopic matches for each mass)
Elements Used:
C: 10-15 H: 5-10 N: 0-5 O: 0-5 F: 1-1 S: 0-2
Q2R (6-F) 14 (0.438) Cm (1:61)
TOF MS ES-

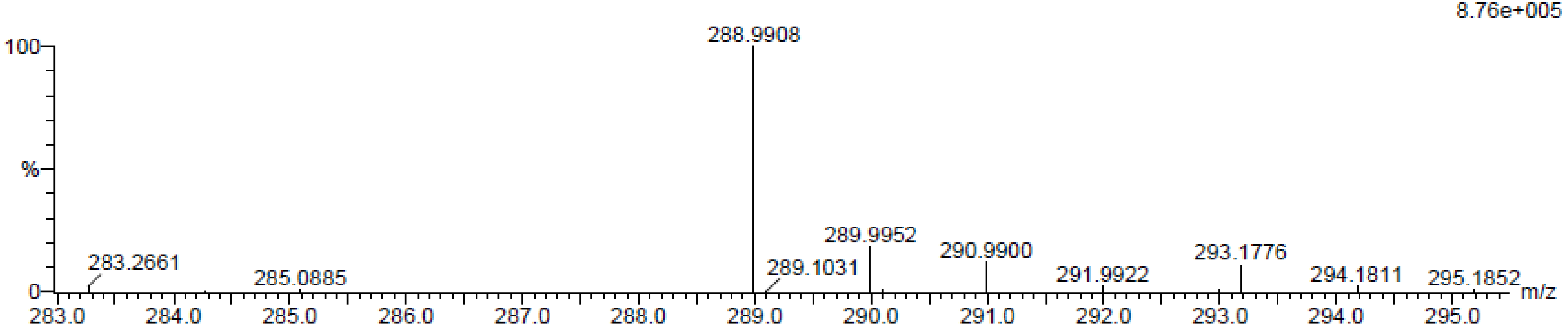

Minimum:				-1.5			
Maximum:		5.0	5.0	100.0			
Mass	Calc. Mass	mDa	PPM	DBE	i-FIT	i-FIT (Norm)	Formula
288.9908	288.9906	0.2	0.7	11.5	54.3	0.0	C13 H6 N2 O F S2

High resolution mass spectrum of **C5f**

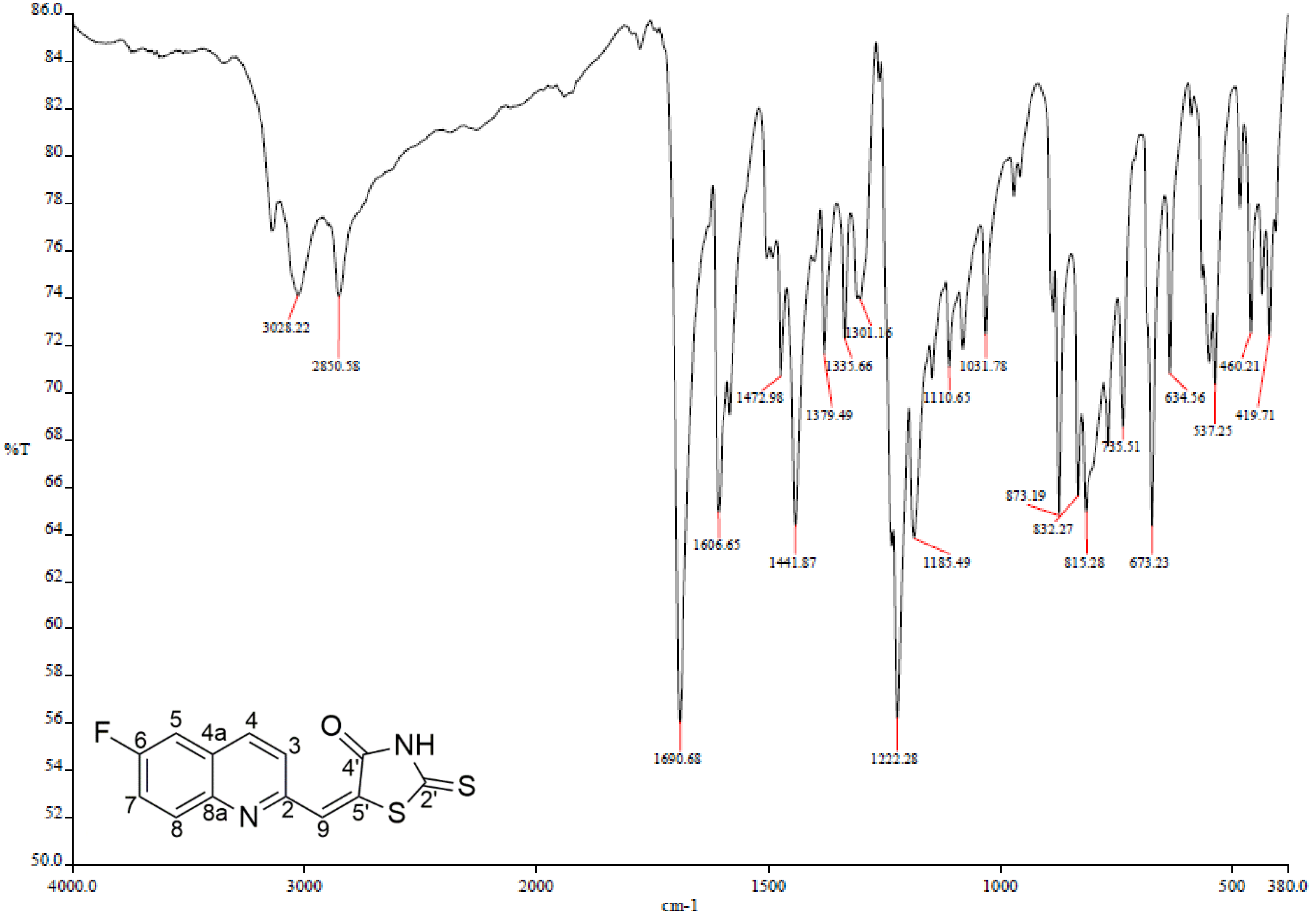

FTIR spectrum of **C5f**

Overlay Spectrum Graph Report

06/10/2017 11:32:23 AM

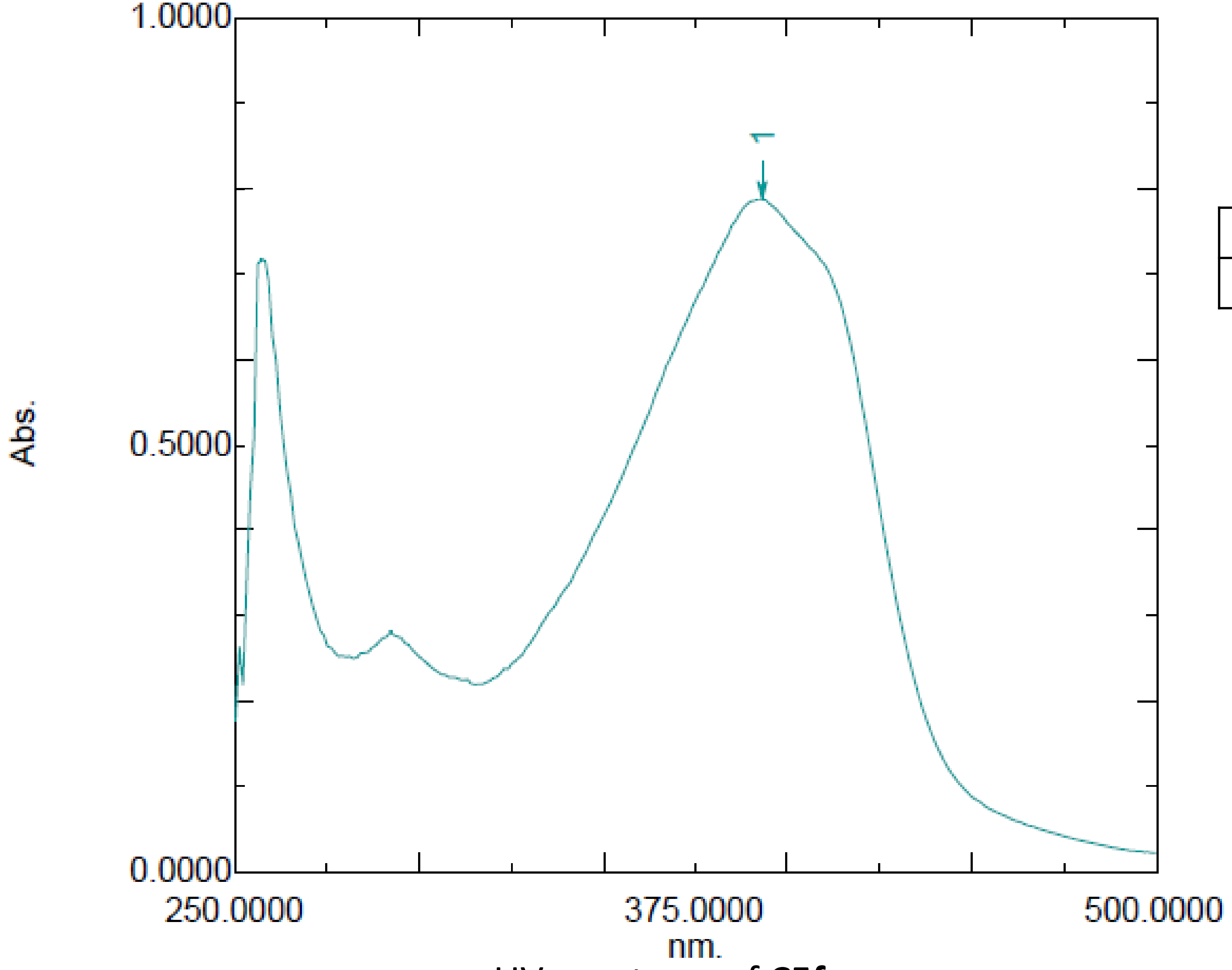

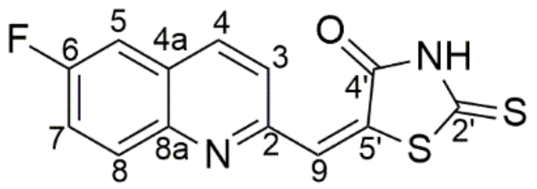

λ	absorbance	logε
393	0.788	4.66

UV spectrum of **C5f**

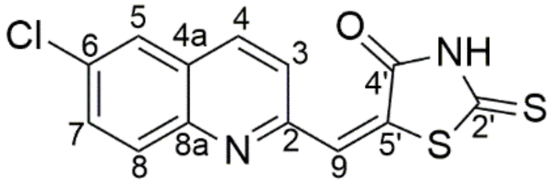

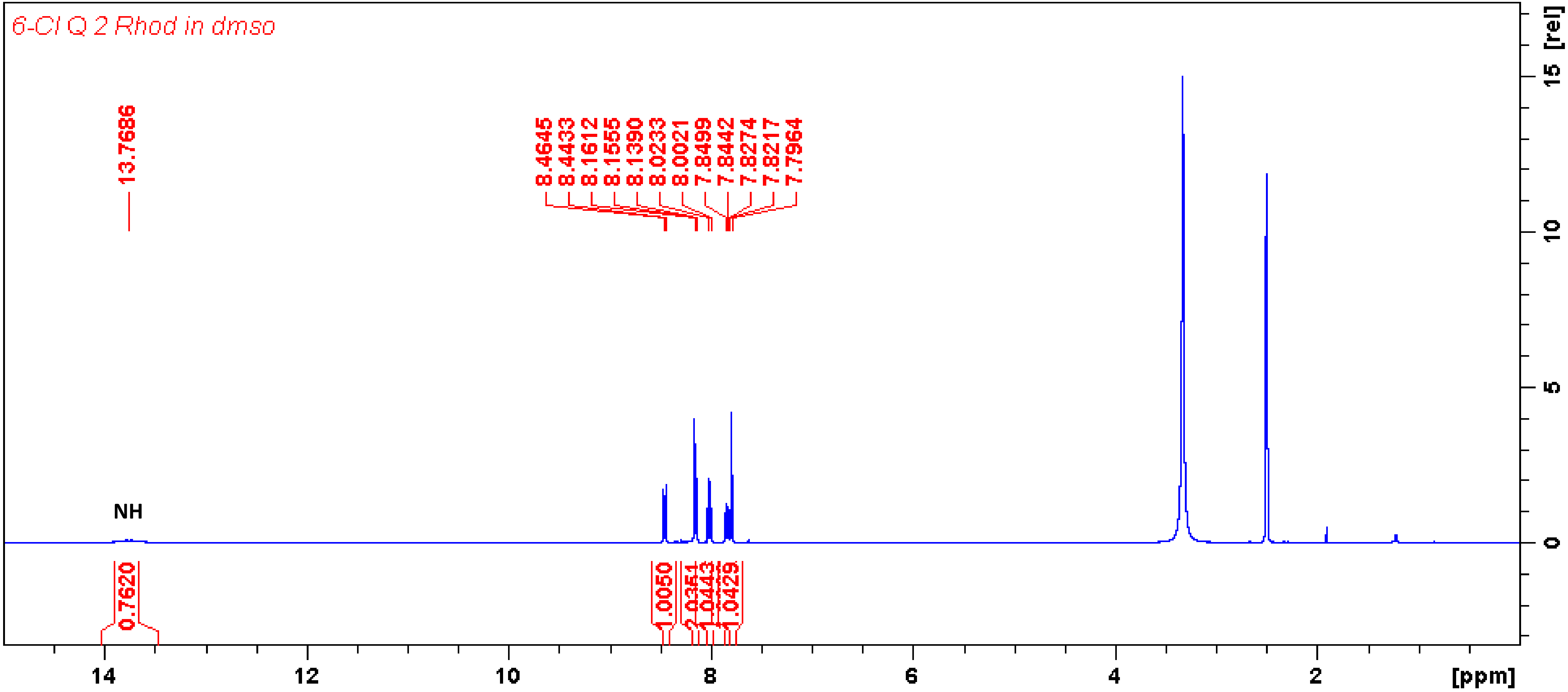

^{1}H NMR spectrum of **C5g**

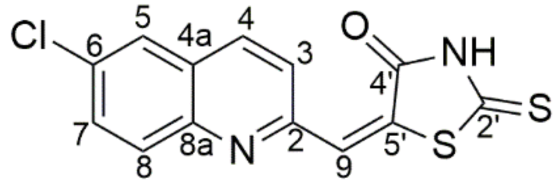

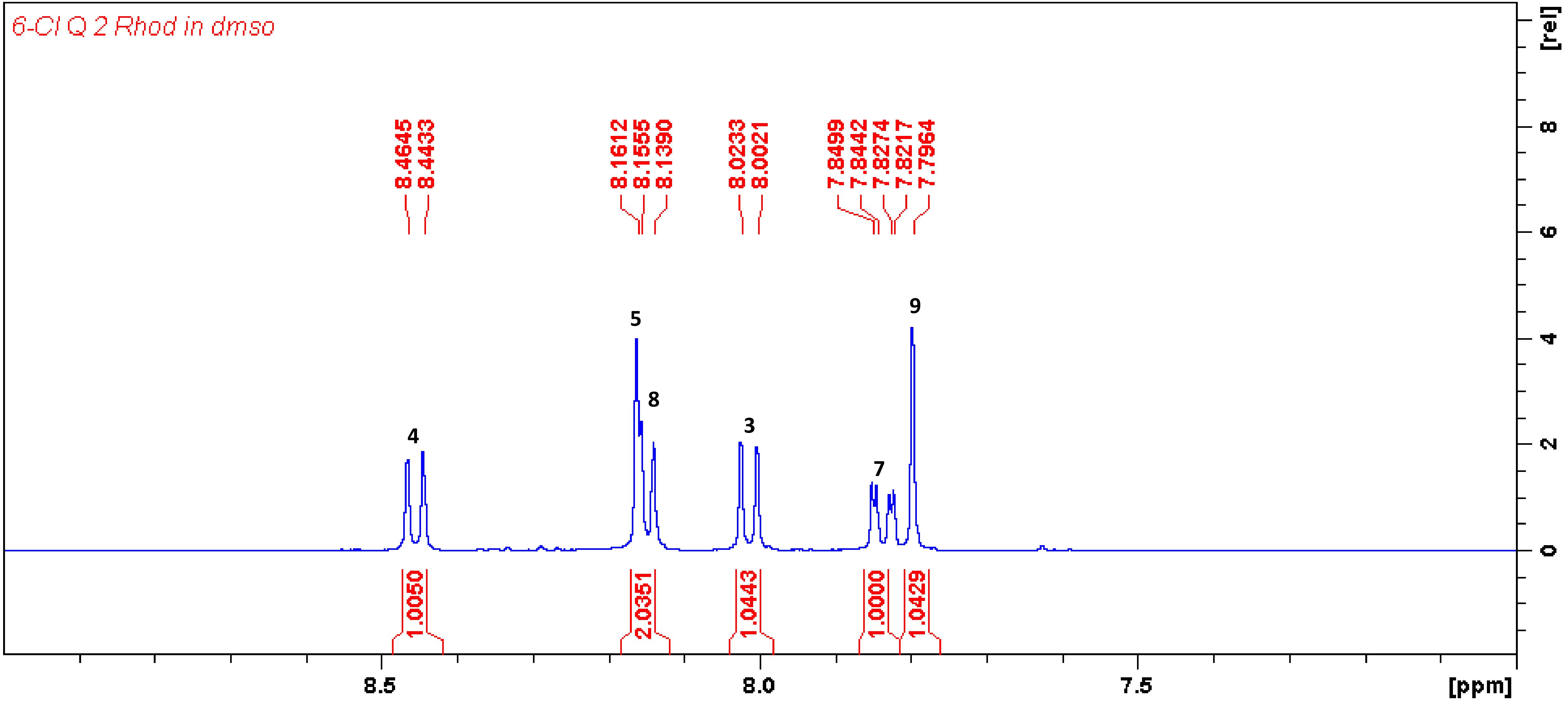

Expanded ^{1}H NMR spectrum of **C5g**

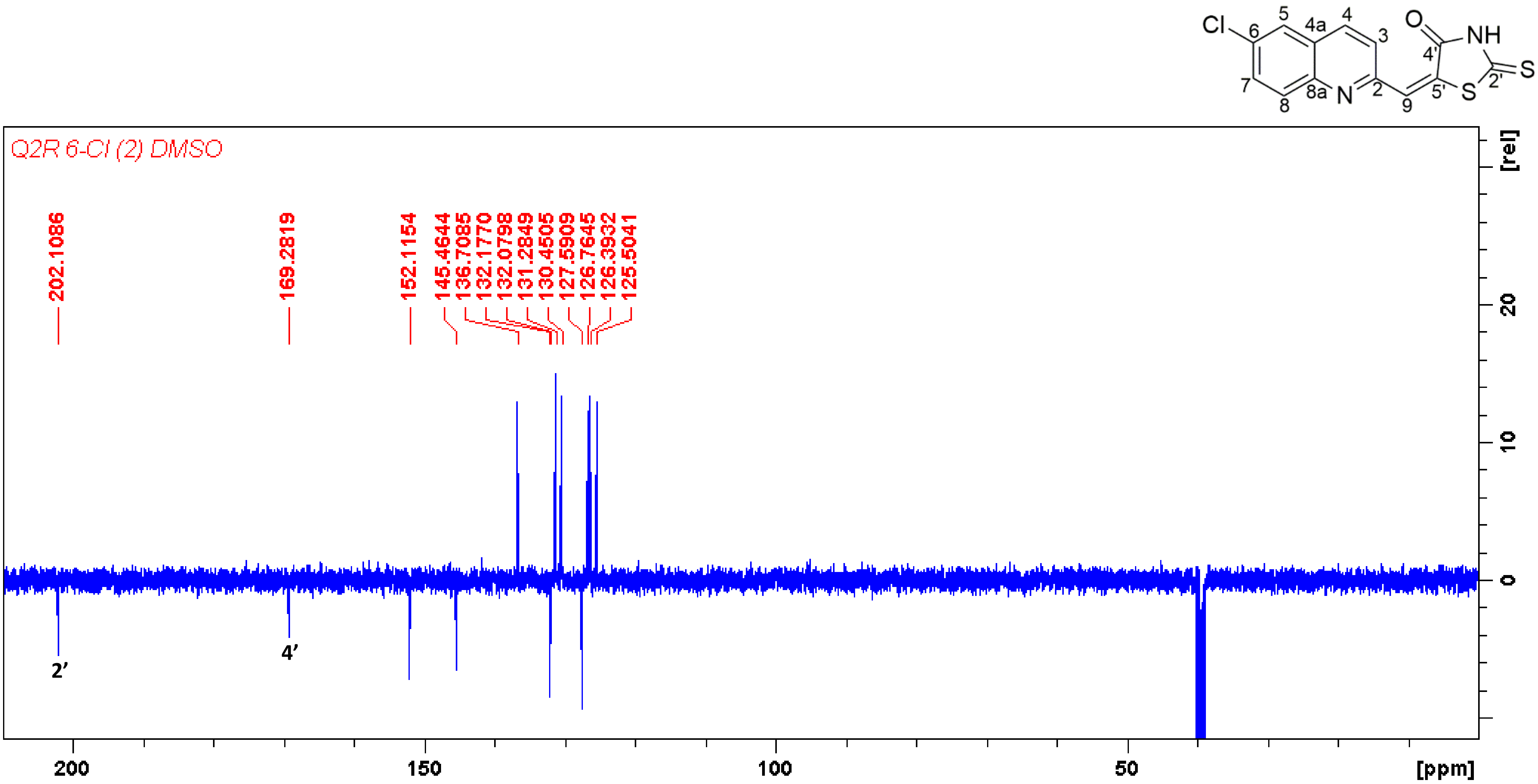

^{13}C NMR spectrum of **C5g**

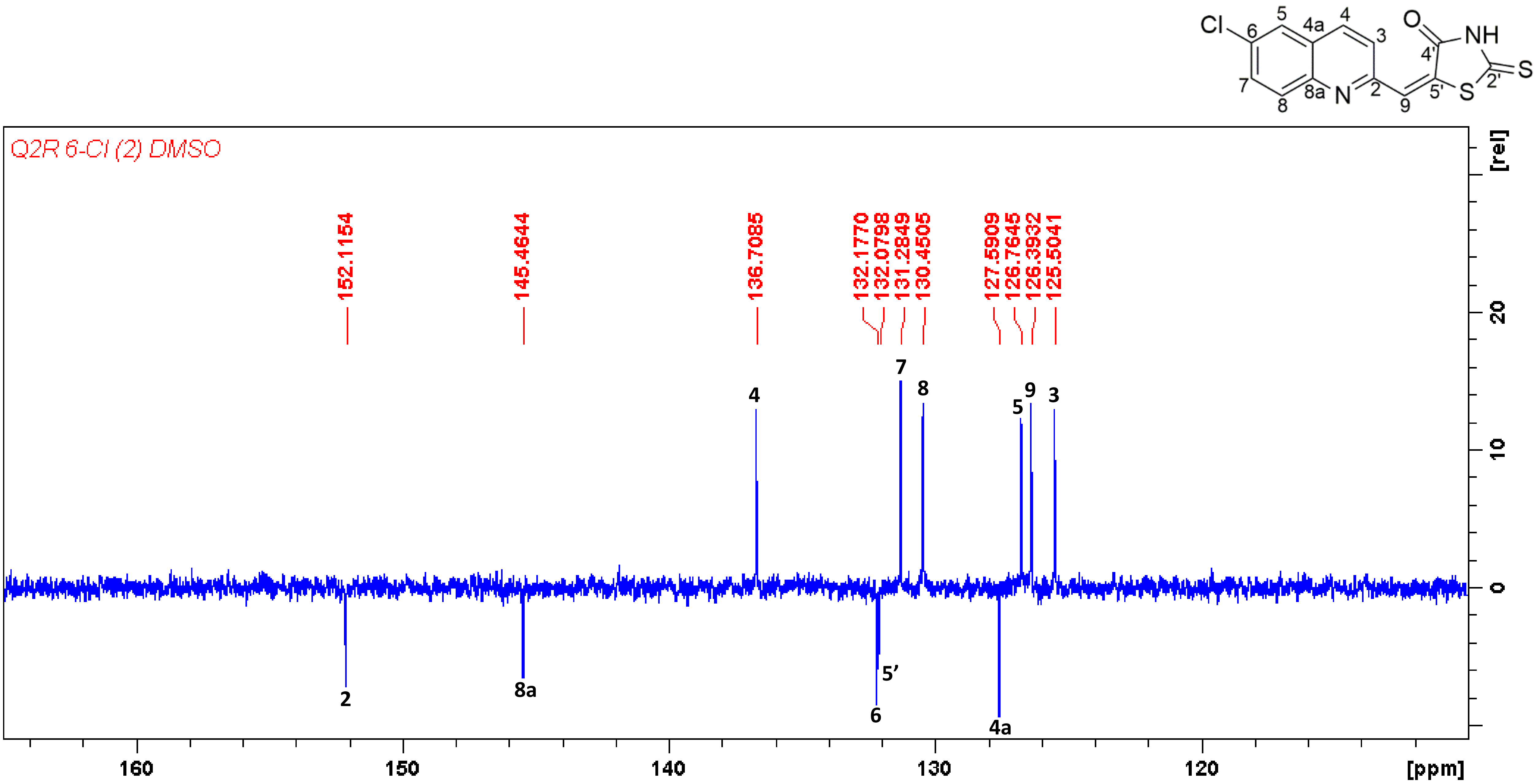

Expanded ^{13}C NMR spectrum of **C5g**

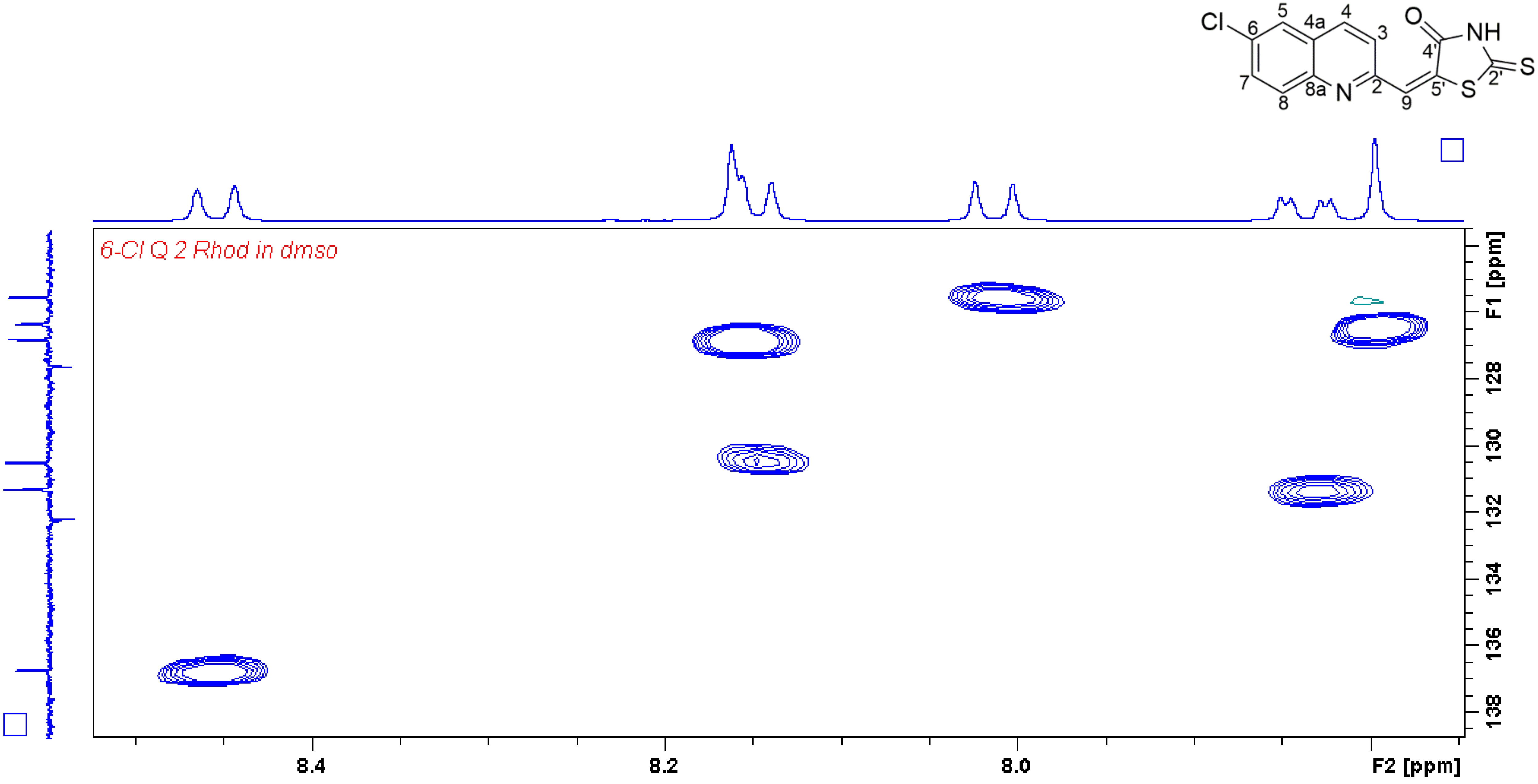

Cl
6
5
4a
4
3
O
NH
4'
S
2'
5'
S
9
2
N
8a
8
7
6-Cl Q 2 Rhod in dmso
F1 [ppm]
128
130
132
134
136
138
8.4
8.2
8.0
F2 [ppm]

HSQC of **C5g**

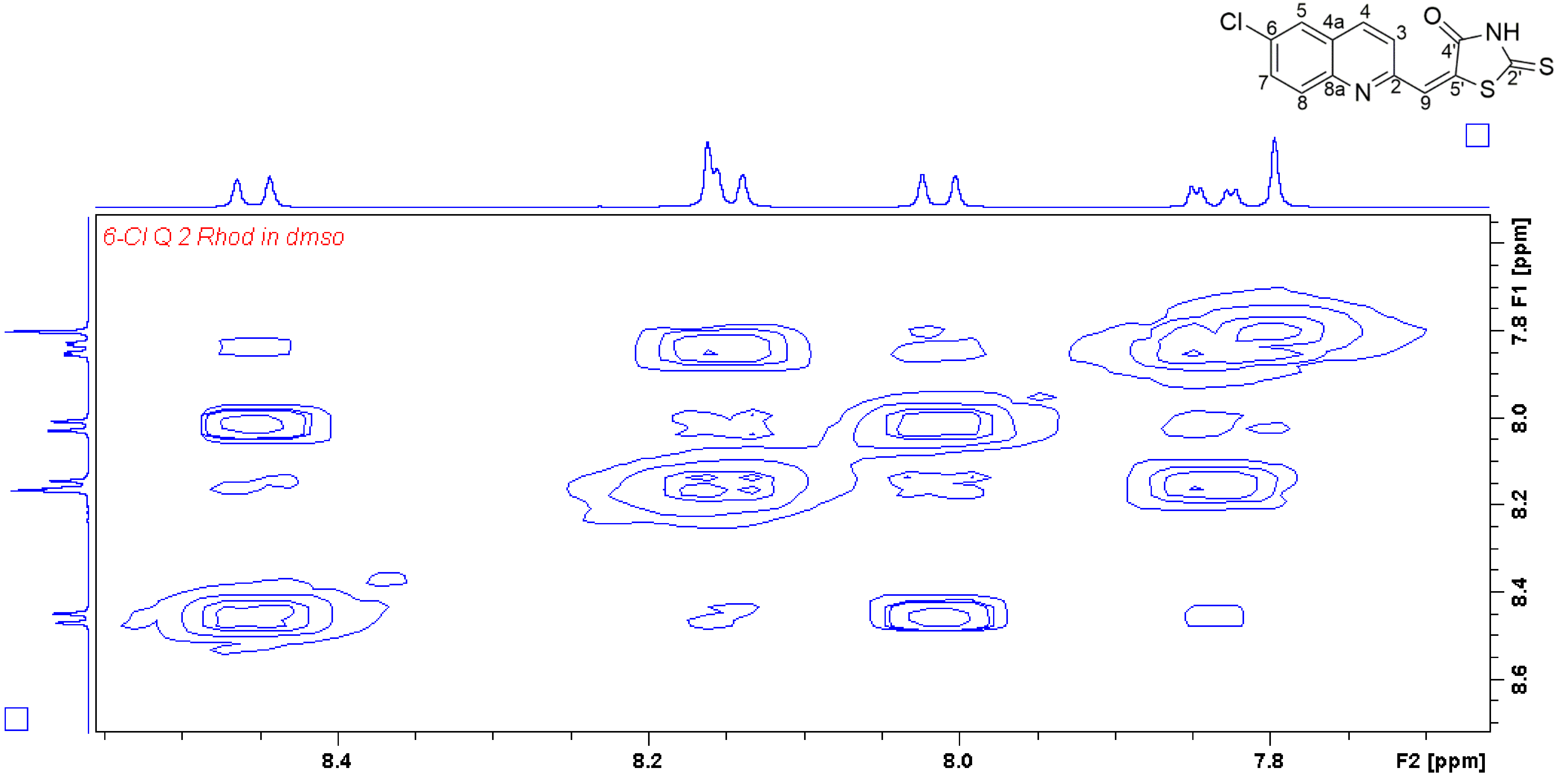
6-Cl Q 2 Rhod in dmso
Cl
6
5
4a
4
3
7
8
8a
N
2
9
5'
4'
O
NH
2'
S
S
8.4
8.2
8.0
7.8
F2 [ppm]
7.8
8.0
8.2
8.4
8.6
F1 [ppm]

COSY of **C5g**

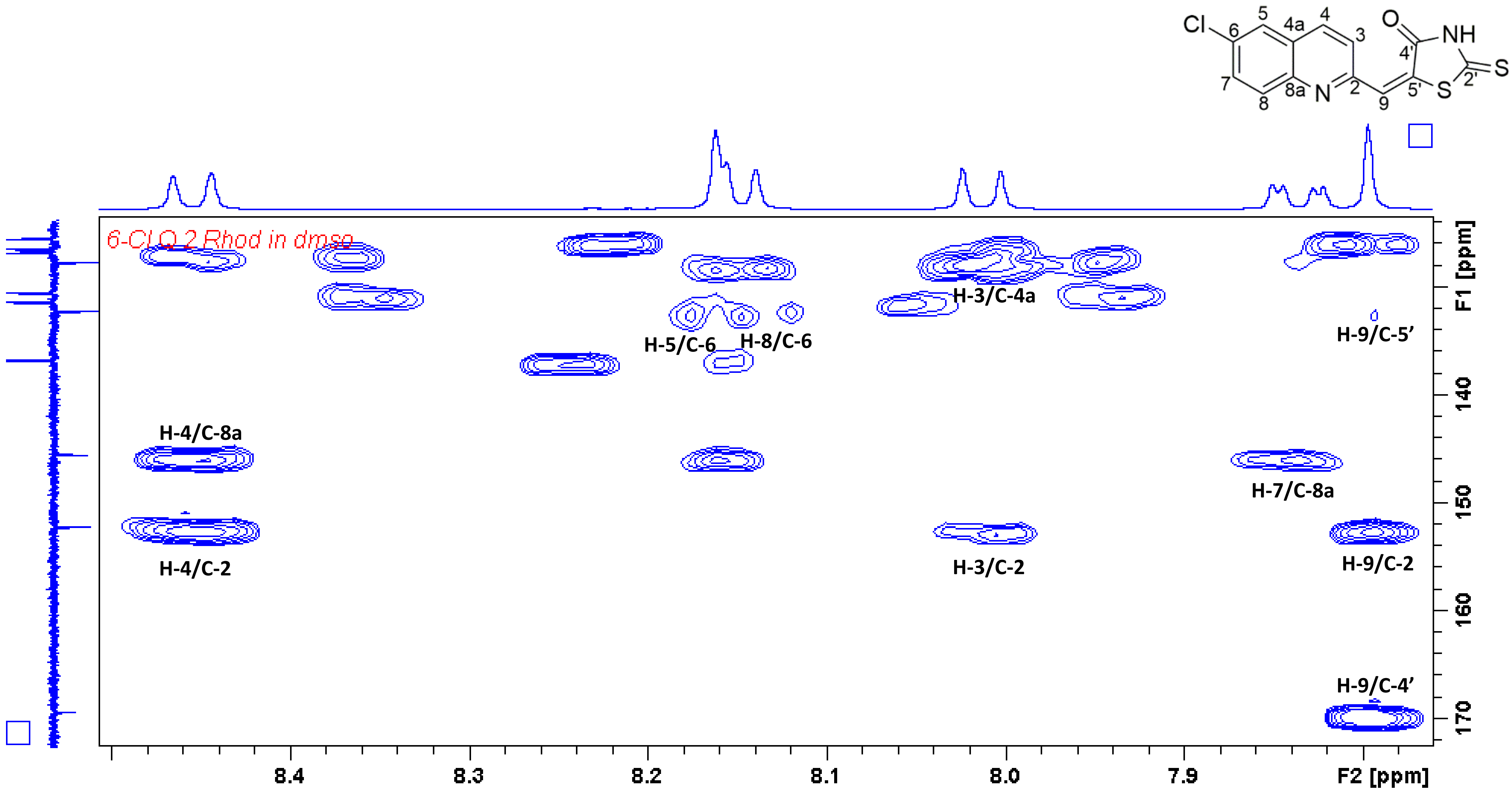

6-ClQ 2 Rhod in dmso
H-3/C-4a
H-5/C-6
H-8/C-6
H-9/C-5’
H-4/C-8a
H-7/C-8a
H-4/C-2
H-3/C-2
H-9/C-2
H-9/C-4’
F1 [ppm]
F2 [ppm]

HMBC of **C5g**

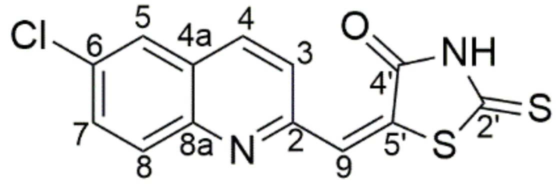

Elemental Composition Report

Single Mass Analysis

Tolerance = 5.0 PPM / DBE: min = -1.5, max = 100.0
Element prediction: Off
Number of isotope peaks used for i-FIT = 2

Monoisotopic Mass, Even Electron Ions
110 formula(e) evaluated with 1 results within limits (up to 20 best isotopic matches for each mass)
Elements Used:
C: 10-15 H: 5-10 N: 0-5 O: 0-5 S: 0-2 Cl: 0-1
Q2R (6-Cl) 35 (1.146) Cm (1:61)
TOF MS ES-

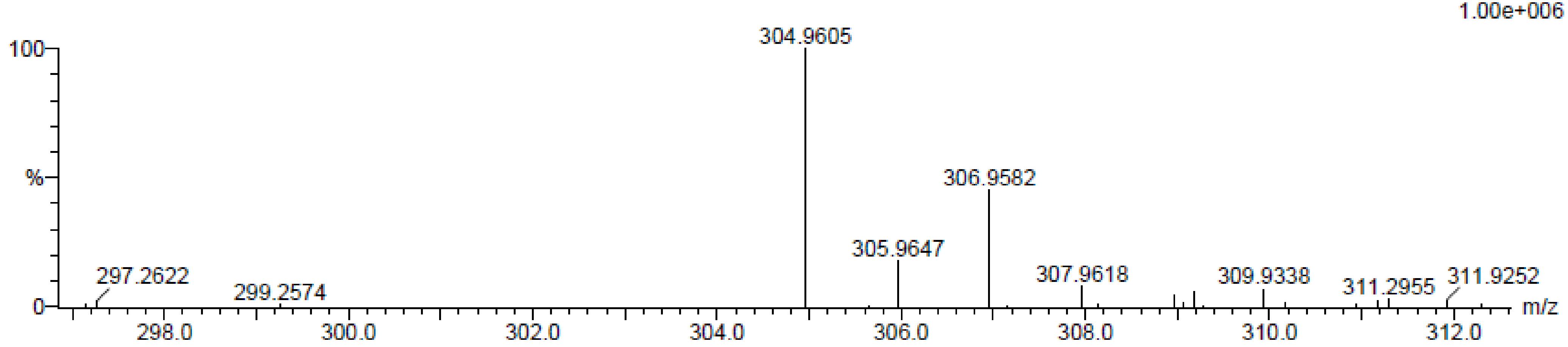

	Mass	Calc. Mass	mDa	PPM	DBE	i-FIT	i-FIT (Norm)	Formula
Minimum:					-1.5			
Maximum:			5.0	5.0	100.0			
	304.9605	304.9610	-0.5	-1.6	11.5	35.5	0.0	C13 H6 N2 O S2 Cl

High resolution mass spectrum of **C5g**

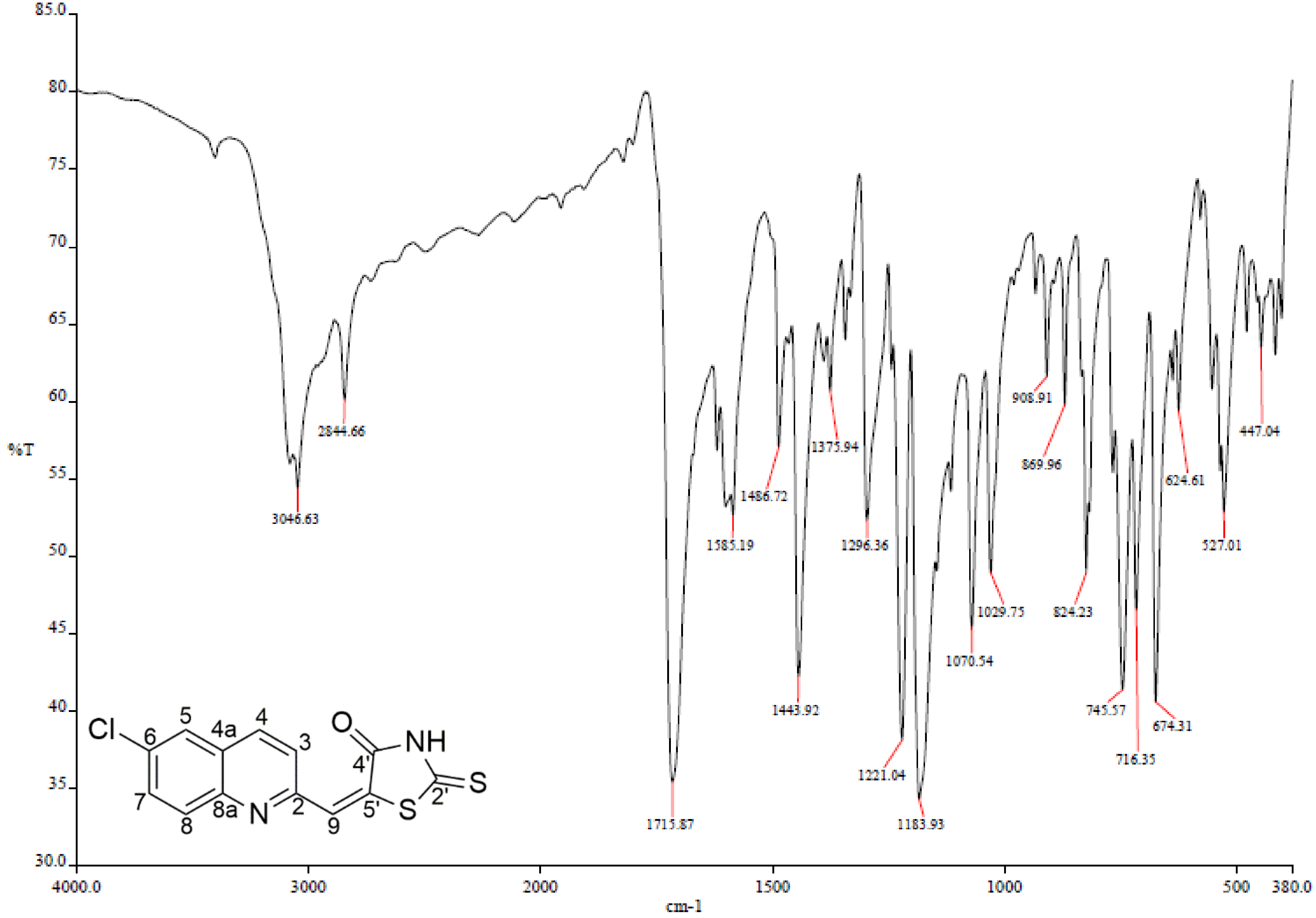

FTIR spectrum of **C5g**

Overlay Spectrum Graph Report

06/10/2017 11:32:59 AM

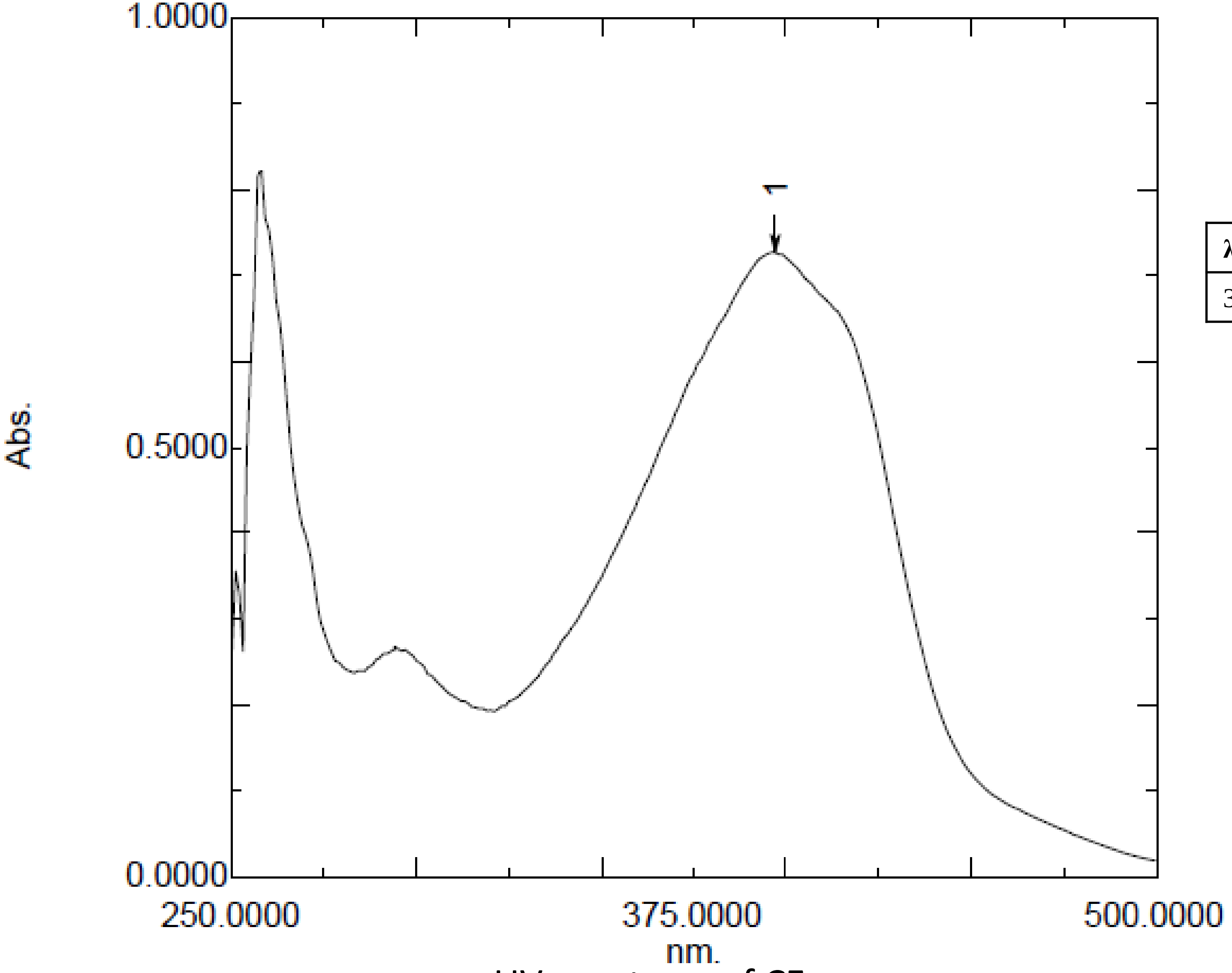

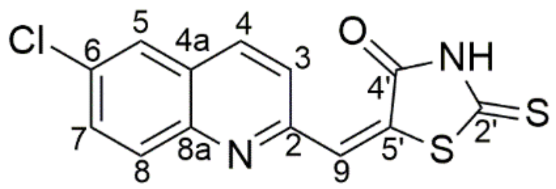

λ	**absorbance**	**logε**
397	0.727	4.65

UV spectrum of **C5g**

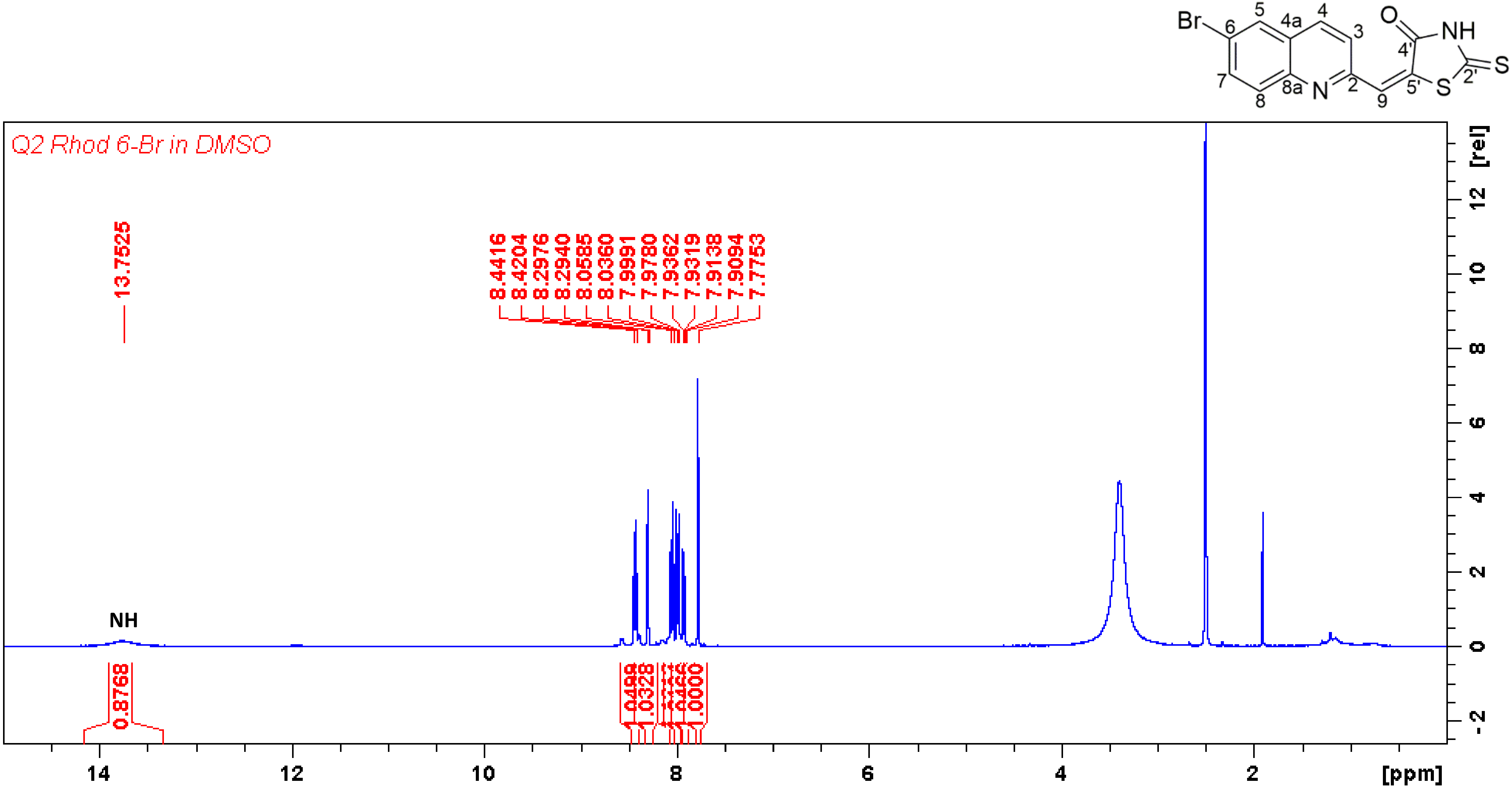

^{1}H NMR spectrum of **C5h**

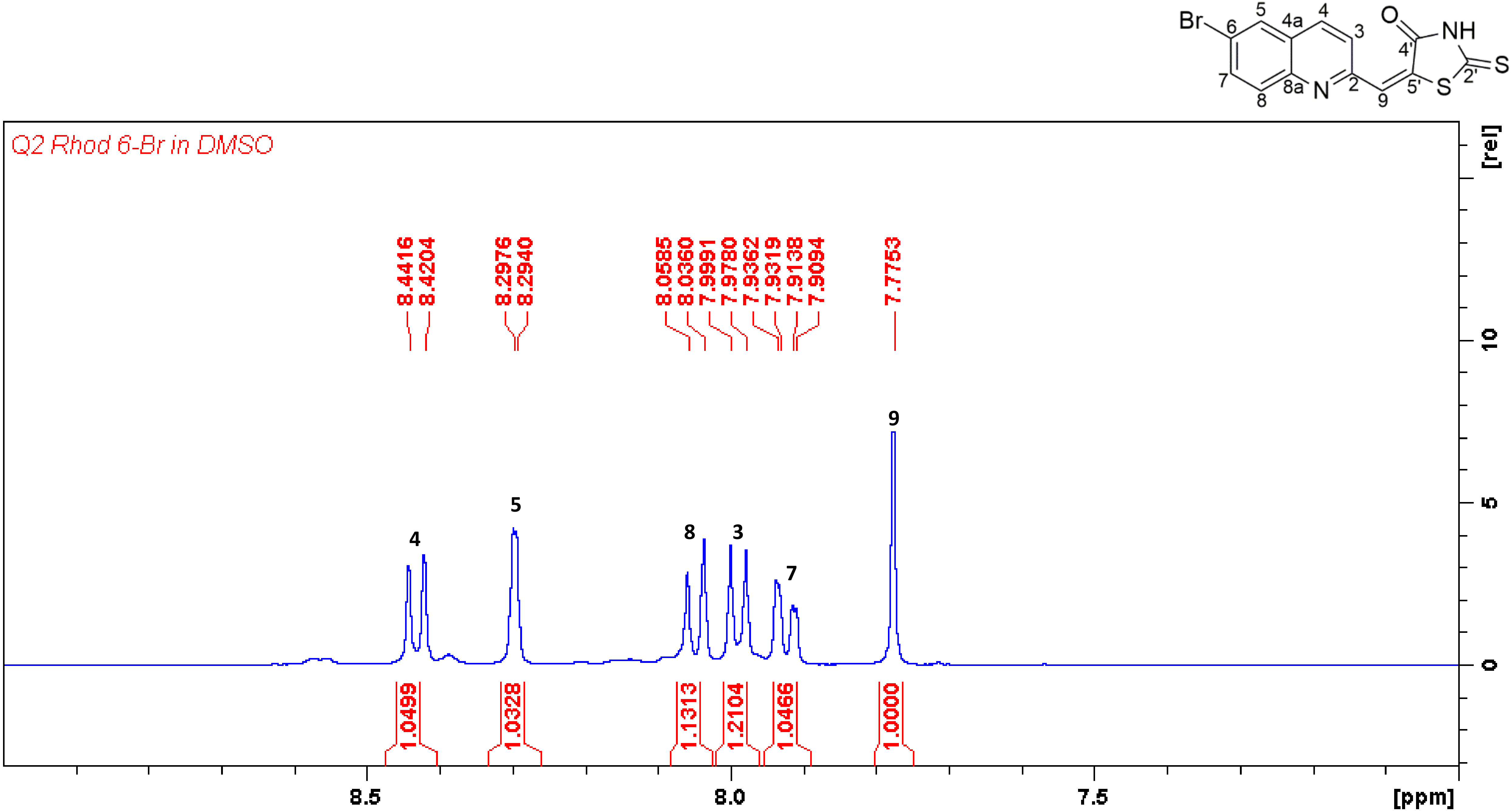

Expanded ^{1}H NMR spectrum of **C5h**

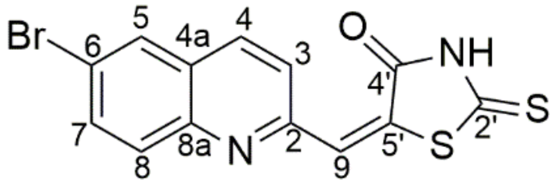

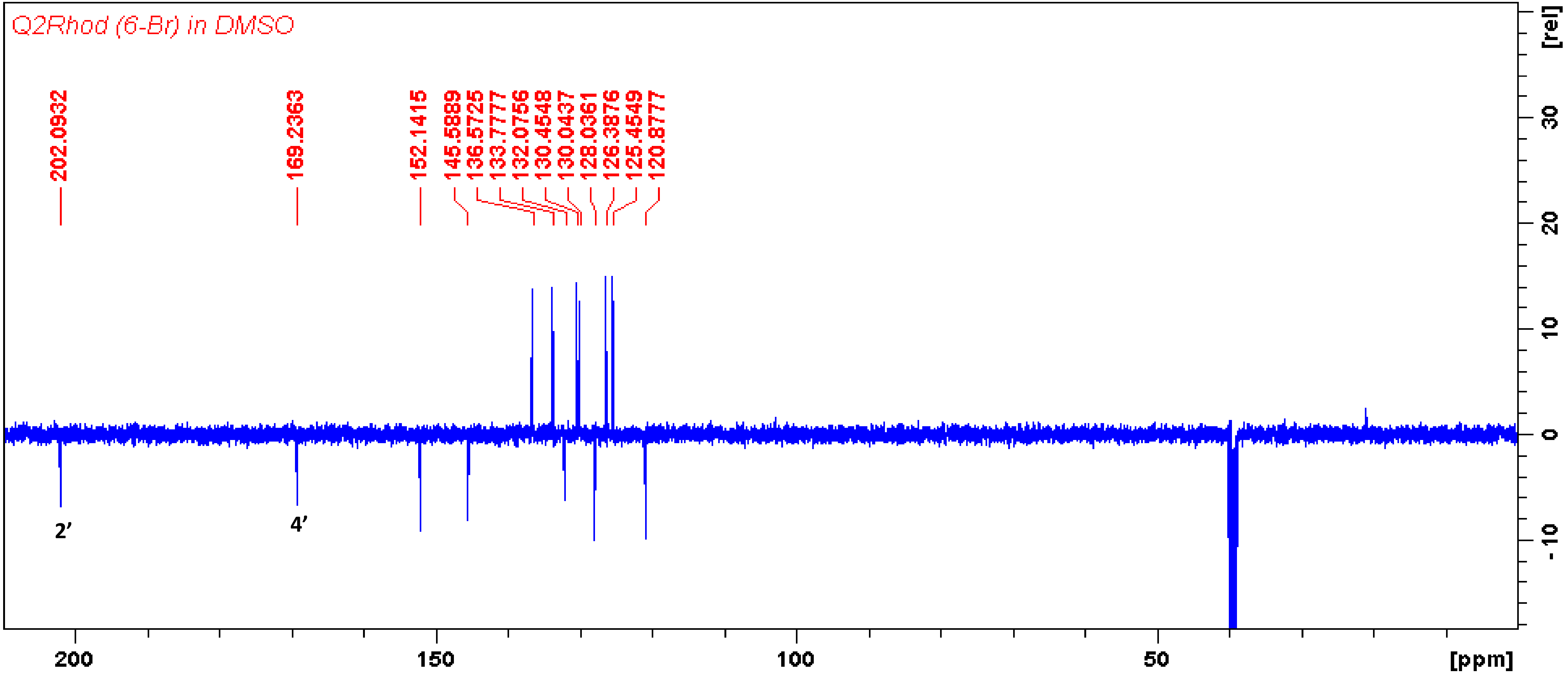

^{13}C NMR spectrum of **C5h**

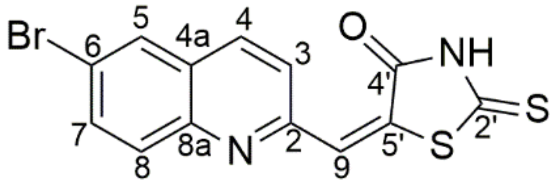

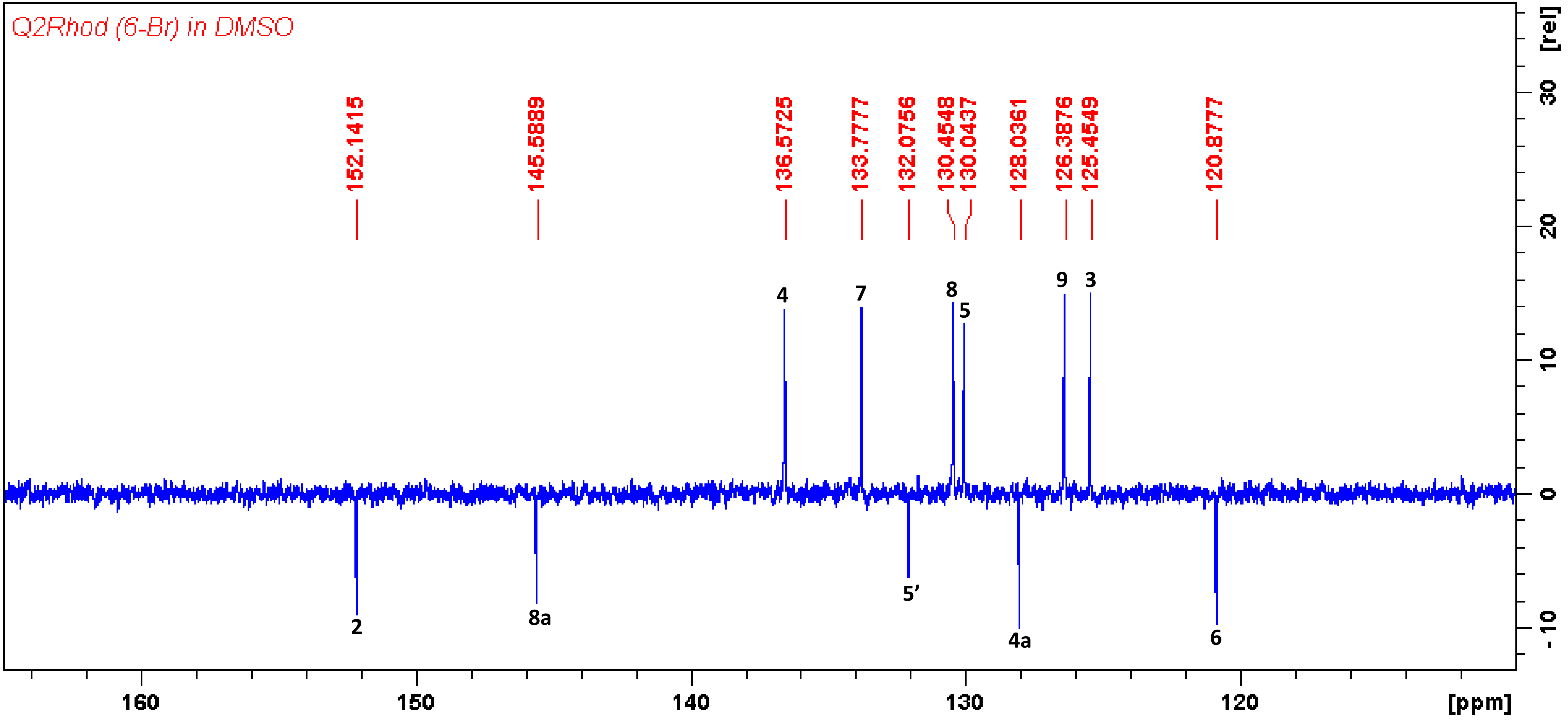

Expanded ^{13}C NMR spectrum of **C5h**

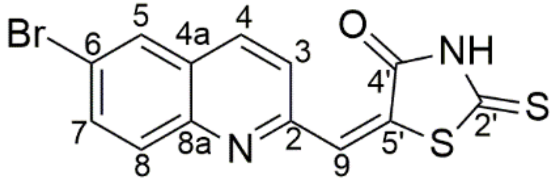

Br
6
5
4a
4
3
O
NH
4'
S
2'
5'
S
7
8
8a
N
2
9

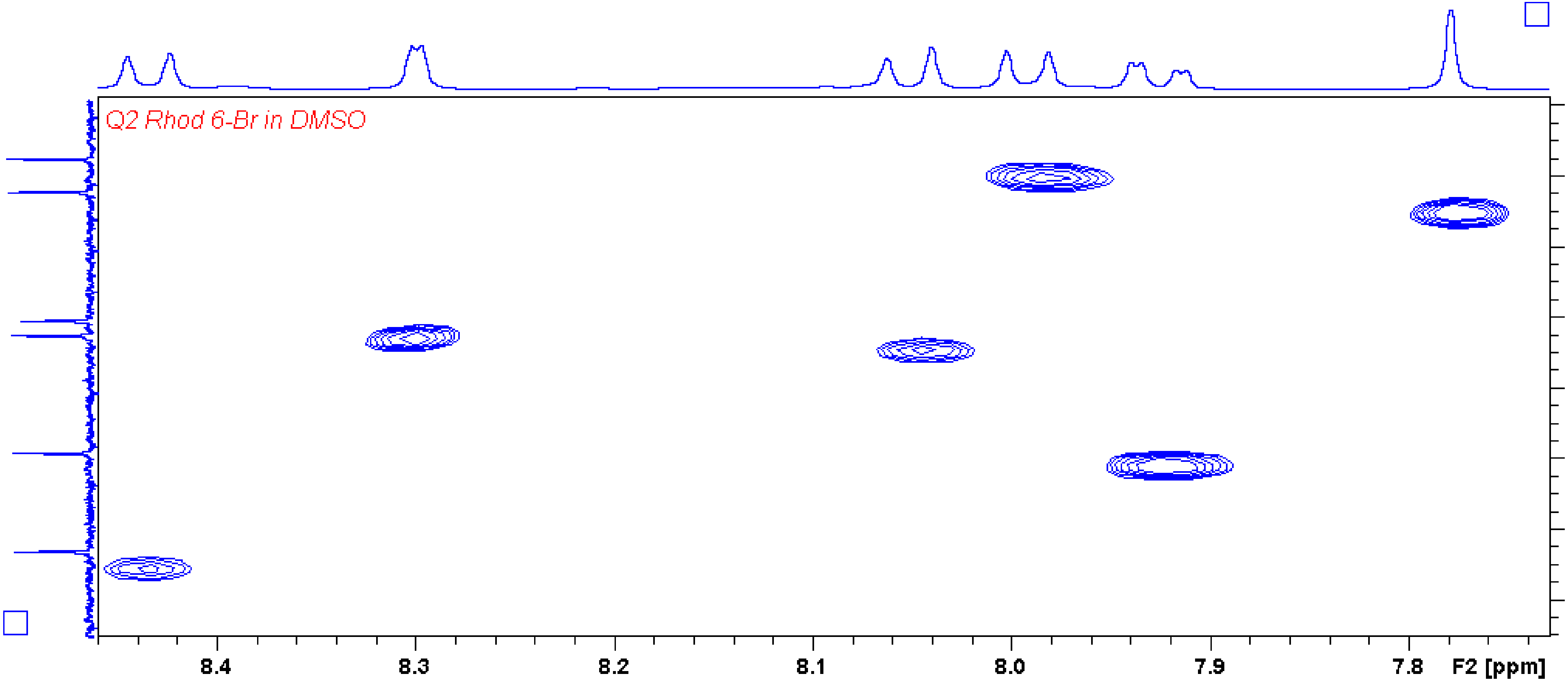

Q2 Rhod 6-Br in DMSO
F1 [ppm]
128
130
132
134
136
138
8.4
8.3
8.2
8.1
8.0
7.9
7.8
F2 [ppm]

HSQC of **C5h**

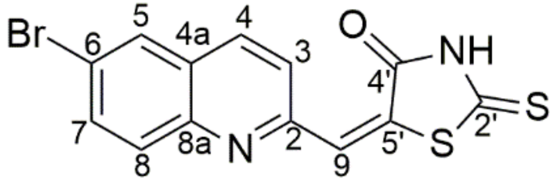

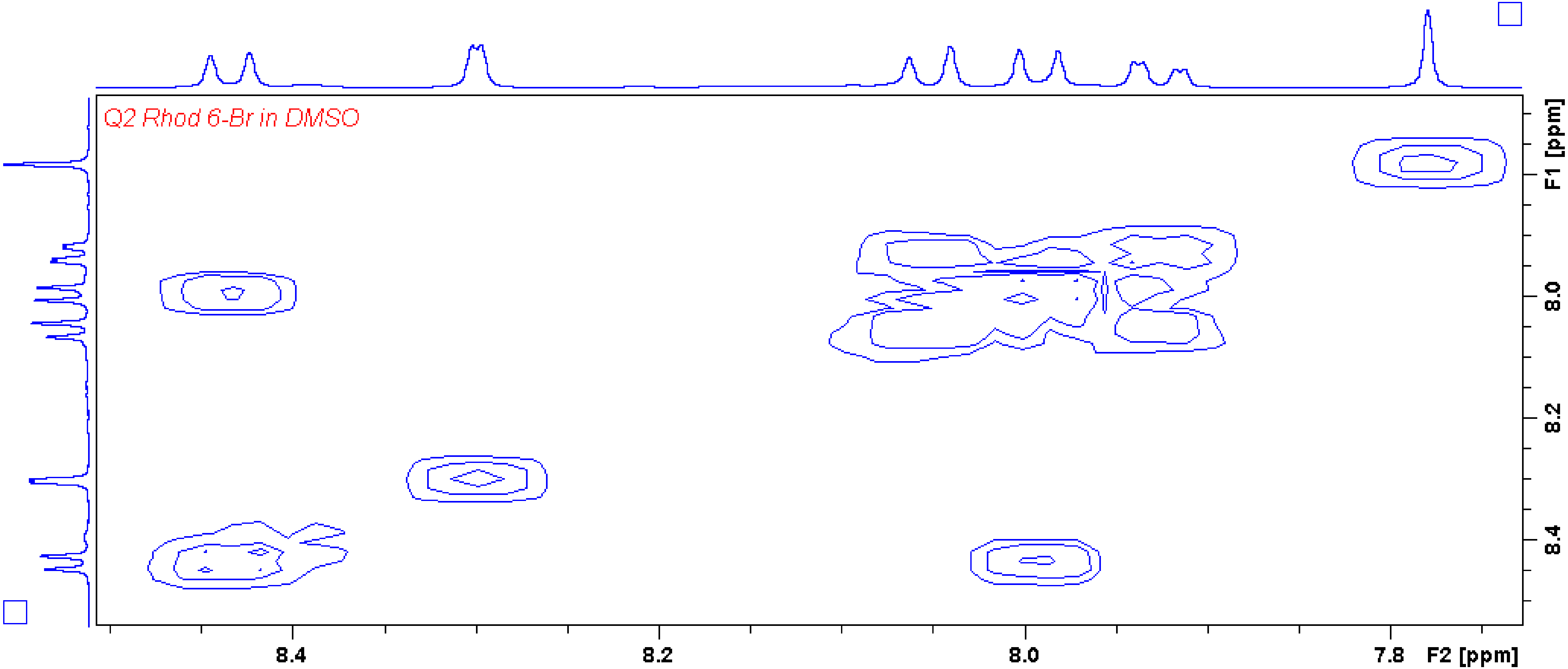

COSY of **C5h**

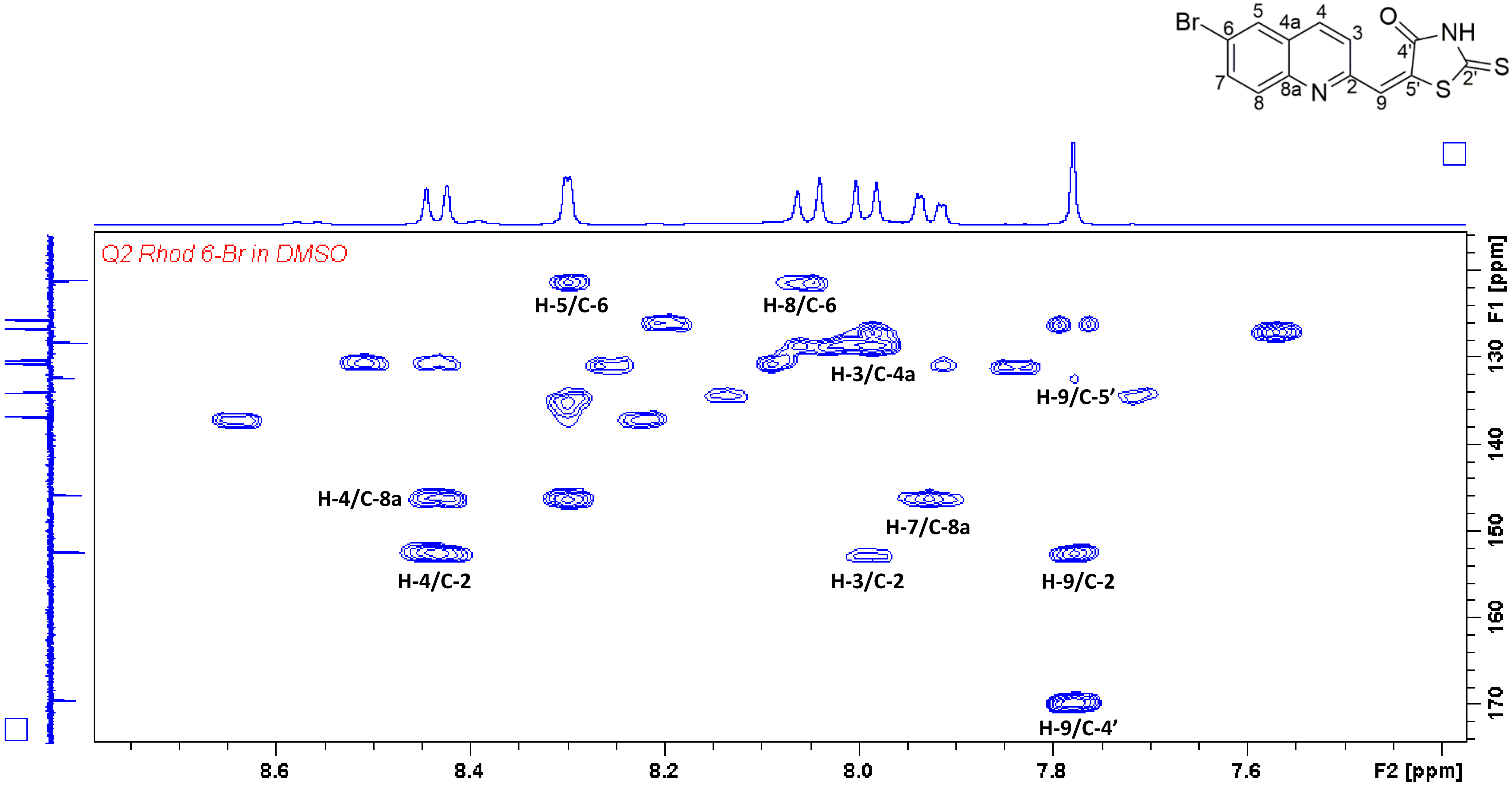
Q2 Rhod 6-Br in DMSO
H-5/C-6
H-8/C-6
H-3/C-4a
H-9/C-5’
H-4/C-8a
H-7/C-8a
H-4/C-2
H-3/C-2
H-9/C-2
H-9/C-4’
F1 [ppm]
130
140
150
160
170
8.6
8.4
8.2
8.0
7.8
7.6
F2 [ppm]

HMBC of **C5h**

Single Mass Analysis

Tolerance = 5.0 PPM / DBE: min = -1.5, max = 100.0
Element prediction: Off
Number of isotope peaks used for i-FIT = 2

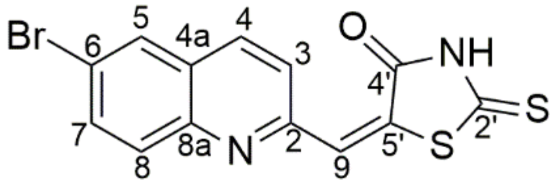

Monoisotopic Mass, Even Electron Ions
130 formula(e) evaluated with 1 results within limits (up to 20 best isotopic matches for each mass)
Elements Used:
C: 10-15 H: 5-10 N: 0-5 O: 0-5 S: 0-2 Br: 0-1

Q2R (6-Br) 19 (0.608) Cm (1:61)
TOF MS ES-

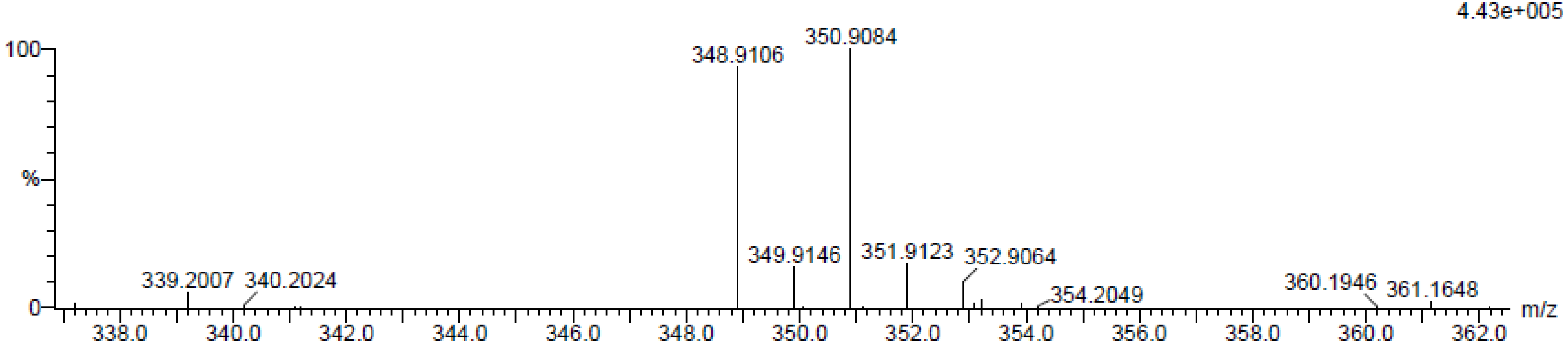

Minimum:				-1.5			
Maximum:		5.0	5.0	100.0			
Mass	Calc. Mass	mDa	PPM	DBE	i-FIT	i-FIT (Norm)	Formula
348.9106	348.9105	0.1	0.3	11.5	26.4	0.0	C13 H6 N2 O S2 Br

High resolution mass spectrum of **C5h**

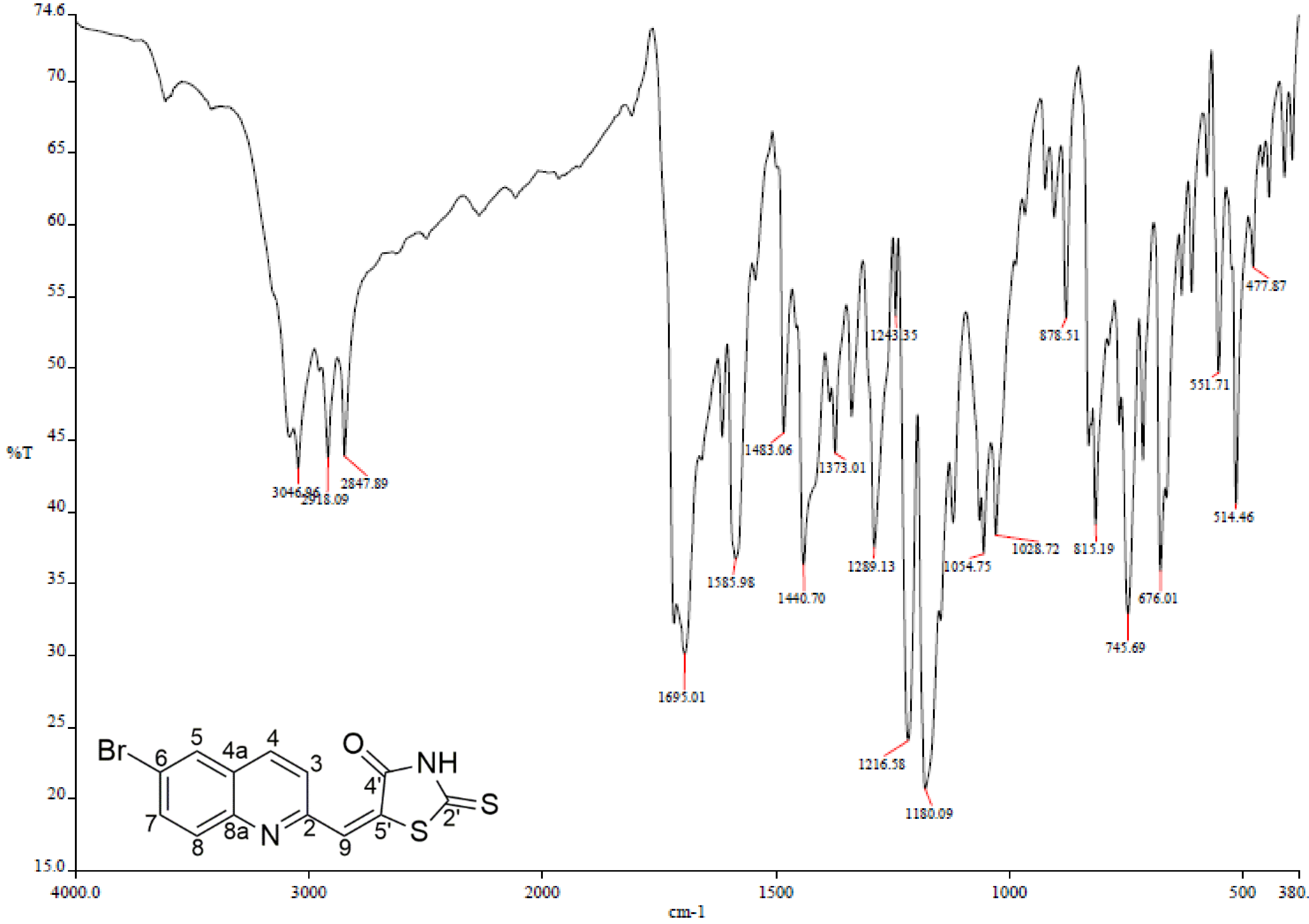

FTIR spectrum of **C5h**

Overlay Spectrum Graph Report

06/10/2017 11:35:36 AM

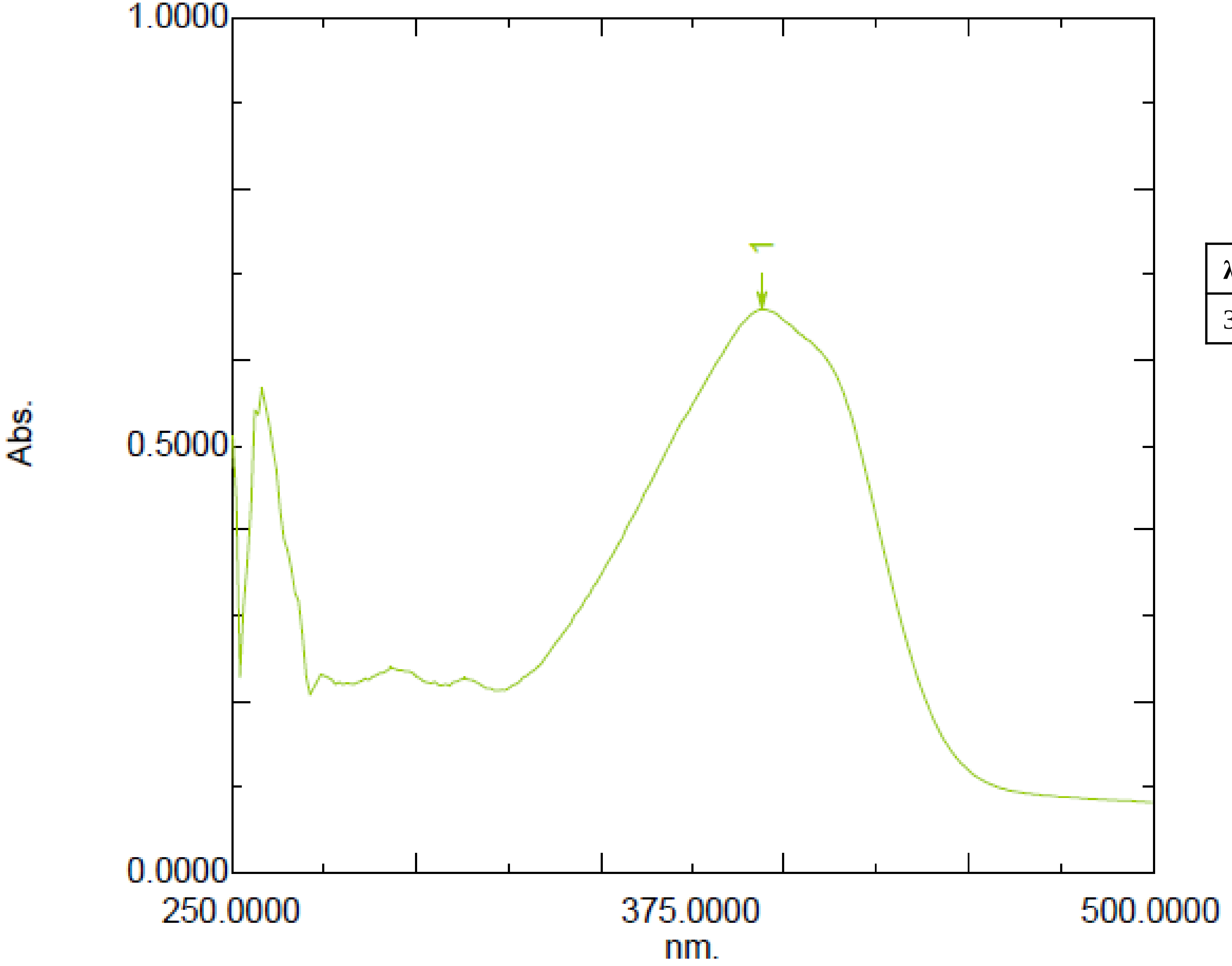

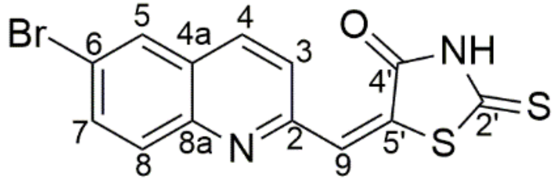

λ	absorbance	logε
394	0.659	4.66

UV spectrum of **C5h**

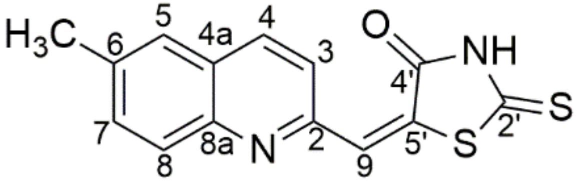

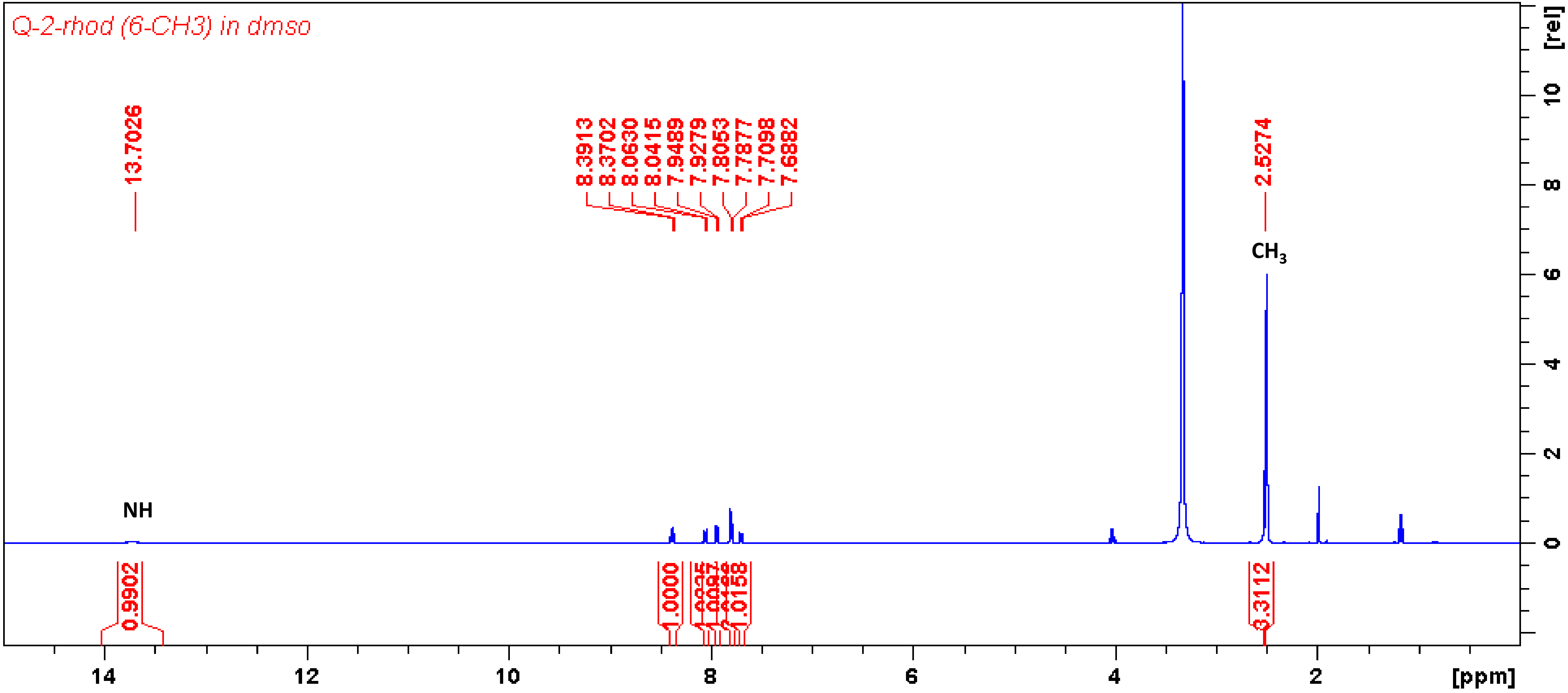

^{1}H NMR spectrum of **C5i**

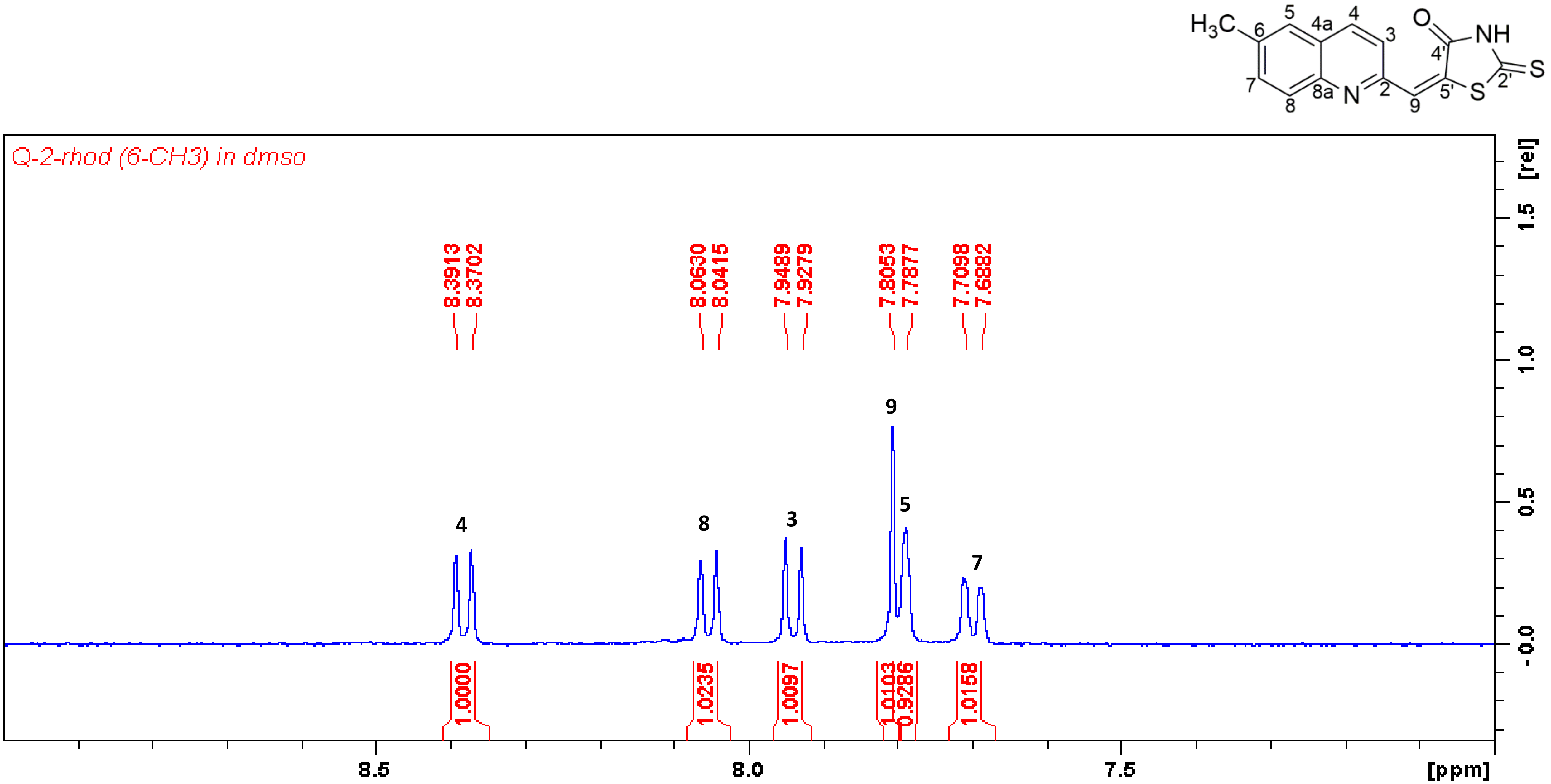

Expanded ^{1}H NMR spectrum of **C5i**

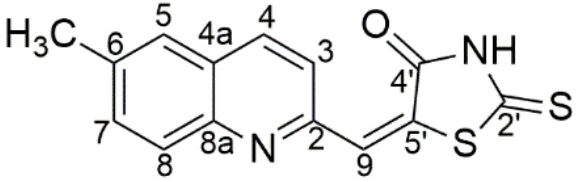

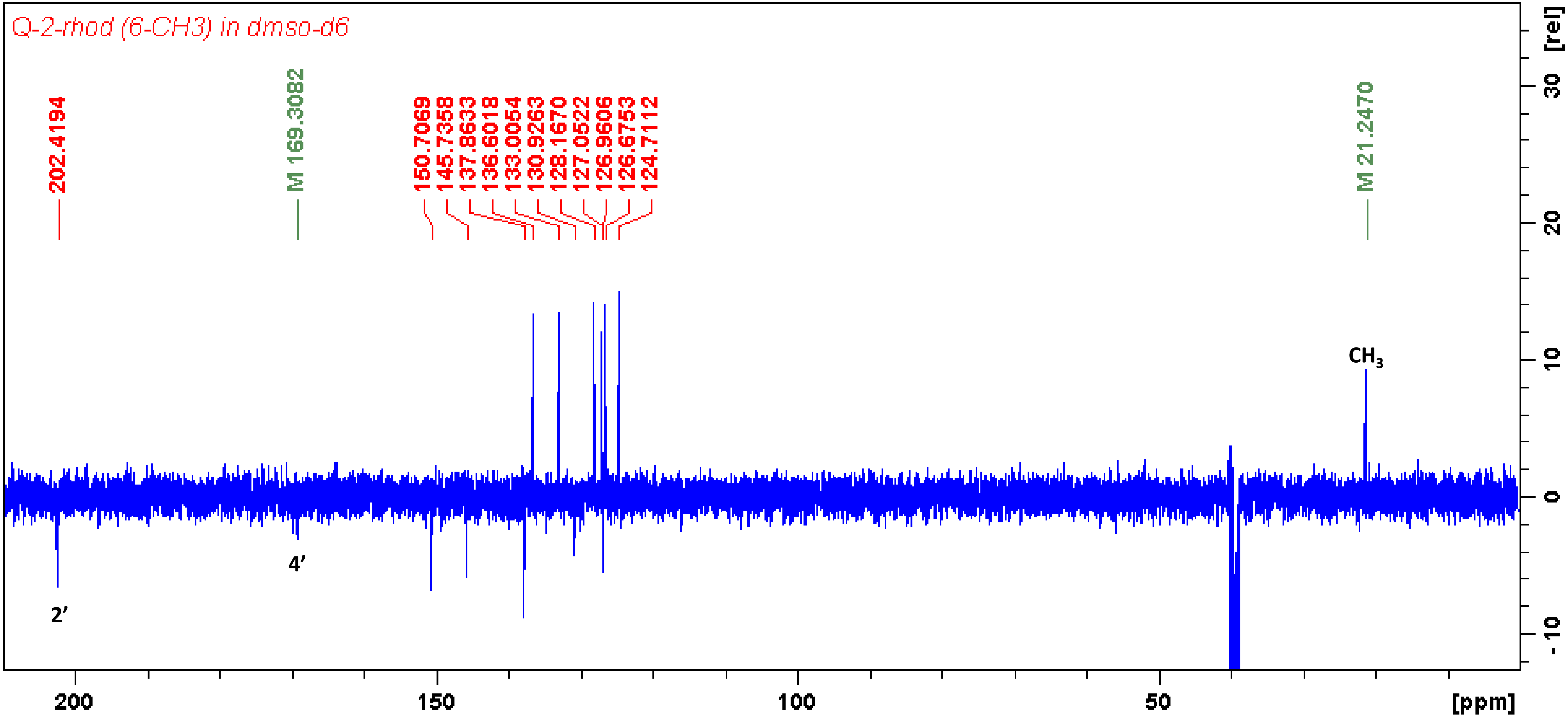

^{13}C NMR spectrum of **C5i**

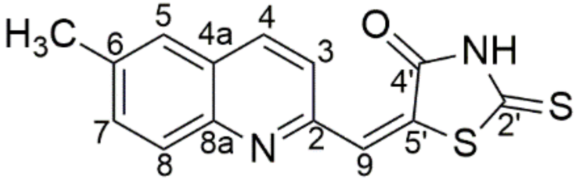

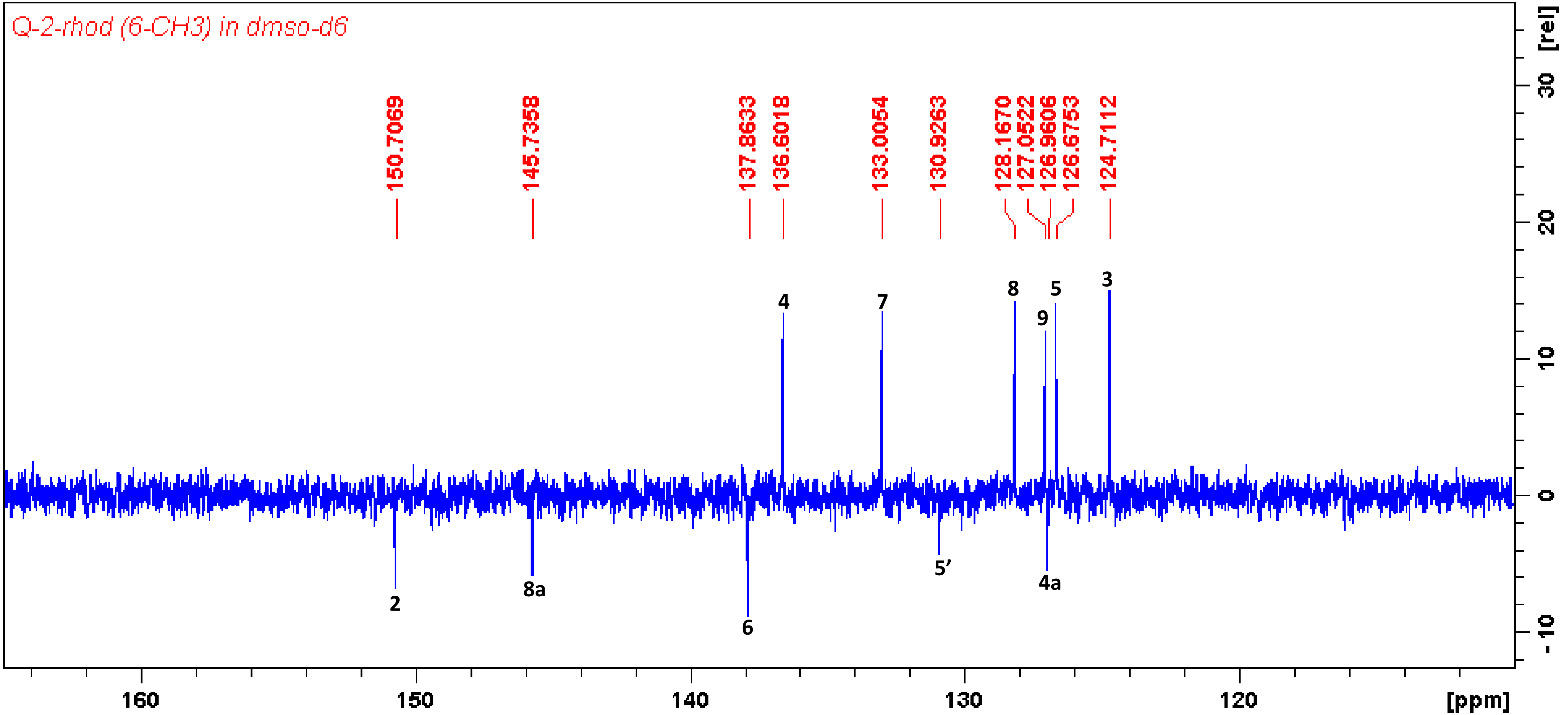

Expanded ^{13}C NMR spectrum of **C5i**

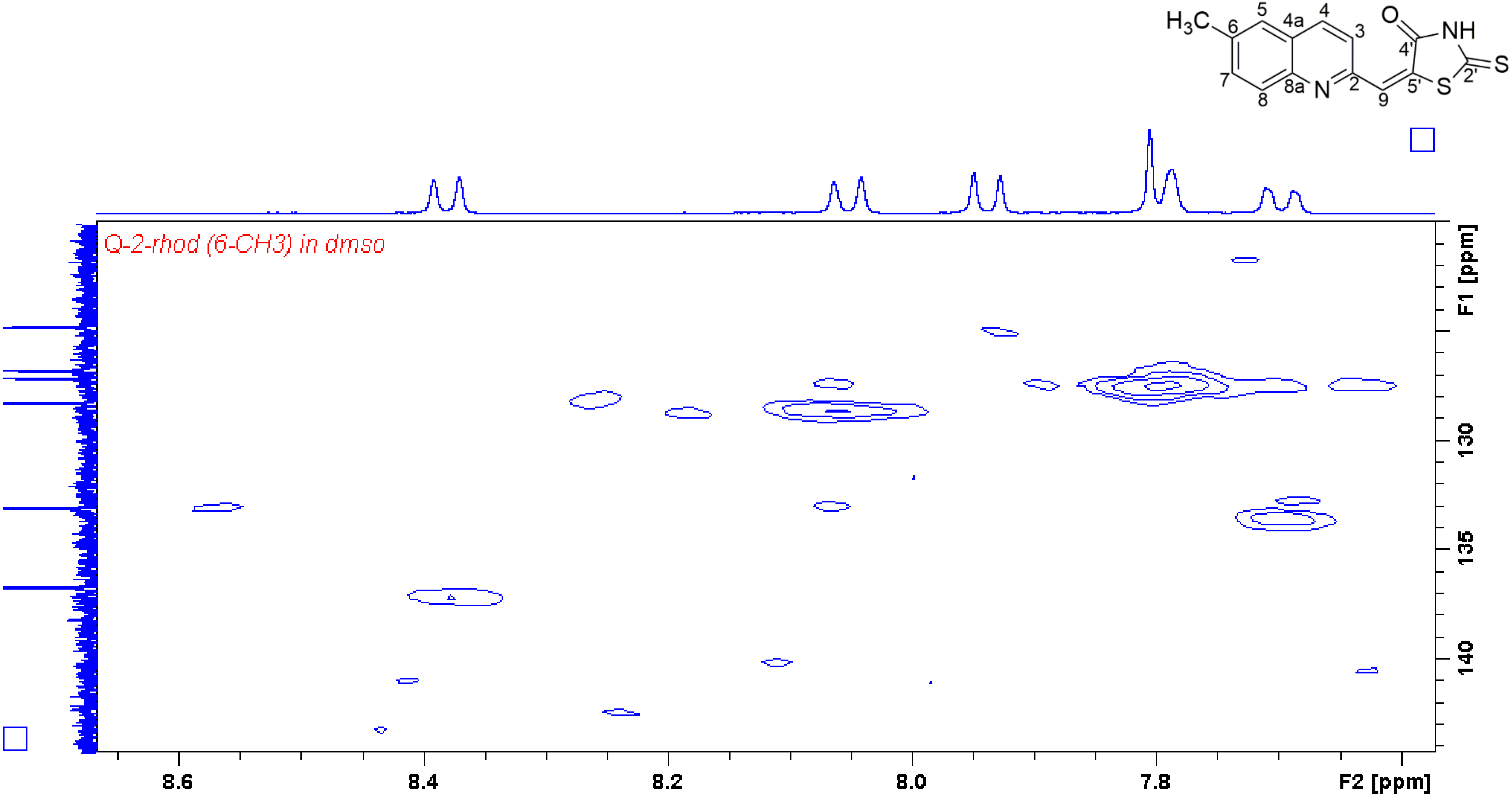

HSQC of **C5i**

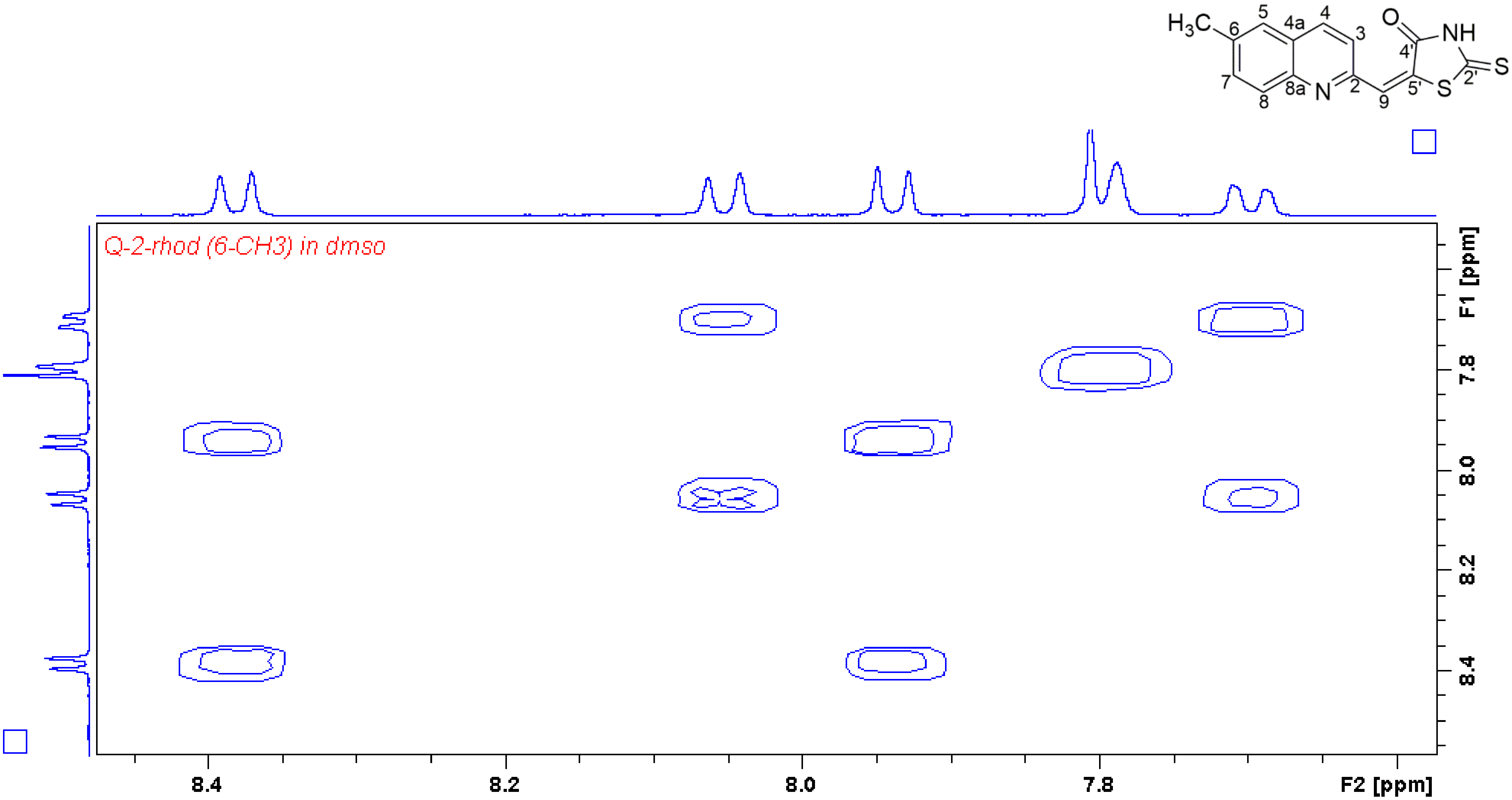

COSY of **C5i**

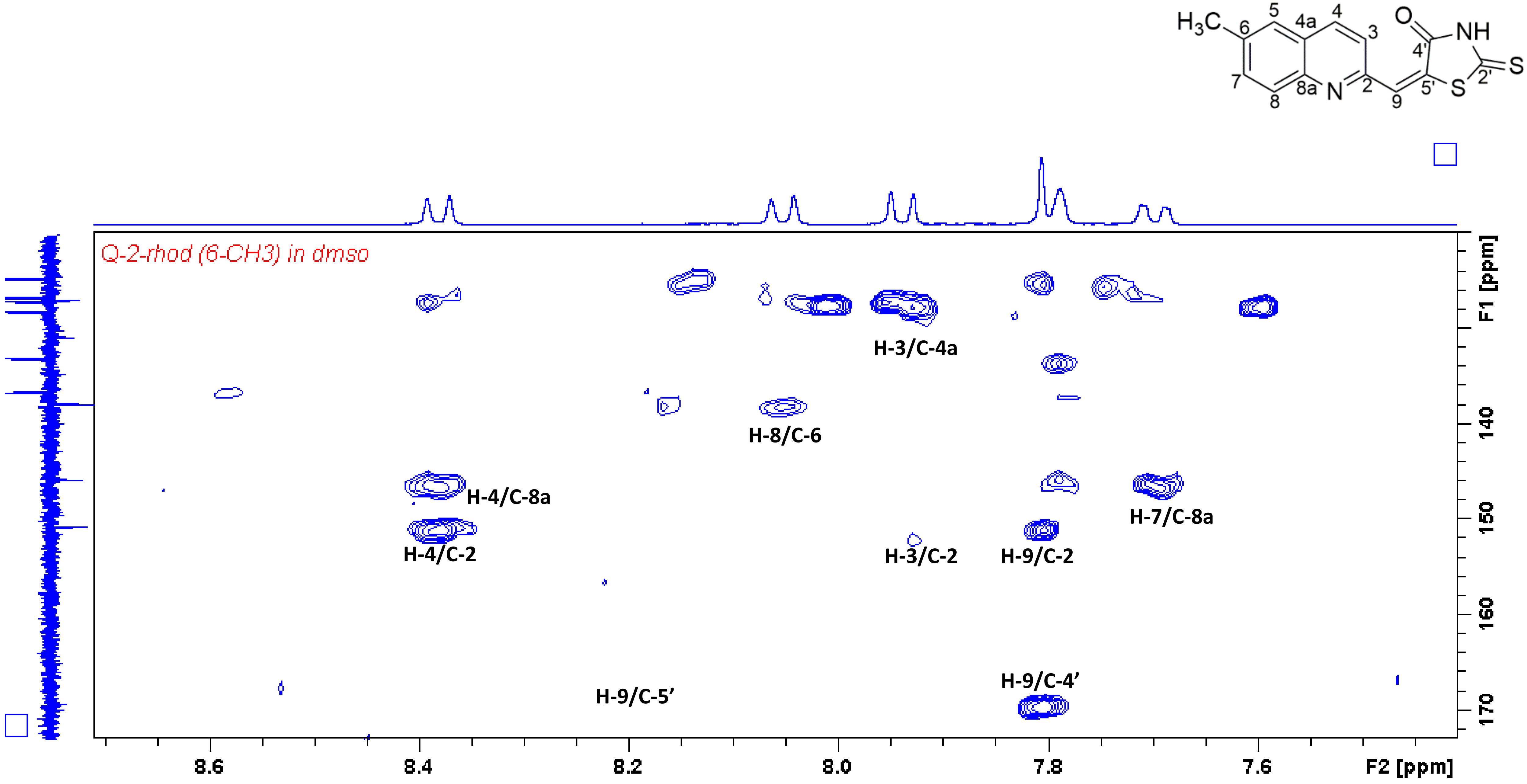
Q-2-rhod (6-CH3) in dmso
H-3/C-4a
H-8/C-6
H-4/C-8a
H-7/C-8a
H-4/C-2
H-3/C-2
H-9/C-2
H-9/C-4'
H-9/C-5'
F1 [ppm]
F2 [ppm]
8.6
8.4
8.2
8.0
7.8
7.6
140
150
160
170

HMBC of **C5i**

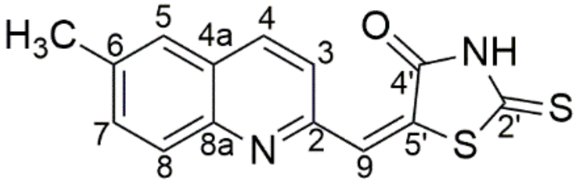

Elemental Composition Report

Single Mass Analysis

Tolerance = 5.0 PPM / DBE: min = -1.5, max = 100.0
Element prediction: Off
Number of isotope peaks used for i-FIT = 2

Monoisotopic Mass, Even Electron Ions
51 formula(e) evaluated with 1 results within limits (up to 20 best isotopic matches for each mass)
Elements Used:
C: 10-15 H: 5-10 N: 0-5 O: 0-5 S: 0-2
Q2R (6-CH3) 9 (0.270) Cm (1:61)
TOF MS ES-

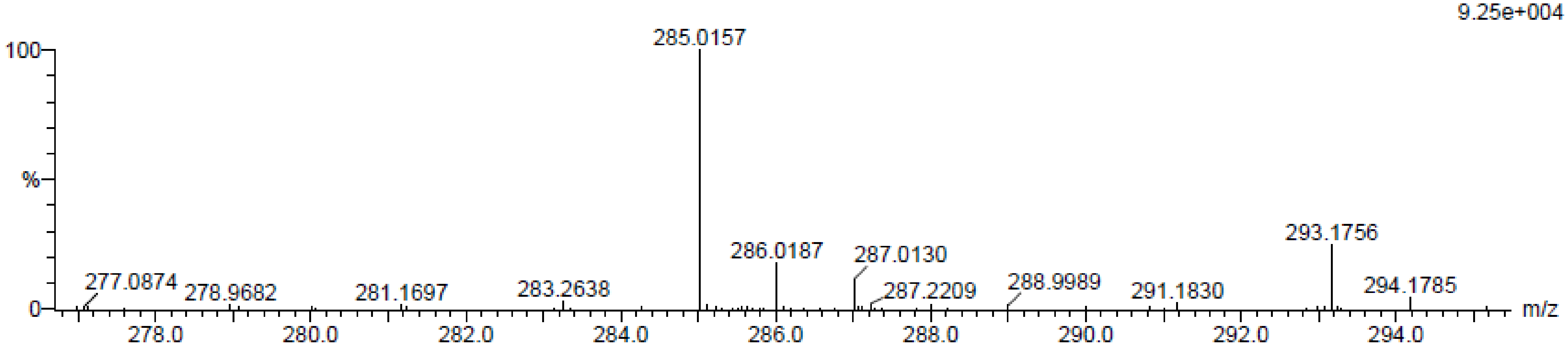

Minimum:				-1.5			
Maximum:		5.0	5.0	100.0			
Mass	Calc. Mass	mDa	PPM	DBE	i-FIT	i-FIT (Norm)	Formula
285.0157	285.0156	0.1	0.4	11.5	167.4	0.0	C14 H9 N2 O S2

High resolution mass spectrum of **C5i**

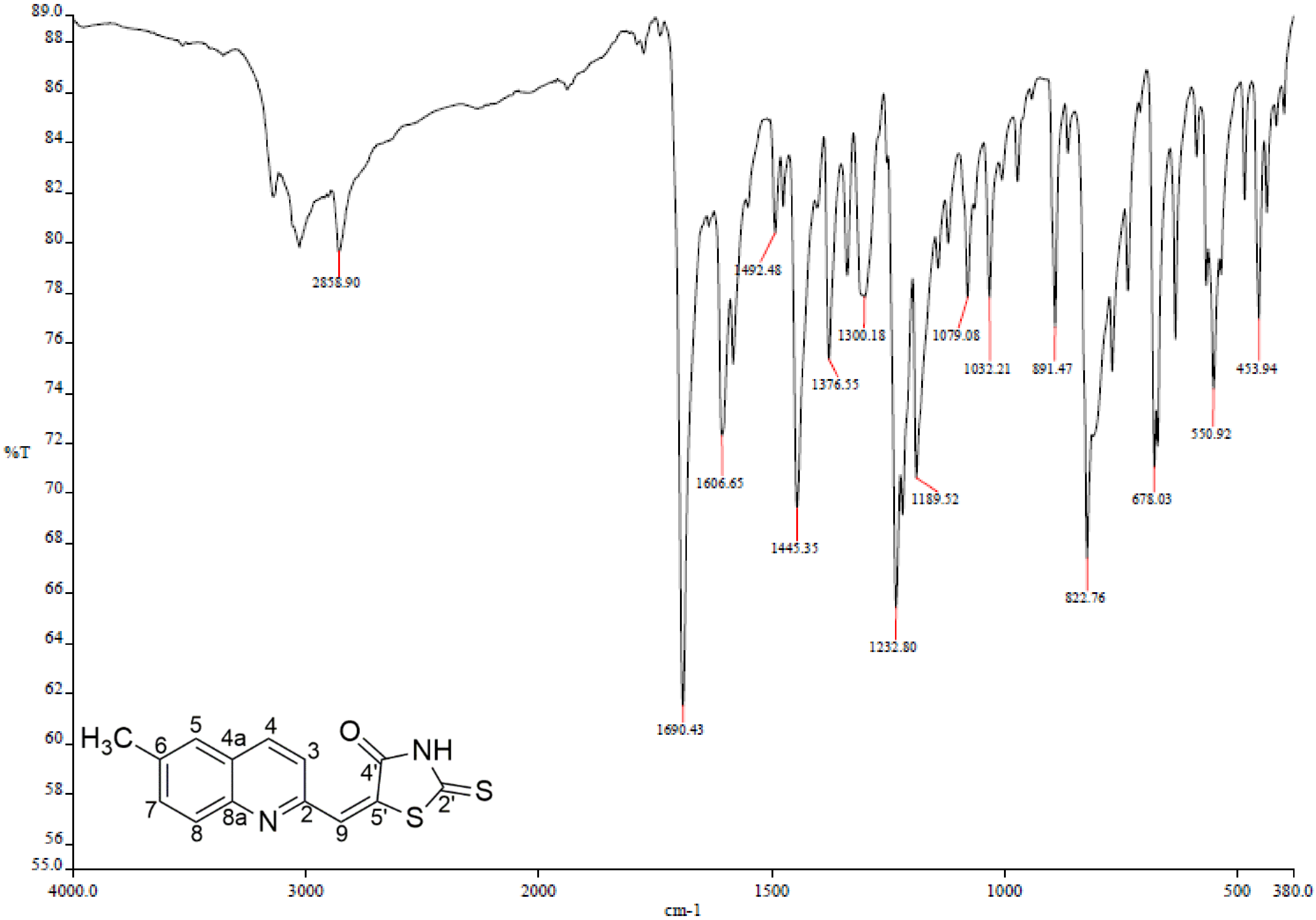

FTIR spectrum of **C5i**

Overlay Spectrum Graph Report

06/10/2017 11:34:37 AM

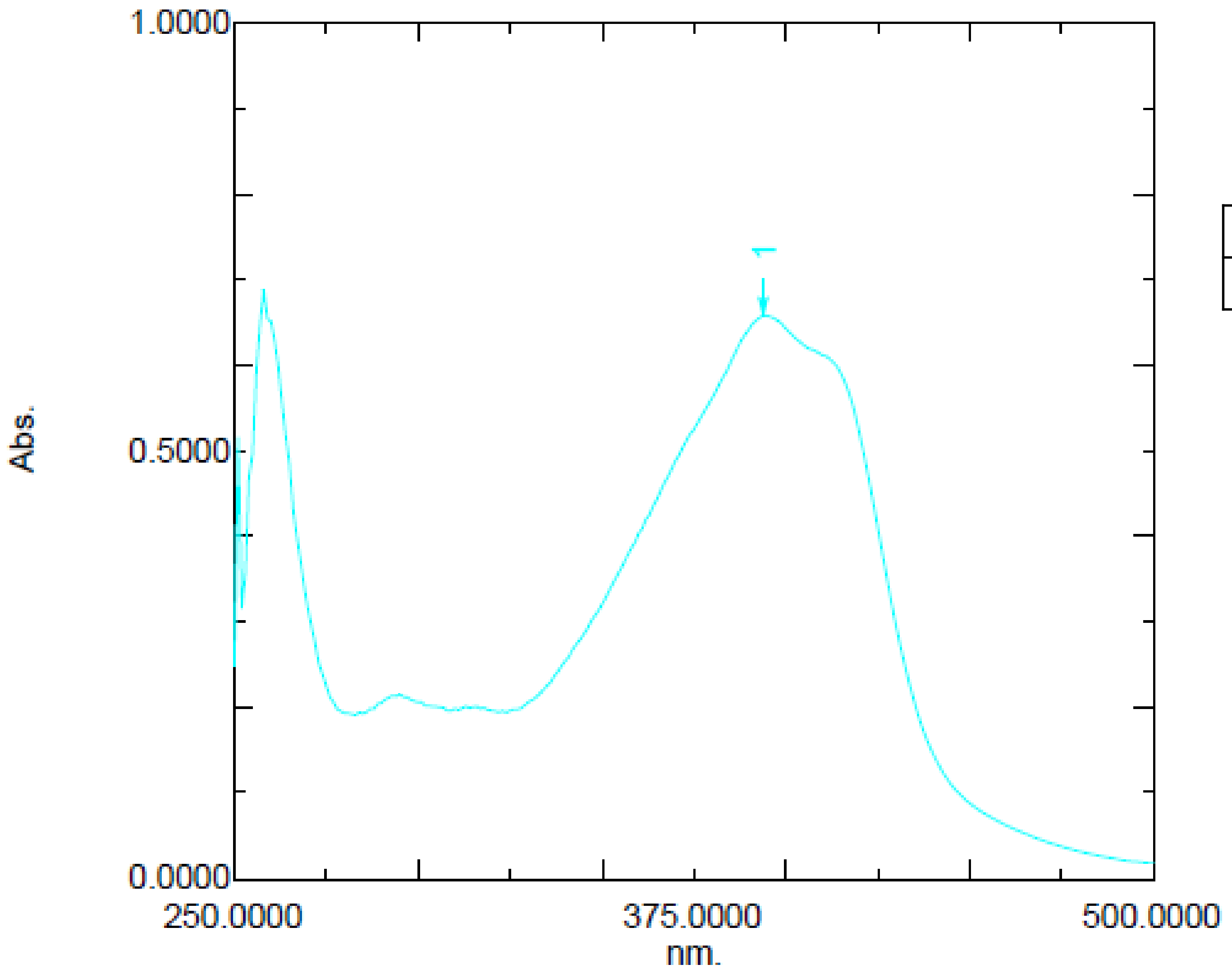

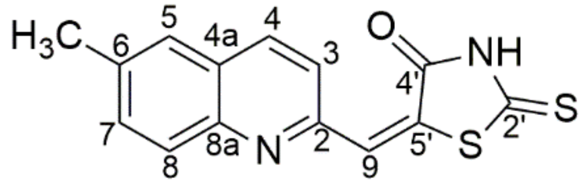

λ	absorbance	logε
394	0.658	4.58

UV spectrum of **C5i**

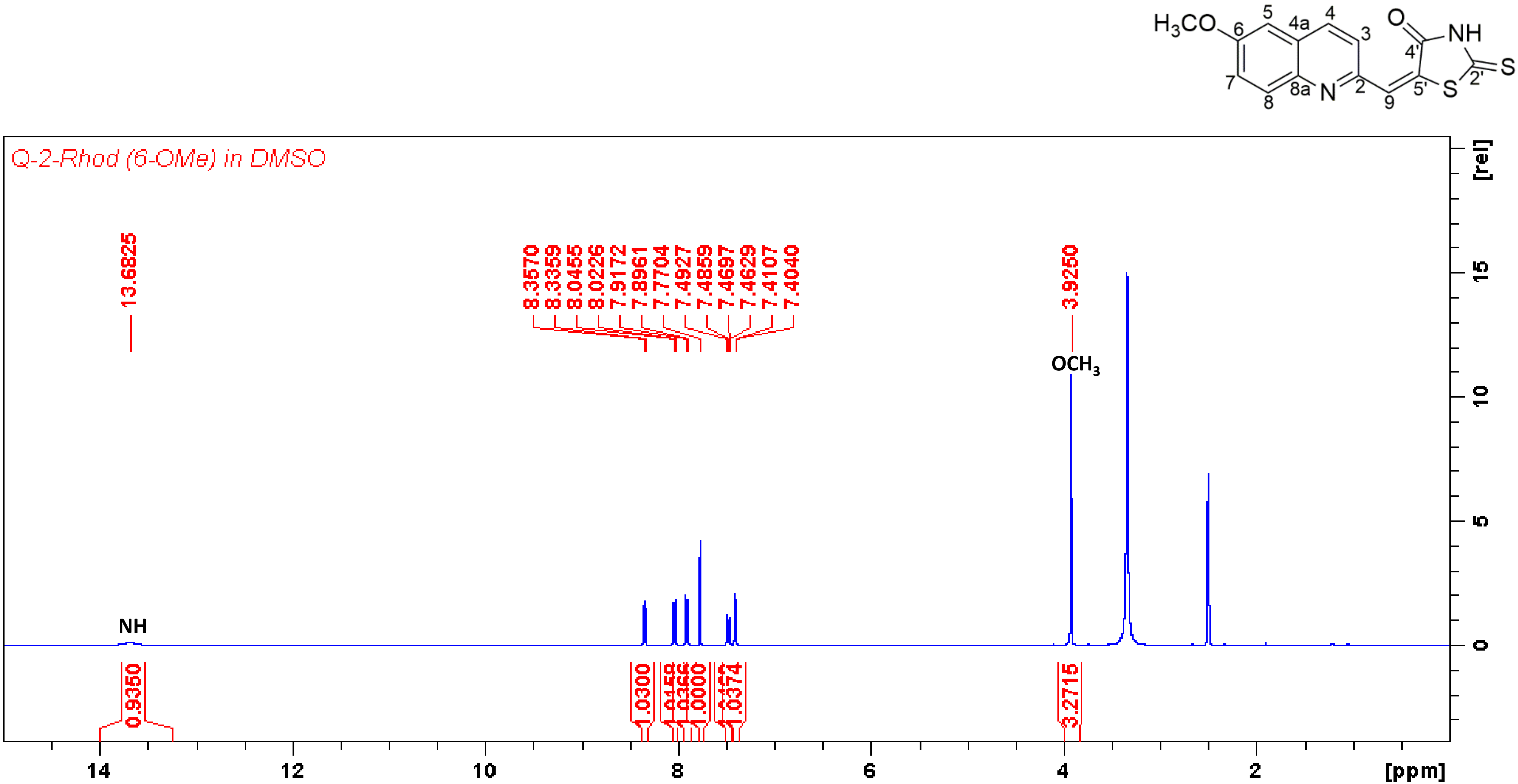

^{1}H NMR spectrum of **C5j**

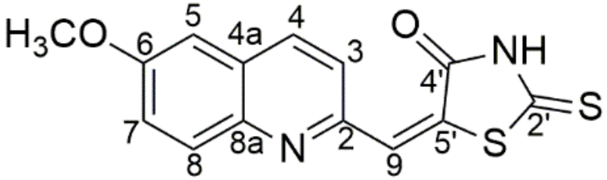

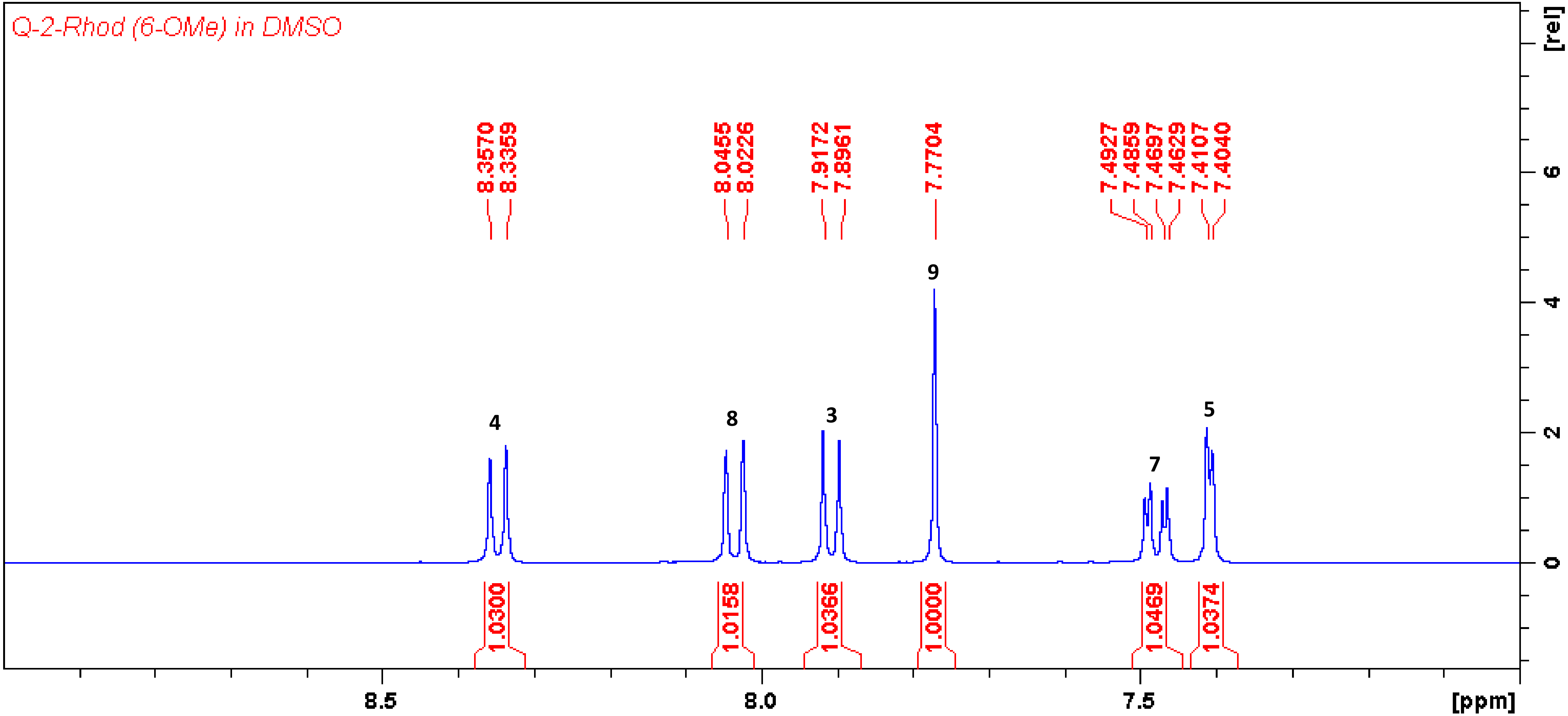

Expanded ^{1}H NMR spectrum of **C5j**

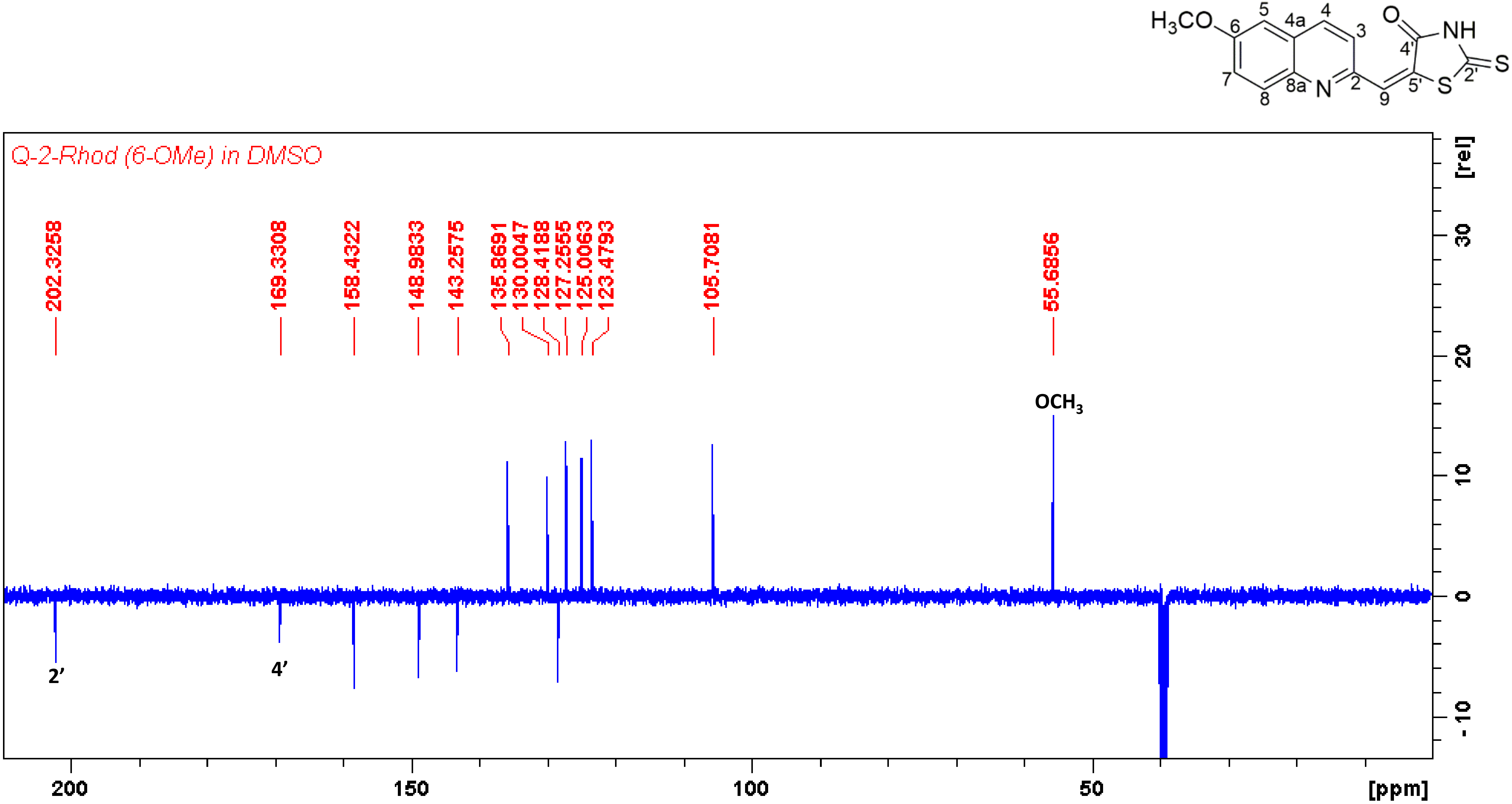

^{13}C NMR spectrum of **C5j**

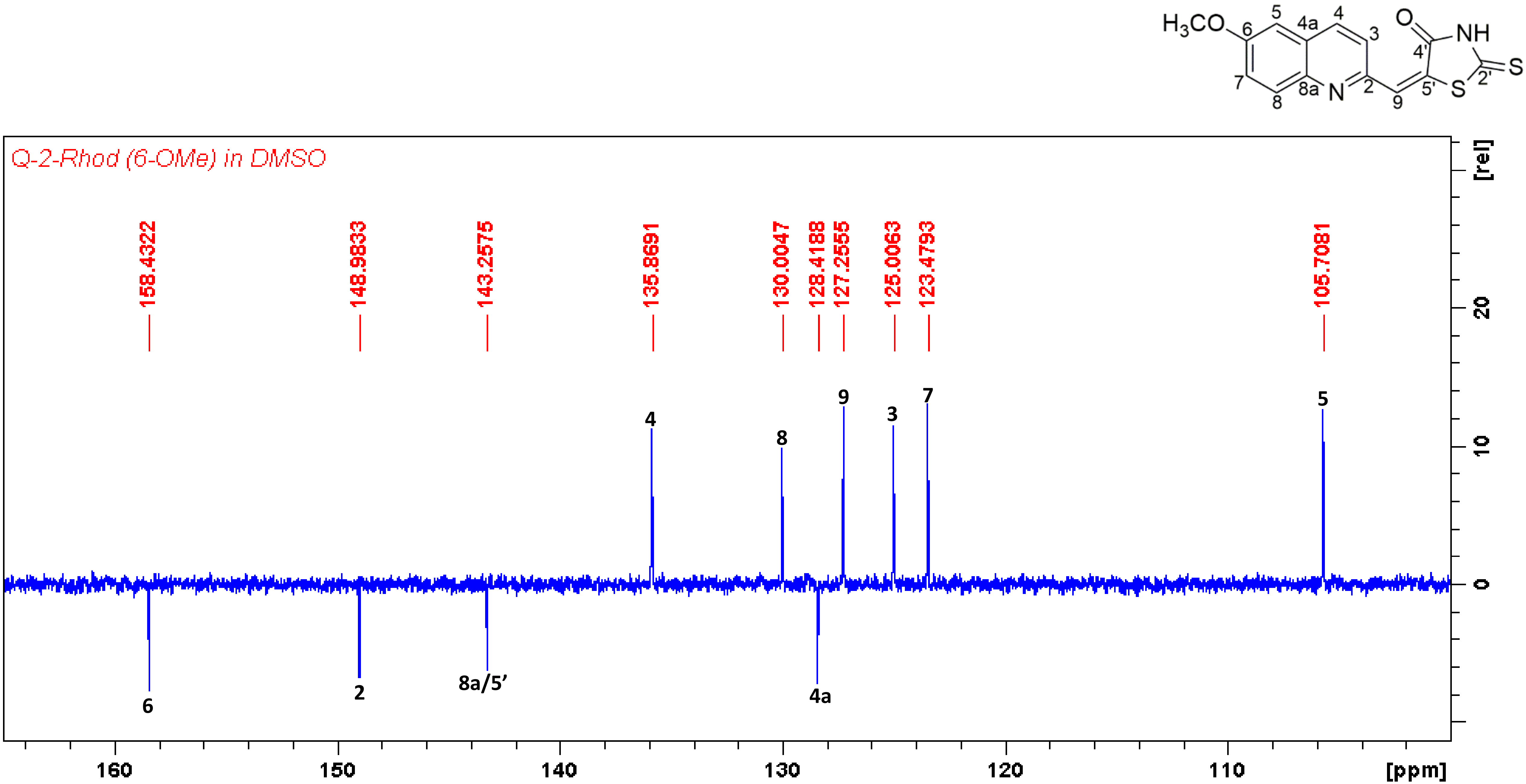

Expanded ^{13}C NMR spectrum of **C5j**

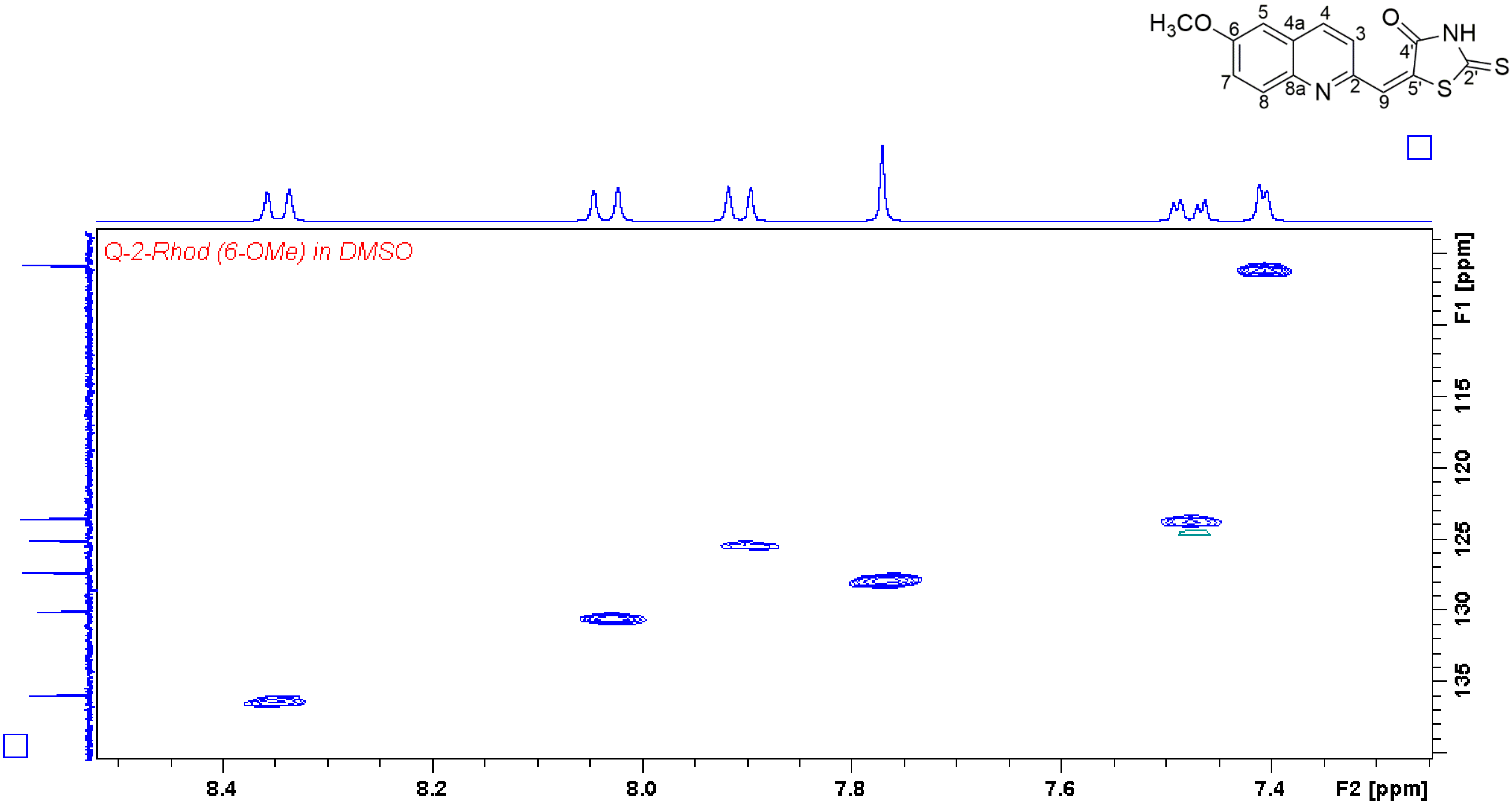

H3CO
6
5
4a
4
3
O
NH
4'
S
2'
7
8
8a
N
2
9
5'
S
Q-2-Rhod (6-OMe) in DMSO
F1 [ppm]
115
120
125
130
135
8.4
8.2
8.0
7.8
7.6
7.4
F2 [ppm]

HSQC of **C5j**

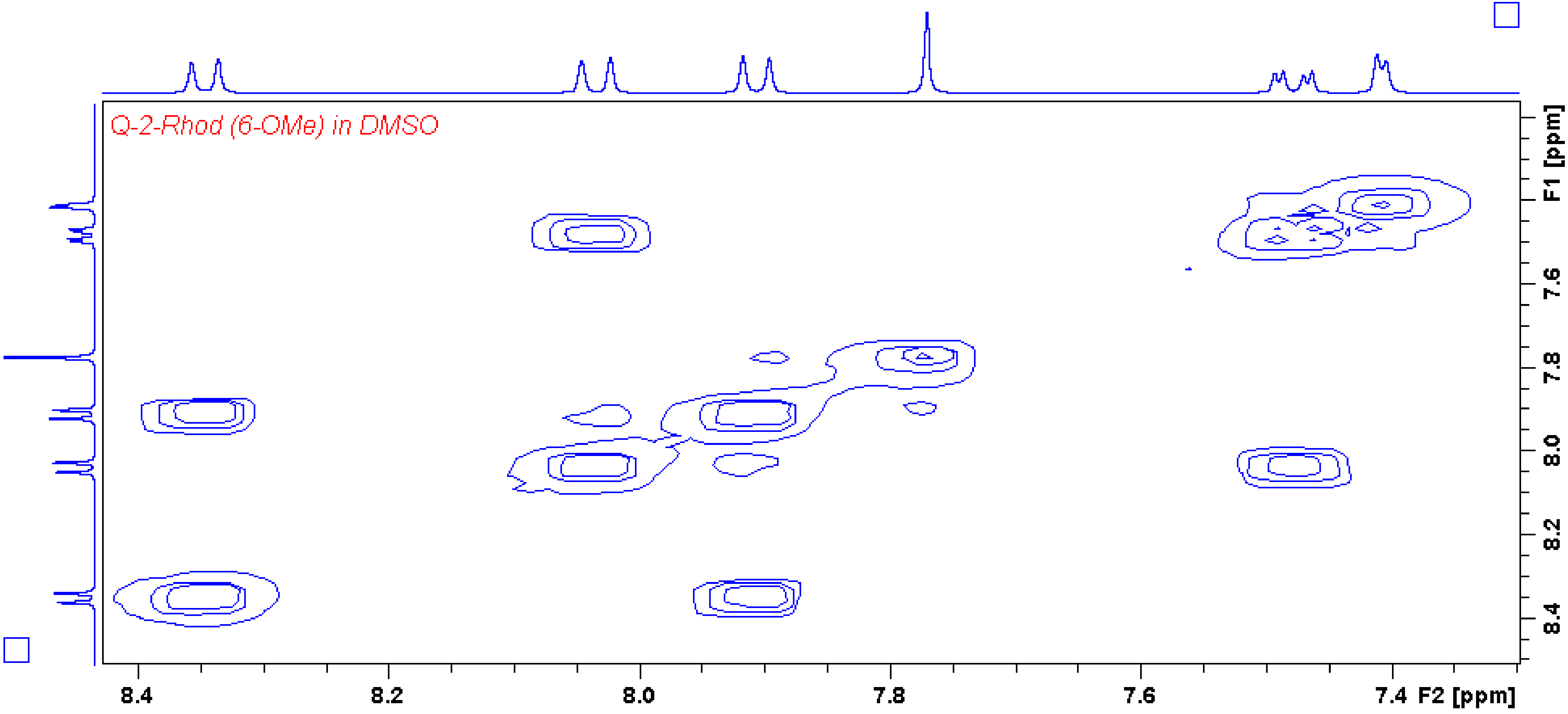

Q-2-Rhod (6-OMe) in DMSO
F1 [ppm]
7.6
7.8
8.0
8.2
8.4
8.4
8.2
8.0
7.8
7.6
7.4 F2 [ppm]

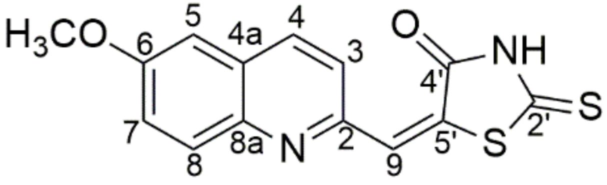

H_3CO
6
5
4a
4
3
7
8
8a
N
2
9
5'
4'
O
NH
2'
S
S

COSY of **C5j**

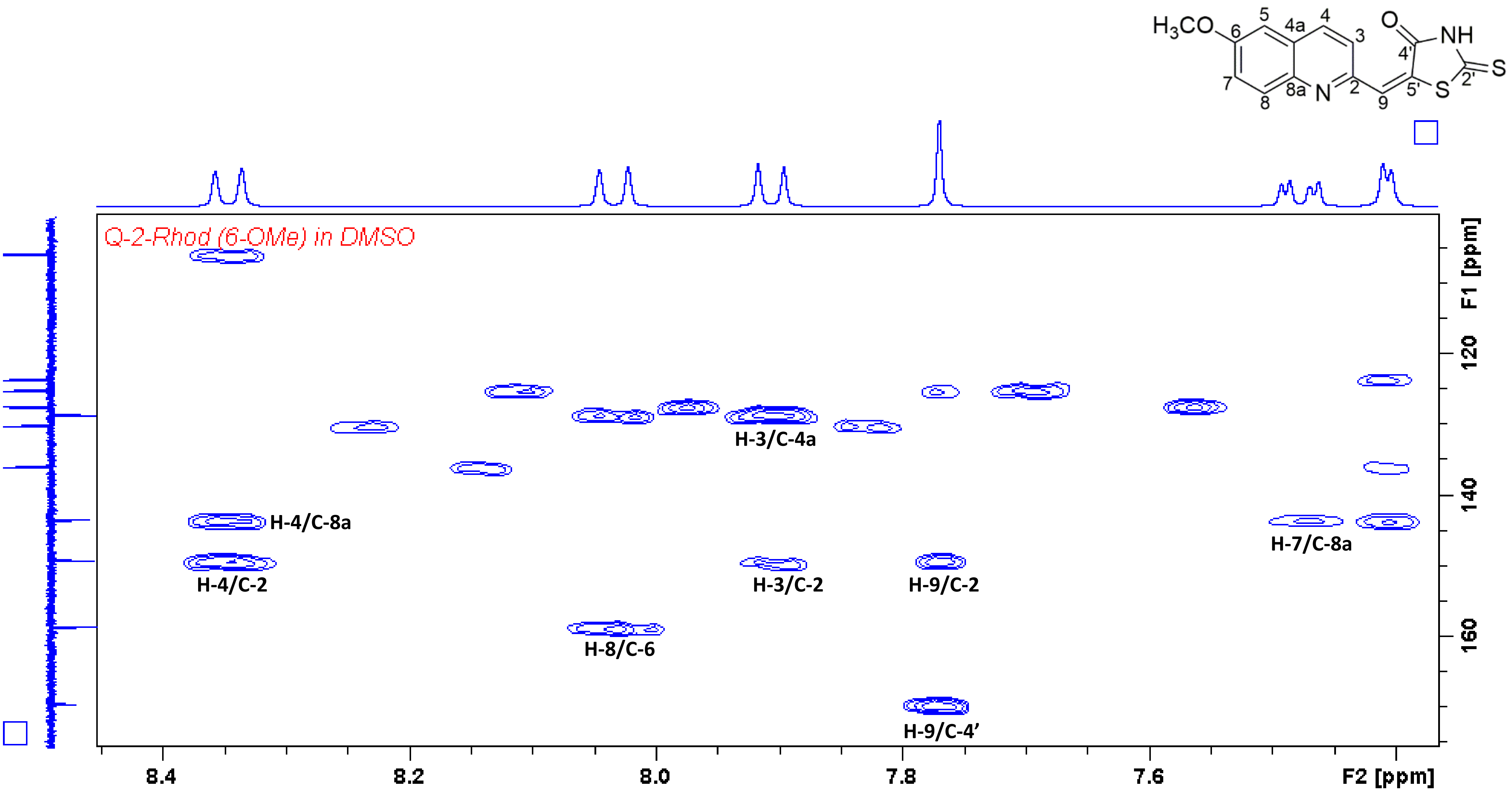

Q-2-Rhod (6-OMe) in DMSO
H-3/C-4a
H-4/C-8a
H-7/C-8a
H-4/C-2
H-3/C-2
H-9/C-2
H-8/C-6
H-9/C-4'
F1 [ppm]
120
140
160
8.4
8.2
8.0
7.8
7.6
F2 [ppm]

HMBC of **C5j**

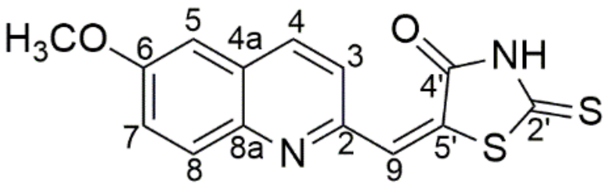

Elemental Composition Report

Single Mass Analysis

Tolerance = 5.0 PPM / DBE: min = -1.5, max = 100.0
Element prediction: Off
Number of isotope peaks used for i-FIT = 2

Monoisotopic Mass, Even Electron Ions
51 formula(e) evaluated with 1 results within limits (up to 20 best isotopic matches for each mass)
Elements Used:
C: 10-15 H: 5-10 N: 0-5 O: 0-5 S: 0-2
Q2R (6-OCH3) 22 (0.709) Cm (1:61)
TOF MS ES-

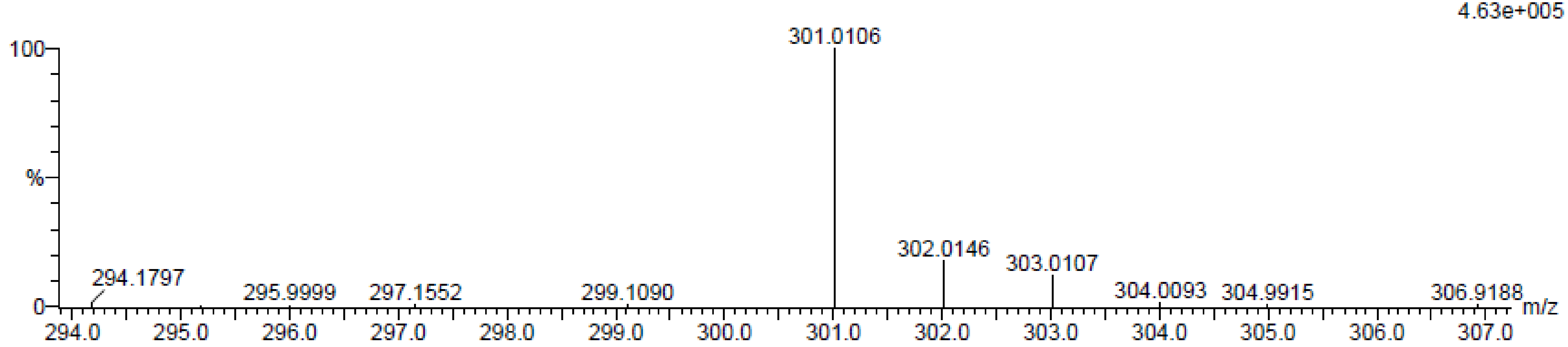

Minimum:				-1.5			
Maximum:		5.0	5.0	100.0			
Mass	Calc. Mass	mDa	PPM	DBE	i-FIT	i-FIT (Norm)	Formula
301.0106	301.0105	0.1	0.3	11.5	13.7	0.0	C14 H9 N2 O2 S2

High resolution mass spectrum of **C5j**

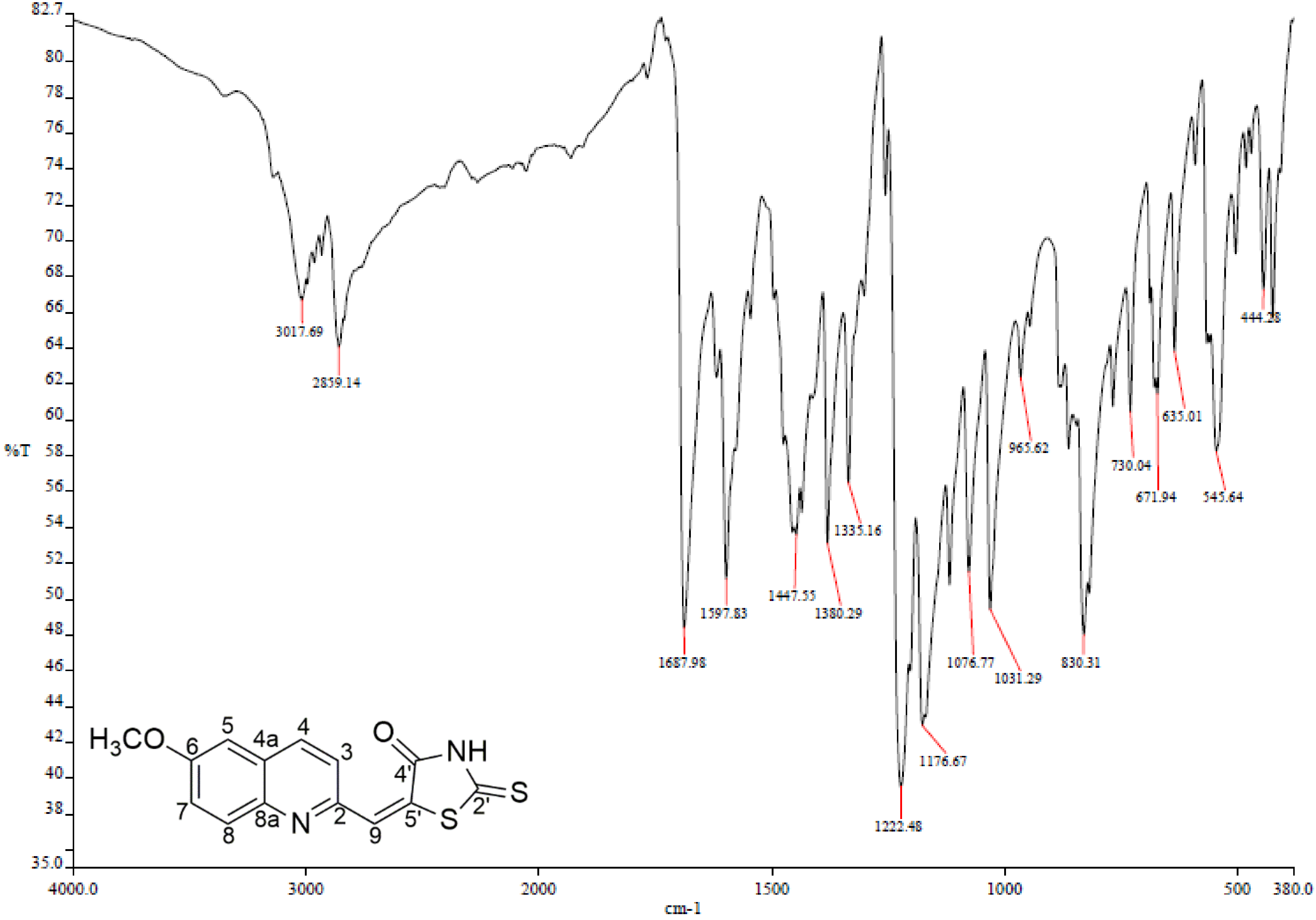

FTIR spectrum of **C5j**

Overlay Spectrum Graph Report

06/10/2017 11:32:23 AM

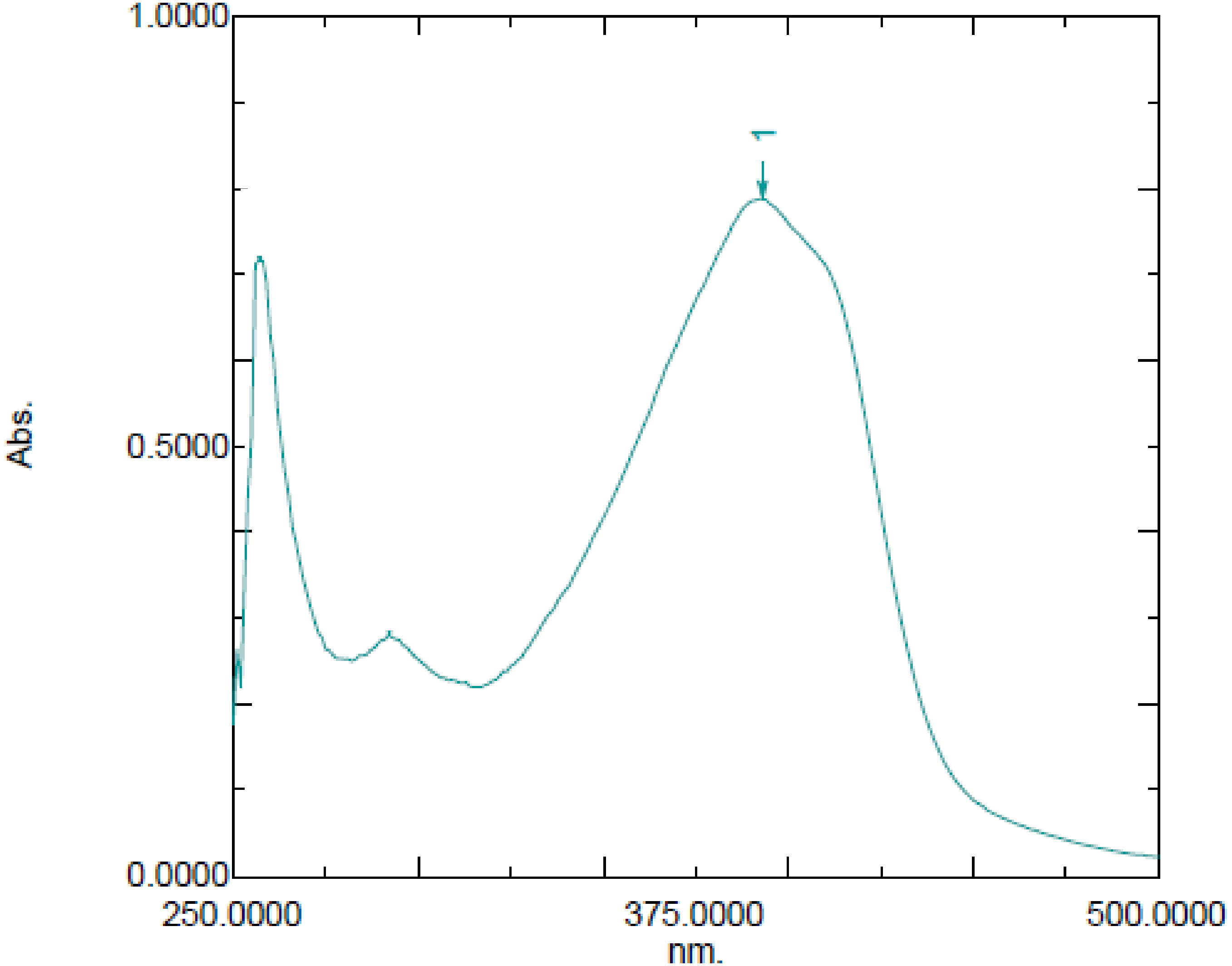

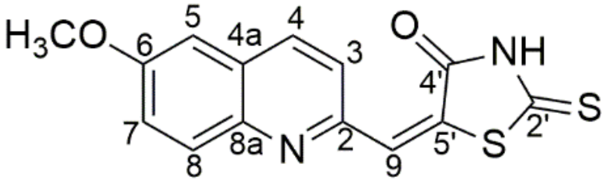

λ	absorbance	logε
419	0.772	4.67

UV spectrum of **C5j**

University of KwaZulu-Natal

Synthesis, Characterisation and Antibacterial Activity of New Quinoline and Quinoxaline Hybrid Molecules

Appendix B : Crystallographic Data

2018

Shirveen Sewpersad

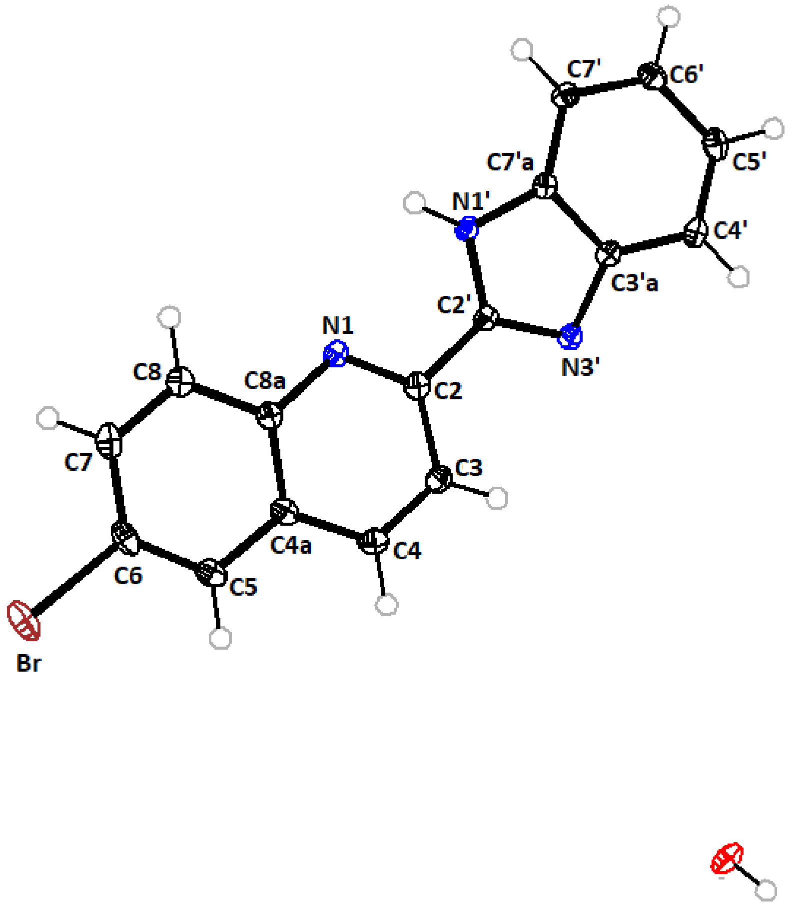

Figure 1: ORTEP diagram of the asymmetric unit of 2-(1H-benzo[d]imidazol-2-yl)-6-bromoquinoline (**A5f**)

Table 1: Crystal data and structure refinement for **A5f**

Identification code	shelx	
Empirical formula	C16 H12 Br N3 O	
Formula weight	342.20	
Temperature	100(2) K	
Wavelength	0.71073 Å	
Crystal system	Monoclinic	
Space group	C 2/c	
Unit cell dimensions	a = 13.1808(7) Å	α= 90°.
	b = 7.4783(4) Å	β= 92.734(2)°.
	c = 28.2736(13) Å	γ = 90°.
Volume	2783.8(2) $Å^3$	
Z	8	
Density (calculated)	1.633 Mg/m^3	
Absorption coefficient	2.955 mm^{-1}	
F(000)	1376	
Crystal size	0.430 x 0.230 x 0.210 mm^3	
Theta range for data collection	2.885 to 28.310°.	
Index ranges	-17<=h<=16, -8<=k<=9, -36<=l<=36	
Reflections collected	17138	
Independent reflections	3395 [R(int) = 0.0301]	
Completeness to theta = 25.242°	100.0 %	
Absorption correction	Semi-empirical from equivalents	
Max. and min. transmission	0.589 and 0.354	
Refinement method	Full-matrix least-squares on F^2	
Data / restraints / parameters	3395 / 3 / 196	
Goodness-of-fit on F^2	1.093	
Final R indices [I>2sigma(I)]	R1 = 0.0271, wR2 = 0.0650	
R indices (all data)	R1 = 0.0335, wR2 = 0.0674	
Extinction coefficient	n/a	
Largest diff. peak and hole	0.393 and -0.652 e.$Å^{-3}$	

.

Table 2: Atomic coordinates (x 10^4) and equivalent isotropic displacement parameters ($Å^2$x 10^3) for **A5f**. U(eq) is defined as one third of the trace of the orthogonalized U^{ij} tensor.

	x	**y**	**z**	**U(eq)**
C(1)	10112(1)	710(2)	6806(1)	19(1)
C(2)	10373(1)	1652(2)	6409(1)	16(1)
C(3)	9758(1)	1430(2)	5995(1)	13(1)
C(4)	9072(1)	1492(2)	5291(1)	12(1)
C(5)	8863(1)	1845(2)	4785(1)	13(1)
C(6)	7882(1)	1219(2)	4110(1)	13(1)
C(7)	7064(1)	257(2)	3889(1)	17(1)
C(8)	6831(1)	453(3)	3415(1)	19(1)
C(9)	7406(2)	1635(2)	3148(1)	18(1)
C(10)	8912(1)	292(2)	5992(1)	13(1)
C(11)	8643(1)	-658(2)	6393(1)	15(1)
C(12)	9263(1)	-428(2)	6799(1)	17(1)
C(13)	9471(1)	3074(2)	4542(1)	16(1)
C(14)	9262(1)	3350(2)	4070(1)	17(1)
C(15)	8450(1)	2415(2)	3836(1)	14(1)
C(16)	8194(1)	2607(2)	3346(1)	16(1)
N(1)	9843(1)	2185(2)	5550(1)	14(1)
N(2)	8093(1)	944(2)	4581(1)	13(1)
N(3)	8490(1)	358(2)	5539(1)	13(1)
O(1S)	13143(1)	11923(2)	4627(1)	21(1)
Br(1)	7060(1)	1861(1)	2493(1)	23(1)

Table 3: Bond lengths [Å] for **A5f.**

C(1)-C(2)	1.382(3)
C(1)-C(12)	1.406(3)
C(1)-H(1)	0.9500
C(2)-C(3)	1.401(2)
C(2)-H(2)	0.9500
C(3)-N(1)	1.390(2)
C(3)-C(10)	1.402(2)
C(4)-N(1)	1.328(2)
C(4)-N(3)	1.359(2)
C(4)-C(5)	1.468(2)
C(5)-N(2)	1.328(2)
C(5)-C(13)	1.418(2)
C(6)-N(2)	1.363(2)
C(6)-C(7)	1.416(2)
C(6)-C(15)	1.419(2)
C(7)-C(8)	1.367(2)
C(7)-H(7)	0.9500
C(8)-C(9)	1.408(3)
C(8)-H(8)	0.9500
C(9)-C(16)	1.366(3)
C(9)-Br(1)	1.8945(17)
C(10)-N(3)	1.373(2)
C(10)-C(11)	1.398(2)
C(11)-C(12)	1.386(2)
C(11)-H(11)	0.9500
C(12)-H(12)	0.9500
C(13)-C(14)	1.364(2)
C(13)-H(13)	0.9500
C(14)-C(15)	1.416(2)
C(14)-H(14)	0.9500
C(15)-C(16)	1.419(2)
C(16)-H(16)	0.9500
N(3)-H(3)	0.8800
O(1S)-H(1H)	0.812(10)
O(1S)-H(2H)	0.820(9)

Symmetry transformations used to generate equivalent atoms:

Table 4: Bond angles [°] for **A5f.**

C(2)-C(1)-C(12)	121.65(16)
C(2)-C(1)-H(1)	119.2
C(12)-C(1)-H(1)	119.2
C(1)-C(2)-C(3)	117.50(16)
C(1)-C(2)-H(2)	121.2
C(3)-C(2)-H(2)	121.2
N(1)-C(3)-C(2)	129.85(16)
N(1)-C(3)-C(10)	109.81(14)
C(2)-C(3)-C(10)	120.33(16)
N(1)-C(4)-N(3)	113.30(15)
N(1)-C(4)-C(5)	124.69(16)
N(3)-C(4)-C(5)	121.99(15)
N(2)-C(5)-C(13)	123.69(16)
N(2)-C(5)-C(4)	115.94(15)
C(13)-C(5)-C(4)	120.37(15)
N(2)-C(6)-C(7)	118.03(16)
N(2)-C(6)-C(15)	122.62(15)
C(7)-C(6)-C(15)	119.35(16)
C(8)-C(7)-C(6)	120.57(17)
C(8)-C(7)-H(7)	119.7
C(6)-C(7)-H(7)	119.7
C(7)-C(8)-C(9)	119.42(17)
C(7)-C(8)-H(8)	120.3
C(9)-C(8)-H(8)	120.3
C(16)-C(9)-C(8)	122.22(16)
C(16)-C(9)-Br(1)	119.72(14)
C(8)-C(9)-Br(1)	118.06(13)
N(3)-C(10)-C(11)	131.89(16)
N(3)-C(10)-C(3)	105.72(14)
C(11)-C(10)-C(3)	122.38(15)
C(12)-C(11)-C(10)	116.44(16)
C(12)-C(11)-H(11)	121.8
C(10)-C(11)-H(11)	121.8
C(11)-C(12)-C(1)	121.69(17)
C(11)-C(12)-H(12)	119.2
C(1)-C(12)-H(12)	119.2

C(14)-C(13)-C(5)	118.71(16)
C(14)-C(13)-H(13)	120.6
C(5)-C(13)-H(13)	120.6
C(13)-C(14)-C(15)	119.65(16)
C(13)-C(14)-H(14)	120.2
C(15)-C(14)-H(14)	120.2
C(14)-C(15)-C(16)	123.10(17)
C(14)-C(15)-C(6)	117.60(16)
C(16)-C(15)-C(6)	119.30(16)
C(9)-C(16)-C(15)	119.14(17)
C(9)-C(16)-H(16)	120.4
C(15)-C(16)-H(16)	120.4
C(4)-N(1)-C(3)	104.35(14)
C(5)-N(2)-C(6)	117.73(15)
C(4)-N(3)-C(10)	106.81(14)
C(4)-N(3)-H(3)	126.6
C(10)-N(3)-H(3)	126.6
H(1H)-O(1S)-H(2H)	106.9(19)

Symmetry transformations used to generate equivalent atoms:

Table 5. Anisotropic displacement parameters ($Å^2$x 10^3)for **A5f**. The anisotropic displacement factor exponent takes the form: $-2\pi^2[h^2a^{*2}U^{11} + ... + 2 h k a^* b^* U^{12}]$

	U^{11}	**U^{22}**	**U^{33}**	**U^{23}**	**U^{13}**	**U^{12}**
C(1)	19(1)	21(1)	15(1)	-3(1)	-4(1)	2(1)
C(2)	13(1)	17(1)	18(1)	-3(1)	-1(1)	-1(1)
C(3)	12(1)	13(1)	14(1)	-2(1)	2(1)	1(1)
C(4)	11(1)	11(1)	14(1)	-1(1)	2(1)	1(1)
C(5)	13(1)	12(1)	14(1)	-2(1)	2(1)	3(1)
C(6)	13(1)	13(1)	15(1)	-1(1)	1(1)	3(1)
C(7)	16(1)	17(1)	17(1)	-1(1)	0(1)	0(1)
C(8)	19(1)	20(1)	18(1)	-4(1)	-4(1)	2(1)
C(9)	23(1)	18(1)	12(1)	-2(1)	-2(1)	8(1)
C(10)	12(1)	13(1)	14(1)	-2(1)	1(1)	2(1)
C(11)	15(1)	15(1)	16(1)	-1(1)	3(1)	-2(1)
C(12)	20(1)	19(1)	13(1)	0(1)	2(1)	1(1)
C(13)	15(1)	14(1)	18(1)	-2(1)	1(1)	-2(1)
C(14)	18(1)	14(1)	18(1)	2(1)	4(1)	-1(1)
C(15)	16(1)	12(1)	14(1)	0(1)	1(1)	4(1)
C(16)	20(1)	14(1)	14(1)	1(1)	3(1)	4(1)
N(1)	13(1)	14(1)	14(1)	-1(1)	0(1)	-1(1)
N(2)	12(1)	13(1)	14(1)	-1(1)	1(1)	0(1)
N(3)	12(1)	14(1)	12(1)	-1(1)	0(1)	-2(1)
O(1S)	13(1)	16(1)	35(1)	-2(1)	5(1)	-4(1)
Br(1)	33(1)	24(1)	13(1)	-2(1)	-4(1)	9(1)

Table 6. Hydrogen coordinates (x 10^4) and isotropic displacement parameters ($Å^2$x 10^3) for **A5f**.

	x	y	z	U(eq)
H(1)	10517	835	7091	22
H(2)	10947	2421	6417	19
H(7)	6674	-531	4071	20
H(8)	6285	-203	3268	23
H(11)	8066	-1420	6388	18
H(12)	9109	-1055	7078	21
H(13)	10012	3693	4704	19
H(14)	9660	4165	3900	20
H(16)	8566	3402	3157	19
H(3)	7947	-222	5430	15
H(1H)	13749(8)	11990(30)	4592(9)	35
H(2H)	12942(17)	12940(18)	4676(9)	35

Table 7. Torsion angles [°] for **A5f**

C(12)-C(1)-C(2)-C(3)	-0.1(3)
C(1)-C(2)-C(3)-N(1)	-179.37(17)
C(1)-C(2)-C(3)-C(10)	0.2(3)
N(1)-C(4)-C(5)-N(2)	176.04(16)
N(3)-C(4)-C(5)-N(2)	-2.2(2)
N(1)-C(4)-C(5)-C(13)	-3.5(3)
N(3)-C(4)-C(5)-C(13)	178.25(16)
N(2)-C(6)-C(7)-C(8)	-178.69(16)
C(15)-C(6)-C(7)-C(8)	1.0(3)
C(6)-C(7)-C(8)-C(9)	-0.6(3)
C(7)-C(8)-C(9)-C(16)	-0.2(3)
C(7)-C(8)-C(9)-Br(1)	179.81(14)
N(1)-C(3)-C(10)-N(3)	0.35(19)
C(2)-C(3)-C(10)-N(3)	-179.26(15)
N(1)-C(3)-C(10)-C(11)	179.73(15)
C(2)-C(3)-C(10)-C(11)	0.1(3)
N(3)-C(10)-C(11)-C(12)	178.79(17)
C(3)-C(10)-C(11)-C(12)	-0.4(3)
C(10)-C(11)-C(12)-C(1)	0.4(3)
C(2)-C(1)-C(12)-C(11)	-0.2(3)
N(2)-C(5)-C(13)-C(14)	-0.4(3)
C(4)-C(5)-C(13)-C(14)	179.14(16)
C(5)-C(13)-C(14)-C(15)	0.1(3)
C(13)-C(14)-C(15)-C(16)	-179.04(17)
C(13)-C(14)-C(15)-C(6)	0.2(3)
N(2)-C(6)-C(15)-C(14)	-0.3(3)
C(7)-C(6)-C(15)-C(14)	-179.93(16)
N(2)-C(6)-C(15)-C(16)	178.96(16)
C(7)-C(6)-C(15)-C(16)	-0.7(2)
C(8)-C(9)-C(16)-C(15)	0.4(3)
Br(1)-C(9)-C(16)-C(15)	-179.53(13)
C(14)-C(15)-C(16)-C(9)	179.18(17)
C(6)-C(15)-C(16)-C(9)	0.0(3)
N(3)-C(4)-N(1)-C(3)	0.61(19)

C(5)-C(4)-N(1)-C(3)	-177.76(16)
C(2)-C(3)-N(1)-C(4)	178.99(18)
C(10)-C(3)-N(1)-C(4)	-0.58(19)
C(13)-C(5)-N(2)-C(6)	0.3(2)
C(4)-C(5)-N(2)-C(6)	-179.26(14)
C(7)-C(6)-N(2)-C(5)	179.73(16)
C(15)-C(6)-N(2)-C(5)	0.1(2)
N(1)-C(4)-N(3)-C(10)	-0.4(2)
C(5)-C(4)-N(3)-C(10)	178.01(15)
C(11)-C(10)-N(3)-C(4)	-179.27(18)
C(3)-C(10)-N(3)-C(4)	0.02(18)

Symmetry transformations used to generate equivalent atoms:

Table 8: Hydrogen bonds for **A5f**.

D-H...A	d(D-H)	d(H...A)	d(D...A)	<(DHA)
N(3)-H(3)...O(1S)#1	0.88	1.92	2.7683(19)	162
O(1S)-H(1H)...N(1)#2	0.812(10)	2.014(12)	2.806(2)	165
O(1S)-H(2H)...N(2)#3	0.820(9)	2.272(15)	3.0108(19)	150
O(1S)-H(2H)...O(1S)#4	0.820(9)	2.49(2)	2.899(3)	112
N(3)-H(3)...O(1S)#1	0.88	1.92	2.7683(19)	162
O(1S)-H(1H)...N(1)#2	0.812(10)	2.014(12)	2.806(2)	165
O(1S)-H(2H)...N(2)#3	0.820(9)	2.272(15)	3.0108(19)	150
O(1S)-H(2H)...O(1S)#4	0.820(9)	2.49(2)	2.899(3)	112

Symmetry transformations used to generate equivalent atoms:

#1 -x+2,-y+1,-z+1   #2 -x+5/2,-y+3/2,-z+1   #3 x+1/2,y+3/2,z

#4 -x+5/2,-y+5/2,-z+1